NEHRP Recommended Revisions to ASCE/SEI 41-17, *Seismic Evaluation and Retrofit of Existing Buildings*

FEMA P-2208 / August 2023

FEMA

nehrp

NEHRP Recommended Revisions to ASCE/SEI 41-17, *Seismic Evaluation and Retrofit of Existing Buildings*

Prepared by
APPLIED TECHNOLOGY COUNCIL
201 Redwood Shores Parkway, Suite 240
Redwood City, California 94065
www.ATCouncil.org

Prepared for
FEDERAL EMERGENCY MANAGEMENT AGENCY
Michael Mahoney, Project Officer (retired)
Christina Aronson, Task Monitor
Andrew Herseth, Task Monitor
William T. Holmes, Technical Advisor
Washington, D.C.

APPLIED TECHNOLOGY COUNCIL
Jon A. Heintz, Project Executive
Justin Moresco, Project Manager

PROJECT TECHNICAL COMMITTEE
Terry Lundeen (Project Tech. Director)
Russell Berkowitz
Wassim Ghannoum
Bret Lizundia
Roy Lobo
Mark Moore
James Parker
Bob Pekelnicky
Peter Somers
Bill Tremayne

PROJECT REVIEW PANEL
Michael Cochran*
Jennifer Goupil
Phil Line
Bonnie Manley
Khaled Nahlawi
Jason Thompson

WORKING GROUP 1, LINEAR ANALYSIS
Bret Lizundia (Team Leader)
Russell Berkowitz
Erick Burgos
Stergios Koutrouvelis
Terry Lundeen
Jie Luo
Garrett Hagen
Bob Pekelnicky
Cynthia Perry

FEMA

nehrp

WORKING GROUP 1, NONLINEAR ANALYSIS
Bob Pekelnicky (Team Leader)
Russell Berkowitz
Rebecca Collins
Greg Deierlein
Wassim Ghannoum
Garrett Hagen
Ron Hamburger
Bret Lizundia
Terry Lundeen
Pearl Ranchal
Charles Roeder
Nick Skok
Bill Tremayne

WORKING GROUP 2, FOUNDATIONS
Roy Lobo (Team Leader)
Ryan Bogart
John Egan
Bruce Kutter
Bret Lizundia
Mark Moore
Bob Pekelnicky
Peter Somers
Kate Spiesman

WORKING GROUP 3, CONCRETE STRUCTURAL WALLS
Wassim Ghannoum (Team Leader)
Saman Abdullah
Garrett Hagen
Afshar Jalalian
Laura Lowes
Mohamed Talaat
John Wallace

WORKING GROUP 4, TIER 1 AND 2
Peter Somers (Team Leader)
James Parker
Russell Berkowitz
Eugene Trahern

WORKING GROUP 6, UNREINFORCED MASONRY
Bret Lizundia (Team Leader)
Rebecca Collins
Terry Lundeen
Cynthia Perry
Bill Tremayne
Kylin Vail

*ATC Board Representative

Notice

Cover photograph – Historic 1893 unreinforced masonry building in Seattle retrofitted with new steel concentrically braced frames in one direction (credit: Coughlin Porter Lundeen).

Foreword

The Federal Emergency Management Agency (FEMA) has the goal of reducing the ever-increasing cost that disasters inflict on our country. Preventing losses before they happen by designing and building to withstand anticipated forces from these hazards is one of the key components of mitigation and is the only truly effective way of reducing the cost of disasters.

As part of its responsibilities under the National Earthquake Hazards Reduction Program (NEHRP), and in accordance with the National Earthquake Hazards Reduction Act of 1977 (PL 94-125, as amended), FEMA is charged with supporting activities necessary to improve technical quality in the field of earthquake engineering. The primary method of addressing this charge has been supporting the investigation of seismic technical issues as they are identified by FEMA, the development and publication of technical design and construction guidance products, the dissemination of these products, and support of training and related outreach efforts.

One of the issues of significant concern for the Program continues to be the risk to the nation presented by older, existing buildings that were constructed prior to the development, adoption, and enforcement of modern building codes. Existing buildings represent a significant percentage of the nation's building stock and their often-poor performance in earthquakes poses a significant risk to the resilience of our nation's communities.

FEMA has supported the development of retrofitting criteria for seismically deficient buildings, dating all the way back to the publication of FEMA 172, *NEHRP Handbook of Techniques for the Seismic Rehabilitation of Existing Buildings*, in 1992 and FEMA 273, *NEHRP Guidelines for the Seismic Rehabilitation of Buildings*, in 1997. However, our goal was always to have this material incorporated into the nation's consensus design standards, and this work culminated in the publication of the American Society of Civil Engineers/Structural Engineering Institute (ASCE/SEI) 41, *Seismic Rehabilitation of Existing Buildings*.

To support the use of ASCE/SEI 41, FEMA contracted with ATC to develop a series of case studies, which FEMA published in June 2018 as FEMA P-2006, *Example Application Guide for ASCE/SEI 41-13 Seismic Evaluation and Retrofit of Existing Buildings with Additional Commentary for ASCE/SEI 41-17*. In developing FEMA P-2006, the team noted several problem areas in ASCE/SEI 41 that needed more work than a typical voluntary committee could provide. For that reason, FEMA funded ATC to put together a series of working groups to address some of the more serious issues. Those working groups prepared 35 recommended changes that were submitted to the ASCE/SEI 41 Update Committee, and all were accepted in some form. Those recommended revisions form the basis of this publication, along with supporting information and commentary, and this publication is intended to be used in conjunction with ASCE/SEI 41-23.

FEMA is indebted to the leadership of Terry Lundeen, Project Technical Director, and to the members of the project working groups for their efforts in the development of this document. The Project Technical Committee, consisting of Russell Berkowitz, Wassim Ghannoum, Bret Lizundia, Roy Lobo,

Mark Moore, James Parker, Bob Pekelnicky, Peter Somers, and Bill Tremayne, led the technical development efforts, and guided the investigations of the working groups.

We also wish to thank the Project Review Panel, which consisted of Michael Cochran, Jennifer Goupil, Phil Line, Bonnie Manley, Khaled Nahlawi, and Jason Thompson. This group provided significant technical advice and consultation over the duration of the work.

Finally, we also wish to thank William Holmes, FEMA Technical Advisor, and the Applied Technology Council, in particular Jon A. Heintz, Project Executive, Justin Moresco, Project Manager, and Veronica Cedillos, Project Manager, for making this publication possible.

The names and affiliations of all who contributed to this report are provided in the list of project participants. Without their dedication and hard work, this publication would not have been possible. The nation will be safer from the next earthquake as a result.

Federal Emergency Management Agency

Preface

The Federal Emergency Management Agency (FEMA) has for many years funded technical studies that address the seismic safety of existing buildings. In 1997, FEMA published FEMA 273, *NEHRP Guidelines for the Seismic Rehabilitation of Buildings*, which presented procedures for performance-based engineering analysis using nonlinear static procedures. This document was superseded by FEMA 356, *Prestandard and Commentary for the Seismic Rehabilitation of Buildings*, which then evolved into the American National Standards Institute-approved consensus standard ASCE/SEI 41-06, *Seismic Rehabilitation of* Existing *Buildings*, published in 2007. The consensus standard has been updated two times, with the latest version, ASCE/SEI 41-17, *Seismic Evaluation and Retrofit of Existing Buildings*, published in 2017, and a third update expected to be published in 2023.

In 2017, the Applied Technology Council (ATC) was awarded the first in a series of task orders under contract HSFE60-17-D-0002 with FEMA to "Update Seismic Retrofit Design Guidance," designated the ATC-140 Project Series. The purpose of this project series was to investigate and propose solutions to technical and procedural issues in the evaluation and retrofit of existing buildings presented in ASCE/SEI 41-17. An important goal of the project series was for the project team to remain in regular contact with relevant subcommittees of the American Society of Civil Engineer's *Seismic Retrofit of Existing Buildings Standards Committee*, which oversees the development of ASCE/SEI 41. This regular contact helped to ensure that the ATC-140 work was current and appropriate and was addressing issues under consideration by the committee.

ATC is indebted to the leadership of Terry Lundeen, who served as the Project Technical Director; Bob Pekelnicky, who served as Working Group 1, Nonlinear Analysis Team Leader; Bret Lizundia, who served as Working Group 1, Linear Analysis and Working Group 6, Unreinforced Masonry Team Leader; Roy Lobo, who served as Working Group 2, Foundations Team Leader; Wassim Ghannoum, who served as Working Group 3 Team Leader; Peter Somers, who served as Working Group 4, Tier 1 and 2 Team Leader, as well as the other members of the Project Technical Committee, including Russ Berkowitz, Mark Moore, James Parker, and Bill Tremayne. The Project Review Panel, consisting of Michael Cochran, Jennifer Goupil, Phil Line, Bonnie Manley, Khaled Nahlawi, and Jason Thompson, provided technical review and advice at key stages of the work.

This work would not have been possible without the contributions from the many working group members. ATC would also like to thank Rebecca Collins, who provided invaluable feedback on early drafts of this report, in particular helping to ensure consistency across the writeups of the various working groups.

ATC also gratefully acknowledges Mike Mahoney (FEMA Project Officer), Christina Aronson (FEMA Task Monitor), Drew Herseth (FEMA Task Monitor), and Bill Holmes (FEMA Technical Advisor) for their input and guidance in the preparation of this report, Veronica Cedillos (ATC) for project management services, and Ginevra Rojahn (ATC) and Kiran Khan (ATC) for report production services. The names and affiliations of all who contributed to this report are provided in the list of Project Participants at the end of this report.

Justin Moresco
ATC Director of Projects

Jon A. Heintz
ATC Executive Director

Table of Contents

Foreword iii

Preface v

List of Figures xix

List of Tables xxxix

Chapter 1: Introduction 1-1

1.1 Background and Purpose 1-1

1.2 Project Organization and Approach 1-1

1.3 Summary of Change Proposals 1-2

1.4 Content and Report Organization 1-5

Chapter 2: Recommendations for Future Studies 2-1

2.1 Overview 2-1

2.2 High-Level Studies 2-1

2.2.1 Introduction 2-1

2.2.2 Revamp Linear Procedures 2-1

2.2.3 Revamp Foundation Chapter Technical Basis 2-2

2.2.4 Functional Recovery Performance Level 2-3

2.2.5 The Right “Break” for Existing Buildings 2-4

2.2.6 Benchmarking 2-5

2.2.7 Revamp Tier 1 Checklists Procedure 2-5

2.2.8 Life Safety Performance Definition and Quantitative Criteria 2-5

2.3 Studies That Are Continuations or Outcomes of Working Group Efforts 2-6

2.3.1 Introduction 2-6

2.3.2 Linear Analysis 2-6

2.3.3 Nonlinear Modeling Parameters 2-7

2.3.4 Foundations 2-7

2.3.5 Tier 1 Analysis 2-9

2.3.6 Masonry 2-10

2.4 Studies That Are Moderate in Scope 2-11

2.4.1 Introduction 2-11

2.4.2 Update Concrete Coupling Beam Acceptance Criteria 2-11

2.4.3 Update Material Properties / Expected Strength for Concrete and Reinforcement 2-12

2.4.4 Primary Research of Cyclic Behavior of Concrete Piers in Tension 2-12

2.4.5 Update Concrete Wall Pier Acceptance Criteria 2-12

2.4.6 Evaluate the Force-Controlled vs. Deformation-Controlled Basis for Subdiaphragms 2-12

2.5 Studies That Are Major in Scope 2-13

2.5.1 Introduction 2-13

2.5.2 Develop Energy-Based Methodology 2-13

2.5.3 Develop Acceptance Criteria for Common Retrofit Components 2-13

2.5.4 Develop Comprehensive, Coordinated, Coherent Strength and Stiffness Values for Wood Diaphragms 2-13

2.5.5 Reorganize/Reformat ASCE/SEI 41 2-13

Part 1

Chapter 1: Revisions to Section 7.3 Linear Limitation Provisions 1-1

1.1 Motivation 1-1

1.2 Summary of Changes Recommended 1-1

1.3 Technical Studies 1-2

1.3.1 Overview 1-2

1.3.2 Case Study Summaries and Findings 1-7

1.3.3 FEMA P-2006 Design Example Summaries and Findings 1-29

1.3.4 Review of Research Studies 1-35

1.3.5 Evolution of the Linear Procedure Limitation Provision 1-37

1.3.6 Observations on Possible Alternative Linear Procedure Limitation Provision Options 1-39

1.3.7 Conclusions and Recommendations 1-41

1.4 Recommended Changes 1-44
1.5 References 1-47

Chapter 2: Adding Acceptance Ratio Term 2-1
2.1 Motivation 2-1
2.2 Summary of Changes Recommended 2-1
2.3 Technical Studies 2-1
2.4 Recommended Changes 2-2
2.5 References 2-3

Part 2

Chapter 1: Nonlinear Analysis Revisions 1-1
1.1 Motivation 1-1
1.1.1 Critical and Ordinary Actions 1-1
1.1.2 Force-Controlled Actions 1-2
1.1.3 Unacceptable Response Drift Limit 1-3
1.1.4 No Unacceptable Responses for Life Safety 1-4
1.1.5 Secondary Components 1-5
1.1.6 Damping 1-6
1.1.7 Accidental Torsion 1-6
1.1.8 Material Property Bounding 1-7
1.2 Summary of Changes Recommended 1-7
1.2.1 Critical and Ordinary Actions 1-7
1.2.2 Force-Controlled Actions 1-7
1.2.3 Unacceptable Response Story Drift Ratio Limit 1-8
1.2.4 No Unacceptable Responses for Life Safety 1-8
1.2.5 Secondary Components 1-9
1.2.6 Damping 1-9
1.2.7 Accidental Torsion 1-10
1.2.8 Material Property Bounding 1-11

1.3 Technical Studies 1-11
1.3.1 Critical and Ordinary Actions 1-14
1.3.2 Force-Controlled Actions 1-15
1.3.3 Unacceptable Response Story Drift Ratio Limit 1-17
1.3.4 No Unacceptable Responses for Life Safety 1-18
1.3.5 Secondary Components 1-19
1.3.6 Damping 1-21
1.3.7 Accidental Torsion 1-26
1.3.8 Material Property Bounding 1-28
1.4 Recommended Changes 1-31
1.4.1 Critical and Ordinary Actions 1-31
1.4.2 Force-Controlled Actions 1-32
1.4.3 Unacceptable Response Drift Limit 1-33
1.4.4 No Unacceptable Responses for Life Safety 1-34
1.4.5 Secondary Components 1-34
1.4.6 Damping 1-35
1.4.7 Accidental Torsion 1-37
1.4.8 Property Bounding 1-39
1.5 References 1-40

Chapter 2: Nonlinear Modeling Parameter and Acceptance Criteria Revisions 2-1
2.1 Motivation 2-1
2.1.1 Modeling Parameter and Acceptance Criteria Revisions 2-1
2.1.2 Fiber Model Requirements 2-1
2.2 Summary of Changes Recommended 2-2
2.2.1 Modeling Parameters and Acceptance Criteria Revisions 2-2
2.2.2 Fiber Model Requirements 2-3
2.3 Technical Studies 2-4
2.3.1 Modeling Parameters and Acceptance Criteria Revisions 2-4
2.3.2 Fiber Model Requirements 2-15
2.4 Recommended Changes 2-21

2.4.1 Modeling Parameters and Acceptance Criteria Revisions 2-22
2.4.2 Fiber Model Requirements 2-35
2.5 References 2-36

Part 3

Chapter 1: Revisions to Chapter 8 Foundation Provisions 1-1
1.1 Motivation 1-1
1.2 Summary of Recommended Changes 1-4
1.2.1 Application of Evaluation Provisions for Shallow Foundations 1-4
1.2.2 Expected Soil Bearing Capacity 1-4
1.2.3 Seismic Overturning Forming Axial Load Action 1-4
1.2.4 Foundation Moment Capacity with Bi-directional Overturning Action 1-5
1.2.5 Determination of Soil Stiffness for Mat Foundations 1-5
1.2.6 Procedures for a Separate Foundation Analysis Using Superstructure Demands from a Fixed-Base Model 1-5
1.2.7 Moment Capacity of Footings Interconnected by Grade Beams 1-5
1.2.8 Limiting Use of Compression-Only Springs When Superstructure Is Modeled as Linear Using Flexible-Base Procedures 1-5
1.2.9 Acceptance Criteria Check for the Structural Footing 1-6
1.2.10 Bounding Requirements for Nonlinear Procedures 1-6
1.3 Technical Studies 1-6
1.3.1 Overview of Case Studies 1-6
1.3.2 Application of Evaluation Provisions for Shallow Foundations 1-16
1.3.3 Expected Soil Bearing Capacity 1-29
1.3.4 Seismic Overturning Forming Axial Load Action 1-31
1.3.5 Foundation Moment Capacity with Bi-directional Overturning Action 1-34
1.3.6 Determination of Soil Stiffness for Mat Foundations 1-50
1.3.7 Procedures for a Separate Foundation Analysis Using Superstructure Demands from a Fixed-Base Model 1-59
1.3.8 Moment Capacity of Footings Interconnected by Grade Beams 1-63

1.3.9 Limiting Use of Compression-Only Springs When Superstructure Is Modeled as Linear Using Flexible-Base Procedures 1-65
1.3.10 Acceptance Criteria Check for the Structural Footing 1-75
1.3.11 Bounding Requirements for Nonlinear Procedures 1-79
1.4 Recommended Changes 1-87
1.4.1 Application of Evaluation Provisions for Shallow Foundations 1-87
1.4.2 Expected Soil Bearing Capacity 1-89
1.4.3 Seismic Overturning Forming Axial Load Action 1-90
1.4.4 Foundation Moment Capacity with Bi-directional Overturning Action 1-91
1.4.5 Determination of Soil Stiffness for Mat Foundations 1-94
1.4.6 Procedures for a Separate Foundation Analysis Using Superstructure Demands from a Fixed-Base Model 1-95
1.4.7 Moment Capacity of Footings Interconnected by Grade Beams 1-96
1.4.8 Limiting Use of Compression-Only Springs When Superstructure Is Modeled as Linear Using Flexible-Base Procedures 1-97
1.4.9 Acceptance Criteria Check for the Structural Footing 1-97
1.4.10 Bounding Requirements for Nonlinear Procedures 1-98
1.5 References 1-100

Part 4

Chapter 1: Revisions to Concrete Structural Wall Stiffness, Modeling Guidance, and Flexure-Controlled Provisions 1-1
1.1 Motivation 1-1
1.2 Summary of Recommended Changes 1-2
1.3 Technical Studies 1-3
1.3.1 Wall Test Database 1-3
1.3.2 Wall Stiffness 1-18
1.3.3 Wall Moment Strength 1-31
1.3.4 Modeling Parameters and Acceptance Criteria 1-35
1.3.5 Conclusions 1-58
1.4 Recommended Changes 1-60

1.4.1 Stiffness Provisions 1-61
1.4.2 Strength Provisions 1-63
1.4.3 Modeling Parameters and Acceptance Criteria 1-63
1.4.4 Analysis Guidance 1-68
1.5 Flexure-Controlled Walls Example 1-71
1.5.1 Overview of Building 1-72
1.5.2 Strength and Stiffness 1-77
1.5.3 Classification 1-78
1.5.4 Evaluation Using Nonlinear Static Procedure 1-79
1.5.5 Discussion and Conclusions 1-100
1.5 References 1-100

Chapter 2: Revisions to Concrete Structural Wall Shear-Controlled Provisions 2-1
2.1 Motivation 2-1
2.2 Summary of Recommended Changes 2-1
2.3 Technical Studies 2-2
2.3.1 Wall Test Database 2-2
2.3.2 Wall Lateral Shear Strengths 2-3
2.3.3 Modeling Parameters and Acceptance Criteria 2-13
2.3.4 Comparison Between ACI 369.1-17 and Proposed Modeling Parameters and Acceptance Criteria 2-25
2.3.5 Conclusions 2-29
2.4 Recommended Changes 2-29
2.4.1 Stiffness Provisions 2-30
2.4.2 Strength Provisions 2-31
2.4.3 Modeling Parameters and Acceptance Criteria 2-32
2.5 Shear-Controlled Walls Example 2-33
2.5.1 Overview of Building 2-34
2.5.2 Evaluation Using Linear Dynamic Procedure 2-41
2.5.3 Evaluation Using Nonlinear Static Procedure 2-44
2.6 References 2-49

Chapter 3: Revisions to Concrete Structural Wall Shear-Friction-Controlled Provisions..... 3-1
3.1 Motivation 3-1
3.2 Summary of Recommended Changes 3-2
3.3 Technical Studies 3-2
3.3.1 Wall Test Database 3-2
3.3.2 Background of Wall Shear-Friction Strength 3-5
3.3.3 Wall Shear-Friction Strengths 3-15
3.3.4 Modeling Parameters and Acceptance Criteria 3-19
3.3.5 Summary and Conclusions 3-24
3.4 Recommended Changes 3-26
3.4.1 Strength Provisions 3-26
3.4.2 Acceptance Criteria and Modeling Parameters 3-27
3.5 Shear Friction-Controlled Walls Example 3-29
3.5.1 Overview of Building 3-29
3.5.2 Evaluation Using Linear Dynamic Procedure 3-35
3.6 References 3-38

Chapter 4: Revisions to Concrete Structural Wall Classification 4-1
4.1 Motivation 4-1
4.2 Summary of Recommended Changes 4-1
4.3 Technical Studies 4-2
4.3.1 Wall Database 4-2
4.3.2 Proposed Wall Classification Approach 4-4
4.3.3 Validation of Proposed Classification Approach and Comparison with ACI 369.1-17 Approach 4-8
4.3.4 Conclusions 4-9
4.4 Recommended Changes 4-9
4.4.1 Strength-Based Classification 4-9
4.5 References 4-11

Part 5

Chapter 1: Update to Common Building Type Definitions 1-1

1.1 Motivation 1-1

1.2 Summary of Changes Recommended 1-1

1.3 Technical Studies 1-1

1.3.1 Updates to ASCE/SEI 41-17 Table 3-1 1-1

1.3.2 Updates to Wood-Framed Common Building Types 1-2

1.4 Recommended Changes 1-3

1.4.1 Provisions and Commentary 1-3

1.4.2 Wood-Frame Buildings 1-4

1.5 References 1-5

Chapter 2: Updates to Tier 1 Diaphragm-Related Provisions 2-1

2.1 Motivation 2-1

2.2 Summary of Changes Recommended 2-1

2.3 Technical Studies 2-1

2.3.1 Story Shear Forces 2-2

2.3.2 Torsion 2-2

2.3.3 Diaphragm Continuity 2-2

2.3.4 Wood and Bare-Steel-Deck Diaphragm Checklist Statements 2-3

2.4 Recommended Changes 2-7

2.4.1 Story Shear Forces 2-7

2.4.2 Torsion 2-7

2.4.3 Diaphragm Continuity 2-8

2.4.4 Wood and Bare-Steel-Deck Diaphragm Checklist Statements 2-8

2.4.5 Tier 2 Diaphragm Updates 2-9

2.4.6 Appendix A Updates 2-10

2.5 References 2-11

Chapter 3: Updates to Tier 1 Foundations and Overturning-Related Provisions 3-1
3.1 Motivation 3-1
3.2 Summary of Changes Recommended 3-1
3.3 Technical Studies 3-1
3.3.1 Overturning Checklist Statement 3-1
3.3.2 Deep Foundation and Sloping Sites Checklist Application 3-4
3.3.3 Deep Foundations 3-5
3.3.4 Sloping Sites 3-5
3.4 Recommended Changes 3-6
3.4.1 Overturning Checklist Statement 3-6
3.4.2 Deep Foundations and Sloping Sites Checklist Application 3-9
3.4.3 Deep Foundations 3-9
3.4.4 Sloping Sites 3-10
3.5 References 3-10

Chapter 4: Guidance for Prioritization of Checklist Statements 4-1
4.1 Motivation 4-1
4.2 Summary of Changes Recommended 4-1
4.3 Technical Studies 4-1
4.4 Recommended Changes 4-2
4.5 References 4-4

Chapter 5: Updates to Tier 2 Retrofit Provisions 5-1
5.1 Motivation 5-1
5.2 Summary of Changes Recommended 5-1
5.3 Technical Studies 5-1
5.3.1 Studies of Representative Tier 2 Retrofit Systems 5-2
5.3.2 Compliance with Deficiency-Based Evaluation 5-4
5.3.3 Additional Evaluation of the Retrofitted Building 5-4
5.3.4 Evaluation of New and Modified Structural Elements and Connections 5-4
5.3.5 Retrofit Design Requirements for Specific Structural Systems 5-5

5.4 Recommended Changes 5-6
5.5 References 5-8

Part 6

Chapter 1: Revised Provisions for New Vertical Elements Chapter 16 1-1
1.1 Motivation 1-1
1.2 Summary of Changes Recommended 1-2
1.3 Technical Studies 1-3
1.3.1 Overview of Working Group 6 Case Studies 1-3
1.3.2 Case Study: Retrofit Situation 1 with New Vertical Elements at Front and Rear Walls 1-15
1.3.3 Case Study: Retrofit Situation 2 with New Vertical Element at Midspan 1-19
1.3.4 Case Study: Retrofit Situation 3 with New Vertical Elements at Open Storefront 1-42
1.3.5 Review of Detailing Requirements 1-51
1.3.6 Conclusions 1-55
1.4 Recommended Changes 1-56
1.5 References 1-59

Chapter 2: Addition of Subdiaphragm Provisions to Chapter 16 2-1
2.1 Motivation 2-1
2.2 Summary of Changes Recommended 2-1
2.3 Technical Studies 2-2
2.3.1 Case Study 2-2
2.3.2 Diaphragm Capacity Studies 2-9
2.3.3 Parametric Study 2-17
2.3.4 Conclusions 2-19
2.4 Recommended Changes 2-20
2.4 References 2-22

Chapter 3: Revisions to Chapter 16 URM Wall Out-of-Plane Provisions 3-1
3.1 Motivation 3-1

3.2 Summary of Changes Recommended 3-1
3.3 Technical Studies 3-1
3.3.1 Penner and Elwood Studies and Method 3-2
3.3.2 ASCE/SEI 41-17 Chapter 11 Updates for Life Safety 3-4
3.3.3 Parametric Study 3-5
3.3.4 Diaphragm Spans and Cross Walls 3-12
3.3.5 Conclusions 3-12
3.4 Recommended Changes 3-12
3.5 References 3-14

Chapter 4: Revisions to Chapter 11 URM Wall Out-of-Plane Provisions 4-1
4.1 Motivation 4-1
4.2 Summary of Changes Recommended 4-1
4.3 Technical Studies 4-1
4.3.1 Penner and Elwood Studies and Method 4-2
4.3.2 ASCE/SEI 41-17 Chapter 11 Updates for Life Safety 4-3
4.3.3 Parametric Study 4-5
4.3.4 Cross Walls 4-11
4.3.5 Other Considerations 4-11
4.3.6 Conclusions 4-12
4.4 Recommended Changes 4-12
4.5 References 4-18

Chapter 5: Addition of Redistribution Provisions for Walls in Section 11.3.2.3.1 5-1
5.1 Motivation 5-1
5.2 Summary of Changes Recommended 5-1
5.3 Technical Studies 5-1
5.3.1 Mixed Modes of Response 5-1
5.3.2 Case Study 5-5
5.3.3 Implementation of Redistribution Concept 5-6
5.3.4 Conclusions 5-7

5.4 Recommended Changes 5-8
5.5 References 5-10

Chapter 6: Revisions to Chapter 11 URM Rocking Axial Stress Provisions 6-1
6.1 Motivation 6-1
6.2 Summary of Changes Recommended 6-1
6.3 Technical Studies 6-1
6.4 Recommended Changes 6-3
6.5 References 6-6

List of Participants A-1

List of Figures

Part 1

Figure 1-1 Working Group 1 RCSW linear model 1-9

Figure 1-2 Working Group 1 RCSW Pattern 1 1-9

Figure 1-3 Working Group 1 RCSW Pattern 2. 1-9

Figure 1-4 Working Group 1 RCSW nonlinear model 1-11

Figure 1-5 Working Group 1, Nonlinear steel moment frame linear model 1-19

Figure 1-6 Working Group 1, Nonlinear braced frame linear model 1-21

Figure 1-7 Working Group 2 cantilever shear wall building foundation and first floor plan 1-22

Figure 1-8 Working Group 2 cantilever shear wall partial elevation of central N-S shear wall 1-23

Figure 1-9 Working Group 3 shear wall first floor plan 1-25

Figure 1-10 Working Group 3 shear wall 3D model 1-27

Figure 1-11 FEMA P-2006 steel moment frame linear model 1-29

Figure 1-12 FEMA P-2006 steel braced frame design example building 1-30

Figure 1-13 FEMA P-2006 steel braced frame design example typical floor 1-31

Figure 1-14 FEMA P-2006 concrete shear wall design example building 1-32

Figure 1-15 FEMA P-2006 concrete shear wall design example typical floor 1-33

Part 2

Figure 1-1 Type 3 Nonlinear force-displacement curve 1-8

Figure 1-2 Moment frame building plan 1-12

Figure 1-3 Moment frame building isometric and elevations 1-13

Figure 1-4 Braced frame building plan 1-13

Figure 1-5 Braced frame elevation 1-14

Figure 1-6 Brace frame model with elastic force-controlled actions 1-15

Figure 1-7 Brace frame model with force-controlled action failure explicitly modeled 1-16

Figure 1-8 Drift comparison with and without force-controlled actions explicitly modeled 1-16

Figure 1-9 Probability of collapse for various COVs 1-19

Figure 1-10 Story drift for moment frame model with and without secondary frames for various seismic hazard levels 1-20

Figure 1-11 Measured percent damping versus building height 1-22

Figure 1-12 Illustration of PEER TBIv2 damping equation 1-22

Figure 1-13 Illustration of spurious damping forces 1-23

Figure 1-14 Story drift for moment frame model with 5% critical damping and with 2% critical damping 1-24

Figure 1-15 Variation of damping ratio with periods of the free vibration modes of the structure per the Rayleigh damping model 1-26

Figure 1-16 Example of building with no torsional resistance 1-27

Figure 1-17 Drift response of Monte Carlo simulation varying the beam strength 1-29

Figure 1-18 Drift response of model with upper-bound, median, and lower-bound beam strength 1-30

Figure 1-19 Comparison of drift response between Monte Carlo simulation and strength bounding cases 1-30

Figure 2-1 FEMA 273 Deformation-controlled component action force-displacement backbone 2-4

Figure 2-2 First cycle versus second cycle backbone curve example 2-6

Figure 2-3 Proposed force-displacement backbone 2-7

Figure 2-4 ASCE/SEI 41-17 and NIST GCR 17-917-45 beam-column hinge and acceptance criteria 2-8

Figure 2-5 Story drift under BSE-2E with ASCE/SEI 41-17 hinges and NIST GCR 17-917-45 hinges 2-9

Figure 2-6 Monte Carlo simulation showing the sensitivity of results to the 'a' parameter when the response is only slightly past the 'a' parameter or significantly past the 'a' parameter 2-10

Figure 2-7 Monte Carlo simulation results for 'a' and 'b' parameter variability 2-11

Figure 2-8 Monte Carlo simulation compared to model with median parameters 2-11

Figure 2-9 Damage control limit change 2-13

Figure 2-10 Proposed backbone curve and acceptance criteria 2-14

Figure 2-11 Default hysteretic pinching shapes 2-15

Figure 2-12 Reinforced concrete column load-response dependence on number of integration points 2-17

Figure 2-13 Load-displacement response of wall specimen as measured and as simulated 2-18

Figure 2-14 Load-displacement simulated response using different numbers of elements per story without material regularization and with material regularization 2-18

Figure 2-15 Rotation gage assignment in four-node wall element 2-19

Figure 2-16 Classification of component pinching response 2-20

Part 3

Figure 1-1 Foundation plan 1-8

Figure 1-2 Retrofit wall and existing structure elevation 1-9

Figure 1-3 Structure boundary conditions 1-10

Figure 1-4 Three-dimensional model of the seven-story reinforced concrete special moment resisting frame building 1-14

Figure 1-5 Proposed foundation evaluation procedures for buildings on shallow foundations 1-17

Figure 1-6 Foundation length for the simplified procedure 1-18

Figure 1-7 Example showing when the simplified procedure may be used as a function of the pseudo seismic axial load 1-19

Figure 1-8 Condition where lateral and vertical soil flexibilities are required to be modeled 1-21

Figure 1-9 Example of a building with less than 15% of weight at the lower foundation level. 1-21

Figure 1-10 Example of a stepped footing where lateral and vertical soil flexibilities are not required to be modeled 1-22

Figure 1-11 Building with lateral force resisting elements of different heights 1-22

Figure 1-12 Figure 2-6 of FEMA P-2091 illustrating impact of soil flexibility 1-23

Figure 1-13 Figure 2-5 of FEMA P-2091 showing the impact of flexible-base modeling 1-24

Figure 1-14 Variation of moment capacity with expected soil bearing capacity 1-30

Figure 1-15 Overturning resisted by coupled axial load actions on footings 1-32

Figure 1-16 Overturning resisted by coupled axial load actions on footings 1-32

Figure 1-17 Overturning resisted by coupled axial load actions on footings 1-33

Figure 1-18 Isolated footing under axial load and moment represented in terms of eccentricity 1-34

Figure 1-19 Isolated footing under axial load and moment represented in terms of eccentricity 1-35

Figure 1-20 Area of footing in contact with the soil based on axial load eccentricity 1-35

Figure 1-21 Eccentricity zones corresponding to soil pressure distribution type 1-36

Figure 1-22 Footing under inherent biaxial loading 1-37

Figure 1-23 Comparison of Options with m-factors multiplying the capacity and of m-factors reducing the demand 1-38

Figure 1-24 Generalized method to define the boundaries of the critical contact area 1-40

Figure 1-25 Critical contact area A_c of a rectangular footing, when the zero-pressure line intersects two opposite edges of the footing 1-42

Figure 1-26 Critical contact area A_c of a rectangular footing, when the zero-pressure line intersects two adjacent edges of the footing 1-43

Figure 1-27 Normalized orthogonal moment capacities for a rectangular footing 1-44

Figure 1-28 Positive M_y moment capacity with positive M_x moment 1-45

Figure 1-29 Positive M_y moment capacity with positive M_x moment 1-46

Figure 1-30 Negative M_y moment capacity with positive M_x moment 1-47

Figure 1-31 Negative M_y moment capacity with positive M_x moment 1-48

Figure 1-32 Comparison of the shapes for the critical contact area with a uniform and triangular soil pressure distribution under for an L-shaped footing 1-49

Figure 1-33 Figure 8-2 from ASCE/SEI 41-17 1-51

Figure 1-34 Variation in soil stiffness values as function of footing width, ASCE/SEI Figure 8-2 1-51

Figure 1-35 Variation in soil stiffness values as function of footing width, ASCE/SEI 41-17 Eq. 8-11 1-52

Figure 1-36 Mat foundation supporting vertical elements spanning multiple bays 1-53

Figure 1-37 Vertical soil pressure profiles for selected points beneath a foundation 1-54

Figure 1-38 Vertical stress σ_z at any point *P* at depth *z* 1-55

Figure 1-39 Soil pressure zones under a mat of footing length, *L*, and width, *B* 1-55

Figure 1-40 Soil pressure zones under a mat of footing length, *L*, and width, *B* 1-56

Figure 1-41 Soil pressure zones under a mat of footing length, *L*, and width, *B* 1-57

Figure 1-42 Soil pressure zones under a mat of footing length, *L*, and width, *B* 1-57

Figure 1-43 Soil pressure zones under a mat of footing length, *L*, and width, *B* 1-58

Figure 1-44 Evaluation process for buildings on combined footings or mat foundations 1-60

Figure 1-45 Evaluation process for buildings using Procedure 1 or Procedure 2 1-62

Figure 1-46 Overturning and resisting forces on an isolated footing with grade beam resistance 1-63

Figure 1-47 Overturning and resisting forces on an isolated footing supporting multiple structural members 1-64

Figure 1-48 Soil takes tension, hazard level BSE-1N max pressure = 12.6 ksf 1-66

Figure 1-49 Soil does not take tension, hazard level BSE-1N max pressure = 15.7 ksf 1-66

Figure 1-50 Soil takes tension, hazard level BSE-2N max pressure = 17.8 ksf. Meets upper bound soil capacity Q_{UB} = 20.4 ksf 1-67

Figure 1-51 Soil does not take tension, hazard level BSE-2N max pressure = 28.2 ksf 1-67

Figure 1-52 Soil does not take tension, hazard level BSE-2N NSP max pressure = 9.24 ksf 1-68

Figure 1-53 Column axial load, load combination (LC): 0.9*D* + *E* (BSE-2N), fixed base..... 1-69

Figure 1-54 Column axial load, LC: 0.9*D* + *E* (BSE-2N), soil no tension, k_{sv} = 0.1 kci 1-69

Figure 1-55 Column axial load, LC: 0.9*D* + *E* (BSE-2N), NSP, k_{sv} = 0.1 kci 1-69

Figure 1-56 Acceptance ratios beam negative moment, ASCE/SEI 7: BSE-1N, fixed base (baseline)..... 1-70

Figure 1-57 Acceptance ratios beam negative moment, ASCE/SEI 41: BSE-2N, fixed base (CP) 1-70

Figure 1-58 Acceptance ratios beam negative moment, ASCE/SEI 41: BSE-2N, soil takes tension (CP) 1-71

Figure 1-59 Acceptance ratios beam negative moment, ASCE/SEI 41: BSE-2N, soil compression only (CP) 1-71

Figure 1-60 Acceptance ratios beam positive moment ASCE/SEI 7: BSE-1N, baseline 1-72

Figure 1-61 Acceptance ratios beam positive moment ASCE/SEI 41: BSE-2N, fixed base (CP) 1-72

Figure 1-62 Acceptance ratios beam positive moment, ASCE/SEI 41: BSE-2N, soil takes tension (CP) 1-73

Figure 1-63 Acceptance ratios beam positive moment, ASCE/SEI 41: BSE-2N, compression only (CP) 1-73

Figure 1-64 Hinge pattern at target displacement, BSE-2N of 32 inches 1-74

Figure 1-65 Soil pressure distribution under the footing used for evaluating the footing strength 1-76

Figure 1-66 Soil pressure distribution under the footing is trapezoidal 1-77

Figure 1-67 Soil pressure distribution under the footing is triangular 1-77

Figure 1-68 Soil pressure distribution under the footing is a rectangle and a triangle 1-78

Figure 1-69 Figure 8-1 in ASCE/SEI 41-17, bounding requirements when soil supports are explicitly modeled 1-80

Figure 1-70 Example moment capacity calculation 1-82

Figure 1-71 Column moments per story from left to right, starting with top story on the left to bottom story on the right 1-85

Figure 1-72 Column axial load per story from left to right, starting with top story on the left to bottom story on the right 1-85

Figure 1-73 Beam negative moments per story from left to right 1-86

Figure 1-74 Beam positive moments for the various analysis cases 1-86

Part 4

Figure 1-1 Typical wall backbone curve contained in RC wall database 1-5

Figure 1-2 Reported axial failure of a wall test reported by Altheeb (2016) 1-5

Figure 1-3 Reported axial failure of a wall test reported by Segura and Wallace 1-5

Figure 1-4 Out-of-plane instability and concrete crushing of a wall test reported by Dashti et al 1-6

Figure 1-5 Histograms of the dataset used for flexural stiffness studies 1-7

Figure 1-6 Histograms of the first dataset for walls with conforming detailing 1-10

Figure 1-7 Histograms of the second dataset for walls with nonconforming detailing 1-12

Figure 1-8 Definition of uncracked flexural stiffness 1-13

Figure 1-9 Contribution of shear deformation to total deformation at *General Yield* point 1-14

Figure 1-10 Definition of effective first yield flexural stiffness 1-15

Figure 1-11 Idealized backbone relations to model hinge region of flexure-controlled walls 1-16

Figure 1-12 Displacement profiles of flexure-controlled walls 1-18

Figure 1-13 Histograms of contribution of computed hinge elastic flexural rotation to: a) the wall total elastic rotation, and b) the total hinge rotation capacity 1-18

Figure 1-14 Comparison of calculated (Eq. 1-11) and experimental $E_{cE}I_{eff}$ 1-21

Figure 1-15 Comparison of experimental and calculated (Eq. 1-10) $E_{cE}I_{eff}$ 1-22

Figure 1-16 Comparison of experimental and calculated (Eq. 1-11) $E_{cE}I_{eff}$ 1-22

Figure 1-17 Comparison of experimental and calculated (Eq. 1-14) $E_{cE}I_{eff}$ considering an h_1 of 7 ft for one-half scale (14 ft for full scale) where I_{sp} calculated from Eq. 1-15 and multiplied by: (a) 2.0, and (b) 1.0 1-23

Figure 1-18 Influence axial load, concrete strength, and shear-span-ratio on $E_{cE}I_{uncr}$. (Note: R = correlation coefficient) 1-24

Figure 1-19 Influence of key parameters on $E_{cE}I_{eff}$. (Note: R=correlation coefficient) 1-25

Figure 1-20 Sensitivity of $E_{cE}I_{eff}$ to the reduction factor used in Eq. 1-8: a) 0.6, b) 0.7, and c) 0.8 1-26

Figure 1-21 Linear regression lines to the data and the proposed model for $E_{cE}I_{uncr}$ 1-27

Figure 1-22 Linear regression lines to the data and the proposed model for $E_{cE}I_{eff}$ 1-28

Figure 1-23 Influence of longitudinal reinforcement ratio ($\rho_{l,BE}$) on $E_{cE}I_{eff}$ 1-29

Figure 1-24 Comparison of experimental and calculated $E_{cE}I_{eff}$. from Eq. 1-17 1-30

Figure 1-25 Effective shear modulus results from the dataset of 64 wall tests 1-31

Figure 1-26 Ratio of calculated-to- experimental yield moment strength ($M_{yE,cal}/M_{yE,exp}$) for the conforming wall dataset 1-32

Figure 1-27 Ratio of experimental ultimate to yield moment strength ($M_{ult,exp}/M_{yE,cal}$) for the conforming wall dataset 1-32

Figure 1-28 Proposed models for Parameter c_{nl} for conforming flexure-controlled walls 1-33

Figure 1-29 Ratio of calculated-to-experimental yield moment strength ($M_{yE,cal}/M_{yE,exp}$) for the nonconforming wall dataset 1-34

Figure 1-30 Ratio of experimental ultimate-to-yield moment strength ($M_{ult,exp}/M_{yE,cal}$) for the nonconforming wall dataset 1-34

Figure 1-31 Proposed models for Parameter c_{nl} for nonconforming flexure-controlled walls 1-35

Figure 1-32 Examples of boundary transverse reinforcement configurations of conforming walls 1-36

Figure 1-33 Impact of detailing variables on drift capacity of conforming walls 1-37

Figure 1-34 Proposed models for Parameter dnl for conforming flexure-controlled walls 1-38

Figure 1-35 Definition of width (b) and length (c) of flexural compression zone 1-38

Figure 1-36 Proposed models for *Parameter* d'_{nl} for conforming flexure-controlled walls 1-39

Figure 1-37 Proposed models for Parameter e_{nl} for conforming walls 1-40

Figure 1-38 Impact of l_{wc}/b^2, $P/(A_g f'_{cE})$, and $V_{max}/\sqrt{f'_{cE}}$ on Parameter d_{nl} for nonconforming walls 1-42

Figure 1-39 Impact detailing parameters on Parameter d_{nl} of nonconforming walls 1-42

Figure 1-40 Comparison of Proposed models for Parameter d_{nl} with experimental data for nonconforming walls 1-43

Figure 1-41 Proposed models for Parameter d'_{nl} for nonconforming walls 1-44

Figure 1-42 Proposed models for Parameter e_{nl} for conforming walls 1-44

Figure 1-43 Proposed model for Parameter d_{nl} of nonconforming walls with $\rho_{lw} < 0.0025$ 1-46

Figure 1-44 Distribution of ratios of experimental-to-predicted *d* and *e*, along with normal and lognormal distributions associated with the means and standard deviations of the datasets 1-49

Figure 1-45 Approximate location of acceptance criteria on backbone shape 1-51

Figure 1-46 Variation of yield curvature (ϕ_y) computed from analytical sectional analysis as a function of wall length (l_w) 1-52

Figure 1-47 Comparison of ASCE/SEI 41-17 Parameter a_{nl} for walls with confined boundaries with test data 1-56

Figure 1-48 Impact of axial load ratio and longitudinal reinforcement on Parameter a_{nl} for walls with confined boundaries 1-57

Figure 1-49 Impact of axial load ratio on Parameter a_{nl} for walls with no confined boundaries 1-57

Figure 1-50 Comparison of proposed acceptance criteria with acceptance criteria in ASCE/SEI 41-17 for conforming walls 1-58

Figure 1-51 Comparison of proposed acceptance criteria with acceptance criteria in ASCE/SEI 41-17 for nonconforming walls 1-58

Figure 1-52. Building floor plan 1-72

Figure 1-53 Elevations of transverse structural walls along grid lines 3 and 5 1-73

Figure 1-54 Elevations of transverse structural walls along grid lines 6 and 8 1-74

Figure 1-55 Cross-section details for wall on grid line 3 first floor 1-75

Figure 1-56 Cross-section details for wall on grid lines 5 and 6 at first floor 1-76

Figure 1-57 Exploded view of analysis model showing transverse walls 1-80

Figure 1-58 FE model of LFRS along grid line 3 1-81

Figure 1-59 FE model of LFRS along grid lines 5 and 6 1-82

Figure 1-60 FE model of LFRS along grid line 8 1-83

Figure 1-61 Perform3D material data for new concrete in hinge zones A 1-85

Figure 1-62 Perform3D material data for new concrete in hinge zones B 1-86

Figure 1-63 Perform3D material data for new concrete in hinge zones C 1-87

Figure 1-64 Perform3D material data for existing concrete in hinge zones 1-88

Figure 1-65 Perform3D material data for new steel bars in hinge zones A 1-89

Figure 1-66 Perform3D material data for new steel bars in other hinge zones 1-91

Figure 1-67 Perform3D material data for existing steel bars in hinge zones 1-90

Figure 1-68 Pushover curve from Perform3D 1-92

Figure 1-69 Comparison of grid line 5 wall backbone curve modeling parameters 1-94

Figure 1-70 Wall cracked flexural stiffness determination 1-95

Figure 1-71 Grid line 3 wall post-yield backbone modeling parameters 1-95

Figure 1-72 Rotation gauge definition for grid line 3 wall 1-97

Figure 1-73 Rotation gauge definition for grid line 5 wall 1-97

Figure 1-74 Moment-rotation curves for wall on grid line 3 1-99

Figure 1-75 Moment-rotation curves for wall on grid line 5 1-99

Figure 2-1 Examples of backbone curves derived from experimental force-displacement relations 2-3

Figure 2-2 Idealized backbone relations to model shear behavior of shear-controlled walls 2-3

Figure 2-3 Parameters impacting cracking shear strength of walls 2-5

Figure 2-4 Comparison of measured and predicted cracking shear strength 2-6

Figure 2-5 Definition of wall cross-section shape 2-6

Figure 2-6 Measured yield strength normalized by measured peak strength 2-7

Figure 2-7 Influence of various parameters on yield shear strength 2-8

Figure 2-8 Influence of $V_{CWall318E}/V_{MCyDE}$, axial load, and web horizontal reinforcement ratio on yield shear strength 2-8

Figure 2-9 Comparison of model for yield shear strength with experimental data 2-9

Figure 2-10 Impact of $V_{CWall318E}/V_{MCyDE}$, axial load, and web horizontal reinforcement ration of peak shear strength 2-10

Figure 2-11 Comparison of peak shear strength model with experimental data 2-11

Figure 2-12 Parameters impacting residual shear strength 2-12

Figure 2-13 Proposed models for residual shear strength 2-12

Figure 2-14 Normalized uncracked shear stiffness for a small subset of data with measured shear cracking load and deformation 2-13

Figure 2-15 Measured drift at yield strength 2-14

Figure 2-16 Measured drift capacity at 20% lateral strength loss 2-15

Figure 2-17 Proposed relations for drift capacity at lateral strength loss 2-16

Figure 2-18 Parameters impacting drift capacity at residual strength 2-17

Figure 2-19 Proposed relations for drift capacity at residual strength 2-17

Figure 2-20 Impact of axial load on drift capacity at axial failure for the small dataset of 45 walls 2-19

Figure 2-21 Impact of axial load on drift capacity at axial failure for the dataset of 90 walls 2-19

Figure 2-22 Proposed models for drift capacity at axial failure 2-20

Figure 2-23 Distribution of the error ratio of measured-to-predicted values of parameters d_{nl} and e_{nl} 2-23

Figure 2-24 Comparison between existing and proposed values for Modeling Parameter d_{nl} and e_{nl} 2-26

Figure 2-25 Comparison of nonlinear acceptance criteria for Immediate Occupancy (IO) 2-27

Figure 2-26 Comparison of nonlinear acceptance criteria for Life Safety (LS) 2-27

Figure 2-27 Comparison of nonlinear acceptance criteria for Collapse Prevention (CP) 2-27

Figure 2-28 Comparison of linear acceptance criteria for Immediate Occupancy (IO) 2-28

Figure 2-29 Comparison of linear acceptance criteria for Life Safety (LS) 2-28

Figure 2-30 Comparison of linear acceptance criteria for Collapse Prevention (CP) 2-29

Figure 2-31 Perimeter concrete bearing walls and interior concrete column lines 2-34

Figure 2-32 Existing pile reinforcement 2-35

Figure 2-33 End wall under consideration 2-36

Figure 2-34 Acceleration response spectra 2-37

Figure 2-35 LDP building drift comparison 2-42

Figure 2-36 Proposed provision LDP BSE-2E shear-only *DCR/m* 2-43

Figure 2-37 Nonlinear shear backbone 2-45

Figure 2-38 Proposed provision pushover results. 2-46

Figure 2-39 Proposed provision CP-DCR's at BSE-2E target displacement 2-47

Figure 2-40 ASCE/SEI 41-17 global north-south pushover results 2-48

Figure 2-41 ASCE/SEI 41-17 CP-DCR's at BSE-2E target displacement 2-49

Figure 3-1 Sample force-displacement relationships for shear-friction-controlled wall tests 3-4

Figure 3-2 Idealized backbone relations to model translational behavior of shear-controlled walls 3-5

Figure 3-3 Push-off test setups used to study shear-friction strength 3-6

Figure 3-4 Development of the sliding shear mechanism 3-7

Figure 3-5 Influence of interface roughness on behavior of shear-friction-controlled walls..... 3-9

Figure 3-6 Influence of flanges on behavior of shear-friction-controlled wall tests 3-10

Figure 3-7 Influence of dowels on changing the location of sliding failure plane 3-11

Figure 3-8 Influence of longitudinal reinforcement yield strength on shear-friction strength .. 3-12

Figure 3-9 Measured longitudinal reinforcement strains at wall-foundation interface of a shear-friction-controlled wall test 3-12

Figure 3-10 Impact of measured longitudinal reinforcement yield on strength shear-friction strength 3-13

Figure 3-11 Comparison of measured peak shear friction strength from the dataset with the ACI 318-19 limits in Table 3-1 3-14

Figure 3-12 Variation of measured shear friction strength from the dataset and the ACI 318-19 limits in Table 3-1 versus clamping stress 3-15

Figure 3-13 Variation of predicted-to-measured yield shear-friction strength versus shear-friction to flexural strength ratios) and shear span ratios 3-16

Figure 3-14 Comparison of estimated and tested yield shear-friction strengths: (a) comparison of model with data, and (b) statistics of the ratio of predicted-to-tested yield strength 3-17

Figure 3-15 Variation of the ratio of estimated (Eq. 3-1) to tested shear-friction yield strengths as a function of: (a) $V_{CyfWallSE}/V_{MCyDE}$ and (b) M/Vl_w 3-18

Figure 3-16 Variation of measured residual strength to yield strength as function of: (a) $V_{CyfWallSE}/V_{MCyDE}$ and (b) clamping stress 3-19

Figure 3-17 Comparison of Parameter anl versus interface type and $V_{CyfWallSE}/V_{MCyDE}$ with the proposed models 3-20

Figure 3-18 Comparison of Parameter a_{nl} and Parameter a'_{nl} 3-21

Figure 3-19 Comparison of proposed models for Parameter a'_{nl} with experimental data in the dataset 3-21

Figure 3-20 RC and PT structures tested at E-Defense shake table 3-29

Figure 3-21 E-Defense RC Building—typical floor plan and member nomenclature 3-30

Figure 3-22 E-Defense RC Building—elevations and member nomenclature 3-31

Figure 3-23 Reinforcement details 3-31

Figure 3-24 Truncated Ground Motion Records for 100% JMA-Kobe 3-32

Figure 3-25 Response Spectra for 100% JMA-Kobe 3-33

Figure 3-26 Drift demands using proposed provisions to ACI 369.1 relative to ASCE/SEI 41-17 provisions and experimental recorded data 3-36

Figure 3-27 Wall acceptance ratios 3-37

Figure 4-1 Wall flexural failure modes: (a) bar buckling and concrete crushing, (b) bar fracture, and (c) lateral instability 4-3

Figure 4-2 Wall shear failure modes: (a) diagonal tension, (b) diagonal compression, and (c) shear-sliding 4-3

Figure 4-3 Wall flexure-shear failure modes: (a) flexure-diagonal tension, (b) flexure-diagonal compression, and (c) flexure-shear-sliding 4-3

Figure 4-4 Histograms of wall tests in the dataset used in this study 4-4

Figure 4-5 Wall failure mode results from a dataset of over 1,100 wall tests: failure modes separated 4-5

Figure 4-6 Wall failure modes results from a dataset of over 1,100 wall tests: failure modes combined 4-6

Figure 4-7 Wall classification: blue region = flexure-controlled, red region= shear-controlled and yellow region= shear sliding at the base 4-6

Figure 4-8 Variation of wall failure mode versus shear-span-ratio and shear-flexure strength ratio 4-9

Part 5

Part 6

Figure 1-1 Isometric view showing example building with perimeter URM bearing walls, URM parapets, and wood frame roof and floor diaphragms with south wall at left 1-5

Figure 1-2 Example building (a) side wall elevation, (b) rear (north) wall elevation, and (c) front (south) wall elevation 1-6

Figure 1-3 Example building plans for (a) first floor and (b) second floor 1-7

Figure 1-4 Example building roof plan 1-7

Figure 1-5 3D ETABS model of example unretrofitted two-story URM building at left and one of the retrofit situations with a steel moment frame shown at right 1-8

Figure 1-6 3D ETABS model of example one-story URM building used to study out-of-plane behavior of URM walls 1-9

Figure 1-7 3D ETABS model of example six-story URM building used for case studies; this figure includes the steel moment frame used as one of the retrofit situations 1-10

Figure 1-8 Retrofit Situations 1, 2a, 2b, 3a, and 3b used in case studies 1-11

Figure 1-9 Retrofit Situation 1 and 2 before retrofit showing URM wall demands at front and rear transverse walls 1-12

Figure 1-10 Retrofit Situation 3 before retrofit showing URM wall demand at rear transverse wall 1-13

Figure 1-11 Figure showing Retrofit Situation 1 plan 1-16

Figure 1-12 Figure showing Retrofit Situation 1 Elevation – rear wall 1-16

Figure 1-13 Figure showing wall demands per ASCE/SEI 41-13 before the retrofit, per ASCE/SEI 41-13 after the retrofit, per ASCE/SEI 41-17 with no *m*-factor after the

retrofit, and per ASCE/SEI 41-17 with m-factors after the retrofit for use with concrete and masonry 1-17

Figure 1-14 Situation 2 with new vertical element placed in middle of the structure 1-19

Figure 1-15 Load distribution for Retrofit Situation 2b with steel moment frame per ASCE/SEI 41-13 (left) vs. ASCE/SEI 41-17 (right) 1-20

Figure 1-16 Figure showing Retrofit Situation 2a plan 1-21

Figure 1-17 Figure showing wall demands per ASCE/SEI 41-13 before the retrofit per ASCE/SEI 41-13 after the retrofit, per ASCE/SEI 41-17 with no *m*-factor after the retrofit, and per ASCE/SEI 41-17 with *m*-factors after the retrofit 1-21

Figure 1-18 Figure showing concrete wall design per ASCE/SEI 41-13 (left) vs. ASCE/SEI 41-17 (right) 1-22

Figure 1-19 Figure showing Retrofit Situation 2b plan 1-23

Figure 1-20 Figure showing wall demands per ASCE/SEI 41-13 before the retrofit, per ASCE/SEI 41-13 after the retrofit, per ASCE/SEI 41-17 with no *m*-factor after the retrofit, and per ASCE/SEI 41-17 with m-factors after the retrofit 1-23

Figure 1-21 Figure showing moment frame design governed by strength and moment frame required to meet 2% drift limit 1-26

Figure 1-22 Figure showing moment frame required to meet 1.5% drift limit with heavier sections than shown in Figure 1-21 1-26

Figure 1-23 Figure showing moment frame required to meet 1% drift limit with heavier sections than either Figure 1-21 or Figure 1-22 (Case 4-13) 1-27

Figure 1-24 Figure showing moment frame required to meet 1.5% drift limit with *m*-factor 1-28

Figure 1-25 Figure showing moment frame required to meet 1.5% drift limit with no *m*-factor 1-28

Figure 1-26 ETABS element shears in steel moment frame from 3D models with membrane elements without and thin shell elements with out-of-plane wall stiffness for longitudinal masonry walls in two-story building 1-31

Figure 1-27 Six 3D ETABS unretrofitted models used for out-of-plane wall stiffness study 1-32

Figure 1-28 Process used to determine appropriate drift limit provision and to define diaphragm span length 1-34

Figure 1-29 Proposed ASCE/SEI 41-23 Figure 16-1 1-35

Figure 1-30 Figure showing moment frame required to meet ASCE/SEI 41-13 Special Procedure with 0.75% drift limit with heavier sections than Figure 1-23 above 1-36

Figure 1-31 Isometric views of unretrofitted and retrofitted and 2D view of frame used for 3D ETABS analysis of two-story Retrofit Situation 2b 1-37

Figure 1-32 RISA-2D model for six-story moment frame retrofit design using ASCE/SEI 41-13 Special Procedure and a drift limit of 0.75% 1-39

Figure 1-33 Isometric views of unretrofitted (top left) and retrofitted (top right) and 2D view of OMF used for 3D ETABS analysis of six-story Retrofit Situation 2b 1-40

Figure 1-34 Figure showing open front first floor for Retrofit Situation 3 1-43

Figure 1-35 Figure showing Retrofit Situation 3a with new steel chevron braced frame 1-43

Figure 1-36 Figure showing wall demands per ASCE/SEI 41-13 before the retrofit as, per ASCE/SEI 41-13 after the retrofit, per ASCE/SEI 41-17 with no *m*-factor after the retrofit, and per ASCE/SEI 41-17 with *m*-factors after the retrofit 1-44

Figure 1-37 Figure showing Retrofit Situation 3b with new steel moment frame 1-45

Figure 1-38 Figure showing wall demands per ASCE/SEI 41-13 before the retrofit, per ASCE/SEI 41-13 after the retrofit, per ASCE/SEI 41-17 with no *m*-factor after the retrofit, and per ASCE/SEI 41-17 with m-factors after the retrofit 1-45

Figure 1-39 Figure showing moment frame governed by strength design 1-46

Figure 1-40 Figure showing moment frame required to meet 2.5% drift limit per ASCE/SEI 7-10 with C_d = 5.5 1-47

Figure 1-41 Figure showing moment frame required to meet 1.5% drift limit with *m*-factor 1-47

Figure 1-42 Figure showing moment frame required to meet 1.5% drift limit per ASCE/SEI 41-17 with no *m*-factor 1-48

Figure 1-43 Retrofit Situation 3b RISA-2D model for MF at front wall of two-story building 1-49

Figure 1-44 Retrofit Situation 3b ETABS model with undeformed shape and deformed shape 1-50

Figure 1-45 Displaced Shape of Story 2 and Story 1 diaphragms from ETABS model with displacements shown in inches 1-50

Figure 1-46 Comparison of flexible MF designed with ASCE/SEI 41-13 with no drift limit and stiffer MF designed with proposed provisions and 0.75% drift limit 1-52

Figure 2-1 Subdiaphragm case study building layout 2-2

Figure 2-2 Subdiaphragm options in transverse direction 2-5

Figure 2-3 Subdiaphragm calculations in transverse direction 2-6

Figure 2-4 Subdiaphragm options in longitudinal direction 2-7

Figure 2-5 Subdiaphragm calculations in longitudinal direction 2-9

Figure 2-6 Wood flooring over straight sheathing—transverse direction 2-10

Figure 2-7 Wood flooring over straight sheathing—longitudinal direction 2-12

Figure 2-8 Wood flooring over diagonal sheathing 2-13

Figure 2-9 Plywood over straight sheathing 2-15

Figure 2-10 Straight sheathing 2-16

Figure 2-11 Diagonal sheathing 2-17

Figure 3-1 S_a at collapse for Penner and Elwood reference configuration 3-3

Figure 3-2 Coefficient of variation for varying period, T_{im}, at which the intensity measure, S_a, is evaluated for varying wall-diaphragm system period, T_s 3-3

Figure 3-3 Comparison of h/t vs S_{X1} for “All Other Walls” category 3-7

Figure 3-4 Comparison of h/t vs S_{X1} for “First Story of Multi-Story Building” category 3-9

Figure 3-5 Comparison of h/t vs S_{X1} for “Top Story of Multi-Story Building” category 3-10

Figure 3-6 Comparison of h/t vs S_{X1} for “One-Story Building” category 3-11

Figure 4-1 Comparison of h/t vs S_{X1} for “All Other Walls” category 4-7

Figure 4-2 Comparison of h/t vs S_{X1} for "First Story of Multi-Story Building" category 4-8

Figure 4-3 Comparison of h/t vs S_{X1} for "Top Story of Multi-Story Building" category 4-9

Figure 4-4 Comparison of h/t vs S_{X1} for "One-Story Building" category 4-10

Figure 5-1 Archetypical wall line 5-2

Figure 5-2 Mixed modes: all deformation-controlled 5-3

Figure 5-3 Mixed modes: deformation-controlled and force-controlled 5-3

Figure 5-4 Mixed modes: deformation-controlled and force-controlled, considering ASCE/SEI 41-17 Section 11.3.2.3: exclude rocking wall piers 5-4

Figure 5-5 Case study: mixed modes: deformation and force-controlled 5-5

Figure 5-6 All rocking-controlled (deformation-controlled), f'_m = 900 psi 5-6

Figure 5-7 Redistribution example 5-7

Figure 6-1 *m*-factor versus axial load ratio 6-2

List of Tables

Table 1-1 Summary of Change Proposals 1-3

Part 1

Table 1-1 Possible Case Studies with Nonlinear Dynamic Procedure Analyses 1-5

Table 1-2 Possible Case Studies with Nonlinear Static Procedure Analyses 1-5

Table 1-3 Working Group 1, Linear RCSW S_{XS} = 1.0 and S_{XS} = 1.5 Case Study: Linear Procedure Limitation Provision Summary 1-12

Table 1-4 Working Group 1, Linear RCSW S_{XS} = 1.0 and S_{XS} = 1.5 Case Study: Pattern 1 Analysis Results 1-13

Table 1-5 Working Group 1, Linear RCSW S_{XS} = 1.0 and S_{XS} = 1.5 Case Study: Pattern 2 Analysis Results 1-14

Table 1-6 Working Group 1 RCSW S_{XS} = 0.67 and S_{XS} = 1.0 Case Study: Linear Procedure Limitation Provision Summary 1-15

Table 1-7 Working Group 1, Linear RCSW S_{XS}=0.67 and 1.0 Case Study: Pattern 1 Analysis Results 1-16

Table 1-8 Working Group 1, Linear RCSW S_{XS} = 0.67 and S_{XS} = 1.0 Case Study: Pattern 2 Analysis Results 1-17

Table 1-9 Comparison of Possible Alternative Linear Procedure Limitation Provision Options 1-39

Part 2

Part 3

Table 1-1 Existing Interior Column - Moment Acceptance Ratios (CP Limit State) 1-25

Table 1-2 Existing Interior Column - Shear Acceptance Ratios (CP Limit State) (For Nonlinear Cases Acceptance Ratio is the Same as the Moment Acceptance Ratio) 1-26

Table 1-3 Retrofit Shear Wall - Shear Acceptance Ratios (CP Limit State) 1-26

Table 1-4 Retrofit Shear Wall - Moment Acceptance Ratios (CP Limit State) 1-27

Table 1-5 Existing Slab – Flexure Acceptance Ratios (CP Limit State) 1-27

Table 1-6 Story Drift – Drift per Story (in.) 1-28

Table 1-7 Story Drift – Drift Ratio per Story 1-28

Table 1-8 Drift Summary for Various Models – BSE-2N Seismic Hazard Level. 1-74

Table 1-9 Summary of Moment Capacity and Acceptance Ratio Using Upper Bound Soil Bearing Capacity 1-82

Table 1-10 Summary of Moment Capacity and Acceptance Ratio Using Lower Bound Soil Bearing Capacity 1-83

Part 4

Table 1-1 Definition of Backbone Response Points 1-3

Table 1-2 Statistics of the Ratios of Predicted-to-Experimental $E_{cE}I_{eff}/E_{cE}I_g$ Values 1-20

Table 1-3 Proposed Values for Uncracked Wall Flexural Stiffness ($E_{cE}I_{uncr}$) 1-27

Table 1-4 Existing Models for Flexural Stiffness of Uncracked Walls or Walls with Limited Cracking 1-27

Table 1-5 Proposed Values for Effective Flexural Stiffness ($E_{cE}I_{eff}$) 1-28

Table 1-6 Proposed Values for $E_{cE}I_{eff}$ as a Function of $P/(A_g f'_{cE})$ and $\rho_{l,BE}$ 1-29

Table 1-7 Modeling Parameters for Conforming RC Structural Walls Controlled by Flexure 1-39

Table 1-8 Statistics of the Modeling Parameters Given in Table 1-7 1-41

Table 1-9 Modeling Parameters for Nonconforming RC Structural Walls Controlled by Flexure 1-46

Table 1-10 Statistics of the Modeling Parameters Given in Table 1-9 1-47

Table 1-11 Recommended Acceptance Criteria for Conforming and Nonconforming Flexure-Controlled Concrete Structural Walls 1-51

Table 1-12 *m*-factors for Reinforced Concrete Walls Based on Provisions of ASCE/SEI 41-17 Section 7.6.3 1-52

Table 1-13 Alternate Numerical Acceptance Criteria for Linear Procedures: Conforming Reinforced Concrete Structural Walls Controlled by Flexure 1-53

Table 1-14 Alternate Numerical Acceptance Criteria for Linear Procedures: Nonconforming Reinforced Concrete Structural Walls Controlled by Flexure 1-54

Table 1-15 Partial View of ASCE/SEI 41-17 Table 10-19 for Nonlinear Modeling Parameters of Flexure-Controlled Structural Walls 1-55

Table 1-16 Wall Moment Capacities and Corresponding Axial Loads [kip, ft units] 1-78

Table 1-17 Backbone Curve Parameter Values for Grid Line 5 Wall 1-94

Table 2-1 Proposed Cracking Shear Strength Models 2-5

Table 2-2 Proposed Values for Modeling Parameter c_{nl} 2-13

Table 2-3 Proposed Values for MP d_{nl} as Function of Cross-Section Shape and Shear Strength to Shear Demand at Flexural Yielding Strength Ratio 2-16

Table 2-4 Proposed Values for Parameter d'_{nl} as a Function of Cross-Section Shape and Shear Strength to Shear Demand Ratio 2-18

Table 2-5 Proposed Values for Parameter e_{nl} 2-20

Table 2-6 Proposed Nonlinear Modeling Parameters 2-21

Table 2-7 Statistics of the Proposed Modeling Parameters 2-22

Table 2-8 Nonlinear Acceptance Criteria for Shear-Controlled Structural Walls 2-22

Table 2-9 Proposed Nonlinear Acceptance Criteria for Shear-Controlled Walls 2-23

Table 2-10 Relations for Linear Acceptance Criteria 2-24

Table 2-11 Proposed *m*-Factors for Shear-Controlled Walls (Linear Acceptance Criteria) 2-24

Table 2-12 ACI 369.1-17 Modeling Parameters and Acceptance Criteria for Shear-Controlled Walls 2-25

Table 2-13 Unfactored Demands 2-38

Table 2-14 Wall Moment Strength 2-39

Table 2-15 Shear Strengths 2-39

Table 2-16 Shear Strength Ratio $V_{CE}/\omega_v V_{MCultE}$ 2-40

Table 2-17 Shear Strength Ratio $V_{CE}/\omega_v V_{MCultE}$ 2-41

Table 2-18 Proposed Provision Linear Acceptance Criteria 2-42

Table 2-19 LDP *DCR/m* Comparison 2-44

Table 3-1 Shear-Friction Coefficients and Strength Upper-Bounds of ACI 318-19 3-6

Table 3-2 Modeling Parameters for Reinforced Concrete Structural Walls and Associated Components Controlled by Shear-Friction 3-23

Table 3-3 Statistical Values for Modeling Parameters of Walls Controlled by Shear-Friction 3-23

Table 3-4 Nonlinear Acceptance Criteria for Reinforced Concrete Structural Walls and Associated Components Controlled by Shear-Friction 3-24

Table 3-5 Numerical Acceptance Criteria for Linear Procedures: Reinforced Concrete Structural Walls and Wall Segments 3-24

Table 3-6 Characteristic Axial Demands and Moment Capacities in Wall Sections 3-33

Table 3-7 Wall Classification 3-34

Table 3-8 Wall Demand-to-Capacity Ratios using Simple Shear-Friction Strength Equation 3-35

Table 3-9 Shear Friction Modeling and Acceptance Criteria 3-36

Table 4-1 Wall Failure Modes in Database 4-2

Table 4-2 Criteria for Determining the Expected Wall Dominant Behavior 4-7

Table 4-3 Predicted Versus Experimental Failure Modes 4-8

Part 5

Table 2-1 Scope of Diaphragm-Related Checklist Statements 2-3

Table 2-2 Summary of Working Group 4 Study Scope 2-4

Table 3-1 Recommended Revisions to the Overturning Checklist Statement 3-2

Table 3-2 Applicability of Foundation-Related Checklist Statements (ASCE/SEI 14-17) 3-4

Part 6

Table 1-1 Summary of Retrofit Situations and Case Studies 1-14

Table 1-2 Retrofit Situation 2b Load Resisted by Moment Frame Based on Drift Limit and Provisions of ASCE/SEI 41-13 1-27

Table 1-3 Retrofit Situation 2b Load Resisted by Moment Frame Based on Drift Limit Using Provisions of both ASCE/SEI 41-13 and ASCE/SEI 41-17 1-29

Table 1-4 Retrofit Situation 2b Moment Frame Beams and Columns Required to Meet Various Drift Limits 1-29

Table 1-5 Distribution of Loads for Six Unretrofitted Structures from 3D ETABS Models for Loading in Transverse (E-W) Direction 1-33

Table 1-6 Midspan Drift Comparison for Two-story Unretrofitted URM Building and MF Retrofit from RISA and ETABS 1-37

Table 1-7 Story Shears Ratio to Forces from Special Procedure for Two-story Unretrofitted URM Building and Moment Frame Retrofit from ETABS 1-38

Table 1-8 Drift from Six-Story RISA-2D Analysis of Moment Frame Retrofit Situation 2b 1-39

Table 1-9 Midspan Displacement and Drift Comparison for Six-story Unretrofitted URM Building and OMF Retrofit from RISA and ETABS 1-41

Table 1-10 ETABS Story Shear Comparison for Six-story Unretrofitted URM Building and OMF Retrofit 1-41

Table 1-11 Story Shears Ratio to Forces from Special Procedure for Six-story Unretrofitted URM Building and OMF Retrofit from ETABS 1-42

Table 1-12 Retrofit Situation 3b Moment Frame Beams and Columns Required to Meet Various Drift Limits 1-48

Table 1-13 Drift and Displacement Comparison for RISA-2D vs. 3D ETABS Models for Stiff MF Designed with Drift Limit 0.75% 1-51

Table 1-14 Situation 3b Distribution of Loads for Two 3D ETABS Models for Loading in Transverse (E-W) Direction with Different Out-of-Plane Modeling of Longitudinal Walls 1-51

Table 1-15 *R*-factors of Common Ordinary vs. Special Systems from ASCE/SEI 7-16 1-53

Table 2-1 Case Study Weights 2-3

Table 2-2 Partial Code Parametric Study—10-foot Anchor Development 2-19

Table 2-3 Partial Code Parametric Study—8-foot Anchor Development 2-19

Table 3-1 Exposure Factor, C_e, from Penner and Elwood (2016b) 3-4

Table 3-2 Proposed Performance Level Factor, C_{pl}, Adapting Penner and Elwood's C_e Factor 3-6

Table 4-1 Exposure Factor, C_e, from Penner and Elwood (2016b) 4-3

Table 4-2 Proposed Performance Level Factor, C_{pl}, Adapting Penner and Elwood's C_e Factor 4-5

Chapter 1: Introduction

1.1 Background and Purpose

This report documents the work and technical studies of the ATC-140 Project Series, "Update Seismic Retrofit Design Guidance." This multi-year project was funded by the Federal Emergency Management Agency (FEMA) with the goal of investigating and developing change proposals for incorporation into ASCE/SEI 41-23, *Seismic Evaluation and Retrofit of Existing Buildings* (ASCE, 2023).

ASCE/SEI 41 is the consensus national standard for the seismic evaluation and retrofit of existing buildings. This standard was first published in 2007 (ASCE, 2007) and then updated in 2008 with Supplement Number 1 (ASCE, 2008), in 2014 (ASCE, 2014), and again in 2017 (ASCE, 2017). In 2014, FEMA initiated a project to develop example applications of the procedures presented in ASCE/SEI 41-13 (the version available at the time). The project led to the publication of FEMA P-2006, *Example Application Guide for ASCE/SEI 41-13 Seismic Evaluation and Retrofit of Existing Buildings with Additional Commentary for ASCE/SEI 41-17* (FEMA, 2018), which contains case study examples of various structural system types, as well as application of more general procedures. The development of FEMA P-2006 revealed the need for technical and procedural improvements in ASCE/SEI 41 that, due to their complexity and scale, were considered beyond the typical scopes of the all-volunteer committees working on updating ASCE/SEI 41. The identification of these needed improvements provided the motivation for the ATC-140 Project Series.

1.2 Project Organization and Approach

During the first phase of the project, the need for additional technical and procedural improvements for ASCE/SEI 41-23 were identified and considered alongside those highlighted during the development of FEMA P-2006. Improvements were prioritized, and the most pressing were assigned to six working groups:

- Working Group 1, Linear Analysis: responsible for reviewing and preparing change proposals related to the linear analysis provisions contained in Chapter 7 of ASCE/SEI 41-17.
- Working Group 1, Nonlinear Analysis: responsible for reviewing and preparing change proposals related to the nonlinear analysis provisions contained in Chapter 7 of ASCE/SEI 41-17.
- Working Group 2, Foundations: responsible for reviewing and preparing change proposals related to the foundation provisions contained in Chapter 8 of ASCE/SEI 41-17.
- Working Group 3, Concrete Structural Walls: responsible for reviewing and preparing change proposals related to the concrete structural wall provisions contained in Chapter 10 of ASCE/SEI 41-17.

- Working Group 4, Tier 1 and 2: responsible for reviewing and preparing change proposals related to the Tier 1 screening procedure and the Tier 2 deficiency-based evaluation procedure contained in Chapter 4 and Chapter 5, respectively, in addition to the checklists in Chapter 17 of ASCE/SEI 41-17.

- Working Group 5, Design of Retrofits: although initially identified and named, this working group was never implemented.

- Working Group 6, Unreinforced Masonry (URM): responsible for reviewing and preparing change proposals related to the unreinforced masonry provisions contained in Chapter 11 and Chapter 16 of ASCE/SEI 41-17.

Each working group designed and implemented technical studies related to their topical focus and used the results of these studies to guide the development of change proposals. The technical studies and change proposals were reviewed by a Project Technical Committee, consisting of the working group leads and other engineers with extensive experience developing prior versions of ASCE/SEI 41, as well as by a Project Review Panel, consisting of representatives from material industries, trade associations, and the American Society of Civil Engineers (ASCE). The draft change proposals were revised based on review feedback and, once finalized, submitted to relevant subcommittees of ASCE's *Seismic Retrofit of Existing Building Standards Committee*, which oversees the development of ASCE/SEI 41. The names and affiliations of all who contributed to the project are provided in the List of Participants at end of the report.

1.3 Summary of Change Proposals

In total, 35 change proposals were prepared and submitted for consideration of adoption into ASCE/SEI 41-23. This report documents the motivations, methods, modeling details, results, conclusions, and recommendations of the technical studies that led to the development of these change proposals. Table 1-1 lists the working groups that developed the change proposals, the change proposal topics, the ASCE/SEI 41-17 chapters and sections affected, and the location in this report where the technical studies that led to the change proposals are described. In all cases, the change proposals included associated commentary, but the affected commentary sections are not listed in the table. In some cases, related change proposals have been grouped together and presented in the same chapter because the same technical study led to those change proposals.

The change proposals are organized in this report by the working groups that developed them. For example, all documentation for Working Group 1, Linear Analysis is contained in the two chapters of Part 1, and all documentation for Working Group 4, Tier 1 and 2 is contained in the five chapters of Part 5.

Note about Change Proposals

This report documents aspects of change proposals as they were submitted to subcommittees of ASCE's *Seismic Retrofit of Existing Building Standards Committee*. Often, these change proposals were revised, in some cases substantively, by these subcommittees before they were adopted into ASCE/SEI 41-23. Readers should not rely on this report for information about the final version of provisions in ASCE/SEI 41-23.

Table 1-1 Summary of Change Proposals

Working Group	Change Proposal Topic	ASCE/SEI 41-17 Chapters and Sections Affected	Documentation Supporting Change Proposal
1, Linear Analysis	Linear analysis limitation provisions	7.3.1.1	Part 1, Chapter 1
1, Linear Analysis	Acceptance ratio term for linear analysis	7.5.2.2	Part 1, Chapter 2
1, Nonlinear Analysis	Nonlinear analysis revisions, including critical and ordinary actions, force-controlled actions, unacceptable drift limit, no unacceptable responses for life safety, secondary components, damping, accidental torsion, property bounding	6.2.4, 7.2.3, 7.4.4, 7.5.1, 7.5.3	Part 2, Chapter 1
1, Nonlinear Analysis	Nonlinear modeling parameter and acceptance criteria	7.4.3, 7.4.4, 7.5.1, 7.5.3, 7.6	Part 2, Chapter 2
2, Foundations	Reorganization of foundations chapter and significant technical improvements	8.4.1, 8.4.2, 8.4.4.1, 8.4.5.2	Part 3, Chapter 1
3, Concrete Structural Walls	Flexure-controlled wall modeling parameters and acceptance criteria, wall stiffness, modeling guidance	10.7[1]	Part 4, Chapter 1
3, Concrete Structural Walls	Shear-controlled wall modeling parameters and acceptance criteria	10.7[1]	Part 4, Chapter 2

Table 1-1 Summary of Change Proposals (continued)

Working Group	Change Proposal Topic	ASCE/SEI 41-17 Chapters and Sections Affected	Documentation Supporting Change Proposal
3, Concrete Structural Walls	Shear-friction controlled wall modeling parameters and acceptance criteria	10.7[1]	Part 4, Chapter 3
3, Concrete Structural Walls	Wall classification procedures	10.7[1]	Part 4, Chapter 4
4, Tier 1 and 2	Common Building Type definitions	3.2	Part 5, Chapter 1
4, Tier 1 and 2	Tier 1 diaphragm-related provisions	4.4.2.2, 5.6.2, 5.6.3, Chapter 17 (various tables)	Part 5, Chapter 2
4, Tier 1 and 2	Tier 1 foundations and overturning-related provisions	Chapter 17 (various tables)	Part 5, Chapter 3
4, Tier 1 and 2	Prioritization of checklist statements	A.1	Part 5, Chapter 4
4, Tier 1 and 2	Tier 2 retrofit provisions	5.8	Part 5, Chapter 5
6, URM	Chapter 16 new vertical element provisions	16.2.3, 16.2.5	Part 6, Chapter 1
6, URM	Chapter 16 URM subdiaphragm provisions	16.2.4.3	Part 6, Chapter 2
6, URM	Chapter 16 URM wall out-of-plane provisions	16.2.4.2	Part 6, Chapter 3
6, URM	Chapter 11 URM wall out-of-plane provisions	11.3.3.3	Part 6, Chapter 4
6, URM	Chapter 11 redistribution of forces between URM wall piers	11.3.2.3	Part 6, Chapter 5
6, URM	Chapter 11 URM rocking axial stress provisions	11.3.2.3	Part 6, Chapter 6

(1) ACI 369.1 is the source document for the concrete provisions in Chapter 10 of ASCE/SEI 41. In ACI 369.1, chapter numbers correspond to main section numbers of Chapter 10 of ASCE/SEI 41. Section 10.7 of ASCE/SEI 41-17 is Chapter 7 of ACI 369.1-17 and contains the structural wall provisions. This chapter has been re-organized for the ACI 369.1-22 edition, whereby content has been redistributed into different sections from those in the 2017 edition of the standard.

1.4 Content and Report Organization

This report documents the motivations, technical studies, and recommendations for change proposals that were submitted for consideration of adoption into ASCE/SEI 41-23.

Chapter 2 describes recommendations for future studies with the goal of developing change proposals for future editions of ASCE/SEI 41.

Part 1 describes the motivations, technical studies, and recommendations related to linear analysis provisions.

Part 2 describes the motivations, technical studies, and recommendations related to nonlinear analysis provisions.

Part 3 describes the motivations, technical studies, and recommendations related to foundation provisions.

Part 4 describes the motivations, technical studies, and recommendations related to concrete structural wall provisions.

Part 5 describes the motivations, technical studies, and recommendations related to the Tier 1 screening procedure and its associated checklists, as well as the Tier 2 deficiency-based evaluation procedure.

Part 6 describes the motivations, technical studies, and recommendations related to unreinforced masonry provisions.

1.5 References

ASCE, 2007, *Seismic Rehabilitation of Existing* Buildings, ASCE/SEI 41-06, American Society of Civil Engineers, Structural Engineering Institute, Reston, Virginia.

ASCE, 2008, *Supplement to Seismic Rehabilitation of Existing Buildings* (ASCE/SEI 41-06), ASCE/SEI 41-06 Supplement No. 1, American Society of Civil Engineers, Structural Engineering Institute, Reston, Virginia.

ASCE, 2014, *Seismic Evaluation and Retrofit of Existing Buildings,* ASCE/SEI 41-13, American Society of Civil Engineers, Structural Engineering Institute, Reston, Virginia.

ASCE, 2017, *Seismic Evaluation and Retrofit of Existing Buildings,* ASCE/SEI 41-17, American Society of Civil Engineers, Structural Engineering Institute, Reston, Virginia.

ASCE, 2023, *Seismic Evaluation and Retrofit of Existing Buildings,* ASCE/SEI 41-23, American Society of Civil Engineers, Structural Engineering Institute, Reston, Virginia.

FEMA, 2018, *Example Application Guide for ASCE/SEI 41-13 Seismic Evaluation and Retrofit of Existing Buildings with Additional Commentary for ASCE/SEI 41-17*, FEMA P-2006, prepared by the Applied Technology Council for the Federal Emergency Management Agency, Washington, D.C.

Chapter 2: Recommendations for Future Studies

2.1 Overview

This section describes recommendations for studies with the goal of developing change proposals for future editions of ASCE/SEI 41. The recommendations emerged from the technical studies conducted by working groups developing change proposals for the ASCE/SEI 41-23 update cycle and documented in Part 1 through Part 6 of this report. Some recommended studies are natural extensions of this completed work, whereas some are broad, high-level topics with the potential for leading to significant changes to current practice. In many cases, these recommended studies could connect the work of other codes and standards organizations, other federally funded programs, or university research programs with future versions of ASCE/SEI 41.

These recommendations were collected, collated, and organized into four categories:

- High-level studies,
- Studies that are continuations or outcomes of working group efforts documented in this report,
- Studies that are moderate in scope, and
- Studies that are major in scope.

This chapter provides summaries of these recommended future studies.

2.2 High-Level Studies

2.2.1 Introduction

These recommended studies are high level and broad in scope. In general, they would investigate aspects of the basic assumptions and processes of ASCE/SEI 41, many of which date back decades to FEMA 273, *NEHRP Guidelines for the Seismic Rehabilitation of Buildings* (FEMA, 1997), which have since been questioned by the profession. Although based on specific topics, the recommended studies have implications throughout ASCE/SEI 41 and therefore would benefit from being completed early in the next update cycle.

2.2.2 Revamp Linear Procedures

Users and working groups (e.g., linear analysis, foundations, concrete) have questioned if the linear procedures require too much effort and precision for the accuracy they provide.

Working Group 1, Linear Analysis addressed some of the concerns this cycle with case studies comparing linear and nonlinear analysis results for several common building types. This work resulted in a change proposal to update the limitations on linear analysis.

In general, the linear procedures tend to be overly conservative, but in some critical cases, they can be unconservative (for example, tall buildings with higher modes, and non-ductile buildings where deformations are concentrated at one or more stories). There are also provisions that effectively require users to run a linear analysis to evaluate whether the linear procedure is permitted.

When engineers are polled, they report that most of their ASCE/SEI 41 work uses linear procedures (often over 80%). Over the decades, much work has been dedicated to nonlinear procedures with limited studies on linear procedures. This represents a significant disconnect between the amount of usage linear procedures receive and the amount of research and funding that has been dedicated to them. Lack of confidence by engineers in the linear procedures is counterproductive to regional seismic retrofit programs.

As an example, ASCE/SEI 41 linear procedures are frequently not used in Southern California because practitioners and especially building officials find them too cumbersome and do not think their results are reliable. It is currently common for building officials to require engineers to use 75% of design forces for new buildings. This is a procedure fraught with its own inaccuracies and goes against the impetus behind ASCE/SEI 41, which is to have a separate standard that addresses existing buildings with their archaic materials and noncompliant modern seismic detailing. The Structural Engineers Association of Southern California felt compelled to submit a formal letter to the City of Los Angeles encouraging the use of ASCE/SEI 41 in lieu of the 75% new code alternative.

It is recommended to consider a comprehensive review of the linear procedures in the next cycle. The procedures date back to FEMA 273 and fundamentally try to mimic the comprehensive nonlinear procedures, which may or may not have been the right direction to take. This work could be as expansive in scope as FEMA P-2018, *Seismic Evaluation of Older Concrete Buildings for Collapse Potential* (FEMA, 2018a), which took a fresh look at the problem from the ground up and had many similar goals. The work scope could also be narrower, for instance the development of a more robust 75% code approach for a broad range of common, simpler structures in ASCE/SEI 41.

2.2.3 Revamp Foundation Chapter Technical Basis

The foundation provisions in FEMA 273 through ASCE/SEI 41-06, *Seismic Rehabilitation of Existing Buildings* (ASCE, 2007), permitted unlimited deformations in the subsurface media due to bearing capacity failure if the stiffness of the subsurface or subsurface-foundation interaction was explicitly modeled in a linear or nonlinear analysis. These provisions were applicable to shallow foundations, end bearing caissons, and skin friction along the shaft of piles and caissons. A major change occurred in ASCE/SEI 41-13, *Seismic Evaluation and Retrofit of Existing Buildings* (ASCE, 2014), where limits were placed on the deformations in the subsurface media due to bearing capacity failure. The updated provisions for the shallow foundation provisions were based on research conducted on a square or rectangular footing with a single cantilevered structural element

protruding out from it (Kutter et al., 2016). These provisions created challenges for users assessing foundations with different loading conditions, such as direct axial load due to seismic as well as for assessing combined footings and mat foundations. The most recent update work documented in this report showed the challenges to extrapolating that simplified condition to more complicated common foundation geometries.

An alternate approach to attempting to idealize complicated foundation components as an equivalent rectangular foundation would be to directly track stress and deformation of the subsurface media.

There are two primary benefits to treating the subsurface media as an independent deformation-controlled action. First, it would permit the direct assessment of settlement and how that settlement translates into additional deformations in the superstructure and permanent settlement, which could affect conformance with higher performance levels like Immediate Occupancy and Damage Control. Second, directly tracking stress versus settlement would permit assessment of mat foundations and irregular combined footings directly.

The deep foundation provisions have remained unchanged from FEMA 273, permitting unlimited deformations in the subsurface media or the subsurface-foundation interface. This approach should be revisited and potentially revised.

2.2.4 Functional Recovery Performance Level

There has been considerable discussion in the profession about shifting the design intent from safety-based objectives that seek to prevent collapse to recovery-based objectives that seek to limit the time after the earthquake the building is not functional for both new and existing buildings. FEMA P-2090 / NIST SP-1254, *Recommended Options for Improving the Built Environment for Post-Earthquake Reoccupancy and Functional Recovery Time* (FEMA, 2021), makes the case for functional recovery and identifies retrofitting existing buildings to meet recovery-based objectives as one of the primary recommendations. Currently, ASCE/SEI 41 has two performance levels targeted at something other than safety. The Immediate Occupancy performance level is intended to provide very short time to resume function, essentially no downtime. The Damage Control performance level seeks to minimize damage but does not provide for a specific downtime.

Because ASCE/SEI 41 is tied to ASCE/SEI 7, *Minimum Design Loads and Associated Criteria for Buildings and Other Structures* (ASCE, 2022), through the Basic Performance Objective Equivalent to New Building Performance (BPON) and by calibrating the Basic Performance Objective for Existing (BPOE) Buildings to be provide similar performance, but at lower hazards, there will be a need to develop provisions for functional recovery in the next edition of ASCE/SEI 41 that mirror any provisions that are proposed for the next edition of ASCE/SEI 7.

Current efforts to incorporate a functional recovery performance objective into the methodology of FEMA P-58, *Seismic Performance Assessment of Buildings* (FEMA, 2018b), could inform the functional recovery time for existing buildings and could inform this work.

In the 2022 EERI Distinguished Lecture, "*From Ductility to Repairability: Evolution of Building Design in the Wake of the Christchurch Earthquake,*" Ken Elwood proposed introducing a Repairable Damage performance level to improve functional recovery. As an example, he proposed limiting ductile concrete beam rotations to 2% at the BSE-1N hazard level. His research indicates that this relatively simple approach, which is consistent with the current ASCE/SEI 41 methodology, could result in repairable buildings with little downtime following major events. This approach could also be considered and inform this potential future study.

2.2.5 The Right "Break" for Existing Buildings

Since the 1970s, engineers have accepted a higher level of risk or lower performance for an existing building than a new building. Historically, existing buildings were permitted to be evaluated for 75% of the forces used to design a new building. This is still permitted as an option in the *International Existing Building Code* (IEBC). ASCE/SEI 31-03, *Seismic Evaluation of Existing Buildings* (ASCE, 2003a), also contained a 0.75 factor to differentiate evaluating an existing building from the design of a new building. In the Tier 1 and 2 procedures, the Design Earthquake of ASCE/SEI 7-02, *Minimum Design Loads and Associated Criteria for Buildings and Other Structures* (ASCE, 2003b), was used as the hazard, but the *m*-factors were increased by 4/3rd (=1/0.75). In the Tier 3 procedure, ASCE/SEI 31-03 permitted the use of ASCE/SEI 7-02 or FEMA 356, *Prestandard and Commentary for the Seismic Rehabilitation of Buildings* (FEMA, 2000), which was the pre-standard to ASCE/SEI 41-06, with the hazard multiplied by 0.75.

When ASCE/SEI 31-03 and ASCE/SEI 41-06 were combined into one standard, the committee chose to maintain the philosophy of allowing a lower performance objective for existing buildings than new buildings. Instead of using a uniform factor of 0.75, the committee chose to adopt lower return period hazards, similar to the approach of the 2007 *California Building Code.* The BSE-2E hazard became the 975-year return period, in contrast to the ASCE/SEI 7-05 Maximum Considered Earthquake (MCE), which had a 2,475-year return period. The BSE-1E hazard became the 225-year hazard under the assumption that the Design Earthquake of 2/3*MCE was about a 475-year hazard. In coastal California, the 975-year and 225-year hazard spectral acceleration parameters were approximately 75% of the 2,475-year and 475-year hazard spectral acceleration parameters respectively.

However, the spectral acceleration parameters have changed significantly in ASCE/SEI 7 since the publication of ASCE/SEI 41-06. For example, the MCE changed to be risk targeted in ASCE/SEI 7-10, *Minimum Design Loads for Buildings and Other Structures* (ASCE, 2010); the ground motion models further evolved in ASCE/SEI 7-16, *Minimum Design Loads and Associated Criteria for Buildings and Other Structures* (ASCE, 2017a); and in ASCE/SEI 7-22, *Minimum Design Loads and Associated Criteria for Buildings and Other Structures* (ASCE, 2021), the hazard definition moved to multi-period spectra with site effects directly from the ground motion models.

These changing hazards warrant a study of the appropriate reduction in performance or increased collapse risk that is acceptable for an existing building. This study could investigate the collapse risk implied by ASCE/SEI 41-23 provisions and compare it to ASCE/SEI 7-22. Then the study could look

at whether that risk is acceptable when compared to other risks people encounter on a daily basis, similar to the work completed in ATC-3-06, *Tentative Provisions for the Development of Seismic Regulations for Buildings* (ATC, 1978 and 1984) nearly 40 years ago.

Additionally, this study could be integrated with the functional recovery task. If the next version of ASCE/SEI 7 adopts functional recovery provisions, the natural question for the next ASCE/SEI 41 committee will be what reduced level of functional recovery objectives is acceptable for an existing building.

2.2.6 Benchmarking

There is a need to add comprehensive commentary that clarifies why the benchmark dates were chosen for common building types. This commentary should include the rationale for selecting dates and could include relevant building code updates or other factors that contribute to the selection of the benchmark code edition. The benchmark dates seem to constantly increase in more recent codes; this increase has a significant impact on what is viewed as a seismic concern. Therefore, these dates need a strong rationale.

2.2.7 Revamp Tier 1 Checklists Procedure

The current Tier 1 Screening is set up to fail a building if any checklist statement is flagged as noncompliant. Not all checklist statements carry the same weight when assessing the collapse potential of a building. In some cases, checklist statement noncompliance only matters if other checklist statements are also noncompliant.

Investigate a shift of the Tier 1 Screening from a simple binary process (compliant/non-compliant) to rank and weight items found non-compliant. One option is to utilize the approach of FEMA P-154, *Rapid Visual Screening of Building for Potential Seismic Hazards* (FEMA, 2015), where the screening process results in a score the is based on the overall risk of not meeting the selected performance objective. Tier 1 could also be based on the probability of collapse where each noncompliant statement alters a base building probability of collapse, so one can differentiate the impact of different potential deficiencies, similar to the HAZUS AEBM method (CBSC, 2007). There is also a need to assess situations where you can pass a Tier 1 but fail a Tier 2. One example where this situation is an issue is with respect to wood diaphragms.

2.2.8 Life Safety Performance Definition and Quantitative Criteria

The Life Safety structural performance level is defined as a margin of safety against collapse, with Section 7.6 defining that margin as 4/3rd (= 1/0.75). There has been discussion by engineers that this performance level provides safety against aftershocks, which differentiates it from Collapse Prevention. However, there is no explicit acknowledgement in ASCE/SEI 41 that Life Safety provides protection against aftershocks. This is an important performance level in the standard, as it appears in both BPON and BPOE. Using the FEMA P-58 methodology, this study could investigate what the Life Safety performance level in ASCE/SEI 41 provides in terms of risk to collapse, probability of red

tag, time to functional recovery, and time to full recovery. The study might also investigate what performance ASCE/SEI 7 provides at the Design Earthquake to understand whether ASCE/SEI 41 Life Safety provides analogous performance.

As an alternative approach, the potential for replacing the Life Safety performance level with a Repairable Damage performance level as suggested in the 2022 EERI Distinguished Lecture could be investigated.

2.3 Studies That Are Continuations or Outcomes of Working Group Efforts

2.3.1 Introduction

These studies are predominantly associated with the efforts of working groups documented in this report. The studies are envisioned as continuations or extensions of work completed in this ASCE/SEI 41 update cycle. These studies could be completed with moderate or even minimal effort in some cases during the next update cycle of ASCE/SEI 41. Priority levels were assigned by the working group leads.

2.3.2 Linear Analysis

The following two studies were identified by Working Group 1, Linear Analysis. Note that many of these would be incorporated into or superseded by the major foundation study recommended in Section 2.4.2.

2.3.2.1 RECONSIDER 25% REDUCTION IN ALLOWABLE NONLINEAR DEFORMATIONS [HIGH PRIORITY]

Initially, the provisions in FEMA 273 were intended to be for nonlinear pushover analysis. Recognizing the need for linear procedures, the displacement-based philosophy of the pushover was extended to linear procedures using displacement amplification of the unreduced earthquake force applied on a structure. The linear acceptance criteria were determined creating a factor based on the ratio of the nonlinear displacement limit at the performance level to the yield displacement multiplied by 0.75. The 0.75 multiplier on the analogous nonlinear acceptance criteria was based on judgement of the team tasked with developing FEMA 273. There are other conservative limits placed on the linear procedures, specifically the requirement that the collapse prevention point be moved from the “b point” to the “a point” (for an illustration of these parameters, see Figure 9-2 in ASCE/SEI 41-17). There has never been a comprehensive study to determine if the 0.75 factor is appropriate due to inaccuracies in the linear procedures or if it provides a potentially unnecessary level of conservatism.

2.3.2.2 SIMPLIFY/CONSOLIDATE *M*-FACTOR TABLES [MEDIUM PRIORITY]

Since FEMA 273, the ASCE/SEI 41 *m*-factor tables have contained the same number of entries and same discretization of component actions as the nonlinear procedures. In the Tier 2 procedure, ASCE/SEI 31-03 reduced the *m*-factors for all material component actions down to a one-page table. The level of precision conveyed by the voluminous number of *m*-factors and, in some cases, the complicated equations or interpolations one must do to determine them is potentially out-of-line with the accuracy of the linear procedures. A thorough review of all the material chapter component action *m*-factors should be undertaken and consideration should be given to consolidating the tables to something simpler that is more in line with the actual precision and reliability of the linear procedures.

2.3.3 Nonlinear Modeling Parameters

The following two studies were identified by Working Group 1, Nonlinear Analysis.

2.3.3.1 CYCLIC PROVISIONS [MEDIUM PRIORITY]

In the ASCE/SEI 41-23 update cycle, the foundation was laid for providing clearer guidance for how to generate cyclic simulation models. The provisions need to be more specific by material and component type. Working Group 1, Nonlinear Analysis proposed energy ratio categories, while ACI 369.1-17, *Standard Requirements for Seismic Evaluation and Retrofit of Existing Concrete Buildings and Commentary* (ACI, 2017), has provided general cyclic behavior shapes. Investigate putting numbers to those shapes. The ideal outcome would not be heavily prescriptive but rather provide ranges of energy ratios in each modeling parameter table in the Standard that vary depending on failure mode and component properties. Such an approach would facilitate implementation in a wider range of analysis software that may use varying cyclic behavioral models. The work from NIST GCR 22-917-50, *Benchmarking Evaluation Methodologies for Existing Reinforced Concrete Buildings* (NIST, 2022), indicated that there is a big difference in building outcomes when different cyclic models are used.

2.3.3.2 VALID RANGE OF MODELING UPDATES [MEDIUM PRIORITY]

Significant updates to Section 7.6 were made to better define the valid range of modeling when someone establishes or modifies modeling parameters. Updates in ASCE/SEI 7-22 and ASCE/SEI 41-23 defined the valid range of modeling as the largest deformation in ASCE/SEI 41-23 or other reference standards, typically the “b point” on the component force vs. deformation curve. Consider adding better criteria on the modeling parameters and acceptance criteria to define the range for specific components.

2.3.4 Foundations

The following seven studies were identified by Working Group 2. Note that many of these would be incorporated into or superseded by the major foundation study recommended in Section 2.4.3.

2.3.4.1 REVISE/UPDATE PROVISIONS FOR DEEP FOUNDATIONS [HIGH PRIORITY]

Investigate updating the deep foundations provisions, similar to the work completed for shallow foundations by Working Group 2.

2.3.4.2 INVESTIGATE COMBINED FOOTING ACCEPTANCE CRITERIA [HIGH PRIORITY]

Compare foundation and superstructure evaluation acceptance criteria for linear procedures using Procedure 1 and Procedure 2 from the current work summarized in Part 3 for buildings modeled as a fixed-base or flexible-base.

2.3.4.3 INCORPORATE FOUNDATION ASPECTS OF COMPLETED ARCHETYPE BUILDING STUDIES FROM OTHER WORKING GROUPS [MEDIUM PRIORITY]

Evaluate the foundation provisions and their impact on the superstructure for buildings modeled as a fixed base and as a flexible base using both linear and nonlinear procedures for various archetype buildings. Use the analytical work already completed by various working groups on concrete shear wall buildings, braced frame buildings, moment frame buildings, and flat slab buildings retrofitted with reinforced concrete shear walls.

2.3.4.4 DEVELOP TIER 1 CHECKLIST REQUIREMENTS FOR CAPACITIES OF DEEP FOUNDATIONS, PARTICULARLY WOOD AND HYBRID WOOD/CONCRETE [MEDIUM PRIORITY]

Consider adding checklists for deep foundations as there are currently no checklist statements for capacity, only for foundation detailing, and these checks only address certain foundation types. An overall foundation lateral and/or vertical capacity check of deep foundations should be considered. In addition, it has been suggested to find a way to explicitly incorporate a check for wood piles and hybrid wood piles (e.g., wood that transitions to concrete) in the Tier 1 foundations checklist.

2.3.4.5 INVESTIGATE INTERACTION OF SLIDING AND OVERTURNING FOR DIFFERENT BUILDING GEOMETRIES USING NONLINEAR PROCEDURES [LOW PRIORITY]

Investigate the impact of sliding using upper-bound and lower-bound soil properties on superstructure response for buildings of different aspect ratios and/or building types using nonlinear dynamic time history procedures. Does sliding appreciably increase or decrease the demands from overturning on the elements of the seismic-force-resisting system? In addition, maximum building drifts and floor accelerations should be evaluated for each case study comparison. Evaluate the impact of sliding for flexible buildings such as moment resisting frames and for rigid buildings with reinforced concrete shear walls.

2.3.4.6 INVESTIGATE SITE CLASS D AND E STIFFNESS UNDER HIGH GROUND MOTIONS [LOW PRIORITY]

Determine soil stiffness values for buildings on Site Class D and Site Class E soils in regions where design ground motion is high. These stiffness values are not well defined in ASCE/SEI 41-17.

2.3.4.7 INVESTIGATE DYNAMIC STIFFNESS OF LARGE MAT FOUNDATIONS [LOW PRIORITY]

Determine an appropriate footing width to calculate the dynamic soil stiffness for buildings supported on large mat foundations. Consideration should be given to account for the flexibility of the mat foundation relative to the soil, stiffness of the soil layers under the mat, and the applied loads on the mat.

2.3.5 Tier 1 Analysis

The following four studies were identified by Working Group 4.

2.3.5.1 UPDATE OVERTURNING CHECKLIST ITEMS, PARTICULARLY CALIBRATION OF $0.6S_A$ [HIGH PRIORITY]

Investigate calibrating the $0.6S_a$ limit for the Tier 1 overturning checklist item. This topic was previously reviewed but given other priorities, the application of the checklist statement was revised to limit the types of buildings affected. However, the criteria for the statement itself were not reviewed.

2.3.5.2 CONTINUE PREVIOUS IMPROVEMENTS TO TIER 1 PROVISIONS [HIGH PRIORITY]

Improvements were made to the Tier 1 checklist provisions, but additional items needing improvement were identified during this process. Investigate including semi-quantitative checks related to lateral strength of flexible diaphragms (more rigorous than the current span and aspect ratio limitations) and a check of the flexural capacity of shear walls (especially slender walls). The shear wall item was based on recommendations from Working Group 3. These revised checklist items may lead to addition updates for the Tier 2 procedures. The complication for Tier 1 is developing something simple enough for Tier 1 level screening but rigorous enough to provide reasonable results.

2.3.5.3 CONTINUE UPDATES TO COMMON BUILDING TYPES W1 AND W2 [MEDIUM PRIORITY]

Continue updates made in the ASCE/SEI 41-23 cycle to Common Building Types W1 and W2. Even after the proposals were developed, these wood structures continue to be the only types that are defined more by occupancy than structural system. It is recommended that a more comprehensive review of the building type, the structural systems, and potential vulnerabilities be reviewed for the purpose of potentially updating the Common Building Types, Benchmark Building years, and Tier 1 checklists. An important checklist development topic concerns wood buildings with lateral systems other than shear walls (for example knee-bracing or cantilever columns), as these buildings are included in the W2 definition but there are not specific checklist statements related to these lateral systems.

2.3.5.4 IMPROVE STEEL STRONG COLUMN-WEAK BEAM PROVISIONS [LOW PRIORITY]

The Quick Check statement says if there are more than 50% of the connections that fail the strong column test, then it is non-compliant. But there is no clear guidance on what the test is in ASCE/SEI 41-17 Chapter 4. There is a Tier 2 reference to ASCE/SEI 41-17 Section 5.5.2.1.5, which has some guidance but refers to Section 5.2.5, which is a generic requirement to essentially follow Chapter 7 through Chapter 12. ASCE/SEI 41-17 Chapter 9 seems to be missing guidance on this. Investigate adding more specific guidance in Chapter 4 and Chapter 5. The issue is that if the AISC 341-16, *Seismic Provisions for Structural Steel Buildings* (AISC, 2016), equation for strong column-weak beam is used, column capacity is reduced by axial demand and axial demand includes seismic loads. But since ASCE/SEI 41-17 provisions do not reduce the earthquake demands by the *R*-factor, as assumed in AISC 341, the column capacity can be severely reduced in many situations, and therefore ASCE/SEI 41-17 would be much more conservative than ASCE/SEI 7. In addition, Tier 1 does not have a simple, yet accurate method for determining earthquake axial loads on columns.

2.3.6 Masonry

The following five studies were identified by Working Group 6.

2.3.6.1 INCORPORATE FEMA 306/307 RESEARCH FOR SPECIAL PROCEDURE [HIGH PRIORITY]

Consider incorporating the research of FEMA 306/307, *Evaluation of Earthquake Damaged Concrete and Masonry Wall Buildings* (FEMA, 1998a,b), which found that, for some wall geometries and piers, test results for in-plane wall behavior could be better predicted than that from FEMA 273. These cases include modes where behavior moves from one type to another as the displacement increases, forming a sequence of behavior similar to what is often seen in moderate ductility concrete walls and columns. ASCE/SEI 41-17, however, largely retains the original FEMA 273 provisions.

2.3.6.2 PIER HEIGHT DEFINITIONS AND CORNER PIERS [MEDIUM PRIORITY]

Consider clarifying pier height and adding corner pier provisions. Chapter 11 has commentary discussing refinements for pier heights to address openings of different heights on each side of the pier. This issue is not discussed or required in Chapter 16. The Chapter 11 commentary in ASCE/SEI 41-13 discussed some of the issues but it did not provide clear guidance. The commentary was revised in ASCE/SEI 41-17 to be clearer and provide two alternatives. However, there are still several issues that are not addressed, such as whether a sloping pier base can cross a diaphragm level and the tributary flange length at corner piers.

2.3.6.3 CLARIFY NONLINEAR STATIC PROCEDURE FOR IN-PLANE BEHAVIOR [LOW PRIORITY]

Nonlinear provisions from ASCE/SEI 41-17 Table 11-4 for analyzing in-plane wall behavior depend on the seismic shear force associated with the onset of toe crushing after rocking initiates and the

lateral displacement at the onset of toe crushing. Neither of these parameters has an explicit equation, and both appear to be dependent on a moment-curvature analysis for which there is no clear guidance.

Consider developing more explicit requirements and guidance (commentary) for evaluating the toe crushing displacement and defining the valid range of modeling. Additionally, investigate developing a truly simplified approach that does not require the toe crushing displacement to be explicitly determined and modeled, for example by limiting the Collapse Prevention acceptance criteria to a more conservative limit.

2.3.6.4 IN-PLANE AND OUT-OF-PLANE INTERACTION [LOW PRIORITY]

In-plane and out-of-plane unreinforced masonry (URM) wall evaluations are conducted independently. There is concern that in-plane damage can weaken out-of-plane capacity and vice versa. The acceptance criteria currently do not explicitly consider this interaction, except for an in-plane drift limit that was established in ASCE/SEI 41-13 based on limited testing reviewed at that time. Review existing research to determine if there is any relevant testing or analysis on this issue and develop an interaction procedure if there is sufficient data.

2.3.6.5 TWO WAY BENDING CONSIDERATIONS FOR OUT-OF-PLANE BEHAVIOR [LOW PRIORITY]

Consider provisions to account for two-way bending of URM walls, where applicable. These provisions will be beneficial for evaluating walls that do not conform to the one-way bending limits in ASCE/SEI 41-17 Chapter 11 and Chapter 16, where perpendicular URM walls occur at corner and interior conditions. A literature review could be conducted to determine if there is any relevant testing or analysis of this issue. This should include a detailed review of the Australian Standard, AS 3700: 2018 (Standards Australia, 2018), which has provisions for two-way bending of masonry walls.

2.4 Studies That Are Moderate in Scope

2.4.1 Introduction

These studies were identified as valuable improvements to ASCE/SEI 41-17. However, as contrasted to those in Section 2.3, these studies are not directly connected to the work completed in this ASCE/SEI 41 update cycle.

2.4.2 Update Concrete Coupling Beam Acceptance Criteria

Investigate updating coupling beam modeling parameters and acceptance criteria to make them more aligned or consistent with recent significant changes to concrete shear wall provisions. Coupling beams often control building outcomes under the current ASCE/SEI 41 approach, but there is limited evidence that coupling beam failure causes collapse.

2.4.3 Update Material Properties / Expected Strength for Concrete and Reinforcement

Investigate updating the expected strength factors for concrete and reinforcement. The material properties of concrete and reinforcing steel have not been updated for several cycles. Particularly the blanket factors of 1.5 for concrete and 1.25 for streel reinforcement to convert from nominal to expected material properties can be substantially in error depending on the materials and the era of construction.

2.4.4 Primary Research of Cyclic Behavior of Concrete Piers in Tension

There is a need for experimental research of cyclic behavior of reinforced concrete piers in tension. This need emerged from a study by Working Group 1. It is unclear if there is any experimental research of this condition.

2.4.5 Update Concrete Wall Pier Acceptance Criteria

Investigate updating the concrete wall pier acceptance criteria in Tables 10-19, 10-20, 10-21, and 10-22 in ASCE/SEI 41-17, which currently vary modeling and acceptance criteria for concrete walls and piers by the axial stress ratio. In Table 10-20 and Table 10-22, there is a low and a high axial stress category. However, it is not clear whether tension belongs in the low or the high category. In general, when axial-moment interaction curves are generated and tension is considered, moment capacity can be significantly reduced. When the unreduced ASCE/SEI 41-17 values are used, this reduction can be more severe than those from ASCE/SEI 7. The acceptance criteria should be modified to bring it into closer consistency with ASCE/SEI 7.

2.4.6 Evaluate the Force-Controlled vs. Deformation-Controlled Basis for Subdiaphragms

ASCE/SEI 41-17 Section 7.2.11 covers wall anchorage and indicates related actions shall be force-controlled. Section 7.2.11.1 requires the wall anchorage to be developed into the diaphragm and indicates subdiaphragms can be used as a possible method. In a wood diaphragm, this would imply that the wood subdiaphragm, which is a deformation-controlled element in other portions of the standard, must be checked as force controlled. Since the wall anchorage forces are at the unreduced level and some design guides indicate that the *J*-factor is not to be applied to wall anchorage, the subdiaphragm would need to be checked for very high loads. Since failing the Tier 1 checklist question on wall anchorage leads to Section 5.2.4.12, which sends the designer to Section 7.2.11, Tier 2 deficiency-based retrofits would trigger these provisions as well. Consider evaluating the Section 7.2.11 subdiaphragm provisions to determine if revisions should be made to address force-controlled vs. deformation-controlled assumptions within the development path.

2.5 Studies That Are Major in Scope

2.5.1 Introduction

The studies identified in this section are large in scope. These studies can be distinguished from those in Section 2.2 in that they do not necessarily impact the entire standard and could be treated as standalone efforts.

2.5.2 Develop Energy-Based Methodology

Consider looking more closely at energy-based methods. Less ductile materials are more susceptible to the duration of shaking and the amount of energy that must be dissipated. Energy methodologies that address these issues have been proposed for years but have never been considered within ASCE/SEI 41.

2.5.3 Develop Acceptance Criteria for Common Retrofit Components

Investigate adding modeling parameters and acceptance criteria for typical retrofit techniques (for example, fiber-reinforced polymer jacketed columns) that are commonly used yet not presently addressed in ASCE/SEI 41. In addition, there is not clear guidance about the process for checking a retrofit scheme. The scope of this topic can be substantial as it can cover the overall retrofit procedure, as well as detailing, modeling parameters, and acceptance criteria for a wide range of components of various materials that are retrofitted using various schemes and materials. Investigate adding guidance about the scope of what should be checked (for example, materials and connections) at different tiers.

2.5.4 Develop Comprehensive, Coordinated, Coherent Strength and Stiffness Values for Wood Diaphragms

There are several long-standing issues with wood diaphragms that are present in ASCE/SEI 41. These issues are mostly related to the inherent duplication of specifications in Chapter 12 (Wood Light Frame) and Section 16.2 (Special Procedure for Unreinforced Masonry) and include differences in definitions of materials and configurations, missing or conflicting information for specific diaphragm configurations, and variation in definitions of what constitutes a diaphragm chord. Investigate updating ASCE/SEI 41 with comprehensive, coordinated, coherent strength and stiffness values for wood diaphragms.

2.5.5 Reorganize/Reformat ASCE/SEI 41

ASCE/SEI 41 was written originally as a report (FEMA 273) and then a pre-standard (FEMA 356) and finally converted to a standard (ASCE/SEI 41). The language in many cases is not as clear as required for an enforceable legal document. Commentary is often too extensive for a standard and is not up to date in many cases. Consider re-organizing and consolidating ASCE/SEI 41. Such an effort would make the standard more easily useable and understandable by the engineering profession,

lowering the learning bar for newer users. In addition, improving the language would reduce ambiguity and enhance enforceability of the standard.

2.6 References

ACI, 2017, Standard Requirements for Seismic Evaluation and Retrofit of Existing Concrete Buildings and Commentary, ACI 369.1-17, American Concrete Institute, Farmington Hills, Michigan.

AISC, 2016, *Seismic Provisions for Structural Steel Buildings*, ANSI/AISC 341-16, American Institute of Steel Construction, Chicago, Illinois.

ASCE, 2003a, *Seismic Evaluation of Existing Buildings*, ASCE/SEI 31-03, American Society of Civil Engineers Structural Engineering Institute, Reston, Virginia.

ASCE, 2003b, *Minimum Design Loads and Associated Criteria for Buildings and Other Structures*, ASCE/SEI 7-02, American Society of Civil Engineers Structural Engineering Institute, Reston, Virginia.

ASCE, 2006, *Minimum Design Loads and Associated Criteria for Buildings and Other Structures*, *Including Supplement No. 1*, ASCE/SEI 7-05, American Society of Civil Engineers Structural Engineering Institute, Reston, Virginia.

ASCE, 2007, *Seismic Rehabilitation of Existing Buildings*, ASCE/SEI 41-06, American Society of Civil Engineers Structural Engineering Institute, Reston, Virginia.

ASCE, 2010, *Minimum Design Loads and Associated Criteria for Buildings and Other Structures*, ASCE/SEI 7-10, American Society of Civil Engineers Structural Engineering Institute, Reston, Virginia.

ASCE, 2014, *Seismic Evaluation and Retrofit of Existing Buildings*, ASCE/SEI 41-13, American Society of Civil Engineers Structural Engineering Institute, Reston, Virginia.

ASCE, 2017a, *Minimum Design Loads and Associated Criteria for Buildings and Other Structures*, ASCE/SEI 7-16, American Society of Civil Engineers Structural Engineering Institute, Reston, Virginia.

ASCE, 2017b, *Seismic Evaluation and Retrofit of Existing Buildings*, ASCE/SEI 41-17, Structural Engineering Institute of American Society of Civil Engineers, Reston, Virginia.

ASCE, 2021, *Minimum Design Loads and Associated Criteria for Buildings and Other Structures*, ASCE/SEI 7-22, American Society of Civil Engineers Structural Engineering Institute, Reston, Virginia.

ATC, 1978, Tentative Provisions for the Development of Seismic Regulations for Buildings, ATC-3-06, Applied Technology Council, Palo Alto, California.

ATC, 1984, *Tentative Provisions for the Development of Seismic Regulations for Buildings*, ATC-3-06 (Amended), second printing, Applied Technology Council, Redwood City, California.

ATC, 2021, Seismic Performance Assessment of Buildings, Volume 8—Methodology for Assessment of Functional Recovery Time, Preliminary Report, ATC-138-3, prepared by Applied Technology Council for the Federal Emergency Management Agency, Washington, D.C.

CBSC, 2007, 2007 California Building Code, California Code of Regulations, Title 24, Volume 1 and 2 of Part 2, 2007 CBC, California Building Standards Commission, Sacramento, California.

Elwood, K. J., 2022, *"From Ductility to Repairability: Evolution of Building Design in the Wake of the Christchurch Earthquake,"* 2022 EERI Distinguished Lecture, 12th National Conference on Earthquake Engineering, June 29, 2022, Earthquake Engineering Research Institute, Oakland, California.

FEMA, 1997a, *NEHRP Guidelines for the Seismic Rehabilitation of Buildings*, FEMA 273, prepared by the Building Seismic Safety Council for the Federal Emergency Management Agency, Washington, D.C.

FEMA, 1997b, *NEHRP Commentary for the Seismic Rehabilitation of Buildings*, FEMA 274, prepared by the Building Seismic Safety Council for the Federal Emergency Management Agency, Washington, D.C.

FEMA, 1998a, *Evaluation of Earthquake Damaged Concrete and Masonry Wall Buildings*, *Basic Procedures Manual*, FEMA 306, prepared by Applied Technology Council for the Federal Emergency Management Agency, Washington, D.C.

FEMA, 1998b, *Evaluation of Earthquake Damaged Concrete and Masonry Wall Buildings*, *Technical Resources*, FEMA 307, prepared by Applied Technology Council for the Federal Emergency Management Agency, Washington, D.C.

FEMA, 2000, *Prestandard and Commentary for the Seismic Rehabilitation of Buildings,* FEMA 356, prepared by the American Society for Civil Engineers for the Federal Emergency Management Agency, Washington, D.C.

FEMA, 2015, *Rapid Visual Screening of Buildings for Potential Seismic Hazards: A Handbook*, FEMA P-154, prepared by Applied Technology Council for the Federal Emergency Management Agency, Washington, D.C.

FEMA, 2018a, *Seismic Evaluation of Older Concrete Buildings for Collapse Potential*, FEMA P-2018, prepared by Applied Technology Council for the Federal Emergency Management Agency, Washington, D.C.

FEMA, 2018b, *Seismic Performance Assessment of Buildings, Second Edition*, Volumes 1 through 7, FEMA P-58, prepared by the Applied Technology Council for the Federal Emergency Management Agency, Washington, D.C.

FEMA, 2021, *Recommended Options for Improving the Built Environment for Post-Earthquake Reoccupancy and Functional Recovery Time*, FEMA P-2090/NIST SP-1254, prepared by the Applied Technology Council for the National Institute of Standards and Technology, Gaithersburg, Maryland, and the Federal Emergency Management Agency, Washington, D.C.

Kutter, B. L., Moore, M., Hakhamaneshi, M., and Champion, C., 2016, "Rationale for shallow foundation rocking provisions in ASCE 41-13," *Earthquake Spectra*, 32(2), 1097-1119.

NIST, 2022, *Benchmarking Evaluation Methodologies for Existing Reinforced Concrete Buildings*, GCR 22-917-50, prepared by the Applied Technology for the National Institute of Standards and Technology, Gaithersburg, Maryland.

Standards Australia, 2018, *Masonry Structures*, AS 3700:2018, prepared by Committee BD-004 Masonry Structures for Standards Australia Limited.

Part 1

Chapter 1: Revisions to Section 7.3 Linear Limitation Provisions

1.1 Motivation

The purpose of this revision proposed for ASCE/SEI 41-23 Section 7.3 is to clarify the limitations on the use of linear analysis procedures for building evaluation using the Tier 3 methodology described in ASCE/SEI 41 Chapter 7. Previous editions of ASCE/SEI 41 have required substantial effort in accordance with Section 7.3.1.1 and effectively required a linear evaluation be performed to determine if linear procedures are permitted. A literature search and a series of case studies were undertaken to study whether these linear procedure limitations could be simplified, at least for some building types or some circumstances. This effort resulted in proposed revisions to Section 7.3.1.1 that will 1) exempt several simple common building types from any requirement to perform nonlinear analysis, 2) clarify that nonlinear analysis is not required when linear evaluation has shown the structure to be inadequate, and 3) make substantial revisions and additions to the commentary. The exempt common building types include wood frame buildings (W1, W1a, and W2), cold-formed steel light-frame construction (CFS1 and CFS2), and unreinforced masonry (URM buildings meeting the requirements to qualify for use of the Chapter 16 special procedure). The provisions will continue to require a test for applicability of the linear analysis procedures for all other building types and circumstances with the result that nonlinear analysis procedures are required when there are high ductility demands coupled with either a weak story irregularity or a torsional strength irregularity for non-exempt common building types.

1.2 Summary of Changes Recommended

The changes are proposed for ASCE/SEI 41-23 Section 7.3.1.1 and will introduce two new exemptions to the linear limitation provisions. The first exemption is for listed common building types that include wood frame buildings (W1, W1a, and W2), cold-formed steel light-frame construction (CFS1 and CFS2), and unreinforced masonry (URM buildings meeting the requirements to qualify for use of the Chapter 16 special procedure). These exempt buildings may be evaluated using the linear procedures without limits or qualifications. The second exemption states that nonlinear analysis is not required when linear analysis has shown the structure is inadequate or does not comply with a Performance Objective, even where nonlinear analysis would be required to show compliance with a particular Performance Objective.

The following provisions from Section 7.3.1.1 of ASCE/SEI 41-17 are proposed not to be revised in ASCE/SEI 41-23. They do not allow linear procedures to be used when both of the following are true:

- *A structural component has a DCR that exceeds the lesser of 3.0 and the m-*factor *for the component action*. DCR is defined as Q_{UD} / Q_{CE}. DCR is a measure of component ductility demand. It does not use the factored capacity, which is $m \kappa Q_{CE}$.

- *The building has a weak story irregularity or a torsional strength irregularity.* Per Section 7.3.1.1.3, a weak story irregularity exists if the ratio of the average shear DCR for elements in any story to that of an adjacent story in the same direction exceeds 1.25. Per Section 7.3.1.1.4, a torsional strength irregularity exists when the ratio of the critical element DCR on one side of the center of resistance of a story to the critical element DCR on the other side exceeds 1.5.

1.3 Technical Studies

1.3.1 Overview

1.3.1.1 SCOPE OF WORK

There are three different procedure limitation provisions in ASCE/SEI 41. The first is Section 7.3.1.1, which applies to both the linear static procedure (LSP) and the linear dynamic procedure (LDP). The second is in Section 7.3.1.2 which, assuming linear procedures are permitted by Section 7.3.1.1, determines whether the LSP is permitted or whether period and stiffness characteristics that can affect the distribution of loads require that the LDP be used. The third is Section 7.3.2.1, which establishes whether the nonlinear static procedure (NSP) can be used when nonlinear analysis is conducted or whether concentrated local ductility and higher mode effects not well captured by the NSP require that the nonlinear dynamic procedure (NDP) be used. The NDP can always be used, but it requires the most engineering effort. Although the Section 7.3.1.2 provisions were evaluated in some of the case studies for this project in passing, the focus and scope of the study is on the Section 7.3.1.1 provision. The conclusions of these studies resulted in proposed changes to ASCE/SEI 41-23 Section 7.3.1.1, but Section 7.3.1.2 and Section 7.3.2.1 are proposed to remain unchanged.

The primary questions addressed in these studies were:

- Is the Section 7.3.1.1 limitation provision reasonably conservative?
- Are there alternative options to the provision that are simpler and that are reasonably conservative?

ASCE/SEI 41 has four analysis procedures: LSP, LDP, NSP, and NDP. The preferred evaluation approach for this study has a model of a realistic existing building, where LSP and/or LDP evaluation results can be compared against NDP evaluation results, and there is a clear determination of DCRs and linear procedure limitation provisions. A less desirable, but still valuable approach, compares LSP and/or LDP results with NSP results, instead of NDP results. Case studies with both approaches were utilized, depending on whether NSP or NDP results were available.

Note on terminology: It is common practice in engineering to use the term demand-to-capacity ratio or demand-capacity ratio (DCR) as a measure of acceptability where a value of less than unity is defined as acceptable and a value equal or greater than unity is defined as unacceptable. However, ASCE/SEI 41 Eq. 7-16 defines DCR as Q_{UD} / Q_{CE}, which is a measure of ductility demand, not

acceptability. In this chapter, acceptability is defined using the Acceptance Ratio. For linear procedures and for deformation-controlled actions, the Acceptance Ratio is equal to $Q_{UD} / m\kappa Q_{CE}$. For force-controlled actions, the Acceptance Ratio is equal to $Q_{UF} / \kappa Q_{CL}$. An Acceptance Ratio less than unity is acceptable; an Acceptance Ratio equal to or greater than unity is unacceptable. The term Acceptance Ratio was initiated and defined in FEMA P-2006, *Example Application Guide for ASCE/SEI 41-13 Seismic Evaluation and Retrofit of Existing Buildings with Additional Commentary for ASCE/SEI 41-17* (FEMA, 2018a). A change proposal was submitted to add it to ASCE/SEI 41-23, as discussed in Part 1, Chapter 2. For nonlinear procedures, in this chapter, the Acceptance Ratio depends on the metric being used for the nonlinear elements. If it is the total drift ratio such as for shear walls in shear, then the Acceptance Ratio is the drift at the seismic hazard level divided by the acceptable total drift.

1.3.1.2 SOURCES OF INFORMATION INVESTIGATED

The following sources of information were investigated in the study. They include cases studies, design examples, research studies, and past evaluation and rehabilitation recommended provisions and standards that led to ASCE/SEI 41-17. Each case study or source listed in the bullets below is described in the following sections.

Case Studies (See Heading 1.3.2 Below)

- Working Group 1 (WG1) Linear Punctured Reinforced Concrete Shear Wall (RCSW): This case study includes LSP, NSP, and NDP modeling. Two geometries were evaluated, and two levels of seismic demand were evaluated, in order to produce different results.

- WG1 Steel Moment Frame (SMF): This case study includes LDP and NSP modeling. The focus was on proposed modifications to nonlinear modeling and acceptance criteria, but the case study also provides information on the limitation provisions.

- WG1 Steel Braced Frame: The focus was on different nonlinear modeling and acceptance criteria, but the case study also provides information on the limitation provisions. LDP and NDP analyses were run.

- WG2 Cantilever RCSW: This case study includes LSP and NSP modeling of a cantilever shear wall building. Five LSP variations and one NSP model were evaluated. The focus was on foundation flexibility, but the case study also provides information on the limitation provisions.

- WG3 RCSW: This case study includes LSP, LDP, and NSP modeling of a seven-story concrete shear wall building. The focus of the case study was on evaluating proposed revisions to the modeling and acceptance provisions for reinforced concrete elements controlled by shear, but the case study also provides some information on the limitation provisions.

Design Examples in FEMA P-2006, Example Application Guide for ASCE/SEI 41-13 Seismic Evaluation and Retrofit of Existing Buildings with Additional Commentary for ASCE/SEI 41- 17 (See Heading 1.3.3 Below)

- Pre-Northridge Steel Moment Frame: LSP, LDP, and NSP.
- Steel Braced Frame: LSP and NSP.
- Cantilever RCSW: LSP and NSP.

Research Studies (See Heading 1.3.4 Below)

- FEMA P-2012, *Assessing Seismic Performance of Buildings with Configuration Irregularities: Calibrating Current Standards and Practices* (FEMA, 2018b).
- FEMA P-807, *Seismic Evaluation and Retrofit of Multi-Unit Wood-Frame Buildings with Weak First Stories* (FEMA, 2009b).
- FEMA 440, *Improvement of Nonlinear Static Seismic Analysis Procedures* (FEMA, 2005a).

Seismic Evaluation and Rehabilitation Recommended Provisions and Standards (See Heading 1.3.5 Below)

- ATC-14, *Evaluating the Seismic Resistance of Existing Buildings* (ATC, 1987).
- FEMA 178, *NEHRP Handbook for the Seismic Evaluation of Existing Buildings* (FEMA, 1992).
- ASCE 31-03, *Seismic Evaluation of Existing Buildings* (ASCE, 2003)
- FEMA 310, *Handbook for the Seismic Evaluation of Buildings: A Prestandard* (FEMA, 1998).
- FEMA 273, *NEHRP Guidelines for the Seismic Rehabilitation of Buildings* (FEMA, 1997a).
- FEMA 274, *NEHRP Commentary for the Seismic Rehabilitation of Buildings* (FEMA, 1997b).
- FEMA 356, *Prestandard and Commentary for the Seismic Rehabilitation of Buildings* (FEMA, 2000).
- ASCE/SEI 41-06, *Seismic Rehabilitation of Existing Buildings* (ASCE, 2007).
- ASCE/SEI 41-13, *Seismic Rehabilitation of Existing Buildings* (ASCE, 2014).

1.3.1.3 COVERAGE OF RELEVANT PERMUTATIONS OR BINS

Studies that were reviewed have been categorized in the following two tables. Table 1-1 includes studies with LSP/LDP and more desirable NDP evaluations. Table 1-2 includes studies with LSP/LDP and NSP evaluations. The tables identify all the possible permutations or "bins," and which bins are of high value to study.

Table 1-1 Possible Case Studies with Nonlinear Dynamic Procedure Analyses

LSP/LDP Result[1]	NDP Result[1]	Linear Permitted?	Limitation Provision Result is Appropriate	Was the Case Studied?[2]	Value of Case to Study
OK	OK	Yes	Yes	No	Low
		No	No	No	High
OK	Not OK	Yes	No	No	High
		No	Yes	Working Group 1 RCSW S_{XS} =0.67 and 1.0	High
Not OK	OK	Yes	Conservative	No	Low
		No	Possibly	No	High
Not OK	Not OK	Yes	Yes	No	Low
		No	No, but unnecessary	Working Group 1 RCSW S_{XS} =1.0 and 1.5, Working Group 1 SMF, Working Group 1 OBF	Low

[1] "OK" for LSP/LDP Result and NDP Result means the performance objective is met. "Not OK" means the performance objective is not met.
[2] Case studies identified are described ahead.

Table 1-2 Possible Case Studies with Nonlinear Static Procedure Analyses

LSP/LDP Result[1]	NSP Result[1]	Linear Permitted?	Limitation Provision Result is Appropriate	Was the Case Studied?[2]	Value of Case to Study
OK	OK	Yes	Yes	No	Low
		No	No	No	High
OK	Not OK	Yes	No	Working Group 2 Fixed Base	High
		No	Yes	No	High
Not OK	OK	Yes	Conservative	Working Group 3 RCSW	Low
		No	Possibly	FEMA P-2006 RCSW	High
Not OK	Not OK	Yes	Yes	FEMA P-2006 SMF	Low
		No	No, but unnecessary	Working Group 2 Flexible Base, FEMA P-2006 OBF Rigid Base	Low

[1] "OK" for LSP/LDP Result and NSP Result means the performance objective is met. "Not OK" means the performance objective is not met.
[2] Case studies identified are described ahead.

1.3.1.4 LINEAR PROCEDURE LIMITATION PROVISION REVISION OPTIONS CONSIDERED

The following eight options were initially considered for revisions to the limitation provision.

- *Revise weak story irregularity to be strength-only:* The definition of "weak story" in Section 7.3.1.1.3 of ASCE/SEI 41-17 is when the ratio of the average shear DCR for elements in any story to the average DCR of an adjacent story exceeds 1.25. By comparison, in ASCE/SEI 7-16 (ASCE, 2017a), the weak story definition is where the "story lateral strength is less than 80% of the story above," and the extreme weak story is where "the story lateral strength is less than 65% of the story above." Thus, ASCE/SEI 41-17 compares DCRs, but ASCE/SEI 7-16 compares only strength. One option is to revise the limitation provision to only check strength ratios and not demand-capacity ratios, which requires less effort.

- *Increase DCR:* The Section 7.3.1.1 threshold for DCRs is when the DCR of any elements exceeds the lesser of 3.0 and the *m*-factor for a component action. To reduce the likelihood of the limitation provision triggering and reduce conservatism, the value of 3.0 can be increased to a higher value, such as 4.0 or 5.0. This will only make a difference if the *m*-factor is greater than the value chosen.

- *Remove m-factor test:* To reduce the likelihood of the limitation provision triggering and reduce conservatism, the *m*-factor test can be removed so the DCR threshold only depends on a single value. With the current provision value of 3.0, this will make a difference if the *m*-factor is less than 3.0.

- *Remove DCR = 3.0 test:* To reduce the likelihood of the limitation provision triggering and reduce conservatism, the test with DCR = 3.0 test can be removed, while preserving the *m*-factor test. With the current provision value of 3.0, this will make a difference if the *m*-factor is greater than 3.0.

- *Disproportionate DCR:* An underlying concern with linear procedures is that there may be an element or story with a disproportionately large DCR where energy dissipation and damage will concentrate. A version of this option considered in this study is to trigger the limitation when the average story shear DCR of any story is more than 1.5 times the average story DCR values.

- *More conservative linear procedure Acceptance Ratio:* Rather than limit the use of linear procedures, an option is to simply make their provisions more conservative. This can be done in general or as an exception to the current limitation provision. In this study, this option is an exception to the current limitation provision. This can be done by reducing the allowed Acceptance Ratio from 1.0 or greater, to a lower value, such as 0.75. This can be written as AR $\leq$ 0.75 or $Q_{UD} \leq 0.75 m \kappa Q_{CE}$.

- *Combine a relaxed weak story irregularity criterion with a more conservative linear procedure Acceptance Ratio:* This option recognizes that the weak story irregularity in ASCE/SEI 41-17 is more conservative than it is in ASCE/SEI 7-16. The weak story criterion using the ratio of DCRs between stories is relaxed from 1.25 to 1.5. However, it also recognizes that demands could

concentrate in the lowest story in an ASCE/SEI 7-16 compliant structure. This is addressed similar to the previous option by reducing the allowed Acceptance Ratio from 1.0 or greater, to a lower value, such as 0.75. This can be written as AR ≤ 0.75 or $Q_{UD} \leq 0.75 m \kappa Q_{CE}$. This can be done in general or as an exception to the current limitation provision. In this study, this option is an exception to the current limitation provision.

- *Exempt select model building types:* A final option is to exempt select model building types from the linear analysis limitation provision, such as wood frame buildings.

1.3.2 Case Study Summaries and Findings

The five studies listed above are summarized in this section below. The most extensive of these studies is described first under Section 1.3.2.1 and focused on punctured shear walls. This study is summarized below, but additional detailed information is provided in Part 1, Appendix A, which can be found at http://femap2208.atcouncil.org/.

1.3.2.1 WORKING GROUP 1 RCSW WITH S_{XS} = 1.0 AND S_{XS} = 1.5 CASE STUDY

Building Description: The case story building is a modified version of the concrete shear wall design example in FEMA P-2006. It is three stories, with punctured shear walls in one direction and cantilever shear walls in the other direction. The focus is on the punctured shear wall direction.

Seismic Demand and Structural Performance Levels: This was the first case study conducted. The case study building was designed to meet the 1961 UBC seismic provisions (ICBO, 1961) using Z=1.0 and K=1.0, but not meet the ASCE/SEI 7-16 seismic provisions, in order to represent a realistic existing building. A typical seismic demand in coastal California outside the near field zone for short-period buildings (S_{XS} = 1.0) was used for the lower seismic hazard level. This was assumed to be the BSE-1N level, with S_{XS} = 1.5 at the BSE-2N level. The use of BSE-1N/BSE-2N instead of BSE-1E/BSE-2E was made initially for potential ease of comparison with designs for new buildings. However, as long as the same seismic hazard level is used with each procedure, differences can be appropriately compared. Demands at the S_{XS} = 1.0 level are compared against the Life Safety Structural Performance Level, and demands at the S_{XS} = 1.5 level are compared against the Collapse Prevention Structural Performance Level.

For NDP runs, a suite of 11 ground motions were scaled to the target spectral acceleration. These were provided by the Working Group 1, Nonlinear per request. Cases were evaluated with $1.0GA_v$ (per ASCE/SEI 41-17 Table 10-5) for shear wall shear rigidity and at $0.25GA_v$ to address the effect of more flexible shear response due to cracking as it was known that reductions to shear wall shear rigidity were being considered by ACI 369 and Working Group 3. It is a very stiff building, and the periods range from 0.27–0.35 seconds in punctured shear wall direction of interest. Thus, per ASCE/SEI 41-17 Section 2.4.3.3 and ASCE/SEI 7-16 Section 16.2.3.1, the $0.2T$ to $1.5T$ range would be 0.2 x 0.27 sec = 0.05 sec to 1.5 x 0.35 sec = 0.53 sec. ASCE/SEI 41-17 Section 2.4.3.3 has a minimum on the upper end of 1 second which is not in ASCE/SEI 7-16. Using ASCE/SEI 41-17, the scaling range is 0.05–1.0 seconds. The suite included 4 pulse records.

Analysis Procedures: LSP, NSP, and NDP analyses were conducted.

Linear structural models for the prototype buildings were created using ETABS following the provisions in Section 7.2.3 and Chapter 10 of ASCE/SEI 41-17. Some of the characteristics of the models are listed as follows:

- The structural models are three-dimensional.
- Section 7.2.3.3 of ASCE/SEI 41-17 states that the total initial lateral stiffness of secondary components, i.e., the gravity-carrying frame in this case, shall not exceed 25% of the total initial lateral stiffness of the primary components. Accordingly, the percentage of lateral loads resisted by the primary components has been checked to make sure that less than 25% of the total lateral loads are resisted by the secondary components.
- Expected material properties are assigned to structural components in the model.
- Effective sectional stiffness has been assigned to structural components according to Table 10-5 of ASCE/SEI 41-17 and other applicable specifications such as ACI 318-14.
- Rigid diaphragms are used.
- Pinned supports are assigned to the base of shear walls. Soil-structure interaction effects are not part of the study.
- P-Delta effects are included.
- Gravity loads are uniformly distributed over the diaphragms.
- Seismic mass of floors is uniformly distributed over the diaphragms.
- Accidental torsional effects were checked per Section 7.2.3.2 of ASCE/SEI 41-17 but were not triggered.
- Load combinations for ASCE/SEI 41-17 are per Section 7.2.2 for linear analysis which includes:
    - $1.1D + 1.1 \times (0.25L) + 1.0E = 1.1D + 0.275L + 1.0E$, where L is the unreduced design live load from ASCE/SEI 7
    - $0.9D + 1.0E$

Figure 1-1, Figure 1-2, and Figure 1-3 illustrate the general layout of the ETABS finite element models that have been studied.

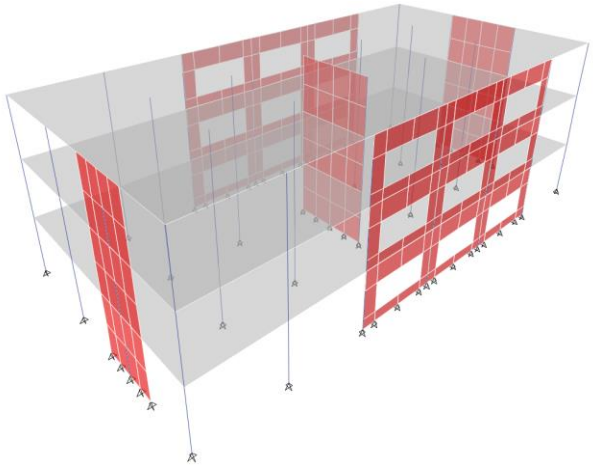

Figure 1-1 Working Group 1 RCSW linear model.

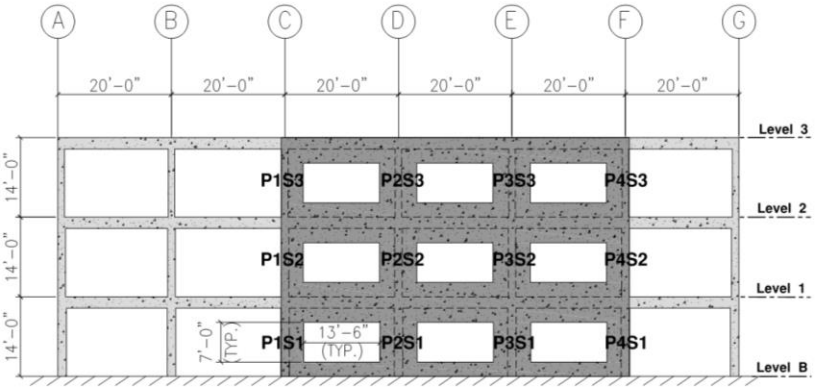

Figure 1-2 Working Group 1 RCSW Pattern 1.

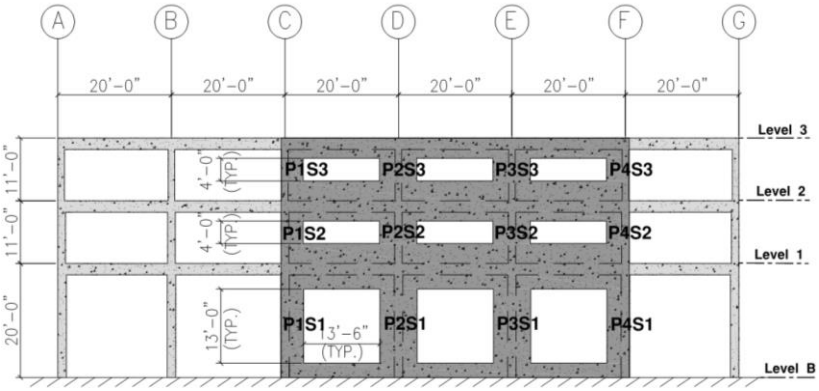

Figure 1-3 Working Group 1 RCSW Pattern 2.

Nonlinear structural models were created using PERFORM-3D following the provisions in Section 7.2.3 and Chapter 10 of ASCE/SEI 41-17. Some of the characteristics of the models are listed as follows:

- The structural models are three-dimensional.
- Per Section 7.2.3.3 of ASCE/SEI 41-17, both primary and secondary components, i.e., shear walls, diaphragms, and columns, are included in the model.
- Uniaxial stress-strain relations of reinforcing steel and concrete materials are created for implementing fiber-discretized sections.
- Fiber-discretized sections for capturing inelastic axial-flexural interactions are assigned to selected wall piers. Columns embedded in the walls have been incorporated into the fiber sections.
- Shear stress-strain relations have been determined according to Table 10-20 of ASCE/SEI 41-17 and assigned to selected wall piers and spandrels.
- Rigid diaphragms are used.
- Pinned supports are assigned to the base of shear walls and columns. Soil-structure interaction effects are not part of the study.
- Gravity columns are included to help capture P-Delta effects.
- Gravity loads are applied to the top of columns according to the tributary area.
- Lateral seismic floor mass is lumped at the master node of the rigid floor constraint.
- A linear elastic gravity analysis is conducted prior to any nonlinear seismic analysis and the gravity loads at the end of the gravity analysis remain constant in the seismic analysis.
- Seismic displacements are applied parallel to the punctured shear wall direction of interest.
- Vertical seismic effects are not considered.
- The load combination for ASCE/SEI 41-17 is per Section 7.2.2 for nonlinear analysis which is:
    - $1.0D + 0.25L + 1.0E$, where L is the unreduced design live load from ASCE/SEI 7
- For the NSP, response spectra are scaled to reach the desired seismic demand.
- For the NDP, earthquake ground motions are scaled to reach the desired seismic demand.

Figure 1-4 illustrates the general layout of the PERFORM-3D finite element models that have been studied.

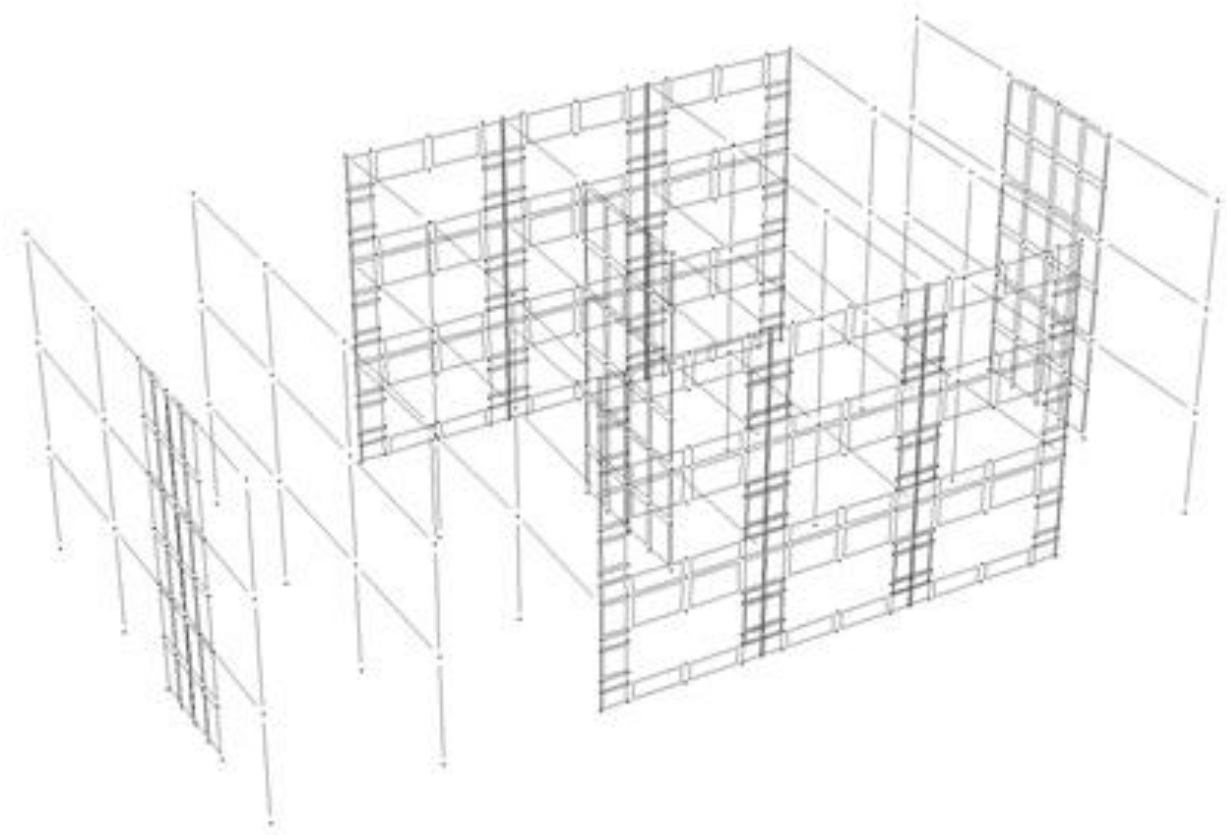

Figure 1-4 Working Group 1 RCSW nonlinear model.

Linear Procedure Limitation Provision Status: The linear limitation provision was evaluated for both Pattern 1 and Pattern 2 and at the BSE-1N and BSE-2N levels, for a total of four permutations. The limitation provision was triggered for both patterns, and linear procedures are not permitted. Table 1- 3 shows a summary.

Table 1-3 Working Group 1, Linear RCSW S_{XS} = 1.0 and S_{XS} = 1.5 Case Study: Linear Procedure Limitation Provision Summary

Pattern	S_{XS}	Ratio of Maximum Story DCR to Adjacent Story DCR	Weak Story?	Component DCR_{max}	Associated *m*-factor	Linear Permitted at Hazard Level?	Linear Permitted for Performance Objective?
1	1.0	1.7	Yes	3.0	2.0	No	No
				3.2	2.5		
	1.5	1.7	Yes	4.7	3.0	No	
2	1.0	1.9	Yes	3.5	2.0	No	No
				3.0	2.5		
	1.5	1.9	Yes	5.2	3.0	No	

Analysis Results: Table 1-4 summarizes the analysis results for each code or standard for Pattern 1. The Acceptance Ratio results exceed 1.0 for ASCE/SEI 7-16, LSP, NSP, and the NDP. The moment Acceptance Ratio results from the LSP are ignored because the capacity is significantly reduced when the full unreduced earthquake tension is used in the P-M interaction equations. This is judged to be a flaw needing correction in ASCE/SEI 41-17 as it is significantly inconsistent with ASCE/SEI 7-16. Because the Acceptance Ratios exceed 1.0, the performance objectives are not met. For the NDP, in the S_{XS} = 1.0 run, two out of 11 ground motions lead to one or more piers reaching the full shear capacity and thus failing. For the S_{XS} = 1.5 run, this happens in three out of 11 ground motions. Because the LSP and the NSP and NDP all do not meet the performance objective, the triggered limitation provision is judged unnecessary. A conclusion using the LSP results that the building is inadequate would be sufficient.

Table 1-4 Working Group 1, Linear RCSW S_{XS} = 1.0 and S_{XS} = 1.5 Case Study: Pattern 1 Analysis Results

Code/Standard	S_{XS}	Shear Acceptance Ratio	Moment Acceptance Ratio	Meets Performance Objective	LSP Bounds NSP	LSP Bounds NDP	LSP Permitted	Limitation Provision Result is Appropriate
1961 UBC	—	0.6	—	Yes	—	—	—	—
ASCE 7-16	1.0	1.5	1.3	No	—	—	—	—
LSP	1.0	1.7	2.8[1]	No	—	—	Not Permitted	—
	1.5	1.7	3.9[1]		—	—		—
NSP	1.0	3.2	—	No	No: 1<1.7<3.2	—	—	Unnecessary
	1.5	7.6	—		No: 1<1.7<7.6	—	—	Unnecessary
NDP	1.0	Fail[2]	—	No	—	Possibly	—	Unnecessary
	1.5	Fail[3]	—		—	Possibly	—	Unnecessary

(1) Moment Acceptance Ratio ignored for LSP, as it is due to low capacity from unreduced EQ tension.
(2) In two out of 11 motions, the piers reached an Acceptance Ratio of 1.0 failure in shear.
(3) In three out of 11 motions, the piers reached an Acceptance Ratio of 1.0 failure in shear.

Table 1-5 provides a similar summary for Pattern 2. While the Acceptance Ratios are slightly different, the results are similar in most cases, except for the S_{XS} = 1.0 level. For the NSP run at this level, the Acceptance Ratios are below 1.0. This is because the overall target displacement for Pattern 2 is similar to Pattern 1, the nonlinear deformations concentrate in the ground story piers, and the ground story pier are taller in Pattern 2, so the shear strains are less for the same displacement. This unanticipated result that a tall first story performs better is not borne out by the NDP runs. As the NDP results are considered more reliable, then the anomaly for the NSP S_{XS} = 1.0 level is not considered determinative.

Table 1-5 Working Group 1, Linear RCSW S_{XS} = 1.0 and S_{XS} = 1.5 Case Study: Pattern 2 Analysis Results

Code/Standard	S_{XS}	Shear Acceptance Ratio	Moment Acceptance Ratio	Meets Performance Objective	LSP Bounds NSP	LSP Bounds NDP	LSP Permitted	Limitation Provision Result is Appropriate
1961 UBC	—	0.6	—	Yes	—	—	—	—
ASCE 7-16	1.0	1.7	2.4	No	—	—	—	—
LSP	1.0	1.4	5.0[1]	No	—	—	Not Permitted	—
	1.5	1.7	8.5[1]		—	—		—
NSP	1.0	0.5	0.8	No	No: 0.8<1<1.4	—	—	Possibly not
	1.5	2.1	—		Yes: 1<1.7<2.1	—	—	Unnecessary
NDP	1.0	Fail[2]	—	No	—	Possibly	—	Unnecessary
	1.5	Fail[2]	—		—	Possibly	—	Unnecessary

(1) Moment Acceptance Ratio ignored for LSP, as it is due to low capacity from unreduced EQ tension.
(2) In six out of 11 motions, the piers reached an Acceptance Ratio of 1.0 failure in shear.

Alternative Linear Procedure Limitation Provision Option Results: This case study result goes in the bin for LSP "Not OK," NDP "Not OK," and linear procedures not permitted. As the limitation provision is unnecessary, there is little reason to explore alternatives to the provision. A "permission clause" is proposed to be added to the limitation provision that says if Acceptance Ratios are greater than or equal to unity, then a nonlinear analysis is not required to state that the building does not meet the standard.

Conclusions: Either the demand should be reduced or the capacity can be increased to determine if performance objectives can be met with any of the ASCE/SEI 41-17 methodologies. The simpler approach of reducing the demand by a factor of 2/3 was chosen to apply to the next case study.

1.3.2.2 WORKIGN GROUP 1 RCSW WITH S_{XS} = 0.67 AND S_{XS} = 1.0 CASE STUDY

Building Description: This is the same building described in Section 2.1.3.2.1 but with the S_{XS} = 0.67 and S_{XS} = 1.0 demands.

Seismic Demand and Structural Performance Levels: This was the second case study conducted. In order to increase the likelihood that performance objectives might be met and help achieve more

pronounced results between procedures, the demands were reduced by a factor of 2/3. Thus, demands at the S_{XS} = 0.67 level were compared against the Life Safety Structural Performance Level, and demands at the S_{XS} = 1.0 level were compared against the Collapse Prevention Structural Performance Level. For NDP, the ground motions of the first phase with S_{XS} = 1.0 and S_{XS} = 1.5 described in Section 1.3.2.1 were scaled down by multiplying them by 2/3.

Analysis Procedures: The same full suite of analysis procedures run for the S_{XS} = 1.0 and S_{XS} = 1.5 case study were also run for the S_{XS} = 0.67 and S_{XS} = 1.0 case study.

Linear Procedure Limitation Provision Status: The linear limitation provision was evaluated for both Pattern 1 and Pattern 2 and at the BSE-1N and BSE-2N levels, for a total of four permutations. The limitation provision was triggered for both patterns. Table 1-6 shows a summary.

Table 1-6 Working Group 1 RCSW S_{XS} = 0.67 and S_{XS} = 1.0 Case Study: Linear Procedure Limitation Provision Summary

Pattern	S_{XS}	Ratio of Maximum Story DCR to Adjacent Story DCR	Weak Story?	Component DCR_{max}	Associated *m*-factor	Linear Permitted at Hazard Level?	Linear Permitted for Performance Objective?
1	0.67	1.70	Yes	1.8	2.0	Yes	No
				2.1	2.5		
	1.0	1.70	Yes	3.2	3.0	No	
2	0.67	1.77	Yes	1.9	2.0	Yes	No
				2.2	2.5		
	1.0	1.77	Yes	3.2	3.0	No	

Analysis Results: Table 1-7 summarizes the analysis results for each code or standard for Pattern 1, and Table 1-8 summarizes Pattern 2. The Acceptance Ratio results are close to 1.0 for ASCE/SEI 7-16 and the LSP. The moment Acceptance Ratio results from the LSP are ignored because the capacity is significantly reduced when the full unreduced earthquake tension is used in the P-M interaction equations. (This is a separate issue this study helped bring to light that should be evaluated in future ASCE/SEI 41 updates.) However, the Acceptance Ratios for the NSP at the S_{XS} = 1.0 level and for both levels for the NDP are exceeded. Thus, the limitation provision result of not permitted is appropriate because it prevents a misleading, unconservative conclusion from being drawn based on the LSP.

Table 1-7 Working Group 1, Linear RCSW S_{XS}=0.67 and 1.0 Case Study: Pattern 1 Analysis Results

Code/Standard	S_{XS}	Shear Acceptance Ratio	Moment Acceptance Ratio	Meets Performance Objective	LSP Bounds NSP	LSP Bounds NDP	LSP Permitted	Limitation Provision Result is Appropriate
1961 UBC	—	0.57	—	Yes	—	—	—	—
ASCE 7-16	0.67	1.1	1.0	Close	—	—	—	—
LSP	0.67	0.9	2.0[1]	Close	—	—	Not Permitted	—
	1.0	1.1	2.8[1]		—	—		—
NSP	0.67	0.4	—	No	Yes: 0.9 > 0.4	—	—	Yes
	1.0	2.9			No: 1.2 < 2.9	—	—	Yes
NDP	0.67	Fail[2]	—	No	—	Possibly	—	Yes
	1.0	Fail[3]	—		—	Possibly	—	Yes

(1) Moment Acceptance Ratio ignored for LSP, as it is due to low capacity from unreduced EQ tension.
(2) In five out of 11 motions, the piers reached an Acceptance Ratio of 1.0 failure in shear.
(3) In five out of 11 motions, the piers reached an Acceptance Ratio of 1.0 failure in shear.

Table 1-8 Working Group 1, Linear RCSW S_{XS} = 0.67 and S_{XS} = 1.0 Case Study: Pattern 2 Analysis Results

Code/Standard	S_{XS}	Shear Acceptance Ratio	Moment Acceptance Ratio	Meets Performance Objective	LSP Bounds NSP	LSP Bounds NDP	LSP Permitted	Limitation Provision Result is Appropriate
1961 UBC	—	0.54	—	Yes	—	—	—	—
ASCE 7-16	0.67	1.0	1.6	No	—	—	—	—
LSP	0.67	1.0	1.7[1]	Close	—	—	Not Permitted	—
	1.0	1.1	2.3[1]		—	—		—
NSP	0.67	0.4	---	No	Yes: 1.0 > 0.4	—	—	Conservative
	1.0	1.2			Close: 1.1 < 1.2	—	—	Yes
NDP	0.67	Fail[2]	—	No	—	No	—	Yes
	1.0	Fail[3]	—		—	No	—	Yes

(1) Moment Acceptance Ratio ignored for LSP, as it is due to low capacity from unreduced EQ tension.
(2) In six out of 11 motions, the piers reached an Acceptance Ratio of 1.0 failure in shear.
(3) In six out of 11 motions, the piers reached an Acceptance Ratio of 1.0 failure in shear.

Alternative Linear Procedure Limitation Provision Option Results: This case study result goes in the bin for LSP (almost) "OK," NDP "Not OK," and linear procedures not permitted. As the LSP is shown to be close to satisfying the performance objective and limitation provision is triggered, alternatives to the provision are explored.

- Revise weak story irregularity to strength only: The pier geometry and reinforcing are the same at each story, so the story strengths are all equal in both Patterns 1 and 2. This revision would thus eliminate the weak story irregularity and thus permit the LSP. Since the building fails the NDP, the revised provision would not lead to the desired result. This is not a good option.

- Increase DCR: In this option, the trigger for both Pattern 1 and Pattern 2 would still be the DCR exceeding the *m*-factor of 3 for Collapse Prevention at the S_{XS} = 1.0 level. Thus, increasing the DCR will not make any difference.

- Remove *m*-factor test: If the *m*-factor requirement were removed, but the DCR = 3.0 test was still required, then there would not be any difference, as the DCRs for the S_{XS} = 1.0 level exceed 3.0.

- Remove DCR = 3.0 test: In this option, the trigger for both Pattern 1 and Pattern 2 would still be the DCR exceeding the *m*-factor of 3.0 for Collapse Prevention at the S_{XS} = 1.0 level. Thus, removing the DCR = 3.0 test will not make any difference.

- Disproportionate DCR: For Pattern 1 at the S_{XS} = 0.67 level, the average shear DCRs for the third, second, and first stories are 1.0, 1.7, and 2.0. The average would be 1.6. The highest ratio would be 2.0/1.6 = 1.3 which is less than the proposed 1.5 threshold for the option. At the S_{XS} = 1.0 level, the highest ratio would be 1.3 as well. The same disproportionate ratios would apply for Pattern 2 at both hazard levels. Thus, this trigger would not be met, and the LSP would be permitted. Since the building fails the NDP, the revised provision would not lead to the desired result. This is not a good option.

- More conservative linear procedure AR: As the Acceptance Ratios for the LSP are at (or just above) the 1.0 threshold, reducing the AR limit for linear procedures to 0.75 would cause the LSP results to clearly fail. This would then match the NDP results, so this would be a possible option for this case.

- Combine a relaxed weak story irregularity criterion with a more conservative linear procedure Acceptance Ratio: The change in the ratio of the maximum story DCR to adjacent story DCR from 1.25 to 1.5 does not impact the results, since the value is 1.77 for this case study. Linear procedures would still not be permitted which is the appropriate result.

Conclusions:

- The alternative limitation provision options generally to not improve or change the situation for this case study, with the exception of applying a more conservative Acceptance Ratio limit.

- The case study is showing that the walls meet (or are close to meeting) the requirement for ASCE/SEI 7-16, but it fails the NDP requirements. This is a more concerning problem that needs further study.

Additional details of this case study are provided in Part 1, Appendix A, which can be found at http://femap2208.atcouncil.org/.

1.3.2.3 WORKING GROUP 1, NONLINEAR STEEL MOMENT FRAME CASE STUDY

Building Description: The case study building is four stories with a pre-Northridge Earthquake steel moment frame. It was designed to the 1985 Uniform Building Code (ICBO, 1985). It is located in San Francisco on Site Class D soil. The focus of the case study was to evaluate proposed changes to nonlinear modeling and acceptance criteria, but it can be used to help study the linear procedure limitation provisions as well. Figure 1-5 shows a 3-D view of the linear model. There is an offset in the building with a four-story portion of one end and a three-story portion at the other end. Information on this case study comes from Working Group 1, Nonlinear.

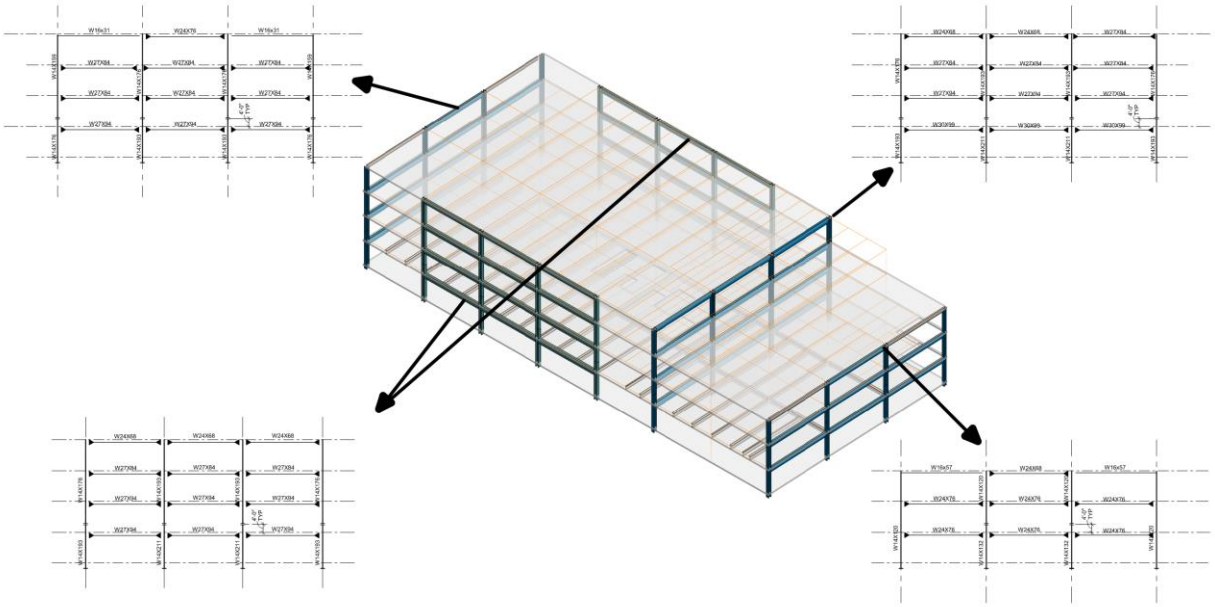

Figure 1-5 Working Group 1, Nonlinear steel moment frame linear model.

Seismic Demand and Structural Performance Levels: Analyses were run for the BSE-1E and BSE-1N Seismic Hazard Levels with the Life Safety Structural Performance Level and for the BSE-2E and BSE-2N Seismic Hazard Levels with the Collapse Prevention Structural Performance Level. Thus, the building was effectively evaluated for both the Basic Performance Objective for Existing Buildings (BPOE) and the Basic Performance Objective Equivalent to New Building Standards (BPON).

Analysis Procedures: LDP and NDP analyses were conducted. There were NDP runs for both ASCE/SEI 41-17 modeling and acceptance criteria lumped plasticity, and for proposed revisions based on ATC-114 (NIST, 2017a, b, c, d) for lumped plasticity and for fiber models. The focus here is on the ASCE/SEI 41-17 runs for comparison with the LDP analyses. The ASCE/SEI 41-17 NDP model included the gravity frame and the partially restrained connections created by the shear tab connections of the gravity columns and composite beams. Models were run with and without panel zone hinges.

Linear Procedure Limitation Provision Status: The building has a torsional strength irregularity as the DCR values on the three-story line are significant less than those at the opposite end on the four-story side. As Acceptance Ratios exceed 1.0, then DCRs are greater than the associated *m*-factor (κ is assumed to be 1.0), so the linear procedure limitation provision is triggered, and linear procedures are not permitted.

Analysis Results:

- Plots for the LDP run show maximum Acceptance Ratios between 1.0 and 1.5 for the BSE-1E and over 1.5 for the BSE-2E.

- For the NDP runs with panel zone hinges, panel zone hinging protected the beam-column connections. At the BSE-1E, maximum Acceptance Ratios for panel zones, columns, and beam-column connections were all below 1.0, but the column splices reach maximum Acceptance Ratios of over 2.0. At the BSE-2E, maximum Acceptance Ratios are between 1.0 and 1.5 for panel zones and columns and up to 2.0 for column splices.

- For the NDP runs without the panel zone hinges, at the BSE-1E, beam-column connections had maximum Acceptance Ratios between 0.75 and 1.0, and columns had maximum Acceptance Ratios between 1.0 and 1.5. At the BSE-2E, beam-column connections had maximum Acceptance Ratios between 1.0 and 1.5, and columns had maximum Acceptance Ratios over 1.5.

Alternative Linear Procedure Limitation Provision Option Results: This case study result goes in the bin for LDP "Not OK," NDP "Not OK," and linear procedures not permitted. As a result, the limitation provision is unnecessary, and alternatives were not investigated. A "permission clause" is proposed to be added to the limitation provision that says if Acceptance Ratios are greater than or equal to unity, then a nonlinear analysis is not required to state that the building does not meet the standard.

Conclusions: The results for the LDP were reasonably similar to the NDP. The case study highlighted the many subtleties of NDP modeling.

1.3.2.4 WORKING GROUP 1, NONLINEAR STEEL BRACED FRAME CASE STUDY

Building Description: The case study building uses steel braced frames, designed to the 1985 Uniform Building Code (ICBO, 1985). It is four stories at one end and three stories at the other end due to a grade change. It was damaged in the 1994 Northridge Earthquake. The case study was developed by the WG1 (Nonlinear) group to evaluate different approaches to nonlinear modeling and compare results against the damage in the earthquake. Figure 1-6 shows a 3-D view of the linear model. Information on this case study comes from Working Group 1, Nonlinear.

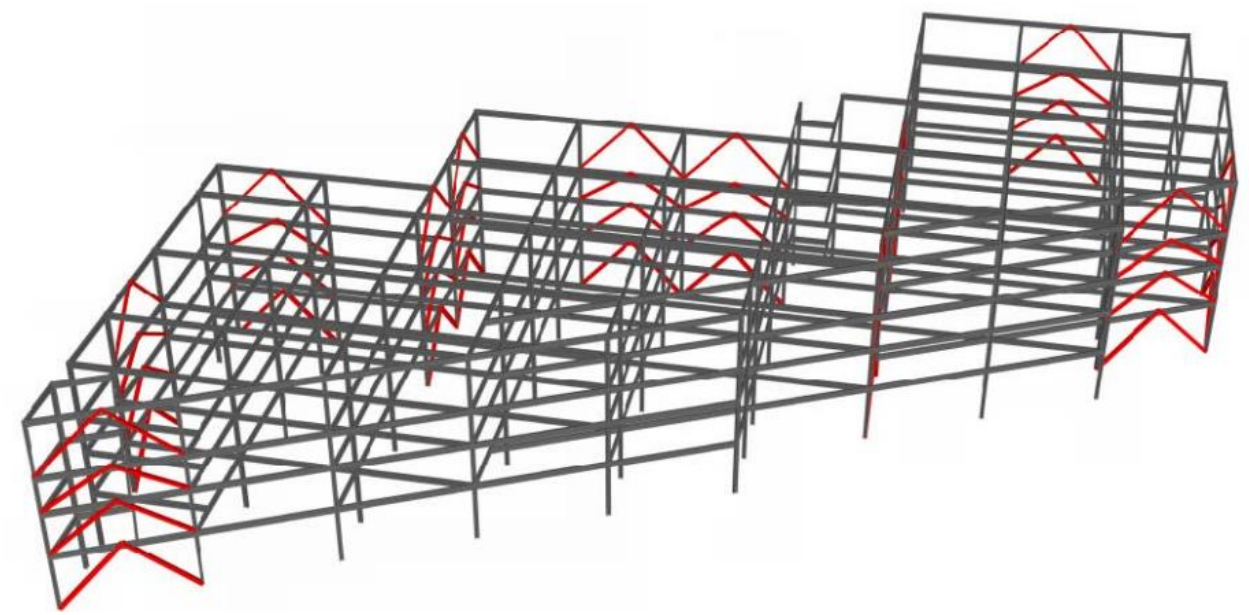

Figure 1-6 Working Group 1, Nonlinear braced frame linear model.

Seismic Demand and Structural Performance Levels: The building was evaluated at the BPOE and also using records from nearby sites in the 1994 Northridge Earthquake. For NDP runs, a suite of 11 ground motions were developed and scaled between a period range of 0.15-1.0 seconds.

Analysis Procedures: One linear and three different nonlinear NDP models were developed. All models had fixed base foundation boundary conditions. The linear model follows the provisions of ASCE/SEI 41-17. The first nonlinear model is per ASCE/SEI 41-17 with forced-controlled actions for the connections, and the chevron beam which was not designed to take unbalanced loading from the yielding tension and buckling compression braces. The second nonlinear model is per ASCE/SEI 41-17 but with brace-to-frame connections modeled with Type 3 behavior and chevron beams allowed to yield with hinges at midspan and the ends. The third nonlinear model uses ATC 114 / AISC 342 lumped plasticity modeling and acceptance criteria.

Linear Procedure Limitation Provision Status: The linear procedure limitation provision is triggered because there is a weak story irregularity and there are DCR values between 2 and 4 that exceed the lesser of 3.0 and the *m*-factor for the associated component action.

Analysis Results: In the linear model, the building does not meet the BPOE. Connection fracture governs. The second story is predicted to be the weakest story, and this matches earthquake damage observations. Maximum Acceptance Ratios for the braces are well over 1.0 and range from 3 to 4. Inclusion of the gravity frame and the partially restrained connections between the composite gravity beams and gravity columns did not affect the linear procedure results. In the NDP runs, there were local components that failed to meet the acceptance criteria.

Alternative Linear Procedure Limitation Provision Option Results: This case study result goes in the bin for LSP “Not OK,” NDP “Not OK,” and linear procedures not permitted. As a result, the limitation

provision is unnecessary, and alternatives were not investigated. A "permission clause" is proposed to be added to the limitation provision that says if Acceptance Ratios are greater than or equal to unity, then a nonlinear analysis is not required to state that the building does not meet the standard.

Conclusions: The case study highlighted many issues related to nonlinear modeling approaches for brittle connections and chevron beam configurations. To discern more meaningful differences between linear and NDP runs, reductions of the seismic demands would likely be needed.

1.3.2.5 WORKING GROUP 2 CANTILEVERED RCSW CASE STUDY

Building Description: The case study building is a 1920s five-story slab-column moment frame building founded on spread footings that is retrofit with cantilever shear walls. The focus was on foundation flexibility, but the case study also provides information on the limitation provisions. Information on the case study comes from Working Group 2. It is consistent with the case study of the same system discussed in Part 3 of this report. Figure 1-7 shows the foundation and first floor plan; Figure 1-8 shows a partial elevation of the central shear wall. The focus of the case story at the time of the report was on the central shear wall in the north-south direction.

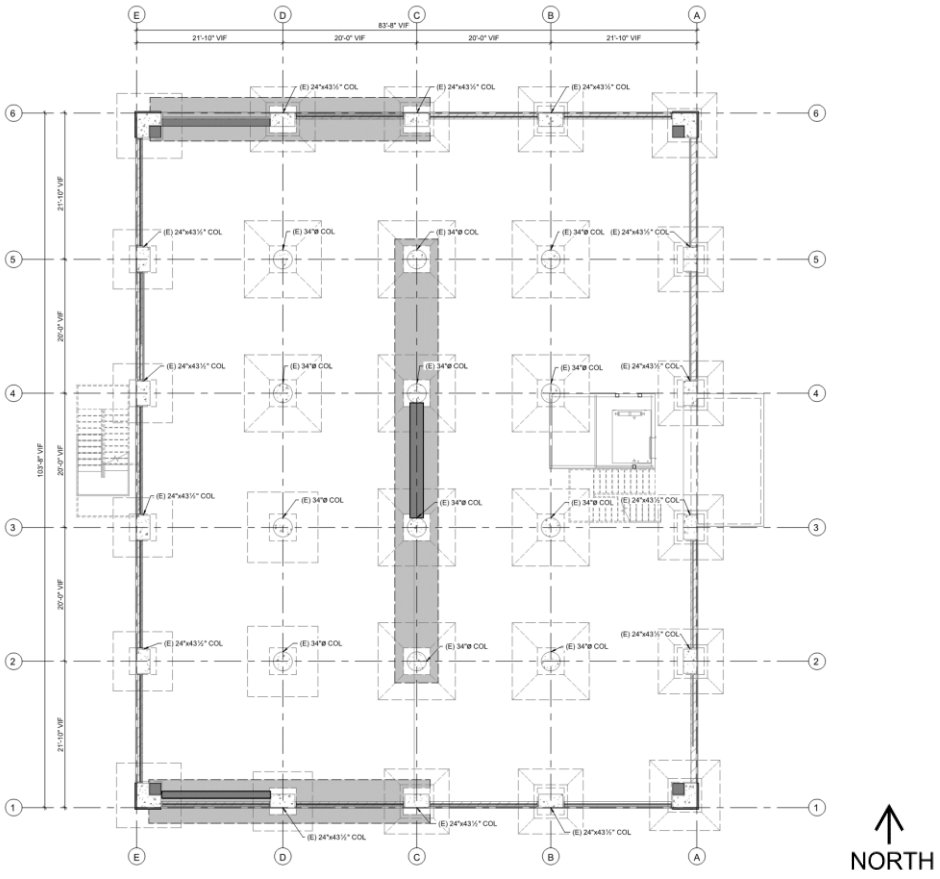

Figure 1-7 Working Group 2 cantilever shear wall building foundation and first floor plan.

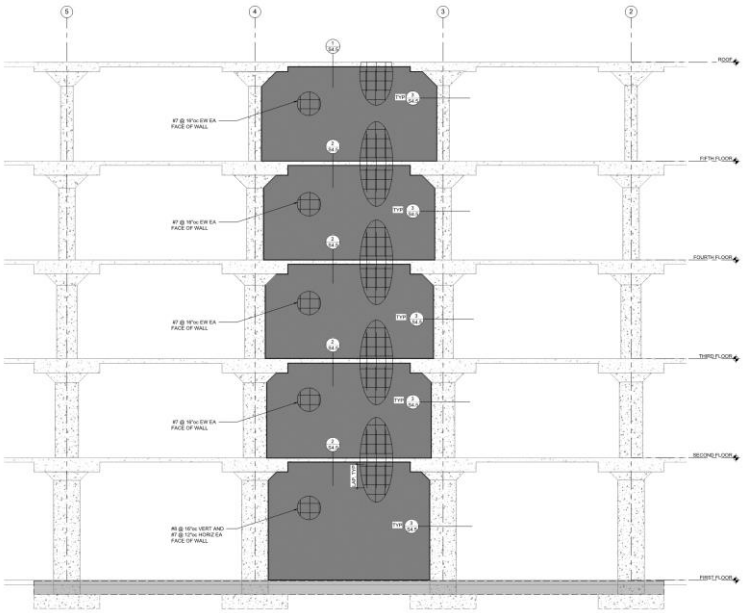

Figure 1-8 Working Group 2 cantilever shear wall partial elevation of central N-S shear wall. Only three of five bays are shown. The gray slab and shear wall were added in the retrofit.

Seismic Demand and Structural Performance Levels: Demands levels appear to use a value of S_{XS}=1.0 with the Collapse Prevention Structural Performance Level. ASCE/SEI 7-10 analyses were also done with S_a=1.0 and R=6.

Analysis Procedures: This case study includes LSP and NSP models. Five LSP variations and one NSP model were evaluated. For the LSP variations, the first was a fixed base model. The other four had a flexible base with different types of concentrated ASCE/SEI 41-17 Method 1 springs to represent foundation and soil flexibility. These include the straight ASCE/SEI 41-17 Method 1 springs with low and high stiffness bounds, and a variation on the low and high stiffness bounds using the K50 method in "Validation of ASCE 41-13 Modeling Parameters and Acceptance Criteria for Rocking Shallow Foundations" (by Hakhamaneshi et al. dated May 2016). For the NSP model, ASCE/SEI 41-17 Method 3 distributed springs were used.

Linear Procedure Limitation Provision Status: Using the retrofit shear wall's shear DCR values provided in the 6 May 2021 email, there is a weak story in all five LSP cases, as the 4th story DCR is more than 1.25 times the 5th story DCR. The ratios are fixed base case (1.83 DCR at 4th story/0.88 DCR at 5th story = 2.08); Method 1 lower bound springs case (1.46/0.60 = 2.43); Method 1 upper bound springs case (1.65/0.74 = 2.23); K50 lower bound springs case (1.25/0.44 = 2.84); and K50 upper bound springs case (1.40/0.55 = 2.55). For the fixed base case, the maximum DCR is always less than or equal to the lesser of 3 or the component *m*-factor. Thus, the linear procedure limitation provision is not triggered. For the flexible base cases, the DCR does exceed the lesser of 3 or the component *m*-factor in every case. For example, for the Method 1 lower bound springs case, the 4th story DCR for the existing slab in flexure is 4.37 which exceeds 3 and the *m*-factor of 3.14. Thus, the linear procedure limitation provision is triggered.

Analysis Results: For the LSP fixed base case, all Acceptance Ratios are at or below 1.0, with the largest at the first story shear wall at 1.00 and then 0.77 at the slab-to-column connection. For the LSP flexible base models, the shear wall Acceptance Ratios are all below 1.0, but the interior columns have Acceptance Ratios between 1.06 and 1.57 and the slabs have Acceptance Ratios between 0.95 and 1.89. In the NSP model, the wall remains elastic, but the slab-to-column connections have an Acceptance Ratio of 1.29.

Alternative Linear Procedure Limitation Provision Option Results: Based on the LSP *flexible base* model results vs. NSP model results, case study pairings go in the bin for LSP "Not OK," NSP "Not OK," and linear procedures not permitted. A "permission clause" is proposed to be added to the limitation provision that says if Acceptance Ratios are greater than or equal to unity, then a nonlinear analysis is not required to state that the building does not meet the standard.

However, based on the LSP *fixed base* model results vs. NSP model results, this case study pairing goes in the bin for LSP "OK," NSP "Not OK," and linear procedures permitted. As this is an inappropriate result, alternatives to the provision are explored.

- Revise weak story irregularity to strength only: Changing to a strength only criterion for the weak story would eliminate the weak story irregularity. The wall geometry is the same at every story and the shear reinforcing is larger at the lower three stories, so there are no stories with weaker capacities that the story above. Since the building fails the NSP, the revised provision would not lead to the desired result. This is not a good option.

- Increase DCR: The DCRs already are below the lesser of 3 and the associated *m*-factor of 3 for Collapse Prevention. Thus, increasing the DCR will not make any difference.

- Remove *m*-factor test: If the *m*-factor requirement were removed, but the DCR = 3.0 test was still required, then there would not be any difference, as the DCR are less than 3.0.

- Remove DCR = 3.0 test: The DCRs are already below the lesser of 3 and the associated *m*-factor of 3 for Collapse Prevention. Thus, removing the DCR = 3.0 test will not make any difference.

- Disproportionate DCR: The average story shear DCR for all five stories is 2.06, and the maximum is 2.79 at the 2nd story. Thus, maximum to average ratio is 2.79/2.06 = 1.35 which is below the proposed criterion of 1.5. Thus, a disproportionate DCR is not identified, and there would be no change in permitting linear procedures.

- More conservative linear procedure AR: As the maximum Acceptance Ratios for the LSP is 1.00, reducing it to 0.75 would mean the performance objective would not be met with the linear procedure which would match the NSP result. While this appears to lead to a desirable result, the more fundamental finding of the case study comparisons is incorporating foundation flexibility in the linear model and nonlinear model reduces demands on the shear wall, but the rocking increases demands on the columns and slab-to-column connection.

- *Combine a relaxed weak story irregularity criterion with a more conservative linear procedure Acceptance Ratio:* The change in the ratio of the maximum story DCR to adjacent story DCR from 1.25 to 1.5 does not impact the results, since the value is 2.08 for this case study. Reducing the requirement from AR < 1 to AR < 0.75 would trigger the provision since there are several Acceptance Ratios between 0.75 and 1.0. Thus, linear procedures would not be permitted which is the appropriate result.

Conclusions: The options using reduced Acceptance Ratios would lead to the desired result, but incorporating foundation flexibility even with simple springs in linear models leads to more realistic response and more consistency between linear and nonlinear results.

1.3.2.6 WORKING GROUP 3 SHEAR-CONTROLLED COMPONENT RCSW CASE STUDY

Building Description: The building considered is a seven-story, reinforced concrete (RC) structure designed in accordance with the 1964 Uniform Building Code and constructed in 1967. The lateral force resisting system consists of concrete wall piers and coupling beams located primarily at the perimeter of the building. The gravity system is a combination of the concrete bearing walls at the perimeter of the building, and a line of concrete columns at the center of the building. A plan view is included for a typical floor level in Figure 1-9 below. The focus of the case study was on evaluating proposed revisions the modeling and acceptance provisions for reinforced concrete elements controlled by shear, but the case study also provides some information on the limitation provisions.

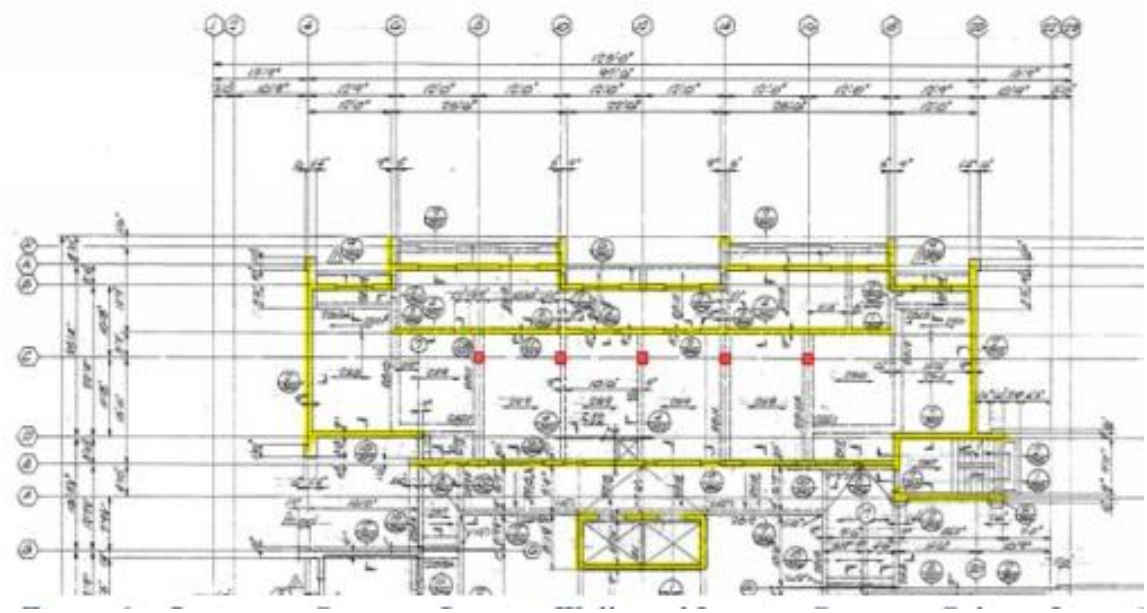

Figure 1-9 Working Group 3 shear wall first floor plan (red squares are the columns while the yellow shaded areas are the shear walls).

Seismic Demand and Structural Performance Levels: The BPOE was the performance objective. The building is located on Site Class C soil in southern California.

Analysis Procedures: This case study includes one LSP, three LDP, and two NSP models. One LDP model used ASCE/SEI 41-17 provisions as written; one revised the stiffness per proposed changes; and the third was done with revised linear modeling and acceptance criteria. Because the revised modeling and acceptance criteria are direction dependent for flanged walls, an LSP run was done. For the NSP, one model was done using provisions in ASCE/SEI 41-17, and the other used revised shear wall nonlinear modeling and acceptance criteria. The focus was on the revised shear wall modeling criteria, but the case study also provides information on the limitation provisions. For the discussion here, the runs using the provisions of ASCE/SEI 41-17 as written were used.

Linear Limitation Provision Status: For the LDP model with ASCE/SEI 41-17 provisions as written, the maximum reported shear wall in shear DCR / *m* (or Acceptance Ratio since $\kappa = 1.0$) is 1.5 at the BSE-2E seismic hazard level which is associated with the Collapse Prevention Structural Performance Level. The *m*-factor for shear walls in shear at the Collapse Prevention Level is 3.0. Thus, this means, the maximum DCR = *m* x (DCR / *m*) = 3 x 1.5 = 4.5. This of course exceeds the *m*- factor of 3 for Collapse Prevention. Whether there is a weak story irregularity or torsional strength irregularity is not reported. If there is one of these irregularities, coupled with the DCR exceeding the *m*- factor of 3, then the linear procedure limitation provision would be triggered. If there is no weak story or torsional strength irregularity, then the linear procedure limitation provision would not be triggered.

Analysis Results: For the ASCE/SEI 41-17 LDP run, the Acceptance Ratios exceed 1.2. This is shown in Figure 1-10. The highest value as noted above is 1.5. For the ASCE/SEI 41-17 NSP run, the maximum Acceptance Ratio is 0.78.

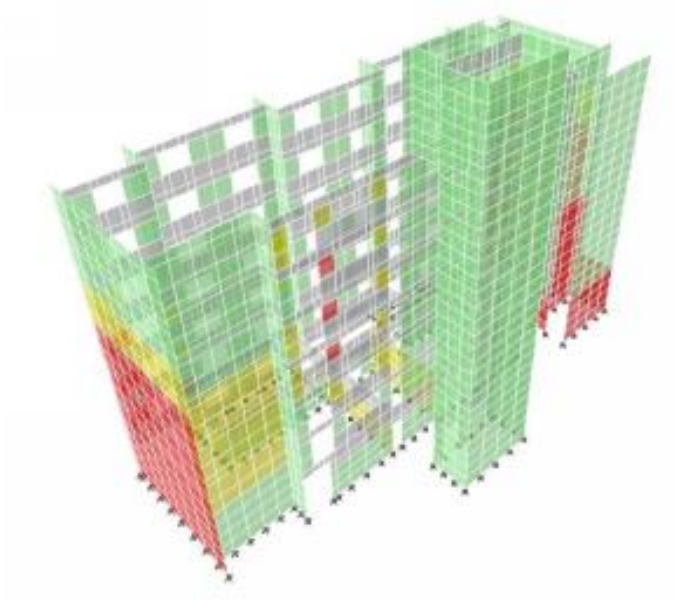

Figure 1-10 Working Group 3 shear wall 3D model (colors are the DCRs for shear in the shear walls at the BSE-2E level). Even though the legend uses "DCR," the values reported are not for the ASCE/SEI 41-17 Section 7.3.1.1 definition of DCR. The values represent the traditional definition in the standard of practice, so they are Acceptance Ratios as defined in this chapter. DCR key: green (less than or equal to 1.0); yellow (greater than 1.0 and less than 1.2); red (greater or equal to 1.2).

Alternative Linear Procedure Limitation Provision Option Results: Based on the LDP model results vs. NSP model results, case study pairings go in the bin for LDP "Not OK," NSP "OK," and linear procedures either permitted (if there is no weak story or torsional strength irregularity) or in the bin for not permitted (if there is a weak story or torsional strength irregularity). The implications of each scenario are discussed below.

- Assuming there is no weak story or torsional strength irregularity: In this case, the linear procedures would be permitted, and they would conservative since the LDP shows the performance objective is not met, but the building passes with the NSP. The linear procedure limitation clause is not relevant, and revisions do not need to be explored.

- Assuming there is a weak story or torsional strength irregularity: In this case, the linear procedures would not be permitted. Since the LDP shows the performance objective is not met, the linear procedure limitation provision is not providing any protection against an inappropriate conclusion. While the designer would be able to use the NSP procedure, forcing them into it does not seem fair. A "permission clause" is proposed to be added to the limitation provision that says if Acceptance Ratios are greater than or equal to unity, then a nonlinear analysis is not required to state that the building does not meet the standard. Since the building did pass the NSP, it is interesting to explore the alternative linear procedure limitation options to see how they apply to this case.

- Revise weak story irregularity to strength only: Since details on story strength were not reported, it is not possible to discuss this option.

- Increase DCR: The DCR threshold would have to rise to over 4.5 in this case to avoid the linear procedure limitation trigger. This may be unconservative for other buildings.

- Remove *m*-factor test: If the *m*-factor requirement were removed, but the DCR = 3.0 test was still required, then there would not be any difference, as the maximum DCR at 4.5 is already over the DCR = 3.0 threshold.

- Remove DCR = 3.0 test: The DCRs are already above the associated *m*-factor of 3 for Collapse Prevention. Thus, removing the DCR = 3.0 test will not make any difference.

- Disproportionate DCR: The details of DCR distribution are not reported by story. Figure 1- 10 shows there are concentrated locations. Qualitatively, it is likely that use of disproportionate DCR might trigger a linear procedure limitation.

- More conservative linear procedure AR: As the maximum Acceptance Ratio for the LDP is 1.5, reducing the linear procedure limitation threshold to 0.75 would not have any effect; it would still be exceeded.

- Combine a relaxed weak story irregularity criterion with a more conservative linear procedure Acceptance Ratio: This would not have any effect either, since the Acceptance Ratios already exceed the threshold.

Conclusions:

- *Assuming there is no weak story or torsional strength irregularity*: In this case, the linear procedures would be permitted, and they would conservative since the LDP shows the performance objective is not met, but the building passes with the NSP. The linear procedure limitation clause is not relevant.

- *If there is a weak story or torsional strength irregularity:* In this case, the linear procedures would not be permitted. Since the LDP shows the performance objective is not met, the linear procedure limitation provision is not providing any protection against an inappropriate conclusion. While the designer would be able to use the NSP procedure, forcing them into it does not seem fair. A "permission clause" is proposed to be added to the limitation provision that says if Acceptance Ratios are greater than or equal to unity, then a nonlinear analysis is not required to state that the building does not meet the standard. Alternative linear procedure limitation options either do not apply or might be unconservative or other buildings.

1.3.3 FEMA P-2006 Design Example Summaries and Findings

1.3.3.1 PRE-NORTHRIDGE STEEL MOMENT FRAME DESIGN EXAMPLE

Building Description: The design example building is five stories with a perimeter pre-Northridge Earthquake steel moment frame. It was designed to the 1982 Uniform Building Code (ICBO, 1982). Figure 1-11 shows a 3-D view of the linear model.

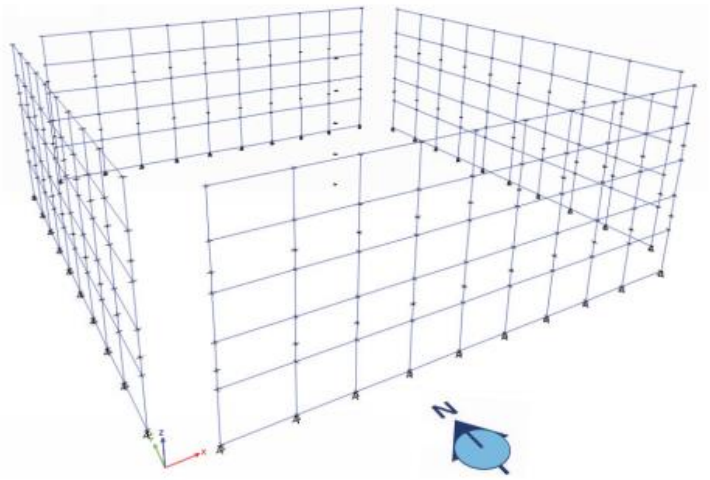

Figure 1-11 FEMA P-2006 steel moment frame linear model.

Seismic Demand and Structural Performance Levels: This building was evaluated using the BPOE. As it is a Risk Category II building and was evaluated at the Tier 2 level, per ASCE/SEI 41-13, only one evaluation level is required, which is the BSE-1E Seismic Hazard Level and the Life Safety Structural Performance Level. The BSE-1E spectral accelerations are S_{XS} = 1.096 and S_{X1} = 0.337. In ASCE/SEI 41-17, this check would be made at the BSE-2E Seismic Hazard Level and the Collapse Prevention Structural Performance Level.

Analysis Procedures: LSP, LDP, and NSP analyses were conducted.

Linear Procedure Limitation Provision Status: The governing DCR_{max} is 2.20, and the associated *m*-factor is 1.43. Thus, the DCR_{max} exceeds to the lesser of 3 and the *m*-factor. However, there is no weak story irregularity or torsional strength irregularity, so the linear analysis limitation provision is not triggered, and linear provisions are permitted.

Analysis Results: In the LSP, the beams are adequate, but the beam-column connections fail, with a maximum Acceptance Ratio of 1.53. The beam-column connections exceed an Acceptance Ratio of 1.0 at all levels, except the roof. The maximum column flexural Acceptance Ratio is 1.31 for the end columns; interior columns have ratios below 1.0. In the LDP, the Acceptance Ratios reduce to 1.25 for the beam-column connections and 0.90 for the columns. In the NSP, only the beam-column connections at the second floor have Acceptance Ratios over 1.0.

Alternative Linear Procedure Limitation Provision Option Results: This case study result goes in the bin for LSP/LDP "Not OK," NSP "Not OK," and linear procedures permitted. As a result, the limitation provision is not inappropriate, and alternatives were not investigated.

Conclusions: The lack of a linear procedure limitation trigger for this example is not inappropriate, since the linear procedure results are similar to the NSP results. A need to change the procedure is not identified.

1.3.3.2 STEEL BRACED FRAME DESIGN EXAMPLE

Building Description: The design example building is a three-story 1980s ordinary steel braced frame in Charlotte, North Carolina. Figure 1-12 and Figure 1-13 show a 3-D image and a typical floor plan.

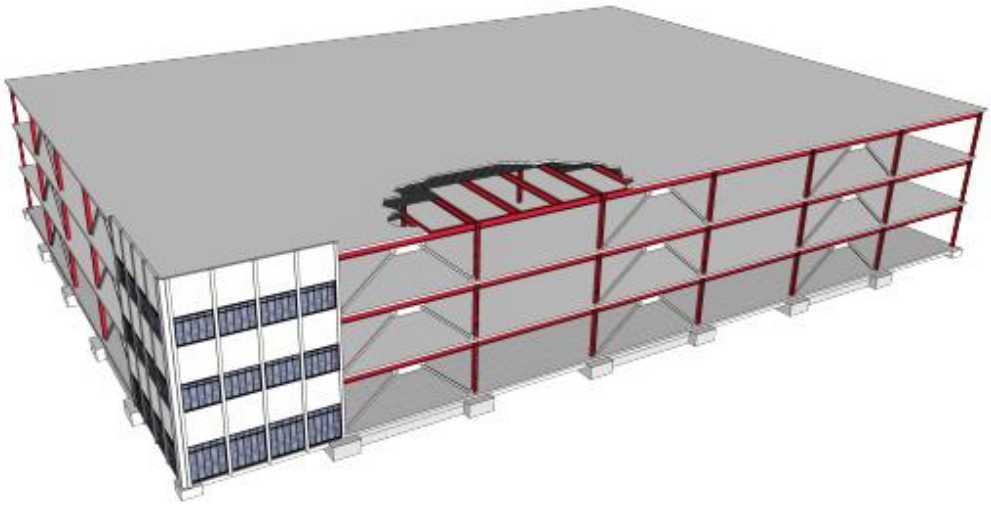

Figure 1-12 FEMA P-2006 steel braced frame design example building.

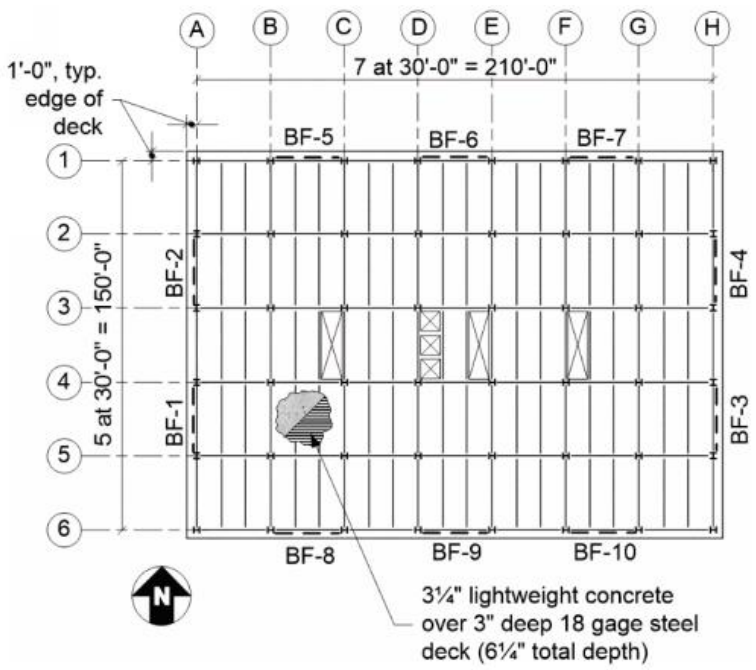

Figure 1-13 FEMA P-2006 steel braced frame design example typical floor.

Seismic Demand and Structural Performance Levels: This building was evaluated using an enhanced performance objective which is the Immediate Occupancy Structural Performance Level with the BSE-1N Seismic Hazard Level. The BSE-1N spectral accelerations are $S_{XS} = 0.26$ and $S_{X1} = 0.16$.

Analysis Procedures: LSP and NSP analyses were conducted. The LSP model assumed a fixed base. For the NSP, two models were used—one with a fixed base and one with vertical springs to account for foundation flexibility.

Linear Procedure Limitation Provision Status: The governing $DCR_{max} = 4.87$ and the associated *m*-factor is effectively 1.0, as the component action of beam compression is force-controlled. Thus, the DCR_{max} exceeds to the lesser of 3 and the *m*-factor. The ratio of the average shear DCR at the second story to the third story is 1.76/1.08 = 1.63. As this exceeds 1.25, there is a weak story irregularity, so the linear analysis limitation provision is triggered, and linear procedures are not permitted.

Analysis Results: In the LSP fixed base case, the braces, beams, and brace connections all have Acceptance Ratios over 1.0, with the braces in compression at 2.24, beams in combined axial compression and bending at 4.87, and brace-to-gusset welds against brace tension at 1.30. In the NSP run with the fixed base, the braces have Acceptance Ratios well over 1.0, but in the flexible base model, the brace frames rock, and Acceptance Ratios are below 1.0.

Alternative Linear Procedure Limitation Provision Option Results: For the rigid base model, the bin is LSP "Not OK," NSP "Not OK," and linear procedures not permitted. As the limitation provision is unnecessary, alternatives to the provision are not explored. A "permission clause" is proposed to be

added to the limitation provision that says if Acceptance Ratios are greater than or equal to unity, then a nonlinear analysis is not required to state that the building does not meet the standard. For the flexible base model, a conclusion cannot be drawn without a parallel LSP flexible base to go with the NSP flexible base.

Conclusions

- There is no need to change the provision in the fixed base case.
- In the flexible base case, and LSP evaluation with springs would be needed to evaluate the provision and alternatives.

1.3.3.3 CONCRETE SHEAR WALL DESIGN EXAMPLE

Building Description: The design example building is a three-story 1950s concrete shear wall building in Seattle. It has a full basement. Figure 1-14 shows a 3-D image, and Figure 1-15 shows a typical floor plan.

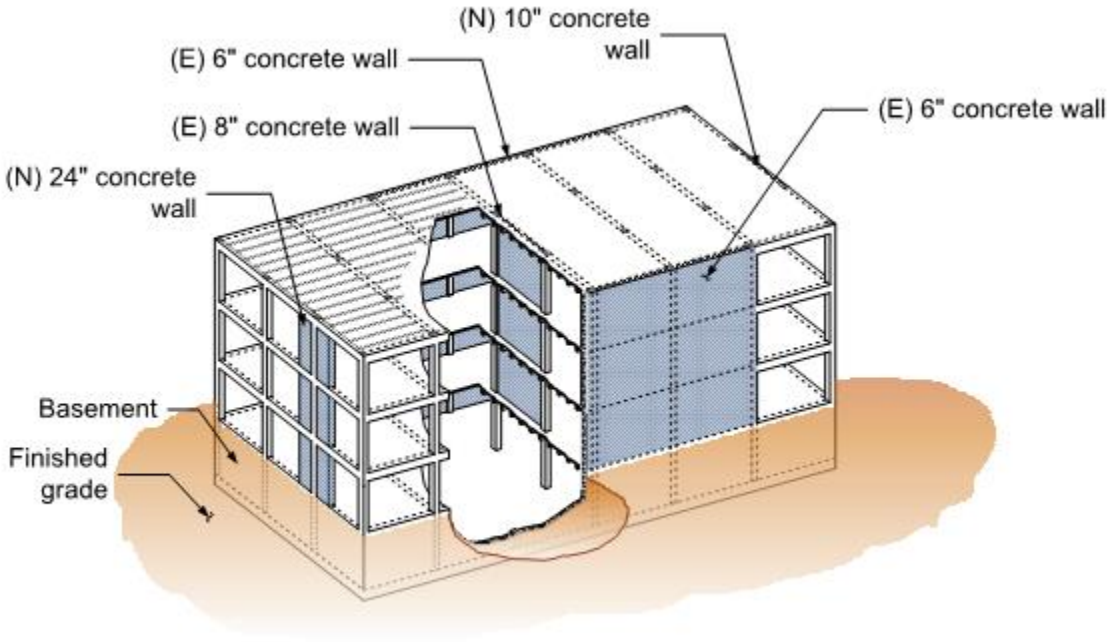

Figure 1-14 FEMA P-2006 concrete shear wall design example building.

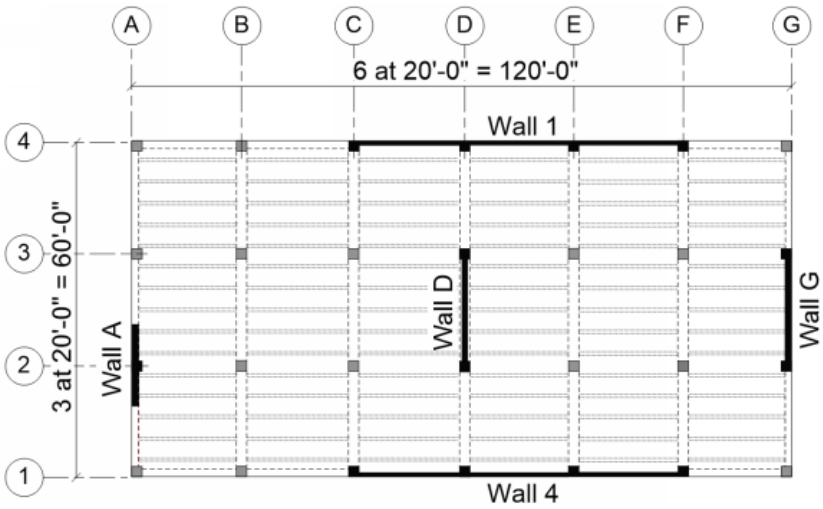

Figure 1-15 FEMA P-2006 concrete shear wall design example typical floor.

Seismic Demand and Structural Performance Levels: This building was evaluated for the BPOE. The BSE-1E spectral accelerations are S_{XS} = 0.69 and S_{X1} = 0.38. The BSE-2E spectral accelerations are S_{XS} = 1.08 and S_{X1} = 0.62.

Analysis Procedures: LSP and NSP analyses were conducted. The LSP model assumed a fixed base. For the NSP, two models were used—one with a fixed base and one with vertical springs to account for foundation flexibility.

Linear Procedure Limitation Provision Status: For the BSE-2E level, the governing DCR_{max} = 4.56 for foundation overturning, and there is a DCR = 3.74 for shear wall flexure on Gridline A at the first story, and then 1.61 for the Gridline 1 and 4 shear walls at the first story. The associated *m*- factors are 4 for foundation overturning, 6 for the shear wall in flexure, and effectively 1.0 for the Gridline 1 and Gridline 4 shear walls, as the walls are force-controlled because their reinforcing ratio is too low. Thus, the DCR_{max} exceeds to the lesser of 3 and the *m*-factor, in all of these cases. The shear capacities in the shear walls at each story are the same, and ratio of the average shear DCR at the third, second, and first stories can be calculated from the Table 10-10 demands as 1.63 x (991 k / 2,477 k) = 0.65, 1.63 x (1,981 k / 2,477 k) = 1.31, and 1.63, respectively. The ratio of second story to the third story is 1.31/0.65 = 2.0. As this exceeds 1.25, there is a weak story irregularity, so the linear analysis limitation provision is triggered, and linear procedures are not permitted. At the BSE- 1E level, the DCR_{max} = 1.05 which is just over the *m* = 1.0 value, so linear procedures are not permitted either (barely).

Analysis Results: In the LSP, at the BSE-1E level, the Gridline 1 and 4 walls have the maximum Acceptance Ratio of 1.16, which is over 1.0. At the BSE-2E level, the maximum Acceptance Ratio rises to 1.81. In the NSP run with the fixed base, the maximum Acceptance Ratios drop to 0.78 for the BSE-1E and 0.93 for the BSE-2E.

Alternative Linear Procedure Limitation Provision Option Results: This case study result goes in the bin for LSP "Not OK," NSP "OK," and linear procedures not permitted. As a result, limitation provision alternatives were investigated.

- Revise weak story irregularity to strength only: The wall geometry, shear reinforcing, and shear capacities are the same at all stories, so the weak story irregularity would be eliminated, and linear procedures would be permitted. In theory, this could be appropriate, since the LSP result would be conservative.

- Increase DCR: All of the governing *m*-factors are effectively 1.0 as they are from force- controlled actions. The *m*-factors are thus the trigger, and increasing the DCR will not make any difference.

- Remove *m*-factor test: If the *m*-factor requirement were removed, the DCR_{max} = 4.56 and next lowest DCR at 3.75 would exceed the DCR = 3.0 test, so there would be no difference.

- Remove DCR = 3.0 test: If the DCR = 3.0 test was removed, the *m*-factor test would still govern for many actions which have DCRs greater than their associated *m*=1 values. The *m*-factors are thus the trigger, and increasing the DCR will not make any difference.

- Disproportionate DCR: The shear wall DCRs for the third, second, and first stories are 0.65, 1.31, and 1.63, as noted above. The average is 1.20. The highest ratio is 1.63/1.20 = 1.36 which is less than the proposed 1.5 threshold for the option. Thus, this trigger would not be met, and the LSP would be permitted. In theory, this could be appropriate, since the LSP result would be conservative.

- More conservative linear procedure AR: The Acceptance Ratios for the LSP are above the 1.0 threshold, and reducing the AR limit for linear procedures to 0.75 would not change the result. They would need to be reduced to (1/1.81) = 0.55 to cause a change. This is too severe, and so this is not a good option.

- Combine a relaxed weak story irregularity criterion with a more conservative linear procedure Acceptance Ratio: The change in the ratio of the maximum story DCR to adjacent story DCR from 1.25 to 1.5 does not impact the results, since the value is 2.0 for this case study. Reducing the requirement from AR < 1 to AR < 0.75 would not make any difference since the Acceptance Ratios are already well over 1.0. Thus, option does not change the result.

Conclusions: Two of the options would permit use of the linear procedures, as the linear procedure would give a conservative result, indicating that the building does not meet the performance objective when the NSP shows that it does.

1.3.4 Review of Research Studies

1.3.4.1 FEMA P-2012

FEMA P-2012 evaluated the impact of configuration irregularities on collapse potential. FEMA P695 (FEMA, 2012) analyses were used to compare the effect of building without and with varying degrees of different irregularities to determine if refinements in code requirements and analytical practices are warranted. Studies included both the weak story irregularity and the torsional strength irregularity.

For the weak story irregularity, a set of four-story ordinary reinforced concrete moment frames and a set of eight-story, 12-story, and 20-story special reinforced concrete moment buildings were studied. Weak stories that are 0.6 and 0.8 times the story above were located at different elevations. Significant reductions in the collapse potential from weak story irregularities were not observed. The study found:

- *The soft/weak archetypes in this study differ from many of the soft/weak story buildings for which poor performance has been observed in past earthquakes because many of those buildings had a story that was too soft/weak to meet current code requirements.*

- *Soft/weak story irregularities do not appear to pose a problem in code-conforming moment frame buildings. This is partially because, as long as the building is code-conforming, "weak story" really means "strong adjacent stories"; the "weak" story still must be strong enough to resist the design lateral force demand per code requirements.*

- *It is reasonable to think that the expected collapse performance may decline when the weak story causes the damage distribution over height to change from several stories to just one or two, as has been observed in the poor seismic performance of non-current-code-conforming soft/weak story buildings in past earthquakes. However, in this study of code-conforming irregular buildings, such a reduction in collapse resistant is not observed; rather, the negative effects of having more concentrated damage are offset by the positive effects of having strengthened members in the adjacent stories.*

Thus, it is not really possible to draw conclusions from FEMA P-2012 regarding the weak story irregularity for non-code conforming buildings.

For the torsional strength irregularity, 12-story reinforced concrete moment frames and two-story wood shear wall buildings were evaluated. A number of recommendations were made regarding revisions to torsion requirements in ASCE/SEI 7, most of which move in the direction of relaxing the code requirements. ASCE/SEI 7 and ASCE/SEI 41 define torsional irregularities differently, with ASCE/SEI 7 focusing on ratios of displacement from rotational vs. translation and ASCE/SEI 41- 17 focusing on torsional strength imbalances. The study found "that special treatment of buildings with 'torsional strength irregularity,' as defined by demand/capacity ratios in ASCE/SEI 41, is not necessary for new building design."

Again, because the focus of the assessment was on case study buildings that were otherwise code compliant, it is difficult to draw conclusions from FEMA P-2012 regarding the torsional strength irregularity for non-code conforming buildings, and a case study with was not pursued.

1.3.4.2 FEMA P-807

FEMA P-807 is a methodology to evaluate and retrofit multi-unit wood frame buildings with weak first stories, such as those with tuck under parking. As the Foreword notes:

> *These seismic retrofitting guidelines are the first to focus solely on the weak first story and to provide just enough additional strength to protect the first floor from collapse but not so much as to drive earthquake forces into the upper stories, placing them at risk of collapse. They are also the first to take into account the strength provided by existing non-structural walls.*

The methodology was based on a rigorous application of Incremental Dynamic Analysis using the FEMA P695 suite of records to a series of archetypes. By determining parameters such as the ratio of first story to second story strength and the strength of the second story with respect to the demand, equations can be used to determine the probability of the onset of strength loss with and without retrofit.

While there is substantial thoughtful analytical work, the underlying method is based on nonlinear force-displacement relationships. There is no direct comparison of linear and nonlinear analyses and when linear results could be misleading. As such, there does not appear to be a clear way to apply the FEMA P-807 findings without further case study work. For example, a case study wood building could be evaluated using ASCE/SEI 41-17 linear procedures and then analyzed using FEMA P-807. A correlation would need to be established between a FEMA P-807 probability of exceedance and an ASCE/SEI 41-17 performance objective. As FEMA P-807 Section 2.3.3 notes:

> *With a drift limit probability of exceedance (POE) of 20 percent, the Guidelines default objective is expected to be similar to an [ASCE 41-06 (ASCE, 2007)] objective of "Collapse Prevention in a BSE-2 event." No correlation or performance equivalence studies between the Guidelines and "Collapse Prevention in a BSE-2 event," however, have been made as part of the effort to develop these Guidelines.*

The BSE-2 event referenced from ASCE/SEI 41-06 is one with a 2% probability of exceedance in 50 years.

The potential FEMA P-807 case study with was not pursued given project resources.

1.3.4.3 FEMA 440

The focus of FEMA 440 is on improving the nonlinear static procedures. The linear procedure limitation provision is not discussed. However, in FEMA 440 Section 2.3, there is this statement, which provides some insight into the concerns with linear procedures.

The primary decision is whether to choose inelastic procedures over more conventional linear elastic analysis. In general, linear procedures are applicable when the structure is expected to remain nearly elastic for the level of ground motion of interest or when the design results in nearly uniform distribution of nonlinear response throughout the structure. In these cases, the level of uncertainty associated with linear procedures is relatively low. As the performance objective of the structure implies greater inelastic demands, the uncertainty with linear procedures increases to a point that requires a high level of conservatism in demand assumptions and/or acceptability criteria to avoid unintended performance. Inelastic procedures facilitate a better understanding of actual performance. This can lead to a design that focuses upon the critical aspects of the building, leading to more reliable and efficient solutions.

1.3.5 Evolution of the Linear Procedure Limitation Provision

The history of the evolution of the linear procedure limitation provision is summarized below. First, the evaluation-only methodologies are discussed, then the rehabilitation/retrofit methodologies, and finally the merged methodologies that cover both evaluation and retrofit in one standard, beginning with ASCE/SEI 41-13.

1.3.5.1 EARLY EVALUATION-ONLY METHODOLOGIES

The development of ASCE/SEI 41-17 can be traced back to ATC-14. ATC-14 contained one analytical procedure, the equivalent lateral force procedure. It was based on ATC-3-06 (ATC, 1978, 1984) and was similar to the provisions in the 1985 SEAOC Bluebook (SEAOC, 1985). It was a working stress procedure using R_w factors, allowable stress design, and capacity over demand (C/D) ratios to account for a lack of modern detailing. It was not intended for retrofit, and there were no limitation provisions.

ATC-14 was followed by FEMA 178. "FEMA 178 used an analysis procedure based on the *1988 NEHRP Provisions* [FEMA, 1988] equivalent lateral force procedure using *R* factors and ultimate strength design. Nonconforming structural systems that did not have proper detailing were assigned lower *R* factors to account for their lack of ductility (ASCE, 2002)."

FEMA 178 was followed by FEMA 310, ASCE 31-02, and then ASCE 31-03. The analysis procedures in FEMA 310 are similar to ASCE 31-02/ASCE 31-03. The commentary noted above in ASCE 31-02 is the same in FEMA 310. ASCE 31-02 contains the four analysis procedures: LSP, LDP, NSP, and NDP. It does not have a limitation provision on the linear procedures, but there is a commentary that notes: "The linear procedures represent a rough approximation of the nonlinear behavior of the actual structure and ignore redistribution of forces and other nonlinear effects. In certain cases, alternative acceptable approaches are presented that may provide wide variation in the results. This is expected, considering the limitations of the linear analysis procedures." ASCE 31-03 was similar to ASCE 31-02.

1.3.5.2 FEMA 273/274

FEMA 273 was the first of the performance-based seismic design documents to focus on seismic rehabilitation, and it contains the four current analysis procedures: LSP, LDP, NSP, and NDP. It was the first of the documents reviewed here to have a limitation provision for linear analyses, which is in its Section 2.9.1.1. Linear procedures are not permitted if there are DCRs greater than 2.0, and there was any of the following irregularities: in-plane discontinuity (unless it is checked as force-controlled with $J = 1.0$), out-of-plane discontinuity (unless it is checked as force-controlled with $J = 1.0$), severe weak story irregularity (defined the same as ASCE/SEI 41-17), or a severe torsional strength irregularity (defined the same as ASCE/SEI 41-17).

FEMA 274 provides a general commentary on the applicability of the linear procedures, stating that:

> *[L]inear procedures, while easy to apply to most structures, are most applicable to buildings that actually have sufficient strength to remain nearly elastic when subjected to design earthquake demands, and buildings with regular geometries and distributions of stiffness and mass… Buildings that have relatively limited inelastic demands under a design earthquake may be evaluated with sufficient accuracy by linear procedures, regardless of their configuration. If the largest component DCR calculated for a structure does not exceed 2.0, the structure may be deemed to fall into this category.*

1.3.5.3 FEMA 356

FEMA 356 contains a linear limitation provision in its Section 2.4.1.1. It is the same as the provision in FEMA 273, except that the option of using a $J = 1.0$ factor was removed. The commentary is significantly abbreviated from that of FEMA 274 (like much of the rest of FEMA 356), so the rationale for the provision was effectively removed.

1.3.5.4 ASCE/SEI 41-06

ASCE/SEI 41-06 contains a linear limitation provision in its Section 2.4.1.1. It is the same as the provision in FEMA 356, and the commentary (or lack of commentary) is the same as well. A note appears later in ASCE/SEI 41-06 commentary Section C3.2.1 that says "linear procedures are appropriate where the expected level of nonlinearity is low. This is measured by component demand capacity ratios (DCRs) of less than 2.0."

1.3.5.5 ASCE/SEI 41-13

ASCE/SEI 41-13 merged the evaluation focus from ASCE 31-03 and the rehabilitation focus from ASCE/SEI 41-06. The same four analysis procedures—LSP, LDP, NSP, and NDP—are included. ASCE/SEI 41-06 contains a linear limitation provision in its Section 7.3.1.1. It is the same as the ASCE/SEI 41-17 provision. The commentary provides no discussion about the rationale for the provision or about the notable change to a less conservative approach by raising the DCR threshold to the lesser of 3.0 and the *m*-factor for the component action and eliminating the triggers with the in-plane discontinuity irregularity and out-of-plane discontinuity irregularity.

1.3.6 Observations on Possible Alternative Linear Procedure Limitation Provision Options

Case study results evaluating the possible quantitative alternative linear procedure limitation provision options are summarized in Table 1-9.

Table 1-9 Comparison of Possible Alternative Linear Procedure Limitation Provision Options

Case Study[1]	Possible Alternative Linear Procedure Limitation Provision Option							
	Reason to study?	Revise weak story definition	Increase DCR	Remove *m*-factor test	Remove DCR=3.0 test	Disproportionate DCR	Reduce Acceptance Ratio	Relax weak story and reduce AR
WG1 RCSW S_{XS}=1.0 and 1.5	No	—	—	—	—	—	—	—
WG1 RCSW S_{XS}=0.67 and 1.0	Yes	Not good	No impact	No impact	No impact	Not good	Possible	Possible
WG1 SMF	No	—	—	—	—	—	—	—
WG1 OBF	No	—	—	—	—	—	—	—
WG2 RCSW Fixed Base	Yes	Not good	No impact	No impact	No impact	No impact	Possible	Possible
WG2 RCSW Flexible Base	No	—	—	—	—	—	—	—
WG3 RCSW – no irregularity[2]	No	—	—	—	—	—	—	—
WG3 RCSW – with irregularity[2]	Yes	Unknown	Not good	No impact	No impact	Unknown	No impact	No impact
FEMA P-2006 SMF	No	—	—	—	—	—	—	—
FEMA P-2006 OBF Fixed Base	No	—	—	—	—	—	—	—
FEMA P-2006 RCSW	Yes	Conserv-ative	No impact	No impact	No impact	Conserv-ative	Not good	No impact

(1) WG1, WG2 and WG3 refer to Working Group 1, Working Group 2, and Working Group 3, respectively.
(2) See Section 1.3.2.6 for discussion on the WG3 RCSW case study permutations for with and without a weak story or torsional strength irregularity.

In general, the summary shows that none of the alternatives is clearly preferable in all of the case studies, and some generally lead to undesirable results, such as permitting a linear procedure when the linear procedure would show the building meeting the performance objective, but the nonlinear procedure shows it does not meet the performance objective.

Likelihood of trigger: The trigger can only be met if the DCR exceeds the lesser of 3.0 and the *m*-factor for the component action. For many situations, this trigger will be met only when Acceptance Ratios exceed 1.0, and thus the building would not meet the performance objective anyway. For example, with concrete walls and piers in shear, the *m*-factor at the Life Safety Structural Performance Level is 2.5 for low axial loads and 2.0 for high axial loads. At the Collapse Prevention Performance Level, the *m*-factor is 3.0 for both low axial loads and high axial loads. Start with the Collapse Prevention Level. If $\kappa = 1.0$, and the DCR = 3.1, then the Acceptance Ratio is $3.1/(1.0 \times 3.0) = 1.03 > 1.0$, so the performance objective is not met. The limitation provision would be triggered since DCR = 3.1 > 3 and $m = 3$. On the other hand, if the DCR is 2.9, then the Acceptance Ratio is $2.9/3.0 = 0.97 < 1.0$, so the performance objective is met, and the limitation provision is not triggered since DCR = 2.9 < 3 and $m=3$. At the Life Safety Level with a low axial stress pier, with DCR = 2.6, then the Acceptance Ratio would be $2.6/2.5 = 1.04 > 1.0$, so the performance objective is not met. The limitation provision would be triggered since DCR = 2.6 > lesser of $m = 2.5$ and 3.0. On the other hand, if the DCR is 2.4, then the Acceptance Ratio is $2.4/2.5 = 0.96 < 1.0$, so the performance objective is met, and the limitation provision is not triggered since DCR = 2.4 < 2.5 < 3.0. This pattern covers all force-controlled actions with an effective *m*-factor of 1.0 and many other component actions.

Exempt select model building types: A final alternative considered is to exempt select model building types. Some are effectively already exempt. One-story buildings cannot have a weak story irregularity. Flexible diaphragm buildings cannot have a torsional strength irregularity. Thus, one-story buildings with flexible diaphragms cannot trigger the linear limitation provision. As a result, one-story PC1 tilt-up buildings, one-story W1 and W2 wood frame buildings, and S3 metal building frames are effectively exempt from the provision.

The multi-story wood frame building situation is more complicated. One way to approach it is to redefine the weak story definition. The definition of “weak story” in ASCE/SEI 41-17 Section 7.3.1.1.3 is when the ratio of the average shear DCR for elements in any story to the average DCR of an adjacent story exceeds 1.25. By comparison, in ASCE/SEI 7-16 (ASCE, 2017), the weak story definition is where the “story lateral strength is less than 80% of the story above,” and the extreme weak story is where “the story lateral strength is less than 65% of the story above.” Thus, the standard compares DCRs, but ASCE/SEI 7-16 compares only strength. An example is a wood framed building that has a uniform layout of shear walls at each story. Per ASCE/SEI 7-16, the building would not have a weak story since the strength would be equal at each story. Per the standard, though, since the story shears increase at lower levels of the building, the DCRs increase as well, and it is common for the 1.25 ratio to be exceeded. For example, in a short period, two-story wood frame building with equal mass at the roof and second floor and equal first and second story heights, then ASCE/SEI 41-17 Equation 7-25 would have a story shear of 2/3 of the base shear at the second story and the full base shear at the first story. With equal strength at each story, the ratio of

the shear strength DCR at the first story to the second story would be (1.0*V*/ 0.67*V*) = 1.5 which exceeds 1.25.

Detailed case studies have not been done to determine the point at which a weak story would pass a linear evaluation and fail a nonlinear evaluation. However, both new and existing wood frame buildings have traditionally been analyzed using linear procedures. Based on engineering judgement, it is believed that linear procedures are adequate to evaluate wood frame buildings, even those with weak story irregularities, and high ductility demands, and it is considered unnecessary to require nonlinear analysis for wood frame buildings.

1.3.7 Conclusions and Recommendations

Based on the documents reviewed and the case studies there were conducted, we draw the following conclusions and recommendations.

- There is no clear justification for a revision to the provision. In some cases, the provision provides the desired protection against drawing an unconservative conclusion that a linear analysis finding of meeting the performance objective is not borne out in a more detailed nonlinear analysis. In other cases, it does not. The alternative options do not always lead to the desired result. More fundamentally, there are many permutations between outcomes and building archetypes and variants, and more studies would need to be done of variants to see if there is a consistent pattern.

- There are fewer examples than expected of cases where the limitation provision prevents use of a linear procedure that matches the result of the nonlinear procedure.

- When the portion of the provision requiring the DCR to be greater than the lesser of 3.0 and the *m*-factor of the component action is met and the limitation is triggered, the building will often have already failed the linear evaluation due to Acceptance Ratios that are exceeded. Thus, even though the linear procedure is not permitted theoretically, it does not matter from a practical point of view. The engineer could reasonably conclude that a building does not meet the performance objective with a linear evaluation. A nonlinear evaluation could show the building does or does not meet the performance objective.

- The ASCE/SEI 41-17 commentary on the linear limitation provision is brief and somewhat misleading. An expanded discussion of the rationale behind the provision would be beneficial and could describe, in abbreviated form, the study findings. This includes:

    - Incorporating some of the commentary from FEMA 274.

    - When the limitation provision is triggered, but when linear procedures show the building does not meet the performance objective, there is no need to require a further nonlinear analysis to prove the point. This should be clarified in both the provisions and the commentary.

- There are often relatively narrow bounds between triggering the linear procedure limitation provision and not failing the linear procedure Acceptance Ratios. When the portion of the limitation provision requiring the DCR to be greater than the lesser of 3.0 and the *m*- factor of the component action is met, the limitation is triggered, and linear procedures are not permitted, then the building will often have already failed the linear evaluation due to Acceptance Ratios that exceed 1.0. Thus, even though the linear procedure is not permitted theoretically, it does not matter from a practical point of view. The engineer could reasonably conclude that a building does not meet the performance objective with a linear procedure evaluation. A nonlinear procedure evaluation could show the building does or does not meet the performance objective should the engineer choose to pursue such a more detailed evaluation.

- Boundary conditions can be important in any analysis procedure, including linear procedures. For buildings sensitive to foundation rocking, adding springs even to a linear model can yield a more realistic assessment of superstructure component and system behavior.

- High DCRs in linear procedure results that do not trigger the linear limitation provision still highlight areas of high ductility and areas where further investigation and scrutiny could be desirable.

- The *m*-factor test in the linear procedure limitation provision requires a *m*-factor, but force-controlled components do not have an explicit *m*-factor. The *m*-factor is effectively 1.0. This means that when there are force-controlled elements and associated Acceptance Ratios that exceed 1.0, then the linear procedure limitation will be triggered by definition for buildings with weak story and torsional strength irregularities.

- Wood frame buildings should be exempted from the linear procedure limitation provision. Both new and existing wood frame buildings have traditionally been analyzed using linear procedures. Based on engineering judgement, it is believed that linear procedures are adequate to evaluate wood frame buildings, even those with weak story irregularities, and high ductility demands, and it is considered unnecessary to require nonlinear analysis for wood frame buildings. Similarly, the same thinking was applied to cold-formed steel light-frame construction (CFS1 and CFS2). In addition, unreinforced masonry bearing walls buildings have traditionally been analyzed using linear procedures. They were also proposed to be exempted from the linear procedure limitation provision, provided they meet the requirements needed to qualify for the Chapter 16 special procedure to eliminate buildings with notable deficiencies that would compromise the analysis.

- In the course of the study, three issues were identified that are outside the scope of the effort, but they are worth further investigation and potential revision to the standard provisions and/or commentary.

  - P-M interaction with tension

- Nonlinear modeling when modeling parameters vary as the earthquake-induced axial load on the component changes.
- Torsion studies from FEMA P-2012.

- Additional case studies would be beneficial in future work, particularly to investigate bins deemed of high value, but for which case studies were not available. In addition, refining or augmenting the existing cases studies would provide valuable information. Examples include:
  - Working Group 1, Linear punctured RCSW cases studies
    - Further reduce the demands until it passes NDP.
    - Revise the modeling and acceptance criteria using the Working Group 3 shear and flexural provision proposals.
    - Increase the strength of one of the punctured wall lines to create a torsional strength irregularity and examine alternative option proposals.
    - Vary ground motions in the NDP runs to determine the sensitivity of results to ground motions.
  - Working Group 3 shear-controlled component RCSW case study: Coordination and examination of the linear limitation procedure provision was not able to be completed during the project effort due to project resources, though it was nearly finished. This could be completed in the future.
  - Evaluate the FEMA P-2006 ordinary braced frame building using a flexible base LSP for comparison with the flexible base NSP.
  - Highrise steel moment frame.
  - Similar approach used in FEMA P-2012 to evaluate the effect of configuration irregularities, but with older non-code conforming buildings.
  - Evaluate linear procedure limitation provisions as applied to the ATC-134 building case studies.

1.4 Recommended Changes

Note about Change Proposals

This report documents aspects of change proposals as they were submitted to subcommittees of ASCE's *Seismic Retrofit of Existing Building Standards* Committee. Often, these change proposals were revised, in some cases substantively, by these subcommittees before they were adopted into ASCE/SEI 41-23. Readers should not rely on this report for information about the final version of provisions in ASCE/SEI 41-23.

The strikeout/underline proposed changes to ASCE/SEI 41-23 Section 7.3.1.1 and Commentary Section C7.3.1.1, Method to Determine Limitations on the Use of Linear Procedures, are shown below. New or modified text is shown in blue.

SCOPE – ASCE 41-17 Section 7.3.1.1. and C7.3.1.1 Method to Determine Limitations on the Use of Linear Procedures

7.3.1.1 Method to Determine Limitations on Use of Linear Procedures. Linear procedures shall be permitted for the following.

Buildings classified as W1, W1a, W2, CFS1, or CSF2 Common Building Types.

Buildings classified as URM Common Building Type, provided they have all of the following characteristics:

Flexible diaphragms at all levels above the base of the structure;

Vertical elements of the seismic-force-resisting system consisting of unreinforced masonry shear walls or a combination of predominantly unreinforced masonry and incidental concrete shear walls;

A minimum of two lines of walls in each principal direction, except for single-story buildings with an open front on one side; and

A maximum of six stories above the base of the structure.

For all other buildings, the ~~The~~ method presented in this section shall be used to determine the applicability of linear analysis procedures based on four configurations of irregularity defined in Section 7.3.1.1.1 through Section 7.3.1.1.4. The determination of irregularity shall be based on the configuration of the original or retrofit structure. A linear analysis to determine irregularity shall be performed by either an LSP in accordance with Section 7.4.1 or an LDP in accordance with Section 7.4.2. The results of this analysis shall be used to identify the magnitude and uniformity of distribution of inelastic demands on the primary elements and components of the seismic-force-resisting system. The magnitude and distribution of inelastic demands for existing and added primary elements and components shall be defined by demand–capacity ratios (DCRs) and computed in accordance with Eq. (7-16):

$$\text{DCR} = Q_{UD} / Q_{CE} \quad (7\text{-}16)$$

where

Q_{UD} = Force caused by gravity loads and earthquake forces calculated in accordance with Section 7.5.2; and

Q_{CE} = Expected strength of the component or element, calculated as specified in Chapters 8 through 13.

DCRs shall be calculated for each action (such as axial force, moment, or shear) of each primary component. The critical action for the component shall be the one with the largest DCR. The DCR for this action shall be termed the critical component DCR. The largest DCR for any element at a particular story is termed the critical element DCR at that story. If an element at a particular story contains multiple components, then the component with the largest computed DCR shall define the critical component for the element at that story.

If a component DCR exceeds the lesser of 3.0 and the *m*-factor for the component action and any irregularity described in Section 7.3.1.1.3 or Section 7.3.1.1.4 is present, then linear procedures are not applicable and shall not be used.

A nonlinear analysis shall not be required to demonstrate nonconformance with a Performance Objective, even where nonlinear analysis is required to demonstrate compliance.

~~***C7.3.1.1 Method to Determine Limitations on Use of Linear Procedures.*** The magnitude and distribution of inelastic demands are indicated by demand–capacity ratios (DCRs). These DCRs are not used to determine the acceptability of component behavior. The adequacy of structural components must be evaluated using the procedures contained in this chapter along with the acceptance criteria provided in Chapters 8 through 12. DCRs are used only to determine a structure's potential for inelastic response and irregularity. It should be noted that for complex structures, such as buildings with perforated shear walls, it may be easier to use one of the nonlinear procedures than to ensure that the building has sufficient regularity to permit use of linear procedures.~~

~~If all of the computed controlling DCRs for a component are less than or equal to 1.0, then the component is expected to respond elastically to the earthquake ground shaking being evaluated. If one or more of the computed DCRs for a component are greater than 1.0, then the component is expected to respond inelastically to the earthquake ground shaking.~~

C7.3.1.1 Method to Determine Limitations on Use of Linear Procedures. The magnitude and distribution of inelastic demands are indicated by demand–capacity ratios (DCRs). These DCRs represent local ductility demands on component actions. A provision to limit the use of linear procedures appeared first in FEMA 273 (FEMA, 1997a) with commentary in FEMA 274 (FEMA, 1997b). FEMA 274 noted that:

"Linear procedures, while easy to apply to most structures, are most applicable to buildings that actually have sufficient strength to remain nearly elastic when subjected to design earthquake demands, and buildings with regular geometries and distributions of stiffness and mass…. Buildings that have relatively limited inelastic demands under a design earthquake may be evaluated with sufficient accuracy by linear procedures, regardless of their configuration. If the largest component DCR calculated for a structure does not exceed 2.0, the structure may be deemed to fall into this category."

Linear procedures were not permitted when the DCR for a component action exceeded 2.0 and any of the following irregularities were present: in-plane discontinuity (unless it was checked as force- controlled with J=1.0), out-of-plane discontinuity (unless it was checked as force-controlled with J=1.0), severe weak story irregularity, or a severe torsional strength irregularity.

Revisions were made in FEMA 356 (FEMA, 2000) and then in ASCE/SEI 41-06, Supplement 1 (ASCE, 2007) which remained unchanged in ASCE/SEI 41-17 (ASCE, 2017b). The revisions made the limitation provision less restrictive in some cases as the triggering irregularities were reduced to

only the weak story irregularity and torsional strength irregularity, and the DCR was revised to trigger when the DCR for a component action exceeded the lesser of 3.0 and the m-factor for the component action. In a building with a weak story irregularity or a torsional strength irregularity, the deflected shape of the structure when analyzed using linear procedures may not represent the actual deflected shape of the structure accurately, and as a result the local demands used to check acceptance may not capture actual demands.

The linear procedure limitation provision was placed in the standard based on engineering judgment, but a recent study documented in FEMA (2022) validates the provision. The study included case study evaluations of a set of alternative options to the linear procedure limitation provision and did not find a clear basis for modifying the provision for the buildings studied. However, the study did recommend exempting woodframe, cold-formed steel light-frame, and URM buildings meeting the requirements of the Chapter 16 special procedure; clarifying that a nonlinear analysis is not required when a linear evaluation has shown the structure to be inadequate; and making revisions to the commentary, which have been incorporated here as follows.

- Consistency between the results of linear procedures and nonlinear procedures varies due to many reasons in addition to ductility demands and irregularities, such as component modeling and acceptance criteria, boundary conditions at the foundation, the Seismic Hazard Level, and the characteristics of ground motions used in nonlinear response history modeling.
- When the limitation provision is triggered, and linear procedures show the building does not meet the performance objective, there is no need to require a further nonlinear analysis to prove the point. However, the distribution of demands obtained from the linear procedures cannot be relied upon, and a nonlinear analysis may be required if a more accurate assessment of the location and extent of elements with inadequate capacities is desired.
- There are often relatively narrow bounds between triggering the linear procedure limitation provision and not failing the linear procedure Acceptance Ratios (as defined in Section 7.5.2.2). When the portion of the limitation provision requiring the DCR to be greater than the lesser of 3.0 and the m-factor of the component action is met, the limitation is triggered, and linear procedures are not permitted, then the building will often have already failed the linear evaluation due to Acceptance Ratios that exceed 1.0. Thus, even though the linear procedure is not permitted theoretically, it does not matter from a practical point of view. The engineer could reasonably conclude that a building does not meet the performance objective with a linear procedure evaluation. A nonlinear procedure evaluation could show the building does or does not meet the performance objective should the engineer choose to pursue such a more detailed evaluation.
- For buildings sensitive to foundation rocking, adding springs even to a linear model will yield a more realistic assessment of superstructure component and system behavior.
- High DCRs in linear procedure results that do not trigger the linear limitation provision still highlight areas of high ductility demands and areas where further investigation and scrutiny could be desirable.
- The definition of "weak story" in Section 7.3.1.1.3 of the standard is when the ratio of the average shear DCR for elements in any story to the average DCR of an adjacent story exceeds 1.25. By comparison, in ASCE/SEI 7-16 (ASCE, 2017a), the weak story definition is where the "story lateral strength is less than 80% of the story above," and

the extreme weak story is where "the story lateral strength is less than 65% of the story above." Thus, the standard compares DCRs, but ASCE/SEI 7-16 compares only strength. Studies show that the definition used by the standard is more conservative, but often more appropriate for existing buildings that may not have sufficient strength and leads to results that are more consistent with nonlinear analysis findings.

- Wood frame, cold-formed steel light-frame, and URM buildings consistent with the Chapter 16 special procedure were exempted from the linear procedure limitation provision in the revisions for this edition of the standard. Both new and existing buildings of these types have traditionally been analyzed using linear procedures. Based on engineering judgement, it is believed that linear procedures are adequate to evaluate these building types, even those with weak story irregularities, and high ductility demands, and it is considered unnecessary to require nonlinear analysis for these building types.

1.5 References

ATC, 1978, *Tentative Provisions for the Development of Seismic Regulations for Buildings*, ATC-3-06 Report, Applied Technology Council, Palo Alto, California.

ATC, 1984, *Tentative Provisions for the Development of Seismic Regulations for Buildings*, ATC-3-06 Report (Amended), second printing, Applied Technology Council, Palo Alto, California.

ATC, 1987, *Evaluating the Seismic Resistance of Existing Buildings*, ATC-14 Report, Applied Technology Council, Redwood City, California.

ASCE, 2002, *Seismic Evaluation of Existing Buildings*, ASCE/SEI 31-02 Report, American Society of Civil Engineers Structural Engineering Institute, Reston, Virginia.

ASCE, 2003, *Seismic Evaluation of Existing Buildings*, ASCE/SEI 31-03 Report, American Society of Civil Engineers Structural Engineering Institute, Reston, Virginia.

ASCE, 2007, *Seismic Rehabilitation of Existing Buildings*, ASCE/SEI 41-06 Report, American Society of Civil Engineers Structural Engineering Institute, Reston, Virginia.

ASCE, 2014, *Seismic Rehabilitation of Existing Buildings*, ASCE/SEI 41-13 Report, American Society of Civil Engineers Structural Engineering Institute, Reston, Virginia.

ASCE, 2017a, *Minimum Design Loads and Associated Criteria for Buildings and Other Structures*, ASCE/SEI 7-16 Report, American Society of Civil Engineers Structural Engineering Institute, Reston, Virginia.

ASCE, 2017b, *Seismic Evaluation and Retrofit of Existing Buildings*, ASCE/SEI 41-17 Report, American Society of Civil Engineers Structural Engineering Institute, Reston, Virginia.

BSSC, 1992, *NEHRP Handbook for the Seismic Evaluation of Existing Buildings*, FEMA 178 Report, developed by the Building Seismic Safety Council for the Federal Emergency Management Agency, Washington, D.C.

FEMA, 1988, *NEHRP Recommended Provisions for the Development of Seismic Regulations for New Buildings*, Part 1: Provisions, prepared by the Building Seismic Safety Council for the Federal Emergency Management Agency, Washington, D.C.

FEMA, 1997a, *NEHRP Guidelines for the Seismic Rehabilitation of Buildings*, FEMA 273 Report, prepared by the Building Seismic Safety Council for the Federal Emergency Management Agency, Washington, D.C.

FEMA, 1997b, *NEHRP Commentary for the Seismic Rehabilitation of Buildings*, FEMA 274 Report, prepared by the Building Seismic Safety Council for the Federal Emergency Management Agency, Washington, D.C.

FEMA, 1998, *Handbook for the Seismic Evaluation of Buildings: A Prestandard*, FEMA 310 Report, prepared by the American Society for Civil Engineers for the Federal Emergency Management Agency, Washington, D.C.

FEMA, 2000, *Prestandard and Commentary for the Seismic Rehabilitation of Buildings,* FEMA 356 Report, prepared by the American Society for Civil Engineers for the Federal Emergency Management Agency, Washington, D.C.

FEMA, 2005a, *Improvement of Nonlinear Static Seismic Analysis Procedures*, FEMA 440 Report, prepared by the Applied Technology Council for the Federal Emergency Management Agency, Washington, D.C.

FEMA, 2009b, *Seismic Evaluation and Retrofit of Multi-Unit Wood-Frame Buildings with Weak First Stories*, FEMA P-807 Report, prepared by the Applied Technology Council for the Federal Emergency Management Agency, Washington, D.C.

FEMA, 2012, *Quantification of Building Seismic Performance Factors*, FEMA P695 Report, prepared by the Applied Technology Council for the Federal Emergency Management Agency, Washington, D.C.

FEMA, 2018a, *Example Application Guide for ASCE/SEI 41-13 Seismic Evaluation and Retrofit of Existing Buildings with Additional Commentary for ASCE/SEI 41-17*, FEMA P-2006 Report, prepared by the Applied Technology Council for the Federal Emergency Management Agency, Washington, D.C.

FEMA, 2018b, *Assessing Seismic Performance of Buildings with Configuration Irregularities: Calibrating Current Standards and Practices*, FEMA P-2012 Report, prepared by the Applied Technology Council for the Federal Emergency Management Agency, Washington, D.C, in progress.

ICBO, 1961, *Uniform Building Code*, 1961 Edition, International Conference of Building Officials, Whittier, CA.

ICBO, 1964, *Uniform Building Code*, 1964 Edition, International Conference of Building Officials, Whittier, CA.

ICBO, 1982, *Uniform Building Code*, 1982 Edition, International Conference of Building Officials, Whittier, CA.

ICBO, 1985, *Uniform Building Code*, 1985 Edition, International Conference of Building Officials, Whittier, CA.

NIST, 2017a, Recommended Modeling Parameters and Acceptance Criteria for Nonlinear Analysis in Support of Seismic Evaluation, Retrofit, and Design, NIST GCR 17-917-45 Report, prepared by the Applied Technology Council as ATC-114 for the National Institute of Standards and Technology, Gaithersburg, Maryland.

NIST, 2017b, *Guidelines for Nonlinear Structural Analysis and Design of Buildings, Part I-General*, NIST GCR 17-917-46v1 Report, prepared by the Applied Technology Council as ATC-114 for the National Institute of Standards and Technology, Gaithersburg, Maryland.

NIST, 2017c, *Guidelines for Nonlinear Structural Analysis and Design of Buildings, Part IIa-Steel Moment Frames*, NIST GCR 17-917-46v2 Report, prepared by the Applied Technology Council as ATC-114 for the National Institute of Standards and Technology, Gaithersburg, Maryland.

NIST, 2017d, *Guidelines for Nonlinear Structural Analysis and Design of Buildings, Part IIb-Reinforced Concrete Moment Frames*, NIST GCR 17-917-46v3 Report, prepared by the Applied Technology Council as ATC-114 for the National Institute of Standards and Technology, Gaithersburg, Maryland.

SEAOC, 1985, *Tentative Lateral Force Requirements*, Structural Engineers Association of California Seismology Committee, known informally as the “Blue Book.”

Chapter 2: Adding Acceptance Ratio Term

2.1 Motivation

The purpose of this revision in ASCE/SEI 41 Chapter 7 is to clarify the terminology used to define the acceptance criteria for linear analysis procedures and to avoid conflicting usage of the term demand-to-capacity ratio (DCR). It is common practice in engineering to use the term demand-to-capacity ratio or demand-capacity ratio (DCR) as a measure of acceptability where a value of less than unity is defined as acceptable and a value equal or greater than unity is defined as unacceptable. However, ASCE/SEI 41-17 Eq. 7-16 defines DCR as Q_{UD} / Q_{CE}, which is a measure of ductility demand, not acceptability. Since ASCE/SEI 41 uses the term DCR differently than the standard of practice, significant confusion has been commonly observed in seismic evaluations using ASCE/SEI 41 as to whether the engineer was reporting Q_{UD} / mKQ_{CE} as would be typically meant or Q_{UD} / Q_{CE}, which is the ASCE/SEI 41-17 Eq. 7-16 definition. To preserve the DCR usage in Eq. 7-16, a new term, Acceptance Ratio, is introduced for Eq. 7-36 and Eq. 7-37. The term Acceptance Ratio is defined by the standard such that an Acceptance Ratio less than unity is acceptable; an Acceptance Ratio equal to or greater than unity is unacceptable. The term Acceptance Ratio was initiated and defined in FEMA P-2006, *Example Application Guide for ASCE/SEI 41-13 Seismic Evaluation and Retrofit of Existing Buildings with Additional Commentary for ASCE/SEI 41-17* (FEMA, 2018), to address this issue, and this proposal formally adds the definition to the standard.

2.2 Summary of Changes Recommended

The proposed changes occur in ASCE/SEI 41 Section 7.5.2.2, which defines acceptance criteria for linear procedures. Specifically, the changes occur in Eq. 7-36, which defines the Acceptance Ratio for deformation-controlled actions and in Eq. 7-37, which defines the Acceptance Ratio for force-controlled actions.

2.3 Technical Studies

The change was proposed to clarify the terminology used for the acceptance criteria and differentiate the new term Acceptance Ratio from the term demand-capacity ratio (DCR) that is used in ASCE/SEI 41 Eq. 7-16 as a measure of ductility demand. No technical studies were conducted as background for this proposed change of terminology.

2.4 Recommended Changes

Note about Change Proposals

This report documents aspects of change proposals as they were submitted to subcommittees of ASCE's *Seismic Retrofit of Existing Building Standards* Committee. Often, these change proposals were revised, in some cases substantively, by these subcommittees before they were adopted into ASCE/SEI 41-23. Readers should not rely on this report for information about the final version of provisions in ASCE/SEI 41-23.

The strikeout/underline proposed changes to ASCE/SEI 41 Section 7.5.2.2, Acceptance Criteria for Linear Procedures, shown below were proposed to the ASCE 41 Standards Committee for their consideration. New or modified text is shown in blue.

7.5.2.2.1 *Acceptance Criteria for Deformation-Controlled Actions for LSP or LDP.* ~~Deformation-controlled actions in primary and secondary components shall satisfy Eq. (7-36).~~ The Acceptance Ratio for deformation-controlled actions shall be defined as $Q_{UD} / m\kappa Q_{CE}$.

$$~~m\kappa Q_{CE} \geq Q_{UD}~~ \qquad ~~(7\text{-}36)~~$$

where

m = Component capacity modification factor to account for expected ductility associated with this action at the selected Structural Performance Level. m-factors are specified in Chapters 8 through 12, 14, and 15;

Q_{CE} = Expected strength of component deformation-controlled action of an element at the deformation level under consideration. Q_{CE}, the expected strength, shall be determined considering all coexisting actions on the component under the loading condition by procedures specified in Chapters 8 through 15; and

κ = Knowledge factor defined in Section 6.2.4.

Deformation-controlled actions in primary and secondary components shall satisfy Eq. (7-36).

$$Q_{UD} / m\kappa Q_{CE} \leq 1 \qquad (7\text{-}36)$$

7.5.2.2.2 *Acceptance Criteria for Force-Controlled Actions for LSP or LDP.* ~~Force-controlled actions in primary and secondary components shall satisfy Eq. (7-37):~~ The Acceptance Ratio for force-controlled actions shall be defined as $Q_{UF} / \kappa Q_{CL}$.

$$~~\kappa Q_{CL} \geq Q_{UF}~~ \qquad ~~(7\text{-}37)~~$$

where

Q_{CL} = Lower-bound strength of a force-controlled action of an element at the deformation level under consideration. Q_{CL}, the lower-bound strength, shall be determined considering all coexisting actions on the component under the loading condition by procedures specified in Chapters 8 through 12, 14, and 15.

Force-controlled actions in primary and secondary components shall satisfy Eq. (7-37):

$$Q_{UF} / \kappa Q_{CL} \leq 1.0 \qquad (7\text{-}37)$$

Commentary is added to Section C7.5.2.2 to go with the changes in provisions.

C7.5.2.2 Acceptance Criteria for Linear Procedures. It is common practice in engineering to use the term demand-to-capacity ratio or demand-capacity ratio (DCR) as a measure of acceptability. A value of less than unity is defined as acceptable; a value equal or greater than unity is defined as unacceptable. However, Equation 7-16 defines DCR as Q_{UD} / Q_{CE}, which is a measure of ductility demand, not acceptability. To preserve the standard's definition of DCR, but to avoid confusion, the term Acceptance Ratio is defined by the standard. An Acceptance Ratio less than unity is defined as acceptable; an Acceptance Ratio equal to or greater than unity is defined as unacceptable.

2.5 References

FEMA, 2018, *Example Application Guide for ASCE/SEI 41-13 Seismic Evaluation and Retrofit of Existing Buildings with Additional Commentary for ASCE/SEI 41-17*, FEMA P-2006 Report, prepared by the Applied Technology Council for the Federal Emergency Management Agency, Washington, D.C.

Part 2

Chapter 1: Nonlinear Analysis Revisions

1.1 Motivation

The overarching goal of the project was to propose changes to improve usability, increase efficiency, and improve accuracy of the nonlinear analysis procedures, then confirm those changes provided the intended improvements through review of past research and case studies. Use of nonlinear analysis procedures under ASCE/SEI 41 has increased significantly in the past ten years, specifically the use of nonlinear response history procedures (referred to in ASCE/SEI 41 as the Nonlinear Dynamic Procedures, NDP). The 2017 edition of ASCE/SEI 41 was updated to align with significant work done by the NEHRP Provisions Update Committee in the 2015 edition of the *Provisions* (FEMA, 2015) and subsequent modification of those updates by the ASCE/SEI 7 committee for the 2016 edition of that standard. However, the project team identified a number of issues where the provisions in ASCE/SEI 41-17 could be improved further.

The report presents a discussion of the motivation for the recommended changes to the nonlinear analysis procedures, followed by a discussion of pertinent research and case studies performed to examine the effects of the proposed change, and finally the resulting change proposal. All changes were considered primarily for their effect on the Nonlinear Dynamic Procedure (NDP). Peripherally, effects of the proposed changes on the Nonlinear Static Procedure (NSP), commonly referred to as pushover analysis, were considered. This chapter discusses eight changes that affect how one conducts the NDP and determines conformance with a specified ASCE/SEI 41 Structural Performance Level. Another chapter presents changes made to the modeling parameters used in developing a nonlinear analysis model.

1.1.1 Critical and Ordinary Actions

The 2016 edition of ASCE/SEI 7 introduced the concept of critical, ordinary, and noncritical for force-controlled and deformation-controlled actions. Critical actions were defined as those whose failure would lead to a disproportionate collapse beyond the individual bay the element is a part of or have significant impact on the response of the structure's seismic force resisting system. Noncritical actions do not cause local collapse when they fail or result in significant detrimental changes to the seismic force resisting system. Ordinary actions could lead to local collapse of the floor tributary to the component if the action fails, but not more than one-bay of one story of the structure. Ordinary actions also do not have a significant impact on the response of the seismic force resisting system.

ASCE/SEI 41-17 only adopted the concept of critical, ordinary, and noncritical for force-controlled actions. ASCE/SEI 41-17 dropped the significant effect on the seismic force resisting system response criteria for classifying an action as critical and focused on collapse due to loss of gravity load support. The ASCE 41-17 provisions treat critical force-controlled component actions differently

than ordinary and non-critical. Ordinary and non-critical force-controlled actions are assessed by comparing the mean of the maximum value of the component action demand from each record in the suite that produces an acceptable response to the component action capacity calculated using lower-bound material properties. There are more requirements for critical actions. If any critical force-controlled component action that is modeled elastically exceeds its expected strength in one ground motion record response history analysis, it is considered an unacceptable response. The seismic force component of the suite mean of the component action is amplified by 1.3 before being checked against the lower-bound capacity to provide greater reliability that the force-controlled action will not fail.

There are several issues with the current provisions. First, the definitions of critical, ordinary, and non-critical are defined in the commentary, not the body of the standard. This creates enforcement issues, since there are no explicit provisions in the body of the standard on how one should delineate between critical, ordinary, and non-critical. Second, only force-controlled actions are delineated as critical, ordinary, or noncritical. The deformation-controlled component actions can produce the same consequences, or lack of consequences, when they are pushed to the point that they lose the ability to support gravity loads. Third, while ordinary and non-critical elements are distinct, there are no differences in how the two different types of component actions are evaluated. Finally, the definition of critical actions in ASCE 41 differs from ASCE 7, because ASCE 41 only focuses on collapse and does not address significant changes to the behavior of the lateral force resisting system as considered by ASCE 7. By exempting actions that could significantly alter the behavior of the seismic force resisting system, the intended reliability of the analysis procedure may be compromised.

While parity with ASCE/SEI 7 is desirable, the main motivation for revising how ASCE/SEI 41 addresses analysis response acceptability and component action acceptance criteria is to make sure they are providing the desired reliability, which per the ASCE/SEI 41 commentary is a 90% reliability of achieving the desired performance level. FEMA 274 alluded to there being some small chance that the standard would not achieve the performance level under a given seismic hazard intensity. As analytical tools increased, which allowed more in-depth study of the variability of seismic hazard demand and our understanding of seismic hazard uncertainties expanded, it became possible to quantify the variability. This is essentially in alignment with the reliability of the seismic provisions in ASCE/SEI 7, which seeks to provide a maximum 10% probability of collapse at the MCE_R hazard shaking intensity for a Risk Category II building. ASCE/SEI 41 requires Collapse Prevention structural performance at the MCE_R (BSE-2N) hazard level in the Basic Performance Objective Equivalent to New Building Performance (BPON) for a Risk Category II building. The critical action criteria were specifically calibrated to provide approximately 90% reliability of achieving collapse prevention (Haselton et al., 2017).

1.1.2 Force-Controlled Actions

ASCE/SEI 41 classifies structural element actions, such as response to shear, moment, or axial force, as either force-controlled or deformation-controlled. Deformation-actions are permitted, and often expected, to deform nonlinearly as the structure responds to earthquake excitation.

Force-controlled actions are typically brittle and incapable of sustaining force or deformations beyond the actions' capacity. In linear analysis, the distinction between force-controlled and deformation-controlled actions is very clear. The distinction is not as clear in nonlinear procedures because ASCE/SEI 41 allows force-controlled actions to be reclassified as deformation-controlled actions and explicitly included in the analysis. Also, ASCE/SEI 41 does not explicitly state that all component actions included in an NSP or NDP model with only linear force-displacement relationships should be treated as force-controlled actions, regardless of whether they could be classified as force- or deformation-controlled actions. That has led to misinterpretation of the standard, where these actions are checked outside of the model using linear deformation-controlled criteria. Such practice is not correct and potentially unconservative.

In ASCE/SEI 41-17, overstress of a critical force-controlled action relative to its expected strength is considered an unacceptable response, unless the action is explicitly modeled with a nonlinear force-deformation relationship that represents sudden loss of lateral and/or gravity resistance at overstress and the user confirms that failure of the component action doesn't cause a loss of gravity support, either through direct simulation in the model, or otherwise. The rationale being that if a critical force-controlled action fails in the model and the model cannot adapt to reflect the consequence of that failure, a potential collapse may not be identified, hence analysis results are invalid after the timestep the failure occurs. There is concern that overstress of ordinary and noncritical force-controlled actions can create a disconnect between the analysis model, which assumes the action can continue to resist force elastically, and the actual structure's performance and should be treated similar to critical actions with respect to their overstress in the analysis.

The current ASCE/SEI 41 provisions only require evaluation of ordinary and noncritical force-controlled actions for the mean of the maximum demand from each ground motion record against their capacity derived using nominal or lower-bound properties. This approach means that actions that meet the acceptance criteria of the mean demand being greater than the capacity calculated using lower-bound capacities may actually be overstressed in a number of ground motion records. In some cases the difference in strength when derived from expected versus nominal or lower-bound material properties is only 10%. So, an element where the demand from the mean of the ground motion suite is about equal to the lower-bound capacity could mean that the expected capacity is exceeded in almost half the records in the ground motion suite. Such overstress could lead to failure of the action and alter the performance of the building, potentially invalidating the results of the model. A model with elastic elements that actually have little to no ability to resist lateral forces because they've been overstressed can lead to underestimation of the deformation and force demands on the remaining lateral forces resisting elements or may lead to loss of gravity load support that is not picked up in the model.

1.1.3 Unacceptable Response Drift Limit

ASCE/SEI 41 does not have drift limits, which is a major difference from ASCE/SEI 7. In ASCE/SEI 7 all buildings are subject to drift limits, regardless of whether the analysis used is the equivalent lateral force, modal response spectrum or nonlinear response history. Additionally, PEER TBI v2.0 and ASCE/SEI 7-22 contain peak transient and residual drift limits based on the mean and

maximum values from the suite of ground motions. Initially there was discussion whether to include drift limits in ASCE 41. ASCE/SEI 7 uses system factors, configuration limitations, and special detailing adopted via material standards, hence global drift requirements are part of the design process to attain the performance objective. Existing buildings were not designed with any or with a constant set of system factors, configuration limitations, and detailing to provide uniform ductility; hence ASCE/SEI 41 relies on a component level assessment to measure the global performance. The project team explored whether drift limits should be added to ASCE 41 or if there was another method to capture the intent of the drift limits in the other documents.

1.1.4 No Unacceptable Responses for Life Safety

Unacceptable response can indicate the potential for collapse of the structure in that record. ASCE/SEI 41-17 permits one unacceptable response per eleven records for the Life Safety, Limited Safety and Collapse Prevention structural performance levels. The permission of one unacceptable response stems from research conducted to support revisions to Chapter 16 of ASCE 7 by the BSSC PUC (Haselton et al., 2017). Haselton et al. (2017) demonstrated that one unacceptable response per eleven records could be permitted if the provisions were targeting a 10% probability of collapse at a given seismic hazard intensity level. 10% probability of collapse under MCE_R shaking intensity is ASCE/SEI 7's target reliability for Risk Category II structures. ASCE/SEI 7 does not permit an unacceptable response for structures assigned to Risk Category III and IV, where the probability of collapse under the MCE_R shaking intensity is 5% and 2.5%, respectively. The analogous ASCE 41 performance objective for buildings assigned to Risk Category II in the BPON is Collapse Prevention in the BSE-2N (MCE_R). Based on that, it was determined that the provisions should target 10% or less probability of not meeting the performance level being considered.

ASCE/SEI 41's predecessor document, FEMA 274, discusses the reality that one cannot obtain with complete certainty the attainment of a performance objective:

> "It is the intent of the Guidelines that most, although not necessarily all, structures designed to attain a given performance at a specific earthquake demand would exhibit behavior superior to that predicted. However, there is no guarantee of this. There is a finite possibility that—as a result of the variances described above, and other factors—some rehabilitated buildings would experience poorer behavior than that intended by the [Performance] Objective."

The Life Safety structural performance level is intended to be better than the Collapse Prevention performance level. There should be a lower likelihood of collapse in a building meeting that level than the Collapse Prevention level. The Life Safety acceptance criteria are intended to be taken as 75% of the Collapse Prevention criteria, quantitatively defined as a 4/3rds margin against collapse. If the Collapse Prevention performance level has a 10% probability of collapse under the seismic hazard level used, buildings meeting the Life Safety structural performance level should have a probability of collapse significantly less than 10%.

In addition, the team identified a potentially confusing provision on how to calculate the component action demands when there is an unacceptable response. The current provisions require the larger

of the mean of values from remaining acceptable responses or 120% of the median from all the responses be used. An issue was raised with how one should compute the median when there is an unacceptable response. Sometimes, specific response parameters can have a low value in the cases with unacceptable response, compared to the cases with acceptable response. For example, an instability is encountered early in the response or a critical element's action exceeds its valid range of modeling while all the other elements show low levels of response. Inclusion of the low values from the unacceptable response would reduce the median, potentially in an artificial manner. If the unacceptable response is an indicator of collapse, the component response parameters should be very large, because the structure has effectively "collapsed."

1.1.5 Secondary Components

ASCE/SEI 41 requires that all components, primary and secondary, be included in the analysis model. This has been a requirement since the original guideline document (FEMA, 1997). The reason for the requirement is concern that the omission of secondary components in the analytical model could substantially alter the structure's predicted response, rendering the analysis results unreliable for performance prediction.

A survey of practitioners found that this requirement was commonly ignored. Many practitioners perform nonlinear analysis using only primary components, particularly for steel framed buildings. ASCE/SEI 7 does not have this same requirement that every structural element, including the gravity load supporting elements, be modeled, nor does it classify structural elements as primary or secondary components. ASCE/SEI 7 stipulates that "all elements that significantly affect seismic response when subjected to MCE_R ground motions shall be included." So, elements of the gravity framing need not be modeled in a nonlinear response history analysis if they do not contribute to the seismic response. Elements not explicitly modeled are checked to confirm that the elements are capable of supporting gravity loads at the mean displacement from the nonlinear response history the analysis.

Additionally, ASCE/SEI 41 requires nonstructural components be reclassified as primary components and included in the analysis model if their stiffness is greater than 10% of the total stiffness of the primary components. This provision is intended to flag nonstructural components that span story-to-story, such as cladding and stairs. Cladding, especially if it is concrete or another stiff and strong material, and stairs in older buildings were often detailed without a mechanism to accommodate story drift. In some instances, these elements can resist seismic forces and introduce torsion and other irregularities into the structure's response. By requiring an explicit check of their stiffness relative to the primary system, users have the ability to discern if they will significantly affect the response. If they do affect the response, they should be included in the primary model.

In many cases modeling all the secondary components can add significant effort to the project, while not changing the results of the analysis. An example of this is not including the gravity framing in a steel moment frame or braced frame building. While inclusion of that framing may lead to a more accurate representation of building performance, it does not necessitate doing so because typically, such framing is very flexible compared to the primary lateral force resisting elements. On the other

hand, there are situations, particularly in reinforced concrete buildings, where the inclusion of the secondary components may change the response of the building and lead to failure mechanisms that would be missed if the elements were not modeled.

1.1.6 Damping

Numerous studies have been undertaken on the amount of damping inherent in buildings and how that should be represented in nonlinear analysis (PEER/ATC 72-1, 2010). Issues that have been observed and that ASCE/SEI 41-17 does not address include:

- Damping is related to structure height
- Damping may need to have a cap or floor, depending on the performance level
- Spurious damping forces have been observed depending on the plasticity models and damping assumptions

The goal of the proposal is to update ASCE/SEI 41-23 to include more recent research.

1.1.7 Accidental Torsion

ASCE/SEI 41 requires consideration of accidental torsion in the NSP and NDP. The provisions require the center of mass be shifted in each of the four orthogonal directions, quadrupling the analysis runs and data that must be processed. The standard does provide some relief by allowing the lower hazard(s) to be conducted without accidental torsion, provided the higher or highest hazard evaluation includes accidental torsion. Additionally, the standard has a provision that allows the user to amplify the deformations from a nonlinear analysis without accidental torsion instead of performing four analyses. It is desirable to reduce the amount of analyses and eliminate steps which require additional effort, but do not yield substantially different results than using one model. However, there are issues with the current provisions:

- ASCE/SEI 41-17 only requires accidental torsion in the highest hazard when the Performance Objective requires multiple hazards, which may be unconservative if the hazard levels are not far enough apart or the Performance Level in the lower hazards is Damage Control or Immediate Occupancy.
- Potential issues with the provision that permits an amplification factor to account for accidental torsion in the NDP and the current provision not being written in enforceable code language.

The goal of the proposed changes is to reduce the number of times that engineers must consider accidental torsion in their analysis to the cases where not considering it would lead to a misclassification of the building's performance.

1.1.8 Material Property Bounding

ASCE/SEI 41-17 requires significant material testing to determine in situ strength of the construction materials when a nonlinear analysis is performed. Although the standard permits preliminary evaluations to proceed without testing, it requires material testing prior to implementing a retrofit or finalizing an evaluation report. This proposal permits the use of bounding analyses in lieu of material testing for nonlinear analysis. In practice, comprehensive material testing programs can be very intrusive to building occupants and can often become prohibitively expensive for the building owners.

1.2 Summary of Changes Recommended

The project team developed eight proposed changes to the nonlinear analysis procedures. All of the changes were made with the primary intent of improving the nonlinear dynamic procedure, but the team also considered the effect of these changes on the nonlinear static procedure.

1.2.1 Critical and Ordinary Actions

These changes provide better clarity on defining critical actions and eliminate an unnecessary additional classification. Because ordinary and noncritical actions have the same criteria in ASCE/SEI 41, the recommendation is to eliminate one of the terms. The definitions of critical and ordinary actions are moved into the body of the standard. The provisions are agnostic with respect to force-controlled or deformation-controlled actions. This was done intentionally to permit other change proposals to invoke different requirements for critical and ordinary deformation-controlled actions.

The definition of critical actions is expanded to include provisions when the action's failure could lead to significant changes in the structure's response. Instead of using a subjective term like significant, the proposed change invokes the weak story or torsional strength irregularity already defined in ASCE/SEI 41 Section 7.3.1.1. If the failure of the action leads to the building having a weak story or torsional strength irregularity, that action should be considered critical. By using already defined irregularities that can be explicitly calculated, the change proposal provides a means to clearly assess if the component action's failure will significantly alter the behavior of the seismic force resisting system.

1.2.2 Force-Controlled Actions

To address the potential ambiguity regarding treatment of elements that could be classified as deformation-controlled but are not explicitly modeled with nonlinear properties in an analysis, the change proposal adds text to clearly require that any component action that does not have an explicit nonlinear force-deformation curve in the analysis model should be considered as a force-controlled action.

To address the concerns that overstress of any force-controlled action in a NDP analysis could significantly change the response of the structure and affect the performance objective, this proposal changes the unacceptable response criteria to be overstress in *any* force-controlled action

modeled elastically in the nonlinear model. The proposal also clarifies how force-controlled actions can be explicitly included in the model by being reclassified as deformation-controlled using a Type 3 force-displacement curve (Figure 1-1) for the action based on expected strength of the component action and allowing the model to adapt after failure of that action. If required, loss of vertical load support should also be captured in the model or post-processed.

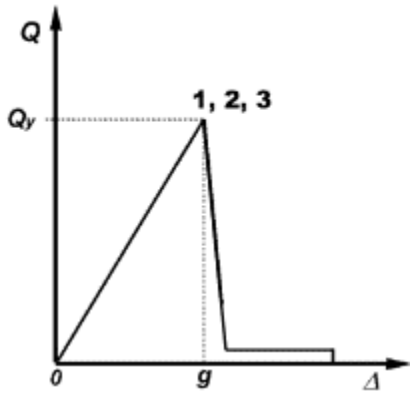

Figure 1-1 Type 3 Nonlinear force-displacement curve (from FEMA 356).

1.2.3 Unacceptable Response Story Drift Ratio Limit

This proposal introduces a maximum peak transient story drift, which would also define unacceptable response. There is concern that current commercially available software may not provide meaningful results at large displacements and large story drifts. It is unclear if programs can process dynamic stability at large displacements and may provide results that indicate a stable structure when it is not. Six percent is proposed as a reasonable limit based on the judgement of the project team and is more liberal than the 4.5% limit in PEER TBI v2.0. This is consistent with requirements in ASCE/SEI 7-22 where the peak transient drift of all analyses must be less than 150% of the limit on mean of 2 times the Design Earthquake drift in Chapter 12, which for Risk Category I and II buildings is 1.5x2x2% = 6% for most buildings. These requirements are based on judgement of committee members.

1.2.4 No Unacceptable Responses for Life Safety

The change proposal eliminates the ability to have one unacceptable response when targeting the Life Safety Performance Level. While having an unacceptable response may still provide the desired reliability for Collapse Prevention or Limited Safety, it does not assure this for Life Safety.

This proposal also clarifies how to calculate component action demands when there is an unacceptable response. The provision now states that the unacceptable response should be treated as being larger than the median when computing the median. This serves to force the median parameter to be between the fifth and sixth acceptable response as opposed to the fourth and fifth acceptable response when 11 motions are used.

1.2.5 Secondary Components

The proposed change permits excluding secondary components from the nonlinear analysis model provided it can be justified excluding those elements will not adversely affect the response of the primary component model. If the demands in the primary components are larger with the secondary components included in the model, the secondary components that cause that demand increase must be classified as primary components and included in the model. However, if exclusion of the secondary components results in no change or an increase in the demands on the primary components, exclusion of those elements is permitted, provided the other rules are followed.

The threshold for when secondary components must be included in linear models is slightly reduced from 25% to 20% of the initial stiffness of the primary system. It is assumed this requirement should be used for nonlinear models as well. The change proposal assumed that users will use a linear model to assess whether the secondary components are stiff enough or affect the torsional stiffness of the story enough to warrant reclassification as primary components. This reduction from 25% to 20% was based on judgement of the Project Team.

The criteria when nonstructural components should be modeled as primary components is increased from 10% to 20% of the initial stiffness of the primary system to align with the secondary component criteria.

Additionally, a new criterion is added that secondary components and nonstructural components cannot cause a shift in the center of rigidity of the story by more than 10%. This was deemed necessary to prevent exclusion of secondary components or reclassification of primary components to miss torsional response. Similar to the rules for when secondary elements should be classified as primary based on overall stiffness, the torsional response limits were based on judgement of the Project Team.

The proposal requires that secondary components not included in the nonlinear response history model be evaluated using the linear static procedures or nonlinear static procedure with deformations from the analysis with the maximum response, as opposed to the suite mean. The intent is that a user would develop a subassemblage model of the secondary components or a representative subset of the secondary components and enforce displacements on that model linearly or nonlinearly using the maximum deformations from the nonlinear static or nonlinear dynamic model. The secondary components' actions would then be checked for forces or deformations arising from the subassemblage's response to the enforced displacement.

1.2.6 Damping

This change proposal concerns ASCE 41-17 Sections 7.2.3.6 and 7.4.4.4 and seeks to aggregate existing guidance with new guidance for the use of damping models in the nonlinear dynamic procedure (NDP). To collect all damping related guidance for the NDP under Section 7.4.4.4, a note concerning the estimation of target elastic effective viscous damping ratio for the NDP is moved from Section 7.2.3.6, which provides general guidance on damping for both linear and nonlinear procedures, to Section 7.4.4.4, which provides damping related guidance specific to the NDP.

This change proposal eliminates the requirement that the target elastic effective viscous damping ratio (β) not exceed 3% and introduces an equation proportional to the building height. Limits on the damping are capped at 5%, like PEER TBI. For Life Safety, Limited Safety and Collapse Prevention performance levels, there is a 2.5% floor on damping, even though the equation can predict lesser values. Immediate Occupancy and Damage Control do not invoke that floor because structures are more likely to behave similar to an elastic structure at those high-performance levels. The change proposal also introduces commentary to make the user aware of spurious damping forces.

Section 7.4.4.4 is also modified to explicitly permit the use of the modal damping model in addition to the Rayleigh damping model. This section also lists conditions for setting up damping models for the NDP. While these conditions are mostly related to the commonly used Rayleigh damping model, they are also relevant for situations where Rayleigh damping is used in conjunction with modal damping.

1.2.7 Accidental Torsion

This change proposal updates the requirements to consider accidental torsion in nonlinear analysis. The proposal permits the analyst to neglect accidental torsion except in specific identified cases where accidental torsion may have significant impact on the analysis. The most important focus of the change proposal is the requirement that buildings that have a torsional strength irregularity must consider accidental torsion. Unlike ASCE/SEI 7, ASCE/SEI 41 uses relative strength of the primary lateral force-resisting elements on each side of the center of rigidity to determine if there is an irregularity. If one side has demand-to-capacity ratios disproportionately larger than the other side, there is a potential for one side to yield and cause significant torsional response. For buildings with a torsional irregularity as defined by ASCE/SEI 41, accidental torsion must be considered, but only in the direction where there is a torsional strength irregularity.

The nonlinear analysis updates to accidental torsion include the following:

- Buildings with a torsional strength irregularity as defined by ASCE/SEI 41 must consider accidental torsion but may only need to consider it in one direction.
- Accidental torsion may be excluded if the eta factor is low.
- Accidental torsion may be excluded if there is already significant inherent torsion
- In the NDP, only the more critical offsets are required when considering accidental torsion, rather than all four.
- In an analysis using two or more hazard levels, permission to exclude accidental torsion from the lower ground motion has been eliminated.

In addition, the commentary discussion about sensitivity studies is deleted. The revised provisions provide more concise direction to help establish whether accidental torsion is significant in the body of the provisions, where it is enforceable.

1.2.8 Material Property Bounding

This change proposal concerns ASCE 41-17 Section 6.2.4.3 – Nonlinear Procedures, which currently requires that comprehensive data collection related to material properties be performed when using nonlinear procedures.

In lieu of mandating inconvenient testing programs that can impede the evaluation and retrofit process, this change proposal permits the user to perform multiple nonlinear analyses to bound the range of material properties present in the building. This change proposal requires one model to be based on lower-bound assumptions and another to be based on upper-bound assumptions. Recognizing that there are situations where having upper-bound properties and lower-bound properties in the same model could produce the largest component demands, the change proposal contains language indicating other combinations may be needed for special circumstances. Commentary is proposed that discusses situations where combining lower- and upper-bound material properties is warranted, specifically for the evaluation of elements supporting discontinuous walls.

The change proposal also permits mixing material testing and bounding analyses.

The scope of this change proposal, however, does not extend to buildings with unreinforced masonry (URM) components because such building are not considered appropriate for such property bounding analysis given the large amount of test variation and deviation of as-built conditions. Comprehensive testing will still be required for URM buildings prior to finalizing an evaluation or retrofit.

Where the standard already requires bounding analyses, such as seismic isolation and supplemental energy dissipation device properties, the change proposal requires that the material bounding properties shall be aligned with the other bounding properties.

The proposal also eliminates the non-standard language about doing trial analyses before doing material testing. Such language might have been appropriate for a guideline document or a commentary but is not appropriate for a standard.

1.3 Technical Studies

Nonlinear response history analyses were run on two different building models. One building was a four-story steel moment frame (Figures 1-2 and 1-3) building originally designed to the 1985 Uniform Building Code for Zone 4. The other building was a four-story steel braced frame building (Figures 1-4 and 1-5), also designed to the 1985 Uniform Building Code for Zone 4. Both buildings exhibit common seismic deficiencies found in older steel construction – moment frame connections subject to premature fracture, partial penetration column splices weaker than the column yield moment, thin-walled brace sections susceptible to premature fracture, chevron beams that cannot resist unbalanced forces from one brace buckling, and brace connections weaker than the braces.

Analyses of each building were performed based on the existing provisions in ASCE/SEI 41-17. The buildings were analyzed using all four analysis procedures in ASCE/SEI 41 – Linear Static (LSP), Linear Dynamic (LDP) using modal response spectrum, Nonlinear Static (NSP), and Nonlinear Dynamic (NDP) using response history with direct integration. The focus of the studies was on the NDP. The NDP analysis was compared against the two linear procedures and the NSP, with the belief that the NDP should provide the most reliable assessment of building performance given the significant increase in complexity.

The seismic hazards used for the analysis were based on a Site Class D in the San Francisco Financial District. Ground motion suites were developed for the BSE-1E, BSE-1N, BSE-2E, and BSE-2N hazards. Analyses used either the BSE-1E and BSE-2E hazards or all four hazards. Part 2, Appendix A, which can be found at http://femap2208.atcouncil.org/, presents a detailed summary of the building evaluations conducted as part of this project. The analysis models were used to assess changes as discussed in the following sections.

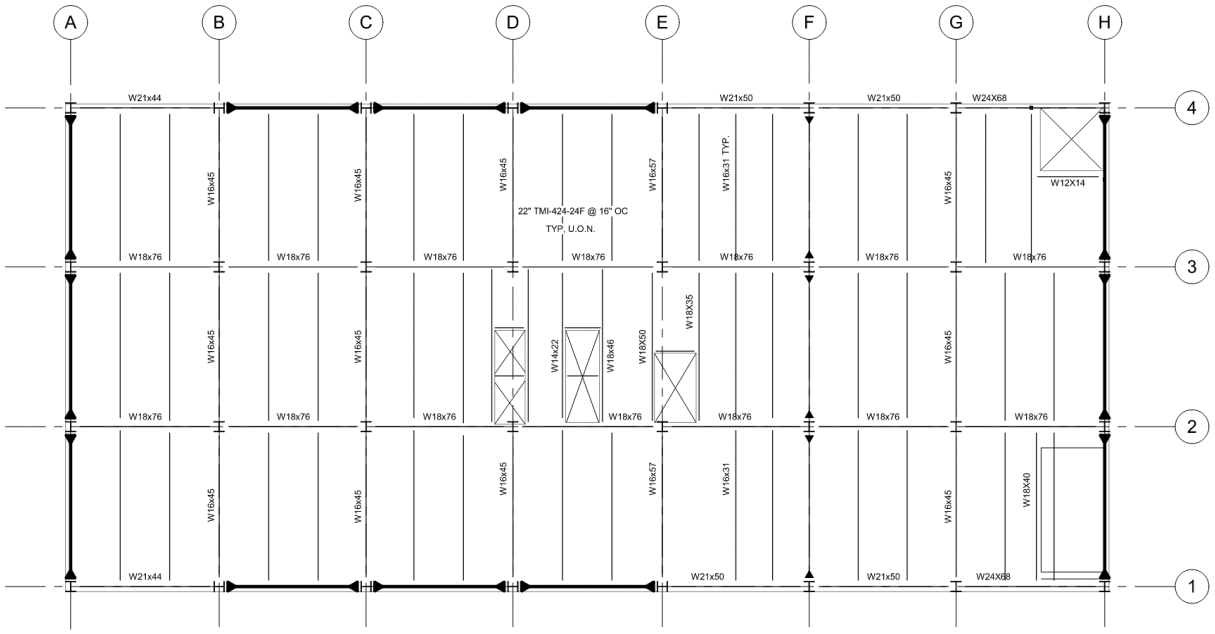

Figure 1-2 Moment frame building plan.

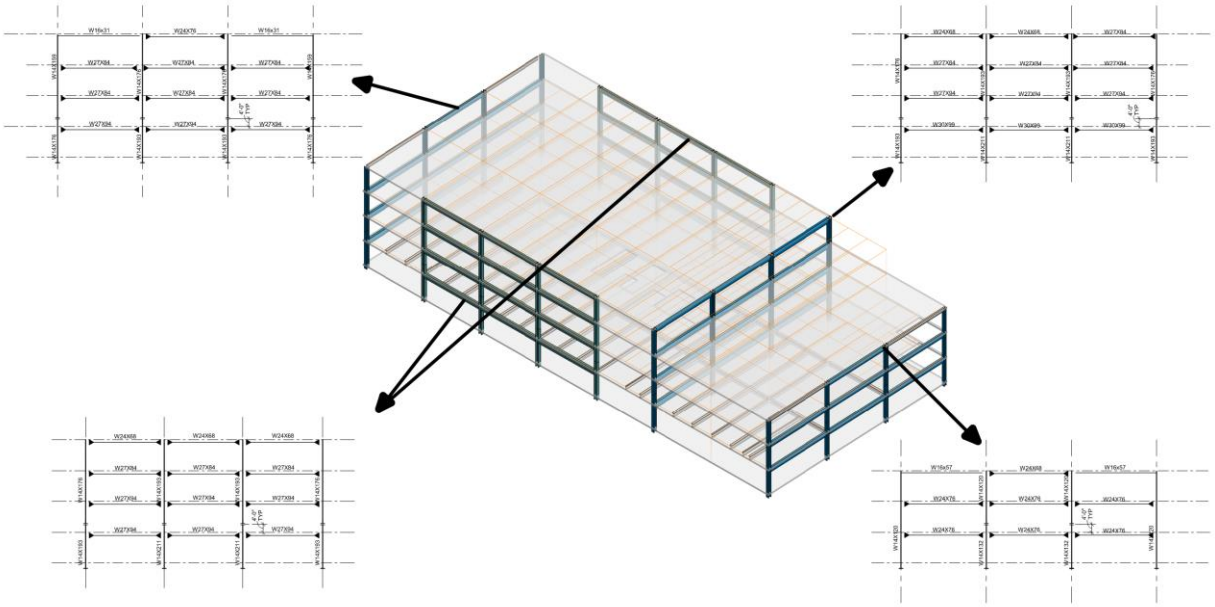

Figure 1-3 Moment frame building isometric and elevations.

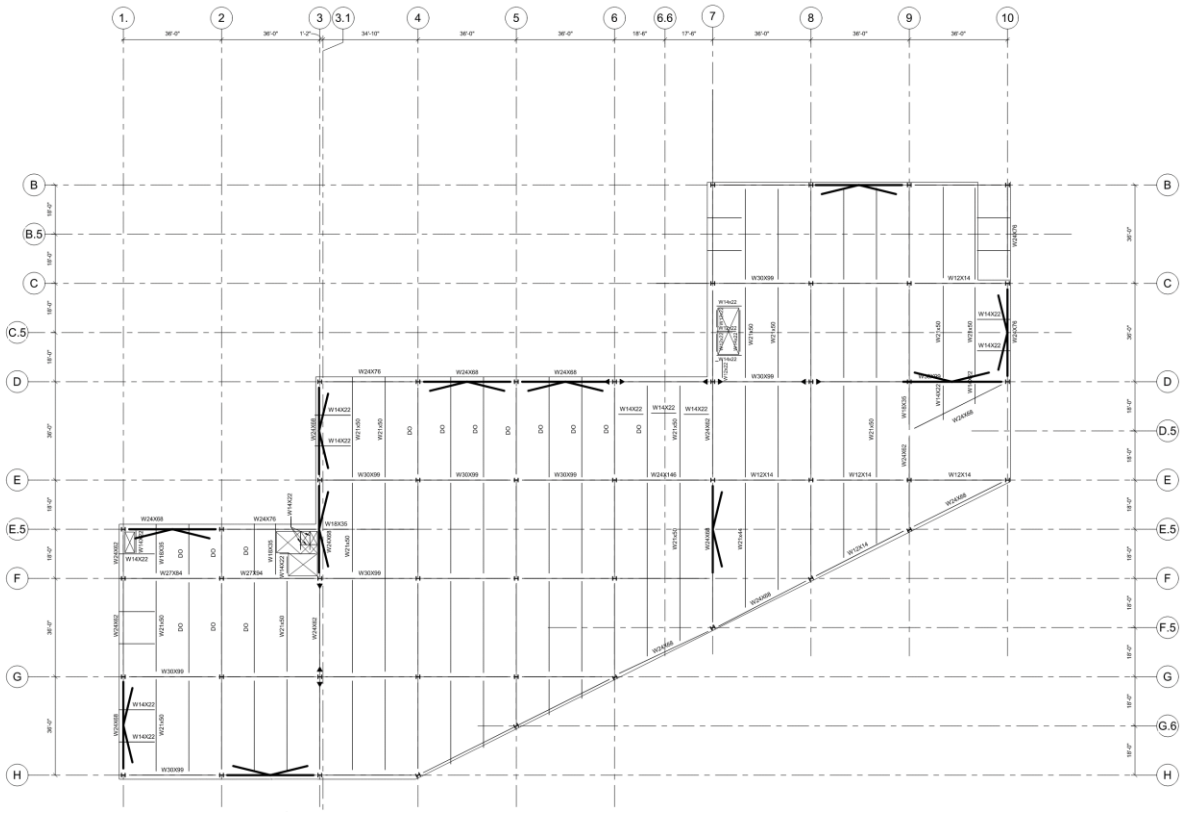

Figure 1-4 Braced frame building plan.

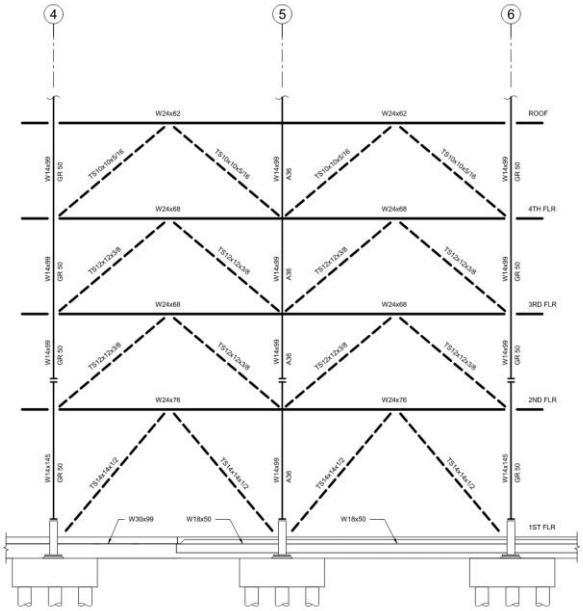

Figure 1-5 Braced frame elevation.

1.3.1 Critical and Ordinary Actions

The proposed change to eliminate noncritical as a designation and consolidate to either a critical or ordinary action was assessed by reviewing the ASCE/SEI 41-17 provisions and determining that the technical provisions do not require anything different for the ordinary and noncritical actions. Looking at the response of actions classified as ordinary or noncritical in the various analyses of the two existing buildings did not provide any indication that there should be different criteria for either. For both ordinary and noncritical force-controlled actions, failure of either has an impact on the response of the structure. It was observed that if force-controlled actions were explicitly modeled with a nonlinear curve representing almost immediate strength degradation once the action's strength is reached, the performance of the building can change and provide a different result than if the action was modeled elastically, regardless of whether the action is critical, ordinary, or noncritical.

When looking at the braced frame building, if a brace connection's failure led to loss of a brace capacity, and that brace's capacity loss then created a weak story, the nonlinear analysis would amplify that weak story. However, if the brace connections were simply included in the model elastically, that weak story would not occur, and the analysis would provide potentially unconservative estimates of performance.

CONCLUSIONS

The fact that explicitly modeling failure of force-controlled actions showed a change in the building performance relative to modeling them elastically and assessing them outside of the model demonstrated a need to place heightened requirements on those actions when they can change the structure's response significantly. After looking at different ways to identify what would be significant,

it was determined that if an action's failure introduced a torsional strength irregularity or weak-story irregularity, it would lead to a significant change in response.

1.3.2 Force-Controlled Actions

As stated previously, in ASCE 41-17, overstress of a critical force-controlled actions relative to its expected strength is considered an unacceptable response, unless the action is explicitly modeled with a nonlinear force-deformation relationship that represents sudden loss of resistance at overstress and the user confirms that failure of the component action doesn't cause a gravity load collapse that is not captured in the model. To study the consequences of failure of force-controlled actions, the braced frame model was run 1) with the brace connections modeled elastically and 2) with the brace connections modeled using a Type 3 force-displacement relationship with the maximum strength based on the connection strength computed with expected material properties. Figure 1-6 shows the story drift plots for the model where the chevron beam and the brace connections are modeled elastically. Figure 1-7 shows the drift plot for the model with the connection failure and flexural yielding of the chevron beam explicitly included in the model with nonlinear force-deformation relationships. Figure 1-8 shows an overlay of the drifts without fracturing connections (dashed lines) and the drifts with fracturing connections (solid lines). The figures show that the behavior of the building is significantly affected by the nonlinear behavior of the force-controlled elements.

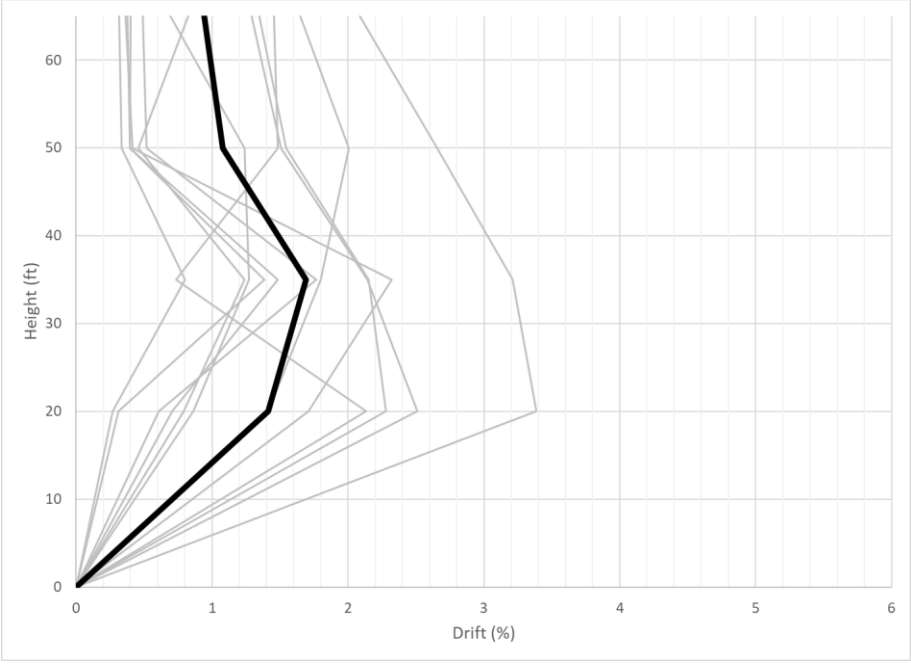

Figure 1-6 Brace frame model with elastic force-controlled actions.

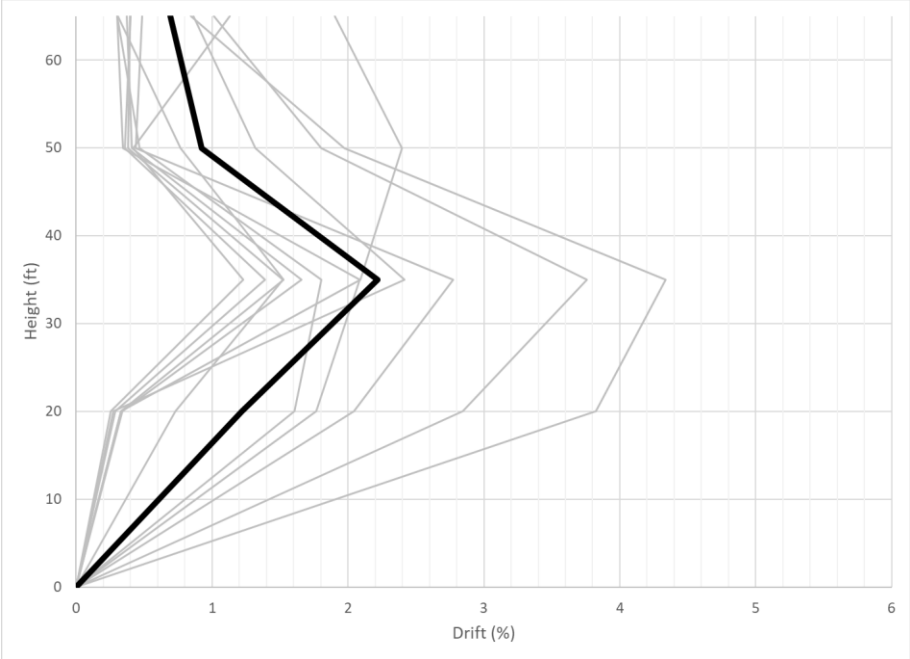

Figure 1-7 Brace frame model with force-controlled action failure explicitly modeled.

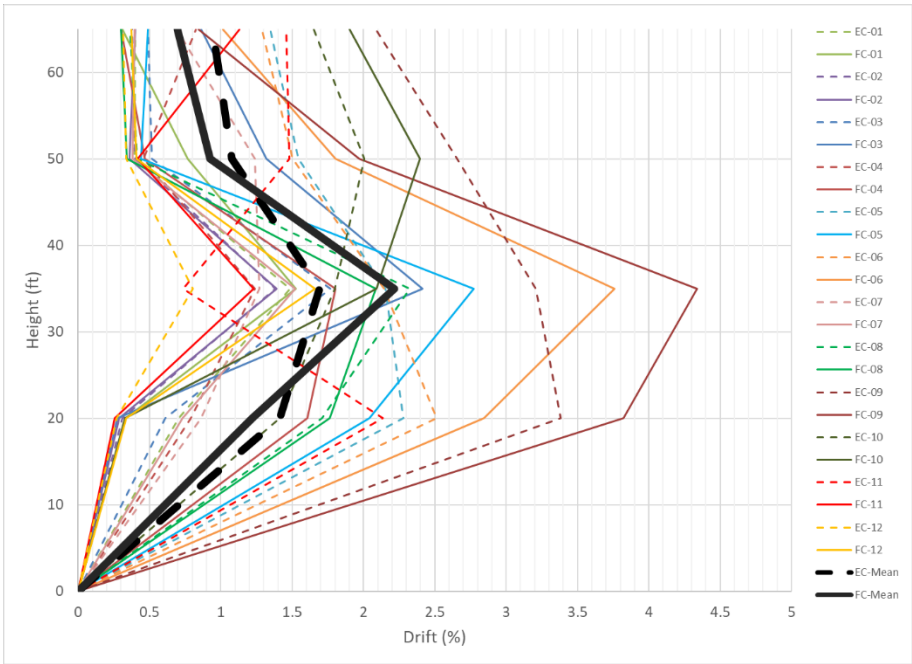

Figure 1-8 Drift comparison with (solid) and without (dashed) force-controlled actions explicitly modeled.

CONCLUSIONS

Because ordinary force-controlled actions are only checked using lower-bound properties, which in some cases are only 10% less than the expected, against the mean response, there can be a

substantial number of records in the suite where the ordinary force-controlled actions are overstressed, leading to significantly different behavior of the model. When the force-controlled actions were explicitly modeled with nonlinear properties, the mean story drift increased by 25% and the maximum story drift increased by about 40%. Drift increases of 25% and 40% are significant and illustrate how allowing force-controlled actions to remain elastic in the model can lead to unconservative demands on the deformation-controlled actions and other force-controlled actions in the model. Therefore, the decision to change the unacceptable response provisions to consider overstress of any force-controlled action, instead of just critical force-controlled actions was the correct choice.

1.3.3 Unacceptable Response Story Drift Ratio Limit

Initially there was discussion about whether to include drift limits in ASCE 41. The project team ultimately chose not to recommend mean drift limits akin to those in ASCE/SEI 7. The primary reason was that there was not good information on what appropriate drift limits would be for existing systems. ASCE/SEI 7 and the material standards referenced therein set forth numerous prescriptive requirements on configuration layout (definition and limitation on irregularities), redundancy factor, types of systems, and the detailing of structural members, which in turn provides for some uniformity in ductility and system response. Existing buildings often do not have such uniformity, which would require very conservative drift limits or provisions for drift limits based on detailing. It was felt that if drift limits needed to be based on local component detailing, the existing component acceptance criteria were sufficient for performance prediction. Another reason for drift limits is to control damage of nonstructural components and systems. ASCE/SEI 41's nonstructural provisions require explicit evaluation of the nonstructural components at the peak drift. The project team believed this was a more direct approach than having uniform structural drift limits.

The project team did not believe that residual drift limits should be included in the standard at this time. An agreed upon process for determining residual drift does not exist and if the team were to introduce a limit, procedures to compute it would be required.

However, the project team did feel that a maximum drift beyond which the analysis should be considered unacceptable was prudent. An unacceptable response can be an indicator of global instability of the structure or a local collapse. The existing unacceptable response provisions list four conditions that would deem a nonlinear response unacceptable. The present conditions under which a response is unacceptable include:

1. Nonconvergence of analysis solution, which could indicate collapse or other problems with the software or model,
2. When the deformation in a deformation-controlled element exceeds the valid range of modeling, which could be an indication that the model's results are unreliable because the component action may not behave as the analytical model predicts beyond the valid range of modeling,

3. When a critical force-controlled element that is modeled as linear elastic exceeds its expected capacity, which can lead to a model predicting performance differently than it would have if the force-controlled action was modeled to lose its ability to resist forces in the analysis, and
4. When other nonmodeled elements, mainly gravity elements, exceed their gravity load capacities or cannot maintain load carrying capacity at maximum displacements in the response.

The proposed change adds a fifth, a maximum transient drift limit beyond which the analysis results should be considered invalid, and a hidden collapse mechanism likely exists. The 6% value is based on judgement of the project team, based on knowledge of the limitations of commercial software. While mathematical solvers available in commercial software packages purport capability of producing nonlinear solutions well beyond 6%, the elements available within these software packages often have limited reliability for simulating nonlinear behavior beyond the 4-6% story drift range. For example: only a few elements available in one of the more common software packages can simulate total loss of strength and stiffness at Point E of the backbone. All the remaining elements cannot. Where such total strength and stiffness loss can be modeled, it is often the case that total loss is triggered for both directions of loading even though the component may only have reached Point E in one of the two directions of loading. These limitations may not adequately permit simulating nonlinear behavior at large drifts under asymmetric loading and strength/stiffness properties. In some of the analytical iterations performed, instability was observed when the components were modeled with this strength degradation beyond the E point, while the responses where they did not have that showed stable drifts in excess of 6%.

To further validate the 6% value, the analysis results of all the models with drifts in excess of 6% were studied. In the case of both the moment frame and braced frame buildings, records with drifts in excess of 6% also showed significant deformations in deformation-controlled components, often beyond the valid range of modeling.

CONCLUSIONS

The project team felt that 6% was a reasonable limit to use as a maximum transient story drift above which the results should be considered unacceptable. In all instances where the drift exceeded 6% in a story in the case study buildings, a number of issues were identified that would lead to the user determining that the specific response was unacceptable. It was rare to find a situation where a response exceeded 6% drift and one of the other four unacceptable response conditions was also not met. While this is redundant, the project team felt that having the 6% limit could also serve as a simplified way to determine that response is unacceptable.

1.3.4 No Unacceptable Responses for Life Safety

If Collapse Prevention means a 10% probability of collapse given the specific seismic hazard intensity, a 4/3 factor of safety beyond that point would imply that the Life Safety performance level means a 10% probability of collapse given 1.33 times the specific seismic hazard intensity being considered. Figure 1-9 presents a graph of probability of collapse with respect to spectral acceleration for different coefficients of variation assuming a lognormal distribution. The fragility

curve assumed for new buildings with a β = 0.6 is provided along with curves for two smaller values of β. In general, existing buildings are typically more brittle than new buildings that have been designed, detailed, and inspected to achieve ductile components. These ductile components have been achieved through decades of evolving ductile detailing provisions in the material standards. The lack of ductility and configuration limitations in existing buildings can lead to a collapse fragility that is less sensitive to record-to-record variability, therefore having a lower coefficient of variation. For all three curves, the probability of collapse is less than 5% for a spectral acceleration taken as 75% of the value which provides a 10% probability of collapse. Haselton et al. (2017) demonstrated through statistical analysis that one ground motion out of a suite of eleven being unacceptable and possibly indicating a collapse would not provide a 5% probability of collapse.

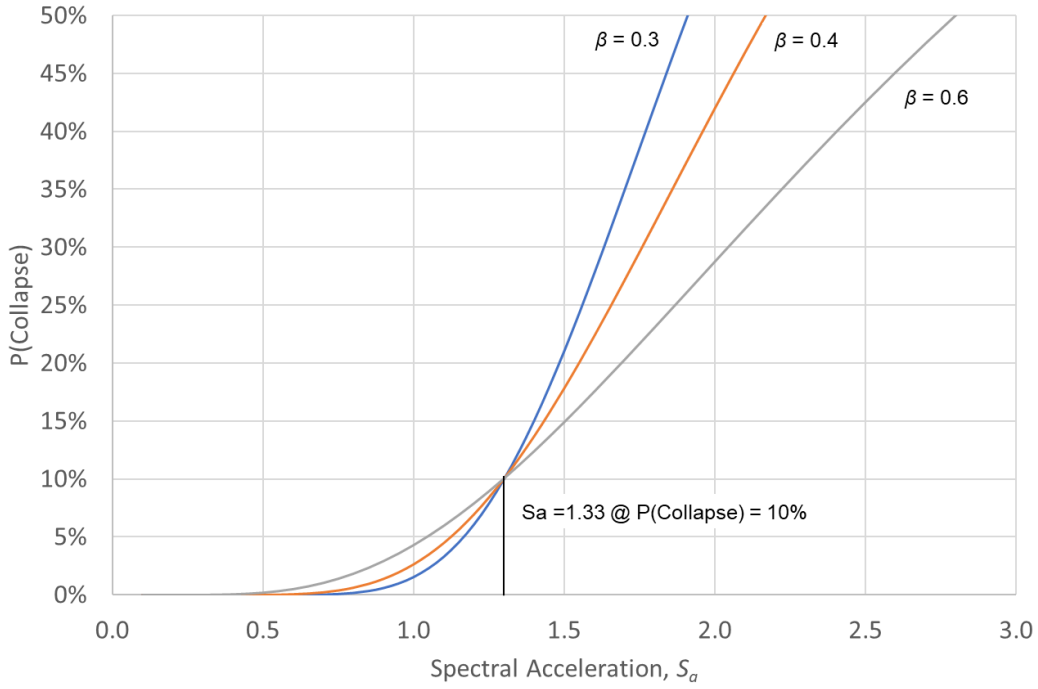

Figure 1-9 Probability of collapse for various COVs.

CONCLUSIONS

Based on the above analysis, to provide the additional protection against collapse implied by the Life Safety performance level, no unacceptable responses out of a suite of eleven ground motion records should be permitted.

1.3.5 Secondary Components

To evaluate the contribution of the secondary system, the moment frame model was modified to remove the secondary PR frames. The building met the criteria of the proposal—the stiffness of the PR frames created by the gravity beam to column shear tab connections are less than 20% of the stiffness of the primary components and the exclusion of the secondary components doesn't shift

the center of rigidity on any of the floors by more than 10%. Figure 1-10 show drift plots for moment frame building with and without the secondary components. In each case, the secondary components reduced the overall drift in the building.

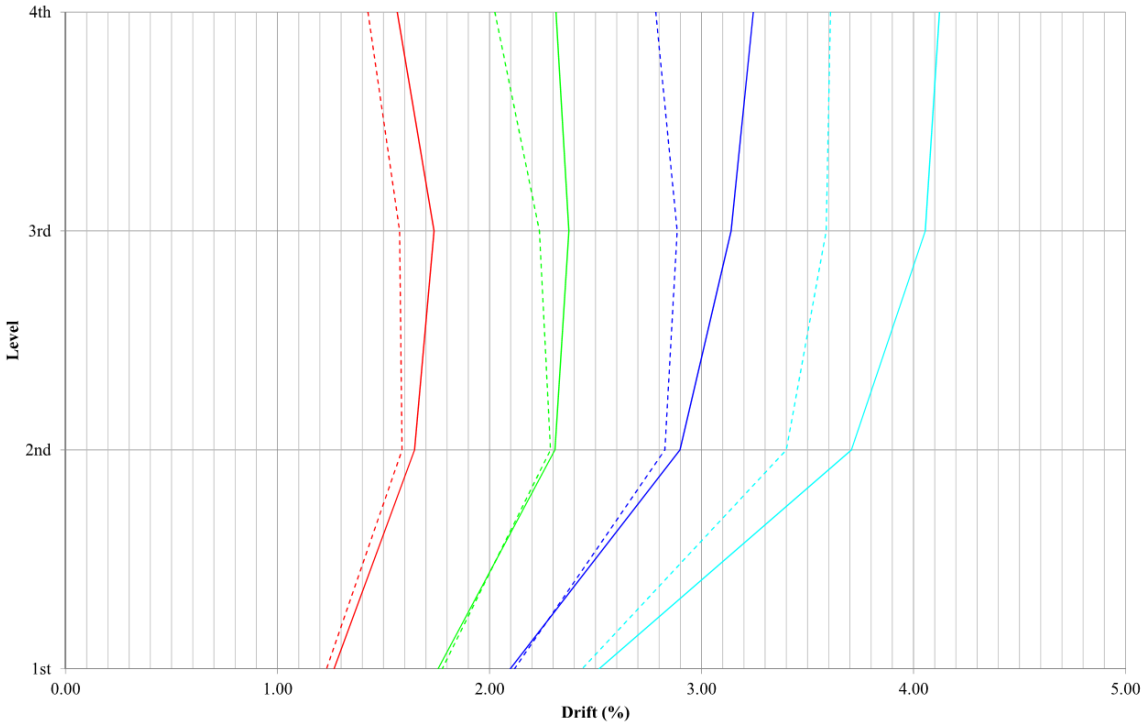

Figure 1-10 Story drift for moment frame model with (dashed lines) and without (solid lines) secondary frames for various seismic hazard levels.

CONCLUSIONS

The presence of the secondary components reduces the overall drift in the building, providing for better performance. Similar response was seen in the braced frame building. So, an analysis conducted for each building that only included the primary components would result in a conservative result, possibly indicating retrofit where it is not needed. Since the intent of the standard is to set a minimum level of work required to demonstrate compliance or noncompliance with a performance objective, the project team felt that it would be acceptable to permit nonlinear analysis without secondary components, provided their exclusion didn't adversely affect the performance or lead to an unconservative result.

There was concern that the secondary components may be excluded at a limit of 25%, while the limit for nonstructural components is at 10% in ASCE/SEI 41-17. The Project Team believed that nonstructural components should be reclassified as primary components using the same thresholds as the secondary components used. In order to align these two, the secondary components exclusion was reduced from 25% to 20% based on judgement of the Project Team. The nonstructural component exclusion was raised from 10% to 20% based on the judgement of the Project Team.

However, uses should not ignore the combined effect of secondary components and nonstructural components and allow a situation where the combination of secondary components and nonstructural components have a combined stiffness of more than 20%.

Along with allowing secondary components to be excluded from modeling, a new criterion that the secondary and nonstructural components cannot cause a shift in the center of rigidity of the story by more than 10% is added. This was deemed necessary to prevent exclusion of secondary components or reclassification of primary components to miss torsional response. Similar to the rules for when secondary elements should be classified as primary based on overall stiffness, the torsional response limits were based on judgement of the Project Team.

For components that are not included in the nonlinear model, they must be evaluated using the linear static procedures or nonlinear static procedure with deformations from the analysis with the maximum response, as opposed to the suite mean. Maximum deformations were chosen rather than the average deformations because the standard requires consideration of unacceptable responses in each record. Using the maximum deformations is the simplest method to evaluate the demands on secondary components outside of the model to confirm that deformation-controlled actions within the secondary components have not exceeded their acceptance criteria or valid range of modeling, that force-controlled actions within the secondary components have not been stressed beyond their expected capacity, or that any other potential unacceptable response have occurred in the subassemblage.

1.3.6 Damping

PREVIOUS STUDIES

Goel and Chopra (1997) and others have identified a relationship of damping versus structure height (Figure 1-11). PEER TBI v2.03 (2014) recommends the following equation for the maximum damping in a building. The equation is represented graphically in Figure 1-12. PEER TBI caps damping at 5%. For the MCE_R evaluation, PEER TBI also sets a floor on the damping of 2.5%. For the Service Level Earthquake, it does not put a floor on the damping.

$$\zeta_{critical} = \frac{0.36}{\sqrt{H}} \leq 0.05 \tag{1-1}$$

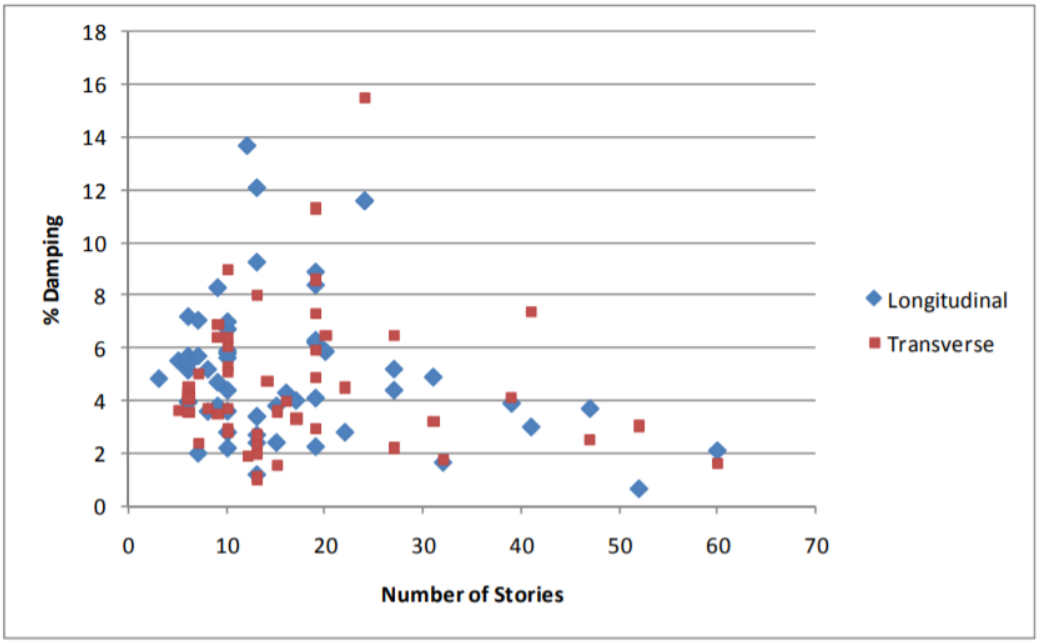

Figure 1-11 Measured percent damping versus building height (PEER/ATC-72-1, 2010).

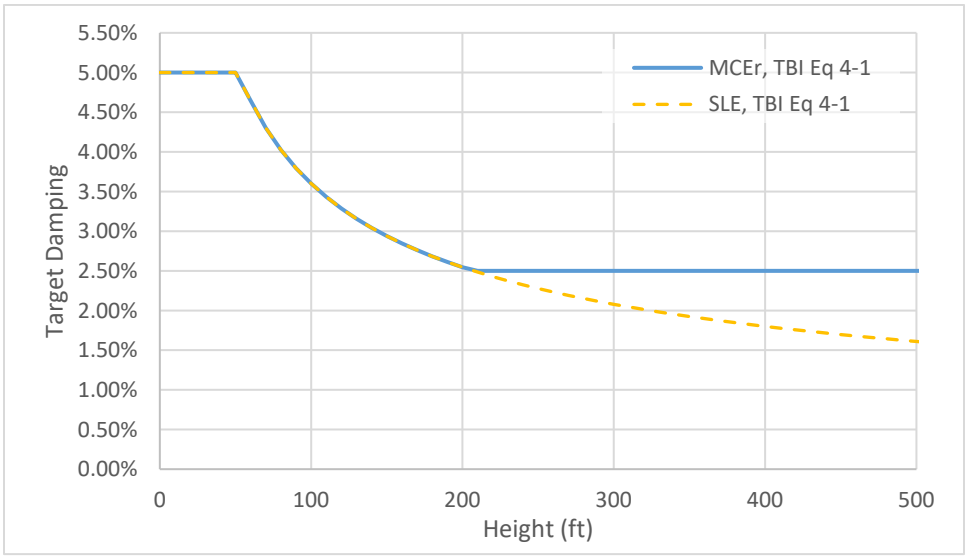

Figure 1-12 Illustration of PEER TBIv2 (2014) damping equation.

Chopra (2016) discusses a phenomenon of spurious damping forces, which could adversely impact the validity of analysis results. In the context of choosing a damping model to employ in response history analysis, consideration should be given to plasticity models and viscous damping assumptions. Response of models employing concentrated or lumped plasticity (zero length) elements have been shown to be sensitive to damping model assumptions. Spurious damping forces have been observed in concentrated plasticity models when used in conjunction with initial-stiffness-proportional Rayleigh damping models (Figure 1-13). Such spurious damping forces can result in effective viscous damping exceeding the target damping, on the order of three times

the yield moment of adjoining structural elements (Chopra, 2016), which can in turn lead to an underestimation of dynamic response. Although the use of tangent-stiffness-proportional Rayleigh damping may substantially diminish such spurious damping forces, this approach is not recommended as it lacks physical basis and has difficult conceptual implications, such as negative damping coefficients associated with the negative tangent stiffness of degrading components. Use of modal damping, which employs a damping matrix constructed by superposition of modal damping matrices, may eliminate spurious damping forces. When such modal damping is employed, damping ratios must be specified for all modes that are expected to contribute significantly to structural response (Chopra, 2016). Response of distributed plasticity elements has been shown to be less sensitive to damping assumptions compared to concentrated plasticity elements. However, even such elements may become more sensitive to damping assumptions at deformation responses approaching collapse (Chopra, 2016; Hall, 2016).

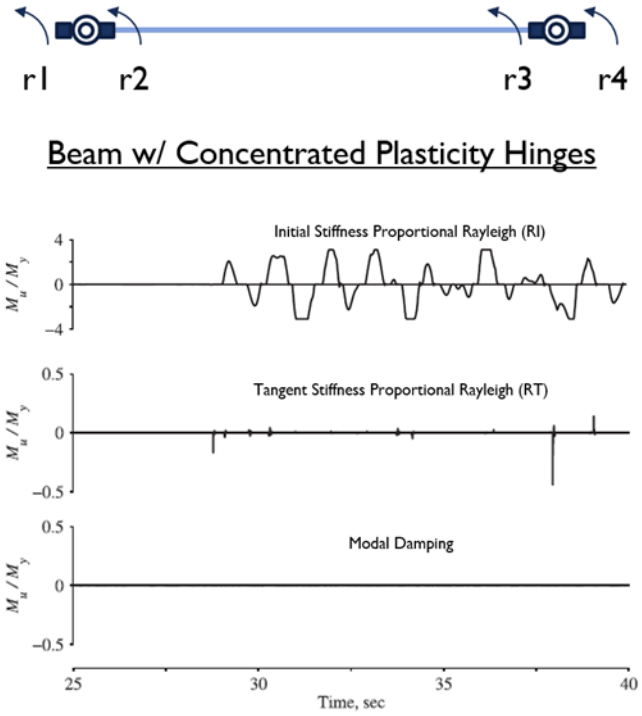

Figure 1-13 Illustration of spurious damping forces.

Use of the mass-proportional damping terms may lead to unrealistically large forces, and an underestimation of response, in structures with large rigid body motion. This effect may be significant in analyses of tall buildings, where drifts in the upper portions of the building are due, in part, to deformations that occur in lower levels of the building (Hall, 2005 via PEER/ATC-72-1, 2010).

CURRENT STUDIES

As the effects of damping are most significant for flexible structure, the moment frame building model was the ideal candidate to assess the effects of the changes in damping formulation. Using

the proposed equation from PEER TBI, the maximum damping for the building is 5% as opposed to the 3% maximum permitted by ASCE/SEI 41-17. The model was run with both damping ratios, using 0.5% Rayleigh damping and the remaining as modal damping. Figure 1-14 shows a plot of two of the seismic hazard suites using the 5% limit on critical damping. The dashed line shows the mean for the 5% damping model and the solid line shows the mean for a model with 2%. Two percent was chosen over the current ASCE/SEI 41 maximum of 3% to further illustrate the global and local effects of changes in damping. As can be seen in Figure 1-14, the change in drift for a 2.5x increase in the damping is about 20% in both the BSE-1E and BSE-2E hazard The 20% change in drift and other response parameters due to the revised damping equation did not lead to a significant change in the building's performance assessment in this case.

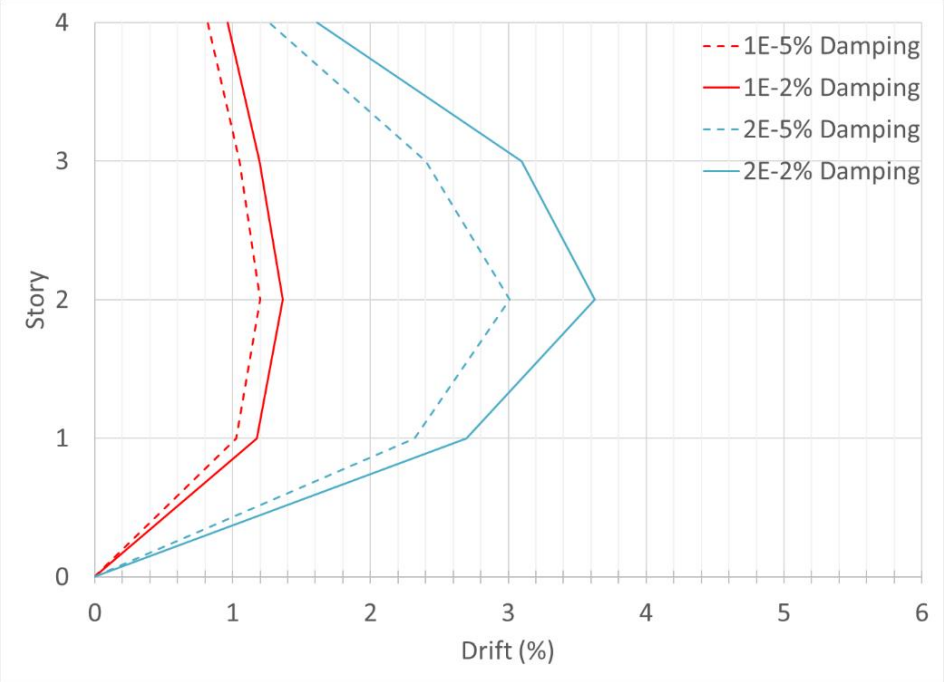

Figure 1-14 Story drift for moment frame model with (solid lines) 5% critical damping and with 2% critical damping (solid lines).

CONCLUSIONS

This change proposal eliminates the requirement that the target elastic effective viscous damping ratio (β) not exceed 3% and introduces the following equation for determining β. This equation is based on research performed by Goel and Chopra in 1997 by analyzing earthquake response data obtained from instrumented buildings. This equation is also adopted by PEER TBI.

$$\beta = 0.36/\sqrt{h} \leq 0.05 \quad (1\text{-}2)$$

where:

h = height of the roof above the grade plane, ft.

Like PEER TBI, damping is capped with an upper-bound of 5%. For Life Safety, Limited Safety, and Collapse Prevention performance levels, there is a 2.5% floor on damping, even though the equation can predict lesser values, similar to what is done in PEER TBI for the MCE_R analysis. Immediate Occupancy and Damage Control do not invoke that floor because structures are more likely to behave similar to an elastic structure at those high-performance levels, similar to what is done in PEER TBI for the service level earthquake analysis. The change proposal also introduces commentary to make the user aware of spurious damping forces.

Section 7.4.4.4 is also modified to explicitly permit the use of the modal damping model in addition to the Rayleigh damping model. This section also lists two conditions for setting up damping models for the NDP. While these conditions are mostly related to the commonly used Rayleigh damping model, they are also relevant for situations where Rayleigh damping is used in conjunction with modal damping.

When Rayleigh damping is employed alone or in conjunction with other damping models, the damping ratio generally varies with the periods of the various free vibration modes of the structure, i.e., each mode is ascribed a different damping ratio (see Figure 1-15).

Thus, the first condition presently listed under Section 7.4.4.4 requires that the average equivalent viscous damping ratio, weighted by mass participation over the modes required to achieve 90% mass participation, does not exceed the target equivalent viscous damping ratio determined using the equation above.

The second condition presently listed under Section 7.4.4.4 requires that the free vibration modes required to achieve 90% mass participation be those with periods no less than one-eighth of the fundamental period. This condition ensures that the overdamping characteristic of Rayleigh damping for higher modes does not influence the response of the nonlinear model.

As part of this change proposal, a third condition is added to ensure that the parabolic variation of Rayleigh damping curve remains anchored at a damping value for periods corresponding to 0.2 times and 1.5 times the fundamental period in each direction that when added to whatever modal damping is included totals the maximum damping value (see Figure 1-15). This ensures that the model remains appropriately damped once the nonlinear model yields and its fundamental period begins to elongate. Without this condition, the yielded structure risks overdamping when the Rayleigh damping model is employed as part of the nonlinear dynamic procedure. The commentary in Section C7.4.4.4 is updated to explain the introduction of this newly introduced third condition.

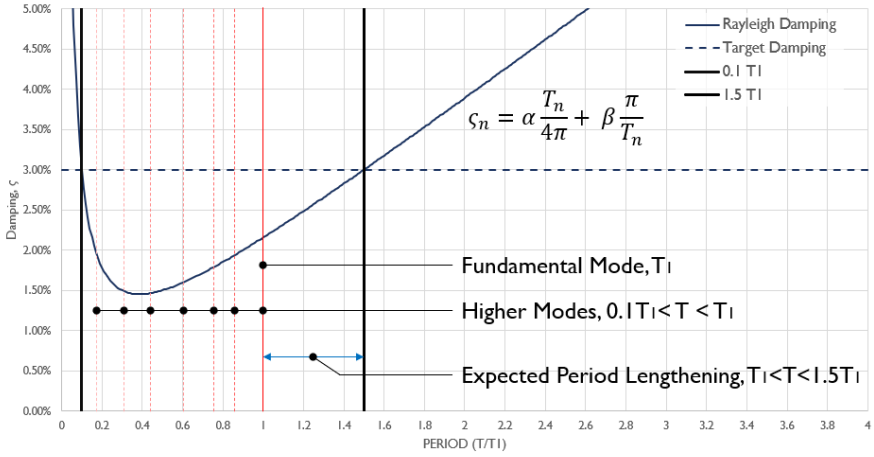

Figure 1-15 Variation of damping ratio with periods of the free vibration modes of the structure per the Rayleigh damping model.

Commentary in Section C7.4.4.4 is also updated to provide guidance related to the use of initial-stiffness and tangent-stiffness matrices as part of the Rayleigh damping model. Recent research (Chopra and McKenna, 2016) has highlighted the role of "spurious damping forces" when initial-stiffness-proportional Rayleigh damping is used in conjunction with models utilizing concentrated plasticity models and how such spurious forces can lead to an underestimation of the nonlinear dynamic response. Also, in line with the research recommendations, the commentary is updated to suggest the use of the modal damping model in lieu of Rayleigh damping when spurious damping forces are expected to affect the response of the nonlinear model. Other minor updates to the commentary are also provided based of recent research.

1.3.7 Accidental Torsion

OVERVIEW

The concept of only requiring accidental torsion in the highest hazard when the Performance Objective requires consideration of multiple hazard intensities is based on the idea that if the building is sensitive to accidental torsion, it will be more pronounced in the higher hazard. So, quadrupling the analyses in both hazard levels is unnecessary. This reasoning is valid if the hazards are far enough apart in intensity and the acceptance criteria for the different performance objectives are not too far apart. In the BPON, the hazards are different by a factor of 1.5. In the BPOE, the difference between the two hazards is at least 1.5 times and can be as high as seven times. Similarly, the difference between the Life Safety and Collapse Prevention acceptance criteria is typically a factor of 1.3. However, when the hazards are closer together or the performance level acceptance criteria further apart, there may be issues excluding accidental torsion from the lower hazard.

There are potential issues with the provision that allows an amplification factor to account for accidental torsion in the NDP. Establishing the amplification factors often requires running some

mass offset permutations. The commentary to Section 7.2.3.2.2 of ASCE/SEI 41-17 acknowledges that there are instances where accidental torsion can increase deformations and trigger mechanisms that would change the response of the building beyond what could be captured with a simple factor. Recognizing this, the project team decided to look at ways to identify when a building is sensitive to accidental torsion and where it should be included to accurately assess the performance objective and not included when it does not substantially affect the analysis results.

The original impetus for accidental torsion requirements in building codes provisions was to ensure that buildings had some level of torsional stiffness and, thus, strength. When engineers were performing analysis by hand and idealizing the structures as two independent orthogonal structures, it would have been possible to design a building with little to no torsional stiffness or strength, such as a cruciform core illustrated in Figure 1-16. Requiring a mass offset that creates torsion would force a designer to change this building to provide some torsional stiffness, which in turn would also provide torsional strength.

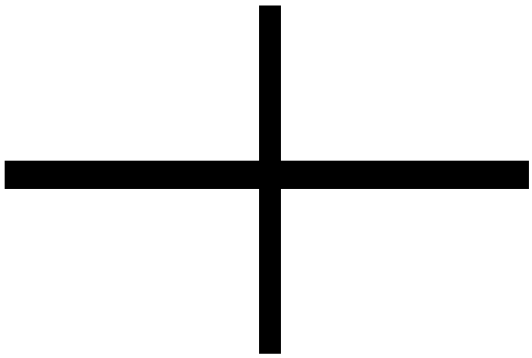

Figure 1-16 Example of building with no torsional resistance.

There are many reasons that a building that appears symmetric could experience torsion (Chopra, 1994):

- The existing mass distribution in the building could be asymmetric. The secondary system could introduce enough stiffness to shift the center of rigidity slightly (note that this is addressed in a separate proposal).
- The inherent variability in actual material properties and construction tolerances could lead to a shifting center of rigidity during response.
- Ground motions can be out of phase over the base of the building, leading to torsional input motion.

CONCLUSIONS

Technical studies were not performed on the accidental torsion provisions. Anecdotal evidence from project team members formed the basis of the assessment of the provisions.

The change proposal incorporates an exemption first proposed in PEER TBI which allows for the exclusion of accidental torsion if the building's twisting due to actual and accidental torsion is low, as measured by the eta parameter, defined as the ratio of the maximum displacement of a point on the diaphragm in the direction of load divided by the average displacement of the diaphragm. It also includes an exemption that allows accidental torsion to be excluded if there is already significant inherent torsion, where inherent torsion is quantified using building stiffness consistent with ASCE 7 analysis procedures. Currently, when accidental torsion needs to be considered, the center of mass is varied positively and negatively in both the principal directions of the structure at every floor. This requirement makes considering accidental torsion in NDP unnecessarily complicated. Generally, it's simple enough to tell which one of the four offset conditions will govern the analytical response. Thus, the new provisions permit the use of one or two offsets instead of four when considering accidental torsion in NDP.

The proposal also eliminates the permission to exclude consideration of accidental torsion in the lower ground motion intensity when one does a two-hazard level analysis. This is done for two reasons. First, when the lower hazards seek higher performance levels like Damage Control or Immediate Occupancy, accidental torsion can have an influence on the buildings response due to factors discussed in the updated commentary. There have been changes to the Life Safety criteria—specifically related to amplified demands on force-controlled actions and eliminating the ability to have an unacceptable response—which warrant doing the evaluation with accidental torsion when it can affect the response. Note that the proposal significantly reduces the conditions when accidental torsion needs to be considered in general, so when one includes accidental torsion, it is likely to have a significant influence on the results.

1.3.8 Material Property Bounding

ASCE/SEI 41 linear procedures allow a reduction in capacity in lieu of material testing for Damage Control, Life Safety, and Collapse Prevention. The project team discussed if a similar approach could be used for the nonlinear procedures. In nonlinear analysis, using only the lower strengths does not always provide a conservative answer. Key components having a higher yield strength can lead to increased demands on other components in the load path.

In order to evaluate the influence of material variability on building response, the project team ran Monte Carlo simulations of the moment frame building by varying the strength of the steel, which impacts when the beam-column connection would fracture. The coefficient of variation was selected to represent both variability due to connection fracture and variability due to material strength. The variability due to connection fracture was taken as 0.15 from NIST GCR 17-917-45. The coefficient of variation of material strength being different than expected based on the ASTM designation was taken as 0.1 based on judgement. Ten different permutations were run with each of the eleven ground motion records. Figure 1-17 presents the drifts from the Monte Carlo simulation, showing the median plus the 10^{th} and 90^{th} percentile drifts.

Similar models were run modifying the beam strengths by 0.75 and 1.25 times the expected (median) capacity as recommended in the change proposal. The factors of 0.75 and 1.25 were

based on a conservative coefficient of variation of 0.25. The bounding analysis showed similar median values (Figure 1-18), but significantly different mean values and differences in the records that produced the largest drifts.

The Monte Carlo simulation results showed considerable variability in the response. However, the median of the results was similar to the median of the results when only run with mean or median material properties (Figure 1-19). Where the Monte Carlo simulations showed unacceptable responses that the mean model did not capture, a model using lower-bound material properties instead of median material properties did capture the unacceptable response.

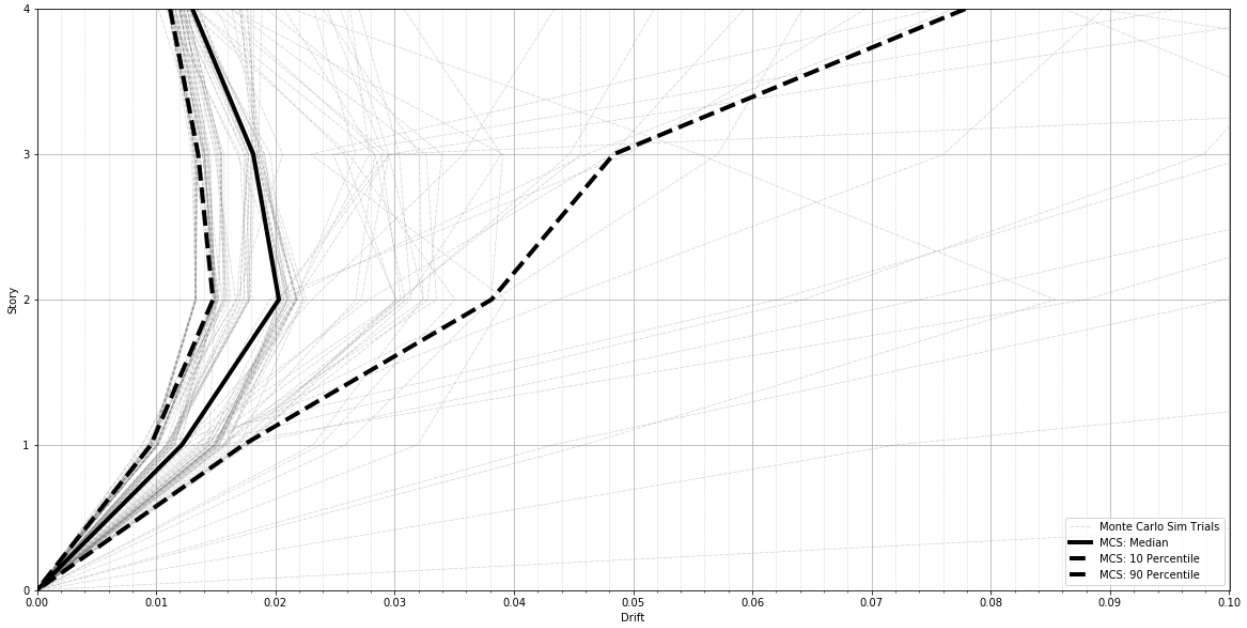

Figure 1-17 Drift response of Monte Carlo simulation varying the beam strength.

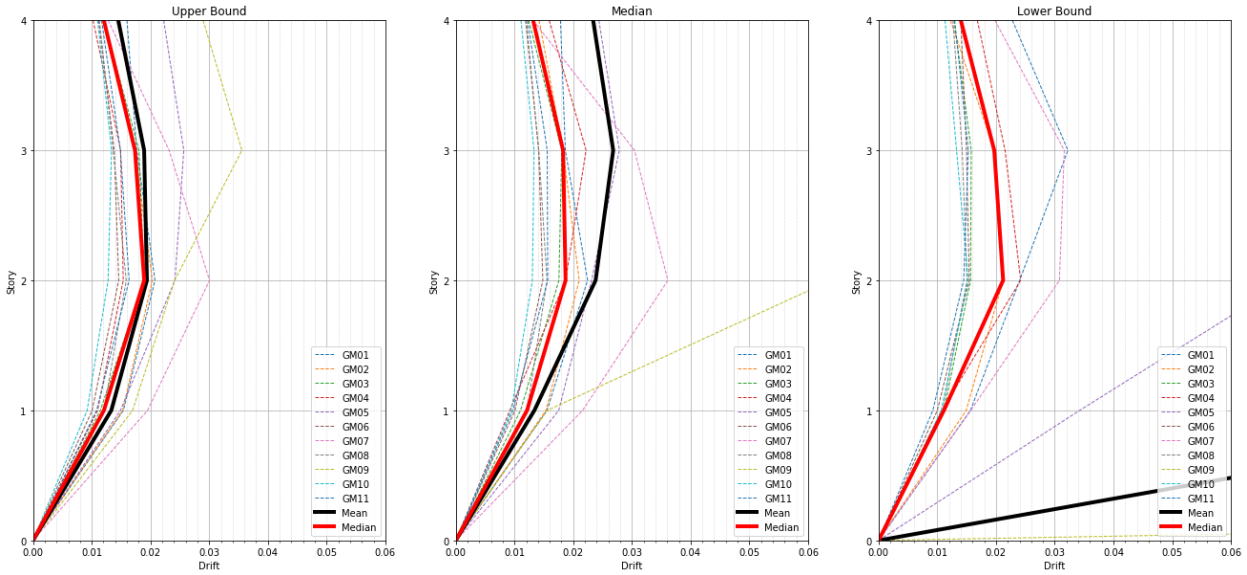

Figure 1-18 Drift response of model with upper-bound, median, and lower-bound beam strength.

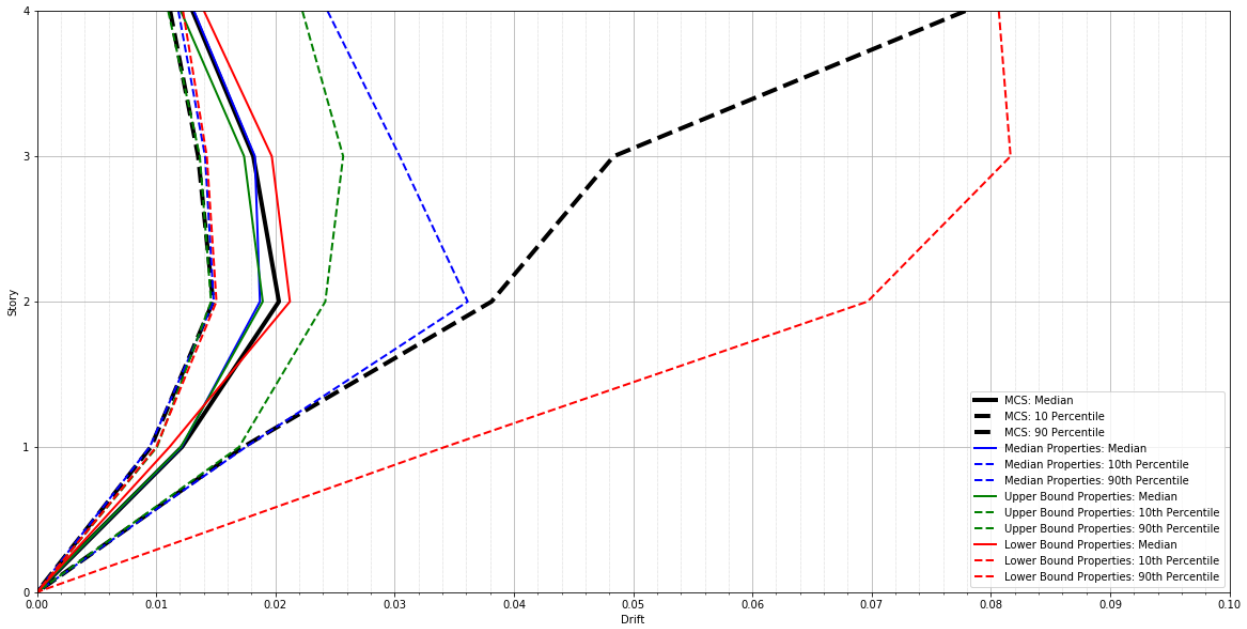

Figure 1-19 Comparison of drift response between Monte Carlo simulation and strength bounding cases.

CONCLUSIONS

Based on the above studies, allowing the user to perform multiple nonlinear analyses to bound the range of material properties appears reasonable. At a minimum, one model should be based on lower-bound assumptions and another based on upper-bound assumptions. Language on when to

combine the properties, as there are special circumstances where a combination may produce the worst-case results, will be included.

The Monte Carlo simulation showed that if there was uncertainty in the material properties, it is possible that modeling only using median or expected properties may not capture some of the more extreme response conditions, possibly missing unacceptable responses. Incorporating a lower-bound material property model does appear to capture the extreme conditions, albeit potentially in a conservative manner. Additionally, the upper-bound material property model provided the highest demands on force-controlled components not modeled explicitly in the analysis.

Mixing material testing and bounding analysis is permitted because there may be some components where the performance of the building relies on the best knowledge of material properties while other components are not sensitive to material strengths. For example, in a concrete wall building the performance of the building could be very sensitive to whether the wall is shear or flexure controlled. However, the concrete diaphragms are robust enough that the material strength could be half what is specified on the drawings and the diaphragms have sufficient capacity. In this case, it would be prudent to perform material testing on the walls, but not on the diaphragm.

Where bounding analyses are already required, such as seismic isolation and supplemental energy dissipation device properties, material bounding properties should be aligned with the other bounding parameters. For example, lower-bound material properties should be used in conjunction with lower-bound isolator properties and vice-versa. As an exception, certain configurations, such as a discontinuous wall, may necessitate a combination of upper-bound properties on one component (the wall) and lower-bound properties (the column or beam supporting the wall) and vice-versa.

The project team felt that bounding analyses should not be allowed for unreinforced masonry (URM) components because there is a large amount of variation in as-built conditions. Comprehensive testing will still be required for URM buildings prior to finalizing an evaluation or retrofit.

1.4 Recommended Changes

Note about Change Proposals

This report documents aspects of change proposals as they were submitted to subcommittees of ASCE's Seismic Retrofit of Existing Building Standards Committee. Often, these change proposals were revised, in some cases substantively, by these subcommittees before they were adopted into ASCE/SEI 41-23. Readers should not rely on this report for information about the final version of provisions in ASCE/SEI 41-23.

1.4.1 Critical and Ordinary Actions

This section describes recommended changes to ASCE/SEI 41-17 Section 7.5.1.2. The proposed change introduces definitions of critical actions and defines anything that does not meet that definition as ordinary. New or modified text is shown in blue.

7.5.1.2 Deformation-Controlled and Force-Controlled Actions

All actions shall be classified as either deformation controlled or force controlled using the component force versus deformation curves shown in Fig. 7-4.

[…]

A component action shall be classified as critical if its failure would result in the collapse of more than one structural bay on one or more stories or a reduction in strength of the lateral force resisting system that results in a weak story or torsional irregularity per Section 7.3.1.1. All other actions shall be classified as ordinary.

1.4.2 Force-Controlled Actions

This section describes recommended changes to ASCE/SEI 41-17 Section 7.5.1.2 and 7.5.3.2.1. The proposed change to Section 7.5.1.2 clarifies that any action not included in the nonlinear analysis with an explicit force-deformation relationship should be considered force-controlled and how one can include a force-controlled action explicitly in the nonlinear model using a Type 3 force-displacement relationship. The change in Section 7.5.3.2.1 makes the overstress of any elastically modeled force-controlled action an unacceptable response.

7.5.1.2 Deformation-Controlled and Force-Controlled Actions

All actions shall be classified as either deformation controlled or force controlled using the component force versus deformation curves shown in Fig. 7-4.

[…]

The Type 3 curve depicted in Fig. 7-4 is representative of a brittle or nonductile behavior where there is an elastic range (points 0 to 1 on the curve) followed by loss of seismic-force-resisting capacity at point 3 and loss of gravity-load-resisting capacity at the deformation associated with point 4. Primary component actions exhibiting this behavior shall be classified as force controlled. Secondary component actions exhibiting this behavior shall be classified as deformation controlled if $f \geq 2g$; otherwise, they shall be classified as force controlled.

When nonlinear procedures are used, any action not explicitly represented in the mathematical model with a Type 1, Type 2, Type 3 or other nonlinear response curve conforming to Section 7.6 shall be classified as a force-controlled action. For nonlinear procedures, force-controlled ~~components~~ actions ~~defined in Chapters 8 through 12~~ may be reclassified as ~~Type 3~~ deformation-controlled ~~components~~ actions if represented in the mathematical model using a Type 3 curve, provided the following criteria are met:

(1) The component action being reclassified exhibits the Type 3 ~~deformation controlled performance~~ behavior defined in this section;

(2) The gravity-load-resisting load path is not altered, or if it is altered, an alternate load path is provided to ensure local stability is maintained in accordance with the load combinations of Section 7.2.2 at the anticipated maximum displacements predicted by the analysis;

(3) The total gravity load supported by all components that are reclassified from force controlled to deformation controlled does not exceed 5% of the total gravity load being supported at that story; and

~~(4) All remaining deformation-controlled components meet the acceptance criteria to achieve the target performance level and all remaining force-controlled components are not overstressed.~~

Where overstrength of Type 3 components alters the expected mechanism in the building, the analysis shall be repeated with the affected Type 3 component strengths increased by the ratio Q_{CE}/Q_y, and all components shall be rechecked.

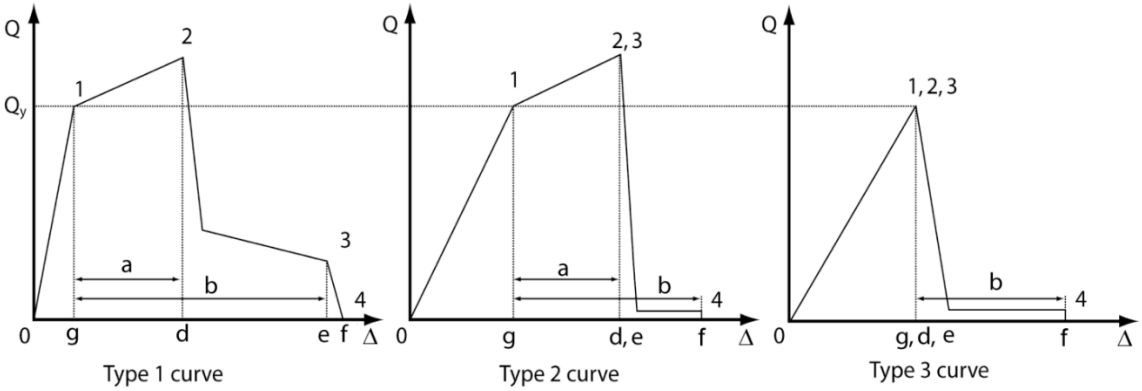

Figure 7-4. Component Force Versus Deformation Curves

Notes:

1. Only secondary component actions permitted between points 2 and 4;
2. The force, Q, after point 3 diminishes to approximately zero.

7.5.3.2 Acceptance Criteria for Nonlinear Procedures

7.5.3.2.1 Unacceptable Response for NDP

Unacceptable response to ground motion shall not be permitted for NDP. Any one of the following shall be deemed to be an unacceptable response:

(1) Analytical solution fails to converge,

(2) Predicted demands on deformation-controlled elements exceed the valid range of modeling,

(3) Predicted demands on force-controlled critical actions that are ~~modeled elastically, as defined in Section 7.5.3.2.3~~ not explicitly included in the mathematical model with a nonlinear force-displacement curve exceed the expected element capacity, or

(4) Predicted deformation demands on elements actions not explicitly modeled exceed the deformation limits at which the members are no longer able to carry their gravity loads.

1.4.3 Unacceptable Response Drift Limit

This section describes recommended changes to ASCE/SEI 41-17 Section 7.5.3.2.1. The proposed change states that if any story reached six percent peak transient drift in an analysis, that analysis should be considered an unacceptable response.

7.5.3.2 Acceptance Criteria for Nonlinear Procedures

7.5.3.2.1 Unacceptable Response for NDP

Unacceptable response to ground motion shall not be permitted for NDP. Any one of the following shall be deemed to be an unacceptable response:

(1) ~~Analytical~~ Computational solution fails to converge,

(2) Predicted demands on deformation-controlled elements exceed the valid range of modeling,

(3) Predicted demands on force-controlled critical actions that are modeled elastically, as defined in Section 7.5.3.2.3 exceed the expected element capacity, or

(4) Predicted deformation demands on elements actions not explicitly modeled exceed the deformation limits at which the members are no longer able to carry their gravity loads.

(5) Peak transient story drift exceeds 6% in a story.

1.4.4 No Unacceptable Responses for Life Safety

This section describes recommended changes to ASCE/SEI 41-17 Section 7.5.3.2.1. The proposed change eliminates the ability to have any unacceptable response when targeting the Life Safety structural performance level and clarifies how to compute the parameter of 120% of the median when the engineer does have an unacceptable response.

7.5.3.2 Acceptance Criteria for Nonlinear Procedures

7.5.3.2.1 Unacceptable Response for NDP

Unacceptable response to ground motion shall not be permitted for NDP. Any one of the following shall be deemed to be an unacceptable response:

[…]

Exception: For ~~Life Safety or lower~~ Limited Safety and Collapse Prevention Performance Levels, not more than one ground motion per 11 analyses shall be permitted to produce unacceptable response. When a ground motion produces unacceptable response, the average response shall be computed as 120% of the median value of all records considering unacceptable responses being larger than the median, but not less than the mean value obtained from the suite of analyses producing acceptable response.

1.4.5 Secondary Components

This section describes recommended changes to ASCE/SEI 41-17 Section 7.2.3.3. The most significant part of the proposed change is the relaxation on needing to include all secondary components in a nonlinear analysis. The change proposal specifies conditions where secondary components must be included and revises the criteria when components can be classified as secondary.

7.2.3.3 Primary and Secondary Components

Components shall be classified as primary or secondary as defined in Section 7.5.1.1. Primary components shall be evaluated for earthquake-induced forces and deformations in combination with gravity load effects. Secondary components shall be evaluated for earthquake-induced deformations in combination with gravity load effects.

Mathematical models for use with linear analysis procedures shall include the stiffness and resistance of only the primary components. If the total initial lateral stiffness of secondary components in a building exceeds ~~25%~~ 20% of the total initial lateral stiffness of primary components or the inclusion of the secondary components causes the center of rigidity of any story to shift by more than 10% in any direction, except when the diaphragm can be classified as flexible, some secondary components shall be reclassified as primary to reduce the total stiffness of secondary components to less than ~~25%~~ 20% of the primary components or the inclusion of the secondary components change in the diaphragm center of rigidity to less than 10% in all directions. If the inclusion of a secondary component increases the force or deformation demands on a primary component by more than 10%, the secondary component shall be reclassified as primary and included in the model.

Mathematical models for use with nonlinear procedures shall include the stiffness and resistance of primary and secondary components. The strength and stiffness degradation of primary and secondary components shall be modeled explicitly. It is permitted to exclude the secondary components from the nonlinear mathematical model unless omission of the secondary components decreases deformation or force demand on the primary components by more than 10%. If secondary components are not included in the mathematical model, they shall be evaluated at the target displacement in the nonlinear static procedure or the maximum of the maximum deformation from each record in the nonlinear dynamic procedure using a linear static or nonlinear static analysis.

Nonstructural components shall be classified as structural components and shall be included in mathematical models if their lateral stiffness or strength exceeds ~~10%~~ 20% of the total initial lateral stiffness or expected strength of a story, respectively, or causes the center of rigidity of any story to shift by more than 10% in any direction except when the diaphragm can be classified as flexible.

A. Components shall not be selectively designated primary or secondary to change the configuration of a building from irregular to regular.

1.4.6 Damping

This section describes recommended changes to ASCE/SEI 41-17 Section 7.2.3.6 and 7.4.4.4. The most significant part of the proposed change is the adoption of a height-based maximum damping value instead of the standard 3% value. All the damping provisions for the NDP are relocated from Section 7.2.3.6 to 7.4.4.4 to eliminate having requirements in two different sections.

7.2.3.6: Damping

For linear static, linear dynamic, and nonlinear static procedures, 5% damped response spectra shall be used for the analysis of all buildings except those meeting the following criteria:

(1) For buildings without either exterior cladding or nonstructural interior partitions, an effective viscous damping ratio, β, equal to 2% of critical damping ($\beta = 0.02$) shall be assumed;

(2) For buildings with wood diaphragms and cross walls that interconnect the diaphragm levels at a maximum spacing of 40 ft (12.2 m) on center transverse to the direction of motion, an effective viscous damping ratio, β, equal to 10% of critical damping (β = 0.10) shall be permitted;

(3) For buildings using seismic isolation technology or enhanced energy dissipation technology, an equivalent effective viscous damping ratio, β, shall be calculated using the procedures specified in Chapters 14 and 15; or

(4) There is sufficient analysis or test data based on the specific characteristics of the building to substantiate the use of a damping ratio other than 5% (β = 0.05).

Damping of the building system shall be implemented in the analysis procedure in accordance with the requirements of Sections 7.4.1.4 and 7.4.2.4 for linear procedures, Section 7.4.3.4 for the nonlinear static procedure, and as augmented by soil–structure interaction per Section 8.5.2.

~~For the nonlinear dynamic procedure, the target elastic effective viscous damping ratio shall not exceed 3% (β = 0.03), except for buildings meeting any of the follow criteria:~~

~~(1) For buildings without exterior cladding, the target effective elastic viscous damping ratio shall not exceed 1% (β = 0.01)~~

~~(2) Higher target elastic effective viscous damping ratios shall be permitted if substantiated through analysis or test data.~~

Damping for the building system shall be implemented in the nonlinear dynamic analysis procedure in accordance with the requirements of Section 7.4.4.4.

For buildings using seismic isolation technology or enhanced energy dissipation technology, the effects of added viscous damping shall be incorporated directly in the nonlinear dynamic analysis in accordance with the procedures specified in Chapters 14 and 15.

7.4.4.4 Damping for NDP

For the nonlinear dynamic procedure, the target elastic effective viscous damping ratio shall be permitted to be calculated using Eq. (7-XX), except for buildings meeting any of the follow criteria:

(1) For buildings without exterior cladding, the target effective elastic viscous damping ratio shall not exceed 1% (β = 0.01).

(2) Higher target elastic effective viscous damping ratios shall be permitted if substantiated through analysis or test data.

$$\beta = 0.025 \le 0.36/\sqrt{h} \le 0.05 \qquad (7\text{-XX})$$

Damping shall be modeled using Rayleigh damping, modal damping, or other rational methodology. ~~Target equivalent elastic viscous damping ratios shall be determined in accordance Section 7.2.3.6.~~ Where damping is implemented using mass and stiffness proportional methods, the target equivalent viscous damping ratios shall be applied such that: ~~the total elastic viscous damping in the range of 0.2 times and 1.5 times the fundamental period in each direction is the first translational mode in each direction, including expected period lengthening under nonlinear response, is damped by no more than the target equivalent viscous damping ratio and~~

(1) The average equivalent viscous damping ratio, weighted by mass participation over the modes required to achieve 90% mass participation, shall not exceed the target equivalent viscous damping ratio; and

(2) No more than eight times the first translational mode damping is provided in the highest translational mode required to achieve 90% mass participation, unless substantiated through analysis or test data; and.

(3) The total elastic effective viscous damping ratio in the range of 0.2 times and 1.5 times the fundamental period in each direction is no more than the target elastic effective viscous damping ratio.

1.4.7 Accidental Torsion

This section describes the recommended changes to ASCE/SEI 41-17 Section 7.2.3.2.2 and introduces a new Section 7.2.3.2.3. The changes relate to how the user considers accidental torsion in their analysis. Section 7.2.3.2.2 is adjusted to be limited in scope to the provisions for linear procedures, without any substantive changes. The new Section 7.2.3.2.3 addresses when and how to consider accidental torsion when performing a nonlinear analysis procedure. The proposed changes seek to reduce how frequently engineers need to include accidental torsion via mass offset in nonlinear analyses.

7.2.3.2 Torsion.

The effects of torsion shall be considered in accordance with this section. Torsion need not be considered in buildings with flexible diaphragms as defined in Section 7.2.9.

7.2.3.2.1 Total Torsional Moment.

The total torsional moment at a story shall be equal to the sum of the actual torsional moment and the accidental torsional moment calculated as follows:

(1) The actual torsional moment at a story shall be calculated by multiplying the seismic story shear force by the eccentricity between the center of mass and the center of rigidity measured perpendicular to the direction of the applied load. The center of mass shall be based on all floors above the story under consideration. The center of rigidity of a story shall include all vertical seismic-force-resisting elements in the story.

(2) The accidental torsional moment at a story shall be calculated as the seismic story shear force multiplied by a distance equal to 5% of the horizontal dimension at the given floor level measured perpendicular to the direction of the applied load.

~~(3) When two or more Seismic Hazard Levels are evaluated using nonlinear procedures and a three-dimensional model is used, accidental torsion need only be included in the analysis for the higher hazard level.~~

Refer to Chapters 14 and 15 for accidental torsional requirements for nonlinear analysis of seismically isolated and supplementary damped structures, respectively.

7.2.3.2.2 Consideration of Torsional Effects for Linear Procedures.

Effects of torsion shall be considered in accordance with the following requirements:

(1) Increased forces and displacements caused by actual torsion shall be calculated for all buildings.

(2) The torsional amplification multiplier for displacements, η, for each level x shall be calculated as the ratio of the maximum displacement at any point on the level x diaphragm to the average displacement $\eta = \delta_{max}/\delta_{avg}$. Displacements shall be calculated for the applied forces.

(3) Increased forces and displacements caused by accidental torsion need not be considered if either of the following conditions apply: (a) the accidental torsional moment is less than 25% of the actual torsional moment, or (b) the ratio of the displacement multiplier η caused by the actual plus accidental torsion and the displacement multiplier caused by actual torsion is less than 1.1 at every floor.

(4) For linear analysis procedures, forces and displacements caused by accidental torsion shall be amplified by a factor, A_x, as defined by Eq. (7-4), where the displacement multiplier η caused by actual plus accidental torsion exceeds 1.2 at any level.

$$A_x = (\eta/1.2)^2 \leq 3.0 \qquad (7\text{-}4)$$

(5) If the displacement multiplier η caused by actual plus accidental torsion at any level exceeds 1.5, two-dimensional models shall not be permitted and three-dimensional models that account for the spatial distribution of mass and stiffness shall be used.

(6) Where two-dimensional models are used, ~~the effects of torsion~~ forces and displacements shall be amplified by the maximum value of η calculated ~~as follows:~~ for the building.

~~(6.1) For the LSP and the LDP, forces and displacements shall be amplified by the maximum value of η calculated for the building;~~

~~(6.2) For the NSP, the target displacement shall be amplified by the maximum value of η calculated for the building;~~

~~(6.3) For the NDP, the amplitude of the ground acceleration record shall be amplified by the maximum value of η calculated for the building.~~

~~(7) For dynamic analyses using nonlinear three-dimensional models, it shall be permitted to establish amplification (η) factors using a parametric study that captures the effects of accidental torsion on individual forces, drifts, and deformations. These factors may then be applied to center-of-mass analysis results to envelop all of the mass-eccentric cases.~~

(7) The effects of accidental torsion shall not be used to reduce force and deformation demands on components.

7.2.3.2.3 Consideration of Torsional Effects for Nonlinear Procedures.

(1) The mathematical model shall consider the effect of actual torsion due to eccentricities between the center of mass of the diaphragm and the center of rigidity of the diaphragm at each floor level.

(2) For NSP using three-dimensional models, accidental torsion shall be considered by multiplying the target displacement by the ratio of the factor η calculated using actual and accidental

torsion in the direction perpendicular to the direction of the target displacement producing the larger torsional moment to the factor η calculated using only actual torsion.

(3) For NSP using two-dimensional models, accidental torsion shall be considered by multiplying the target displacement by factor η calculated using actual and accidental torsion in the direction perpendicular to the direction of the target displacement producing the larger torsional moment.

(4) For NDP using a three-dimensional model with ground motion records consisting of concurrent orthogonal pairs of acceleration records, accidental torsion shall be considered by modifying the mathematic model to shift the center of mass a distance equal to 5% in the direction that produces the largest value of η in a linear model or the direction that has a torsional strength irregularity per Section 7.3.1.1.4. If both directions have a torsional strength irregularity, the mathematical model shall be modified to consider a shift in the center of mass in each orthogonal direction in the direction that produces the maximum value of η in a linear model.

(5) If all accidental torsion is considered in all four directions, η need not be computed.

(6) The effects of accidental torsion shall not be used to reduce force and deformation demands on components below the forces and deformations determined without including accidental torsion.

(7) It is permitted to exclude accidental torsion if the structure does not have a torsional irregularity defined in Section 7.3.1.1.4 and one of the following conditions apply:

a. The accidental torsional moment is less than 25% of the total torsional moment based on Section 7.2.3.2.1, or

b. The value of maximum value of η when computed per Section 7.2.3.2.1 including accidental torsion is less than 1.2 at every level based on a linear analysis.

1.4.8 Property Bounding

This section describes recommended changes to ASCE/SEI 41-17 Section 6.2.4. The change proposal provides an option to perform bounding analyses in lieu of material testing.

6.2.4 Knowledge Factor

[…]

6.2.4.3 Nonlinear Procedures.

Where nonlinear procedures are used, data collection consistent with either the usual or comprehensive levels of knowledge shall be performed. ~~Nonlinear procedures may be used in preliminary evaluations without testing as long as the required testing is performed before implementing the retrofit. If the evaluation does not require retrofit, the testing shall be performed before finalizing the evaluation report.~~ Alternatively, it shall be permitted to perform bounding analyses to envelope the range of material properties in lieu of material testing for all buildings except those containing unreinforced masonry as a primary or secondary component. The

bounding analyses shall include at least two different mathematical models with representative lower and upper-bound material properties. At a minimum, an analysis with all lower-bound property assumptions and one with all upper-bound property assumptions shall be performed. Where the standard already requires bounding of properties, the lower-bound properties of that analysis should be incorporated with the lower bound properties of the material properties and vice-versa for upper-bound properties. Additional analyses shall be performed if there is a situation where a combination of lower-bound and upper-bound properties produces significantly different results than the lower-bound and upper-bound only models. Each analysis shall be assessed separately and the worst-case result for each component taken from the different bounding cases.

When determining the appropriate bounds for material properties of the deformation controlled components the following shall be considered:

(1) The variation of the material property from information specified on the design document.

(2) The variation in the component action capacity based on the material property.

Unless other parameters are substantiated by analysis or testing the following factors shall be used to establish the lower and upper-bound properties

	Lower-bound	**Upper-bound**
Yield Strength	0.75	1.25

Force controlled actions shall be checked with lower-bound capacities.

1.5 References

FEMA, 1997, *NEHRP Commentary for the Seismic Rehabilitation of Buildings*, FEMA 274, prepared by the Building Seismic Safety Council for the Federal Emergency Management Agency, Washington, D.C.

Haselton, C.B., Fry, A., Hamburger, R.O., Baker, J.W., Zimmerman, R.B., Luco, N., Elwood, K.J., Hooper, J.D., Charney, F.A., Pekelnicky, R.G. and Whittaker, A.S., 2017, "Response history analysis for the design of new buildings in the NEHRP provisions and ASCE/SEI 7 standard: Part II-Structural analysis procedures and acceptance criteria," *Earthquake Spectra*, 33(2), pp.397-417.

Chopra, A.K., and McKenna, F., 2015, "Modeling viscous damping in nonlinear response history analysis of buildings for earthquake excitation," *Earthquake Engineering & Structural Dynamics 2016*, 45:193–211.

Goel, R.K., and Chopra, A.K., 1997, "Vibration Properties of Buildings Determined from Recorded Earthquake Motions," UCB/EERC Report 97/14, University of California, Berkeley, California.

Goings, C.B., Weaver, B., Singhania, A., and Ranchal, P., 2020, "Industrial Scale NLRH Analysis Using OpenSees and Comparison with Perform3D," *Proceedings of the 2020 SEAOC Convention*, Paper No. 83, SEAOC, Sacramento, California.

Hall, J.F., 2016, "Discussion of 'Modeling viscous damping in nonlinear response history analysis of buildings for earthquake excitation' By Anil K. Chopra and Frank McKenna," *Earthquake Engineering & Structural Dynamics 2016*, 45:2229–2233.

PEER/ATC, 2010, "Modeling and acceptance criteria for seismic design and analysis of tall buildings," ATC-72-1 Report, Applied Technology Council, Redwood City, California.

Chapter 2: Nonlinear Modeling Parameter and Acceptance Criteria Revisions

2.1 Motivation

Nonlinear analysis is predicated on accurate representation of the nonlinear behavior of the individual deformation-controlled component actions. ASCE/SEI 41 and its predecessor documents, FEMA 273 and FEMA 356, provide parameters to construct nonlinear force-deformation relationships for most component actions in a building. In addition to modeling parameters, ASCE/SEI 41 has acceptance criteria specific to the various structural performance levels in the standard. In many cases, the modeling parameters and acceptance criteria in ASCE/SEI 41-17 have not been changed since originally proposed in FEMA 273. Furthermore, the only place that one can find direction on how to develop nonlinear modeling parameters and acceptance criteria is in a section intended for project-specific testing of a small number of components. Nowhere in the standard does it explicitly spell out how to go about updating the modeling parameters and acceptance criteria for general use. However, it has been understood that the project-specific procedures were what should be used, given the available data in determining the standard values, and have generally been used when modeling parameters and acceptance criteria have been updated.

This project focused on an overall update of the section on how to derive modeling parameters and acceptance criteria to expand it to be applicable to both general use parameters and project specific testing. In addition, provisions were developed specific to fiber models.

2.1.1 Modeling Parameter and Acceptance Criteria Revisions

The project team felt that Section 7.6 in ASCE/SEI 41-17 should be expanded to cover both project-specific testing, as it does now, and the development of modeling parameters for general use. The section should also serve as the rules that other standards developing organizations, such as AISC and ACI, and vendors of proprietary products should use to develop modeling parameters and acceptance criteria for components that can be used with the ASCE/SEI 41 standard.

2.1.2 Fiber Model Requirements

Fiber models offer an alternative to lumped plasticity elements to establish nonlinear force-displacement relationships of component actions. The fiber model tracks stress and strain of discrete elements, called “fibers,” of a component’s cross-section. Explicit modeling of stress and strain in individual fibers can provide a more accurate representation of the cyclic force-displacement relationship of the component action, as well as the effects of strain hardening,

hinge growth, member length change, cyclic pinching and degradation, and other effects of plasticity. Initially, fiber models were used to represent flexure or axial-flexure relationships in concrete beam, column, and wall components. However, their use has expanded to represent additional elements such as the pre- and post-fracture of pre-Northridge moment connections (NIST GCR 17-917-46v2) and buckling in steel columns and braces (NIST GCR 17-917-45). A key difference in using fiber elements is that nonlinear behavior is portrayed directly in terms of plastic strain, as opposed to plastic rotations, plastic elongations, etc.

ASCE/SEI 41 does not have any clear provisions regulating the use of fiber models and acceptance criteria when such models are used. As discussed in the preceding section, all of the modeling parameter information contained in ASCE/SEI 41 assumes lumped plasticity models are used. The only place where the standard even mentions strain limits is in Section 10.3.3.1 where maximum compression strain in concrete and maximum tension and compression strain in reinforcing steel is provided. However, these strain limits are intended to be indicative of maximum usable material strains and were not intended to inform component-level modeling. Even with those provisions, the commentary cautions engineers when using these limits to develop moment and axial strength relationships and acceptance criteria.

2.2 Summary of Changes Recommended

This project developed two proposed changes to the nonlinear modeling criteria. Proposed changes to the requirements for developing modeling parameters and acceptance criteria are far reaching and will have a profound impact on future editions of the standard. It is hoped that these changes will inspire more laboratory testing to failure of the component, which is essential for developing accurate modeling parameters. The proposed changes for fiber modeling introduce clear provisions for using such models, including requirements to calibrate them against test data or already developed force-deformation relationships.

2.2.1 Modeling Parameters and Acceptance Criteria Revisions

The change proposal significantly expands Section 7.6 on the development of modeling parameters and acceptance criteria by separating project-specific subassemblage testing and the development of modeling parameters for general use into separate sections, with both relying on the same provisions to determine acceptance criteria.

The significant changes to Section 7.6 including the following:

- A section for development of modeling parameters and acceptance criteria based on large data sets for general use is added. Project-specific testing is now a separate section.
- Use of monotonic testing to develop backbone curves is no longer permitted, except in the case where it is used to calibrate an adaptive hinge.

- The Damage Control component for nonlinear procedures is explicitly set at the C-point on the generalized force-displacement curve.
- A new point is added to the backbone curves—the loss of vertical load carrying capacity, point F, which may be significantly larger than the point at which the component stops resisting lateral deformation, E. The loss of vertical load carrying capacity point can be used to determine Life Safety and Collapse Prevention acceptance criteria.
- Local acceptance criteria for Collapse Prevention of ordinary elements are eliminated.
- Default hysteretic shapes are introduced.
- Relaxation on what constitutes a force-controlled action and how that action's capacity is developed.

In addition to the major revisions to Section 7.6, there are ancillary changes to Sections 7.4.4.2.1 and 7.5.1.2 based on the concepts embodied in the revisions to Section 7.6.

2.2.2 Fiber Model Requirements

This section adds language to ASCE/SEI 41-17 Chapter 7 sections that describe general nonlinear component modeling and acceptance criteria and adds more explicit information for fiber models. Although ASCE/SEI 41 never prohibited fiber modeling, the proposal explicitly recognizes fiber models as an alternative modeling method and provides more requirements for how load-deformation response of elastic and nonlinear components should be treated in the analytical model to capture appropriate load and local deformation distributions and related strength degradation. The proposal recognizes nonlinear components may employ distributed plasticity models in place of traditional lumped hinge models and provides the user with direction for calibrating and assigning acceptance criteria for such models.

In applying fiber modeling in nonlinear analysis, the proposal identifies three requirements:

1. Calibration of fibers such that component-level load-deformation relationships match either ASCE/SEI 41-provided backbone curves or testing is required.
2. Acceptance criteria for the fiber model also must be aligned with component behavior.
3. Hysteretic pinching effects and the cyclic response must be considered in calibrating the fiber model.

2.3 Technical Studies

2.3.1 Modeling Parameters and Acceptance Criteria Revisions

OVERVIEW

When FEMA 273 was written, few engineers were performing nonlinear analyses on a routine basis. If an engineer performed a nonlinear analysis in the mid-1990s, they typically performed a pushover analysis either following the ASCE/SEI 41 Nonlinear Static Procedure (NSP) or a similar approach. A nonlinear pushover analysis requires force-deformation relationships for the deformation-controlled component actions modeled nonlinearly in the pushover analysis. FEMA 273 was groundbreaking because it provided parameters for engineers to develop those nonlinear force-deformation relationships for most deformation-controlled component actions found in existing buildings. Tables in each of the material chapters contained values to construct the force-displacement relationships, parameterized as shown in Figure 2-1, depending on the material of construction.

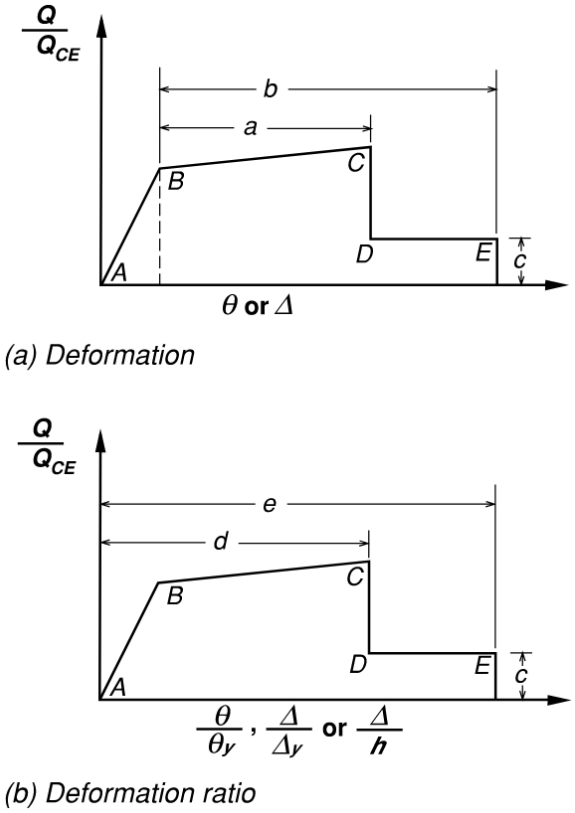

Figure 2-1 FEMA 273 Deformation-controlled component action force-displacement backbone (FEMA 273).

The FEMA 273 force-displacement relationships were derived on the available data. Much, but not all, of this data was obtained from tests using fully reversed cyclic loading, conducted using the ATC-24 or similar loading protocols. A second cycle backbone curve was drawn through the points

where the first cycle at each deformation increment intersected the second cycle to the same increment (Figure 2-2). The primary reason for doing this was to capture the effects of cyclic degradation on a component action because the pushover analysis, which is monotonic, cannot explicitly capture such effects. Each of the four construction materials covered in FEMA 273 and foundation components had a team assigned to review available test data and propose modeling parameters for common component actions based on the component's geometry, detailing, or loading conditions, which did result in inconsistencies between material chapters. While the teams did their best to mine available research data, invariably gaps were present, and the teams used judgement extrapolating from the available material to augment parameters where cyclic test data did not exist.

In general, there was significantly more test data available to determine the 'a' or 'd' parameter in Figure 2-1 than to develop the 'b' or 'e' parameter. This is due in large part to the concern of researchers to push tests too far beyond the point of strength degradation for risk of damaging their equipment or physical limitations of the equipment. The acceptance criteria for Life Safety and Collapse Prevention are derived from 'b' and 'e' parameters for nonlinear analysis. Therefore, underestimation of those points creates a conservative bias in the standard. Additionally, if the 'a' or 'd' parameter is underestimated, the component action may drop load sooner in the analysis than it would in reality, potentially underestimating demands on force-controlled actions in the load path of the deformation-controlled action.

FEMA 273 contained provisions that described how to develop backbone curves from experimental tests. In FEMA 356, a subsection was added to the section on backbone curve derivation to discuss the necessary experimental setup required to obtain information to develop a backbone curve. Specifically, the section required a minimum of three tests for a specific subassemblage. The addition of this information implied the section was to be used in developing project-specific criteria rather than parameters for general use, even though it was intended for general use parameters too.

Supplement No. 1 to ASCE/SEI 41-06 revised the section on determining backbone curves by requiring the backbone curve to envelope the cyclic test. The committee felt that second-cycle curves over-predicted cyclic degradation in many instances and biased the standard in an unnecessarily conservative manner. This shift from second cycle to first cycle envelope increased the deformation capacity of most component actions, as shown in Figure 2-2. However, none of the other published parameters in ASCE/SEI 41 were updated to reflect this change. Only new parameters for concrete columns were based on first cycle envelope.

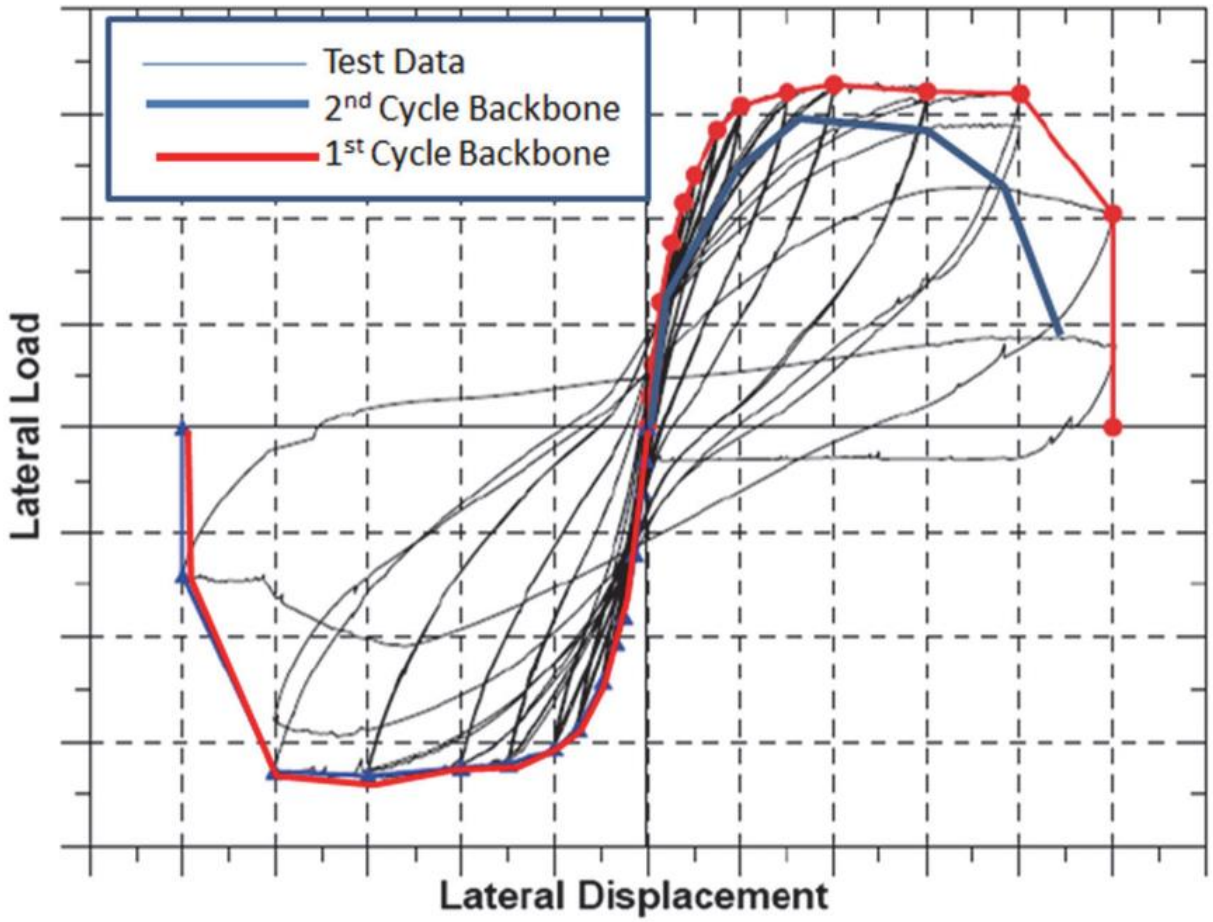

Figure 2-2 First cycle versus second cycle backbone curve example (NIST GCR 17-917-45).

In the 2017 update of ASCE/SEI 41, a change was made to the section on alternate backbone development to explicitly permit loading protocols other than fully reverse cyclic. The commentary to Supplement No. 1 of ASCE/SEI 41-06 discussed other loading protocol use, but the changes in ASCE/SEI 41-17 went further to drop the requirement in the standard text that the loading protocol be "*fully* reverse cyclic" and that it only need be "cyclic." Additionally, the revisions permitted the use of one monotonic test in addition to two cyclic tests in determining backbone curves. The commentary of ASCE/SEI 41-17 went on to discuss the potential conservatism in fully reversed cyclic loading protocols, with it often being different from the actual loading that a component action undergoes in a real earthquake.

NIST GCR 17-917-45 identified a number of issues with the current provisions in ASCE/SEI 41 related to development of modeling parameters and acceptance criteria. One of the most significantly is the fact that most of the parameters in the standard have not been updated to incorporate new research conducted over the past twenty years or to account for the change from second cycle to first cycle envelope. NIST GCR 17-917-45 proposed a modified force-deformation relationship that introduces a new point, labeled the loss of vertical load carrying capacity, Δ_{LVCC} (Figure 2-3).

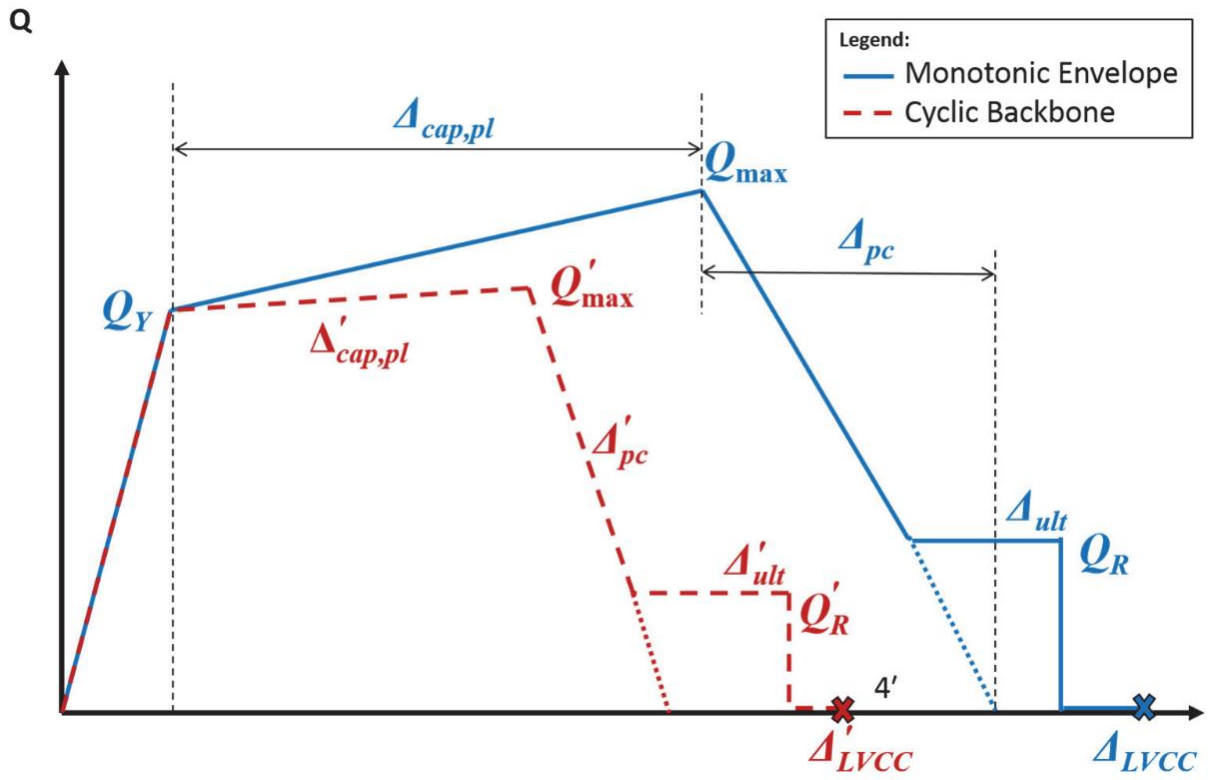

Figure 2-3 Proposed force-displacement backbone (NIST GCR 17-917-45).

Another item identified in NIST GCR 17-917-45 was the lack of guidance on developing modeling parameters for use in nonlinear response history analyses. Because the backbone curves were originally developed to be used in pushover analyses, ASCE/SEI 41 directs the engineer to consider hysteretic behavior in developing their modeling parameters, but lacks guidance on how to develop modeling parameters that express cyclic and hysteretic behavior. With the now commonplace use of nonlinear response history analysis, the project team felt the standard should provide direction on hysteretic properties.

NIST GCR 17-917-45, GCR 17-917-46v2, and GCR 17-917-46v3 all describe in detail proposed updates to the modeling parameters for most of the component actions in ASCE/SEI 41. Many of these new modeling parameters were developed using data regression similar to what is described in the commentary to the new section on general use parameters in the change proposal. The reader is referred to those documents for a detailed technical discussion on the development of modeling parameters from large suites of test data, including specifics about how one should go about adjusting conditions to bin test results.

CURRENT STUDIES

Several studies were undertaken to illustrate the importance of the shape of the backbone curve using the moment frame building discussed in the preceding chapter. The beam-column connection backbone curve was modeled using the provisions in ASCE/SEI 41 and then, in a different model,

using the provisions in NIST GCR 17-917-45. Figure 2-4 illustrates the different backbones, with the ASCE/SEI 41-17 curve dashed and the NIST GCR 17-917-45 as a solid line. The NIST GCR 17-917-45 curve has a slightly lower yield point and a significantly smaller plastic deformation before strength degradation, the 'a' parameter. Figure 2-5 shows the building response using the different beam-column hinges. It is clear that reducing the 'a' parameter has a significant effect on the response. The drifts and deformations using the reduced 'a' parameter are significantly increased with the NIST relationships due to the beam-column hinges degrading sooner in the response than the ASCE/SEI 41-17 model.

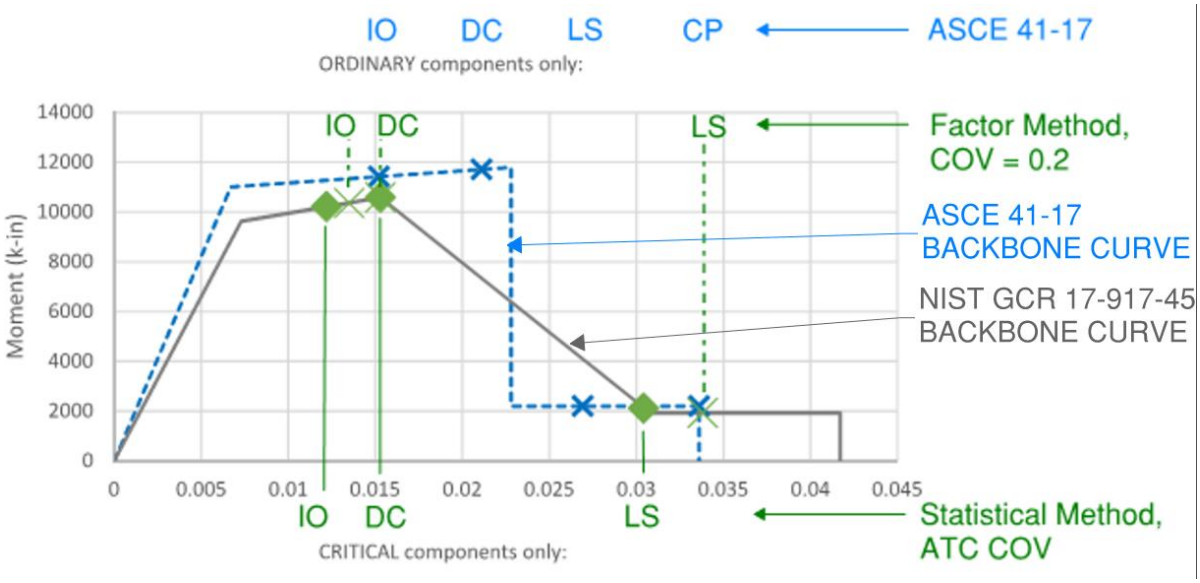

Figure 2-4 ASCE/SEI 41-17 and NIST GCR 17-917-45 beam-column hinge and acceptance criteria.

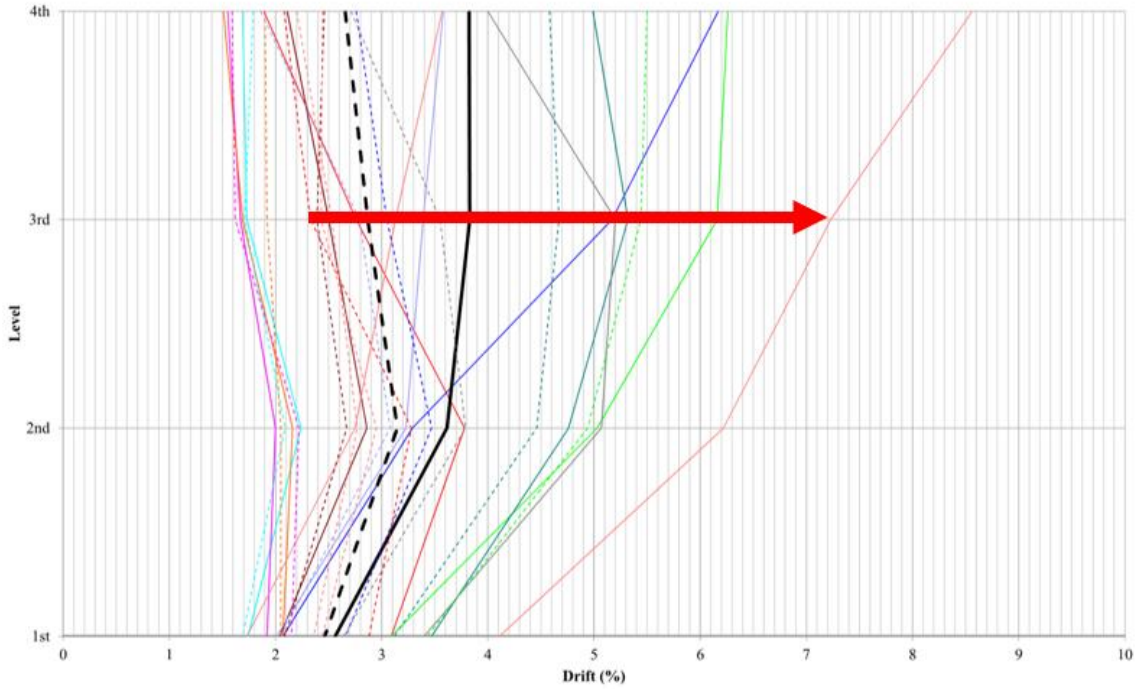

Figure 2-5 Story drift under BSE-2E with ASCE/SEI 41-17 hinges (dashed) and NIST GCR 17-917-45 hinges (solid).

Figure 2-4 overlays three different methods of determining the acceptance criteria. The statistical method is what was included in the change proposal, where Life Safety is based on 10th percentile of the loss of vertical load carrying capacity, point F, which is taken as the maximum deformation in the standard if not explicitly provided. The factor method, which used the same percentiles but with a coefficient of variation of 0.2 instead of the coefficient of variation for the specific point referenced in NIST GCR 17-917-45, was explored but ultimately abandoned. This was proposed as an alternate to the percentile method because many points have very high COVs. A high COV coupled with a conservative 'b' parameter (the maximum deformation) resulted in performance points significantly more conservative than the current performance limits in ASCE/SEI 41-17. Similar trends were observed for concrete components.

A Monte Carlo simulation was conducted using the ASCE/SEI 41-17 modeling parameters and varying the 'a' parameter based on a coefficient of variation of 0.6 as reported in FEMA 355d. Figure 2-6 shows the variability in the response for one ground motion record when the deformations are near the 'a' parameter versus pushing the hinge past the 'a' parameter. When the deformation is less than the 'a' parameter, the response is less sensitive to the 'a' parameter, but if it is near the median, then it becomes more sensitive. That sensitivity is exacerbated by the large coefficient of variation of the 'a' parameter. Most of the component actions in NIST GCR 17-917-45 have coefficients of variation greater than 0.4 for the 'a' parameter.

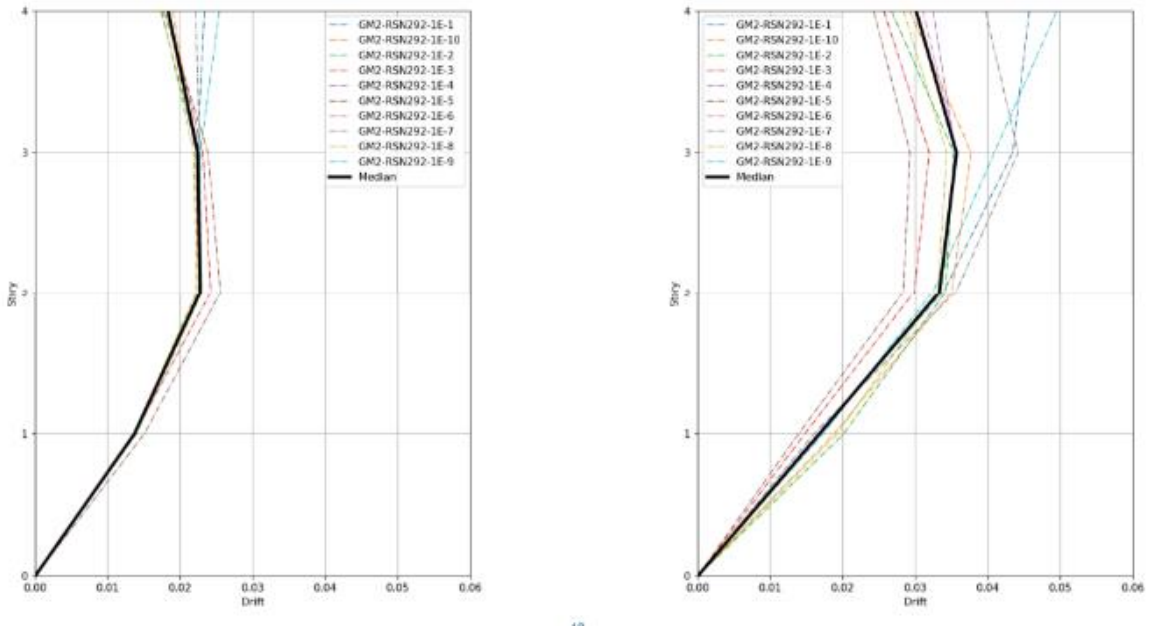

Figure 2-6 Monte Carlo simulation showing the sensitivity of results to the 'a' parameter when the response is only slightly past the 'a' parameter (left) or significantly past the 'a' parameter (right).

Figure 2-7 shows the results of the full Monte Carlo simulation when the 'a' and 'b' parameters were varied. Figure 2-8 overlays the median, 10th and 90th percentile drifts for the same model when only median properties are used (blue line). Comparing the figures shows that using median parameters provides a reasonable, if slightly conservative, estimate of the building's response when compared to the Monte Carlo simulation. In addition to the median drift being close between the two models, the 10th and 90th percentile drifts are also. This appears to affirm the direction in the standard to base the backbone curve off the median estimate of each point when aggregating test data.

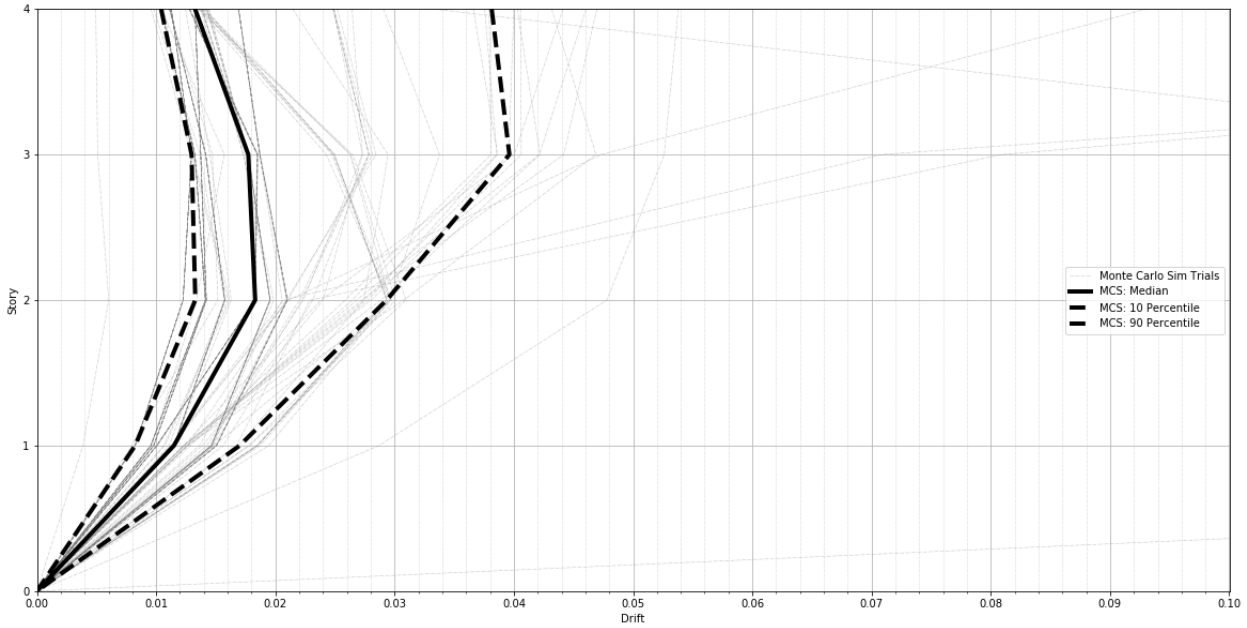

Figure 2-7 Monte Carlo simulation results for ‘a’ and ‘b’ parameter variability.

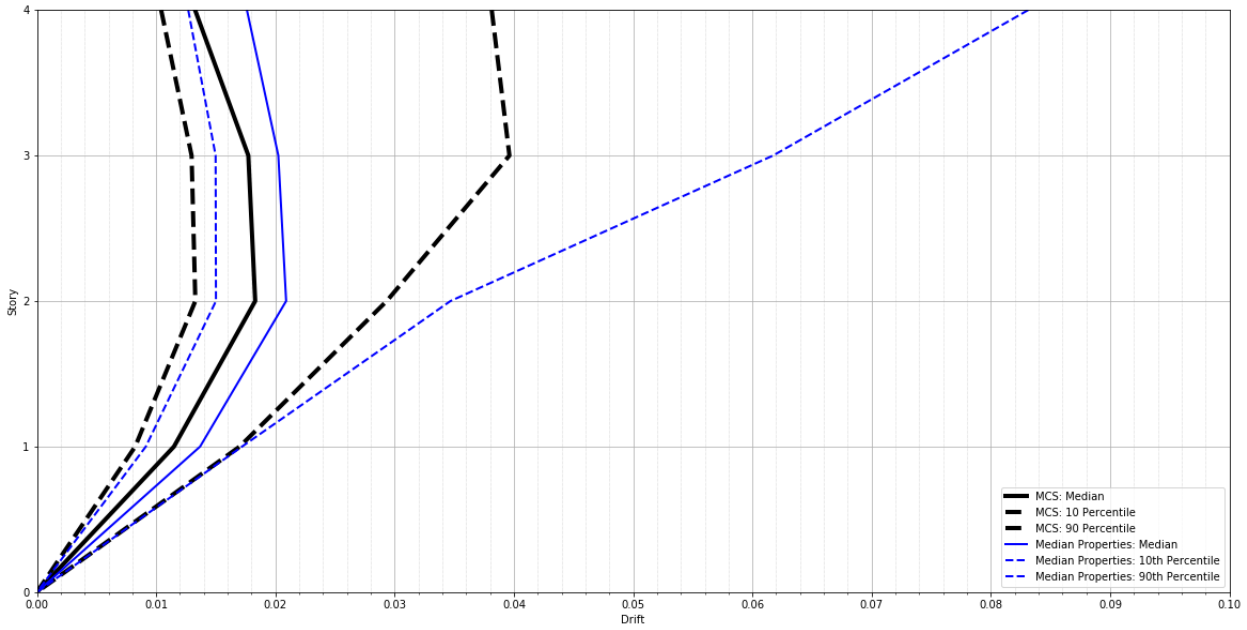

Figure 2-8 Monte Carlo simulation compared to model with median parameters.

The exercise discussed in the preceding paragraphs illustrates the importance of the ‘a’ parameter. This parameter is also sensitive to loading protocol (FEMA 440a), which could explain why aggregating a significant number of tests as was done in NIST GCR 17-917-45 would yield large coefficients of variation. This is why it is necessary to have rules that different groups can follow to develop consistent modeling parameters and why it is important for the ASCE/SEI 41 committee to update the modeling parameters from the second cycle to first cycle at a minimum.

While the high coefficient of variation is one contributor to the significant conservatism in developing performance points using statistics, the other issue is the likely conservatism in the 'b' parameter. FEMA 355d discusses how many of the pre-Northridge, post-Northridge, and retrofit beam-column connections ultimate rotation limits were proposed based on judgement because there was not sufficient test data where the beam-column connections were pushed to the point where they fractured all the bolts in the shear tab or had other failure mechanisms that would indicate a loss of vertical load carrying capacity. NIST GCR 17-917-45 also discusses the lack of information leading to coefficients of variation on the order of 0.6 to 1.1 for the 'b' parameter. Until significantly more testing is done to produce more accurate estimates of the 'b' parameter and to reduce the coefficient of variation of that point, the statistical approach is unlikely to provide a good measure of performance. Nevertheless, the project team chose to include that option in the proposed change in the hope that it would inspire additional testing.

CONCLUSIONS

The first major change is the creation of a section specific to the development of modeling parameters and acceptance criteria based on large data sets for general use. This is done to set the "rules" for how to develop new modeling parameters and acceptance criteria, to update existing values provided in the standard, for other standards that are intended to be used with this standard, or for values provided in product literature for a proprietary component. The proposed requirements for developing general use parameters is different than the directions for project-specific testing found in the 2017 and earlier editions of the standard. Ideally one would have sufficient test data for the specific component action over all possible boundary conditions and for all possible configurations of the component. The test data may be augmented by analytical modeling, but the parameters cannot be based solely on analytical modeling.

Backbone curves for general use parameters should be based on the median of test data aggregated together to develop the parameters. The Monte Carlo simulations showed that this provides an adequate representation of the response with respect to both the median response and the 10th percentile upper- and lower-bound responses.

The second major change is the elimination of the use of monotonic test data, except where such data are used to calibrate an adaptive hinge. Adaptive hinges are capable of replicating the force-deformation behavior of a nonlinear action that is sensitive to the loading history and should be able to represent both fully reversed cyclic behavior as well as monotonic behavior, as well as any other loading specific to the response of a structure in a particular earthquake.

Monotonic testing can provide an unconservative estimate of a component ductility, often missing failure modes or phenomena that negatively impact the ductility of a structural component action related to cyclic behavior. For example, Sen et al. (2017) demonstrated significant reduction in tension ductility for an HSS brace with a high d/t ratio when first subjected to one cycle of compression. A monotonic tension test would predict significant ductility. Even in earthquakes where there is a significant pulse, there is typically some level of cyclic excitation before the large pulse, making only monotonic testing an unrealistic loading protocol. (The figures added as part of the

change to permit monotonic testing illustrate the significantly different behavior between the monotonic and any of the cyclic tests.) The provision recognized that there is a place for monotonic testing, when being used as one of several tests to calibrate an adaptive hinge model.

The third major change is to explicitly set the Damage Control limit for nonlinear procedures at the C point on the generalized force-displacement curve. This change was done in recognition of the imprecision and potentially unconservative outcome of setting Damage Control as the mean between Immediate Occupancy and Life Safety. For example, consider a pre-Northridge moment frame where the flange fractures at 1.5% story drift (Point C) but does not lose the ability to support gravity load or lateral forces until 6%. Assuming yield at 1%, IO would be taken as 0.25% plastic rotation and Life Safety would be taken at 3.75% plastic rotation, meaning Damage Control would be 2% plastic rotation or 3% total rotation, as shown in Figure 2-9. At that rotation, there would be fracture of at minimum the bottom flange and loss of several bolts in the shear tab. Such deformation is based on the median curve. This is likely too much damage to meet the spirit of Damage Control. Therefore, a decision was made to restrain the damage to the median point of strength degradation (likely coupled with the transition from minor/moderate damage to more substantial damage).

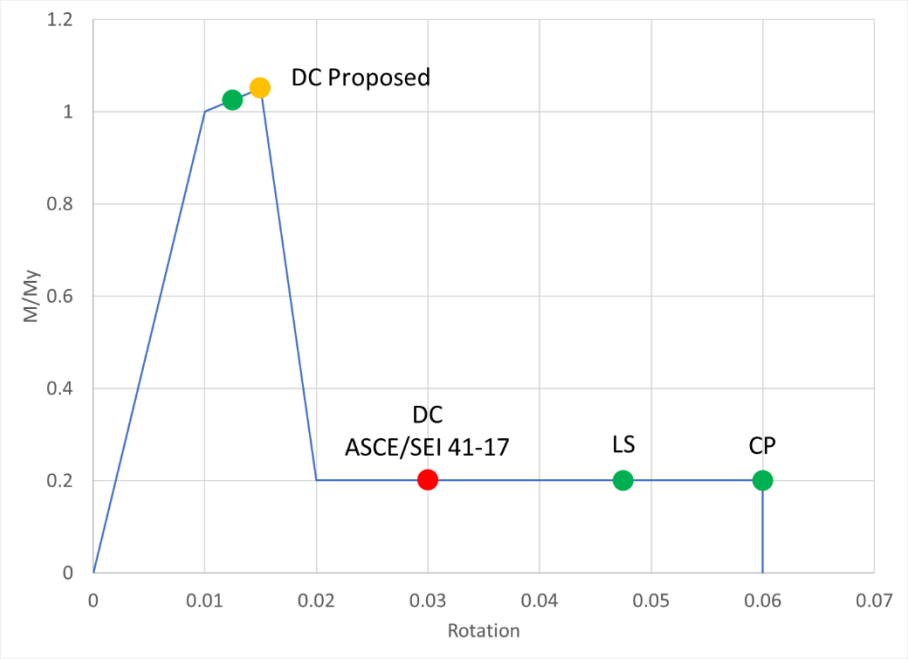

Figure 2-9 Damage control limit change.

The fourth major change is to permit the introduction of the loss of vertical load carrying capacity point, F, which may be significantly larger than the point at which the component stops resisting lateral deformation, E. The introduction of this point coincides with a permission to set the Life Safety limit at the 5th percentile of the loss of vertical load carrying capacity, point F, as an alternate to the existing definition of 75% of the deformation at point E, and to set the Collapse Prevention point for critical elements at the 10th percentile of the loss of vertical load carrying capacity, point F, as an

alternate to the deformation at point E. The existing definitions of Life Safety and Collapse Prevention are retained in recognition of there being very little test data that actually identifies the point at which components lose the ability to carry vertical loads (point F). Figure 2-10 shows the revised backbone curve from the change proposal and the ranges of the acceptance criteria for various Performance Levels.

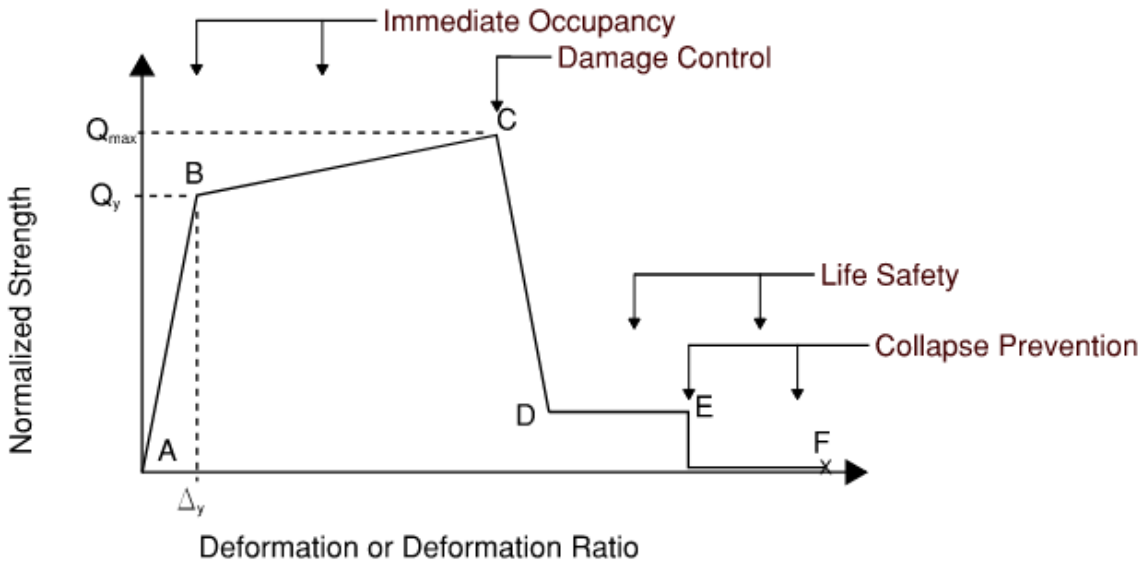

Figure 2-10 Proposed backbone curve and acceptance criteria.

The fifth change is the elimination of local acceptance criteria for Collapse Prevention of ordinary elements. Since Collapse Prevention is based on overall system stability, local element deformation only matters if the failure of that individual element could contribute to a partial collapse. Those elements would be classified as critical.

The sixth change is the introduction of default hysteretic shapes showing in Figure 2-11. Since nonlinear response history is commonplace in engineering practice now, the project team felt strongly that rules should be provided for default hysteretic shapes. The change proposals identify four different shapes ranging from nearly elastic-plastic to hysteresis with significant pinching. The intent of these four options is that over time the material chapters will adopt these designations and identify which hysteretic shape should be used for each entry in the modeling parameter table. The four designations are based on the amount of the area encompassed by the hysteretic envelope to the plot of the hysteretic curve of the element if it exhibited elastic plastic response without any reduction in area in the second and fourth quadrants of the four-quadrant plot.

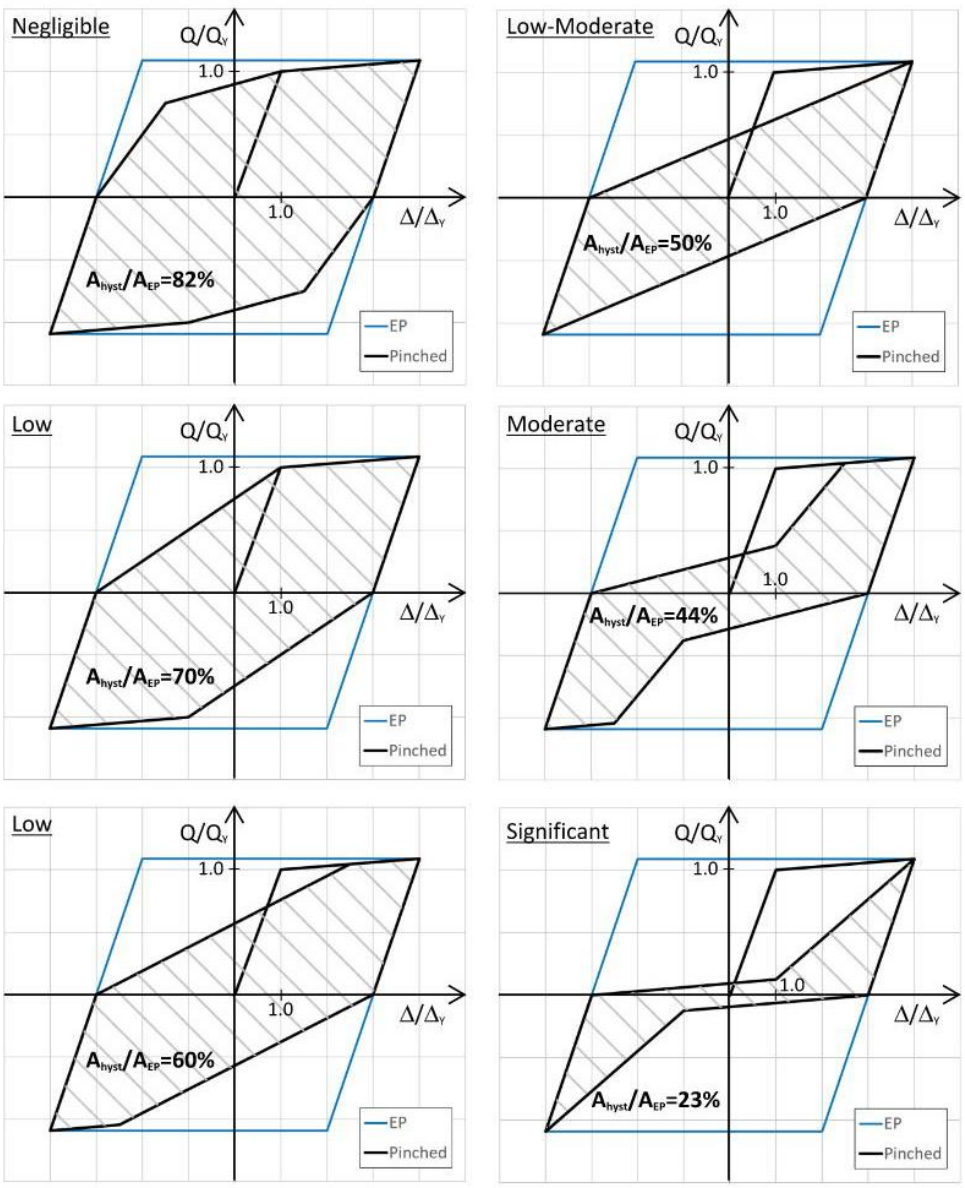

Figure 2-11 Default hysteretic pinching shapes.

The final change is the relaxation on what constitutes a force-controlled action and how that action's capacity is determined. The revisions to Section 7.6.3 discuss that a component action must have Type 3 behavior and have very little residual capacity before complete loss of lateral force resisting or vertical load carrying capacity.

2.3.2 Fiber Model Requirements

Fiber models are becoming more commonplace in practice given their ability to explicitly capture complex interactions with axial and flexural wall demands, bidirectional effects, and shifting neutral axis effects on strain demands and wall rotation capacity. Although ASCE/SEI 41 never prohibited

fiber modeling, it never explicitly recognizes the models, nor does it provide guidance. The following studies and recommendations were developed to allow distributed plasticity models for nonlinear components in place of traditional lumped hinge models and provide guidance on their implementation.

In applying fiber modeling in nonlinear analysis, the proposal identifies three essential considerations: calibration of fiber models, defining acceptance criteria for fiber models, and the energy dissipation captured by the nonlinear action.

CALIBRATION

NIST GCR 17-917-45 discusses the need to calibrate fiber models back to testing or established force-displacement relationships to confirm that the fiber model will provide an accurate representation of the component action's force-displacement relationship. ASCE/SEI 41 does not currently have this requirement, but given the increasing use of fiber models, the project team felt that a calibration requirement is warranted.

Calibration of load-deformation response of fiber hinges is required beyond solely relying on material stress-strain relationships for fibers. Neglecting to calibrate material fibers can result in overestimating component load-deformation response by overlooking critical failure modes, for example local buckling of reinforcement or shear-flexure interaction. Further, variations in meshing along the component length and over the component cross section can affect the component-level load-deformation response. Such variations have well been documented in past literature.

Coleman and Spacone (2001) showed how modifying the number of integration points along the component height or length can substantially affect the load-deformation response. Their work proposes regularization based on a constant fracture energy or alternatively geometric scaling effects to appropriately capture post-peak response and avoid inappropriate localization effects. Figure 2-12 below demonstrates sensitivity of component-level load-deformation response to the number of integration points used along a concrete column height despite identical material stress-strain relationships in the fibers and identifies the need for an objective approach to fiber models.

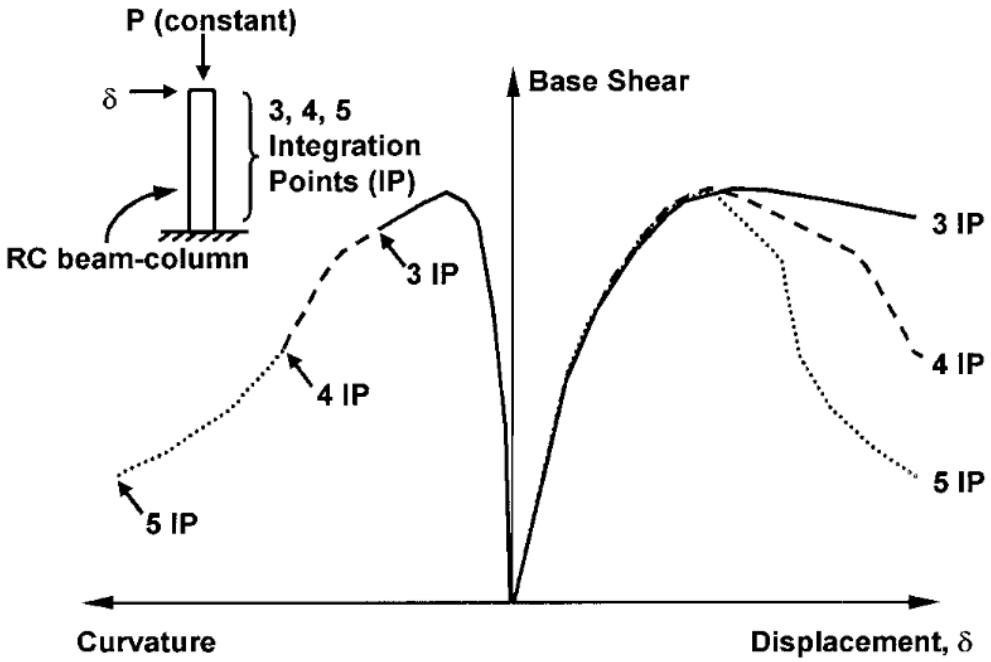

Figure 2-12 Reinforced concrete column load-response dependence on number of integration points.

Lowes and Baker (2016) demonstrate similar sensitivity of fiber modeling in commercially available software, exhibiting that the commonly used PERFORM-3D four-node wall models are not immune to the effects selection of integration points along the component length and discretization along the element cross section. Lowes and Baker showed how response can be overestimated if not regularized and how similar fracture-energy regularization techniques can be applied to commercially available software models. Figure 2-13 below demonstrates cyclic load-deformation response in a non-regularized wall component model (in blue) relative to the measured experimental lab specimen response (in black). The simulated response overestimates the drift at which lateral strength loss occurs by roughly 100% and provides a poor representation of cyclic response.

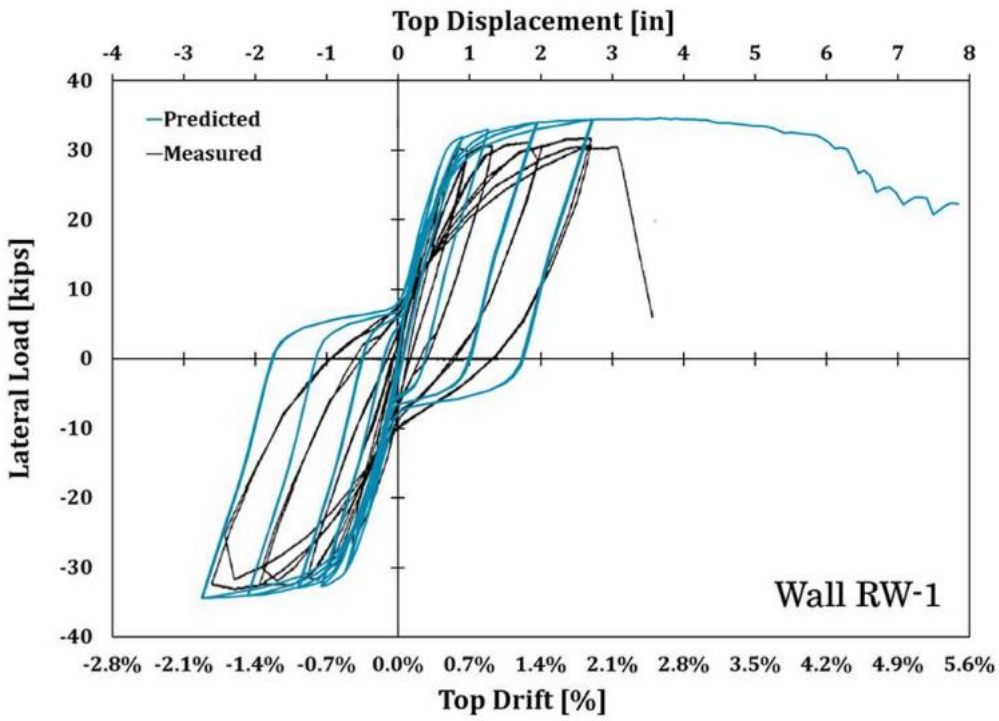

Figure 2-13 Load-displacement response of wall specimen as measured and as simulated.

Further, Lowes and Baker (2016) demonstrate the sensitivity of component mesh for the simulated wall component with and without fiber material regularization. In Figure 2-14A, element mesh is varied using consistent fiber material properties, and substantial variability is observed in load-deformation response. Figure 2-14B then demonstrates accurate simulation of drift capacity and negligible mesh sensitivity after material regularization.

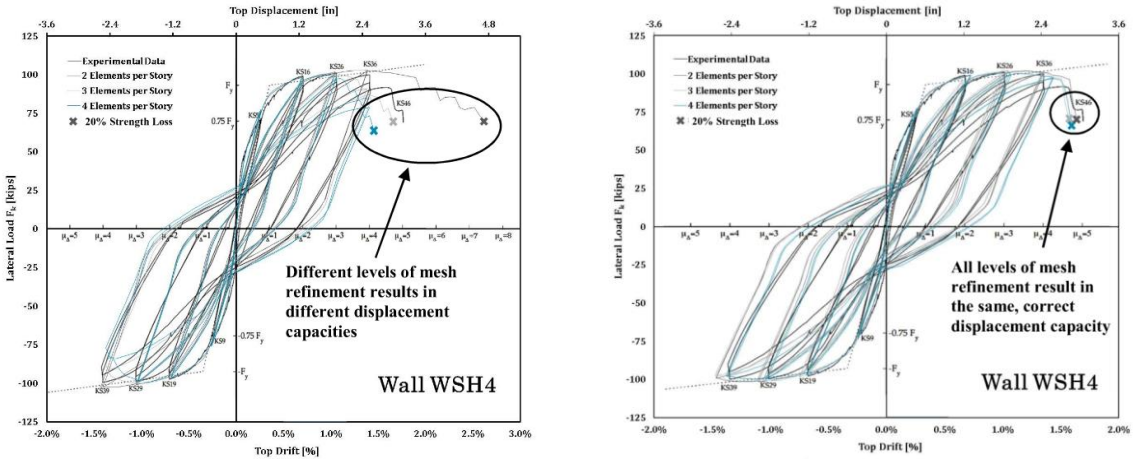

Figure A **Figure B**

Figure 2-14 Load-displacement simulated response using different numbers of elements per story without material regularization (left) and with material regularization (right).

ACCEPTANCE CRITERIA

The change proposal defines requirements for fiber model acceptance criteria. As with load-deformation response, acceptance criteria must consider component-level response and not solely rely on strain limits of fibers based on local material behavior. The definition of gage length over which strains or component rotation are measured must consider overall component response: defining the strain or rotation gage length too long can result in underestimation of strain or rotation measures compared against shorter gage lengths, and ultimately acceptance criteria should rely on global component degradation points in its load-deformation response as defined in Section 7.5. Figure 2-15 demonstrates how a four-node rotation gage is applied in a commercial software, extending over the length of the plastic hinge as defined by ASCE/SEI 41. The fiber material models and/or mesh should be regularized such that the monitored gage rotations correspond to component strength degradation states and associated acceptance limits defined by ASCE/SEI 41 tables for flexure-controlled walls or by Section 7.6 for experimentally derived acceptance criteria.

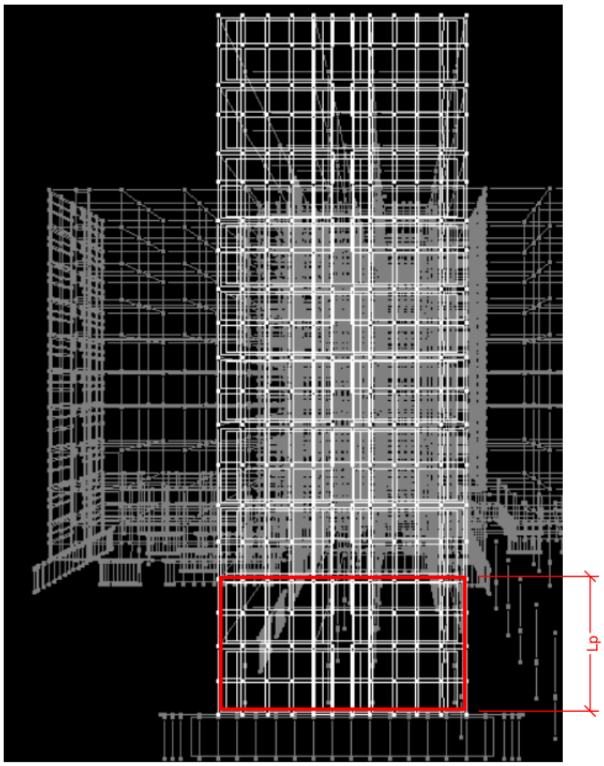

Figure 2-15 Rotation gage assignment in four-node wall element.

HYSTERETIC PINCHING

Hysteretic pinching effects must also be reviewed in the context of component response and identified as low, moderate, or significant pinching to confirm appropriate response is captured. Failing to capture effects of pinching could result in overestimation of energy dissipation leading to unconservative deformation response in buildings with shorter periods and lower global strength (FEMA P440A).

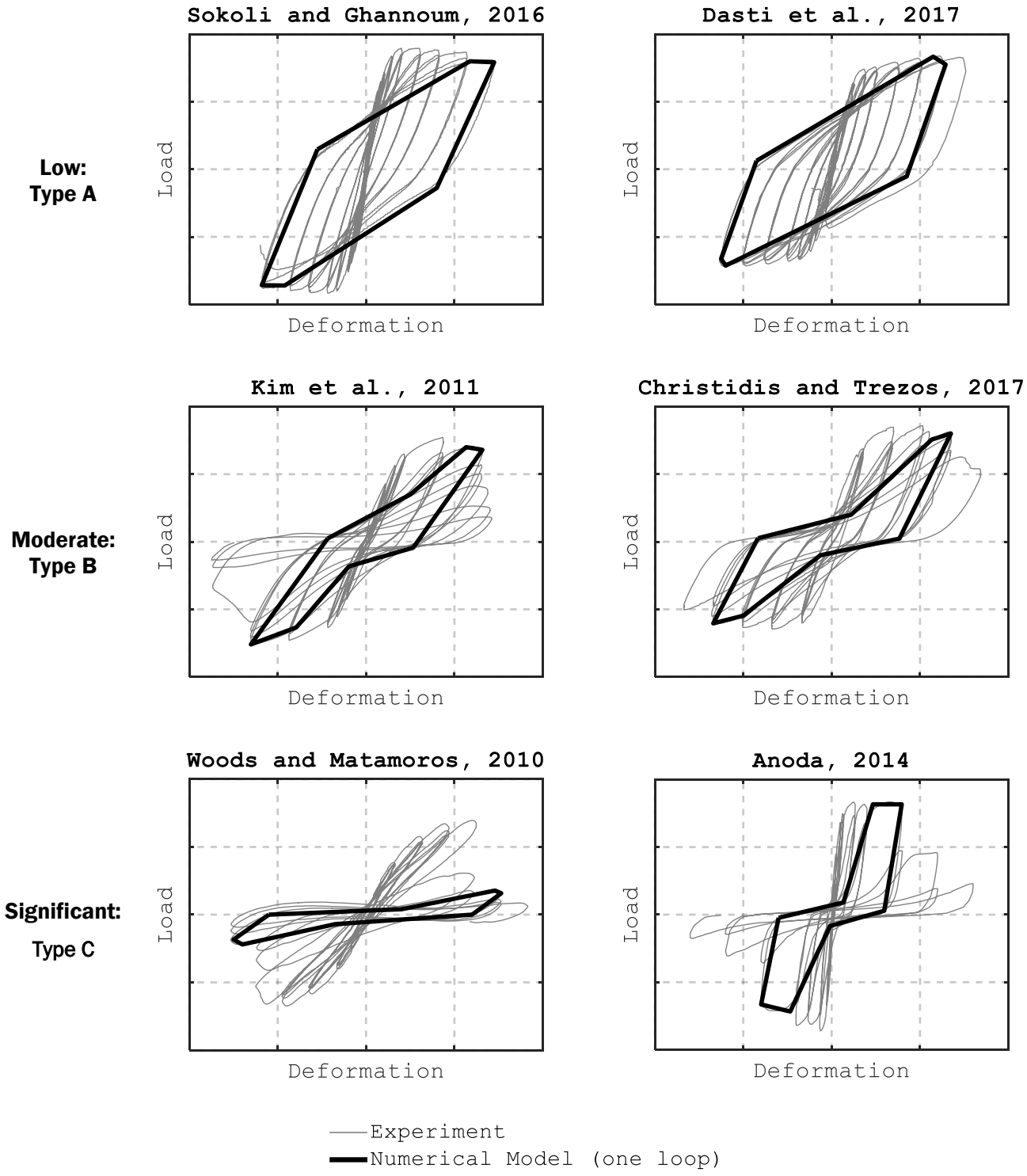

Figure 2-16 Classification of component pinching response.

In addition to regularizing fiber material response for appropriate strength degradation at the component level, pinching can be regularized by adjusting the cycle-to-cycle stress-strain response of

the material fibers. The capability for precisely mimicking experimental component response may be limited by software capabilities; however, the proposed updates focus on categorizing the component response into the three identified levels of pinching (Figure 2-16). The emphasis is on the area within the fully cycled load-deformation response and at least a qualitative consideration of such modeling to avoid inappropriate hysteretic modeling in nonlinear response history analysis.

CONCLUSIONS

Relying solely on material stress-strain relationships is not sufficient for fiber modeling. Calibration of fibers such that component-level load-deformation relationships match either ASCE/SEI 41-provided lumped plasticity modeling or testing is required. Such calibration is critical for both in-cycle and cyclic behavior.

Consistent with fiber calibration for modeling component behavior, acceptance criteria for the fiber model also must be aligned with component behavior. Correspondingly, the gage length over which strains or component hinge rotation must be determined based on either ASCE/SEI 41-provided lumped hinge acceptance criteria or ASCE/SEI 41 Section 7.6 criteria for the component load-deformation response when based on experimental testing.

Pinching effects must also be considered in calibrating the fiber model. Traditionally, there has been little guidance on quantifying appropriate energy dissipation in hysteretic behavior when performing nonlinear response history analysis. The chosen hysteresis and associated pinching can have effects on maximum displacement response, residual displacements after cycles of earthquake acceleration and associated ratcheting effects, as well as degradation in strength. Although peak displacements can be similar for buildings with fundamental periods greater than 1 second, these differences can be more pronounced when building periods are shorter and as the global lateral strength decreases where equal displacement rules tend to not capture peak displacement demands as accurately as equal energy concepts (FEMA P440A). The modeling improvements proposals aim to guide the user to qualitatively categorize the type of pinching and confirm appropriate energy dissipation in the fiber model.

2.4 Recommended Changes

Note about Change Proposals

This report documents aspects of change proposals as they were submitted to subcommittees of ASCE's Seismic Retrofit of Existing Building Standards Committee. Often, these change proposals were revised, in some cases substantively, by these subcommittees before they were adopted into ASCE/SEI 41-23. Readers should not rely on this report for information about the final version of provisions in ASCE/SEI 41-23.

2.4.1 Modeling Parameters and Acceptance Criteria Revisions

This section describes recommended changes to ASCE/SEI 41-17 Section 7.6. The proposed changes expand the section to cover general use parameters in addition to project specific testing. There are some ancillary changes in Section 7.4.4.2.1 and 7.5.1.2 based on the concepts embodied in the revisions to Section 7.6. New or modified text is shown in blue.

Subassemblage – A representative assembly of components or of a specific component that is used to perform laboratory testing of a component's response to lateral forces or of a specific action within the component's response to lateral forces.

7.6 ~~ALTERNATIVE~~ EXPERIMENTALLY DERIVED MODELING PARAMETERS AND ACCEPTANCE CRITERIA

~~It shall be permitted to derive required~~ Modeling parameters and acceptance criteria for component actions not specifically addressed in this standard or as alternatives to those provided in this standard shall be derived using the experimentally obtained cyclic response characteristics of ~~a~~ subassembly tests, determined in accordance with this section. It is permitted to augment subassembly test data with analytical models provided the analytical models have been calibrated to subassembly cyclic test data. Where ~~relevant data~~ the modeling parameters are intended for general use, the procedures of Section 7.6.1 shall be followed. Where the modeling parameters are intended to be used on ~~the inelastic force–deformation behavior for a structural subassembly are not available, such data shall be obtained from experiments consisting of physical tests of representative subassemblies as specified in this section~~ an individual project application, the procedures of Section 7.6.2 shall be followed. The provisions of this section do not apply to seismic isolation or supplemental damping components. Chapters 14 and 15 provide specific requirements for establishing modeling parameters and acceptance criteria for seismic isolation and supplemental damping components.

7.6.1. Criteria for General Use Parameters.

Development of modeling parameters and acceptance criteria for specific component actions or for specific conditions not listed in this standard or to be used as an alternate to those listed in this standard shall be permitted subject to the requirements of this section. The criteria for the component action shall be based on data from experimental tests of sub-assemblages of the component. It is permitted to supplement experimental test data with analytical results to augment information. Analytical results shall not be used without being validated with physical sub-assemblage testing. Load-deformation behavior for a structural subassembly shall be normalized to permit the development of modeling parameters and acceptance criteria per Section 7.6.3. Parameters that affect the deformation capacity of the component action shall be identified and their effect on the modeling parameters quantified. When multiple component actions affect the deformation of a subassemblage, they shall be discretized, or provisions shall be provided to account for the influence of both actions in one of the two action's force-deformation curve. Ranges of component configurations and the parameters affecting the component action shall be stipulated.

Tests and analytical results used to develop the modeling parameters shall be selected based on a), b), and c).

a) Where modeling parameters are developed per Section 7.6.3 for use with mathematical models that do not adapt behavior based on loading history, experimental tests having at least two cycles at each target drift level shall be included. For each component action, a minimum of three tests for a given member size and specific component action is required. Where a sufficient number of tests based on cyclic loading are not available, such data shall be obtained from experiments consisting of physical tests of representative subassemblies as specified in this section.monotonic tests are permitted to be included in the data set if it can be demonstrated that cyclic loading protocols would not significantly affect the component action, or the monotonic test is modified by factors to represent the effects of cyclic loading. The use of monotonic tests only is not permitted.

b) Tests shall be conducted to the point at which the component cannot resist lateral forces through the action being tested or the component cannot support gravity loads. It is permitted to include tests that have not been conducted to failure, provided the maximum deformation tested is recorded as the valid range of modeling and treated as Point E in Section 7.6.3, unless Point E be extrapolated from other similar tests or a combination of similar tests and analytical simulations.

c) Where modeling parameters are developed per Section 7.6.4 or 7.6.5 for use with mathematical models that explicitly adapt behavior based on loading history, tests covering the range of expected cyclic loading demands and histories shall be included.

7.6.2. Criteria for Individual Project Testing.

Development of modeling parameters and acceptance criteria for specific component actions or for specific conditions on an individual project based on subassemblage testing is permitted subject to the requirements of this section. The subassemblage test shall be based on the provisions of Section 7.6.2.1 and the development of modeling parameters and acceptance criteria from the test shall be based on Section 7.6.3. The boundary conditions of the subassembly shall reasonably represent the stiffness of the boundary conditions within the structure. Peer review of this process shall be conducted by an independent engineer ~~(~~or engineers~~)~~ approved by the Authority Having Jurisdiction. The reviewers shall be experienced with the use of test data in design and analysis of structures~~, in accordance with the requirements of Section 1.5.10 as applicable to construction of the component for lab testing~~. Upon completion of the review~~, and before the issuance of the final permit,~~ the reviewer(s) shall provide the Authority Having Jurisdiction and the registered design professional a letter attesting to the scope of the review performed, concurrence with the alternative modeling parameters and acceptance criteria resulting from the test program~~, and any items that require resolution~~ limits on the applicability of the proposed parameters and criteria and inspection requirements, if required.

7.6.2.1 Experimental Setup.

Each tested subassembly shall be an identifiable portion of the structural element or component, the stiffness and strength of which is required to be modeled as part of the structural analysis process. The objective of the experiment shall be to estimate the seismic-force-displacement relationships. These properties shall be used in developing an analytical model of the structure to calculate its response to selected earthquake shaking and other hazards and in developing acceptance criteria for strength and deformations. The limiting strength and deformation capacities shall be determined from an experimental program using multiple tests performed for the same configuration. ~~A number of~~ Three or more tests~~, but not fewer than three,~~ shall be performed to

determine the component behaviors throughout its expected range of performance. ~~The number of tests shall be agreed upon by the peer review and approved by the Authority Having Jurisdiction.~~

The experimental setup shall replicate the construction details, support and boundary conditions, and loading conditions expected in the building. In cases where deformation components (e.g., flexure or shear) are modeled separately, test instrumentation shall be provided to enable backbone curves for each action to be derived from the overall test force–deformation relations. The tests shall include cyclic loading protocols with the number of cycles and displacement levels based on the expected response of the structure. ~~At least two tests shall utilize the same cyclic loading protocol. Tests using monotonic loading shall be permitted to supplement the cyclic tests.~~ Preference shall be given to established loading protocols in other reference standards. At least two tests shall utilize the same cyclic loading protocol. Loading protocols shall be representative of the seismic hazard, including but not limited to site effects, expected ground motions, component loading history that change material properties or preloading condition, and strong shaking duration. Loading protocols shall test components to the point where the action under consideration ceases to resist lateral forces or, where applicable, can no longer resist gravity loads supported by the component. If the loading protocol does not test the component to failure, the report should note that and the maximum deformation of the component test be identified as the valid range of modeling.

Tests using monotonic loading are permitted to develop an adaptive model or as an augmentation to at least three cyclic tests.

7.6.2.2 Data Reduction and Reporting.

A report shall be prepared for each ~~experiment~~ series of subassembly tests. The report shall include the following:

(1) Description of the subassembly being tested;

(2) Description of the experimental setup, including the following:

(2.1) Details on fabrication of the subassembly,

(2.2) Location and date of testing,

(2.3) Description of instrumentation used,

(2.4) Name of the person in responsible charge of the test, and

(2.5) Photographs of the specimen, taken before testing;

(3) Description of the loading protocol used, including the following:

(3.1) Increment of loading (or deformation) applied,

(3.2) Rate of loading application, and

(3.3) Duration of loading at each stage;

(4) Description, including photographic documentation, and limiting deformation value for all important behavior states observed during the test, including the following, as applicable:

(4.1) Elastic range with effective stiffness reported,

(4.2) Plastic range,

(4.3) Onset of visible damage,

(4.4) Loss of seismic-force-resisting capacity,

(4.5) Loss of vertical-load-resisting capacity,

(4.6) Force–deformation plot for the subassembly (noting the various behavior states), and

(4.7) Description of limiting behavior states defined as the onset of specific damage mode, change in stiffness or behavior (such as initiation of cracking or yielding), and failure modes.

7.6.3 ~~Analysis~~ Modeling Parameters and Acceptance Criteria for ~~Subassemblies~~ Component Actions Based on Experimental Data for Non-Adaptive Lumped Plasticity Mathematical Models.

The following procedure shall be followed to develop ~~structural~~ modeling parameters and acceptance criteria for ~~subassemblies~~ component actions based on experimental data for use in non-adaptive lumped plasticity simulation tools.

(1) An idealized force–deformation curve shall be developed from the experimental data. The backbone curve shall be plotted in a single quadrant. If the component action exhibits significantly different response in opposite quadrants, separate backbone curves shall be plotted and parameters developed for direction specific actions. ~~In cases where deformation components (e.g., flexure or shear) are modeled separately, test instrumentation must be provided to enable backbone curves for each deformation component to be derived from the overall test force–deformation relations.~~ The backbone curves shall be constructed as follows:

(1.1) Envelope curves shall be drawn through each point of peak displacement during the first cycle of each increment of loading (or deformation), as indicated in Fig. 7-5. A smooth "backbone" curve shall be drawn through the average of the envelope curves as depicted in Fig. 7-6~~a~~. The ultimate deformation (E) is the point at which the component action degrades to the point where resistance to lateral loads is less than 5% of the maximum strength of the component action or shall not exceed the maximum displacement used in the tests, nor shall it exceed the peak displacement from any cyclic test in which the component experienced ~~in-cycle~~ rapid strength loss~~. Rapid strength loss when~~ defined by the component in-cycle tangent stiffness attains a large negative value, as depicted in Figure 7-5b~~.~~, and the reduction in strength is to a residual level. The deformation at point F shall be the point at which the component loses the ability to support gravity load if the component supports gravity load.

~~(1.2) It shall be permitted to construct backbones from a combination of monotonic and cyclic data, provided that in-cycle rapid strength loss did not occur during any cyclic test, as depicted in Fig. 7-6b. For this case, the ultimate deformation need not be limited by that from the cyclic tests. The ultimate deformation shall not exceed 1.5 times the monotonic test capping displacement (at which the tangent stiffness becomes negative), nor shall it exceed the maximum displacement attained in the monotonic test. When multiple monotonic tests are performed, the ultimate deformation shall be the average from the tests.~~

(1.~~3~~2) The backbone ~~curve so derived~~ shall be approximated by a smooth curve or a series of linear segments, drawn to form a multisegmented curve conforming to one of the types indicated in Fig. 7-4. When the backbone curve is idealized as a series of linear segments, it shall conform to Figure 7-7.

For Figure 7-7a, the points are defined as follows:

Point B – The effective yield point of the component action.

Point C – The deformation where the resistance begins to deteriorate significantly due to approaching failure modes and in which the resistance is never larger than the resistance at C. It is permitted to use the point where the strength is 80% of the maximum strength on the backbone curve with a corresponding strength equal to the maximum strength.

Point D – The deformation at which strength degradation levels out and a residual strength resisting lateral forces is reached.

Point E – As defined above.

Point F – As defined above.

For Figure 7-7b, the points are defined as follows:

Point B – The effective yield point of the component action.

Point C' – The deformation at which the maximum strength is reached. The deformation where the resistance begins to deteriorate significantly due to approaching failure modes and in which the resistance is never larger than the resistance at C.

Point C – The deformation where the resistance begins to deteriorate significantly due to approaching failure modes and in which the resistance is never larger than the resistance at C. It is permitted to use the point where the strength is 80% of the maximum strength on the backbone curve with a corresponding strength equal to the maximum strength.

Point D – The deformation at which strength degradation levels out and a residual strength resisting lateral forces is reached.

Point E – As defined above.

Point F – As defined above.

(1.3) The component action backbone curve shall be represented by the mean of the backbone curves of each test of similar configurations. Where the test data represent different sub assemblages, the points shall be normalized based on the effective yield point, point 1 in Figure 7-4. Backbone curves derived from monotonic tests, shall only be included where permitted in Section 7.6.1 or 7.6.2. Even if the component action backbone curve is idealized as a smooth curve, the points on the curve in Figure 7-7 shall be derived to allow computation of the acceptance criteria in this section.

(1.4) The component cyclic parameters shall be represented by one of the levels of pinching specified in Section 7.4.4.2.5.1 or by explicitly reporting A_{hyst}/A_{EP}.

~~(2) The backbone curve so derived shall be explicitly agreed upon by the peer review and approved by the Authority Having Jurisdiction, considering all aspects of the test program, building configuration, and seismic hazard, including but not limited to site effects, expected ground motions, and strong shaking duration.~~

(~~3~~2)The stiffness of the subassembly for use in linear procedures shall be taken as the slope of the first segment of the composite curve. The composite multilinear force–deformation curve shall be used for modeling in nonlinear procedures.

(~~4~~3)For the purpose of determining acceptance criteria, subassembly actions shall be classified as being either force controlled or deformation controlled as defined in Section 7.5.1.2. Subassembly actions shall be classified as ~~force~~ deformation-controlled unless ~~any~~ the component exhibits Type 3 behavior and either of the following ~~applies~~ conditions apply:

- The ~~full backbone curve, including strength degradation and~~ residual strength, is modeled less than 20% of Q_{CE}; or
- The ~~composite multilinear force-~~deformation ~~curve for the subassembly, determined in accordance with requirements above, conforms to either Type 1, Type 2, or Type 3 as indicated in Fig. 7-4~~ at point E is less than 2 times the deformation at Point B in Figure 7-7; ~~and~~
- ~~The component action is classified as deformation controlled in accordance with Section 7.5.1.2.~~

(~~5~~4)The strength capacity, Q_{CL}, for force-controlled actions evaluated using either the linear or nonlinear procedures shall be taken as ~~the mean minus one standard deviation strength QyL determined from the series of representative subassembly tests~~ the strength of the force-controlled action calculated from the reference material standards in Chapter 8 through 12 using lower-bound material properties for the specific material. If the strength under consideration cannot be ascertained by the material standards, Q_{CL} shall be taken as 0.8 times the mean determined from the subassembly tests.

(~~6~~5)The acceptance criteria for deformation-controlled actions used in nonlinear procedures shall be the deformations corresponding with the following points on the curves of Fig. 7-7:

(~~6~~5.1) Immediate Occupancy:

The deformation at which permanent, visible damage occurred in the experiments but not greater than ~~0.67~~ 0.5 times the deformation ~~limit for Life Safety specified in item 7.2.1 as follows~~ at point C.

(5.3) Damage Control: The deformation at Point C.

(~~6~~5.~~2~~3) Life Safety:

The larger of the 10th percentile of the plastic deformation at Point F but not less than 0.75 times the deformation at point E.

(~~6~~5.~~3~~4) Collapse Prevention – Critical Elements Only:

The 25th percentile of the plastic deformation at point F, but not less than ~~1.0 times~~ the deformation at point E on the curve.

Acceptance criteria derived using percentile of deformation limits is only permitted if there are more than thirty tests for the component action to develop the component action backbone curve.

(~~7~~6)The m-factors used as acceptance criteria for deformation-controlled actions in linear procedures shall be determined as follows: (a) obtain the deformation acceptance criteria given in items 7.1 through 7.3; (b) then obtain the ratio of this deformation to the deformation at

yield, represented by the deformation parameter B in the curves shown in Fig. 7-7; (c) then multiply this ratio by a factor 0.75 to obtain the acceptable m-factor.

(~~7~~6.1) Immediate Occupancy: Primary and secondary components

The deformation at which permanent, visible damage occurred in the experiments but not greater than ~~0.67~~ 0.50 times the deformation limit ~~for Life Safety specified in item 7.2.1 as follows~~ at point C.

(6.2) Damage Control: Primary and secondary components

1.5 times the deformation at which permanent, visible damage occurred in the experience, but not greater than 0.63 times the deformation at Point C on the curves.

(~~7~~6.~~2~~3) Primary components:

(~~7~~6.~~2~~3.1) Life Safety: 0.75 times the deformation at point C on the curves, but not greater than 0.55 times the deformation at point E.

(~~7~~6.~~2~~3.2) Collapse Prevention: The deformation at point C on the curves but not greater than 0.75 times the deformation at point E.

(~~7~~6.~~3~~4) Secondary components:

(~~7~~6.~~3~~4.1) Life Safety: 0.75 times the deformation at point E.

(~~7~~6.~~3~~4.2) Collapse Prevention: 1.0 times the deformation at point E on the curve.

(~~8~~7)~~Where performing NDP requires additional~~ ~~h~~Hysteretic parameters to define the expected behavior of the component shall be identified. ~~, e.g., reloading,~~ Specifically, the action shall be identified as having stiffness degradation, strength and stiffness degradation, and whether there is in-cycle strength degradation~~, self-centering, or pinching behavior, the mathematical model of~~ In addition, the component action shall be identified as exhibiting negligible pinching, low pinching, moderate pinching or significant pinching in accordance with 7.4.4.2.5.1 ~~result in reasonable agreement between the shape of the nominal and test hysteresis loop for each component type and the dissipated hysteretic energy. The modeled hysteresis should be checked against the measured hysteresis throughout the range of expected deformation demands. Separate properties shall be computed for the lower selected Seismic Hazard Level displacements and also the higher selected Seismic Hazard Level displacements where warranted~~.

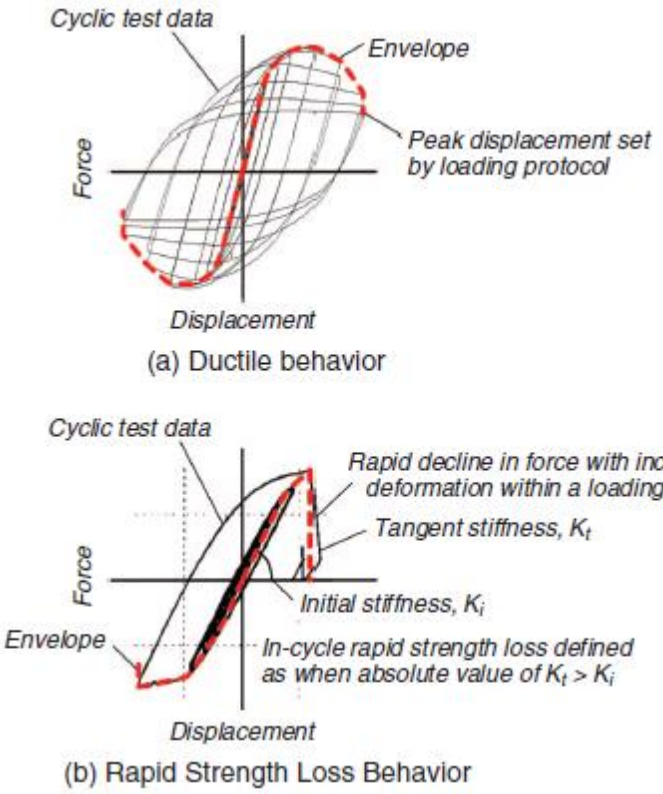

Figure 7-5. Illustration of Envelopes from Experimental Test Data

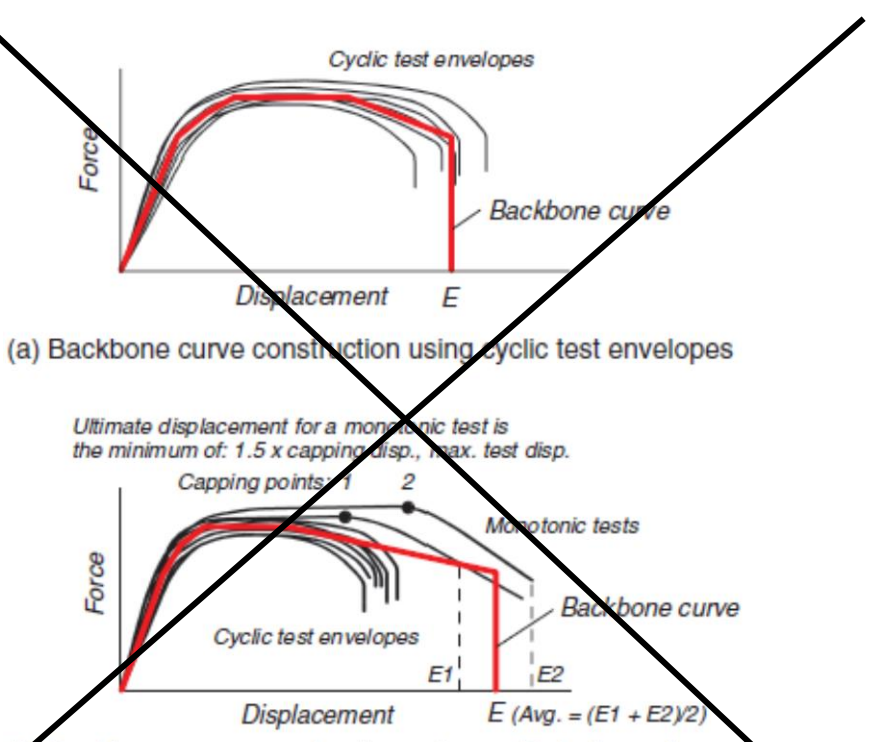

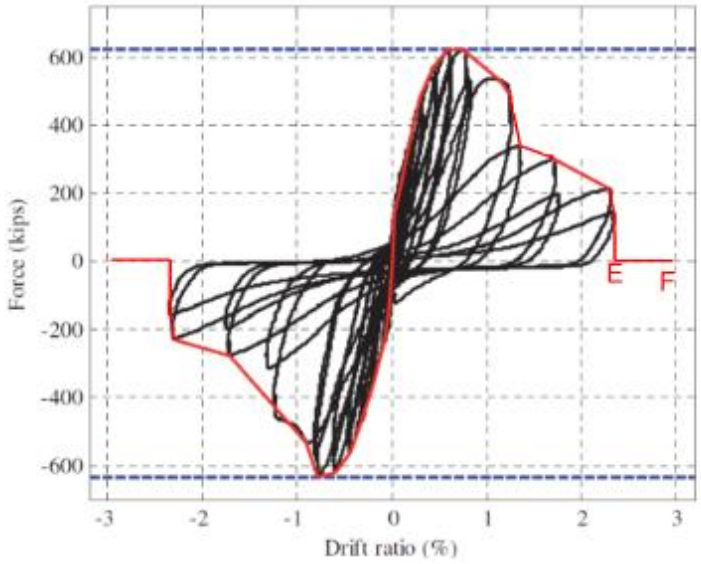

Figure 7-6. Illustration of Backbone Curves Derived from Envelopes of Experimental Test Data (from Luna et al.)

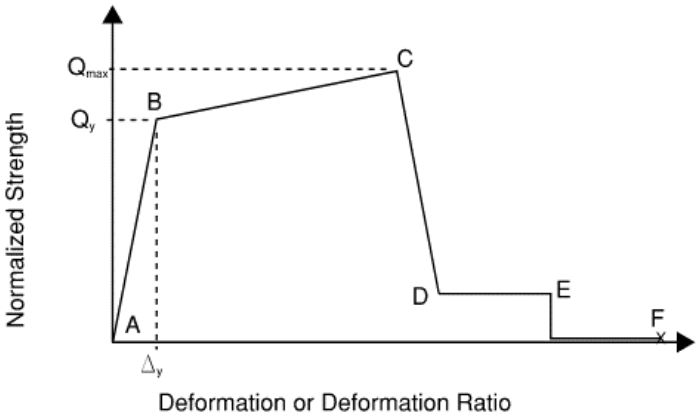

(a) Common Idealization

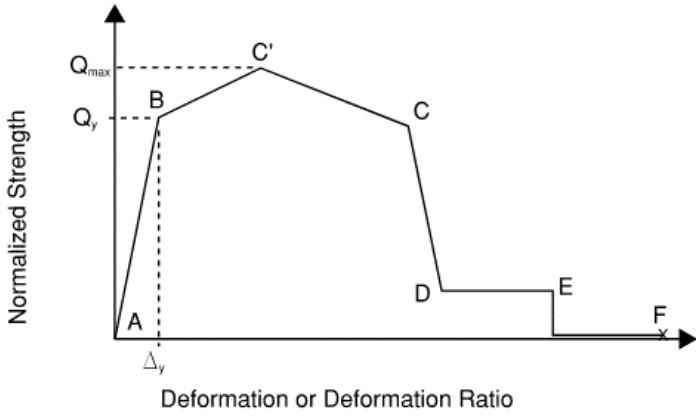

(b) Idealization Including Maximum Strength

Figure 7-7. Multi-segment Linear Idealized Backbone Curve

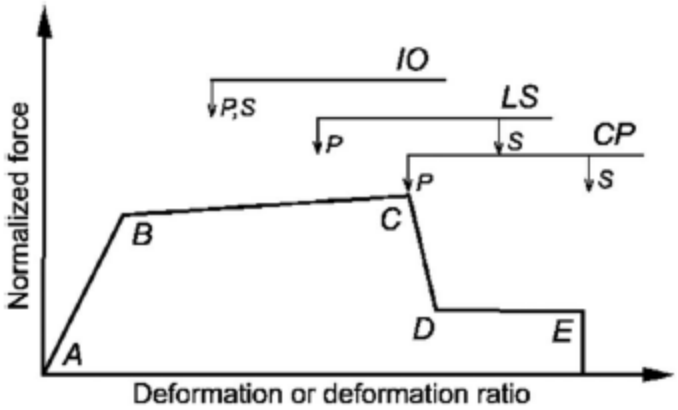

Figure 7-~~7~~8. Acceptance Criteria Illustration for Linear Procedures

~~The above requirements do not apply to buildings using seismic isolation and energy dissipation systems. See Chapter 14 for the specific requirements of these systems.~~

[Note to the reviewer: The following sections are being placed out of numerical order because the changes are due to modifications in Section 7.6, which is the primary focus of this change proposal.]

7.4.4.2 Modeling and Analysis Considerations for NDP

7.4.4.2.1 General Requirements for NDP.

The modeling and analysis requirements specified in Section 7.4.3.2 for the NSP shall apply to the NDP, excluding considerations of control node and target displacements.

The mathematical model of the component action shall result in reasonable agreement between the shape of the nominal and test hysteresis loop for each component type and the dissipated hysteretic energy. The modeled hysteresis should be checked against the measured hysteresis throughout the range of expected deformation demands.

7.4.4.2.5.1 Cyclic Response in Nonlinear Dynamic Procedure

Cyclic force-deformation envelopes of nonlinear components shall incorporate unloading and reloading stiffness that capture effects of hysteretic pinching for the representative inelastic action in the component. The enveloped force-deformation behavior shall be shown to capture related effects on hysteretic energy dissipation. Component hysteretic behavior actions shall be identified as one of the following:

(1) Negligible Pinching: The hysteretic shape is 90% or more of the hysteretic shape assuming fully elastic-plastic behavior in all four quadrants of the force-displacement plot when displaced cyclically to the 'a' parameter.

(2) Low Pinching: The hysteretic shape envelopes 70% of the hysteretic shape assuming fully elastic-plastic behavior in all four quadrants of the force-displacement plot when displaced cyclically to the 'a' parameter.

(3) Moderate Pinching: The hysteretic shape envelopes 50% of the hysteretic shape assuming fully elastic-plastic behavior in all four quadrants of the force-displacement plot when displaced cyclically to the 'a' parameter.

(4) Significant Pinching: The hysteretic shape envelops 30% of the hysteretic shape assuming fully elastic-plastic behavior in all four quadrants of the force-displacement plot. In a significantly pinched hysteretic shape, there is virtually no envelope of the force-displacement response in the second and fourth quadrants of the force-displacement plot.

As an alternate to the four level listed above, the level of pinching shall be based on the ratio of the area enclosed by the actual hysteresis, A_{hys}, should be compared to the area enclosed by an elastic-plastic hysteresis, A_{EP}. It shall be permitted to represent pinching by the ratio of A_{hys}/A_{EP} when substantiated by test data.

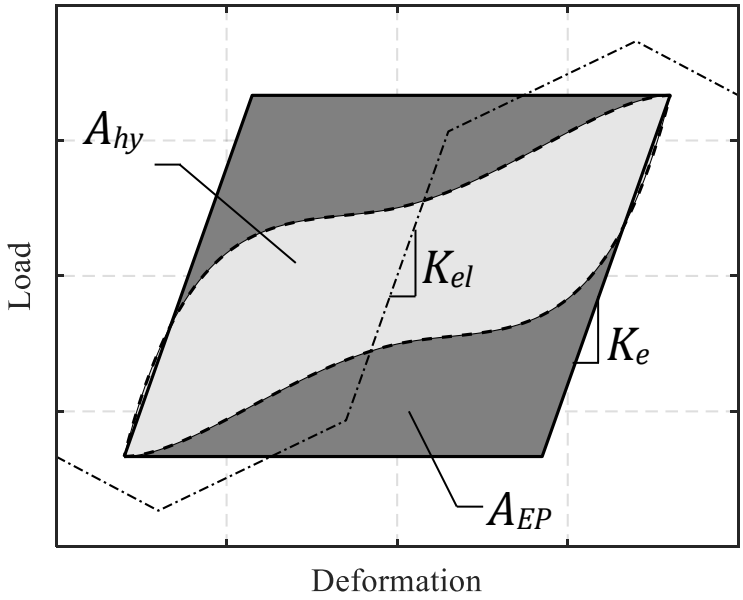

Figure 7-X. Hysteretic Area versus Elastic-Perfectly Plastic Hysteretic Area

It is permitted to represent inelastic actions as having Moderate Pinching behavior where experimental data is not available for the component type and the material chapters do not provide sufficient information for the inelastic action being modeled.

7.5.1.2 Deformation-Controlled and Force-Controlled Actions.

All actions shall be classified as either deformation controlled or force controlled using the component force versus deformation curves shown in Fig. 7-4.

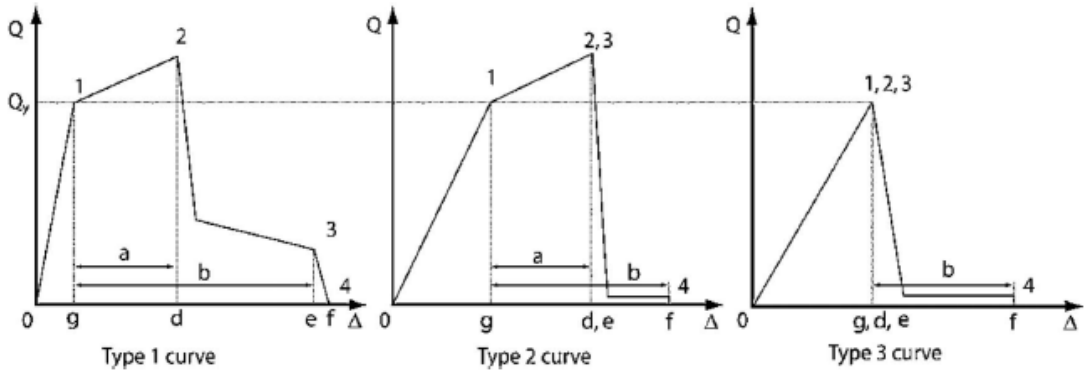

Figure 7-4. Component Force Versus Deformation Curves

~~*Notes:*~~

~~1. Only secondary component actions permitted between points 2 and 4;~~
~~2. The force, Q, after point 3 diminishes to approximately zero.~~

Deformation-controlled actions are defined in Chapters 8 through 12 of this standard by the designation of linear and nonlinear acceptance criteria. Where linear and nonlinear acceptance

criteria are not specified in the standard and component testing in accordance with Section 7.6 is not performed, actions shall be taken as force controlled.

The Type 1 curve depicted in Fig. 7-4 is representative of ductile behavior where there is an elastic range (points 0 to 1 on the curve) and a plastic range (points 1 to 3), followed by loss of seismic-force-resisting capacity at point 3 and effective loss of ~~gravity-load~~ lateral force-resisting capacity at point 4. The plastic range can have either a positive or negative post-elastic slope (points 1 to 2) and a strength-degraded region with nonnegligible residual strength to resist seismic forces and gravity loads (points 2 to 3). Primary component actions exhibiting this behavior shall be classified as deformation controlled if the plastic range is such that $d \geq 2g$; otherwise, they shall be classified as force controlled. Secondary component actions exhibiting this behavior shall be classified as deformation controlled for any d/g ratio.

The Type 2 curve depicted in Fig. 7-4 is representative of ductile behavior where there is an elastic range (points 0 to 1 on the curve) and a plastic range (points 1 to 3). The plastic range can have either a positive or negative post-elastic slope (points 1 to 3) followed by substantial loss of seismic-force-resisting capacity at point 3. Loss of seismic force resisting capacity or gravity-load-resisting capacity takes place at the deformation associated with point 4. Primary component actions exhibiting this behavior shall be classified as deformation controlled if the plastic range is such that $e \geq 2g$; otherwise, they shall be classified as force controlled. Secondary component actions exhibiting this behavior shall be classified as deformation controlled if $f \geq 2g$; otherwise, they shall be classified as force controlled.

The Type 3 curve depicted in Fig. 7-4 is representative of a brittle or nonductile behavior where there is an elastic range (points 0 to 1 on the curve) followed by loss of seismic-force-resisting capacity at point 3 and loss of gravity-load-resisting capacity at the deformation associated with point 4. Primary component actions exhibiting this behavior shall be classified as force controlled. ~~Secondary component actions exhibiting this behavior shall be classified as deformation controlled if $f \geq 2g$; otherwise, they shall be classified as force controlled.~~

For nonlinear procedures, force-controlled components defined in Chapters 8 through 12 may be reclassified as Type 3 deformation-controlled components, provided the following criteria are met:

(1) The component action being reclassified exhibits the Type 3 deformation-controlled performance defined in this section;

(2) The gravity-load-resisting load path is not altered, or if it is altered, an alternate load path is provided to ensure that local stability is maintained in accordance with the load combinations of Section 7.2.2 at the anticipated maximum displacements predicted by the analysis;

(3) The total gravity load supported by all components that are reclassified from force controlled to deformation controlled does not exceed 5% of the total gravity load being supported at that story; and

(4) All remaining deformation-controlled components meet the acceptance criteria to achieve the target performance level and all remaining force-controlled components are not overstressed.

Where overstrength of Type 3 components alters the expected mechanism in the building, the analysis shall be repeated with the affected Type 3 component strengths increased by the ratio Q_{CE}/Q_y, and all components shall be rechecked.

2.4.2 Fiber Model Requirements

This section describes recommended changes to ASCE/SEI 41-17 Sections 7.4 and 7.6 having to do with fiber modeling. The changes clarify requirements for modeling nonlinear actions and calibrating fiber models.

7.4.3.2.2 Component Modeling for NSP

Nonlinear component modeling using lumped or distributed plasticity models shall represent component force-deformation relationships specified in material Chapters 8 through 15 or otherwise be shown to represent experimentally obtained cyclic response characteristics in accordance with Section 7.6. The nonlinear model shall be discretized such that any identified locations of inelastic action represent all potential local mechanisms that affect component response.

Material load-deformation response and meshing in nonlinear fiber sections are permitted in lieu of the lumped plasticity models described in Section 7.5.1.2. Fiber models shall be normalized, within the expected range of behavior, to represent load-deformation response in accordance with component-level behavior prescribed in the material chapters or alternatively experimental derived behavior in accordance with Section 7.6. Fiber element models shall exhibit similar load-deformation response in the complete building analysis to the normalized component-level model.

Components not explicitly represented in the nonlinear model shall be evaluated outside the nonlinear model for potential inelastic actions and acceptance criteria per 7.5.3.2, and representative stiffness in the nonlinear model shall capture load distribution effects and any potential inelastic mechanisms on modeled components. Elastic components in the nonlinear model shall represent effective stiffness prescribed in the respective material chapters to appropriately capture load distribution and acceptance criteria for those elements shall be in accordance with 7.5.3.2.3.

7.5.3.2.2 Acceptance Criteria for Deformation-Controlled Actions for NSP or NDP.

Primary and secondary components shall have expected deformation capacities not less than maximum deformation demands calculated at target displacements. Primary and secondary component demands shall be within the acceptance criteria for nonlinear components at the selected Structural Performance Level. Expected deformation capacities shall be determined considering all coexisting forces and deformations in accordance with Chapters 8 through 15.

Fiber element section acceptance criteria shall be normalized such that deformations over the component length in which inelastic action is expected does not exceed acceptance criteria limits prescribed in material Chapters 8 through 12. It is permitted to develop acceptance criteria for fiber models based on strain limits, if such limits have been calibrated to test data per Section 7.6.

7.6.4 Distributed Plasticity Analysis Parameters and Acceptance Criteria for Component Actions on Experimental Data.

(1) Backbone Calibration: An idealized load-deformation backbone curve shall be developed from the component experimental data as prescribed in Section 7.6.3. Material stress-deformation relationships and analytical component discretization (i.e., element mesh or integration points) in distributed plasticity models shall be adjusted such that the enveloped load-deformation relationship of the component or sub-assemblage is in substantial agreement with the experimental backbone curve, and stiffness and strength loss effects of non-material

fiber-related mechanisms, for example, shear-flexure interaction and local or global buckling, are captured.

(2) Fiber Acceptance Criteria: The subassembly experimental backbone shall be used to classify component behavior as force-controlled or deformation-controlled, and acceptance criteria shall be developed for the subassembly action in accordance with Section 7.6.3. Local deformation acceptance criteria, for example rotation, curvature, or strain, in distributed plasticity models shall be developed for a defined hinge length, or otherwise normalized component length. The local deformation acceptance criteria shall be based on the corresponding experimental subassembly backbone deformations and related acceptance criteria.

(3) Cyclic Response in Nonlinear Dynamic Procedure: The subassembly action shall be identified as exhibiting low pinching, moderate pinching, or significant pinching. Cyclic force-deformation envelopes of distributed plasticity models shall capture such effects of hysteretic pinching, i.e., unloading and reloading stiffness, for the representative inelastic action in the component. The enveloped force-deformation behavior shall be shown to capture related effects on hysteretic energy dissipation.

2.5 References

Coleman and Spacone, 2001, "Localization issues in force-based frame elements," *J. Struct. Eng.*, 127 (11), 1257–1265.

Hagen, 2012, "Performance-Based Analysis of a Reinforced Concrete Wall Building," *M.Sc. Thesis,* California Polytechnic State University at San Luis Obispo, San Luis Obispo, California.

Lowes, L. and Baker, C., 2016, "Recommendations for modeling the nonlinear response of slender of slender reinforced concrete walls using PERFORM-3D," *Proceedings of the 2016 Structural Engineers Association of California Convention*, Maui, Hawaii.

FEMA, 1997, *NEHRP Guidelines for the Seismic Rehabilitation of Buildings*, FEMA 273, prepared by the Building Seismic Safety Council for the Federal Emergency Management Agency, Washington, D.C.

FEMA, 2000a, *State of the Art Report on Connection Performance*, FEMA 355D, prepared by SEAOC, ATC, and CUREE Joint Venture for the Federal Emergency Management Agency, Washington, D.C.

FEMA, 2000b, *Prestandard and Commentary for the Seismic Rehabilitation of Buildings,* FEMA 356, prepared by the American Society for Civil Engineers for the Federal Emergency Management Agency, Washington, D.C.

FEMA, 2009, *Effects of Strength and Stiffness Degradation on Seismic Response*, FEMA P-440A, prepared by the Applied Technology Council for the Federal Emergency Management Agency, Washington, D.C.

NIST, 2017a, *Recommended Modeling Parameters and Acceptance Criteria for Nonlinear Analysis in Support of Seismic Evaluation, Retrofit, and Design*, NIST GCR 17-917-45, prepared by the Applied Technology Council for the National Institute of Standards and Technology, Gaithersburg, Maryland.

NIST, 2017b, *Guidelines for Nonlinear Structural Analysis and Design of Buildings, Part IIa -- Steel Moment Frames*, NIST GCR 17-917-46v2, prepared by the Applied Technology Council for the National Institute of Standards and Technology, Gaithersburg, Maryland.

NIST, 2017c, *Guidelines for Nonlinear Structural Analysis and Design of Buildings, Part IIb -- Reinforced Concrete Moment Frames*, NIST GCR 17-917-46v3, prepared by the Applied Technology Council for the National Institute of Standards and Technology, Gaithersburg, Maryland.

Part 3

Chapter 1: Revisions to Chapter 8 Foundation Provisions

1.1 Motivation

Working Group 2 was tasked with evaluating the shallow foundation provisions in the ASCE/SEI 41-17 standard for clarity, usability, and technical content and with providing recommendations and code change proposals as input for deliberation by the ASCE/SEI 41-23 committee to be incorporated into the next update to the standard.

To provide historical context, ASCE/SEI 41-06 foundation provisions utilized linear procedures to incorporate soil-structure interaction, which included kinematic and foundation damping. However, for flexible base modeling, both FEMA 356 and ASCE/SEI 41-06 allowed for infinite ductility if a spring was added in modeling; the soil strength need not be evaluated – no acceptance criteria was provided for the flexible base modeling case. Research has shown that this bearing area with infinite ductility assumption can be correct up to a point. However, it is not always the case and can cause an underestimation of deformations in the superstructure. ASCE/SEI 41-06 also decoupled the rocking and yielding mechanisms and had separate checks for them, despite that they do not occur independently.

In ASCE/SEI 41-13, the de-coupled rocking issue was addressed with the addition of *m*-factor tables and nonlinear acceptance criteria for these actions that are a function of the soil stiffness and gravity loads on the foundations. In addition, ASCE/SEI 41-13 revised the soil-foundation-structure interaction provisions and added limitations. The fundamental concept of both the ASCE/SEI 41-13 and the ASCE/SEI 41-17 provisions is that if the Acceptance Criteria of the foundation chapter are satisfied, then the foundation deformations are accurate enough, and the analysis is suitable for determining the component level Acceptance Criteria of the superstructure. This philosophy is retained in the changes proposed for ASCE/SEI 41-23. However, several issues with the ASCE/SEI 41-17 foundation chapter have been identified:

- Navigation through the foundations chapter in ASCE/SEI 41-17 is complicated as requirements for linear and nonlinear procedures were intermixed within the standard.
- There are large gaps in the linear procedure process including:
    - Lack of clarity for when a fixed-base assumption is permitted, which leads to confusion about what analysis provisions to follow.
    - In order to proceed with the correct analysis method, per the provisions, it must be determined if a footing is rigid relative to the soil. However, the method provided for that determination is in the commentary section and does not consider that soil separates from the footing during rocking action.

  - Linear provisions for footings that are flexible relative to the soil are not provided (former Method 3 was missing for the linear procedures).

- In some cases, acceptance criteria and direction for items such as bounding and stiffness are provided in narrative form. This led to confusion in applying the provisions and reduced the useability and clarity of the chapter. Tabulated acceptance criteria would be easier to follow.

- Some of the provisions required a flexible-base analysis to be performed in addition to a fixed base analysis to determine if the results from the fixed base procedures could be used.

- The prescriptive soil properties permitted to be used when soils information is not available was very small, such that it would most certainly require soil exploration to be conducted for evaluation of the foundations for almost all buildings regardless of its foundation capacity or level of seismicity. Further, the prescriptive bearing capacities are inconsistent between the two methods provided; expected bearing capacities based on the calculated gravity loads to existing footings per ASCE/SEI 41-17 Equation 8-3 are too conservative when compared to expected bearing capacity based on Equation 8-1.

- Acceptance criteria for overturning compression in the absence of moment is not addressed.

- Soil bearing acceptance is expressed only in terms of ultimate bearing capacity for an isolated rectangular footing resisting axial load and uniaxial moment. This left out a lot of cases and necessitated the use of engineering judgement, which potentially resulted in inconsistencies and misapplication in the use of the standard. *m*-values provided in ASCE/SEI 41-17 were derived based on axial and overturning actions but were incorrectly applied to soil bearing. The intent is that these *m*-values should not be applied to soil bearing but to the overturning moment capacity.

- Use of the fixed-base method results in unusually large footings for a normal-sized superstructure. The results are also unusually large compared to footings using the other methods or ASCE/SEI 7-16 for similar-sized superstructures.

- Foundation acceptance is only provided for soil bearing with little guidance provided for evaluation of the foundation structural component.

- Bounding for stiffness and bearing capacities is required because soil is inherently less homogeneous and has greater variations in material properties than other materials such as steel or concrete, However, the 2017 version eliminated nearly the entirety of the clarification on what to use for these capacities. Additionally, the limits of doubling and halving strength and stiffness may not be appropriate. The high and low bounding needs to provide significant results to merit the additional analysis requirements. Bounding should consider soil variation, uplifting foundations, overturning stability, liquefaction, and modeling sophistication. Moreover, there are discrepancies between the stiffness values of ASCE/SEI 41-17 Figure 8-1 equations, which are based on a rigid structural footing and elastic soil response where the soil remains in contact with the footings, and those stiffness values derived using the modulus of subgrade reaction and

methods that embrace and incorporate soil separation from the footing as well as flexible and yielding structural footings. There is potential to bound and calibrate springs on the wrong solution – the too stiff solution.

- Further smaller-scale technical concerns:
  - Definitions of select key terms, such as uplift, are not clear, leading to confusion and misuse of provisions. Uplift in the context of these provisions is the pure axial force causing the entire footing to separate from the soil as opposed to some soil separation as the footing rotates due to rocking action.
  - Determination of the effective footing width (B_f) for a mat foundation was missing,
  - Where footing overturning action cannot be idealized as a rectangular or I-shaped footing, such as combined footings and mat foundations, the analysis method required engineering judgement.
  - ASCE/SEI 41-17, Equation 8-10 for determining the upper bound moment capacity of a rigid shallow rectangular footing is confusing to users and therefore could lead to implementation issues without clarification of its origins.

$$M_{CE} = \frac{L_f P_{UD}}{2}\left(1 - \frac{q}{q_c}\right)$$

  - The overturning action is very dependent upon the transient axial load level, so when using the pseudo elastic force methods, determining a realistic seismic axial load is very difficult. This issue is not limited to foundations; it applies to linear procedures of other material chapters.
  - The intent of Equation 7-2 of ASCE/SEI 41-17 is to use 0.9 times the expected dead load, not the load combinations. Incorrectly applying the load combinations resulted in yet another type of bounding that leads to more unnecessary work. Even the FEMA P-2006 examples incorrectly used the load combinations where intent was just to use expected dead load, indicating the error is common.
  - There is a discrepancy between Chapter 10 (Concrete) and the intent of Chapter 8. Chapter 10 requires footings to be designed as force controlled.

These numerous issues were the catalyst for providing proposed provision and commentary changes for consideration by the ASCE/SEI 41 committee. The priorities were to derive a shallow foundation provision structure that was user friendly and to address all the above gaps, as well as new items as discovered during the case study work.

New sections are added to guide the user though the proper use of the standard to provide a more logical flow based on the level of analysis performed, in the application of the standard. Gaps in the

existing provisions for evaluation of buildings on shallow foundations have been addressed with the new added provisions. Existing provisions have also been carefully examined for accuracy and applicability through case studies and parametric studies on individual aspects in the provisions. Existing provisions that were not widely used or where it can be shown to be too conservative, corroborated by outcomes from individual parametric or full building analysis case studies have been deleted.

This chapter provides the technical justification for the proposed changes to Chapter 8 of ASCE/SEI 41-17 to achieve these goals. The foundation acceptance criteria and corresponding superstructure acceptance criteria were evaluated, and results were compared for reasonableness assuming the building was designed to meet the requirements of new buildings designed using ASCE/SEI 7.

1.2 Summary of Recommended Changes

ASCE/SEI 41 Chapter 8 was reorganized to separate the linear and nonlinear provisions. This resulted in completely different section numbers between ASCE/SEI 41-23 and ASCE/SEI 41-17. A summary of the case studies and the major technical changes are noted below.

1.2.1 Application of Evaluation Provisions for Shallow Foundations

Added a new section 8.4.1 to ASCE/SEI 41-23, to specify when modeling the building as a fixed-base is permitted and when it is not permitted without having to perform a fixed-base and a flexible-base analysis to determine the outcome. This section replaced the requirement where fixed-base procedures are not permitted when the superstructure is sensitive to base rotations when evaluated at the Immediate Occupancy level.

1.2.2 Expected Soil Bearing Capacity

Revised terminology for upper- and lower-bound properties to expected ultimate capacities and eliminated bounding requirement for linear analysis procedures. There was no net change in regulatory effect.

Updated the soil bearing capacity when information on the soil properties is not available either in the construction documents or in a geotechnical report.

1.2.3 Seismic Overturning Forming Axial Load Action

A new section was added to ASCE/SEI 41-23 Section 8.4.4.1.1.2 to evaluate foundations where overturning action is resisted by axial action, coupled tension and compression, and where the overturning moment action on the foundation is low. Currently in ASCE/SEI 41-17 there is acceptance criteria for overturning uplift action, but it is silent for overturning compression action in the absence of moment. This added section addresses the issue. The exception to considering foundations as force-controlled when seismic axial load exceeds 3 times the gravity loads or A_c/A exceeds 0.6 was deleted and adjustments were made to the *m*-factors instead.

1.2.4 Foundation Moment Capacity with Bi-directional Overturning Action

Currently in the Standard, overturning acceptance is addressed only for unidirectional moment for a rectangular or I-shaped footing. A new methodology is proposed in ASCE/SEI 41-23 Section 8.4.4.1.1.1 and described in the commentary for evaluating foundations where the footing is required to resist overturning moments simultaneously about the two horizontal principal axes of the footing. This methodology is applicable to isolated footings of any plan geometry. Section 8.4.4.1.1.1 also provides clarifications for the calculation of the expected vertical load on the soil at the footing interface, P_{UF}, including an increase in the DCR_m limit from $2C_1C_2$ to $3C_1C_2$.

1.2.5 Determination of Soil Stiffness for Mat Foundations

Formulations for determination of the soil stiffness or modulus of subgrade reaction are provided for rigid isolated footings or strip footings. Extending these stiffness formulations as representative for buildings on large mat foundations results in unreasonably low values of stiffness. Multiple alternate methods for determination of the soil stiffness for mat foundations have therefore been proposed in ASCE/SEI 41-23 Section 8.4.4.1.2.1 using rational judgment and are based on the actual loaded area immediately below the vertical elements supported by the mat.

1.2.6 Procedures for a Separate Foundation Analysis Using Superstructure Demands from a Fixed-Base Model

A common practice for new buildings designed using ASCE/SEI 7 is to use an elastic, fixed-base building model to design the superstructure, and a separate elastic model of the foundation on compression-only springs to design the foundation. A similar approach is proposed in ASCE/SEI 41-23 Section 8.4.4.1.2, and alternate procedures are provided when different platforms are used to check foundations and superstructure for foundations modeled as a fixed base.

1.2.7 Moment Capacity of Footings Interconnected by Grade Beams

Acceptance criteria for foundation overturning capacity in the standard are based on the moment capacity for an isolated footing. Footings that are interconnected by a grade beam have additional capacity that is not accounted for. New provisions are proposed in ASCE/SEI 41-23 Section 8.4.4.1.2.3 to permit increasing the overturning moment capacity, M_{CE}, of the footing by the resistance provided by the grade beam beyond the boundaries of the isolated footings. The resistance from the grade beam is computed by principles of mechanics considering a free body diagram of the footing.

1.2.8 Limiting Use of Compression-Only Springs When Superstructure Is Modeled as Linear Using Flexible-Base Procedures

For linear analysis flexible base procedures, when the foundations supporting soil and superstructure are modeled together in a single computer model, the supporting soil is also to be modeled as elastic in ASCE/SEI 41-23 Section 8.4.5.2. Combining nonlinear uplifting foundations

with an elastic superstructure is now explicitly not permitted unless superstructure elements are expected to remain essentially elastic under the applied seismic demands.

1.2.9 Acceptance Criteria Check for the Structural Footing

There is currently no specific requirement or acceptance criteria for checking the structural footing in Chapter 8. Evaluation of the foundation structural component is specified in the material chapters where demands to the foundation are treated as force-controlled. Specific requirements have been introduced in ASCE/SEI 41-23 Section 8.4.4.1.1.3.2 specifying the magnitude and application of the soil pressures as loads to the footing.

1.2.10 Bounding Requirements for Nonlinear Procedures

Earlier versions of the standard required bounding on soil strength and stiffness to be considered when soil properties were explicitly modeled. The proposed requirements eliminate the need for modeling using upper- and lower-bound soil properties and permitting modeling of the soil using the expected values for strength and stiffness.

1.3 Technical Studies

1.3.1 Overview of Case Studies

Working Group 2 evaluated the current provisions in the ASCE/SEI 41-17 standard for clarity, usability, and technical content and provided recommendations and code change proposals to be incorporated in the next standard update. The working group focused on investigation of strategically selected technical topics, resolution of which is achieved through quantitative case studies of the overall foundation analysis and design process, as opposed to opinion-based approaches. To achieve this, independent computer models of two archetype buildings were developed: one was for a five-story slab-column moment frame building, Archetype Building 1, and one was for a seven-story reinforced concrete moment frame building, Archetype Building 2. The models created were used in a myriad of parametric case studies to investigate selected topics related to overturning actions on shallow foundations. The foundation acceptance criteria and corresponding superstructure acceptance criteria were evaluated, and results were compared for reasonableness assuming the building was designed to meet the requirements of new buildings designed using ASCE/SEI 7-10. The results from the case studies formed the basis of the proposed changes to ASCE/SEI 41-17. A brief description of the modeling and analysis approach used in each case study is presented below. Results for the case study that justified the change are presented in the relevant sections where the change is proposed. Additional details on the case studies are presented in the supporting documentation for each case study.

1.3.1.1 ARCHETYPE BUILDING 1 CASE STUDY

This case study investigated the use of ASCE/SEI 41-17 Chapter 8 for clarity, usability, and technical content as part of Working Group 2 objectives. Individual aspects in the standard were isolated and

quantitatively investigated. Because of the interrelation between each provision, it was difficult to study one provision without understanding the implications of other assumptions. The collective impact of the variations of the isolated provisions were tracked in terms of superstructure and foundation acceptance, and recommended changes were proposed based on the findings.

Building Description

The 1920s existing building selected as the archetype building for this study is a five-story, 55-foot-tall reinforced concrete structure that measures approximately 104 feet by 84 feet (5 by 4 bays) in plan. Concrete columns occur on an approximate 20-foot square grid throughout the building, and the structure is supported at its base on shallow isolated footings. Floor and roof slabs are reinforced concrete; the core for the existing elevator and stair are non-structural infill walls. The existing lateral force-resisting system is slab-column moment resisting frame (Concrete Moment Frame, C1), and with new shear walls added, Concrete Shear Walls with Rigid Diaphragms (C2). The retrofit consists of adding shear walls at strategic locations: one in the center of the building for north-south loading and two in the orthogonal direction at the ends of the building to provide shear resistance and plan torsion stability (see Figures 1-1 and 1-2). The intent is to perform studies by applying unidirectional loading in the north-south direction only.

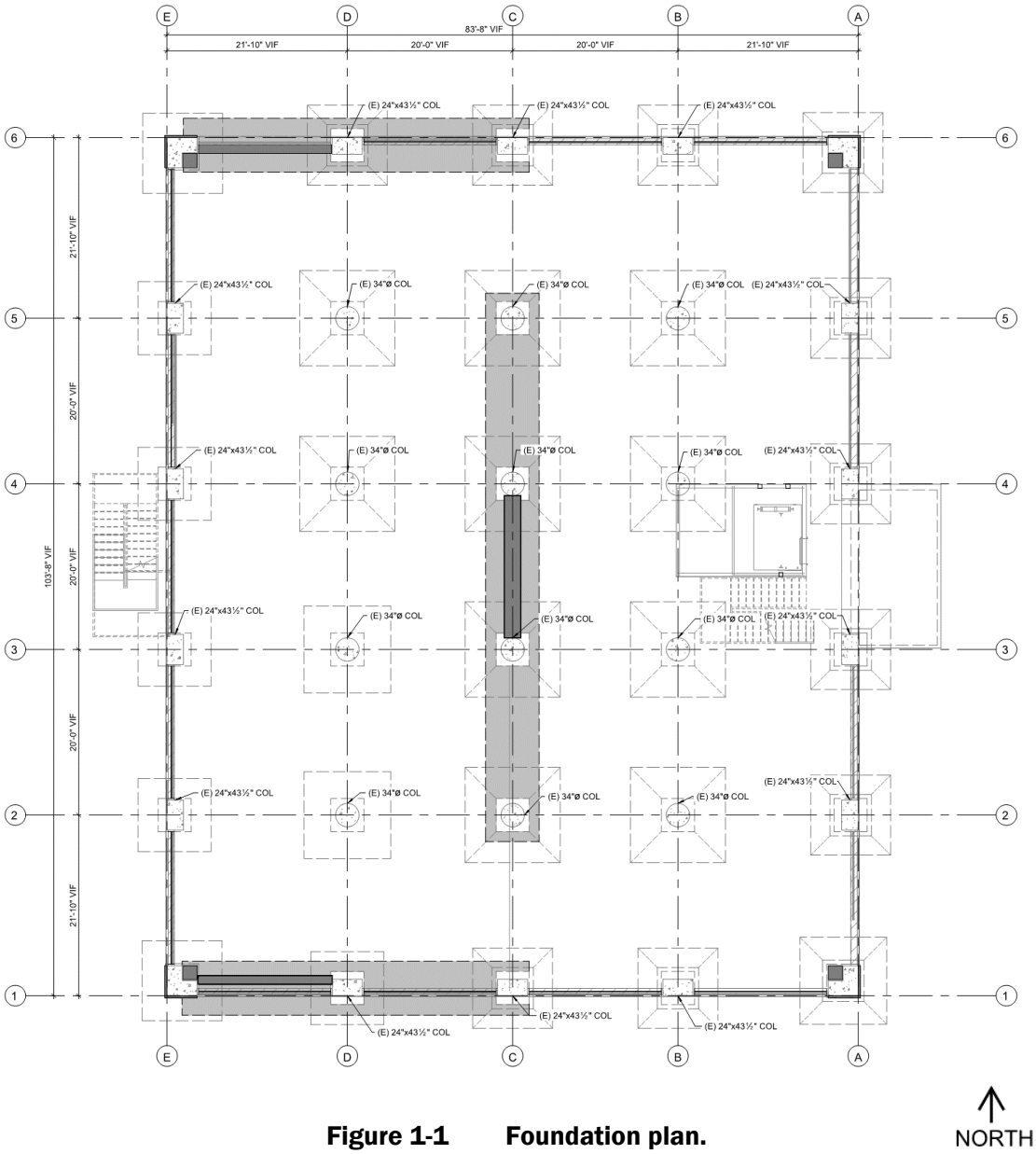

Figure 1-1 Foundation plan.

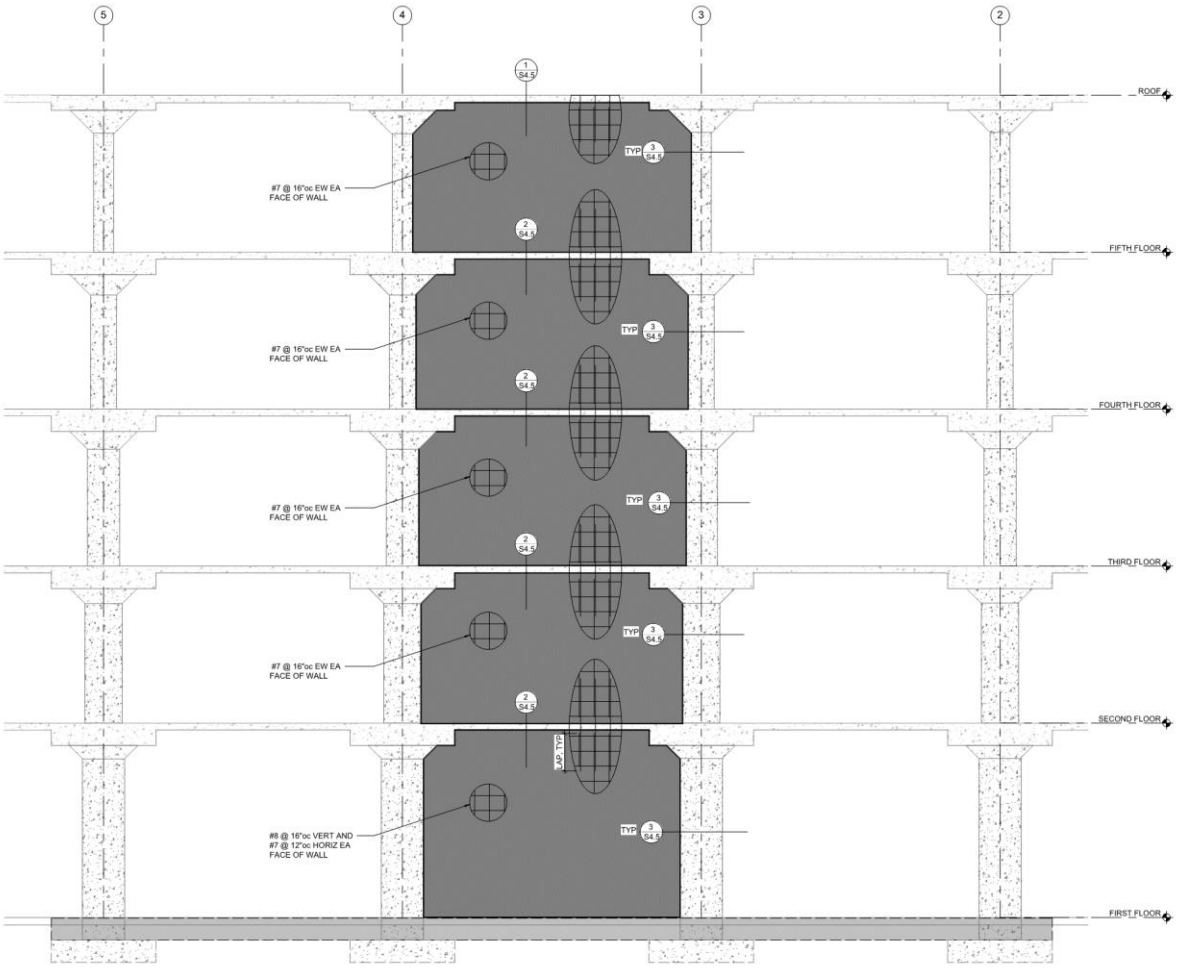

Figure 1-2 Retrofit wall and existing structure elevation (3 of 5 bays shown). The grey slab and shear wall were added in the retrofit.

Soil Conditions

A geotechnical investigation was performed on the site. The soil consists of medium stiff clayey fill underlain by stiff to very stiff clay and claystone bedrock. New and existing footings are founded on the claystone bedrock with a N_{60} (penetration blow count corrected to an equivalent hammer energy efficiency of 60%) equal to 25 per the geotechnical engineer. The initial shear modulus is calculated per ASCE/SEI 41-17 Section 8.4.2.2, and the effective shear modulus is determined based on the ratio in ASCE/SEI 41-17 Table 8-2.

Case Study Approach

Analysis Model

The finite element analysis program ETABS 18 by Computers and Structures, Inc., a widely used structural engineering software by the engineering community, was used as the analysis platform in

this case study. The analysis model is a 3D model for all cases and consists of analysis objects including joints objects, frame objects, and area objects.

Where nonlinear characteristics are included in the analysis, lumped plasticity, user-defined hinge properties are input in ETABS and assigned to frame elements. Fiber modeling is not utilized in this analysis as the nonlinear aspects of the elements are adequately captured by the nonlinear hinges applied to frame elements. Walls and slabs that are typically defined as shell elements in linear models are defined as frame elements in the nonlinear models for assignment of frame hinges.

For fixed-base analysis, the base of each column (including each end of shear walls) is restrained against translation and rotation. This setup was compared to a model with base of the columns pinned (base of columns restrained against translation but not rotation). The fundamental period of the two models was within 5% of each other, indicating that the column base fixity does not have a large effect on overall building response.

In the analysis models with foundation components explicitly modeled (flexible base), overturning action on the soil is modeled as either a single rotational spring or coupled axial springs.

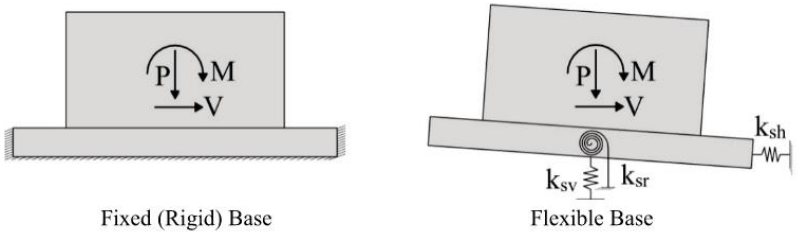

Figure 1-3 Structure boundary conditions.

Accidental torsion was not investigated within these analyses. The building plan is symmetric in the north-south direction with the retrofit wall at the plan center of the building. The retrofit in the east-west direction provides walls on the west side on the north and south ends of the structure as shown in Figure 1-1. Torsional building response is ignored for these investigations.

Analysis Procedures

Linear and nonlinear analysis procedures from ASCE/SEI 41-17 Chapter 7 were utilized in this study. Many of the objectives seek to compare linear results from the linear static procedure (LSP) to nonlinear results from the nonlinear static procedure (NSP) or the nonlinear dynamic procedure (NDP). In these comparisons, the nonlinear results are utilized as the benchmark for the studies and the linear procedures were calibrated to it. Nonlinear procedures are not presumed to precisely estimate the real building performance; this study did not seek to prove accuracy of nonlinear modeling compared to true building performance. Other research has been conducted to calibrate nonlinear results to testing data, which is the basis of the nonlinear hinge methodology in ASCE/SEI 41. For this study, it is assumed the nonlinear analyses are more accurate in determining structural response and provide sufficient data to examine the various aspects related to linear analyses.

General Overview of ASCE/SEI 41-17 Chapter 8 Soil Modeling Methodologies

There are three "methods" for foundation modeling in ASCE/SEI 41-17. There are two methodologies included within Method 1. Method 1 fixed base models do not have soil springs and are restrained against translation and global rotation at the soil-structure interface. Acceptance criteria for the fixed base models are per ASCE/SEI 41-17 Section 8.4.2.3.2.1, which includes provisions for soil bearing and overturning stability of individual foundation elements. Method 1 flexible base models uses uncoupled moment, shear, and axial springs to model rigid foundations such that the moment and shear behaviors are independent of the axial load. Method 1 soil springs can be utilized for both linear and non-linear analysis methods but is only applicable to footings assumed rigid compared to the soil. Method 2 is also for shallow footings considered rigid compared to the soil but can only be utilized with nonlinear analysis methods. Method 2 provides an alternative approach for rigid footings that uses a bed of nonlinear springs that accounts for coupling between vertical loads and moment. Method 2 is the preferred approach when there is significant variation in axial load. The moment-rotation and vertical load-deformation characteristics are modeled as a beam on a nonlinear Winkler foundation with stiffer vertical springs at the end regions of the foundation to allow for tuning of the springs to approximately match the elastic vertical and rotational stiffness provided in Method 1. This method may also be used to account for settlement and permanent deformations. Method 3 is the only method allowed for shallow foundations where the structural component (footing) is not rigid relative to soil, and it is only applicable to nonlinear analysis procedures. Method 3 uses a similar methodology to Method 2 with Winkler springs beneath the foundations, except that a uniform distribution of soil stiffness and strength is applied. Deep foundation provisions were not investigated as part of this case study.

Analyses Performed

Numerous studies of the building were conducted to investigate the applications of ASCE/SEI 41-17 Chapter 8 methods.

- ASCE 7-10 (for comparison purposes)
- ASCE/SEI 41-17 Linear Static Procedure
  - Fixed Base
  - Flexible Base (Method 1, upper and lower bound)
  - Flexible Base (K_{50} Stiffness, $300M_{c,foot}$ and $550M_{c,foot}$)
- ASCE/SEI 41-17 Nonlinear Static Procedure
  - Flexible Base (Methods 1)
  - Flexible Base (Method 2, non-tuned and tuned)
  - Flexible Base (Method 3, force-controlled and deformation controlled)

- Fixed Base

These models were used to investigate these major ASCE ASCE/SEI 41-17 Chapter 8 methods:

- Bearing Capacity Investigation
  - Investigate multiple methods for determining the expected soil bearing capacity and investigate LSP soil bearing capacity bounding
- Foundation Overturning Capacity: Clarification of the Expected Vertical Load by calculating the effects of different P_{UD} calculations on $M_{C.}$ (LSP)
- Seismic Overturning Resisted by Axial and Moment Action: Analyses to define bi-direction overturning moment and acceptance criteria for bidirectional loading
  - Fixed Base
  - Bi-directional Loading
  - Rectangular and L-shaped retrofit footings
  - with previous case studies
- Acceptance Criteria for the Structural Footing
- Soil Stiffness for Shallow Foundations: Simplify modeling approaches and eliminate unnecessary options
  - Spring Derivation Comparisons:
  - Effects on superstructure and foundation methodologies for deriving soil springs
- Isolated Spread Footings Soil Strength and Stiffness
- Acceptance Criteria for Isolated Spread Footings with Foundation Interface Modeled as a Flexible Base
  - Foundations evaluated as deformation and force-controlled
- Combined footings and mat foundations
  - Parametric study of spring stiffness with tension/compression springs
- Nonlinear static procedure
  - Stiffness Derivations for springs and their respective effects on analysis results and acceptance criteria

- Determination of allowable rotation at the footing-soil interface

1.3.1.2 ARCHETYPE BUILDING 2 CASE STUDY

Introduction

The case study for Archetype Building 2 is similar to the case study for Archetype Building 1. It investigates the application of some of the methods specified in ASCE/SEI 41-17 Chapter 8 for clarity, usability, and technical content. Various combinations of shallow foundation modeling options are created, to evaluate the shallow foundation provisions related to overturning actions. Sliding is not considered in this case study example and sliding is assumed as fixed for all modeling cases. A baseline model was created where superstructure and foundations are designed to meet the requirements of ASCE/SEI 7-10. Parametric case studies are then performed to investigate selected topics related to overturning actions on shallow foundations using ASCE/SEI 41-17. Foundation acceptance criteria and corresponding superstructure acceptance criteria are evaluated, and results compared for reasonableness assuming the building was designed to meet the requirements of the new building designed using ASCE/SEI 7.

The case study chosen for Archetype Building 2 is a seven-story reinforced concrete moment frame building. The model created was used in a myriad of parametric case studies to investigate selected topics related to overturning actions on shallow foundations. The foundation acceptance criteria and corresponding superstructure acceptance criteria are evaluated, and results compared for reasonableness assuming the building was designed to meet the requirements of the new building designed using ASCE/SEI 7.

Planned Approach

Prior to creating the case study models, a roadmap was developed to establish a step-by-step approach of what the working group was going to do with a list of assumptions and get agreement before embarking on actual computational work. The roadmap was used as a guide to execute the parametric case studies.

Goals of the Case Study

- Evaluate and revise current provisions for clarity, technical accuracy, optimal computations, and ease of use.
- Calibrate *m*-factor approach such that it shows acceptable performance analytically consistent with engineering judgment.
- Determine if simplifications in the analysis methods are possible and that they are reasonably conservative.
- Determine the impact of foundation modeling variations on the superstructure.

Building Description

The subject building is a modified existing seven-story reinforced concrete special moment frame building located in a region of high seismicity (Van Nuys, California). The study building is supported on shallow foundations and designed to satisfy the requirements in ASCE/SEI 7-10 for a new building in Risk Category 2. This case study considers the building to be on individual/spread footings to investigate the shallow foundation provisions of ASCE/SEI 41-17.

The gravity system consists of reinforced concrete flat slabs supported by interior concrete columns and perimeter concrete beams supported by concrete columns. The concrete slabs are 10 inches thick at the second floor, 8.5 inches thick at the third through seventh floors, and 8 inches thick at the roof. The typical framing consists of columns spaced at approximately 20-foot centers in the transverse (north-south) direction and 18 feet 9 inches on center in the longitudinal direction.

Lateral forces in each direction are resisted by the interior column-slab frames, and by the perimeter column-spandrel beam frames. Interior columns are 18 inches square and exterior columns are 14 inches by 20 inches.

A complete three-dimensional mathematical model of the building (Figure 1-4) was created for this building incorporating the stiffness, strength and deformation characteristics as specified in ASCE/SEI 41.

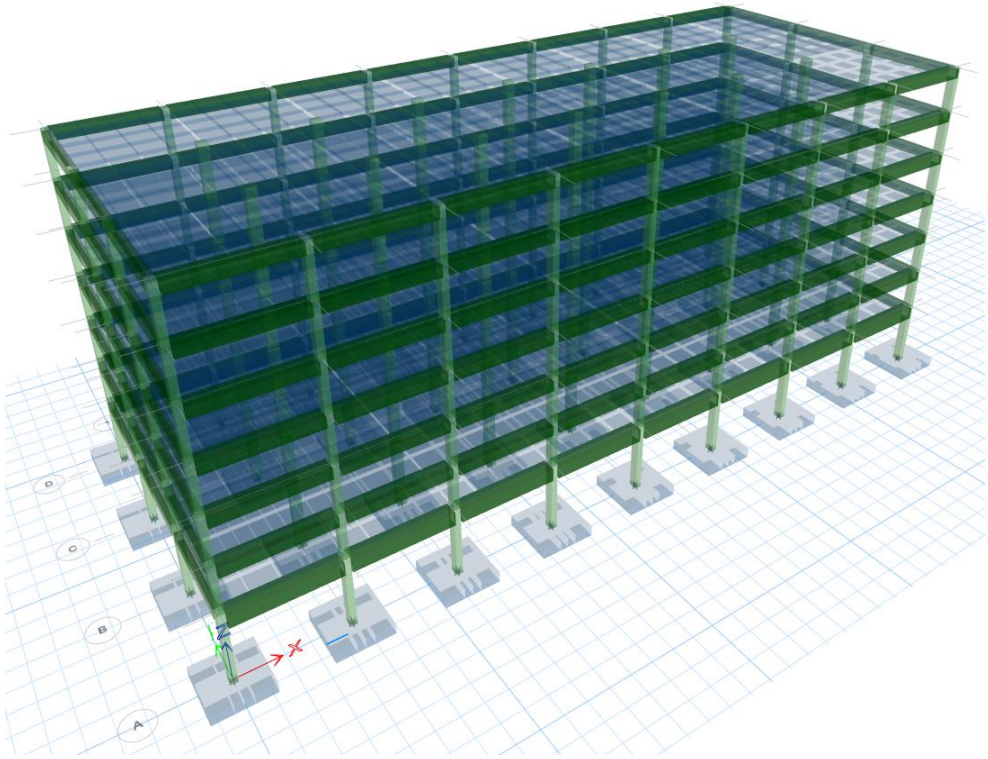

Figure 1-4 Three-dimensional model of the seven-story reinforced concrete special moment resisting frame building.

General Assumptions

- Model is 3D but only symmetric loading in the longitudinal direction is considered in the analysis, and effects of torsion are ignored.
- Soil properties are uniform over the footprint of the building. Variable soil properties or liquefaction potential are not considered.
- For flexible base option, the building is modeled on area springs with assumed properties for stiff clay with a modulus of subgrade reaction of 0.1 ksi.
- Deformations due to sliding are ignored.
- Diaphragms are modeled as rigid.
- Ground motions are the mapped values for the site (Van Nuys, California).
- Section properties modifiers used per ASCE/SEI 41-17 Table 10-5.
- Beam reinforcement is designed to meet the detailing requirements of ACI 318-14 for qualification as a special reinforced concrete moment frame.
- Column reinforcement is not designed, but moment capacities adjusted to meet the strong column-weak beam check.

Building Demand Parameters of Interest

The following demand parameters are tracked for comparison between the methods: A) for foundation and B) for superstructure.

- Foundation
  - Bearing pressure
  - Settlement
  - Demands on the footing
  - Acceptance criteria for soil and foundation
- Superstructure
  - Base shear demand
  - Building displacement and story drift
  - Acceptance ratio in elements of the lateral-force-resisting system per story for each element type

Analyses Performed

To execute the parametric case studies, linear and nonlinear analysis procedures were conducted with the following boundary conditions for the foundation:

- Linear Static Procedure (LSP)
  - Fixed base model
  - Model on foundation area springs
- Nonlinear Static Procedure (NSP)
  - Fixed base model
  - Model on foundation area springs

1.3.2 Application of Evaluation Provisions for Shallow Foundations

The consensus is that many building configurations and lateral-seismic-force-resisting systems should not experience excessive rocking of the foundation to result in damage or failure of the superstructure elements for buildings on nonliquefiable sites. However, the decision of how and when to model the shallow foundation's flexibility requires engineering judgment and an understanding of the impacts this decision has on the behavior of the structural components in the building. The determination of whether foundation movement is an important consideration for a myriad of building types and configurations is such a complicated and complex question that it is impractical to develop prescriptive code provisions, similar to those of ASCE/SEI 7-16, for each case. A flowchart of the various evaluation procedures to be followed is shown in Figure 1-5.

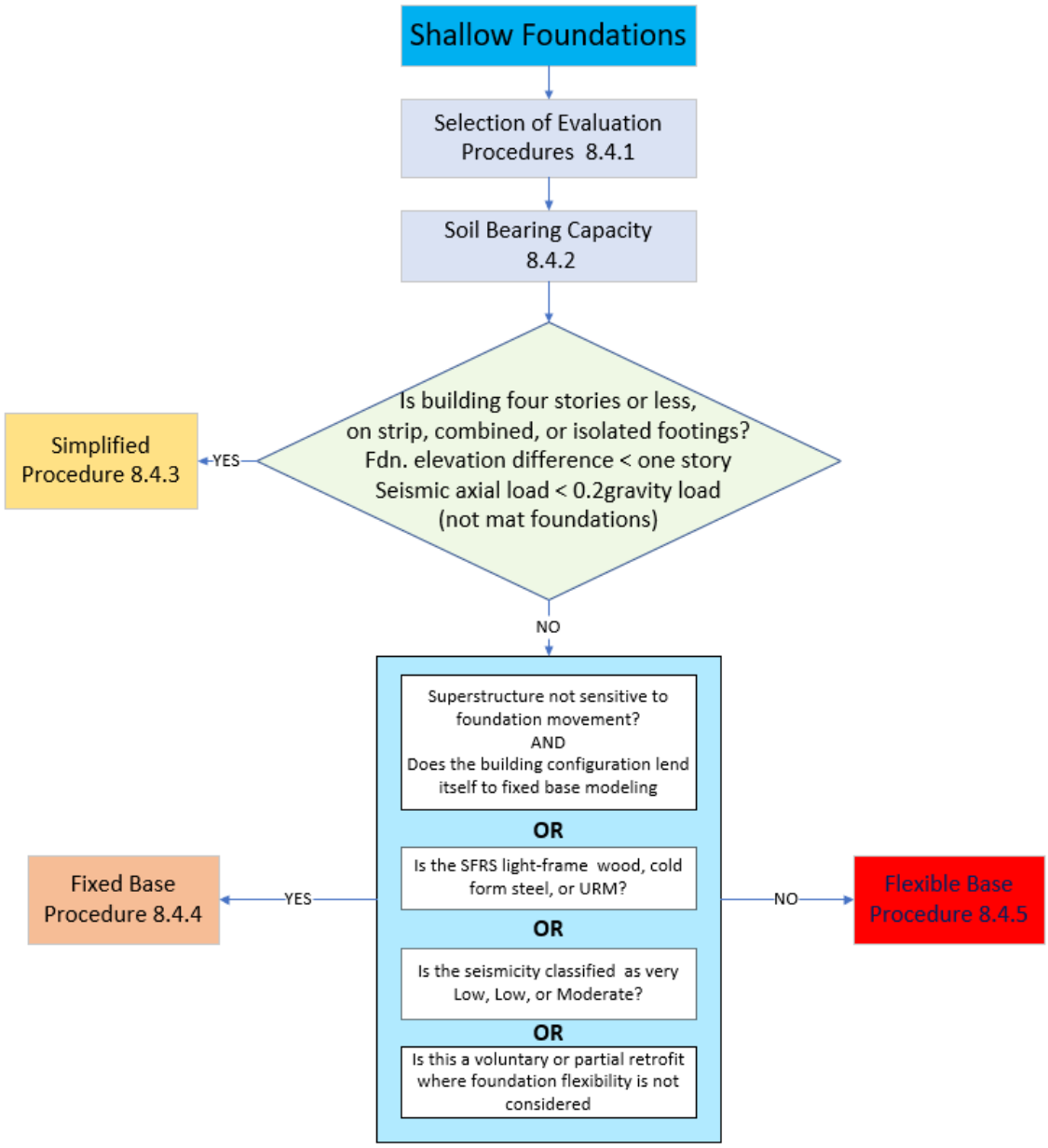

Figure 1-5 Proposed foundation evaluation procedures for buildings on shallow foundations.

There are three overarching procedures (Section 8.4.3, Section 8.4.4, and Section 8.4.5) that can be used to evaluate the foundation system. Evaluation procedures for the majority of existing buildings are generally covered by the Simplified Procedure, ASCE/SEI 41-23 Section 8.4.3. For the remaining buildings, the decision of how to model foundation fixity is paramount to an accurate analysis.

1.3.2.1 SIMPLIFIED PROCEDURE

A simplified procedure is introduced for evaluation of the foundation system of buildings on shallow foundations on relatively level ground to allow the user to avoid the complexities of the rest of the

chapter. Foundation acceptance in ASCE/SEI 41-17 is limited to the *m*-factor amplified moment capacity of isolated footings being less than pseudo seismic force demand. New recommended provisions have been introduced to extend this provision to apply to footings interconnected by grade beams and to strip footings, where the resistance provided by the grade beam increased the moment capacity of the footing using the principles of mechanics. This concept has been utilized to implement the fixed base procedure. It is intended to be more conservative than the fixed-base or flexible-base provisions but was deemed appropriate for buildings four stories or less on relatively level ground or gently sloping ground. The use of the simplified procedure is therefore limited to buildings four stories or less on strip, combined, or isolated footings (not mat foundations) where the elevation of the bottom of the footings is nominally the same. In this procedure where the foundation consists of strip footings supporting gravity and lateral loads at multiple locations along the footing, the footing should be discretized into rectangular segments supporting the elements of the lateral-force-resisting system without consideration of the bends at corners or other foundation plan geometric irregularities, as shown in Figure 1-6.

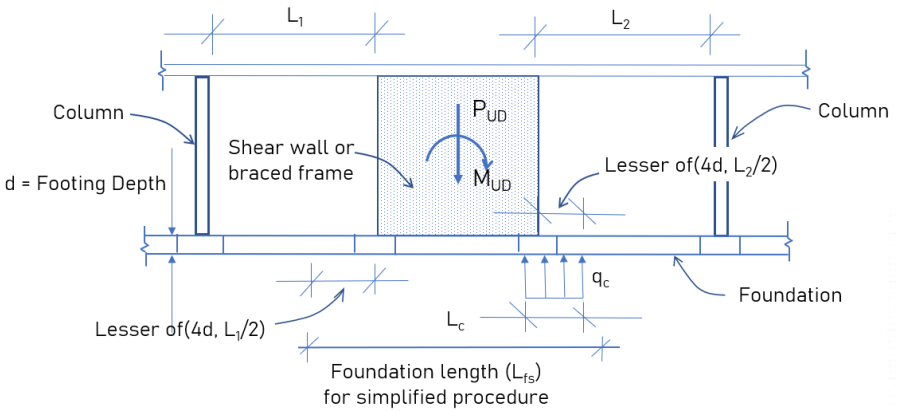

(a) Intermediate Condition

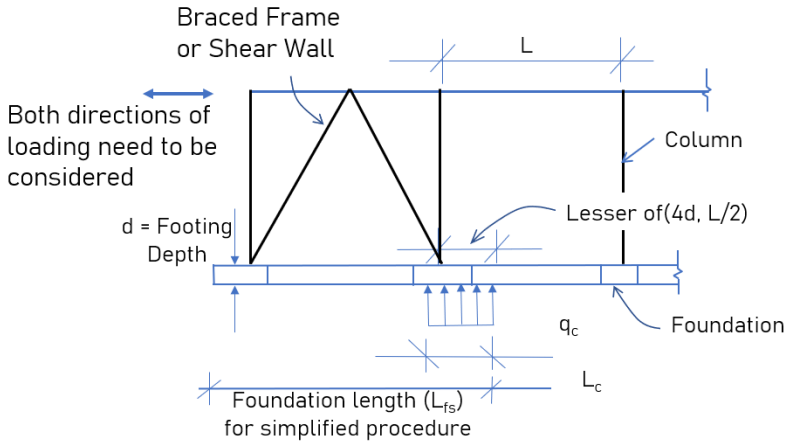

(b) End Condition

Figure 1-6 Foundation length for the simplified procedure.

Soil acceptance occurs when the gravity axial load and foundation overturning demand on the segment of footing are less than the *m*-factor times the moment capacity of that footing. The structural integrity of the footing is determined based on the ability of the footing to resist demands using a bearing pressure q_c under the footing. Footing acceptance is evaluated depending on the action (moment or shear) on the footing with the requirements in the material chapters.

While there is a discrepancy between the requirements for overturning stability or soil bearing and the evaluation of the footing, case studies have shown this approach to give reasonable outcomes. It should be noted that the demands on the foundation are the pseudo seismic forces demands, and do not reflect a reduction due to inelastic deformations in the superstructure. In addition, concentration of the resisting soil pressure applied at the ends of the footing results in the maximum demand at the critical sections of the footing.

Since the foundation moment capacity is dependent on the applied axial load on the footing, this procedure is not permitted when the pseudo-seismic axial demands on individual isolated footings exceeds 0.2 times the gravity load on the footing, as shown in Figure 1-7. For these conditions the foundation should be evaluated using the fixed-base or flexible-base procedures.

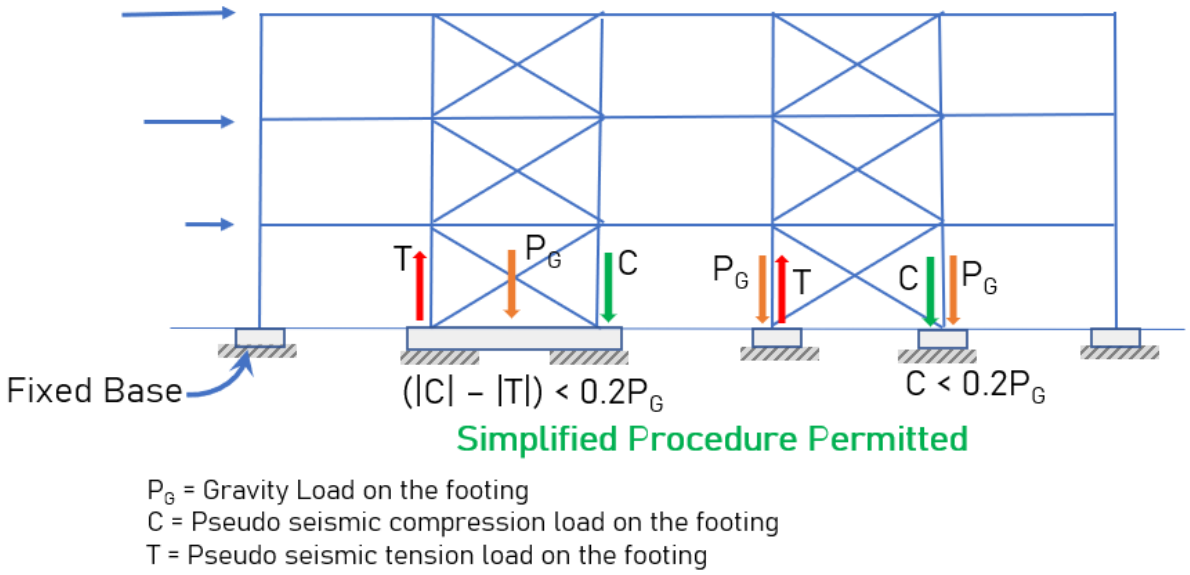

Figure 1-7 Example showing when the simplified procedure may be used as a function of the pseudo seismic axial load.

1.3.2.2 FOUNDATION DEGREE OF FIXITY: FIXED VERSUS FLEXIBLE

The following section provides the reasoning, discussion, and examples of where fixed-base procedures are deemed acceptable and flexible-base procedures would be prudent. Building types, including foundation configurations, that are clear cases where the fixed-base assumptions capture accurate performance outcomes are identified and permitted to always be modeled as a fixed-base.

For example, buildings using the partial retrofit provisions of ASCE/SEI 41-17 Section 2.2.5 (where a voluntary or a partial retrofit is performed) could exclude foundation evaluation from the scope and use a fixed-base model without considering the additional limitations. Also, limitations to the use of fixed-base procedures do not apply when buildings are evaluated at seismicity's classified as Very Low, Low, or Moderate from ASCE/SEI 41-17 Table 2-4, as not modeling the foundation flexibility may not significantly impact the deformations of the superstructure when the ground motion is relatively small.

Modeling of foundation flexibility is also not mandated for buildings of light-frame construction, (wood or cold-formed steel) where the superstructure is flexible relative to the foundation nor for buildings constructed of Unreinforced Masonry (URM) where yielding/failure of the superstructure is likely to occur prior to the rotation of the foundation due to soil yielding.

There are buildings, however, that do not lend themselves to fixed-base modeling. Foundation deformations that can cause additional inelastic deformations in the superstructure may not be assessed in a fixed-based model. Potential collapse mechanisms of superstructure secondary components may be overlooked. These cases where fixed-base procedures are not recommended are subdivided into two categories: Category A buildings where differential lateral restraints at the ground are provided and Category B buildings where foundation rocking adversely impacts drift sensitive components.

Category A

Buildings where base support configurations require modeling of foundation lateral and vertical flexibility include:

1. Buildings where the superstructure lateral force resisting elements are simultaneously supported on deep and shallow foundations. In this situation, overturning deformations from the lateral force resisting elements supported on deep foundation elements which resist uplift or compression settlement is expected to be less than where the lateral force resisting elements are supported on shallow foundation elements. This could cause differential settlements not accounted for when the building is modeled as a fixed base.

   However, where a majority of elements have their lateral forces resisted by either the shallow or deep foundation elements, it is expected that superstructure demands due to differential settlement can be accommodated by redistribution of forces such that the targeted performance objective is maintained. Therefore an 80/20 split in the base shear demands to each foundation type was selected as being a reasonable cut off for the exception. For this configuration, an additional exception is added where the retrofit consists of adding micropiles or deep foundation elements to resist overturning uplift. This is because non-battered micropiles resist mostly rocking action and provide little lateral resistance such that the differential lateral movement is limited, and superstructure deformations caused by rocking behavior is small.

2. Buildings where the elevation difference between the bottom of any unconnected footings supporting lateral load resisting elements in the building equals or exceeds one story height (see

Figure 1-8). When this building support condition exists, if the building is modeled as a fixed base, the lateral force demands would mostly get resisted at the highest level based on building flexibility. Therefore, the foundation lateral flexibility is required to be included in the model. Since modeling of the soil lateral flexibility is required, the requirement for modeling the vertical flexibility in the model is also required.

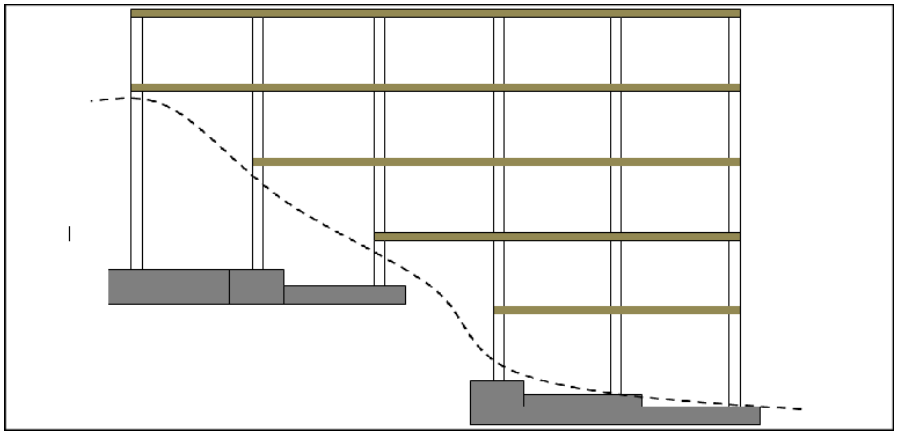

Figure 1-8 Condition where lateral and vertical soil flexibilities are required to be modeled.

Exceptions to this provision have been added when a majority of the building being evaluated is supported at the upper elevation and a small portion of the building has an overhang and the lateral demands are effectively resolved by the foundations and superstructure at the upper level (see Figure 1-9) and for buildings on box stepped foundations of wood or light frame construction where design of these foundation systems make them rigid relative to the superstructure and the added complexity of foundation flexibility is not required (see Figure 1-10).

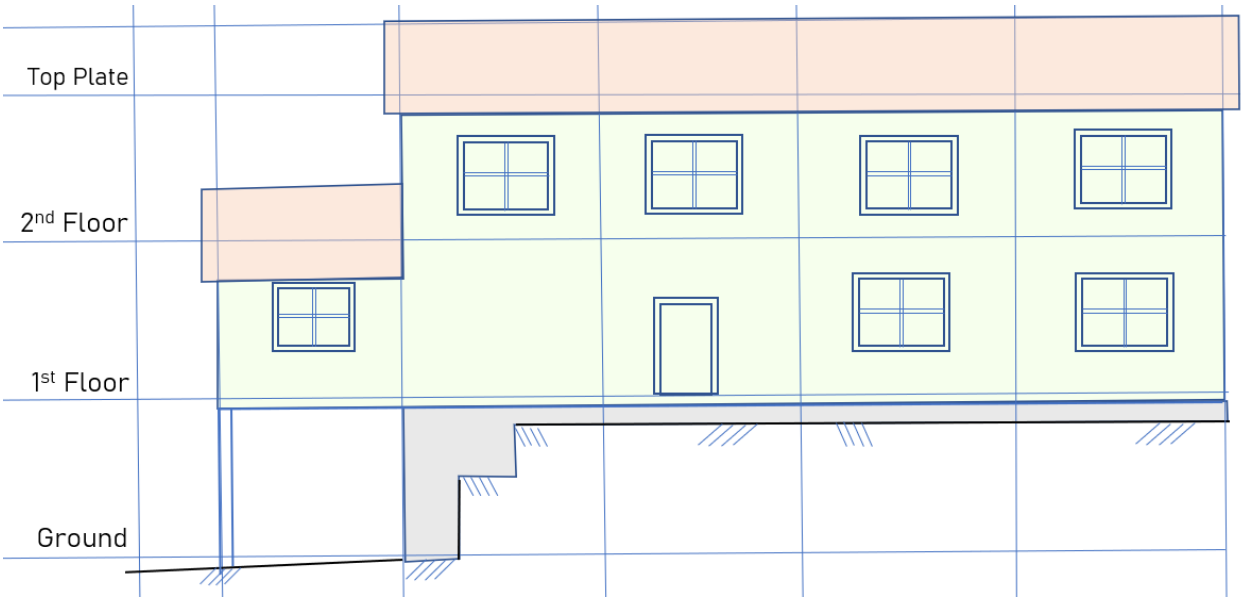

Figure 1-9 Example of a building with less than 15% of weight at the lower foundation level.

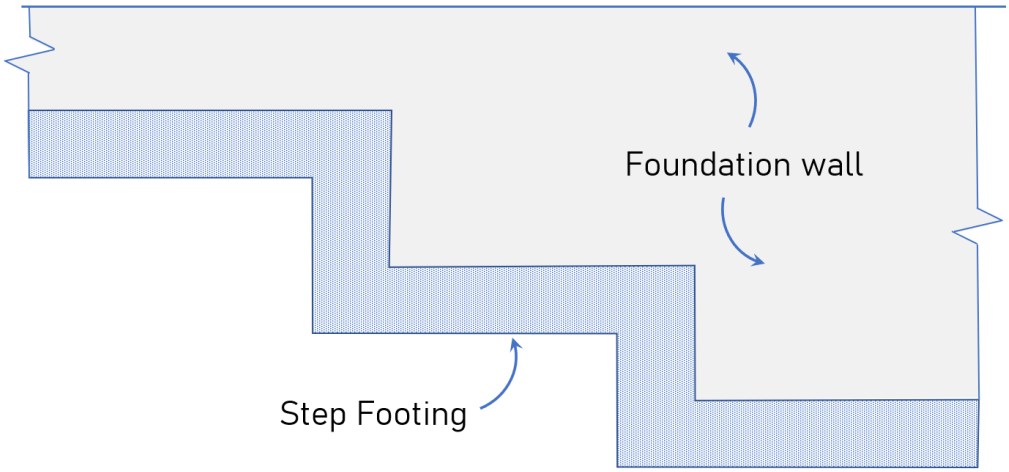

Figure 1-10 Example of a stepped footing where lateral and vertical soil flexibilities are not required to be modeled.

Category B

Buildings where superstructure elements are sensitive to base rotations include:

1. Cantilever concrete shear wall or steel braced frame buildings with different wall or bracing heights: Buildings with such configurations can result in large deformation demands in in the shorter walls with low axial load where overturning resistance at the foundation is not appropriately captured in a fixed-base model (Figure 1-11).

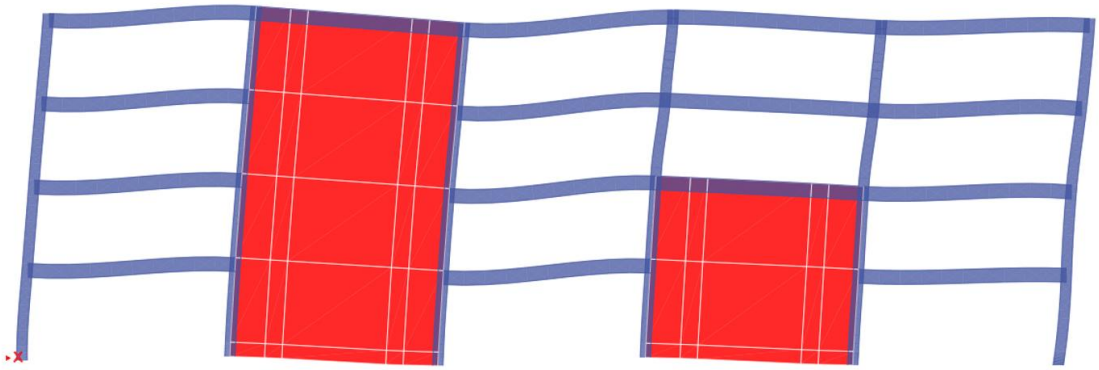

Figure 1-11 Building with lateral force resisting elements of different heights.

Exceptions to this requirement to include the flexibility of the soil within the model and when the fixed-base procedure may be used, is where the superstructure response is minimally affected by foundation flexibility modeling assumptions. The following cases are such examples:

- The shorter wall/bracing elements resist a small portion of the base shear of the building, or less than 25 percent of the base shear of the building, implying that the taller more flexible elements still resist a majority of the overturning demand on the structure.

- The foundation of the short wall or short braced frame is not the governing mechanism (in other words, stronger relative to the shear wall/braced frame strength capacity). When a foundation is undersized, there will be significant rotation of the footing prior to the yielding of the intended superstructure elements, necessitating modeling foundation flexibility.

2. Fixed-base procedures are not recommended where the seismic-force-resisting system is comprised of full height cantilever or coupled shear walls, unless the secondary elements in the superstructure can be demonstrated to maintain deformation compatibility. Failure of these secondary components could cause partial or total collapse of the building. Assessing the secondary components as primary components may be a means to demonstrate this ability. Since *m*-factors are a measure of component ductility, a low *m*-factor indicates inability of the component to resist large deformations beyond yield. To account for the additional rotation demand, secondary components having m-factors less than three are required to be evaluated using the primary m-factors. However, there are cases where the inelastic demand on secondary elements resulting from foundation movement will cause even the primary component acceptance criteria to be exceeded. For example, fixed-base models for concrete shear walls on independent spread footings may maximize deformation demands on the walls themselves, but could underestimate the demands on other secondary components in the buildings, such as beams and columns in moment frames, which may be sensitive to additional building movement as shown in Figure 1-12.

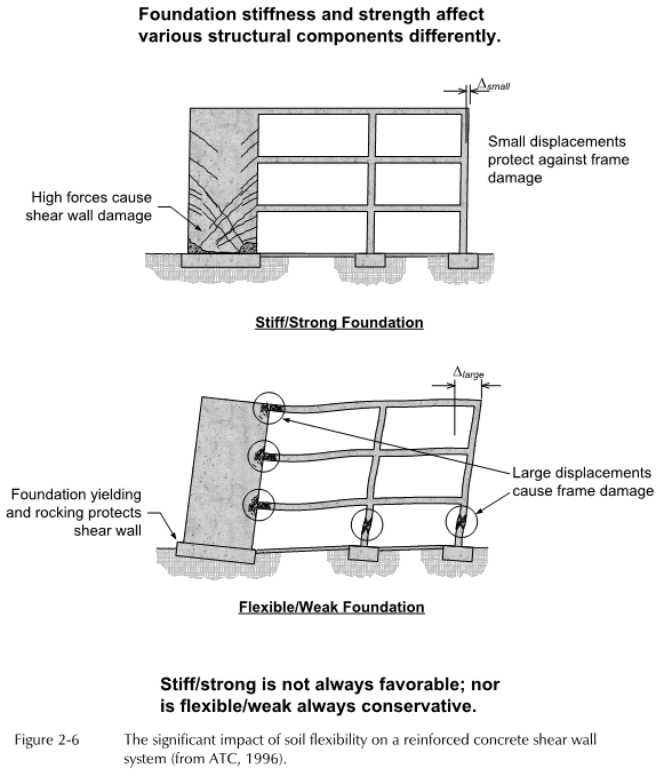

Figure 1-12 Figure 2-6 of FEMA P-2091 illustrating impact of soil flexibility.

Exceptions to the limitations on the use of the fixed-base procedure are included where it can be readily demonstrated that for robust foundations or by modeling techniques the demands in the superstructure are minimally affected by the inclusion or exclusion of the foundation flexibility such that it would not satisfy the intended performance objective. The exceptions only apply when any of the following conditions addressing that limitation is met:

- The building has a full basement with a complete system of perimeter basement walls, at least one-story in height, that can resist the overturning and sliding actions. Here the rigidity of the basement permits foundations to rotate as a rigid body limiting inelastic deformations in the superstructure, provided the walls are sufficiently strong to accommodate the demands.

- The foundation plan is included in the model and where foundation elements are interconnected in the form of grade beams, foundation structural slab or foundation tie beams. The soil support is idealized a as a single vertical pin support under the gravity load bearing element and flexural deformations of the interconnecting foundation elements are not restrained. This exemption does not apply to shear walls with multiple pin supports not directly under gravity columns or wall centerlines.

Flexible-base models provide a more accurate result than a fixed-base model. The primary question is if that accuracy is important to the building in question. In some cases, flexible-base foundation models are able to provide both improved accuracy and also a more economical footing. Nonlinear modeling where foundation rocking occurs has been shown to improve the performance of the building by lowering demands on the primary seismic-force-resisting elements, provided that secondary elements have sufficient ductility to accommodate the additional foundation movement (Figure 1-13).

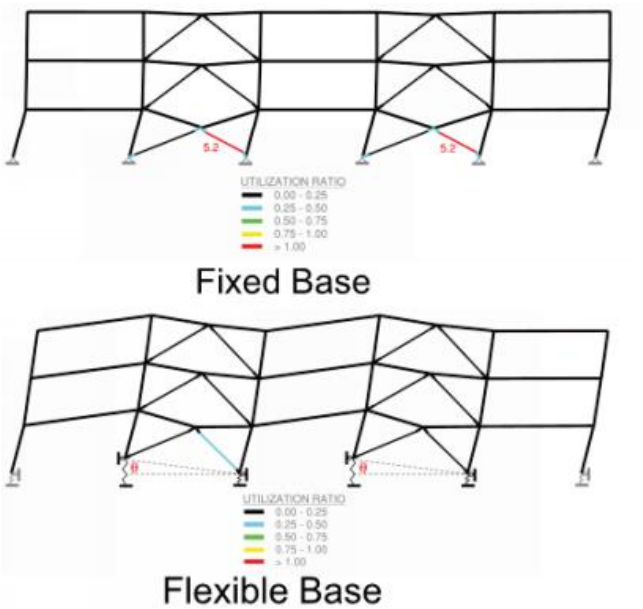

Figure 1-13 Figure 2-5 of FEMA P-2091 showing the impact of flexible-base modeling.

Results from the case study for Archetype Building 1 corroborate the reasons for the change proposals. A summary of the findings from that study is given below. Additional information is presented in Part 3, Appendix B, which can be found at http://femap2208.atcouncil.org/.

1.3.2.3 ARCHETYPE BUILDING 1: RESULTS OF SOIL MODELING ON SUPERSTRUCTURE

The resulting effects of the soil modeling assumptions on the superstructure were captured for each analysis case. Acceptance ratios were calculated for columns, shear walls, and slabs, as shown in Table 1- through Table 1-. The LSP acceptance ratios compare the analysis demand to the deformation-controlled capacity in accordance with ASCE/SEI 41-17 Equation 7-36. None of the superstructure elements shown in the tables below have been evaluated as force-controlled. The acceptance ratios for the NSP analyses compare the hinge rotation to the acceptance criteria for Collapse Prevention as specified in ASCE/SEI 41-17 Chapter 10. If there is no inelastic rotation in the hinge at the target displacement, the acceptance criteria are listed as 0.00. Maximum values for each action and analysis have been highlighted.

Similar to the soil foundation acceptance ratios, the superstructure results indicate a nominal difference in forces in the superstructure between lower- and upper-bound stiffness for each flexible foundation analysis. The K_{50} analysis procedures have higher acceptance ratios than the Method 1 analyses, because of the increased flexibility in the soil springs.

Table 1-1 Existing Interior Column - Moment Acceptance Ratios (CP Limit State)

Existing Interior Columns – Moment Acceptance Ratios by Story						
Analysis Model	**1st Story**	**2nd Story**	**3rd Story**	**4th Story**	**5th Story**	**Outcome**
LSP - Fixed Base	0.77	0.62	0.26	0.41	0.60	OK
LSP - Method 1 Lower Bound (Rigid Footing)	1.22	0.86	0.39	0.60	0.82	NG
LSP - Method 1 Upper Bound (Rigid Footing)	1.06	0.76	0.33	0.51	0.75	NG
LSP - K50 $300M_{c,foot}$ (Rigid Footing)	1.57	0.76	0.50	0.51	0.77	NG
LSP - K50 $550M_{c,foot}$ (Rigid Footing)	1.52	0.73	0.45	0.45	0.70	NG
NSP - Method 3	0.54	0.00	0.15	0.35	0.66	OK

Note: A DCR equal to 0.00 indicates no inelastic behavior occurs at the target displacement

Table 1-2 Existing Interior Column - Shear Acceptance Ratios (CP Limit State) (For Nonlinear Cases Acceptance Ratio is the Same as the Moment Acceptance Ratio)

Existing Interior Columns – Shear Acceptance Ratios by Story						
Analysis Model	**1st Story**	**2nd Story**	**3rd Story**	**4th Story**	**5th Story**	**Outcome**
LSP - Fixed Base	0.34	0.45	0.20	0.34	0.49	OK
LSP - Method 1 Lower Bound (Rigid Footing)	0.64	0.72	0.31	0.51	0.67	OK
LSP - Method 1 Upper Bound (Rigid Footing)	0.51	0.59	0.26	0.43	0.62	OK
LSP - K50 $300M_{c,foot}$ (Rigid Footing)	0.89	0.80	0.41	0.43	0.63	OK
LSP - K50 $550M_{c,foot}$ (Rigid Footing)	0.83	0.68	0.36	0.38	0.57	OK
NSP - Method 3	See moment acceptance ratios for nonlinear cases above					

Table 1-3 Retrofit Shear Wall - Shear Acceptance Ratios (CP Limit State)

Retrofit Shear Walls – Shear Acceptance Ratios by Story						
Analysis Model	**1st Story**	**2nd Story**	**3rd Story**	**4th Story**	**5th Story**	**Outcome**
LSP - Fixed Base	0.85	0.93	0.75	0.61	0.29	OK
LSP - Method 1 Lower Bound (Rigid Footing)	0.53	0.82	0.63	0.49	0.20	OK
LSP - Method 1 Upper Bound (Rigid Footing)	0.74	0.85	0.69	0.55	0.25	OK
LSP - K50 $300M_{c,foot}$ (Rigid Footing)	0.14	0.80	0.57	0.42	0.15	OK
LSP - K50 $550M_{c,foot}$ (Rigid Footing)	0.28	0.83	0.61	0.47	0.18	OK
NSP - Method 3	0.00*	0.00*	0.00*	0.00*	0.00*	OK

Note: A DCR equal to 0.00 indicates no inelastic behavior occurs at the target displacement

Table 1-4 Retrofit Shear Wall - Moment Acceptance Ratios (CP Limit State)

Retrofit Shear Walls – Moment Acceptance Ratios by Story						
Analysis Model	**1st Story**	**2nd Story**	**3rd Story**	**4th Story**	**5th Story**	**Outcome**
LSP - Fixed Base	1.00	0.83	0.55	0.78	0.30	OK
LSP - Method 1 Lower Bound (Rigid Footing)	0.79	0.76	0.46	0.59	0.20	OK
LSP - Method 1 Upper Bound (Rigid Footing)	0.96	0.82	0.51	0.69	0.25	OK
LSP - K50 $300M_{c,foot}$ (Rigid Footing)	0.52	0.71	0.40	0.48	0.14	OK
LSP - K50 $550M_{c,foot}$ (Rigid Footing)	0.64	0.76	0.44	0.56	0.18	OK
NSP - Method 3	0.00*	0.00*	0.00*	0.00*	0.00*	OK

Note: A DCR equal to 0.00 indicates no inelastic behavior occurs at the target displacement

Table 1-5 Existing Slab – Flexure Acceptance Ratios (CP Limit State)

Existing Slab – Flexure Acceptance Ratios by Story						
Analysis Model	**1st Story**	**2nd Story**	**3rd Story**	**4th Story**	**5th Story**	**Outcome**
LSP - Fixed Base	0.42	0.59	0.68	0.77	0.49	OK
LSP - Method 1 Lower Bound (Rigid Footing)	1.28	1.38	1.39	1.32	0.75	NG
LSP - Method 1 Upper Bound (Rigid Footing)	0.80	0.92	0.95	0.94	0.51	OK
LSP - K50 $300M_{c,foot}$ (Rigid Footing)	1.83	1.89	1.89	1.77	1.00	NG
LSP - K50 $550M_{c,foot}$ (Rigid Footing)	1.46	1.53	1.54	1.44	0.83	NG
NSP - Method 3	1.33	1.29	1.29	1.17	0.83	NG

Table 1-6 Story Drift – Drift per Story (in.)

Story Drift					
Analysis Model	**2nd Story**	**3rd Story**	**4th Story**	**5th Story**	**Roof**
LSP - Fixed Base	0.51	0.79	0.94	1.02	1.06
LSP - Method 1 Lower Bound (Rigid Footing)	1.31	1.48	1.62	1.66	1.73
LSP - Method 1 Upper Bound (Rigid Footing)	0.83	1.11	1.27	1.34	1.39
LSP - K50 $300M_{c,foot}$ (Rigid Footing)	1.77	1.85	1.96	1.99	2.06
LSP - K50 $550M_{c,foot}$ (Rigid Footing)	1.43	1.59	1.72	1.76	1.83
NSP - Method 3	1.86	1.63	1.63	1.62	1.68

Table 1-7 Story Drift – Drift Ratio per Story

Story Drift – Ratios by Story					
Analysis Model	**2nd Story**	**3rd Story**	**4th Story**	**5th Story**	**Roof**
LSP - Fixed Base	0.003	0.006	0.007	0.008	0.008
LSP - Method 1 Lower Bound (Rigid Footing)	0.008	0.012	0.013	0.013	0.013
LSP - Method 1 Upper Bound (Rigid Footing)	0.005	0.009	0.010	0.011	0.011
LSP - K50 $300M_{c,foot}$ (Rigid Footing)	0.011	0.015	0.016	0.016	0.016
LSP - K50 $550M_{c,foot}$ (Rigid Footing)	0.009	0.013	0.014	0.014	0.014
NSP - Method 3	0.012	0.013	0.013	0.013	0.013

1.3.2.4 CONCLUSIONS

This heavily updated ASCE/SEI 41 section was proposed to guide the user to select the appropriate modeling and analysis procedure to evaluate the building and its foundation system, depending on the building type, foundation site characteristics, and impact of foundation flexibility on superstructure demands. The language in the existing provisions was vague and required both a fixed-base and a flexible-base analysis to be performed to decide whether the fixed-base solution

was adequate. New proposed language identifies the cases when a fixed-base analysis is adequate or when a flexible-base analysis is required. This section is intended to replace the requirement where fixed-base procedures are not permitted when the superstructure is sensitive to base rotations when evaluated at the Immediate Occupancy level.

A simplified procedure was also added for a select class of buildings where inclusion of the foundation flexibility in the analysis is not required, and at the same time, permit the user to quickly evaluate the foundations without getting into the complexities of the remainder of the chapter. Use of this procedure only applies to buildings on strip, combined, or isolated footings (not mat foundations) where the elevation of the bottom of the footings is nominally the same.

1.3.3 Expected Soil Bearing Capacity

ASCE/SEI 41-17 Section 8.4.1.1 provides prescriptive bearing capacity values when information is available on the construction documents and when information is not available. There is a big difference in these values when soils information is available and when they are not, as the prescriptive values are very conservative. This study attempts to align these two values so that a soils report may not be required for all evaluations where soil information is not available by accounting for the parameters used to estimate soil strength in the original design.

Geotechnical engineers have generally made assumptions based on limiting settlement that may be conservative in terms of the bearing capacities of the soil. Traditionally, a factor of 3 was often used as a minimum acceptable factor of safety against bearing failure. Since allowable pressures were controlled by long-term settlements, allowable pressures are expected to be much smaller than the expected soil bearing capacities under dynamic loading situations. The actual factor of safety used in the determination of the expected capacities would, however, be the best predictor of the expected bearing capacity.

In projecting expected soil bearing capacities, it is also important to consider the bearing pressures that the foundations are exhibiting under the building gravity loads or have experienced during past seismic loading conditions and whether the foundations have performed adequately.

ASCE/SEI 41-17 provided an alternate method to estimate soil bearing capacity when information on the soil bearing capacity is not provided in the construction documents or in a geotechnical report. The bearing capacity was limited to 1.5 times gravity dead and live loads. However, this factor did not account for the fact that foundations traditionally have been designed with a factor of safety of 3 for gravity loads. Therefore, given the absence of any visible distress in the superstructure due to differential foundation settlement, a reasonable assumption on the factor of safety of 2.5 on the sustained dead load plus 0.4 of the unreduced live load, which is a general approximation of the reduced live load for a multistory building of typical occupancy, was made as an estimate of the soil bearing capacity. The previous factor of $1.5Q_G$ in ASCE/SEI 41-17 was judged to be too conservative and not consistent with the factors of safety used in the design. Since the expected capacity under each footing varies as a function of gravity load, in lieu of determining a long-duration expected bearing capacity, q_c, for each footing, it was judged reasonable to assume an average value of

expected soil bearing capacity, q_c, based on the sustained dead load plus 0.4 of the unreduced live load for the entire building divided by the sum of the areas of all the footings supporting the load.

The expected long-term soil bearing capacities, q_c, under static loads are further amplified by a factor of two for short duration loading soil strength, q_{cDA}, from the prescriptive bearing capacity to account for the strength increase in soils due to loading rate effects. This factor was chosen to be consistent with the upper-bound soil strengths and associated *m*-factors for fixed-base or flexible-base linear analysis procedures. However, this value can range anywhere from say 1.3 to 2.0 depending on the type of soil and moisture content. It should also be noted that rate-sensitivity of the strength of non-cohesive soils is known to be less than that for cohesive soils. However, for shallow foundations on non-cohesive soils, the allowable loads, q_{allow}, are usually based upon settlement considerations not on capacity considerations; hence there is additional anticipated conservatism in the q_c value for non-cohesive soils.

A plot showing the variation of foundation moment capacity with expected soil bearing capacity, q_c, for different constant axial loads is shown in Figure 1-14. From the figure a change in dynamic amplification factor from 2.0 to 1.5 would result is a bearing capacity of 18 ksf instead of 24 ksf from an assumed q_c of 12 ksf. This change in expected bearing capacity has a negligible impact on the foundation moment capacity for a given axial load.

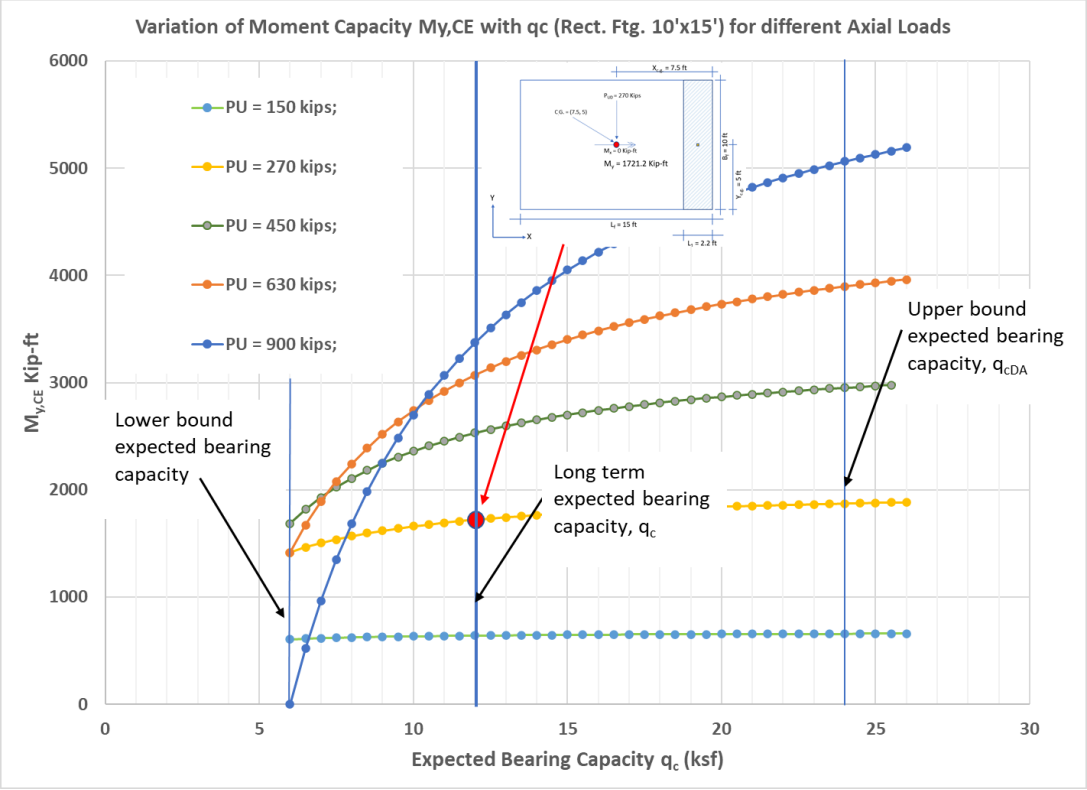

Figure 1-14 Variation of moment capacity with expected soil bearing capacity.

Example: For 15 ft × 10 ft rectangular footing supporting an axial load of 540 kips, using a q_c = 24 ksf, the A_c/A_f ratio = (540 kips)/{(15 ft)(10 ft)(24 ksf)} = 0.15. The moment capacity is 3442.5 kip-ft. If the bearing capacity for the same axial load instead used the short term expected bearing capacity q_c = 18 ksf, the moment capacity is 3240.0 kip-ft. Using the higher amplification resulted in a 6% increase in moment capacity.

Since this difference in moment capacity is small and given the uncertainty in the variation of soil properties, the dynamic amplification factor of 2.0 was selected for consistency with the upper-bound expected bearing capacities already permitted in the standard. If a lower-bound value of strength is used, this alters the A_c/A_f ratio and the change in the moment capacity is significant. For the same 540 kips, using a q_c of 6 ksf, the moment capacity is 1620 kip-ft, a reduction of 47% from the upper-bound capacity, which is unjustified based on initial design assumptions for the soil properties having a minimum factor of safety of 3.0. For this reason. the existing provisions for expected bearing capacities were revised when geotechnical information is not available to have a minimum factor of safety of 2.5 on the dead plus 0.4 of the unreduced live load instead of the 1.5 factor on the existing gravity dead plus live loads.

Case study results from Archetype Building 1, shown in Section 1.3.11, also confirm that lower-bound strengths do not provide acceptable results for the flexible-base procedure. Upper-bound strength could still be conservative for soil bearing when foundations are modeled as fixed-base compared to when foundations are modeled as a flexible-base.

CONCLUSIONS

The upper-bound soil bearing capacity in ASCE/SEI 41-17 was traditionally taken as $q_c(1+C_v)$, where C_v is the coefficient of variation of the soil bearing capacity and C_v was assumed to be 1.0. This resulted in an upper-bound strength of $2.0q_c$ for soil bearing capacity. For linear analysis procedures, ASCE/SEI 41-17 permitted use of upper-bound strength for buildings modeled as a fixed-base or a flexible-base. Therefore, the term upper-bound was dropped in favor of expected bearing capacity for short duration loads such as earthquakes and was represented by the symbol q_{cDA}, where q_{cDA} = $2.0q_c$. This change results in the same acceptance criteria for soil bearing but is more transparent to the user as to what value is permitted be used.

The other proposed change to this section was to increase the prescriptive soil bearing capacity when geotechnical information on allowable soil bearing capacities is not available. The 1.5 factor on gravity was deemed to be too conservative when traditionally the allowable factor of safety used in the design was 3.0. A factor of 2.5 on the calculated design gravity loads was therefore deemed appropriate.

1.3.4 Seismic Overturning Forming Axial Load Action

There are conditions where compression or uplift caused by overturning on isolated footings is associated with coupled foundations such as those supporting columns in a braced or moment

frame (Figure 1-15). In these cases, overturning demand results in axial actions, tension and compression, on the foundation. This action is not adequately addressed in ASCE/SEI 41-17.

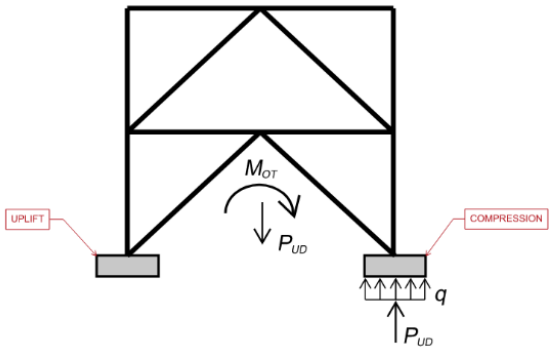

Figure 1-15 Overturning resisted by coupled axial load actions on footings.

The acceptance criteria in ASCE/SEI 41-17 are based on the overturning moment demand on the foundation being less than the resisting capacity. The corresponding failure mode of the foundation is by rocking action with bearing failure by plowing action occurring over a relatively small area (Figure 1-16).

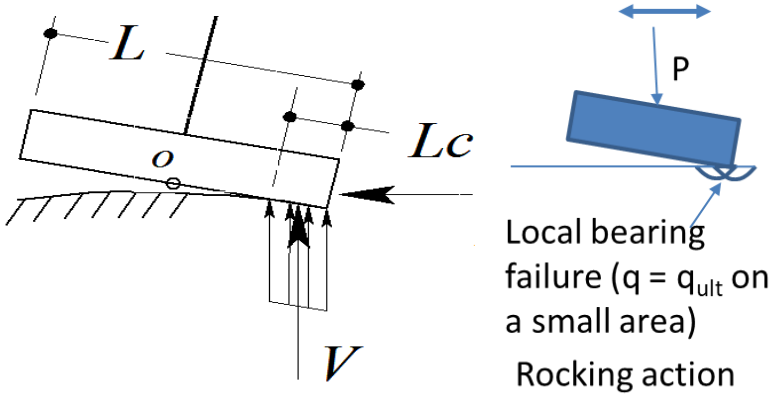

Figure 1-16 Overturning resisted by coupled axial load actions on footings.

As such this failure mode does not adequately address the foundation resistance when the seismic overturning resulted in coupled compression and tension action. The failure mode for axial compression results in bearing capacity failure for load distributed over a large area by plunging resulting in settlement of the footing (Figure 1-17),

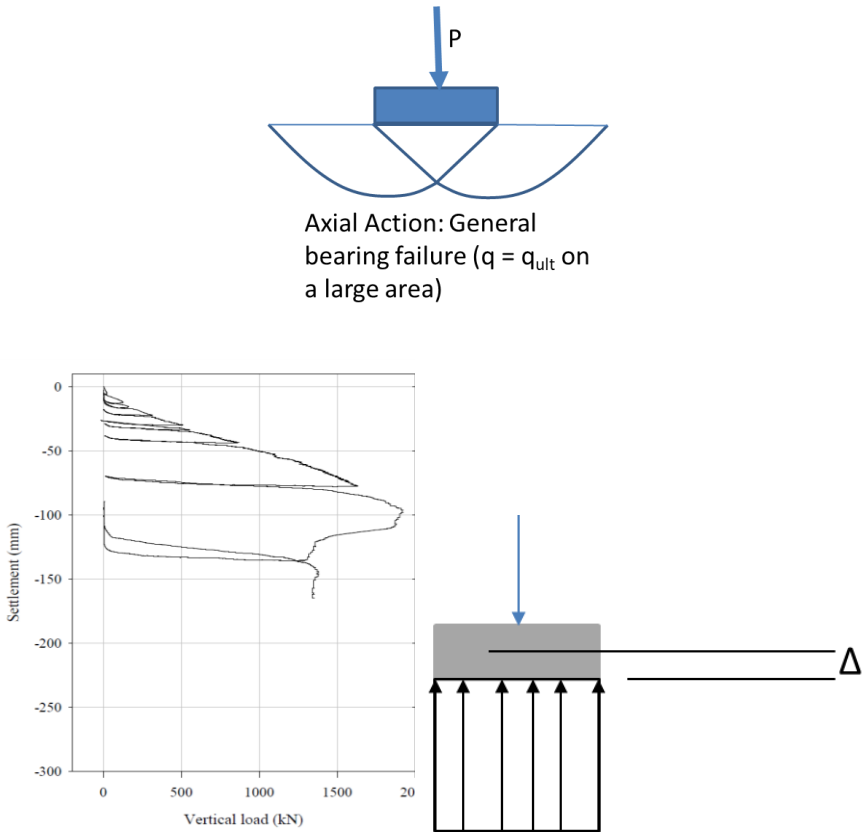

Figure 1-17 Overturning resisted by coupled axial load actions on footings.

1.3.4.1 PROPOSED REQUIREMENTS FOR SEISMIC OVERTURNING FORMING AXIAL LOAD ACTION

To address this issue, a new section was added to evaluate foundations where overturning action is resisted by axial action, coupled tension and compression, and where the overturning moment action is low. A threshold when the moment demand on the isolated footing, M_{OT}, is less than 20% of associated *m*-factor times the moment capacity of the foundation was selected as a reasonable cutoff to consider the seismic overturning action as axial load action, and where the localized overturning moment action could be ignored.

Smaller axial compression *m*-factors were suggested based on judgment for the axial compression action. Foundation acceptance is evaluated by assessing axial compressive demand acting over the full area of the footing with the *m*-factor times the soil bearing capacity. Overturning stability is assessed by comparing uplift (or tension) demand with the gravity dead load multiplied by the associated *m*-factor with the condition that the vertical element in net tension is able to engage the dead load of the footing and slab-on-grade tributary to the footing.

Adding this new section with the revised *m*-factors addresses the condition where seismic overturning is resisted by axial load action. ASCE/SEI 41-17 had addressed this condition by exception, where foundation overturning action was treated as force-controlled when seismic axial

compression force exceeded 3 times gravity or A_c/A exceeded 0.6. This exception in ASCE/SEI 41-17 Section 8.4.2.3.1 is therefore deleted as the action it addressed is resolved with addition of this new section.

1.3.4.2 CONCLUSION

This proposed new section addresses a gap in the existing provisions where the acceptance criteria for overturning action only accounted for overturning resistance due to rocking action. The existing provisions precluded the cases where overturning action is resisted by coupled tension and compression on isolated footings. The existing *m*-factors were also specific to overturning produced by rocking action. The new proposed language and associated *m*-factors provided in ASCE/SEI 41-23 Section 1.4.3 rectifies this issue.

1.3.5 Foundation Moment Capacity with Bi-directional Overturning Action

It is common for engineers to use analysis software to determine bearing stresses and uplift for evaluation of foundations. This option is not recognized in ASCE/SEI 41-17. Instead, foundation acceptance is based on overturning moment capacity of the foundation, which is addressed simplistically only for uni-directional moment for a rectangular or I-shaped footing (Figure 1-18) given by ASCE/SEI 41-17 Equation 8-10, as shown below.

$$M_{CE} = \frac{L_f P_{UD}}{2}\left(1 - \frac{q}{q_c}\right) \qquad \text{(ASCE/SEI 41-17 Eq. 8-10)}$$

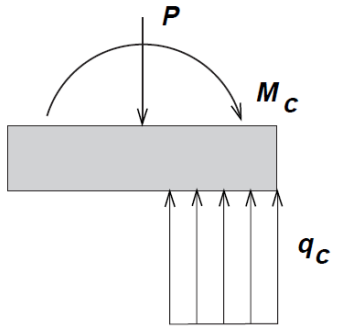

Figure 1-18 Isolated footing under axial load and moment represented in terms of eccentricity.

However, there are many cases where the moment on the footing acts concurrently in both the x and y directions. For such cases, the combined axial load and moment demand on the footing can be represented as an axial load that is offset from the centroid of the footing with an eccentricity in the x or y directions or both as shown in Figure 1-19.

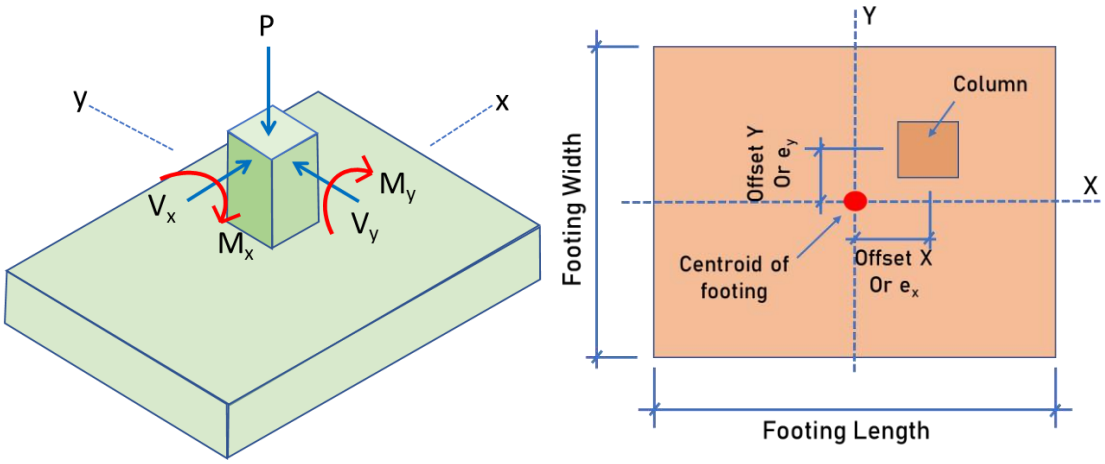

Figure 1-19 Isolated footing under axial load and moment represented in terms of eccentricity.

Based on the eccentricity of loading in the first quadrant, five different area shapes can be mapped on the footing, where the footing remains in contact with the soil as shown in Figure 1-20.

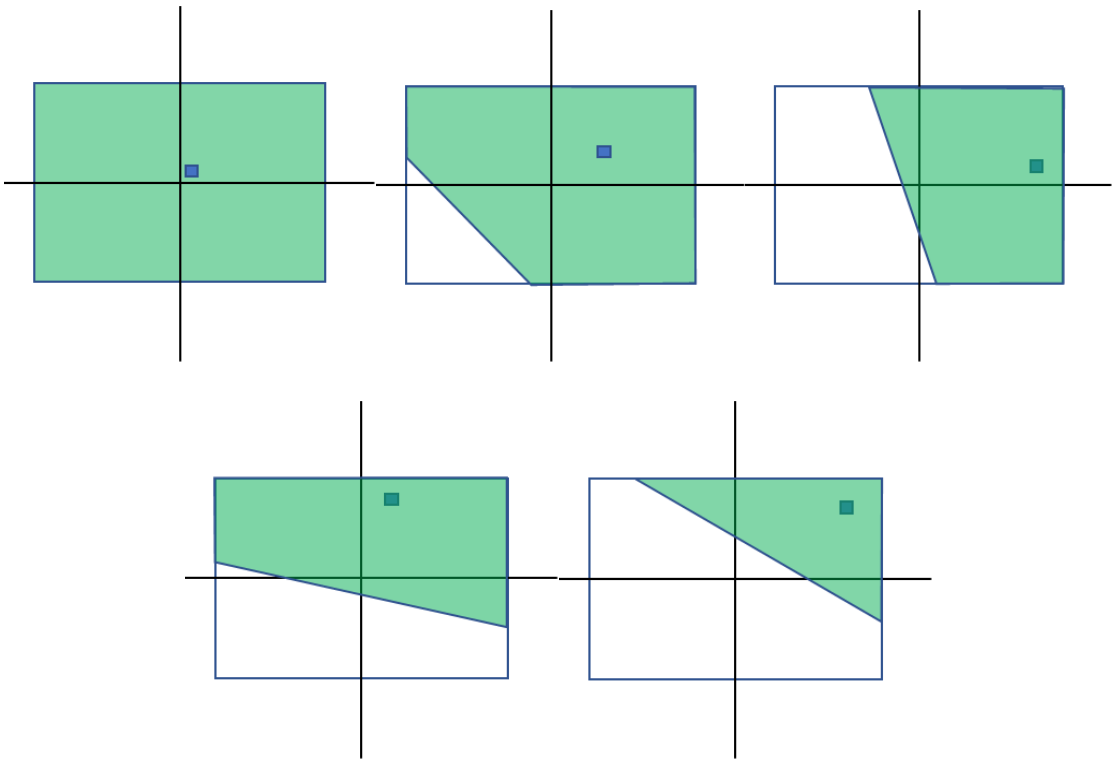

Figure 1-20 Area of footing in contact with the soil based on axial load eccentricity.

Using equations developed by John Bellos and Nikolaos Bakas (2017), which assume a triangular soil pressure distribution and where the soil does not resist tension, a map of eccentric zones can be generated as shown in Figure 1-21. If the eccentricity of the load falls within that zone, the shape of the loaded area will correspond to the type shown in Figure 1-20.

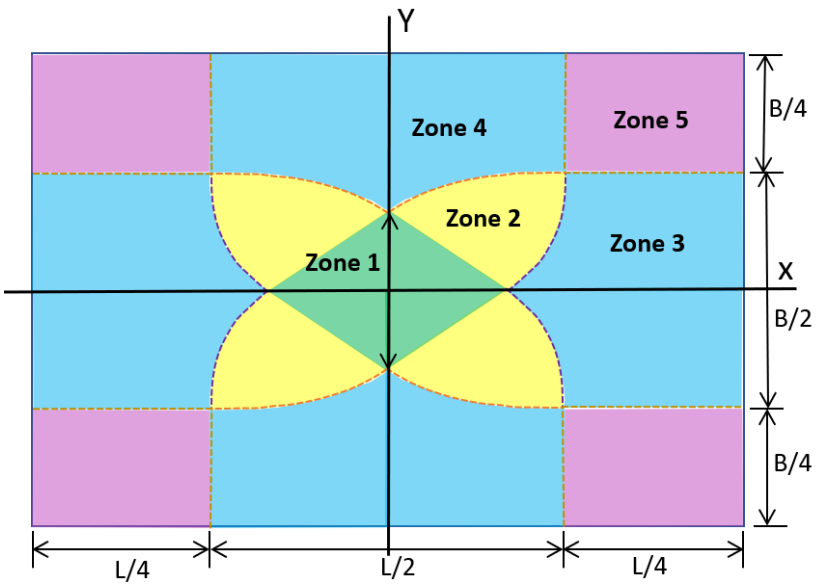

Figure 1-21 Eccentricity zones corresponding to soil pressure distribution type.

This map of the eccentricity zones generated using the footing eccentricity map available at (https://www.desmos.com/calculator/vnzzynunae) makes it easy to see which part of the footing remains in contact with the soil and where the eccentricity falls. When the eccentricity falls with Zones 1 through 4, ASCE/SEI 41-17 Equation 8-10 may give a reasonable estimate of the moment capacity. However, when the eccentricity falls within Zone 5, the equation is unconservative for loads acting in both directions and bi-directional loading needs to be considered.

Acceptance for soil bearing for footing under bi-directional loads is revised to:

$$\left(\frac{M_{OT,x}}{m\kappa M_{CE,x\_uniaxial}}\right)^2+\left(\frac{M_{OT,y}}{m\kappa M_{CE,y\_uniaxial}}\right)^2\le 1.0 \qquad (1\text{-}1)$$

Where the overturning moment demand M_{OT} is:

$$M_{OT}=\sqrt{M_{OT,x}^2+M_{OT,y}^2}$$

However, this acceptance criterion is inaccurate for footings of irregular plan shape as shown in Figure 1-22, which may occur at a building corner. Even with the application of uniaxial overturning moments, the critical contact area will almost always result in non-rectangular soil bearing pressure areas and hence the uniaxial moment capacity cannot be determined.

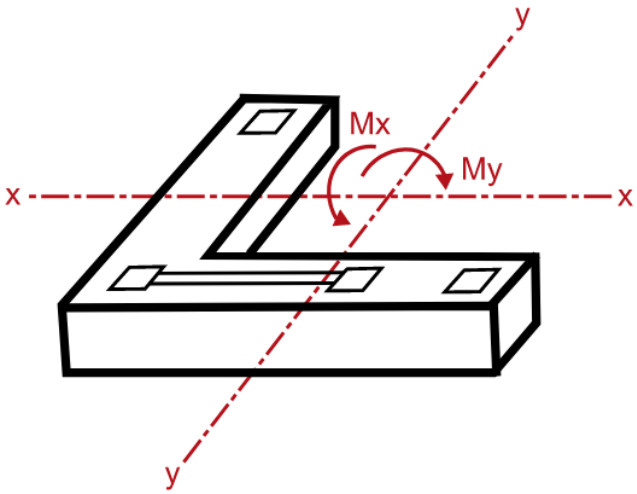

Figure 1-22 Footing under inherent biaxial loading.

Because of the limitations in the current acceptance criteria, alternate solutions were investigated as engineers will continue to use foundation design software to evaluate the foundations rather than determine the foundation moment capacity because these solutions get quite complex when bi-directional moment are applied to the footing or for footings of irregular shape. A literature search to determine the ultimate moment capacity of isolated footing subjected to bi-directional overturning demands did not reveal any results where the pressure distribution under the footing is uniform. Various options were investigated starting with the equations of equilibrium of axial loads and moments. As the solution for overturning capacity also included the overturning stability, the overturning demands where required to be reduced by the *m*-factor or superstructure DCR to convert the pseudo forces to the actual estimated loads to arrive at a feasible solution as shown in the next section.

1.3.5.1 GENERAL METHODOLOGY TO DETERMINE MOMENT CAPACITY FOR ISOLATED FOOTINGS

A new methodology is proposed for evaluating foundations for load eccentricities not covered by ASCE/SEI 41-17 where the footing is required to resist overturning moments simultaneously about the two horizontal principal axes of the footing and for footings of irregular plan shape. This methodology is currently addressed by the standard only in general terms in ASCE/SEI 41-17 Section 8.4.2.3.1, as given below:

> For nonrectangular footings, the moment capacity shall be obtained by determining the critical contact area, A_c, and integrating the product of the bearing capacity times the distance from the neutral axis of the footing over the critical contact area.

Steps in the Methodology:

1. Divide the weak axis moment by the *m*-factor for the corresponding performance level

In this method, the pseudo seismic overturning moment demands in one of the orthogonal directions, x or y, have to first be reduced by the *m*-factor for overturning, and the moment capacity in the orthogonal direction is the derived by simultaneously solving the equations of equilibrium for axial load and moment to define the boundaries of the critical contact area. This division by the *m*-factor is required because there is interaction of the moment capacities when simultaneous bi-directional moments are present, as opposed to the formulation of the uniaxial moment capacity which only depends on the seismic axial load on the footing. Amplification of the moment capacity by an *m*-factor and comparing that with the pseudo seismic overturning demand results in the same acceptance ratio.

Example: The Acceptance Ratio (AR) for two options, for gravity and overturning actions creating axial load and uniaxial moment on a 10 ft by 12 ft footing are shown in Figure 1-23. In Option 1, the *m*-factor amplifies the capacity and in Option 2, the demands are divided by the *m*-factor. For both options, the ARs are the same which demonstrates that m-factor can amplify the capacity which is consistent with the methodology of the standard, or the demands may be reduced by the m-factor, without changing the result.

Footing	**B_f (ft)**	10
12'x10'x2'	**L_f (ft)**	12
	H_{ftg} (ft)	**2**
Axial Load	**P_G (kips)**	350
	P_{seism} (kips)	400
Max DCR	**DCR_{max}**	**2**
Overturning Moment	**M_{OT} (kip-ft)**	8500
Performance Level CP	**m-factor**	**4**
Soil bearing pressure, allowable (D+L)	**q_{allow} (ksf)**	3

	P_U	M_{OT}	DCR_{max}	q_{allow}	q_{cDA}	q	M_{CE}	m	κ	$mκM_{CE}$	M_{OT}/mkM_{CE}
Option 1	550	8500	2	3	18	4.58	2460	4	1	9839	0.86
	P_U	M_{OT}/m	DCR_{max}	q_{allow}	q_{cDA}	q	M_{CE}	m	κ	$κM_{CE}$	M_{OT}/kM_{CE}
Option 2	550	2125	2	3	18	4.58	2460	4	1	2460	0.86

Figure 1-23 Comparison of Options with *m*-factors multiplying the capacity and of m-factors reducing the demand.

where:

$P_U = P_G + P_{seism} / DCR_{max}$

and

$$M_{CE} = \frac{P_U L_f}{2}\left(1 - \frac{q}{q_{cDA}}\right)$$

2. Assume a shape for the trial critical contact area A_c

Draw a straight line on the footing that will approximately define the shape of the critical contact area such that area formed multiplied by the short-term soil bearing capacity q_{cDA} equals the applied axial load P_U on the footing (Figure 1-24). This line is henceforth referred to as the zero-pressure line.

3. Solve simultaneously the equations of equilibrium for axial load and moment

If the soil pressure block under the footing resisting the applied loads is discretized into individual segments, the moment capacity is a sum of the volume of soil pressure for the area multiplied by the distance of the centroid of the individual soil pressure blocks from the centroid of the footing cross section. The equations of equilibrium for axial load and moment about the x axis can then be written as:

$$q_{cDA}\sum_{i=1}^{n} A_i = P_U \tag{1-2}$$

and

$$q_{cDA}\sum_{i=1}^{n} A_i y_i - P_U Y_{c.g.} + \frac{M_{OT,x}}{m} = 0 \tag{1-3}$$

where:

A_i = Area of cross section i resisting axial load PU

y_i = Distance from centroid of cross section i of the footing to the x axis

x_i = Distance from centroid of cross section i of the footing to the y axis

n = Total number of areas resisting the axial load P_U

$Y_{c.g.}$ = Distance from the centroid of the footing to the edge of the footing in the direction of loading along the y axis

$M_{OT,x}$ = Component of applied moment in the x direction or minor axis of overturning

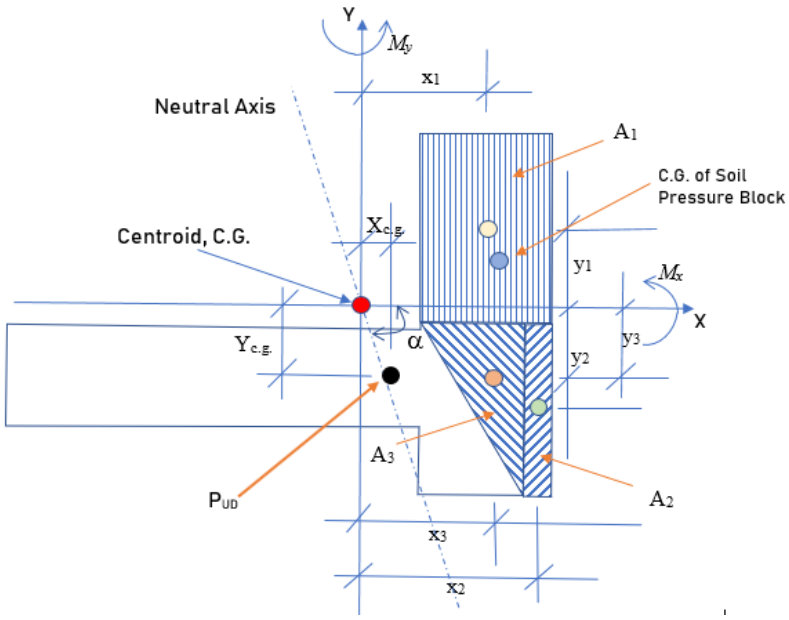

Figure 1-24 Generalized method to define the boundaries of the critical contact area.

4. Check if solution is feasible for the assumed critical contact area

If the selected shape of the critical contact area is correct, the boundaries of the critical contact area will lie within the footing geometry. If the boundaries of the critical contact area are outside of the edges of the footing, alternate trial shapes are required until a feasible solution is obtained. If no solution is obtained, the footing is unstable under the applied combination of axial load and weak direction moment.

5. Determine the ultimate moment capacity

Given the boundaries of the critical contact area, the moment capacity $M_{CE,y}$ is obtained from the expression:

$$M_{CE,y} = q_c \sum_{i=1}^{n} A_i x_i - P_U X_{c.g.} \tag{1-4}$$

Therefore, the total moment capacity of the foundation can be written as:

$$M_{CE} = \sqrt{\left(M_{OT,x}/m\right)^2 + \left(M_{CE,y}\right)^2} \tag{1-5}$$

And the moment demand on the footing defining the critical contact area in the x direction becomes its capacity, or:

$$M_{CE,x} = M_{OT,x}/m \tag{1-6}$$

where:

$X_{c.g.}$ = Distance from the centroid of the footing to the edge of the footing in the direction of loading along the x axis.

$M_{CE,x}$ = Moment capacity of the foundation in the x direction.

$M_{CE,y}$ = Moment capacity of the foundation in the y direction.

$M_{OT} = \sqrt{M_{OT,x}^2 + M_{OT,y}^2}$

Acceptance can then be written in the general form:

$$M_{OT} \leq mkM_{CE} \tag{1-7}$$

1.3.5.2 MOMENT CAPACITY FOR RECTANGULAR FOOTING SUBJECTED TO BI-DIRECTIONAL OVERTURNING MOMENTS

The moment capacity for rectangular footing subjected to bi-directional overturning moments for two of the most common shapes of the critical contact area, A_c, forming the soil pressure block with a bearing capacity q_c is shown below. Additional information and moment capacities for less common patterns and for footings with an angled cross-section can be found in Lobo (2021).

CASE 1: Moment Capacity of a Rectangular footing where the zero-pressure line intersects two opposite edges of the footing.

The critical contact area, A_c, under the footing required to resist the axial load can be discretized into an area consisting of a rectangular and a triangular block as shown in Figure 1-25.

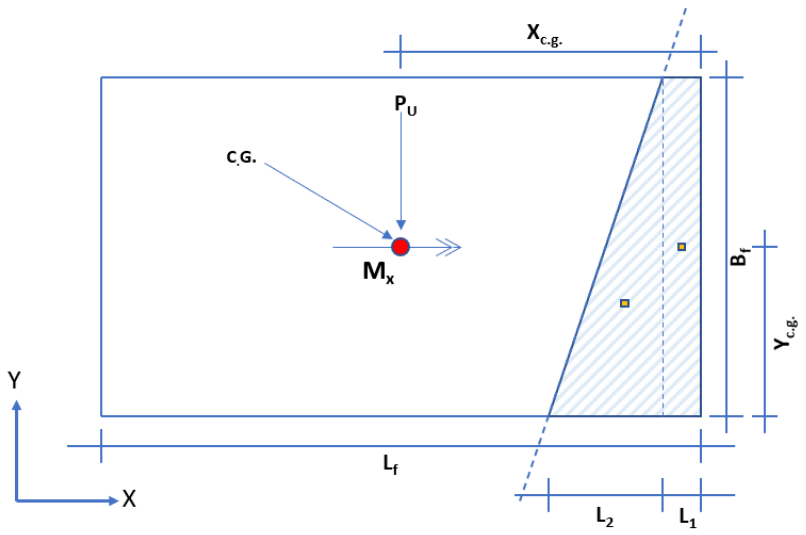

Figure 1-25 Critical contact area A_c of a rectangular footing, when the zero-pressure line intersects two opposite edges of the footing.

Given:

P_U = Axial load on the footing, applied at the centroid of the section

M_x = Minor axis moment

q_c = Bearing capacity of the soil

From Figure 1-25, the equations of equilibrium can be written as:

$$q_c\left(L_1 B_f + \left(\frac{1}{2}\right)L_2 B_f\right) = P_U \tag{1-8}$$

and

$$q_c\left(L_1 B_f\left(\frac{B_f}{2}\right) + \left(\frac{1}{2}\right)L_2 B_f\left(\frac{B_f}{3}\right)\right) = P_U Y_{c.g.} - M_x \tag{1-9}$$

Rearranging the terms in Eq. 1-9 we get:

$$L_1 = \frac{2(P_U Y_{c.g.} - M_x)}{q_c B_f^2} - \frac{L_2}{3} \tag{1-10}$$

and from Eq. 1-8 we get:

$$L_1 = \frac{P_U}{q_c B_f} - \frac{L_2}{2} \tag{1-11}$$

subtracting Eq 1-9 from Eq 1-10:

$$\frac{L_2}{2} - \frac{P_U}{q_c B_f} = \frac{L_2}{3} - \frac{2(P_U Y_{c.g.} - M_x)}{q_c B_f^2} \tag{1-12}$$

therefore:

$$L_2 = \frac{6}{q_c B_f}\left(P_U - \frac{2(P_U Y_{c.g.} - M_x)}{q_c B_f}\right) \tag{1-13}$$

If L_1 and L_2 are both greater than zero and $L_1 + L_2 < L_f$, the solution is valid and the major axis moment capacity $M_{y,CE}$ is calculated as:

$$M_{y,CE} = q_c B_f \left\{ L_1 \left(X_{c.g.} - \frac{L_1}{2} \right) + \frac{1}{2} L_2 \left(X_{c.g.} - L_1 - \frac{L_2}{3} \right) \right\} \tag{1-14}$$

CASE 2: Moment Capacity of a Rectangular footing where the zero-pressure line intersects two adjacent edges of the footing.

If the zero-pressure line of the soil pressure block intersects two adjacent edges of the footing as shown in Figure 1-26, the ultimate moment in the orthogonal direction is given by the following expressions:

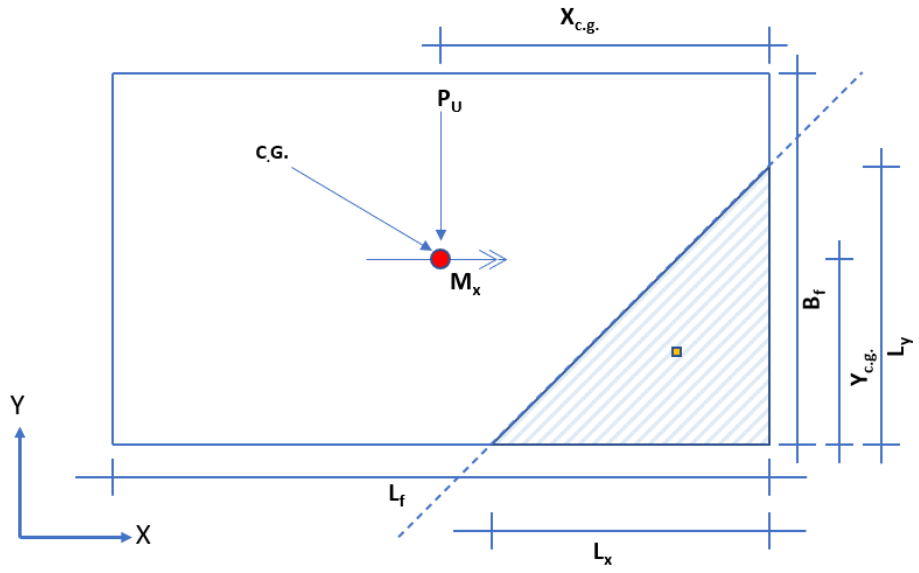

Figure 1-26 Critical contact area *Ac* of a rectangular footing, when the zero-pressure line intersects two adjacent edges of the footing.

$$M_{y,CE} = \frac{1}{2} q_{cDA} L_x L_y \left(X_{c.g.} - \frac{L_x}{3} \right) \quad (1\text{-}15)$$

$$L_y = 3(Y_{c.g.} - M_x/P_U) \quad (1\text{-}16)$$

$$L_x = 2P_U/(q_c L_y) \quad (1\text{-}17)$$

1.3.5.3 NORMALIZED MOMENT CAPACITY FOR DIFFERENT A_C/A RATIOS FOR A RECTANGULAR FOOTING

For a given axial load, the normalized moment capacities in each orthogonal direction for a footing of rectangular section, is shown in Figure 1-27. From the figure, there is a minimal reduction in moment capacity where moments in the orthogonal direction are less than 20% of the moment capacity in that direction. Therefore, the effects of bi-directional moments are permitted to be ignored for orthogonal moments less than 20% of the capacity in that direction.

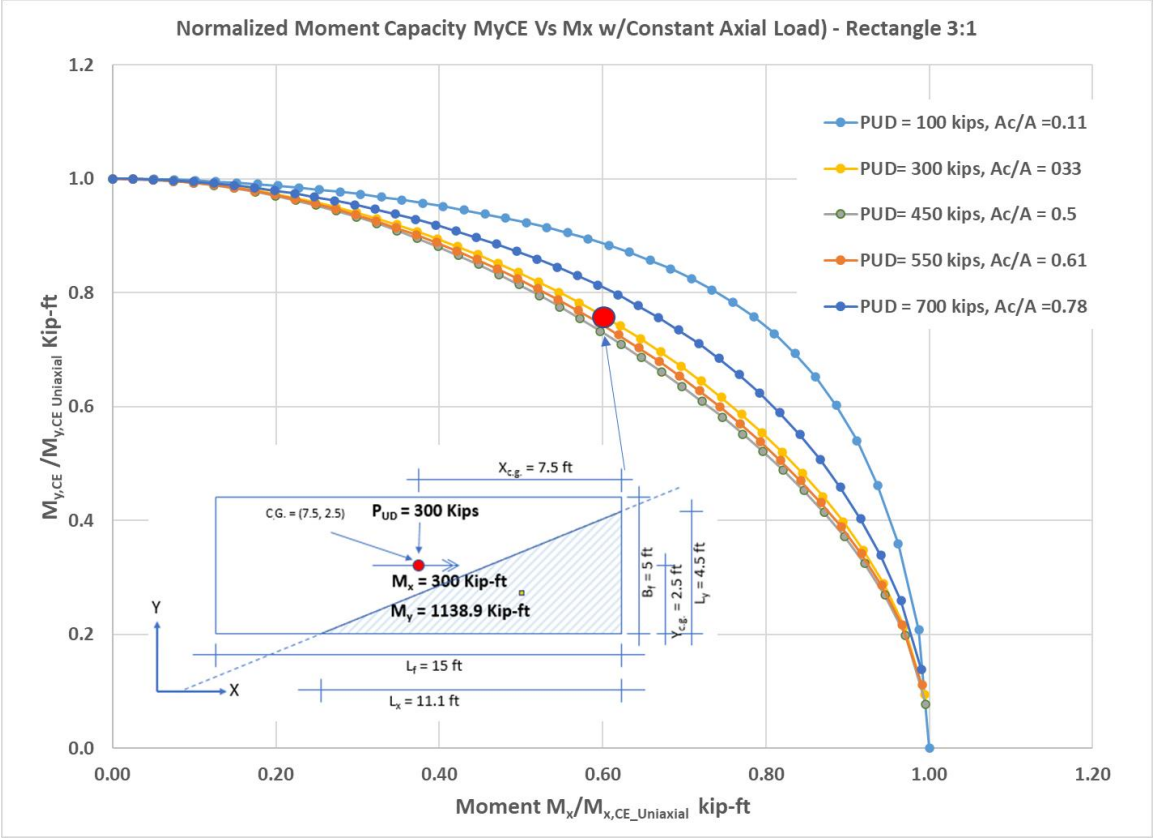

Figure 1-27 Normalized orthogonal moment capacities for a rectangular footing.

1.3.5.4 MOMENT CAPACITY FOR AN L-SHAPED FOOTING

The moment capacity for L-shaped footings for positive and negative moments about each axis for four different patterns of the critical contact area, A_c, forming the soil pressure block with a bearing

capacity q_c is shown below. Additional information and moment capacities can be found in Lobo (2021).

CASE 1

For the applied loading (P_{UD} and M_x) and footing geometry shown in Figure 1-28, where the resisting soil pressure that satisfies the equations of equilibrium results in a pattern represented by the hatched area shown in Figure 1-28, for a positive M_y moment capacity, $M_{y,CE}$ is given as:

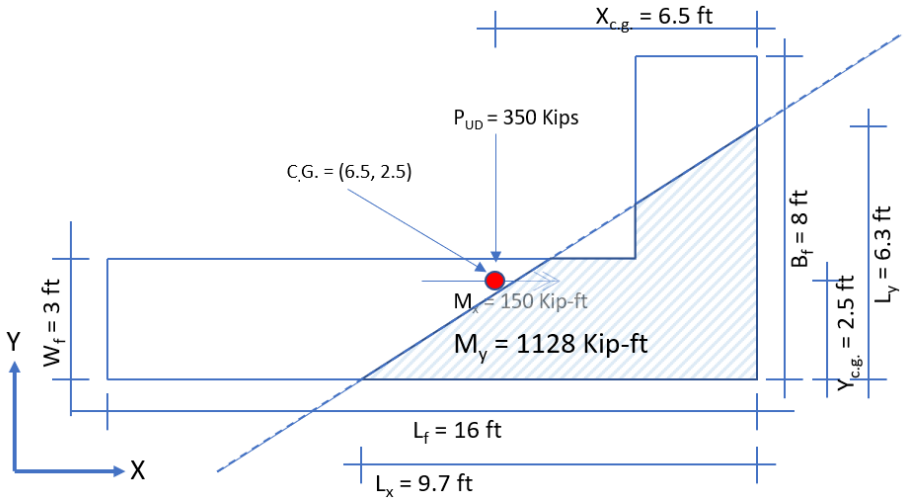

Figure 1-28 Positive M_y moment capacity with positive M_x moment.

Major axis moment capacity M_{yCE} can be written as:

$$M_{y,CE} = q_c \frac{1}{2} L_x L_y \left(X_{c.g.} - \frac{L_x}{3} \right) - q_c \frac{1}{2} \xi_1 \xi_2 \left(X_{c.g.} - W_f - \frac{\xi_1}{3} \right) \quad (1\text{-}18)$$

where:

$$\xi_1 = L_x - W_f(L_x/L_y) - W_f \quad (1\text{-}19)$$

$$\xi_2 = L_y - W_f(L_y/L_x) - W_f \quad (1\text{-}20)$$

L_x and L_y are determined iteratively, such that the equations for M_x and P_{UD} are simultaneously satisfied.

$$M_x = -\left\{ \frac{q_c \frac{1}{2} L_x L_y^2}{3} - P_{UD} Y_{c.g.} - q_c \frac{1}{2} \xi_1 \xi_2 \left(W_f + \frac{\xi_2}{3} \right) \right\} \quad (1\text{-}21)$$

$$P_{UD} = q_c \frac{1}{2} L_x L_y - q_c \frac{1}{2} \xi_1 \xi_2 \tag{1-22}$$

CASE 2

For the applied loading (P_{UD} and M_x) and footing geometry shown in Figure 1-29, where the resisting soil pressure that satisfies the equations of equilibrium results in a pattern represented by the hatched area shown in Figure 1-29, for a positive M_y moment capacity, $M_{y,CE}$ is given as:

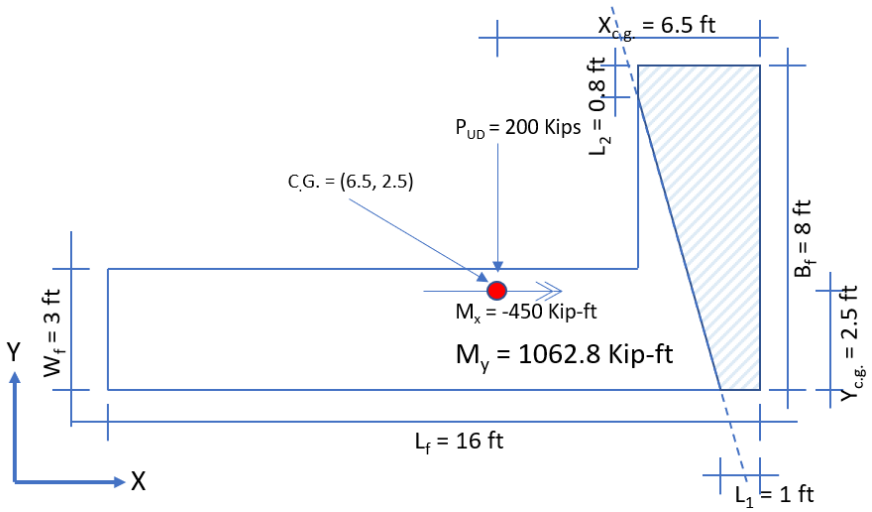

Figure 1-29 Positive M_y moment capacity with negative M_x moment.

$$M_{y,CE} = q_c(W_f - L_1)\left\{\frac{L_1 B_f}{W_f - L_1}\left(X_{c.g.} - \frac{L_1}{2}\right) + L_2\left(X_{c.g.} - L_1 - \frac{W_f - L_1}{2}\right) + \frac{B_f - L_2}{2}\left(X_{c.g.} - L_1 - \frac{W_f - L_1}{3}\right)\right\} \tag{1-23}$$

where:

$$L_2 = \frac{3\left(\frac{P_{UD} Y_{c.g.} - M_x}{q_c} - \frac{B_f^2 W_f}{3}\right) - \frac{P_{UD} B_f}{q_c} + \frac{W_f B_f^2}{2}}{W_f B_f - P_{UD}/q_c} \tag{1-24}$$

$$L_1 = \frac{2P_{UD}/q_c - W_f B_f - L_2 W_f}{B_f - L_2} \tag{1-25}$$

CASE 3

For the applied loading (P_{UD} and M_x) and footing geometry shown in Figure 1-30, where the resisting soil pressure that satisfies the equations of equilibrium results in a pattern represented by the hatched area shown in Figure 1-30, for a positive M_y moment capacity, $M_{y,CE}$ is given as:

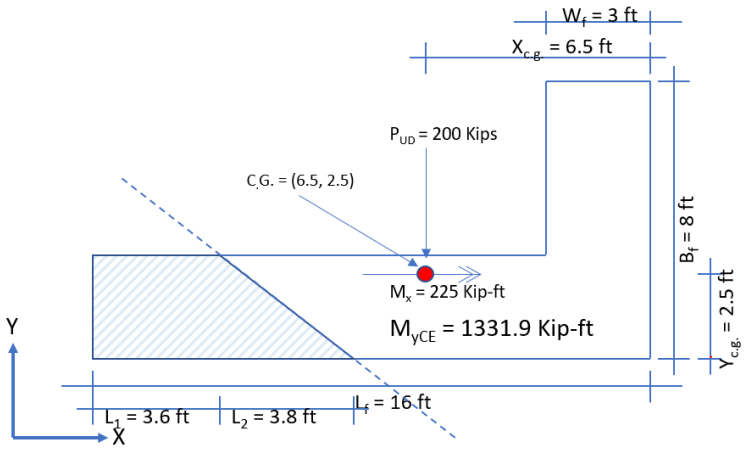

Figure 1-30 Negative M_y moment capacity with positive M_x moment.

$$M_{y,CE} = -W_f\left\{L_1\left(L_f - X_{c.g.} - \frac{L_1}{2}\right) + \frac{L_2}{2}\left(L_f - X_{c.g.} - L_1 - \frac{L_2}{3}\right)\right\} \quad (1\text{-}26)$$

where:

$$L_2 = \frac{6}{q_c W_f}\left(P_{UD} - \frac{2\left(P_{UD}Y_{c.g.} - M_x\right)}{W_f}\right) \quad (1\text{-}27)$$

$$L_1 = \frac{P_{UD}}{q_c W_f} - \frac{1}{2}L_2 \quad (1\text{-}28)$$

CASE 4

For the applied loading (P_{UD} and M_x) and footing geometry shown in Figure 1-31 where the resisting soil pressure that satisfies the equations of equilibrium results in a pattern represented by the hatched area shown in Figure 1-31, for a positive *My* moment capacity, $M_{y,CE}$ is given as:

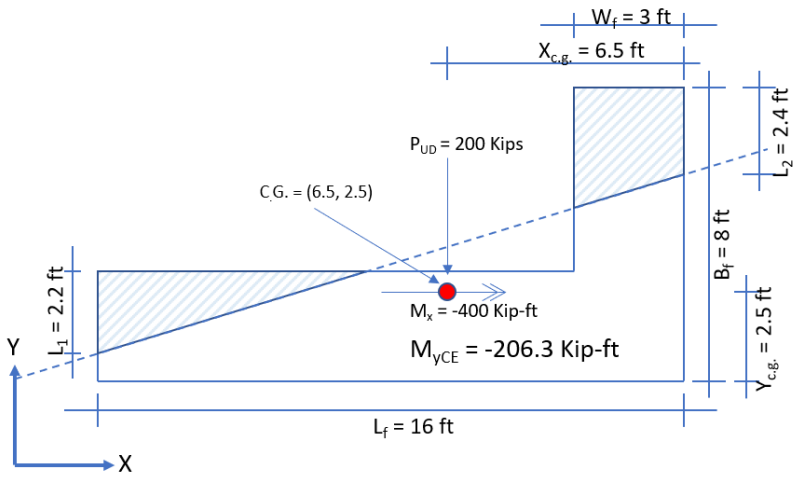

Figure 1-31 Negative M_y moment capacity with negative M_x moment.

$$M_{y,CE} = -q_c \left\{ \frac{1}{2} L_1 X \left(L_f - X_{c.g.} - \frac{X}{3} \right) - W_f L_2 \left(X_{c.g.} - \frac{W_f}{2} \right) - \frac{1}{2} W_f Y \left(X_{c.g.} - \frac{2}{3} W_f \right) \right\} \quad (1\text{-}29)$$

where,

$$B' = B_f - L_2 - W_f + L_1 \quad (1\text{-}30)$$

$$X = L_1 (L_f / B') \quad (1\text{-}31)$$

$$Y = W_f (B' / L_f) \quad (1\text{-}32)$$

1.3.5.5 COMPARISON OF THEORETICAL MOMENT CAPACITIES WITH FINITE ELEMENT ANALYSIS

The formulations have been compared with finite element analysis and give a one-to-one correlation on the maximum soil bearing pressure when appropriate adjustments are made to account for the fact the above equations are derived assuming a uniform soil pressure under the footing, while the finite element analysis assumes a triangular pressure distribution. Since both methods have to satisfy statics, the centroid of the resulting soil pressure distribution under the footing, whether it is uniform or triangular, for the two cases is the same. Using this fact, the adjustment factor can be determined by equating the volumes of the soil pressure for the given boundary of the critical contact area. This adjustment factor ranges from 1.33 where the zero-pressure line is parallel to an edge and 1.69 where the zero-pressure line intersects two adjacent edges at a corner.

Example verification shapes of the critical contact area for various axial loads and directions of applied moment on the footing are presented below (Figure 1-32).

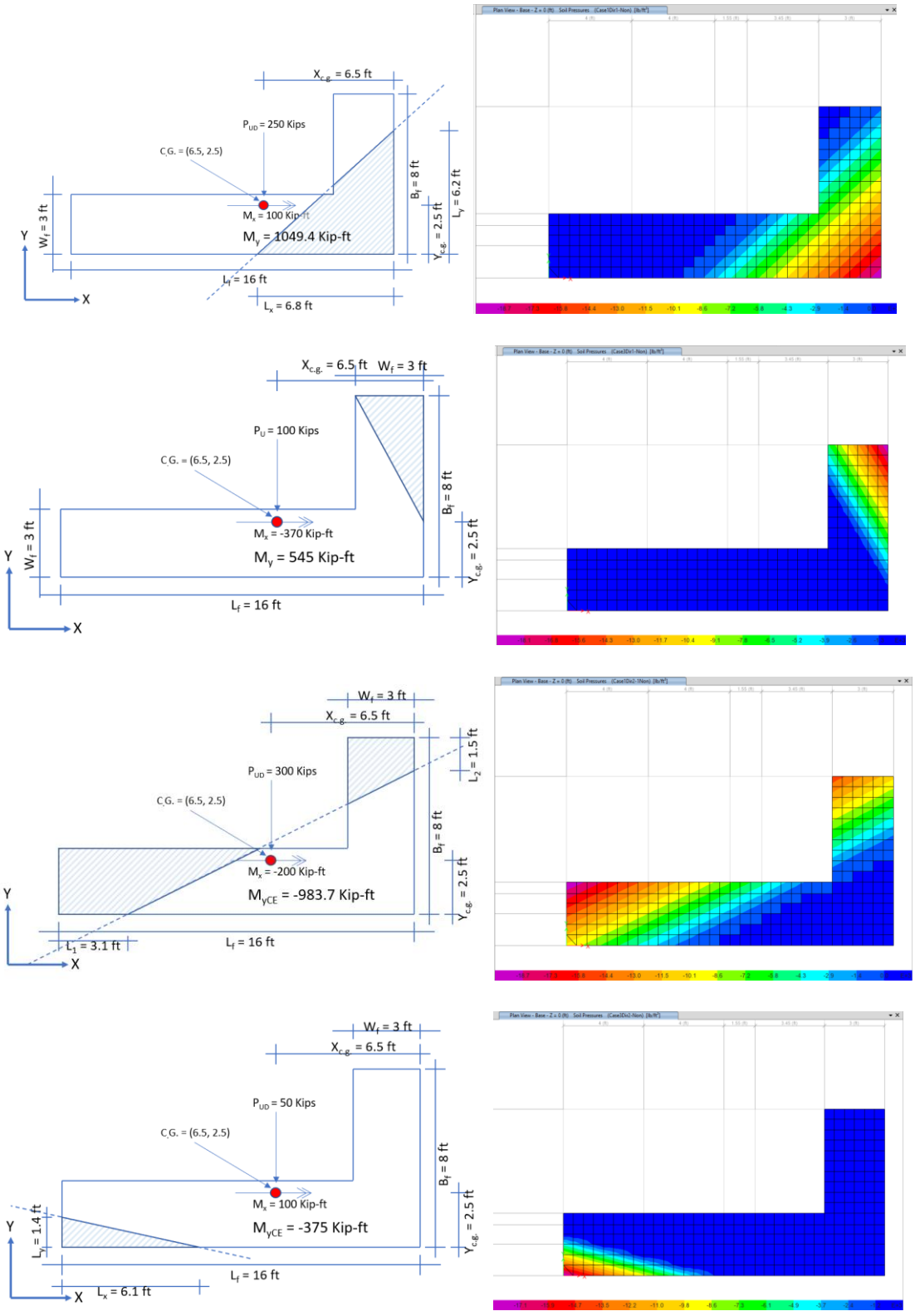

Figure 1-32 Comparison of the shapes for the critical contact area with a uniform and triangular soil pressure distribution under for an L-shaped footing.

1.3.5.6 CONCLUSION

This proposal addresses a limitation in the moment capacity equation in ASCE/SEI 41-17 which provides a general equation for determination of moment capacity on an isolated footing subjected to axial load and uniaxial overturning moment. For footings of irregular or non-rectangular shape, and for bi-directional overturning moments on the footing, the solution is presented in general terms based on principles of mechanics. This is not useful for practicing engineers, who may not be able to quickly derive the moment capacity of an irregular-shaped footing by means of integration, and in some cases a closed form solution may not be available. To circumvent this problem, engineers use foundation analysis software to determine maximum bearing stresses in the soil. This solution is not well suited with the current provisions in the standard, where foundation acceptance is measured against the moment capacity of the footing.

The new methodology proposed demonstrates how the moment capacity can be established for footings of any geometry under a given axial load and overturning moment. However, deriving a solution for each non-rectangular footing shape is complex and is not recommended for general foundation evaluation of existing buildings, but creates the framework under which an equivalent acceptance criterion is created that uses the maximum bearing pressures under the footing as determined from finite element analysis to estimate the ultimate moment capacity of the footing. With appropriate modeling of the footing and adjustment factors, the finite element solution can estimate the ultimate moment capacity of the footing with reasonable accuracy and is in-keeping with the general philosophy of ASCE/SEI 41. The proposed acceptance criteria for the finite element option are conservative as it does not include what the adjustment factor should be, which is between 1.33 and 1.69. It is up to the user to further justify a higher soil bearing pressure value when footing acceptance criteria is not satisfied but is within the margin of the acceptance ratio.

1.3.6 Determination of Soil Stiffness for Mat Foundations

Formulations for determination of the soil stiffness are provided in ASCE/SEI 41-17 for rigid isolated footings relative to soil (Figure 1-33, ASCE/SEI 41-17 Figure 8-2) where stiffness translation of the footing along the z axis, K_{z_sur}, is converted to unit stiffness k_{z_sur}, as shown in Figure 1-34, or as a modulus of subgrade reaction for strip footings (ASCE/SEI 41-17 Eq. 8-11). These equations are used by geotechnical engineers when estimating the dynamic soil stiffness values for use in modeling the soil support beneath the foundation. Figure 1-34 and Figure 1-35 show the variation in effective soil stiffness values as a function of footing widths ranging from 5 feet to 50 feet for the two methods.

Degree of Freedom	Stiffness of Foundation at Surface	Note
Translation along x-axis	$K_{x\_sur} = \frac{GB}{2-\nu}\left[3.4\left(\frac{L}{B}\right)^{0.65} + 1.2\right]$	
Translation along y-axis	$K_{y\_sur} = \frac{GB}{2-\nu}\left[3.4\left(\frac{L}{B}\right)^{0.65} + 0.4\frac{L}{B} + 0.8\right]$	
Translation along z-axis	$K_{z\_sur} = \frac{GB}{1-\nu}\left[1.55\left(\frac{L}{B}\right)^{0.75} + 0.8\right]$	
Rocking about x-axis	$K_{xx\_sur} = \frac{GB^3}{1-\nu}\left[0.4\left(\frac{L}{B}\right) + 0.1\right]$	
Rocking about y-axis	$K_{yy\_sur} = \frac{GB^3}{1-\nu}\left[0.47\left(\frac{L}{B}\right)^{2.4} + 0.034\right]$	
Torsion about z-axis	$K_{zz\_sur} = GB^3\left[0.53\left(\frac{L}{B}\right)^{2.45} + 0.51\right]$	

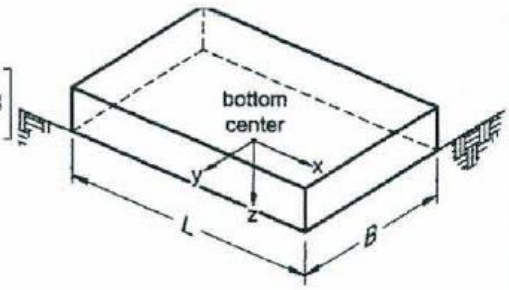

Orient axes such that $L > B$. If $L = B$, use x-axis equations for both x-axis and y-axis.

Figure 1-33 Figure 8-2 from ASCE/SEI 41-17.

Poison's Ratio	ν =	0.25	
Shear wave velocity	V_{s0} =	300	m/s
		984	ft/sec
Soil density	γ =	120	pcf
Initial soil shear modulus	$G_0 = \frac{\gamma V_{s0}^2}{g}$	3608	ksf
Effective shear modulus ratio	G/G0 =	0.5	Table 8-2 of ASCE 41
Effective shear modulus	G =	1804	ksf

L_f/B_f = 1

Footing Length L_f (ft)	Footing width B_f (ft)	k_{z_sur} pci
5	5	654
10	10	327
15	15	218
20	20	164
25	25	131
30	30	109
35	35	93
40	40	82
45	45	73
50	50	65

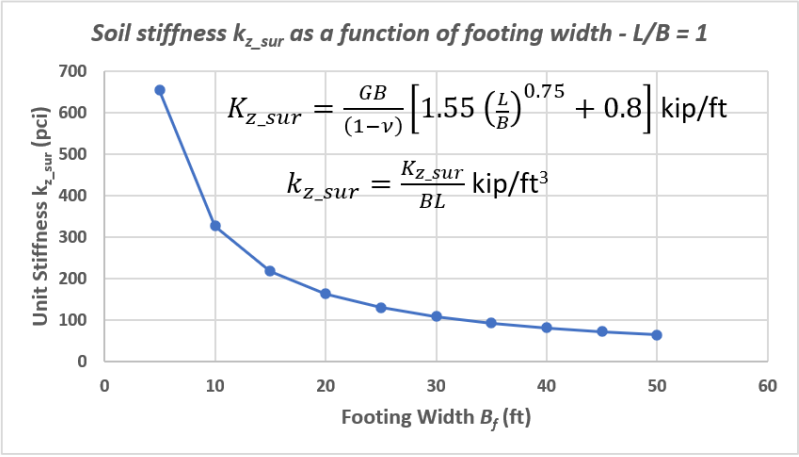

Figure 1-34 Variation in soil stiffness values as function of footing width, ASCE/SEI Figure 8-2.

Poison's Ratio	ν =	0.25	
Shear wave velocity	V_{s0} =	300	m/s
		984	ft/sec
Soil density	γ =	120	pcf
Initial shear modulus	$G_0 = \frac{\gamma V_{s0}^2}{g}$	3608.4	ksf
Effective shear modulus ratio	G/G_0 =	0.5	Table 8-2 of ASCE 41
Effective shear modulus	G =	1804	ksf

Footing width (ft)	k_{sv} pci
5	362
10	181
15	121
20	90
25	72
30	60
35	52
40	45
45	40
50	36

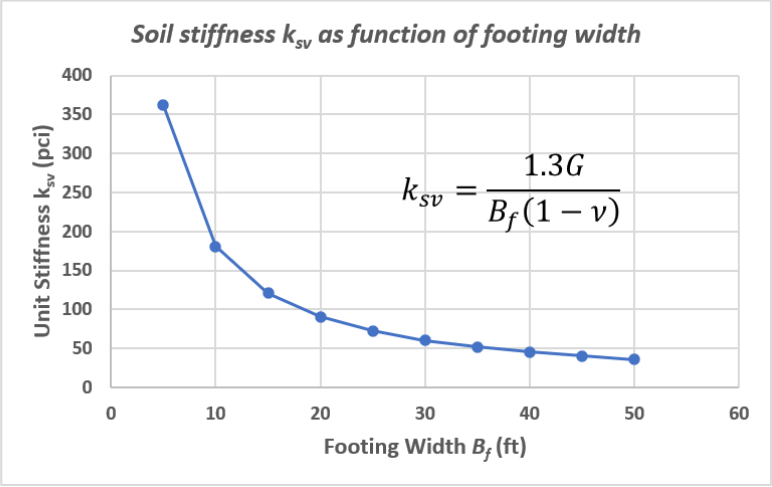

Figure 1-35 Variation in soil stiffness values as function of footing width, ASCE/SEI 41-17 Eq. 8-11.

Extending these stiffness formulations as representative for buildings on large mat foundations results in unreasonably low values of stiffness. Multiple alternate methods for determination of the soil stiffness for mat foundations are therefore proposed using rational judgment and are based on the actual loaded area immediately below the vertical elements supported by the mat.

When the entire building or portion thereof is supported by a mat foundation over multiple bays (Figure 1-36), the modulus of subgrade reaction using the whole width of the mat foundation using the two methods shown above gives unrealistically low values for the soil spring stiffness per unit tributary area of foundation. Four alternate methods are proposed that establish an equivalent width to be used in the determination of the soil spring stiffness. Capping the width should result in a reasonable estimate for the stiffness of the soil under the mat without loss of accuracy than if more sophisticated methods are used.

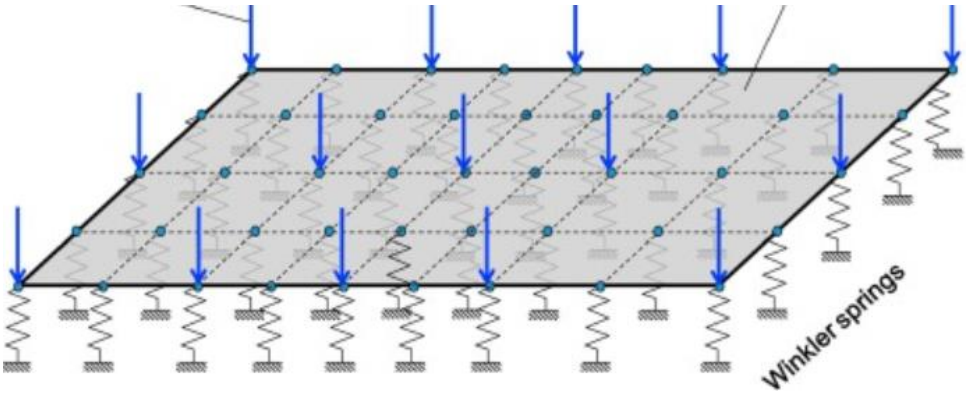

Figure 1-36 Mat foundation supporting vertical elements spanning multiple bays.

1.3.6.1 METHOD 1

The effective width may be zoned to coincide with the column grid lines and limited by the typical bay width. Widths for end bays are typically less than the interior bays resulting in greater stiffness at the perimeter than in the center portion of the mat. In addition, the center portion of the mat foundation may be further reduced based on methods using the procedures in ACI 336.2R-88.

The ACI 336.2R method to determine the spring stiffness is based on the soil pressure profile as a function of depth. The pressure profiles are given for 5 points from the edge of the footing towards the center at the one-eighth points for three different *B/L* ratios in Table 6-1 of ACI 336.2R-88, as shown in Figure 1-37. This table is copied from ACI 336.2R-88 and represents the soil pressure at various depths under a footing obtained from Newmark's influence chart for vertical stress distribution in the soil under a footing where the soil pressure dissipates with depth from the surface.

Example: for *B/L* =1, pressure ratio at the surface is 1.0, at a depth of 0.5*B* it is 0.4 of the value. At 4*B* the pressure is 3% of the pressure applied at the surface.

For a reference stiffness, k_s, at the edge, the stiffnesses at any point *i* in the interior of the mat can be calculated as:

$$k_{si} = k_s(DQ_e/DQ) \quad (1\text{-}33)$$

where:

DQ = Average pressure under the mat at point *i*

DQ_e = Average pressure at the edge of the mat

Table 6.1-Vertical pressure profiles by Newmark's 1935 method (in Bowles 1985) for selected points beneath a foundation as shown

B/L = 1

PRESSURE PROFILE FOR POINTS:					
DY	1	2	3	4	5
0.00 B	1.000	1.000	1.000	1.000	1.000
0.50B	0.400	0.530	0.628	0.683	0.701
1.00B	0.240	0.278	0.309	0.329	0.336
1.50B	0.146	0.160	0.170	0.177	0.179
2.00B	0.095	0.100	0.105	0.107	0.108
2.50B	0.066	0.068	0.070	0.071	0.072
3.00B	0.048	0.049	0.050	0.050	0.051
3.50B	0.036	0.037	0.037	0.038	0.038
4.00B	0.028	0.028	0.029	0.029	0.029
AVERAGE PRESSURE INCREASE					
DQ =	0.193	0.217	0.235	0.246	0.250

B/L = 2

PRESSURE PROFILE FOR POINTS:					
DY	1	2	3	4	5
0.00B	1.000	1.000	1.000	1.000	1.000
0.50B	0.408	0.648	0.757	0.792	0.800
1.00B	0.270	0.362	0.431	0.469	0.481
1.50B	0.186	0.229	0.263	0.285	0.293
2.00B	0.135	0.157	0.175	0.186	0.190
2.50B	0.101	0.113	0.123	0.129	0.131
3.00B	0.078	0.085	0.090	0.094	0.095
3.50B	0.061	0.066	0.069	0.071	0.072
4.00B	0.049	0.052	0.054	0.056	0.056
AVERAGE PRESSURE INCREASE					
DQ =	0.220	0.273	0.304	0.319	0.324

B/L = 3

PRESSURE PROFILE FOR POINTS:					
DY	1	2	3	4	5
0.00B	1.000	1.000	1.000	1.000	1.000
0.50B	0.409	0.718	0.796	0.811	0.814
1.00B	0.274	0.408	0.486	0.517	0.525
1.50B	0.195	0.262	0.312	0.340	0.348
2.00B	0.147	0.185	0.216	0.235	0.241
2.50B	0.115	0.138	0.157	0.170	0.174
3.00B	0.092	0.107	0.119	0.127	0.130
3.50B	0.075	0.085	0.093	0.098	0.100
4.00B	0.062	0.069	0.075	0.078	0.079
AVERAGE PRESSURE INCREASE					
DQ =	0.230	0.305	0.340	0.355	0.359

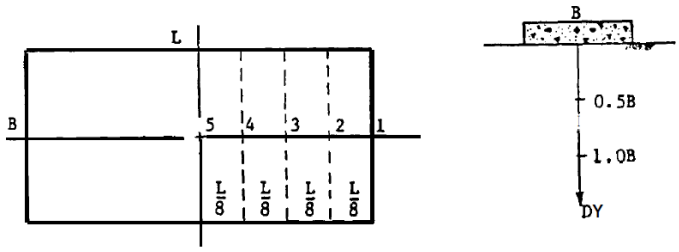

Figure 1-37 Vertical soil pressure profiles for selected points beneath a foundation (ACI 336.2R).

These influence charts are based on the Boussinesq equation to determine the vertical stress σ_z at any point *P* at a depth *z* as a result of a surface point load *Q*.

$\sigma_z = 3Q/2\pi z^2(1/[1+(r/z)^2]^{5/2}$, where r is the horizontal distance between any point P below the surface and the vertical axis through the point load Q, z is the vertical depth of point P from the surface.

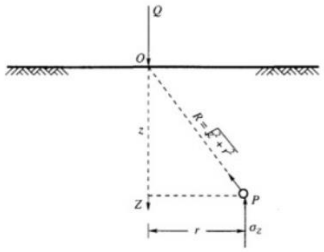

Figure 1-38 Vertical stress σ_z at any point *P* at depth *z*.

Example: Mat with a *L/B* ratio of 2.

For a given edge zone stiffness, k_s = 100 pci, the stiffnesses in the interior, Zone 2 and Zone 3 shown in Figure 1-39 are determined using Table 6-1 of ACI 336.2R as follows:

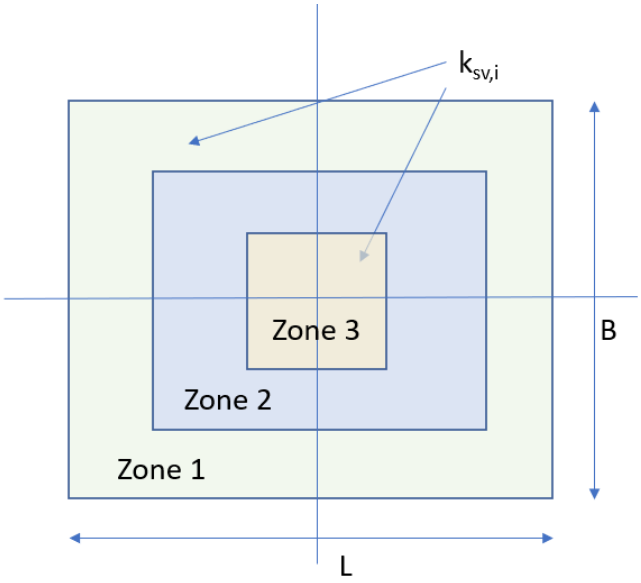

Figure 1-39 Soil pressure zones under a mat of footing length, *L*, and width, *B*.

Stiffness determination for Zone 2:

From ACI 336.2R Table 6-1, for B/L =2, DQ = 0.22 at point 1, and 0.304 at point 3. Therefore, the stiffness for zone 2 is:

$$k_{s\_zone\ 2} = (100\ \text{pci})(0.22/0.304) = 72.4\ \text{pci}$$

Stiffness determination for Zone 3, Center zone:

$k_{s\_zone\ 3}$ = (100 pci)(0.22/0.324) = 67.9 pci.

The variation of soil stiffness assuming five pressure zones for the mat for three different *L/B* ratios is shown in Figure 1-40:

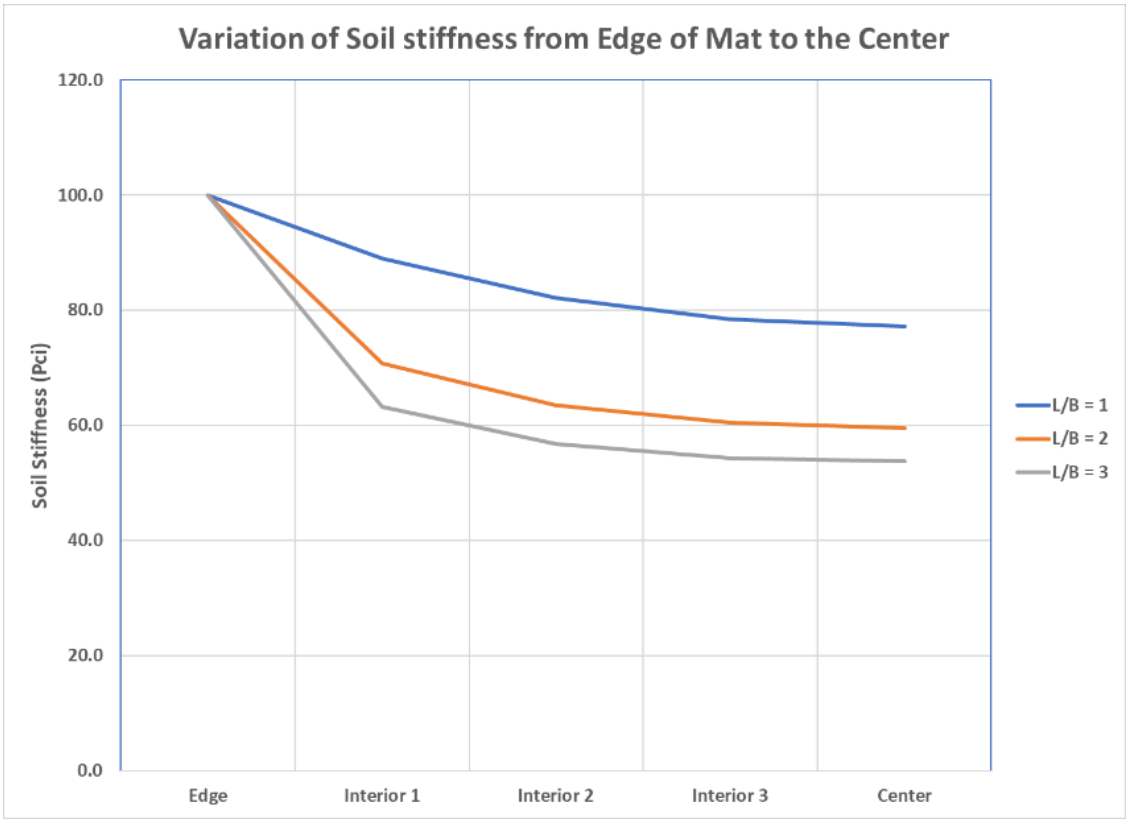

Figure 1-40 Soil pressure zones under a mat of footing length, *L*, and width, *B*.

1.3.6.2 METHOD 2

The effective width B'_f used to determine the soil spring stiffness is determined based on the minimum footing area required to support 1.5 times the gravity axial load at each location of the vertical structural component on the mat and the allowable soil pressure.

The width is calculated on the allowable soil bearing pressure, which is assumed to have a built-in factor of Safety of 3.0. Therefore, the width calculated as 1.5 of the gravity load is a reasonable assumption where the influence of soil pressure to the settlement of the footing from the adjacent footing is minimal. For overlapping widths, the total width is required to be used.

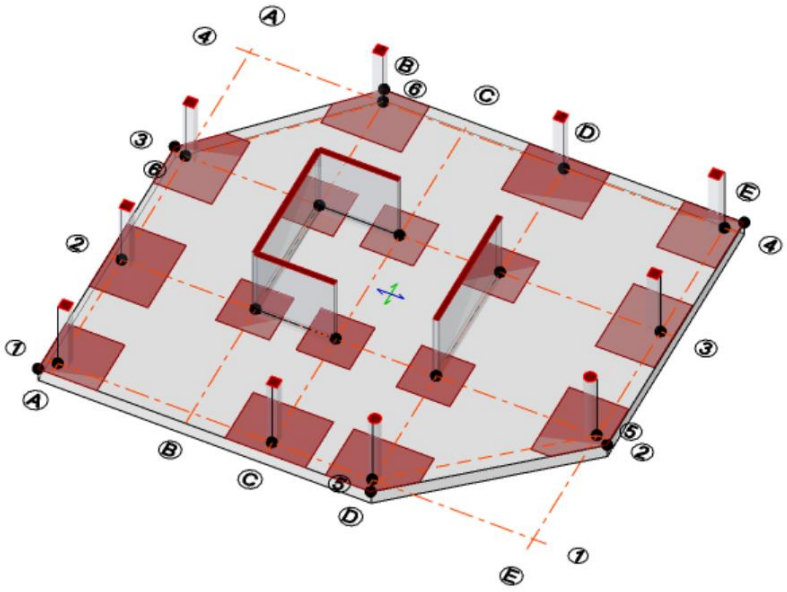

Figure 1-41 Soil pressure zones under a mat of footing length, *L*, and width, *B*.

1.3.6.3 METHOD 3

The effective width is based on the geometry and spacing of the vertical structural components on the mat and the thickness of the mat. The effective footing width is taken as 4 times the footing depth on each side of the vertical element but not more than the actual footing size. The assumption is the thicker the mat, the larger the gravity load, and the distribution is spread out over a larger area. In this method, overlapping areas are not considered in the estimation of soil stiffness.

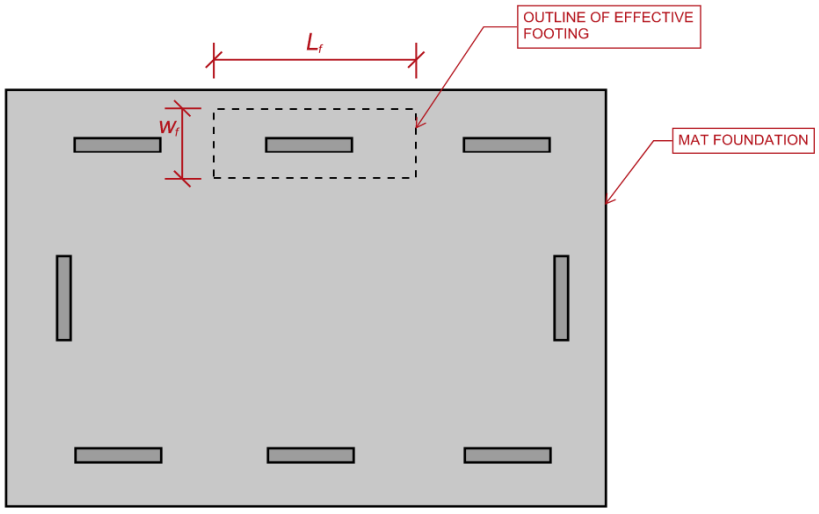

Figure 1-42 Soil pressure zones under a mat of footing length, *L*, and width, *B*.

1.3.6.4 METHOD 4

Other rational procedures are based on settlement of the mat from finite element modeling of the soil continuum that include the geometry and rigidity of the mat. Geotechnical engineers often use software where the loads from the structure are input on the foundation plan as concentrated or area loads on the soil. The stiffness is then back-calculated from the settlement and the applied load. The foundation settlement increases with footing width applied over a large area, which is expected, however the rate at which settlement happens diminishes as the area increases. An example of the footing pressure versus settlement plot as a function of the width B of the footing, used in estimation of the soil stiffness for a large building on a mat foundation is shown in Figure 1-43.

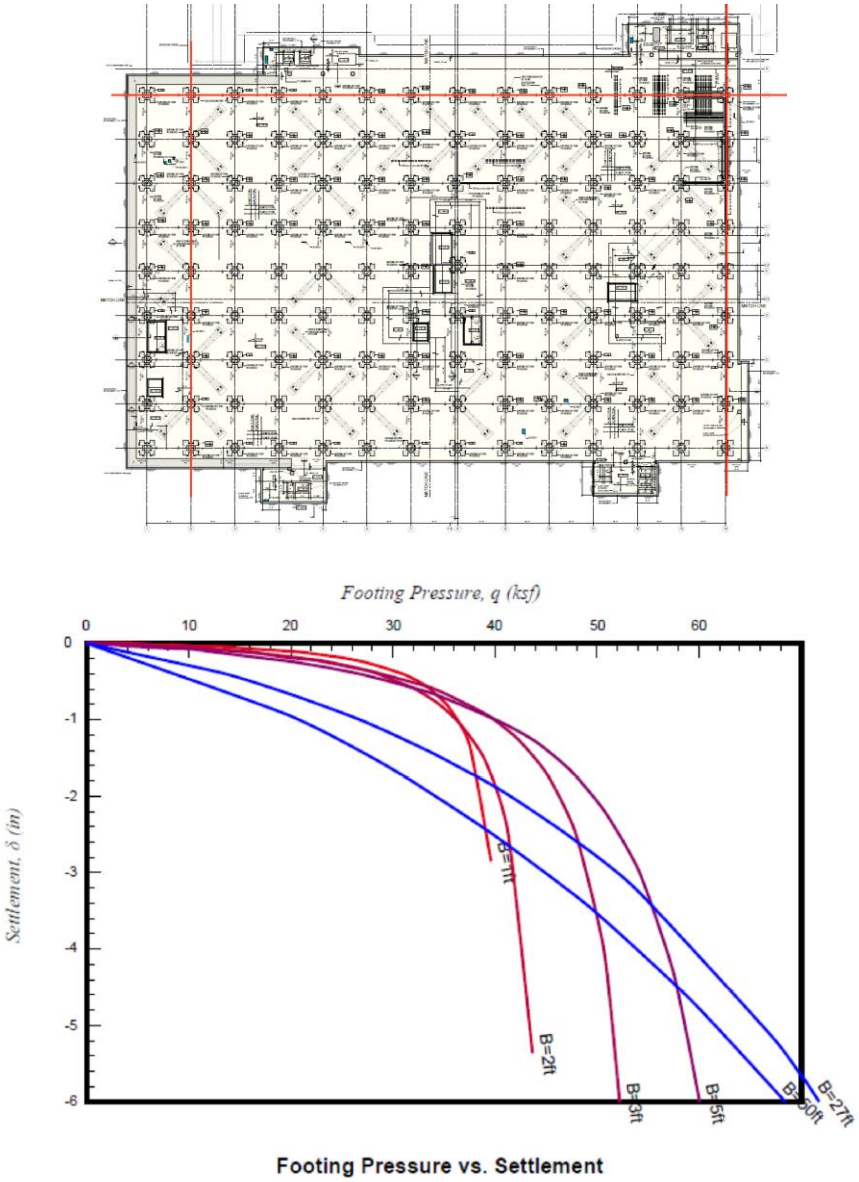

Figure 1-43 Soil pressure zones under a mat of footing length, *L*, and width, *B*.

1.3.6.5 CONCLUSIONS

The equations to calculate the stiffness of the foundations in ASCE/SEI 41-17 were established for single isolated footings considered rigid relative to soil, or for strip footings of finite width supporting a single row of vertical gravity and lateral-force-resisting elements. These equations are not suitable for the estimation of stiffnesses of larger mat foundations that span multiple bays and extend over several hundred feet. There is currently no consensus in the structural engineering or geotechnical community as to what the appropriate width should be to estimate the stiffness of the soil supporting a mat. Several options are proposed based on engineering judgment that all give a reasonably conservative dynamic stiffness for large mat foundations. The thinking is that the gravity loads resulting in settlement of the mat foundation would have already occurred prior to a large seismic event. There would therefore be selected areas where large axial overturning loads would be applied at lateral-force-resisting column locations or wall boundaries. Based on the thickness of the mat and the magnitude of the axial load at the column or wall boundary element, suggests there is a limited width which is required to resist that additional load. The proposed methods limit the width required to be used when using the stiffness equations in Chapter 8 of ASCE/SEI 41. It should also be noted that a stiffer subgrade reaction may result in higher base shear demands in the superstructure. It is up to the user to select the method which is the most appropriate.

1.3.7 Procedures for a Separate Foundation Analysis Using Superstructure Demands from a Fixed-Base Model

A common practice for new buildings designed using ASCE/SEI 7 is to use an elastic, fixed-base building model to design the superstructure, and a separate elastic model of the foundation on compression-only springs to design the foundation. Different proprietary software programs are typically used for this two-step analysis approach; the structure is modelled with a fixed-base in one program and the reactions are then transferred to another foundation-analysis program to determine the soil bearing pressure distribution and to design the foundation structure.

The demands are based on forces, as determined through the application of a global force reduction factor or response modification factor, *R*, and compression-only soil springs are used to represent the soil and soil-structure interface.

For existing building evaluation and retrofit using ASCE/SEI 41-17, the standard uses unreduced force-demands and treats each component action as either force- or deformation-controlled. For deformation-controlled actions, the capacity is increased by an *m*-factor that varies depending on its ductility capacity. The unreduced demand is then compared to an amplified capacity on a component action basis. See Chapter 2 of FEMA P-2006 for a discussion of the differences between ASCE/SEI 7 and ASCE/SEI 41 provisions. This historically caused problems in practice, particularly when elastic demands are applied to foundations where footing uplift is unrestrained. While the linear procedures are meant to be elastic procedures, engineering practice has the tools and propensity to incorporate geometric nonlinearity (soil separation from footing) into the design process. Therefore, the standard has addressed this by permitting two alternate procedures, namely Procedure 1 and Procedure 2.

Where a fixed-base assumption is used and the foundation consists of combined footings or mat foundations, demands from the superstructure are extracted and analyzed outside of the model used for evaluation of the superstructure to check the foundation. Because of the indeterminate nature of foundation systems with combined footings and mat foundations, they are typically analyzed using computer models where the footings are supported on individual vertical soil springs or distributed area springs, also called Winkler springs, as a beam on elastic foundation. The foundation model with springs is analyzed elastically where the springs resist tension and compression, Procedure 1, with associated soil modeling and acceptance criteria, or nonlinearly with yielding or nonyielding compression-only springs, Procedure 2, with associated soil modeling and acceptance criteria.

A flowchart of the steps for evaluation of buildings on combined footings or mat foundations is shown in Figure 1-44.

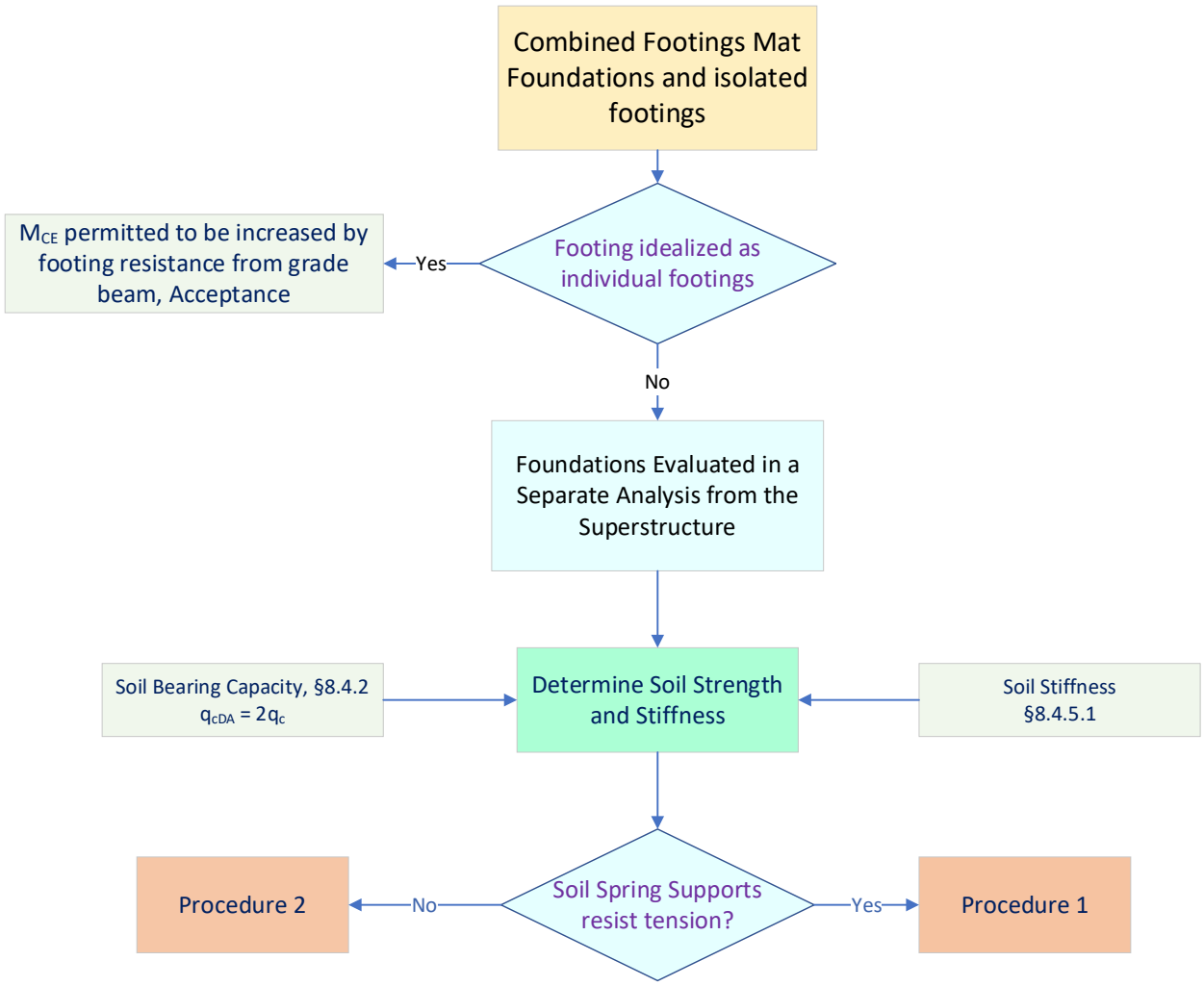

Figure 1-44 Evaluation process for buildings on combined footings or mat foundations.

1.3.7.1 PROCEDURE 1: SOIL SPRINGS RESIST TENSION AND COMPRESSION

In this procedure, unreduced, pseudo-elastic demands, and elastic compression-tension soil springs are used. The soil pressure distribution and structural actions of the foundation are based on the soil remaining in contact with the footing. Soil spring stiffnesses or modulus of subgrade reaction used in the analysis model, which act in both tension and compression are derived from ASCE/SEI 41-17 Figure 8-2 by discretizing a continuous or mat foundation into individual "effective" footings that are interconnected, or as provided by the geotechnical engineer. With the mat foundation now represented with flexural and shear flexibility and the distributed springs, the pseudo-elastic reaction forces from the base of the building are applied.

The total foundation rotation demand is obtained at the base of the wall, or from the bottom of two columns that form a braced frame. To assess the soil bearing, the rotation demand is compared directly to the total rotation acceptance displacement acceptance values.

1.3.7.2 PROCEDURE 2: SOIL SPRINGS ARE COMPRESSION-ONLY

This procedure is an alternate to Procedure 1, where only the pseudo force earthquake demands from a fixed-base analysis are divided by the appropriate *m*-factor and are superimposed with the gravity loads per the applicable load combinations in ASCE/SEI 41 Chapter 7.

In this procedure, if the spring capacity in compression is not capped or does not yield, the soil pressure distribution is triangular with the maximum pressure occurring at the edge of the footing when the footing is rigid relative to the soil. Since the soil pressure distribution is triangular, the maximum soil pressure at the loaded edge of the footing can be increased as limiting it to the maximum soil pressure is conservative. A study by Lobo (2021) has shown that, for uniaxial and biaxial loading on the footing with appropriate meshing of the footing, an adjustment factor between 1.33 and 1.69 gives a one-to-one correspondence when the soil pressure gradient is parallel to the loaded edge and when the maximum pressure is at the corner and goes to zero along the two adjacent edges of the corner. These factors can be easily derived by equating the volumes of the soil pressure blocks for the uniform and triangular pressure distributions given the fact that the centroids of the soil pressure forming the critical contact area, A_c, for the two soil pressure distributions are at the same location.

A flowchart of the methodology adopted for the two procedures is shown in Figure 1-45.

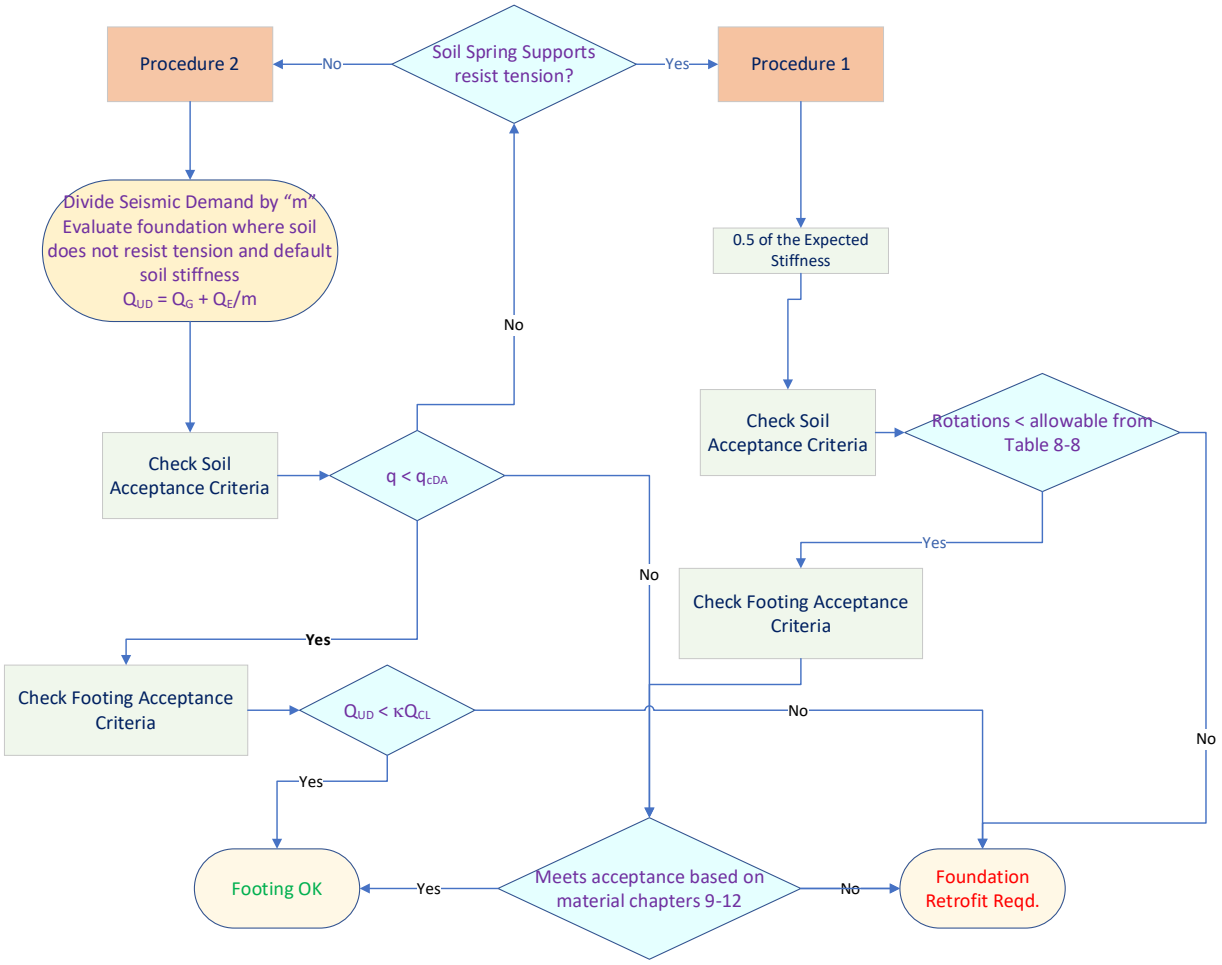

Figure 1-45 Evaluation process for buildings using Procedure 1 or Procedure 2.

1.3.7.3 CONCLUSIONS

There is currently no guidance in the standard using linear analysis procedures for evaluating foundation systems comprising of combined footings nor mat foundations when a fixed-base assumption is used. This could lead to inconsistencies in the evaluation. To address this deficiency, two new procedures are proposed when evaluating combined footings or mat foundations using demands from a linear analysis fixed-base model. Both procedures require a separate foundation analysis model different from the superstructure to analyze the foundation system.

In Procedure 1, the foundation stiffness is multiplied by 0.5 to account for the fact that foundation uplift is restrained. Soil bearing acceptance is based on rotation demands and the foundation structural component is evaluated using the *m*-factors from the material chapters, or as force-controlled elements.

In Procedure 2, the foundation is modeled with spring supports which act nonlinearly as compression only springs, in other words they do not resist tension. The superstructure seismic demands from the fixed-base analysis are divided by the *m*-factors prior to the foundation analysis

where soil does not resist tension. Soil bearing acceptance is based on the maximum soil pressure being less than the expected bearing capacity for short duration loading, q_{cDA}. The footing structural component is evaluated using the resisting soil pressure as the demands on the footing. No additional *m*-factor reduction is permitted when evaluating the foundation structural element.

1.3.8 Moment Capacity of Footings Interconnected by Grade Beams

Acceptance criteria for foundation overturning capacity in the current ASCE/SEI 41 standard is based on moment capacity for an isolated footing. In many cases, footings are interconnected by a grade beam and have additional capacity that is not taken into account. For these cases where the grade beam or spandrel beam at grade (as shown in Figure 1-46) provides additional overturning resistance beyond the boundaries of the individual footing in question, principles of mechanics can be used to determine the overturning moment capacity of the footing by summing all restoring actions, including gravity loads as shown below.

$$\Sigma M_A = 0 \rightarrow M_{CE} = P_{UD}(L_f/2 - L_c/2) + V_{GB1}(L_f - L_c/2) + V_{GB2}(L_c/2) \quad (1\text{-}34)$$

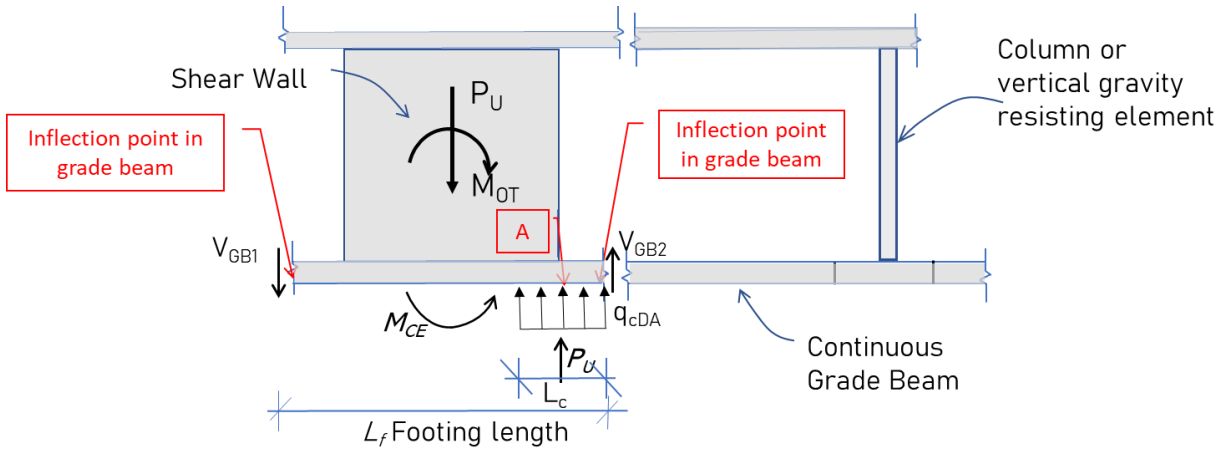

Figure 1-46 Overturning and resisting forces on an isolated footing with grade beam resistance.

For shallow strip or isolated footings supporting multiple structural members (Figure 1-47), either principles of mechanics or explicit mathematical modelling can be used to evaluate the overturning demand and capacity.

Where principles of mechanics are used, and the combined footing is rigid relative to the soil for foundations supporting multiple structural members, the overturning demand action, M_{OT}, is calculated as the sum of individual overturning axial forces on each member. The expected gravity load, P_U, is the sum of vertical loads on each member. The resisting moment capacity is the summation of all restoring loads multiplied by their eccentricity to the center of rotation.

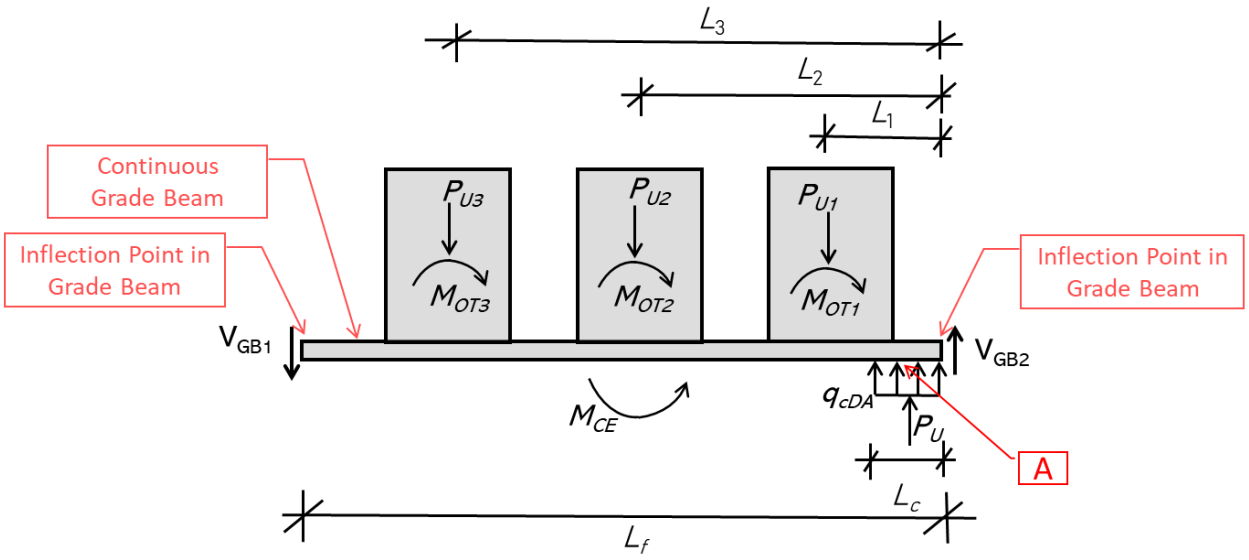

Figure 1-47 Overturning and resisting forces on an isolated footing supporting multiple structural members.

$$M_{OT} = M_{OT1} + M_{OT2} + M_{OT3} \quad (1\text{-}35)$$

$$P_U = P_{U1} + P_{U2} + P_{U3} \quad (1\text{-}36)$$

$$\Sigma M_A = 0$$

$$M_{CE} = P_{U1}(L_1 - L_c/2) + P_{U2}(L_2 - L_c/2) + P_{U3}(L_3 - L_c/2) + V_{GB1}(L_f - L_c/2) + V_{GB2}(L_c/2) \quad (1\text{-}37)$$

Adding these provisions allows the user to quickly estimate if the combined footing has adequate capacity. However, the above-mentioned proposed changes are applicable when combined footings are evaluated using simple hand calculations. These procedures would not apply when foundations are evaluate using a separate foundation analysis computer program.

1.3.8.1 CONCLUSIONS

There are conditions where it may not be economical to create a separate foundation model to check the foundation resisting capacity of a combined footing when a simple hand check will suffice. New provisions are therefore proposed to permit the additional resistance provided by the footings extending beyond the boundaries of the isolated footings by means of a grade beam. These provisions apply when using the newly proposed Simplified Procedure or where the combined footing is idealized as individual isolated footings. It should be noted that analyzing the foundation system for a large building using either Procedure 1 or Procedure 2 in the combined footings section is more efficient.

1.3.9 Limiting Use of Compression-Only Springs When Superstructure Is Modeled as Linear Using Flexible-Base Procedures

Case studies on the two archetype buildings, one a nonductile concrete flat slab building retrofit with shear walls including a shallow foundation retrofit beneath the new shear walls, Archetype Building 1, and one a special reinforced concrete moment frame building designed to the requirements of ASCE/SEI 7-10, Archetype Building 2, have shown that for linear analysis procedures when the foundation and superstructure are modeled together in a single computer model, with foundations supported on nonlinear compression only springs, force demands in the foundations superstructure elements are inconsistent with demands when the superstructure and foundation are modeled using nonlinear procedures. The following is a documentation of the case study results that provides the justification for this proposed change. Additional details and modeling assumptions used in the case study models are documented in Part 3, Appendix B and Appendix C, which can be found at http://femap2208.atcouncil.org/.

1.3.9.1 CASE STUDY ARCHETYPE BUILDING 2

Several parametric studies were performed on Archetype Building 2, the special reinforced concrete moment frame building starting with a fixed-base model designed to satisfy the requirements of a new building using the prescriptive requirements of ASCE/SEI 7-10 and ACI 318-14. The following analyses were performed to evaluate the building superstructure and foundation performance to confirm the fundamental concept: If the building foundation is sufficiently robust and satisfies the acceptance criteria of ASCE/SEI 41 for the selected performance level, the superstructure demands are reasonable. Example: A new building designed using ASCE/SEI 7 should also satisfy the Basic Safety Objective for New buildings (BPON).

To execute the parametric case studies, linear and nonlinear analysis procedures were conducted with the following boundary condition for the foundation:

- Linear Static Procedure (LSP)
  - Fixed-base model
  - Model on foundation area springs
- Nonlinear Static Procedure (NSP)
  - Fixed-base model
  - Model on foundation area springs

Lower-bound soil stiffness was used for the models where foundations were modeled as flexible and soil resists tension. Expected soil properties were used for all other cases where the foundation was modeled as flexible on nonlinear compression-only springs.

Comparison of Foundation Soil Pressure Distribution from the Various Models – LSP and NSP

For the models with flexible-base foundations, and LSP, the soil pressure distribution in the foundations for ASCE/SEI 41-17 demands at the BSE-1N and BSE-2N earthquake hazard levels considering the springs as elastic (both tension and compression) and nonlinear as compression only, are as shown in Figure 1-48 through Figure 1-51. Soil pressure distribution for the NSP at the BSE-2N earthquake hazard level is shown in Figure 1-52.

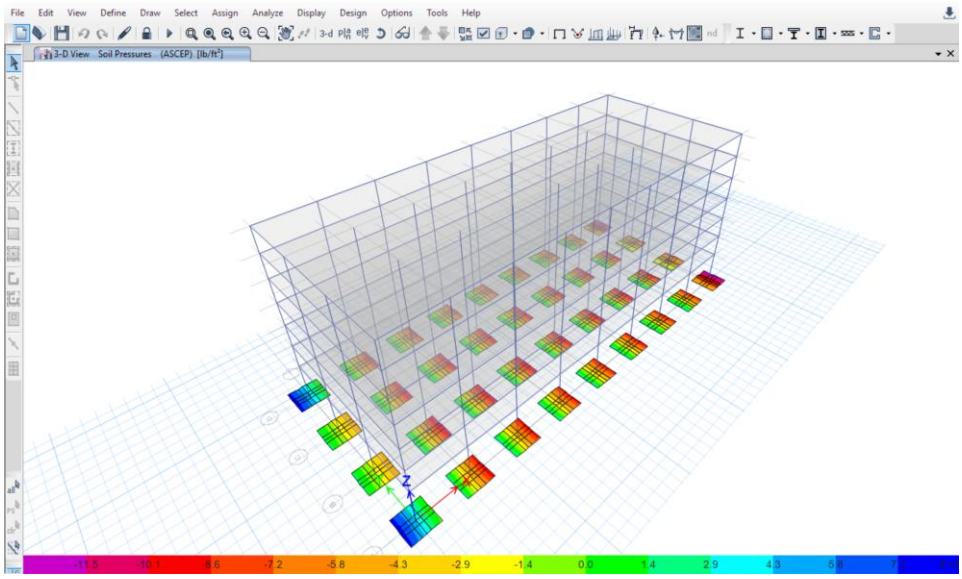

Figure 1-48 Soil takes tension, hazard level BSE-1N max pressure = 12.6 ksf.

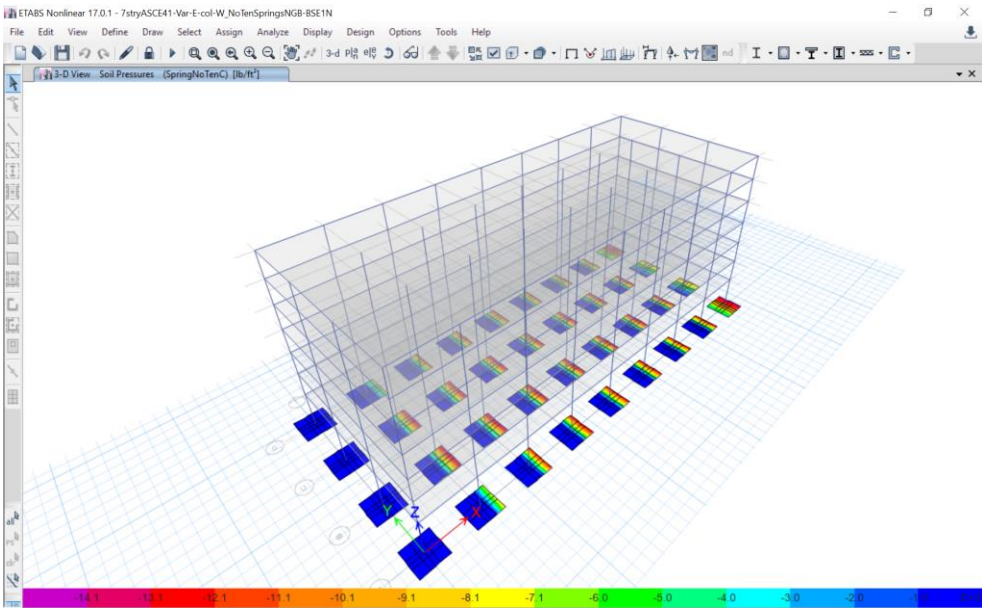

Figure 1-49 Soil does not take tension, hazard level BSE-1N max pressure = 15.7 ksf.

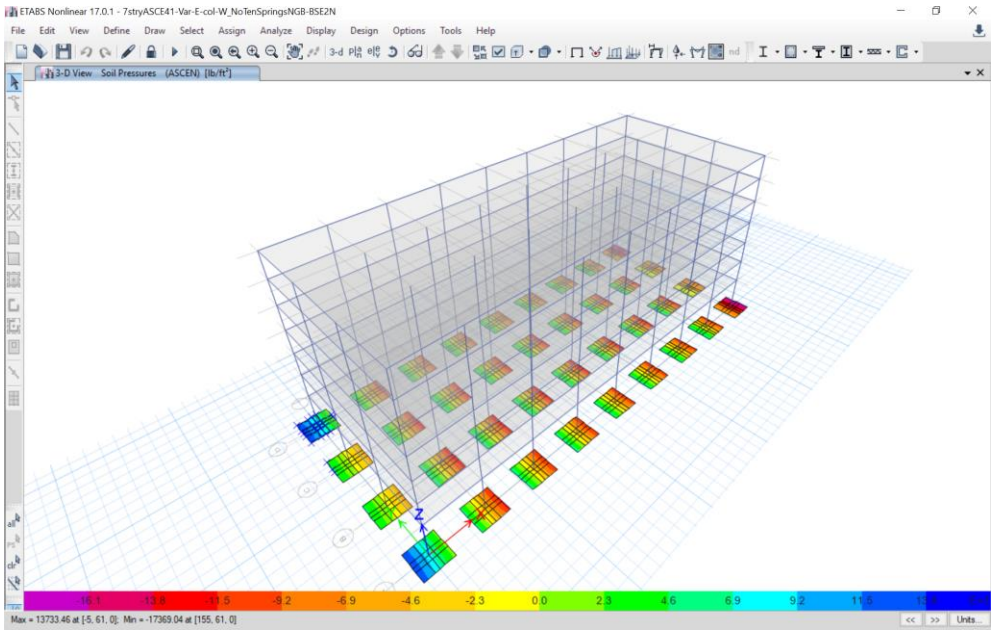

Figure 1-50 Soil takes tension, hazard level BSE-2N max pressure = 17.8 ksf. Meets upper bound soil capacity Q_{UB} = 20.4 ksf.

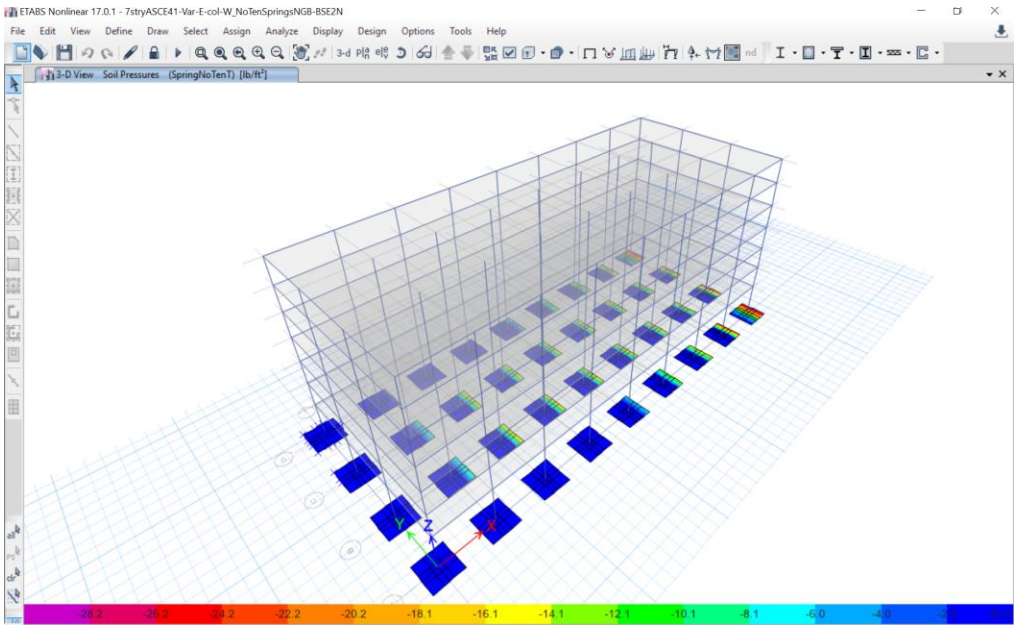

Figure 1-51 Soil does not take tension, hazard level BSE-2N max pressure = 28.2 ksf.

Foundation Demands – NSP

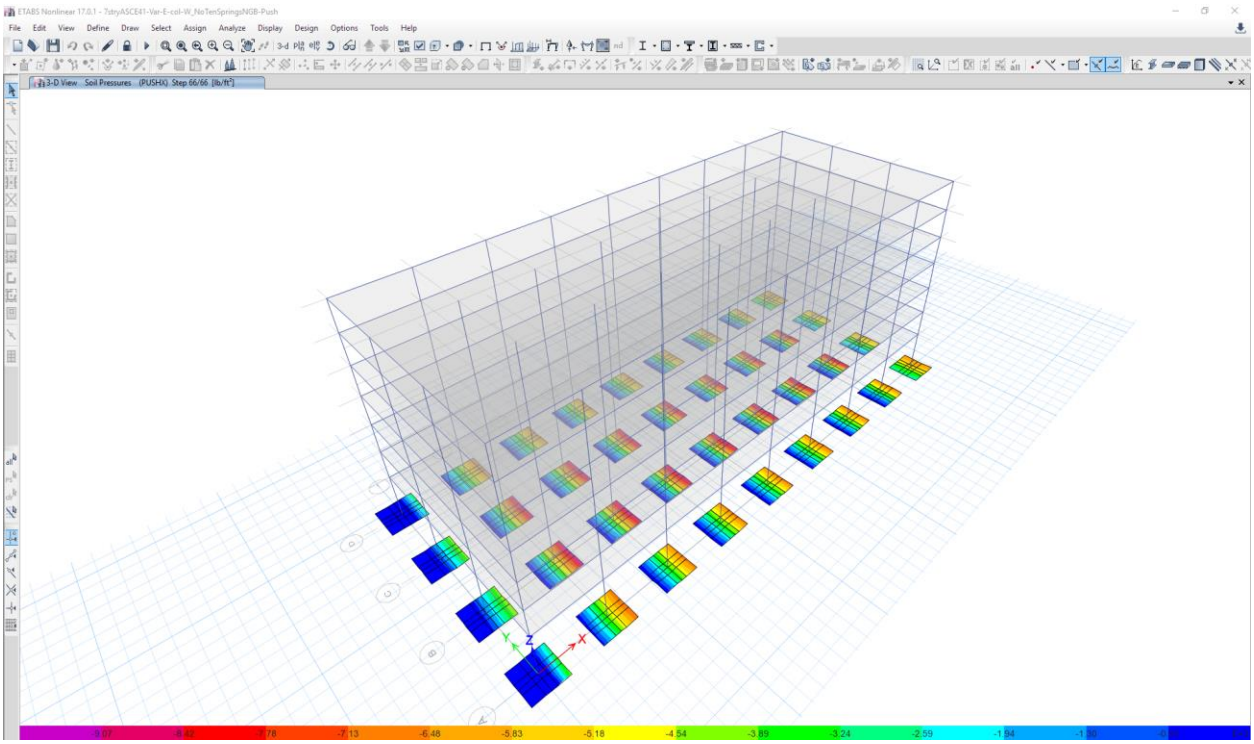

Figure 1-52 Soil does not take tension, hazard level BSE-2N NSP max pressure = 9.24 ksf.

Observation of the soil pressures from the LSP shows that when the superstructure is modeled as elastic, and the soil is modeled as nonlinear compression-only springs, as the seismic overturning demand increases, there is a large uplift and shifting of the loads so that only a few footings are in contact with the soil. This outcome is unrealistic considering the geometry and flexibility of the building. The soil bearing pressures when the superstructure is permitted to yield shows a very different soil bearing pressure profile but would be similar to the bearing pressure profile for the baseline demands using ASCE/SEI 7-10. Results from the NSP show that the foundation meets the acceptance criteria for soil bearing, without additional superstructure deformation as inelastic deformations in the superstructure govern the response.

Comparison of Superstructure Column Axial Loads LSP and NSP

The superstructure column axial loads for x-direction loading at the BSE-2N earthquake hazard level for the Load Combination (LC) where gravity and seismic are counteracting for the various analyses performed are shown in Figure 1-53 through Figure 1-55. These include the fixed-base and flexible-base analysis where the soil springs are elastic and resist tension and the column axial loads for the nonlinear static procedure. From the results the column axial loads are the highest for the fixed-base analysis. It also shows a large net tension demand in the end column which does not materialize in the nonlinear analysis model. The resulting column axial load pattern where the superstructure is elastic and the soil springs act nonlinearly and do not resist tension, shows all the

gravity load to shift in the direction of overturning. Where lateral-force-resisting system of the superstructure is flexible, this pattern is unrealistic.

Figure 1-53 Column axial load, load combination (LC): 0.9*D* + *E* (BSE-2N), fixed base.

Figure 1-54 Column axial load, LC: 0.9*D* + *E* (BSE-2N), soil no tension, k_{sv} = 0.1 kci.

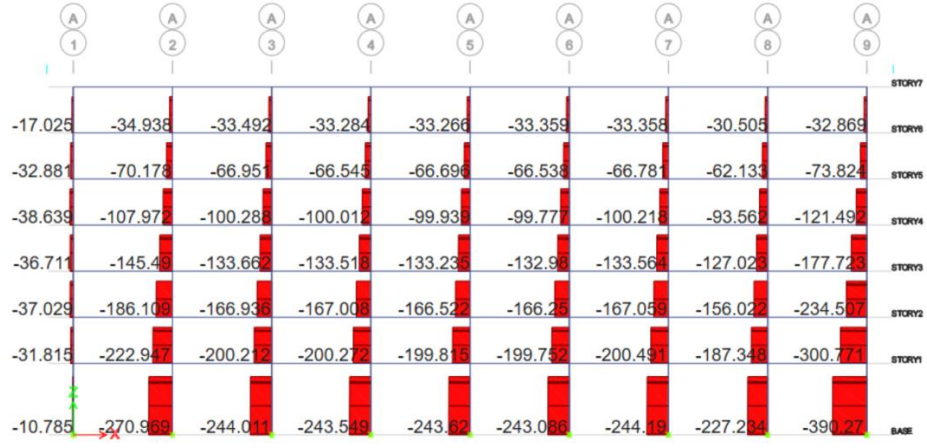

Figure 1-55 Column axial load, LC: 0.9*D* + *E* (BSE-2N), NSP, k_{sv} = 0.1 kci.

Comparison of Superstructure Acceptance Ratios: LSP - Beams

The acceptance ratios between the various cases run for beam negative and positive moments are given in Figure 1-56 through Figure 1-63. Observation of the beam negative and positive acceptance ratios for the different analyses shows very different results compared to baseline ASCE/SEI 7-10 results. Beam acceptance ratios from the fixed-base or flexible-base analysis where soil takes tension seems to give the best approximate pattern with the baseline. Modeling the superstructure as elastic with nonlinear foundation compression-only springs gives a different distribution of acceptance ratios with much higher maximums. Results when compared to the hinge pattern from the NSP shown in Figure 1-64, confirm that modeling the superstructure as elastic with nonlinear compression only springs give inconsistent acceptance ratios for the superstructure elements.

Figure 1-56 Acceptance ratios beam negative moment, ASCE/SEI 7: BSE-1N, fixed base (baseline).

Figure 1-57 Acceptance ratios beam negative moment, ASCE/SEI 41: BSE-2N, fixed base (CP).

Figure 1-58 Acceptance ratios beam negative moment, ASCE/SEI 41: BSE-2N, soil takes tension (CP).

Figure 1-59 Acceptance ratios beam negative moment, ASCE/SEI 41: BSE-2N, soil compression only (CP).

Figure 1-60 Acceptance ratios beam positive moment ASCE/SEI 7: BSE-1N, baseline.

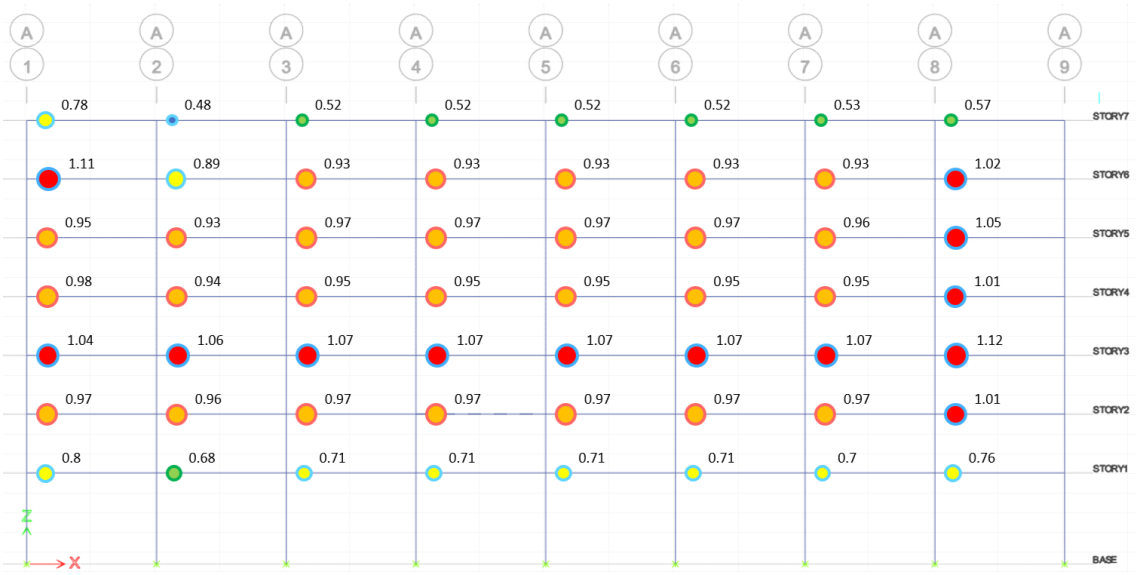

Figure 1-61 Acceptance ratios beam positive moment ASCE/SEI 41: BSE-2N, fixed base (CP).

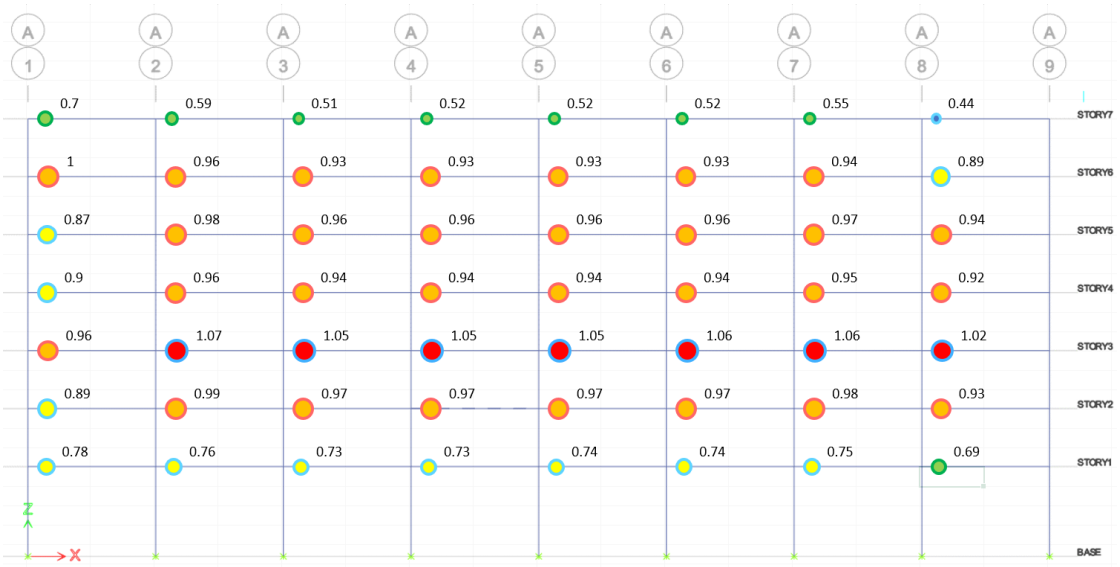

Figure 1-62 Acceptance ratios beam positive moment, ASCE/SEI 41: BSE-2N, soil takes tension (CP).

Figure 1-63 Acceptance ratios beam positive moment, ASCE/SEI 41: BSE-2N, compression only (CP).

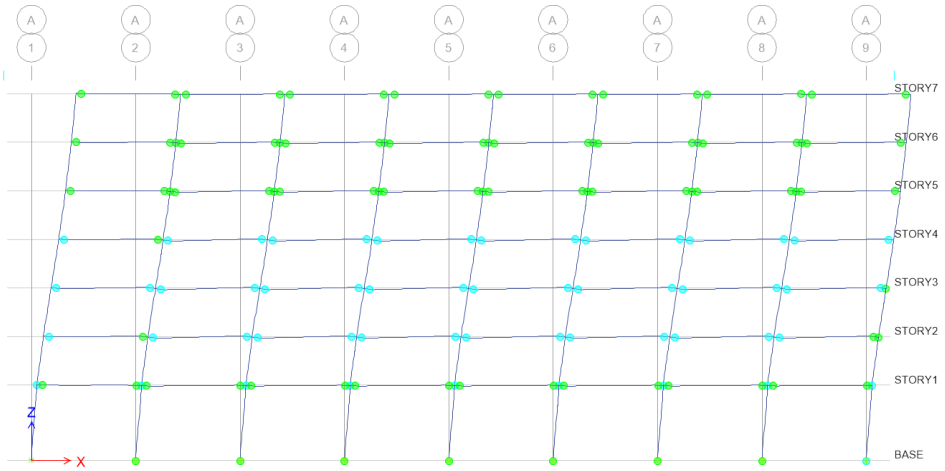

Figure 1-64 Hinge pattern at target displacement, BSE-2N of 32 inches.

Building Displacements (Drifts)

The superstructure displacements at each story for the various models are compared with the displacements from the Nonlinear Static Procedure (NSP) Table 1-8. The displacement demands at each story for the fixed-base and flexible-base where the soil resists tension track well with the superstructure displacements from the nonlinear static procedure. The displacements where soil does not resist tension are at many stories over twice as high as the displacements from the NSP.

Table 1-8 Drift Summary for Various Models – BSE-2N Seismic Hazard Level.

Foundation Fixity & Analysis Type	Spring No Tension k_{sv} =0.1kci (NSP)	Fixed-Base (LSP)	Spring take Tension k_{sv} = 0.05kci (LSP)	Springs take Tension k_{sv} = 0.1 kci (LSP)	Spring No Tension k_{sv}= 0.1 kci (LSP)
Period (sec)	1.626	1.574	1.665	1.626	1.626
Base shear (Kips)	3428	8022	7583	7765	7765
Story	Displacement (in)				
7	32	35.56	36.94	36.36	63.85
6	28.64	31.84	33.21	32.64	57.65
5	24.55	27.04	28.47	27.87	50.37
4	19.68	21.45	22.99	22.34	42.25
3	14.29	15.93	17.56	16.87	34.14
2	8.9	10.58	12.3	11.57	26.05
1	4.26	5.74	7.38	6.69	17.63

Summary

Comparing the results from the various analysis, using the linear static procedure (LSP) with the results from the nonlinear static procedure (NSP), shows that when the elements of the superstructure are ductile relative to the foundation system, combining results from a linear superstructure with a nonlinear foundation can give incorrect results and overestimate the demands in the superstructure and foundation elements. For this reason, for LSP, modeling the foundations as nonlinear uplifting springs is not recommended. Results from the LSP with all elements modeled as elastic and the NSP gave reasonable correlation with the baseline ASCE/SEI 7-10 analysis model.

1.3.9.2 CONCLUSIONS

Observations from the case studies for both archetype buildings show that modeling the foundations as nonlinear compression-only springs combined with an elastic superstructure results in superstructure force distributions that are unrealistic and may be too conservative when overturning demands are high. For low-magnitude earthquakes where the superstructure is likely to remain essentially elastic, the results are more reasonable. It is therefore permitted to model the foundation supports as nonlinear compression-only springs for linear analysis flexible-base procedures when the likelihood of the superstructure elements to remain elastic is high, or the maximum DCRs as defined in ASCE/SEI 41-17 are below 1.5.

1.3.10 Acceptance Criteria Check for the Structural Footing

There is currently no specific requirement or acceptance criteria for checking the structural footing in ASCE/SEI 41 Chapter 8. A new requirement for evaluation of the structural footing for rocking action is added which adopts a capacity-based approach. Internal forces in the footing are determined based on the application of the expected soil bearing capacity, without the increase for short-term loading, by a rectangular compression block at the end of the rocking footing equal to the axial load P_{UF} on the footing, as shown in Figure 1-65. Component actions on the structural foundation are then evaluated depending on whether the action is force-controlled or deformation-controlled, using these demands in accordance with the appropriate material chapters.

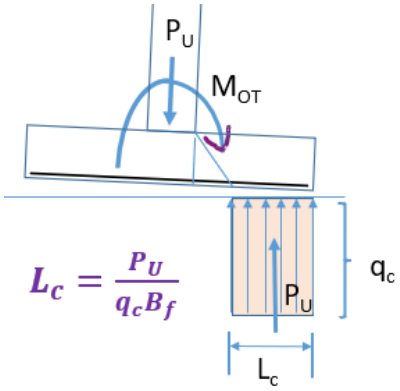

Figure 1-65 Soil pressure distribution under the footing used for evaluating the footing strength.

If the structural footing does not have adequate strength to provide overturning for the component actions in the structure, foundation strengthening of the footing is required or the footing may be further evaluated based on the actual demands and soil pressure distribution under the footing, adjusted by the *m*-factor for the required performance objective.

The shear and moment demand on the footing may be further evaluated such that the acceptance criteria for soil bearing is still satisfied. This is illustrated below for rectangular footings, where the footing should be evaluated considering following cases as applicable:

1.3.10.1 CASE 1: UNIFORM OR TRAPEZOIDAL DISTRIBUTION OF SOIL PRESSURE

This condition is applicable when the soil pressure, *q,* distribution under the footing (as shown in Figure 1-66) along the length from Q_{max} to Q_{min} satisfies the requirement that no portion of the soil is in tension. In other words, $Q_{min} > 0$ and $Q_{max} < q_{cDA}$. Foundation demands on the structural foundation are evaluated at the critical section for moment and shear as deformation-controlled or force-controlled actions respectively for concrete footings. Additional examples for determining the foundation demands are documented in Part 3, Appendix C, which can be found at http://femap2208.atcouncil.org/.

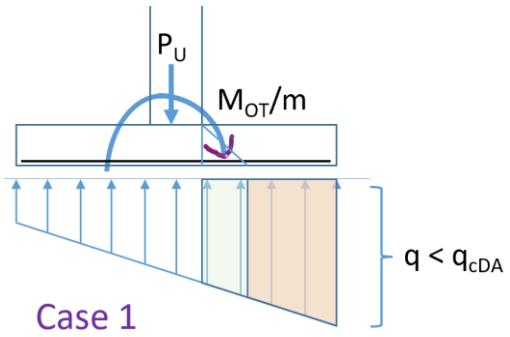

Figure 1-66 Soil pressure distribution under the footing is trapezoidal.

$0 \le q < q_{cDA}$, where:

$$Q_{max/min} = \frac{P_U}{A_f}\left(1 \pm \frac{6e_{AC}}{L_f}\right)$$

and when:

$e_{AC} = M_{CE}/P_U \le L_f/6$

1.3.10.2 CASE 2: TRIANGULAR DISTRIBUTION OF SOIL PRESSURE

This condition is applicable when the soil pressure, *q,* distributed under the footing (as shown in Figure 1-67) along the length goes from Q_{max} to zero and satisfies the requirement that $Q_{max} < q_{cDA}$. Foundation demands and acceptance criteria are determined similar to Case 1.

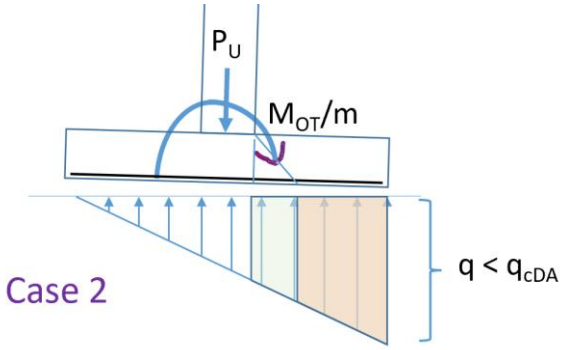

Figure 1-67 Soil pressure distribution under the footing is triangular.

$0 \le q < q_{cDA}$, where:

$$Q_{max} = \frac{2P_U}{3B_f\left(L_f/2 - e_{AC}\right)}$$

and when:

$L_f/6 \le e_{AC} \le L_f/2$

$Q_{min} = 0$ at $L' = 3(L_f/2 - e_{AC}) \le L_f$

1.3.10.3 CASE 3: RECTANGULAR AND TRIANGULAR DISTRIBUTION OF SOIL PRESSURE

This condition may be used if the soil pressure distribution of the seismic demands are not satisfied using either Case 1 or Case 2 (Figure 1-68).

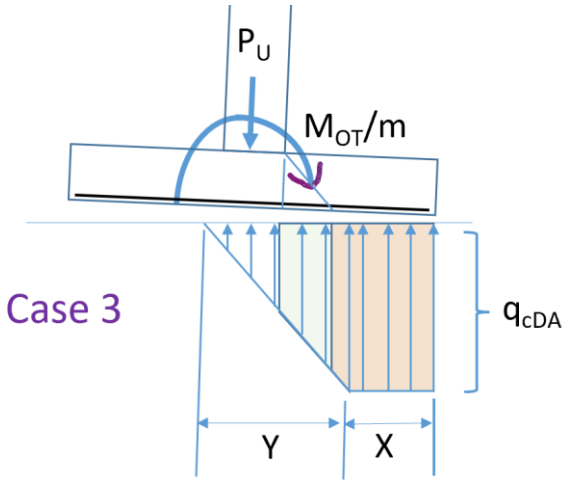

Figure 1-68 Soil pressure distribution under the footing is a rectangle and a triangle.

A rectangular distribution of soil pressure with $q = q_{cDA}$ is be applied over an area for a distance X from the footing end towards the neutral axis, followed by a triangular distribution over a distance Y with $q_{cDA} \ge q \ge 0$, where:

$$X = \frac{P_U}{q_{cDA} B_f} - \frac{1}{2} Y$$

$$Y = \sqrt{12\left(P' L_f - 2M' - P'^2\right)} > 0$$

and

$X + Y < L_f$

where:

$$P' = \frac{P_U}{q_{cDA} B_f}$$

and

$$M' = \frac{\left(M_{OT}/m\right)}{q_{cDA}B_f}$$

Derivation of the equations for the determination of dimensions *X* and *Y* above is given in Part 3, Appendix A, which can be found at http://femap2208.atcouncil.org/. However, it should be cautioned that, since this proposal recommends use of q_c at the soil pressure, this option may not give a more favorable result.

1.3.10.4 CONCLUSIONS

This added provision identifies the need that foundation acceptance includes a check on the foundation structural component, as well as on soil bearing. A simple capacity-based approach is provided by which the strength of an isolated footing may be evaluated. Alternative solutions account for the demand reduction in soil pressure as a function of the target performance level. This approach accounts for the fact that foundation demands may be reduced by superstructure yielding for lower target performance levels.

1.3.11 Bounding Requirements for Nonlinear Procedures

Earlier versions of ASCE/SEI 41 required bounding on soil strength and stiffness to be considered when soil properties were explicitly modeled. Case studies for Archetype Building 1 (Flat slab reinforced concrete moment frame building retrofit with reinforced concrete shear walls), and Archetype Building 2 (Special reinforced concrete moment frame building), have shown that modeling using the upper- and lower-bound stiffness values do not have appreciable effects on the superstructure demands. However, variations in strength could have a significant impact on the outcome, and the conservatism in the design to account for the uncertainty in the properties of the soil is already built-in with factors of safety of around three traditionally used in the estimation of the soil bearing capacity. While there is a lot of uncertainty in the soil properties, the halving and doubling of the strength and stiffness did not account for actual designs where the factors of safety are already accommodated in the design for strength, and consolidation over time accounts for additional stiffness gain not accounted for in the bounding provisions.

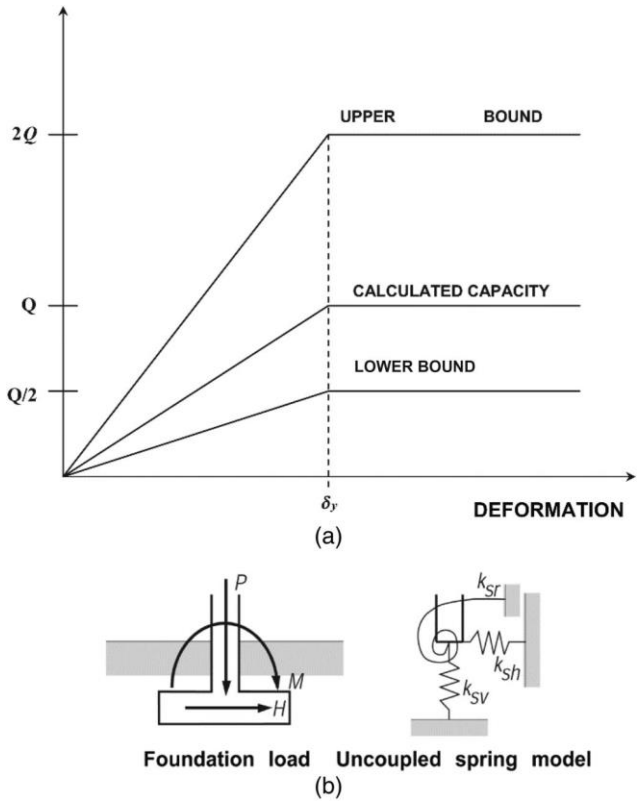

Figure 1-69 Figure 8-1 in ASCE/SEI 41-17, bounding requirements when soil supports are explicitly modeled.

The requirement for bounding has been proposed to be removed in ASCE/SEI 41-23 for strength and stiffness for the following reasons:

1.3.11.1 BOUNDING ON STRENGTH

Geotechnical engineers generally provided recommendations using a lower-bound strength to account for the uncertainty in soil properties. For sands the allowable values were based on minimizing settlement, and there is additional strength before soil failure occurs. For clays, the ultimate strength is lower; however, there is a difference between immediate settlement and long-term settlement. Consolidated soils have higher strength than unconsolidated soil. In addition, soils have been shown to exhibit an increased bearing capacity at failure when subjected to sort-term earthquake loads of about one-and-a-half to two times the static values.

The provisions already adjust the initial stiffness to a degraded stiffness as a function of the seismic ground shaking intensity. This adjustment is equivalent to starting from a lower-bound strength for the soil. Having bounding on top of that, with a difference between the upper- and lower-bound soil strengths differing by a factor of four, appears unjustified as this initial reduction is not considered in the current bounding provisions. The lower-bound strength does not account for the dynamic increase in soil bearing capacity and further cuts into an already conservative factor of safety. This

reduction due to bounding on strength could indicate a potential soil bearing capacity failure, requiring unnecessary foundation retrofit.

For linear procedures using fixed-base or flexible-base assumptions, upper-bound values are already permitted. This implies there is a different set of rules for linear versus nonlinear procedures for soil strength. The case study results from Archetype Building 1 justify the use of upper-bound soil strengths.

Findings Archetype Building 1: Investigation of Soil Bearing Capacity Bounding

Methodology

Strength bounding was investigated to determine its effect on overturning moment capacity acceptance ratios for the retrofit footing designed using ASCE/SEI 7-10. Current ASCE/SEI 41-17 provisions permit the use of upper-bound bearing capacity for both fixed-base (ASCE/SEI 41-17 Section 8.4.2.3.2.1) and flexible-base (ASCE/SEI 41-17 Section 8.4.2.3.2.2) procedures. Table 1-9 and Table 1-10 summarize the results of utilizing upper- and lower-bound bearing capacity when calculating overturning moment capacity.

The *m*-factors in ASCE/SEI 41-17 Table 8-3 were calibrated for rocking behavior to get allowable rotation demand, $q_{allowable}$, considering gradual accumulation of settlement with the number of cycles as a localized bearing failure converted to *m*-factors through $m \sim (q_{allowable} \times K50) / M_{capacity}$. The actual magnitude of the elastic stiffness of the springs is determined iteratively using a monotonic pushover analysis, so that the secant rotational stiffness of the foundation corresponding to 50% mobilization of the foundation moment capacity, M_{cf}, is equal to $300M_{cf}$ (Deng et al., 2014) as an expected stiffness. The secant rotational upper bound stiffness is approximately 550 M_{cf}. The *m*-factors given in ASCE/SEI 41-17 Table 8-3 vary as a function of the A_c/A and b/L_c ratios which result in low *m*-factors using the lower bound soil bearing capacity as these ratios are higher. Thus, the difference in *m*-values used in Table 1-9 and 1-10 using upper bound and lower bound soil bearing capacities.

Figure 1-70 provides an example calculation for the LSP fixed-base utilizing upper-bound bearing capacity.

P_{UD} =	1660	kips
q =	2.71	ksf
qc =	21.0	ksf, upper-bound
A_f =	612	ft^2
L_f =	70.5	ft
M_{CE} =	50,948	k-ft
M_{base} =	269,427	k-ft (ETABS)
required m =	**5.3**	
allowable m =	4.0	Section 8.4.2.3.2.1
Acceptance ratio =	1.32	

Figure 1-70 Example moment capacity calculation.

Results Summary

The use of upper-bound soil bearing strength for fixed-base analysis provides reasonable results compared to ASCE/SEI 7-10 with an acceptance ratio relatively close to 1.0 as shown in Table 1-9. The use of lower-bound soil bearing strength does not provide acceptable results for flexible-base analyses, with acceptance ratios greater than 1 for the LSP—Method 1, using both upper or lower bound spring stiffness properties as shown in Table 1-10. Results using lower bound strength properties are shown for illustrative purposes. For linear procedures, ASCE/SEI 41-17, Section 8.4.2.3.2.2 permits use of upper bound values for soil strength when the foundation interface is modeled as flexible.

Table 1-9 Summary of Moment Capacity and Acceptance Ratio Using Upper Bound Soil Bearing Capacity

Model	P_{UD} (kip)	q (ksf)	M_{base} (k-ft)	Upper Bound Strength				
				q_c (ksf)	M_{CE} Upper (k-ft)	Required *m*	Allowable *m*	Acceptance Ratio
LSP - Fixed Base	1,660	2.71	269,427	21.0	50,948	5.29	4.0	1.32
LSP - Method 1 Lower Bound (Rigid Footing)	1,586	2.59	177,978	21.0	49,002	3.63	6.0	0.61
LSP - Method 1 Upper Bound (Rigid Footing)	1,611	2.63	224,538	21.0	49,672	4.52	6.0	0.75
LSP - K_{50} 300$M_{c,foot}$ (Rigid Footing)	1,586	2.59	111,809	21.0	49,003	2.28	6.0	0.38
LSP - K_{50} 550$M_{c,foot}$ (Rigid Footing)	1,586	2.59	146,138	21.0	49,002	2.98	6.0	0.50

Table 1-10 Summary of Moment Capacity and Acceptance Ratio Using Lower Bound Soil Bearing Capacity

Model	P_{UD} (kip)	q (ksf)	M_{base} (k-ft)	Lower Bound Strength				
				q_c (ksf)	M_{CE} Lower (k-ft)	Required m	Allowable m	Acceptance Ratio
LSP - Fixed Base	1,660	2.71	269,427	5.25	28,284	9.53	4.0	2.38
LSP - Method 1 Lower Bound (Rigid Footing)	1,586	2.59	177,978	5.25	28,310	6.29	2.1	3.05
LSP - Method 1 Upper Bound (Rigid Footing)	1,611	2.63	224,538	5.25	28,314	7.93	2.0	3.97
LSP - K_{50} 300$M_{c,foot}$ (Rigid Footing)	1,586	2.59	111,809	5.25	28,310	3.95	2.1	1.92
LSP - K_{50} 550$M_{c,foot}$ (Rigid Footing)	1,586	2.59	146,138	5.25	28,310	5.16	2.1	2.51

Conclusions

For the fixed-base analysis procedure, the use of upper-bound soil bearing strength provides reasonable results compared to ASCE/SEI 7-10. If the expected or lower-bound soil bearing strength were to be used instead, the *m*-factor would have to be increased to provide comparable results. Note that if the *m*-factors for the fixed-base procedures are increased, they could become equal to or greater than the *m*-factors used for the flexible-base procedure (ASCE/SEI 41-17 Table 8-3), which is counterintuitive to the general concept that the fixed-base procedure should provide a more conservative design. Therefore, we suggest that the soil bearing strength equivalent to the upper-bound strength continue to be used for the fixed-base procedure, in which case the terminology will be revised to specify the use of the expected soil bearing strength with a factor of 2 to account for transient, seismic loading effects.

Lower-bound soil bearing strengths do not provide acceptable results for the flexible-base procedure. In any case, design of the structural foundation should be performed with the expected bearing capacity.

1.3.11.2 BOUNDING ON STIFFNESS

Soil stiffness values as used in the standard are already reduced for site class when the G/G_0 ratio is applied. These values represent the secant stiffness for fully degraded soil at higher ground shaking magnitudes for Site Class D and higher. Therefore, the stiffness values are low to begin with and

using and additional factor of 2 would lead to excessive superstructure deformations, again resulting in unnecessary costly retrofits beyond the intended performance level of the building for the specified hazard.

Lower-bound stiffness for elastic analysis for flexible-base is used to counteract the fact that gapping is prevented, in other words, when soil resists tension. For the condition where the soil does not resist tension, the rotation value is in line with the values in Table 8-4 of ASCE/SEI 41-17 when soil does not get too soft. For higher values of S_{DS}, for Site Class D or E from Table 8-2 of ASCE/SEI 41-17, the G/G_0 ratios appear to be too small already. Case studies for Archetype Building 2, have shown that buildings on reasonably firm sites the presence or absence of modeling the flexibility of the soil does not have a big impact on the superstructure deformations.

Findings Archetype Building 2: Investigation of Soil Stiffness Bounding

Parametric studies were performed on Archetype Building 2, the Special Reinforced Concrete Moment Frame building, designed to the requirements of ASCE/SEI 7-10 with an *R* of 8. Several base fixities were considered in the study, including the modeling of the foundation system as a fixed-base and flexible-base using both upper-bound (UB) and lower-bound (LB) soil stiffness values. For the linear elastic procedure, the soil and superstructure were modeled as elastic, in other words the soil resists tension. For the analysis using the nonlinear elastic procedure, nonlinearity was permitted at the soil foundation interface, in other words the soil supports were compression-only springs. The results from the study for each element of the superstructure, are presented in Figure 1-71 through Figure 1-74 starting with the top story on the left and the bottom story on the right. The loading for each case was for demands applied in the positive x-direction, the longitudinal direction of the building. Observation of the column axial loads at the bottom story shown in Figure 1-72, shows that the higher axial load demands from the column to foundation correspond to the fixed-base analysis. Foundation demands from the columns are a minimum when lower-bound spring stiffness are used.

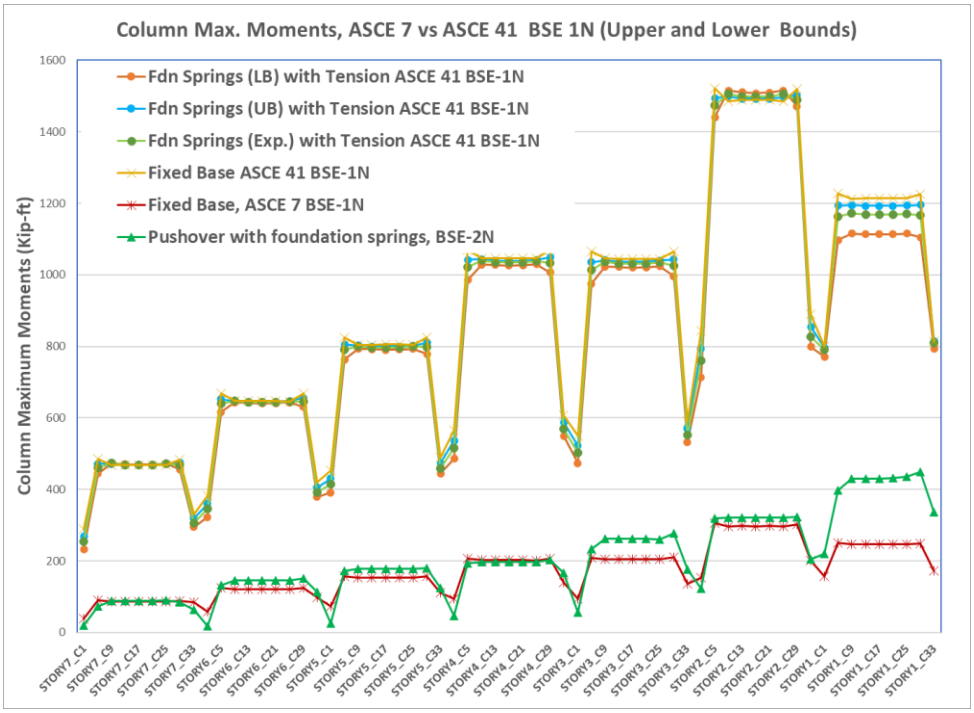

Figure 1-71 Column moments per story from left to right, starting with top story on the left to bottom story on the right.

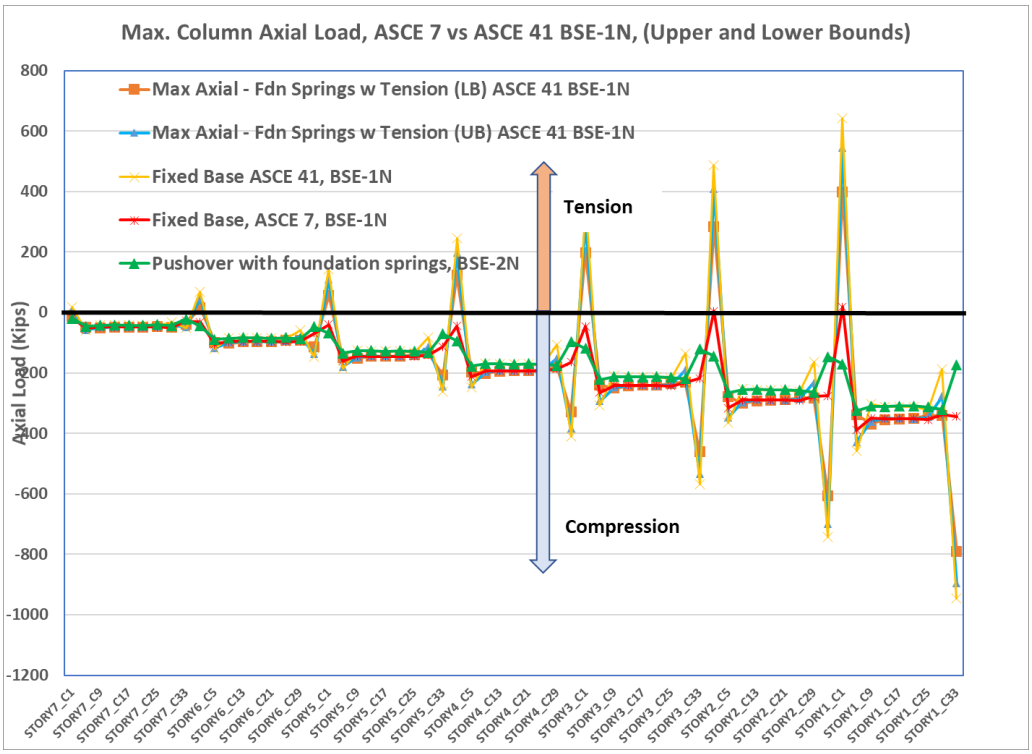

Figure 1-72 Column axial load per story from left to right, starting with top story on the left to bottom story on the right.

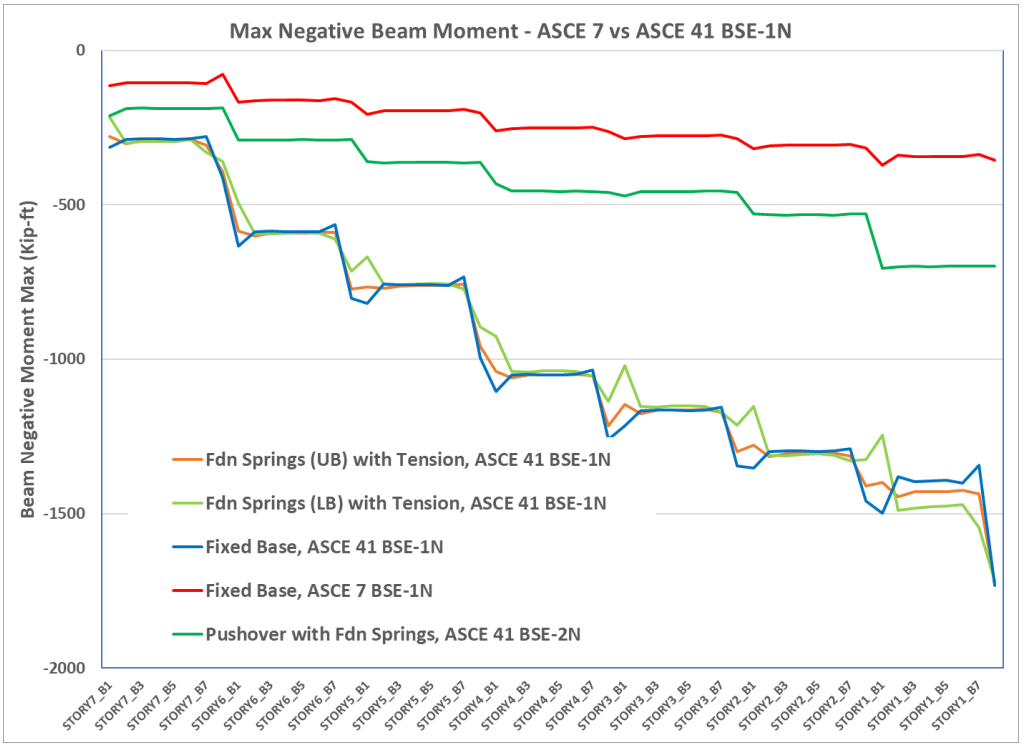

Figure 1-73 Beam negative moments per story from left to right.

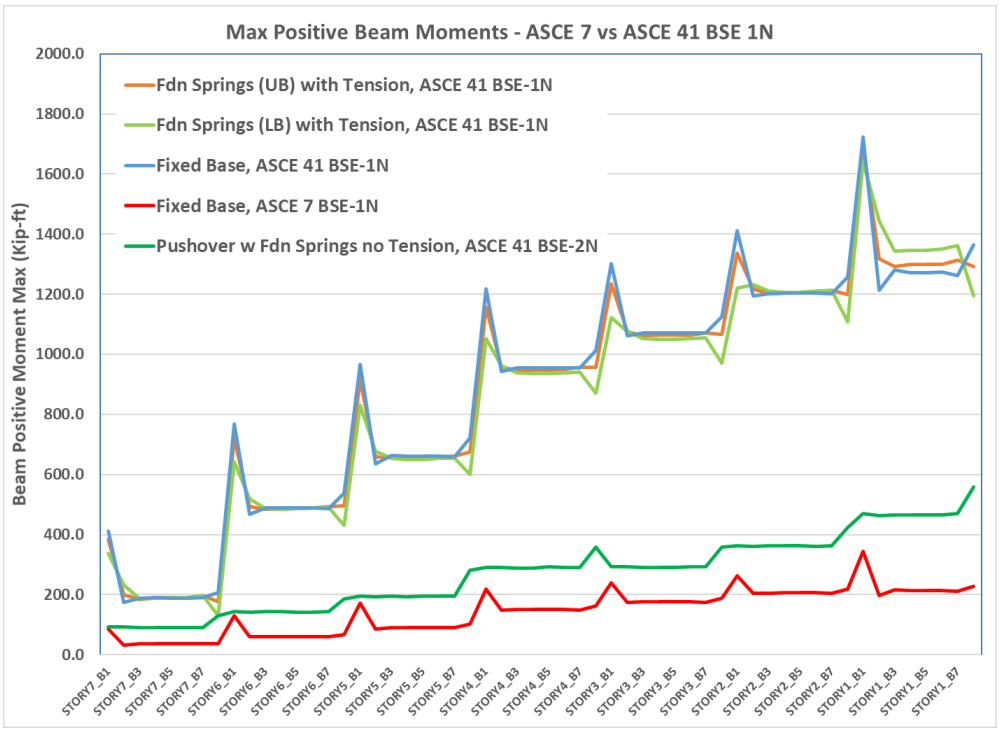

Figure 1-74 Beam positive moments for the various analysis cases.

1.3.11.3 CONCLUSIONS

It is well recognized that soils supporting foundations have a high degree of uncertainty in their estimation. To account for this, traditionally geotechnical engineers provided conservative allowable bearing values to limit short-term and long-term foundation settlement. This conservatism resulted in a minimum factor of safety of 3. The requirements for bounding in ASCE 41-17 and earlier versions of the standard did not consider this fact when the bounding provisions were introduced. The halving and doubling of the soil strength and stiffness when foundations are explicitly modeled results in soil strengths and stiffnesses well below their actual soil bearing capacity or stiffness values. This also does not account for consolidation over time for clayey soils. Sandy soils inherently have higher strength and stiffness values, and soil bearing values are typically based on settlement, not on strength. Using these low values for strength could potentially translate to very conservative designs and require superstructure or foundation retrofit that may not be necessary to achieve the selected performance objective for the building. The case study results also showed minimal variation in superstructure response when the bounding provisions are applied to soil stiffness values for linear analysis procedures. It should be noted that the provisions require the elastic stiffness to be modified by the G/G_0 ratio, which accounts for a fully degraded sub-medium based on the magnitude of the shaking. It was therefore decided that a further reduction on stiffness was not required. There is a potential un-conservativeness introduced with the elimination of the upper-bound stiffness, but the impact on the expected target performance of the building with the elimination of bounding is expected to be minimal.

1.4 Recommended Changes

Note about Change Proposals

This report documents aspects of change proposals as they were submitted to subcommittees of ASCE's *Seismic Retrofit of Existing Building Standards* Committee. Often, these change proposals were revised, in some cases substantively, by these subcommittees before they were adopted into ASCE/SEI 41-23. Readers should not rely on this report for information about the final version of provisions in ASCE/SEI 41-23.

1.4.1 Application of Evaluation Provisions for Shallow Foundations

Working Group 2 recommends adding a new section to ASCE/SEI 41-23 for buildings on shallow foundations for when a fixed-base or flexible-base procedure can be used for evaluation of the building. Guidance is based on the building type, configuration, foundation system, and site characteristics. Site characteristics include whether the site is flat or sloping and the level of seismicity. The proposed language is given below. New or modified text is shown in blue.

8.4.1 Application of Evaluation Procedures

Buildings shall not be permitted to be evaluated as a fixed base when prohibited by Section 8.4.1.2 and the requirements given in Section 8.4.1.1 items 1 through 3 do not apply.

8.4.1.1 Fixed Base Procedure Permitted

The fixed base procedure shall be permitted for any of the following conditions:

(1) Buildings where the Level of Seismicity is defined as Very Low, Low, or Moderate in accordance with Section 2.5.

(2) Buildings where the seismic-force-resisting system consists only of light-frame wood or cold-formed steel construction.

(3) Buildings where the seismic-force-resisting system consists only of unreinforced masonry construction.

The fixed base procedure shall also be permitted where the building, foundation, or the analysis satisfies one of the following requirements:

(4) Building in which the secondary elements are assigned *m*-factors less than 3, shall have these secondary elements evaluated using the *m*-factors as primary components.

(5) Buildings with a full basement having a complete system of perimeter basement walls that are at least 8 feet tall.

(6) The foundation consists of interconnected footings where the foundation elements are included in the model without fixed flexural deformation restraints and the soil resistance is idealized as a single vertical pin support (free to rotate) under the gravity columns or single shear walls.

8.4.1.2 Fixed Base Procedure Not Permitted

The fixed base procedure shall not be used where any of the following conditions exist, unless the foundation satisfies the additional requirements of this section:

(1) Buildings with mixed deep and shallow foundation systems where the base shear resisted by either the shallow or deep foundation elements is greater than 20%, but less than 80%, of the total base shear.

Exception: Shallow foundation buildings where deep foundation elements are added as part of a retrofit solely for the purpose of increasing overturning resistance.

(2) Buildings where the elevation difference between the bottom of individual footings that support elements of the seismic-force-resisting system is greater than or equal to the typical story height.

Exception: Where this condition occurs, the fixed base procedure shall be permitted where the following conditions apply:

a. Building where gravity loads to the footings at the lower elevation are less than 15% of the total weight of the building.

b. Stepped foundations with a level, top of foundation wall.

(3) Multistory buildings where the seismic-force-resisting system consists of cantilever shear walls or braced frames that have different heights.

> **Exception**: Where this condition occurs, the fixed base procedure shall be permitted where the following conditions apply:
>
> a. The walls or braced frames with heights less than the average height of the walls or braces in the building, resist less than 25% of the base shear of the building.
>
> b. The governing foundation DCR of all walls or braced frames with heights less than the average height of the walls or braced frames that resists more than 10% of the total base shear exceeds the governing superstructure DCR of that wall or braced frame.

This section replaces the requirement in ASCE/SEI 41-17 where fixed base procedures are not permitted when the superstructure is sensitive to base rotations when evaluated at the immediate occupancy level. The following clause is deleted:

> ~~A fixed-base assumption shall not be used for buildings being evaluated or retrofitted to the Immediate Occupancy Performance Level that are sensitive to base rotations or other types of foundation movement that would cause the structural components to exceed their acceptance criteria.~~

1.4.2 Expected Soil Bearing Capacity

This section describes recommended changes to ASCE/SEI 41-17 Section 8.4.1.1, Prescriptive Expected Capacities. Existing provisions for prescriptive soil bearing capacity when information on the soil properties is not available, either in the construction documents or in a geotechnical report, were deemed too conservative and inconsistent with the prescriptive bearing capacities when soil bearing values are available. Item 3 in ASCE/SEI 41-17 Section 8.4.1.1 is a proposed deletion and is replaced with revised recommendations where geotechnical information necessary to evaluate the foundation is not available. In addition, a new term q_{cDA} is defined to represent the short-term bearing capacity resistance to dynamic loading such as earthquakes. The proposed language is shown below.

8.4.2 Expected Soil Bearing Capacities

…

(1) The prescriptive expected bearing capacity, q_c, for a spread footing shall be calculated using Eq. (8-7):

$$q_c = 3q_{allow} \quad (8\text{-}7)$$

where q_{allow} = allowable long-term bearing pressure specified in available documents for the dead load including self-weight of the footing plus design live load;

(2) Where geotechnical reports are not available and soil bearing capacity is not included in available construction documents, the prescriptive expected capacity, q_c of any foundation is permitted to be calculated using Eq. (8-8):

$$q_c = 2.5(D + 0.4L)/A_f \quad (8\text{-}8)$$

where:

D = Calculated dead load including self-weight of the footing;

L = the unreduced live load from the original construction period, and

A_f = area of the footing.

Prescriptive expected bearing capacities q_c shall be permitted to be multiplied by a seismic amplification factor for short-duration seismic loading and are represented by the symbol q_{cDA} using Eq. 8-9:

$$q_{cDA} = 2.0q_c \quad (8\text{-}9)$$

Exception:

Where the expected bearing capacity for short-duration seismic loading q_{cDA} is provided by the geotechnical engineer in an approved report, and includes the effects of seismic loading, no additional increase shall be permitted.

1.4.3 Seismic Overturning Forming Axial Load Action

Working Group 2 recommends adding a new section in ASCE/SEI 41-23 for evaluating foundations where the overturning is resisted primarily by axial load action on the footing. This includes changes to how the acceptance criteria is calculated for axial compression of uplift on the footing. New *m*-factors for foundation axial compression failure are proposed. Currently acceptance criteria are only addressed for overturning rocking action (ASCE/SEI 41-17 Section 8.4.2.3). However, there are many foundation conditions where the overturning action is resisted by coupled action, tension, and compression. Adding this new section addresses the gap in the existing provisions. The recommended change is given below.

8.4.4.1.1.2 Seismic Overturning Resisted by Axial Load Action

For foundations where seismic overturning is resisted by axial compression and tension action and when Eq. (8-15) is satisfied, the requirements of this section shall apply.

$$M_E < 0.2\ mM_{CE} \quad (8\text{-}15)$$

where,

M_E = The moment demand on the footing determined from Eq. (7-34)

M_{CE} = The moment capacity of the footing, determined using $P_{UF} = P_G$, and

m = The value from Table 8-2b

For load combinations where the seismic axial demands on the foundation are additive to gravity, acceptance criteria for soil bearing shall be evaluated using the axial compression m-factor from Table 8-2a and satisfy Eq. (8-16).

$$P_{UF} \leq mkq_{cDA}A_f \quad (8\text{-}16)$$

The structural footing shall be evaluated as force controlled using a uniform soil pressure distribution under the footing with axial load demand P_{UF} from Eq. (8-12), or by substituting the DCR_m in Eq. (8-12) with the m-factor in Table 8.2a.

For load combinations where the seismic axial demands on the foundation subtract from gravity, and the axial load demand P_{UF}, is less than zero the foundation shall be evaluated using the uplift *m*-factor from Table 8-2a and satisfy Equation 8-17. If this condition is not satisfied, a fixed base procedure cannot be used.

$$P_E \leq mP_G \quad (8\text{-}17)$$

where:

P_G = Action caused by gravity load at the soil footing interface determined using Eq. (7-2) and includes the weight of the footing.

P_E = The axial demand on the footing determined from Eq. (7-34)

Table 8-2a m-factors for Overturning from Axial Action

Action	Performance Level		
	IO	LS	CP
Axial Compression	1.25	2	2.5
Axial Uplift	4	6	8

1.4.4 Foundation Moment Capacity with Bi-directional Overturning Action

This section describes recommended changes to ASCE/SEI 41-17 Section 8.4.2.3 by adding new provisions for determining foundation overturning capacity where the footing is non-rectangular and for bi-directional moments on the footing. Currently in the standard, overturning acceptance is addressed simplistically only for unidirectional moment for a rectangular or I-shaped footing. A new methodology is outlined in the proposed commentary for evaluating foundations where the footing is

required to resist overturning moments simultaneously about the two horizontal principal axes of the footing. This methodology is applicable to isolated footings of any plan geometry. The recommended change is given below:

8.4.4.1.1.1 Foundation Overturning Capacity

For isolated footings (rectangular, I shaped or nonrectangular footings), the overturning moment capacity, M_{CE} shall be obtained using the procedures specified in this section. The overturning moment capacity, M_{CE} is obtained by determining the critical contact area, A_c, and integrating the product of the bearing capacity times the distance from the centroid-of the footing over the critical contact area. The critical contact area, A_c, defined as the footing area required to support the expected vertical load and shall be calculated using Eq. (8-11) as:

$$A_c = P_{UF}/q_{cDA} \quad (8\text{-}11)$$

Where the expected vertical load on the soil at the footing interface P_{UF} is the maximum action that can be developed by gravity and seismic loads based on a limit-state analysis considering the expected strength of the components delivering force to the footing; alternatively, the expected vertical load is permitted to be determined using Eq. 8-12.

$$P_{UF} = P_G \pm P_E/DCR_m \quad (8\text{-}12)$$

where:

q_{cDA} = Bearing capacity determined in Section 8.4.1.

P_G = Gravity load at the soil footing interface determined using Eq. 7-1 which includes the footing weight.

DCR_m = Maximum demand–capacity ratio *of the elements of the lateral force resisting system in the direct load path of the footing being evaluated contributing to the seismic axial load* as defined in Section 7.3.1.1, which need not be taken as less than C_1C_2 and shall not be taken as greater than $3C_1C_2$; where C_1 and C_2 are as defined in Section 7.4.1.3.1.

P_E = Q_E *as defined in* Eq. (7-34).

For rectangular footings, for rocking about a principal axis, the moment capacity M_{CE} shall be determined using Eq. (8-13)

$$M_{CE} = (L_f P_{UD}/2)(1 - q/q_{cDA}) \quad (8\text{-}13)$$

where:

$q = P_{UD}/(B_f L_f)$ = vertical bearing pressure;

B_f = width of footing (parallel to the axis of rocking);

L_f = length of footing in the direction perpendicular to the axis of rocking;

The moment capacity for all other cases is determined using Eq. (8-14).

$$M_{CE} \sqrt{\left(\frac{M_{OT,x}}{m}\right)^2 + \left(M_{CE,y}\right)^2} \quad (8\text{-}14)$$

where:

$M_{CE,y}$ = Moment capacity of the foundation in the y- direction (see Figure 8-2 for axis direction), determined from the critical contact area A_c that corresponds to the axial load P_{UF} and moment $M_{OT,x}/m$ acting simultaneously on the footing.

$M_{OT,x}$ = Component of applied moment determined using Eq. (7-34) in the x- direction or minor axis of overturning.

m = m-factor from Table 8.2b for the required performance objective.

...

8.4.4.4.1.1.3 Seismic Overturning Resisted by Axial and Moment Action

Foundation overturning action, not satisfying the requirements of Section 8.4.4.1.1.1, shall satisfy the requirements of this section. The overturning demand $Q_{UD} = M_{OT}$ shall be determined using Eq. (7-34).

8.4.4.1.1.3.1 Acceptance Criteria for Soil Bearing and Overturning

Where the overturning moment demand M_{OT} results in concurrent loading in the x- and y-direction, such that $M_{OT,x}$ and $M_{OT,y}$ are both independently divided by the m-factor in Table 8-2b exceeds 20% of the unidirectional moment capacity determined using Eq. (8-12) in each direction, bi-directional effects shall be considered. M_{OT} is represented as the square root of the sum of the squares of the pseudo force moment demand along two orthogonal axes x, and y.

$$M_{OT} = \sqrt{M_{OT,x}^2 + M_{OT,y}^2} \quad (8\text{-}18)$$

Where seismic axial loads are additive to gravity, acceptance criteria for soil bearing shall satisfy the requirements of Eq. (8-19) or Eq. (8-20) using the moment/rotation m-factor values from Table 8-2b. For overturning demands where the seismic axial load subtracts from gravity, the moment capacity shall be determined using P_G, defined in Section 8.4.2.1.1 as the axial load on the footing.

$$M_{OT} = \sqrt{\left(\frac{M_{OT,x}}{mkM_{CE,x}}\right)^2 + \left(\frac{M_{OT,y}}{mkM_{CE,y}}\right)^2} \le 1.0 \quad (8\text{-}19)$$

$$M_{OT} \le mkM_{CE} \quad (8\text{-}20)$$

Table 8-2b m-factors(1) for Overturning Moment Action

Action	Performance Level		
	IO	LS	CP
Moment/Rotation	2	3	4

Where $A_c/A_f > 0.4$, the m-factors from Table 8-3 shall be used.

Table 8-3. Modeling Parameters and Numerical Acceptance Criteria for Linear Procedures

	m-Factors[a]		
	Performance Level		
Footing Shape	IO	LS	CP
i. Rectangle			

b/L_c	$(A_{rect}-A_f)/A_{rect}$	A_c/A_f			
≥ 10	0	0.20	5	8	10
		0.5	3	5	6
		1	1	1	1
3	0	0.20	4	6	8
		0.5	2	3	4
		1	1	1	1
0.3	0	0.20	2	4	5
		0.5	1	1.5	2
		1	1	1	1
ii. I-Shape					
b/L_c	$(A_{rect}-A_f)/A_{rect}$	A_c/A_f			
$1 \le b/L_c \le 10$	0.3	0.20	3	5	7
		0.5	1.5	2.5	3.5
		1	1	1	1
$1 \le b/L_c \le 10$	0.6	0.20	2.5	4.5	5.5
		0.5	1	2	2
		1	1	1	1
$1 \le b/L_c \le 10$	1	0.20	2	3.5	4.5
		0.5	1	1.5	1.5
		1	1	1	1

[a] Linear interpolation between values listed in the table shall be permitted.

1.4.5 Determination of Soil Stiffness for Mat Foundations

A new section is proposed in ASCE/SEI 41-23 that provides guidance on determining the minimum width of a large mat foundation when extrapolating the soil stiffness obtained from ASCE/SEI 41-17 Figure 8-2 or ASCE/SEI 41-17 Equation 8-11. Four different rational methods are proposed using judgment. These are based on the actual loaded area immediately below the vertical elements supported by the mat and considering that settlement and consolidation of the soil would have already occurred prior to a large seismic event. Therefore, only elements resisting large overturning demands would see increased axial forces. These additional forces would dissipate within a finite area under the mat in the vicinity of the applied additional load. The proposed change language is given below:

8.4.4.1.2 Combined Footings and Mat Foundations

…

When the entire building or portion thereof is supported by a mat foundation, over multiple bays, the modulus of subgrade reaction shall be based on one of the following:

(1) The effective width B'_f used to determine the spring stiffness from Section 8.4.5.1 shall be zoned to coincide with the column grid lines and is permitted to be limited by the typical bay width. Widths for end bays shall extend from the edge of the footing to half the distance between the vertical elements at the perimeter of the building to the vertical elements of the first interior bay.

(2) Soil spring stiffnesses shall be determined at each location in the mat footing supporting a vertical structural component. At each location, the effective width B'_f used to determine the spring stiffness from Section 8.4.5.1 is permitted to be reduced based on a minimum bearing area $A'_{cf} = B'_f L'_f$ required to support 1.5 times the design dead and live loads resisted by the allowable bearing pressure q_{allow} defined in Section 8.4.2. The bearing area shall extend equally from all sides of the vertical element supported by the mat unless terminated by the edge of the footing or mat. If the individual bearing areas from multiple vertical elements overlap, the whole area required to support the combined load shall be used in the determination of B'_f.

(3) Soil spring stiffnesses shall be determined at each location in the mat footing supporting a vertical structural component from Section 8.4.5.1. At each location, an effective footing length, L_f, shall be taken as either: the length from points of flexural inflection on either side of the vertical structural component, or from the ¼ points of the span on either side of the vertical structural component, whichever is greater. L_f shall not be longer than the actual footing length. The effective footing width shall be taken as 4 times the footing depth on each side of the vertical element but not more than the actual footing size.

(4) Other rational procedures where equivalent foundation stiffnesses is determined based on settlement of the mat from finite element modeling of the soil continuum with applied loads on mat that include geometry and rigidity of the mat.

1.4.6 Procedures for a Separate Foundation Analysis Using Superstructure Demands from a Fixed-Base Model

The proposed recommended change is intended to align the evaluation of foundations in ASCE/SEI 41-23 with common practice used in the design of foundations for new buildings using ASCE/SEI 7, where an elastic, fixed-base building model is used to design the superstructure, and a separate elastic model of the foundation on compression-only springs is used to design the foundation. Two alternate procedures are proposed to check foundations using a different analysis platform from the superstructure where the foundations are modeled as a fixed base. In Procedure 1, the soil is modeled using elastic tension and compression springs, while in Procedure 2, the soil is modeled as compression-only springs. The proposed language is given below:

8.4.4.2.1 Combined Footings and Mat Foundations

…

8.4.4.1.2.3 Acceptance Criteria for Soil Bearing and Overturning

Buildings where the superstructure is modeled as a fixed base using Section 7.4.1 or 7.4.2 where the foundation plan consists of combined footings, grade beams resisting bearing pressures or mat foundations, the foundation evaluation shall comply with the requirements in this section. The foundation soil supports shall be represented by Winkler springs, and the foundation shall be evaluated for superstructure demands from the fixed base analysis.

Procedure 1: Soil Springs Resist Tension and Compression

Pseudo seismic forces from the fixed-base building analysis are applied to the structural foundation, which is modelled with elastic properties and supported by discrete springs representing the soil which resists tension and compression without gapping occurring between the soil and the footing. Each spring shall represent a tributary area of contact and be distributed uniformly across the footing-soil interface. The spring stiffness values used in the model shall be the soil stiffness values determined in accordance with Section 8.4.5.2.1.2 for linear procedures.

Foundation rotation demands at each column or wall location is obtained at the base of the wall, or from the bottom of two columns that form a brace frame. The soil bearing is satisfied if the rotation demand is less than 0.75 times the rotation acceptance values in Table 8-4.

Procedure 2: Soil Springs Resist Only Compression

When the structural combined footing or mat foundation is analyzed including gapping (nonlinearly), soil springs do not resist tension, the seismic demands from the superstructure are permitted to be divided by the applicable m-factor from Table 8-2c prior to the foundation analysis evaluation. Acceptance criteria for the soil bearing is satisfied if the maximum soil bearing pressure at any point under the footing is less than q_{cDA}.

Table 8-2c m-factor(1) for Overturning Action

Action	Performance Level		
	IO	LS	CP
Compression or Uplift	2	3	4

Where $A_c/A_f > 0.4$, the m-factors from Table 8-3 shall be used.

1.4.7 Moment Capacity of Footings Interconnected by Grade Beams

A new provision is proposed in ASCE/SEI 41-23, which permits the moment capacity of isolated footings to be increased by the resistance of an interconnecting grade beam or spandrel when present. Acceptance criteria for foundation overturning capacity in ASCE/SEI 41-17 Section 8.4.2.3.2 is based on the moment capacity for an isolated footing. This condition leaves out a lot of foundation configurations where the individual isolated footings are interconnected by grade beams. Footings that are interconnected by a grade beam have additional capacity that is not accounted for in the moment capacity equation in ASCE/SEI 41-17, Eq. 8-10. The proposed change is given below:

8.4.4.1.2.3 Acceptance Criteria for Soil Bearing and Overturning

Acceptance criteria for soil bearing shall satisfy the requirements of either a) or b).

a. Isolated footings interconnected by foundation structural elements are permitted to be discretized as individual footings at the points of contraflexure of the interconnecting structural element. Acceptance shall be in accordance with Section 8.4.4.1.1 except the foundation moment capacity M_{CE} shall be determined using principles of mechanics taking the summation of the overturning resistance about the centroid of the soil footing contact area.

b. When a two-dimensional analysis is permitted and used, overturning resistance of orthogonal framing may be included to resist overturning but shall not exceed the allowed flange width of the shear wall, nor the moment and shear capacity of the orthogonal members. When a three-dimensional analysis is required, such as with concurrent seismic effects of Section 7.2.5.1, overturning resistance of orthogonal framing shall be limited by the excess strength of the framing member beyond that required to resist design loads.

1.4.8 Limiting Use of Compression-Only Springs When Superstructure Is Modeled as Linear Using Flexible-Base Procedures

This section recommends clarifying the analysis procedure in ASCE/SEI 41-17 Section 8.4.2.3 when linear analysis procedures are used. New language is added where it is not permitted to analyze the superstructure as linear and permit the foundations to act nonlinearly with gapping permitted in the same analysis model. Combining a nonlinear uplifting foundation where superstructure elements are modeled as elastic and where the ductility *m*-factors for primary or secondary components are high gives unrealistic and incorrect results for the superstructure and foundation demands as demonstrated in the case study for Archetype Building 2. The proposed language is given below:

8.4.5 Flexible Base Procedure

…

8.4.5.2 Linear Procedures

For linear analysis procedures, the soil is assumed to be in contact with the footing or has the same stiffness and strength in tension or compression. The analysis shall be performed using the soil stiffness and strength as defined in this section. Nonlinear uplifting foundations are not permitted to be used with linear procedures unless Procedure 2 in Section 8.4.4.1.2 is used in a separate analysis from the superstructure.

1.4.9 Acceptance Criteria Check for the Structural Footing

There is no specific requirement or acceptance criteria for checking the structural footing in Chapter 8 of ASCE/SEI 41-17. Evaluation of the foundation structural component is specified in the material chapters. Since a majority of foundations are concrete, these provisions follow Chapter 10 of ASCE/SEI 41-17, where demands to the foundation are required to be evaluated as force controlled. Case studies on Archetype Building 1 have shown that this requirement could be overly conservative

and evaluation of the foundation should be either deformation-controlled or force-controlled depending on the action. Specific requirements have been proposed specifying the magnitude and application of the soil pressures as loads to check the adequacy of the footing. The text of the proposal is shown below:

> **Acceptance Criteria for the Structural Footing**
>
> Rectangular shaped isolated footings shall be evaluated in accordance with the material chapters for demands generated by an upward rectangular soil pressure distribution q_c as defined in Section 8.4.2 applied at the bottom of the footing starting from the edge towards the centroid over a length L_c such that $L_c = P_{UF} / q_c B_f$.
>
> Alternatively, for all footing geometries and loading, it shall be permitted to evaluate the structural footing as force-controlled for the soil pressure distribution using a rectangular soil pressure block for an axial demand P_{UF} and overturning moment M_{OT} divided by m (M_{OT}/m), where P_{UF}, M_{OT} and m, are the same values used for soil bearing in Section 8.4.4.1.1.2.1. The soil pressure distribution shall be obtained using a rational procedure where footing uplift is unrestrained.

1.4.10 Bounding Requirements for Nonlinear Procedures

This section proposes deleting the bounding requirements in ASCE/SEI 41-17 Section 8.4.2 when building foundations are explicitly modeled in the mathematical model of the building. While it is recognized that there is uncertainty in the soil properties, the halving of the strength and stiffness does not consider the factors of safety already introduced in the design for soil bearing capacity or the short-term strength amplification factor. In addition, consolidation over time accounts for additional strength and stiffness gain not accounted for in the bounding provisions. Case study results from Archetype Building 1 have shown that using lower bound properties for strength is unrealistic, and incompatible with the inherent safety factors in the original design of the building. Case study results from Archetype Building 2 have demonstrated minimal impact on superstructure demands due to bounding on stiffness. Therefore, the following requirements for bounding on strength and stiffness are proposed to be deleted:

> ~~8.4.2.3 Shallow Footings Considered Rigid (Method 1)~~
>
> ~~*8.4.2.3.1 Expected Strength and Stiffness.*~~
>
> ~~Expected nonlinear sliding and bearing behavior of foundations shall be represented by a bilinear elastic, perfectly plastic load–deformation relationship unless another approved relationship is available. The initial elastic stiffness may be calculated using elastic solutions in Fig. 8-2 with expected shear modulus and Poisson's ratio determined according to Section 8.4.2.2.~~
>
> ~~Where foundation components are modeled explicitly, the analysis shall be performed using the expected load–deformation characteristics and also using the upper- and lower-bound load–deformation characteristics, as illustrated in Fig. 8-1(a). The expected moment capacity, M_{CE}, shall be calculated using Eq. (8-10) with expected values of L_f, P_{UD}, q, and q_c. The upper- and lower-bound values for bearing, sliding, and rocking stiffness and for bearing and sliding capacity shall be obtained by multiplying and dividing by $(1 + C_v)$ where the coefficient of variation, C_v, is~~

~~defined as the standard deviation divided by the mean. C_v shall be taken as 1 unless specific data are available to show otherwise. In no case shall the value of C_v be taken as less than 0.5.~~

~~8.4.2 Load-Deformation Characteristics for Shallow Foundations.~~

~~If building foundations are explicitly modeled in the mathematical model of the building, the load-deformation characteristics shall be calculated in accordance with Sections 8.4.2.3 to 8.4.2.5 for shallow bearing foundations.~~

~~For the nonlinear dynamic procedure (NDP), nonlinear sliding and overturning behavior of foundations shall be represented by an equivalent elastoplastic load-deformation relationship.~~

~~Where foundation components are modeled explicitly, the analysis shall be performed using upper- and lower-bound load-deformation characteristics of foundations as illustrated in Fig. 8-1(a) and defined in this section. Where foundation components are not modeled explicitly, the analysis shall be bounded by the upper- and lower-bound foundation capacity as defined in this section. In lieu of explicit evaluation of uncertainties in foundation characteristics, it shall be permitted to take the upper-bound stiffness and bearing capacity values and shear-sliding and axial load-settlement relationships as two times the expected values and the lower-bound stiffness and capacity values as one-half of the expected values.~~

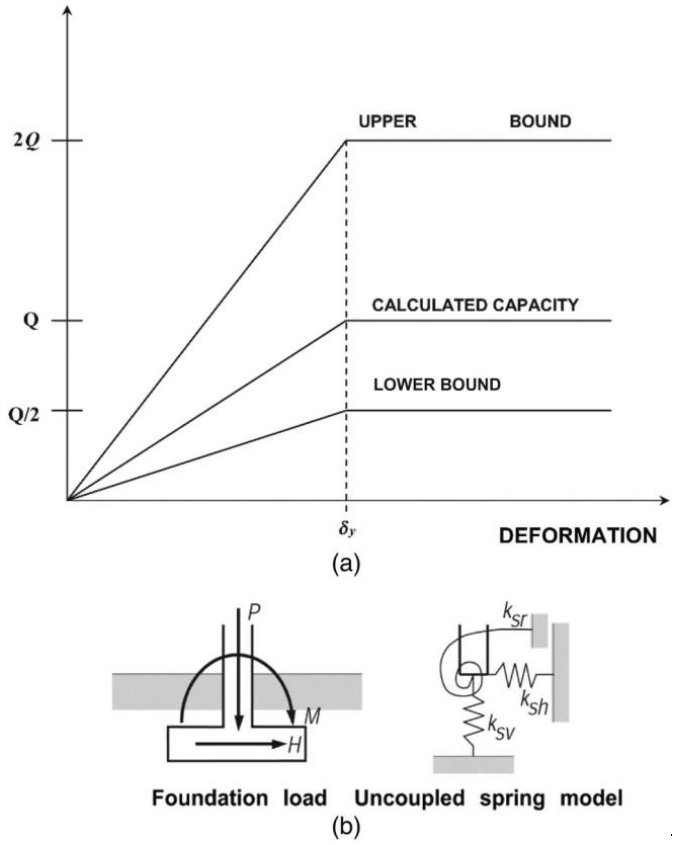

~~Figure 8-1. (a) Idealized Elastoplastic Load-Deformation Behavior for Soils; (b) Uncoupled Spring Model for Rigid Footings~~

1.5 References

ACI, 1988, ACI committee 336, 336.2R-88, Suggested Analysis and Design Procedures for Combined Footings and Mats, Reapproved (2002).

ACI, 2014, Building Code Requirements for Structural Concrete and Commentary on Building Code Requirements, ACI 318-14, American Concrete Institute, Farmington Hills, Michigan.

ASCE, 2010, *Minimum Design Loads for Buildings and Other Structures*, ASCE/SEI 7-10, American Society of Civil Engineers, Reston, Virginia.

ASCE, 2016, *Minimum Design Loads for Buildings and Other Structures*, ASCE/SEI 7-16, American Society of Civil Engineers, Reston, Virginia.

ASCE, 2017, *Seismic Evaluation and Retrofit of Existing Buildings*, ASCE/SEI 41-17 Report, American Society of Civil Engineers Structural Engineering Institute, Reston, Virginia.

Bellos, J. and Bakas, N., 2017, "Complete analytical solution for linear soil pressure distribution under rectangular spread footings," *International Journal of Geomechanics*, July 2017, Volume 17, Issue 7, American Society of Civil Engineers, Reston, Virginia.

Deng, L., Kutter, B., and Kunnath, S., 2014. *"Seismic design of rocking shallow foundations: displacement-based methodology," J. Bridge Eng*., Volume 19, Issue 11, American Society of Civil Engineers, Reston, Virginia.

FEMA, 2011. *Quantification of Building Seismic Performance Factors: Component Equivalency Methodology,* FEMA P-795, prepared by the Applied Technology Council for the Federal Emergency Management Agency, Washington, D.C.

FEMA, 2018, Example Application Guide for ASCE/SEI 41-13 Seismic Evaluation and Retrofit of Existing Buildings with Additional Commentary for ASCE/SEI 41-17, FEMA P-2006, prepared by the Applied Technology Council for the Federal Emergency Management Agency, Washington, D.C.

FEMA, 2020, *A Practical Guide to Soil-Structure Interaction*, FEMA P-2091, prepared by the Applied Technology Council for the Federal Emergency Management Agency, Washington, D.C.

Lobo, R.F., Tokas, C.V. and Hale, T, 2021, "General methodology for determining foundation moment capacity of rigid footings of any plan under P-M-M Loading," *Proceedings, Structural Engineering Association of California, SEAOC 2021 Convention*, Carlsbad, California.

Part 4

Chapter 1: Revisions to Concrete Structural Wall Stiffness, Modeling Guidance, and Flexure-Controlled Provisions

1.1 Motivation

Most of the provisions for concrete structural walls in ASCE/SEI 41-17 were developed in the late 1990s based on limited experimental data and judgement (FEMA 273/247-1997). The only exceptions are the modeling parameters (MP) and acceptance criteria (AC) of shear-controlled walls, which were updated for the ASCE/SEI 41-06 Supplement 1 (Elwood et al., 2007).

Studies assessing the accuracy of the MPs for flexure-controlled walls have indicated that the MPs tend to be overly conservative and are influenced by variables that are not considered in ASCE/SEI 41-17 (for example, Abdullah and Wallace (2019), Birely et al. (2014), Motter et al. (2018), Segura and Wallace (2018), Tran (2012), and Wallace (2006)). Moreover, procedures for classifying walls into flexure- or shear-controlled behaviors are not specified in the provisions of ASCE/SEI 41-17, with only commentary provided indicating that the wall height-to-length aspect ratio could be used to differentiate behaviors. This recommendation for classifying wall behavior is shown in this document to have limited accuracy. Other shortcomings include lack of provisions for wall sliding mechanisms, and limited guidance on modeling techniques for walls, particularly fiber-section based techniques that are increasingly used for walls.

An extensive database developed by Abdullah (2019) with over 1,100 wall tests spurred a comprehensive review of all structural wall provisions and the addition of new provisions related to wall sliding and wall modeling. The outcome, presented here in Part 4, includes: a restructuring of the structural wall Chapter 7 in ACI 369.1-17, which was reproduced as Section 10.7 in ASCE/SEI 41-17; updated wall classification procedures based on the relative strengths of various mechanisms; updated MP and AC for flexure-controlled, shear-controlled, and shear friction-controlled walls; and new modeling guidance for structural walls. Three example assessments for flexure-controlled, shear-controlled, and shear friction-controlled walls in low- to mid-rise buildings also are presented. Assessment outcomes between the provisions of ASCE/SEI 41-17 and the proposed provisions are compared.

In Chapter 1, the wall database is presented, including methods used to extract necessary force and deformation metrics for updating stiffness, strength, and deformation capacities for walls controlled by flexural modes of degradation. Proposed wall stiffness provisions, as well as Acceptance Criteria (AC) and Modeling Parameters (MP) for flexure-controlled walls are presented. In addition, new

provisions and commentary for modeling walls using lumped-plasticity or fiber-section methods are given in this chapter. At the end of the chapter, an example assessment of a building with flexure-controlled walls is presented based on existing ASCE/SEI 41-17 provisions and the proposed provisions. Comparisons between the outcomes of the existing and proposed provisions are discussed.

Note about the Relation Between the ASCE/SEI 41 and ACI 369.1 Standards

The concrete wall provisions contained in Section 10.7 of ASCE/SEI 41-17 were reproduced from Chapter 7 of the new ACI 369.1-17 Standard, based on a Memorandum of Understanding between ACI and ASCE. In 2021, however, the ASCE/SEI 41 Standard Committee elected to reference the next version of ACI 369.1 directly, without replicating its contents, making ACI 369.1 the reference standard for concrete members for ASCE/SEI 41. The proposed changes were, therefore, submitted to ACI's *Seismic Repair and Rehabilitation* Code committee 369 for possible adoption.

1.2 Summary of Recommended Changes

Due to the extensive nature of the proposed changes to the concrete structural wall provisions, a restructuring of the concrete wall Chapter 7 of ACI 369.1-17 (Section 10.7 in ASCE/SEI 41-17) is proposed to improve the flow of information. In addition, the following technical changes, covered in this chapter, are proposed for concrete walls:

(a) Wall stiffness: improvements to wall stiffness provisions are recommended based on test data. Flexural rigidity is proposed to vary with axial force, as is the case for concrete columns. Shear rigidities are reduced for cracked walls. A median estimate of member stiffness is targeted with the proposed rigidities, to avoid skewing the response in analyses.

(b) Flexure-controlled walls: updated linear and nonlinear AC and MP are proposed based on test data. In addition, the definition of peak wall moment strength is updated. Guidance for how to treat flanged walls and variable axial loads is also proposed.

(c) Wall modeling: fiber-section representations are often used in seismic analyses as they can easily capture the stiffness and flexural strength of walls, while accounting for variations in axial loads. However, AC and MP provided in tables of the standard are based on lumped-plasticity deformations (for example, concentrated rotational or shear/translational deformations at hinges). Guidance is proposed to assist users in adjusting material properties in fiber analyses to obtain realistic deformations (particularly during strength degradation), and for converting deformations obtained from fiber-section elements to deformations that are compatible with AC and MP tables.

1.3 Technical Studies

1.3.1 Wall Test Database

1.3.1.1 OVERVIEW

A comprehensive database (Abdullah, 2019; Abdullah and Wallace, 2019) that includes detailed data on more than 1,100 reinforced concrete (RC) wall tests surveyed from more than 260 programs reported in the literature was utilized in this study. The database includes three major clusters of data: 1) information about the test specimen, test setup, and axial and lateral loading protocols, 2) analytically computed data, for example, moment-curvature relationships (depth of neutral axis, c; nominal moment, M_n; first yield moment, M_y; curvature at M_n, ϕ_n; and first yield curvature, ϕ_y) and wall shear strengths according to ACI 318-19, and 3) experimental data, for example, backbone relations and failure modes. Database information related to the objectives of this study is briefly presented below; however, detailed information about the database can be found elsewhere (Abdullah, 2019; Abdullah and Wallace, 2019).

Figure 1-1 provides example backbone relations for the experimental base shear versus total top displacement, which includes deformations due to curvature, shear, and bar slip/extension, from two wall tests. Table 1-1 provides the definition of each response point provided in the database as shown in Figure 1-1 and the approach used by the database developers to derive these points from the experimental load-deformation relationships.

The database was filtered to obtain separate datasets to study stiffness (flexure and shear), and modeling parameters and acceptance criteria for flexure-controlled walls, as described in the following sections.

Table 1-1 Definition of Backbone Response Points

Point	Definition	Data Used to Define the Point
Cracking	Represents the state at which horizontal flexural cracks are first observed in the test.	The cracking load and displacement are available for the majority of the tests in the database based on information reported by the authors who performed the tests. However, in cases where this information is not reported, the cracking point was identified using the load-displacement relation, i.e., the point at which a significant change in stiffness is observed. If a significant change in stiffness was not observed, then information related to cracking is not reported in the database, and a data point was not included for the specific test.

Table 1-1 Definition of Backbone Response Points (continued)

Point	Definition	Data Used to Define the Point
General Yield	Represents yielding of most of the boundary longitudinal reinforcement or the onset of concrete nonlinearity in compression-controlled walls.	This point is visually identified as the point where the hysteretic loops (or the response curve in case of monotonic loading) demonstrate an abrupt reduction in stiffness. This point is easily identified for walls where yield point is defined by yielding of boundary longitudinal reinforcement, as shown in Figure 1-1. It is noted that this point does not necessarily correspond to the first yield of boundary longitudinal reinforcement, but rather is associated with yielding of most of the boundary longitudinal bars. For compression-yielding walls (i.e., walls tested under significant axial loads or walls with T- or L-shaped cross-section loaded with the flange in tension), stiffness degradation is typically more gradual, leading to a more subjective assessment of the yield point. For these walls, a consistent approach was used by the database developers (Abdullah, 2019; Abdullah and Wallace, 2019).
Peak	Represents maximum lateral strength	This point is taken as the maximum lateral strength observed on the backbone relation.
Ultimate	Represents a significant loss in lateral strength (i.e., lateral failure)	This point is identified as the point at which lateral strength degrades by 20% from the peak load during the first cycle to a lateral displacement that exceeds the lateral displacement at the peak load. This definition is widely used in literature and in developing MP for members in ASCE/SEI 41.
Residual	Represents the residual lateral strength	This point is defined as the point at which the wall reaches its residual lateral strength (residual strength plateau, for example, Figure 1-2), if a residual strength is observed or reported for the tests. Many tests, especially tests conducted prior to about the year 2000, do not report residual strength because the test was terminated after modest strength reduction was observed.
Collapse/ Axial failure	Represents the loss of axial-load-carrying capacity	The Axial Failure point was identified based on: (1) reported axial failure from the tests (For example, Figure 1-2 and Figure 1-3), (2) observed concrete crushing along the entire length of the wall, or (3) out-of-plane instability along a majority of the wall length (For example, Figure 1-4). If axial failure occurred at a deformation smaller than the maximum deformation reached (in a prior cycle), then the maximum deformation reached in the prior cycle is reported as the deformation for axial failure (For example, Figure 1-3*c*). Similar to the residual point, for many wall tests, especially tests conducted prior to about the year 2000, the test was terminated prior to reaching a residual strength value.

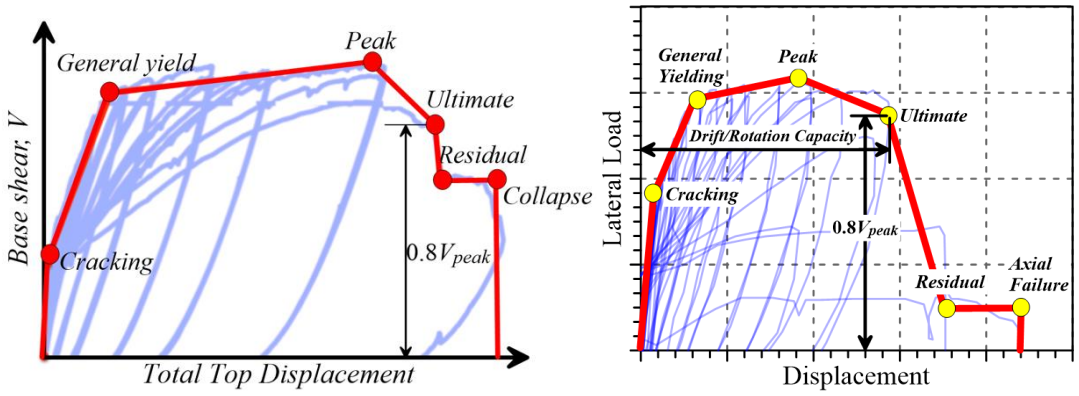

(a) Test by Tran (2012) **(b) Test by Albidah (2016)**

Figure 1-1 Typical wall backbone curve contained in RC wall database.

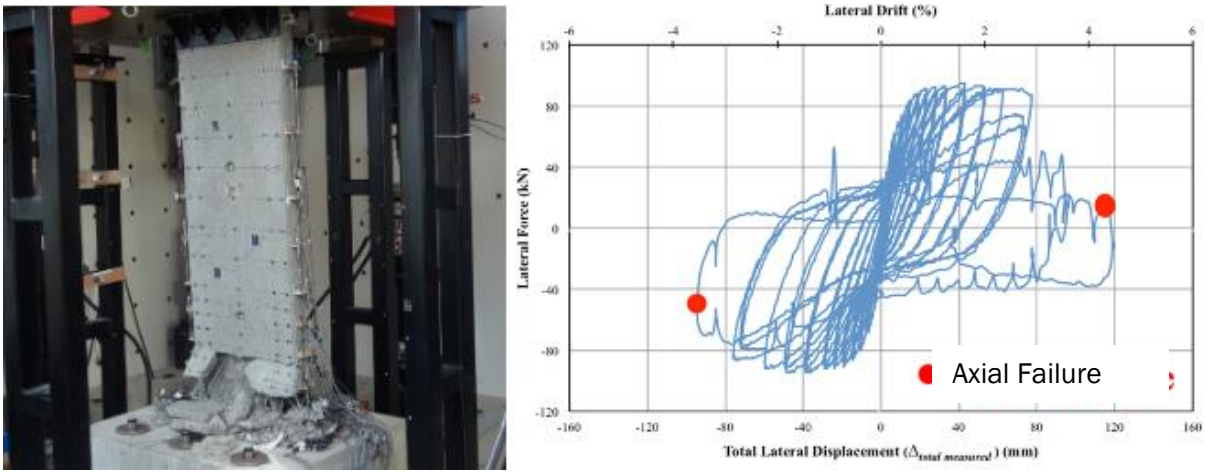

Figure 1-2 Reported axial failure of a wall test reported by Altheeb (2016).

(*a*) South view (*b*) North view (*c*) Load-displacement response

Figure 1-3 Reported axial failure of a wall test reported by Segura and Wallace (2018a).

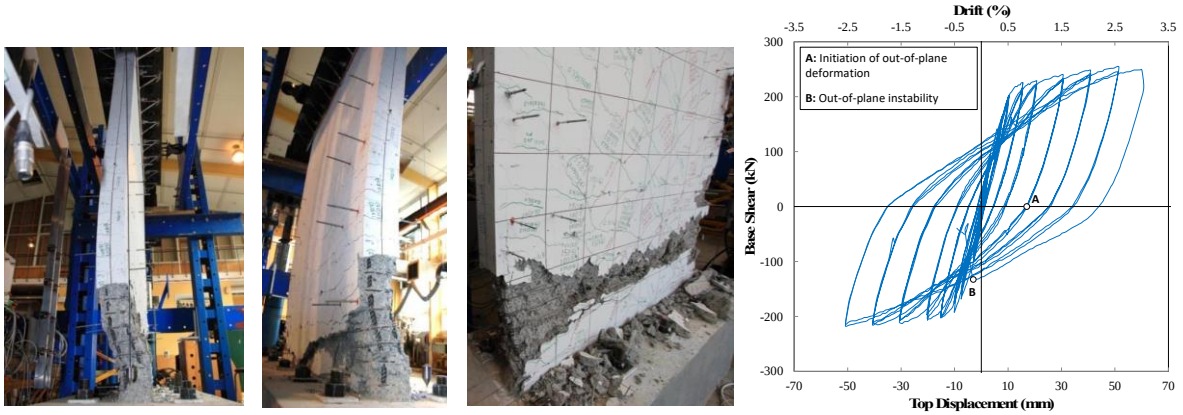

Figure 1-4 Out-of-plane instability and concrete crushing of a wall test reported by Dashti et al. (2018).

1.3.1.2 DATASETS FOR WALL STIFFNESS STUDIES

Flexural Stiffness

For the purpose of extracting flexural stiffness values (uncracked and effective), the main database was filtered to obtain a subset of wall tests that satisfied the following criteria:

- Flexure-controlled walls (i.e., ratio of shear capacity to shear demand based on yield moment strength, $V_{CE}/V_{MCyDE} \geq 1.15$; see Chapter 4 for wall classification criteria),
- Walls tested under quasi-static, monotonic, or cyclic loading (in-plane or bi-directional),
- Walls containing one or two curtains of web reinforcement,
- Walls with conforming or nonconforming seismic detailing, and
- Walls with different cross-section shapes (i.e., rectangular, barbell, I-shaped, T-shaped, L-shaped, or half-bar bell).

Based on the selected filters, a total of 527 wall tests were identified. Histograms for various dataset parameters are shown in Figure 1-5, where $P/A_g f'_{cE}$ is the sustained axial load applied during the experiment normalized by tested concrete compressive strength (f'_{cE}) and gross concrete area (A_g), $M/(Vl_w)$ is the ratio of base moment-to-base shear reported for the test normalized by wall length (l_w), $\rho_{l,BE}$ and $\rho_{l,web}$ are the longitudinal reinforcement ratios at the wall boundary and for the web, respectively, $f_{y,BE}$ is the tested yield strength of the boundary longitudinal reinforcement, t_w is the wall web thickness, and b is the width of flexural compression zone. Walls tested under monotonic or bidirectional loading are included because it is assumed that the loading protocol does not have a significant influence on the wall behavior prior to the yield point. Nonetheless, walls tested under monotonic and bidirectional loading constitute only 6% and 2.5%, respectively, of the walls in the dataset of 527 walls, as shown in Figure 1-5l. This dataset includes walls from the Conforming and Nonconforming datasets (described later for modeling parameters and acceptance criteria) and additional tests that were excluded for these two datasets, for example, wall tests without noticeable

lateral strength loss, which are appropriate for stiffness studies, but not for deriving modeling parameters.

Due to the lack of information for the cracking point for 132 of the 527 wall tests, the dataset for determination of uncracked flexural stiffness included 395 tests.

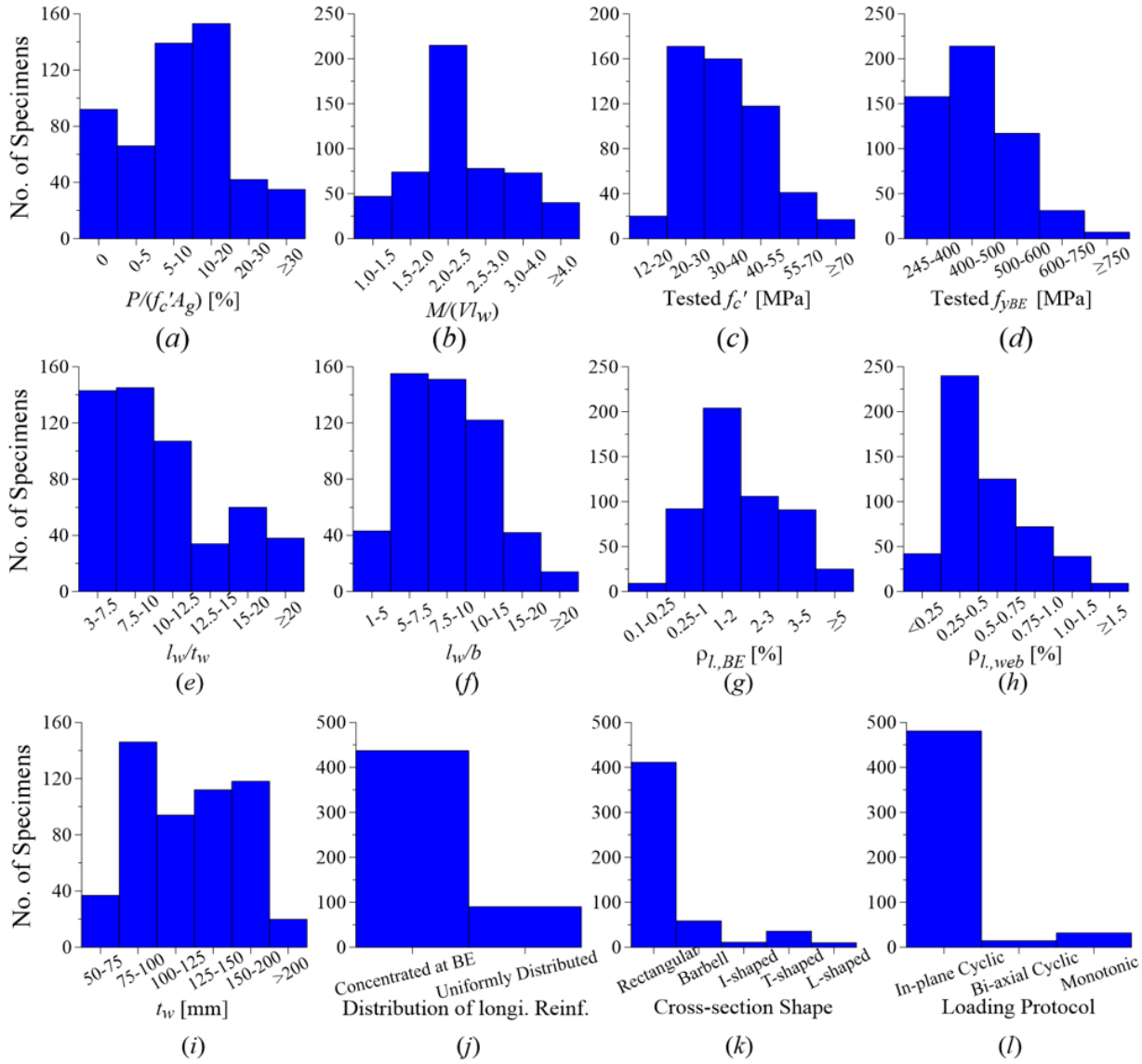

Figure 1-5 Histograms of the dataset (527 wall tests) used for flexural stiffness studies.

For the results presented in this study, the flexural stiffness (rigidity) values are normalized by gross section flexural stiffness ($E_{cE}I_g$), in which Young's Modulus of concrete (E_{cE}) is computed from Equation 1-1 (ACI 318-19 Equation 19.2.2.1a) for normal strength concrete (NSC) and Equation 1-2 (ACI 363R-10) for high strength concrete (HSC) using the tested concrete compressive strength (f'_{cE}). ACI CT-13 defines high strength concrete as concrete that has a specified compressive strength of 8000 psi or greater. However, Equation 1-1 is intended to only be used for concrete compressive

strength up to 6000 psi. Therefore, the break point between normal and high strength concrete was adopted as 6000 psi for the purpose of calculating E_{cE} using tested f'_{cE}. I_g is the gross section moment of inertia, for which presence of reinforcement in the cross-section is ignored, consistent with the I_g definition given in ACI 369.1-17.

$$E_{cE} = w_c^{1.5} 33 \sqrt{f'_{cE}\text{psi}} \quad \left(= w_c^{1.5} 0.043 \sqrt{f'_{cE}\text{MPa}} \right) \qquad \text{Normal strength concrete (1-1)}$$

$$E_{cE} = 40000 \sqrt{f'_{cE}\text{psi}} + 10^6 \quad \left(= 3320 \sqrt{f'_{cE}\text{MPa}} + 6900 \right) \qquad \text{High strength concrete (1-2)}$$

Where w_c is unit weight of concrete, assumed to be equal to 150 pcf (24 kN/m^3) and 120 pcf (19.2 kN/m^3) for normal weight and light weight concretes, respectively.

Shear Stiffness

To study effective shear stiffness of flexure-controlled walls, the dataset of 527 walls described in the previous section was further filtered to identify wall tests that had also included instrumentation to enable the measurement of load-shear deformation backbone relations. As a result, a reduced dataset of 64 wall tests was obtained and was used to develop wall recommendation for shear stiffness.

1.3.1.3 WALL DATASETS FOR MODELING PARAMETERS AND ACCEPTANCE CRITERIA

Flexure-controlled walls are classified into two categories based on the level of detailing provided: conforming walls and nonconforming walls. For each category, a dataset is filtered from the main database and is then used to propose updated modeling parameters and acceptance criteria. In ASCE 41-17 the term “Confined Boundary” is used for walls that have boundaries with transverse reinforcement exceeding 75% of the requirements given in ACI 318-19 and spacing of transverse reinforcement not exceeding $8d_b$. In the proposed updates, the terms “confined boundary” and “no confined boundary” are replaced with conforming and nonconforming walls, respectively. This is because the criteria used for conforming walls include more than just detailing in the boundary element (For example, two curtains of web bars), as will be discussed next.

Conforming Wall Dataset

Design of reinforced concrete structural walls is currently governed by the requirements of ASCE/SEI 7-16 and ACI 318-19, which includes provisions for special structural walls with special boundary elements (SBE) according ACI 318-19 Section 18.10.6.4 for buildings assigned to Seismic Design Category D, E, or F. Detailing requirements for SBEs have changed over the years and are likely to keep changing in the future; therefore, the main database was filtered to obtain a dataset of “Conforming Walls” using the criteria given below, which are slightly less restrictive than the detailing requirements of ACI 318-19 Section 18.10.6.4 for SBEs:

(a) General criteria:

- Flexure-controlled walls, (i.e., $V_{CE}/V_{MCyDE} \geq 1.15$, see Chapter 4)
- Walls with different cross-sections were included (i.e., rectangular, barbell, H-shaped, T-shaped, L-Shaped, or half-bar bell),
- Walls tested under quasi-static, reversed cyclic loading (i.e., no monotonic tests),
- Walls were excluded if noticeable lateral strength loss was not observed or if walls failed due to inadequate lap-splices,
- Walls with measured concrete compressive strength, $f'_{cE} \geq 3$ ksi,
- Walls with ratio of measured tensile-to-yield strength for boundary longitudinal reinforcement, f_{uE}/f_{yE}, ≥1.2, and
- Walls with web thickness, t_w, ≥ 3.5 in.

(b) Detailing criteria:

- Two curtains of web vertical and horizontal reinforcement,
- Boundary longitudinal reinforcement ratio, $\rho_{l,BE} \geq 6\sqrt{f'_{cE}(\text{psi})}/f_{yE}$,
- Minimum ratio of provided-to-required (per ACI 318-19 Section 18.10.6.4) area of boundary transverse reinforcement, $A_{sh,provided}/A_{sh,required} \geq 0.7$,
- Ratio of vertical spacing of boundary transverse reinforcement to minimum diameter of longitudinal boundary reinforcement, $s/d_b < 8.0$, and
- Centerline distance between laterally supported boundary longitudinal bars, h_x, between 1.0 in. and 9.0 in.

A limit of 3 ksi was specified on f'_{cE} in accordance with requirements of ACI 318-19 Section 18.2.5 for conforming seismic systems. At least two curtains of web reinforcement were specified to be consistent with ACI 318-19 Section 18.10.2.2. Walls with t_w less than 3.5 in. were not included because use of two curtains of web reinforcement along with realistic concrete cover is not practical in such thin walls. The limit on ratio f_{uE}/f_{yE} is slightly less restrictive than the limit of 1.25 specified in ACI 318-19 Section 20.2.2.5. The specified limits on $s/d_b \leq 8.0$ and $A_{sh,provided}/A_{sh,required} \geq 0.7$ are slightly less restrictive than the current limits in ACI 318-19 Section 18.10.6.4 of 6.0 and 1.0, respectively. The limit on $\rho_{l,BE}$ was included based on ACI 318-19 Section 18.10.2 (to avoid brittle tension failures). ACI 318-19 Section 18.10.6.4e requires $h_{x,max}$ not exceeding the lesser of 14 in. or $2b/3$; however, most of the tests in the database were conducted at less than full scale (typically 25 to 50%). Therefore, $h_{x,max}$ for the wall tests should generally be between 3.5 to 7.0 in. for the 14 in.

limit. Based on the range of h_x used to filter the data, 95% of the specimens have $h_x \leq 6$ in., which is reasonable, whereas the histogram for h_x/b presented in Figure 1-6f indicates that a majority of the tests have $h_x/b < 3/4$, which is only slightly higher than the current limit of $h_x/b < 2/3$.

Based on the above selected filters, a total of 188 wall tests were identified that included information on lateral strength loss (i.e., 20% lateral strength loss from peak strength) and 101 of these tests had reported information on axial failure. Histograms for various dataset parameters for the 188 tests are shown in Figure 1-6, where $P/A_g f'_{cE}$ is the compressive axial load normalized by the measured concrete compressive strength (f'_{cE}) and gross concrete area (A_g), M/Vl_w is the ratio of base moment to base shear normalized by wall length (l_w), b is the width of flexural compression zone, and c is the depth of neutral axis computed at concrete compressive strain of 0.003.

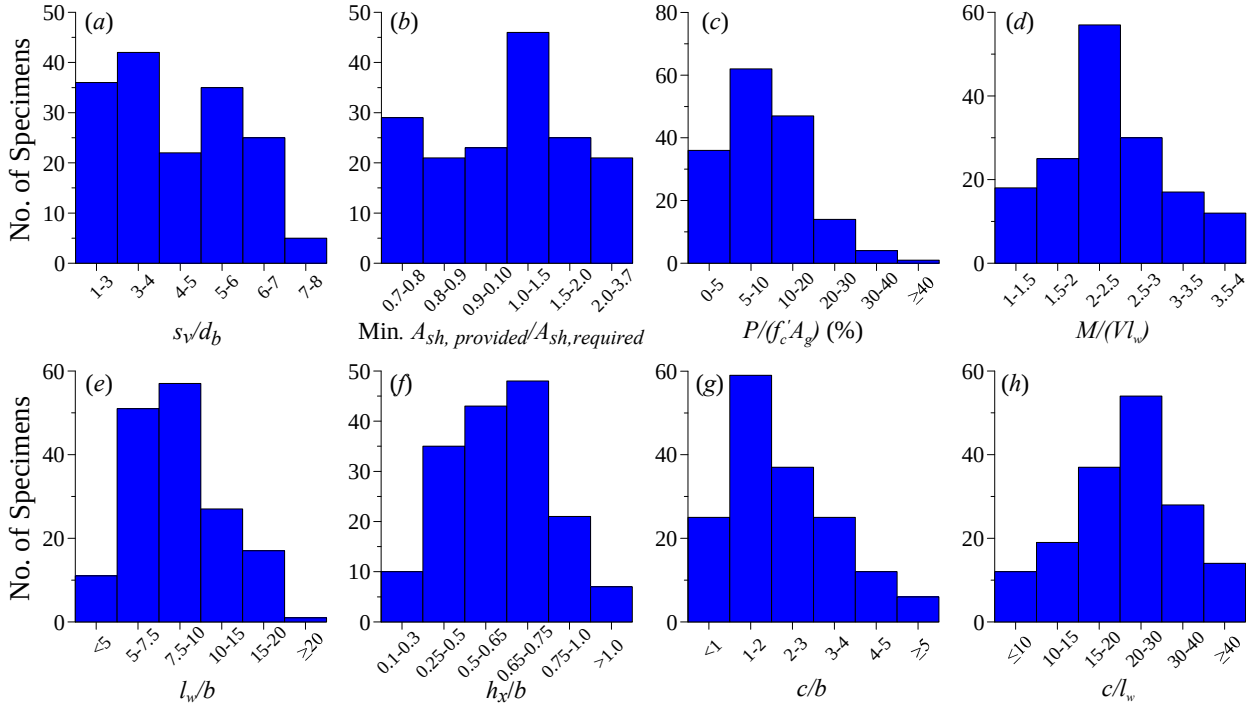

Figure 1-6 Histograms of the first dataset (188 tests) for walls with conforming detailing.

Nonconforming Wall Dataset

Walls with detailing not conforming to special structural wall provisions are common in older construction designed prior to the establishment of detailing requirements for structural walls, which were introduced in ACI 318-77 and were updated significantly in ACI 318-83, 318-99 and ACI 318-14. Additionally, the special detailing requirements of ACI 318-19 are relaxed where wall displacement or force demands are low; however, if the boundary longitudinal reinforcement ratio exceeds $400/f_y$, modest detailing is required by ACI 318-19 Section 18.10.6.5 (introduced in ACI 318-99 in Section 21.6.6.5) to prevent bar buckling at smaller deformation demands. These walls are sometimes referred to as walls with Ordinary Boundary Elements, or OBEs (For example, see

NIST (2011)). Based on these considerations, the following criteria were used to obtain a dataset of "Nonconforming Walls":

(a) General criteria:

- Flexure-controlled walls, (i.e., $V_{yE}/V_{MyE} \geq 1.15$, see Chapter 4)
- Walls with different cross-sections were included (i.e., rectangular, barbell, I-shaped, T-shaped, L-Shaped, or half-bar bell),
- Walls tested under quasi-static, reversed cyclic loading (no monotonic tests), and
- Walls were excluded if noticeable lateral strength loss was not observed, or if walls failed due to inadequate lap-slices.

(b) Detailing criteria:

- Walls with one or more curtains of web vertical and horizontal reinforcement,
- Minimum ratio of provided-to-required (per ACI 318-19 Section 18.10.6.4) area of boundary transverse reinforcement $A_{sh,provided}/A_{sh,required} < 0.7$, and/or ratio of vertical spacing of boundary transverse reinforcement to minimum diameter of longitudinal boundary reinforcement, $s/d_b \geq 8.0$.

Based on the above selected filters, a total of 256 wall tests were obtained. Histograms for various dataset parameters for those 256 wall tests are shown in Figure 1-7. Out of the 256 wall tests, 118 tests had reported information on axial failure point in the database.

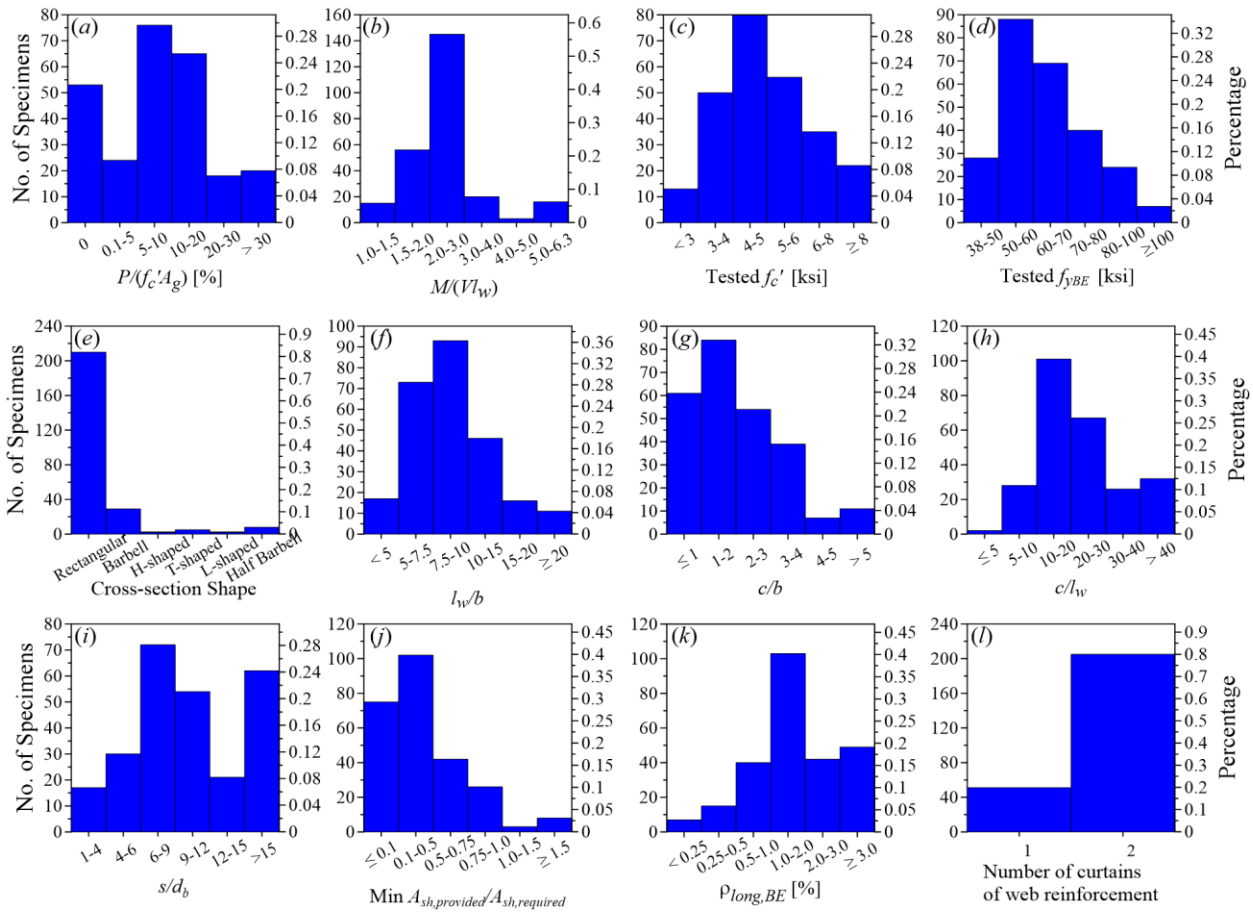

Figure 1-7 Histograms of the second dataset (256 tests) for walls with nonconforming detailing.

1.3.1.4 DATA EXTRACTION FOR STIFFNESS

In this study, uncracked and effective "cracked" flexural stiffnesses of the walls in the stiffness dataset are derived from the experimental backbone curves, with some approximations and assumptions, as discussed below.

Uncracked Flexural Stiffness

Not to be confused with the gross sectional stiffness, the uncracked "or initial" stiffness (K_{uncr}) is defined as the slope of the backbone curve from *origin* to a point at which flexural cracking is first observed (reported). However, the deformation at *cracking* point shown in Figure 1-1 includes elastic shear deformation ($\delta_{cr,s}$). Therefore, the $\delta_{cr,s}$ corresponding to the shear at the critical section (base of wall) at flexural cracking is analytically computed using Equation 1-3 using the gross shear stiffness ($G_{gE}A_{cv}$), assuming no shear cracking at this loading stage has occurred. Then, $\delta_{cr,s}$ is subtracted from the total experimental cracking deformation ($\delta_{cr,t}$) to obtain the cracking flexural deformation ($\delta_{cr,f}$) using Equation 1-4 (Figure 1-8):

$$\delta_{cr,s} = \frac{V_{cr} h_w f}{A_{cv} G_{gE}} \tag{1-3}$$

$$\delta_{cr,f} = \delta_{cr,t} - \delta_{cr,s} \tag{1-4}$$

Where V_{cr} is the base of wall shear corresponding to cracking moment of the wall (experimental), h_w is the wall height, A_{cv} is the shear resisting (web) area of the wall ($l_w t_w$), G_{gE} is the gross shear modulus taken as $0.4E_{cE}$, E_{cE} is the concrete Young's modulus computed from Equation 1-1 or Equation 1-2 using tested f'_{cE}, and f is a shape factor allowing the non-uniform distribution of shear stresses in the cross-section and is taken as 1.2 for rectangular sections and 1.0 for flanged or barbell-shaped sections.

The uncracked flexural stiffness ($E_{cE}I_{uncr}$) is then computed for a cantilever wall with a fixed base and a single lateral load applied near the top of the wall using Equation 1-5. A similar approach is used for non-cantilever (For example, panel or partial height) wall tests.

$$E_{cE} I_{uncr} = \frac{V_{cr} h_w^3}{3\delta_{cr,f}} \tag{1-5}$$

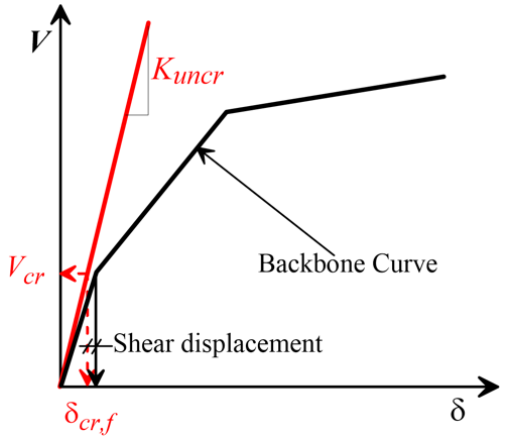

Figure 1-8 Definition of uncracked flexural stiffness.

Effective "Cracked" Flexural Stiffness

The effective "cracked" stiffness (K_e) is commonly defined as the slope of a straight line, passing through *origin* and a point on the experimental backbone curve at which first yielding of longitudinal reinforcement or the onset of concrete nonlinearity (i.e., maximum extreme fiber concrete compressive strain of 0.002) occurs, whichever is reached first. This is consistent with the definition of wall effective flexural stiffness given in ASCE/SEI 41-17 and ACI 369.1-17. However, as noted earlier, the database contains total displacements and base of wall shears at the *General Yield* point ($\delta_{y,g}$, $V_{y,g}$), which is defined as the point where the hysteretic loops (or the response curve in case of monotonic loading) begin to abruptly lose stiffness, as shown in Figure 1-8. Therefore, *General Yield* does not correspond to the first yielding of longitudinal bars, but rather to yielding of most of the

longitudinal bars in the tension boundary region. Furthermore, the *General Yield* displacement includes shear deformations. To address these issues, the following two adjustments and simplifications were made:

i. The shear deformation ($\delta_{y,s}$) corresponding to the base shear at *General Yield* is subtracted from the total deformation at this point ($\delta_{y,g}$) using Equation 1-6 to obtain the flexural displacements ($\delta_{y,f}$) (curvature and bar slip/extension deformations):

$$\delta_{y,f} = \delta_{y,g} - \delta_{y,s} \tag{1-6}$$

Where $\delta_{y,s}$ is analytically approximated using Equation 1-7, with an effective shear modulus of $G_{gE}/3$ used for the entire dataset. This value was selected based on an analysis of test results of 64 flexure-controlled walls for which the base shear-shear displacement backbones were available in the database, as discussed later.

$$\delta_{y,s} = \frac{V_{y,g} h_w f}{A_{cv}(G_{gE}/3)} \tag{1-7}$$

Figure 1-9 shows the contribution of shear deformation to total deformation at *General Yield* against normalized shear stress at *General Yield* and test shear span ration (M/Vl_w). This figure indicates that shear displacement increases with increase in shear stress and with decrease in M/Vl_w. It also shows that shear displacement contribution to total yield displacement generally falls with the range of 4% to 25% (based on a best fit line, Figure 1-9), which is considered reasonable for flexure-controlled walls.

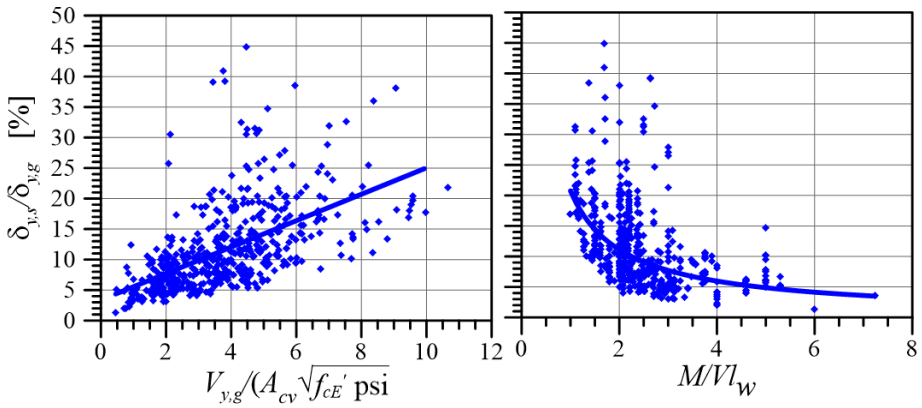

Figure 1-9 Contribution of shear deformation to total deformation at *General Yield* point.

ii. The flexural displacements at *General Yield* ($\delta_{y,f}$) are reduced by 30% to approximately obtain effective stiffness corresponding to first yield, as illustrated in Figure 1-10. This approximation was verified against a subset of 20 wall tests for which first yield of longitudinal reinforcement is identified from strain gage readings and the results were found to be relatively insensitive where modestly higher and lower reduction factors were considered, as discussed later. Therefore, the

effective flexural rigidity ($E_{cE}I_{eff}$) is computed as follows for cantilever walls (Equation 1-8), as an example:

$$E_{cE}I_{eff} = \frac{V_{y,g}h_w^3}{3(0.7\delta_{y,f})} \tag{1-8}$$

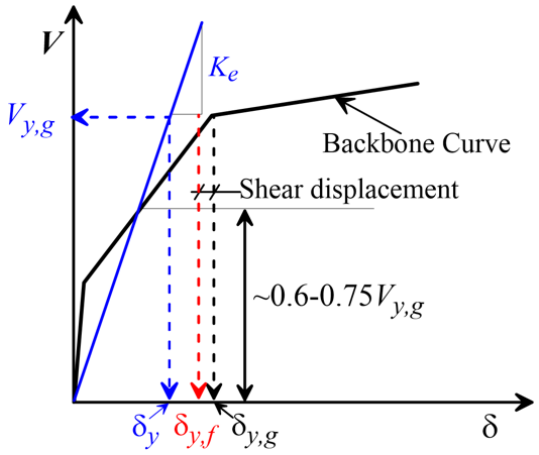

Figure 1-10 Definition of effective first yield flexural stiffness.

The above approach to obtain $E_{cE}I_{eff}$ is similar to approaches used by other researchers for walls and other concrete elements (For example, Elwood and Eberhard, 2009; Fenwick and Bull, 2000; Paulay and Priestley, 1992; Adebar et al., 2007) and ASCE/SEI 41-17, where effective stiffness is defined as the slope of a line from *origin* passing through a point on the response curve corresponding to 0.6 to 0.75 $V_{y,g}$.

Effective "Cracked" Shear Stiffness

For the small dataset of wall tests used for cracked shear stiffness, the effective shear modulus ($G_{eff,E}$) was computed using Equation 1-9:

$$G_{eff,E} = \frac{V_{y,g}h_w f}{A_{cv}\delta_{y,s}} \tag{1-9}$$

Where $V_{y,g}$ and $\delta_{y,s}$ are the experimental base shear and the corresponding shear displacement at *General Yield* point on backbone (Figure 1-1), respectively.

1.3.1.5 DATA EXTRACTION FOR MODELING PARAMETERS

The ACI 369/1-17 nonlinear deformation-based modeling parameters (i.e., Parameters a_{nl} and b_{nl}) are given as plastic hinge rotations (Figure 1-11a). Where a lumped plasticity model is used, the hinge region, which is typically at or near the base of a wall, is modeled as a near-rigid spring with effectively no elastic deformation. However, in this study, a new backbone relation is proposed, as shown in Figure 1-11*b*, where the deformation-based modeling parameters are given as total hinge

rotation capacities, which include both the elastic and plastic deformations in the hinge region. This approach is proposed because: (1) modeling parameters are not sensitive to approaches (or assumptions) used to calculate yield rotation, θ_y, (2) modeling parameters are consistent with the total drift ratio or chord rotation used to define modeling parameters for shear-controlled walls and coupling beams, respectively, and (3) modeling parameters can be converted to strain limits by dividing by an assumed hinge length, which is convenient where fiber models are used, which is becoming increasingly popular in engineering practice.

For the proposed backbone relation shown in Figure 1-11b, two new modeling parameters are introduced, Parameters c'_{nl} and d'_{nl}, to represent the post-yield strength gain (i.e., ratio of ultimate strength to yield strength, $V_{@Mult}/V_{@MyE}$) and the total hinge rotation capacity once the residual strength is reached. Additionally, the ordinate and abscissa for Point C are set equal to the ultimate (peak) lateral strength ($V_{@Mult}$) normalized by $V_{@MyE}$ (i.e., Parameter c'_{nl}) and the total hinge rotation capacity at 20% lateral strength loss from $V_{@Mult}$ (i.e., Parameter d_{nl}), respectively. Therefore, the value for peak strength is defined at the hinge rotation capacity associated with 20% loss in lateral strength.

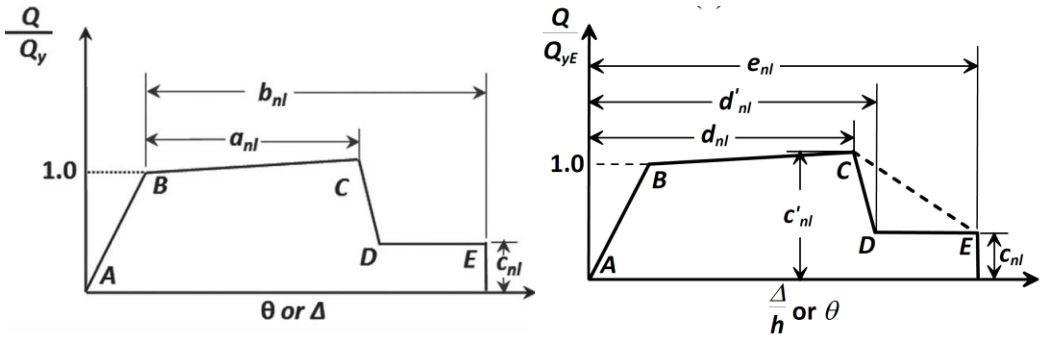

(*a*) ACI 369.1-17 backbone **(*b*) Proposed backbone**

Figure 1-11 Idealized backbone relations to model hinge region of flexure-controlled walls.

The following approach was used to obtain the total hinge rotation capacities from the experimental backbone relations. The steps are given for a typical cantilever wall test (Figure 1-12a), and a similar approach was used for panel or partial height walls. For cases where only the hinge region of the wall was tested, or where hinge rotations were measured in the tests, the approach outlined below was not necessary:

- Modeling parameter d_{nl} (Hinge rotation capacity at Point C, i.e., at 20% lateral strength loss from peak strength):
    - A plastic hinge length (l_p) of half the wall length ($l_w/2$) was assumed for all the walls in the dataset (Figure 1-12*a*). This is consistent with ASCE 41-17 ACI 369.1-17 Section 7.2.2.2. Since wall specimens are typically tested as cantilever or panel walls without story prototype, the limit of one-story height in Section7.2.2.2 was not applicable here.

- The plastic displacement, δ_p, (Figure 1-12c) is obtained by subtracting the elastic first yield displacement, δ_e, (Figure 1-12d) from the total displacement, δ_t, (Figure 1-12b). The plastic rotation capacity, θ_p, is calculated as δ_p divided by the wall height between the center of the hinge (located at $l_w/4$ from the base) and top of the wall.

- The elastic flexural rotation contributed by the hinge region, $\theta_{h,f}$, (Figure 1-12e) is calculated analytically using Equation 1-10. Figure 1-13a shows the contribution of the elastic hinge rotation to the total wall elastic rotation for the Conforming wall dataset. The high values (>60%) are for panel or partial height walls where only the bottom portion of the wall was tested. The figure also shows that a significant part of the total elastic rotation is from the hinge region, which is consistent with the elastic curvature profile, which has a triangular shape with the highest values at the hinge region.

$$\theta_{h,f} = \frac{M_{h,ave}}{E_{cE} I_{eff}} l_p \tag{1-10}$$

  Where $M_{h,ave}$ is the average moment over the hinge region, and $E_{cE}I_{eff}$ is the effective flexural stiffness taken as 0.20 $E_{cE}I_g$ and 0.50 $E_{cE}I_g$ for $P/A_g f'_{cE} \leq 0.05$ and ≥ 0.50, respectively, and linear interpolation is applied for $0.05 < P/A_g f'_{cE} < 0.50$), as proposed in the next section.

- The total hinge rotation capacity is calculated as the sum of θ_p (item *ii* above and Figure 1-12c) and $\theta_{h,f}$ (item *iii* above and Figure 1-12e). Figure 1-13b shows the contribution of the hinge elastic flexural rotation to the total hinge rotation capacity ($\theta_{h,f}/\theta_f$) for the conforming wall dataset. Examination of Figure 1-13b reveals that for the majority of the walls in the dataset, hinge elastic rotation contributes less than 10% of the total hinge rotation capacity.

- Modeling parameter d'_{nl} and e_{nl} [Hinge rotation capacity at Point D (residual strength) and Point E (axial failure)]:

  At these two points, the total hinge rotation capacity was calculated as the total wall displacement (Figure 1-12b) divided by the wall height between the center of the hinge and the top of the wall, assuming a plastic hinge length of $l_w/2$ from the base of the wall. That is, for Points D and E, the elastic deformation contributed by the wall above the hinge is not subtracted as was done for Point C. Therefore, all wall deformation is assumed to be associated with plastic rotation concentrated in the hinge region. Shear displacements at this stage are expected to be small, and are ignored (i.e., not subtracted from total displacement).

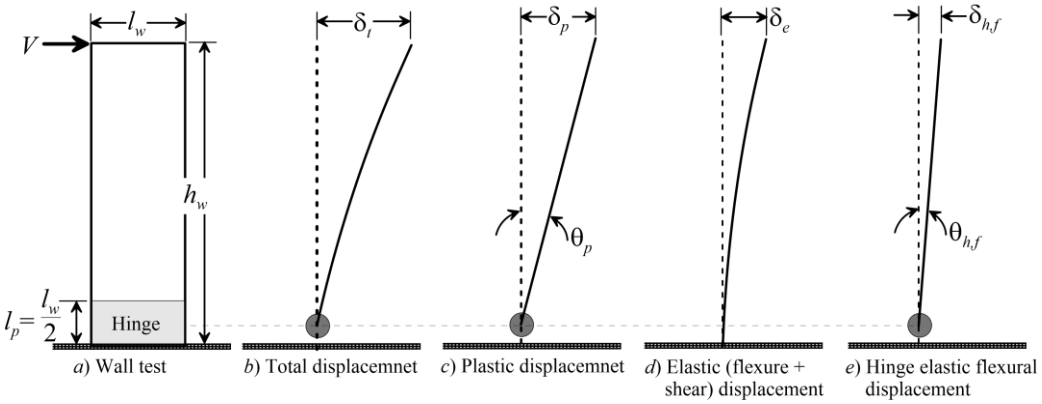

Figure 1-12 Displacement profiles of flexure-controlled walls.

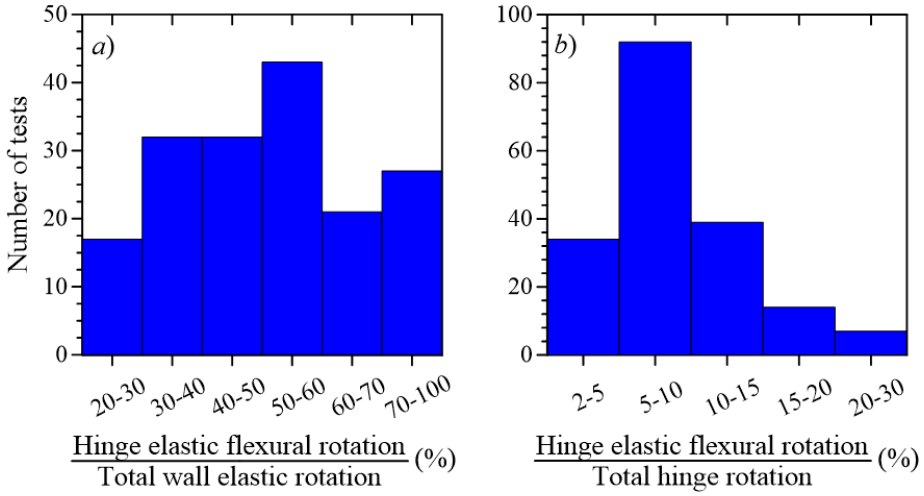

Figure 1-13 Histograms of contribution of computed hinge elastic flexural rotation to: a) the wall total elastic rotation, and b) the total hinge rotation capacity.

1.3.2 Wall Stiffness

1.3.2.1 PROVISIONS AND COMMENTARY OF ACI 369.1-17

Overview

As noted earlier, ACI 369.1-17 Section 7.2.2 Table 5 allows wall $E_{cE}I_{eff}$ to be calculated as 35% of the gross flexural stiffness (Equation 1-11):

$$E_{cE}I_{eff} = 0.35\ E_{cE}I_g \tag{1-11}$$

Where E_{cE} is modulus of elasticity of concrete evaluated using expected material properties and I_g is the moment of inertia of gross concrete section about centroidal axis, neglecting reinforcement.

The following three alternative approaches to compute $E_{cE}I_{eff}$ are given in the commentary of ACI 369.1-17 (C7.2.2):

First: For flexural deformations without the effect of bond slip, $E_{cE}I_{eff}$ can be calculated in accordance with Equation 1-12 (ACI 369.1-17 Eq. C5):

$$E_{cE}I_{eff} = \frac{M_{yE}}{\phi_{yE}} \tag{1-12}$$

Where M_{yE} is the yield moment strength evaluated per ACI 318-19 using expected material properties and applied sustained gravity axial load (N_{UG}), and ϕ_{yE} is the curvature associated with M_{yE}. Curvature may be approximated as $\phi_{yE} = 2f_{ylE}/(l_w E_s)$ planar walls with $N_{UG}/(A_g f'_{cE}) \leq 0.15$ and $\rho_l \leq 0.01$, where f_{ylE} and E_s are the expected yield strength and Young's Modulus of the longitudinal reinforcement, respectively.

Second: $E_{cE}I_{eff}$ can be computed from analytical moment-curvature analysis of the cross-section using Equation 1-13 (ACI 369.1-17 Eq. C6).

$$E_{cE}I_{eff} = \frac{M_{fyE}}{\phi_{fyE}} \tag{1-13}$$

Where M_{fyE} and ϕ_{fyE} are the moment and curvature at first yield, defined when the yield strain of the reinforcing steel is first reached in tension, or when a concrete strain of 0.002 is reached in compression, evaluated using expected material properties and N_{UG}.

Third: For continuous walls, ACI 369.1-17 C7.2.2 provides an approach for capturing the effects of bond slip, where a reduction factor is used to modify $E_{cE}I_{eff}$ of the wall in the story directly above the wall-foundation interface (hinge region) as follows:

$$E_{cE}I_{eff} = \frac{M_{fyE}}{\phi_{fyE}}\left(\frac{h_1}{h_1 l_{sp}}\right) \tag{1-14}$$

Where h_1 is the first-floor height, and l_{sp} is the strain penetration depth approximated using Equation 1-15:

$$l_{sp} = \frac{1}{48}\frac{f_{ylE}}{\sqrt{f'_{cE}}}d_b \tag{1-15}$$

ACI 369.1-17 C7.2.2 provides lower and upper bounds on $E_{cE}I_{eff}$ obtained from Equation 1-11 through Equation 1-14, which are $0.15E_{cE}I_g$ and $0.5E_{cE}I_g$, respectively.

Finally, ACI 369.1-17 Section 7.2.2 Table 5 allows wall shear stiffness to be calculated as "uncracked" gross shear stiffness (Equation 1-16):

$$G_{eff,E}A_w = G_{gE}A_w = 0.4\,E_{cE}A_w \quad (1\text{-}16)$$

Where G_{gE} is concrete gross shear modulus taken as $0.4E_{cE}$, and A_w is area of the wall web cross section.

Evaluation of Provisions and Commentary of ACI 369.1-17

The effective flexural stiffness values ($E_{cE}I_{eff}$) of the 527-wall dataset, as defined in Figure 1-10, are used to evaluate the ACI 369.1-17 stiffness provisions and recommendations summarized in the preceding section. Table 1-2 presents the statistics of the predicted (calculated) $E_{cE}I_{eff}$ values from Equation 1-11 through Equation 1-14, normalized by the $E_{cE}I_{eff}$ values (ratios of calculated-to-experimental $E_{cE}I_{eff}$ values). Figure 1-14 through Figure 1-17 present comparison of the calculated and the experimental $E_{cE}I_{eff}$ results. Discussion of the results is given below.

Figure 1-14(*a*) shows that ASCE 41-17 (Equation 1-11) significantly overestimates $E_{cE}I_{eff}$ at low axial loads ($P/(A_g f'_{cE}) < 0.05$) and significantly underestimates $E_{cE}I_{eff}$ at high axial loads ($P/(A_g f'_{cE}) > 0.20$), with significant dispersion (Table 1-2). It will be shown later that this poor correlation is because using a constant value for $E_{cE}I_{eff}$ ignores the influence of key parameters, such as axial load and boundary longitudinal reinforcement ratio.

Table 1-2 Statistics of the Ratios of Predicted-to-Experimental $E_{cE}I_{eff}/E_{cE}I_g$ Values

Equation	Equation 1-11	Equation 1-12	Equation 1-13[1]	Equation 1-14	
				(a)[2]	(b)[3]
Mean	1.33	1.16	1.12	0.93	1.02
STDV	0.59	0.39	0.35	0.28	0.31
COV	0.44	0.34	0.31	0.31	0.30
Max	3.15	2.74	2.32	1.98	2.13
Min	0.31	0.32	0.28	0.25	0.27
Median	1.26	1.09	1.08	0.9	0.97

[1] ϕ_{yE} is computed as $2f_{ylE}/l_w E_s$
[2] I_{sp} calculated from Equation 1-15 multiplied by 2.0 to account for the influence of reduced scale.
[3] I_{sp} calculated from Equation 1-15 multiplied by 1.0 to account for the influence of reduced scale.

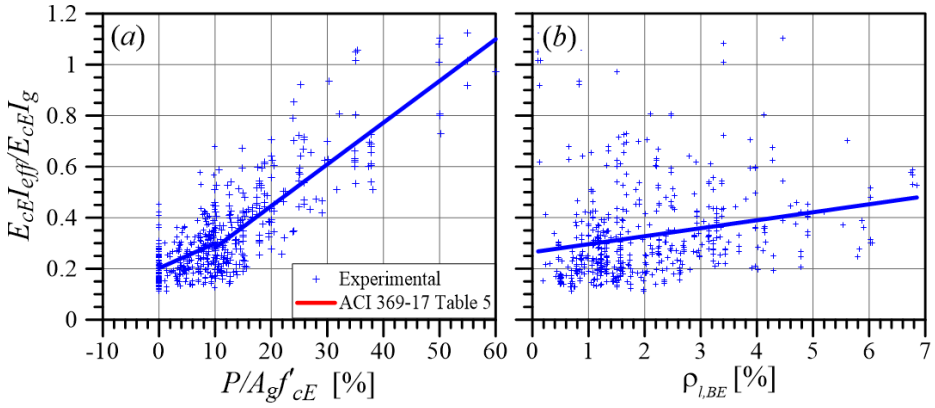

Figure 1-14 Comparison of calculated (Equation 1-11) and experimental $E_{cE}I_{eff}$.

Figure 1-15(*a*) indicates that, for walls with $P/(A_g f'_{cE}) < 0.15$, use of Equation 1-12 results in moderate overestimation of $E_{cE}I_{eff}$, with relatively high dispersion. This is attributed to the fact that with decrease in $P/(A_g f'_{cE})$, the depth of the neutral axis reduces and, consequently, the stress in the tension reinforcement increases, which results in larger lateral displacement contributed by bar slip/extension from the foundation that is not captured by moment-curvature analysis of the cross-section. Motter et al. (2018) observed 15% to 35% reduction in $E_{cE}I_{eff}$ as a result of slip/extension of longitudinal reinforcement from the foundation block for walls subjected to $P/(A_g f'_{cE}) < 0.05$. For higher $P/(A_g f'_{cE})$ values, the contribution of slip/extension from the foundation could approach zero (For example, see Elwood and Eberhard, 2009 for columns), and the wall might be above the balance point on the P-M interaction diagram, which would result in a reduction in moment capacity. In addition, the concrete stress-strain model used to compute moment capacity does not incorporate the influence of concrete confinement. Given that most walls with high $P/(A_g f'_{cE})$ are likely to have some level of confinement, computing moment capacity without the influence of confinement might slightly underestimate the nominal moment capacity and, thus, result in underestimation of effective stiffness.

Additionally, Figure 1-15(*b*) indicates that use of Equation 1-12 for walls with high $\rho_{l,BE}$ (i.e., > 0.02) results in a slight overestimation of $E_{cE}I_{eff}$. This could be attributed to the fact that increase in $\rho_{l,BE}$ helps in spreading of yielding not just over a larger height of the wall but also into the foundation support, which means more contribution from bar slip deformation to yield displacement.

Equation 1-13, which is based on analytical moment and curvature values corresponding to first yield, produces similar results as Equation 1-12, as seen in Figure 1-16 and Table 1-2, with slightly less overestimation and dispersion for walls with $P/(A_g f'_{cE}) < 0.15$. This is because the results indicate that the ratios M_{yE} to M_{fyE} (general yield to first yield) and ϕ_{yE} to ϕ_{fyE} are approximately the same (i.e., ≈1.24). The factors leading to the offsets between the calculated (Equation 1-13) and experimental results are discussed in the preceding paragraphs for results from Equation 1-12.

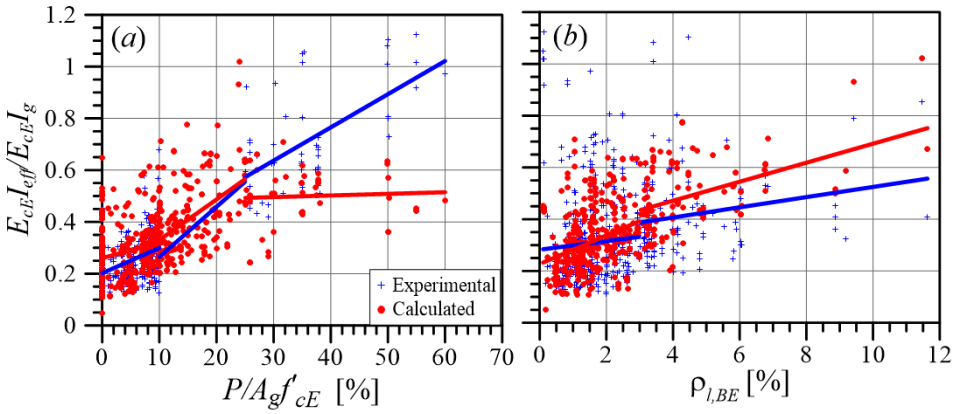

Figure 1-15 Comparison of experimental and calculated (Equation 1-10) $E_{cE}I_{eff}$.

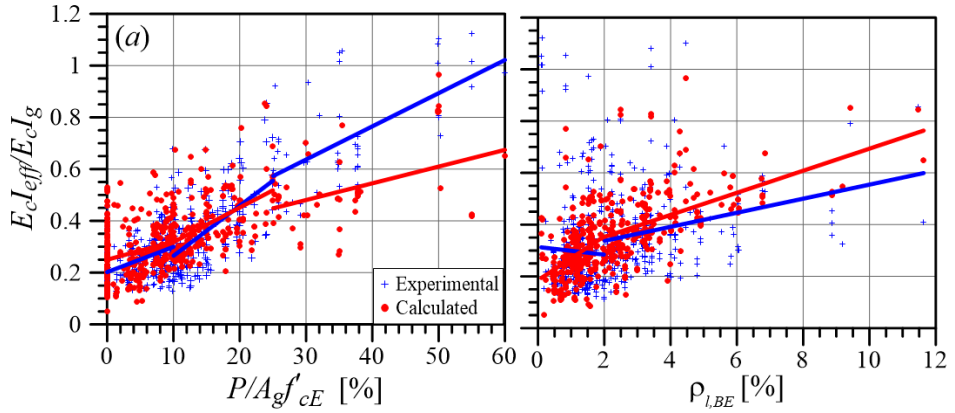

Figure 1-16 Comparison of experimental and calculated (Equation 1-11) $E_{cE}I_{eff}$.

It may not be appropriate to evaluate Equation 1-14, which includes a reduction factor to account for the influence of bond slip on effective stiffness, using results from the dataset because: (1) the reduction factor includes h_1 (first story height), while most tests in the dataset do not have a prototype wall and thus the database does not include story heights, (2) walls are typically tested in laboratories at reduced scales, where in addition to geometry, bar sizes are also scaled down, which influences the contribution of slip/extension deformation to yield deformation and, consequently, the l_{sp} (strain penetration depth) calculated from Equation 1-15. To account for these limitations, two assumptions were made: (1) h_1 is taken as 7 ft, which, assuming a one-half-scale for the entire dataset results in h_1 =14 ft for a full-scale prototype wall, 2) the l_{sp} calculated from Equation 1-15 is multiplied by a factor of 2.0, assuming again a one-half scale for the walls, to account for the reduced scale of the bars. Furthermore, multiplying the l_{sp} calculated from Equation 1-15 by a factor of 1.0 was also considered to highlight the sensitivity of the results to l_{sp}.

The results are presented in Table 1-2 and Figure 1-17. Considering the assumptions made, it can be seen that Equation 1-14 produces results that are in good agreement with the experimental results for walls with $P/(A_g f'_{cE}) < 0.15$ or 0.20. For walls with high $P/(A_g f'_{cE})$, applying this reduction factor leads to further underestimation of $E_{cE}I_{eff}$ relative to Equation 1-12 and Equation 1-13

because, as noted previously, these walls likely experience little or no bar slip/extension. Therefore, no reduction factor should be considered for such walls. Furthermore, Figure 1-17 reveals that the results are only slightly sensitive to the strain penetration depth (l_{sp}).

To conclude, Equation 1-11 through Equation 1-13 overestimate $E_{cE}I_{eff}$ by 12% to 33%, with relatively moderate dispersions. Equation 1-14 produces results with median values better matching the experimental results and dispersions comparable to Equation 1-12 and Equation 1-13; however, these equations require a fair amount of calculations to compute $E_{cE}I_{eff}$. Therefore, simplified $E_{cE}I_{eff}$ values are proposed in the subsequent sections.

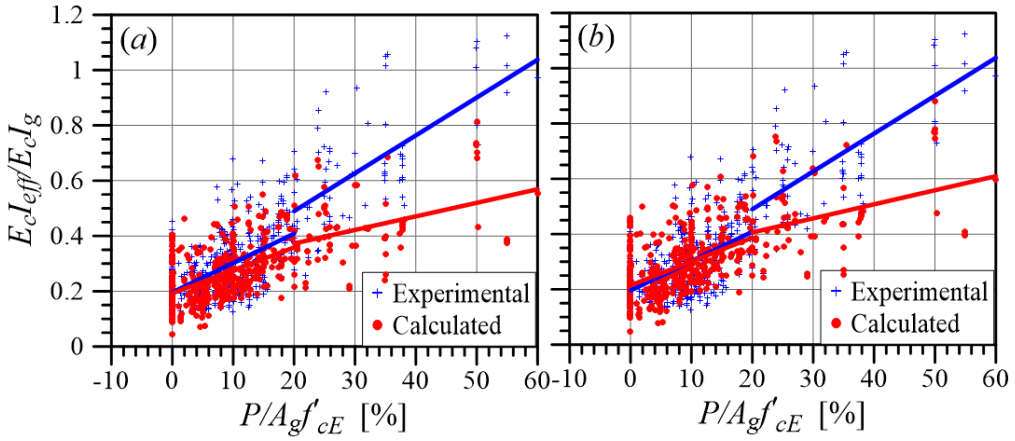

Figure 1-17 Comparison of experimental and calculated (Equation 1-14) $E_{cE}I_{eff}$ considering an h_1 of 7 ft for one-half scale (14 ft for full scale) where l_{sp} calculated from Equation 1-15 and multiplied by: (*a*) 2.0, and (*b*) 1.0.

1.3.2.2 PARAMETERS INFLUENCING WALL FLEXURAL **STIFFNESS**

Uncracked Flexural Stiffness

To identify parameters that are likely to have a significant influence on $E_{cE}I_{uncr}$, review of available literature and a series of linear regression analyses were conducted. It was found that the most influential parameter is axial load ratio, $P/(A_gf'_{cE})$, with a correlation coefficient (R) of 0.58, as shown in Figure 1-18(*a*). This is because presence of axial load leads to an increase in cracking moment capacity, while cracking curvature is not influenced by axial load. It can also be seen from Figure 1-18(*a*) that uncracked flexural stiffness ranges (on average) from 0.50 to 1.40 of the gross section stiffness ($E_{cE}I_g$) as $P/(A_gf'_{cE})$ increases from 0.0 to 0.60. The low values, which are mostly for walls with low to moderate $P/(A_gf'_{cE})$, might be due to the influence of microcracks and shrinkage. The values of $E_{cE}I_{uncr}/E_{cE}I_g > 1.0$ might be due to presence of longitudinal reinforcement in the cross-section that is ignored in the calculation of I_g.

Concrete compressive strength (f'_{cE}) has some influence on $E_{cE}I_{uncr}$ because of its influence on tension stiffening, elastic modulus, and modulus of rupture. However, the influence, with an R of 0.23, is not significant (Figure 1-18*b*) and is already included in the $P/(A_gf'_{cE})$ parameter.

Figure 1-18(c) indicates that M/Vl_w also has a significant influence on $E_{cE}I_{uncr}$; however, this is not a causal relationship. Most slender walls (with high M/Vl_w) have moderate to high axial loads, as indicated by Figure 1-18(c); therefore, the parameter that drives the trend in Figure 1-18(**c**) is primarily $P/(A_g f'_{cE})$, not M/Vl_w.

It should be noted that, for most walls in the dataset, cracking deformation is very small (ranging from < 0.04 to 0.1 in. (1 to 2.5 mm)), and that accurate measurement of such small displacements is difficult. Additionally, this damage state in the database is based on visual observation of first flexural cracks reported by the authors who conducted the tests, which might also include some subjectivity. These two factors, among others, might contribute to the significant dispersion of the data.

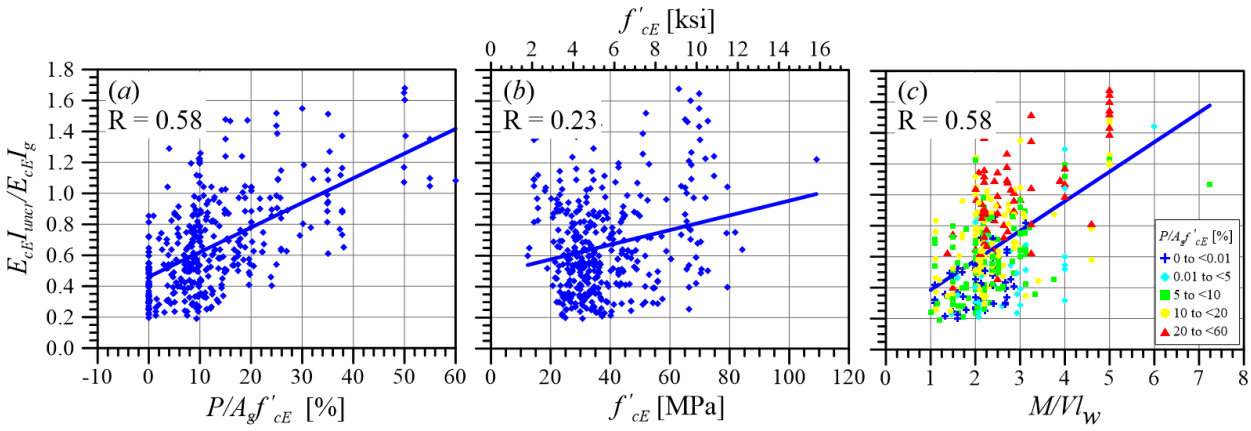

Figure 1-18 Influence axial load, concrete strength, and shear-span-ratio on $E_{cE}I_{uncr}$. (Note: R = correlation coefficient)

Effective "Cracked" Flexural Stiffness

Parameters that were found to influence $E_{cE}I_{eff}$ include $P/(A_g f'_{cE})$, yield strength and quantity of longitudinal reinforcement in the boundary region (f_{yE} and $\rho_{l,BE}$), and f'_{cE}, as shown in Figure 1-19. The influence of axial load on stiffness of concrete members is widely recognized in many research studies and design codes/guidelines (For example, Elwood and Eberhard, 2009; Khuntia and Ghosh, 2004a; Fenwick and Bull, 2000; Adebar et al., 2007; NZS 3101: Part 2:2006; ACI 318-19 Table 6.6.3.1.1*b*). As shown in Figure 1-19(*a*), $P/(A_g f'_{cE})$ has the strongest correlation with $E_{cE}I_{eff}$, with an R of 0.82. The trend shown in Figure 1-19a is similar to that observed by Elwood and Eberhard (2009) for columns.

An increase in longitudinal reinforcement ratio in the tension zone ($\rho_{l,BE}$) results in spread of yielding and development of secondary cracks over a larger height of the wall, as opposed to a one or two major cracks at or near the critical section. Furthermore, doubling $\rho_{l,BE}$, assuming everything else is constant, would be expected to have little influence on yield curvature (ϕ_y) since ϕ_y is primarily a function of wall length and reinforcement yield strain, i.e., $\phi_y \approx 2f_y/l_w E_s$ or $\phi_y \approx (0.0025 \text{ to } 0.0035)/l_w$ (Thomsen and Wallace, 2004), but would theoretically be expected to approximately double the yield

flexural strength and thereby increase $E_{cE}I_{eff}$ by the same amount (ATC 72, 2010). It is this reasoning that gives rise to the concept of "stiffness is proportional to strength" (Priestley and Kowalsky, 1998; Priestley et al., 2007; Paulay, 2002). However, the trend in Figure 1-19b does not show as big of an influence as the above concept suggests, even for slender walls. This is likely due to: (1) the influence of other parameters (For example, axial load) which cause large dispersion in the data, and (2) with increase in $\rho_{l,BE}$, the wall flexural strength increases, which results in flexural cracking spreading over a larger zone along the wall height from the foundation support. This stiffness loss reduces the stiffness gain due to large $\rho_{l,BE}$ in the lower portions of the wall. Figure 1-19c shows that the influence of $\rho_{l,BE}$ on $E_{cE}I_{eff}$ is more pronounced for walls subjected to low-to-moderate $P/(A_g f'_{cE})$.

Yield strength of longitudinal reinforcement (f_{yE}) has a limited influence on $E_{cEE}I_{eff}$ since f_{yE} is one of the factors affecting both first yield moment and curvature (i.e., $\phi_y \approx 2f_y/(l_w E_s)$). Walls with high yield strength reinforcement have higher yield moment and higher yield curvature (due to higher yield strain) and, consequently, the value of $E_{cE}I_{eff}$ is largely insensitive to changes in f_{yE}, as suggested by Figure 1-19d.

Use of high strength concrete modestly increases E_{cE}, tension stiffening, tensile strength, and wall flexural strength. However, the impact of f'_{cE} on $E_{cE}I_{eff}/E_{cE}I_g$ is statistically insignificant, as shown in Figure 1-19e. The influence of f'_{cE} is more noticeable on $E_{cE}I_{uncr}$ than $E_{cE}I_{eff}$.

Figure 1-19f shows the combined influence of f'_{cE}, f_{yE}, and $\rho_{l,BE}$ on $E_{cE}I_{eff}$, with an R of 0.29, which does not improve the correlation compared to the influence of $\rho_{l,BE}$ alone in Figure 1-19b.

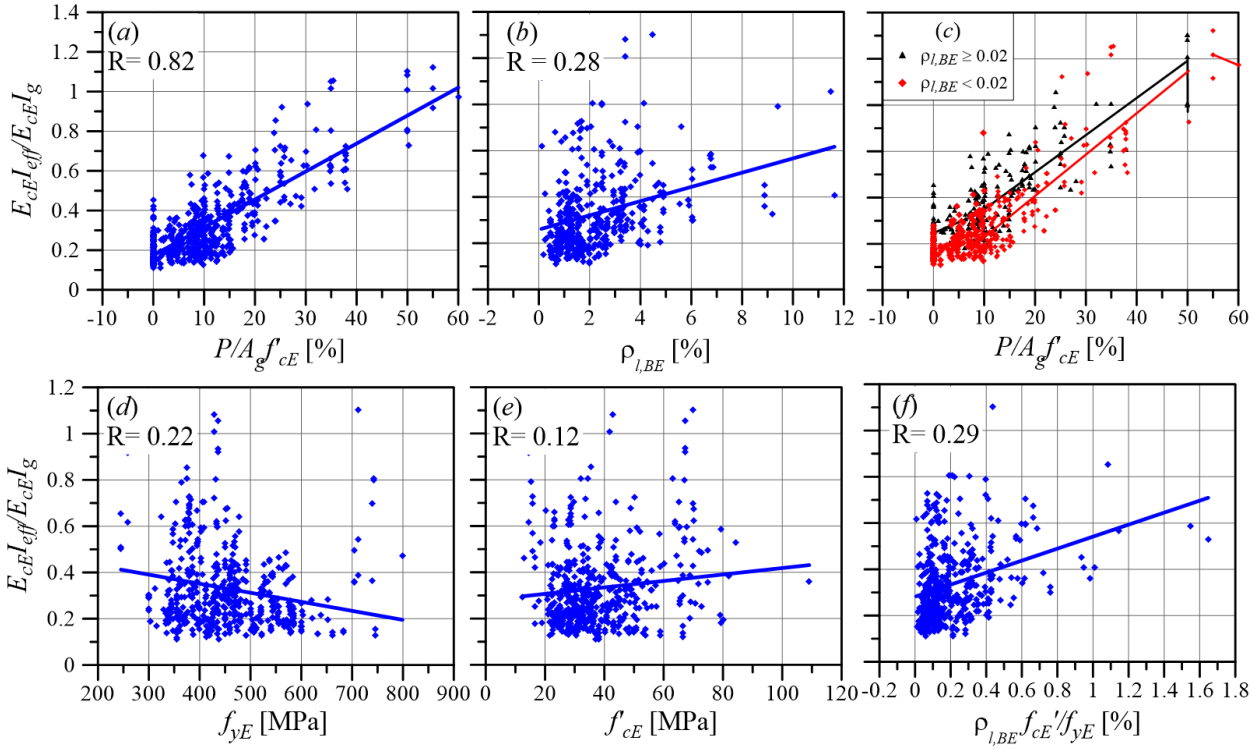

Figure 1-19 Influence of key parameters on $E_{cE}I_{eff}$. (Note: R=correlation coefficient).

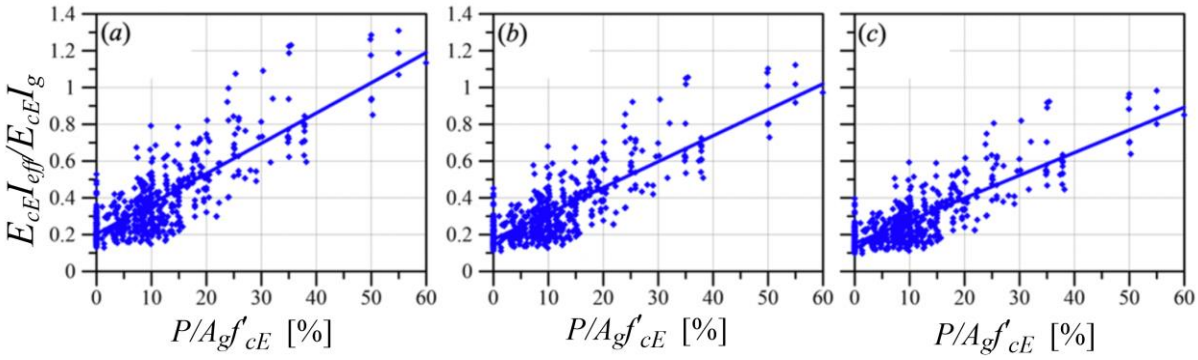

Figure 1-20 Sensitivity of $E_{cE}I_{eff}$ to the reduction factor used in Equation 1-8: a) 0.6, b) 0.7, and c) 0.8.

Figure 1-20 presents sensitivity of $E_{cE}I_{eff}$ to the reduction factor used in Equation 1-8 to convert secant stiffness corresponding to general yield to effective stiffness corresponding to first yield. Given the dispersion in the data and other uncertainties (i.e., modeling and loading), changing this reduction factor does not produce significant changes in the correlation. Therefore, the 0.7 reduction factor was adopted in this study to compute $E_{cE}I_{eff}$, which was backed by some limited experimental data, as noted earlier.

1.3.2.3 PROPOSED RECOMMENDATIONS FOR FLEXURAL AND SHEAR RIGIDITIES

Uncracked Flexural Rigidity

Flexural cracking is assumed to occur where the moment demand exceeds the cracking moment strength calculated using the modulus of rupture provided in ACI 318-19 using the expected material properties. Based on the results presented earlier, the model shown in Figure 1-17 (black line) is proposed, for which $E_{cE}I_{uncr}/(E_{cE}I_g)$ ranges on average from 0.50 to 1.00 for $P/(A_g f'_{cE})$ increasing from 0.0 to 0.30. If wall tests with no axial load are excluded, the blue trend line will move closer to the model (black line). This model results in a mean and COV of 1.12 and 0.42, respectively. The model is also presented in a tabulated format in Table 1-3.

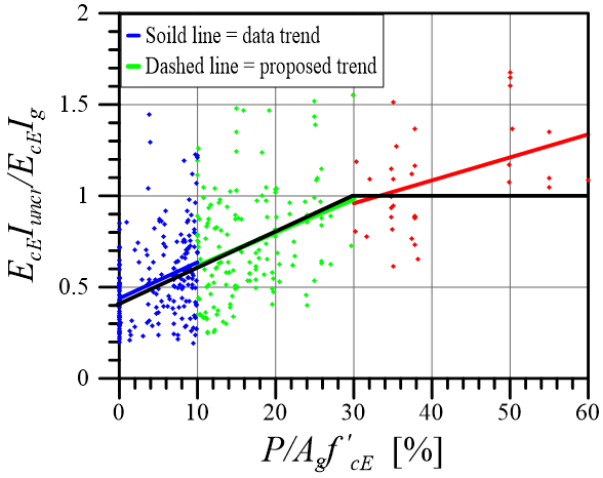

Figure 1-21 Linear regression lines to the data and the proposed model for $E_{cE}I_{uncr}$.

Table 1-3 Proposed Values for Uncracked Wall Flexural Stiffness ($E_{cE}I_{uncr}$)

$\frac{P}{A_g f'_{cE}}$	$\frac{E_{cE}I_{uncr}}{E_{cE}I_g}$
≤ 0.00	0.50
≥ 0.30	1.00

Note: Values between those listed should be determined by linear interpolation

As noted earlier, ACI 369.1-17 currently does not provide provisions to estimate wall flexural stiffness for cases where little or no cracking is expected to occur. Such provisions, however, can be found in other codes and documents (i.e., ACI 318-19 Table 6.6.3.1.1a; CSA A23.3-14; FEMA 356 Table 6-5; NZS 3101: Part 2:2006; Eurocode 8-2004). For comparison with the proposed model, these existing models were reviewed and evaluated using the dataset, and the results are presented in Table 1-4.

Table 1-4 Existing Models for Flexural Stiffness of Uncracked Walls or Walls with Limited Cracking

Model	ACI 318-19-Table 6.6.3.1.1a CSA A23.3-14	FEMA 356 Table 6-5	NZS 3101: Part 2:2006 Serviceability limit (μ=1.25)	NZS 3101: Part 2:2006* Serviceability limit (μ=3)	Eurocode 8-2004	PEER/TBI-10* LATBSDC-14 (Service level)	Proposed Model
$\frac{E_{cE}I_{uncr}}{E_{cE}I_g} =$	0.7	0.8	1.0	$0.7 \geq \left(0.5 + \frac{P}{A_g f'_{cE}}\right) \geq 0.5$	0.5	0.75	$1.0 \geq \left(0.5 + \frac{P}{A_g f'_{cE}}\right) \geq 0.5$

Table 1-4 Existing Models for Flexural Stiffness of Uncracked Walls or Walls with Limited Cracking (continued)

Model	ACI 318-19-Table 6.6.3.1.1a CSA A23.3-14	FEMA 356 Table 6-5	NZS 3101: Part 2:2006 Serviceability limit (μ=1.25)	NZS 3101: Part 2:2006* Serviceability limit (μ=3)	Eurocode 8-2004	PEER/TBI-10* LATBSDC-14 (Service level)	Proposed Model
Mean	1.32	1.51	1.89	1.11	0.95	1.42	1.12
STDV	0.65	0.75	0.93	0.49	0.47	0.70	0.38
COV	0.49	0.49	0.49	0.44	0.49	0.49	0.42
MAX	3.65	4.17	5.21	3.09	2.60	3.91	3.42
MIN	0.42	0.48	0.60	0.37	0.30	0.45	0.39
Median	1.17	1.33	1.66	1.01	0.83	1.25	1.07

Note: A limited level of cracking is expected at service loading.

Effective "Cracked" Flexural Rigidity

As noted previously, $P/(A_g f'_{cE})$ is the most influential parameter on $E_{cE}I_{eff}$. Therefore, a model, which takes the form of a piece-wise line, seems to fit the regression lines well, as shown in Figure 1-22, where the colored lines are regression lines of the data, and the black line is the proposed model. This model is also shown in a tabulated format in Table 1-5.

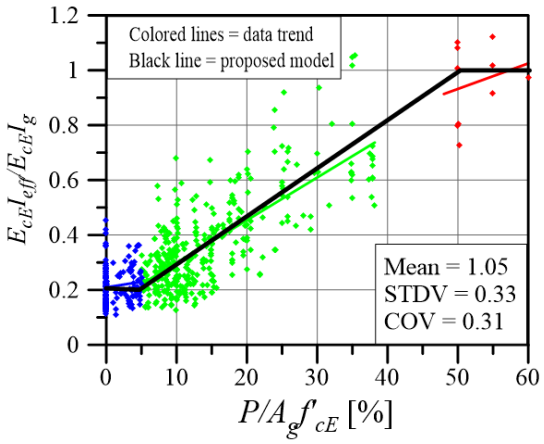

Figure 1-22 Linear regression lines to the data and the proposed model for $E_{cE}I_{eff}$.

Table 1-5 Proposed Values for Effective Flexural Stiffness ($E_{cE}I_{eff}$)

$\frac{P}{A_g f'_{cE}}$	$\frac{E_{cE}I_{eff}}{E_{cE}I_g}$
≤ 0.05	0.20
≥ 0.50	1.00

Note: Values between those listed should be determined by linear interpolation

A more detailed model that includes the $\rho_{l,BE}$ as a secondary parameter in addition to axial load is proposed as given in Equation 1-17 and Table 1-6. Use of this refined model leads to slightly more accurate results, especially for walls with low to moderate axial loads. As seen in Figure 1-23b, $E_{cE}I_{eff}$ for walls with $P/(A_g f'_{cE}) \leq 0.20$ increases by factors of about 1.5 to 2 on average when $\rho_{l,BE}$ increases from 0.01 to 0.03.

$$\frac{E_{cE}I_{eff}}{E_{cE}I_g} = 0.10 + 1.5\,\frac{P}{A_g f'_{cE}} + 3.5\rho_{l,BE} \leq 1.0 \qquad (1\text{-}17)$$

Comparison of predicted (Equation 1-17) and experimentally obtained $E_{cE}I_{eff}$, along with the statistics, are presented in Figure 1-24. The comparison indicates that the detailed model only modestly reduces the prediction error compared to the simplified model (Figure 1-22).

Table 1-6 Proposed Values for $E_{cE}I_{eff}$ as a Function of $P/(A_g f'_{cE})$ and $\rho_{l,BE}$

$\frac{P}{A_g f'_{cE}}$	$\rho_{l,BE}$	$\frac{E_{cE}I_{eff}}{E_{cE}I_g}$
≤ 0.05	≥ 0.01	0.20
	≤ 0.03	0.30
≥ 0.50	≥ 0.01	0.90
	≤ 0.03	1.00

Note: Values between those listed should be determined by linear interpolation

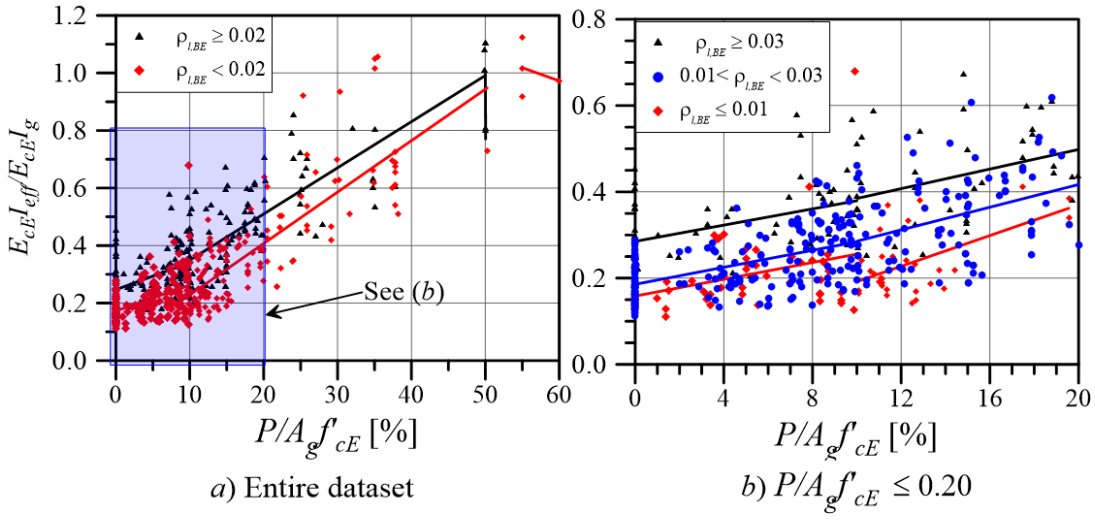

Figure 1-23 Influence of longitudinal reinforcement ratio ($\rho_{l,BE}$) on $E_{cE}I_{eff}$.

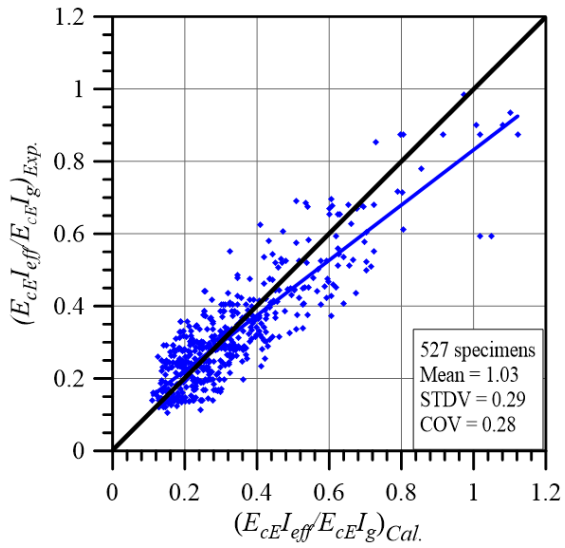

Figure 1-24 Comparison of experimental and calculated $E_{cE}I_{eff}$ from Equation 1-17.

Uncracked Shear Rigidity

Shear cracking is assumed to occur where the wall shear stress demand exceeds $2\sqrt{f'_{cE}}$ (psi). For upper stories of a flexure-controlled wall, where shear demands are $<2\sqrt{f'_{cE}}$ (psi), it is proposed that the shear response of the wall be modeled using the gross shear modulus (G_{gE}) taken as $0.4E_{cE}$.

Cracked Shear Rigidity

For cracked shear rigidity ($G_{eff,E}$), the dataset of 64 flexure-controlled wall tests described earlier with measured shear force-shear deformation backbones were reviewed. Figure 1-25 presents $G_{eff,E}$ of the dataset normalized by the gross shear modulus (G_{gE}) taken as $0.4E_{cE}$, which indicates that shear stress at *General Yield* point for all the walls in the dataset exceeded the cracking shear strength of

concrete [$V_{cE} = 2\sqrt{f'_{cE}}$ (psi)]. Based on the results of Figure 1-25, a constant $G_{eff,E}$ of $G_{gE}/3$ is proposed to be used to model shear response of flexure-controlled walls.

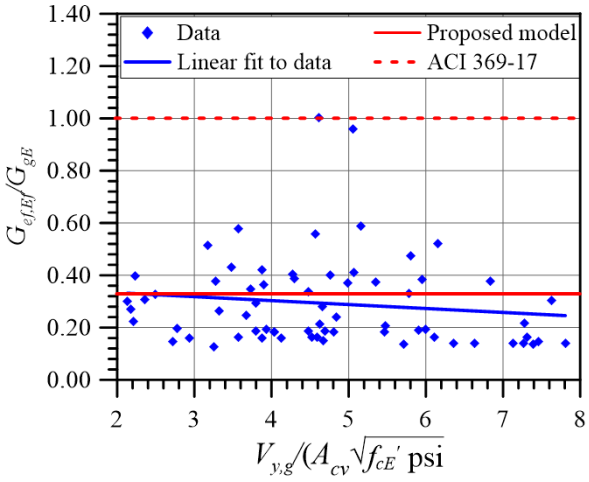

Figure 1-25 Effective shear modulus results from the dataset of 64 wall tests.

1.3.3 Wall Moment Strength

In this section, moment strength values and relations for each point on the backbone curve are explored in the order they appear on the idealized backbone presented in Figure 1-11.

1.3.3.1 CONFORMING WALLS

The moment strength of each point on the backbone curve is developed in the following subsections using the experimental results from the conforming wall dataset.

Yield Strength at Point B

The calculated yield moment strength, $M_{yE,cal}$, is evaluated as defined in ACI 369.1-17 and ASCE/SEI 41-17 based on the ACI 318-19 approach but using expected material properties. Figure 1-26 presents the ratio of the calculated yield moment strength ($M_{yE,cal}$) to the experimental (observed) yield moment strength ($M_{yE,exp}$). It can be seen that use of $M_{yE,cal}$ accurately captures the strength at yield ($M_{yE,exp}$) with a mean and coefficient of variation (COV) of 1.01 and 0.12, respectively.

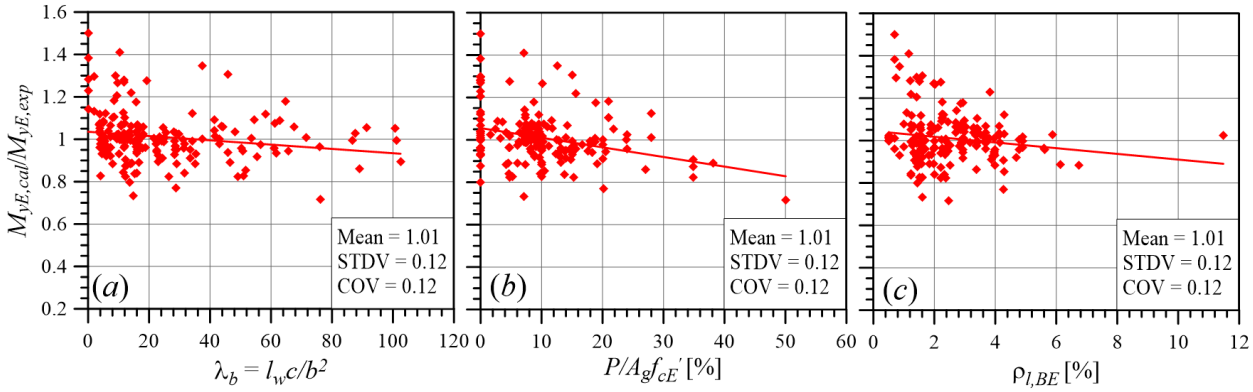

Figure 1-26 Ratio of calculated-to- experimental yield moment strength ($M_{yE,cal}/M_{yE,exp}$) for the conforming wall dataset.

Peak Strength at Point C

As noted previously, this point has an ordinate equal to the ultimate (peak) lateral strength ($V_{@Mult}$) normalized by $V_{@MyE}$ (i.e., Parameter c'_{nl}). Figure 1-27 shows the ratio of the experimental wall ultimate moment strength ($M_{ult,exp}$) to the calculated $M_{yE,cal}$ and indicates that, on average, $M_{ult,exp}$ is 14% higher than $M_{yE,cal}$. Therefore, Parameter c'_{nl} is taken as 1.15 (i.e., M_{ultE} =1.15 M_{yE}) for simplicity and to be consistent with Parameter c'_{nl} for nonconforming walls, as discussed later.

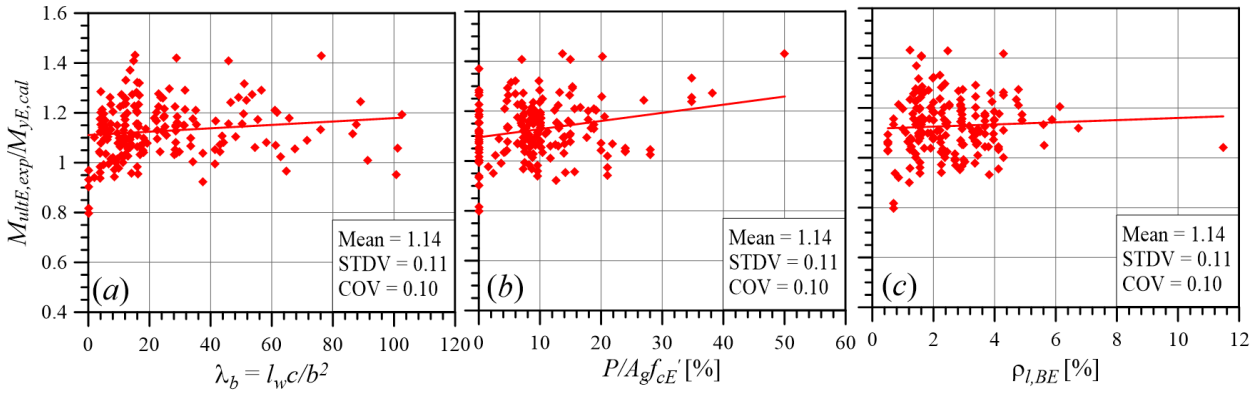

Figure 1-27 Ratio of experimental ultimate to yield moment strength ($M_{ult,exp}/M_{yE,cal}$) for the conforming wall dataset.

Residual Strength at Point D

As shown in Figure 1-11, Point D defines the slope of the strength degrading branch of the backbone relation and has an ordinate equal to the wall residual lateral strength ratio (Parameter c_{nl}). The reduced subset of 101 walls that included information on axial failure was studied to identify parameters that influence residual strength ratio (Parameter c_{nl}). Figure 1-28 shows the variation of experimental residual moment strength, $M_{residual}$, of the dataset normalized by the yield moment strength, M_{yE}, which is equal to Parameter c_{nl}, against λ_b. It is clear that residual strength does not correlate well with parameters such as the slenderness parameter $\lambda_b = l_w c/b^2$ (where c = depth of

neutral axial, as defined previously) and $P/(A_g f'_{cE})$, which significantly impact deformation at this point (Parameter d'_{nl}), as will be shown later. However, from Figure 1-28 (*a*), it can be seen that the walls with $P/A_g f'_{cE} \geq 0.2$ (~ 20 walls) have little or no residual strength, and that walls with $\lambda_b > 70$ have no residual strength regardless of the level of axial load or shear stress (i.e., little or no post-peak deformation capacity). Additional study may provide improved relations; however, the models shown in Figure 1-28 (*a*) are proposed to derive Parameter c_{nl} for conforming walls.

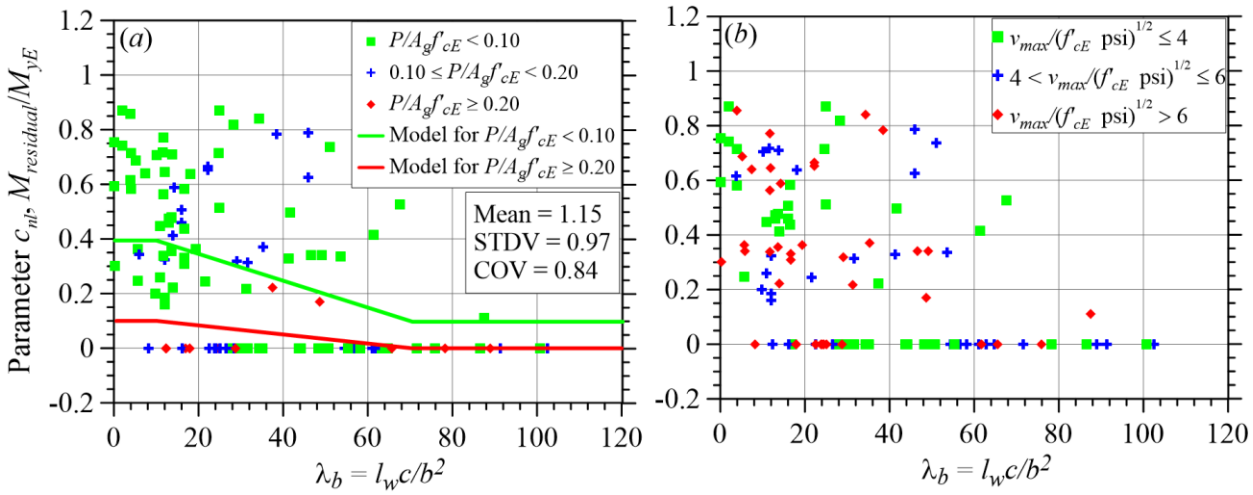

Figure 1-28 Proposed models for parameter c_{nl} for conforming flexure-controlled walls.

1.3.3.2 NONCONFORMING WALLS

Similar to conforming walls, the strength of each response point on the idealized backbone relation (Figure 1-11) is developed in the following subsections using the experimental results from the nonconforming wall dataset.

Yield Strength at Point B

The calculated yield moment strength, $M_{yE,cal}$, is evaluated as defined in ACI 369.1-17 and ASCE/SEI 41-17 based on the ACI 318-19 approach but using expected material properties. Figure 1-29 presents the ratio the calculated yield moment strength ($M_{yE,cal}$) to the experimental (observed) yield moment strength ($M_{yE,exp}$) for the nonconforming dataset. It can be seen that the calculated M_{yE} on average only slightly underpredicts the yield moment strength ($M_{yE,exp}$), except for walls with $P/(A_g f'_{cE}) > 0.40$. Given that nonconforming walls encountered in practice typically have axial loads below $0.2A_g f'_{cE}$, taking strength at Point B as $M_{yE,cal}$ is proposed, similar to conforming walls.

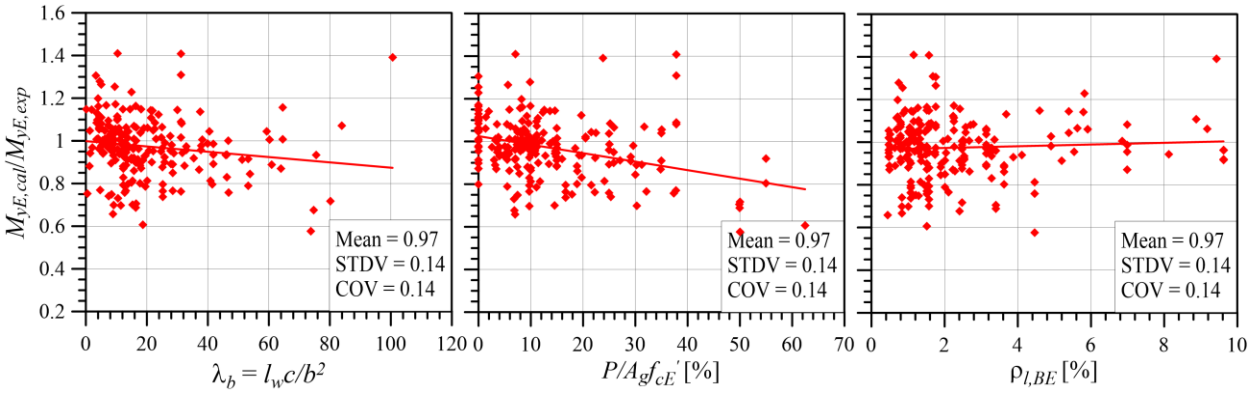

Figure 1-29 Ratio of calculated-to-experimental yield moment strength ($M_{yE,cal}/M_{yE,exp}$) for the nonconforming wall dataset.

Peak Strength at Point C

Figure 1-30 presents the ratio of the ultimate moment strength obtained during the test ($M_{ultE,exp}$) to the calculated $M_{yE,cal}$ for the nonconforming dataset, which shows that, on average, $M_{ultE,exp}$ is 18% higher than $M_{yE,cal}$. This value is slightly larger than that of conforming walls. Based on these results and results of the conforming wall dataset, Parameter c'_{nl} is taken as 1.15 (i.e, M_{ultE} =1.15 M_{yE}).

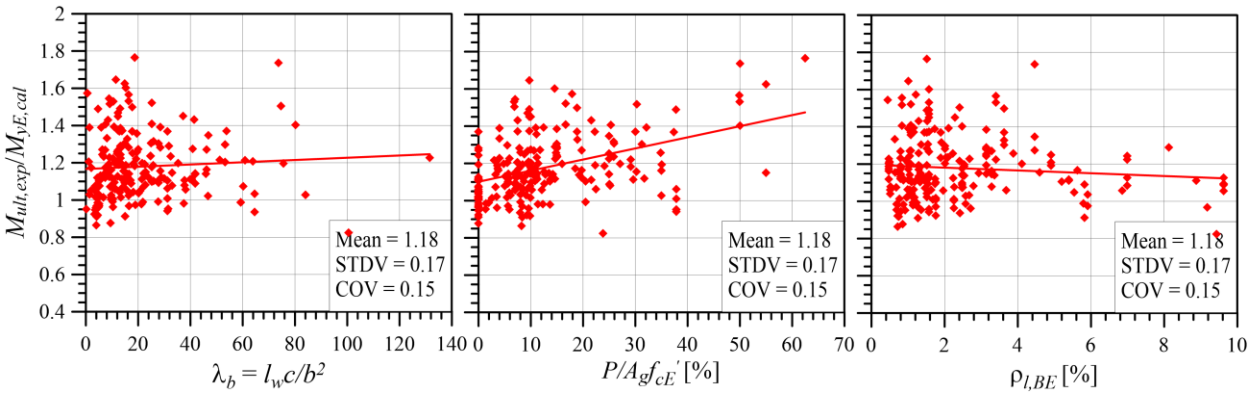

Figure 1-30 Ratio of experimental ultimate-to-yield moment strength ($M_{ult,exp}/M_{yE,cal}$) for the nonconforming wall dataset.

Residual Strength at Point D

Figure 1-31 shows the residual moment strength ($M_{residual}$) of the dataset normalized by M_{yE} (i.e., Parameter c_{nl}), and reveals that, similar to conforming walls, Parameter c_{nl} does not correlate well with the parameters that significantly impact Parameter d'_{nl} (as will be shown later) such as λ_b and $P/(A_g f_{cE})$. In the absence of additional studies, the piecewise best-linear fits (models) shown in Figure 1-31 are proposed to derive Parameter c_{nl} for nonconforming walls.

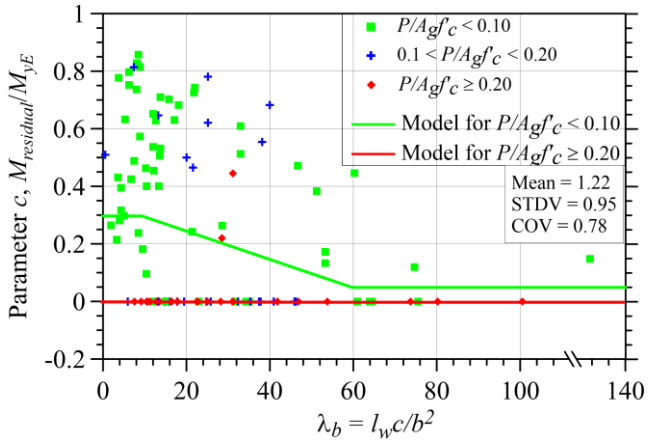

Figure 1-31 Proposed models for Parameter c_{nl} for nonconforming flexure-controlled walls.

1.3.4 Modeling Parameters and Acceptance Criteria

1.3.4.1 NONLINEAR MODELING PARAMETERS

Conforming Walls

The total hinge rotation capacity of each point on the proposed backbone in Figure 1-11 are presented in the following sections using the experimental results from the conforming wall dataset.

Parameter d_{nl} (Hinge rotation Capacity at Point C)

As discussed previously, this point is assumed to have an ordinate that is equal to the peak lateral strength ratio (Parameter c'_{nl}), whereas the abscissa is equal to the hinge rotation capacity corresponding to 20% lateral strength loss (Parameter d_{nl}).

Abdullah and Wallace (2019) analyzed the Conforming Wall dataset and found that the following parameters had a significant impact on lateral drift capacity at 20% lateral strength loss: (1) ratio of wall neutral axis depth-to-width of compression zone (slenderness of the compression zone), c/b, (2) ratio of wall length-to-width of compression zone (slenderness of the cross-section), l_w/b, (3) ratio of maximum wall shear stress to the square root of tested concrete compressive strength, $V_{max}/\sqrt{f'_c}$, and (4) configuration of the boundary transverse reinforcement used, i.e., use of overlapping hoops (Figure 1-32i) versus a single perimeter hoop with intermediate legs of crossties (Figure 1-32ii). They also concluded that use of a combined cross-sectional slenderness parameter $\lambda_b = l_w c/b^2$ provided an efficient means to account for slenderness of the cross section (l_w/b) and the slenderness of the compression zone on the cross section (c/b). Parameter $\lambda_b = l_w c/b^2$ considers the impact of concrete and reinforcement material properties, axial load, wall cross-section geometry, and quantities and distributions of longitudinal reinforcement at the boundary and in the web.

Furthermore, Abdullah and Wallace (2019) also investigated the impact of other parameters deformation capacity at this point such as the: (1) area ratio of provided-to-required (per ACI 318-19 Section 18.10.6.4) boundary transverse reinforcement, $A_{sh,provided}/A_{sh,required}$, (2) ratio of vertical spacing of boundary transverse reinforcement to the diameter of the smallest longitudinal reinforcement, s/d_b, (3) distance between laterally supported boundary longitudinal reinforcement, h_x, normalized by $h_{x,max}$ or width of compression zone, b, and (4) degree of lateral support provided (support for all boundary longitudinal bars versus every other bar). It was concluded that these detailing parameters did not significantly impact wall lateral drift capacity at 20% lateral strength loss (Figure 1-33) for walls with well-detailed boundary elements. A more in-depth discussion of these parameters can be found in Abdullah and Wallace (2019) and Abdullah (2019).

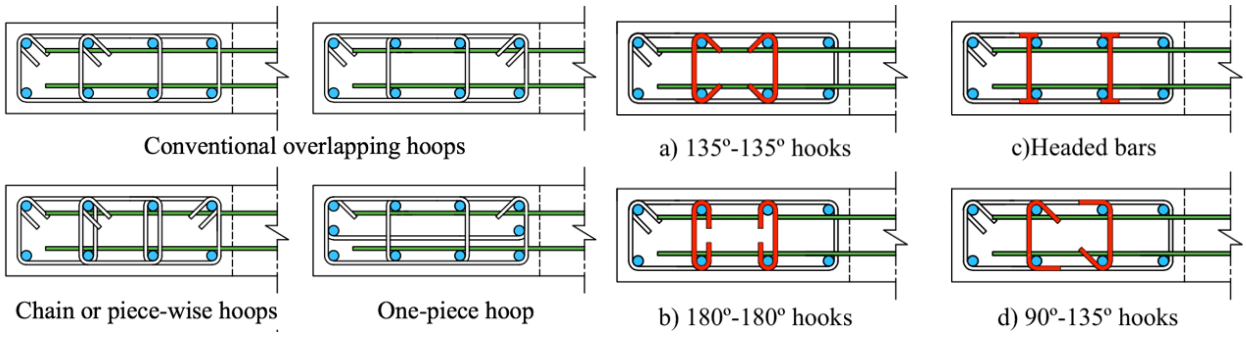

i) Overlapping hoops **ii) Perimeter hoop with crossties**

Figure 1-32 Examples of boundary transverse reinforcement configurations of conforming walls.

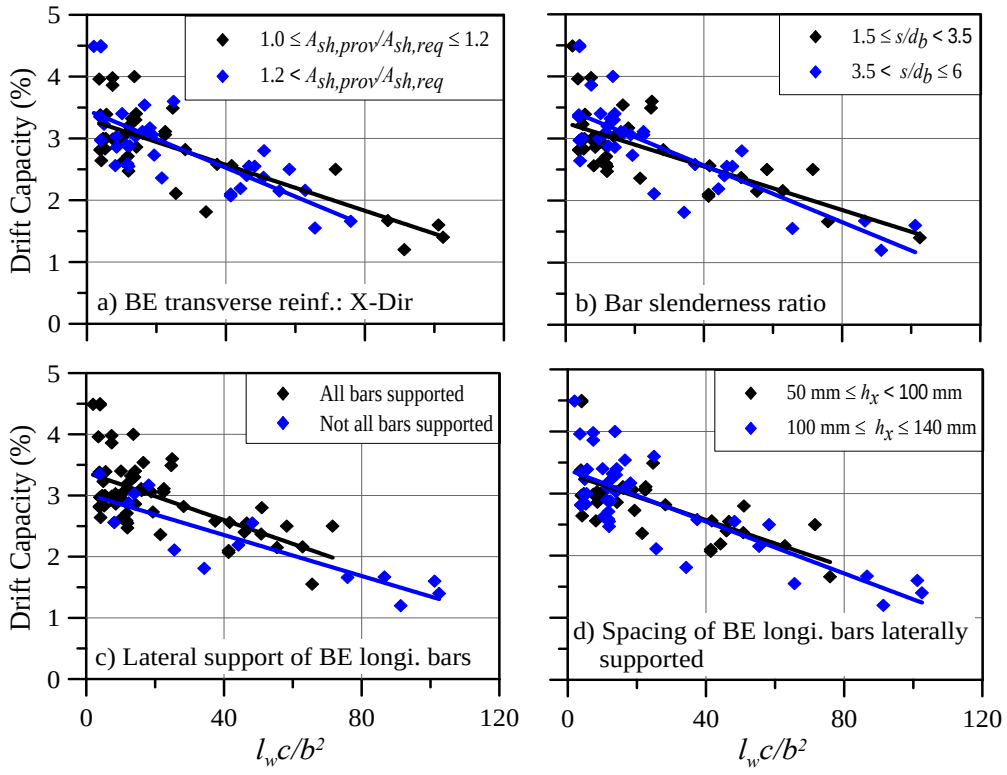

Figure 1-33 Impact of detailing variables on drift capacity of conforming walls (Note 1 mm = 0.0394 in.).

Figure 1-34 shows variation of Parameter d_{nl} of the conforming dataset as a function of the aforementioned four significant parameters (i.e., $\lambda_b = l_w c/b^2$, $V_{max}/\sqrt{f'_{cE}}$, and overlapping hoops), with piecewise best-linear fits of the data (proposed models) to derive the updated Parameter d_{nl} values. Figure 1-34a reveals that use of overlapping hoops for values of $\lambda_b > 40$ (i.e., walls with slender cross-sections and large compression depths) results in a significant increase in hinge rotation capacity because the behavior of walls with small compression zones ($c/b < 1$) tends to be controlled by bar fracture rather than flexural compression failure. It is noted that for walls with overlapping hoops and high shear stresses, only three tests exist for $\lambda_b > 40$ (Figure 1-34b). A detailed discussion on the impact of overlapping hoops on wall deformation capacity can be found in Abdullah and Wallace (2019), Abdullah (2019), and Segura and Wallace (2018a).

The term b represents the width of the flexural compression zone of the wall section. For a planar wall, b_s is equal to t_w. The width of the flexural compression zone, b, for other conditions is illustrated in Figure 1-35. For cases with a large b, such as where the barbell or flange of a wall is in compression, deformation capacity is likely to be relatively large. However, cases with a barbell or flange in tension and a thin wall web in compression may result in large values of $l_w c/b^2$ and higher shear demands such that lower deformation capacities are likely. For cases where b_s varies over c, or where c varies over b, representative or weighted average values of b and c should be used, as illustrated in Figure 1-35.

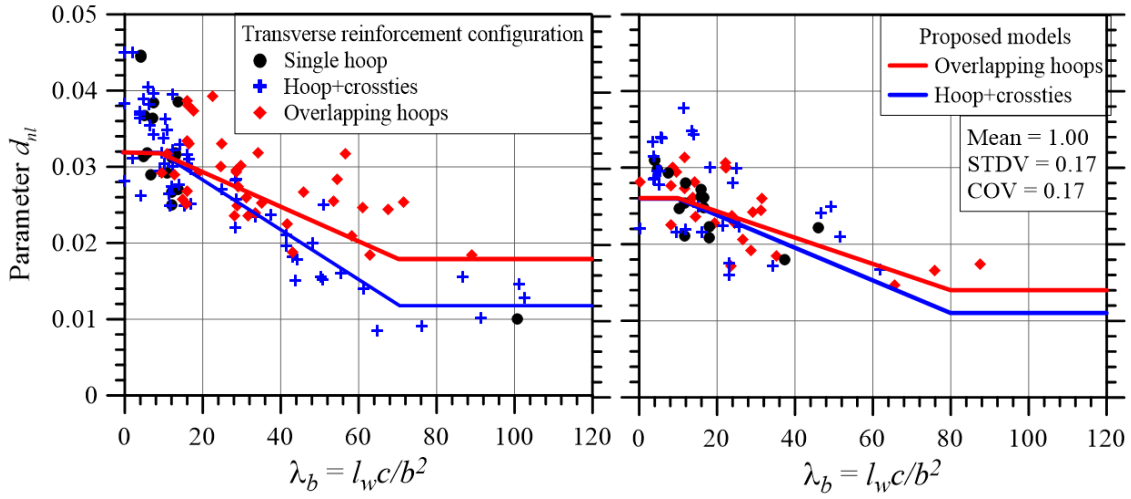

(a) $v_{max}/\sqrt{f'_{cE}(psi)} \le 4$ $\left(\le 0.33\sqrt{f'_{cE}(MPa)}\right)$ **(b)** $v_{max}/\sqrt{f'_{cE}(psi)} > 6$ $\left(> 0.50\sqrt{f'_{cE}(MPa)}\right)$

Figure 1-34 Proposed models for Parameter d_{nl} for conforming flexure-controlled walls (Note: the statistics shown are for the ratios of predicted-to-experimental values).

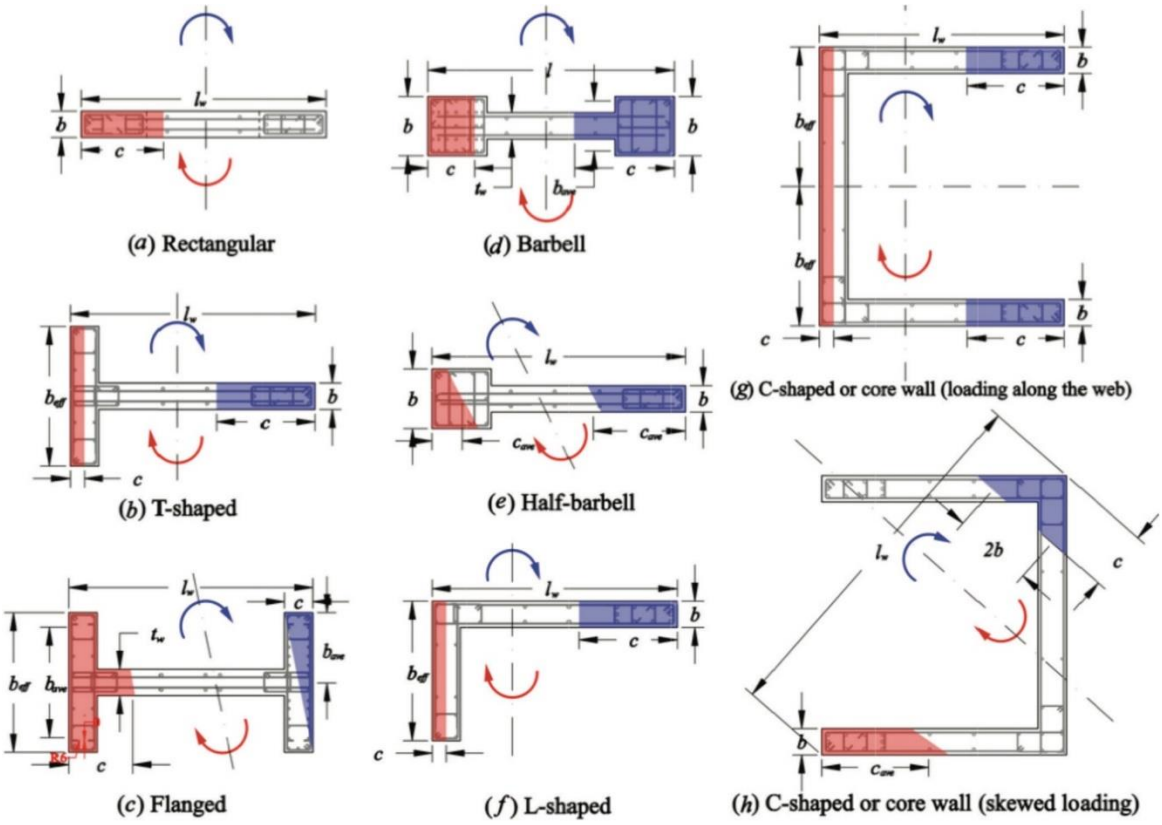

Figure 1-35 Definition of width (*b*) and length (*c*) of flexural compression zone (Abdullah and Wallace 2020). (b_{ave} = average width of compression zone, c_{ave}= average depth of neutral axis, and b_{eff}= effective with of wall flange; the blue and red arrows indicate the direction of bending).

Parameter d'_{nl} (Hinge Rotation Capacity at Point D, Residual Strength)

Figure 1-36 shows that, in addition to $\lambda_b = l_w c/b^2$, $P/(A_g f'_{cE})$ produces a significant influence on Parameter d'_{nl}. This is because, once strength degradation starts, the level of axial load accelerates the rate of deterioration such that walls with high $P/(A_g f'_{cE})$ have a steep post-peak slope on the backbone relation, where no or little additional deformation capacity beyond Point C is achieved prior to axial failure (i.e., no residual strength plateau, Figure 1-11). Insufficient data existed to evaluate if the use of overlapping hoops in the boundary elements would influence Parameter d'_{nl}. Therefore, λ_b and $P/(A_g f'_{cE})$ are used as predictor variables to select Parameter d'_{nl} based on the piecewise best-linear fits (models) shown on Figure 1-36.

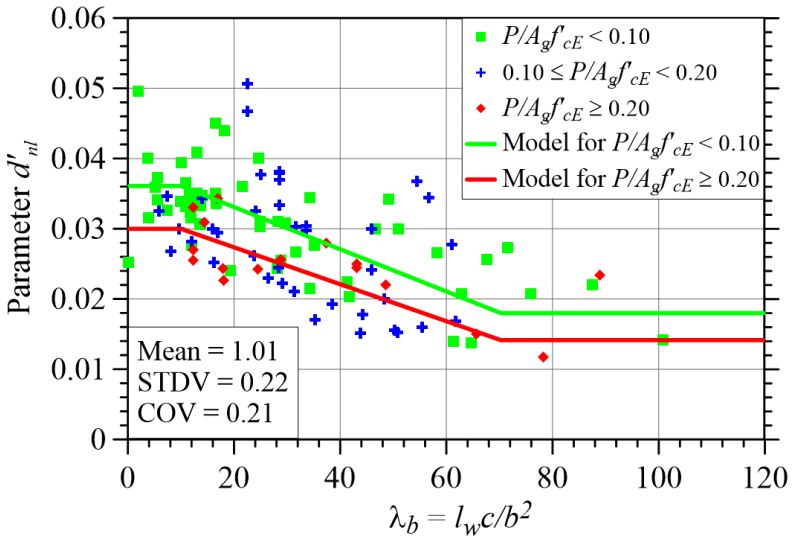

Figure 1-36 Proposed models for *Parameter d'_{nl}* for conforming flexure-controlled walls (Note: the statistics shown are for the ratios of predicted-to-experimental values).

Parameter e_{nl} (Hinge Rotation Capacity at Point E, Axial Failure)

As shown in Figure 1-11, this point is assumed to have an ordinate that is equal to the wall residual lateral strength ratio (Parameter c_{nl}), whereas the abscissa is equal to the hinge rotation capacity corresponding to the onset of axial failure (Parameter e_{nl}).

The reduced subset of 101 walls with reported information on axial failure was studied to identify parameters that influence hinge rotation capacity (Parameter d'_{nl}) at Point E. Similar to Parameter d'_{nl}, $\lambda_b = l_w c/b^2$ and $P/(A_g f'_{cE})$ significantly influence Parameter e_{nl}. Data and the proposed models are presented in Figure 1-37. Segura and Wallace (2018a) reported that providing lateral restraint in the form of crossties for the web longitudinal bars increased the rotation capacity of conforming walls at axial failure; however, tests on walls with crossties in the web region are rare and would not allow statistical analysis. More detailed discussion on axial failure of RC structural walls can be found in Abdullah and Wallace (2021).

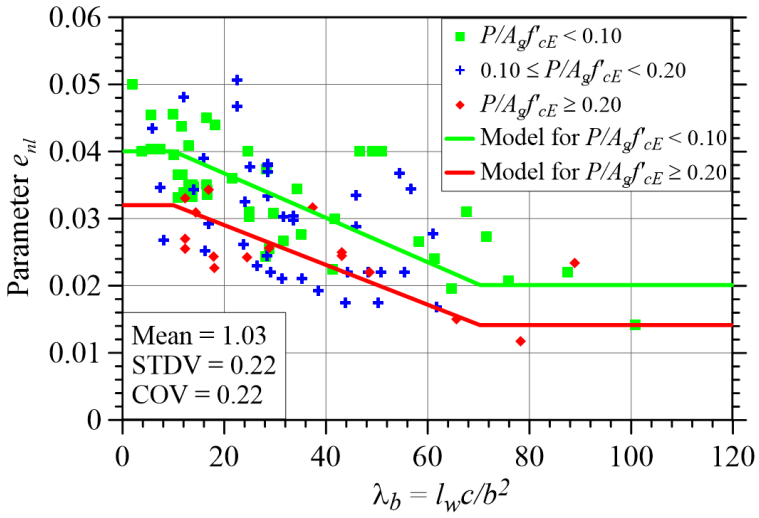

Figure 1-37 Proposed models for Parameter e_{nl} for conforming walls (Note: the statistics shown are for the ratios of predicted-to-experimental values).

Summary of Proposed Nonlinear Modeling Parameters for Conforming Walls

Based on the results and proposed models presented in the preceding sections, updated modeling parameters for flexure-controlled conforming walls are presented in Table 1-7. The statistics of each parameter are presented in Table 1-8.

Table 1-7 Modeling Parameters for Conforming RC Structural Walls Controlled by Flexure

Conditions[d]			
$l_w c_{DE}/b_s^2$	$\frac{w_v V_{MCultDE}}{A_{cv}\sqrt{f'_{cE}}}$[c]	Overlapping hoops[a] used?	d_{nl}
≤ 10	≤ 4	Yes	0.032
≤ 10	≥ 6	Yes	0.026
≥ 70	≤ 4	Yes	0.018
≥ 70	≥ 6	Yes	0.014
≤ 10	≤ 4	No	0.032
≤ 10	≥ 6	No	0.026
≥ 70	≤ 4	No	0.012
≥ 70	≥ 6	No	0.011

Table 1-7 Modeling Parameters for Conforming RC Structural Walls Controlled by Flexure (continued)

Conditions[d]					
$I_w c_{GE}/b_s^2$	$N_{UD}/(A_g f'_{cE})$	c_{nl}	c'_{nl}	d'_{nl} [b]	e_{nl} [b]
≤ 10	≤ 0.10	0.5	1.15	0.036	0.040
≤ 10	≥ 0.20	0.1		0.030	0.032
≥ 70	≤ 0.10	0.0		0.018	0.020
≥ 70	≥ 0.20	0.0		0.014	0.014

[a] Overlapping hoop definition shall be per ACI 318-19
[b] Parameters d'_{nl} and e_{nl} shall not be taken smaller than parameter d_{nl}.
[c] The shear amplification factor ω_v need not be applied if $V_{MCultDE}$ is obtained from nonlinear analyses procedures.
[d] Linear interpolation between the values given in the table shall be permitted; however, interpolation between the values specified for Conforming walls and Nonconforming walls shall not be permitted.

Table 1-8 Statistics of the Modeling Parameters Given in Table 1-7

Parameter	Mean	Median	Standard Deviation	Coefficient of Variation, COV
$M_{yE,cal}/M_{yE}$	1.01	1.00	0.12	0.12
c'_{nl}	1.03	1.02	0.10	0.10
c_{nl}	1.15	0.84	0.97	0.84
d_{nl}	0.98	0.95	0.17	0.17
d'_{nl}	1.01	1.01	0.22	0.21
e_{nl}	1.03	1.01	0.22	0.21

Note: The statistics are for the ratios of predicted-to-experimental modeling parameter values.

Nonconforming Walls

Similar to conforming walls, the total hinge rotation capacities of each response point on the idealized backbone relation (Figure 1-11) are developed in the following subsections using the experimental results from the nonconforming wall dataset.

Parameter d_{nl} (Hinge Rotation Capacity at Point C)

The nonconforming wall dataset was studied to identify parameters that influence Parameter d_{nl}. Figure 1-38 shows variation of Parameter d_{nl} against $\lambda_b = I_w c/b^2$ for three levels of $P/(A_g f'_{cE})$ and wall shear stress ratio ($V_{max}/\sqrt{f'_{cE}}$). It is clear that, similar to conforming walls, Parameter d_{nl} is highly influenced by $\lambda_b = I_w c/b^2$, but the influence of $P/(A_g f'_{cE})$ and $V_{max}/\sqrt{f'_{cE}}$ is not clear. As noted

previously, $P/(A_g f'_{cE})$ does not correlate well with wall lateral deformation capacity at 20% lateral strength loss (Figure 1-38*a*). Figure 1-38(*b*) shows that the impact of $V_{max}/\sqrt{f'_{cE}}$ is not as apparent as it was for walls in the conforming dataset, which might suggest that walls with nonconforming detailing might fail due to lack of proper detailing before the negative impact of shear stress takes effect. It is also noted that there are relatively few walls in the dataset with high shear stresses ($V_{max}/\sqrt{f'_{cE}} > 6$) at $l_w c/b^2 > 20$ (Figure 1-38*b*).

Additionally, a series of linear regression analyses were conducted on the nonconforming dataset and revealed that detailing parameters such as provided A_{sh}, s/d_b, and $\rho_{l,BE}$ play a key role in the value of Parameter d_{nl}, as shown in Figure 1-39. It is noted that $\rho_{l,BE}$ is computed in accordance with ACI 318-19 R18.10.6.5, and the dataset includes walls with $\rho_{l,BE} \geq 0.004$ (Figure 1-29 and Figure 1-30). Walls with very low $\rho_{l,BE}$ and low $P/(A_g f'_{cE})$ could have significantly less deformation capacity because such walls may develop one or two major cracks at or near the base (critical section) with little or no secondary cracks, which leads to strain concentration at the major cracks and eventual abrupt bar fracture.

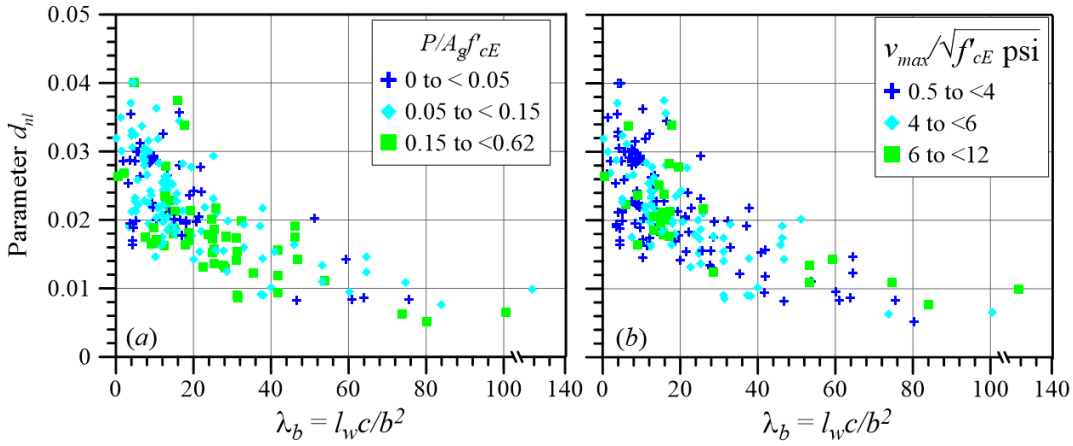

Figure 1-38 Impact of $l_w c/b^2$, $P/(A_g f'_{cE})$, and $V_{max}/\sqrt{f'_{cE}}$ on Parameter d_{nl} for nonconforming walls.

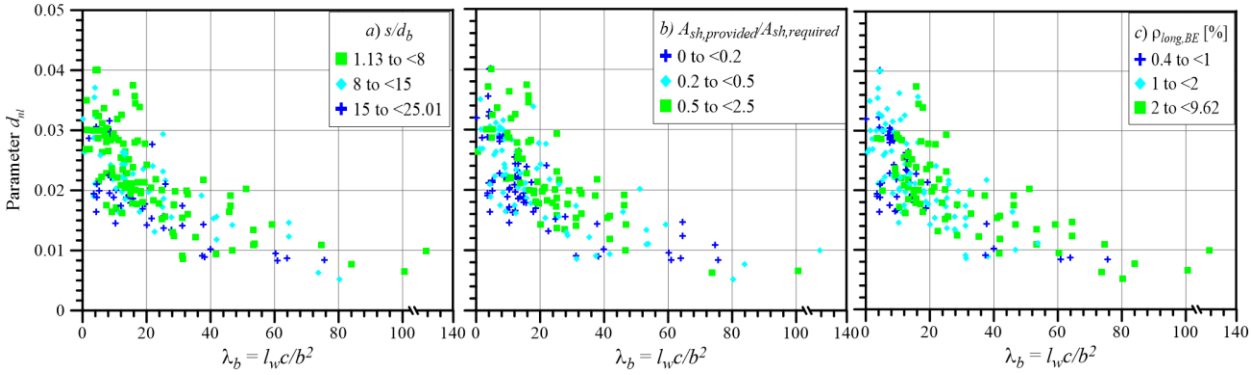

Figure 1-39 Impact detailing parameters on Parameter d_{nl} of nonconforming walls.

Figure 1-40 shows the combined impact of A_{sh} and s/d_b along with the proposed models for Parameter d_{nl}. It can be seen that the dispersion of the data at $\lambda_b < 20$ is significant. In this region, walls tend to have different flexure-failure modes. For example, deformation capacity of walls with slender cross-sections ($l_w/b > 12$) and small compression zones ($c/b < 1.5$) tends to be limited by tensile strains that develop in the boundary longitudinal reinforcement (For example, a T-shaped wall loaded with the flange in compression), where providing additional transverse reinfrcement does not result in increased deformation capacity. These walls typically have rotation capacities larger than 0.02 unless they are reinforced with brittle (non-ductile) longitudinal reinforcement, or their longitudinal reinforcement ratio in the boundary region is small (i.e., < 0.0025). On the other hand, for walls that have squat cross-sections ($l_w/b < 8$) and moderate compression demands ($c/b > 2$), most of the non-confroming walls fall into this category (Figure 1-7), the deformation capacity tends to be limited by flexure compression failures, for which increased transverse reinforcement and bar restraint would likely lead to increased deformation capacity by providing improved lateral restraint against rebar buckling. Walls with $\lambda_b > 60$, which are characterized with slender cross-sections and high compression demands (i.e., thin walls), are typically controlled by brittle compression failures and/or out-of-plane instability.

Figure 1-40 also compares results for walls with one curtain of web reinforcement, which, except for seven walls, all had no transverse reinforcement within the boundary region, with walls with two curtains of web reinforcement, and reveals that walls with one curtain of web reinforcement have rotation capacities comparable to those with two curtains of web reinforcement. Therefore, it is proposed that nonconforming walls with one curtain of web reinforcement be treated similar to nonconforming walls with two curtains of web reinforcement for backbone modeling parameters.

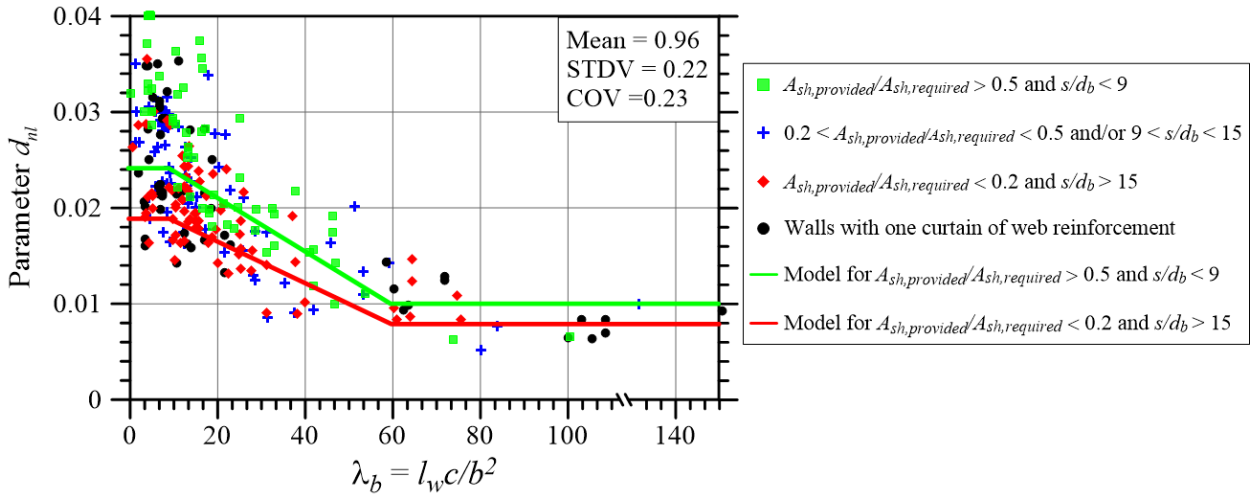

Figure 1-40 Comparison of proposed models for Parameter d_{nl} with experimental data for nonconforming walls.

Parameter d'_{nl} (Hinge Rotation Capacity at Point D)

Additionally, similar to conforming walls, λ_b and $P/(A_g f'_{cE})$ were found to have a considerable influence on Parameter *d'*, as shown in Figure 1-41. Therefore, these two parameters are used as predictors for selecting Parameter *d'* based on the models shown in Figure 1-41.

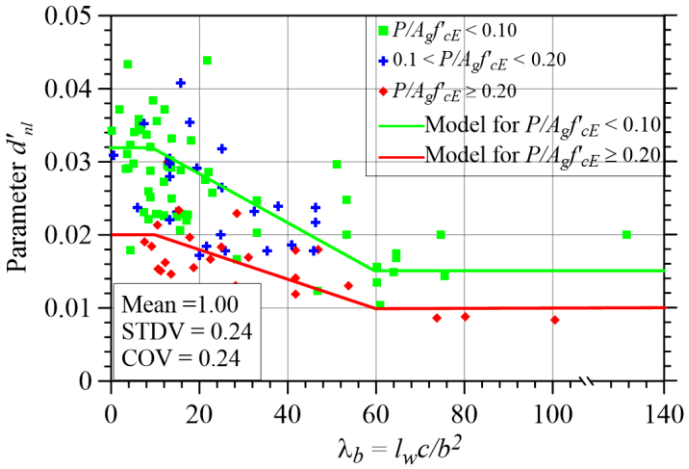

Figure 1-41 Proposed models for Parameter d'_{nl} for nonconforming walls.

Parameter e_{nl} (Hinge Rotation Capacity at Point E, Axial Failure)

Similar to Parameter *d'*, λ_b, and $P/(A_g f'_{cE})$ significantly influence Parameter e_{nl}. The results of the dataset, along with the proposed models, are presented in Figure 1-42. More detailed discussion on axial failure of RC structural walls can be found in Abdullah and Wallace (2021).

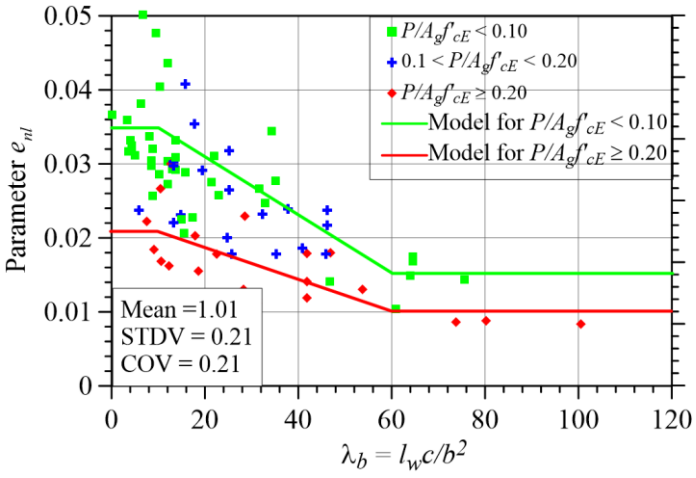

Figure 1-42 Proposed models for Parameter e_{nl} for conforming walls.

Nonconforming walls with Low Longitudinal Reinforcement Ratios

As noted previously, the nonconforming dataset contains walls with longitudinal reinforcement ratios in the boundary region (ρ_{lw}) equal to, or greater than, 0.0025 (minimum web longitudinal

reinforcement ratio of ACI 318-19). However, walls with distributed longitudinal reinforcement ratios < 0.0025 are commonly found in buildings constructed prior 1970s. Furthermore, walls with longitudinal reinforcement ratios < 0.0015 are currently treated as force-controlled components/actions (ASCE/SEI 41-17 Section 10.7.2.3), which makes it virtually impossible to meet the strictly defined performance objectives at the BSE-2E hazard level when no ductility capacity is permitted, especially in wall buildings, since the strength limit is reached at relatively low drift demands.

To address this issue, the database was filtered to identify walls with distributed longitudinal reinforcement ratios (ratio of area of total longitudinal reinforcement to gross concrete area perpendicular to the reinforcement), ρ_{lw}, < 0.0025, where ρ_{lw} is ratio of area of total longitudinal reinforcement to gross concrete area perpendicular to that reinforcement in a wall or wall segment) and a subset of 11 walls were identified with $0.001 < \rho_{lw} < 0.0025$. For those 11 wall tests, only data up to lateral strength loss is available (i.e., Parameter d_{nl}). The limited data are presented in Figure 1-43 along with the models of Figure 1-40 (nonconforming walls with longitudinal reinforcement ratio ≥ 0.0025). This figure suggests that nonconforming walls with such low longitudinal reinforcement ratios can perform significantly worse than those with higher reinforcement ratios when subjected to relatively low compression demands (i.e., $l_w c/b^2 < 10$), for which the failure mode is typically more tension-fracture of longitudinal bars due to the significant tensile strains expected to be developed in the extreme tension bars. This figure also reveals that walls with $\rho_{lw} < 0.0025$ and moderate-to-high compression demands perform similar to the data presented in Figure 1-40 (i.e., walls with $\rho_{lw} \geq 0.0025$) because the deformation capacity of such walls is not particularly limited by tension-fracture of longitudinal bars, but rather by concrete crushing and bar buckling. Therefore, the following is proposed until further data and information on walls with $\rho_{lw} < 0.0025$ become available.

The models presented in Figure 1-40, Figure 1-41, and Figure 1-42 do not apply to walls with $\rho_{lw} < 0.001$ and a reduction factor should be applied for ρ_{lw} between 0.001 and 0.0025 and for low values of the parameter $l_w c/b^2$. A reduction factor of 0.4 for $\rho_{lw} = 0.001$ and $l_w c/b^2 \leq 10$ and 1.0 for $\rho_{lw} = 0.0025$ and $l_w c/b^2 \geq 20$ should be applied to the hinge rotation capacity values obtained from models shown in Figure 1-40, Figure 1-41, and Figure 1-42. Linear interpolation of the reduction factor with respect to ρ_{lw} and $l_w c/b^2$ should be permitted for intermediate values. This proposed approach is shown in Figure 1-43 (broken red line) with the limited test data and models of Figure 1-40.

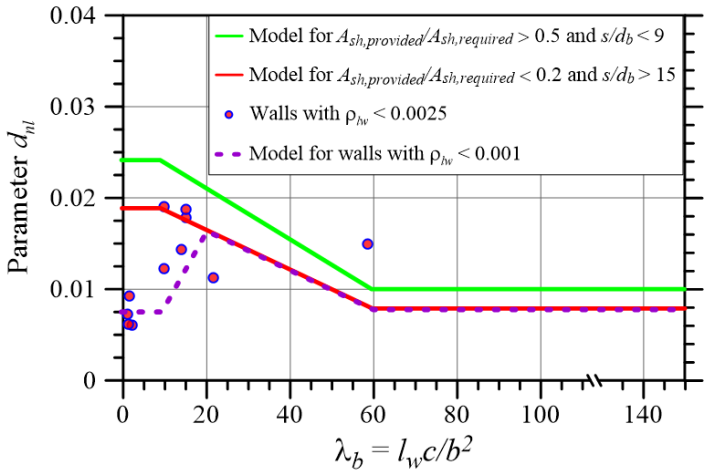

Figure 1-43 Proposed model for Parameter d_{nl} of nonconforming walls with $\rho_{lw} < 0.0025$.

Summary of Proposed Nonlinear Modeling Parameters for Nonconforming Walls

Based on models and results presented in the preceding sections, updated modeling parameters for nonconforming flexure-controlled walls are given in Table 1-9. The statistics of the parameters are given in Table 1-10. These statistics allow users to select appropriate modeling rules and acceptance criteria other than those recommended for the ACI 369.1 Standard.

Table 1-9 Modeling Parameters for Nonconforming RC Structural Walls Controlled by Flexure

Conditions[d,e]		
$\frac{l_w c_{DE}}{b_s^2}$	Detailing[a,b,c,g]	d_{nl}
≤ 10	$A_{sh,provided}/A_{sh,required} \geq 0.5$ and $s/d_b \leq 9$	0.024
≤ 10	$A_{sh,provided}/A_{sh,required} < 0.2$ and $s/d_b > 15$	0.019
≥ 60	$A_{sh,provided}/A_{sh,required} \geq 0.5$ and $s/d_b \leq 9$	0.010
≥ 60	$A_{sh,provided}/A_{sh,required} < 0.2$ and $s/d_b > 15$	0.008

Table 1-9: Modeling Parameters for Nonconforming RC Structural Walls Controlled by Flexure (continued)

Conditions[d]					
$\frac{I_w c_{DE}}{b_s^2}$	$\frac{N_{UD}}{A_g f'_{cE}}$	c_{nl}	c'_{nl}	$d'_{nl}{}^{f}$	$e_{nl}{}^{f,h}$
≤ 10	≤ 0.10	0.4	1.15	0.032	0.035
≤ 10	≥ 0.20	0.1		0.020	0.021
≥ 60	≤ 0.10	0.0		0.015	0.015
≥ 60	≥ 0.20	0.0		0.010	0.010

[a] $A_{sh,required}$ should be as calculated per ASCI 318-19 Chapter 18. In case of boundary elements with transverse reinforcement in the form spiral or circular hoop, the term $A_{sh,provided}/A_{sh,required}$ should be replaced with $\rho_{s,provided}/\rho_{s,required}$, where $\rho_{s,required}$ is calculated per ACI 318-19 Chapter 18.

[b] If values of both $A_{sh,provided}/A_{sh,required}$ and s/d_b fall between the limits given in the table, linear interpolation should independently be performed for both $A_{sh,provided}/A_{sh,required}$ and s/d_b, and the lower resulting value of parameter d_{nl} should be taken.

[c] Values of $A_{sh,provided}/A_{sh,required}$ and s/d_b should be provided over a horizontal distance that extends from extreme compression fiber at least $c_{DE}/3$.

[d] This table applies to walls and wall segments with $\rho_{lw} \geq 0.001$. For $0.0025 \geq \rho_{lw} \geq 0.001$ and $I_w c_{DE}/b_s^2 \leq 20$, modeling parameters d_{nl}, d'_{nl} and e_{nl} should be multiplied by a reduction factor. The reduction factor shall be 0.4 for $\rho_{lw} = 0.001$ and $I_w c_{DE}/b_s^2 \leq 10$ and 1.0 for $\rho_{lw} = 0.0025$ and $I_w c_{DE}/b_s^2 = 20$. Linear interpolation of the reduction factor with respect to ρ_{lw} and $I_w c_{DE}/b_s^2$ is permitted for intermediate values.

[e] This table applies to walls with one or multiple curtains of web reinforcement.

[f] Parameters d'_{nl} and e_{nl} should not be taken smaller than parameter d_{nl}.

[g] Linear interpolation between the values given in the table is permitted; however, interpolation between the values specified for Conforming walls and Nonconforming walls is not permitted.

[h] For walls with no boundary transverse reinforcement and $N_{UD} > 0.08 A_g f'_{cE}$, e_{nl} and d'_{nl} should be multiplied by 0.8 but should not be taken less than d_{nl}.

Table 1-10: Statistics of the Modeling Parameters Given in Table 1-9

Parameter	Mean	Median	Standard Deviation	Coefficient of Variation
$M_{yE,cal}/M_{yE}$	0.97	0.97	0.14	0.14
c'_{nl}	1.03	0.97	0.15	0.15
c_{nl}	1.22	1.00	0.95	0.78
d_{nl}	0.95	0.93	0.22	0.23
d'_{nl}	1.01	0.97	0.24	0.24
e_{nl}	1.01	1.02	0.21	0.21

Note: The statistics are for the ratios of predicted-to-experimental modeling parameter values.

1.3.4.2 ACCEPTANCE CRITERIA

General

Acceptance criteria are limiting values of deformation demands for deformation-controlled actions and strength demands for force-controlled actions, which are used to determine the conformance of a structure with the design requirements or performance objectives. ASCE/SEI 41-17 Section 7.5.1.2 gives guidance on classifying actions as either deformation-controlled or force-controlled. In general, deformation-controlled actions are those for which the component can undergo measurable inelastic deformations without compromising the ability to maintain its load-carrying capacity, whereas force-controlled actions are those for which the component loses its load-carrying capacity once the elastic limit (yield strength) is exceeded (no ductility). In ASCE/SEI 41-17, actions are defined as deformation-controlled by the standard if linear and nonlinear acceptance criteria are designated to them. In cases where linear and nonlinear acceptance criteria are not specified in the standard, actions should be classified as force-controlled, unless component testing is performed to demonstrate otherwise.

Currently, both shear and flexure actions in RC structural walls are treated as deformation-controlled actions, with acceptance criteria specified for linear approaches in the form of deformation-based *m*-factors and for nonlinear approaches in the form of plastic hinge rotations. Other actions, such as axial, base shear sliding, as well as shear in walls with a transverse reinforcement ratio < 0.0015 (ASCE/SEI 41-17 Section 10.7.2.3), flexure in walls where the cracking moment strength exceeds the yield strength (ASCE/SEI 41-17 Section 10.7.2.3), and shear in walls with axial load ratio greater than 0.15 are currently treated as force-controlled actions, unless component testing is performed to demonstrate otherwise. The acceptance criteria proposed in this chapter do not result in changes to the designation of force- and deformation-controlled actions for flexure-controlled walls.

Distribution of Data for Parameters d_{nl} and e_{nl}

Figure 1-44 presents the distribution of the data for the ratios of experimental-to-predicted Parameter d_{nl} and e_{nl}, along with normal and lognormal distributions associated with the means and standard deviations of the data. It can be seen that the error data are better fit using a lognormal distribution. The error data for Parameter e_{nl} is not as well-fit using a lognormal distribution as Parameter d_{nl}, and using normal distribution is not much better, either. This could be a limitation of the data set size (smaller) and the selected bin widths. For both distributions, the lower tail is more important, since this is the side of the distribution that affects the acceptance criteria. For Parameter d_{nl}, the lognormal distribution does a better job capturing that lower tail than the normal distribution. Furthermore, to be consistent with distributions used for other components in the standard and to avoid negative values of acceptance criteria, lognormal distribution is assumed for deriving the acceptance criteria, as shown below.

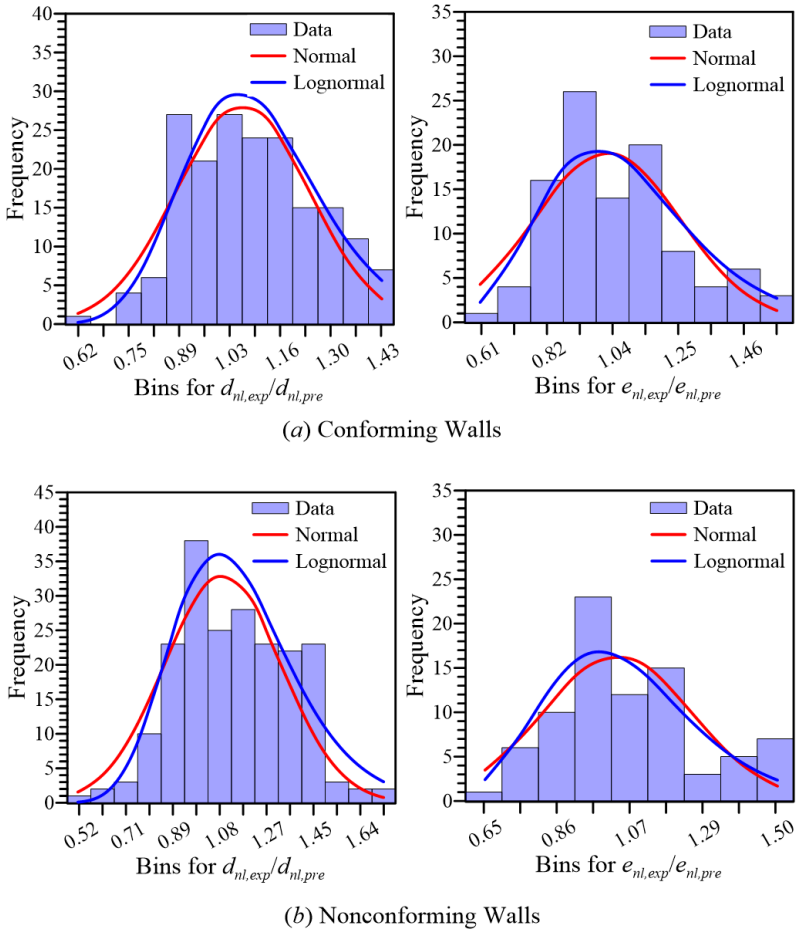

Figure 1-44 Distribution of ratios of experimental-to-predicted *d* and *e*, along with normal and lognormal distributions associated with the means and standard deviations of the datasets.

Proposed Nonlinear Acceptance Criteria

The ASCE/SEI 41-17 Section 7.6.3 provides a procedure for defining acceptance criteria based on experimental data. For both primary and secondary components, the standard defines acceptance criteria for the Immediate Occupancy (IO) performance objective as the deformation at which permanent, visible damage occurred in the experiments (acceptable damage), but not greater than 2/3 of the deformation limit (acceptance criteria) for Life Safety (LS). For both secondary and primary members, ASCE/SEI 41-17 Section 7.6.3 defines acceptance criteria as 75% of Parameter e_{nl} for LS and 100% of Parameter e_{nl} for Collapse Prevention (CP). It is noted that nonlinear acceptance criteria in ASCE/SEI 41-17 are based on Secondary Component metrics since the designation of Primary and Secondary Components for nonlinear analyses was dropped in that edition of the standard. The acceptance criteria for Primary Components are extracted as they were used to develop the linear acceptance criteria that maintain the Primary/Secondary designation.

Current modeling parameters in the standard, however, are overly conservative, as shown later; therefore, by taking acceptance criteria as fractions of Parameter e_{nl} or d_{nl}, the standard in essence

aims at deformation limits smaller than values at which lateral strength loss or axial failure occur. For LS and CP performance objectives, for which structural stability and safety are of significant concern, ensuring a fixed probability of exceeding the deformation corresponding to the onset of lateral-strength degradation (Parameter d_{nl}) or the onset of axial failure (Parameter e_{nl}) is more appropriate and is consistent with performance objectives targeted for concrete columns in ACI 369.1-17 (Ghannoum and Matamoros, 2014). As a result, the following acceptance criteria for nonlinear procedures are recommended for RC structural walls:

1. It is proposed that acceptance criteria for IO be based on a percentage of the plastic hinge rotation value (d_{nl} - θ_{yE}) plus the yield rotation. A conservative value of θ_{yE} + 0.10 (d_{nl} – θ_{yE}) is selected as the limiting deformation at which a reinforced concrete wall is deemed to need repair and no longer satisfy the IO performance objective.
2. For LS of primary members, it is proposed that total hinge rotations should not exceed the 20th percentile of Parameter d_{nl}. For a member critical to the stability of a structure, satisfying the acceptance criteria for LS would indicate an 80% level of confidence that the member under consideration has not initiated lateral strength degradation.
3. For CP of primary members, it is proposed that total hinge rotations should not exceed the 35th percentile of Parameter d_{nl}.
4. For LS of secondary members, it is proposed that total hinge rotations should not exceed the 10th percentile of Parameter e_{nl} nor be less than acceptance criteria for LS of primary members. Due to the more critical nature of the behavioral milestone identified by Parameter e_{nl}, a lower percentile was selected for this acceptance criteria than for primary members.
5. For CP of secondary members, total hinge rotations should not exceed the 25th percentile of Parameter e_{nl} nor be less than acceptance criteria for CP of primary members.
6. In all cases, the acceptance criteria for primary members should not be larger than those for secondary members.

Assuming lognormal distribution for the errors on Parameters d_{nl} and e_{nl}, the fractions of d_{nl} and e_{nl} that produced the percentiles stated above were determined for conforming and nonconforming walls. However, the acceptance criteria fractions for conforming and nonconforming walls were found to be similar and a single set of acceptance criteria for both cases is proposed, as presented in Table 1-15. The approximate locations of acceptance criteria on the proposed backbone shapes are shown in Figure 1-45.

Table 1-11 Recommended Acceptance Criteria for Conforming and Nonconforming Flexure-Controlled Concrete Structural Walls

Performance Level	Component Type	Acceptance Criteria
IO	Primary and Secondary	$\theta_{yE}+0.1(d_{nl} - \theta_{yE})$
LS	Primary	$0.90d_{nl}$
	Secondary	$0.75e_{nl} \geq 0.90d_{nl}$
CP	Primary	$1.00d_{nl}$
	Secondary	$0.85e_{nl} \geq 1.00d_{nl}$

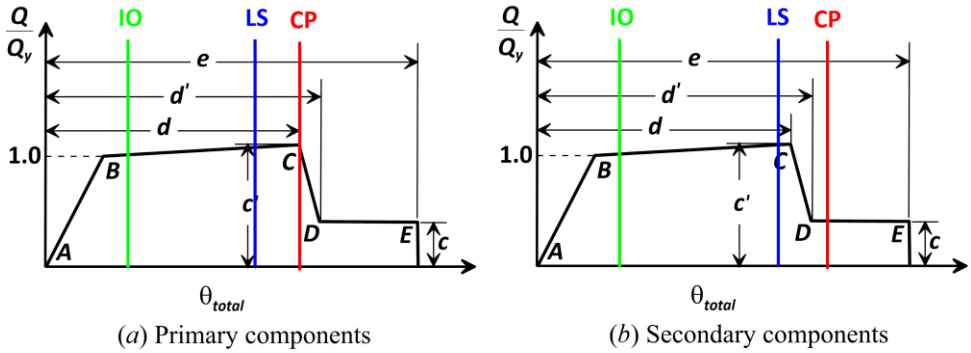

Figure 1-45 Approximate location of acceptance criteria on backbone shape.

Proposed Linear Acceptance Criteria

As noted in the previous section, for acceptance criteria in nonlinear procedures, deformation limits are used. However, for the acceptance criteria in the linear procedures, these deformation limits are converted to *m*-factors, defined as component capacity modification factors to account for the expected ductility associated with the action at the selected performance level. Since deformation (drifts or rotation) demands are not explicitly evaluated for ASCE/SEI 41 linear procedures, the *m*-factors are used as a proxy for limiting allowable deformations.

Provisions of ASCE/SEI 41-17 Section 7.6.3 stipulate that *m*-factors be selected based on the nonlinear modeling parameters d_{nl} and e_{nl} from experimental data according to the relationships shown in Table 1-16. Because these *m*-factors are defined in terms of nonlinear modeling parameters d_{nl} and e_{nl}, the relationships in Table 1-16 are applicable to all types of walls, regardless of the level of detailing (conforming or nonconforming).

Table 1-12 *m*-factors for Reinforced Concrete Walls Based on Provisions of ASCE/SEI 41-17 Section 7.6.3

Component Type	Performance Level		
	IO	LS	CP
Primary	$\frac{3}{8}\left(\frac{d_{nl}}{\theta_y}\right)$	$\frac{9}{16}\left(\frac{d_{nl}}{\theta_y}\right)$	$\frac{9}{16}\left(\frac{e_{nl}}{\theta_y}\right)$
Secondary	$\frac{3}{8}\left(\frac{e_{nl}}{\theta_y}\right)$	$\frac{9}{16}\left(\frac{e_{nl}}{\theta_y}\right)$	$\frac{3}{4}\left(\frac{e_{nl}}{\theta_y}\right)$

The θ_y in Table 1-16 is the average hinge rotation corresponding to the first yield of longitudinal reinforcement and is computed from sectional analysis of the wall as yield curvature (ϕ_y) times the assumed plastic hinge length (l_p). Figure 1-46 presents variation of yield curvature computed from sectional analysis for a dataset of 978 walls versus wall length (l_w). A best fit model in the form of $\phi_y = 0.00375/l_w$ results in a mean of 1.02 and a coefficient of variation of 0.21, as shown in the figure. The upper- and lower-bounds shown in Figure 1-46 represent roughly the mean plus and minus two standard deviations, respectively. Assuming an l_p of $l_w/2$ and uniform distribution of curvature over l_p, a mean value of θ_y of 0.188% can be obtained. For deriving *m*-factors, it might be more appropriate to use the upper-bound yield curvature, which results in a θ_y of 0.25%, producing conservative values of *m*-factors. It is noted that these yield rotation values do not consider the increase in yield rotation (flexibility) as a result of bar slip/extension into the foundation, which could arguably increase θ_y by another 5% to 20% for walls with low-to-moderate axial loads (more axial load results in less bar slip/extension, as was noted previously). Therefore, use of θ_y of 0.30% is recommended.

The alternative *m*-factors drived from Table 1-16 and use of a θ_y of 0.30% are presented in Table 1-17 and Table 1-18 for conforming and non-conforming walls, respectively.

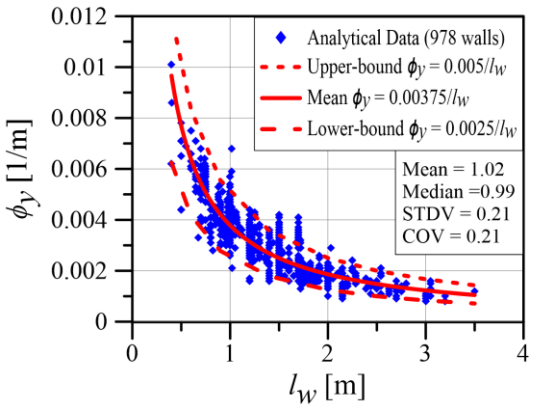

Figure 1-46 Variation of yield curvature (ϕ_y) computed from analytical sectional analysis as a function of wall length (l_w).

Table 1-13 Alternate Numerical Acceptance Criteria for Linear Procedures: Conforming Reinforced Concrete Structural Walls Controlled by Flexure

Conditions			*m*-factors	
			Performance Level	
$\frac{I_w c_{DE}}{b_s^2}$	$\frac{w_v V_{MCultDE}}{A_{cv}\sqrt{f'_{cE}}}$	Overlapping hoops used?	Primary	
			IO	LS
≤ 10	≤ 4	YES	2.0	6.0
≤ 10	≥ 6	YES	1.8	4.9
≥ 70	≤ 4	YES	1.5	3.4
≥ 70	≥ 6	YES	1.4	2.6
≤ 10	≤ 4	NO	2.0	6.0
≤ 10	≥ 6	NO	1.8	4.9
≥ 70	≤ 4	NO	1.3	2.3
≥ 70	≥ 6	NO	1.3	2.1

Conditions		*m*-factors		
		Performance Level		
$\frac{I_w c_{GE}}{b_s^2}$	$\frac{N_{UD}}{A_g f'_{cE}}$	Primary	Secondary	
		CP	LS	CP
≤ 10	≤ 0.10	7.5	7.5	10.0
≤ 10	≥ 0.20	6.0	6.0	8.0
≥ 70	≤ 0.10	3.8	3.8	5.0
≥ 70	≥ 0.20	2.6	2.6	3.5

Table 1-14 Alternate Numerical Acceptance Criteria for Linear Procedures: Nonconforming Reinforced Concrete Structural Walls Controlled by Flexure

Conditions		*m*-factors	
		Performance Level	
$\frac{l_w c_{DE}}{b_s^2}$	Detailing	IO	Primary
			LS
≤ 10	$A_{sh,provided}/A_{sh,required} \geq 0.5$ and $s/d_b \leq 9$	1.7	4.5
≤ 10	$A_{sh,provided}/A_{sh,required} < 0.2$ and $s/d_b > 15$	1.5	3.6
≥ 60	$A_{sh,provided}/A_{sh,required} \geq 0.5$ and $s/d_b \leq 9$	1.2	1.9
≥ 60	$A_{sh,provided}/A_{sh,required} < 0.2$ and $s/d_b > 15$	1.2	1.5

Conditions		*m*-factors		
		Performance Level		
$\frac{l_w c_{GE}}{b_s^2}$	$\frac{N_{UD}}{A_g f'_{cE}}$	Primary	Secondary	
		CP	LS	CP
≤ 10	≤ 0.10	6.6	6.6	8.8
≤ 10	≥ 0.20	3.9	3.9	5.3
≥ 60	≤ 0.10	2.8	2.8	3.8
≥ 60	≥ 0.20	1.9	1.9	2.5

1.3.4.3 COMPARISON OF ACI 369.1-17 (ASCE/SEI 41-17) AND PROPOSED MODELING PARAMETERS AND ACCEPTANCE CRITERIA

In this section, the ACI 361.1-71 or ASCE/SEI4 1-17 Parameter a_{nl} (i.e., plastic hinge rotation capacity at 20% strength loss) of walls with "Confined Boundaries" is evaluated using the results of the conforming wall dataset to highlight the conservatism associated with the current structural wall modeling parameters of ASCE/SEI 41. ASCE/SEI 41-17 Table 10-19, which gives modeling parameters for flexure-controlled RC structural walls, is partially shown in Table 1-19. It is noted that the walls in the conforming dataset satisfy the criteria for walls with "Confined Boundary" in ASCE/SEI 41-17 (Table 1-19).

For the walls in the conforming dataset, Parameter a_{nl} was computed as the plastic displacement (total experimental displacement at 20% lateral strength loss minus the experimental yield displacement) divided by plastic hinge length (l_p) of $l_w/2$. The experimental results of Parameter a_{nl} are compared with those from Table 1-19 (from the first four rows for conforming walls) in Figure 1-47. Two primary observations result from a review of Figure 1-47: (1) the current modeling

parameter a_{nl} for walls with "confined boundaries" constitutes a conservative lower-bound estimate of wall deformation capacity at 20% lateral strength loss, and (2) the predictor variable given in the first column of the Table 1-19 (i.e., $[(A_s - A'_s)f_{yE} + P]/(A_g f'_{cE})$ does not correlate well with Parameter a_{nl} and thus produces large dispersions.

The $[(A_s - A'_s)f_{yE} + P]/(A_g f'_{cE})$ parameter considers the impact of axial load ratio ($P/(A_g f'_{cE})$) and longitudinal reinforcement ratio and yield strength ($(A_s - A'_s)f_{yE}/(A_g f'_{cE})$). Figure 1-48a shows that there is no significant trend between $P/(A_g f'_{cE})$ (ranging from 0.0 to 0.35) and Parameter a_{nl}. This observation relates to the fact that $P/(A_g f'_{cE})$ alone does not indicate much about the stability of the compression zone, and its influence on deformation capacity is best accounted for through neutral axis depth of a wall section, as was shown previously. The impact of $(A_s - A'_s)f_{yE}/(A_g f'_{cE})$ is shown in Figure 1-48b, which interestingly shows that an increase in this parameter results in an increase of Parameter a_{nl} for walls subjected to low shear stress values ($V_{max}/\sqrt{f'_{cE}(\text{psi})} \le 4$). This is because the value of $(A_s - A'_s)f_{yE}/(A_g f'_{cE})$ is the largest for walls with small depth of neutral axis (more reinforcement are in tension), and deformation capacities of such walls are typically limited by fracture of tension reinforcement. Thus, such walls tend to have large deformation capacities (Segura and Wallace, 2018b). Figure 1-48b also shows that there is no clear trend between $(A_s - A'_s)f_{yE}/(A_g f'_{cE})$ and plastic rotation capacity for walls with high shear stresses.

Table 1-15: Partial View of ASCE/SEI 41-17 Table 10-19 for Nonlinear Modeling Parameters of Flexure-Controlled Structural Walls

Modeling Parameters and Numerical Acceptance Criteria for Nonlinear Procedures

			Plastic Hinge Rotation (radians)		Residual Strength Ratio	Acceptable Plastic Hinge Rotation[a] (radians)		
						Performance Level		
Conditions			***a***	***b***	***c***	**IO**	**LS**	**CP**
i. Structural walls and wall segments								
$\frac{(A_s - A'_s)f_{yE} + P}{t_w l_w f'_{cE}}$	$\frac{V}{t_w l_w \sqrt{f'_{cE}}}$	Confined Boundary[b]						
≤0.1	≤4	Yes	0.015	0.020	0.75	0.005	0.015	0.020
≤0.1	≥6	Yes	0.010	0.015	0.40	0.004	0.010	0.015
≥0.25	≤4	Yes	0.009	0.012	0.60	0.003	0.009	0.012
≥0.25	≥6	Yes	0.005	0.010	0.30	0.0015	0.005	0.010
≤0.1	≤4	No	0.008	0.015	0.60	0.002	0.008	0.015
≤0.1	≥6	No	0.006	0.010	0.30	0.002	0.006	0.010
≥0.25	≤4	No	0.003	0.005	0.25	0.001	0.003	0.005
≥0.25	≥6	No	0.002	0.004	0.20	0.001	0.002	0.004

Table 1-15 Partial View of ASCE/SEI 41-17 Table 10-19 for Nonlinear Modeling Parameters of Flexure-Controlled Structural Walls (continued)

Numerical Acceptance Criteria for Linear Procedures

			***m*-Factors[a]**				
			Performance Level				
				Component Type			
				Primary		**Secondary**	
Conditions			**IO**	**LS**	**CP**	**LS**	**CP**
i. Structural walls and wall segments $\frac{(A_s - A'_s)f_{yE} + P}{t_w l_w f'_{cE}}$[b]	$\frac{V^c}{t_w l_w \sqrt{f'_{cE}}}$	Confined Boundary[d]					
≤0.1	≤4	Yes	2	4	6	6	8
≤0.1	≥6	Yes	2	3	4	4	6
≥0.25	≤4	Yes	1.5	3	4	4	6
≥0.25	≥6	Yes	1.25	2	2.5	2.5	4
≤0.1	≤4	No	2	2.5	4	4	6
≤0.1	≥6	No	1.5	2	2.5	2.5	4
≥0.25	≤4	No	1.25	1.5	2	2	3
≥0.25	≥6	No	1.25	1.5	1.75	1.75	2

For structural walls and wall segments where inelastic behavior is governed by shear, the axial load on the member must be ≤ 0.15 $A_g f'_{cE}$; otherwise, the member must be treated as a force-controlled component.

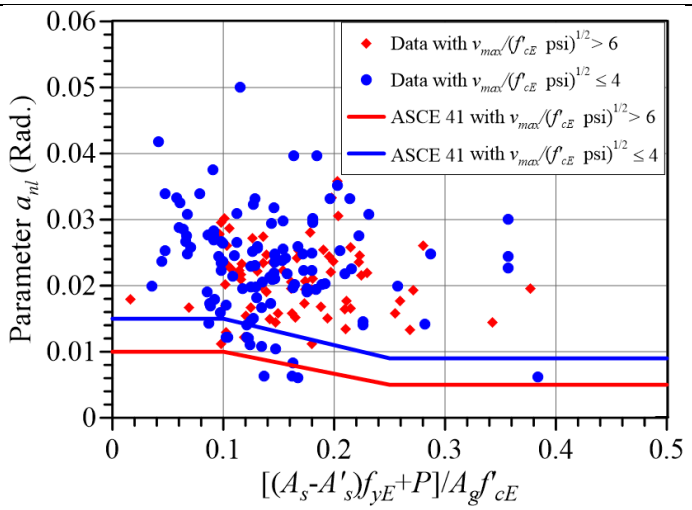

Figure 1-47 Comparison of ASCE/SEI 41-17 Parameter a_{nl} for walls with confined boundaries with test data.

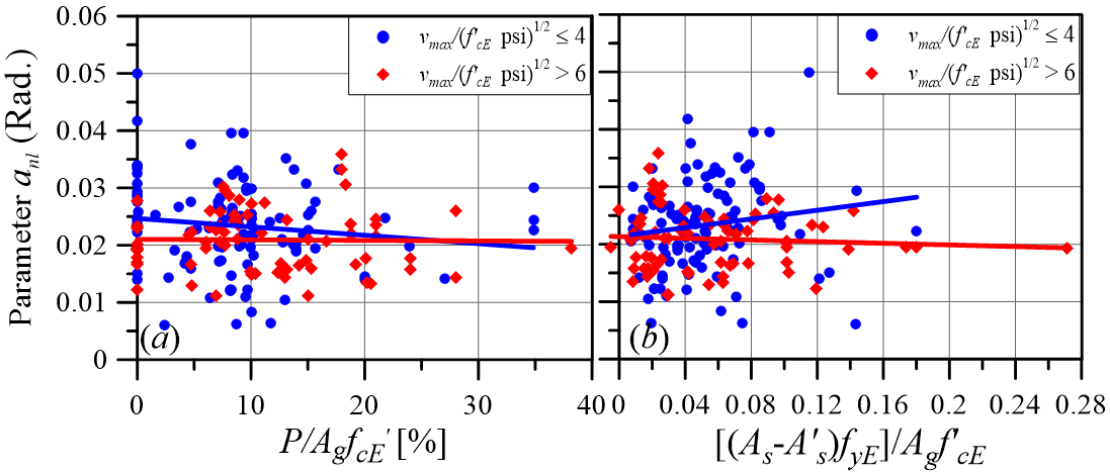

Figure 1-48 Impact of axial load ratio and longitudinal reinforcement on Parameter a_{nl} for walls with confined boundaries.

Comparable results are observed for tests with "No Confined Boundaries" from the second dataset of nonconforming walls, as shown Figure 1-49. For such walls, this figure shows that there is only a moderate trend of Parameter a_{nl} as a function of $P/(A_g f'_{cE})$ for walls with low shear stresses, and no clear trend for walls with high shear stresses.

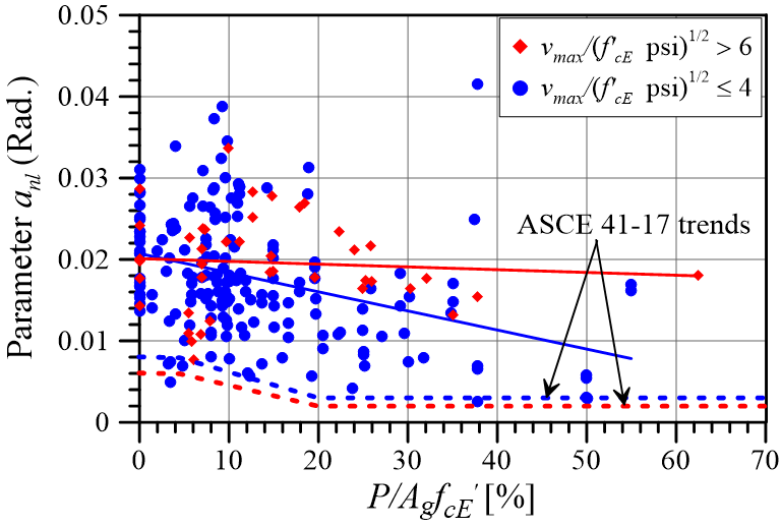

Figure 1-49 Impact of axial load ratio on Parameter a_{nl} for walls with no confined boundaries (Note: the break points for the ASCE/SEI 41-17 trends shown are approximate since X-axis does not include $(A_s-A'_s)f_{yE}/(A_g f'_{cE})$).

Figure 1-50 and Figure 1-51 compare the proposed linear acceptance criteria (*m*-factors) with acceptance criteria from ASCE/SEI 41-17 for conforming and nonconforming walls, respectively, and indicate that the proposed values are almost always significantly higher, especially for walls with cross-section aspect ratios (l_w/b) smaller than 10. It is also noted that the difference between proposed and existing values is typically higher for nonconforming walls than conforming walls.

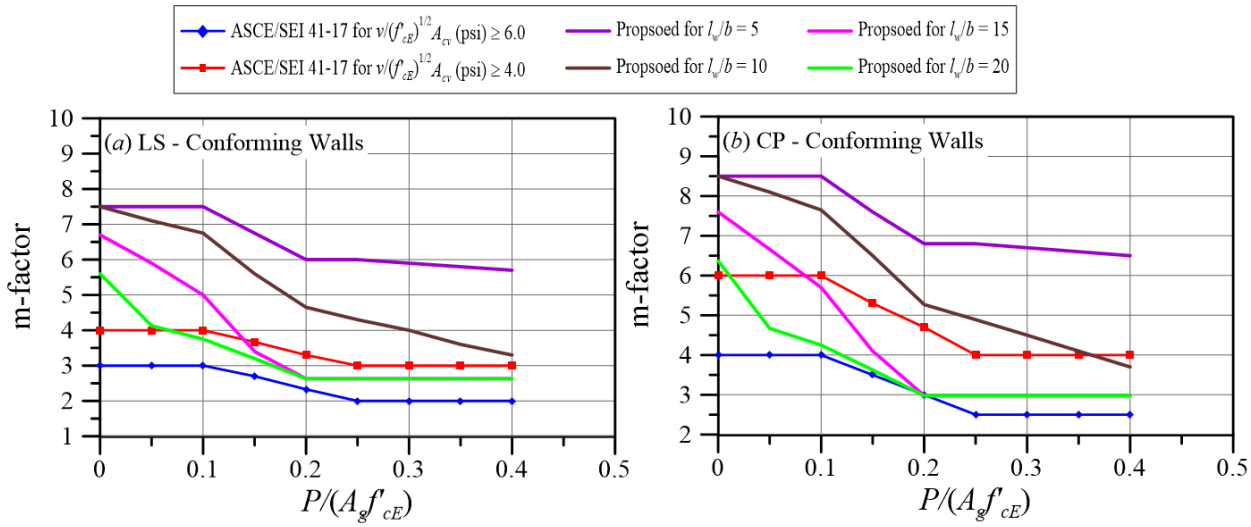

Figure 1-50 Comparison of proposed acceptance criteria with acceptance criteria in ASCE/SEI 41-17 for conforming walls.

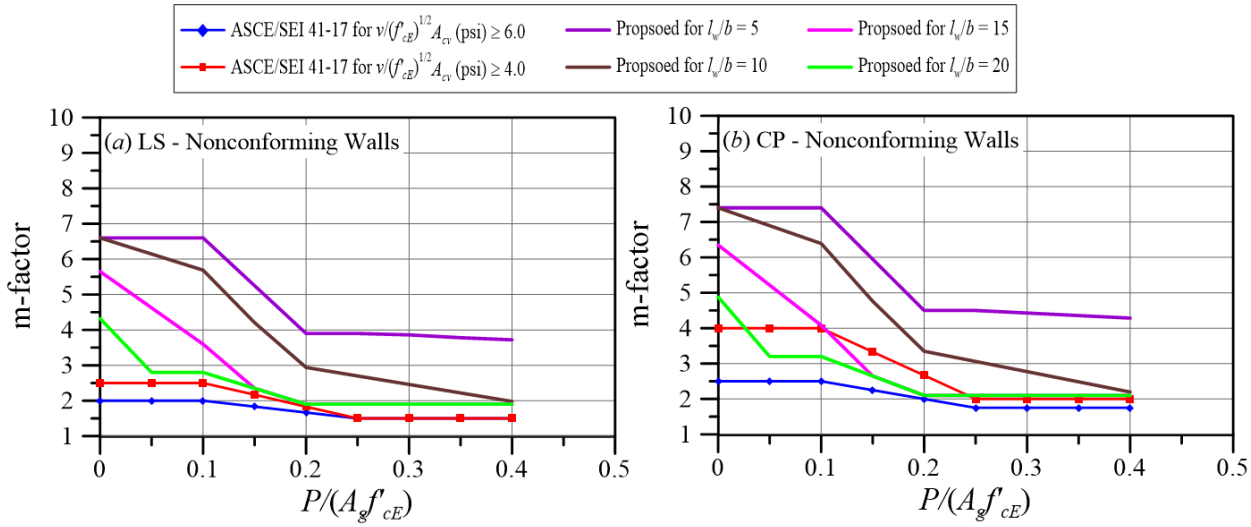

Figure 1-51 Comparison of proposed acceptance criteria with acceptance criteria in ASCE/SEI 41-17 for nonconforming walls.

1.3.5 Conclusions

Available experimental data and new information on performance of RC structural walls were utilized to develop updated provisions and recommendations for wall stiffness, modeling parameters, and acceptance criteria for seismic evaluation and retrofit of flexure-controlled reinforced concrete structural walls in the ACI 369.1 and ASCE/SEI 41 standards. An extensive database that includes detailed data on more than 1,100 RC wall tests reported in the literature was utilized. For stiffness evaluation, a subset of 527 test of flexure-controlled walls was filtered from the main database. The dataset was first used to evaluate the current stiffness provisions of ASCE/SEI 41-17 (ACI 369.1-17), and the results revealed that: 1) use of a constant value of "cracked" effective flexural stiffness (i.e., $E_{cE}I_{eff} = 0.35E_{cE}I_g$) does not adequately consider variables that influence wall effective flexural

stiffness, and 2) use of 100% of the gross "uncracked" shear stiffness ($0.4E_{cE}A_w$) to model shear response in flexure-controlled walls overly estimates shear stiffness. Subsequently, parameters that significantly influence uncracked and cracked effective flexural and shear stiffnesses of walls were identified. It was found that axial load has the greatest impact on wall flexural stiffness (uncracked and cracked), and that the longitudinal reinforcement ratio produced a significant impact on cracked effective flexural stiffness at low axial load ratios (i.e., < 0.10 $A_g f'_{cE}$). Based on these results, wall flexural stiffness relations (cracked and uncracked) are proposed. For shear stiffness, based on results from a subset of 64 wall tests whose base shear versus shear deformation backbones were available in the database, a constant effective shear modulus of one-third of the gross shear modulus (i.e., $G_{eff,E} = G_{gE}/3$) is proposed to be used to model shear response of shear-cracked flexure-controlled walls.

The current ASCE/SEI 41-17 nonlinear deformation-based modeling parameters (i.e., Parameters *a* and *b*) are given as plastic hinge rotations. Where a lumped plasticity model is used, the hinge region, which is typically at or near the base of the wall, is modeled as a near-rigid spring with effectively no elastic deformation. However, in this study, the deformation-based modeling parameters are given as total hinge rotation capacities, which include both the elastic and plastic deformations of the hinge region taken as $l_w/2$. By using total hinge rotation capacities: 1) modeling parameters are not sensitive to approaches (or assumptions) used to calculate yield rotation, 2) modeling parameters are consistent with the total drift ratio or chord rotation used to define modeling parameters for shear-controlled walls and coupling beams, respectively, and 3) modeling parameters can be converted to strain limits by dividing by an assumed hinge length, which is convenient where fiber models are used, which is becoming increasingly popular in engineering practice.

Two subsets of tests were filtered from the main database, one for walls with conforming or "special" detailing and the other for walls with non-conforming or "ordinary" detailing. The datasets were used to evaluate the current modeling parameters of ASCE/SEI 41-17 (ACI 369.1-17), and the results revealed that the current modeling parameters for walls constitute a conservative lower-bound estimate of wall deformation capacities. Additionally, the predictor variable $[(A_s - A'_s)f_{yE} + P]/(A_g f'_{cE})$ used to select modeling parameters does not correlate well with the modeling parameters and thus produces large dispersions. Subsequently, the two datasets were studied to identify parameters that influence each modeling parameter. Based on the results, two sets of modeling parameters are proposed, one for walls with conforming detailing (i.e., nearly ACI 318-19 code compliant) and the other for walls with nonconforming (or ordinary) detailing. The proposed modeling parameters, which represent roughly median values of experimental data, produce relatively low dispersions (coefficients of variation ranging from 0.18 to 0.25). Nonlinear and linear acceptance criteria were derived for flexure-controlled walls, as was done for concrete columns in ACI 369.1-17, by targeting percentiles of exceeding threshold modeling parameters rather than fixed percent values of these parameters.

The updates are expected to significantly reduce conservatism in current modeling parameters and acceptance criteria for most flexure-controlled walls.

1.4 Recommended Changes

Note about Change Proposals

This chapter documents aspects of change proposals as they were submitted to ACI's *Seismic Repair and Rehabilitation* Code Committee 369 for possible adoption. Often, these change proposals were revised, in some cases substantively, by this committee before they were adopted into ACI 369.1-22. Readers should not rely on this chapter for information about the final version of provisions in ACI 369.1-22.

1.4.1 Stiffness Provisions

The change proposal for the upcoming ACI 369.1 standard for wall stiffness contains changes to:

- Flexural, shear, and axial stiffnesses for uncracked walls based on axial load ratio (Table 5).
- Flexural, shear, and axial stiffnesses for cracked walls (Table 5).
- Alternative and more detailed flexural stiffness values based on axial load ratio and boundary longitudinal reinforcement ratio (Table 18).

Due to the re-organization of the wall Chapter 7 in ACI 369.1-17, much of the existing standard text was moved, with some being modified, some being deleted, and some new text introduced. To aid in identifying existing and new text, the following color scheme is used. Green text is existing text in ACI 369.1-17, which was moved in the new organization. Blue text indicates text that was either modified or newly introduced.

Table 5–Effective Stiffness Values

Component	Flexural Rigidity	Shear Rigidity	Axial Rigidity
Beams—nonprestressed[*a]	$0.3E_{cE}I_g$	$0.4E_{cE}A_w$	—
Beams—prestressed[*a]	$E_{cE}I_g$	$0.4E_{cE}A_w$	—
Columns with compression caused by design gravity loads $\geq 0.5A_gf_c'$[†b]	$0.7E_{cE}I_g$	$0.4E_{cE}A_w$	$E_{cE}A_g$
Columns with compression caused by design gravity loads $\leq 0.1A_gf_c'$ or with tension[†b]	$0.3E_{cE}I_g$	$0.4E_{cE}A_w$	$E_{cE}A_g$ (compression) E_sA_s (tension)
Beam–column joints	Refer to Section 4.2.2.1		$E_{cE}A_g$
Flat slabs—nonprestressed	Refer to Section 4.4.2	$0.4E_{cE}A_g$	—
Flat slabs—prestressed	Refer to Section 4.4.2	$0.4E_{cE}A_g$	—

Walls-uncracked with compression caused by design gravity loads $\geq 0.3A_g f_c'$[b,c]	$1.0E_{cE}I_g$	$0.4E_{cE}A_w$	$E_{cE}A_g$
Walls-uncracked with zero compression caused by design gravity loads or with tension[b,c]	$0.5E_{cE}I_g$	$0.4E_{cE}A_w$	$E_{cE}A_g$
Walls-cracked[‡b,c]	~~$0.35E_{cE}I_g$~~ Refer to Sections 7.3 and 7.4	0.15~~0.4~~$E_{cE}A_w$	$E_{cE}A_g$ (compression) E_sA_s (tension)

[*a] For T-beams, I_g can be taken as twice the value of I_g of the web alone. Otherwise, I_g shall be based on the effective width as defined in Section 3.1.3.

[‡b] For columns and walls with axial compression falling between the limits provided, flexural rigidity shall be determined by linear interpolation. If interpolation is not performed, the more conservative effective stiffnesses shall be used. An imposed axial load N_{UG} is permitted to be used for stiffness evaluations

[‡] ~~See Section 7.2.2~~

[c] Wall cracking in flexural actions is determined where flexural demands exceed McrE and in shear actions where shear stress demands exceed $2\sqrt{f'_{cE}}$. It shall be permitted to assume all walls to be cracked.

7.3—Linear static and dynamic procedures for structural walls and wall segments

7.3.1 Modeling—The analytical model for a structural wall ~~element~~ and wall segment shall represent ~~the~~ component stiffness~~, strength, and deformation capacity of the wall,~~ considering axial, flexural, and shear actions. Potential yielding action ~~failure~~ in flexure, shear, and reinforcement development at any point in the wall shall be considered. Interaction with other structural and nonstructural components shall be included.

The effective stiffness of structural walls and wall segments shall satisfy Section 3.1.2. The effective stiffness values given in Tables 5 and 18 shall be permitted unless alternative stiffness values are determined by a more detailed analysis. For closed and open wall cross-section shapes, such as box, T, L, I, H, and C sections, the effective tension or compression flange widths shall be as specified in Section 3.1.3 for stiffness evaluations, except that the fourth limit shall be changed to one tenth of the wall height. The calculated strength to be used in assessment shall be in accordance with Section 7.2.

When linear static or linear dynamic procedures are used, it shall be permitted to take the flexural rigidity of structural walls as $0.25\ E_{cE}I_g$.

Table 18–Effective stiffness values for cracked structural walls

$N_{UG}/(A_g f'_{cE})$	ρ_l[a,]	Flexural Rigidity[b]
≤ 0.05	≤ 0.01	$0.20\ E_{cE}I_g$
	≥ 0.03	$0.30\ E_{cE}I_g$
≥ 0.50	≤ 0.01	$0.90\ E_{cE}I_g$

	≥ 0.03	1.00 $E_{cE}I_g$

[a] It shall be permitted to use a default ρ_{lb} value of 0.02.

[b] For walls with axial compression and reinforcement ratios falling between the limits provided, flexural rigidity shall be determined by linear interpolation. If interpolation is not performed, the more conservative effective stiffnesses shall be used.

~~Slender~~ Structural walls and wall segments shall be permitted to be modeled as equivalent beam–column elements in which ~~that include~~ both flexural and shear deformations are simulated but flexural strength and deformation capacity is decoupled from shear response. The flexural strength of beam–column elements shall include the interaction of axial load (N_{UF} or N_{UD}) and bending and shall be calculated based on lower bound or expected material properties as applicable to force- or deformation-controlled actions, respectively. The rigid connection zone at beam connections to this equivalent beam–column element shall represent the distance from the wall centroid to the edge of the wall at the location where the beam is connected to the wall. ~~Unsymmetrical wall sections shall be modeled with the different bending capacities for the two loading directions.~~

Joints between structural walls and frame elements shall be modeled as stiff components or rigid components, as appropriate. The diaphragm action of concrete slabs that interconnect ~~shear~~ structural walls and frame columns shall be represented in the model.

To calculate the effective stiffness to yield of flexure-controlled walls, the 2013 version of ASCE 41 recommended using an effective stiffness of 0.5 times the gross moment of inertia (Ig). However, experimental studies of slender walls pushed to yield-level drifts have shown lower stiffness reduction factors, in the range of 0.15 to 0.25 times the gross moment of inertia (PEER 2010; Panagiotou and Restrepo 2007; Priestley et al. 2007). ~~An important limitation of this type of approach is that the calculated effective wall stiffness is independent of parameters such as the The 2020 version of this Standard updated the wall stiffness values to account for the~~ axial load and longitudinal reinforcement ratio.

Results of a large dataset of flexure-controlled wall tests (Abdullah 2019) revealed that cracked effective flexural stiffness is significantly influenced by axial load such that with axial load increasing from zero to 0.5Agf'cE, cracked effective flexural stiffness increases, on average, by a factor of five (i.e., from 0.2 to 1.0 EcEIg). The results also showed that longitudinal reinforcement ratio has a significant influence on cracked effective stiffness, especially for walls with low to moderate axial loads. The modifications to Table 5 and addition of Table 18 reflect the statistics and results of the dataset and provide a closer estimate of cracked effective flexural stiffness than a constant fraction of EcEIg as has traditionally been used.

1.4.2 Strength Provisions

A new Section 7.2 is introduced that contains all the wall strength relations for all wall classifications. The change proposal for wall flexural strength is presented below.

7.2—Strength of Reinforced Concrete Structural Walls, Wall Segments, and Coupling Beams

Component strengths shall be computed according to the general requirements of Section 3.2, with the additional requirements of this section. Strength shall be determined considering the potential for ~~failure~~ yielding action at any point in flexure, shear, shear friction sliding, or

reinforcement development under combined gravity and lateral load, and the controlling actions of components shall be classified as identified in 7.3.2 and 7.4.1.

For all ~~flexural~~ strength calculations, ~~the yield~~ material strengths ~~of the longitudinal reinforcement~~ shall be taken as lower bound or expected material properties as applicable to force-controlled or deformation-controlled actions, respectively.

7.2.1 *Flexural Strength* – The flexural yield strength of structural walls or wall segments, M_{Cy}, as represented by Point B in Fig. 1(*b*), shall be determined using the fundamental principles given in Chapter 22 of ACI 318-19, without using a strength reduction factor. For calculation of flexural strength, the effective compression and tension flange widths defined in Section ~~7.2.2~~ 3.1.3 shall be used, except that the first limit shall be changed to one tenth of the wall height. Where calculating the maximum inelastic flexural strength of the wall, M_{Cult}, as represented by Point C in Fig. 1(~~a~~b), the effects from strain hardening shall be accounted for by ~~substituting f_{yIE} with $1.25f_{yIE}$~~ taking the tensile strength of the reinforcement to be 1.15 times the yield strength. Alternatively, M_{Cult} may be taken as $1.15M_{Cy}$.

Splice lengths for primary longitudinal reinforcement shall be evaluated using the procedures given in Section 3.5. Reduced flexural strengths shall be evaluated at locations where splices govern the usable stress in the reinforcement.

1.4.3 Modeling Parameters and Acceptance Criteria

1.4.3.1 LINEAR PROCEDURES

The change proposal for ACI 369.1 pertaining to linear procedure of flexure-controlled walls contains the following updates:

- Provisions for shear amplification for linear procedures
- Two sets of m-factors are proposed: (a) a table with expressions for deriving m-factors based on nonlinear modeling parameters, and (b) two tables for m-factor values for conforming and nonconforming walls.

A strength-based wall classification approach was also proposed. This classification approach and the change proposal that is associated with it are presented in Chapter 4 of this Part of the document. Change proposal text in Section 7.3.2 (below) that pertains to wall classification are presented in Chapter 4 and not shown here.

7.3.2 Acceptance Criteria –

[Note: Wall classification text removed here and presented in Part 4, Chapter 4]

Design actions (flexure, shear, axial, or force transfer at reinforcing bar anchorages and splices) on components shall be determined as prescribed in Chapter 7 of ASCE 41-17. Where determining the appropriate value for the design actions, proper consideration shall be given to gravity loads and to the maximum forces that can be transmitted considering nonlinear action in adjacent components. Design actions shall be compared with strengths in accordance with Section 7.5.2.2 of ASCE 41-17. Tables 20 and 21 specify m-factors for use in Equation (7-36) of ASCE 41-17. Alternatively, in

place of Table 20, it shall be permitted to use applicable m-factor values from Tables 22 and 23 for wall controlled by flexure. Alternate m-factors shall be permitted where justified by experimental evidence and analysis.

Table ~~21~~20–Numerical acceptance criteria for linear procedures: reinforced concrete structural walls controlled by flexure

Component Type	m-factors[a,b]		
	Performance level		
	IO	LS	CP
Primary	$\frac{\theta_{yE}+0.1(d_{nl}-\theta_{yE})}{\theta_{yE}}$	$\frac{9}{16}\left(\frac{d_{nl}}{\theta_{yE}}\right)$	$\frac{9}{16}\left(\frac{e_{nl}}{\theta_{yE}}\right)$
Secondary	$\frac{\theta_{yE}+0.1(d_{nl}-\theta_{yE})}{\theta_{yE}}$	$\frac{9}{16}\left(\frac{e_{nl}}{\theta_{yE}}\right)$	$\frac{9}{16}\left(\frac{e_{nl}}{\theta_{yE}}\right)$

[a] θ_{yE} s hall be calculated per Equation 6. It shall be permitted to take θ_{yE} as 0.003 rad in this table, in lieu of using Equation 6. m-factors for LS or CP shall not be smaller than those for IO or LS, respectively. m-factors for LS shall not be greater than those for CP. m-factors shall not be smaller than 1.0.

[b] The acceptance criteria for primary members shall not be taken larger than those for secondary members

Table 22– Alternate numerical acceptance criteria for linear procedures: Conforming reinforced concrete structural walls controlled by flexure

Conditions[a]			m-factors	
			Performance Level	
$\frac{l_w c_{DE}}{b_s^2}$	$\frac{w_v V_{MCultDE}}{A_{cv}\sqrt{f'_{cE}}}$	Overlapping hoops used?	IO	Primary LS
≤ 10	≤ 4	YES	2.0	6.0
≤ 10	≥ 6	YES	1.8	4.9
≥ 70	≤ 4	YES	1.5	3.4
≥ 70	≥ 6	YES	1.4	2.6
≤ 10	≤ 4	NO	2.0	6.0
≤ 10	≥ 6	NO	1.8	4.9
≥ 70	≤ 4	NO	1.3	2.3
≥ 70	≥ 6	NO	1.3	2.1

Conditions[a]		m-factors		
		Performance Level		
$\frac{l_w c_{GE}}{b_s^2}$	$\frac{N_{UD}}{A_g f'_{cE}}$	Primary	Secondary	
		CP	LS	CP

≤ 10	≤ 0.10	7.5	7.5	10.0
≤ 10	≥ 0.20	6.0	6.0	8.0
≥ 70	≤ 0.10	3.8	3.8	5.0
≥ 70	≥ 0.20	2.6	2.6	3.5

[a] See Table 22a for criteria to apply to conditions

Table 23— Alternate numerical acceptance criteria for linear procedures: Non-conforming reinforced concrete structural walls controlled by flexure

Conditions[a]		m-factors	
		Performance Level	
$\frac{l_w c_{DE}}{b_s^2}$	Detailing		Primary
		IO	LS
≤ 10	$A_{sh,provided}/A_{sh,required} \geq 0.5$ and $s/d_b \leq 9$	1.7	4.5
≤ 10	$A_{sh,provided}/A_{sh,required} < 0.2$ and $s/d_b > 15$	1.5	3.6
≥60	$A_{sh,provided}/A_{sh,required} \geq 0.5$ and $s/d_b \leq 9$	1.2	1.9
≥ 60	$A_{sh,provided}/A_{sh,required} < 0.2$ and $s/d_b > 15$	1.2	1.5

Conditions[a]		m-factors		
		Performance Level		
$\frac{l_w c_{GE}}{b_s^2}$	$\frac{N_{UD}}{A_g f'_{cE}}$	Primary	Secondary	
		CP	LS	CP
≤ 10	≤ 0.10	6.6	6.6	8.8
≤ 10	≥ 0.20	3.9	3.9	5.3
≥ 60	≤ 0.10	2.8	2.8	3.8
≥ 60	≥ 0.20	1.9	1.9	2.5

[a] See Table 22b for criteria to apply to conditions

1.4.3.1 NONLINEAR PROCEDURES

The change proposal for nonlinear procedures of walls controlled by flexure contains:

- Criteria for defining conforming walls. Walls that do not satisfy these requirements are treated as nonconforming.
- Updated tables for modeling parameters and acceptance criteria for conforming and nonconforming walls.

7.4.1.1.1 *Structural walls and wall segments controlled by flexure*

Values for the variables $c_{n\ell}$, $c'_{n\ell}$, $d_{n\ell}$, $d'_{n\ell}$, and $e_{n\ell}$ required to define the location of Points C, D, and E in Fig. 1(b) shall be as specified in Table 22. Walls shall be considered conforming where wall detailing complies with the following requirements:

1. A minimum of two curtains of web vertical and horizontal reinforcement are present,
2. the boundary longitudinal reinforcement ratio, $\rho_{lb} \geq 6\sqrt{f'_{cE}/f_{yE}}$,
3. the minimum ratio of provided area of boundary transverse reinforcement, $A_{sh}/(sb_c)$, is not less than 0.7 times that computed from Equation 7.

$$A_{sh}/sb_c = 0.3\left(\frac{A_g}{A_{ch}}\right)\frac{f'_{cE}}{f_{ytE}} \geq 0.09\frac{f'_{cE}}{f_{ytE}} \quad (7)$$

4. the ratio of vertical center-to-center spacing of boundary transverse reinforcement to the diameter of the smallest longitudinal reinforcement, $s/d_b \leq 8.0$,
5. lap-splice failure of longitudinal reinforcement is precluded.

For the nonlinear dynamic procedure (NDP), the unloading and reloading stiffnesses and strengths, and any pinching of the load-versus-rotation hysteresis loops, shall reflect the behavior experimentally observed for wall elements similar to the one under investigation. Where experimental data are not available to validate complete hysteretic behavior of a component including unloading and reloading stiffness and strength and pinching of the load-deformation response history, the computational models employed shall define response histories in general agreement with the relationships presented in Section 3.1 as specified in Table 24 Use of the generalized load-deformation relation shown in Fig. 1(b) to represent the response envelope ~~relation~~ for the analysis shall be permitted.

Table ~~19~~24a—Modeling parameters and numerical acceptance criteria for nonlinear procedures: conforming reinforced concrete structural walls and associated components controlled by flexure

Conditions[e]				Acceptance Criteria
				Performance Level
$\frac{l_w c_{DE}}{b_s^2}$	$\frac{w_v V_{MCultDE}{}^c}{A_{cv}\sqrt{f'_{cE}}}$	Overlapping hoops[a] used?	d_{nl}	IO
≤ 10	≤ 4	Yes	0.032	$\theta_y + 0.1(d_{nl} - \theta_y)$
≤ 10	≥ 6	Yes	0.026	
≥ 70	≤ 4	Yes	0.018	
≥ 70	≥ 6	Yes	0.014	
≤ 10	≤ 4	No	0.032	
≤ 10	≥ 6	No	0.026	
≥ 70	≤ 4	No	0.012	

≥ 70	≥ 6	No	0.011	

Conditions[e]						Acceptance Criteria	
						Performance Level	
$\frac{l_w c_{GE}}{b_s^2}$	$\frac{N_{UD}}{A_g f'_{cE}}$	c_{nl}	c'_{nl}	d'_{nl}[b]	e_{nl}[b]	LS	CP
≤ 10	≤ 0.10	0.5	1.15	0.036	0.040	0.75 e_{nl}	0.85 e_{nl}
≤ 10	≥ 0.20	0.1		0.030	0.032		
≥ 70	≤ 0.10	0.0		0.018	0.020		
≥ 70	≥ 0.20	0.0		0.014	0.014		

[a] Overlapping hoop definition shall be per ACI 318-19

[b] Parameters d'nl and e nl shall not be taken smaller than parameter dnl.

[c] the shear amplification factor ωv need not be applied if VMCultDE is obtained from nonlinear analyses procedures.

[e] Linear interpolation between the values given in the table shall be permitted; however, interpolation between the values specified for conforming walls (Table 22a) and non-conforming walls (Table 22b) shall not be permitted.

Table ~~1924~~b—Modeling parameters and numerical acceptance criteria for nonlinear procedures: nonconforming reinforced concrete structural walls and associated components controlled by flexure

Conditions[d,e]			Acceptance Criteria
			Performance Level
$\frac{l_w c_{DE}}{b_s^2}$	Detailing[a,b,c,g]	d_{nl}	IO
≤ 10	$A_{sh,provided}/A_{sh,required} \geq 0.5$ and $s/d_b \leq 9$	0.024	$\theta_y+0.1(d_{nl} - \theta_y)$
≤ 10	$A_{sh,provided}/A_{sh,required} < 0.2$ and $s/d_b > 15$	0.019	
≥ 60	$A_{sh,provided}/A_{sh,required} \geq 0.5$ and $s/d_b \leq 9$	0.010	
≥ 60	$A_{sh,provided}/A_{sh,required} < 0.2$ and $s/d_b > 15$	0.008	

Conditions[d,e,g]						Acceptance Criteria	
						Performance Level	
$\frac{l_w c_{DE}}{b_s^2}$	$\frac{N_{UD}}{A_g f'_{cE}}$	c_{nl}	c'_{nl}	d'_{nl}[f]	e_{nl}[f]	LS	CP

≤ 10	≤ 0.10	0.4	1.15	0.032	0.035	0.75 e_{nl}	0.85 e_{nl}
≤ 10	≥ 0.20	0.1		0.020	0.021		
≥ 60	≤ 0.10	0.0		0.015	0.015		
≥ 60	≥ 0.20	0.0		0.010	0.010		

[a] $A_{sh,required}$ shall be as calculated using Equation 7

[b] If values of both $A_{sh,provided}/A_{sh,required}$ and s/d_b fall between or outside the limits given in the table, linear interpolation shall independently be performed for both $A_{sh,provided}/A_{sh,required}$ and s/d_b, and the lower resulting value of parameter d_{nl} shall be taken.

[c] Values of $A_{sh,provided}/A_{sh,required}$ and s/d_b shall be provided over a horizontal distance that extends from extreme compression fiber at least $c_{DE}/2$.

[d] This table applies to walls and wall segments with $\rho_{lw} \geq 0.001$. For $0.0025 \geq \rho_{lw} \geq 0.001$ and $l_w c_{DE}/b_s^2 \leq 20$, modeling parameters d_{nl}, d'_{nl} and e_{nl} shall be multiplied by a reduction factor. The reduction factor shall be 0.4 for $\rho_{lw} = 0.001$ and $l_w c_{DE}/b_s^2 \leq 10$ and 1.0 for $\rho_{lw} = 0.0025$ and $l_w c_{DE}/b_s^2 = 20$. Linear interpolation of the reduction factor with respect to ρ_{lw} and $l_w c_{DE}/b_s^2$ shall be permitted for intermediate values.

[e] This table applies to walls with one or multiple curtains of web reinforcement.

[f] Parameters d'_{nl} and e_{nl} shall not be taken smaller than parameter d_{nl}.

[g] Linear interpolation between the values given in the table shall be permitted; however, interpolation between the values specified for conforming walls (Table 22a) and non-conforming walls (Table 22b) shall not be permitted.

1.4.4 Analysis Guidance

Within the change proposal, guidance on constructing lumped-plasticity and fiber-section models was provided. Requirements for extracting deformation measures that are consistent with nonlinear modeling parameters and acceptance criteria for walls are provided.

General guidance for wall modeling using linear and nonlinear procedures is proposed as follows. Where guidance is proposed only in commentary, the appropriate commentary sections of the change proposal are provided below. Where requirements are proposed, changes to the appropriate clauses are provided.

C3.1.2.2 Nonlinear Procedures

In real structures and in finite element analyses of structures, softening-type response results in large deformations and reduced strength within a localized region. In analysis models, the length over which the deformations localize is determined by the size of the finite element mesh. If material models are not regularized, using mesh dependent lengths, then simulated deformation capacity becomes mesh dependent, with reduced element size resulting in reduced deformation capacity and increasingly rapid strength loss. Pugh et al. (2017) and Lowes et al. (2016) provide guidance on regularization of concrete and steel material models to minimize mesh-sensitivity in models that comprise solid element, layered and fiber shell element, and beam-column element with fiber-type sections.

Within this Standard, rotation is the primary measure used to define component response and acceptance criteria. When the nonlinear response of a structure is simulated using a modeling

approach other than a concentrated hinge, defined by a moment-rotation or story shear-deflection history, it is necessary to convert between the rotations specified in this Standard and the deformation measures employed within the model. To make these conversions, it is recommended that the component rotations specified within this Standard be compared with a rotation computed using i) curvature at the critical section and, as needed, curvature computed at additional sections, as well as ii) a hinge length (l_p) equivalent to that specified within this Standard or justified by experimental evidence for the hinge rotation being considered. Figure XXX shows an example of this conversion for a wall modeled using multiple approaches.

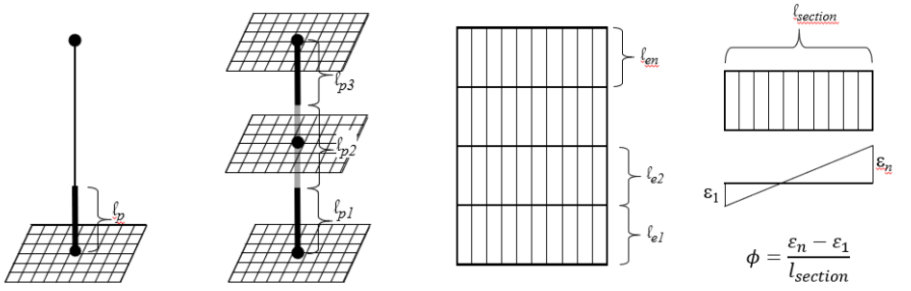

Figure C1a: lumped-plasticity beam-column line-element, 2D fiber section element located at element critical section

Figure C1b: distributed-plasticity beam-column line-element, 2D fiber sections located at element ends and distributed within element

Figure C1c: fiber shell element model of planar wall; mesh comprises a single element along the horizontal length of the wall and multiple elements along the vertical height of the wall

Figure C1d: calculation of fiber section curvature from extreme fiber strains

$$\theta = \phi_{e1} * l_p \text{ for } lp < l_{e1}$$
$$\theta = \phi_{e1} * l_{e1} + \phi_{e2} * (l_p - le_1) \text{ for } le_1 < l_p < le_1 + le_2$$

Fig. XXX—Nonlinear wall modeling options.

7.3—Linear static and dynamic procedures for structural walls and wall segments

7.3.1 *Modeling*—

~~Slender~~ Structural walls and wall segments shall be permitted to be modeled as equivalent beam–column elements in which ~~that include~~ both flexural and shear deformations are simulated but flexural strength and deformation capacity is decoupled from shear response. The flexural strength of beam–column elements shall include the interaction of axial load (N_{UF} or N_{UD}) and bending and shall be calculated based on lower bound or expected material properties as applicable to force- or deformation-controlled actions, respectively. The rigid connection zone at beam connections to this equivalent beam–column element shall represent the distance from the wall centroid to the edge of the wall. ~~Unsymmetrical wall sections shall be modeled with the different bending capacities for the two loading directions.~~

Joints between structural walls and frame elements shall be modeled as stiff components or rigid components, as appropriate. The diaphragm action of concrete slabs that interconnect ~~shear~~ structural walls and frame columns shall be represented in the model.

7.4—Nonlinear static and dynamic procedures for structural walls and wall segments

7.4.1 *Modeling*

It shall be permitted to simultaneously use decoupled rotational and translational elements to simulate the flexure and shear nonlinear behaviors, respectively, of structural walls and wall segments in accordance with 7.4.1.1. However, story drifts at wall critical sections shall be evaluated to confirm that that the onset of lateral strength loss is not shifted to occur at a drift value

corresponding to the lower value of modeling parameter d_{pl} of the rotational and translational elements given in Tables 19 and 20. In addition, story drift acceptance criteria at wall critical sections shall be limited to a value corresponding to the lower acceptance criteria permitted in Tables 19 and 20, for the applicable Performance Objective.-Alternatively, it shall be permitted to model structural walls and wall segments using solid elements or layered shell elements that couple flexural and shear behaviors in accordance with 7.4.1.2.

Walls that are asymmetrical about the centerline of the cross-section in terms of geometry, reinforcement ratio, and/or detailing, shall be modeled with different force-deformation responses in the two loading directions.

The controlling behavior for structural walls and wall segments shall be in accordance with Table 7. The shear amplification factor ω_v need not be applied in Table 7 if V_{MCultE} is obtained from nonlinear analyses procedures. Structural walls with h_w/l_w smaller than 1.0 shall be permitted to be classified as shear-controlled.

1.4.4.1 LUMPED PLASTICITY APPROACH

Specific guidance for modeling walls using the lumped-plasticity approach is provided in the change proposal as follows:

7.4.1.1 *Nonlinear static and dynamic procedures employing lumped-plasticity load-deformation models*—Nonlinear load-deformation relations for use in analysis by nonlinear static and dynamic procedures shall comply with the requirements of Section 3.1.2. Monotonic and cyclic load-deformation relationships for analytical models that represent structural walls and wall segments shall be in accordance with the generalized relations defined in Section 3.1 and shown in Fig. 1 Tables 5 and 18 shall be permitted for determining the initial stiffness from Point A to Point B in Fig. 1.

7.4.1.1.1 *Structural walls and wall segments controlled by flexure*—For structural walls and wall segments that have inelastic behavior under lateral loading that is controlled by flexure, the following approach shall be permitted. The load-deformation relationship in Fig. 1(b) shall be used with the X-axis of the figure taken as the rotation over the plastic hinging region (l_p) at the end of the member, as shown in Fig. 4. The hinge rotation at Point B in Fig. 1(b) corresponds to the yield hinge rotation (θ_y) and shall be calculated in accordance with Eq. (6~~5~~)

$$\theta_{yE} = \left(\frac{M_{CyGE}}{E_{cE}I_{eff}}\right) l_p \qquad (6\text{~~5~~})$$

where $E_{cE}I_{eff}$ is the effective flexural stiffness computed per Section 7.3.1~~7.2.2~~, M_{CyGE} is computed per Section 7.2.1, and l_p is the assumed plastic hinge length. The value of l_p shall be set equal to the lesser of 0.5 times the ~~effective flexural depth~~ total length of the wall and 0.5 times the height of the story at the location of the hinge. For ~~analytical~~ computational models of wall segments, the value of l_p shall be set equal to the lesser of 0.5 times the effective flexural depth of the member and 50 percent of the element length.

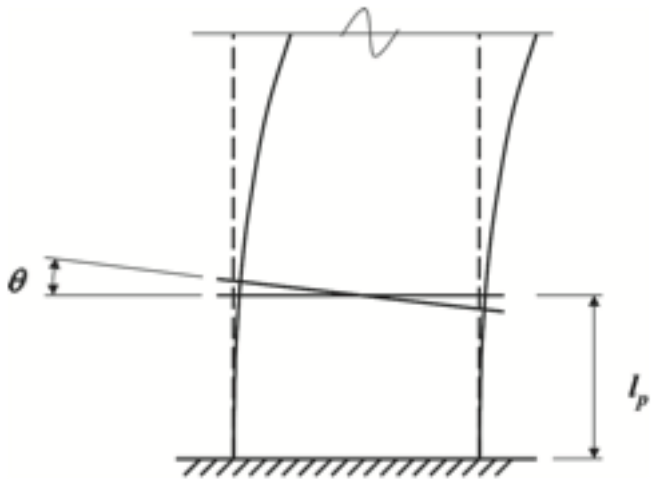

Fig. 4– Plastic hinge rotation in structural wall where flexure dominates inelastic response.

1.4.4.2 FIBER-SECTION APPROACH

Specific guidance for modeling walls using the fiber-section approach is provided in the change proposal as follows:

7.4.1.2 *Nonlinear static and nonlinear dynamic procedures employing models other than lumped-plasticity load-deformation models* – It shall be permitted to model structural walls and wall segments using solid elements or layered shell elements in accordance with Section 3.1.2. It shall be permitted to model structural walls and wall segments responding primarily in flexure using, solid elements, fiber or layered shell elements, or beam-column elements with fiber-type section models in accordance with Section 3.1.2. Where simulation results generated using these modeling procedures cannot be validated using experimental data, the stress-strain models that compose these models shall be modified such that predicted response is in general agreement with the generalized load-deformation values in 7.4.1.1.

1.5 Flexure-Controlled Walls Example

This section presents an analysis and evaluation example for a lateral force resisting system (LRFS) of a building structure comprising flexure-controlled reinforced concrete walls. The example uses a modified version of an existing building that was seismically evaluated and retrofitted following the nonlinear static procedure (NSP) provisions of ASCE/SEI 41-13. The LFRS of the retrofitted building in the transverse direction consists primarily of four new flexure-controlled reinforced concrete walls.

The example summarizes the building structure, configuration, seismic loading, wall classification, and mathematical modeling and analysis using the computer software Perform3D. The example presents calculation reports and evaluation results for an example wall using the proposed MPs and ACs and compares them to evaluation outcomes using the ASCE/SEI 41-13 and ASCE/SEI 41-17 provisions.

1.5.1 Overview of Building

The building is a reinforced concrete structure located in Southern California. It is approximately 50 ft × 150 ft in plan and 144 ft high above the ground level. The building has twelve stories above ground and one basement level. There is a mezzanine between the ground and second floors. The columns are arranged in a 3 × 9 bay pattern, with each bay roughly 17 ft square. The gravity system consists of reinforced concrete slabs, beams, columns, and walls. The foundation consists of reinforced concrete isolated spread footings at interior columns and continuous footings under the walls. Figure 1-52 shows a typical plan of the building. Figure 1-53 and Figure 1-54 show structural wall elevations in the transverse direction.

The original LFRS in the transverse direction consisted of a reinforced concrete moment frame. The retrofit design included the addition of 12 in. or 16 in. thick structural walls in either one or two bays along grid lines 3, 5, and 6, and 8. The existing construction has what is commonly referred to as non-ductile detailing. The new construction (i.e., structural members and connections added for retrofit) has relatively ductile detailing but is not "conforming" per the proposed provisions. The 12 in. thick walls on grid lines 5 and 6 are about 16 ft long (one bay) and nearly identical. The walls on grid lines 3 and 8 are 12 in. and 16 in. thick, respectively. They are two bays long each and have generally similar configurations, but the latter has a large opening that spans one bay (about 16 ft) between the ground and second floors. In addition to the new walls, new columns were added adjacent to some existing columns (Section 1.5.2.2). This example focuses on the performance assessment of retrofitted walls in the transverse directions.

In the longitudinal direction, the existing LFRS consists of a perforated structural wall along grid line A. This wall is continuous up the height of the building and is shear-controlled. Evaluation of this wall is not part of this example.

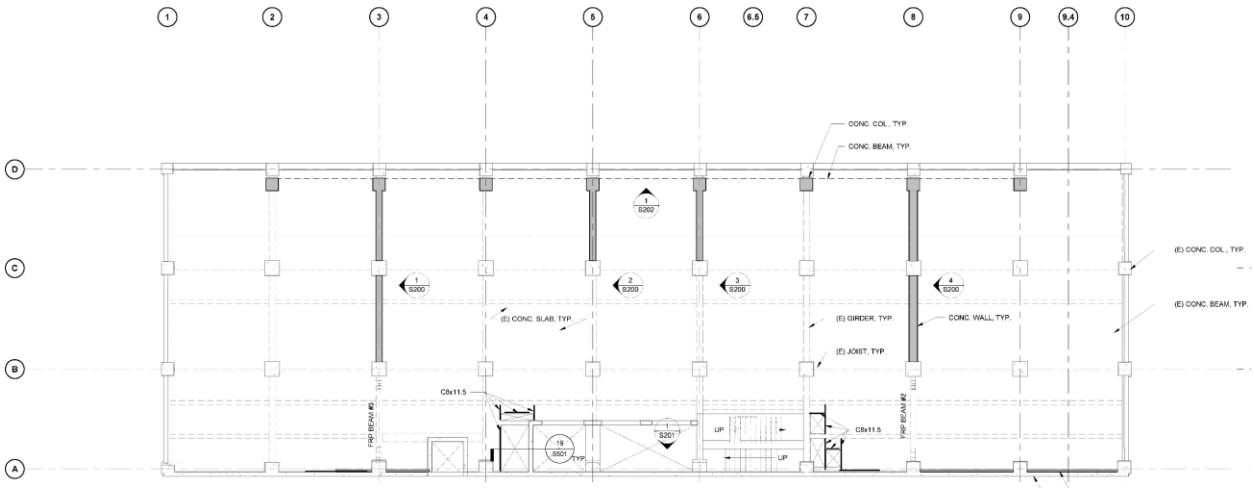

Figure 1-52 Building floor plan (north is upward).

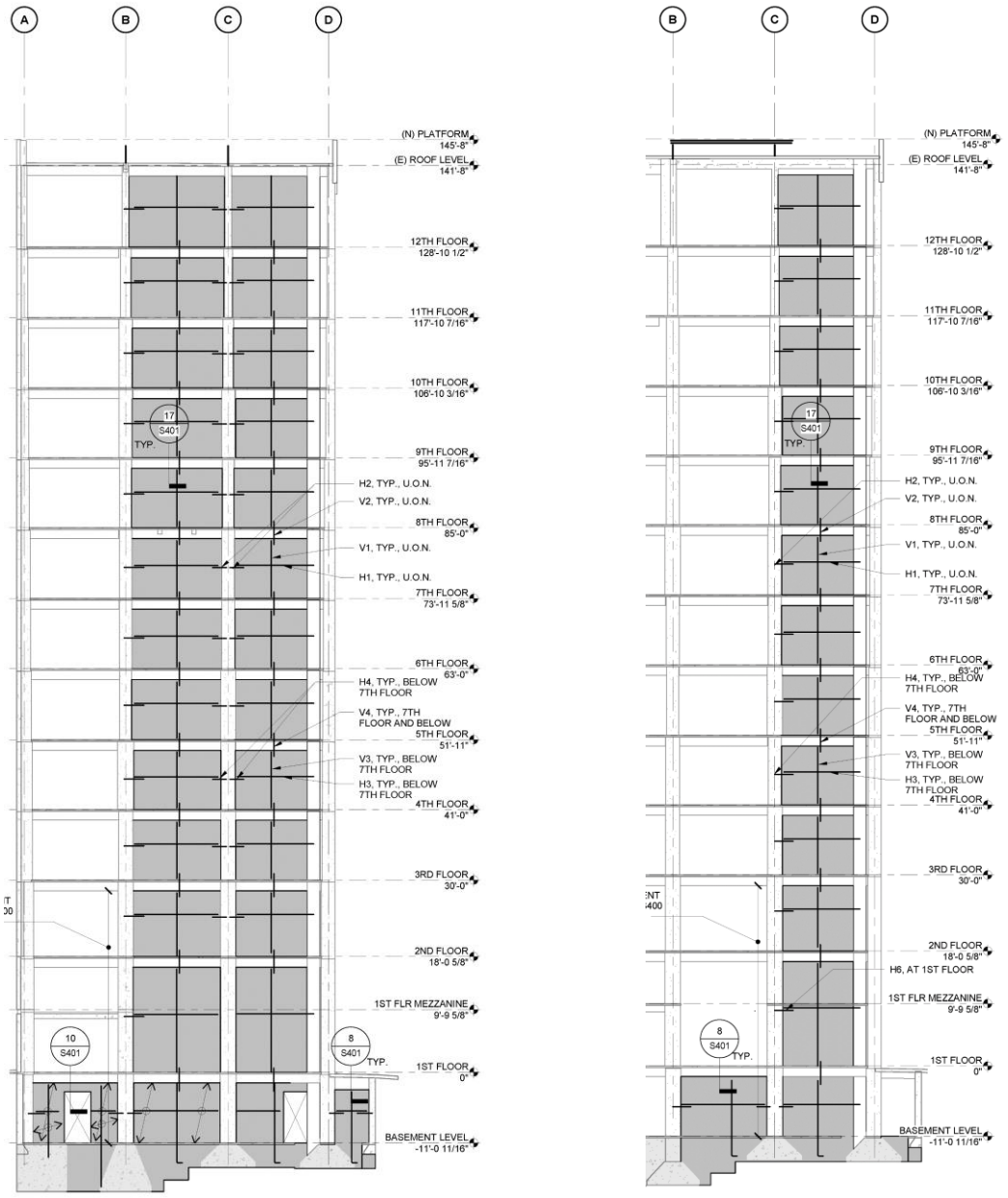

Figure 1-53 Elevations of transverse structural walls along grid lines 3 (left) and 5 (right).

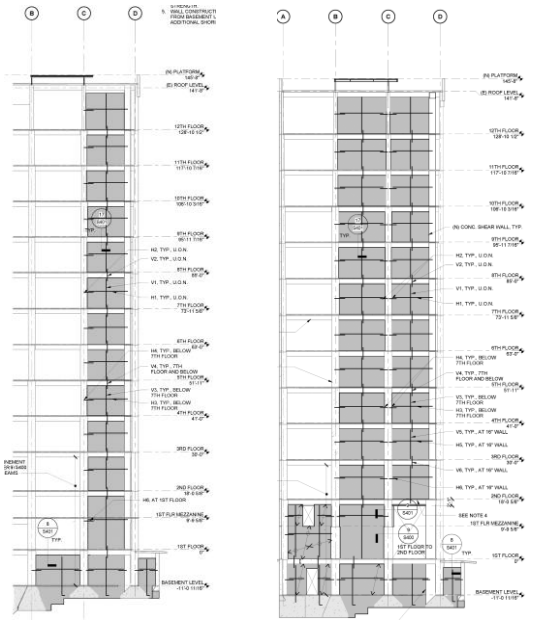

Figure 1-54 Elevations of transverse structural walls along grid lines 6 (left) and 8 (right).

1.5.1.1 WALL CONFIGURATION

Figure 1-55 shows the cross-section of the added wall on grid line 3. The wall is 12 in. thick and spans two bays that are about 16 ft long each. It contains two curtains of reinforcement, one on each face, with transverse steel bars placed on the outside. The wall longitudinal and transverse reinforcement ratios are 1.1% and 0.8%, respectively. The wall cross-section ends with a new column added near grid line D. The new column is 24 in.×24 in. with 2.8% longitudinal reinforcement ratio. Three existing columns with dimensions of 28 in.×28 in, 28 in.×28 in., and 25 in.×25 in. are located at grid lines B, C, and D, with longitudinal reinforcement ratios of 2.2%, 1.5%., and 2.4%, respectively. The new walls and columns are concentric with the existing columns and girders. Shear dowels between the new walls and columns and the adjacent columns and girders provide load path continuity throughout the height of the building.

Figure 1-56 shows the cross-sections of the walls on grid lines 5 and 6. Except for the shorter overall wall length, the wall and new column dimensions and reinforcement ratios are the same as the grid line 3 wall. The existing columns, at grid lines C and D, have similar dimensions to the ones along grid line 3, and their longitudinal reinforcement ratios are 1.7% and 2.6%, respectively.

Figure 1-55(a) and Figure 1-56(a) show the wall dimensions and identify slight adjustments adopted in constructing the computer analysis model due to constraints of the finite element (FE) mesh. The fiber sections shown in Figure 1-55(b) and Figure 1-56(b) were used to compute the section moment strengths including the effect of axial-flexure interaction.

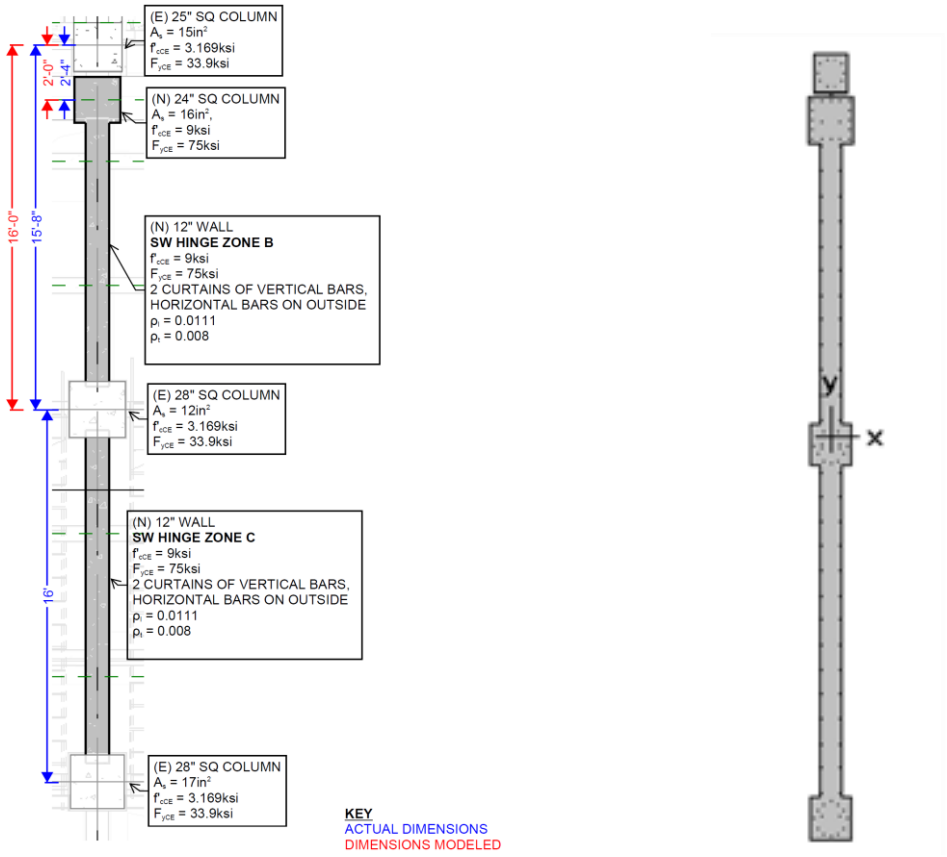

(a) Geometry and Reinforcement **(b) Fiber Section Model**

Figure 1-55 Cross-section details for wall on grid line 3 first floor.

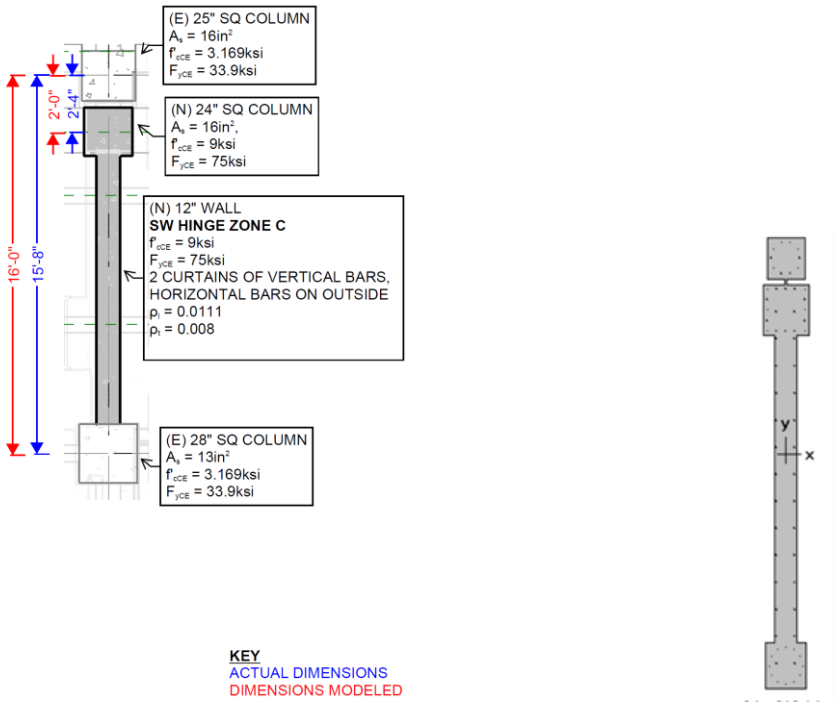

(a) Geometry and Reinforcement **(b) Fiber Section Model**

Figure 1-56 Cross-section details for wall on grid lines 5 and 6 at first floor.

1.5.1.2 MATERIALS

The nominal material strengths of the materials used in the retrofit design are as follows:

- Concrete f'_c = 6 ksi
- Steel reinforcing bars f_y = 60 ksi

The material specifications for the original concrete and steel materials were not available. Their expected strengths were determined based on ASCE/SEI 41-13 Usual Testing requirements, and are as follows:

- Concrete f'_{cE} = 3.17 ksi
- Steel reinforcing bars f_{yE} = 33.9 ksi

The Young's modulus of elasticity was determined as follows:

- Concrete E_{cE} = 57,000sqrt(f'_{cE}) [psi]
- Steel reinforcing bars E_{sE} = 29,000 ksi

The concrete uncracked stiffness modulus used the expected compressive strength, f'_{cE} (Section 1.5.4). The transverse reinforcement in the new columns meet the ACI 318-14 detailing

requirements for Special Moment Frame columns, and the confined concrete strength is thus used in the model. Unconfined strength is used for the existing concrete based on review of the existing column details.

1.5.1.3 EARTHQUAKE LOADING

The ground motion input for the performance evaluation was taken following the ASCE/SEI 7-10 design spectrum shape. The site-specific spectral accelerations defining this spectrum for the basic safety earthquake (BSE)-1E and BSE-2E were as follows:

S_{xs} = 0.88g (BSE-1E) and 1.75g (BSE-2E)

S_{x1} = 0.44g (BSE-1E) and 0.80g (BSE-2E)

For this example, the BSE-2E hazard level was constrained with the minimum of 0.75×BSE-2N. The BSE-1E hazard level was not constrained by a minimum value. Response of the structure in the transverse direction is the subject of this example. The transverse axis is oriented along the north-south direction. The elastic and effective first-mode periods for the structure in the north-south direction were calculated to be:

T_i = 1.39 s

T_e = 1.70 s

The corresponding spectral acceleration at the effective period is therefore:

S_a = 0.26g (BSE-1E) and 0.47g (BSE-2E)

The NSP loading sequence consisted of applying gravity load followed by lateral pushover analysis. Gravity load consisted of dead load and 25% of the design live load. The target roof displacements for BSE-1E and BSE-2E were determined according to ASCE/SEI 41-13. These displacements corresponded to average drift ratios of 0.49% and 0.83%, respectively, between the roof and the ground. The lateral pushover analysis was performed using the normalized displacement profile of the fundamental mode, which results in essentially a triangular loading pattern. Seismic loading towards the south direction was found to govern the wall performance evaluation, and its results are the focus of this example.

1.5.2 Strength and Stiffness

The axial load ratio from gravity, N_{UG}, on all walls is lower than $0.05A_g f'_{cE}$. In this example, the NSP provisions are used, with lateral load applied monotonically in only one direction. Review of the Perform3D output indicated that the NSP loading imposes an increasing net compressive axial force on the transverse walls for the governing loading direction. The maximum axial load demands in the transverse walls during pushover ranged from 1.8 times to 2.3 time the axial load from gravity. A representative axial load level of $2N_{UG}$ was used in the strength calculation for all walls.

The moment yield strengths were computed according to ASCE/SEI 41 and the proposed MP provisions. The computation used computer program spColumn v6.00, which models the axial-flexure interaction using fiber section representation (Figure 1-55b and Figure 1-56b). A representative total axial load of $2N_{UG}$ due to earthquake loading was used to determine the moment strengths. The effective yield moment in ASCE/SEI 41-13, 41-17, and the proposed provisions is the same. The ultimate moment strength is considered to be equal to the yield moment in ASCE/SEI 41-13 and 41-17 (in the NSP execution, a modest strength gain is typically added for numerical convergence). The proposed provisions consider the ultimate moment strength to be 1.15 times the yield moment.

Table 1-16 lists the expected wall moment strengths determined using computer program spColumn. The walls are flexure-controlled, as demonstrated in Section 1.5.3. Therefore, shear strengths are not used in this example.

Wall stiffness is discussed in Section 1.5.4.3.1.

Table 1-16 Wall Moment Capacities and Corresponding Axial Loads [kip, ft units]

Wall Grid Line	3	5	6	8
Push Direction	South	South	South	South
N_{UG}	1,860	1,280	1,290	1,240
N_{UD} ($=2N_{UG}$)	3,720	2,560	2,580	2,480
M_{CyDE}	156,100	54,400	54,500	125,400
M_{CultDE} ($=1.15M_{CyDE}$)	179,500	62,600	62,700	144,200

1.5.3 Classification

ASCE/SEI 41-13 and 41-17 classify structural walls with aspect ratios higher than 3 as slender walls controlled by flexure.

The proposed provisions classify structural walls according to the ratio of expected shear strengths to the shear force corresponding to moment strength. The four walls have aspect ratios of about 4.5 or higher. It could be determined by judgment that they are flexure-controlled. The following calculations are shown for illustration for the wall on grid line 5.

Wall Height, H	140 ft	
Number of stories, n_s	13	
Shear amplification, ω_v	1.73	$= 1.3 + n_s / 30$
Moment strength, M_{CultE}	54,400 kip-ft	(Section 1.5.2)

Flexural hinge length, l_p	9 ft	$= l_w / 2$
Corresponding shear, V_{MCultE}	612 kip	$= M_{CultE} / (2H/3 - 0.5l_p)$

The wall shear strength is controlled by diagonal tension. The shear strength using ACI 318-19 provisions and expected material properties, V_{C318E}, was calculated to be about 2,500 kips using conservatively biased simplifications since it is only used for screening.

Wall shear strength, V_{CE}	2,500 kip	
Check $V_{CE} / (\omega_v V_{MCultE})$	$= 2.36 > 1.0$	Confirms that wall is flexure-controlled

1.5.4 Evaluation Using Nonlinear Static Procedure

1.5.4.1 ANALYSIS MODEL

Geometry

Figure 1-57 shows an exploded view of the Perform3D analysis model. Figure 1-58 through Figure 1-60 show elevation views of the FE models for the LFRS at grid lines 3, 5, 6, and 8. Cyan and pink lines identity the new and existing columns, respectively. Light black lines identify the coupled moment frame beams and columns. The walls were represented by shell elements. The shell elements were assigned composite fiber sections for flexure-axial response and nonlinear shear panel sections for in-plane shear response. The embedded columns were represented using frame elements with fiber sections and tied to wall nodes at floor elevations. The A, B, and C monikers in Figure 1-58 through Figure 1-60 identify the assignment of material properties to wall segments, which is discussed below.

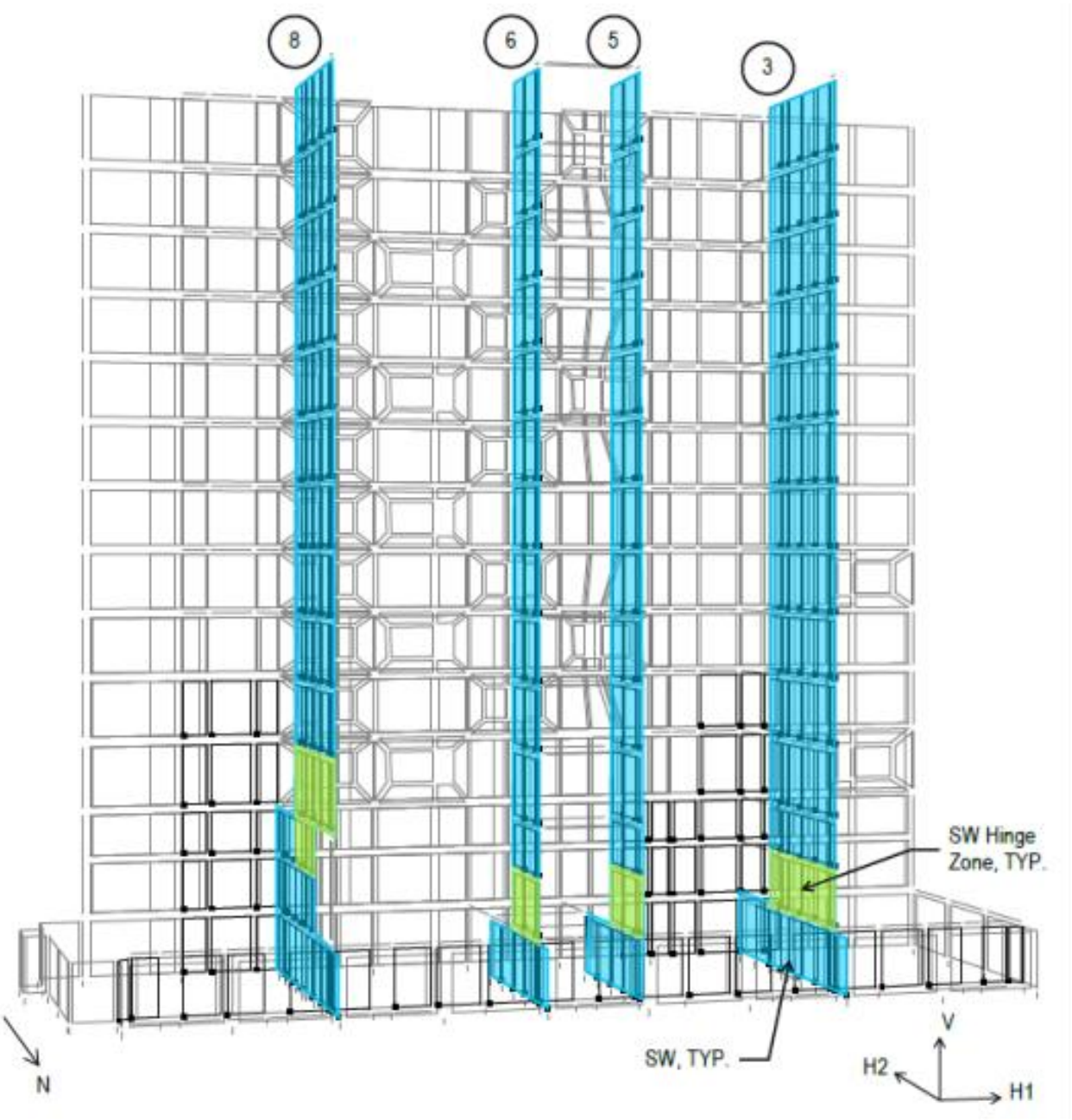

Figure 1-57 Exploded view of analysis model showing transverse walls.

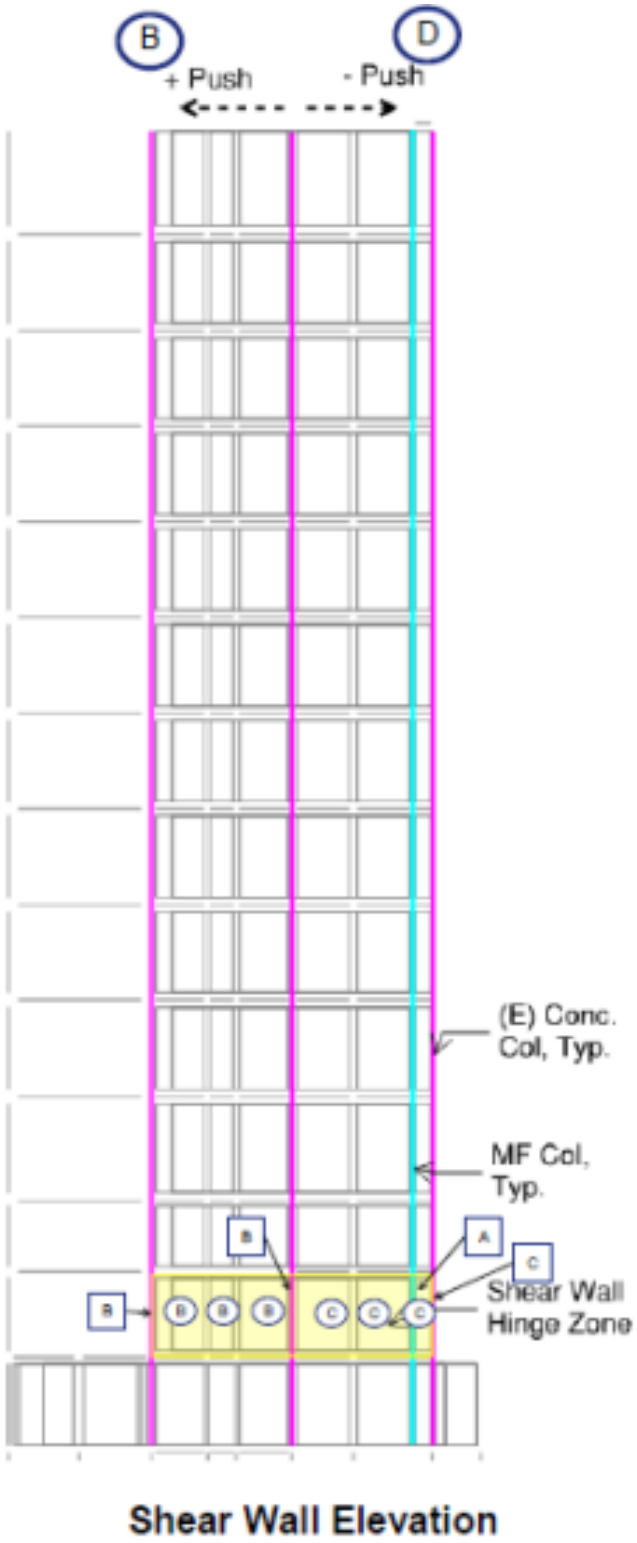

Figure 1-58 FE model of LFRS along grid line 3.

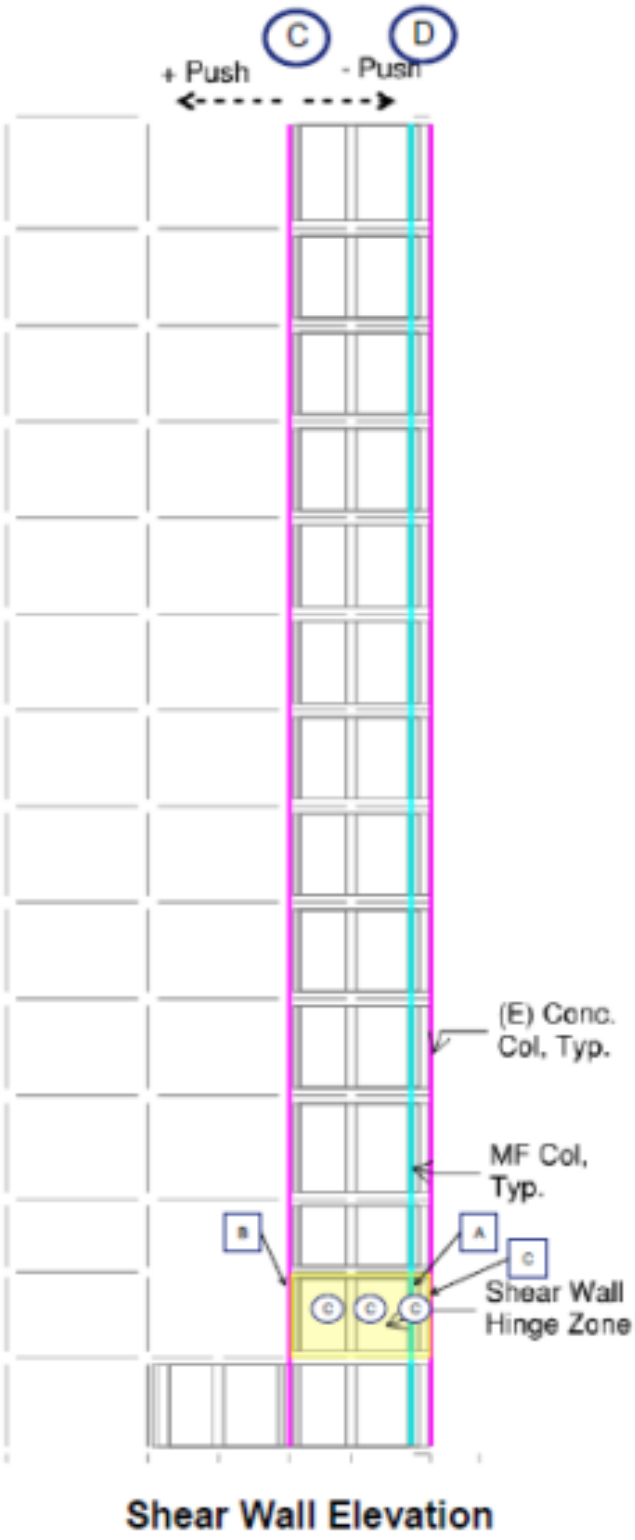

Figure 1-59 FE model of LFRS along grid lines 5 and 6.

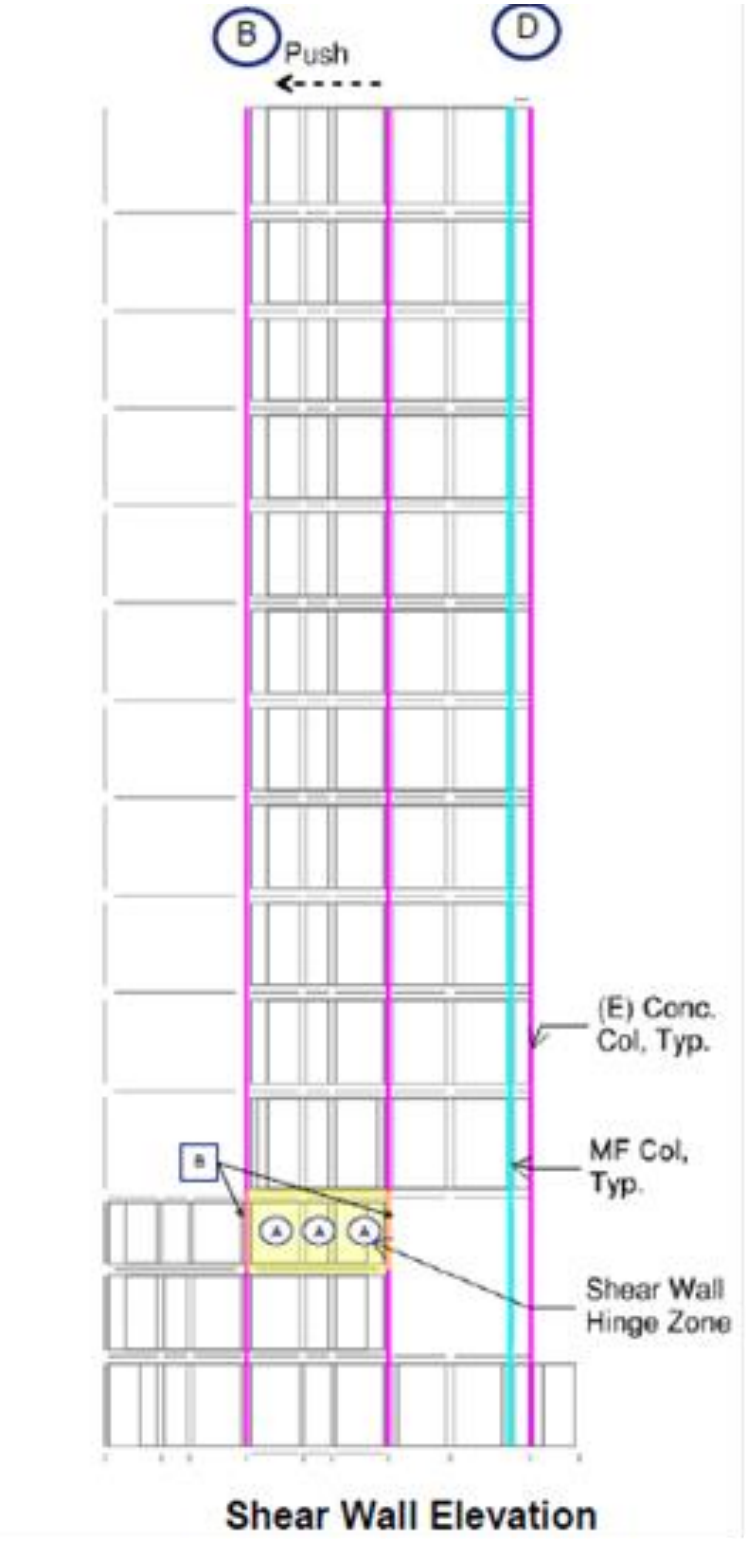

Figure 1-60 FE model of LFRS along grid line 8.

Material and Cross-Section Modeling

Figure 1-61 through Figure 1-63 show the Perform3D material curve data for new concrete materials assigned to shear wall hinge zones A, B, and C (Figure 1-58 through Figure 1-60). The ascending branch of the concrete compression stress-strain curve was represented by a bilinear profile, anchored by ultimate strength (FU) and an effective yield stress (FY). The ultimate strength is taken equal to f'_{cE}. The initial Young's modulus was taken equal to 57,000sqrt(f'_{cE}). The ultimate strength was prescribed to be at 0.003 strain (DU). Prescribed strain at the onset of strength loss (DL) varied from 0.004 to 0.005 depending on location and confinement effectiveness. Prescribed strain at residual strength (DR) varied correspondingly from 0.0052 to 0.0065. Residual strength was taken to be effectively zero. Tension strength was ignored.

Figure 1-64 shows the Perform3D material curve data for existing concrete materials assigned to the existing columns in shear wall hinge zones. The parameters used to define this curve are similar to the ones introduced in Figure 1-61.

Figure 1-65 shows the Perform3D material curve data for new steel reinforcing bars assigned to shear wall hinge zones A. These reinforcing bars are not expected to buckle in compression within the hinge zone due to confinement by the adjacent wall pier between grid lines A and B (Figure 1-60). Its assigned strain-strain curve is therefore bilinear and symmetric in tension and compression, with Young's Modulus of 29,000 ksi and post-yield modulus ratio of about 1.3%.

Figure 1-66 and Figure 1-67 show the Perform3D material curve data for new steel bars in shear wall hinge zones B and C and existing steel bars, respectively. These stress-strain curves are asymmetric in tension and compression. The tension branch represents yield, post-yield hardening, subsequent strength loss, and ultimate fracture. The compression branch represents strength loss due to buckling shortly after yield.

These material definitions were assigned to the fiber sections for shell and frame elements representing the walls and columns. Nonlinear shear materials were assigned to wall shell elements to represent in-plane shear behavior. The in-plane shear modeling details are not discussed in this flexure-controlled shear wall example.

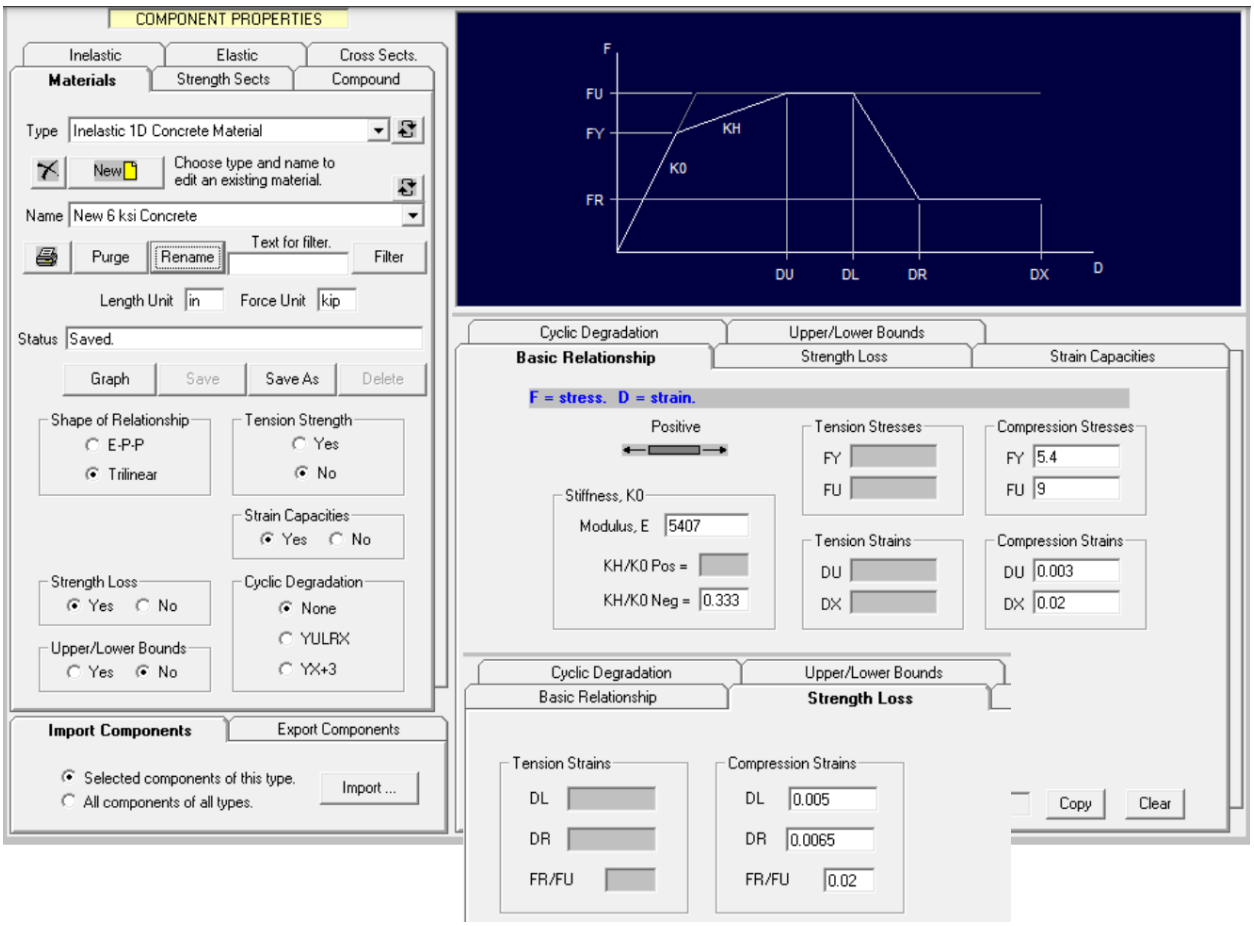

Figure 1-61 Perform3D material data for new concrete in hinge zones A.

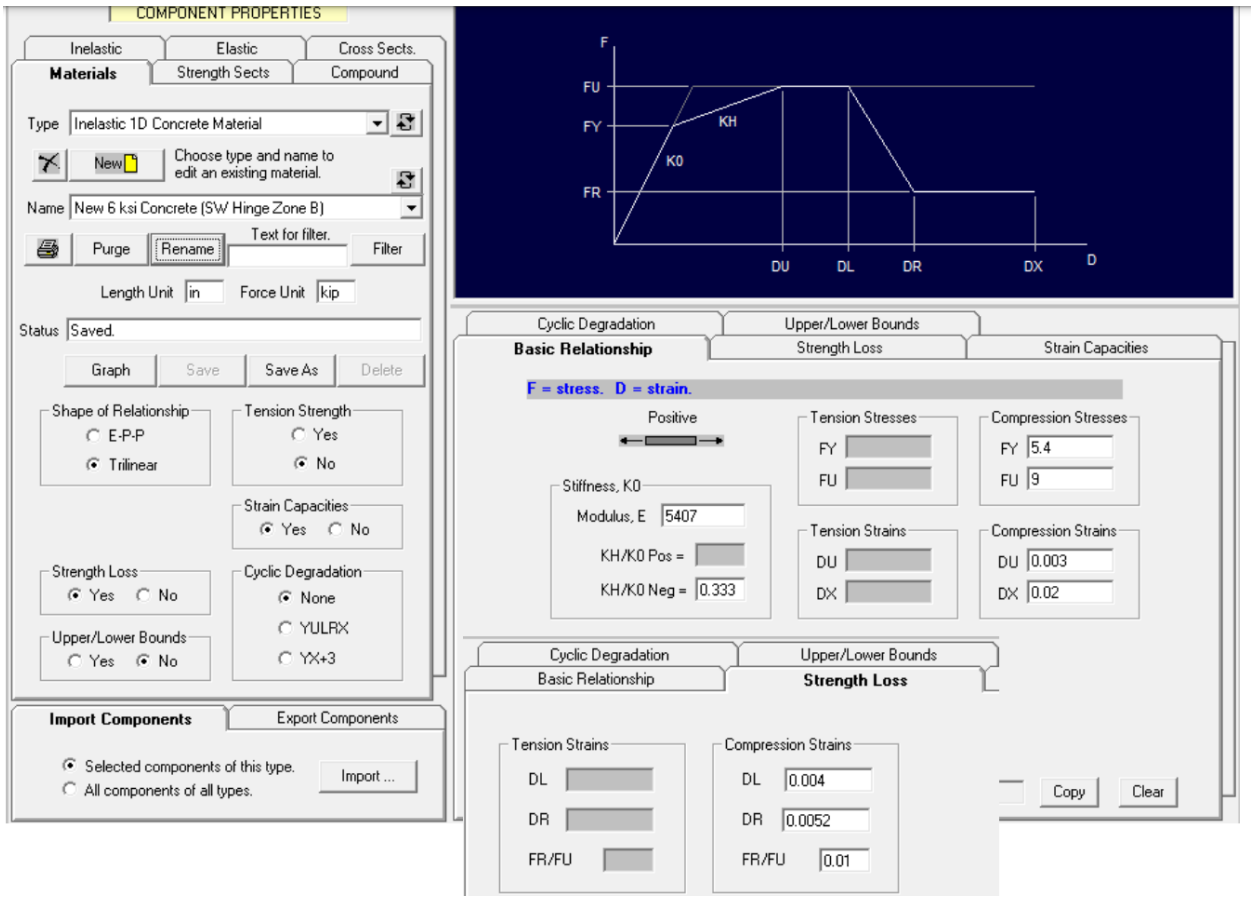

Figure 1-62 Perform3D material data for new concrete in hinge zones B.

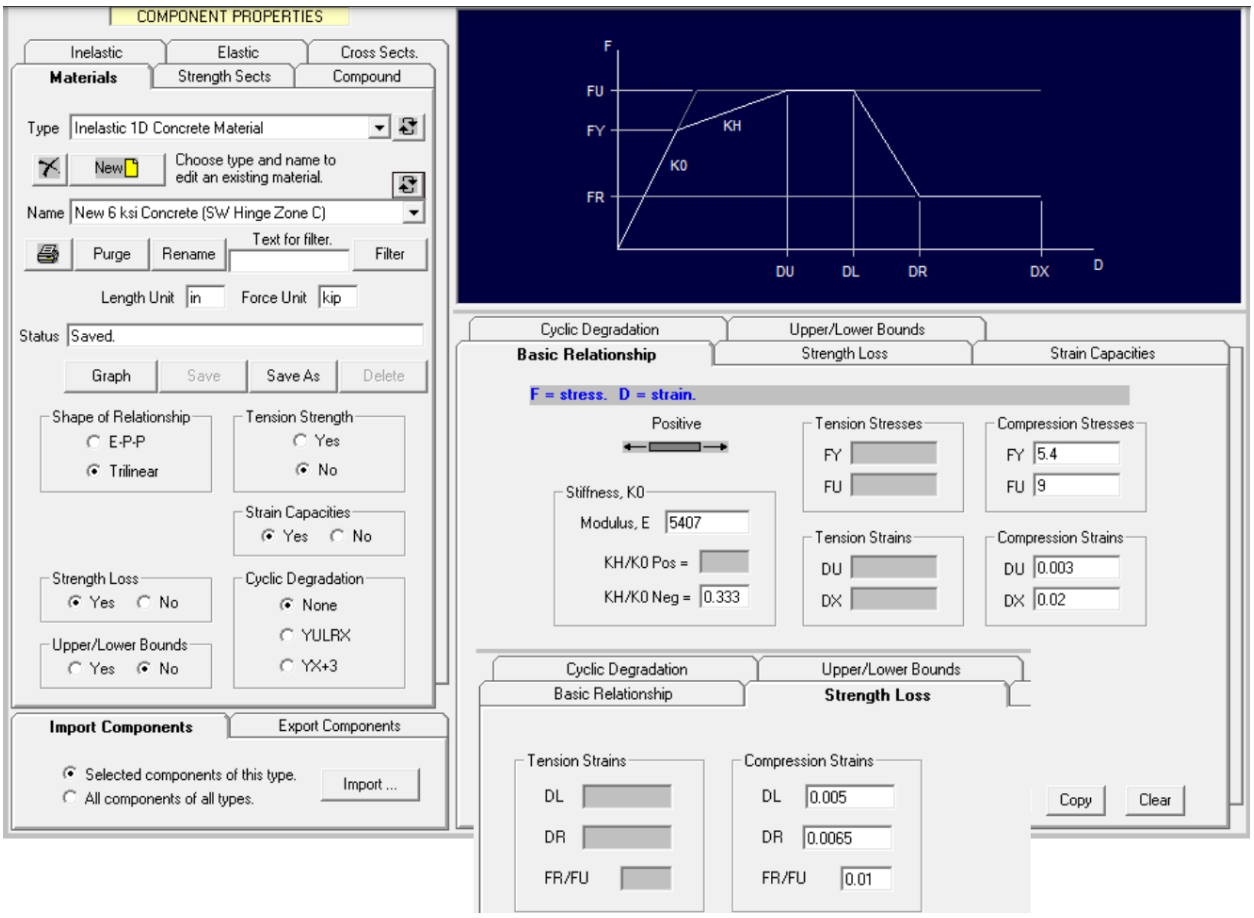

Figure 1-63 Perform3D material data for new concrete in hinge zones C.

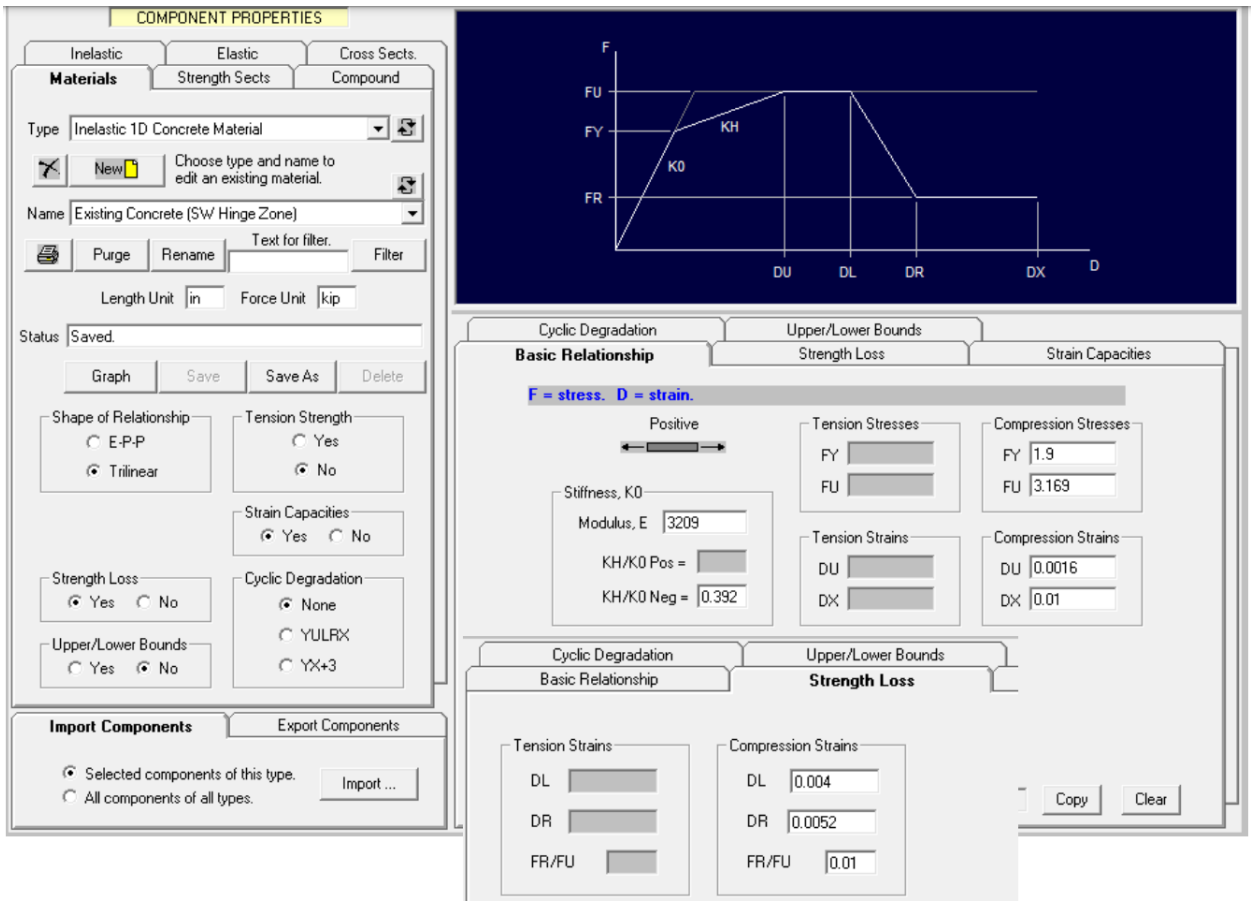

Figure 1-64 Perform3D material data for existing concrete in hinge zones.

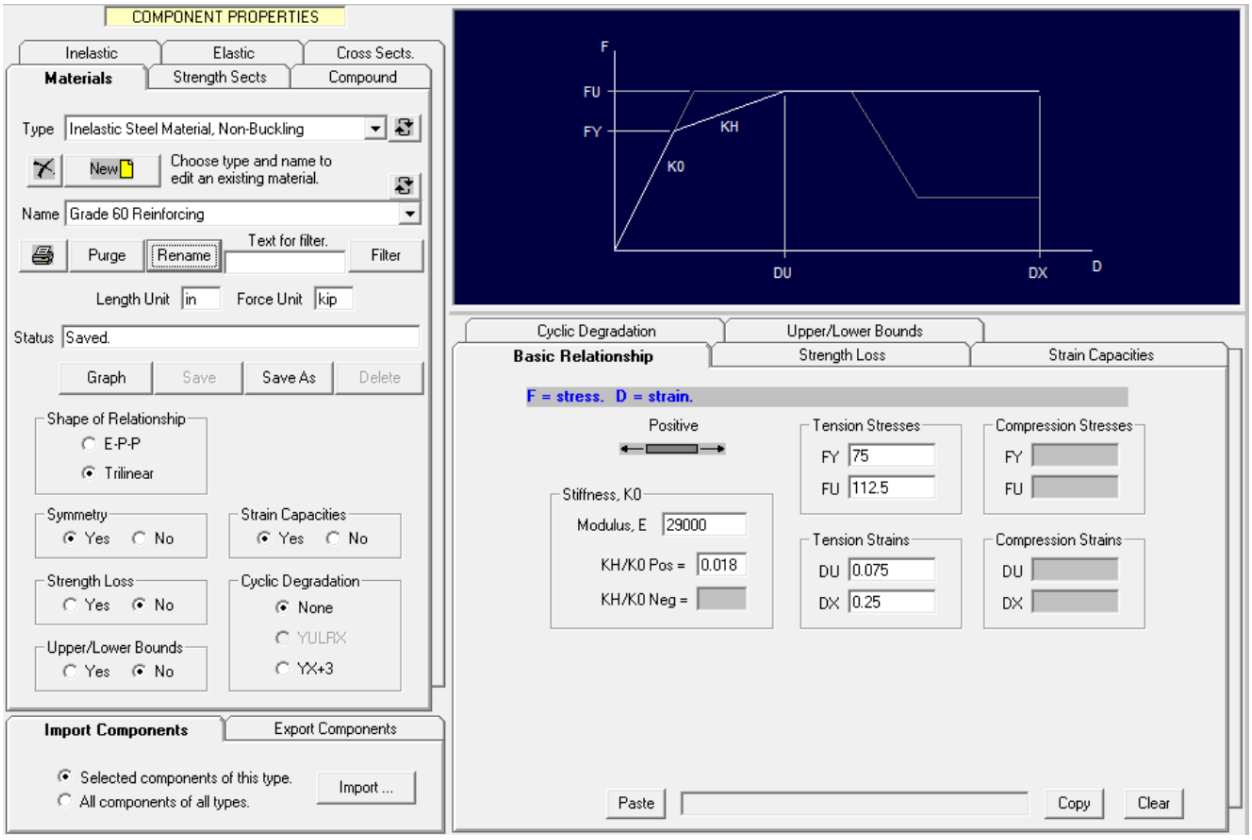

Figure 1-65 Perform3D material data for new steel bars in hinge zones A.

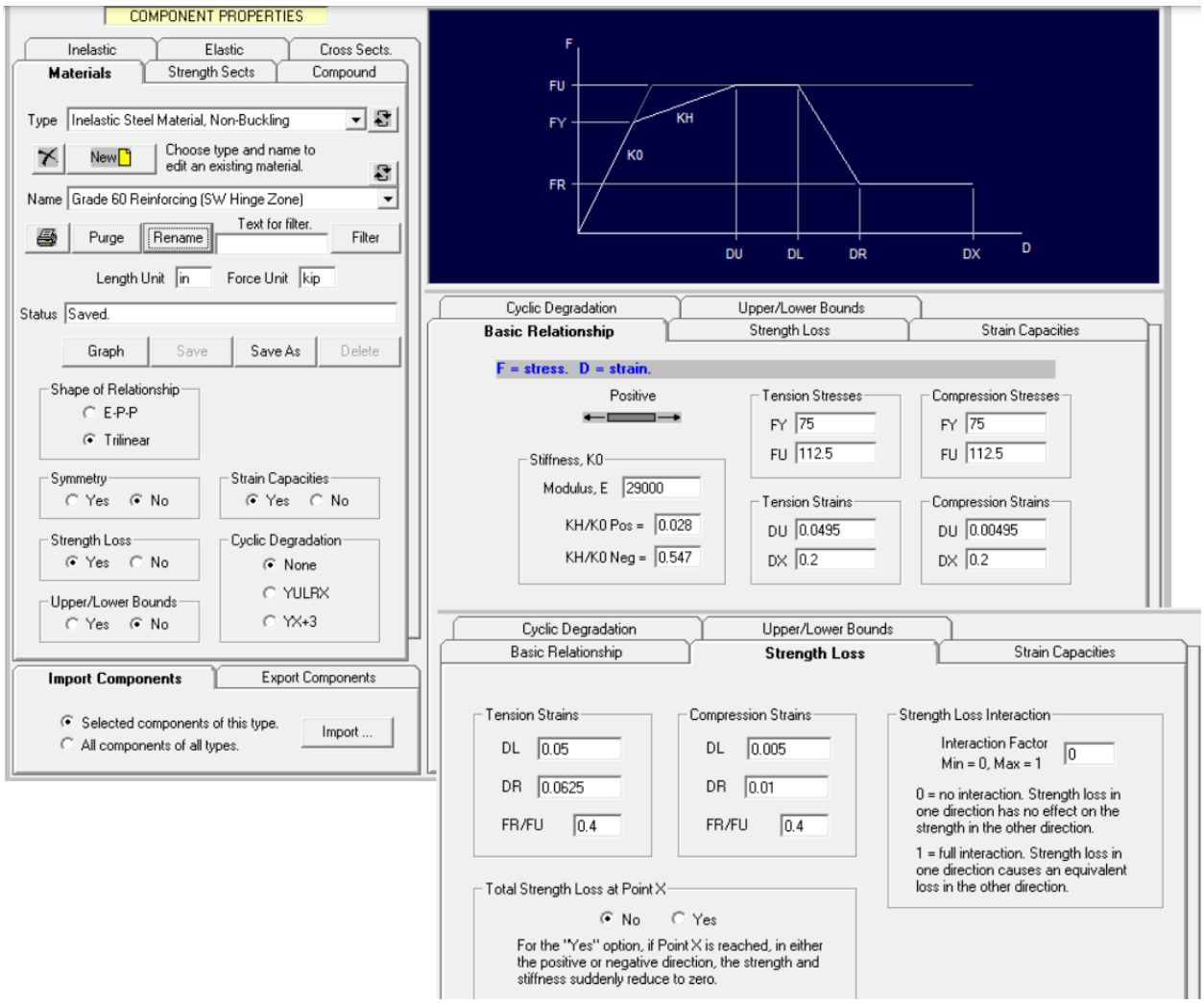

Figure 1-66 Perform3D material data for new steel bars in other hinge zones.

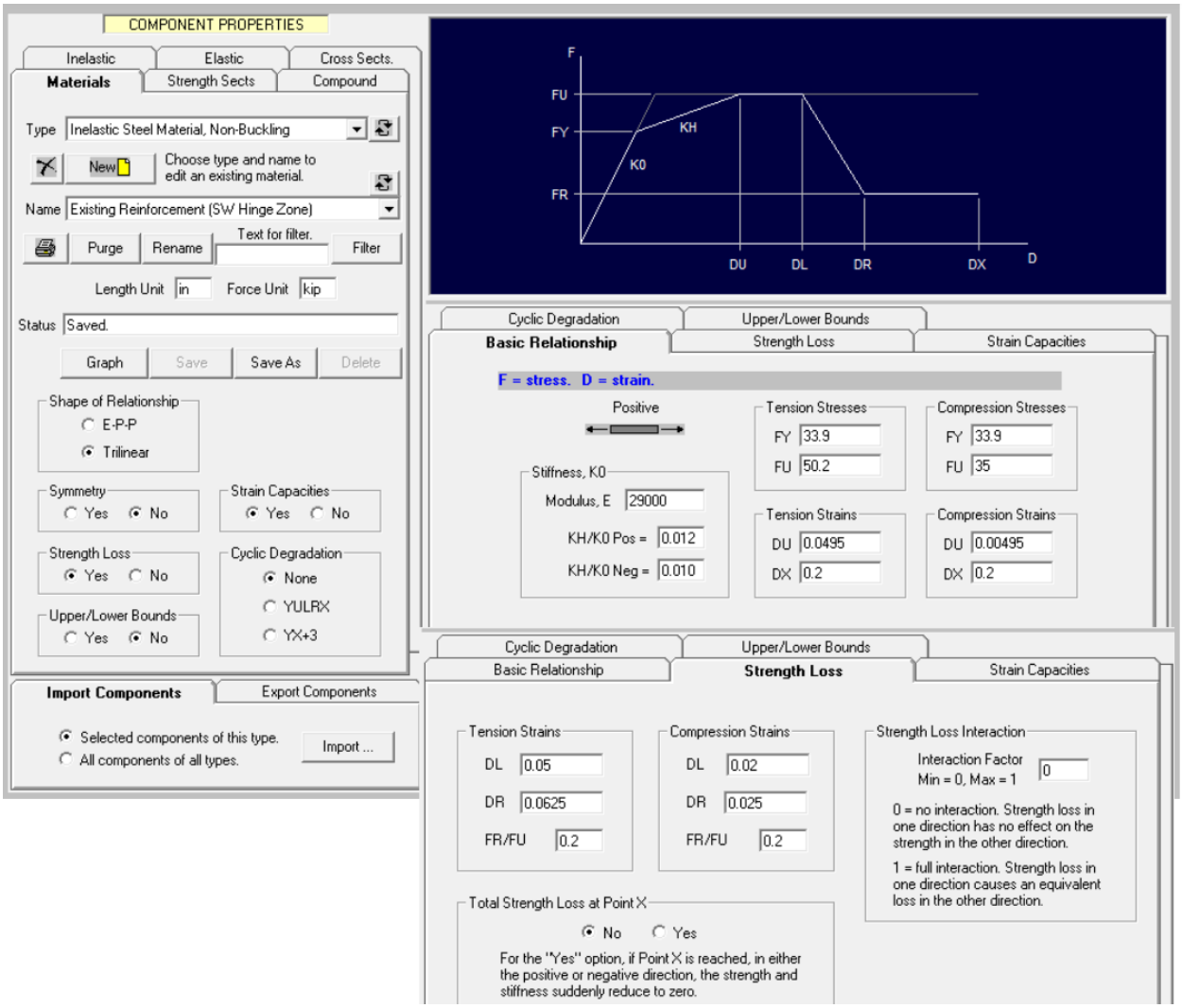

Figure 1-67. Perform3D material data for existing steel bars in hinge zones.

Boundary Conditions

As discussed previously, the seismic load distribution for the governing load case is essentially an inverted triangular load pattern in the south direction. This load pattern was applied as a series of forces acting at each story up the height of the building. After gravity load is applied, the magnitude of the total lateral load is adjusted, to achieve increasing lateral displacement demand. The resulting overturning moment on the building subjects the new columns to tension. The wall boundary in compression consists of existing columns only (Figure 1-58 through Figure 1-60).

The wall cross-sections for base shear extraction were defined above the basement level. Rotational flexibility due to reinforcement yield penetration into the wall foundations was ignored. Foundation rocking flexibility due to soil-structure interaction (SSI) was represented by adding horizontal and vertical soil springs (compression-only) below grade. The specific details of the SSI modeling are not

discussed in this example and do not affect the comparison of the wall performance to the acceptance criteria of the different ASCE/SEI 41 versions.

1.5.4.2 ANALYSIS RESULTS

Figure 1-68 shows the transverse base shear-roof displacement pushover curve extracted from a preliminary analysis of the building using Perform3D. The global pushover curve represents the overall building nonlinear response up to a roof displacement of about 20 in. This response was idealized using a trilinear curve, with initial yield point at about 3,000 kips. The idealized backbone curve was used, along with the effective spectral acceleration and period (Section 1.5.1.3), to calculate the target displacements for the BSE-1E and BSE-2E levels according to the provisions of ASCE/SEI 41-13. Review of the individual wall responses indicated that grid line 3 and 8 walls together resist about 80% of the total base shear while the other two walls resist about 20%.

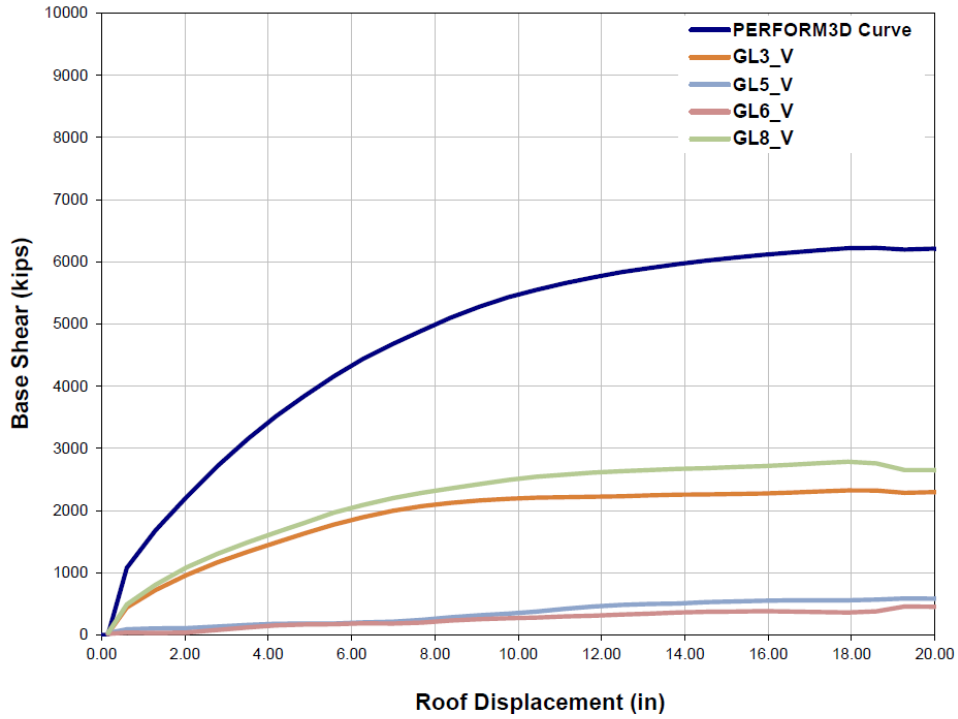

Figure 1-68. Pushover curve from Perform3D.

1.5.4.3 WALL PERFORMANCE ASSESSMENT

Modeling Parameters for Wall Backbone

Table 1-17 shows the backbone MPs for the grid line 5 wall according to ASCE/SEI 41-13, 41-17, and the proposed provisions. Figure 1-69 plots the tabulated values and shows the idealized wall flexure backbone curve and defines each MP. Note that the backbone curve in the previous versions of ASCE/SEI 41 did not explicitly define MPs c'_{nl} and d'_{nl}.

The yield and ultimate moment strengths were calculated as discussed in Section 1.5.2. Yield rotation was computed by dividing the yield moment by the cracked effective flexural stiffness and a flexural hinge length of one half the wall length. ASCE/SEI 41-13 and 41-17 specify effective flexural stiffnesses of $0.5EI_{gross}$ and $0.35EI_{gross}$, respectively, for cracked walls. The proposed provisions specify the effective stiffness as a function of axial load and reinforcement ratio at the wall boundary and recommend using the effect of gravity as the axial load to determine stiffness since the seismic axial load is expected to reverse directions during earthquake loading with a time-averaged value close to zero. The boundary reinforcement is that of longitudinal reinforcement in tension. The effective stiffness according to the proposed provisions for grid line 5 was determined as follows:

Gross flexural stiffness, $E_{cE}I_g$	6.22E+8 kip-ft^2
N_{UG} / A_g f'_{cE}	0.045
Boundary reinforcement ratio, ρ_{lb}	0.028
Cracked stiffness multiplier	0.29 by linear interpolation, Figure 1-70
Effective flexural stiffness	1.80E+8 kip-ft^2
Yield rotation, θ_y	0.0027 rad

As discussed in Section 1.5.4.3.2, the cracked effective stiffness was also calculated using an axial load of $2N_{UG}$ for comparison purposes. This stiffness for grid line 5 was determined as follows:

$2N_{UG}$ / A_g f'_{cE}	0.09
Cracked stiffness multiplier	0.35 by linear interpolation, Figure 1-70
Effective flexural stiffness	2.18E+8 kip-ft^2
Yield rotation, θ_y	0.0022 rad

The post-peak MPs were calculated according to Figure 1-71. The wall configurations were non-conforming according to the proposed provisions since the pushover direction to the south is such that the wall boundary in compression consist only of existing columns, which have poor seismic detailing. The following parameters were calculated:

Distance to neutral axis, c_{DE}	67 in.
Wall thickness, b_s	12 in.
Wall length, l_w	168 in.
l_w c_{DE} / b_s^2	78.2

N_{UD} / A_g f'_{cE} 0.09

Table 1-17 Backbone Curve Parameter Values for Grid Line 5 Wall

Provisions –>	ASCE/SEI 41-13		ASCE/SEI 41-17		ATC-140 Proposed Provisions	
Point	**θ**	**M**	**θ**	**M**	**θ**	**M**
B	0.0108	54,400	0.0023	54,400	0.0027 for N_{UG} 0.0022 for $2N_{UG}$	54,400
C	0.0088	54,400	0.0093	54,400	0.0080	62,600
D	0.0131	28,800	0.0139	28,800	0.0150	0
E	0.0148	28,800	0.0153	28,800	0.0150	0

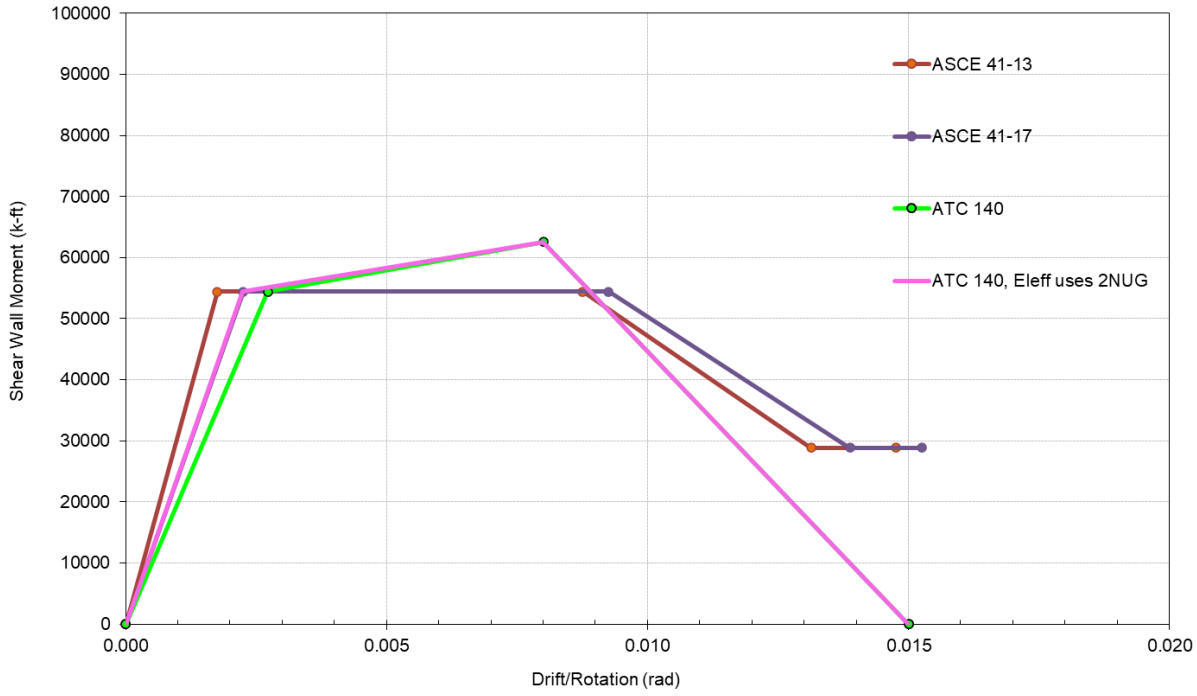

Figure 1-69 Comparison of grid line 5 wall backbone curve modeling parameters.

$\frac{N_{UG}}{A_g f'_{cE}}$	ρ_{lb}[a,b]	Flexural Rigidity[c]
≤ 0.05	≤ 0.01	$0.20\ E_{cE}I_g$
	≥ 0.03	$0.30\ E_{cE}I_g$
≥ 0.50	≤ 0.01	$0.90\ E_{cE}I_g$
	≥ 0.03	$1.00\ E_{cE}I_g$

Figure 1-70. Wall cracked flexural stiffness determination.

$\frac{l_w c_{DE}}{b_s^2}$	Conditions[d,e] Detailing[a,b,c,g]	d_{nl}	Acceptance Criteria Performance Level IO
≤ 10	$\frac{A_{sh,provided}}{A_{sh,required}} \geq 0.5$ and $\frac{s}{d_b} \leq 9$	0.024	$\theta_{yE}+0.1(d_{nl} - \theta_{yE})$
≤ 10	$\frac{A_{sh,provided}}{A_{sh,required}} < 0.2$ and $\frac{s}{d_b} > 15$	0.019	
≥ 60	$\frac{A_{sh,provided}}{A_{sh,required}} \geq 0.5$ and $\frac{s}{d_b} \leq 9$	0.010	
≥ 60	$\frac{A_{sh,provided}}{A_{sh,required}} < 0.2$ and $\frac{s}{d_b} > 15$	0.008	

$\frac{l_w c_{DE}}{b_s^2}$	Conditions[d,e,g] $\frac{N_{UD}}{A_g f'_{cE}}$	c_{nl}	c'_{nl}	d'_{nl}[f]	e_{nl}[f,h]	Acceptance Criteria Performance Level LS	CP
≤ 10	≤ 0.10	0.4	1.15	0.032	0.035	$0.75\ e_{nl}$	$0.85\ e_{nl}$
≤ 10	≥ 0.20	0.1		0.020	0.021		
≥ 60	≤ 0.10	0.0		0.015	0.015		
≥ 60	≥ 0.20	0.0		0.010	0.010		

Figure 1-71 Grid line 3 wall post-yield backbone modeling parameters.

Wall Moment-Rotation Response Post-processing

The moment-rotation backbone curves in Section 1.5.4.3.1 idealize the wall response as that of a lumped-plasticity frame element with a hinge length along which almost all of the inelastic deformation is accumulated. The hinge response is represented by moment strengths and corresponding rotations that represent the integration of curvature responses along the hinge length.

The fiber section elements used in the analysis model use distributed plasticity, and their backbone curves are therefore different from the idealized backbone curves for lumped-plasticity elements. This section describes the extraction of wall fiber section moment-rotation responses to compare to the idealized backbone curves developed in Section 1.5.4.3.

Perform3D calculates wall section rotations directly from nodes using a rotation gauge element instead of integrating curvatures over a hinge length. These rotation gauge "elements" are response recorders with no stiffness or mass. Advantages of using these elements include versatility and low sensitivity to the actual wall hinge length, which is unknown apriori. Since these rotation gauges extend over a wall height that exceeds one half the wall length, i.e., the plastic hinge zone, the rotations they record may include a contribution from mostly elastic rotations outside the hinge zone, which would be negligible compared to the inelastic rotations. Figure 1-71 and Figure 1-72 show these gauge definitions for two transverse walls.

ASCE/SEI 41-13 and 41-17 provisions recommend a cracked stiffness that is independent of wall axial load. The proposed provisions recommend a cracked stiffness that depends on axial load and uses the gravity load to represent the average axial load during the earthquake duration. In the NSP, lateral pushover proceeds in one direction only, and the average axial load in the walls is about $2N_{UG}$ (Section 1.5.2). For the comparisons shown in this section, this cracked stiffness for the idealized wall backbone was therefore computed and plotted for two different axial load cases: one stiffness case used the wall axial load from gravity in order to show the average effective stiffness that will be assigned using the proposed provisions (most applicable to dynamic analysis with reversible loading), and one stiffness case used twice the wall axial load from gravity, $2N_{UG}$, to compare to the Perform3D fiber section stiffness where the wall axial loads due to lateral displacement in the south direction varied between $1.8N_{UG}$ and $2.3N_{UG}$. These comparisons are shown in Section 1.5.4.3.3.

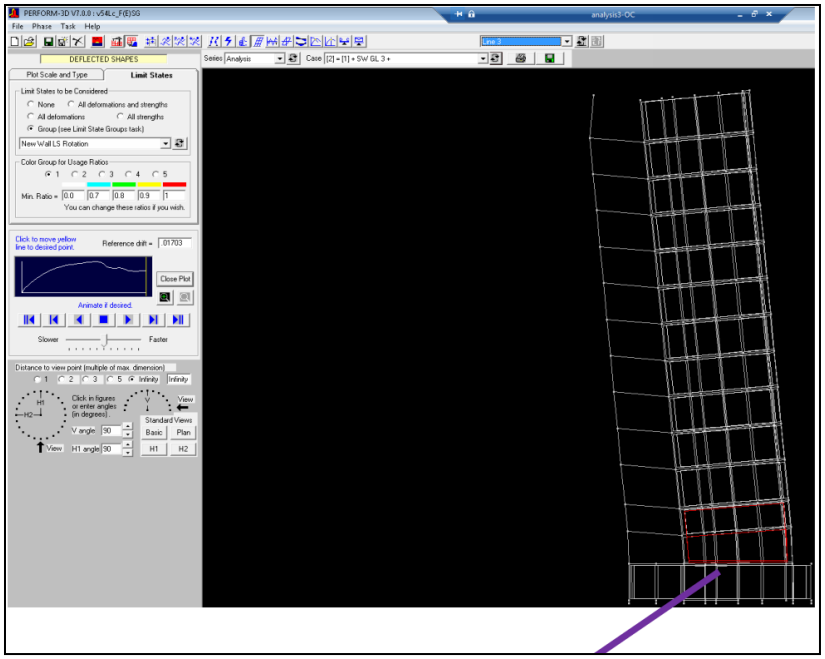

Figure 1-72 Rotation gauge definition for grid line 3 wall.

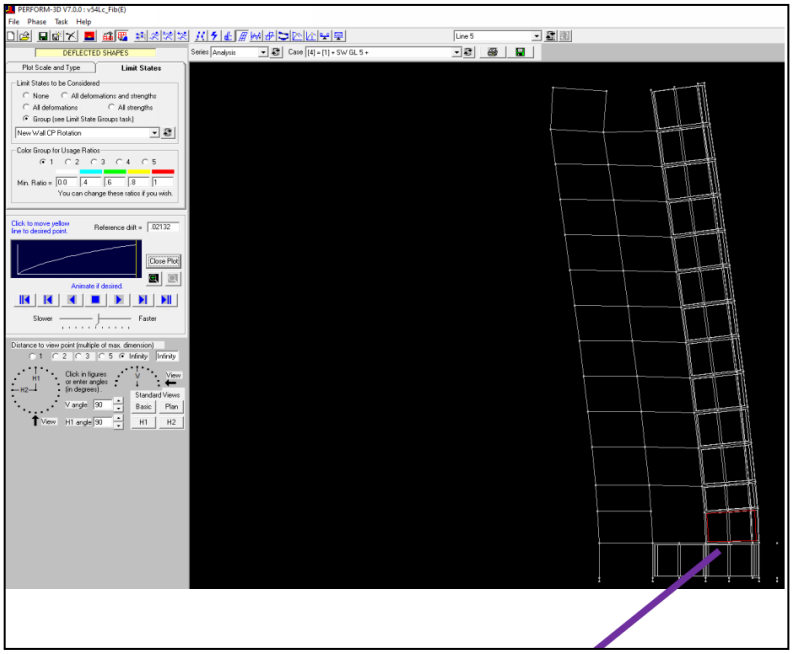

Figure 1-73 Rotation gauge definition for grid line 5 wall.

Wall Acceptance Criteria Assessment

This section compares the wall performance assessment using ASCE/SEI 41-13, 41-17, and the proposed ATC-140 provisions. The proposed ATC-140 acceptance criteria for all walls are determined according to Figure 1-70:

Life Safety (LS) Rotation Limit	0.75 × 0.015 = 0.011 rad
Collapse Prevention (CP) Rotation Limit	0.85 × 0.015 = 0.013 rad

Figure 1-73 and Figure 1-74 show the moment-rotation responses of the walls on grid lines 3 and 5, respectively. The plots denoted "ATC 140" correspond to the proposed provisions. Two "ATC 140" backbones are shown, demonstrating the effective stiffness calculated using axial loads of N_{UG} and $2N_{UG}$, as discussed in the previous sections. The wall rotation acceptance criteria for ASCE/SEI 41-13 and 41-17 correspond to points C (LS) and E (CP) on their respective backbone curves (Table 5.2). The ATC-140 proposed acceptance criteria are identified in each figure as calculated above. A moment-roof drift ratio plot is shown to establish a reference between the moment-rotation response and the global pushover curve. The wall rotation demands at roof drift values corresponding to the BSE-1E and BSE-2E hazard levels are identified by circles on the moment-rotation plot. These wall rotation demands are well below the acceptance criteria for LS and CP in both ASCE/SEI 41 versions and the proposed provisions (which confirms that the retrofit design has significant safety margins for these walls). The proposed ATC-140 acceptance criteria for LS are shown to be less stringent than both ASEC/SEI 41 versions for these walls, while the acceptance for CP are more stringent. These walls are highly slender and have relatively low axial loads. The low axial loads are favorable for the acceptance criteria in the existing ASCE/SEI provisions. The relatively high slenderness is unfavorable for the $I_w c_E / b^2$ parameter in the proposed ATC-140 provisions.

The Perform3D behavior of the grid line 5 wall exhibits numerical instability at rotation demands exceeding 0.01 rad (Figure 1-74). This occurs at roof drift values approaching 2%. At this roof drift, the shear strengths of the major walls on grid lines 3 and 8 will have already severely degraded (Figure 1-73). The observed numerical instability is likely a result of a negative global stiffness of the structure. This excessive roof drift level is not relevant to the wall performance assessment.

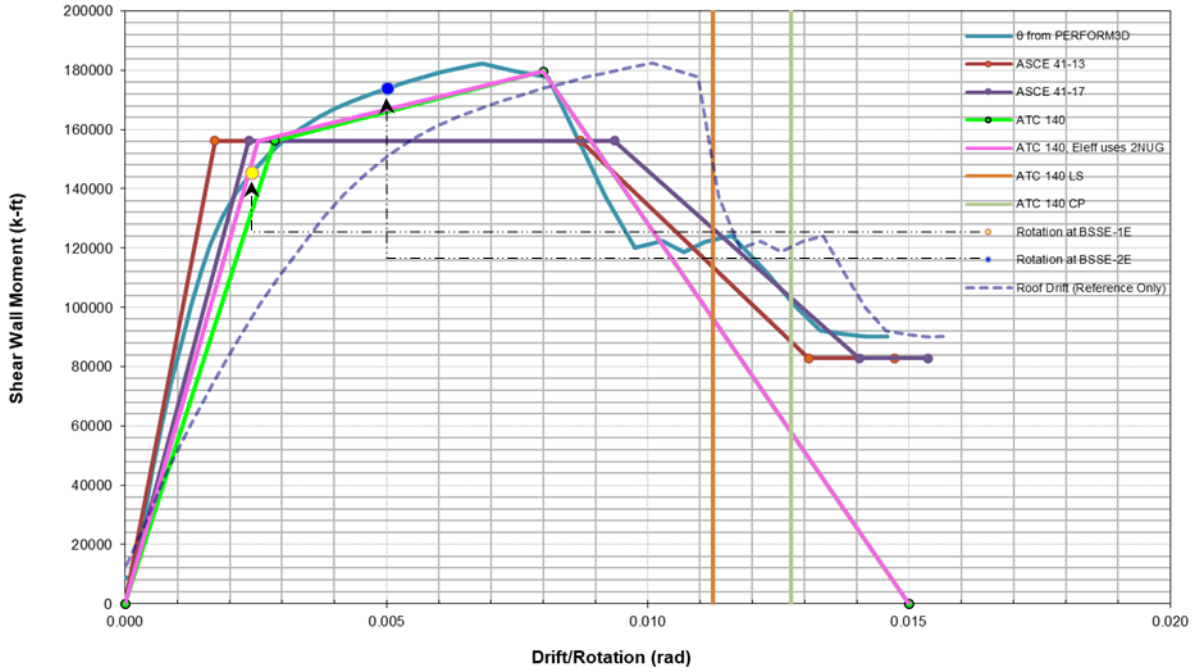

Figure 1-74 Moment-rotation curves for wall on grid line 3.

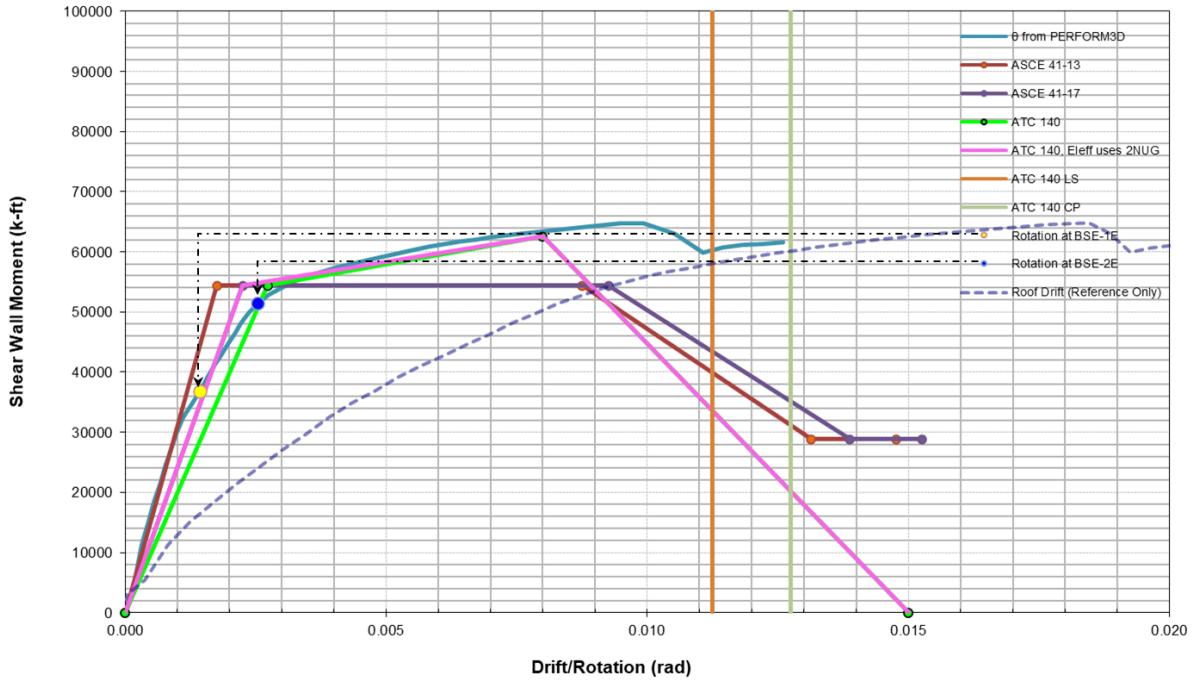

Figure 1-75 Moment-rotation curves for wall on grid line 5 (grid line 6 similar).

1.5.5 Discussion and Conclusions

Comparing the idealized backbone curves for lumped-plasticity wall models to the fiber section moment-rotation output (Section 1.5.4.3) indicates that the overall wall response is generally similar while the Perform3D numerical solution is stable. This general similarity is primarily attributed to the wall axial load levels in this example building, as summarized below. The following observations discuss specific comparisons between the backbone curve details.

ASCE/SEI 41-13 overestimates the effective stiffness compared to the Perform3D model. The ASCE/SEI 41-17 effective stiffness is comparable to the proposed provisions when the representative total axial load of $2N_{UG}$ in the wall is considered. The Perform3D response shows stiffness degradation that is effectively comparable to both. The Perform3D stiffness ignores some minor phenomena, e.g., yield penetration, and may therefore have a slight upward bias.

The proposed provisions predict a slightly lower effective stiffness for wall loading in the south direction if axial load from gravity only is considered. These provisions are likely to estimate a slightly higher stiffness for loading in the north direction; thus, the use of these provisions should be representative of the average stiffness for response to loading in both directions.

The effective yield moment from spColumn compares well with the Perform3D fiber section prediction. The proposed ATC-140 ultimate moment strength and post-yield stiffness compare very well with the Perform3D fiber section output.

For the grid line 3 wall, the maximum axial load during pushover was 15% higher than $2N_{UG}$, which may explain the slightly higher moment strength and lower corresponding rotation in the Perform3D simulation than the backbone parameters computed using $2N_{UG}$ axial load. For the grid line 5 wall, the maximum axial load during pushover was 10% lower than $2N_{UG}$, which may contribute to the higher ductility in the Perform3D simulation.

1.6 References

Abdullah, S. A., 2019, *Reinforced concrete structural walls: Test database and modeling parameters, Ph.D. dissertation,* Dept. of Civil and Environmental Engineering, University of California, Los Angeles, California.

Abdullah S. A., and J. W. Wallace, 2019, “Drift capacity of RC structural walls with special boundary elements,” ACI Structural Journal, Vol. 116, No 1, pp. 183–194. https://doi.org/10.14359/51710864.

Abdullah, S. A., and Wallace, J. W., 2020a, “Reliability-based design methodology for reinforced concrete structural walls with special boundary elements,” *ACI Structural Journal*, Vol. 117, No. 3.

Abdullah S. A., and Wallace J. W., 2021, "Drift capacity at axial failure of RC structural walls and wall piers," *ASCE Journal of Structural Engineering*, DOI: 10.1061/(ASCE)ST.1943-541X.0003009.

ACI, 1977, *Building Code Requirements for Reinforced Concrete*, ACI 318-77, American Concrete Institute, Detroit, MI, 103 pp.

ACI, 1983, *Building Code Requirements for Reinforced Concrete*, ACI 318-83, American Concrete Institute, Detroit, MI.

ACI, 1999, *Building Code Requirements for Structural Concrete*, ACI 318-99, American Concrete Institute, Detroit, MI.

ACI, 2010, *Report on High Strength Concrete*, ACI 363R-10, American Concrete Institute, Farmington Hills, MI.

ACI, 2013, *ACI Concrete Terminology*, ACI CT-13, American Concrete Institute, Farmington Hills, MI.

ACI, 2014, *Building Code Requirements for Structural Concrete*, ACI 318-14, American Concrete Institute, Farmington Hills, MI.

ACI, 2017, *Standard Requirements for Seismic Evaluation and Retrofit of Existing Concrete Buildings*, ACI 369.1-17, American Concrete Institute, Farmington Hills, MI.

ACI, 2019, *Building Code Requirements for Structural Concrete*, ACI 318-19, American Concrete Institute, Farmington Hills, MI.

Adebar, P., Ibrahim, A.M.M., and Bryson, M., 2007, "Test of high-rise core wall: effective stiffness for seismic analysis," *ACI Structural Journal*, vol. 104, pp. 549-559.

Albidah, A., 2016, "Vulnerability and Risks of Collapse of Structural Concrete Walls in Regions of Low to Moderate Seismicity," PhD Dissertation, The University of Melbourne, Melbourne, Australia.

Altheeb, H., 2016, "Seismic Drift Capacity of Lightly Reinforced Concrete Shear Walls," PhD Dissertation, The University of Melbourne, Melbourne, Australia.

ASCE, 2016, *Minimum Design Loads for Buildings and Other Structures*, ASCE/SEI 7-16, American Society for Civil Engineers, Reston, VA.

ASCE, 2017, *Seismic Evaluation and Retrofit of Existing Buildings*, ASCE/SEI 41-17, American Society of Civil Engineers, Reston, VA.

Birely, A. C., Lowes, L. N., and Lehman, D., 2014, "Evaluation of ASCE 41 Modeling Parameters for Slender Reinforced Concrete Structural Walls," *ACI Special Publication*, 297(1-18).

CEN, *Eurocode 8: "Design of Structures for Earthquake Resistance, Part 1: General Rules, Seismic Actions and Rules for Buildings*, *ENV 1998-1:2003,"* Comité Européen de Normalisation, Brussels, Belgium, 2004.

CSA Committee, "*Design of Concrete Structures*, *CSA A23.3-14,"* Canadian Standards Association, Mississauga, Canada, 2014.

Dashti, F., Dhakal, R.P., and Pampanin, S., 2018, "Inelastic Strain Gradients in Reinforced Concrete Structural Walls," Proceedings of the 16th European Conference on Earthquake Engineering, June 18-21, Thessaloniki, Greece.

Elwood, K.J., and M.O. Eberhard, 2009, "Effectiveness of Reinforced Concrete Columns," *ACI Structural Journal*, 106 (4): 476–484.

Elwood, K. J., Matamoros, A. B., Wallace, J. W., Lehman, D. E., Heintz, J. A., Mitchell, A. D., Moore, M. A., Valley, M. T., Lowes, L. N., Comartin, C. D., and Moehle, J. P., 2007, "Update to ASCE/SEI 41 concrete provisions," *Earthquake Spectra*, 23(3), 493-523.

FEMA, 1997a, *NEHRP Commentary on the Guidelines for the Seismic Rehabilitation of Buildings*, FEMA 274, Federal Emergency Management Agency, Washington, D.C.

FEMA, 1997b, *NEHRP Guidelines for the Seismic Rehabilitation of Buildings*, FEMA 273, Federal Emergency Management Agency, Washington, D.C.

FEMA, 2000, *NEHRP Guidelines for the seismic rehabilitation of buildings, FEMA 356*, Federal Emergency Management Agency, Washington, D.C.

Fenwick, R., and Bull, D., 2000, "What is the stiffness of reinforced concrete walls," *SESOC Journal*, Vol. 13, No. 2.

Ghannoum W.M., and Matamoros A.B., 2014, "Nonlinear modeling parameters and acceptance criteria for concrete columns," *ACI Special Publication*, 297, pp. 1-24.

Khuntia, M., and Ghosh, S. K., 2004, "Flexural stiffness of reinforced concrete columns and beams: Experimental Verification," *ACI Structural Journal*, vol. 101, pp. 364-374.

Motter, C.J., Abdullah, S.A., and Wallace, J.W., 2017, "Reinforced concrete structural walls without special boundary elements," *ACI Structural Journal*, (submitted for publication).

NIST, 2011, *Seismic Design of Cast-in-Place Concrete Special Structural Walls and Coupling Beams: A Guide for Practicing Engineers*, NIST GCR 11-917-11 REV-1, NEHRP Consultants Joint Venture, National Institute of Standards and Technology, Gaithersburg, Maryland.

NZS 3101, 2006, Concrete Structures Standard, Part 1: The Design of Concrete Structures: Part 2: Commentary on the Design of Concrete Structures, Standards New Zealand, Wellington, New Zealand.

Paulay, T., and Priestley, M. J. N., 1992, *Seismic Design of Reinforced Concrete and Masonry Buildings*, John Wiley & Sons Inc., New York.

Paulay. T, 2002, "A displacement focused seismic design of mixed building systems," *Earthquake Spectra,* Vol 18, No. 4.

Priestley, M.J.N. and Kowalski, M.J., 1998, "Aspects of drift and ductility capacity of cantilever structural walls," *Bulletin*, NZNSEE 31, 2.

Priestley, M., Calvi, G., and Kowalsky, M., 2007, *Displacement-Based Seismic Design of Structures,* IUSS Press, Pavia, Italy.

Segura, C. L., 2017, "Seismic Performance Limitations and Reinforcement Detailing of Slender RC Structural Walls," PhD Dissertation, University of California, Los Angeles, Los Angeles, CA.

Segura, C. L., and Wallace, W. J., 2018a, "Seismic performance limitations and detailing of slender reinforced concrete walls," *ACI Structural Journal*, V. 115, No. 3, pp. 849-860.

Segura, C. L., and Wallace, W. J., 2018b, "Impact of geometry and detailing on drift capacity of slender walls," *ACI Structural Journal*, V. 115, No. 3, pp. 885–896.

Thomsen, J. H. IV, and Wallace, J. W., 2004, "Displacement-based design of slender reinforced concrete structural walls—experimental verification," *Journal of Structural Engineering*, V. 130, No. 4, pp. 618-630.

Tran, T. A., 2012, "Experimental and analytical studies of moderate aspect ratio reinforced concrete structural walls," Ph.D. dissertation, Dept. of Civil and Environmental Engineering, Univ. of California, Los Angeles.

Wallace, J. W., 2006, "Slender Wall Behavior and Modeling," PEER/EERI Technical Seminar Series, New Information on the Seismic Performance of Existing Concrete Buildings, Berkeley, California.

Chapter 2: Revisions to Concrete Structural Wall Shear-Controlled Provisions

2.1 Motivation

Most of the provisions for concrete structural walls in ASCE/SEI 41-17 were developed in the late 1990s based on limited experimental data and judgement for FEMA 273 (1997a) and FEMA 274 (1997b). The only exceptions were the modeling parameters (MP) and acceptance criteria (AC) of shear-controlled walls, which were updated for the ASCE/SEI 41-06 Supplement 1 (Elwood et al. (2007)).

An extensive database developed by Abdullah (2019) with over 1,100 wall tests spurred a comprehensive review of all structural wall provisions. In this chapter, proposed updates to MP and AC for shear-controlled walls are presented. The previous provisions had been overly conservative for many structures. An example assessment for shear-controlled walls in low- to mid-rise buildings is presented as well. Assessment outcomes between provisions of ASCE/SEI 41-17 and the proposed provisions are compared.

Note about the Relation Between the ASCE/SEI 41 and ACI 369.1 Standards

The concrete wall provisions contained in Section 10.7 of ASCE/SEI 41-17 were reproduced from Chapter 7 of the new ACI 369.1-17 Standard, based on a Memorandum of Understanding between ACI and ASCE. In 2021, however, the ASCE/SEI 41 Standard Committee elected to reference the next version of ACI 369.1 directly, without replicating its contents, making ACI 369.1 the reference standard for concrete members for ASCE/SEI 41. The proposed changes were therefore submitted to ACI's Seismic *Repair and Rehabilitation* Code committee 369 for possible adoption.

2.2 Summary of Recommended Changes

For walls controlled by shear modes of degradation, new shear-strength relations are proposed based on test data. The new relations account for the influence of moment demand on shear strength. Updated linear and nonlinear AC and MP are proposed based on test data. For relatively brittle shear-controlled walls, the proposed provisions do not result is drastic changes in acceptance criteria and modeling parameters from those in ACI 369.1-17. For walls that sustain shear degradation after flexural yielding (flexure-shear controlled), generally larger deformation capacities are provided by the proposed provisions. The provisions do not distinguish explicitly between shear

and flexure-shear-controlled behaviors but do so indirectly by incorporating the ratio of shear strength to shear demand at flexural yielding of walls.

2.3 Technical Studies

2.3.1 Wall Test Database

2.3.1.2 DATASET OF SHEAR- AND FLEXURE-SHEAR-CONTROLLED WALLS

The main database, described in Chapter 1 of Part 4, was filtered to a dataset of 325 shear- and flexure-shear-controlled walls (i.e., $(V_{CWall318E}/V_{MCyDE}) \leq 1.15$) tested under quasi-static, reversed cyclic loading protocols. The dataset included 115 wall tests that experienced limited flexural yielding prior to diagonal shear failure (either diagonal tension or compression failure) and 210 walls that experienced shear failure without flexural yielding. Additionally, a smaller subset that included about 40 wall specimens tested under monotonic loading was added to the dataset for studies related to shear cracking strength and stiffness, as well as shear yield strength and drift, which are not expected to be significantly impacted by the type of the loading protocol (cyclic vs monotonic). Further, the dataset included walls with different cross-section shapes: 48% had rectangular cross-sections, 48% had either barbell or H-shaped cross-sections, and 4% had either L-shaped, half-barbell, or wing-shaped cross-sections. Lastly, it is noted that no detailing criteria were applied to obtain the dataset because boundary detailing variables, such as area of boundary transverse reinforcement (A_{sh}), slenderness ratio of boundary bars (s/d_b), and spacing between laterally supported boundary bars (h_x), are not typically relevant for shear-controlled walls. The walls in the dataset had shear span ratios (M/Vl_w) ranging between 0.3 to 3.0 and axial load ratios ($P/(A_g f'_{cE})$) ranging primarily between zero and 0.25, with only four data points above 0.25.

2.3.1.2 DATA EXTRACTION

As described in Chapter 1, the database includes backbone relations derived from the experimental force-displacement relationships, as shown in Figure 2-1, which include displacement capacity values as measured total displacements at the top of the wall specimen, i.e., the backbone displacement values are displacements contributed by shear distortion, flexural displacement (curvature and bar-slip), and sliding at the base. Since shear-controlled walls are typically modeled using a nonlinear translational spring to capture the shear deformations coupled with a flexural element to capture the flexural deformations, or a panel element that treats shear and flexural deformations independently, the analytically calculated elastic flexural deformation was removed from the total measured displacement values when determining modeling parameters for shear-controlled walls (i.e., shear displacement = total displacement – elastic flexural displacement). The elastic flexural displacements for all the points on the backbone at and beyond the yield point were calculated using the effective flexural stiffness values at *General Yield*, $E_{CE}I_{eff}$, proposed in Chapter 1. The proposed flexural stiffness for walls is a function of $P/(A_g f'_{cE})$ and longitudinal reinforcement ratio ($\rho_{l,BE}$). This approach may result in overestimation of flexural deformation for shear-controlled walls (walls without flexural yielding), because these walls do not experience as

much flexural cracking as flexure-controlled walls at flexural yield. However, this approach produces shear deformations, which combined with calculated flexural deformations, results in the correct total wall drift.

As discussed in Chapter 1 of Part 4, a backbone shape that differs from the one in ACI 369.1-17 is assumed for test data, with additional modeling parameters extracted (Figure 2-2). Namely the additional parameters are c'_{nl} and d'_{nl}. Similar to flexure-controlled walls, when determining modeling parameters (Section 2.3.3), an approximation is made for Point C such that this point has an ordinate and abscissa that are respectively equal to the peak lateral strength (i.e., Parameter c'_{nl}) and the drift capacity at 20% lateral strength loss from peak strength (i.e., Parameter d_{nl}). Based on this assumption, the value for peak strength is defined at the drift capacity associated with 20% loss in lateral strength.

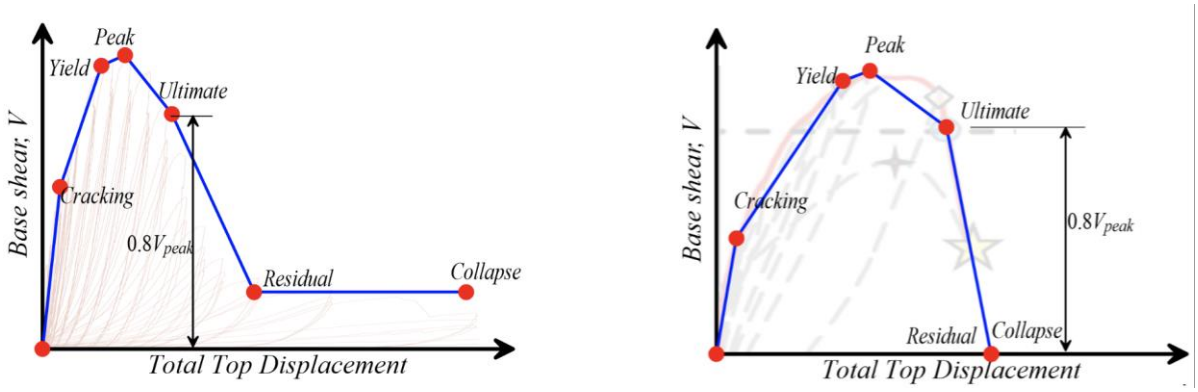

(*a*) Terzioglu (2011) **(*b*) Looi (2017)**

Figure 2-1 Examples of backbone curves derived from experimental force-displacement relations.

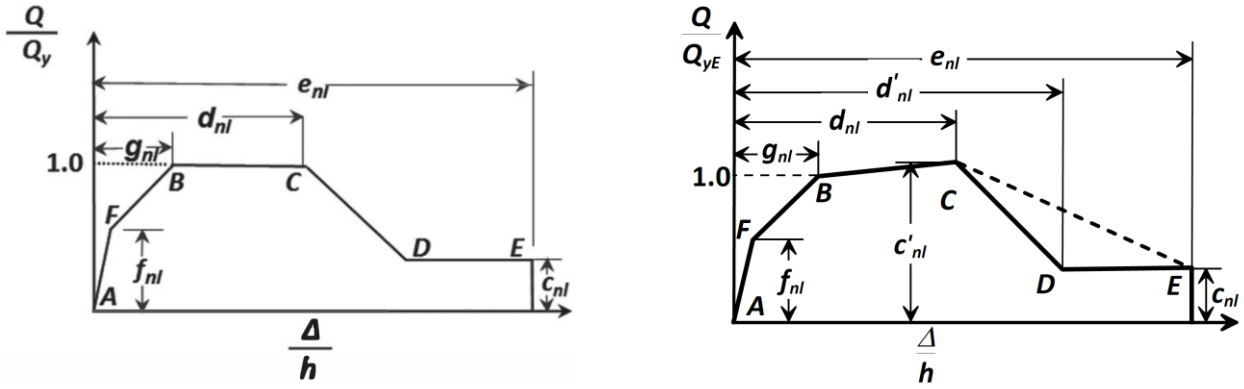

(*a*) ASCE/SEI 41-17/ACI 369-17 backbone **(*b*) Proposed backbone**

Figure 2-2 Idealized backbone relations to model shear behavior of shear-controlled walls.

2.3.2 Wall Lateral Shear Strengths

In this section, the strength relations for each point on the backbone curve are proposed in the order they appear on the proposed backbone (Figure 2-2b). For each strength at each point, the impact of several variables was investigated. However, only the most relevant variables are discussed next for brevity.

2.3.2.1 CRACKING STRENGTH

In ACI 369.1-17, the cracking shear strength (V_{crE}) is defined as 60% of yield strength V_{nE}, regardless of characteristics of the wall such as cross-section shape. However, cracking strength was found to correlate better with the concrete contribution to shear strength ($V_{c,ACI}=\alpha_c\lambda\sqrt{f'_{cE}}A_{cv}$, where α_c and λ are as defined later in Equation 2-1 and ACI 318-19 Equation 18.10.4.1).

Figure 2-3 presents results for experimentally observed strength at shear cracking ($V_{cr,test}$) normalized by $\alpha_c\lambda\sqrt{f'_{cE}}A_{cv}$ Figure 2-3a shows a strong correlation of $V_{cr,test}/\alpha_c\lambda\sqrt{f'_{cE}}A_{cv}$ with cross-section shape of the wall. It has been observed that walls with flanged cross-sections (barbell-shaped and H-shaped) have significantly higher peak shear strength than walls with rectangular cross-sections (e.g., Gulec and Whittaker, 2011; Kabeyashawa et al., 2008; Park et al., 2015). The data presented here indicates that this observation also holds true for cracking strength. Figure 2-3a also indicates that there is moderate correlation between $V_{cr,test}/\alpha_c\lambda\sqrt{f'_{cE}}A_{cv}$ and axial load ratio ($P/A_g f'_{cE}$). Limited correlation can be observed between shear cracking strength and M/Vl_w (Figure 2-3b).

Based on data analysis results, the approach given in Table 2-1 is proposed for expected shear strength at cracking ($V_{CcrWall}$), which, for simplicity, only depends on wall cross-section shape (rectangular vs. barbell and flanged walls). Figure 2-4 shows that this model slightly overpredicts data mean by 9% for shear- and flexure-shear-controlled walls. This could be addressed by using a factor of 1.9 or 1.8 for barbell and flanged walls, respectively, instead of 2.0; however, given the uncertainties in the measured data at cracking level and for simplicity, a factor of 2.0 is recommended. The proposed model results in a mean of 1.01 if only shear-controlled walls are considered (Figure 2-4). Inclusion of flexure-shear data increases dispersion (COV increases from 0.27 to 0.37). This may be attributed to flexural cracking, which tends to precede diagonal shear cracking for such walls.

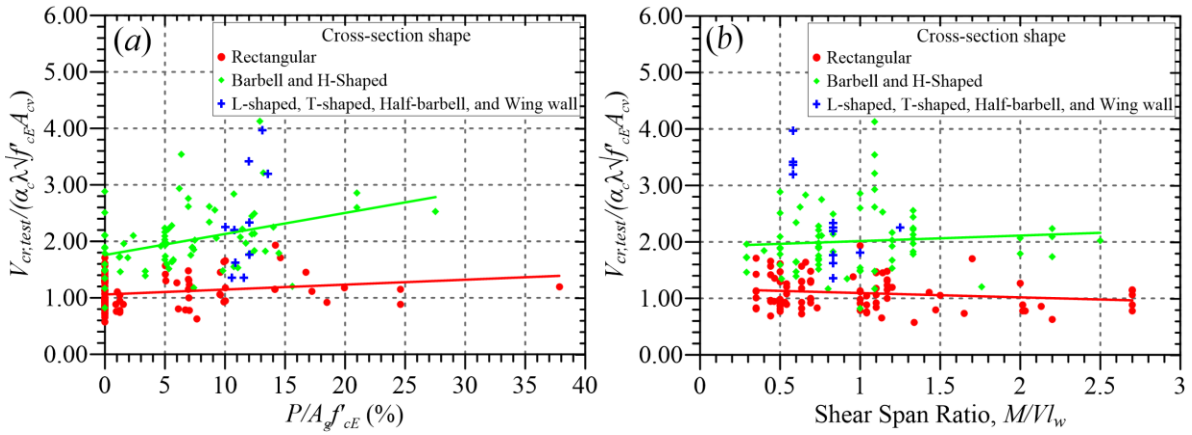

Figure 2-3 Parameters impacting cracking shear strength of walls.

In order for the proposed approach in Table 2-1 to be adopted in a standard, an objective method for distinguishing between walls with rectangular and flanged cross-sections was needed. Due to the varied geometries of flanged walls, including barbell, C-shaped, T-shaped and L-shaped, a method based on the ratio of gross moment of inertia of the cross-section to the gross moment of inertia of the rectangular web the cross section was adopted (I_{g_flange}/I_{g_rect}). Figure 2-5 presents the ratio of I_{g_flange}/I_{g_rect} of the wall tests in the dataset. Walls with I_{g_flange}/I_{g_rect} = 1.0 are rectangular (planar) walls, whereas walls with $I_{g\_flange}/I_{g\_rect} \geq 1.5$ are considered as flanged walls. Linear interpolation between the parameters for rectangular and flanged sections are recommended based on the ratio of moments of inertia.

Walls that are non-symmetric about a bending axis, in terms of geometry, reinforcement ratio, detailing, and/or applied axial loads, are recommended to be modeled considering non-symmetric behavior in the two directions of loading about that axis.

Table 2-1 Proposed Cracking Shear Strength Models

Cross-section Shape	$V_{CcrWall}$ (1)(2)(3)
Rectangular	$1.0\ A_{cv}\left(\alpha_c\lambda\sqrt{f'_{cE}(\text{psi})}\right)$
Barbell or Flanged	$2.0\ A_{cv}\left(\alpha_c\lambda\sqrt{f'_{cE}(\text{psi})}\right)$

(1) Walls with I_{g_flange}/I_{g_rec} = 1.0 are defined as rectangular (planar) walls, whereas walls with $I_{g\_flange}/I_{g\_rec} \geq 1.5$ are defined as flanged walls (including barbell-shaped walls).
(2) α_c and λ are as defined later in Equation 2-1 and ACI 318-19 Equation 18.10.4.1.
(3) Linear interpolation can be used for in-between values.

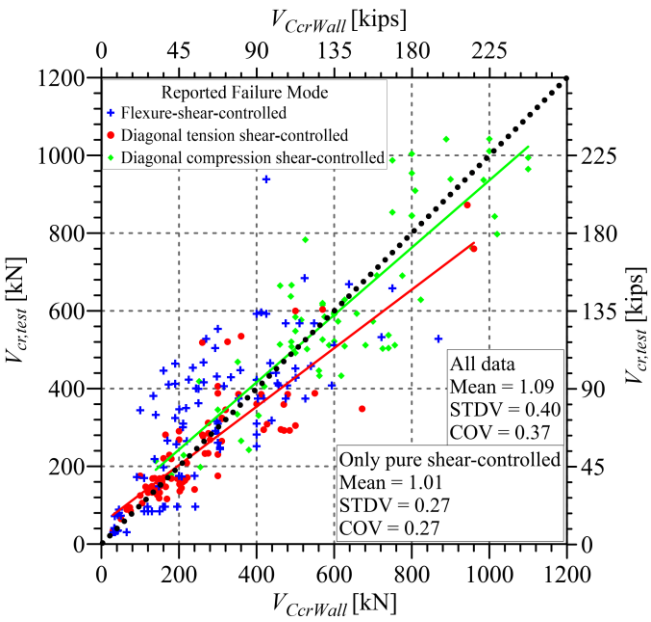

Figure 2-4 Comparison of measured and predicted (Table 2-1) cracking shear strength ($V_{CcrWall}$).

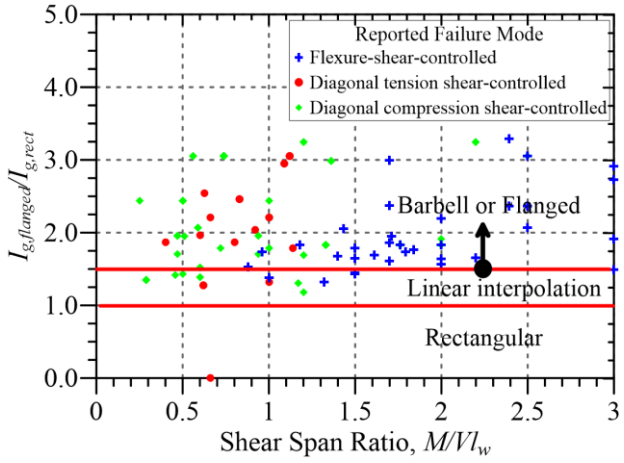

Figure 2-5 Definition of wall cross-section shape.

2.3.2.2 YIELD SHEAR STRENGTH

Yield shear strength of shear-controlled walls in ACI 369.1-17 is calculated using Equation 2-1, which is taken from ACI 318-19 Equation 18.10.4.1. Experimental data shown in Figure 2-6 for measured yield-to-peak strength ratios ($V_{y,test}/V_{peak,test}$) indicate a moderate increase in shear strength from Point B (yield) to Point C (peak) (Figure 2-2), with a mean value of $V_{y,test}/V_{peak,test} \approx 0.9$ (i.e., ~11% hardening) and a COV of 0.08. Therefore, the approach taken here was to develop a relation for yield strength and take peak shear strength at Point C equal to a multiplier times the yield shear strength.

$$V_{CWall318E} = A_{cv}\left(\alpha_c\sqrt{f'_{cE}} + \rho_{web,h}f_{ytE}\right) \le 10A_{cv}\sqrt{f'_{cE}} \quad (2\text{-}1)$$

Where A_{cv} is the gross area of concrete section bounded by web thickness and wall length ($A_{cv}= t_w l_w$), f'_{cE} is the tested concrete compressive strength, $\rho_{web,h}$ is the web transverse (horizontal) reinforcement ratio, f_{ytE} is the tested yield strength of the web transverse reinforcement, and α_c is a coefficient that depends on h_w/l_w of the wall, where α_c is taken as 3.0 for $h_w/l_w \le 1.5$, as 2.0 for $h_w/l_w \ge 2.0$, and varies linearly between 3.0 and 2.0 for h_w/l_w between 1.5 and 2.0.

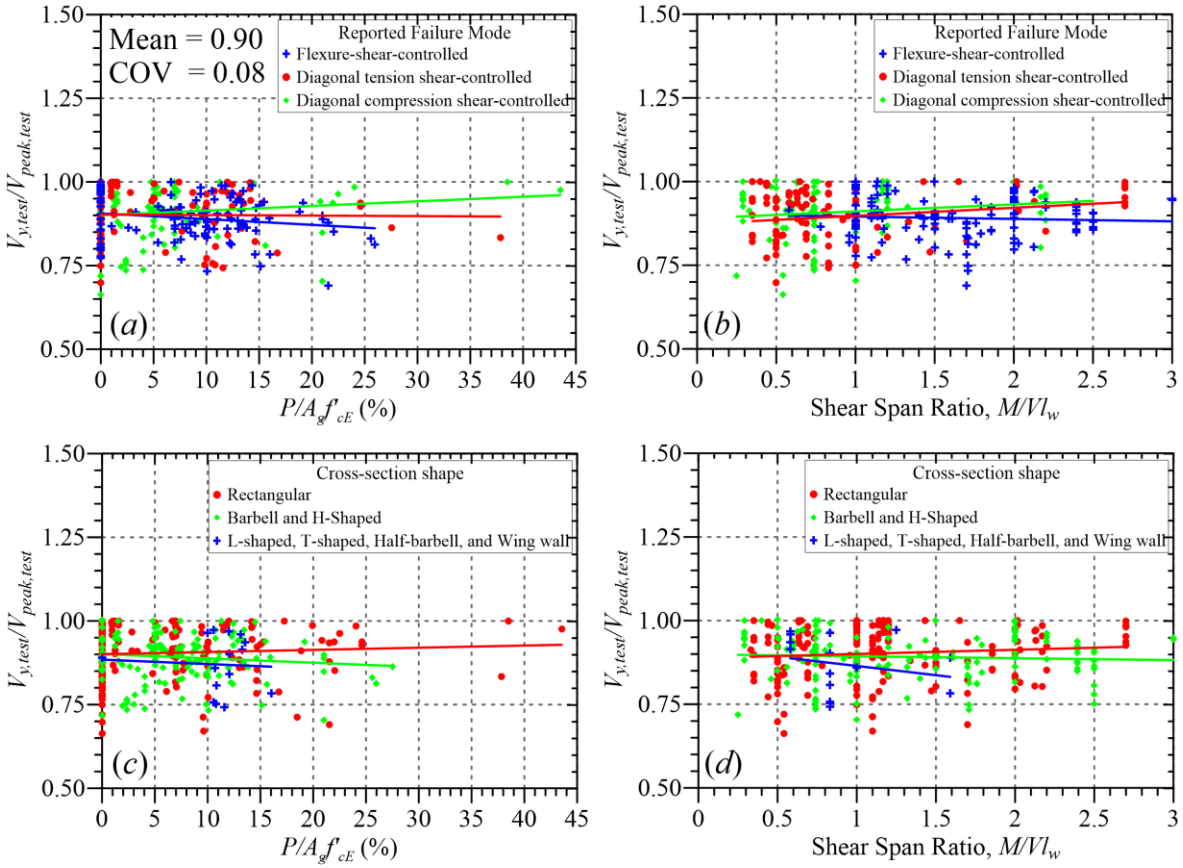

Figure 2-6 Measured yield strength ($V_{y,test}$) normalized by measured peak strength ($V_{peak,test}$).

Figure 2-7 shows the variation of the ratio of measured yield strength to shear strength calculated from Equation 2-1 ($V_{y,test}/V_{CWall318E}$), against likely influential parameters. The results show that the ratio of $V_{CWall318E}/V_{MCyDE}$ produces the highest correlation with $V_{y,test}/V_{CWall318E}$. The reason for the significant correlation of yield shear strength with $V_{CWall318E}/V_{MCyDE}$ is that this term accounts for the shear demands at flexural yielding (V_{MCyDE}), which, through the expected flexural yield strength M_{CyDE}, accounts for various other parameters that are not represented in Equation 2-1 such axial load, amount and distribution of longitudinal reinforcement in the boundaries and web, and cross-section shape. Additionally, Figure 2-7 shows that increasing axial load results in an increase in yield shear strength for walls with flexure-shear and diagonal tension failure modes and a reduction for walls with diagonal compression failure mode because larger axial loads increase shear strength along the diagonal shear crack for diagonal tension-controlled walls, whereas in case of diagonal

compression-controlled walls, larger axial loads result in more compression demands on the diagonal compression strut, resulting in crushing of the diagonal compression strut.

Further attempts were made to reduce dispersion of the data by isolating the impact of other parameters such as web horizontal and vertical reinforcement ratios ($\rho_{web,h}$ and $\rho_{web,v}$) and $P/A_g f'_{cE}$, in addition to $V_{CWall318E}/V_{MCyDE}$. The results showed that only moderate improvements could be made by considering $\rho_{web,h}$ and $P/A_g f'_{cE}$, as shown in Figure 2-8.

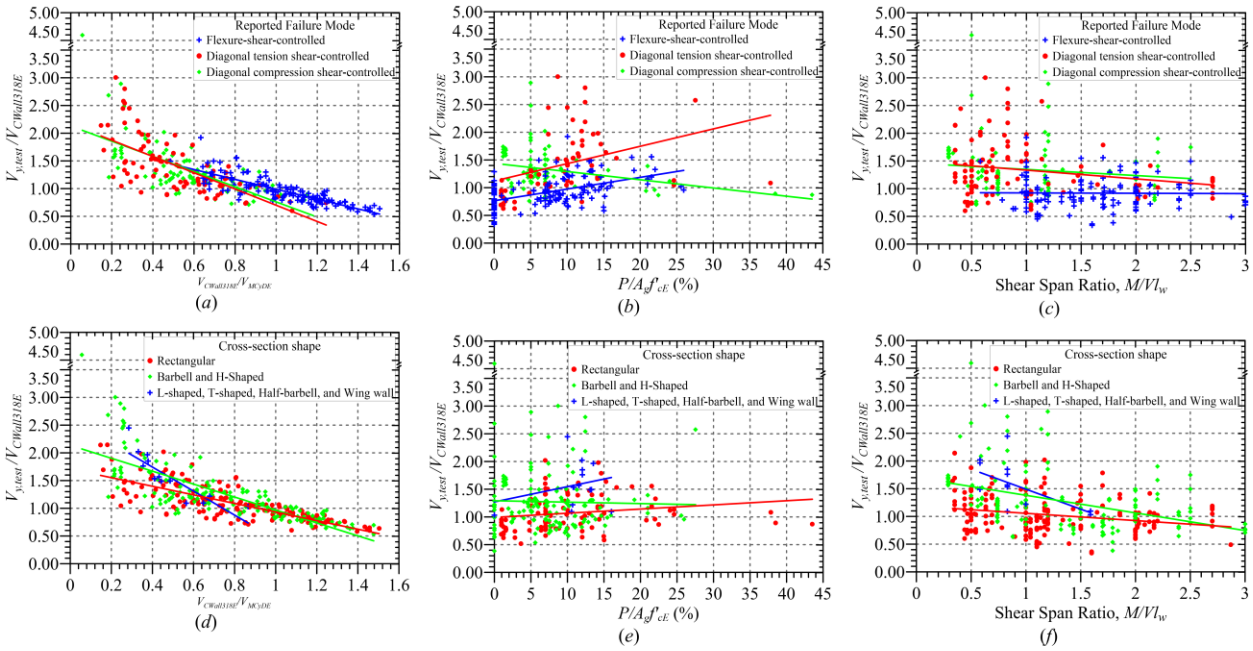

Figure 2-7 Influence of various parameters on yield shear strength.

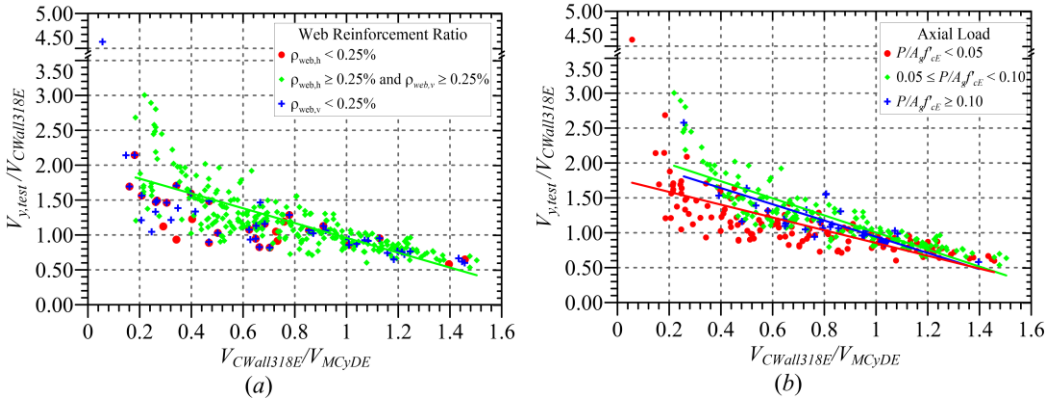

Figure 2-8 Influence of $V_{CWall318E}/V_{MCyDE}$, axial load, and web horizontal reinforcement ratio on yield shear strength.

Since Equation 2-1 is familiar to engineers and is relatively simple to implement, a modified version of this equation is proposed as opposed to generating new equation. Based on the results presented in Figure 2-8, a predictive model for yield shear strength is proposed as given by Equation 2-2, which

depends on the $V_{CWall318E}/V_{MCyDE}$ and the shear strength ($V_{CWall318E}$) from Equation 2-1. Figure 2-9 compares results from Equation 2-2 with the experimental data and shows that the model well matches the experimental data. From this figure, it can also be observed that walls with web horizontal reinforcement ratios, $\rho_{web,h}$, less than 0.0015, have on average slightly less yield shear strength than values predicted from Equation 2-2; therefore, a reduction factor of 0.85 is recommended to be applied to results from Equation 2-2 for walls with $\rho_{web,h}$ less than 0.0015.

$$V_{CydWallE} = \left(2.0 - 1.10 \times \frac{V_{CWall318E}}{V_{MCyDE}}\right) V_{CWall318E} \tag{2-2}$$

Where $V_{CydWallE}$ should be not be larger than 1.8 $V_{CWall318E}$ or smaller than 0.8$V_{CWall318E}$.

Several nonlinear modeling parameters in this report, including stiffness and strength parameters (e.g., $V_{CWall318E}$), are related to the applied axial load on the member. Where axial loads vary significantly due to earthquake effects, these modeling parameters need to adapt to the changing axial loads. However, most element models in structural analysis software cannot adapt their behavior with changing axial load. If such models are used, the effects of earthquake axial load on the force-deformation backbone relations can be incorporated by applying differing modeling parameters in each loading direction that correspond to the earthquake axial loads in each direction. The earthquake axial loads should be estimated in either direction of loading at anticipated drift levels. This process may be iterative as the model needs to be run with assumed modeling parameters based on gravity loads to obtain estimates of seismically induced axial loads. The modeling parameters would then be updated based on those axial loads. This process results in non-symmetric backbone relations with respect to direction of loading.

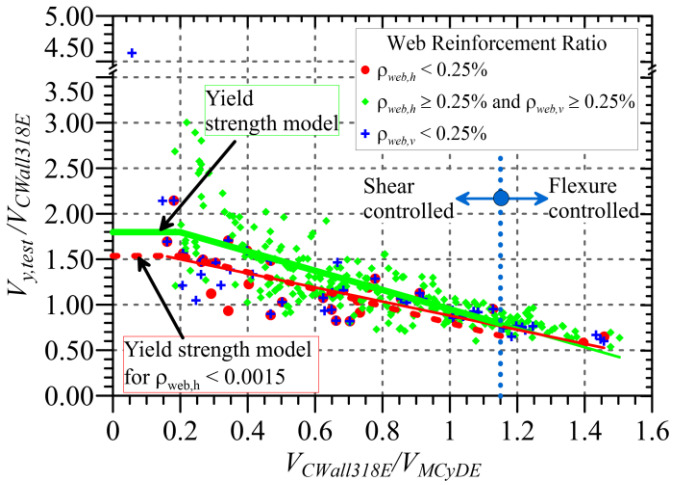

Figure 2-9 Comparison of model for yield shear strength with experimental data.

2.3.2.3 PEAK SHEAR STRENGTH

Figure 2-10 presents results for ratios of shear strength from Equation 2-1 to measured peak strength ($V_{CWall318E}/V_{peak,test}$) and shows that, similar to yield shear strength, there is a significant

correlation between $V_{peak,test}$ and $V_{CWall318E}/V_{MCyDE}$. Figure 2-11 compares the $V_{peak,test}$ from the dataset with the yield shear strength model (Equation 2-2) and indicates that peak shear strength can be obtained by multiplying the yield shear strength (V_{CWallE}) by a factor of 1.10, i.e., Parameter c'_{nl} = 1.15.

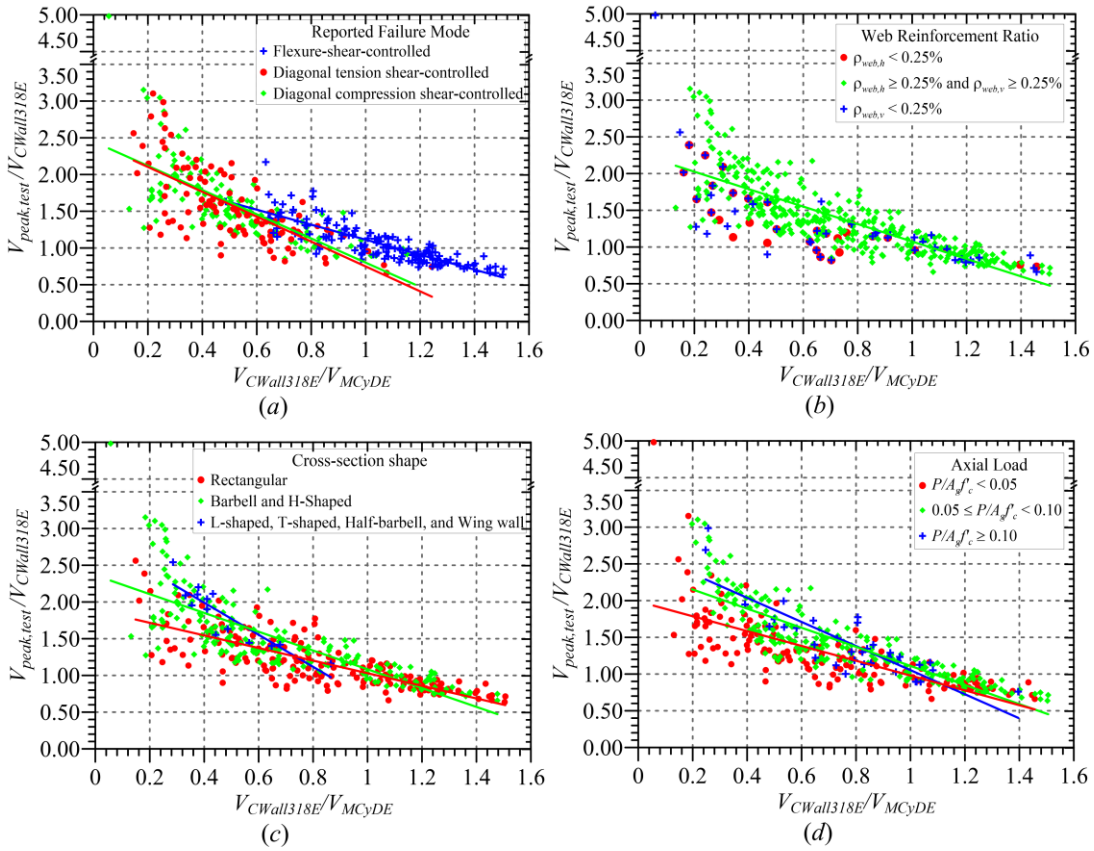

Figure 2-10 Impact of $V_{CWall318E}/V_{MCyDE}$, axial load, and web horizontal reinforcement ration of peak shear strength.

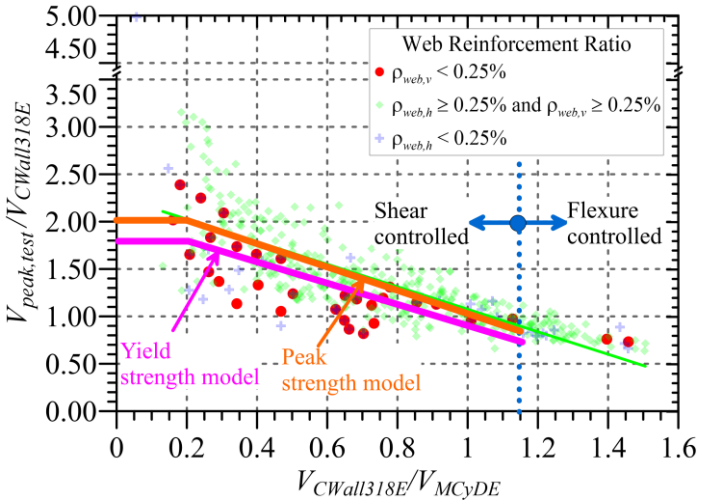

Figure 2-11 Comparison of peak shear strength model with experimental data.

2.3.2.4 RESIDUAL STRENGTH

Residual shear strength in ACI 369.1-17 depends on the axial load and longitudinal reinforcement ratio and ranges from zero to 0.20. The results presented in Figure 2-12 indicate that residual strength is significantly impacted by axial load ratio and wall cross-section shape. Shear-span-ratio does not seem to have a significant correlation with residual strength. Therefore, the relations illustrated in Figure 2-13 are proposed for residual strength. Tabulated values for Parameter c_{nl} are given in Table 2-2. The limited data in Figure 2-13 also indicates that walls with horizontal web reinforcement ratios less than 0.0015 tend to have little to no residual strength, i.e., Parameter $c_{nl} = 0$.

As shown in Figure 2-2b, it is assumed that the wall maintains its residual strength from the point of initiation of residual strength to the point of initiation of axial failure. Therefore, strength at Point E is taken equal to strength at Point D.

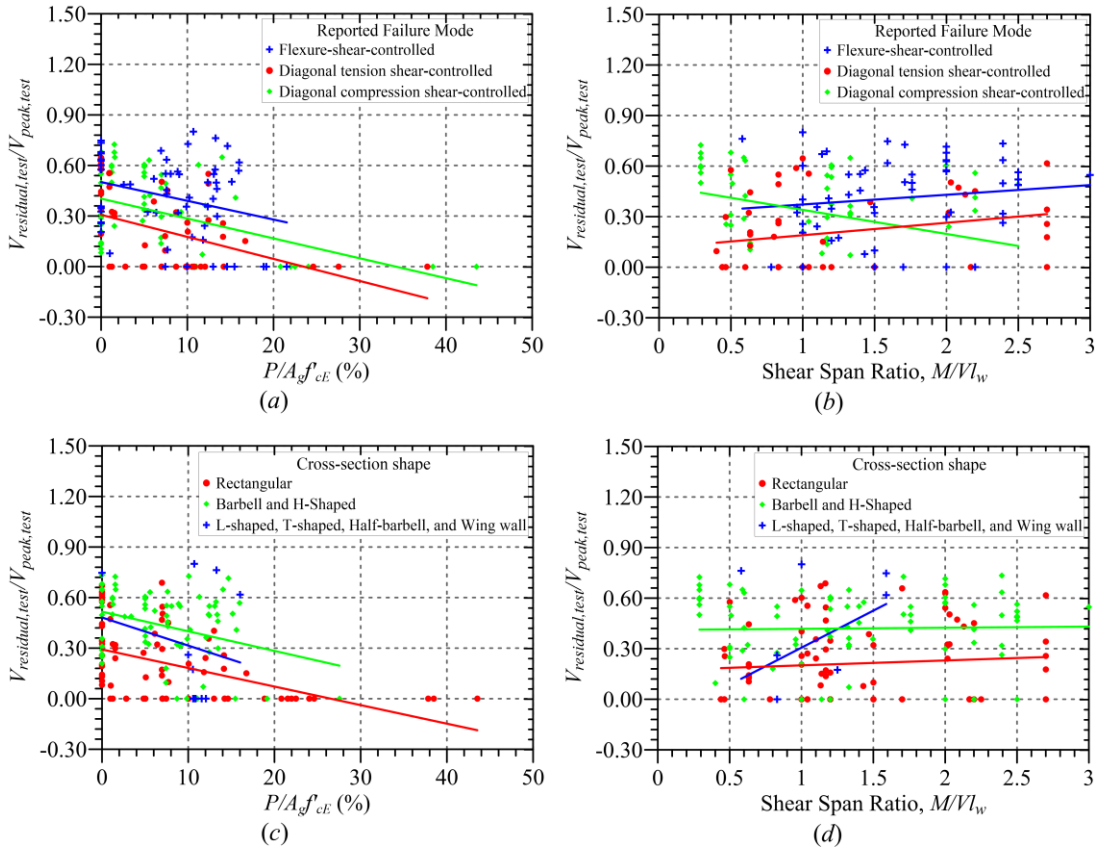

Figure 2-12 Parameters impacting residual shear strength.

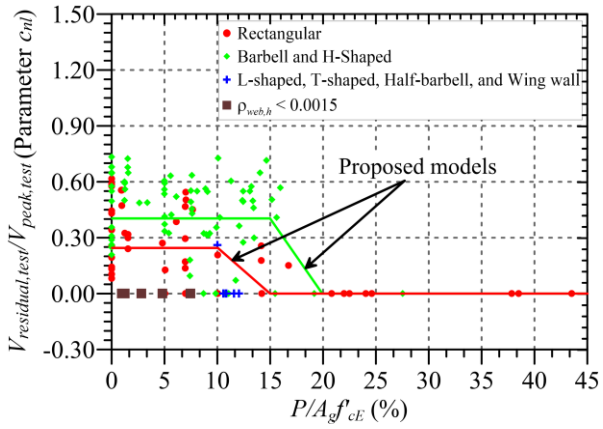

Figure 2-13 Proposed models for residual shear strength.

Table 2-2 Proposed Values for Modeling Parameter c_{nl}

Cross-section shape	$P/A_g f'_{cE}$	Parameter c_{nl}[1][2]
Planar	≤ 0.10	0.25
	> 0.15	0.00
Barbell or flanged	≤ 0.15	0.40
	> 0.20	0.00

[1] Linear interpolation between limits

[2] For walls with $\rho_{web,h}$ < 0.0015, Parameter *c* shall be taken as zero.

2.3.3 Modeling Parameters and Acceptance Criteria

2.3.3.1 NONLINEAR MODELING PARAMETERS

In this section, the modeling parameters for each point on the backbone curve are developed in the order they appear on the backbone using the experimental dataset. The impact of several variables was investigated on modeling parameters, however, only the most relevant results are presented here for brevity.

Cracking Shear Stiffness

Shear deformations prior to shear cracking are relatively minor compared with other deformations, particularly flexural ones. The approach of subtracting flexural deformation from total deformation in this case did not yield reliable results. Therefore, a second dataset of 34 walls, for which GA_{uncrE} (cracked shear stiffness) is determined based on reported cracking load and measured cracking shear deformation. The results from the second dataset are presented in Figure 2-16 and indicate that there is significant dispersion in the data. However, Figure 2-14 shows that on average GA_{uncrE} is about 0.70 $G_{gE}A_{cv}$ (gross shear stiffness) for all cross-section shapes. These results are used to propose GA_{uncrE} = 0.7*0.4$E_{cE}A_{cv}$ = 0.28 $E_{cE}A_{cv}$ ≈ 0.30 $E_{cE}A_{cv}$ for both linear and nonlinear analysis procedures.

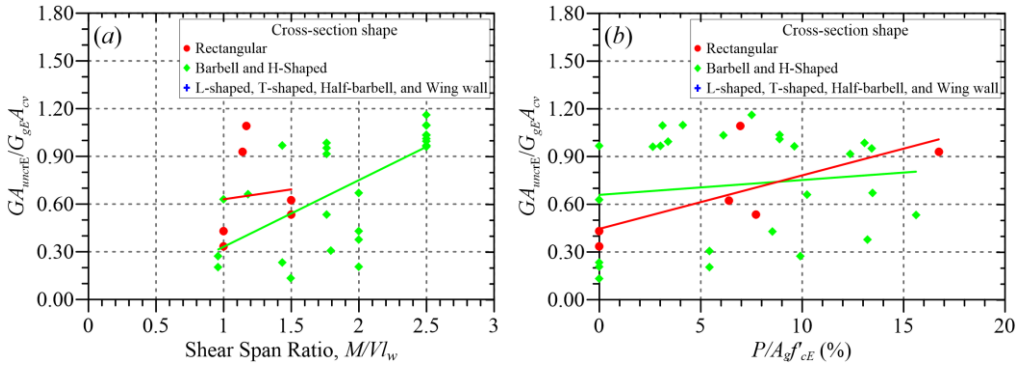

Figure 2-14 Normalized uncracked shear stiffness for a small subset of data (34 walls) with measured shear cracking load and deformation.

Parameter g_{nl} (Drift at Point B, Yield)

Figure 2-15 presents the variation of measured yield drift of the dataset against axial load, shear span ratio, and cross-section shape. This figure indicates no apparent trend between yield drift and axial load, cross-section shape, or shear-span ratio. Figure 2-15 also highlights the average yield drift across the dataset of 0.36% with a standard deviation of 0.14 and COV of 0.39. ACI 369.1-17 uses a value of 0.40% for yield drift of shear-controlled walls. The evidence therefore supports maintaining that yield drift be taken as 0.40%, regardless of cross-section shape and other wall characteristics.

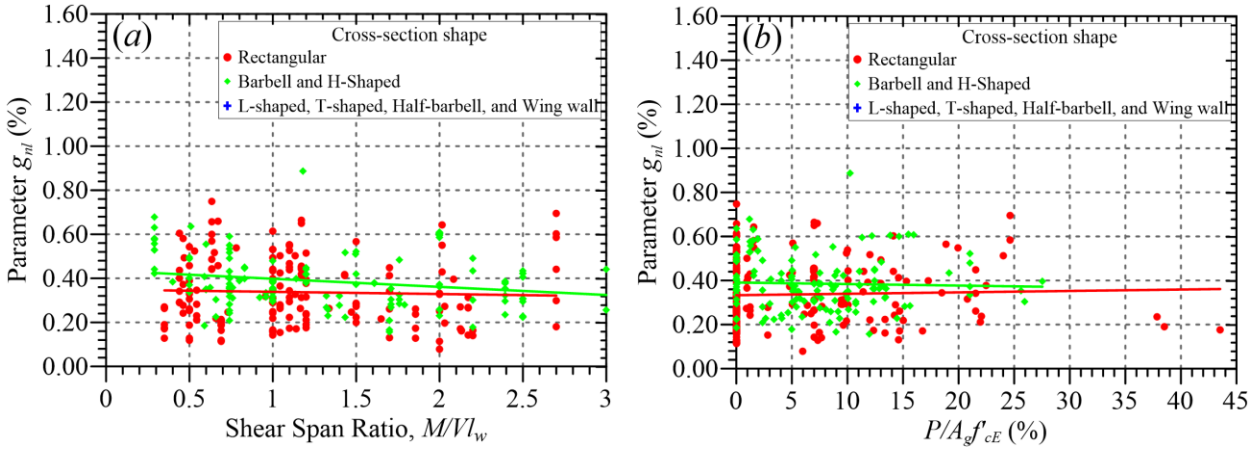

Figure 2-15 Measured drift at yield strength (Parameter g_{nl}).

Parameter d_{nl} (Drift at Point C, Initiation of Lateral Strength Loss)

As noted previously, Point C is taken at the point where a loss of 20% in lateral strength from peak strength occurs. In ACI 369.1-17, the drift ratio value at Point C (Parameter d_{nl}) is given as a function of the axial load ratio and the difference between the tension and compression reinforcement ratios. It ranges from 0.75% to 1.0%. The influence of various parameters on the drift at Point C was investigated through test data. Figure 2-16 shows that the shear-to-flexure strength ratio ($V_{CWall318E}/V_{MCyDE}$) has the most significant impact on d_{nl}. Walls that experience flexural yielding prior

to shear failure have a larger drift capacity because they have a larger contribution from inelastic flexural deformations, which is not captured by $E_{CE}I_{eff}$. Figure 2-16 also shows that an increase in M/Vl_w results in an increase in drift capacity, again, due to larger contribution from flexure for more slender walls. Furthermore, Figure 2-16 indicates that flanged walls tend to have larger drift capacities than rectangular wall, especially for walls with $M/Vl_w > 1.0$. Therefore, a relation for d_{nl} is proposed as a function of $V_{CWall318E}/V_{MCyDE}$ and cross-section shape.

Figure 2-17 presents the proposed relations for Parameter d_{nl} compared with experimental data. As noted on the figure, flanged walls that have confinement in the form of hoops and/or crossties in the web exhibit larger drift capacity. Possibly, web confinement increases the ductility of the diagonal compression strut of flanged walls, which typically fail due to crushing of the diagonal compression strut. Proposed values of Parameter d_{nl} are given in Table 2-3.

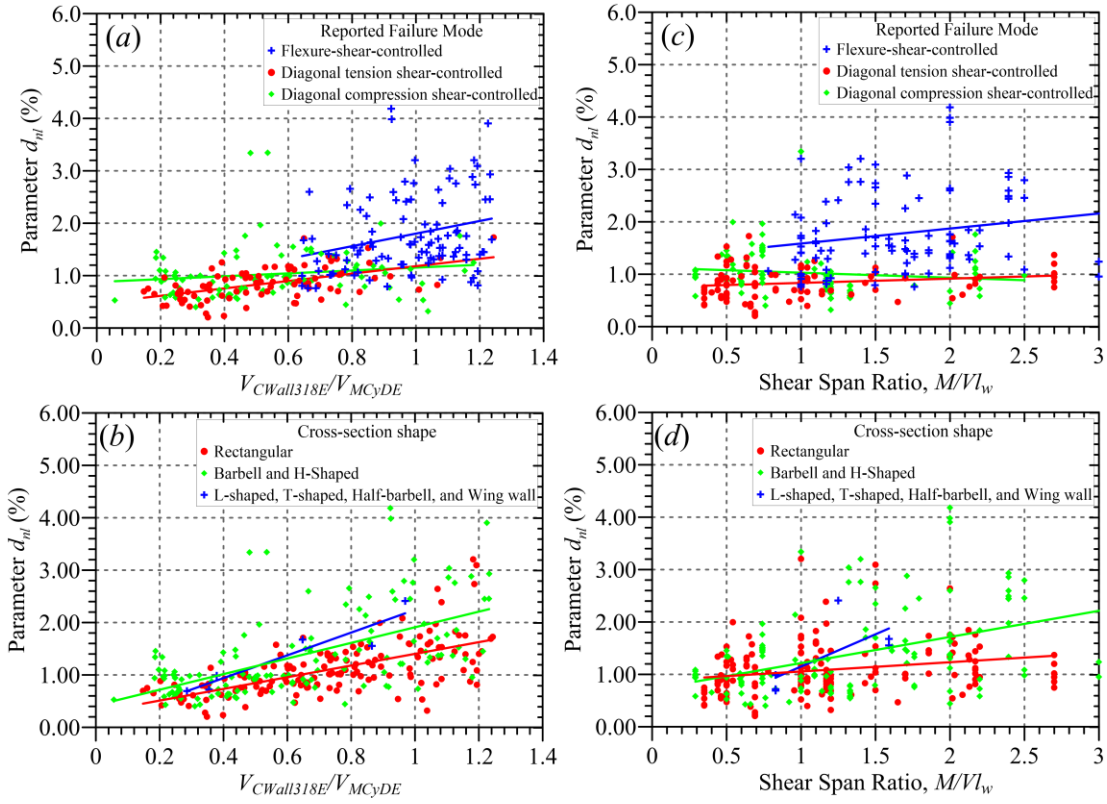

Figure 2-16 Measured drift capacity at 20% lateral strength loss (Parameter d_{nl}).

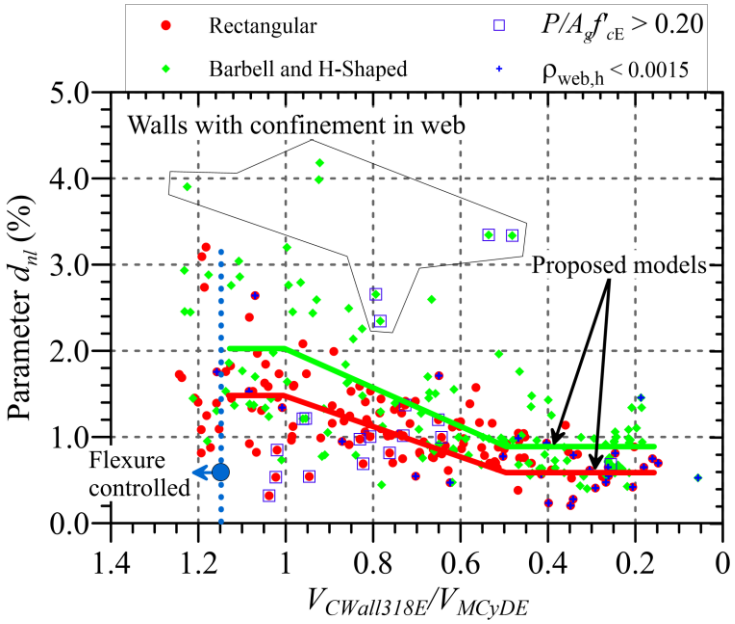

Figure 2-17 Proposed relations for drift capacity at lateral strength loss.

Table 2-3 Proposed Values for MP d_{nl} as Function of Cross-Section Shape and Shear Strength to Shear Demand at Flexural Yielding Strength Ratio

Shape	$\frac{V_{CWall318E}}{V_{MCyDE}}$	Parameter d_{nl} (1)(2)
Rectangular	> 1.0	0.015
	≤ 0.5	0.006
Barbell and Flanged	> 1.0	0.020
	≤ 0.5	0.009

(1) Linear interpolation between limits

(2) If $P/A_g f'_{cE} \geq 0.20$ and $V_{CWall318E}/V_{MCyDE} > 0.80$, then d shall be taken as 0.5%.

Parameter d'_{nl} (Drift at Point D, Residual Strength)

There is no deformation-based modeling parameter for Point D in ACI 369.1-17. Figure 2-18 shows that the important parameters impacting the drift at Point D (Parameter d'_{nl}) include axial load ratio ($P/A_g f'_{cE}$) and the shear strength to shear demand ratio ($V_{CWall318E}/V_{MCyDE}$). Again, the impact of $V_{CWall318E}/V_{MCyDE}$ is partly due to contributions from inelastic flexural deformation to the drift at residual strength. Therefore, $P/A_g f'_{cE}$ and $V_{CWall318E}/V_{MCyDE}$ are used as predictor variables to obtain Parameter d'_{nl} (Figure 2-19 and Table 2-4)

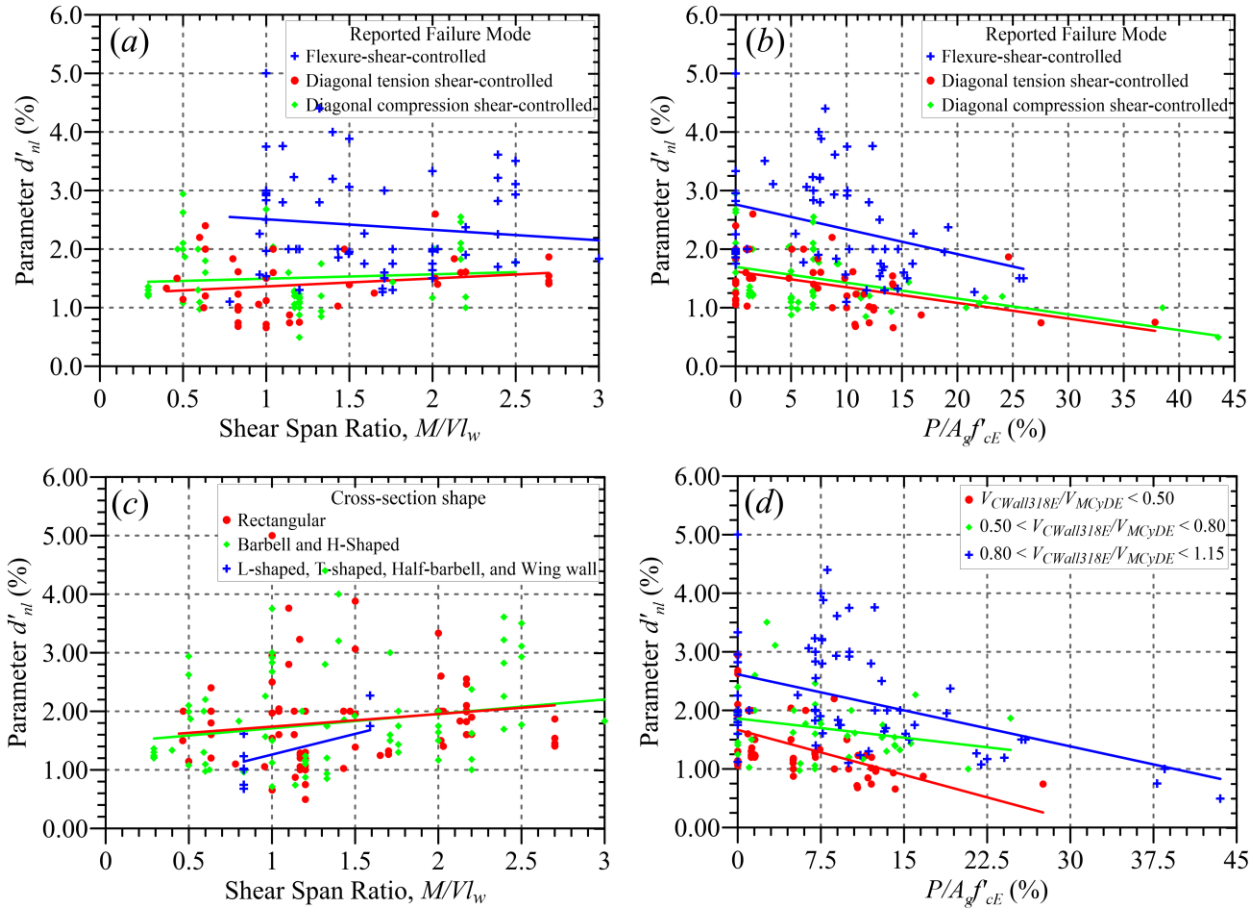

Figure 2-18 Parameters impacting drift capacity at residual strength (Parameter d'_{nl}).

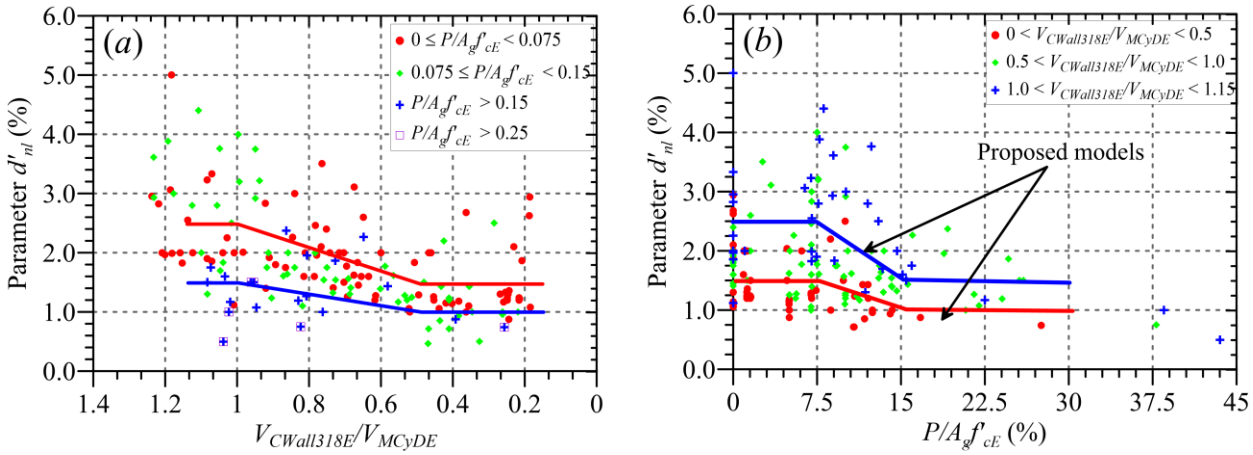

Figure 2-19 Proposed relations for drift capacity at residual strength (Parameter d'_{nl}).

Table 2-4 Proposed Values for Parameter d'_{nl} as a Function of Cross-Section Shape and Shear Strength to Shear Demand Ratio

$P/A_g f'_c$	$\frac{V_{CWall318E}}{V_{MCyDE}}$	Parameter d'_{nl} (1)(2)
≤ 0.075	> 1.0	0.025
	≤ 0.5	0.015
> 0.150 < 0.30	> 1.0	0.015
	≤ 0.5	0.01
> 0.30	Force-controlled	

(1) Linear interpolation between limits
(2) d'_{nl} shall not be taken less than d_{nl}

Parameter e_{nl} (Drift at Point E, Axial Failure)

Axial failure in shear-controlled walls results from sliding along a critical crack extending diagonally over the height of the wall, when the shear friction demand exceeds the shear friction capacity along the diagonal crack (Abdullah and Wallace (2021)).

To evaluate drift capacity at axial failure (Parameter e_{nl}), two datasets were used. The first dataset includes 45 wall tests with reported axial failure (Abdullah and Wallace, 2021; Abdullah, 2019). One limitation of this dataset is that it lacks enough data on flexure-shear-controlled walls. The second dataset includes 90 wall tests, which include the 45 wall tests from the first dataset and another 45 walls with lower-bound drift capacities at axial failure (i.e., axial failure not reported). This dataset was only used to evaluate the deformation capacity of flexure-shear-controlled walls.

The observed drift capacities at axial failure (Parameter e_{nl}) of the wall tests in the first dataset (45 walls) are plotted against $P/A_g f'_{cE}$ in Figure 2-20, along with logarithmic and power trend lines fitted to the data. This figure shows that the trend lines for walls with diagonal tension and compression failure modes are only slightly different, and there is significant scatter in the data for walls with flexure-shear failure modes, although the drift capacities of the flexure-shear-controlled walls are higher. It is noted that there are only seven data points with flexure-shear failure modes, five of which are wing walls; therefore, the data for wing walls are not considered. Extrapolating the trends in Figure 2-20 indicates that drift capacity reaches about zero at $P/A_g f'_{cE}$ of approximately 0.85 (i.e., axial stress of ~$0.85f'_{cE}$), which is commonly used as the maximum pure axial compression strength of compression members, as in ACI 318-19, ignoring the presence of the longitudinal reinforcement.

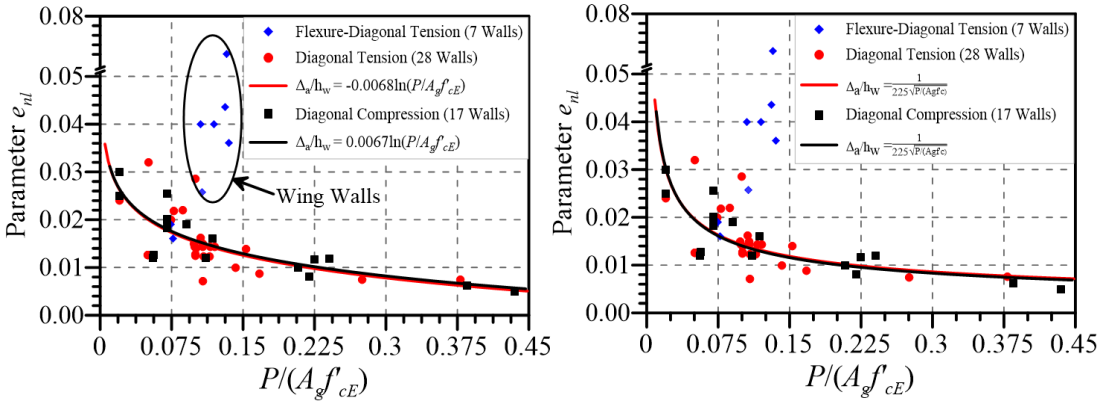

Figure 2-20 Impact of axial load on drift capacity at axial failure (Parameter e_{nl}) for the small dataset of 45 walls.

To address the lack of data on flexure-shear-controlled walls in the first dataset, the second dataset was investigated. The observed Parameter e_{nl} of the wall tests (90 walls) are plotted against $P/A_g f'_{cE}$ for different ranges of $V_{CWall318E}/V_{MCyDE}$ in Figure 2-21. This figure indicates that, in addition to axial load, $V_{CWall318E}/V_{MCyDE}$ has a significant impact on Parameter e_{nl}. Walls that experience flexural yielding prior to shear failure have larger drift capacities. Therefore, the relations shown in Figure 2-22, which are function of $P/A_g f'_{cE}$ and $V_{CWall318E}/V_{MCyDE}$, are proposed for Parameter e_{nl}. Drift capacity values from these relations are tabulated in Table 2-5.

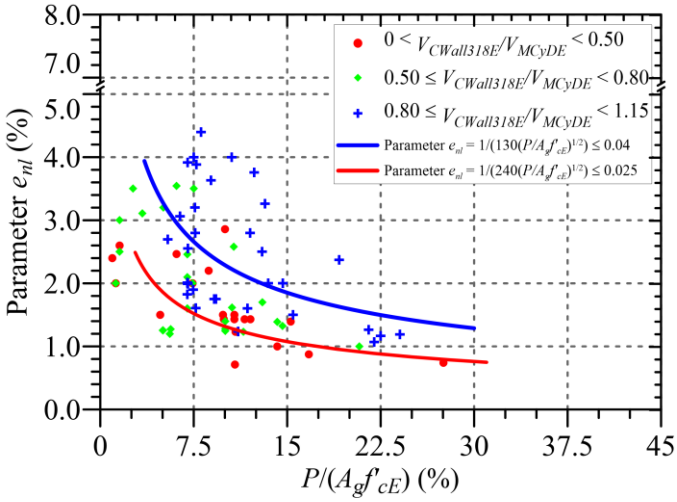

Figure 2-21 Impact of axial load on drift capacity at axial failure (Parameter e_{nl}) for the dataset of 90 walls.

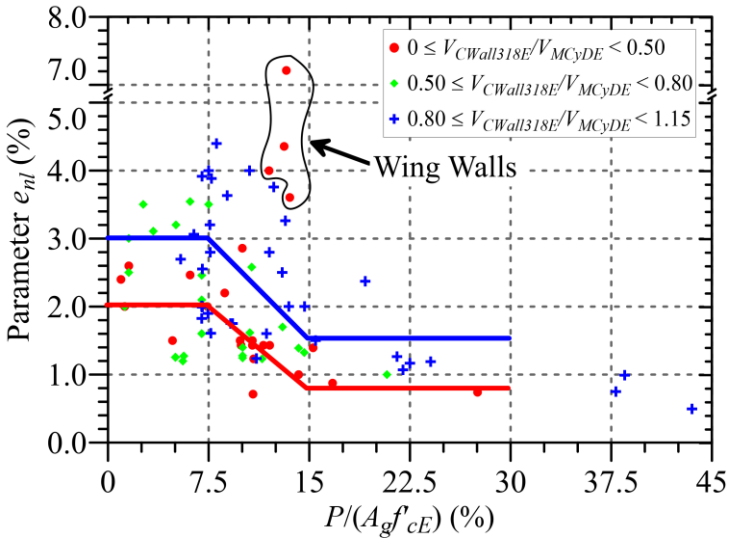

Figure 2-22 Proposed models for drift capacity at axial failure (Parameter e_{nl}).

Table 2-5 Proposed Values for Parameter e_{nl}

$\frac{N_{UD}}{A_g f'_{cE}}$	$\frac{V_{CWall318E}}{V_{MCyDE}}$	Parameter e_{nl}
≤ 0.075	> 0.80	0.03
	≤ 0.50	0.02
> 0.15 ≤ 0.30	> 0.80	0.015
	≤ 0.50	0.008
> 0.30	Force-controlled	

Note: Linear interpolation for values between limits

Summary of Proposed Nonlinear Modeling Parameters

Table 2-6 presents the proposed nonlinear backbone modeling parameters for shear-controlled walls. The error statistics of the proposed modeling parameters are given in Table 2-7.

Table 2-6 Proposed Nonlinear Modeling Parameters[a]

Condition		g_{nl}	d_{nl}[c]
Cross-section shape[bf]	$\frac{V_{CWall318E}}{V_{MCyDE}}$		
Rectangular	≥ 1.0	0.004	0.015
	≤ 0.5		0.006
Flanged	≥ 1.0		0.020
	≤ 0.5		0.009

Condition[bf]		d'_{nl}[d]	e_{nl}[d]
$\frac{N_{UD}}{A_g f'_{cE}}$	$\frac{V_{CWall318E}}{V_{MCyDE}}$		
≤ 0.075	≥ 1.0	0.025	0.03
	≤ 0.5	0.015	0.02
≥ 0.150 ≤ 0.30	≥ 1.0	0.015	0.015
	≤ 0.5	0.010	0.010

Condition		c_{nl}[e]	c'_{nl}
Cross-section shape[bf]	$\frac{N_{UD}}{A_g f'_{cE}}$		
Rectangular	≤ 0.10	0.25	1.10
	≥ 0.15	0.00	
Flanged	≤ 0.15	0.40	
	≥ 0.20	0.00	

[a] Linear interpolation between values listed in the table is permitted.

[b] Linear interpolation between values listed in the table based on I_{g_flange}/I_{g_rect} is permitted for walls and wall segments between wall and flanged designations with $1.0 < I_{g\_flange}/I_{g\_rect} < 1.5$.

[c] d_{nl} is taken as 0.005 when $P/(A_g f'_{cE}) \geq 0.20$ and $V_{CWall318E}/V_{MCyDE} \geq 0.8$ or when ρ_t and ρ_l are less than 0.0015 and $V_{CWall318E}/V_{MCyDE} \leq 0.5$.

[d] d'_{nl} and e_{nl} should not be taken less than d_{nl}.

[e] c_{nl} should be taken as zero where ρ_t is less than 0.0015.

[f] walls with P greater than 0.30 $A_g f'_{cE}$, shall be considered as force controlled.

Table 2-7 Statistics of the Proposed Modeling Parameters

Parameter	Mean	Median	Standard Deviation	Coefficient of Variation, COV
$V_{CcrWall}$	1.09	1.01	0.40	0.37
$V_{CydWall}$	1.01	1.00	0.25	0.24
c'_{nl}	1.01	1.00	0.20	0.19
g_{nl}	1.31	1.15	0.60	0.46
d_{nl}	1.04	0.96	0.40	0.38
d'_{nl}	1.10	1.06	0.39	0.36
e_{nl}	1.06	1.04	0.37	0.35

Note: The statistics are for the ratios of estimated-to-experimental values.

2.3.3.2 ACCEPTANCE CRITERIA

Proposed Nonlinear Acceptance Criteria

For the nonlinear acceptance criteria, the same approach used for flexure-controlled walls is followed, where the acceptance criteria are taken as percentiles of Parameters d_{nl} and e_{nl} for LS and CP, and acceptance criteria for IO as yield drift + 10% of the inelastic deformation to Point C, as shown in the Table 2-8.

Table 2-8 Nonlinear Acceptance Criteria for Shear-Controlled Structural Walls

Performance Level	Component Type	Acceptance Criteria
IO	-	$g_{nl}+0.1(d_{nl}-g_{nl})$
LS	Primary	20^{th} of d_{nl}
	Secondary	10^{th} of e_{nl}
CP	Primary	35^{th} of d_{nl}
	Secondary	25^{th} of e_{nl}

Figure 2-23 compares the distribution of error data (ratio of predicted-to-measured) for Parameters d_{nl} and e_{nl} with Normal and LogNormal distributions. A LogNormal distribution is assumed for the

error data as it provides a better fit for the lower tail, which affects the acceptance criteria. Using a LogNormal distribution parameters that best fit the error data and the criteria given in Table 2-8, the nonlinear acceptance criteria were computed as provided in Table 2-9.

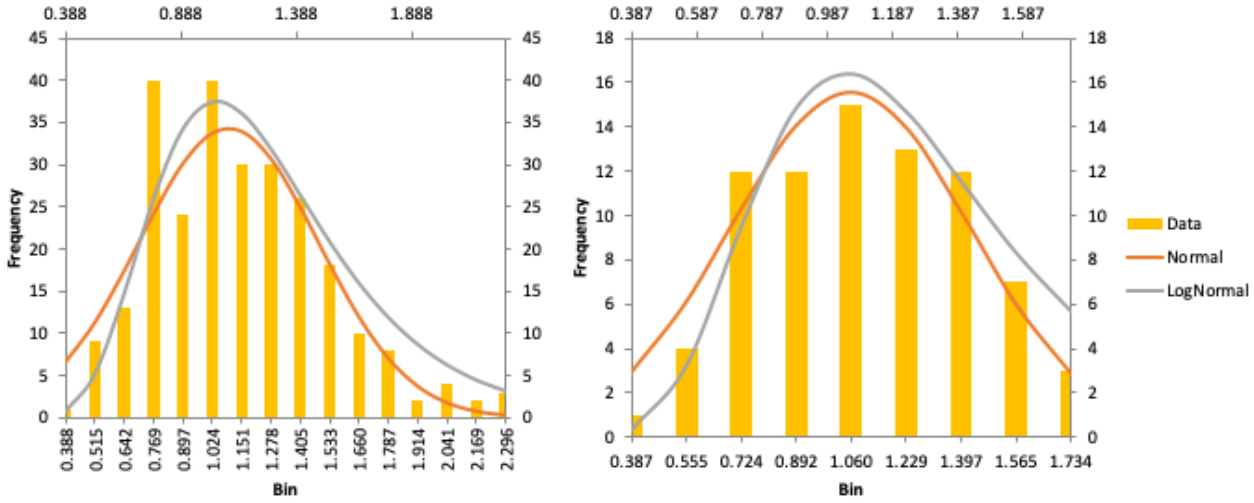

(*a*) Parameter d_{nl} **(*b*) Parameter e_{nl}**

Figure 2-23 Distribution of the error ratio of measured-to-predicted values of parameters d_{nl} and e_{nl}.

Table 2-9 Proposed Nonlinear Acceptance Criteria for Shear-Controlled Walls

Condition		g_{nl}	d_{nl}	Acceptance Criteria
				Performance Objective
Cross-Section Shape	$\frac{V_{CWall318E}}{V_{MCyDE}}$			IO
Rectangular	≥ 1.0	0.004	0.015	$g_{nl}+0.1(d_{nl}-g_{nl})$
	≤ 0.5		0.006	
Flanged	≥ 1.0		0.020	
	≤ 0.5		0.009	

Condition		d'_{nl}	e_{nl}	Acceptance Criteria	
				Performance Objective	
$\frac{N_{UD}}{A_g f'_{cE}}$	$\frac{V_{CWall318E}}{V_{MCyDE}}$			LS	CP
≤ 0.075	≥ 1.0	0.025	0.03		

	≤ 0.5	0.015	0.02	0.65 e_{nl}	0.80 e_{nl}
≥ 0.150	≥ 1.0	0.015	0.015		
	≤ 0.5	0.010	0.010		

Proposed Linear Acceptance Criteria

The *m*-factors are derived from the nonlinear modeling parameters using the expressions given in Table 2-10. This table is similar to the table provided in Chapter 1 for *m*-factors for flexure-controlled walls, except for some rounding up of the coefficient for CP and the use of Parameter g_{nl} instead of θ_{yE}. Using the same method for converting nonlinear modeling parameters across wall classifications ensures consistency between the *m*-factors for flexure- and shear-controlled walls. Using the expressions from Table 2-10 and g_{nl} of 0.004, the values shown in Table 2-11 are obtained.

Table 2-10 Relations for Linear Acceptance Criteria

Component Type	*m*-factors		
	Performance level		
	IO	LS	CP
Primary	$\frac{g_{nl}+0.1(d_{nl}-g_{nl})}{g_{nl}}$	$\frac{3}{4}\ \frac{3}{4}\left(\frac{e_{nl}}{g_{nl}}\right)$	$\frac{3}{4}\ \frac{17}{20}\left(\frac{e_{nl}}{g_{nl}}\right)$
Secondary		$\frac{3}{4}\left(\frac{e_{nl}}{g_{nl}}\right)$	$\frac{17}{20}\left(\frac{e_{nl}}{g_{nl}}\right)$

Table 2-11 Proposed *m*-Factors for Shear-Controlled Walls (Linear Acceptance Criteria)

Conditions		*m*-factors				
		Performance Level				
			Primary		Secondary	
$\frac{N_{UD}}{A_g f'_{cE}}$	$\frac{V_{CWall318E}}{V_{MCyDE}}$	IO	LS	CP	LS	CP
≤ 0.075	≥ 1.0	1.3	4.2	4.8	5.6	6.4
	≤ 0.5	1.1	2.8	3.2	3.8	4.3
≥ 0.150 < 0.300	≥ 1.0	1.3	2.1	2.4	2.8	3.2
	≤ 0.5	1.1	1.4	1.6	1.9	2.1

2.3.4 Comparison Between ACI 369.1-17 and Proposed Modeling Parameters and Acceptance Criteria

The modeling parameters and acceptance criteria for shear-controlled walls in the change proposal are compared with the existing values from ACI 369.1-17, which are shown in Table 2-12. It should be noted that modeling parameters and acceptance criteria in ACI 369.1-17 are given as total drifts, whereas the updated values are only for the translational (or shear) component of drifts. Moreover, actions on shear-controlled walls with axial loads larger than 0.15 $A_g f'_{cE}$ are considered force-controlled (see footnote in Table 2-12), whereas, in the proposed provisions, this axial load limit is increased to 0.30 $A_g f'_{cE}$ for force-controlled designation.

Table 2-12 ACI 369.1-17 Modeling Parameters and Acceptance Criteria for Shear-Controlled Walls

Conditions		Total drift ratio (%), or chord rotation, rad*			Strength ratio		Acceptable total drift (%) or chord rotation, rad(1)		
							Performance level		
		d_{nl}	e_{nl}	g_{nl}	c_{nl}	f_{nl}	IO	LS	CP
i: Shear walls and wall segments(2)									
$\frac{(A_s - A'_s) f_{yE} + P}{t_w \ell_w f'_{cE}} \le 0.05$		1.0	2.0	0.4	0.20	0.6	0.40	1.5	2.0
$\frac{(A_s - A'_s) f_{yE} + P}{t_w \ell_w f'_{cE}} > 0.05$		0.75	1.0	0.4	0.0	0.6	0.40	0.75	1.0
ii: Shear wall coupling beams(3)									
Longitudinal reinforcement and transverse reinforcement(4)	$\frac{V}{t_w \ell_w \sqrt{f'_{cE}}}$								
Conventional longitudinal reinforcement with conforming transverse reinforcement	≤3	0.02	0.030		0.60		0.006	0.020	0.030
	≥6	0.016	0.024		0.30		0.005	0.016	0.024
Conventional longitudinal reinforcement with nonconforming transverse reinforcement	≤3	0.012	0.025		0.40		0.006	0.010	0.020
	≥6	0.008	0.014		0.20		0.004	0.007	0.012

(1) For shear walls and wall segments, use drift; for coupling beams, use chord rotation.
(2) For shear walls and wall segments where inelastic behavior is governed by shear, the axial load on the member must be less than or equal to $0.15 A_g f_c'$; otherwise, the member must be treated as a force-controlled component.
(3) For coupling beams spanning less than 8 ft 0 in., with bottom reinforcement continuous into the supporting walls, acceptance criteria values shall be permitted to be doubled for LS and CP performance.
(4) Conventional longitudinal reinforcement consists of top and bottom steel parallel to the longitudinal axis of the coupling beam. Conforming transverse reinforcement consists of: (a) closed stirrups over the entire length of the coupling beam

at a spacing less than or equal to $d/3$; and (b) strength of closed stirrups $V_s \geq 3/4$ of required shear strength of the coupling beam.

2.3.4.1 NONLINEAR MODELING PARAMETERS AND ACCEPTANCE CRITERIA

As shown in Table 2-12, existing values of Parameters d_{nl} and e_{nl} range from 0.75% to 1.0% and 1.0% to 2.0%, respectively. Figure 2-24 compares the proposed and existing values of Parameters d_{nl} and e_{nl}. Figure 2-24a shows that the proposed values for Parameter d_{nl} are smaller for rectangular walls with $V_{CWall318E}/V_{MCyDE} < 0.5$ by 20 to 40%, and proposed Parameter d_{nl} values could be either smaller (10%) or larger (20%) for barbell/flanged walls with $V_{CWall318E}/V_{MCyDE} < 0.5$. However, proposed values of Parameter d_{nl} are significantly larger for walls with $V_{CWall318E}/V_{MCyDE} \geq 1.0$ (by a factor of 1.5 to 2.67). Figure 2-24b indicates that the proposed values for Parameter e_{nl} are either the same or higher than existing values for walls with $V_{CWall318E}/V_{MCyDE} < 0.5$, and that proposed values are larger by a factor of about 1.5 for walls with $V_{CWall318E}/V_{MCyDE} \geq 1.0$.

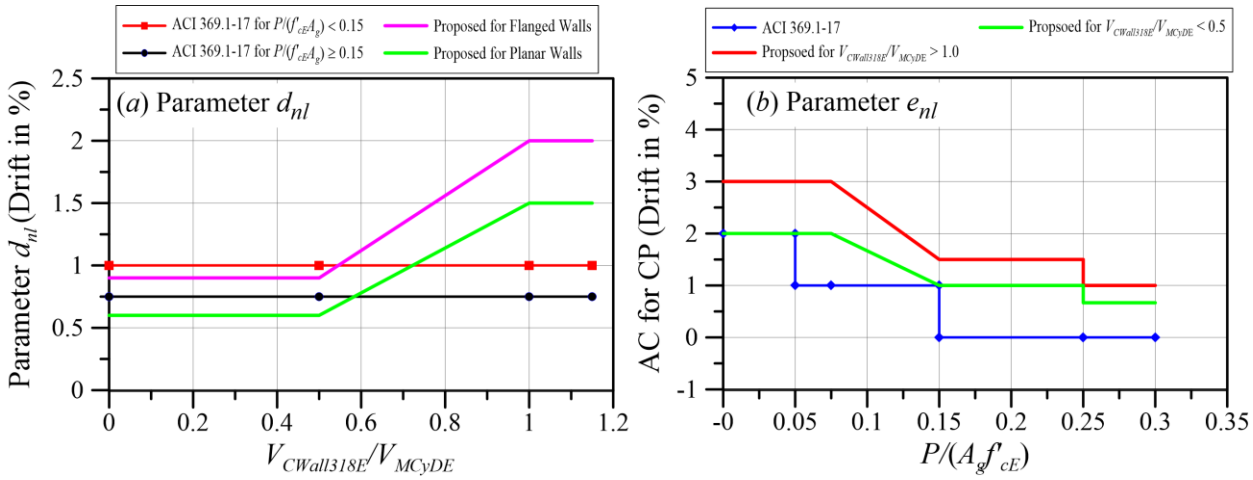

Figure 2-24 Comparison between existing and proposed values for Modeling Parameter d_{nl} and e_{nl}.

Figure 2-25 through Figure 2-27 compare the proposed and existing nonlinear acceptance criteria. For Immediate Occupancy (IO), the proposed values are always greater than existing values, especially for walls with $V_{CWall318E}/V_{MCyDE} > 0.50$. Similarly, for Life Safety (LS) and Collapse Prevention (CP), the proposed values are almost always larger than the existing values, especially for walls with $V_{CWall318E}/V_{MCyDE} > 0.50$.

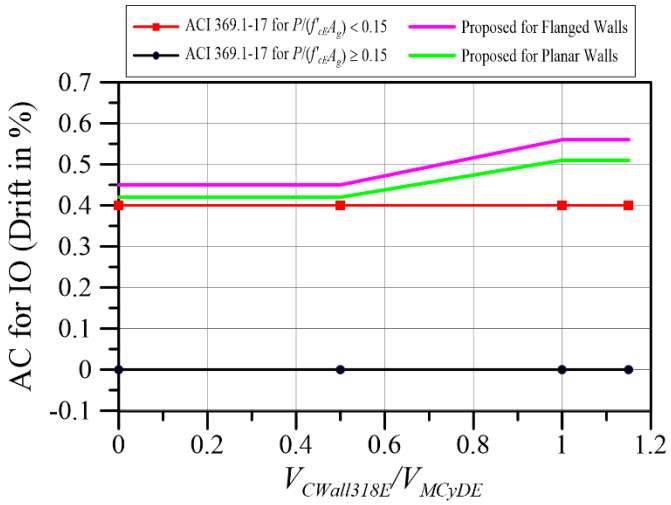

Figure 2-25 Comparison of nonlinear acceptance criteria for Immediate Occupancy (IO)

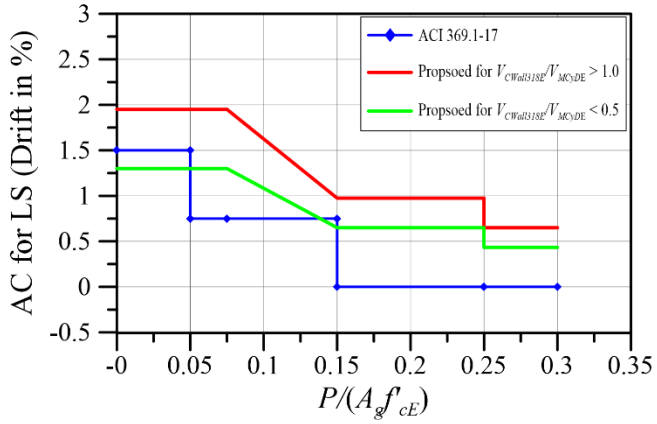

Figure 2-26 Comparison of nonlinear acceptance criteria for Life Safety (LS).

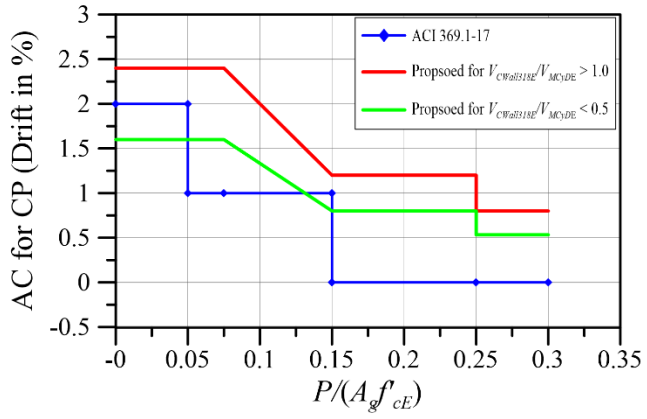

Figure 2-27 Comparison of nonlinear acceptance criteria for Collapse Prevention (CP).

2.3.4.2 LINEAR ACCEPTANCE CRITERIA (m-factors)

Figure 2-28 through Figure 2-30 compare the proposed and existing m-factors for linear procedures. For LS, the proposed *m*-factors are greater than the *m*-factors in ACI 369.1-17 for the most part, especially for primary components. For CP, most proposed *m*-factors are greater than the existing *m*-factors for primary components. For secondary components, the proposed *m*-factors are either higher or lower depending on the values of $P/A_g f'_{cE}$ and $V_{CWall318E}/V_{MCyDE}$.

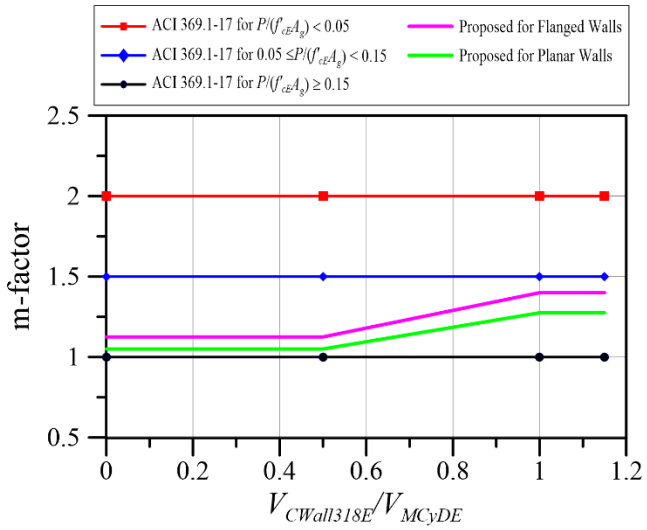

Figure 2-28 Comparison of linear acceptance criteria for Immediate Occupancy (IO).

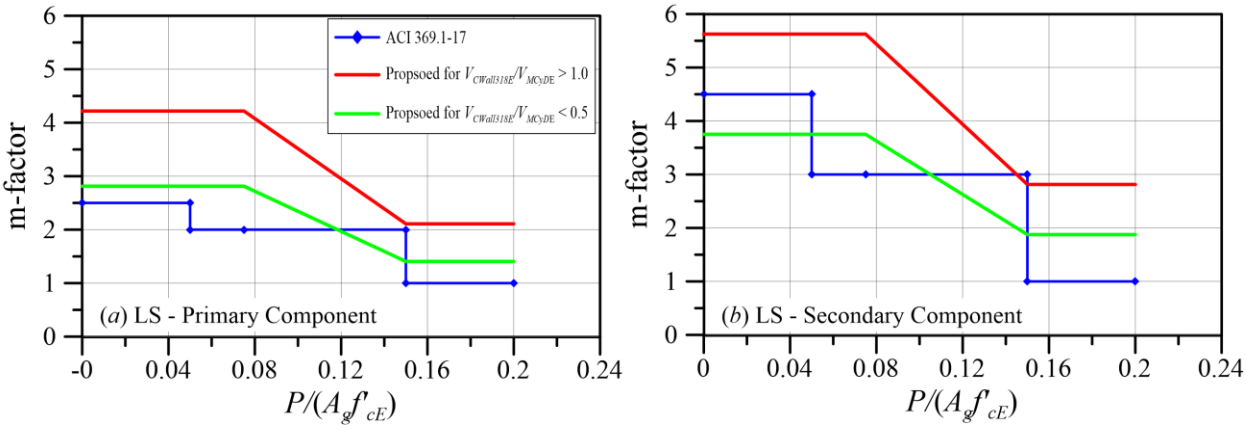

Figure 2-29 Comparison of linear acceptance criteria for Life Safety (LS).

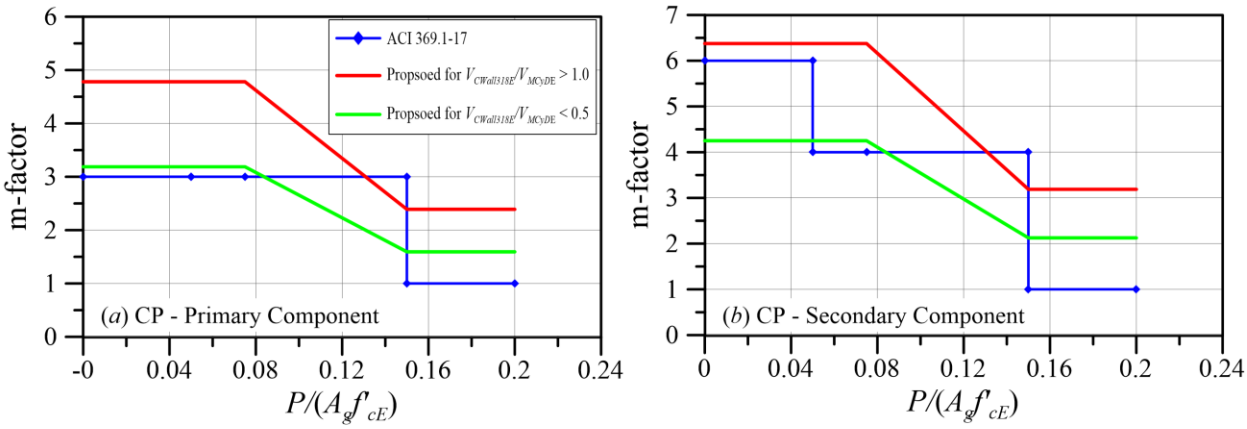

Figure 2-30 Comparison of linear acceptance criteria for Collapse Prevention (CP).

2.3.5 Conclusions

A change proposal was developed to modify ACI 369.1-17 with updated modeling parameters and acceptance criteria for shear-controlled structural walls. A dataset of more than 300 shear-controlled concrete wall tests was filtered from an extensive database of 1,100 wall tests reported in the literature. A modified backbone relation, which includes a post-yield hardening slope and a deformation-based modeling parameter at the initiation of residual strength is proposed. The dataset was studied to identify parameters that correlate with each modeling parameter on the backbone curve. An updated set of modeling parameters and strength relations are proposed. The proposed modeling parameters represent roughly median values of experimental data, with reported dispersions for each backbone point. New shear strength relations are proposed that account for moment demand on shear strength. The proposed relations produce larger shear strengths than existing relations at low moment demands (up to 80% larger) and slightly lower strengths at large moment demands (up to 20% smaller). Generally, deformation capacities increase in the change proposal over existing values, especially for walls with shear strength approaching shear demand at flexural yielding (flexure-shear walls).

2.4 Recommended Changes

Note about Change Proposals

This chapter documents aspects of change proposals as they were submitted to ACI's *Seismic Repair and Rehabilitation* Code Committee 369 for possible adoption. Often, these change proposals were revised, in some cases substantively, by this committee before they were adopted into ACI 369.1-22. Readers should not rely on this chapter for information about the final version of provisions in ACI 369.1-22.

Re-numbering in ACI 369.1

ACI 369.1-17 underwent significant changes during the code cycle leading to the next edition. In the process, figure and table numbers were modified to follow the number of the section that contains them. This change proposal follows the new figure and table numbering, whereas the change proposal presented in Chapter 1 of Part 4 followed the numbering in ACI 369.1-17.

2.4.1 Stiffness Provisions

The change proposal for shear-controlled walls was developed after the one for flexure-controlled walls presented in Chapter 1 of Part 4. This change proposal, where new or modified text is shown in blue, further modifies the shear rigidities for walls for nonlinear procedures, as follows:

- Uncracked shear stiffness is taken as $0.3E_{cE}A_w$, regardless of axial load.
- The cracked effective shear stiffness at yielding is captured through modeling parameter g_{nl}, which is given in Table 7.4.1.1.2 that provides the nonlinear modeling parameters for shear-controlled walls.

Table 3.1.2.2.4 —Effective stiffness values for nonlinear analysis[1]

Component	Flexural rigidity	Shear rigidity	Axial rigidity
Beams—nonprestressed[2]	$0.2E_{cE}I_g$	$0.4E_{cE}A_w$	$1.0E_{cE}A_g$
Beams—prestressed[2]	$1.0E_{cE}I_g$	$0.4E_{cE}A_w$	$1.0E_{cE}A_g$
Columns with compression caused by design gravity loads ≥ $0.5A_gf_c'$[3]	$0.7E_{cE}I_g$	$0.4E_{cE}A_w$	$1.0E_{cE}A_g$
Columns with compression caused by design gravity loads ≤ $0.1A_gf_c'$ or with tension[3]	$0.2E_{cE}I_g$	$0.4E_{cE}A_w$	$1.0E_{cE}A_g$ (compression) $1.0E_sA_s$ (tension)
Diaphragms (in-plane) — nonprestressed[4]	$0.25E_{cE}I_g$	$0.25E_{cE}A_g$	$0.25E_{cE}A_g$
Diaphragms (in-plane) — prestressed[4]	$0.5E_{cE}I_g$	$0.4E_{cE}A_g$	$0.5E_{cE}A_g$
Walls-uncracked with compression caused by design gravity loads ≥ $0.3A_gf_{cE}'$[3,5]	$1.0E_{cE}I_g$	$0.3E_{cE}A_w$	$1.0E_{cE}A_g$
Walls-uncracked with compression caused by design gravity loads ≤ $0.05A_gf_{cE}'$ or with tension[3,5]	$0.5E_{cE}I_g$	$0.3E_{cE}A_w$	$1.0E_{cE}A_g$

Walls—cracked[5,6]	$0.25E_{cE}I_g$	$0.15E_{cE}A_w$ for flexure-controlled; See Table 7.4.1.1.2 for shear-controlled	$1.0E_{cE}A_g$ (compression) $1.0E_sA_s$ (tension)
Coupling beams with longitudinal or diagonal reinforcement	$0.05\ (l_n/h)\ E_{cE}I_g \le 0.20\ E_{cE}I_g$	$0.2E_{cE}A_w$	$1.0E_{cE}A_g$

[1] Tabulated values for axial, flexural, and shear shall be applied jointly in defining effective stiffness of an element, unless alternative combinations are justified. For other elements not covered in this table, it shall be permitted to use values in Table 3.1.2.1.

[2] For T-beams, I_g can be taken as twice the value of I_g of the web alone. Otherwise, I_g shall be based on the effective width as defined in 3.1.3.

[3] For columns and walls with axial compression falling between the limits provided, flexural rigidity shall be determined by linear interpolation. If interpolation is not performed, the more conservative effective stiffnesses shall be used. An imposed axial load N_{UG} is permitted to be used for stiffness evaluations.

[4] In-plane diaphragm effective stiffness values apply where diaphragm flexibility is considered in accordance with 10.2.2

[5] Walls are permitted to be considered cracked due to earthquake demands in flexural actions where flexural demands exceed M_{crE} and/or in shear actions where shear force demands exceed the cracking shear strength defined in 7.2.2 . It shall be permitted to assume all walls to be cracked.

[6] Alternative stiffness values dependent on axial load and boundary longitudinal reinforcement ratio shall be permitted in accordance with 7.3.

2.4.2 Strength Provisions

For strength of shear-controlled walls, the following changes are proposed:

- Cracking shear strength is provided that is based on the cross-section shape of a wall and taken as a multiple of the concrete contribution to shear strength from ACI 318-19.
- Two equations for shear yield strength are proposed: one detailed equation and a simplified lower-bound equation.
- Peak shear strength is estimated using a hardening factor of 1.1 applied to the yield strength.

7.2.2 Shear Strength – The cracking shear strength of a structural wall or wall segment, $V_{CcrWall}$, corresponding to Point F in Fig. 3.1.2.2.3(c) shall be evaluated using Eq. 7.2.2(a) or (b).

$$V_{CcrWall} = \alpha_c \lambda \sqrt{f'_c} A_{cv} \text{ for rectangular sections} \qquad \text{Eq. 7.2.2(a)}$$

$$V_{CcrWall} = 2\alpha_c \lambda \sqrt{f'_c} A_{cv} \text{ for flanged sections} \qquad \text{Eq. 7.2.2(b)}$$

Where:

$$\alpha_c = 3 \text{ for } h_w/l_w \le 1.5$$

$$\alpha_c = 2 \text{ for } h_w/l_w \ge 2.0$$

α_c varies linearly between 3 and 2 for $1.5 < h_w/l_w < 2.0$

Linear interpolation between Eq. 7.2.2 (a) and (b) based on I_{g_flange}/I_{g_rect} shall be permitted for the cracking shear strength of walls and wall segments with $1.0 < I_{g\_flange}/I_{g\_rect} < 1.5$.

The shear strength of a structural wall or wall segment, $V_{CydWall}$, corresponding to Point B in Fig. 3.1.2.2.3(c) shall be determined using Eq. 7.2.2(c).

$$V_{CydWall} = \left(2.0\text{-}1.10\frac{V_{CWall318E}}{V_{MCyDE}}\right)V_{CWall318} \quad \le 1.8\,V_{CWall318} \quad \ge 0.8\,V_{CWall318} \qquad \text{Eq. 7.2.2(c)}$$

Where

$$V_{CWall318} = \left(\alpha_c \lambda \sqrt{f'_{cE}} + \rho_t f_{ytE}\right)A_{cv} \qquad \text{Eq. 7.2.2(d)}$$

Alternatively, it shall be permitted to evaluate $V_{CydWall}$ using Eq. 7.2.2(e).

$$V_{CydWall} = 0.8\,V_{CWall318} \qquad \text{Eq. 7.2.2(e)}$$

$V_{CydWall}$ shall be multiplied by 0.85 where ρ_t is less than 0.0015.

2.4.3 Modeling Parameters and Acceptance Criteria

The following changes are proposed:

- Updated *m*-factors for linear procedures
- Updated modeling parameters and acceptance criteria for nonlinear procedures.

Table 7.3.2c—Numerical acceptance criteria for linear procedures: reinforced concrete structural walls and associated components controlled by shear

Conditions		m-factors[a]				
		Performance Level				
			Primary		Secondary	
$\frac{N_{UD}}{A_g f'_{cE}}$	$\frac{V_{CWall318E}}{V_{MCyDE}}$	IO	LS	CP	LS	CP
≤ 0.075	≥ 1.0	1.3	4.2	4.8	5.6	6.4
	≤ 0.5	1.1	2.8	3.2	3.8	4.3
≥ 0.150	≥ 1.0	1.3	2.1	2.4	2.8	3.2
	≤ 0.5	1.1	1.4	1.6	1.9	2.1

[a] Linear interpolation between values listed in the table shall be permitted.

Table 7.4.1.1.2 —Proposed modeling parameters and numerical acceptance criteria for nonlinear procedures: reinforced concrete structural walls and associated components controlled by shear[a]

Condition		γ_{nl}	δ_{nl}[c]	Acceptance Criteria
Cross-section shape[b]	$\frac{V_{CWall318E}}{V_{MCyDE}}$			IO
Rectangular	≥ 1.0	0.004	0.015	$\gamma_{nl}+0.1(\delta_{nl}-\gamma_{nl})$
	≤ 0.5		0.006	
Flanged	≥ 1.0		0.020	
	≤ 0.5		0.009	

Condition		δ'_{nl}[d]	ε_{nl}[d]	Acceptance Criteria	
$\frac{N_{UD}}{A_g f'_{cE}}$	$\frac{V_{CWall318E}}{V_{MCyDE}}$			LS	CP
≤ 0.075	≥ 1.0	0.025	0.03	0.65 ε_{nl}	0.80 ε_{nl}
	≤ 0.5	0.015	0.02		
≥ 0.150 < 0.30	≥ 1.0	0.015	0.015		
	≤ 0.5	0.010	0.010		

Condition		γ_{nl}[e]	γ'_{nl}
Cross-section shape[b]	$\frac{N_{UD}}{A_g f'_{cE}}$		
Rectangular	≤ 0.10	0.25	1.10
	≥ 0.15	0.00	
Flanged	≤ 0.15	0.40	
	≥ 0.20 < 0.30	0.00	

[a] Linear interpolation between values listed in the table shall be permitted.

[b] Linear interpolation between values listed in the table based on $I_{g\ flange}/I_{g\ rect}$ shall be permitted for walls and wall segments between wall and flanged designations with $1.0 < I_{g\ flange}/I_{g\ rect} < 1.5$

[c] For non-symmetric flanged sections, modeling parameters and acceptance criteria shall be taken from flanged values when the flanged side is compressed due to moment and shear actions and from rectangular values when the rectangular end is compressed.

[d] δ_{nl} shall be taken as 0.005 when $N_{UD}/(A_g f'_{cE}) \geq 0.20$ and $V_{CWall318E}/V_{MCyDE} \geq 0.8$ or when ρ_t and ρ_l are less than 0.0015 and $V_{CWall318E}/V_{MCyDE} \leq 0.5$

[e] δ'_{nl} and ε_{nl} shall not be taken less than δ_{nl}

[f] γ_{nl} shall be taken as zero where ρ_t is less than 0.0015.

2.5 Shear-Controlled Walls Example

This section presents an analysis and evaluation example of a shear-controlled reinforced concrete wall building. The example uses a modified version of an existing building that was seismically

evaluated and retrofitted following the linear dynamic (LDP) and nonlinear static procedure (NSP) provisions of ASCE/SEI 41-17.

The example summarizes the building structure configuration, seismic loading, wall classification, and mathematical modeling and analysis using computer software Perform3D. The example presents calculation reports and evaluation results for an example wall using the proposed modeling parameters (MP's) and acceptance criteria (AC) and compares them to evaluation outcomes using the ASCE/SEI 41-17 provisions. The governing failure mode for the controlling walls in the example building (i.e., wall classification) is shear for the various load combinations examined. It is noted that varying wall classifications would be identified in the case the more complex proposed shear strength provisions are considered in combination with shear friction updates and varying load combinations, however the shear-controlled classification case is the focus of this example.

2.5.1 Overview of Building

The building was a seven-story, reinforced concrete (RC) structure designed in accordance with the 1964 Uniform Building Code and constructed in 1967. The lateral force resisting system consists of concrete wall piers and coupling beams located primarily at the perimeter of the building. The gravity system is a combination of the concrete bearing walls at the perimeter of the building, and a line of concrete columns at the center of the building. A plan view is included for a typical floor level in Figure 2-31 below.

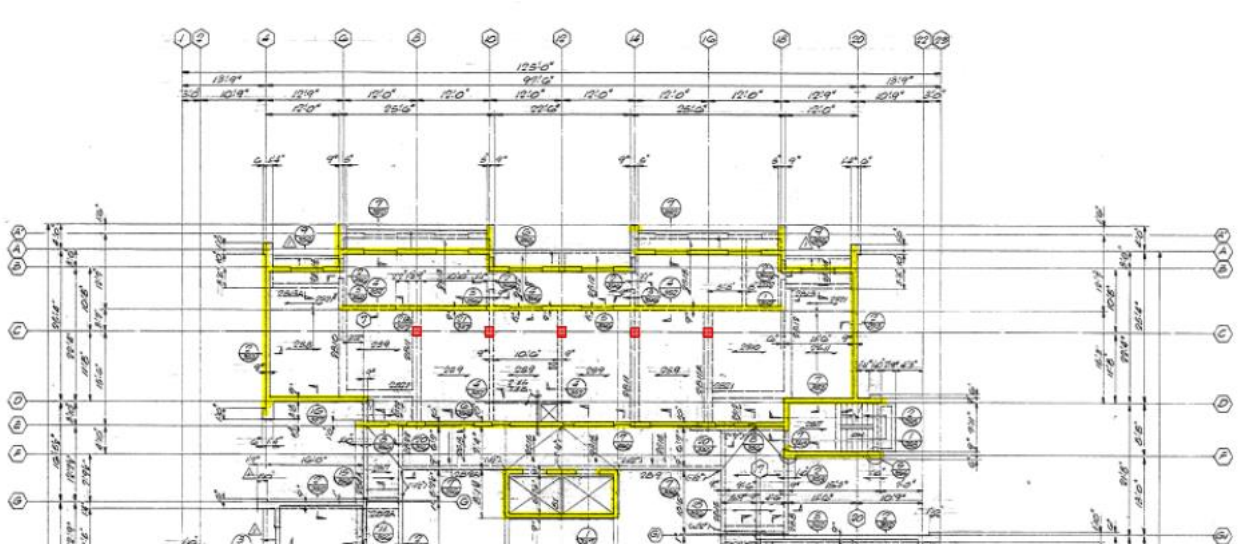

Figure 2-31 Perimeter concrete bearing walls and interior concrete column lines (excerpt from the original construction documents). The red squares are the columns while the yellow shaded areas are the shear walls.

The concrete wall piers and columns are founded on pile-caps with cast-in-place concrete piles. The dowels of the wall piers and columns, as well as the longitudinal reinforcements of the piles, extend into the pile caps. The piles are detailed with heavy transverse reinforcement over their bending length,

which is expected to provide ductility when the piles are subject to lateral earthquake induced deformations (see Figure 2-32).

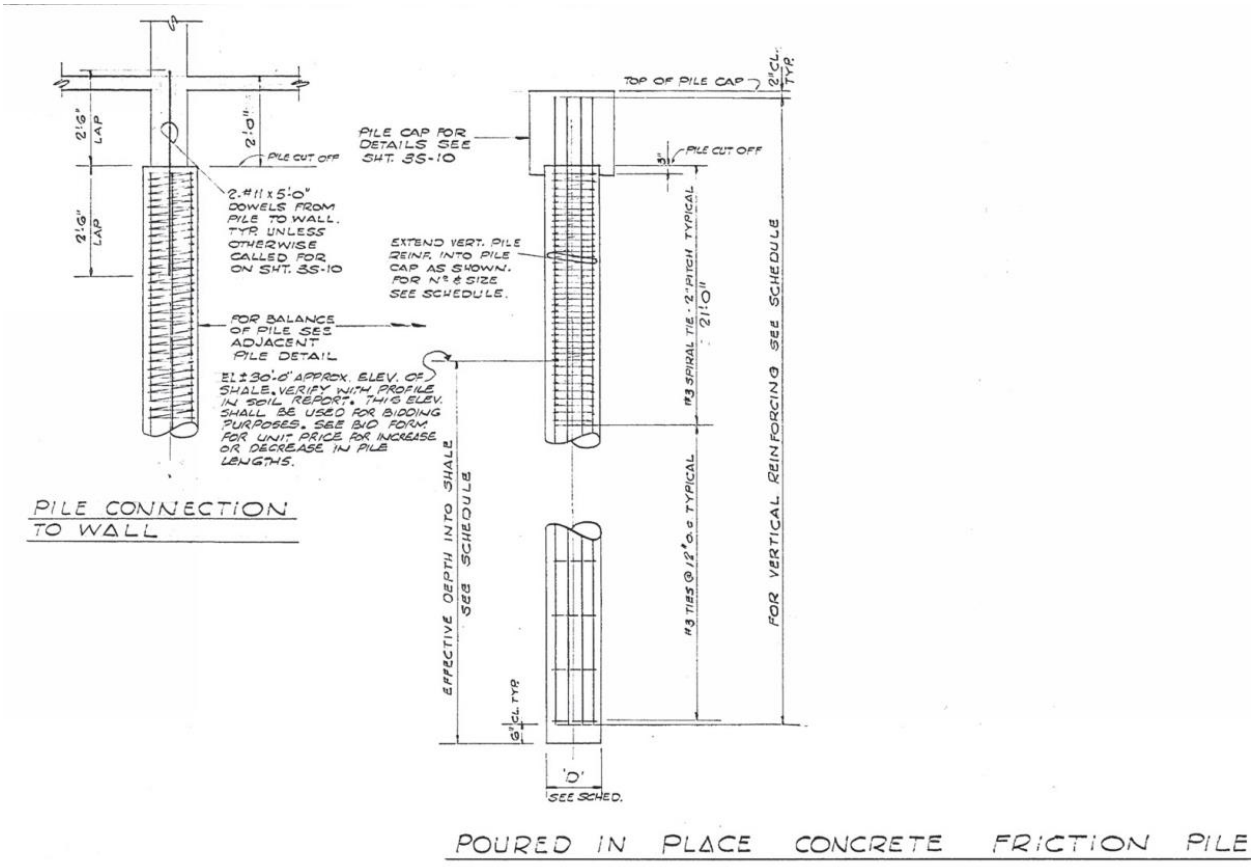

Figure 2-32 Existing pile reinforcement (excerpt from the original construction documents).

2.5.1.1 WALL CONFIGURATION

Sample calculations utilize the end wall on the south side of the building to illustrate critical steps in the analysis process (grid line 4 in plan, Figure 2-33 below). The wall is 9 inches thick and has two #4 bars spaced at 18 inches on center each way (horizontally and vertically). The plan view is provided in Figure 2-33 below in which the highlighted region outlines the effective flange of the return wall in the east direction. On the north side, there is no substantive return wall at the base level but rather coupling beams above.

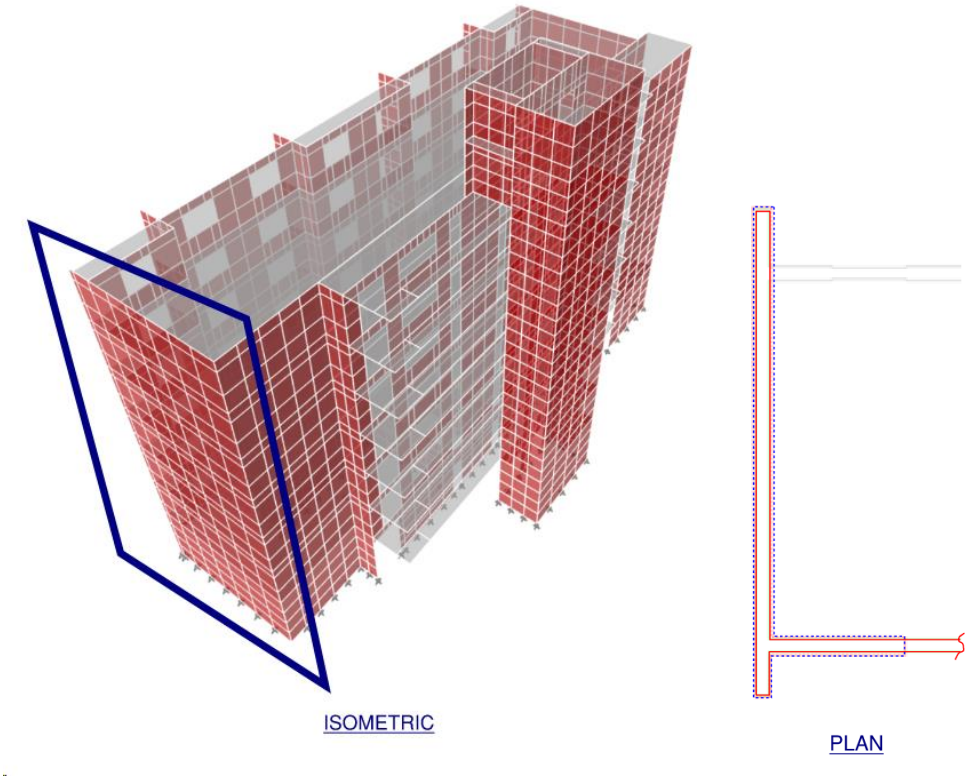

Figure 2-33 End wall under consideration.

2.5.1.2 MATERIALS

The reported concrete strength and reinforcement strength from the as-built structural drawings were 3,000 psi and 40,000 psi, respectively. The ASCE/SEI 41-17 conversion factors for lower-bound to expected material properties were employed resulting in expected concrete strength of 4,500 psi and reinforcement strength of 50,000 psi. Limited "usual" material testing and condition assessment programs were carried out for a knowledge factor of 1.0.

2.5.1.3 EARTHQUAKE LOADING

The building is located in a high seismic region in California. The soil was classified as Site Class C based on geotechnical engineering reports for the site. The existing building hazards were used for seismic evaluation relative to BPOE performance. The acceleration response spectra are reported below in Figure 2-34.

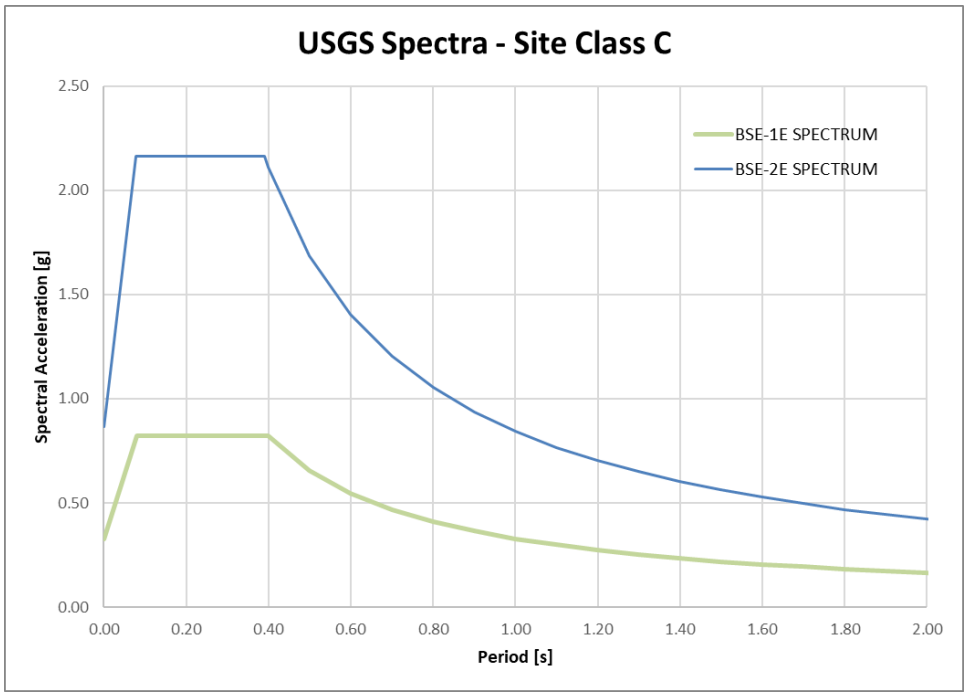

Figure 2-34 Acceleration response spectra.

2.5.1.4 STRENGTH AND STIFFNESS

The stiffness contributions of walls were captured by the three-dimensional wall shell elements and cracked concrete stiffness properties. The updated stiffness provisions allow for 0.25 times the gross moment of inertia for flexural response and 0.15 times the shear area for shear response. The effects of return wall flanges are captured explicitly in the linear analysis model.

Calculations for flexural strength consider the effective flange width and the relevant amount of tension steel to be considered in the wall cross-section. The effective flange is defined in Section 3.1.3 for walls, referring to ACI 318 Chapter 18, as 25 percent of the wall height relative to the section of wall being evaluated, but not to exceed half the distance to the next adjacent wall web. At the base of the wall section for the case study Grid Line 4 wall, the total height is 63 feet. At the south end, because the next adjacent web is 16 feet away, half that distance, 8 feet, governs the effective flange toward the south side of the building. Although there is wall at stories above the base on the north side of the flange, those walls do not continue to the base, so the north side of the wall has no return wall to serve as an effective flange.

In order to calculate wall moment capacity, axial demands must be considered for *P-M* interaction: the unfactored earthquake demands are factored by *Cm*, *C1*, and *C2* and then either divided by the J-factor in compression or the m-factor in tension (an iterative process for m), and the gravity demands must be factored for maximum compression and minimum compression gravity load combinations using ASCE 41-17 Section 7.2.2. The factored axial demands are used to identify where on the *P-M* interaction curve the wall flexure capacity should be based. Because axial compression is considered a force-controlled action, a J-factor is used to divide the earthquake axial compression component,

and an *m*-trial of 2 was used for axial tension. The *m*-trial of 2 for tension is expected to be a conservative lower-bound to estimate flexural strength for the tension condition, and the trial m-factor is iteratively updated based on the m-factor for flexure response. It is noted that neutral axis depths also must be tracked and incorporated dependent on loading for flexure-controlled wall acceptance criteria.

Because loading direction is not retained when using SRSS in response spectrum analysis, a Linear Dynamic Procedure (LDP) using response spectra is not possible when the simplifications for effective flange are not employed, and a Linear Static Procedure (LSP) must be used to retain demands depending on loading direction. The following unfactored demands (Table 2-13) are reported at the base of the wall from ETABS using the LSP and assuming only the north-south loading direction, with plus and minus 5% floor diaphragm mass plan eccentricity of loading, for brevity. Technically, because the effective flange causes the wall to be loaded in both directions, 100% loading in the north-south direction plus 30% loading in the east-west direction is required, the LSP analysis results in four unfactored sets of demands to evaluate, given there are also two hazards to consider, two gravity load combinations, and two accidental eccentricity cases to consider, the rigorous flange-considered approach would result in 32 separate load combinations to evaluate. The added simplifications in the proposal, which consider the worst-case effects of the return wall flanges allow for the user to base the shear strength on the rectangular wall section and the largest wall moment capacity (when south flange is in tension for this case), which greatly simplify the loading cases to be kept track of and allow for the LDP to be used. The associated flexural strengths are reported for the various axial loads using a concrete cross-sectional analysis software, e.g., spCol, in Table 2-14 below.

Table 2-13 Unfactored Demands

Demand	Loading Type		
	LSP 100% +ecc	LSP 100% -ecc	LDP (+/-ecc)
BSE-2E Shear (kips)	664	1140	1030
BSE-2E Moment (kip-ft)	31,600	38,200	37,200
BSE-2E Axial (kip)	976	1160	1170
Gravity Dead (kip)	477		
Gravity Live (kip)	168		

Table 2-14 Wall Moment Strength

Yield Moment Strength (kip-ft)	Loading Type		
	LSP 100% +ecc	LSP 100% -ecc	LDP (+/-ecc)
Maximum Compression (flange in tension)	41,100	42,400	42,600
Maximum Compression (flange in compression)	32,800	33,700	33,800
Minimum Compression (flange in tension)	22,400	20,700	20,600
Minimum Compression (flange in compression)	20,200	19,100	19,000

Although the proposed definition for cracking strength is sensitive to the moment of inertia of the flanged wall, cracked strength is only required in the nonlinear procedures. It is noted that for this wall, the ratio between I_{g_flange} and I_{g_rect} is 1.4, thus it would be permitted to linearly interpolate between Equations 7.2.2(a) and 7.2.2(b) for cracking shear strength.

The shear strength, calculated in accordance with Equation 7.2.2(c), is dependent on the ratio between the ACI 318 shear strength [Eq. 7.2.2(d)] and the shear associated with flexural yielding, multiplied by ω_v from Equation 7.3.2a. Given the building is seven stories, ω_v = 1.53. The shear demand associated with flexural yielding can be taken as the ratio between flexural strengths and flexural demands listed in *Table 2* and *Table 1*, multiplied by the shear demands in *Table 1*. It is noted that the ACI 318 shear strength of the wall is equal to 811 kip, and the simplified expression proposed for shear strength of 0.8 times $V_{CWall318}$ results in 649 kips. The resulting shear strengths in accordance with Equation 7.2.2(c) are reported in Table 2-15 below.

Table 2-15 Shear Strengths

Shear Strength (kip-ft)	Loading Type		
	LSP 100% +ecc	LSP 100% -ecc	LDP (+/-ecc)
Maximum Compression (flange in tension)	1075	1249	1222
Maximum Compression (flange in compression)	936	1152	1117
Minimum Compression (flange in tension)	649	857	793
Minimum Compression (flange in compression)	649	792	723

Although this example is focused on the traditional shear provisions, for completeness, shear friction strength is calculated using, μ=0.6, the axial loads reported above based on the relevant loading condition, and the vertical reinforcement ratio. The strength from Equation 7.2.4 is then amplified based on the ratio between the shear friction strength and the shear demand associated with flexural yielding, per Equation 7.2.3. The resulting wall strength for the base condition is 1116 kips. This example focuses on the shear-controlled conditions and refers the user to the shear friction example for the proposed shear friction provisions, however, it is noted that the shear friction strengths would also have to be compared in the classification section below when carrying out the full updated provisions.

2.5.1.5 CLASSIFICATION

The Shear Strength Ratios, i.e., relative shear demands associated with flexural yielding to shear capacity ratios, are provided in Table 2-16 below. All Shear Strength Ratios are less than 1.15 and thus classified as shear-controlled.

Table 2-16 Shear Strength Ratio ($V_{CE}/\omega_v V_{MCultE}$)

Shear Strength Ratio (kip-ft)	Loading Type		
	LSP 100% +ecc	LSP 100% -ecc	LDP (+/-ecc)
Maximum Compression (flange in tension)	0.81	0.65	0.68
Maximum Compression (flange in compression)	0.89	0.75	0.78
Minimum Compression (flange in tension)	0.90	0.91	0.91
Minimum Compression (flange in compression)	1.00	0.91	0.90

In the previous versions of ACI 369 / ASCE 41-17, the shear strength would have been taken as the ACI 318 equation value of 811 kips, and the Shear Strength Ratios would be mixed as shown in the table below. The updated provisions and more complex shear strength equations are affected similarly by axial load effects and thus result in more consistent trends of shear/flexure classification.

Table 2-17 Shear Strength Ratio ($V_{CE}/\omega_v V_{MCultE}$)

Shear Strength Ratio (kip-ft)	Loading Type		
	LSP 100% +ecc	LSP 100% -ecc	LDP (+/-ecc)
Maximum Compression (flange in tension)	0.75	0.65	0.66
Maximum Compression (flange in compression)	0.87	0.70	0.73
Minimum Compression (flange in tension)	1.25	0.95	1.02
Minimum Compression (flange in compression)	1.25	1.02	1.12

2.5.2 Evaluation Using Linear Dynamic Procedure

2.5.2.1 ANALYSIS MODEL

The ETABS LDP evaluation was performed with an updated model using the proposed modeling and acceptance criteria. All wall and other structural elements were modeled using elastic shell elements. For modeling wall stiffness, cracked wall stiffness was updated with a 0.25 cracked modifier for flexure and using $0.15E_{cE}$ for shear, or effectively a 3/8 modifier on shear modulus in accordance with the updated proposals.

2.5.2.2 ANALYSIS RESULTS

The resulting period increased slightly to 0.27 seconds in the north-south direction and 0.17 seconds in the east-west direction. Despite the modest increase in period, however, the increased flexibility resulted in a noticeable increase in story drifts up the building height, as shown in Figure 2-35 below.

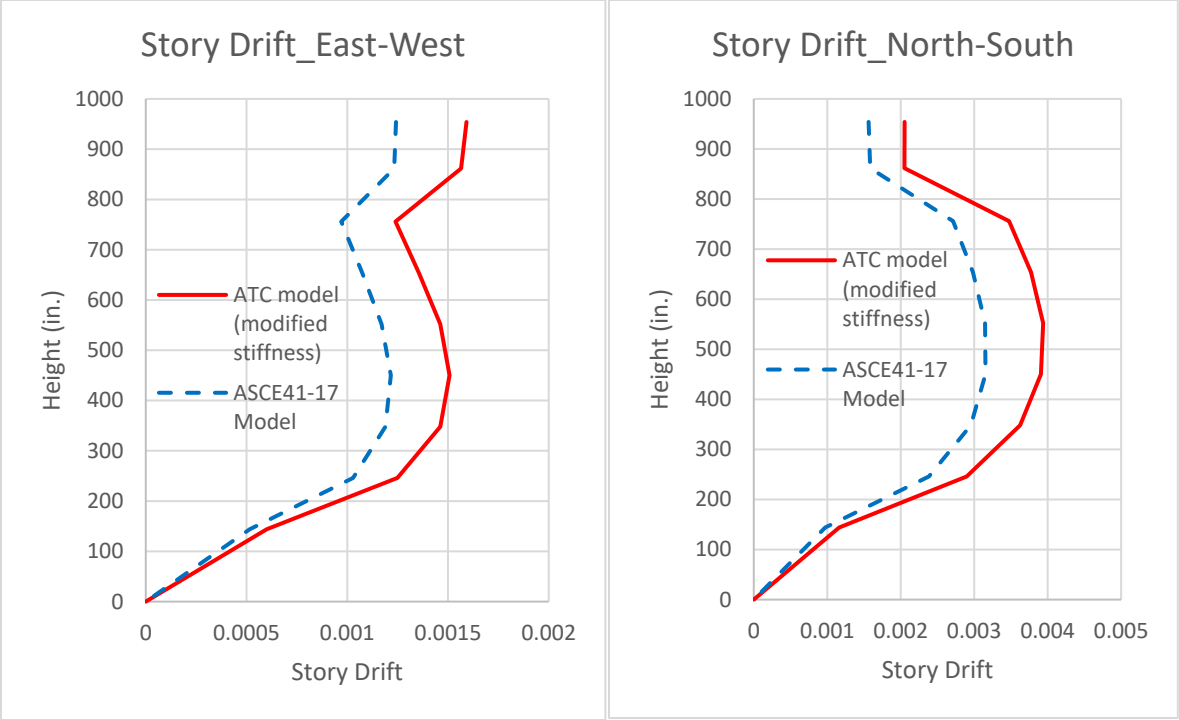

Figure 2-35 LDP building drift comparison.

2.5.2.3 WALL PERFORMANCE ASSESSMENT

The updated provisions for *m*-factors (Table 2-18) rely on ratio of axial load to concrete axial capacity and the ratio of wall shear strength, calculated in accordance with ACI 318, and shear demand associated with flexural yielding.

Table 2-18 Proposed Provision Linear Acceptance Criteria

$\frac{N_{UD}}{A_g f'_{cE}}$	VCwall318E/VMCyDE	e_{nl}	LS	CP
≤ 0.075	≥ 0.80	0.030	4.2	4.8
	≤ 0.5	0.020	2.8	3.2
≥ 0.150	≥ 0.80	0.015	2.1	2.4
	≤ 0.5	0.010	1.4	1.6

The results in Figure 2-36 below are visualized based on the idealized rectangular wall case: the proposed provision *DCR/m* values generally tend to be slightly lower than ASCE/SEI 41-17, but can be larger where shear demand ratios are high, which did not come into play in the past provisions. In

Figure 2-36, green indicates DCR/m less than 1, yellow indicates *DCR/m* between 1 and 1.2, and red indicates *DCR/m* greater than 1.2.

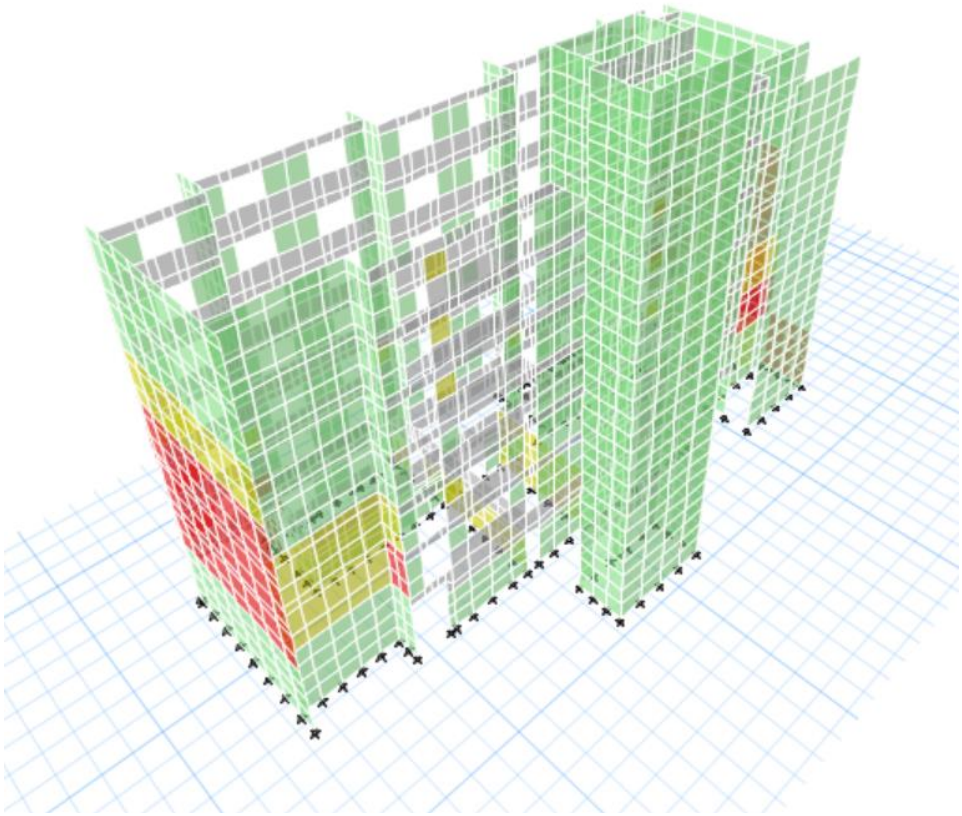

Figure 2-36 Proposed provision LDP BSE-2E shear-only *DCR/m*.

2.5.2.4 DISCUSSION AND CONCLUSIONS

Generally, the resulting *DCR/m* values are not substantially different from the past provisions. A sample of several wall *DCR/m* values are displayed in Table 2-19 for ASCE/SEI 41-17 and proposed-provision linear evaluations, as well as an intermediate DCR using ASCE/SEI 41-17 / ACI 369-17 *m*-factors but proposed stiffness updates to isolate the effects of stiffness updates alone:

Table 2-19 LDP *DCR/m* Comparison

	ASCE 41-17		ASCE 41-17 (Modified Stiffness)		ATC 140	
	BSE-1E	BSE-2E	BSE-1E	BSE-2E	BSE-1E	BSE-2E
	Max Gravity	Max Gravity	Max Gravity	Max Gravity	Max Gravity	Max Gravity
W-S6-10.1-1	0.16	0.27	0.12	0.20	0.12	0.19
W-S6-13.9-1	0.27	0.48	0.12	0.21	0.12	0.19
W-S5-4-1	0.48	1.16	0.49	1.19	0.49	1.15
W-S5-6-1	0.25	0.46	0.24	0.44	0.24	0.43
W-S5-7-1	0.27	0.63	0.35	0.81	0.35	0.77
W-S5-10-1	0.05	0.11	0.04	0.09	0.04	0.08
W-S5-14-1	0.09	0.15	0.04	0.09	0.04	0.09
W-S5-18-1	0.27	0.49	0.25	0.46	0.25	0.44
W-S5-20-1	0.61	1.50	0.56	1.38	0.56	1.32
W-S5-Z2-1	0.14	0.33	0.07	0.17	0.07	0.17
W-S5-Z1-1	0.05	0.09	0.03	0.08	0.03	0.05
W-S5-Z1-2	0.03	0.05	0.02	0.04	0.02	0.04
W-S5-Z1-3	0.05	0.10	0.03	0.07	0.03	0.05
W-S5-F-1	0.03	0.06	0.02	0.04	0.02	0.04
W-S5-E-1	0.54	1.00	0.52	0.97	0.52	0.62
W-S5-E-2	0.65	1.25	0.64	1.21	0.64	0.89
W-S5-E-3	0.54	1.05	0.52	1.02	0.52	0.79
W-S5-E-4	0.16	0.39	0.17	0.41	0.17	0.30
W-S5-E-5	0.18	0.43	0.21	0.50	0.21	0.32
W-S5-E-6	0.47	0.88	0.59	1.15	0.59	0.84
W-S5-E-7	0.30	0.72	0.59	1.13	0.59	0.84

2.5.3 Evaluation Using Nonlinear Static Procedure

2.5.3.1 ANALYSIS MODEL

The Nonlinear Static Procedure was performed using the updated backbones per proposed provisions. Generally, the backbones are similar between the two sets of provisions, however it was found that the cracking strength tends to decrease slightly, and the ultimate shear strength generally increases. An example of the controlling end wall backbone, resulting from component pushover results, is shown in Figure 2-37. It is noted that the controlling wall case is used for the comparison in nonlinear procedures.

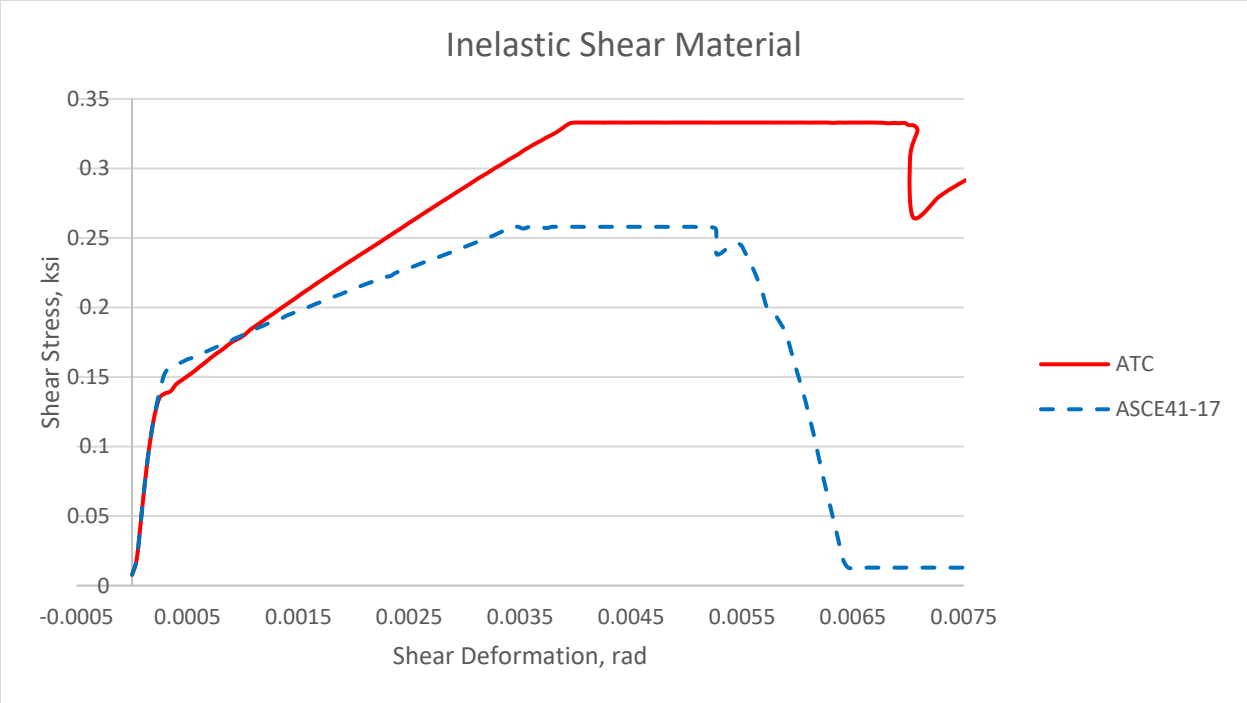

Figure 2-37 Nonlinear shear backbone.

2.5.3.2 ANALYSIS RESULTS

As with the linear procedures, the updated nonlinear provisions allow for taking advantage of the effective flange for shear strength, however this can be time consuming, and simplifications are permitted to only consider the rectangular ACI 318 wall strength and use conservative estimates for the shear demand to shear capacity ratio based on direction of loading. It was again found conservative to idealize as a purely rectangular wall, where the same end wall resulted in a CP limit of 1.7% for the rectangular case versus 2.6% for the flanged wall case. It is noted that this case study wall has symmetric flanges, and this may not be the case when a flange only occurs on one end.

The pushover results for the updated model are shown in Figure 2-38 for the positive and negative loading directions.

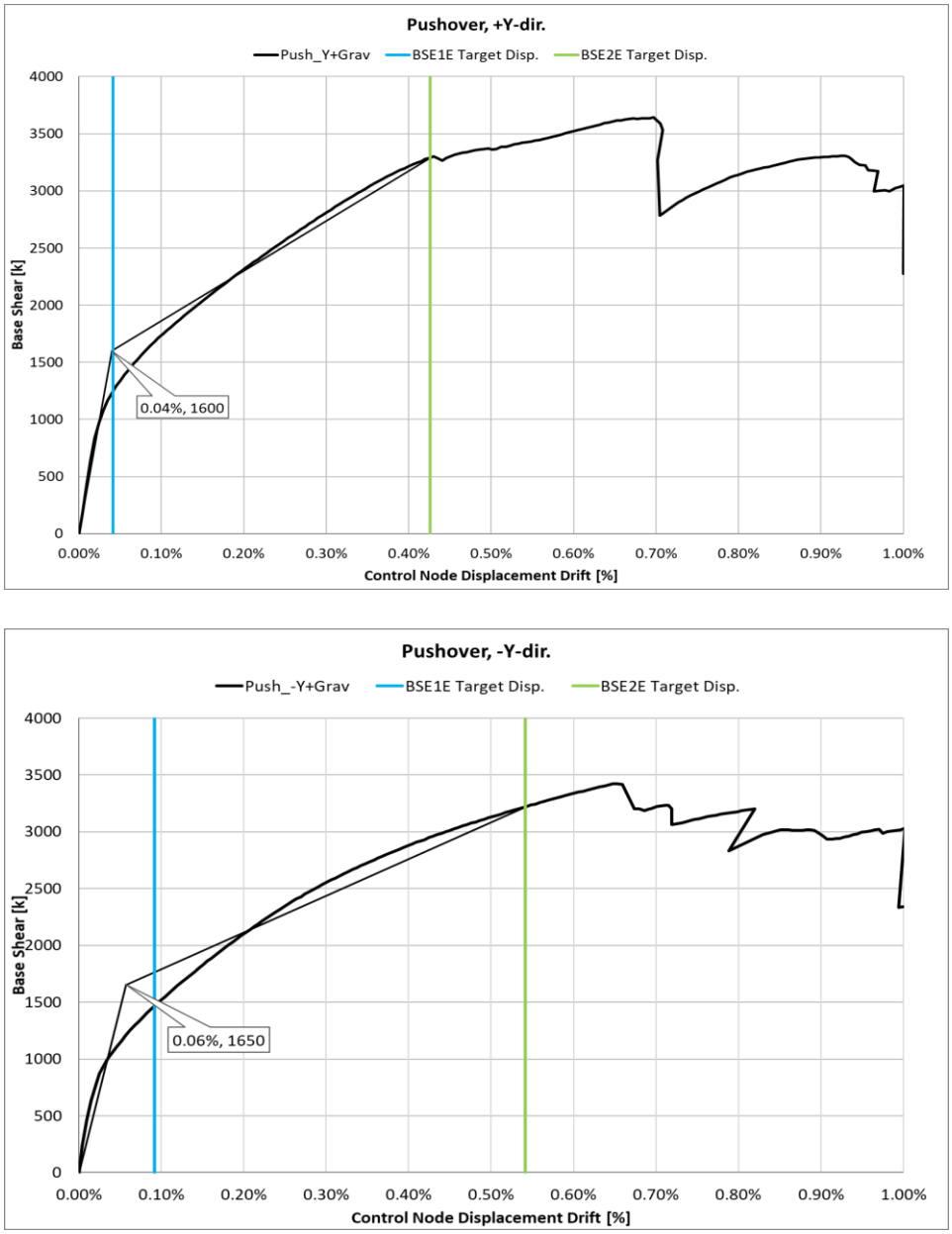

Figure 2-38 Proposed provision pushover results.

2.5.3.3 WALL PERFORMANCE ASSESSMENT

The resulting wall DCR's were found to be lower in the model based on proposed provisions, dropping to 0.6 from 0.78 in the controlling end walls. It is noted that although the local deformation response is sensitive to the size and location of meshing, shear gages are used to monitor structural wall drift across the clear length of vertical elements in order to normalize response relative to monitored acceptance criteria (see Figure 2-39).

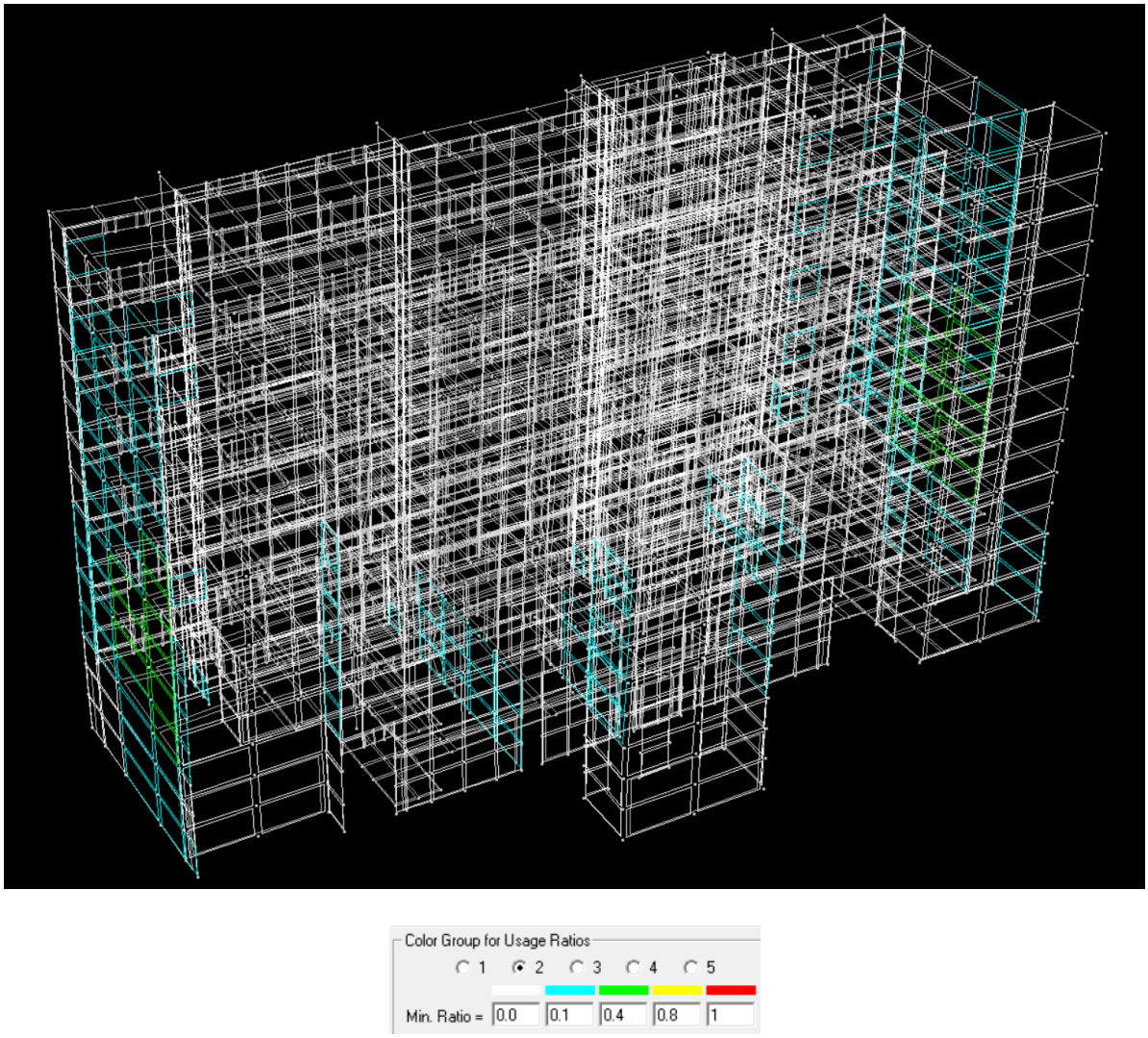

Figure 2-39 Proposed provision CP-DCR's at BSE-2E target displacement.

2.5.3.4 DISCUSSION AND CONCLUSIONS

The global results are not substantially different from those of ASCE/SEI 41-17, but it is noted the ultimate building strength has a noticeable increase. The ASCE/SEI 41-17 global pushovers are shown for reference in Figure 2-40 below, where the peak strength was roughly 3000 kips compared to approximately 3500 kips for the updated provisions. It is noted however that the idealized yield points are not substantially different, leading to similar target displacement demands in the analysis and ultimately similar usage ratios (see Figure 2-41).

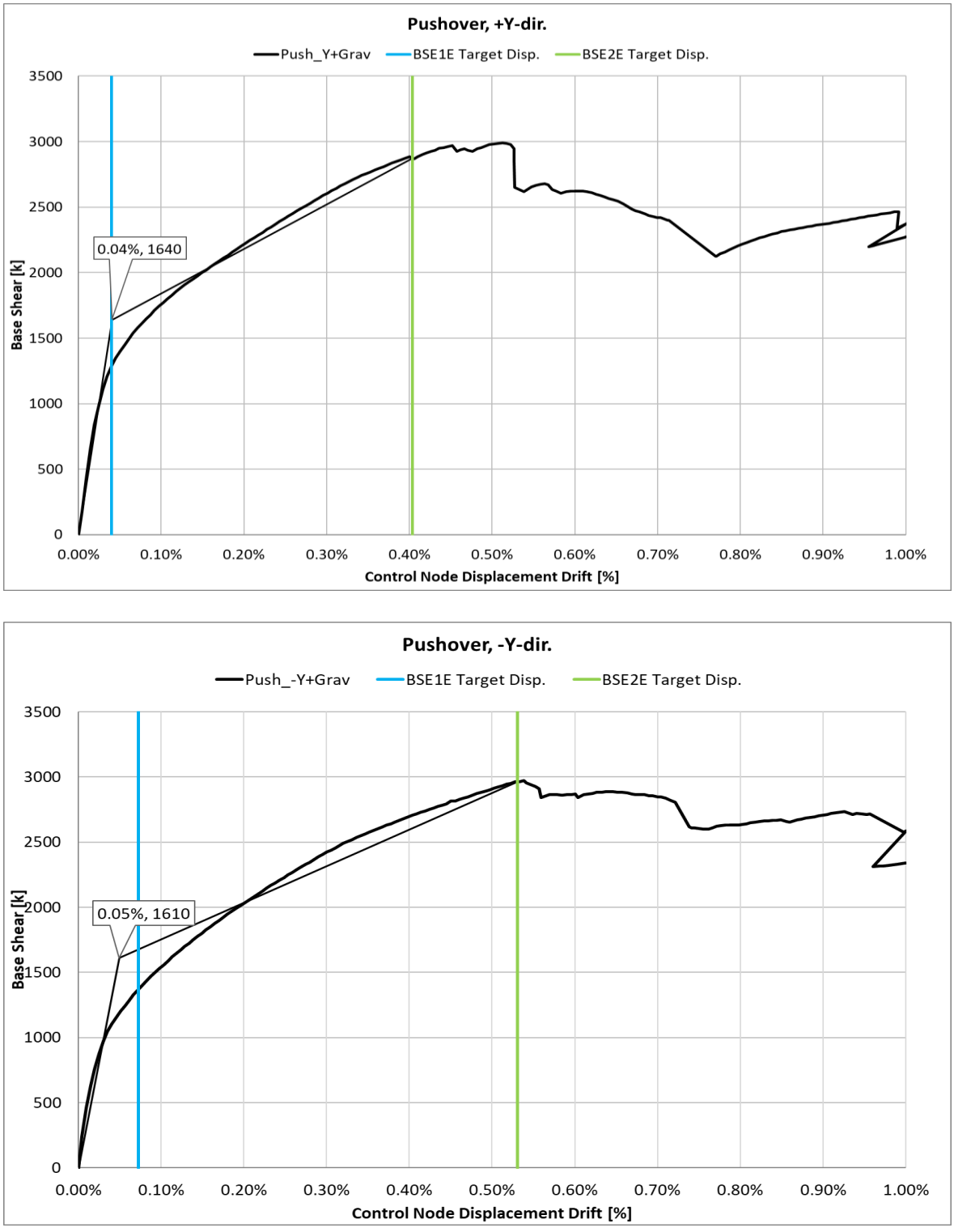

Figure 2-40 ASCE/SEI 41-17 global north-south pushover results.

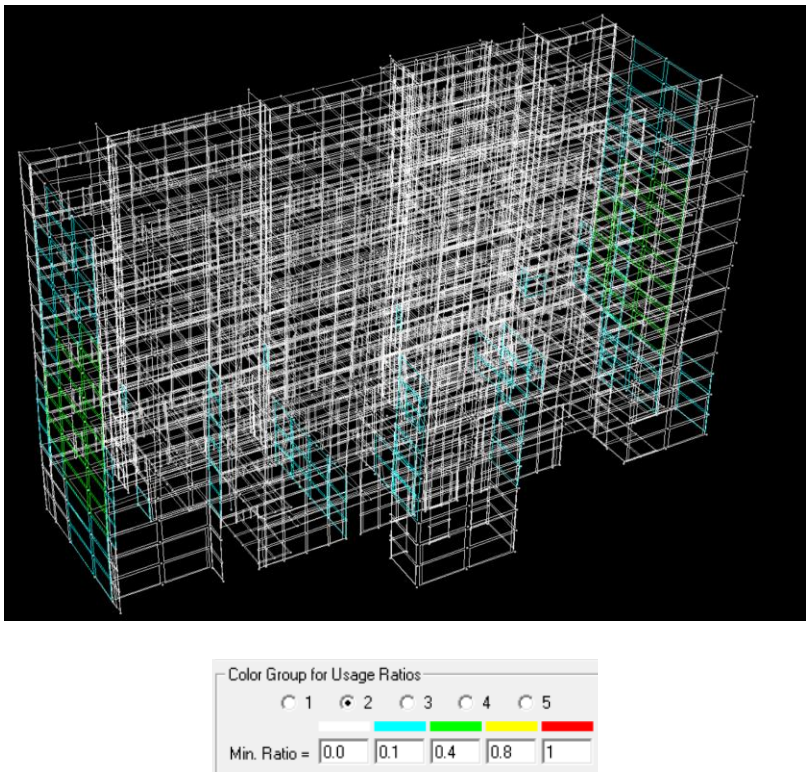

Figure 2-41 ASCE/SEI 41-17 CP-DCR's at BSE-2E target displacement.

2.6 References

Abdullah, S. A., 2019, *Reinforced Concrete Structural Walls: Test Database and Modeling Parameters, Ph.D. dissertation,* Dept. of Civil and Environmental Engineering, University of California, Los Angeles, California.

Abdullah S. A., and Wallace J. W., 2021, "Drift capacity at axial failure of RC structural walls and wall piers," *ASCE Journal of Structural Engineering*, DOI: 10.1061/(ASCE)ST.1943-541X.0003009.

ACI, 1983, *Building Code Requirements for Reinforced Concrete*, ACI 318-83, American Concrete Institute, Detroit, MI.

ACI, 2017, *Standard Requirements for Seismic Evaluation and Retrofit of Existing Concrete Buildings*, ACI 369.1-17, American Concrete Institute, Farmington Hills, MI.

ACI, 2019, *Building Code Requirements for Structural Concrete*, ACI 318-19, American Concrete Institute, Farmington Hills, MI.

Architectural Institute of Japan, 1999, "Design Guidelines for Earthquake Resistant Reinforced Concrete Buildings Based on Inelastic Displacement Concept," Tokyo, Japan.

ASCE/SEI, 2017, *Seismic Evaluation and Retrofit of Existing Buildings*, ASCE/SEI 41-17, American Society of Civil Engineers, Reston, VA.

Barda, F., 1972, *Shear Strength of Low-Rise Walls with Boundary Elements*, Ph.D. Dissertation, Lehigh University Bethlehem, Pennsylvania.

Beekhuis, W. J., 1971, *An Experimental Study of Squat Shear Walls*, M.E. *Report,* Department of Civil Engineering, University of Canterbury, Christchurch, New Zealand.

Benjamin, J. R., and Williams, H. A., 1953, *Investigation of Shear Walls, Part–Experimental and Mathematical Studies of Reinforced Concrete Walled Bents under Static Shear Loading, Report No. 1*, Department of Civil Engineering, Stanford University, Stanford, CA.

Benjamin, J. R., and Williams, H. A., 1954, Investigation of Shear Walls, Part 6–Continued Experimental and Mathematical Studies of Reinforced Concrete Walled Bents under Static Shear Loading, Report No. 4, Department of Civil Engineering, Stanford University, Stanford, CA.

Benjamin, J. R., and Williams, H. A., 1956, *Investigation of Shear Walls, Part 12–Studies of Reinforced Concrete Shear Wall Assemblies, Report No. 10*, Department of Civil Engineering, Stanford University, Stanford, CA.

Elwood, K. J., Matamoros, A. B., Wallace, J. W., Lehman, D. E., Heintz, J. A., Mitchell, A. D., Moore, M. A., Valley, M. T., Lowes, L. N., Comartin, C. D., and Moehle, J. P., 2007, "Update to ASCE/SEI 41 Concrete Provisions," *Earthquake Spectra*, 23(3), 493-523.

FEMA, 1997a, *NEHRP Commentary on the Guidelines for the Seismic Rehabilitation of Buildings*, FEMA 274, Federal Emergency Management Agency, Washington, D.C.

FEMA, 1997b, *NEHRP Guidelines for the Seismic Rehabilitation of Buildings*, FEMA 273, Federal Emergency Management Agency, Washington, D.C.

Galletly, G. D., 1952, *Behavior of Reinforced Concrete Shear Walls Under Static Load, Report Submitted to Office of the Chief of Engineers, Department of the Army*, Department of Civil and Sanitary Engineering, Massachusetts Institute of Technology, Cambridge, MA.

Gulec, C. K., and Whittaker, A. S., 2011, "Empirical equations for peak shear strength of low aspect ratio reinforced concrete walls," *ACI Structural Journal*, V. 108, No. 1, pp. 80-89.

Hirosawa, M., 1975, "Past Experimental Results on Reinforced Concrete Shear Walls and Analysis on Them," *Kenchiku Kenkyu Shiryo,* No. 6, Building Research Institute, Ministry of Construction, Tokyo, Japan, 279 pp. (in Japanese).

Kabeyashawa, T.; Kabeyashawa, T.; Kabeyashawa, T.; Kim, Y.; and Tojo, Y., 2008, "Effects of shapes and reinforcings on shear strength of reinforced concrete walls," *Journal of Structural Engineering*, v. 54B, pp. 423-428.

Kassem, W., 2015, "Shear strength of squat walls: a strut-and-tie model and closed-form design formula," *Engineering Structures*, V. 84, pp. 430-438. doi: 10.1016/j.engstruct.2014.11.027

Loo, D. T. W, 2017, *Seismic Axial Collapse of Short Shear Span Reinforced Concrete Shear Walls*, Ph.D. Dissertation, University of Hong Kong.

Massone L.M., and Wallace J.W., 2004, "Load—deformation responses of slender reinforced concrete walls," *ACI Structural Journal*, Vol 101, No.1, pp 103–113.

Park, H.-G.; Baek, J.-W.; Lee, J.-H.; and Shin, H.-M., 2015, "Cyclic loading tests for shear strength of low-rise reinforced concrete walls with grade 550 MPa bars," *ACI Structural Journal*, V. 112, No. 3, pp. 299-310. doi: 10.14359/51687406

Synge A. J., 1980. *Ductility of Squat Shear Walls*, *Technical Report No. 80-8*, Department of Civil Engineering, University of Canterbury, Christchurch, New Zealand.

Terzioglu, T., 2008, "Experimental evaluation of the lateral load behavior of squat structural walls," Master Dissertation, Boğaziçi University, Istanbul, Turkey, pp. 1- 155.

Chapter 3: Revisions to Concrete Structural Wall Shear-Friction-Controlled Provisions

3.1 Motivation

Most of the provisions for concrete structural walls in ACI 369.1-17 were developed in the late 1990s based on limited experimental data and judgement for FEMA 273 (FEMA, 1997a) and FEMA 274 (FEMA, 1997b). The only exceptions were the modeling parameters (MP) and acceptance criteria (AC) of shear-controlled walls, which were updated for the ASCE/SEI 41-06 Supplement 1 (Elwood et al., 2007).

A comprehensive database for structural wall tests developed by (Abdullah, 2019) with over 1,100 wall tests spurred a comprehensive review of all structural wall provisions and the addition of new provisions related to wall sliding and wall modeling. The outcome, presented in Part 4 Chapter 1, includes: a restructuring of the structural wall Section 10.7 in ASCE/SEI 41-17; updated wall classification procedures based on the relative strengths of various mechanisms; updated MP and AC for flexure-controlled, shear-controlled, and shear friction-controlled walls; and new modeling guidance for structural walls. Three example assessments for flexure-controlled, shear-controlled, and shear friction-controlled walls in low to mid-rise buildings are presented in this Part as well. Assessment outcomes between provisions of ACI 369.1-17 and the proposed provisions are compared.

In this chapter, a brief summary of the wall database is presented, including methods used to extract necessary force and deformation metrics for updating strength and deformation capacities for walls controlled by the shear-friction mode of degradation. The wall database is discussed in more detail in Chapter 1 of Part 4. Proposed wall Acceptance Criteria (AC) and Modeling Parameters (MP) for shear friction-controlled walls are presented. ACI 369.1-17 does not contain provisions for the shear-fiction mode of wall degradation. Therefore, the proposed provisions constitute new additions to the standard, as opposed to modifications on existing content. At the end of the chapter, an example assessment of a building with shear friction-controlled walls is presented based on proposed provisions.

Note about the Relation Between the ASCE/SEI 41 and ACI 369.1 Standards

The concrete wall provisions contained in Section 10.7 of ASCE/SEI 41-17 were reproduced from Chapter 7 of the new ACI 369.1-17 Standard, based on a Memorandum of Understanding between ACI and ASCE. In 2021, however, the ASCE/SEI 41 Standard Committee elected to reference the next version of ACI 369.1 directly, without replicating its contents, making ACI 369.1 the reference standard for concrete members for ASCE/SEI 41. The proposed changes were therefore submitted to ACI's Seismic *Repair and Rehabilitation* Code committee 369 for possible adoption.

3.2 Summary of Recommended Changes

For walls controlled by shear-friction or sliding, new shear-friction strength relations are proposed based on test data. The relations differ from those of ACI 318-19. Relatively low coefficients of friction are proposed compared with ACI 318-19. It is postulated that inelastic cycling at the interface weakens the shear transfer mechanism. However, the new relations also account for the influence of moment demand on shear strength. Interfaces with relatively low moment demands can see their shear friction strength increase beyond the values in ACI 318-19, despite the proposed low coefficients of friction. Updated nonlinear and linear AC and MP are proposed based on test data. Shear-friction is not treated explicitly in ASCE/SEI 41-17 and ACI 369.1-17, and thus is considered a force-controlled action. The proposed AC and MP permit a deformation-controlled designation for shear-friction sliding in walls, and provide deformation capacities for the sliding mechanism.

3.3 Technical Studies

3.3.1 Wall Test Database

3.3.1.1 DATASET OF SHEAR- FRICTION-CONTROLLED WALLS

The main database (Abdullah, 2019), described in Chapter 1 of Part 4, was filtered to obtain a dataset of 71 shear-friction-controlled walls tested under quasi-static, reversed cyclic loading protocols. The dataset includes walls with different cross-section shapes: 58 rectangular, six barbell, five H-shaped, and two L-shaped. Furthermore, the dataset includes walls with different interface conditions at the foundation level or above: cold untreated interfaces (joints), monolithic interfaces, roughened interfaces, and interfaces treated with sealing agents. Similar to the shear-controlled wall dataset, no detailing criteria were applied in filtering to the dataset, because detailing variables such as area of boundary transverse reinforcement (A_{sh}), slenderness ratio of boundary longitudinal bars (s/d_b), and spacing between laterally supported boundary longitudinal bars (h_x) are not typically relevant for shear-friction-controlled walls, i.e., there are no limits placed on these variables in ACI 318-19. The walls in the dataset had shear span ratio (M/Vl_w) ranging between 0.33 to 0.95. Most of the walls in the dataset had no additional applied axial load, whereas for the walls with applied axial load, the axial load did not exceed $0.1A_g f'_c$.

3.3.1.2 DATA EXTRACTION

Review of test results (e.g., Figure 3-1) indicated that shear-friction behavior at an interface is characterized by almost zero slip along the interface until the yield shear-friction strength is exceeded. This indicates that wall top deformations are due to shear and flexural actions over the wall height prior to yield. Figure 3-1 indicates that, as the displacement demands increase, contribution from sliding displacement increases, and that minor inelastic displacements due to shear and/or flexure could be expected at strength loss. Based on these observations, where a lumped-plasticity translational element is used to simulate shear sliding along an interface (but not the deformations in the wall above the interface), the load-deformation relationship shown in Figure 3-2 should be used for the interface element. Prior to yield, the response is captured through the flexure and shear springs, which are assumed to remain linear. Alternatively, if the elastic shear flexibility of the wall or wall segment is aggregated into the lumped-plasticity translational element used to simulate the nonlinear shear-friction behavior, the load-deformation relationship of the element should be defined as presented in Figure 2-3 in Chapter 2 (i.e., backbone of shear-controlled walls) using stiffness values of shear-controlled walls up to Point B (Yield), and parameters illustrated in Figure 3-2 beyond Point B.

As described in Chapter 1 of Part 4, the database includes backbone relations derived from the reported experimental force-displacement relationships, in which the displacement capacities are measured as total displacements at the top of the wall specimen, i.e., the backbone displacement values include sliding at the base (or other weak sections), shear distortion, and flexural displacement (curvature). As previously noted, shear-friction-controlled walls are typically modeled using a nonlinear translational spring to capture the interface sliding displacement and linear translational and rotational springs to capture the shear and flexural deformations over the wall height. Therefore, to be consistent with this approach, elastic shear and flexural deformations were determined analytically based on recommendations of Chapters 1 and 2 of part 4 and subtracted from the total measured displacements for each wall in the dataset (i.e., sliding displacement = total displacement – calculated elastic flexural displacement – calculated elastic shear displacement). The elastic flexural displacements (for all the points on the backbone curve) were calculated using the effective flexural stiffness values, $E_{cE}I_{eff}$, proposed in Table 1-6 of Part 4. At the yield point, elastic shear displacements were calculated using Parameter g_{nl} (= 0.40% drift) for shear-controlled walls. This approach assumes that the wall has reached diagonal shear yielding, which might lead to a slight overestimation of elastic shear displacements and thus conservative shear sliding modeling parameters.

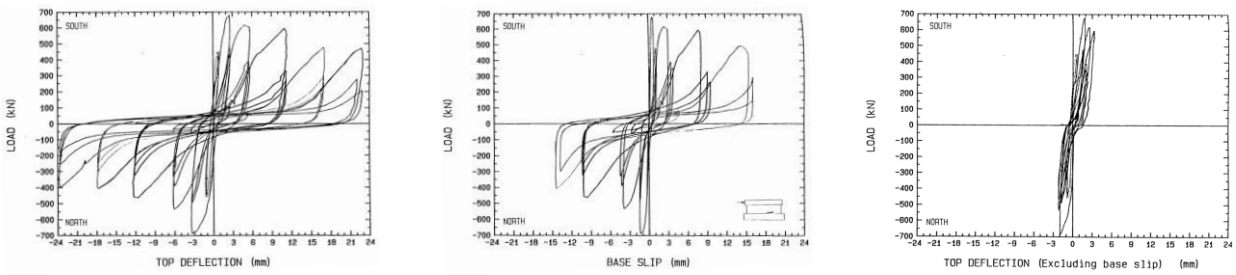

(*a*) Total displacement **(*b*) base sliding** **(*c*) shear and flexural displacement**

(*i*) Test by Wiradinata (1985)

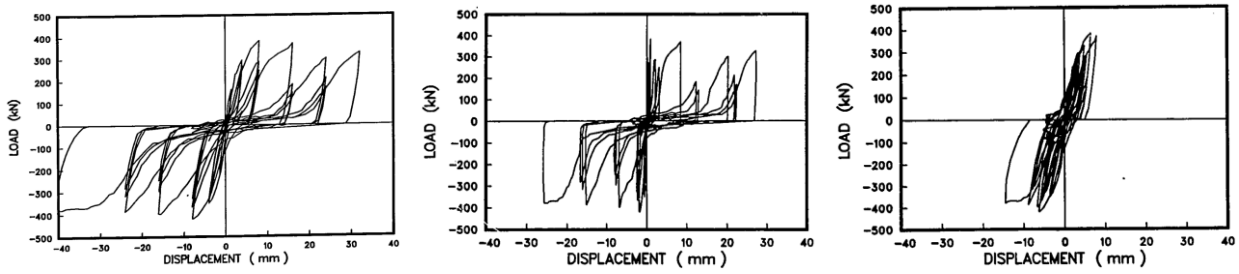

(*a*) Total displacement **(*b*) base sliding** **(*c*) shear and flexural displacement**

(ii) Test by Pilette (1988)

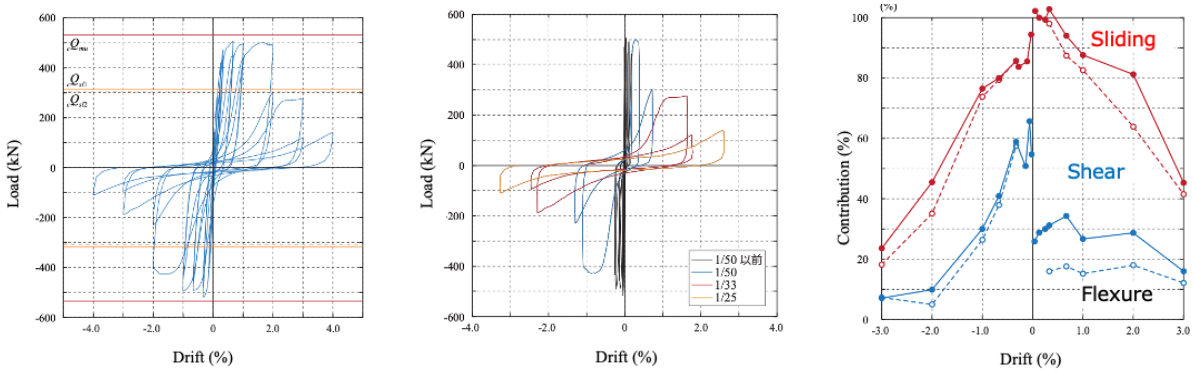

(*a*) Total displacement **(*b*) base sliding** **(*c*) Displacement contributions**

(*iii*) Test by Anoda (2014)

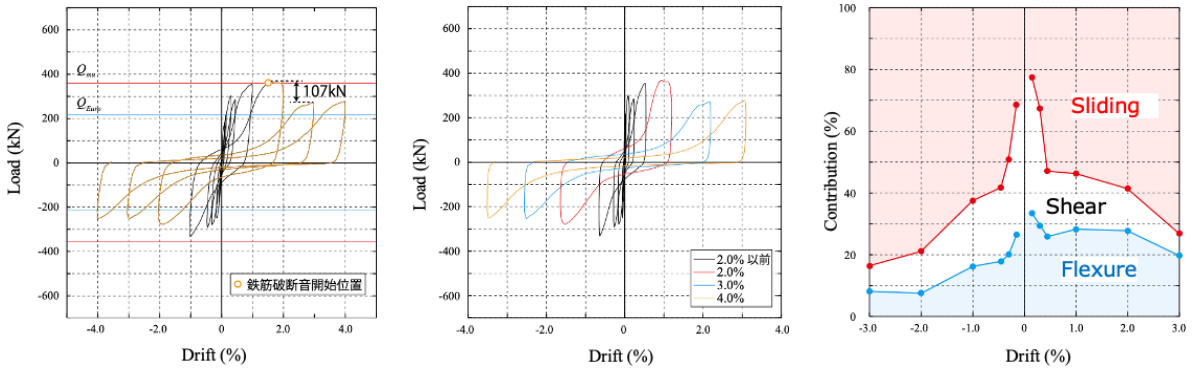

(*a*) Total displacement **(*b*) base sliding** **(*c*) Displacement contributions**

(*iv*) Test by Ramarozatov et al. (2016)

Figure 3-1 Sample force-displacement relationships for shear-friction-controlled wall tests.

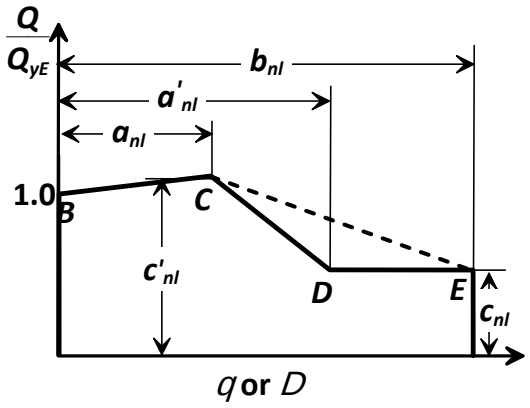

Figure 3-2 Idealized backbone relations to model translational behavior of shear-controlled walls.

3.3.2 Background of Wall Shear-Friction Strength

3.3.2.1 ACI 318 APPROACH TO SHEAR-FRICTION

The concept of shear-friction strength was originally developed in the 1960s (Birkeland and Birkeland, 1966; Hofbeck et al., 1969) to evaluate shear transfer across a concrete-to-concrete interface crossed by reinforcement perpendicular to the interface. The concept has been further studied over the years (Mattock, 1976 and 1977; Kahn and Mitchell, 2002). These studies indicate that shear-friction (interface) strength results from: (a) cohesion between particles (direct bearing of asperities and aggregate interlock), (2) friction between concrete parts or crack faces (ACI 318 approach), and (3) dowel action of the reinforcement crossing the interface (to a minor extent).

ACI 318 first adopted shear-friction provisions in 1971 based on the work of Hofbeck et al. (1969). The ACI 318 approach for shear-friction strength (ACI 318-19 Section 22.9.4), which is given by Equation 3-1, only considers the contribution of friction between concrete surfaces, where A_{vf} is the area of reinforcement crossing the sliding interface, f_y is the design yield strength of the reinforcement, μ is the coefficient of friction accordance with Table 3-1 (ACI 318-14 Table 22.9.4.2), and P is the sustained axial load on the sliding interface if present. In ACI 318-19 Table 22.9.4.2, reproduced as Table 1, the interface type significantly impacts shear-friction strength (strength changes by a factor of 2.33). Cold joints that meet ACI 318 roughness definition (1/4 in. amplitudes) are treated as 1.67 times stronger than their "smooth" counterparts. Monolithic interfaces are treated as 2.33 times stronger than their "smooth" counterparts. As shown Table 3-1, upper-bound limits are applied primarily due the lack of sufficient data when these provisions were adopted.

$$V_n = \mu\left(A_{vf} f_y + P\right) \tag{3-1}$$

Table 3-1 Shear-Friction Coefficients and Strength Upper-Bounds of ACI 318-19

Interface Type	μ	Maximum shear-friction strength, $V_{n,max}$
Monolithic (concrete to concrete)	1.4λ	For normal-weight concrete (monolithic or roughened): Least of $\begin{Bmatrix} 0.2f'_{Ce}A_c \\ (480+0.08f'_{Ce})A_c \\ 1600A_c \end{Bmatrix}$ For all other cases: Lesser of $\begin{Bmatrix} 0.2f'_{cE}A_c \\ 800A_c \end{Bmatrix}$
Roughened (concrete to concrete)	1.0 λ	
Concrete placed against hardened concrete not roughened intentionally	0.60 λ	
Concrete anchored to an as-rolled structural still by headed studs or by reinforcing bars	0.70 λ	

Note: f'_c is the design concrete compressive strength, μ is the coefficient of friction, Ac is the area of concrete section resisting shear transfer, and l is the modification factor to reflect the reduced mechanical properties of lightweight concrete relative to normal weight concrete of the same compressive strength.

One of the principal limitations of the ACI 318 approach for shear-friction strength, as it applies to concrete walls, is that this approach was developed and verified using results from "push-off" tests under primarily monotonic loading. Under earthquake loading, wall interfaces are typically subjected to cyclic moments, shears, and axial loads and the contributions of direct bearing of asperities and reinforcement dowel action are likely reduced under these conditions. Mattock (1977) concluded that repeated cyclic loading degrades shear-friction resistance to roughly 80% of monotonic strength.

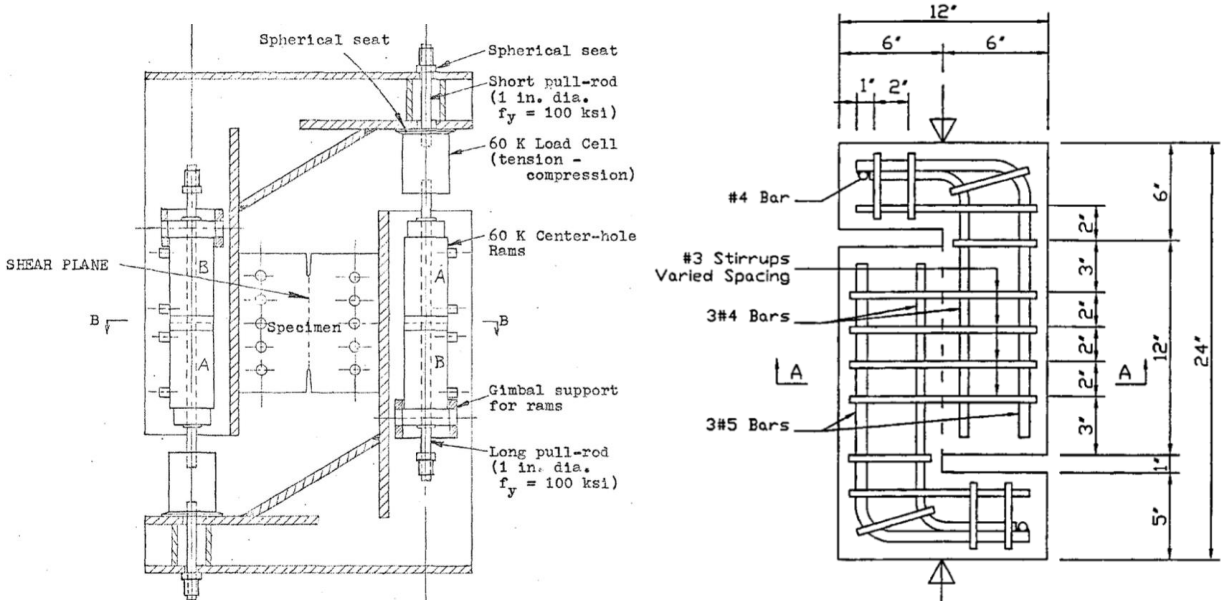

(*a*) Mattock (1976; 1977) **(*b*) Kahn and Mitchell, 2002)**

Figure 3-3 Push-off test setups used to study shear-friction strength.

3.3.2.2 INFLUENCE OF CYCLIC LOADING ON SHEAR-FRICTION STRENGTH

The information provided in this subsection is based on content in Paulay et al. (1982). For concrete walls subjected to earthquake cyclic demands imparting relatively large flexural cracking, most of the shear force is transmitted across the flexural compression zone (prior to sliding), as shown in Figure 4a. Once the load reverses, cracks form across the previous flexural compression zone (Figure 4b). Until the base moment reaches a level sufficient to yield these bars in compression (close the gap), a wide, continuous crack develops along the foundation-wall interface, and large horizontal shear displacements could occur at this stage of the response. Along this crack, shear is transferred primarily by dowel action of the vertical reinforcement. The wall continues to slide until the compression reinforcement yields, leading to closing of the crack at the compression end of the wall and allowing flexural compression stresses to also be transmitted by the concrete (Figure 4c). As a result of the sliding that occurred during this load reversal, the compression in the flexural compression zone is transmitted by uneven bearing across crack surfaces, which reduces both strength and stiffness of the aggregate interlock mechanism along the interface. After a few cycles of reversed loading, sliding displacement can occur along flexural cracks that interconnect and form a continuous, approximately horizontal shear path. At the base of a shear wall, where continuous cracking is likely to be initiated by a construction joint, bending moments also need to be transferred. Consequently, shear transfer along the critical sliding plane is then restricted to the vertical wall reinforcement and flexural compression zone where cyclic opening and closure of cracks will take place. This sliding behavior is quite different than that observed from push-off tests.

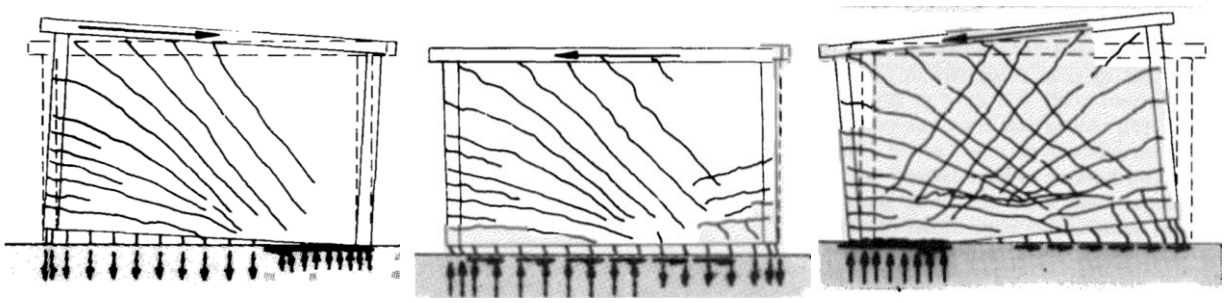

(*a*) (*b*) (*c*)

Figure 3-4 Development of the sliding shear mechanism (Paulay et al., 1982).

3.3.2.3 INFLUENCE OF INTERFACE CONDITION ON SHEAR-FRICTION STRENGTH

Per ACI 318-19, the interface surface condition significantly influences the shear-friction strength. However, the test results reviewed (and discussed later), demonstrate that shear-friction coefficients at concrete interfaces transferring cyclic shear and moment demands are not significantly influenced by the type of the interface. Such interfaces exhibit shear-friction coefficients at the lower end of values specified in ACI 318-19 Section 22.9.4.2. Figure 3-5a presents results isolating the role of interface conditions on shear-friction strength and deformation from a series of wall tests with different interface conditions and longitudinal reinforcement layouts

Test results reported by Anoda (2014) and shown in Figure 3-5a indicate that, according to ACI 318-19, wall W1-M is expected to be 2.33 times stronger than walls W1-Js and W2-J. However, test results show that shear-friction strength was similar for a monolithic connection or a cold joint. It is postulated that during the first cycle prior to any sliding occurring, flexural cracks form at a monolithically cast interface, changing the interface from being monolithic to a cracked interface. Figure 3-5a also suggests that the longitudinal reinforcement layout in the wall section (uniform distribution vs. concentrated at boundaries) does not have a clear impact on shear friction strength.

Similarly, Figure 3-5b shows test results from three identical wall specimens with different interface conditions (Baek et al., 2020), and indicates that walls H0.33OR and H0.33OG with roughened or monolithic interfaces are only about 20% stronger than H0.33OU with an interface that is not intentionally roughened. These tests indicate a coefficient of friction of roughly 0.70 for roughened and monolithic interfaces versus 0.60 for an untreated interface. This modest increase of strength observed for walls H0.33OR and H0.33OG in Figure 3-5b is presumably because these walls have smaller aspect ratios than walls in Figure 3-5(a) (0.33 vs. 0.56), which means less flexural demands and cracking for walls in Figure 3-5b, resulting in more noticeable effect of interface type. The shorter the aspect ratio of the wall, the closer it is to a push-off test condition shown in Figure 3, which was used to develop the coefficients of friction in ACI 318. Figure 3-5b also suggests that failure of roughened and grooved interfaces involves some web crushing at the sliding interface, resulting in reduced ductility.

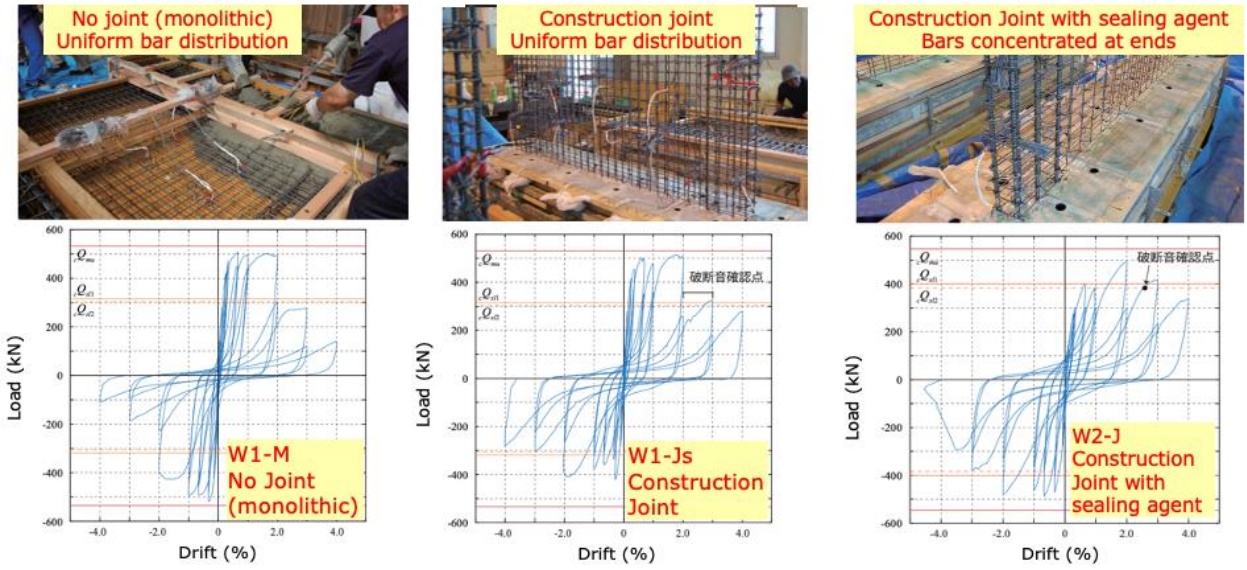

(*a*) Test by Anoda (2014)

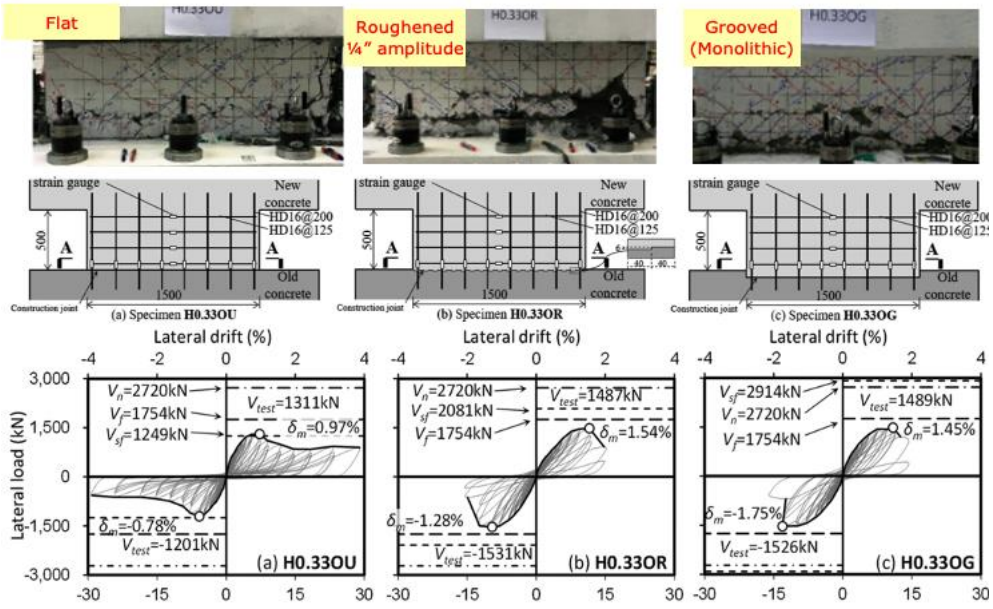

(*b*) Test by Baek et al. (2020)

Figure 3-5 Influence of interface roughness on behavior of shear-friction-controlled walls.

3.3.2.4 INFLUENCE OF FLANGES ON SHEAR-FRICTION STRENGTH

In ACI 318-19, it is not clear whether the longitudinal reinforcement in wall flanges should be consisted in the calculation of shear-friction strength, such that the contribution of longitudinal reinforcement in the flanges is often ignored. However, recent test results suggest that longitudinal bars in wall flanges contribute to shear-friction resistance and should be considered (Kim and Park, 2020; Baek et al., 2020). Figure 3-6a indicates that presence of flanges with vertical reinforcement significantly increases the shear-sliding resistance of walls (40% and 87% increase in the negative and positive directions of loading, respectively). Figure 3-6b presents results from three walls with the same web but different cross-section shapes and indicates that longitudinal bars in flanges significantly increase shear-sliding resistance. For the H-shaped wall shown in Figure 3-6b, it is reported that shear-sliding was limited until diagonal tension cracking through the thickness of the flanges occurred, which was followed by a large slip at the wall-foundation interface; indicating that the flanges restrained shear sliding of the wall web. For the T-shaped wall, when the flange is in tension, sliding resistance is higher partly due to larger compression zone (large neutral axis depth), whereas this effect is not as significant when the flange is in compression (smaller depth of neutral axis).

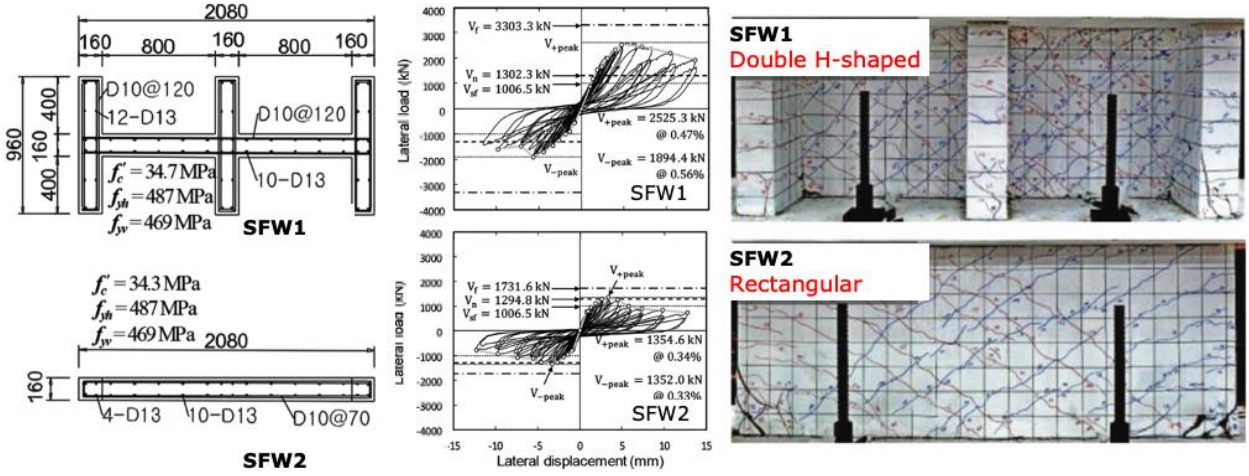

(*a*) Test by Kim and Park (2020)

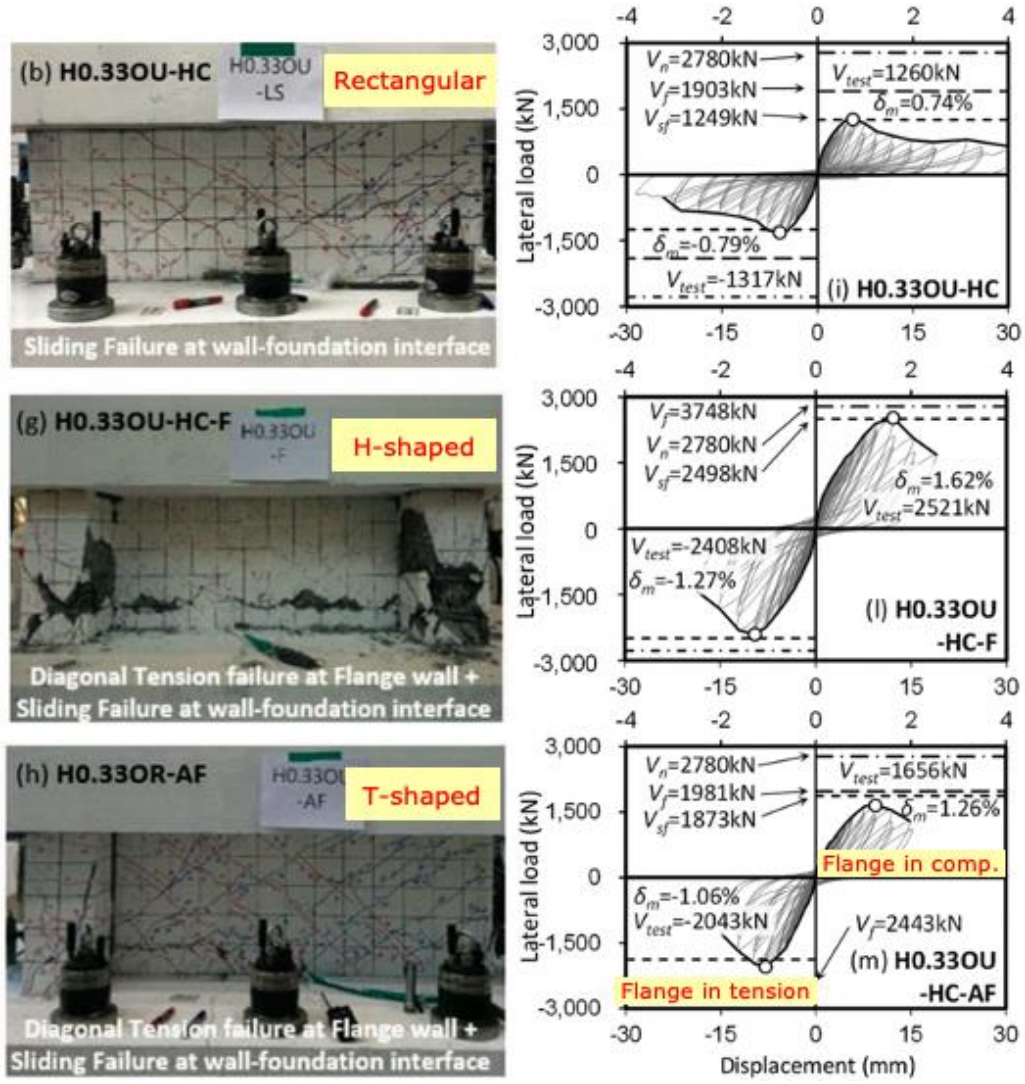

(*b*) Test by Baek et al. (2020)

Figure 3-6 Influence of flanges on behavior of shear-friction-controlled wall tests.

3.3.2.5 INFLUENCE OF DOWELS ON SHEAR-FRICTION STRENGTH

When shear-friction resistance along an interface is not sufficient to resist shear demands, it is common practice to provide dowels crossing the interface with sufficient development length on both sides of the interface. However, test results (Wasiewicz, 1988; Baek et al., 2018) show that it is possible for the failure plane to shift to the end of the dowel bars, as shown in Figure 3-7. These results suggest that shear-friction strength should be evaluated at all possible failure planes along the wall or wall segment height, i.e., at the cold joint and at the plane where the dowels end. An appropriate backbone curve to model shear sliding should be located at each potential sliding plane unless the weaker plane can be identified a priori.

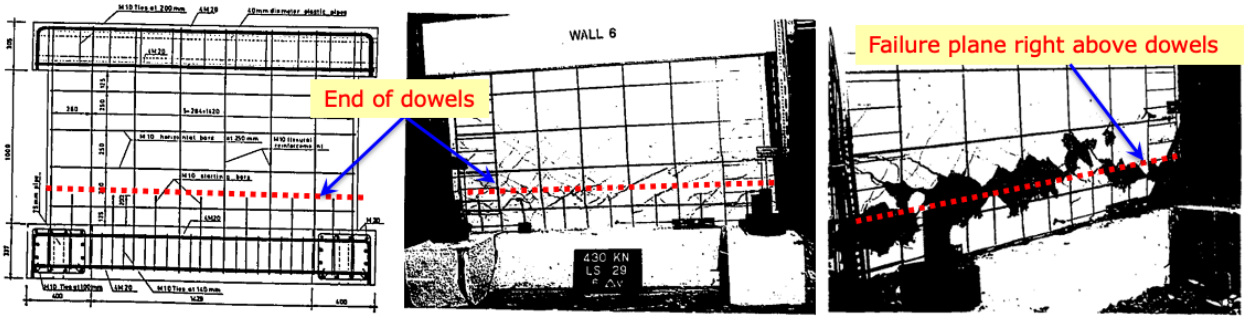

(*a*) Test by Wasiewicz (1988)

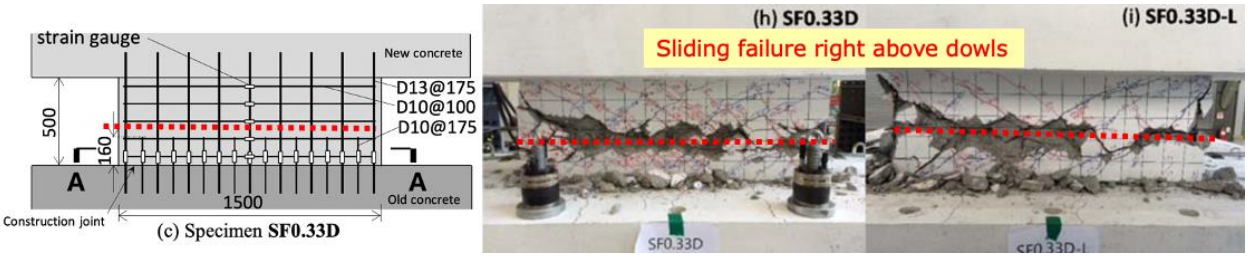

(*b*) Test by Baek et al. (2018)

Figure 3-7 Influence of dowels on changing the location of sliding failure plane.

3.3.2.6 INFLUENCE OF REINFORCEMENT GRADE ON SHEAR-FRICTION STRENGTH

Figure 3-8 shows results from two identical wall tests with roughened interfaces where reinforcement with different yield strength was used across the interface. Nominal yield strengths, f_y, were 400 MPa (~58 ksi) and 600 MPa (87 ksi). Test results indicate that, for interfaces with both steel grades, the measured shear-friction strength was lower than predicted by ACI 318-19, which is denoted as V_{sf} in the plots. This is results is observed despite ACI 318-19 Table 20.2.2.4(a) limiting yield strength of shear-friction reinforcement to 420 MPa (60 ksi). This limit is apparent in Figure 3-8 because the shear-friction strengths for the two walls are identical. Further, test results shown in Figure 3-9 indicate that, at peak strength, limited yielding of reinforcement crossing the shear friction plane is observed. This result is at odds with the ACI 318-19 assumption (Equation 3-1) that all shear-friction bars yield [up to 420 MPa (60 ksi)] when the peak load is reached. Use of higher strength steel for shear friction is permitted by other codes, e.g., Grade 500 MPa (72.5 ksi) in CSA

A23.3-04 and KCI 2012, and Grade 600 MPa (87 ksi) in Eurocode 2, Eurocode 8, and fib Model Code 2010.

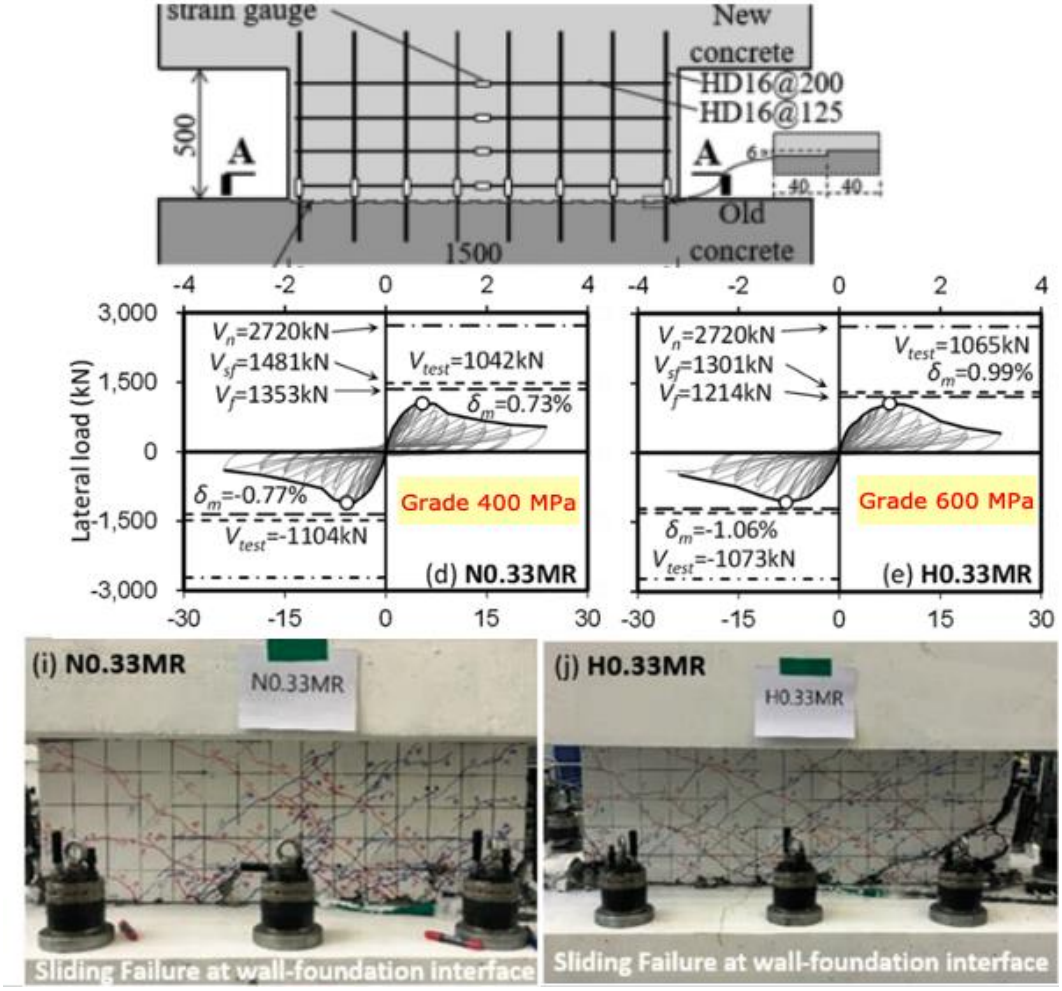

Figure 3-8 **Influence of longitudinal reinforcement yield strength on shear-friction strength (Beak et al., 2020).**

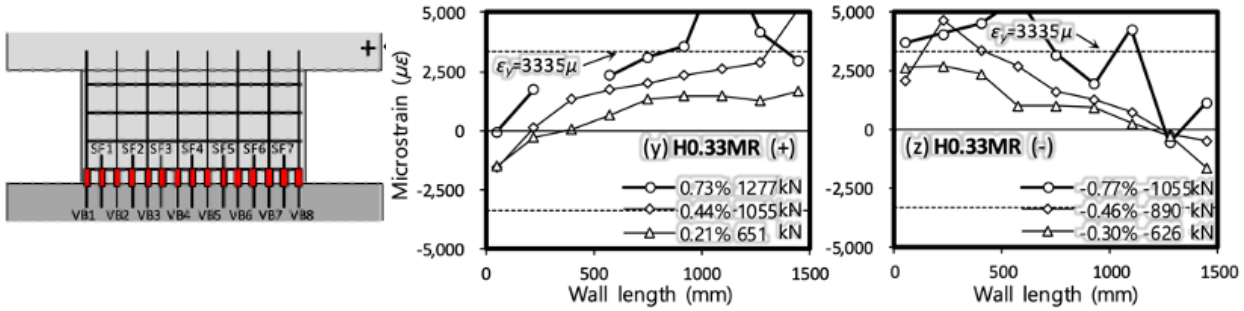

(*a*) Location of strain gages (*b*) Postive loading (*c*) Negative loading

Figure 3-9 **Measured longitudinal reinforcement strains at wall-foundation interface of a shear-friction-controlled wall test (Beak et al., 2017).**

The influence of reinforcement yield strength (steel grade) on shear-friction strength was also investigated using the dataset of 71 wall tests. The results presented in Figure 3-10 represent measured values of reinforcement yield strength, f_{yE}, which ranges from 300 MPa (40 ksi) to 675 MPa (98 ksi). Results shown in Figure 3-10 present shear-friction strength predictions using the ACI 318-19 shear-friction equation, where $V_{CyfWallSE}$ is determined from Equation 3-1 with expected material properties (f'_{cE}, f_{yE}) and without applying the limit on f_{yE} and using $\mu = 0.6$, regardless of the interface type. The figure indicates higher ratios of predicted-to-experimental shear-friction strengths for walls with high strength longitudinal bars ($f_{yE} \geq 480$ MPa, 70 ksi). This is likely because larger strains are required to reach bar yield, potentially requiring a larger separation at the interface when yield strains are reached. This result suggests that either: (a) a lower μ should be used for higher grades of bars, or (b) reinforcement yield strength should be limited, similar to what is used in ACI 318-19. To address this issue, limiting the expected yield strength of reinforcement (f_{yE}) used for shear-friction resistance to 517 MPa (75 ksi) is proposed. This limit is similar to that used in CSA A23.3-04 and KCI 2012 [i.e., Grade 500 MPa (72.5 ksi)].

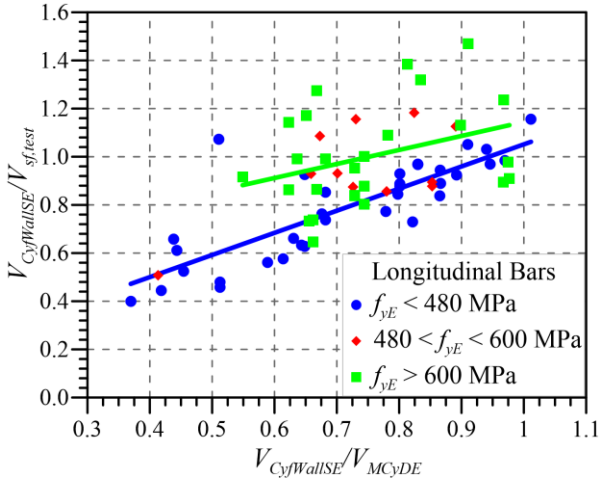

Figure 3-10 Impact of measured longitudinal reinforcement yield on strength shear-friction strength (1 MPa = 145 psi).

3.3.2.7 EVALUATION OF ACI 318-19 PROVISIONS

As noted previously, the provisions of ACI 318-19 for shear-friction strength were developed primarily based on results from "push-off" tests under monotonic loading protocols, which differ from wall loading conditions under earthquake demands.

Figure 3-11 compares the measured peak shear friction strength ($V_{sf,test}$) from the 71 wall dataset with the ACI 318-19 limits. As was shown in Table 3-1, ACI 318-19 includes limits on shear-friction strength. In particular, the 5.5-MPa (800-psi) limit on shear-friction stress for "smooth" cold joints was introduced in ACI 318-71 and has not been revised since. The limited results presented in Figure 3-11, however, indicate that this 5.5-MPa (800-psi) limit may not be justified by experimental evidence, and thus it is recommended to be removed. Further, Figure 3-11 suggests that the effect

of concrete strength on shear-friction strength is not clear, and that the $0.2f'_{cE}\,A_{cv}$ limit for untreated (smooth) interfaces seems to reasonably envelope the data (and thus it is retained here).

Figure 3-12 shows the variation of measured peak shear friction strength ($V_{sf,test}$) from the 71-wall dataset and the ACI 318-19 approach (with assumed μ= 0.6 for all interfaces) versus clamping stress due to longitudinal bars (ρf_{yE}) and axial load (P/A_{cv}). Again, the limited results presented in Figure 3-12 suggest that the 5.5-MPa (800-psi) upper limit underestimates shear-friction strength significantly for high strength concrete, and that Equation 3-1 with μ= 0.6, regardless of the interface type, generally underestimates peak shear-friction strength. The walls with monolithic and roughened interfaces are either on or above the solid line (Equation 3-1) in Figure 3-12, whereas walls with untreated interfaces straddle above and below the solid line, with majority of the data above the line. Moreover, it can be observed from Figure 3-12 that the type of joint/interface has only a slight-to-moderate influence on peak shear-friction resistance. These results reinforce the earlier observation that the ACI 318-19 values for coefficient of frictions (μ) for roughened and monolithic interfaces over-estimate the shear-friction strength of concrete walls.

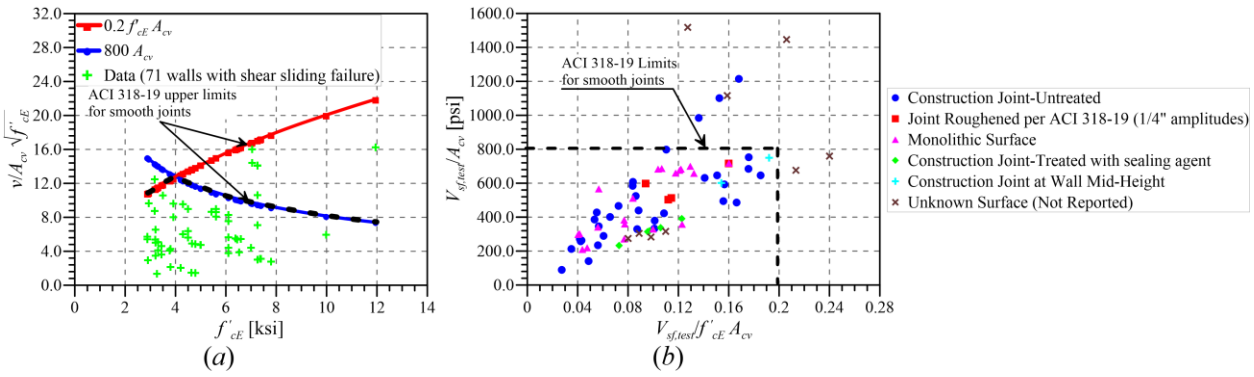

Figure 3-11 Comparison of measured peak shear friction strength ($V_{sf,test}$) from the dataset with the ACI 318-19 limits in Table 3-1.

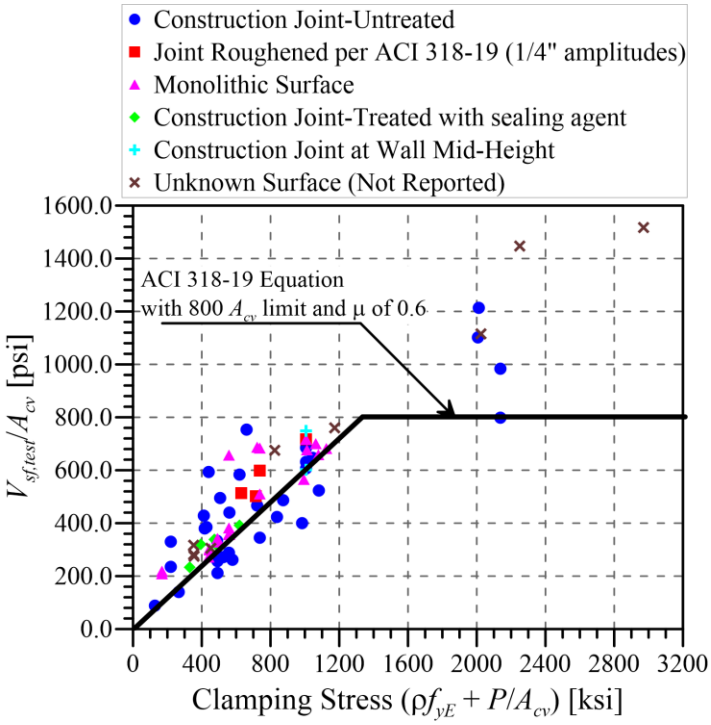

Figure 3-12 Variation of measured shear friction strength ($V_{sf,test}$) from the dataset and the ACI 318-19 limits in Table 3-1 versus clamping stress.

3.3.3 Wall Shear-Friction Strengths

In this section, strength relations for each point on the backbone curve (yield, peak, and residual) are discussed. For each strength, the impact of several variables was investigated; however, only the most relevant variables are discussed here for brevity. It should be noted that the shear-friction strength equations produced are calibrated for walls and wall segments interfaces subjected to reversed cyclic moment and shear. They are not intended for interfaces with differing boundary conditions, such as the vertical interface plane between slab and wall.

3.3.3.1 YIELD STRENGTH

Analysis of the 71-wall dataset, indicated that, yield shear-friction strength ($V_{sfy,test}$) is significantly influenced by the wall flexural demand (Figure 3-10), expressed by either the ratio of shear-friction strength to shear demand at flexural yield ($V_{CyfWallSE}/V_{MCyDE}$), or shear span to length ratio (M/Vl_w), as highlighted in Figure 3-13. Walls with significant flexural yielding and cracking (i.e., high $V_{CyfWallSE}/V_{MCyDE}$ or M/Vl_w) have lower yield shear-friction strength than walls with limited flexural yielding. Figure 3-13 also indicates that a modified ACI 318-19 Equation with no upper stress limit and μ = 0.6, results in a mean predicted-to-experimental yield strength ratio of 1.00 and a coefficient of variation of 0.26.

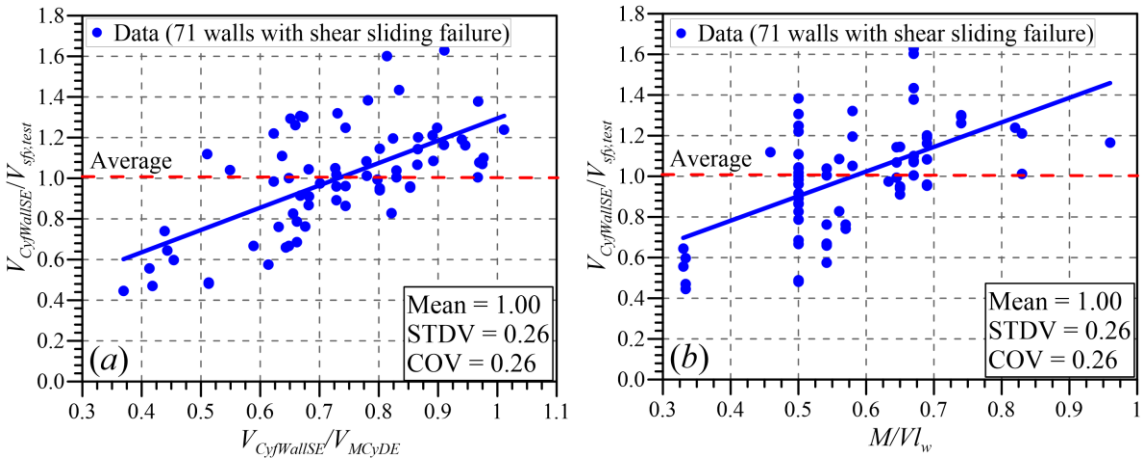

Figure 3-13 Variation of predicted-to-measured yield shear-friction strength versus shear-friction to flexural strength ratios ($V_{CyfWallSE}/V_{MCyDE}$) and shear span ratios (M/Vl_w).

Similar to shear- and flexure-controlled walls, the approach taken here was to develop an equation for yield shear-friction strength with a mean of predicted-to-tested values of 1.0 and then apply an amplification factor to obtain peak shear-friction strength.

Based on these results, a new equation is proposed for shear-friction strength at yielding, which corresponds to Point B on the proposed backbone in Figure 3-2. The expression is given by Equation 3-2.

$$V_{CfyWallE} = \left(2.5 - 2.15\frac{V_{CyfWallSE}}{\omega_v V_{MCyDE}}\right) V_{CyfWallSE} \tag{3-2}$$

Where $V_{CfyWallE}$ should not be taken greater than 1.8 $V_{CyfWallSE}$ or smaller than 0.8 $V_{CyfWallSE}$.

$$V_{CyfWallSE} = \mu\left(A_{vf} f_{yfE} + N_{UG}\right) \leq 0.2 f'_{cE} A_g \tag{3-3}$$

Where μ is the coefficient of shear friction and is taken as 0.7 for concrete cast monolithically or placed against hardened concrete that is intentionally roughened to a full amplitude of approximately 1/4 in, and 0.6 for concrete placed against hardened concrete that is not intentionally roughened, and N_{UG} is the member gravity axial force. These proposed μ values are based on the discussion provided in Section 3.3.2. Shear-friction strength should be evaluated at all possible failure planes along a wall or wall segment height, such as weak interfaces located at the end of dowel bars, at an existing or potential crack, at an interface between dissimilar materials, or at an interface between two concretes cast at different times. It is possible that a construction joint at the foundation-wall interface with dowel bars (μ = 0.6) is stronger than a monolithic interface (μ = 0.7) at the end of the dowel bars. In Equation 3-2, the expected yield strength of shear friction reinforcement, f_{yfE}, should be reduced if the development length is insufficient to develop f_{yfE} and should not be taken greater than 517 MPa (75 ksi). For flanged wall sections, the reinforcing steel crossing the interface, including the reinforcement within the effective flange width defined in ACI

318-19, should be included in A_{vf}. Equation 3-2 and Equation 3-3 assume that reinforcement is normal to the interface. For inclined reinforcement, adjustments to the equation should be made as provided in ACI 318-19.

Figure 3-14 presents results using the yield strength model (Equation 3-2) with the experimental data from the dataset and demonstrates that the model matches the experimental data fairly well, with a mean of 1.0 and a coefficient of variation of 0.17.

As a simplified approach to Equation 3-2, Equation 3-3 can be used. Use of this simplified expression results in increased dispersions (coefficient of variation of ~0.27) compared to Equation 3-2.

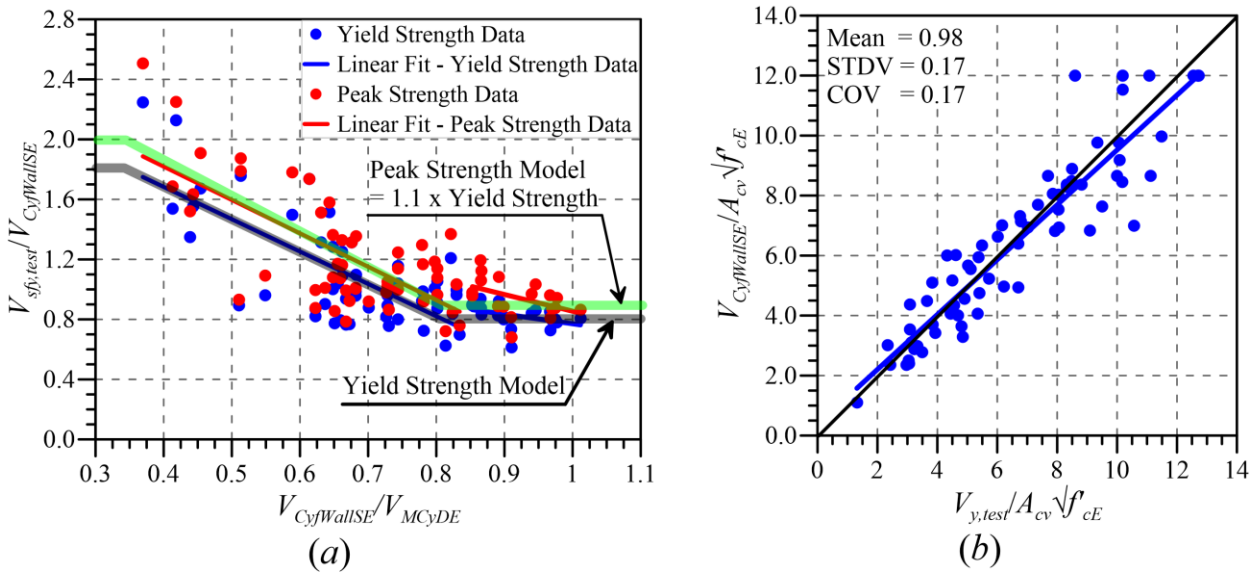

Figure 3-14 Comparison of estimated and tested yield shear-friction strengths: (*a*) comparison of model with data, and (*b*) statistics of the ratio of predicted-to-tested yield strength.

3.3.3.2 PEAK STRENGTH

Review of the peak strength data in the 71-wall dataset revealed that there is modest hardening from yield to peak strength. Figure 3-14a and Figure 3-15 show that, on average, peak strength is about 10% higher than yield strength ($V_{sf,peak}$ = 1.10 $V_{CyfWallSE}$, i.e., Parameter c' = 1.10). Therefore, it is proposed that peak strength at Point C on the backbone be taken as 1.1 times yield strength at point B, which is the same factor used for shear-controlled walls.

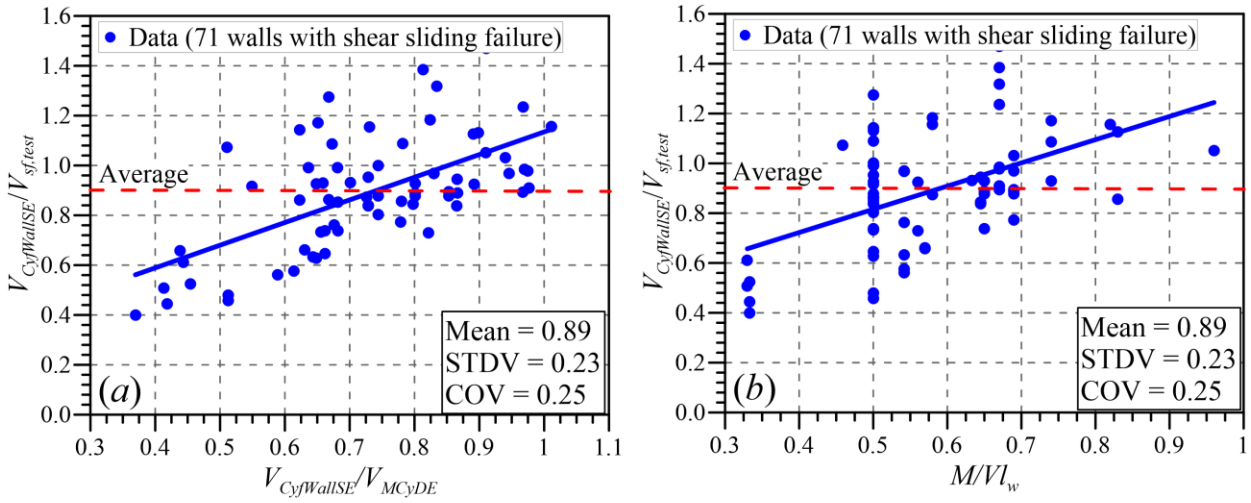

Figure 3-15 Variation of the ratio of estimated (Equation 3-1) to tested shear-friction yield strengths as a function of: (*a*) $V_{CyfWallSE}/V_{MCyDE}$ and (*b*) M/Vl_w.

3.3.3.3 RESIDUAL STRENGTH

Generally, shear-friction-controlled walls have larger residual strength than flexure- or shear-controlled walls. On average, the residual strength of the wall tests in the 71-wall dataset is roughly 0.6 of their yield strength, as shown in Figure 3-16. Figure 3-16a shows a slight correlation of residual strength with $V_{CyfWallSE}/V_{MCyDE}$, whereas Figure 3-16b shows that there is a significant correlation of residual strength with clamping stress and type of interface. For roughened and monolithic interfaces, the residual strength is lower because, as was noted from Figure 3-5b, failure of roughened and grooved/monolithic interfaces involves moderate to significant concrete crushing at the sliding interface, depending on the level of clamping force on the interface, leading to faster degradation of strength once lateral strength loss initiates. Given the uncertainly and dispersion in the data, it is proposed to take the residual strength as 0.5 and 0.6 of yield strength for monolithic/roughened and untreated interfaces, respectively.

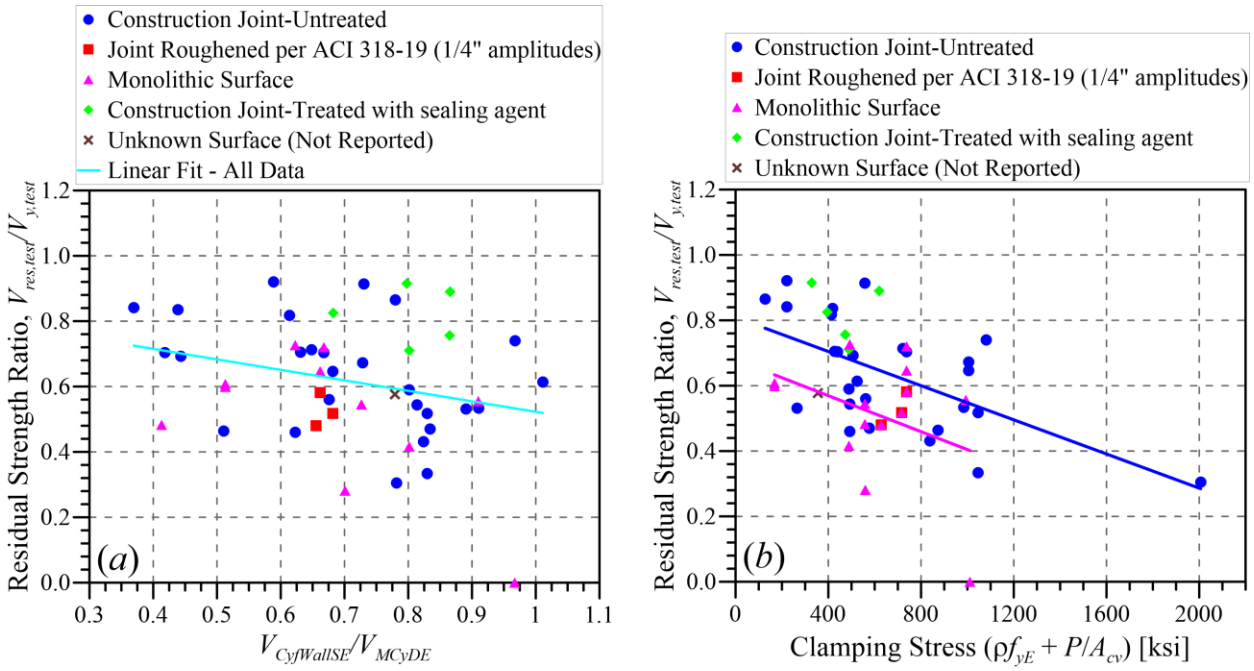

Figure 3-16 Variation of measured residual strength to yield strength as function of: (*a*) $V_{CyfWallSE}/V_{MCyDE}$ and (*b*) clamping stress.

3.3.4 Modeling Parameters and Acceptance Criteria

3.3.4.1 NONLINEAR MODELING PARAMETERS

Since the sliding deformation along an interface is a localized response, and therefore, independent of the wall height, the proposed nonlinear modeling parameters for shear-sliding are given in inches (rather than drift ratio values). The modeling parameters are, for the most part, developed based on the test results of the 71-wall dataset. In cases where there is a lack of test data, such as sliding deformation at axial failure, experience and engineering judgement were exercised to provide recommended values. It should be noted that the proposed modeling parameters are intended for potential interfaces along the wall or wall segment heights and are not intended for use with interfaces having different boundary conditions such as a vertical plane at slab-wall interfaces.

In the following subsections, the modeling parameters for each point on the backbone curve are developed in the order they appear on the backbone using the experimental dataset. Similar to the backbone strengths, detailed data analyses were performed for each parameter, and the impact of many variables was investigated; however, only the most relevant results are presented here for brevity.

Parameter a_{nl} (Sliding Displacement at Point C)

For this parameter, which is defined as displacement at 20% lateral strength loss on the experimental backbone, a series of regression analysis were performed, which revealed that the

most important variables include the interface type and $V_{CyfWallSE}/V_{MCyDE}$. In Figure 3-17, the walls with monolithic or roughened interfaces are in one bin, and the rest are in another bin. As it was noted previously, roughened and monolithic interfaces tend to be less ductile than untreated interfaces due to the significant concrete crushing occurring at monolithic and roughened interfaces under cyclic sliding. Figure 3-17 presents results that show that walls with low flexural demands (i.e., high ratios of $V_{CyfWallSE}/V_{MCyDE}$) tend to have a larger Parameter a_{nl}, partly due to the contribution of inelastic flexural displacement that are not accounted for by analytically removing elastic flexural displacements. Based on these results, the models shown in Figure 3-17 are proposed, which reasonably match the experimental data.

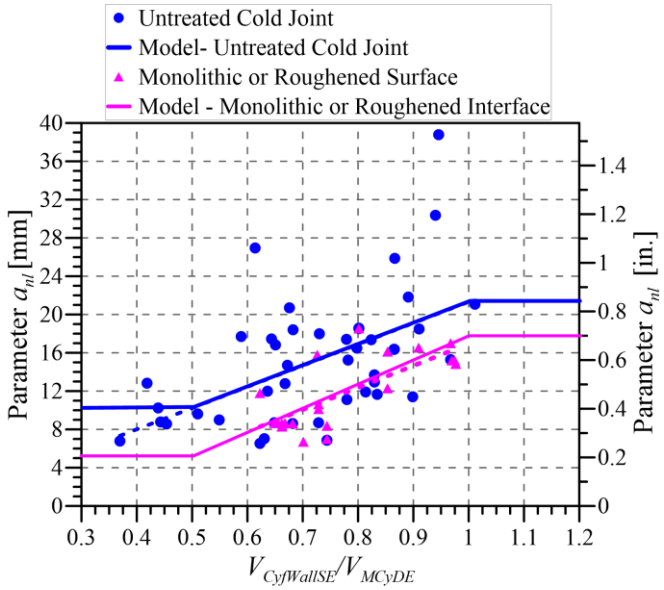

Figure 3-17 Comparison of Parameter a_{nl} versus interface type and $V_{CyfWallSE}/V_{MCyDE}$ with the proposed models.

Parameter a'_{nl} (Sliding Displacement at Point D)

Review of hysteretic behavior of shear-friction-controlled walls in the dataset (e.g., Figure 3-1, Figure 3-5, Figure 3-6, and Figure 3-8) revealed that, although the hysteretic loops are quite pinched, strength loss for these walls tends to be gradual with increasing displacement and that relatively large displacement capacity can be achieved. Figure 3-18 compares the displacement capacities of the dataset at 20% lateral strength loss (Parameter a_{nl}) and at residual strength (Parameter a'_{nl}) and demonstrates that, on average, there is a significant difference between Parameter a_{nl} and Parameter a'_{nl}. Also, Figure 3-18 shows that Parameter a'_{nl} is correlated with $V_{CyfWallSE}/V_{MCyDE}$, but the dispersion is greater than that for Parameter a_{nl}, partly due to the subjectivity in identifying the residual point on the backbone (as discussed in Chapter 1 of Part 4). The limited data presented in Figure 3-19 suggests that walls with a monolithic or roughened interface have lower displacement capacity. at residual than walls with untreated interfaces. Figure 3-19 compares results obtained from the experimental data with results from the proposed models for Parameter a'_{nl}, which are a function o$V_{CyfWallSE}/V_{MCyDE}$f and type of interface, similar to Parameter a_{nl}.

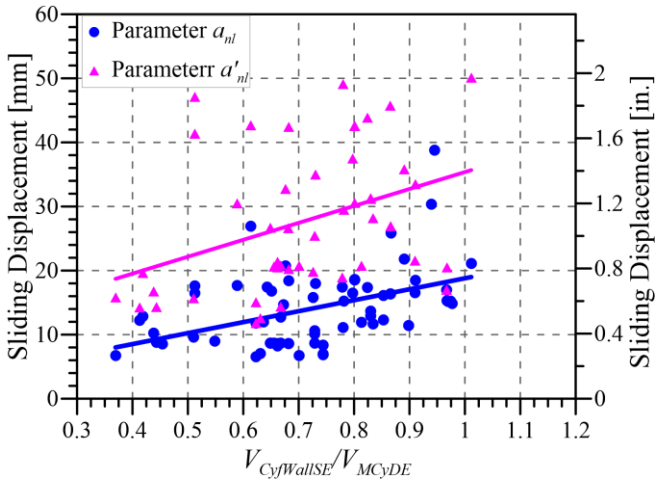

Figure 3-18 Comparison of Parameter a_{nl} (at 20% lateral strength loss) and Parameter a'_{nl} (sliding displacement at residual strength).

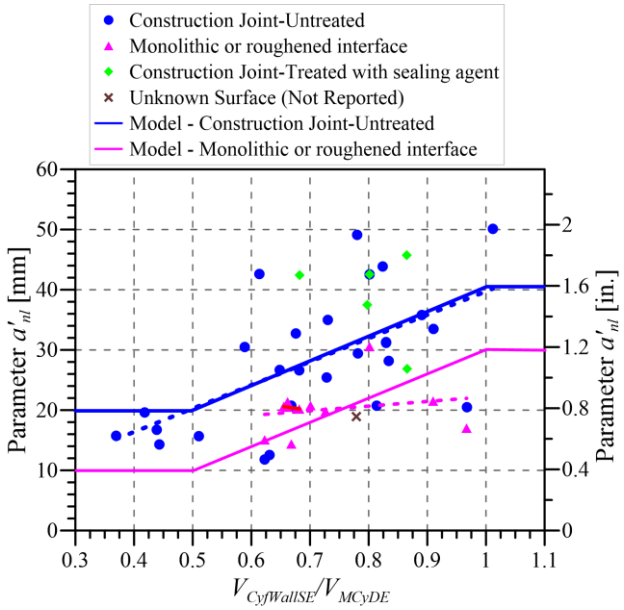

Figure 3-19 Comparison of proposed models for Parameter a'_{nl} with experimental data in the dataset.

Parameter b_{nl} (Sliding Displacement at Axial Failure, Point E)

Review of the test data revealed that axial failure (loss of gravity load-carrying capacity) rarely occurs in shear-friction-controlled walls because: (a) walls exhibiting this failure mode typically have relatively low axial loads (otherwise they do not fail in shear sliding), (b) although sliding failure can involve moderate concrete spalling and crushing along the interface combined with, in some cases, fracture of longitudinal bars due to dowel action, it does not involve out-of-plane instability or sliding along a diagonal crack (both of which can lead to axial failure). Therefore, walls and wall piers sustaining sliding failure at an interface are expected to maintain gravity load carrying capacity to

relatively large sliding displacements. Since the walls in the dataset did not sustain axial failure, they could not be used to define the expected sliding displacement at axial failure (Parameter b_{nl}). Therefore, based on experience and judgement, the sliding displacement at Point E is limited to 4 in. (100 mm). Under sustained transverse (out-of-plane) loads such as earth or fluid loads, or where lateral displacements may occur such as for a weak plane above terminated dowels over a story height, the sliding interface may become unstable. For such case, it is proposed that b_{nl} be limited to a'_{nl}.

Summary of Proposed Nonlinear Modeling Parameters

This section summarizes the proposed modeling parameters for shear-friction-controlled walls. The tabulated modeling parameters are presented in Table 3-2, and the statistics associated with the ratios of predicted-to-experimental values are presented in Table 3-3.

1. Cracking Point
   - Not applicable for shear-friction response
2. Yield Point (Point B)
   - Strength: detailed (Equation 3-2) or simplified (Equation 3-3) expression
   - Sliding displacement at yield is negligible.
3. Peak Point (Point C)
   - Strength: multiply yield strength by 1.1
   - Select Parameter a_{nl} (in inches) based on flexural demand and interface type
4. Residual Point (Point D)
   - Strength = 0.5 or 0.6 times the yield strength for monolithic/roughened and untreated interfaces, respectively.
   - Select Parameter a'_{nl} (in inches) based on flexural demand and interface type
5. Axial Failure Point (Point E)
   - Strength = residual strength at Point D
   - Parameter b_{nl} = 4 in.

Table 3-2 Modeling Parameters for Reinforced Concrete Structural Walls and Associated Components Controlled by Shear-Friction

Conditions		Sliding Displacements[a] (in.)			Strength Ratios	
Interface Type	$\frac{V_{CyfWallSE}}{w_v V_{MCyDE}}$[b]	a_{nl}	a'_{nl}	b_{nl}	c'_{nl}	c_{nl}
Monolithic or roughened to ¼ in. amplitude	≥ 1.0	0.65	1.30	4.0 in.	1.10	0.50
	≤ 0.5	0.20	0.40			
Other	≥ 1.0	0.80	1.60			0.60
	≤ 0.5	0.40	0.80			

[a] Linear interpolation between values listed in the table shall be permitted.
[b] The shear amplification factor ω_v need not be applied if V_{MCyDE} is obtained from nonlinear dynamic analyses procedures.

Table 3-3 Statistical Values for Modeling Parameters of Walls Controlled by Shear-Friction[a]

Parameter	Mean	Median	Lognormal Standard Deviation	Coefficient of Variation, COV
$V_{CyfWallSE}$[b]	1.01	0.97	0.20	0.20
$V_{CyfWallE}$[c]	1.05	1.09	0.26	0.25
c'_{nl}[b]	1.03	1.07	0.25	0.24
c'_{nl}[c]	0.99	0.98	0.20	0.21
c_{nl}	1.03	0.90	0.45	0.44
a_{nl}	1.06	1.07	0.35	0.33
a'_{nl}	1.02	1.00	0.41	0.41

[a] The statistics are for the ratios of estimated-to-experimental values.
[b] For values predicted by Equation3-2.
[c] For values predicted by Equation 3-3.

3.3.4.2 ACCEPTANCE CRITERIA

Proposed Nonlinear Acceptance Criteria

For the nonlinear acceptance criteria, the same approach used for flexure- and shear-controlled walls is followed, where the acceptance criteria are taken as percentiles of Parameter b_{nl} for LS and CP and as 10% of Parameter a_{nl} for IO, as shown in Chapters 1 and 2 of Part 4. The resulting nonlinear acceptance criteria are shown in Table 3-4.

Table 3-4 Nonlinear Acceptance Criteria for Reinforced Concrete Structural Walls and Associated Components Controlled by Shear-Friction

Conditions		Sliding Displacements[a] (in.)		Acceptance Criteria[a]		
Interface Type	$\frac{V_{CyfWallSE}{}_{b}}{w_v V_{MCyDE}}$	a_{nl}	b_{nl}	IO	LS	CP
Monolithic or roughened to ¼ in. amplitude	≥ 1.0	0.65	4.0 in.	0.1 a_{nl}	0.75 b_{nl}	b_{nl}
	≤ 0.5	0.20				
Other	≥ 1.0	0.80				
	≤ 0.5	0.40				

[a] Linear interpolation between values listed in the table shall be permitted.
[b] The shear amplification factor ω_v need not be applied if V_{MCyDE} is obtained from nonlinear analyses procedures.

Linear Acceptance Criteria (*m*-factors)

For linear acceptance criteria (*m*-factors), the same approach used for flexure- and shear-controlled walls is followed. The resulting expressions for linear acceptance criteria are shown in Table 3-5.

Table 3-5 Numerical Acceptance Criteria for Linear Procedures: Reinforced Concrete Structural Walls and Wall Segments

Component Type	*m*-factors[a,b]		
	Performance level		
	IO	LS	CP
Primary	1.2	$\frac{1}{2}\left(\frac{\frac{b_{nl}}{h_s}+g_{nl}{}^{c}}{g_{nl}{}^{c}}\right)$	$\frac{5}{8}\left(\frac{\frac{b_{nl}}{h_s}+g_{nl}{}^{c}}{g_{nl}{}^{c}}\right)$
Secondary		$\frac{3}{5}\left(\frac{\frac{b_{nl}}{h_s}+g_{nl}{}^{c}}{g_{nl}{}^{c}}\right)$	$\frac{4}{5}\left(\frac{\frac{b_{nl}}{h_s}+g_{nl}{}^{c}}{g_{nl}{}^{c}}\right)$

[a] m-factors shall not be smaller than 1.0.
[b] The acceptance criteria for primary members shall not be taken larger than those for secondary members.
[c] g_{nl} shall be from Table 7.4.1.1.2

3.3.5 Summary and Conclusions

This study involves utilizing available experimental data from 71 wall tests and new information on performance of structural walls to develop modeling parameters and acceptance criteria for seismic evaluation and retrofit of shear-friction-controlled reinforced concrete walls. Based on the results, the following conclusions are reached:

1. The ACI 318-19 approach for shear-friction strength developed from "push-off" tests under primarily monotonic loading, does not capture the shear-friction strength at interfaces undergoing inelastic cyclic loading. Under cyclic loading, the contributions of direct bearing of asperities and reinforcement dowel action are both reduced.
2. The ACI 318-19 coefficients of friction (μ) for roughened and monolithic interfaces tend to over-predict the shear-friction strength for concrete wall interfaces subjected to cyclic loading. The interface surface condition does not influence shear-friction strength as significantly as implied by ACI 318-19, possibly because the cyclic moment and shear loading opens interface cracks and weakens the transfer mechanism reducing the coefficient of friction to the lower values in ACI 318-19, regardless of interface treatment. Cycled interfaces exhibit shear-friction coefficients on the lower end of values given in ACI 318-19, with μ = 0.7 or 0.6 for roughened/monolithic and untreated interfaces, respectively.
3. Shear-friction yield strength relations are proposed that modify the ACI 318-19 shear-friction equation with reduced friction coefficients and introducing the effects of the ratio of shear-friction strength to shear demand at flexural yielding ($V_{CyfWallSE}/V_{MCyDE}$). Interfaces with larger flexural demands are given reduced shear-friction strength.
4. Despite the proposed low coefficients of friction for interfaces sustaining cyclic loading, interfaces with relatively low moment demands can see their shear friction strength increase beyond values provided by ACI 318-19.
5. Longitudinal bars in flanges are found to contribute to shear-friction resistance and should be considered in the calculation of shear-friction strength.
6. At peak strength, limited reinforcement yielding occurs in the web, regardless of the reinforcement grade. For high strength bars, a larger separation at the interface is needed for the bars to reach yield and to mobilize the full bar yield strength. Thus, it is proposed that the useable yield strength of reinforcement resisting shear-friction be limited to 517 MPa (75 ksi).
7. Test results indicate that it is possible for the shear-sliding failure plane to shift to the end of wall dowel bars, where the steel area is reduced, and monolithic concrete conditions exist.
8. ACI 318-19 includes limits on friction strength, which are mostly due to lack of experimental data. In particular, the 5.5-MPa (800-psi) limit for "smooth" cold interfaces was introduced in the ACI 318-71 edition and has not been revised since. Results presented indicate that this limit may not be justified by experimental evidence, and thus it is recommended to be removed. The results also revealed that the effect of concrete strength on shear-friction strength is not clear, and that the $0.2f'_c A_{cv}$ limit for untreated (smooth) interfaces seems to well envelope the data, and thus it is recommended to be retained.
9. Review of test results indicate that shear-friction behavior at an interface is characterized by almost zero slip along the interface until the yield shear-friction strength is exceeded.
10. Review of the peak strength data in the database revealed that there is roughly 10% hardening from yield strength to peak strength.

11. The most important variables for sliding displacement capacity of shear-friction-controlled walls include the type of interface and the ratio of shear-friction strength to shear demand at flexural yielding ($V_{CyfWallSE}/V_{MCyDE}$).
12. Roughened and monolithic interfaces tend to be less ductile than untreated interfaces as a result of concrete crushing occurring at monolithic and roughened interfaces due to cyclic sliding.
13. Review of hysteretic behavior of shear-friction-controlled walls in the dataset revealed that, although the hysteretic loops are quite pinched, these walls tend to have significant displacement capacity at residual due to the relatively gradual lateral strength loss.
14. Axial failure (loss of gravity load-carrying capacity) rarely occurs in sliding-shear-controlled walls because: (a) walls exhibiting this failure mode typically have limited axial loads (otherwise, they do not fail in shear sliding), (b) although sliding failure can involve moderate concrete spalling and crushing along the interface combined with fracture of longitudinal bars due to dowel action in some cases, it does not involve out-of-plane instability or sliding along a diagonal crack. Therefore, based on experience and judgement, the sliding displacement capacity at Point E is limited to 4 in. (100 mm).

3.4 Recommended Changes

3.4.1 Strength Provisions

Two equations are provided for shear-friction strength. The simpler Equation 7.2.4 is similar to the shear-friction strength equation in ACI 318-19 Chapter 22 but is applied with lower friction coefficients. Equation 7.2.3 is based on Equation 7.2.4 but accounts for the impact of moment demand on shear-friction strength and provides improved estimates of shear-friction strength for walls and wall segments. Additionally, the upper-limit on shear-friction strength in ACI 31819 Table 22.9.4.4(e) of 5.5-MPa (800-psi) is not considered in Equation 7.2.3 and 7.2.4.

For walls with higher strength bars, the yield strength of the reinforcing bars was observed not to fully mobilize at the interface and is therefore limited to 75,000 psi. Equation 7.2.4 assumes that reinforcement is normal to the interface. For inclined reinforcement, adjustments to the equation should be made as provided in ACI 318-19.

The shear-friction strength equations provided were calibrated for wall and wall segment potential interfaces sustaining cyclic flexural loading. They are not intended for interfaces with differing boundary conditions such as the vertical plane at slab-wall interfaces. New or modified text is shown in blue. Existing text that has been relocated is shown in green.

7.2—Strength of Reinforced Concrete Structural Walls, Wall Segments, and Coupling Beams

7.2.3 *Shear-Friction Strength* – The shear-friction yield strength of a structural wall or wall segment, corresponding to Point B in Fig. 3.1.2.2.3(d), considering shear transfer across any given plane along wall height shall be determined using Eq. 7.2.3 or 7.2.4.

$$V_{CfyWallE} = \left(2.5 - 2.15\frac{V_{CyfWallSE}}{\omega_v V_{MCyDE}}\right) V_{CyfWallSE} \quad \leq 1.8\, V_{CyWallSE} \quad \geq 0.8\, V_{CyWallSE} \tag{7.2.3}$$

$$V_{CyfWallSE} = \mu\left(A_{vf} f_{yfE} + N_{UG}\right) \leq 0.2 f'_{cE} A_g \tag{7.2.4}$$

Where

μ = 0.7 for concrete cast monolithically or placed against hardened concrete that is intentionally roughened to a full amplitude of approximately 1/4 in.

μ = 0.6 for concrete placed against hardened concrete that is not intentionally roughened.

f_{yfE} in Eq. 7.2.4 shall not be taken greater than 75,000 psi and shall be computed considering reductions with respect to anchorage in accordance with 3.5. For flanged wall sections, the reinforcing steel crossing the interface, including the reinforcement within the effective flange width in accordance with 3.1.3, shall be included in A_{vf}.

3.4.2 Acceptance Criteria and Modeling Parameters

Expressions for deriving linear acceptance criteria based on nonlinear modeling parameters is proposed. Additionally, a new table that includes nonlinear modeling parameters and acceptance criteria is proposed.

7.3.2 *Acceptance Criteria* –

...

Table 7.3.2b specifies m-factors for use in Eq. (7-36) of ASCE 41-17 for flexure-, ~~and~~ shear-, and shear friction-controlled structural walls and wall segments. Nonlinear modeling parameters, a_{nl}, b_{nl}, d_{nl}, e_{nl}, and g_{nl}, in Table 7.3.2b shall be determined as specified in Table 7.4.1.1.1a and Table 7.4.1.1.1b for flexure-controlled walls, ~~and~~ Table 7.4.1.1.2 for shear-controlled walls, and Table 7.4.1.1.3 for shear-friction controlled walls, unless otherwise specified. As an alternative to Table 7.3.2b, it shall be permitted to use m-factors from Table 7.3.2c for walls controlled by shear, and Table 7.3.2d and Table 7.3.2e for walls controlled by flexure. ~~It shall be permitted to use m-factors from Table 7.3.2c for wall actions controlled by shear-friction at cold joints located at the interface between walls and foundations having a minimum dowel reinforcement ratio of 0.001.~~ Alternate m-factors shall be permitted where justified by experimental evidence and analysis.

Walls that are non-symmetric about a bending axis, in terms of geometry, reinforcement ratio, ~~and/or~~ detailing, and/or applied axial loads, shall have their non-symmetric behavior considered in the two directions of loading about that axis. For such non-symmetric wall sections, it shall be permitted to use the moment strength from either direction of loading that results in the largest DCR or lowest m-factor from Tables 7.3.2a through Table 7.3.2e.

Table 7.3.2b–Numerical acceptance criteria for linear procedures: reinforced concrete structural walls and wall segments

Controlling Behavior	Component Type	m-factors[a,b]		
		Performance level		
		IO	LS	CP
Shear-Friction	Primary	1.2	$\frac{1}{2}\left(\frac{\frac{b_{nl}}{h_s}+g_{nl}^{\ c}}{g_{nl}^{\ c}}\right)$	$\frac{5}{8}\left(\frac{\frac{b_{nl}}{h_s}+g_{nl}^{\ c}}{g_{nl}^{\ c}}\right)$
	Secondary		$\frac{3}{5}\left(\frac{\frac{b_{nl}}{h_s}+g_{nl}^{\ c}}{g_{nl}^{\ c}}\right)$	$\frac{4}{5}\left(\frac{\frac{b_{nl}}{h_s}+g_{nl}^{\ c}}{g_{nl}^{\ c}}\right)$

[a] m-factors shall not be smaller than 1.0.

[b] The acceptance criteria for primary members shall not be taken larger than those for secondary members.

[c] g_{nl} shall be from Table 7.4.1.1.2

7.4.1.1.3 *Structural walls and wall segments controlled by shear-friction* – For structural walls and wall segments with inelastic behavior under lateral loading that is controlled by shear-friction, in accordance with 7.3.2, the following approaches shall be permitted. The load-deformation relationship in Fig. 3.1.2.2.3(d) shall be used, with the X-axis of the figure taken as the nonlinear sliding displacement of the wall along the sliding plane. Values for the variables a_{nl}, a'_{nl}, b_{nl}, $c_{n\ell}$, and $c'_{n\ell}$ required to define Points C, D, and E in Fig. 3.1.2.2.3(d) shall be as specified in Table 7.4.1.1.3. For walls or wall segments with sustained transverse loading, b_{nl} shall be taken equal to a'_{nl} in Table 7.4.1.1.3.

Table 7.4.1.1.3 —Modeling parameters and numerical acceptance criteria for nonlinear procedures: reinforced concrete structural walls and associated components controlled by shear-friction

Conditions		Sliding Displacements[a] (in.)			Strength Ratios		Acceptance Criteria		
Interface Type	$\frac{V_{CyfWallSE}}{w_v V_{MCyDE}}$[b]	a_{nl}	a'_{nl}	b_{nl}	c'_{nl}	c_{nl}	IO	LS	CP
Monolithic or roughened to ¼ in. amplitude	≥ 1.0	0.65	1.30	4.0 in.	1.10	0.50	0.1 a_{nl}	0.75 b_{nl}	b_{nl}
	≤ 0.5	0.20	0.40						
Other	≥ 1.0	0.80	1.60			0.60			
	≤ 0.5	0.40	0.80						

[a] Linear interpolation between values listed in the table shall be permitted.

[b] The shear amplification factor ω_v need not be applied if V_{MCyDE} is obtained from nonlinear analyses procedures.

3.5 Shear Friction-Controlled Walls Example

This section presents an analysis and evaluation example of a shear friction-controlled reinforced concrete wall building. The example uses a modified version of the E-defense shake table building testing performed in 2010.

The example summarizes the building structure configuration, seismic loading, wall classification, and mathematical modeling and analysis. The example presents calculation reports and evaluation results for an example wall using the proposed modeling parameters (MP's) and acceptance criteria (AC) and compares them to evaluation outcomes using the ACI 369.1-17 provisions.

3.5.1 Overview of Building

The building was a four-story, reinforced concrete (RC) structure tested on the E-Defense shake table in 2010. It was one of two structures tested simultaneously that were nearly identical in dimensions but differed in construction technique and reinforcing design. The objective of the testing program was to compare the seismic performance of traditional concrete construction (RC building on the left in Figure 1) with that of newly developed post-tensioned systems (PT building on the right in Figure 3--20).

Figure 3-20 RC and PT structures tested at E-Defense shake table (ACI 112-S12).

The RC structure considered here has two lines of moment frames in the longitudinal direction and two shear walls in the transverse direction.

Observed damage from that motion consisted of severe shear damage in first floor beam-column joints, limited cracking and spalling of beam and column ends, and cracking and crushing of the

shear walls at their base. The boundary elements of the wall saw considerable crushing damage, and sliding was observed at the base of the walls.

The testing program for the RC and PT buildings is documented extensively in PEER Report 2011/104 by Wallace et al. (2011). The report contains design drawings, testing instrumentation, ground motion information, and weight documentation. Nagae et al. (2015) indicates that the RC building satisfies most of the provisions of ACI 318-14 for special moment frame and special wall systems.

3.5.1.1 WALL CONFIGURATION

The building is structurally regular and has major gridlines spaced 7.2m (23.62ft) apart. It was designed to conform to the seismic design provisions of the Architectural Institute of Japan (AIJ, 1999) and nearly meets the ACI 318-11 provisions (Nagae et al., 2015). Floor heights were 3000mm (118.1 inch). The slab system is a pan joist system with a 130mm (5.12 inch) slab thickness at all levels. The two walls are 250mm (9.84 inch) thick by 2500mm (98.4 inch) long. The columns are 500mm (19.69 inch) square. Beams in the frame direction are 300mm (11.81 inch) wide by 600mm (23.62 inch) deep, while those coupling the walls to the corner columns were 300mm (11.81 inch) wide and deep.

A typical floor plan of the RC building, elevations of the RC building, and reinforcement detailing are presented in Figure 3-21 to Figure 3-23.

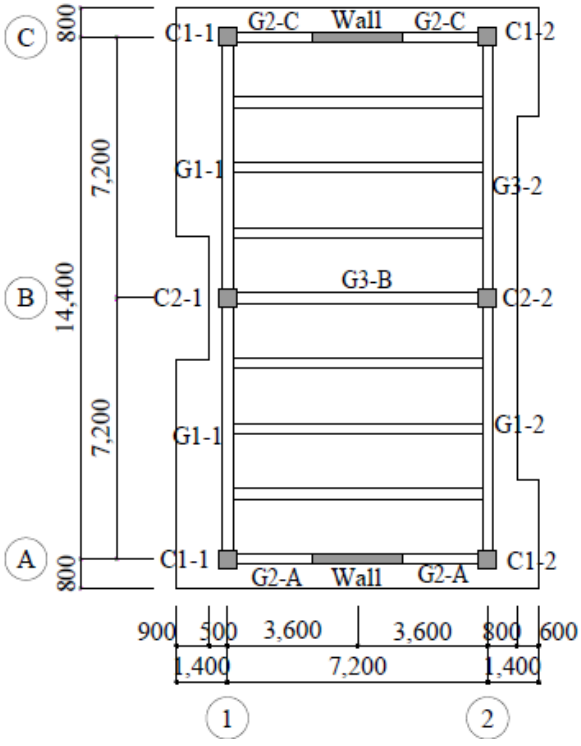

Figure 3-21 E-Defense RC Building—typical floor plan and member nomenclature (mm).

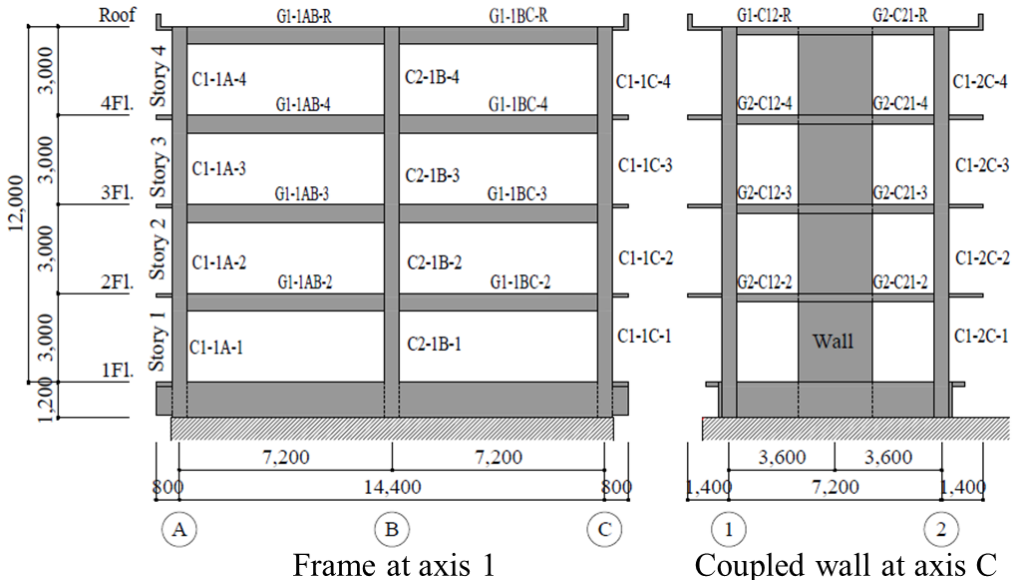

Figure 3-22 E-Defense RC Building—elevations and member nomenclature (mm).

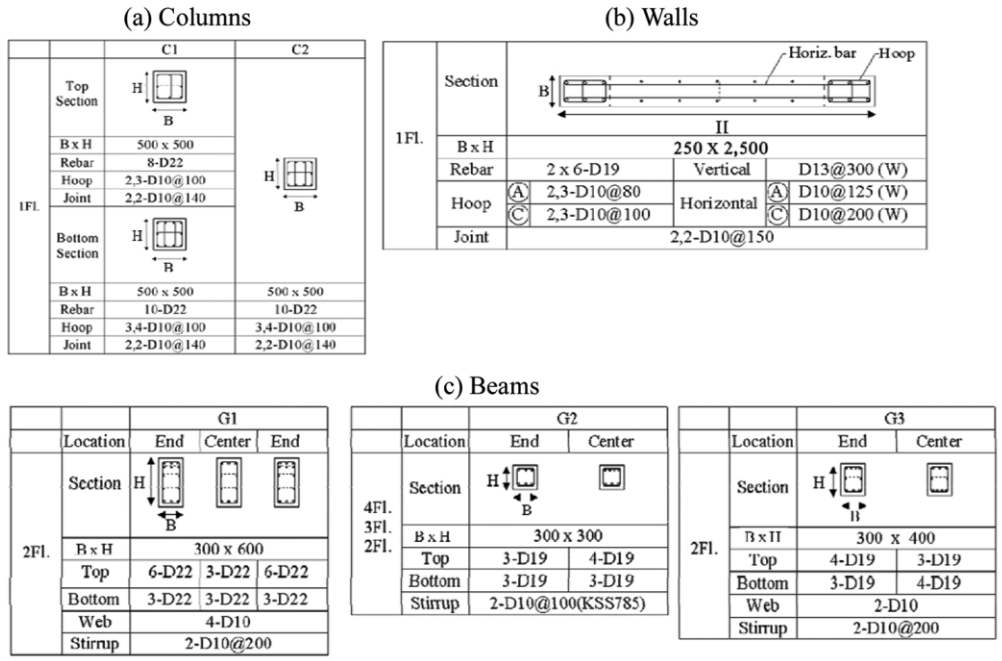

Figure 3-23 Reinforcement details (adapted from Nagae et al., 2015).

3.5.1.2 MATERIALS

The design values and testing results can be found in Wallace et al. (2011). For the purposes of this evaluation, the measured material strengths from testing were used for all elements. The measured mean compressive strengths of the concrete were 39.6 MPa, 39.2 MPa, 30.2 MPa and 41 MPa at

the first story and second floor, second story and third floor, third story and fourth floor, and. fourth story and roof, respectively. D19 (19 mm nominal diameter) and D22 (22 mm nominal diameter) reinforcing bars were the primary longitudinal reinforcement with measured yield strengths of 380 MPa and 370 MPa respectively. D10 bars with a measured yield strength of 388 MPa were the primary transverse reinforcement.

3.5.1.3 EARTHQUAKE LOADING

The structure was tested with two series of increasing ground motion intensities starting with 25%, 50%, and 100% JMA-Kobe followed by 40% and 60% JR-Takatori. The building was subjected to all three components of a ground motion simultaneously (including the vertical component). For the purposes of this study, the 100% JMA-Kobe record was used to evaluate members and for comparison to observed performance because significant nonlinear response was first observed during that test. The acceleration histories of the two horizontal components of the ground motion are shown in Figure 3-24. Figure 3-25 presents the response spectra with 5% damping for these ground motions.

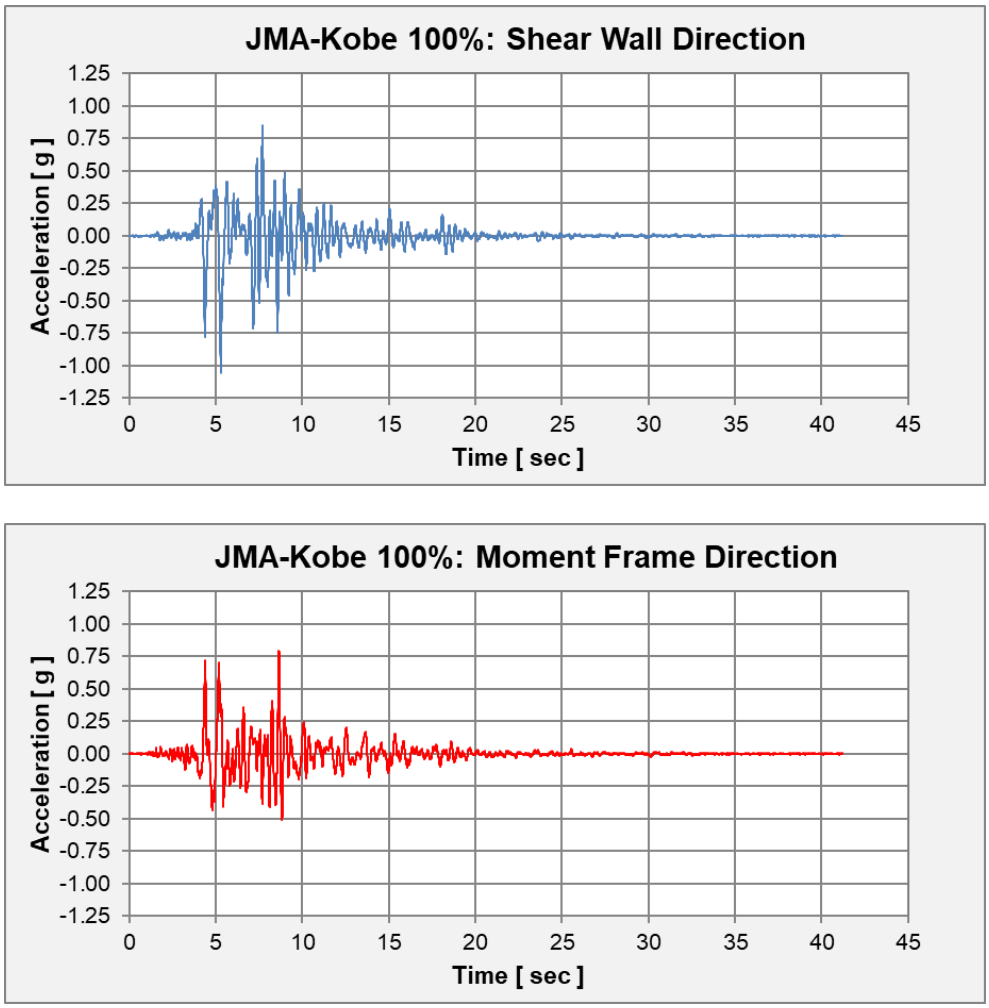

Figure 3-24 Truncated ground motion records for 100% JMA-Kobe (first 10 s truncated).

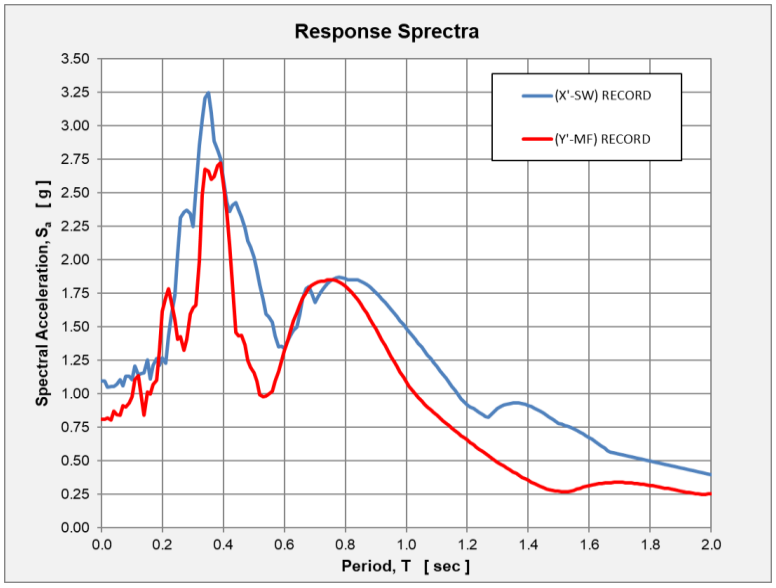

Figure 3-25 Response spectra for 100% JMA-Kobe (5% damping).

3.5.1.4.1 STRENGTH AND STIFFNESS

A linear dynamic analysis was performed using linear shell elements for the walls and linear frame elements for the beams and columns using CSI's ETABS software. Cracked stiffness assumptions were reduced to 0.25 times gross properties for flexural rigidity and using 0.15 times gross shear area.

The relevant demands and moment capacities for the concrete walls are reported in Table 3-6 below. It is noted that axial loads do not vary substantially from earthquake loading on walls.

Table 3-6 Characteristic Axial Demands and Moment Capacities in Wall Sections

Element	Story	N_{UD} (KN)	N_{UG} (KN)	M_{yE} (KN-m)	M_{uE} (KN-m)
Wall	1	333	275	2319	2533
	2	246	196	2252	2471
	3	160	113	2077	2289
	4	76	51	2141	2381

The shear strength is calculated as follows:

$$V_{CE} = \left(\alpha_c \sqrt{f'_{cE}} + \rho_t f_{ytE}\right) A_{cv}$$

$V_{CE} = \left(2\sqrt{5800\text{psi}} + (0.45\%)54{,}000\text{psi}\right)968\text{in}^2$

V_{CE} = 385 kips = 1710 kN

The shear friction strength based on the updated provisions results in 312 kips, where:

$V_{CE} = \mu A_{vf} f_{ylE}$ kips = 1.0(5.78in^2)(54,000psi)=312 kips = 1388 kN

Wall shear demand obtained from linear analysis is amplified by $\omega_v = 0.9 + \frac{4}{10} = 1.3$. With the linear analysis procedure, the shear demand at the base of the wall, scaled based on flexural yielding and then amplified by the shear amplification factor results in (145 kips) (1.3) = 189 kips = 841 kN.

3.5.1.5 CLASSIFICATION

Because the LDP requires an upper-bound and lower-bound gravity load combination which affects the wall moment capacity calculations, the wall demand-to-capacity ratios are higher in flexure in some cases, however shear-friction always governs the expected wall behavior based on ACI 369.1 Table 7.3.2a due to the application of the shear-amplification factor, ω_v. Table 3-7 and Table 3-8 summarize the resulting wall classifications and demand-to-capacity ratios (DCRs) corresponding to the previously identified wall labels. It is interesting to note based on the reported DCRs, the E-Defense building governing wall behavior is at the interface between shear-friction and flexure, which was also exhibited in the shake table experimental results: significant flexure action was intermixed with sliding at the wall base.

Table 3-7 Wall Classification

Wall Pier Definition	Controlling Behavior (M = Moment, V = Shear, S = Shear Friction / Sliding)	
	Load Combination: 0.9QD + QE	Load Combination: 1.1(QD + QL + QS) + QE
W-S2-A-01	S	S
W-S3-A-01	S	S
W-S4-A-01	S	S
W-S5-A-01	S	S
W-S2-C-01	S	S
W-S3-C-01	S	S
W-S4-C-01	S	S
W-S5-C-01	S	S

Table 3-8 Wall Demand-to-Capacity Ratios (DCRs) using Simple Shear-Friction Strength Equation

Wall Pier Definition	DCR			
	Load Combination: $0.9Q_D + Q_E$		Load Combination: $1.1(Q_D + Q_L + Q_S) + Q_E$	
	Shear Friction (S)	Moment (M)	Shear Friction (S)	Moment (M)
W-S2-A-01	7.4	8.9	7.4	7.8
W-S3-A-01	5.1	4.4	4.3	4.0
W-S4-A-01	2.4	2.2	2.3	2.0
W-S5-A-01	1.7	1.5	1.7	1.5
W-S2-C-01	7.4	8.9	7.4	7.8
W-S3-C-01	5.1	4.4	4.3	4.0
W-S4-C-01	2.4	2.2	2.3	2.0
W-S5-C-01	1.7	1.5	1.7	1.5

3.5.2 Evaluation Using Linear Dynamic Procedure

3.5.2.1 ANALYSIS MODEL

The ETABS LDP evaluation was performed with an updated model using the proposed modeling and acceptance criteria. All wall and other structural elements were modeled using elastic shell elements. For modeling using the updated provisions, wall stiffness, cracked wall stiffness was updated with a 0.25 cracked modifier for flexure and using $0.15E_{cE}$ for shear, or effectively a 3/8 modifier on shear modulus in accordance with the updated proposals. The analysis was also conducted using the past ASCE/SEI 41-17 cracked stiffness modifiers which were slightly higher at 0.35 for flexure and uncracked for shear.

3.5.2.2 ANALYSIS RESULTS

Figure 26 compares the drift demands calculated in the previous version in ASCE/SEI 41-17 (and related ACI 369-17 provisions) to the recorded shake table data. The increased drifts in the updated provisions have to do with the added requirement that the C_1 and C_2 coefficients must be calculated using the ASCE/SEI 41 equations as opposed to using default table values, which tends to have a more substantial effect in short-period buildings. The drifts were little different due to the reduced effective stiffness values.

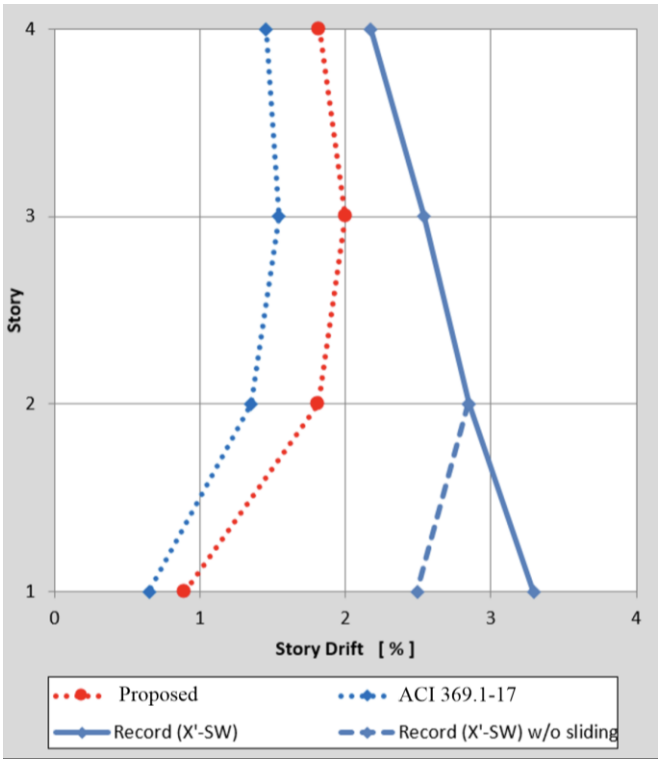

Figure 3-26 Drift demands using proposed provisions to ACI 369.1 relative to ASCE/SEI 41-17 provisions and experimental recorded data.

3.5.2.3 WALL PERFORMANCE ASSESSMENT

The proposed *m*-factors for shear-friction are reduced from the b_{nl}-parameters in the proposed ACI 369.1 Table 7.4.1.1.3 (1/2 and 5/8 for Life Safety and Collapse Prevention, respectively), shown below in Table 3-9. The 3% story drift governs the b_{nl}-parameter for the E-Defense building due to its short story heights, however the upper-bound 4 inches is likely to govern in most buildings.

Table 3-9 Shear Friction Modeling and Acceptance Criteria

Conditions		Sliding Displacements[a] (in.)			Strength Ratios		Acceptance Criteria		
Interface Type	$\frac{V_{CyfWallSE}{}^{b}}{w_v V_{MCyDE}}$	a_{nl}	a'_{nl}	b_{nl}	c'_{nl}	c_{nl}	IO	LS	CP
Monolithic or roughened to ¼ in. amplitude	≥ 1.0	0.65	1.30	$0.03h_s \leq$ 4.0 in.	1.10	0.50	0.1 a_{nl}	0.75 b_{nl}	b_{nl}
	≤ 0.5	0.20	0.40						
Other	≥ 1.0	0.80	1.60			0.60			
	≤ 0.5	0.40	0.80						

[a] Linear interpolation between values listed in the table shall be permitted.
[b] The shear amplification factor ω_v need not be applied if V_{MCyDE} is obtained from nonlinear analyses procedures.

After processing the reported DCRs relative to the proposed *m*-factors, the resulting "acceptance ratios," or DCR/*m*, are reported in Figure 3-27 below for CP *m*-factors and LS *m*-factors, respectively. The acceptance ratios indicate exceedance of the CP limit by 66%, which is high relative to the acceptance ratios using flexure in Section 2 of this report. It is noted however that substantial damage was exhibited in the E-Defense walls, and it appears that the dominant mechanisms are captured well in the updated provisions.

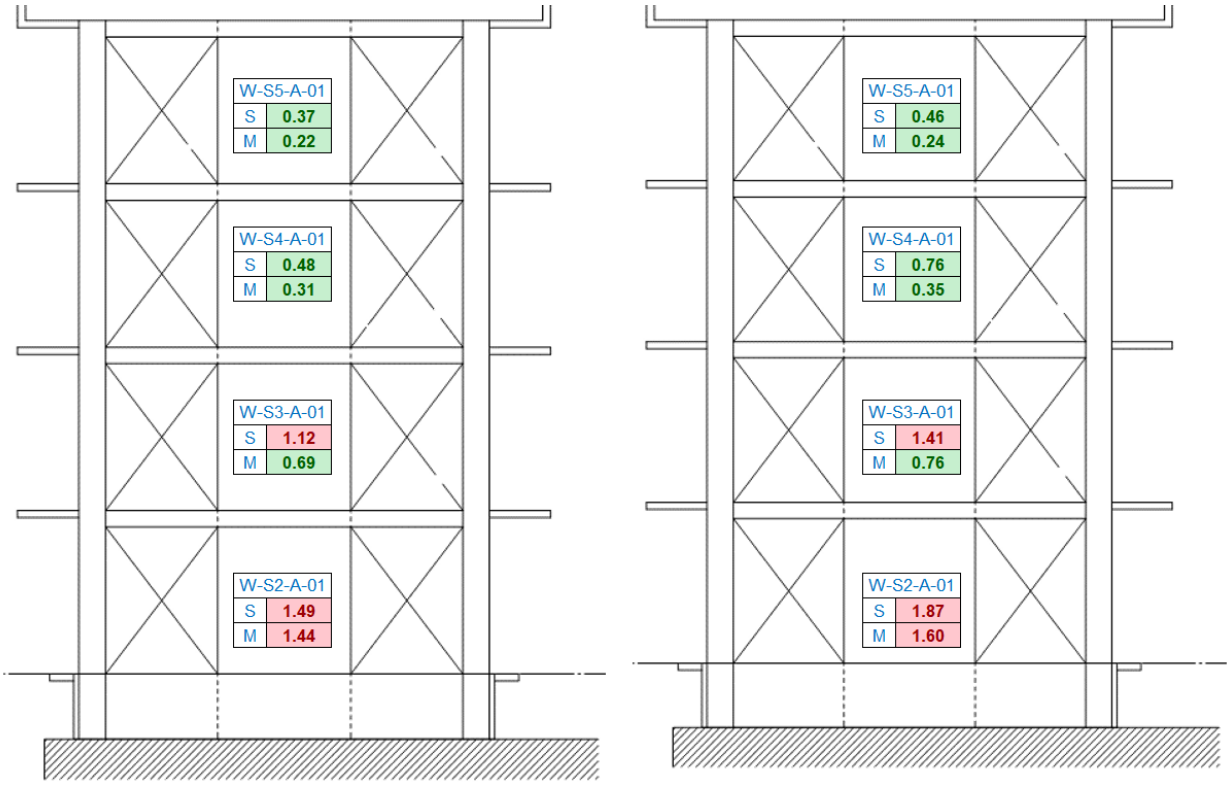

CP (m = 6) **LS (m = 4 ¾)**

Figure 3-27 Wall acceptance ratios.

3.5.2.4 DISCUSSION AND CONCLUSIONS

The previous ASCE/SEI 41-17 provisions would have referenced the ACI 318 equations for shear friction strength, and it would have likely been assumed a coefficient of friction of 1.0 could be used for a roughened cold joint at the wall to foundation interface. As such, flexure would have been the dominant wall classification. Given there was a mixture of flexural rocking and sliding observed from the test data, the mixed failure mode predicted by the separate analyses are both in line with the observed behavior. However, the updated provisions being more likely to predict sliding is likely a positive characteristic given once sliding initiates, it likely dominates the inelastic mode of deformation and performance should be classified accordingly. The updated provisions are likely to be modestly more conservative in most cases.

3.6 References

Abdullah, S. A., 2019, *Reinforced Concrete Structural Walls: Test Database and Modeling Parameters,* Ph.D. Dissertation*,* Dept. of Civil and Environmental Engineering, University of California, Los Angeles, California.

ACI, 1971, Building Code Requirements for Reinforced Concrete, ACI 318-71, Farmington Hills, MI.

ACI, 2017, Standard Requirements for Seismic Evaluation and Retrofit of Existing Concrete Buildings, ACI 369.1-17, Farmington Hills, MI.

ACI, 2019, Building Code Requirements for Structural Concrete, ACI 318-19, Farmington Hills, MI.

Anoda, J., 2014, Effect of Construction Interface and Arrangement of Vertical Bars on Slip Behavior of Shear Walls, Master's Thesis, Nagoya Institute of Technology, Nagoya, Japan. (in Japanese)

ASCE, 2017, Seismic Evaluation and Retrofit of Existing Buildings, ASCE/SEI 41-17, Reston, VA.

Baek, J., Park, H., and Yim, S., 2017, "Cyclic loading test for walls of aspect ratio 1.0 and 0.5 with Grade 550 MPa (80 ksi) Shear Reinforcing Bars," *ACI Structural Journal*, Vol. 114, No. 4, pp. 969-982.

Baek, J.W., Park, H.G., Lee, B.S., Shin, H. M., 2018, "Shear-friction strength of low-rise walls with 550 MPa (80 ksi) reinforcing bars under cyclic loading," *ACI Structural Journal*, V. 115, No. 1, pp. 65-78.

Baek, J., Kim, S., Park, H., and Lee, B., 2020, "Shear-friction strength of low-rise walls with 600 MPa Reinforcing Bars," *ACI Structural Journal*, V. 117, No. 1, pp. 169-182.

Birkeland, P. W., and Birkeland, H. W, 1966, "Connections in precast concrete construction," *ACI Journal Proceedings*, Vol. 63, No. 3, pp. 345-368.

British Standards Institution, 2003, "Eurocode 8: Design of Structures for Earthquake Resistance," European Committee for Standardization, Brussels, Belgium.

British Standards Institution, 2004, "Eurocode 2: Design of Concrete Structures - Part 1-1: General Rules and Rules for Building," European Standard EN-1992-1-1:2004:E, European Committee for Standardization, Brussels, Belgium.

CSA, 2004, *Design of Concrete Structures*, Canadian Standards Association, Rexdale, ON, Canada, 214 pp.

Elwood, K. J., Matamoros, A. B., Wallace, J. W., Lehman, D. E., Heintz, J. A., Mitchell, A. D., Moore, M. A., Valley, M. T., Lowes, L. N., Comartin, C. D., and Moehle, J. P., 2007, "Update to ASCE/SEI 41 concrete provisions," *Earthquake Spectra*, 23(3), 493-523.

FEMA, 1997a, *NEHRP Guidelines for the Seismic Rehabilitation of Buildings*, FEMA 273, Federal Emergency Management Agency, Washington, D.C.

FEMA, 1997b, *NEHRP Commentary on the Guidelines for the Seismic Rehabilitation of Buildings*, FEMA 274, Federal Emergency Management Agency, Washington, D.C.

Hofbeck, J. A., I. O. Ibrahim, and A.H. Mattock, 1969, "Shear transfer in reinforced concrete," *Journal of the American Concrete Institute, Vol* 66, No. 2, pp. 119-128.

International Federation for Structural Concrete (*fib*), 2013, "*fib* Model Code for Concrete Structures 2010," Wilhelm Ernst & Sohn, Berlin, Germany, 402 pp.

Kahn, L .F. and A. D. Mitchell, 2002, "Shear friction tests with high strength concrete," *ACI Structural Journal*, 99 (1): 98-103.

Kim, J.H. and Park, G.P., 2020, "Shear and shear-friction strengths of squat walls with flanges," *ACI Structural Journal*, V. 117, No. 6, pp. 269-280.

Korea Concrete Institute, "Concrete Design Code and Commentary," Kimoondang, Korea, 2012, 599.

Mattock, A. H., 1976, *Shear Transfer under Monotonic Loading Across an Interface Between Concretes Cast at Different Times*, Department of Civil Engineering report SM 76-3, Seattle, WA: University of Washington.

Mattock, A. H., 1977, "Considerations for the design of precast concrete bearing wall buildings to withstand abnormal loads," *PCI Journal*, 22 (3): 105-106.

Paulay, T., Priestley, M.J.N., and Paulay, T., 1982, "Ductility in earthquake resisting squat shear walls," *ACI Structural Journal,* Vol. 79, No. 4, pp. 257-269.

Pilette, C.F., 1988, *Behavior of Earthquake Resistant Squat Shear Walls*, Master's Dissertation, University of Ottawa, Ottawa, Canada, pp. 1-130.

Ramarozatovo, R., Hosono, J., Kawai, T., Takahashi, S., and Ichinose, T., 2016, "Effects of construction interfaces and axial loads on slip behavior of RC shear walls," *Proceedings*, The 5th International Congress on Engineering and Information, Kyoto, Japan, pp. 1-12.

Wasiewicz, Z., 1988, *Sliding Shear in Low Rise Shear Walls under Lateral Load Reversals*, Master's Dissertation, University of Ottawa, Canada, pp. 1-127.

Wiradinata, S., 1985, *Behavior of Squat Walls Subjected to Load Reversals*, Master's Dissertation, University of Toronto, Toronto, Canada, pp. 1-171.

Chapter 4: Revisions to Concrete Structural Wall Classification

4.1 Motivation

The procedures for classifying walls into flexure- or shear-controlled behaviors are not specified in the provisions of ACI 369.1-17 or ASCE/SEI 41-17, with only commentary provided indicating that the wall height-to-length aspect ratio could be used to differentiate behaviors. This recommendation for classifying wall behavior is shown in this chapter to have limited accuracy.

Note about the Relation Between the ASCE/SEI 41 and ACI 369.1 Standards

The concrete wall provisions contained in Section 10.7 of ASCE/SEI 41-17 were reproduced from Chapter 7 of the new ACI 369.1-17 Standard, based on a Memorandum of Understanding between ACI and ASCE. In 2021, however, the ASCE/SEI 41 Standard Committee elected to reference the next version of ACI 369.1 directly, without replicating its contents, making ACI 369.1 the reference standard for concrete members for ASCE/SEI 41. The proposed changes were therefore submitted to ACI's Seismic *Repair and Rehabilitation* Code committee 369 for possible adoption.

4.2 Summary of Recommended Changes

An extensive database developed by Abdullah (2019) with over 1,100 concrete wall tests spurred a comprehensive review of all structural wall provisions, and the addition of new provisions related to wall sliding and wall modeling. Proposed modeling parameters and acceptance criteria are presented for flexure-controlled, shear-controlled, and shear friction-controlled walls are presented in Part 4 Chapter 1, 2, and 3, respectively. Presented in this chapter is the change proposal that introduces new wall classification procedures based on the relative strengths of various mechanisms. Proposed moment, shear, and shear-friction strengths are used to identify the weakest action according to which a wall is classified. Wall classification directs users to the appropriate provisions based on their expected mode of strength degradation. The strengths used for classification are based on expected material properties since all actions with modeling parameters and acceptance criteria are treated as deformation controlled in ACI 369.1-17. Validation of the proposed wall classification provisions is presented in this chapter.

4.3 Technical Studies

4.3.1 Wall Database

The main database described in Chapter 1 of Part 4, which contains detailed information and test results on more than 1,100 wall tests reported in the literature (Abdullah, 2019; Abdullah and Wallace, 2019), was used. Database information related to the objectives of this study are briefly presented below; however, detailed information about the database can be found elsewhere (Abdullah, 2019; Abdullah and Wallace, 2019).

The reported failure modes are classified in the database as presented in Table 4-1 and illustrated in Figure 4-1, Figure 4-2, and Figure 4-3. Abdullah (2019) validated the reported failure mode with observed wall response and damage, before recording that information in the database.

Table 4-1 Wall Failure Modes in Database

Primary Classification	Sub-Classification
Flexure	Bar buckling and concrete crushing Bar fracture Global or local instability
Shear	Diagonal tension Diagonal compression (web crushing) Shear sliding at the base
Flexure-Shear	Yielding in flexure prior to shear degradation
Lap-Splice	-

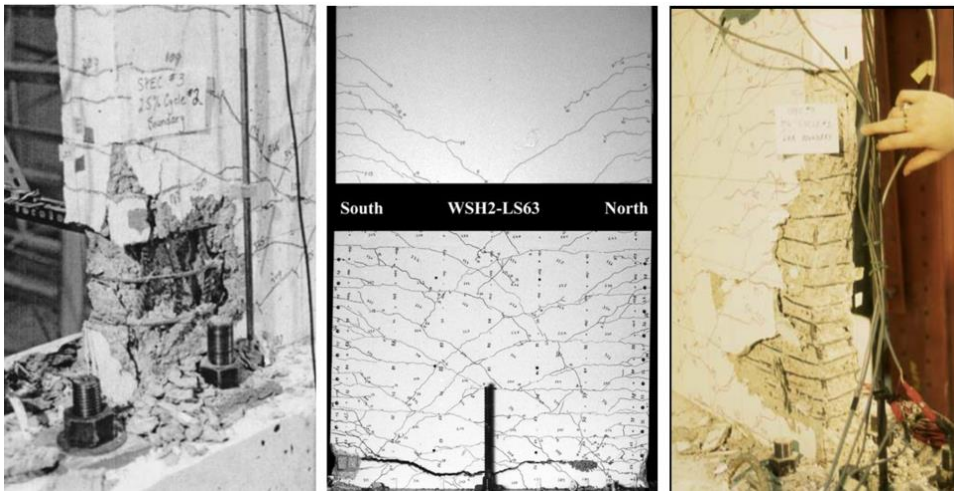

(*a*) (*b*) (*c*)

Figure 4-1 **Wall flexural failure modes: (*a*) bar buckling and concrete crushing (Thomsen and Wallace, 1995), (*b*) bar fracture (Dazio et al., 2009), and (*c*) lateral instability (Thomsen and Wallace, 1995).**

(a) (b) (c)

Figure 4-2 **Wall shear failure modes: (*a*) diagonal tension (Mestyanek, 1986), (*b*) diagonal compression (Dabbagh, 2005), and (*c*) shear-sliding (Luna, 2015).**

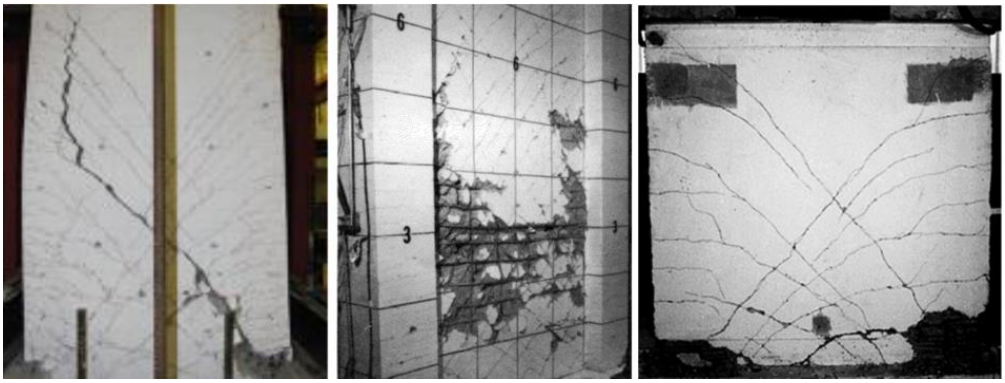

(*a*) (*b*) (*c*)

Figure 4-3 **Wall flexure-shear failure modes: (*a*) flexure-diagonal tension (Tran, 2012), (*b*) flexure-diagonal compression (Oesterle et al., 1976), and (*c*) flexure-shear-sliding (Salonikios et al., 1999).**

For validating the proposed wall classification provisions, the database was filtered to obtain a dataset of approximately 1,000 wall tests with reported flexure, shear, flexure-shear, or shear-friction failure modes. Omitted tests were for walls sustaining lap-splice failure, and walls that were not tested to failure or to at least 10% lateral strength degradation. Figure 4-4 presents histograms of key attributes of the walls in the filtered dataset.

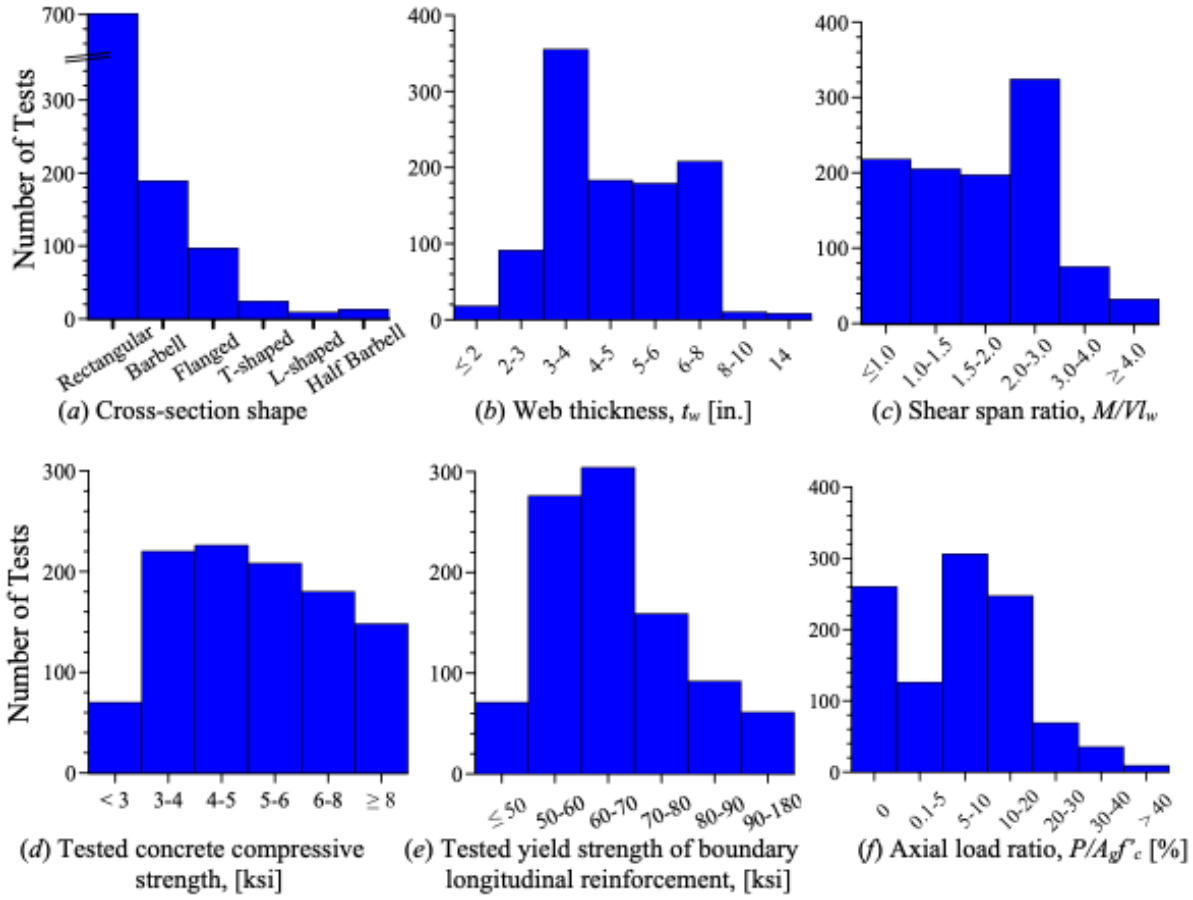

Figure 4-4 Histograms of wall tests in the dataset used in this study.

4.3.2 Proposed Wall Classification Approach

4.3.2.1 DATA ANALYSIS

For each reported failure mode, $V_{peak,test}/V_{MCyDE}$ is plotted versus V_{CE}/V_{MCyDE} in Figure 4-5. Figure 4-6 combines the data in Figure 4-5 into one plot. V_{CE} is the shear yield strength computed using the simplified shear strength equation in Chapter 2 (V_{CE} is the least of $V_{CydWallE}$ and $V_{CyfWallE}$), $V_{peak,test}$ is the peak wall shear measured during a test, and V_{MCyDE} is the shear demand at the yield moment calculated using expected material properties and ACI 318-19 procedures. From these figures, it can be seen that almost all flexure-controlled walls have a shear strength-to shear-demand ratio (V_{CE}/V_{MCyDE}) > 1.0. Walls with failure modes reported as flexure-shear are mainly scattered between 0.7 < V_{CE}/V_{MCyDE} < 1.3 (Figure 4-7*d*). While shear-controlled walls for the most part have (V_{CE}/V_{MCyDE}) < 1.0. Figure 4-6 also reveals that using V_{MCultE} (shear demand at ultimate moment strength as

defined in Chapter 1) instead of V_{MCyDE} or effectively V_{CE}/V_{MCyDE} = 1.15 provides a reasonable delineation between flexure-controlled and flexure-shear controlled walls.

A rearranged presentation of the results is given in Figure 4-7, where the vertical axis corresponds to the shear-friction-strength computed using the simplified equation in Chapter 3 ($V_{CyfWallE}$) normalized by the simplified diagonal shear strength equation from Chapter 2 ($V_{CydWallE}$). It can be seen in the figure that the data are divided between three regions: (1) blue region: flexure-controlled walls with V_{CE}/V_{MCyDE}> 1.0, (2) red region: diagonal shear-controlled walls (due to failure of diagonal tension or compression strut) with $V_{CE}/V_{MCyDE}\leq$ 1.0 and $V_{CyfWallE}/V_{CydWallE} \geq$ 1.0, and (3) yellow region: sliding shear-controlled walls with $V_{CE}/V_{MCyDE}\leq$ 1.0 and $V_{CyfWallE}/V_{CydWallE}$ < 1.0.

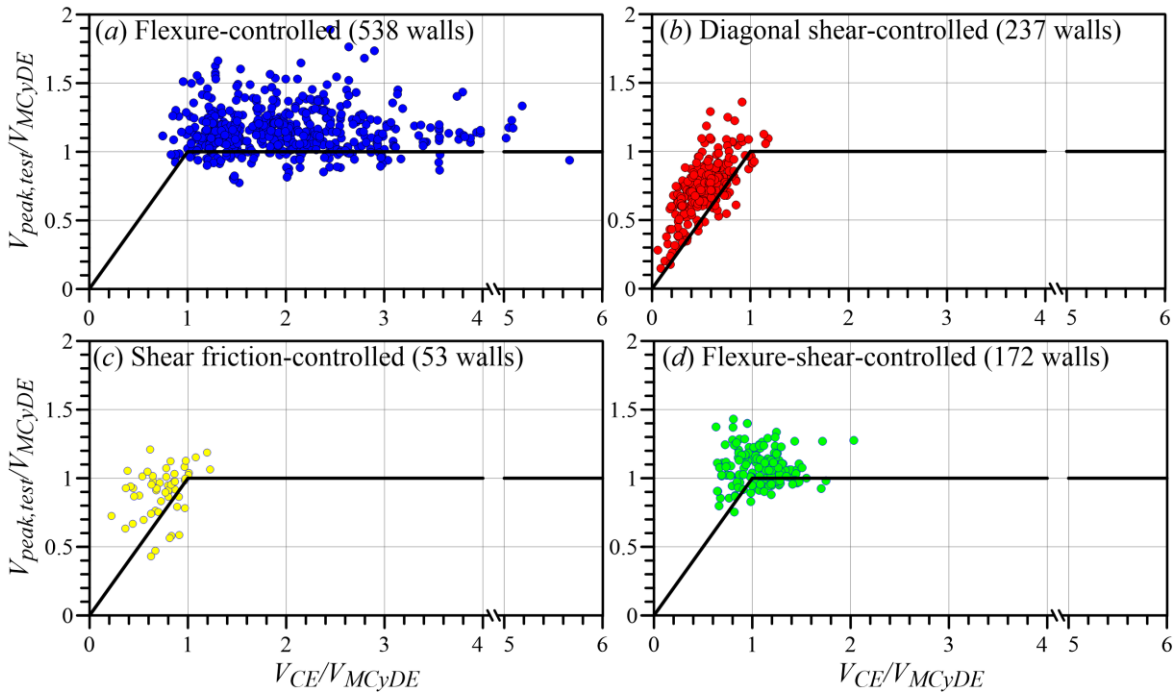

Figure 4-5 Wall failure mode results from a dataset of over 1,100 wall tests: failure modes separated.

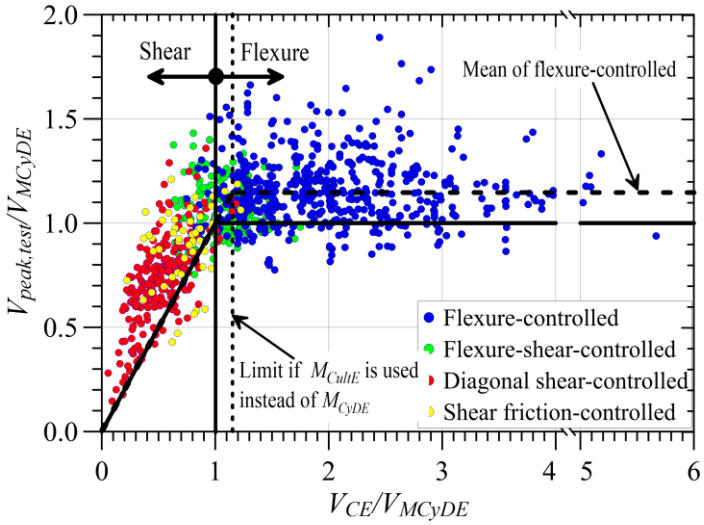

Figure 4-6 **Wall failure modes results from a dataset of over 1,100 wall tests: failure modes combined.**

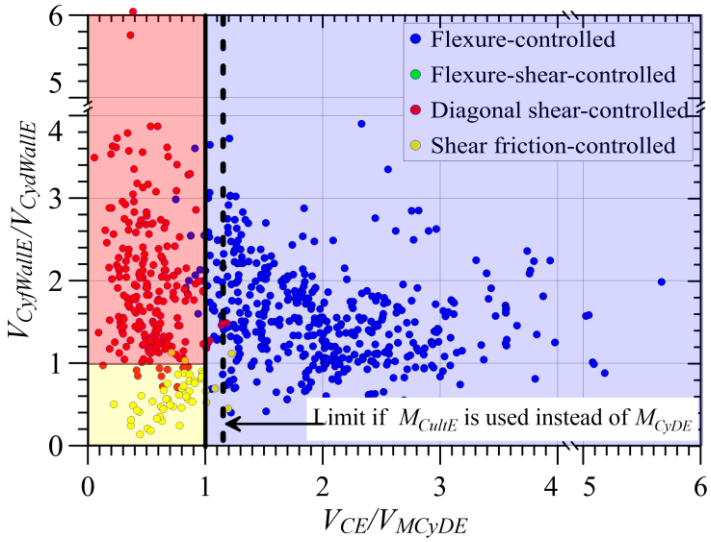

Figure 4-7 **Wall classification: blue region = flexure-controlled, red region= shear-controlled (diagonal tension or compression), and yellow region= shear sliding at the base.**

4.3.2.2 WALL CLASSIFICATION

Experimental results from the database presented in the preceding section indicate that walls can be classified as shear- or flexure-controlled based on their shear strength to shear demand ratio. While delineation between shear and shear-friction (or sliding) modes can be done by identifying the weaker of the diagonal shear strength ($V_{CydWallE}$) or the sliding shear strength ($V_{CyfWallE}$) of a wall.

The approach given in Table 4-2 is therefore proposed to classify wall failure modes and is based on the relative strengths of the various modes. It is noted that to minimize the likelihood of shear-controlled walls being classified as flexure-controlled and be given more liberal drift capacities, the delineating ratio between the two modes $V_{CE}/(\omega_v V_{MCyDE})$ was selected to be equal to and greater

than 1.15 (i.e., $V_{CE}/(\omega_v V_{MCultE}) \geq 1.0$). To use Table 4-2, the user needs to estimate the shear demands at the wall critical section using either linear static or linear dynamic analysis approach, amplify the estimated shear demands to account for the effects of higher modes on shear demands, if using linear analyses, and then compare these demands with the wall shear strengths to determine the expected dominant behavior. According to the expected dominant behavior, wall nonlinearity can be modeled using the applicable modeling parameters proposed in Chapters 1, 2, and 3.

Table 4-2 Criteria for Determining the Expected Wall Dominant Behavior

Criteria		Expected Controlling Behavior
$V_{CE}/(\omega_v V_{MCyE}) < 1.15$	$V_{CydWallE} \leq V_{CyfWallE}$	Shear-controlled
	$V_{CydWallE} > V_{CyfWallE}$	Shear-friction-controlled
$V_{CE}/(\omega_v V_{MCyE}) \geq 1.15$		Flexure-controlled

When the Linear Static Procedure or Linear Dynamic Procedure of ASCE/SEI 41-17 are used, the resulting wall effective height (h_{eff}) that allows the calculating of shear demand at flexural yielding (i.e., $V_{MCyDE} = M_{CyDE}/h_{eff}$) does not fully capture the effects of higher modes. Linear analyses methods do not account for the dynamic amplification of wall shear demands due to higher mode responses of walls, especially those softening due to flexural yielding.

Research has shown that dynamic shear amplification is strongly correlated with building period, which is a function of building height (Paulay (1986), Munshi and Ghosh (2000), Fischinger et al. (2010), Kim and Wallace (2016). Therefore, the following simplified dynamic shear amplification factor (ω_v) computed from Eq. 4-1 is proposed to amplify V_{MCyDE} and V_{MCultE}. This approach, which is aligned with the approaches in New Zealand and Canadian codes (NZS 3101-2006 and CSA A23.3-2014, respectively), has been adopted in ACI 318-19 in Section 18.10.3.

$$w_v = 0.9 + \frac{n_s}{10} \text{ for } n_s \leq 6$$
$$w_v = 1.3 + \frac{n_s}{30} \text{ for } n_s > 6 \quad (4\text{-}1)$$

Where n_s is the number of stories above the critical section and should not be taken less than 0.007 times the wall height above the critical section (h_{wcs}) measured in inches. This limit is imposed on n_s to account for buildings with large story heights (i.e., > 12 ft. (144 in.)).

It is noted that this new provision in ACI 318-19 also includes shear amplification due to moment overstrength. However, since expected material strengths are used to compute M_{CyDE}, and M_{CyDE} is

amplified (by 1.15) to obtain M_{CultE}, the moment overstrength amplification factor is not considered here.

4.3.3 Validation of Proposed Classification Approach and Comparison with ACI 369.1-17 Approach

Table 4-3 compares the predicted failure modes of wall specimens using Table 4-2 with reported failure modes. The figure indicates that the proposed approach accurately captures the dominant behavior (and failure mode) of the wall specimens, especially for flexure- and diagonal shear-controlled walls (more than 90% of the walls are classified accurately). For shear-friction-controlled walls, about 80% of the data was classified accurately. For the flexure-shear-controlled walls, 57% are predicted as shear-controlled, whereas 37% are predicted as flexure-controlled. A flexure-shear classification is not provided in the proposed classification approach. Therefore flexure-shear controlled walls are expected to be split into the shear- and flexure-controlled classifications.

Figure 4-10 shows the distribution of reported failure modes of the walls in the dataset versus test shear-span-ratio (M/Vl_w or h_{eff}/l_w) and V_{CE}/V_{MCyDE}. This figure reveals that M/Vl_w, which is closely related to aspect ratio (h_w/l_w) recommended in ACI 369.1-17 for wall classification, is not as good of an indicator of wall dominant behavior particularly for walls of intermediate aspect ratios with $1.0>M/Vl_w<3.0$. However, this figure also shows that most walls with $M/Vl_w \geq 3.0$ sustained a flexure mode of failure and those with $M/Vl_w < 1.0$ sustained a shear failure mode.

Table 4-3 Predicted (using Table 4-1) Versus Experimental Failure Modes

		Estimated Flexure	Estimated Shear	Estimated Shear-Friction	SUM
Experimental Flexure	No. of Tests	489	33	2	524
	Percentage	**93.3%**	6.3%	0.4%	100%
Experimental Diagonal Shear	No. of Tests	2	241	10	253
	Percentage	0.8%	**95.3%**	4.0%	100%
Experimental Shear-Friction	No. of Tests	3	11	55	69
	Percentage	4.3%	15.9%	**79.7%**	100%
Experimental Flexure-Shear	No. of Tests	74	115	11	200
	Percentage	37.0%	57.5%	5.5%	100%
SUM		568	400	78	1046

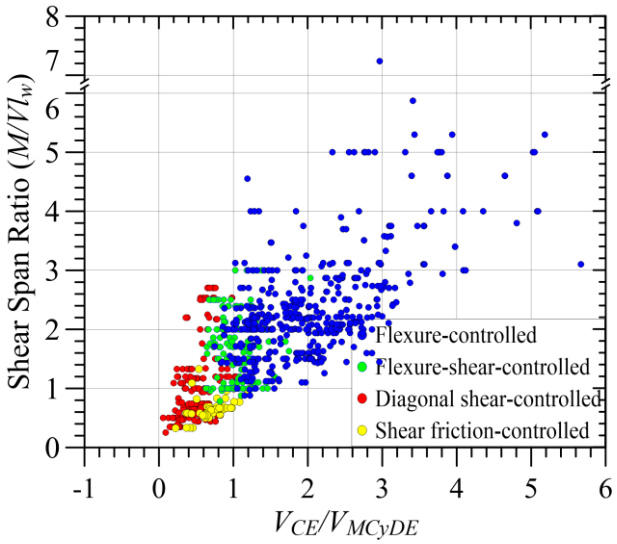

Figure 4-8 Variation of wall failure mode versus shear-span-ratio (M/Vl_w) and shear-flexure strength ratio (V_{CE}/V_{MCyDE}).

4.3.4 Conclusions

A strength-based approach is proposed to quantitatively distinguish between various wall strength degradation modes. The proposed methodology identifies the weakest mode by comparing flexure, shear, and shear-friction strengths of walls to classify them as flexure-controlled, shear-controlled, and shear-friction-controlled. Results from a dataset of about 1,000 concrete wall tests indicated that the shear span ratio (h_{eff}/l_w), which is similar to the aspect ratio (h_w/l_w) that is recommended in ACI 369.1-17 for wall classification, is not a good indicator of the expected wall dominant behavior and failure mode. This is particularly the case for walls with intermediate height-to-length aspect ratios between 1.0 and 3.0.

4.4 Recommended Changes

Note about Change Proposals

This chapter documents aspects of change proposals as they were submitted to ACI's *Seismic Repair and Rehabilitation* Code Committee 369 for possible adoption. Often, these change proposals were revised, in some cases substantively, by this committee before they were adopted into ACI 369.1-22. Readers should not rely on this chapter for information about the final version of provisions in ACI 369.1-22.

4.4.1 Strength-Based Classification

The change proposal for classifying walls based on their expected mode of strength degradation (or failure) is presented below.

Due to the re-organization of the wall Chapter 7 in ACI 369.1-17, much of the existing standard text was moved, with some being modified, some being deleted, and some new text introduced. To aid in identifying existing and new text, the following color scheme is used. Green text is existing text in ACI 369.1-17, which was moved in the new organization. Blue text indicates text that was either modified or newly introduced.

7.3.2 *Acceptance Criteria* –The controlling behavior for structural walls and wall segments shall be in accordance with Table 19. Structural walls with h_w/l_w smaller than 1.0 shall be permitted to be classified as shear controlled.

Table 19–Structural wall and wall segment controlling behavior classification

Criteria		Expected Controlling Behavior
$V_{CE}/(\omega_v V_{MCultE}) < 1.0$	$V_{CydWallE} \le V_{CyfWallE}$	Shear-controlled
	$V_{CydWallE} > V_{CyfWallE}$	Shear-friction-controlled
$V_{CE}/(\omega_v V_{MCultE}) \ge 1.0$		Flexure-controlled

The ~~nominal~~ maximum expected flexural strength of a structural wall or wall segment, M_{CultE}, shall be used to determine the maximum expected shear demand ~~force~~ in structural walls and wall segments, V_{MCultE}, for the purpose of determining the controlling behavior. For cantilever structural walls, the ~~design~~ maximum expected shear demand ~~force~~, V_{MCultE}, shall not be less than the magnitude of the lateral force required to develop the ~~nominal~~ maximum expected flexural strength, M_{CultE}, at the ~~base of the~~ wall~~, assuming that the lateral force is distributed uniformly over the height of the wall~~ critical section ~~using the linear analysis procedures from ASCE/SEI 41-17 Chapter 7 and amplified by the dynamic shear amplification factors in Eq. 8~~, but need not exceed the maximum load that can be delivered to the wall segment. For non-cantilever wall segments, the maximum expected shear demand ~~force~~, V_{MCultE}, shall be equal to the shear corresponding to the development of the positive and negative maximum expected flexural strengths at opposite ends of the wall segment, but need not exceed the maximum load that can be delivered to the wall segment. Shear demands need not exceed the maximum demand from analysis. The dynamic shear amplification factor (ω_v) in Table 19 shall be determined from Equation 5.

$$\omega_v = 0.9 + \frac{n_s}{10} \qquad \text{for } n_s \le 6 \qquad (5a)$$

$$\omega_v = 1.3 + \frac{n_s}{30} \qquad \text{for } n_s > 6 \qquad (5b)$$

Design actions (flexure, shear, axial, or force transfer at reinforcing bar anchorages and splices) on components shall be determined as prescribed in Chapter 7 of ASCE 41-17. Where determining the appropriate value for the design actions, proper consideration shall be given to gravity loads and to the maximum forces that can be transmitted considering nonlinear action in adjacent components. Design actions shall be compared with strengths in accordance with Section 7.5.2.2 of ASCE 41-17. Tables 20 and 21 specify m-factors for use in Equation (7-36) of ASCE 41-17. Alternatively, in place of Table 20, it shall be permitted to use applicable m-factor values from Tables 22 and 23 for wall controlled by flexure. Alternate m-factors shall be permitted where justified by experimental evidence and analysis.

4.5 References

Abdullah, S. A., 2019, *Reinforced Concrete Structural Walls: Test Database and Modeling Parameters,* Ph.D. dissertation, Dept. of Civil and Environmental Engineering, University of California, Los Angeles, California.

Abdullah S. A., and J. W. Wallace, 2019, "Drift capacity of RC structural walls with special boundary elements," *ACI Structural Journal*, Vol. 116, No 1, pp. 183–194. https://doi.org/10.14359/51710864.

ACI, 2017, *Standard Requirements for Seismic Evaluation and Retrofit of Existing Concrete Buildings, ACI 369.1-17*, American Concrete Institute, Farmington Hills, MI.

ACI, 2019, *Building Code Requirements for Structural Concrete*, ACI 318-19, American Concrete Institute, Farmington Hills, MI.

ASCE, 2017, *Seismic Evaluation and Retrofit of Existing Buildings*, ASCE/SEI 41-17, American Society of Civil Engineers, Reston, VA.

Canadian Standards Association (CSA), 2014, *CAN/CSA-A23.3-14 Design of concrete structures*, 352 pp.

Dabbagh, H., 2005, *Strength and Ductility of High-Strength Concrete Shear Walls Under Reversed Cyclic Loading*, Ph.D. Dissertation, School of Civil and Environmental Engineering, The University of New South Wales, Sydney, Australia.

Dazio, A, Beyer, K., and Bachmann, H, 2009, "Quasi-static cyclic tests and plastic hinge analysis of RC structural walls," *Engineering Structures*, Vol.31, No. 7, pp. 1556-1571.

Fischinger M, Rejec K, and Isaković T, 2012, "Modeling inelastic shear response of RC walls," *Proceedings of the 15th World Conference on Earthquake Engineering*, Lisbon, Portugal, No. 2120.

Hognestad, E., 1951, *A Study of Combined Bending and Axial Load in Reinforced Concrete Members*, *Bulletin No. 399*, University of Illinois Engineering Experimental Station, IL.

Kim, S. and Wallace J,W,, 2017, "Shear design of structural walls for tall reinforced concrete buildings," *Proceedings of the 16th World Conference on Earthquake Engineering*, Santiago, Chile, January, 10 pp.

Luna, B. N., 2015, *Seismic Response of Low Aspect Ratio Reinforced Concrete Walls for Building and Safety-Related Nuclear Applications*, Ph.D. Dissertation, Department of Civil, Structural and Environmental Engineering, University at Buffalo.

Mattock, A.H., 2001, "Shear friction and high-strength concrete," *ACI Structural Journal*, Vol. 98, No. 1, pp. 50–59.

Mestyanek, J. M., 1986, *The Earthquake of Resistance of Reinforced Concrete Structural Walls of Limited Ductility*, Master's Thesis, University of Canterbury, Christchurch, New Zealand.

Munshi J, and Ghosh SK, 2000, "Displacement-based design for coupled core walls," *Earthquake Spectra*, 16(3), pp. 621 – 642.

NZS 3101, 2006, *Concrete Structures Standard, Part 1: The Design of Concrete Structures: Part 2: Commentary on the Design of Concrete Structures*, Standards New Zealand, Wellington, New Zealand. ISBN 1-86975-043-8.

Oesterle, R.G., Fiorato, A.E., Johal, L.S., Carpenter, J.E., Russell, H.G., and Corley, W.G., 1976, *Earthquake Resistant Structural Walls–Tests of Isolated Walls, Report to National Science Foundation,* Construction Technology Laboratories, Portland Cement Association, Skokie, IL, 315 pp.

Paulay T, 1986, "The design of ductile reinforced concrete structural walls for earthquake resistance," *Earthquake Spectra*, 2(4), pp. 783–823.

Salonikis, T., Kappos, A., Tegos, I. and Penelis, G., 1999, "Cyclic load behavior of low-slenderness reinforced concrete walls: design basis and test results," *ACI Structural Journal*, Vol. 96, No. 4, pp. 649–661.

Thomsen, J. H. and Wallace, J. W., 1995, *Displacement-Based Design of Reinforced Concrete Structural Walls: Experimental Studies of Walls with Rectangular and T-Shaped Cross Sections, Report No. CU/CEE-95/06*, Department of Civil and Environmental Engineering, Clarkson University, Potsdam, NY.

Tran, T. A., 2012, *Experimental and Analytical Studies of Moderate Aspect Ratio Reinforced Concrete Structural Walls*, Ph.D. Dissertation, University of California, Los Angeles, CA, 300 pp.

Part 5

Chapter 1: Update to Common Building Type Definitions

1.1 Motivation

The Common Building Type (CBT) definitions in ASCE/SEI 41-17 (ASCE, 2017) Chapter 3 have been in ASCE/SEI 41 and its predecessor documents from the time they were initially developed as guidelines for the seismic evaluation of existing buildings. Because of this long history, the definitions have features that are not consistent with standards language requirements, and contain text that is sometimes unclear, inconsistent, or unenforceable. The general goal of this task is to develop improved, standard-compliant text for the CBT definitions in ASCE/SEI 41-17 Table 3-1.

A secondary motivation, identified during the review of ASCE/SEI 41-17 Table 3-1, is to improve the definitions for the three wood-framed CBT (W1, W1a, W2), including eliminating overlaps and gaps in the definitions. The intent is to improve the clarity and consistency of assigning wood-framed buildings to the appropriate CBT.

1.2 Summary of Changes Recommended

In general, the proposed changes include a complete update of ASCE/SEI 41-17 Table 3-1 and creation of a new commentary Table C3-1. The changes are primarily editorial, consisting of moving text from the provisions table to the new commentary table and then making additional updates to the provisions text in ASCE/SEI 41-17 Table 3-1. The main technical change is the elimination of CBT W1a by combining it with W2.

1.3 Technical Studies

1.3.1 Updates to ASCE/SEI 41-17 Table 3-1

As the purpose of this task is largely editorial, intended to improve the text for usability, consistency, and enforceability, there were no specific technical studies associated with this task. The Working Group 4 members focused their efforts on editorial reorganization and rewriting of ASCE/SEI 41-17 Table 3-1 and separating the commentary text into a new Table C3-1.

The process included an initial pass at ASCE/SEI 41-17 Table 3-1 to delete non-standard language and move it to the new commentary table. An additional editorial pass was made to the commentary table to improve the clarity and flow of the text. This necessitated some duplication of the text of Table 3-1 in Table C3-1.

1.3.2 Updates to Wood-Framed Common Building Types

The studies related to the wood-framed CBT primarily involved group discussions related to user experience with the CBT definitions in their practice. These discussions identified the following topics for update and clarification:

- The floor area for the definitions of W1 and W1a in ASCE/SEI 41-17 Table 3-1 were unclear and potentially inconsistent. The definition for W1 indicates "plan areas of less than or equal to 3,000 ft^2 (280 m^2)" whereas the definition of W1a indicates "plan areas on each floor of more than 3,000 ft^2 (280 m^2)." Presumably the intent of W1 is area per floor, but the text is not clear.

- If the area for W1 is per floor and there is no limit on number of stories (the text reads "one or more stories high"), then W1 could in theory include very large dwellings, say 4 stories at 3,000 square feet per floor, which is probably beyond the intent of the W1 definition.

- Many new, large dwellings can have large open spaces, supplemental steel framing, and other features probably not intended by the original definition of W1, so it was judged important to have some upper limit on the size of W1 buildings for this definition.

- As defined in ASCE/SEI 41-17 Table 3-1, W1a appears intended generally for multiunit residential and not simply large, single-family dwellings, so essentially the larger single-family dwellings would not meet any of the CBT definitions.

- As defined in ASCE/SEI 41-17 Table 3-1, W2 only includes commercial and industrial occupancies. However, there are other common occupancies for non-residential wood-framed, for example medical, education, and religious.

- As defined in ASCE/SEI 41-17 Table 3-1, W2 only includes buildings "with a floor area of 5,000 ft^2 (465 m^2) or more." Therefore, smaller, non-residential wood-framed buildings cannot be included in the CBT definitions.

In a practical sense, the only difference in the application of ASCE/SEI 41-17 for the three wood-framed building types is the Benchmark Building criteria. CBT W1 and W1a share the same Tier 1 checklist and W2 has separate checklists but the statements are identical to the others. For benchmarking, in accordance with ASCE/SEI 41-17 Table 3-2, W1 and W2 are benchmarked to the *1976 Uniform Building Code* (UBC) (ICBO, 1976) and other comparable code editions while W1a is benchmarked to the 1997 UBC (ICBO, 1997) and other comparable code editions. The reason for the two different benchmark dates is to avoid benchmarking older W1a multi-unit residential buildings with the potential for soft and/or weak first stories (underscored in the 1994 Northridge earthquake and corrected by provisions introduced into the 1997 UBC).

During discussions to expand the definition of W2 to include other occupancies, it was also reasoned that the types of construction, configurations, and expected seismic performance in the newly expanded W2 definition could be very broad. Therefore, it was judged appropriate to revise the

Benchmark Building code for the W2 buildings. Benchmarking to the 1997 UBC (and other comparable code editions) similar to W1a was judged reasonable and appropriate.

The result of these studies was a recommendation to revise the definition of W1 to include what are essentially small-to-medium dwellings (the original intent of W1 when CBTs were developed) and include all other types of wood-framed buildings in W2, thereby eliminating W1a. Essentially, W1 includes dwellings of the type covered by the *International Residential Code* (IRC) (ICC, 2018), and W2 includes all other wood structures (subject to the limitations of the W2 definition). This has no impact on the checklists, and the only impact on the Benchmark Building criteria is to change W2 to the 1997 UBC instead of the 1976 UBC. The resulting definitions are more clear, consistent, and inclusive.

1.4 Recommended Changes

Note about Change Proposals

This report documents aspects of change proposals as they were submitted to subcommittees of ASCE's *Seismic Retrofit of Existing Building Standards* Committee. Often, these change proposals were revised, in some cases substantively, by these subcommittees before they were adopted into ASCE/SEI 41-23. Readers should not rely on this report for information about the final version of provisions in ASCE/SEI 41-23.

This section describes recommended changes to ASCE/SEI 41-17 Section 3.2.1 and Table 3-1 and the creation of a new commentary Table C3-1. The recommended changes are primarily editorial in nature, intended to keep language in ASCE/SEI 41-17 Table 3-1 that sets criteria for features that must be present to satisfy the definition for each CBT and then create a new commentary Table C3-1 containing descriptions of various components of the buildings, historical information, and other items to help the evaluating engineer better understand the building systems. Additional editorial and technical changes were made to the wood-framed building types. The main technical change involves the classifications of the three wood-framed CBTs (W1, W1a, and W2). Specific revisions are described in the following sections. New or modified text is shown in blue.

1.4.1 Provisions and Commentary

The recommended revisions include editorial updates to all of the individual CBT definitions in ASCE/SEI 41-17 Table 3-1 consisting of deleted and revised text intended to remove commentary language and development of a parallel commentary Table C3-1 which contains much of the text removed from Table 3-1. An example of the proposed changes for a single CBT (C1 was selected as a representative building type) is included below.

Table 3-1. Common Building Types

Concrete Moment Frames C1	These buildings consist of a frame assembly of cast-in-place reinforced concrete beams and columns. Floor and roof framing consists of cast-in-place concrete slabs, concrete beams, one-way joists, two-way waffle joists, or flat slabs. Seismic forces are resisted by concrete moment frames that develop their stiffness through monolithic beam–column connections. ~~In older construction, or in levels of low seismicity,~~ In some conditions, the moment frames ~~are permitted to~~ consist of ~~the~~ slab-column frames ~~strips~~ of two-way flat slab systems. ~~Modern frames in levels of high seismicity have joint reinforcing, closely spaced ties, and special detailing to provide ductile performance. This detailing is usually not present in older construction. The foundation system is permitted to consist of a variety of elements.~~

Table 3-1. Common Building Types

Concrete Moment Frames C1	These buildings consist of a frame assembly of cast-in-place reinforced concrete beams and columns. Floor and roof framing consists of cast-in-place concrete slabs, concrete beams, one-way joists, two-way waffle joists, or flat slabs. Seismic forces are resisted by concrete moment frames that develop their stiffness through monolithic beam–column connections. In older construction, or in levels of low seismicity, the moment frames are permitted to consist of the column strips of two-way flat slab systems. Modern frames in levels of high seismicity have joint reinforcing, closely spaced ties, and special detailing to provide ductile performance. This detailing is usually not present in older construction. The foundation system could consist of a variety of elements.

1.4.2 Wood-Frame Buildings

The recommended reorganization of the wood-frame CBT eliminates W1a, resulting in two CBTs, W1 and W2. The intent is to limit W1 buildings to those smaller structures traditionally considered conventional light-frame construction and to align with the building code definition of these buildings, including those covered by the IRC. The W2 definition was expanded to include larger dwellings that generally do not fall under the conventional construction provisions as well as wood-framed buildings that typically require a fully engineered design. These CBT updates are as follows:

Table 3-1. Common Building Types

Wood Light Frames, Small Residential W1	These buildings are detached one- or two-~~single- or multiple-~~family dwellings one to three ~~or more~~ stories high with plan areas on each level less than or equal to 3,000 ft^2 (280 m^2) and total plan area less than or equal to 6,000 ft^2 (1,520 m^2). ~~Building loads are light, and the framing spans are short.~~ Floor and roof framing consist~~s~~ of wood trusses, joists or rafters on wood studs spaced no more than 24 in. (61 cm) apart or wood post-and-beam construction. The first-floor framing is supported directly on an at-grade ~~the~~ foundation ~~system~~ or slab-on-grade or directly on

	concrete or masonry basement walls or is raised up on cripple studs and post-and-beam supports. ~~The foundation is permitted to consist of a variety of elements. Chimneys, where present, consist of solid brick masonry, masonry veneer, or wood frame with internal metal flues.~~ Seismic forces are resisted by wood framed and sheathed diaphragms and shear walls. Floor and roof diaphragms consist of straight or diagonal lumber sheathing, tongue-and-groove planks, oriented strand board, plywood, or other materials. Shear walls ~~are permitted to~~ consist of straight or diagonal ~~lumber~~ wood sheathing, plank siding, oriented strand board, plywood, stucco, gypsum board, particleboard, fiberboard, or similarly performing materials. ~~Interior partitions are sheathed from floor to floor with plaster or gypsum board. Older construction often has open front garages at the lowest story and is permitted to be split-level.~~
~~W1a~~ ~~(Multistory, Multiunit, Residential)~~	~~These buildings are multistory, similar in construction to W1 buildings, but have plan areas on each floor of more than 3,000 ft^2 (280 m^2). Older construction often has open front garages at the lowest story.~~
Wood Frames, Large Residential, Commercial, and Industrial W2	These buildings are one- or two-family dwellings that exceed the criteria for W1 buildings, multi-unit residential buildings, or commercial, ~~or~~ industrial, or institutional buildings. ~~or large single or multi-unit buildings with a floor plan areas on each level of greater than 3,000 ft^2 (280 m^2) or more. There are few, in any, interior walls. The~~ Elevated floor and roof framing consist~~s~~ of wood or steel trusses, glulam or steel beams, and wood posts or steel columns. Ground or basement floors generally consist of concrete slab-on-grade. ~~The foundation system is permitted to consist of a variety of elements.~~ Seismic forces are resisted by flexible diaphragms and exterior walls sheathed with plywood, oriented strand board, stucco, plaster, or straight or diagonal wood sheathing, or they are permitted to be braced with various forms of wood bracing, such as let-in, knee-braced, or cantilevered columns. Bracing with other materials is considered a mixed-system and is subject to the requirements in Section 3.4.1.2.2. Wall openings for storefronts and garages, where present, are framed by post-and-beam framing. In some cases, these building may be located over a podium level structure with concrete or masonry shear walls and can be evaluated as a mixed system subject to the requirements in Section 3.4.1.2.2.2.

1.5 References

ASCE, 2017, *Seismic Evaluation and Retrofit of Existing Buildings,* ASCE/SEI 41-17, Structural Engineering Institute of American Society of Civil Engineers, Reston, Virginia.

ICC, 2018, *2018 International Residential Code*, International Code Council, Whittier, California.

ICBO, 1976, *1976 Uniform Building Code*, International Conference of Building Officials, Whittier, California.

ICBO, 1997, *1997 Uniform Building Code*, International Conference of Building Officials, Whittier, California.

Chapter 2: Updates to Tier 1 Diaphragm-Related Provisions

2.1 Motivation

The primary purpose of this task is to update the diaphragm-related provisions for Tier 1 screening procedure in ASCE/SEI 41-17 (ASCE 2017a) Chapters 4 and 17 to address the diaphragm components that should be considered for Tier 1 evaluations and to eliminate various editorial inconsistencies with the current text. In particular, this task involved consideration of added Tier 1 screening scope for buildings with heavy walls (concrete and masonry) and flexible diaphragms.

2.2 Summary of Changes Recommended

The scope of recommended updates to the Tier 1 diaphragm-related checklists is primarily related to flexible diaphragm issues—improving clarity, consistency, and adding checklist statements for wood structural panel and bare steel deck diaphragms. Related updates are also proposed for ASCE/SEI 41-17 Section 5.6 addressing Tier 2 evaluations of flexible diaphragms and for ASCE/SEI 41-17 Appendix A updating the commentary for flexible diaphragms. The following is a brief summary of the main substantive changes being recommended:

- Changes are proposed for ASCE/SEI 41-17 Section 4.4.2.2 related to application of story shear forces in a Tier 1 screening.
- The Torsion checklist statement is proposed to only apply to buildings with stiff diaphragms.
- New checklist statements are proposed to be added for buildings with heavy walls and flexible diaphragms.
- The checklist statement covering bare steel deck diaphragms is recommended to apply to the Collapse Prevention performance level instead of just the Immediate Occupancy performance level in ASCE/SEI 41-17.

2.3 Technical Studies

The purpose of this task is a combination of substantive and editorial revisions, but there were no specific analytical studies associated with this task, since the substantive changes were based on the judgment of the Working Group 4 members and on creating consistency with other reference standards as described in the following sections.

The updates for the diaphragm-related checklist application and content are based on a review of ASCE/SEI 41-17 compared to the predecessor documents and the judgment of Working Group 4 as

to the proper application of these items for buildings eligible for the ASCE/SEI 41-17 Tier 1 screening provisions in ASCE/SEI 41-17 Chapters 4 and 17. The following sections describe the rationale behind the main substantive changes to the diaphragm-related checklist statements. Additional editorial updates to the checklists and related updates to the Tier 2 evaluation text in ASCE/SEI 41-17 Section 5.6 and the commentary in ASCE/SEI 41-17 Appendix A are included in Section 2.4.

2.3.1 Story Shear Forces

The Quick Check procedures of ASCE/SEI 41-17 Section 4.4 are generally based on average story forces over any entire level of a structure without determining relative rigidities of specific vertical elements. This allows the quick checks to be performed without modeling the building. For rigid diaphragms it is reasonable to distribute the total story shear evenly among all lines of lateral resistance. However, for flexible diaphragms it is recommended to require tributary area distribution, which is not very difficult to implement for these systems and will lead to more accurate results. Therefore, ASCE/SEI 41-17 Section 4.4.2.2 is proposed to be updated for consistency with the typical application of the Quick Check procedures. In addition, consistent with the recommendation to remove the torsion check for flexible diaphragm buildings (see Section 2.3.2), a tributary area distribution is helpful since a uniform distribution may not capture effects of unbalanced lateral elements.

2.3.2 Torsion

In the judgment of Working Group 4, the torsion check is used both to identify an important irregularity and to validate the use of the Tier 1 screening procedure, in particular when using the Quick Check procedures for rigid diaphragm buildings since these are based on averaging the story forces among all of the lateral elements on a given floor level. Both of these items are important for rigid diaphragm buildings, but for flexible diaphragm buildings neither are a particular concern as long as the Quick Checks are based on tributary area. The torsion check can be used to identify an "open storefront" irregularity in flexible diaphragm buildings, but this concern is more related to a discontinuous lateral element (in multi-story buildings) or a cantilever diaphragm condition (in both single- and multi-story buildings). Therefore, the recommendation is to remove the torsion check from all buildings with flexible diaphragms and to add a cantilever diaphragm check for flexible diaphragm systems in buildings with heavy walls (as discussed in Section 2.3.4).

2.3.3 Diaphragm Continuity

After reviewing the Diaphragm Continuity checklist statement, Working Group 4 concluded that additional clarity could be provided to assist users in applying the statement in a more consistent manner. The statement update specifically lists the types of roof systems that typically create a discontinuity. Roof systems with vertical offsets—such as sawtooths and clerestories—will often lack inherent diaphragm continuity, and therefore a Tier 2 evaluation should be required to pass the building.

2.3.4 Wood and Bare-Steel-Deck Diaphragm Checklist Statements

The main study performed for this task consisted of reviewing the current diaphragm-related provisions for Tier 1 screening in ASCE/SEI 41-17 to determine if modifications or additional checklist statements should be considered and then to develop recommendation for updates to the diaphragm-related Tier 1 provisions.

2.3.4.1 REVIEW OF DIAPHRAGM CHECKLIST SCOPE

Working Group 4 started by identifying the basic scope of checklist statements for various diaphragm systems as summarized in Table 2-1. Note that there are other specific diaphragm-related checks in the Basic Configuration checklists and the checklists for individual Common Building Types (CBTs). This summary only relates to generic screening criteria by diaphragm system.

Table 2-1 Scope of Diaphragm-Related Checklist Statements

Diaphragm System	Collapse Prevention Screening Criteria	Immediate Occupancy Screening Criteria
Wood Straight Sheathing	Span and Aspect Ratio	Span and Aspect Ratio
Wood Diagonal Sheathing	Span and Aspect Ratio	Span and Aspect Ratio
Unblocked Wood Structural Panel	Span and Aspect Ratio	Span and Aspect Ratio
Blocked Wood Structural Panel	None	None
Bare Steel Deck	None	Span and Aspect Ratio
Concrete Slab on Steel Deck	None	None
Precast Concrete	Topping Slab	Topping Slab
Cast-in-Place Concrete	None	None
Horizontal Steel Bracing	None	None
Other Diaphragm Systems	Not Permitted	Not Permitted

After completing the summary of the screening criteria, the working group members proceeded to consider whether any proposed changes to the scope of screening should be considered. The following conclusions were reached based on judgment, experience with previous seismic evaluations, an understanding of the development of the predecessors to the standard, and an understanding of observations from past earthquakes. After detailed discussions, the following general conclusions were reached:

- The pre-modern and generally weaker diaphragm systems (wood sheathing and unblocked wood structural panels) are adequately addressed in the current provisions. Although additional

analytical studies could be performed to validate the span and aspect ratio limits, these were judged not to be a priority for this diaphragm task.

- The lack of specific checklist statement criteria for modern flexible diaphragm systems (wood structural panel and bare steel deck) deserves additional consideration and therefore was considered the priority for this diaphragm study. This conclusion was largely based on experiences with recent seismic evaluations where these types of diaphragm systems were analyzed and found to be significantly deficient with respect to current building code requirements, for example those in ASCE/SEI 7-16 (ASCE, 2017b) and SDPWS (AWC, 2015).

- Concrete diaphragm systems (slab-on-steel deck and cast-in-place concrete) are generally not sources of significant earthquake damage unless there are other systematic irregularities (for example geometric irregularities or discontinuous vertical elements) that are addressed elsewhere in the Tier 1 Screening, and so these systems were judged not to be a priority for this diaphragm task.

- The current provisions for precast concrete diaphragms were judged to be adequate and not a priority for this diaphragm task.

- Horizontal steel braced diaphragms are considered somewhat uncommon for structures eligible for the Tier 1 screening, and the lack of specific Tier 1 screening checklists was judged to not be a priority for this diaphragm task.

- The prohibition of other diaphragm systems for allowing conformance with the Tier 1 Screening was judged adequate.

Table 2-2 summarizes the consensus conclusions that were reached regarding the various diaphragm systems.

Table 2-2 Summary of Working Group 4 Study Scope

Diaphragm System	Study Scope
Wood Straight Sheathing	No additional study warranted since current criteria judged to be adequate
Wood Diagonal Sheathing	No additional study warranted since current criteria judged to be adequate
Unblocked Wood Structural Panel	No additional study warranted since current criteria judged to be adequate
Blocked Wood Structural Panel	Consider added criteria for buildings with heavy walls, no additional study for other buildings
Concrete Slab-on-Steel Deck	No additional study warranted since these systems represent low risk of failure

Table 2-2 Summary of Working Group 4 Study Scope (continued)

Diaphragm System	Study Scope
Bare Steel Deck	Consider added criteria for buildings with heavy walls, no additional study for other buildings
Precast Concrete	No additional study warranted since current criteria judged to be adequate
Cast-in-Place Concrete	No additional study warranted since these systems represent low risk of failure
Horizontal Steel Bracing	No additional study considered since determined to be beyond the scope of this diaphragm study
Other Diaphragm Systems	No additional study warranted since Tier 2 evaluation is appropriate

2.3.4.2 CONCLUSIONS

Focusing then on the requirements for wood structural panel and bare steel deck diaphragm systems, the first consideration was the scope of the screening and the second was on the technical requirements for such a screening.

After deliberation, the consensus was to limit the scope of any added checklist provisions to buildings with heavy walls (concrete and masonry) since those systems represent the greatest risk of collapse due to poor diaphragms. (The greatest risk of the flexible diaphragm/heavy wall system is lack of adequate wall anchorage, followed by diaphragm connections and ties, but if those items are upgraded, then the strength of the diaphragm itself could become the critical component of the lateral load path).

Subsequently, several proposed checklist updates were initially considered:

- Add criteria for blocked wood structural panel diaphragms in heavy wall buildings. These criteria are needed to ensure compliance with the performance assumptions underlying the CBT definitions (maximum span and maximum aspect ratio).
- Add a checklist item for cantilevered wood diaphragms in heavy wall buildings. This is also needed to ensure compliance with the performance assumptions underlying the CBT definitions (maximum span and maximum aspect ratio).
- Copy the bare steel deck diaphragm checklist statement from the Immediate Occupancy checklists to the Collapse Prevention checklists for heavy wall buildings. The potential failure of a nonconforming bare steel deck diaphragm in a building with heavy walls represents a risk of partial collapse, not just ability to occupy a building following an earthquake.

Concluding these revisions were appropriate for a Tier 1 Screening, specific checklist statements were created using the current statements for other flexible diaphragm system as a baseline, specifically including limitations on span and aspect ratios. The limits for both blocked wood structural panel diaphragms and cantilevered wood diaphragms were developed somewhat qualitatively, based partially on building code limitations and the judgment of the working group members. This process is consistent with the development of many of the existing Tier 1 checklist statements, where specific criteria were often based on the judgment of the developers of the original guidelines.

For wood structural panel blocked diaphragms, the screening criteria are proposed to be a maximum span of 120 feet and a maximum aspect ratio of 4-to-1 for Collapse Prevention and a maximum cantilever length of 90 feet and a maximum aspect ratio of 4-to-1 for Immediate Occupancy. The Collapse Prevention criteria are based on the requirements of SDPWS, and the Immediate Occupancy criteria is taken as approximately two-thirds of Collapse Prevention to approximate the Seismic Importance Factor of 1.5 in ASCE/SEI 7-16 Table 1.5-2.

For Cantilevered Wood Diaphragms, the screening criteria for Collapse Prevention are proposed to be a maximum cantilever length of 30 feet and a maximum cantilever to backspan ratio of 1-to-1 if blocked wood structural panel and a maximum span of 20 feet and a maximum cantilever to backspan ratio of 1-to-2 for all others. For Immediate Occupancy the criteria are proposed to be a maximum cantilever length of 25 feet and a maximum cantilever to backspan ratio of 1-to-1.5 if blocked wood structural panel and a maximum span of 15 feet and a maximum cantilever to backspan ratio of 1-to-2.5 for all others. The Collapse Prevention criteria are based on the requirements of SDPWS, and the Immediate Occupancy criteria is taken as approximately two-thirds of Collapse Prevention similar to blocked diaphragms described above.

For the Nonconcrete Filled Diaphragms statement, the criteria for Immediate Occupancy in ASCE/SEI 41-17 are a maximum span of 40 feet and an aspect ratio of 4-to-1. For the new Collapse Prevention checklist statement, the recommendation was to keep the same aspect ratio and to increase the maximum span by a factor of three to 120 feet. This makes the criteria for bare steel deck diaphragms the same as blocked wood structural panel diaphragms. The ratio of Immediate Occupancy to Collapse Prevention is significantly greater than what would be consistent with the Importance Factor of 1.5 in ASCE 7-16, but 120 feet was judged to be a reasonable limit for the Tier 1 Screening—anything less was judged to be too restrictive for an expanded requirement.

2.4 Recommended Changes

Note about Change Proposals

This report documents aspects of change proposals as they were submitted to subcommittees of ASCE's *Seismic Retrofit of Existing Building Standards* Committee. Often, these change proposals were revised, in some cases substantively, by these subcommittees before they were adopted into ASCE/SEI 41-23. Readers should not rely on this report for information about the final version of provisions in ASCE/SEI 41-23.

This section describes recommended changes to ASCE/SEI 41-17 Section 4.4.2.2 and the Chapter 17 Tier 1 Screening checklists for buildings with flexible diaphragms. The recommended changes for these diaphragm-related checklists are described in the following sections. New or modified text is shown in blue.

2.4.1 Story Shear Forces

ASCE/SEI 41-17 Section 4.4.2.2 is proposed to be updated for consistency with the quick check procedures, as shown below.

4.4.2.2 Story Shear Forces.

The pseudo seismic force calculated in accordance with Section 4.4.2.1 shall be distributed vertically in accordance with Eqs. (4-2a and 4-2b). For buildings six stories or fewer high, the value of k shall be permitted to be taken as 1.0.

….

~~For buildings with stiff or rigid diaphragms, t~~The story shear forces shall be distributed to the lateral-force-resisting elements in accordance with the Quick Checks for strength and stiffness in Section 4.4.3~~based on their relative rigidities~~. For buildings with flexible diaphragms ~~(Types S1a, S2a, S5a, C2a, C3a, PC1, RM1, and URM)~~, story shear shall be calculated separately for each line of lateral resistance based on tributary mass.

2.4.2 Torsion

The torsion check for both Collapse Prevention (ASCE/SEI 41-17 Table 17-2) and Immediate Occupancy (ASCE/SEI 41-17 Table 17-3) Basic Checklists is proposed to be revised to apply only to buildings with stiff diaphragms as shown below.

TORSION: For buildings with rigid diaphragms, ~~T~~the estimated distance between the story center of mass and the story center of rigidity is less than 20% of the building width in either plan dimension. This statement does not apply to buildings with flexible diaphragms.

2.4.3 Diaphragm Continuity

The diaphragm continuity check is expanded to include various roof types (as described in the proposed text below) that often lack continuity and therefore should require Tier 2 evaluation. This revision applies to all the checklists containing the Diaphragm Continuity statement.

> **DIAPHRAGM CONTINUITY:** The diaphragms are not composed of split level floors and do not have expansion joints. Roof diaphragm configurations composed of sawtooth, clerestory, or other vertical offset configurations that lack continuity of the diaphragm itself are not used.

2.4.4 Wood and Bare-Steel-Deck Diaphragm Checklist Statements

The proposed updates to the flexible diaphragm related checklists are intended to address the following:

- Editorial revisions to the Straight Sheathing statement and elimination of the Spans statement for all locations where these statements occur for consistency with the statements for other diaphragm types.
- Editorial revisions to change "metal deck" to "steel deck" for consistency with current AISC/AISI terminology in AISC 342-22 (AISC, 2022).
- Added checklist statements for Blocked Diaphragms and Cantilevered Wood Diaphragms for all heavy wall/flexible diaphragm CBTs at both the Collapse Prevention and Immediate Occupancy performance levels.
- Adding the Nonconcrete Filled Diaphragm checklist statement to the Collapse Prevention checklists for heavy wall/flexible diaphragm buildings. This statement currently only applies to Immediate Occupancy.

The proposed editorial revisions to the Collapse Prevention checklists for all CBTs with flexible diaphragms (applying to all occurrences of these statements in the Chapter 17 tables) are as follows:

> STRAIGHT SHEATHING: All straight-sheathed diaphragms have horizontal spans less than 24 ft (7.3m) and aspect ratios less than 2-to-1 in the direction being considered.
>
> ~~SPANS: All wood diaphragms with spans greater than 24 ft (7.3 m) consist of wood structural panels or diagonal sheathing.~~
>
> The proposed added statements to the Collapse Prevention checklists for CBTs with heavy walls and flexible diaphragms (S5a, C2a, C3a, PC1, RM1, and URM) are as follows:
>
> BLOCKED DIAPHRAGMS: All blocked wood structural panel diaphragms have horizontal spans less than 120 ft (36.5 m) and have aspect ratios less than or equal to 4-to-1.

CANTILEVERED WOOD DIAPHRAGMS: All cantilevered wood diaphragms that provide lateral support for concrete or masonry walls consist of wood structural panels and have a maximum cantilever length of 20 ft (6.1 m) if unblocked or 30 ft (9.2 m) if blocked, and a maximum ratio of cantilever length to diaphragm width of 1:2 if unblocked and 1:1 if blocked. In addition, the cantilevered diaphragm has a back-span length equal to or greater than the cantilevered portion.

NONCONCRETE FILLED DIAPHRAGMS: Bare steel deck diaphragms or steel deck diaphragms with fill other than reinforced structural concrete consist of horizontal spans of less than 120 ft (36.5 m) and have aspect ratios less than 4-to-1.

The proposed editorial revisions to the Immediate Occupancy checklists for all CBTs with flexible diaphragms (applying to all occurrences of these statements in the Chapter 17 tables) are as follows:

STRAIGHT SHEATHING: All straight-sheathed diaphragms have horizontal spans less than 12 ft (3.6 m) and aspect ratios less than 1-to-1 in the direction being considered.

~~SPANS: All wood diaphragms with spans greater than 12 ft (3.6 m) consist of wood structural panels or diagonal sheathing.~~

The proposed added statements to the Immediate Occupancy checklist statements for CBTs with heavy walls and flexible diaphragms (S5a, C2a, C3a, PC1, RM1, and URM) are as follows:

BLOCKED DIAPHRAGMS: All blocked wood structural panel diaphragms have horizontal spans less than 90 ft (18.3 m) and have aspect ratios less than or equal to 4-to-1.

CANTILEVERED WOOD DIAPHRAGMS: All cantilevered wood diaphragms that provide lateral support for concrete or masonry walls consist of wood structural panels and have a maximum cantilever length of 15 ft (4.6 m) if unblocked or 25 ft (7.6 m) if blocked, and a maximum ratio of cantilever length to diaphragm width of 1:2.5 if unblocked and 1:1.5 if blocked. In addition, the cantilevered diaphragm has a back-span length equal to or greater than the cantilevered portion.

NONCONCRETE FILLED DIAPHRAGMS: ~~Untopped metal~~ Bare steel deck diaphragms or ~~metal~~steel deck diaphragms with fill other than reinforced structural concrete consist of horizontal spans of less than 40 ft (12.2 m) and have aspect ratios less than 4-to-1.

2.4.5 Tier 2 Diaphragm Updates

Updates to the Tier 2 procedures for wood and metal deck diaphragms (ASCE/SEI 41-17 Sections 5.6.2 and 5.6.3) are proposed for consistency with the related Tier 1 checklists that were added or updated as described in Section 2.4.4. Additional editorial updates are proposed to provide further clarity for the Tier 2 procedures. The proposed revisions are as follows.

5.6.2 Procedures for Wood Diaphragms.

For wood diaphragms with noncompliant spans or aspect ratios, an analysis of the entire diaphragm at each noncompliant level shall be performed in accordance with Section 5.2.4, and the adequacy of the diaphragm system shall be evaluated in accordance with Section 5.2.5. The diaphragm deflection shall be calculated, and the adequacy of the vertical-load-carrying elements at the maximum deflection, including P-delta effects, shall be evaluated.

5.6.3 Procedures for ~~Metal~~Steel Deck Diaphragms.

For ~~untopped metal~~ bare steel deck diaphragms or steel deck diaphragms with fill other than reinforced structural concrete with noncompliant spans or aspect ratios, an analysis of the entire diaphragm shall be performed at each noncompliant level in accordance with Section 5.2.4, and the adequacy of the diaphragm system ~~shear capacity~~shall be evaluated in accordance with Section 5.2.5. ~~Diaphragms shall be evaluated for the forces in Chapter 7. The adequacy of the shear capacity of the metal deck diaphragm shall be evaluated.~~ The diaphragm deflection shall be calculated, and the adequacy of the vertical-load-carrying elements at the maximum deflection, including P-delta effects, shall be evaluated.

5.6.5 Diaphragms Other than Wood, ~~Metal~~Steel Deck, Concrete, or Horizontal Bracing.

An analysis of the diaphragm system shall be performed in accordance with Section 5.2.4, and the adequacy of the system shall be evaluated in accordance with Section 5.2.5 or using available reference standards for the capacity of the diaphragm not covered by this standard.

2.4.6 Appendix A Updates

New subsections are proposed to be added to ASCE/SEI Section A4.2 providing commentary for the proposed new checklist statements. These are included below. Additionally, minor editorial updates (not included below) are proposed for ASCE/SEI Sections A2.2.7, A4.1.1, and A4.2 for consistency with the other checklist updates described in Sections 2.4.2, 2.4.3, and 2.4.4 above.

A4.2.3 Blocked Diaphragms. All blocked wood structural panel diaphragms have horizontal spans less than 120 ft (36.5 m) for Collapse Prevention and less than 90 ft (18.3 m) for Immediate Occupancy and have aspect ratios less than or equal to 4-to-1.

Long-span diaphragms often experience large lateral deflections and diaphragm shear demands. Large deflections in the diaphragm can result in increased damage or collapse of elements laterally supported by the diaphragm. Excessive diaphragm shear demands cause damage and reduced stiffness in the diaphragm.

Compliance can be demonstrated if the diaphragm can be shown to have adequate capacity for the demands in the building being evaluated and vertical- load-carrying elements can be shown to have adequate capacity at maximum deflection.

The shear capacity of blocked diaphragms can be improved with additional fasteners or placing additional new wood structural panels over the existing diaphragm increases the shear capacity. Both of these methods require the partial or total removal of existing flooring or roofing to place and fasten the new overlay or fasten the existing panels to the new blocking. Strengthening of the diaphragm is usually not necessary at the central area of the diaphragm where shear is low.

New vertical elements can be added to reduce the diaphragm span. The reduction of the diaphragm span also reduces the lateral deflection and shear demand in the diaphragm. However, adding new

vertical elements results in a different distribution of shear demands. Additional blocking, nailing, or other retrofit measures may need to be provided at these areas, as indicated in FEMA 172 (1992a), Section 3.4.

A4.2.4 Cantilevered Wood Diaphragms. All cantilevered diaphragms that provide lateral support for concrete or masonry walls consist of wood structural panels and have a maximum cantilever length of 20 ft (6.1 m) if unblocked or 30 ft (9.2 m) if fully blocked for Collapse Prevention and 15 ft (4.6 m) if unblocked or 25 ft (7.6 m) if fully blocked for Immediate Occupancy, and a maximum ratio of cantilever length to diaphragm width of 1:2 if unblocked and 1:1 if blocked for Collapse Prevention and 1:2.5 if unblocked and 1:1.5 if blocked for Immediate Occupancy. In addition, the cantilevered diaphragm has a back span length equal to or greater than the cantilevered portion.

Cantilevered diaphragms can have large lateral deflections and diaphragm shear demands. Large deflections in the diaphragm can result in increased damage or collapse of elements laterally supported by the diaphragm. Excessive diaphragm shear demands cause damage and reduced stiffness in the diaphragm. Short back spans can have high shear demands throughout their length relative to the cantilevered portion.

Compliance can be demonstrated if the diaphragm can be shown to have adequate capacity for the demands in the building being evaluated and vertical- load-carrying elements can be shown to have adequate capacity at maximum deflection.

The shear capacity of blocked diaphragms can be improved with additional fasteners or placing additional new wood structural panels over the existing diaphragm increases the shear capacity. Both of these methods require the partial or total removal of existing flooring or roofing to place and fasten the new overlay or fasten the existing panels to the new blocking.

2.5 References

AISC, 2022, *Seismic Provisions for Evaluation and Retrofit of Existing Structural Steel Buildings,* AISC 342-22, Public Review Draft, American Institute of Steel Construction, Chicago, Illinois.

ASCE, 2017a, *Seismic Evaluation and Retrofit of Existing Buildings,* ASCE/SEI 41-17, Structural Engineering Institute of American Society of Civil Engineers, Reston, Virginia.

ASCE, 2017b, *Minimum Design Loads and Associated Criteria for Buildings and Other Structures*, ASCE/SEI 7-16, Structural Engineering Institute of American Society of Civil Engineers, Reston, Virginia.

AWC, 2015, Special Design Provisions for Wind and Seismic Standard with Commentary, ANSI/AWC SDPWS-2015, American Wood Council, Leesburg, Virginia.

Chapter 3: Updates to Tier 1 Foundations and Overturning-Related Provisions

3.1 Motivation

There are inconsistencies and a lack of clarity with three ASCE/SEI 41-17 (ASCE, 2017) Tier 1 checklist items related to foundations and overturning. These checklist statements include Overturning, Deep Foundations, and Sloping Sites. This task consists of a review of the application of the checklist items (based on seismic hazard level and performance level) and a review of the statements themselves in order to develop potential improvements.

3.2 Summary of Changes Recommended

The recommended changes include elimination of the Overturning checklist statement for all Common Building Types (CBTs) at the Collapse Prevention performance level; elimination of the Overturning checklist statement for select CBTs at the Immediate Occupancy performance level; additional commentary for the Overturning checklist statement; updates to the application of the Deep Foundations and Sloping Sites checklist statements by Seismic Hazard Level; and technical revisions to the Deep Foundations and Sloping Sites checklist statements.

3.3 Technical Studies

The purpose of this scope item is to develop a combination of substantive and editorial revisions, but there were no specific technical studies associated with this task since the substantive changes were based on improving consistency and completeness of the provisions using judgment and consensus of the working group members.

The updates for the Overturning, Deep Foundation, and Sloping Sites checklists, as well as supporting commentary, are based on the studies described in the following sections.

3.3.1 Overturning Checklist Statement

Reviewing the foundation overturning checklist statement, the working group began by considering two primary purposes of this statement:

1. Determine risk for local or global collapse due to foundation rocking
2. Determine risk for excessive deformations of the building superstructure as a result of foundation rotation

The risk of local or global collapse in the first item is judged to be very low for the types of buildings eligible for the Tier 1 screening procedure (limited to a maximum of 8 stories in areas of High Seismicity). Rocking instability (actual overturning) is very unlikely to occur, and the risk of collapse due to excessive deformations of the superstructure is judged to occur only when the superstructure is comprised of brittle members that will be identified by other checklist statements (for example, shear-critical concrete beams and columns). Therefore, the recommendation is to completely remove the Overturning statement from the Collapse Prevention Basic Configuration Checklist.

However, excessive foundation deformation or rotation can lead to increased superstructure deformations and a risk of damage related to achieving Immediate Occupancy performance for some building types. Therefore, the recommendation is to remove the Overturning statement from the Immediate Occupancy Basic Configuration Checklist and move it to specific building system checklists (with application at the Moderate and High Level of Seismicity as in the current standard). For certain building types, for example wood-framed shear wall and cold formed steel-framed buildings, foundation rotations are not the governing behavior as related to deformation-induced damage since the lateral elements tend to be well-distributed and are controlled by shear wall slenderness or the lack of adequate hold-downs. Table 3-1 shows the recommended application for the Overturning checklist statement by CBT.

Table 3-1 Recommended Revisions to the Overturning Checklist Statement

Building Type	Overturning Check?	Discussion
W1, Wood Light Frames	Remove for CP and IO	Foundation overturning or rotation is not a concern. Separate checklist statements for wall stress, aspect ratio, and hold-downs covers element overturning.
W1a, (Multistory, Multiunit, Residential)	Remove for CP and IO	Foundation overturning or rotation is not a concern. Separate checklist statements for wall stress, aspect ratio, and hold-downs covers element overturning.
W2, Wood Frames, Commercial and Industrial	Remove for CP and IO	Foundation overturning or rotation is not a concern. Separate checklist statements for wall stress, aspect ratio, and hold-downs covers element overturning.
S1/S1a Steel Moment Frames	Remove for CP Keep for IO	Concern is not global collapse (CP) but excessive foundation rotation and associated deformations (IO).
S2/S2a Steel Braced Frames	Remove for CP Keep for IO	Concern is not global collapse (CP) but excessive foundation rotation and associated deformations (IO).
S3, Metal Building Frames	Remove for CP and IO	Foundation overturning or rotation is not a concern. Lateral system is well-distributed and buildings not at risk of excessive deformation due to foundation rocking.
S4, Frame Systems with Backup Steel Moment Frames	Remove for CP Keep for IO	Concern is not global collapse (CP) but excessive foundation rotation and associated deformations (IO).

Table 3-1 Recommended Revisions to the Overturning Checklist Statement (continued)

Building Type	Overturning Check?	Discussion
S5/S5a, Steel Frames with Infill Masonry Shear Walls	Remove for CP Keep for IO	Foundation overturning is generally not a concern for these buildings because they tend to have perimeter walls and they will likely pass anyway. Keep for IO for potential deformation compatibility concerns.
CFS1, Cold-Formed Steel Light-Frame Construction (Shear Wall System)	Remove for CP and IO	Foundation overturning or rotation is not a concern. Separate checklist statements for wall stress, aspect ratio, and hold-downs covers element overturning.
CFS2, Cold-Formed Steel Light-Frame Construction (Strap-Braced Wall System)	Remove for CP and IO	Foundation overturning or rotation is not a concern. Separate checklist statements for wall stress, aspect ratio, and hold-downs covers element overturning.
C1, Concrete Moment Frames	Remove for CP Keep for IO	Concern is not global collapse (CP) but excessive foundation rotation and associated deformations (IO).
C2/C2a, Concrete Shear Walls	Remove for CP Keep for IO	Concern is not global collapse (CP) but excessive foundation rotation and associated deformations (IO).
C3/C3a, Concrete Frames with Infill Masonry Shear Walls	Remove for CP Keep for IO	Foundation overturning is generally not a concern for these buildings because they tend to have perimeter walls but they will likely pass anyway. Keep for IO for potential deformation compatibility concerns
PC1/PC1a, Precast or Tilt-Up Concrete Shear Walls	Remove for CP Keep for IO	Foundation overturning is generally not a concern for these buildings because they tend to have perimeter walls and they will likely pass anyway. Keep for IO for potential deformation compatibility concerns.
PC2, Precast Concrete Frames (with Shear Walls)	Remove for CP Keep for IO	Concern is not global collapse (CP) but excessive foundation rotation and associated deformations (IO).
PC2a, Precast Concrete Frames (without Shear Walls)	Remove for CP Keep for IO	Concern is not global collapse (CP) but excessive foundation rotation and associated deformations (IO).
RM1/RM2, Reinforced Masonry Bearing Walls	Remove for CP Keep for IO	Concern is not global collapse (CP) but excessive foundation rotation and associated deformations (IO).
URM/URMa, Unreinforced Masonry Bearing Walls URM	Remove for CP and IO	Foundation overturning is generally not a concern for these buildings because they tend to have perimeter walls and wall strength governs behavior in nearly all cases.

3.3.2 Deep Foundation and Sloping Sites Checklist Application

A study was performed to address what appears to be an unintended change to the application of the Deep Foundation and Sloping Sites checklist statements that occurred in the development of ASCE/SEI 41-13 (ASCE, 2014). In FEMA 178 (FEMA, 1992), FEMA 310 (FEMA, 1998), ASCE/SEI 31-03 (ASCE, 2003), these two checklist statements, in addition to all of the other checklist statements for geotechnical site hazards and foundations, were applicable to all buildings for the Immediate Occupancy Performance Level and at Very Low (VL), Moderate (M), and High (H) Seismicity. When ASCE/SEI 41-13 was created as a combination of ASCE/SEI 31-03 and ASCE/SEI 41-06 (ASCE, 2007), these two checklist statements were moved to building specific checklists, still at Immediate Occupancy performance only, but at varying levels of seismicity. In ASCE/SEI 41-17 there were some updates to applicable building types and levels of seismicity, but these still applied to Immediate Occupancy performance only and still at varying levels of seismicity. Table 3-2 shows the application of these two checklist statements, which appears arbitrary and inconsistent. In the table, NA refers to Not Applicable.

Table 3-2 Applicability of Foundation-Related Checklist Statements (ASCE/SEI 14-17)

Common Building Type	Deep Foundations	Sloping Sites
W1/W1a, Wood Light Frames	IO = VL	IO = VL
W2, Wood Frames, Commercial and Industrial	IO = VL	IO = VL
S1/S1a Steel Moment Frames	IO = H	IO = H
S2/S2a Steel Braced Frames	IO = H	IO = H
S3, Metal Building Frames	IO = H	IO = H
S4, Frame Systems with Backup Steel Moment Frames	IO = H	IO = H
S5/S5a, Steel Frames with Infill Masonry Shear Walls	IO = M	IO = M
CFS1, Cold-Formed Steel Light-Frame Construction (Shear Wall System)	IO = VL	IO = VL
CFS2, Cold-Formed Steel Light-Frame Construction (Strap-Braced Wall System)	IO = VL	IO = VL
C1, Concrete Moment Frames	IO = NA	IO = NA
C2/C2a, Concrete Shear Walls	IO = VL	IO = VL
C3/C3a, Concrete Frames with Infill Masonry Shear Walls	IO = NA	IO = NA
PC1/PC1a, Precast or Tilt-Up Concrete Shear Walls	IO = VL	IO = VL
PC2, Precast Concrete Frames (with Shear Walls)	IO = NA	IO = NA
PC2a, Precast Concrete Frames (without Shear Walls)	IO = NA	IO = NA

Table 3-2 Applicability of Foundation-Related Checklist Statements (ASCE/SEI 14-17) (continued)

Common Building Type	Deep Foundations	Sloping Sites
RM1/RM2, Reinforced Masonry Bearing Walls	IO = VL	IO = VL
URM/URMa, Unreinforced Masonry Bearing Walls URM	IO = VL	IO = VL

To fix the inconsistency of application among CBTs and levels of seismicity, the recommended update is to move these two checklist statements to the Immediate Occupancy Basic Configuration Checklist. The reason is that most, if not all, of the CBTs could be on piles, and the concerns for any building type are similar (except perhaps small and light buildings). This essentially reverts back to the criteria in ASCE/SEI 31-03 except that the checklist statements no longer apply to Low Seismicity. The rational for this change is that these types of foundation concerns are not significant risks in areas of Low Seismicity, so this change prioritizes consistency of application over specific foundation risks. That is, now all the foundation-related checklist statements are grouped by same level of seismicity.

3.3.3 Deep Foundations

The review of the Deep Foundations checklist statement found it to be vague and unenforceable as standards text. The commentary makes it clear that the concern is more about pile connections and detailing. Therefore, this study focused on revisions to the Deep Foundations checklist statement to require a positive connection to the pile cap or other foundation element for all piles and to have limits on pile detailing requirements. The working group determined that the requirements for Seismic Design Category C in Chapter 18 of the *2021 International Building Code* (IBC) (ICC, 2021) were an appropriate lower-bound detailing requirement for this checklist statement. Specifically, using the amount of longitudinal reinforcement and transverse reinforcing required by IBC Section 1810.3.9.4.1 for cast-in-place concrete piles was judged adequate. For precast piles, it is assumed that the detailing requirements for transporting and driving is sufficient to provide at least a minimum amount of ductility and there are not significant ductility concerns (at least as far as this checklist is concerned) for steel and timber piles which are generally constructed with “compact” sections.

3.3.4 Sloping Sites

The review of the Sloping Sites checklist statement also concluded that the statement is somewhat confusing. The original statement in FEMA 178 and FEMA 310 was “The grade difference from one side of the building to another does not exceed one-half story.” The commentary (ASCE/SEI 41-17 Appendix A and all previous versions) makes it clear that the concern is unbalanced soil load. Therefore, the recommended update involves changing the text from foundation embedment to reference the grade surface, since the issue is unbalanced soil load which relates to grade not foundation embedment. Keeping the limit at one story height is consistent with ASCE/SEI 31-03 and more recent versions.

3.4 Recommended Changes

Note about Change Proposals

This report documents aspects of change proposals as they were submitted to subcommittees of ASCE's *Seismic Retrofit of Existing Building Standards* Committee. Often, these change proposals were revised, in some cases substantively, by these subcommittees before they were adopted into ASCE/SEI 41-23. Readers should not rely on this report for information about the final version of provisions in ASCE/SEI 41-23.

This section describes recommended changes to ASCE/SEI 41-17 Chapter 17, Tier 1 Checklists related to overturning and foundations. Recommended changes to the Overturning, Deep Foundations, and Sloping Sites checklists are described in the following sections. New or modified text is shown in blue.

3.4.1 Overturning Checklist Statement

The Overturning Checklist statement is proposed to be eliminated for the Collapse Prevention performance for all CBTs. This is accomplished by deleting the statement from Table 17-2 as shown below. The Overturning Checklist statement is proposed to be eliminated for Immediate Occupancy performance for certain CBTs but retained for others. This is accomplished by deleting the statement from Table 17-3 as shown below and adding it to certain other Chapter 17 Tables, as described in 3.3.1. A representative example of the latter is included below.

Table 17-2. Collapse Prevention Basic. Configuration Checklist

Status	Evaluation Statement	Tier 2 Reference	Commentary Reference
High Seismicity (Complete the Following Items in Addition to the Items for Moderate Seismicity)			
Foundation Configuration			
C NC N/A U	OVERTURNING: The ratio of the least horizontal dimension of the seismic-force-resisting system at the foundation level to the building height (base/height) is greater than $0.6S_a$.	5.4.3.3	A.6.2.1
C NC N/A U	TIES BETWEEN FOUNDATION ELEMENTS: The foundation has ties adequate to resist seismic forces where footings, piles, and piers are not restrained by beams, slabs, or soils classified as Site Class A, B, or C.	5.4.3.4	A.6.2.2

Note: C = Compliant, NC = Noncompliant, N/A = Not Applicable, and U = Unknown.

Table 17-3. Immediate Occupancy Basic Configuration Checklist

Status	Evaluation Statement	Tier 2 Reference	Commentary Reference
Moderate and High Seismicity (Complete the Following Items in Addition to the Items for Low Seismicity)			
Foundation Configuration			
C NC N/A U	OVERTURNING: The ratio of the least horizontal dimension of the seismic-force-resisting system at the foundation level to the building height (base/height) is greater than $0.6S_a$.	5.4.3.3	A.6.2.1
C NC N/A U	TIES BETWEEN FOUNDATION ELEMENTS: The foundation has ties adequate to resist seismic forces where footings, piles, and piers are not restrained by beams, slabs, or soils classified as Site Class A, B, or C.	5.4.3.4	A.6.2.2

Note: C = Compliant, NC = Noncompliant, N/A = Not Applicable, and U = Unknown.

Table 17-23. Immediate Occupancy Structural Checklist for Building Type C1

Status	Evaluation Statement	Tier 2 Reference	Commentary Reference
Low ~~and Moderate~~ Seismicity (Complete the Following Items in Addition to the Items for Very Low Seismicity)			
Seismic-Force-Resisting System			
C NC N/A U	FLAT SLAB FRAMES: The seismic-force-resisting system is not a frame consisting of columns and a flat slab or plate without beams.	5.5.2.3.1	A.3.1.4.3
Moderate and High Seismicity (Complete the Following Items in Addition to the Items for Very Low and Low Seismicity)			
Foundation System			
C NC N/A U	OVERTURNING: The ratio of the least horizontal dimension of the seismic-force-resisting system at the foundation level to the building height (base/height) is greater than $0.6S_a$.	5.4.3.3	A.6.2.1

Note: C = Compliant, NC = Noncompliant, N/A = Not Applicable, and U = Unknown.

Updates to the checklist commentary in Appendix A with the overturning checklist proposal include editorial updates for consistency. Additional commentary was also included to explain the reasoning for the checklist updates. Also, a figure was developed to assist in determining the aspect ratio of

the foundation as required by the overturning checklist statement. The commentary figure, recommended to be added to ASCE/SEI 41-17 Section A6.2.1 is shown below.

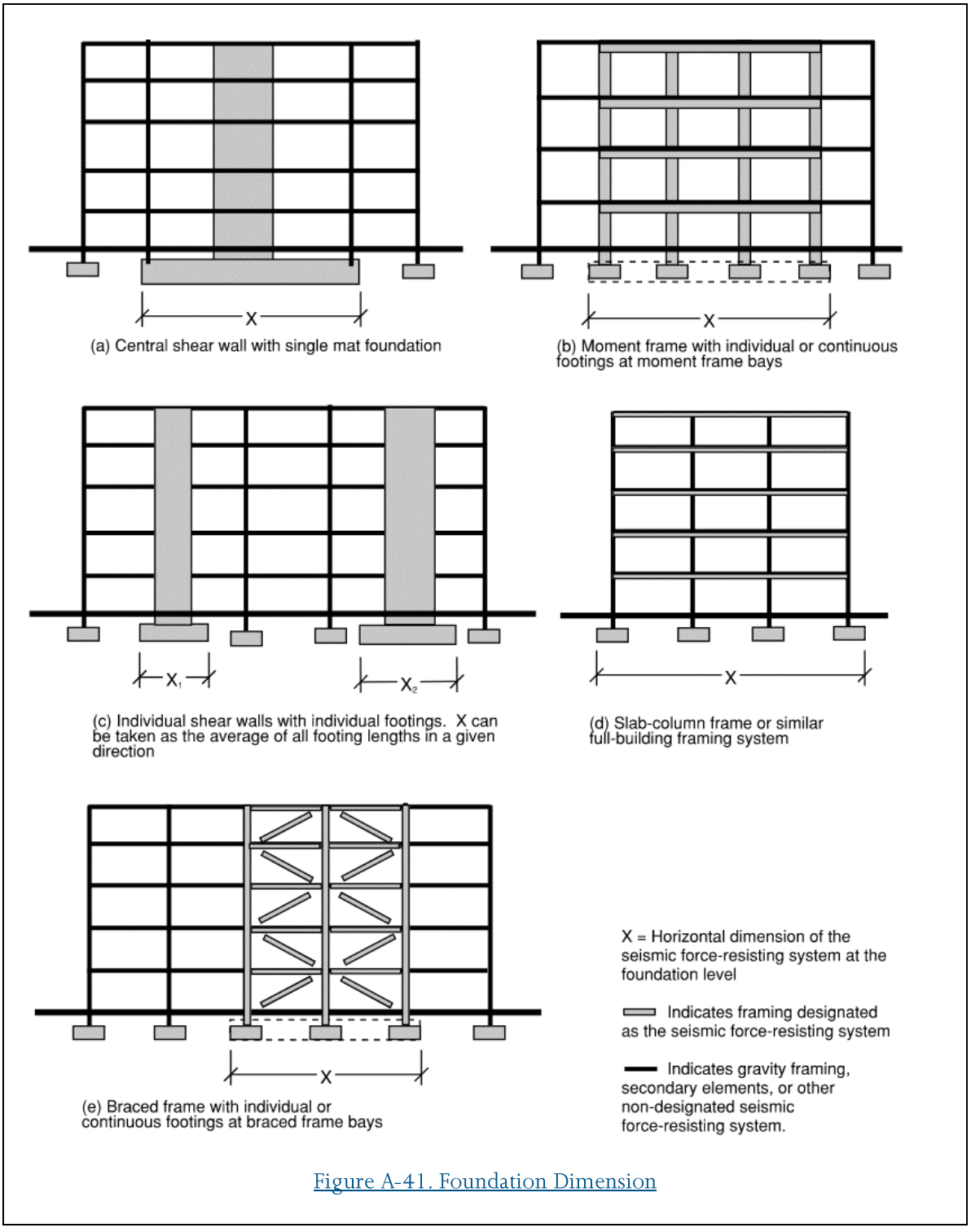

Figure A-41. Foundation Dimension

3.4.2 Deep Foundations and Sloping Sites Checklist Application

This proposal moves the Deep Foundations and Sloping Sites checklist statements to the Immediate Occupancy Basic Configuration Checklist. The proposed change to ASCE/SEI Table 17.3 is included below. The two statements shown added to this checklist are deleted from the Immediate Occupancy checklists for all of the individual CBTs.

Table 17-3. Immediate Occupancy Basic Configuration Checklist

Status	Evaluation Statement	Tier 2 Reference	Commentary Reference
Moderate and High Seismicity (Complete the Following Items in Addition to the Items for Low Seismicity)			
Foundation Configuration			
C NC N/A U	OVERTURNING: The ratio of the least horizontal dimension of the seismic-force-resisting system at the foundation level to the building height (base/height) is greater than $0.6S_a$.	5.4.3.3	A.6.2.1
C NC N/A U	TIES BETWEEN FOUNDATION ELEMENTS: The foundation has ties adequate to resist seismic forces where footings, piles, and piers are not restrained by beams, slabs, or soils classified as Site Class A, B, or C.	5.4.3.4	A.6.2.2
C NC N/A U	DEEP FOUNDATIONS: Piles and piers are capable of transferring the lateral forces between the structure and the soil.		A.6.2.3
C NC N/A U	SLOPING SITES: The difference in foundation embedment depth from one side of the building to another does not exceed one story.		A.6.2.4

Note: C = Compliant, NC = Noncompliant, N/A = Not Applicable, and U = Unknown.

3.4.3 Deep Foundations

The revisions to the Deep Foundations Checklist statement include adding a requirement for a positive connection from the pile to the pile cap or other foundation element for all piles and a minimum amount of longitudinal reinforcement and transverse reinforcing for cast-in-place concrete piles.

DEEP FOUNDATIONS: Piles ~~and piers~~ that are ~~capable of transferring~~ required to transfer ~~the~~ lateral and/or overturning forces between the structure and the soil shall have a positive connection between the pile and the pile cap, foundation mat, grade beam, or other element of the building foundation system. Cast-in-place concrete piles shall have a minimum longitudinal reinforcement ratio of 0.0025 and transverse reinforcing spaced at no more than 6 inches at the upper 10 feet of the pile.

3.4.4 Sloping Sites

The revisions to the Sloping Sites checklist statement are generally considered editorial, to improve clarity of intent. Specifically, this proposal changes the text from foundation embedment to reference the grade surface since the issue is unbalanced soil load, which relates to grade not foundation embedment. The proposed revisions are shown below.

SLOPING SITES: The exterior grade difference ~~in foundation embedment depth~~ from one side of the building to another does not exceed one story in height.

3.5 References

ASCE, 2003, *Seismic Evaluation of Existing Buildings,* ASCE/SEI 31-03, Structural Engineering Institute of American Society of Civil Engineers, Reston, Virginia.

ASCE, 2007, *Seismic Rehabilitation of Existing Buildings (including Supplement 1),* ASCE/SEI 41-06, Structural Engineering Institute of American Society of Civil Engineers, Reston, Virginia.

ASCE, 2014, *Seismic Evaluation and Retrofit of Existing Buildings,* ASCE/SEI 41-13, Structural Engineering Institute of American Society of Civil Engineers, Reston, Virginia.

ASCE, 2017, *Seismic Evaluation and Retrofit of Existing Buildings,* ASCE/SEI 41-17, Structural Engineering Institute of American Society of Civil Engineers, Reston, Virginia.

FEMA, 1992, *NEHRP Handbook for the Seismic Evaluation of Existing Buildings*, FEMA 178, prepared by the Building Seismic Safety Council for the Federal Emergency Management Agency, Washington, DC.

FEMA, 1998, *Handbook for the Seismic Evaluation of Existing Buildings: A Prestandard*, FEMA 310, prepared by the American Society of Civil Engineers for the Federal Emergency Management Agency, Washington, DC.

ICC, 2021, *2021 International Building Code,* International Code Council, Whittier, California.

Chapter 4: Guidance for Prioritization of Checklist Statements

4.1 Motivation

In most cases, when a Tier 1 screening is performed on an existing building, there are at least some non-compliant conditions found to be present. It is recognized that not all non-compliant conditions pose the same level of collapse risk and that some judgement is required to assess the overall relative threat posed by each condition. The goal of this task is to develop text that can assist the engineer in assessing the severity of Tier 1 noncompliant conditions related to risk of structural collapse. This assessment can be useful to create a relative ranking of the non-compliant conditions to better communicate the risk posed by each condition.

4.2 Summary of Changes Recommended

The recommended changes consist of expanded commentary text in ASCE/SEI 41-23 Appendix A, Section A.1. (Appendix A is the commentary for the checklists used in the Tier 1 screening procedure). This commentary text includes a list of deficiencies that are judged to be associated with significant risk of global and local collapse.

4.3 Technical Studies

As the purpose of this task is largely editorial, consisting of added commentary, there were no specific technical studies associated with this task. Instead, the working group members developed the recommendations based on judgment and consensus.

This task developed guidance in the Appendix A commentary for relative collapse risk associated with various Tier 1 checklist items and to help users prioritize non-conformance items in terms of relative risk. The goal of developing the added text is to assist the engineer in assessing the severity of Tier 1 noncompliant conditions related to risk of structural collapse. This assessment can be useful to create a relative ranking of the non-compliant conditions to better communicate to stakeholders the risk posed by each condition.

The methodology is based on a rating system developed by San Francisco engineers for a large-scale assessment of a college campus (SEAONC, 2017). The methodology also utilizes the current ASCE/SEI 41-17 (ASCE, 2017) Chapter 5 commentary and the previous commentary from the ASCE/SEI 41-06 (ASCE, 2007) simplified procedure, as well as various other commentary sections.

The intent is to relocate and expand the commentary and place it in Appendix A, which is the primary source of commentary for the Tier 1 checklists.

In developing the proposed text, the working group members considered a potential ranking of identified deficiencies from a Tier 1 screening in order of severity related to prediction of collapse risk and discussion of when a Tier 2 or Tier 3 evaluation may or may not be likely to "pass" a Tier 1 non-compliance.

The primary result of the study was to develop a list of deficiencies critical to risk of overall lateral instability. The types of items in the list include lack of a proper load path, presence of significant irregularities, significantly low lateral strength, lack of redundancy, and presence of extremely brittle elements. These prioritized deficiencies are based on the materials cited above as well as the working group members' experiences with existing building assessment and post-earthquake reconnaissance.

A second list includes the types of deficiencies that could lead to localized collapse, but that pose a lower risk of global collapse. This list includes primarily items related to lack of proper detailing, again based on the working group members' review of relevant documents and experience.

Finally, the working group considered providing guidance to assist engineers in determining the next steps following a Tier 1 screening. Typically, following Tier 1 evaluation, the engineer must decide whether to move to a Tier 2 or Tier 3 assessment to further evaluate the identified deficiencies, or if they should move directly to development of a seismic retrofit approach. The working group members considered hypothetical buildings and those from their collective experience that would be so non-compliant based on the Tier 1 screening that additional evaluation would not be helpful. Based on this, additional text has been proposed to assist the engineer when judging whether the non-compliant conditions are so severe that the building would be unlikely to pass a Tier 2 or Tier 3 evaluation, and that moving straight to development of retrofit recommendations is advisable.

4.4 Recommended Changes

Note about Change Proposals

This report documents aspects of change proposals as they were submitted to subcommittees of ASCE's *Seismic Retrofit of Existing Building Standards* Committee. Often, these change proposals were revised, in some cases substantively, by these subcommittees before they were adopted into ASCE/SEI 41-23. Readers should not rely on this report for information about the final version of provisions in ASCE/SEI 41-23.

This section describes recommended changes to ASCE/SEI 41-17 Section A.1, which consist of added commentary to this section, which serves as commentary to the Tier 1 Checklist statements.

The text addresses potential ranking of identified deficiencies from a Tier 1 screening in order of severity related to collapse risk and discussion of when a Tier 2 or Tier 3 evaluation may or may not be likely to "pass" a Tier 1 non-compliance. New or modified text is shown in blue.

A.1 GENERAL

This appendix chapter provides commentary to the checklists used for the Tier 1 screening in Chapter 4. This commentary, which is referenced from the checklists contained in Chapter 17, includes each checklist statement, followed by commentary on the potential deficiency represented by the checklist statement and considerations for mitigation of the deficiency. This checklist commentary can also be used for guidance in the further evaluation and potential retrofit of identified deficiencies using the Tier 2 deficiency-based evaluation and retrofit procedures in Chapter 5.

The deficiencies identified by a Tier 1 evaluation at the Collapse Prevention Structural Performance Level can generally be ranked by risk of collapse based on post-earthquake observation of buildings with similar deficiencies. Where major structural irregularities and poor detailing conditions are both present, this could lead to an overall critical deficiency. When judging whether a building will likely require a retrofit based on the Tier 1 deficiencies or estimating the likelihood that a building may pass a Tier 2 or Tier 3 evaluation, it may be helpful to consider the relative risk to collapse posed by the non-compliant conditions.

In general, deficiencies most critical to the overall stability buildings with the potential for global collapse include:

- Lack of proper substantial load path
- Major irregularities
  - Vertical irregularities
  - Extreme torsion
  - Weak or Soft stories
    - Substantial overstress of primary lateral resisting elements
    - Lack of Redundancy when combined with major irregularities
    - Poor detailing resulting in brittle primary lateral resisting elements or relative proportioning of primary lateral resisting elements
  - Inadequate column ties
  - Inadequate brace connections leading to possible story mechanism
  - Inadequate column strength relative to beams

Deficiencies generally related to local collapse include:

- Poor detailing of items at risk for local collapse
  - Inadequate beam ties
  - Lack of continuous beam reinforcing bars through supports
  - Lack of adequate beam-column joint reinforcing

- Inadequate punching shear capacity of flat plates
- Shear critical gravity items / deformation compatibility
- Non-ductile beam-column moment connections
- Non-ductile brace connections
- Anchorage of masonry / concrete walls to flexible diaphragms is inadequate or lacking altogether

The risk to global or partial collapse related to geotechnical site hazards varies widely based on the severity of the hazard. Surface fault rupture, slope failure and liquefaction have caused major structural damage in previous earthquakes, but it is difficult to predict if these conditions will be present at a specific building site or whether the effects will be severe.

When a major irregularity condition is present in combination with failure of the Quick Check of lateral strength on the main lateral elements it may be useful to conduct a supplemental check on the strength of the lateral resisting elements to assist in judging how likely a building is to pass a Tier 2 evaluation.

For example, for the Quick Checks of lateral strength, the shear demand in a story can be checked using the m-factors and expected material strengths used in a Tier 2 evaluation without conducting a full Tier 2 assessment. If the structure is still deficient using this check, there is a low likelihood of passing a Tier 2 evaluation and retrofit is likely required.

Additional commentary on the specific requirements for the Tier 2 analysis procedures is provided in Chapter C5. The appendix is organized as follows:

4.5 References

ASCE, 2007, *Seismic Rehabilitation of Existing Buildings (including Supplement 1),* ASCE/SEI 41-06, Structural Engineering Institute of American Society of Civil Engineers, Reston, Virginia.

ASCE, 2017, *Seismic Evaluation and Retrofit of Existing Buildings,* ASCE/SEI 41-17, Structural Engineering Institute of American Society of Civil Engineers, Reston, Virginia.

SEAONC, 2017, *Earthquake Performance Rating System ASCE 41-13 Translation Procedure,* prepared by the Building Ratings Committee, a subcommittee of the Existing Buildings Committee of the Structural Engineers Association of Northern California, San Francisco, California.

Chapter 5: Updates to Tier 2 Retrofit Provisions

5.1 Motivation

Based on feedback from various ASCE/SEI 41 users and the findings from the development of FEMA P-2006 (FEMA, 2018), the specific intent and requirements for the Tier 2 deficiency-only retrofit can be ambiguous and open to wide interpretation. This is particularly true for the scope of a retrofit and both the design of new elements and the assessment of the existing elements of the retrofitted structure. The goal of this task is to improve the clarity and consistency of the requirements for using Tier 2 to design and assess seismic retrofits of existing buildings.

5.2 Summary of Changes Recommended

In general, the changes proposed include a substantial rewrite and expansion of ASCE/SEI 41-17 (ASCE, 2017) Section 5.8 and commentary Section C5.8. Added subsections to ASCE/SEI 41-17 Section 5.8 address retrofit design criteria including evaluation requirements for select existing elements in the retrofitted building, evaluation requirements for new and modified elements, and detailing requirements for specific retrofit systems and elements.

5.3 Technical Studies

As the purpose of this task is largely editorial, intended to improve the text for usability, consistency, and enforceability, there were no specific technical studies associated with this task.

The development of the proposal followed a multi-step process, the first of which was developing a clear, concise philosophy statement for Tier 2 focusing on the underlying assumptions of the deficiency-based procedures, the expected certainty in the outcomes of these procedures compared to the Tier 3 systematic procedure, and the limitations that need to be in place to ensure uniform application of the procedure. This initial statement provided the basis for the outline, text, and commentary for the revised ASCE/SEI 41-17 Section 5.8.

A critical part of the Tier 2 retrofit procedure involves ensuring that any upgrade work performed on the building does not inadvertently cause harm to the building. This is important in a deficiency-based retrofit because unchanged elements do not require analysis, unlike the Tier 3 procedure where all components of a retrofitted building (existing, new, and altered) are required to be demonstrated to be in compliance with the selected performance objective. This “do no harm” clause is also consistent with the *International Existing Building Code* (IEBC) (ICC, 2021), which is the primary code-based path to referencing ASCE/SEI 41-17 for most jurisdictions in the United States.

The current Tier 2 provisions in Chapter 5 provide substantial guidance on Tier 2 evaluations, but they are somewhat limited in the requirements for Tier 2 retrofits, including detailing requirements for new elements, the extent that new elements need to be connected to the existing building, and what additional evaluation may be required as a result of adding retrofit elements.

In order to develop new provisions, Working Group 4 studied three common retrofit systems: wall anchorage, concrete shear walls, and steel braced frames. The retrofit systems, rather than the Common Building Type (CBT) being retrofitted, were selected as a way of organizing the provisions, since the same retrofit systems are used in many different CBTs.

Using a draft of what the working group called a Tier 2 "retrofit philosophy statement," the IEBC "do no harm" provisions, and draft outline of a generic retrofit design as a starting point, the working group considered expanded text for the scope and requirements of Tier 2 retrofit requirements. The results of these studies and the associated recommended scope for an expansion of the Tier 2 retrofit text is summarized in the following sections.

5.3.1 Studies of Representative Tier 2 Retrofit Systems

To assist with the development of the expanded Tier 2 retrofit provisions, three representative retrofit components were considered. These three items were judged to be both representative of commonly applied retrofit measures and were selected for relative simplicity of application. These studies were qualitative in nature, thinking about the procedure under which a retrofit design would be performed, what a typical retrofit solution might involve, and how that retrofit could impact the remaining elements of the existing structure. Highlights of these studies are summarized here.

5.3.1.1 WALL ANCHORAGE

A wall anchorage retrofit is most often implemented to improve the connection of heavy perimeter walls (concrete or masonry) to flexible diaphragms (wood or steel deck). This type of retrofit is commonly implemented, and the requirements using the Tier 2 retrofit procedure are generally clear. ASCE/SEI 41-17 Section 5.8 points to ASCE/SEI 41-17 Section 5.2.4, which points to ASCE/SEI 41-17 Section 7.2.12, which contains provisions for the design and detailing of wall anchorage retrofits. Therefore, no specific updates to ASCE/SEI 41-17 Section 5.8 were based on this study. In general, the current provisions for implementation of elemental retrofits were judged adequate. Therefore, this task focused primarily on implementation of lateral system retrofits as described in the next two sections.

5.3.1.2 CONCRETE SHEAR WALLS

Introduction of concrete shear walls into a variety of existing building types is a common retrofit procedure. Some of the issues with implementation of this retrofit system identified in this study include the following:

- Introduction of new concrete shear walls can change an existing structure from one CBT to another. For example, an existing concrete moment frame building (C1) with added shear walls

effectively becomes a concrete shear wall building (C2), and so the limitations on deficiency-based procedures in accordance with ASCE/SEI 41-17 Section 3.4.1 should apply to the retrofitted system.

- Introduction of shear walls can change the load distribution to other existing elements and the diaphragm demands (for example if a new shear wall is added in the middle of a long diaphragm span).
- New concrete shear walls can increase the overall seismic mass or reduce the building period, both of which can lead to higher seismic demands for the overall building.
- New concrete shear walls can increase gravity load demands on existing foundations.
- The connection of new concrete shear walls to existing diaphragms, existing columns, or existing walls must be considered.
- The detailing requirements (including reinforcing steel limits, boundary elements, and coupling beams) for new concrete shear walls needs to be considered.
- If constraints require the implementation of new concrete shear walls with discontinuities, for example a new shear wall at one floor supported on columns at the floor below, the evaluation of those columns needs to be considered.

The recommended revisions to ASCE/SEI 41-17 Section 5.8 were developed based on how the above considerations should be addressed in a Tier 2 retrofit as discussed in the following sections.

5.3.1.3 STEEL BRACED FRAMES

Introduction of steel braced frames into a variety of existing building types is a common retrofit procedure. Some of the issues with implementation of this retrofit system identified in this study include the following:

- Introduction of new steel braced frames can change an existing structure from one CBT to another. For example, an existing concrete moment frame building (C1) with added steel braced frames effectively becomes a steel braced frame building (S2) and so the limitations on deficiency-based procedures in accordance with ASCE/SEI 41-17 Section 3.4.1 should apply to the retrofitted system.
- Introduction of steel braced frames can change the load distribution to other existing elements and the diaphragm demands (for example if a braced frame is added in the middle of a long diaphragm span).
- New steel braced frames can reduce the building period, which can lead to higher seismic demands for the overall building.

- The connection of new steel braced frames to existing diaphragms, beams, columns, or other elements must be considered.
- The detailing requirements (including member proportioning and connection detailing) for new steel braced frames needs to be considered.
- If constraints require the implementation of new steel braced frames with discontinuities, for example a new brace at one floor that cannot extend to the floor below, the evaluation of those columns needs to be considered.

The recommended revisions to ASCE/SEI 41-17 Section 5.8 were developed based on how the above considerations should be addressed in a Tier 2 retrofit as discussed in the following sections.

5.3.2 Compliance with Deficiency-Based Evaluation

To be compliant with the Deficiency-Based procedures, any retrofitted building must remain in substantial compliance with the Common Building Types and the limitations for Tier 1 and Tier 2 procedures. In addition, if the building changes from one CBT to another (for example adding steel bracing to a steel moment frame), then the retrofitted structure must comply with limitations for the CBT associated with the retrofit system.

5.3.3 Additional Evaluation of the Retrofitted Building

In support of the "do no harm" philosophy, recommended text was developed to prohibit features that could be considered to do harm to an existing building being retrofitted if not adequately evaluated. These include the following:

- Building Configuration: if a retrofit creates an irregularity that would cause the building to fail Tier 1, that irregularity needs to be evaluated using Tier 2 provisions.
- Gravity Loads: if a retrofit increases gravity loads on an existing element, that element needs to be evaluated using the building code (since ASCE/SEI 41-17 does not address gravity loads). The 5 percent trigger is consistent with the IEBC trigger for evaluating increased gravity loads.
- Increased Demands to Existing Elements: if a retrofit increases seismic demands on an existing lateral element (for example adding a shear wall in the middle of a diaphragm span changes the behavior of the diaphragm), then that element needs to be evaluated using the Tier 2 procedures. The 10 percent trigger is consistent with the IEBC trigger for evaluating increased lateral loads.

5.3.4 Evaluation of New and Modified Structural Elements and Connections

Based on the system studies summarized in Sections 5.3.1.2 and 5.3.1.3, the working group considered it important to explicitly require that the Tier 2 evaluation of the retrofitted building address all new elements and existing structural elements that are modified as part of the retrofit.

Even though this requirement should be readily understood from the current ASCE/SEI 41-17 Section 5.8 text, a more explicit statement was judged prudent.

5.3.5 Retrofit Design Requirements for Specific Structural Systems

A significant aspect of the study was to develop text related to the design and detailing requirements for retrofit systems added to an existing building and the potential impacts on the existing structural systems, based partly on the system studies summarized in Sections 5.3.1.2 and 5.3.1.3. These studies resulted in the development of the following rules for Tier 2 retrofit systems:

- System Detailing: New systems added to a building must be designed as no less than "ordinary" system requirements as specified by ASCE/SEI 7-22 (ASCE, 2022) and applicable material standards, where such system designations are used. While it is not always necessary and appropriate to add a "special" system into a brittle existing building, there should be a minimum level of detailing for all new elements.

- System Design: The minimum m-factor for the design of new systems added to an existing building is 2.0 and not more than 2 times the lowest m-factor of all primary elements in the existing building. While there were not any studies to calibrate or validate these values, the working group, with concurrence from the overall project team, judged these values to be reasonable based on the rationale described below. In addition to the detailing limitations, this requirement places another floor on the level of ductility for a retrofit element. The second part of the provision is effectively a minimum strength requirement for new elements. New elements are to be sized for strength based on an m-factor not greater than 2 times the lowest m-factor of all primary elements of the seismic force resisting system for the selected performance objective(s) in order to assure compatibility with existing elements given the Tier 2 retrofit procedures employ only linear analysis. New elements may be detailed for more ductility consistent with higher m-factors; however, when proportioning the element and checking acceptance, the m-factor is limited in order to assure that the use of the strength-based linear procedures is valid. By setting a maximum m-factor, this provides a reasonable level of confidence that the new elements will not yield too far before any lower ductility elements, which would potentially overload these elements.

- Deformation Compatibility: New components in the vertical elements of the seismic force resisting system must be proportioned and designed using a maximum m-factor of not greater than the minimum m-factor of all secondary components of the existing seismic force resisting system. This requirement is intended to provide adequate projection for secondary elements subjected to nonlinear deformations without explicitly checking these secondary elements.

- Connections: Connections between new elements and existing elements are to be designed as force-controlled elements in order to ensure that the new elements are adequately engaged into the existing structure and that the interconnection is not the weak link. While this may have been understood from the current text, a more explicit requirement was judged prudent.

5.4 Recommended Changes

Note about Change Proposals

This report documents aspects of change proposals as they were submitted to subcommittees of ASCE's *Seismic Retrofit of Existing Building Standards* Committee. Often, these change proposals were revised, in some cases substantively, by these subcommittees before they were adopted into ASCE/SEI 41-23. Readers should not rely on this report for information about the final version of provisions in ASCE/SEI 41-23.

This section describes recommended changes to ASCE/SEI 41-17 Section 5.8. The recommended changes, as summarized in the previous section, are primarily editorial in nature with some technical updates intended to improve clarity and consistency. The completely revised and expanded ASCE/SEI 41-17 Section 5.8 is shown below. New or modified text is shown in blue.

5.8 TIER 2 DEFICIENCY-BASED RETROFIT REQUIREMENTS

~~When a Tier 2 deficiency-based retrofit is to be performed, deficiencies identified by a Tier 1 screening or Tier 2 evaluation shall be mitigated by implementation of retrofit measures in accordance with this standard. The resulting building, including strengthening measures, shall comply with the appropriate Tier 1 screening or with a Tier 2 deficiency-based evaluation for all potential deficiencies that the design professional identifies in the Tier 1 screening. The design professional shall perform Tier 2 analysis and evaluation as necessary to demonstrate the adequacy of all new structural elements, connections, and details added and all existing structural elements, connections, and details modified as part of the rehabilitation. Analysis and acceptance criteria of Section 5.3 shall be used in conjunction with the procedures in Sections 5.4 through 5.8. Compliance with Tier 2 retrofit procedures shall not be based on the Quick Check procedures in Section 4.4.3.~~

Where a Tier 2 deficiency-based retrofit is to be performed to achieve compliance with the selected performance objective(s), deficiencies identified by a Tier 1 screening or Tier 2 evaluation shall be mitigated by implementation of retrofit measures in accordance with this standard. The proposed retrofit measures shall satisfy the requirements of Sections 5.8.1 through 5.8.3. The scope of retrofit measures shall conform with Section 5.8.4.

5.8.1 Compliance with Deficiency-Based Evaluation

The resulting building, including strengthening measures, shall conform to a Common Building Type and to the limitations for use of the Tier 1 and Tier 2 evaluation procedures of Section 3.4.1. A combination of Common Building Types shall be permitted if the provisions of Section 3.4.1.2 are satisfied for the retrofitted building. The retrofitted building shall comply with Tier 2 evaluation requirements for all statements identified in the original building as nonconforming based on a Tier 1 screening and Tier 2 evaluations.

If the modifications to the building for the retrofit change the original building from one Common Building Type to another or creates a combination of Common Building Types different from the original building, the resulting building shall satisfy the limitations of Section 3.4.1 for the use of Tier 2 procedures.

5.8.2 Additional Evaluation of the Resulting Building

5.8.2.1 Building Configuration

If the retrofit creates a building configuration irregularity consisting of a Weak Story, Soft Story, Vertical Irregularity, Geometry, Mass, or Torsion condition as defined by noncompliance with the Building Configuration statements in Tables 17-2 and 17-3, the resulting building shall conform with the Tier 2 evaluation procedures in Section 5.4.2.

The requirements of this section are different from some model building code requirements for voluntary seismic retrofits (for example the IEBC), which prohibit the introduction of any new structural irregularity. Since the Tier 2 procedure is robust enough to adequately assess the seismic performance of buildings with irregularities, it is not necessary to prohibit these irregularities, just require that the building meets the selected performance objective(s) with the irregularities present. It should be noted, however, that the requirements of an adopted building code or local amendments may still govern the assessment of irregularities in a Tier 2 retrofit.

5.8.2.2 Gravity Loads

The retrofit measures shall not increase the gravity load demands to existing structure elements and foundations by more than 5 percent, or reduce the capacity of existing structural elements or foundations to resist gravity loads unless it is demonstrated that the component complies with the applicable building code requirements for gravity loads.

5.8.2.3 Increased Seismic Demands to Existing Elements

If the retrofit increases the seismic demands on any existing structural element, connection, or foundation by more than 10 percent as a result of added seismic mass or a change in seismic load path, such elements shall be demonstrated to be in compliance with Sections 5.2.4 and 5.2.5.

5.8.3 Evaluation of New and Modified Structural Elements and Connections

A Tier 2 analysis and evaluation shall be performed as necessary to demonstrate the adequacy of all new structural elements, connections and foundations added and all existing structural elements and connections modified as part of the retrofit. Tier 2 analysis methods of Section 5.2.4 and acceptance criteria of Section 5.2.3 shall be used in conjunction with the procedures in Sections 5.4 through 5.7.

5.8.4 Retrofit-Specific Requirements

5.8.4.1 General. In addition to compliance with Tier 2 evaluation procedures, the retrofit measures shall conform with this section.

5.8.4.2 Design and Detailing Requirements

New elements added to the seismic force resisting system of a retrofitted building shall conform with the following requirements:

(1) New elements and systems shall conform with, at a minimum, the detailing requirements for "ordinary" systems as prescribed in the applicable material standards referenced in Chapters 9 through 12.

(2) New components in the vertical elements of the seismic force resisting system shall be designed and detailed such that the corresponding element m-factor determined in accordance with Chapters 9 through 12 for a primary element and Collapse Prevention performance is no less than 2.0.

(3) Regardless of the level of detailing and ductility, new components in the vertical elements of the seismic force resisting system shall have strength to achieve the required acceptance criteria using an m-factor that is not more than 2 times the lowest m-factor of all primary elements of the seismic force resisting system for the selected performance objective(s).

(4) New components in the vertical elements of the seismic force resisting system shall be proportioned and designed using a maximum m-factor of not greater than the minimum m-factor of all secondary components of the existing seismic force resisting system for the selected performance objective(s) unless all secondary components are explicitly evaluated in accordance with Sections 5.2.4 and 5.2.5.

(5) Connections between new elements and between new and existing elements in the seismic force resisting system shall be designed to meet force-controlled acceptance criteria for the selected performance objective(s).

5.8.4.3 Scope of Evaluation Requirements for Existing Components

Existing elements of the seismic force resisting system of the resulting building shall be evaluated and demonstrated to be compliant with the selected performance objective(s) using the Tier 2 analysis methods of Section 5.2.4 and acceptance criteria of Section 5.2.5. The minimum scope of evaluation shall include the following:

(1) Existing beams, columns, and connections that form part of new braced frame, moment frame, or shear wall systems.

(2) Existing collectors, collector connections, and the collector connection to the diaphragms along the line of new and modified braced frames, moment frames or shear walls. Connections are to be evaluated as force-controlled elements.

(3) Existing diaphragm shears and connections to a line of new and modified braced frames, moment frames or shear walls.

(4) Existing columns below discontinuous braced frames, moment frames and shear walls shall be evaluated as force-controlled elements.

(5) Existing diaphragm or horizontal elements that transfer forces between vertical elements when new braced frames, moment frames, and shear walls create a horizontal offset.

5.5 References

ASCE, 2017, *Seismic Evaluation and Retrofit of Existing Buildings,* ASCE/SEI 41-17, Structural Engineering Institute of American Society of Civil Engineers, Reston, Virginia.

ASCE, 2022, *Minimum Design Loads and Associated Criteria for Buildings and Other Structures*, ASCE/SEI 7-22, Structural Engineering Institute of American Society of Civil Engineers, Reston, Virginia.

FEMA, 2018, *Example Application Guide for ASCE 41-13 Seismic Evaluation and Retrofit of Existing Buildings with Additional Commentary for ASCE/SEI 41-17*, FEMA P-2006, prepared by Applied Technology Council for the Federal Emergency Management Agency, Washington, D.C.

ICC, 2021, *2021 International Existing Building Code,* International Code Council, Whittier, California.

Part 6

Chapter 1: Revised Provisions for New Vertical Elements in Chapter 16

1.1 Motivation

Many past URM retrofits have performed poorly due to issues of deformation compatibility of the new vertical elements with existing URM walls and with flexible diaphragms. In many instances, moment frames or light braced frames have been used as new vertical elements in URM buildings, but they may be ineffective if they are not stiff enough to attract the intended design loads. Case studies were conducted to investigate these issues.

This change proposal combines several interrelated revisions to ASCE/SEI 41-23 in Chapter 16 that clarify or revise the design and detailing requirements for new vertical elements used to retrofit unreinforced masonry (URM) buildings. The various provisions address issues of relative rigidities between new and existing elements, allocation of shear between new and existing elements, diaphragm span lengths for retrofit structures, drift limits for new vertical elements, and detailing requirements for new elements. The motivation for these revised provisions is to provide an integrated set of provisions for how loads for new elements are determined and shared with existing elements, and to provide requirements for how stiff they need to be with these assumptions. This helps address the deformation compatibility issues directly, resulting in retrofits that utilize new vertical elements with stiffness comparable to the stiffness of the URM elements and stiff enough to reduce the diaphragm spans as intended. The revisions occur in the existing section on analysis, describing the URM special procedures for shear wall and diaphragm analysis requirements, but they also include a new section on detailing requirements that previously was lacking.

To add some historical context, the Special Procedure of ASCE/SEI 41-13 lacked clear guidance on the forces and approach to be used for the design of retrofit elements and how and whether to share load between the new and existing elements. Provisions were added in ASCE/SEI 41-17 to address these issues; however, these provisions were inconsistent with past engineering practice and forces developed in the evaluation, lost the notion of capacity design, and may not have had adequate case study testing. Three different seismic retrofit situations were investigated to illustrate issues with previous code provisions regarding determination of demand, load sharing when new elements are overlaid or in-line with existing elements, and drift limits. This effort resulted in the revised provisions proposed for ASCE/SEI 41-23 for new vertical elements used in URM building retrofits. The revised provisions include Section 16.2.3, Section 16.2.3.2.3, Section 16.2.3.5.4, Section 16.2.3.5.2.1, Section 16.2.3.5.2.2, Section 16.2.3.5.6, and Section 16.2.5. Reasons for revisions in each of the affected sections are described in the following section.

Note on terminology: In this chapter, steel moment frame will be used to generally represent the category of steel moment-resisting frames. A special steel moment frame will be abbreviated as SMF per AISC 341-16 (AISC, 2016). An ordinary steel moment frame will be abbreviated as OMF per AISC 341-16.

1.2 Summary of Changes Recommended

The changes clarify or revise the design and detailing requirements for new vertical elements used to retrofit URM buildings and occur in ASCE/SEI 41-23 Section 16.2.3, in a new Section 16.2.5, and in corresponding sections of the commentary. As the changes occur in several different subsections, a summary of the specific changes is provided below:

- In Section 16.2.3, the proposal clarifies how forces on existing masonry and new elements are shared for the purpose of calculating the demand of each element. The proposal states that forces attracted by relative rigidity are evaluated regardless of the design force used for new vertical elements. Given the potential differences between the strength and stiffness of new vertical elements and existing masonry wall elements, it is possible that a new wall could be designed to carry 100% of the required forces for the wall line but have insufficient stiffness to attract significant loads away from the masonry elements, leading to substantial damage in the masonry before the new elements provided effective resistance. To address this, the standard requires that loads be shared by relative rigidity between the new and existing elements. An explicit requirement was added to emphasize that, after the loads have been distributed, the masonry must be evaluated using the provisions of Section 16.2.2.3.

- In Section 16.2.3.2.3, the proposal also clarifies the diaphragm span length after a new vertical element is added. The new provision includes other systems beyond shear walls as lateral force-resisting elements that divide the diaphragm span. The rationale to exclude all systems besides shear walls was because shear walls are much stiffer than more flexible steel systems, such as a moment frame, and flexible systems may not be sufficient to reduce diaphragm displacements significantly. Case studies using three-dimensional computer models indicate that a moment frame designed to meet the proposed 0.0075 (0.75%) interstory drift limit with the proposed design forces using tributary area/2D modelling substantially reduces the diaphragm deflection from the unretrofitted building at the moment frame location (approximately by half), effectively dividing the span. Therefore, the provision on diaphragm span length should expand beyond shear walls to include other, less stiff systems, like steel moment frames or steel braced frames, provided they meet the 0.75% drift limit.

- In Section 16.2.3.5.2.1, the proposal requires that existing masonry elements be evaluated for the loads they attract, even where new vertical elements are designed for 100% of the design forces.

- In Section 16.2.3.5.2.2, the drift limit is omitted here since it is now included in Section 16.2.3.5.6 for all types of new vertical elements.

- In Section 16.2.3.5.4, the proposal also simplifies application of the Special Procedure on masonry buildings with new vertical elements. Chapter 16 contains a design procedure separate from the rest of ASCE/SEI 41, and therefore demands of new and existing vertical lateral force-resisting elements should also be included in this stand-alone chapter. In an effort to avoid referring to other chapters in ASCE/SEI 41 and using other methods of analysis to determine the demands for new vertical elements, the force determination method is the same for new elements as it is for the masonry walls.

- In Section 16.2.3.5.6, the proposal simplifies the drift limit as well. Previously, moment frames in line with a URM wall could not be used unless the wall had rocking-critical piers, and the moment frames were designed to take 100% of the force tributary to the wall line and the drift was limited to 0.75%. Other new vertical elements of the lateral force-resisting system were limited to a drift of 1.5%. The proposal eliminates the less stringent 1.5% drift limit for non-moment frames elements and applies a 0.75% drift limit to all new vertical elements, regardless of system type. The case studies confirmed that use of this drift limit will provide better performing retrofits without a requirement to do a full-scale 3D analysis, thus simplifying the retrofit process.

- Section 16.2.5 is added to provide detailing requirements that are currently missing in the Special Procedure. The Special Procedure is in a stand-alone chapter with no distinction between deformation-controlled or force-controlled actions. In order to apply special detailing requirements to vertical elements, it is necessary to understand the ductility demand. This is beyond the scope of the Special Procedure. Ductility demands are generally low, and lateral force-resisting systems are typically drift controlled. Adopting additional detailing requirements would be inconsistent with retrofit outcomes of IEBC A1, which has no explicit detailing requirements, and suggests higher performance expectations than CP at the BSE-1E level. Thus, it is easier to refer to the “ordinary” requirements of referenced material standards in Chapters 9 through 12 and keep the Special Procedure separate.

Revisions, additions, and deletions are also found in Commentary Section C16.2.3, Section C16.2.3.2.3, Section C16.2.3.5.1, Section C16.2.3.5.4, Section C16.2.3.5.5, Section C16.2.3.5.6, and Section C16.2.5.

1.3 Technical Studies

1.3.1 Overview of Working Group 6 Case Studies

The Special Procedure in ASCE/SEI 41-13 lacked clear guidance on the forces and approach that should be used for the design of retrofit elements and how and whether to share load between the new and existing elements. Provisions were added in ASCE/SEI 41-17 to address this issue, under Section 16.2.3.5 “New Vertical Elements,” including those in Sections 16.2.3.5.2.1, 16.2.3.5.4, and 16.2.3.5.5.

> 16.2.3.5.2.1 *Lateral Force Distribution.* Lateral forces shall be distributed among the vertical elements in proportion to their relative rigidities….
>
> 16.2.3.5.4 *Forces on New Vertical Elements.* The Linear Static Procedure of Section 7.4.1 shall be used to determine forces on new lateral elements. The building period shall be calculated according to Eq. (7-18) using $C_t = 0.020$ and $\beta = 0.75$. The value of $C_1C_2C_m$ in Eq. (7-21) shall be taken as 1.4.
>
> 16.2.3.5.5 *Acceptance Criteria for New Vertical Elements.* New vertical elements shall satisfy the acceptance criteria provisions of Section 7.5.2.2. The value of m in Eq. (7-16) shall not exceed 4.0

However, these provisions are inconsistent with past engineering practice and forces developed in the evaluation, lose the notion of capacity design, and may not have had adequate case study testing. In addition, it is not explicitly clear if the load sharing of Section 16.2.3.5.2.1 applies to both the new and the existing elements, or only the new elements. Issues with the ASCE/SEI 41-17 provisions are discussed in more detail ahead. The focus of the Working Group 6 effort was to clarify and simplify the Special Procedures of ASCE/SEI 41-23 Chapter 16 and provide for better performing retrofit designs. Numerous 2D and 3D case studies were undertaken to develop these recommendations and alleviate the need for retrofit designers to do 3D evaluations of URM buildings. The hope is that this will stimulate more and better performing URM retrofits.

1.3.1.1 GOALS, APPROACH, AND CASE STUDY BUILDING DESCRIPTIONS

The primary objective of the Working Group 6 effort was to improve the Special Procedure in Chapter 16, to make this a standalone procedure without cross references to other ASCE/SEI 41 code sections, to provide more rational analytical tools, and to provide guidance that would result in better performing URM retrofit designs. The case studies described below included both 2D and 3D analyses of a variety of retrofit situations with one-story, two-story, and six-story configurations. These studies included numerous variables to address retrofit situations, modeling assumptions, building heights, diaphragm stiffness, wall stiffnesses, drift limits, and detailing provisions. Some studies influenced more than one proposed code revision; other code revisions are primarily based on the judgement of the authors and not the direct result of a case study. Where appropriate, the links between the case studies and proposed code revisions are described below.

Two-Story Case Study Building Description

Case study analyses on a representative URM bearing wall building were used to study different situations. Three different basic seismic retrofit situations were investigated to illustrate issues with current code provisions regarding determination of demand, load sharing when new elements are overlaid or in-line with existing elements, and drift limits in ASCE/SEI 41.

The unretrofitted condition for the case study building explored is taken from Chapter 12 of FEMA P-2006, *Example Application Guide for ASCE/SEI 41-13 Seismic Evaluation and Retrofit with Additional Commentary for ASCE/SEI 41-17* (FEMA, 2018), which was in turn drawn from the URM bearing wall example in the *2009 IEBC SEAOC Structural/Seismic Design Manual (*SEAOC, 2012). The design example features a rectangular unreinforced masonry building with flexible wood

diaphragms. This two-story URM structure was utilized in a series of different retrofit situations. The example building is a two-story, unreinforced masonry bearing wall office building located in Los Angeles with an approximately 30-foot by 60-foot floor area as shown in isometric view in Figure 1-1 and in elevations and plans in Figure 1-2 through Figure 1-4. The example building does not represent a specific structure, but it is consistent with prevalent building configurations and has an assumed construction date of 1920.

For each retrofit situation, results from ASCE/SEI 41-13 and ASCE/SEI 41-17 are compared. Although ASCE/SEI 41-13 does not have requirements for new vertical elements, the standard of practice has been to use the demands from the evaluation analyses. This approach is described in the FEMA P-2006 *Design Guide* and is used in this case study exercise.

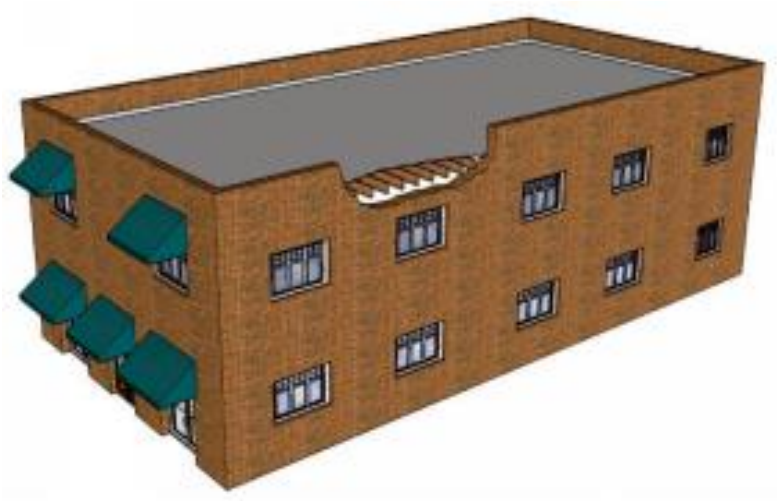

Figure 1-1 Isometric view showing example building with perimeter URM bearing walls, URM parapets, and wood frame roof and floor diaphragms with south wall at left.

The structural system of the building consists of a wood frame roof and second floor that are supported by perimeter unreinforced masonry walls and interior wood stud walls. The roof is constructed with 1× straight sheathing over 2×12 wood joists at 24 in. o.c., and the roof covering is applied directly to the straight sheathing. The second floor is constructed with hardwood flooring and 1× straight sheathing over 2×12 wood joists at 16 in. o.c. The 2×12 roof and floor joists were measured at 1 $^5/_8$ in. × 11 $^1/_2$ in., and typical of older buildings, are larger than the current size of 1-$^1/_2$ in. × 11 $^1/_4$ in. Both the roof and second floor diaphragms can be treated as flexible. The first floor is a concrete slab-on-grade. The unreinforced masonry walls are located around the exterior of the building, and they measure 13 in. thick at the first and second stories and 9 in. thick at the parapet. There are bearing and nonbearing wood stud walls located on the interior. These wood walls are covered with plaster over wood lath on both sides. The building is founded on continuous concrete strip footings.

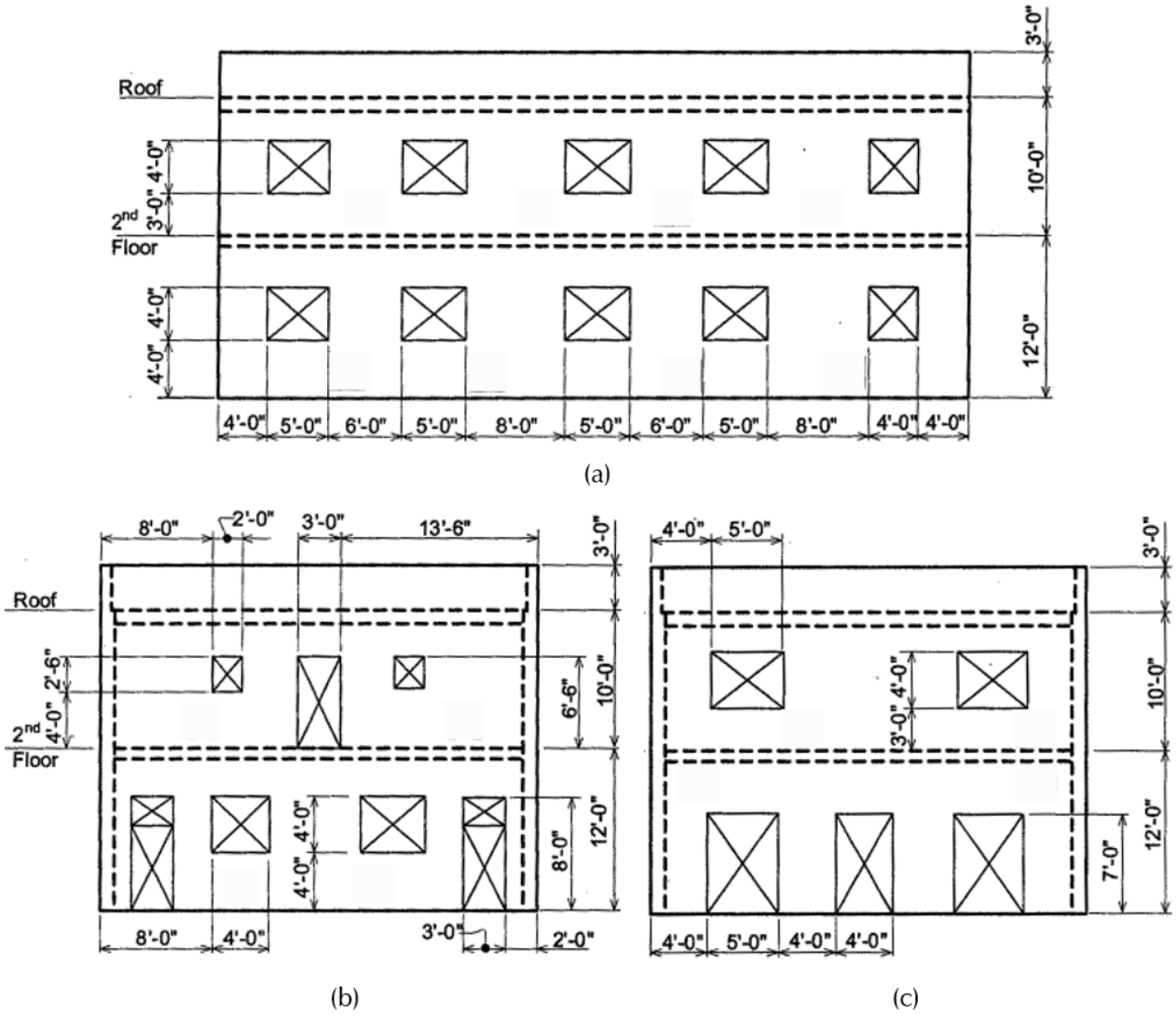

Figure 1-2 Example building (a) side wall elevation, (b) rear (north) wall elevation, and (c) front (south) wall elevation.

Based on the FEMA P-2006 *Design Guide* example, the seismic weight tributary to the roof is 192 kips and the seismic weight tributary to the second floor is 275 kips for a total seismic weight of 467 kips. Per FEMA P-2006, the base shear at the base of the building computed using the Special Procedure of ASCE/SEI 41-13 is 213 kips for each wall in each direction using the equation $V=CS_aW$ where C=1.0 and $S_a = S_{XS,BSE\text{-}1E}$ = 0.913. The value of S_{X1}=0.507 is used for various computations. Wall capacities for the original condition used in the examples below were taken from FEMA P-2006.

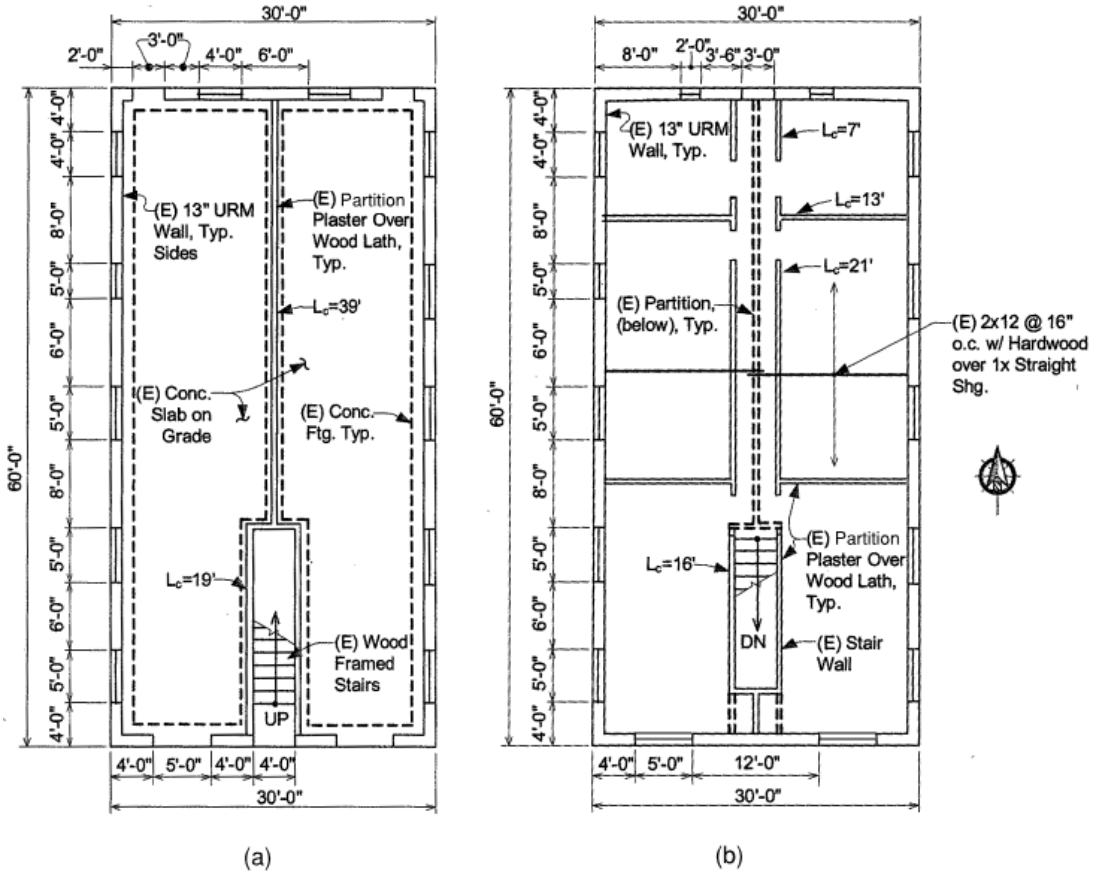

Figure 1-3 Example building plans for (a) first floor and (b) second floor.

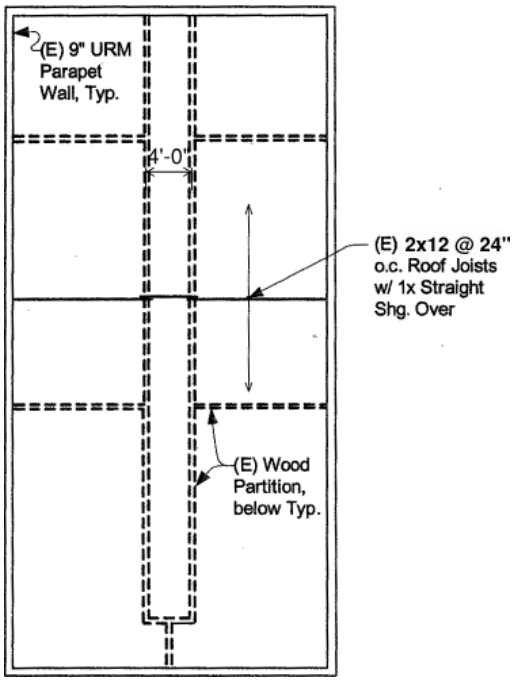

Figure 1-4 Example building roof plan.

The 3D ETABS model of the building is shown in Figure 1-5. Several retrofit options were considered in the case studies, and these were incorporated into the ETABS models. Additional 2D RISA models were created for the retrofit situations and results compared with the 3D ETABS results.

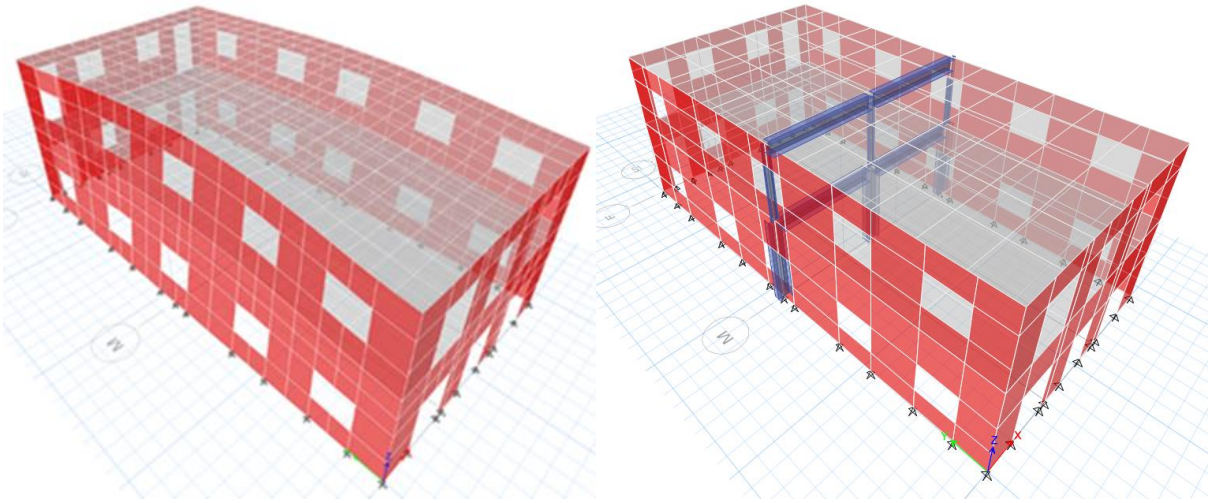

Figure 1-5 3D ETABS model of example unretrofitted two-story URM building at left and one of the retrofit situations with a steel moment frame shown at right.

One-Story Configuration Case Study Description

The bottom story of the two-story building described above was used as a one-story structure for the purposes of an out-of-plane wall investigation. Five different modeling assumptions were used to study the out-of-plane behavior of the one-story configuration. One additional two-story variation was included for comparison. The basic one-story configuration is shown in Figure 1-6. The variations are shown in Figure 1-27 and discussed in detail in Section 1.3.3.3. These models were created to study the 3D effects of out-of-plane wall stiffness by softening walls and diaphragms in isolation. Results from these studies were used to improve the two-story and six-story ETABS models used for the other case studies described below. The various modeling assumptions used for the out-of-plane stiffness investigation were as follows:

- One story, roof (flexible) diaphragm, membrane walls
- One story, roof (flexible) diaphragm, thin shell walls
- One story, floor (10x stiffer) diaphragm, thin shell walls
- One story, roof (flexible) diaphragm, thin shell walls, side walls on rollers
- One story, roof (flexible) diaphragm, thin shell walls, side walls fixed at base

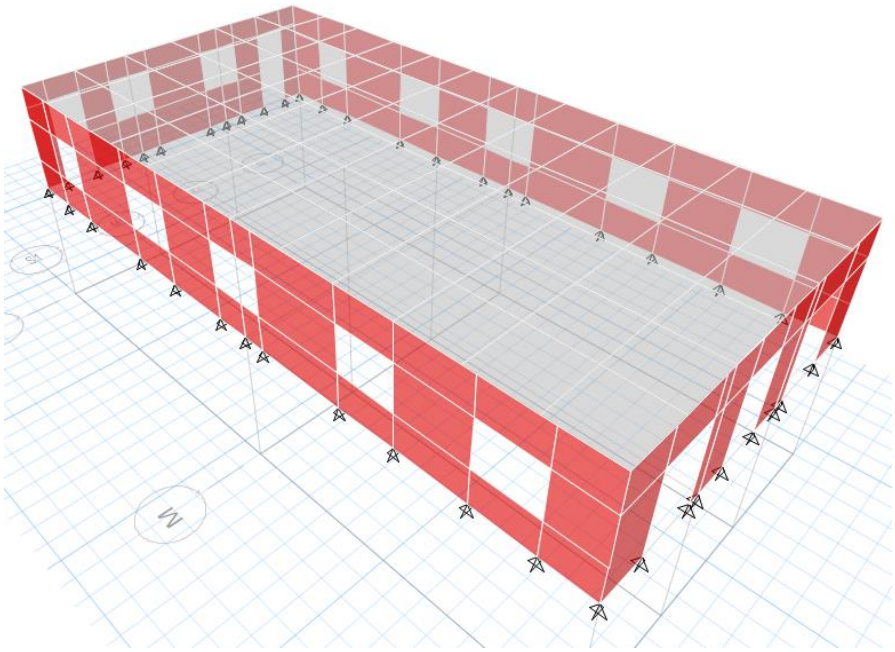

Figure 1-6 3D ETABS model of example one-story URM building used to study out-of-plane behavior of URM walls.

Six-Story Case Study Building Description

A six-story structure was generated by extending the properties of the upper story of the two-story ETABS model for an additional four stories. Figure 1-7 shows the 3D ETABS model including a steel steel moment frame used for one of the retrofit case studies. Additional 2D RISA models were created for the retrofit situations and results compared with the 3D ETABS results. Note that extruding the upper story of the two-story building to create the six-story building is likely not fully representative of a realistic six-story building. The walls at the lower stories would likely grow thicker by one or two wythes. This was done for simplicity. However, the six-story model does still help investigate 3D effects and extend the investigation beyond the primary thrust of evaluation using the two-story models.

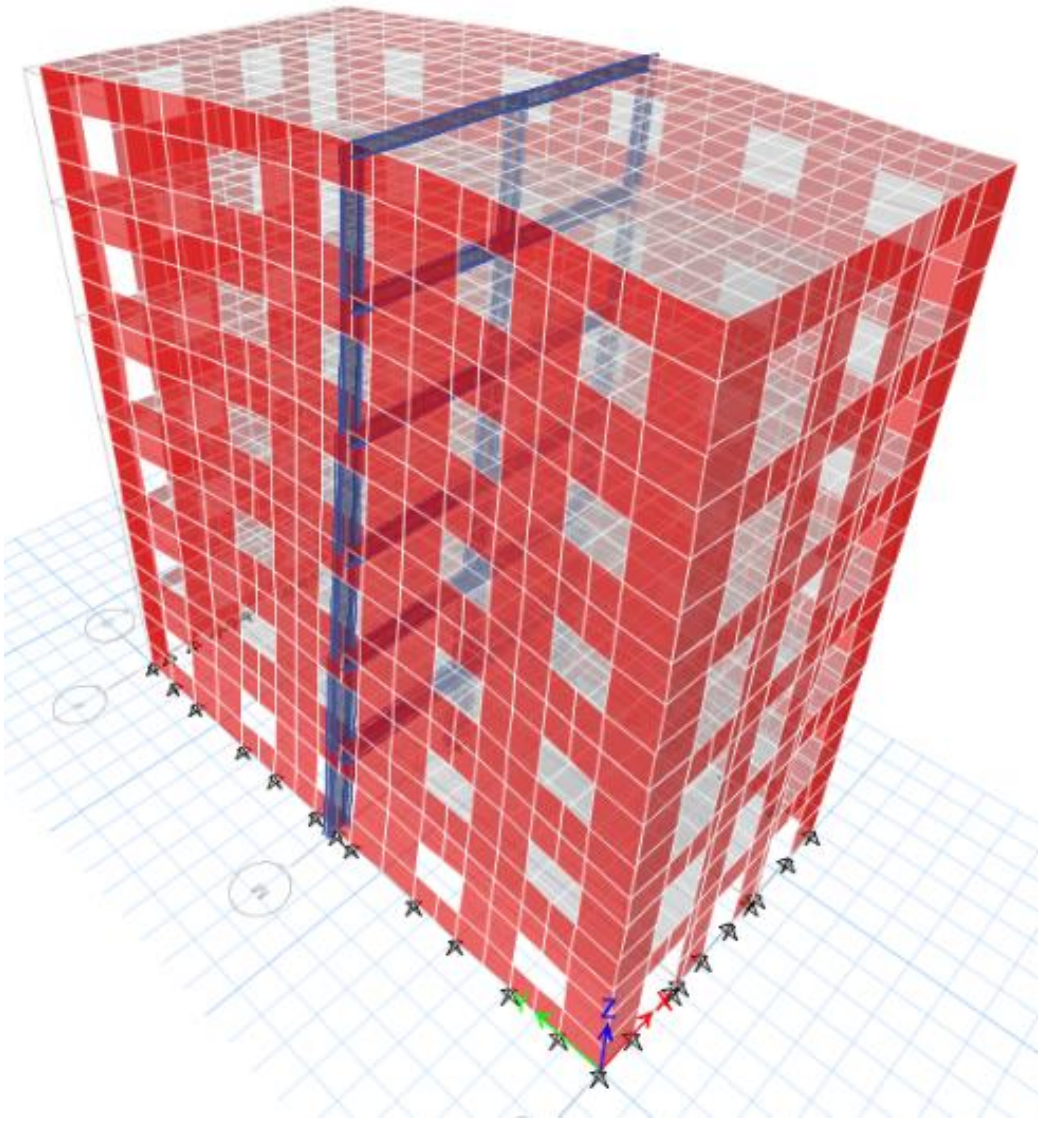

Figure 1-7 3D ETABS model of example six-story URM building used for case studies; this figure includes the steel moment frame used as one of the retrofit situations.

1.3.1.2 RETROFIT SITUATIONS STUDIED

Evaluation of the building using the Special Procedure in Chapter 16 of ASCE/SEI 41-13 and ASCE/SEI 41-17 prior to retrofit reveals the first story front and rear walls have inadequate capacity. The side walls have adequate capacity and will not be addressed any further. To address the deficiencies of the transverse Level 1 walls, three retrofit situations are explored as shown in Figure 1-8. Retrofit Situation 1 involves the addition of new shotcrete on the inside faces of both the front and rear walls. Retrofit Situation 2 involves the addition of new lateral-force-resisting elements at the mid-span of the diaphragm. Retrofit Situation 3 involves the addition of new lateral-force-resisting elements at the weak store-front area at the first floor of the front wall. Retrofit Situations 2 and 3

both include two variations each in the two-story configuration, and Situation 2b with a steel moment frame is considered in both a two-story and six-story configuration.

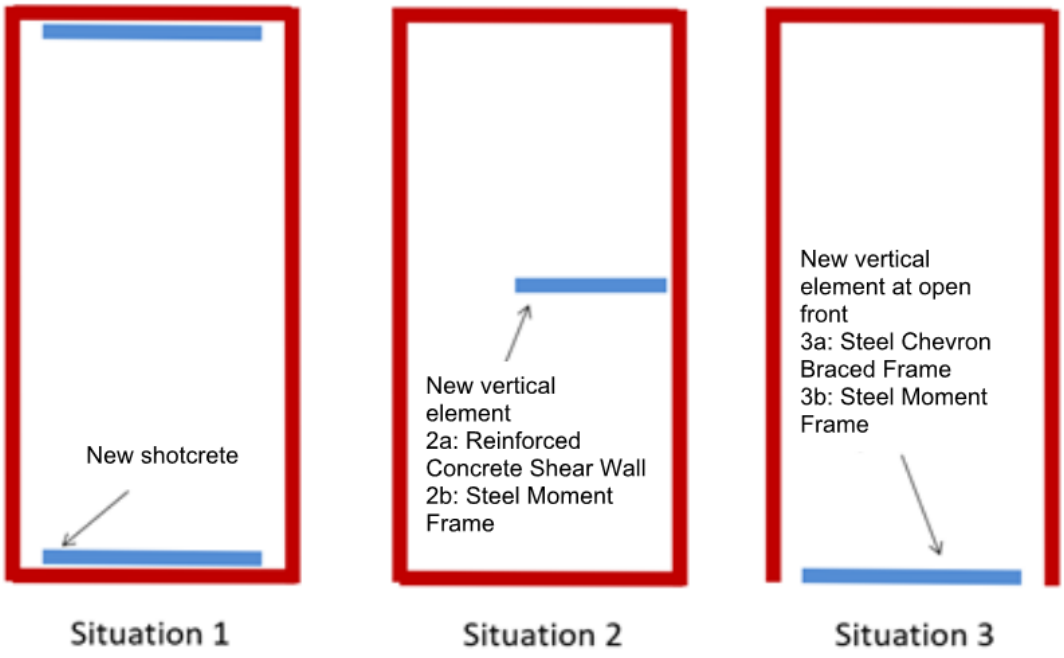

Figure 1-8 Retrofit Situations 1, 2a, 2b, 3a, and 3b used in case studies.

The unretrofitted version of Situation 1 and Situation 2 is identical to the unretrofitted URM building in the FEMA P-2006 *Design Guide*.

- Retrofit Situation 1 involves strengthening the front and rear masonry walls with the addition of shotcrete on the inside face of these walls. Retrofit Situation 1 was studied in the two-story configuration and used to confirm proposed revisions regarding the allocation of forces to new and existing vertical elements. This scheme is described in Section 1.3.2 below.

- For Retrofit Situation 2, a new vertical element is added to the middle of the building, splitting the diaphragm, and redistributing demands on the front and rear walls to the new element in the middle. The two permutations for Retrofit Situation 2 are a new vertical element that is a two-story concrete shear wall (2a - RCSW), and a new element that is a two-story steel moment frame (2b – steel moment frame). Retrofit Situation 2b was studied in both the two-story and six-story configurations. These studies were used to investigate the stiffness required for both diaphragms and new vertical elements in order to obtain reasonable retrofit performance. Both the drift limits and diaphragm span length revisions were influenced by these studies. See Section 1.3.5 regarding review of detailing requirements, such as whether to require an SMF or permit just an OMF for steel moment frames.

- The unretrofitted version of Situation 3 does not have a front wall. Examples of this kind of structure would be open front buildings with a store at the street level and offices or residences

on the upper story. For Retrofit Situation 3, a new vertical element is added to the open front. Retrofit Situation 3 also has two permutations including a new vertical element that is a one-story steel braced frame (3a – Steel BF) and a new element that is a one-story steel moment frame (3b – Steel moment frame).

See Figure 1-9 and Figure 1-10 for first floor plans with initial wall demands prior to retrofit. The demand of 75 kips shown in Figure 1-9 comes from FEMA P-2006 Table 12-8. The 80 kips demand on the rear wall in Figure 1-10 results from the seismic contribution of the front wall weight being added to the rear wall since the front wall is open at the lower level. Retrofit design provisions from both ASCE/SEI 41-13 and ASCE/SEI 41-17 are used in the case studies for comparison.

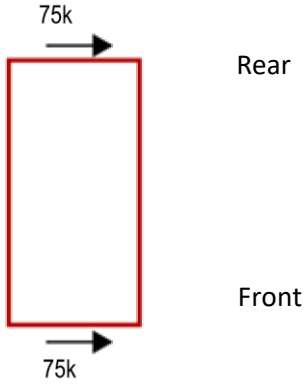

Figure 1-9 Retrofit Situation 1 and 2 before retrofit showing URM wall demands at front and rear transverse walls.

ASCE/SEI 41-17 Section 7.3.1.1 defines demand-capacity ratio (DCR) as Q_{UD} / Q_{CE}. As such, it is a measure of ductility, rather than a measure used in typical structural engineering practice to represent acceptance criteria, where the capacity would be factored, and in the linear procedures of ASCE/SEI 41-17 would include the multipliers *m* and κ on the denominator Q_{CE}. This DCR definition is not used for vertical elements in the ASCE/SEI 41-17 Chapter 16 Special Procedure. Throughout this discussion, the term "acceptance ratio" is used to describe the ratio of demand to capacity in the traditional sense to provide a consistent approach for comparisons. An acceptance ratio of less than one is required to meet the requirements of the provisions. An acceptance ratio in excess of one indicates the demand on the subject element exceeds the capacity allowed by the provisions. Nevertheless, there is some nuance with differing definitions in different parts of each document.

- ASCE/SEI 41-13 and ASCE/SEI 41-17 Special Procedure: In both documents, the Special Procedure of Chapter 16 defines the acceptance criteria for rocking piers as $0.7Vwx/\sum Vr$. For the purpose of this study and as an example, the acceptance ratio is also defined as $0.7Vwx/\sum Vr$. Other materials and related actions are addressed similarly with a demand divided by a capacity in the traditional sense.

- ASCE/SEI 41-17 LSP: Where Chapter 16 refers back to Chapter 7, the acceptance ratio is defined as $Q_{UD}/m\kappa Q_{CE}$ where both the *m* and κ factors are included.

- ASCE/SEI 41-23 as proposed here: This would revert back to the acceptance criteria in the Special Procedure for the element in question without reference to Chapter 7. Acceptance ratios are defined in the same way as the first bullet above.

Wall capacities from FEMA P-2006 Table 12-12 are 45 kips at the rear wall first story for the rocking piers, resulting in an acceptance ratio 0.7(75 kips)/45 kips=1.17. The wall capacity for the front wall was found to be a lower value of 31.9 kips as there are more openings. Governing acceptance ratios from ASCE/SEI 41-17 Equation 16-18:

Front Wall: $0.7V_{wx}/\sum V_r$ = **1.65**

Rear Wall: $0.7V_{wx}/\sum V_r$ = **1.17**

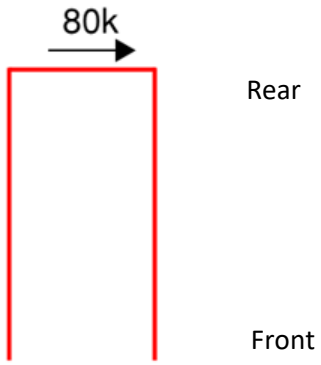

Figure 1-10 Retrofit Situation 3 before retrofit showing URM wall demand at rear transverse wall.

Using the same wall capacity of 45 kips cited above, the governing acceptance ratio is:

Rear Wall: $0.7V_{wx}/\sum V_r$ = **1.24**

1.3.1.3 SUPPLEMENTARY STUDIES

Several additional studies were conducted as part of the overall Working Group 6 effort. In general, these were parametric studies based on one of the Retrofit Situations and will be described below in conjunction with the appropriate Retrofit Situation.

- One-story out-of-plane wall stiffness study: The purpose of this study was to address modeling concerns and identify the most reliable way to incorporate out-of-plane wall stiffness in the 3D models used to evaluate the various retrofit situations. An early version of Retrofit Situation 2b showed that the wall stiffness used in the 3D ETABS model influenced the loads to the moment frame. This study was done by varying the modeling assumptions as described with the one-story structure description above. Results were used to refine the ETABS models used for the other case studies.

- Drift Validation Study: ASCE/SEI 41-17 includes a drift limit of 1.5% for all new vertical elements except moment frames for which the drift limit was reduced to 0.75%. Studies were done using the Retrofit Situation 2a to confirm the adequacy of the steel moment frame design using the Special Procedure demands and to determine the most appropriate drift limit. As a result, the drift limit of 0.75% was extended to all new vertical elements for ASCE/SEI 41-23.

- Diaphragm Span Length Review: The definition of the diaphragm span length was reviewed based on a review of the results from Retrofit Situations 2 and 3 and resulted in revisions to the definition accompanying ASCE/SEI 41-23 Figure 16-1 and Section 16.2.3.2.3.

- Detailing Provisions in Chapter 16 Special Procedure: This effort involved a comparison of detailing requirements for various retrofit types found in other parts of ASCE/SEI 41 to determine whether any of these should be brought into Chapter 16.

Details on these supplementary studies are provided in sections ahead.

1.3.1.4 SUMMARY OF STUDIES

A summary of the various case studies and supplementary studies and findings is shown in Table 1-1 below.

Table 1-1 Summary of Retrofit Situations and Case Studies

Retrofit Situation	Retrofit Description	No. of Stories	Purpose of Case Study	Conclusion
1	6” shotcrete on inside face of front and rear walls, first story only	2	Evaluate 3 methods of allocating forces between the URM and concrete material layers	Designer may choose how to allocate forces, but URM walls must be capable to resist loads they attract by relative rigidity
2a	8” concrete shear wall at midspan of diaphragm, two-story wall	2	Evaluate diaphragm behavior with stiff retrofit element added at midspan; results used for comparison with case 2b	ASCE/SEI 41-13 method limited by diaphragm capacity appears to be the more rational method and results in more cost effective retrofit.

Table 1-1 Summary of Retrofit Situations and Case Studies (continued)

Retrofit Situation	Retrofit Description	No. of Stories	Purpose of Case Study	Conclusion
2b	Steel moment frame at midspan of diaphragm, two-story frame (augmented by drift validation supplemental study)	2	Evaluate several different moment frame designs to assess stiffness and strength required at midspan to effectively reduce diaphragm span to half the building length. Evaluate modeling assumptions about masonry wall out-of-plane properties and diaphragm stiffness.	Steel moment frame must have adequate stiffness otherwise ineffective. Study shows that drift ratio of 0.75% provided moment frame with adequate stiffness and this was recommended for new provisions.
2b	Steel moment frame at midspan of diaphragm, six-story frame	6	Extend moment frame to 6-stories to assess whether 0.75% drift limit still effective for taller structure	Steel moment frames designed with the 0.75% drift limit still had adequate stiffness in the taller structure
3a	Chevron braced frame at the open front, first story only	2	Evaluate effectiveness of braced frame at open front	Study confirmed that braced frame adequate as retrofit for the open front condition
3b	Steel moment frame at open front, first story only	2	Evaluate effectiveness of braced frame at open front when frame designed with 0.75% drift limit	Study confirmed that frame designed with drift limit of 0.75% provided adequate stiffness for the open front condition

1.3.2 Case Study: Retrofit Situation 1 with New Vertical Elements at Front and Rear Walls

This case study was intended to answer two primary questions:

1. Should new vertical elements be designed for 100% of the retrofit design force?
2. Should the original unreinforced masonry walls be checked for the forces attracted due to their relative rigidity?

As a result of this study, the Special Procedure will continue to allow the designer to choose how much load will be resisted by new vertical elements. Nevertheless, provisions were added to explicitly require that the masonry walls be evaluated for the forces attracted due to their relative rigidities, even where new elements are designed to take 100% of the retrofit design forces. This new

language is found in the ballot proposal for ASCE/SEI 41-23 Section 16.2.3.5.2.1. Thus, the answer to both Questions 1 and 2 above is "yes."

In this retrofit situation, walls without adequate capacity must be strengthened. A retrofit consisting of the addition of a shotcrete wall has been selected. Shotcrete will be applied to the inside face of the transverse end walls as shown in blue in Figure 1-11.

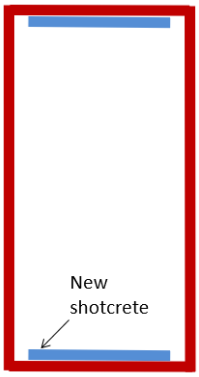

Figure 1-11 Figure showing Retrofit Situation 1 plan.

Since the analysis shows adequate strength in the second story walls, shotcrete will only be applied at the first story (see Figure 1-12). The vertical extent of the shotcrete will be from the existing foundation to just below the straight sheathing at the second-floor diaphragm. The corner Piers 17 and 21 have a length of only 11 in. between the existing doors and the perpendicular walls. Therefore, these piers will be designed as enlarged pilasters with closed ties using a thickness greater than the rest of the shotcrete wall.

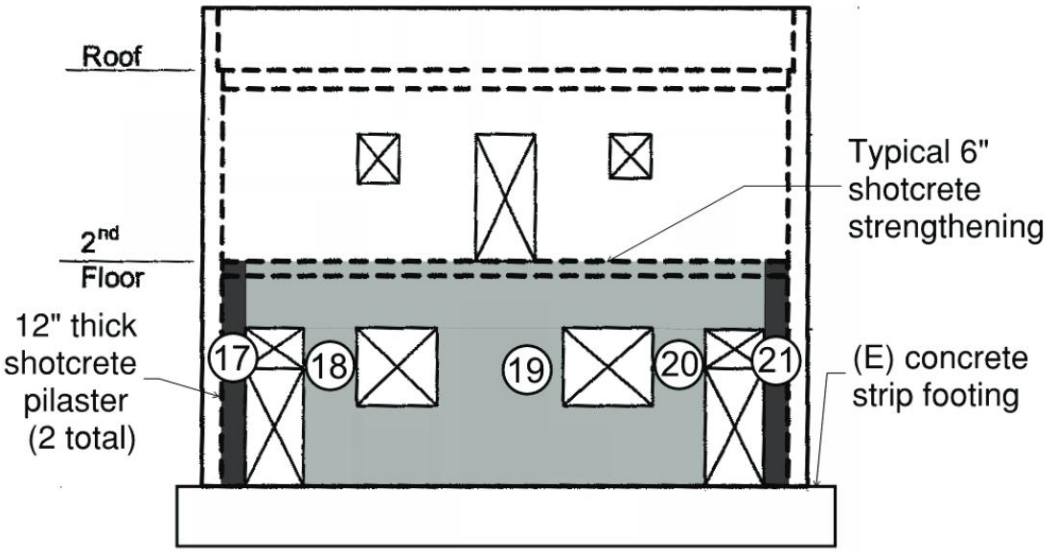

Figure 1-12 Figure showing Retrofit Situation 1 Elevation – rear wall.

In the provision added in ASCE/SEI 41-17 Section 16.2.3.5.4, the Linear Static Procedure of Section 7.4.1 is required to be used to determine forces on new lateral elements. Using the Linear Static Procedure on the demand side requires the use of *m*-factors on the capacity side. Since Chapter 16 does not have *m*-factors, the values from Chapter 11, the unreinforced masonry chapter, are used for the masonry walls. Chapter 10 is used for the concrete elements.

Per ASCE/SEI 41-17 Table 10-22, a shear-controlled concrete shear wall at the Life Safety Building Performance Level has an *m*-factor of 2.5. The masonry walls have a rocking-controlled failure mode with an *m*-factor of 3.75. Thus, 3.75 is the *m*-factor for the masonry that are used for all the following retrofit situations. See Figure 1-13 for demands. Note that with shotcrete applied, the URM piers in the composite shotcrete and masonry walls may no longer be rocking critical. For simplicity, this subtlety was not considered in this comparison study.

Figure 1-13 has four images that show wall capacities per ASCE/SEI 41-13 before the retrofit (same as ASCE/SEI 41-17), per ASCE/SEI 41-13 after the retrofit, per ASCE/SEI 41-17 with no *m*-factor after the retrofit, and per ASCE/SEI 41-17 with *m*-factors after the retrofit for use with concrete (*m*=2.5) and masonry (*m*=3.75). Note that the wall capacity for ASCE/SEI 41-17 of 310 kips is computed using the Linear Static Procedure of Chapter 7 Eq. 7-21 as $V = C_1C_2C_mS_aW$.

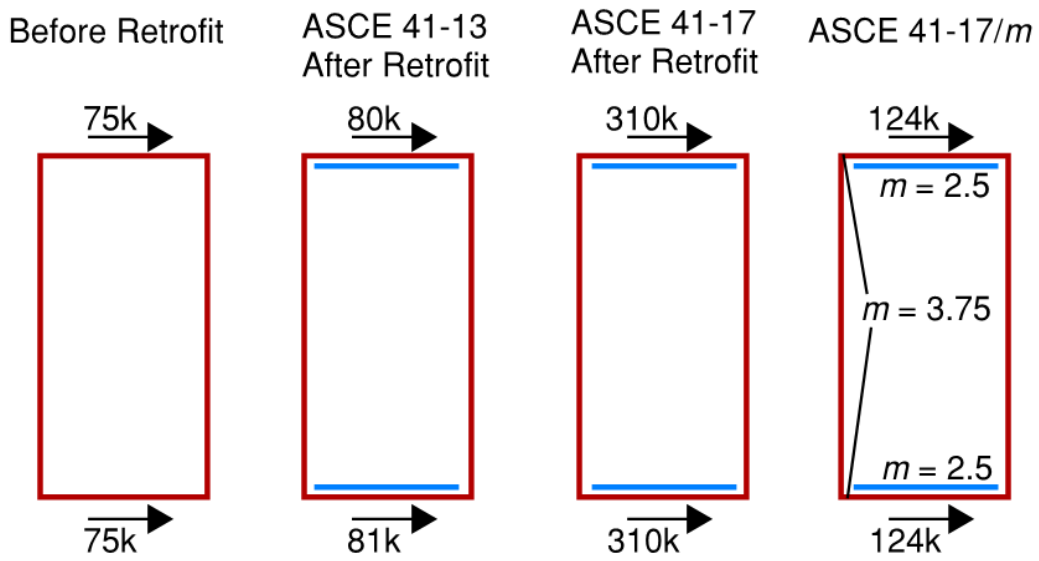

Figure 1-13 Figure showing wall demands per ASCE/SEI 41-13 before the retrofit (same as ASCE/SEI 41-17), per ASCE/SEI 41-13 after the retrofit, per ASCE/SEI 41-17 with no *m*-factor after the retrofit, and per ASCE/SEI 41-17 with *m*-factors after the retrofit for use with concrete (*m*=2.5) and masonry (*m*=3.75).

In order to design the new shotcrete wall, it is necessary to make an assumption about the behavior of the composite wall system. Typically, the design involves assigning shear demands to concrete and masonry piers using a force-design philosophy. The following approaches are commonly used:

- Method #1**:** Assume the shotcrete wall carries 100% of the shear demand and ignore any contribution to strength or stiffness from the existing masonry.

- Method #2: Design the shotcrete wall for 100% of the shear but check the masonry for shear demands based on the relative rigidity of the masonry piers.

- Method #3: Design each concrete and masonry pier for a portion of the total wall shear based on the relative rigidity of each component.

These approaches are discussed further in FEMA 547 (FEMA, 2006) and in FEMA P-2006 (FEMA, 2018). Using Method #2 typically results in the most conservative design for the new shotcrete. Given the limited displacement capacity of the existing masonry, it is possible that if only Method #1 is used, the existing piers will be significantly damaged at the design shear force (particularly with flexure-critical concrete piers). Per ASCE/SEI 41-17 Section 16.2.3.5.2.1, lateral forces are to be distributed among vertical elements in proportion to their relative rigidities which would effectively be Method #3. For minor retrofits, like the one in this example, the cost difference between the approaches may be limited. In larger structures requiring extensive retrofits, the selected design criteria can have significant impact on retrofit cost.

Acceptance ratios for the masonry walls after the shotcrete is applied are consistently higher using ASCE/SEI 41-17 than they are with the method in ASCE/SEI 41-13. Figure 1-12 shows the names for the piers at the rear wall. A similar figure is not provided for the front wall. Demands are determined in the results below for Method #3.

Acceptance ratios are summarized below. For ASCE/SEI 41-13, since the piers are rocking controlled, then ASCE/SEI 41-13 Equation 16-18 is used, and it applies as one value to the wall line. ASCE/SEI 41-17 Section 16.2.3.5.4 and 16.2.3.5.5 send the designer to the Linear Static Procedure of ASCE/SEI 41-17 Section 7.4.1, where there is no similar wall line summation equation, but rather each pier is checked individually.

- ASCE/SEI 41-13: Governing acceptance ratio $0.7V_{wx}/\sum V_r$ = **0.35**

- ASCE/SEI 41-17: Governing acceptance ratio per pier along the front wall line:

  - Pier 25 $Q_{UD}/m\kappa Q_{CE}$ = **0.54**

  - Pier 26 $Q_{UD}/m\kappa Q_{CE}$ = **0.41**

  - Pier 27 $Q_{UD}/m\kappa Q_{CE}$ = **0.41**

  - Pier 28 $Q_{UD}/m\kappa Q_{CE}$ = **0.53**

After the shotcrete retrofit, preliminary masonry results for the *rear wall* are as follows:

- ASCE/SEI 41-13: Governing acceptance ratio $0.7V_{wx}/\sum V_r$ = **0.24**

- ASCE/SEI 41-17: Governing acceptance ratio per pier along the rear wall line:

  - Pier 17 $Q_{UD}/m\kappa Q_{CE}$ = **0.13**

- Pier 18 $Q_{UD}/m\kappa Q_{CE}$ = **0.35**
- Pier 19 $Q_{UD}/m\kappa Q_{CE}$ = **0.61**
- Pier 20 $Q_{UD}/m\kappa Q_{CE}$ = **0.35**
- Pier 21 $Q_{UD}/m\kappa Q_{CE}$ = **0.13**

In summary, thousands of buildings have been retrofit using the methods of design characterized by ASCE/SEI 41-13 and this study did not find a compelling reason to change to the more conservative method of ASCE/SEI 41-17 as interpreted above. As a result of this study, the proposed revisions to the Special Procedure will continue to allow the designer to choose how much load will be resisted by new vertical elements, consistent with the approach in ASCE/SEI 41-13. Nevertheless, provisions are proposed to explicitly require that the masonry walls be evaluated for the forces attracted due to their relative rigidities, even where new elements are designed to take 100% of the retrofit design forces.

1.3.3 Case Study: Retrofit Situation 2 with New Vertical Element at Midspan

Retrofit Situation 2 involves the introduction of a new vertical element at the mid-span of the 60 ft long diaphragm in the transverse direction. Two variations were considered for the new vertical elements, and both the two-story and six-story building configurations were included in the study. These studies prompted a supplementary parametric study to consider the most effective modeling assumptions for the out-of-plane stiffness of the walls in the 3D ETABS models. These Retrofit Situation 2a and 2b case studies were also used to evaluate the drift limits and assumptions about diaphragm spans and lead to proposed revisions in the provisions in each of these areas.

In this retrofit situation, a new vertical element is added in the middle of the building. Since the building has a flexible diaphragm, the intent of the retrofit solution is to draw load away from the front and rear walls.

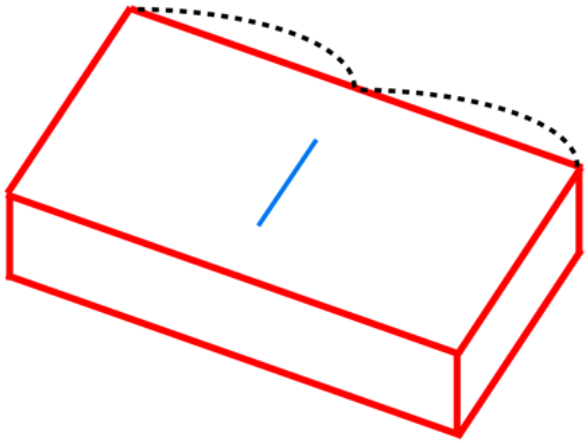

Figure 1-14 Situation 2 with new vertical element placed in middle of the structure.

Conventional flexible diaphragm theory would indicate the masonry walls should resist a quarter of the total seismic load and the new middle element should resist half of the total seismic load. However, the Special Procedure incorporates capacity-based design concepts, and the wall demands are limited by the diaphragm capacity.

Per ASCE/SEI 41-17 Section 16.2.3.5.4, the Linear Static Procedure (LSP) of Section 7.4.1 is used to determine forces on new lateral elements. Unlike the Special Procedure, which has a rectangular load distribution, the LSP has a triangular load distribution and no capacity-based design provisions. Using the Special Procedure in ASCE/SEI 41-13 results in the Level 2 wall demands being limited by roof diaphragm capacity. The second-floor diaphragm is stronger than the roof diaphragm, and the Level 1 wall demands are not limited by diaphragm capacity. Figure 1-15 shows the story force distributions to the new vertical element in the middle of the diaphragm for ASCE/SEI 41-13 and for ASCE/SEI 41-17. Although Figure 1-15 shows a moment frame, there is no difference if the vertical element is a braced frame or shear wall.

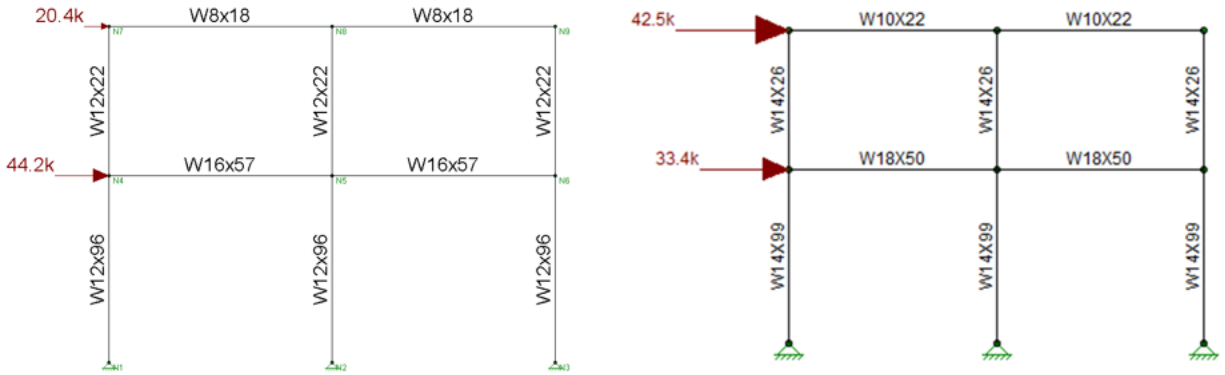

Figure 1-15 Load distribution for Retrofit Situation 2b with steel moment frame per ASCE/SEI 41-13 (left) vs. ASCE/SEI 41-17 (right).

The equations for wall demand in ASCE/SEI 41 are structured to apply to simple rectangular buildings with four sides. The addition of the new vertical element in the middle of the building requires the engineer to alter to code equations based on the new geometry.

$$F_{wx} = 0.8(S_{X1})(W_{wx} + 0.5W_d) \qquad \text{(ASCE/SEI 41-17 Eq. 16-12)}$$

But not exceeding

$$F_{wx} = 0.8(S_{X1})(W_{wx}) + (\nu_u)(D) \qquad \text{(ASCE/SEI 41-17 Eq. 16-13)}$$

For ASCE/SEI 41-17 equation 16-13, D is reduced from 60 ft to 30 ft. Therefore, the wall demand is reduced, but not halved like the Linear Static Procedure. For the ASCE/SEI 41-13 example, the story shear at the roof (20.4 kips) was governed by the diaphragm capacity reflected in Eq. 16-13, while the story shear at the second floor (44.2 kips) was governed by Eq. 16-12. For the ASCE/SEI 41-17 LSP example, half the story shear at the roof was divided by an m-factor of 4 (340 kips/2/4 = 42.5

kips) and half the story shear at the second floor was divided by an *m*-factor of 4 (267 kips/2/4 = 33.4 kips). The weights used for these computations were preliminary and updated values are reflected in Figures 1-21 and Figure 1-23 below.

1.3.3.1 SITUATION 2A – TWO-STORY REINFORCED CONCRETE SHEAR WALL

In this retrofit situation, a new 8-inch concrete shear wall is added in the middle of the building.

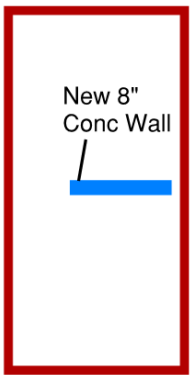

Figure 1-16 Figure showing Retrofit Situation 2a plan.

Per ASCE/SEI 41-17 Table 10-22, a shear-controlled concrete shear wall at the Life Safety Structural Performance Level has an *m*-factor of 2.5. See Figure 1-17 for Level 1 seismic demands.

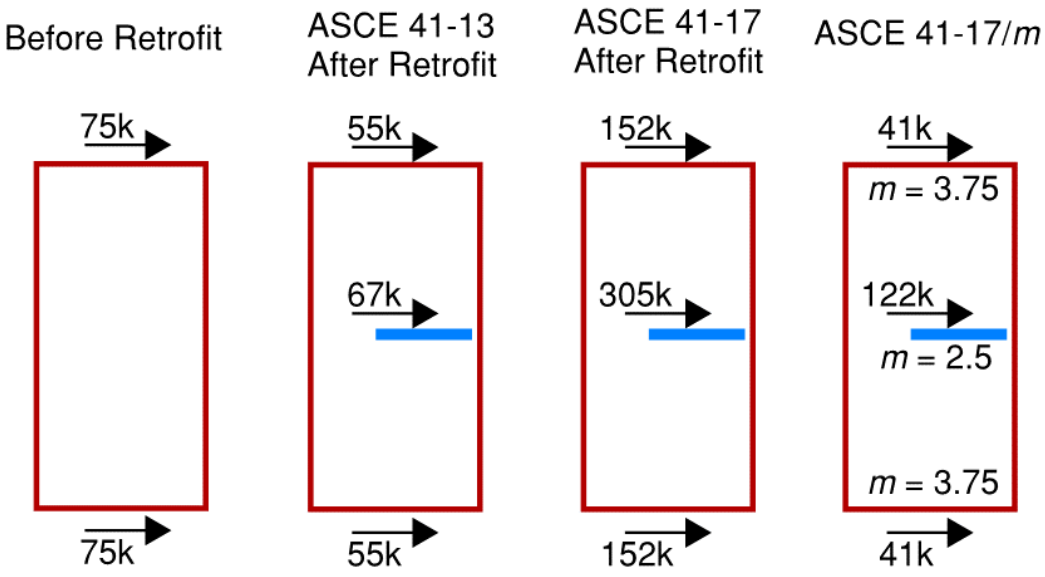

Figure 1-17 Figure showing wall demands per ASCE/SEI 41-13 before the retrofit (same as ASCE/SEI 41-17), per ASCE/SEI 41-13 after the retrofit, per ASCE/SEI 41-17 with no *m*-factor after the retrofit, and per ASCE/SEI 41-17 with *m*-factors after the retrofit (2.5 for the concrete and 3.75 for the masonry).

The ASCE/SEI 41-17 approach using the provisions added in ASCE/SEI 41-17 (Forces LSP) leads to lower demands on the outer masonry walls and higher demands on the new concrete wall in the middle as opposed to the Special Procedure loads from ASCE/SEI 41-13 which are limited by diaphragm capacity.

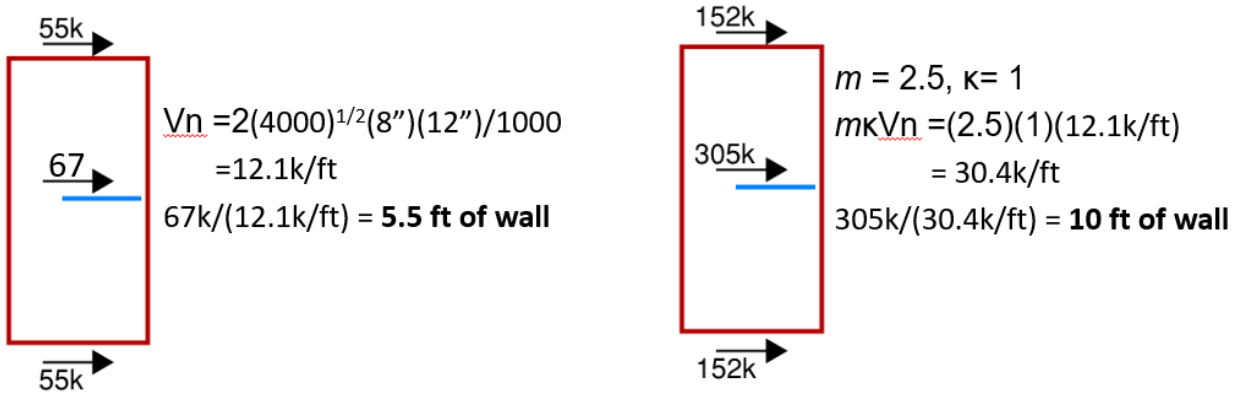

Figure 1-18 Figure showing concrete wall design per ASCE/SEI 41-13 (left) vs. ASCE/SEI 41-17 (right).

Assuming $\kappa = 1$ for this example, the concrete wall design, using ASCE/SEI 41-13 design provisions versus ASCE/SEI 41-17 design provisions results in nearly half the length of wall required as shown in Figure 1-18. Note, there is no φ factor in ASCE/SEI 41-17, or equivalently $\varphi = 1$.

The conclusion from this comparison is that the methodology of ASCE/SEI 41-17 does not take the diaphragm capacity into account and results in a markedly different force distribution between the three walls; twice the wall length is required for the retrofit when compared to ASCE/SEI 41-13. The ASCE/SEI 41-13 method limited by the capacity of vintage wood diaphragms may be more appropriate and result in more cost effective retrofit schemes.

1.3.3.2 SITUATION 2B – STEEL SPECIAL MOMENT FRAME FOR TWO-STORY BUILDING DESIGNED WITH ASCE/SEI 41-13 AND ASCE/SEI 41-17 WITH VARIOUS DRIFT LIMITS

In this retrofit situation, a new steel special moment frame is added in the middle of the building. This initial study prompted a supplementary study of out-of-plane wall stiffness. These initial results are reported here using several different drift limits, followed by results of the supplementary study, and then results from a subsequent RISA-2D design that used a more stringent drift limit of 0.75% to achieve the desired results with a moment frame that would effectively reduce the diaphragm span in half.

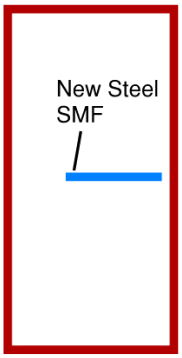

Figure 1-19 Figure showing Retrofit Situation 2b plan.

Per ASCE/SEI 41-17 Table 9-6, the *m*-factors for steel moment frame beams and columns vary between 2 and 6. Since the *m*-factor limit for new elements in a URM retrofit is equal to 4 per ASCE/SEI 41-17 Section 16.2.3.5.5 and the average *m*-factor for beams and columns is also equal to 4, an *m*-factor of 4 is used for all moment frames. See Figure 1-20 for Level 1 seismic demands.

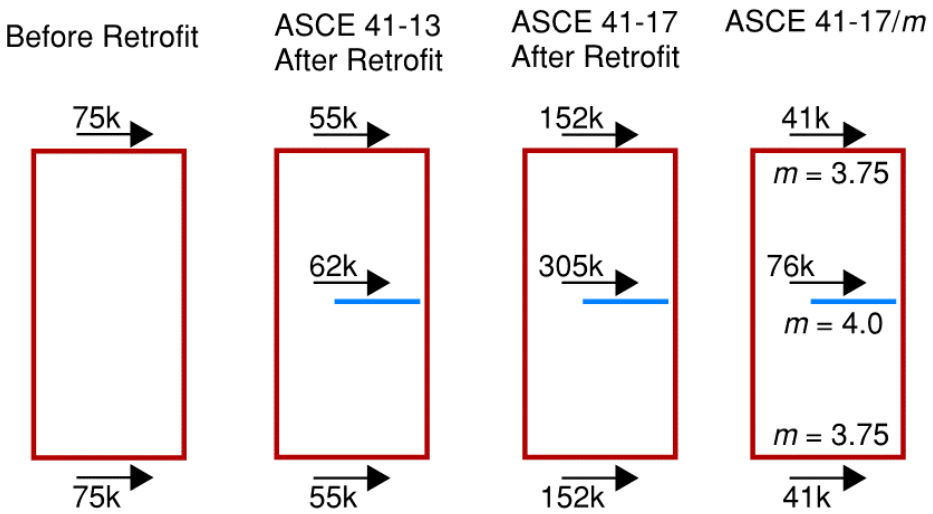

Figure 1-20 Figure showing wall demands per ASCE/SEI 41-13 before the retrofit (same as ASCE/SEI 41-17), per ASCE/SEI 41-13 after the retrofit, per ASCE/SEI 41-17 with no *m*-factor after the retrofit, and per ASCE/SEI 41-17 with *m*-factors after the retrofit (4.0 for the moment frame and 3.75 for the masonry.)

The general workflow for the two-story Retrofit Situation 2b was as follows:

- Step 1: A series of moment frame designs were made for both ASCE/SEI 41-13 and ASCE/SEI 41-17 using different drift criteria, together with the force demands shown above. RISA-2D was used to design the moment frames.

- Step 2: In typical practice with a flexible diaphragm assumption, the effectiveness of the moment frame in resisting the assumed load is not examined. However, for this case study building, the moment frames are much more flexible than the masonry shear walls at the front and rear. They

are all linked by a wood diaphragm that has some stiffness. Once the moment frame was designed, what portion of the demand at midspan is resisted by the diaphragm and what portion is resisted by the new moment frame was investigated.

For Step 2, the midspan stiffness of both the roof and second floor was determined using the equations for diaphragm deflection in SDPWS-2015, *Special Design Provisions for Wind and Seismic Standard with Commentary* (AWC, 2015).

The midspan stiffness was converted to an equivalent spring. The roof and second floor equivalent springs were then applied to the 2-D moment frame models, loads applied, and the contribution of load resisted by the diaphragm springs could be compared against the sum of the load in the moment frame columns.

Per SDPWS-2015 Section 4.2.2, the roof diaphragm deflection is:

$$\delta_{dia} = 5\nu L^3/8EAW + 0.25\nu L/1000G_a + \sum(x\Delta_c)/2W \qquad \text{(AWC SDPWS-2015 Eq. 4.2-1)}$$

where:

E = modulus of elasticity of diaphragm chords, psi

A = area of chord cross-section, in^2

G_a = apparent diaphragm shear stiffness from nail slip and panel shear deformation, kips/in. (From Column A, Tables 4.2A, 4.2B, 4.2C, or 4.2D)

L = diaphragm length, ft

W = diaphragm width, ft

ν = induced unit shear in diaphragm, lbs/ft

x = distance from chord splice to nearest support, ft

Δ_c = diaphragm chord splice, in., at the induced unit shear in diaphragm

In this example, assuming no chord splices:

L = 60 ft

W = 30 ft

E = 1,600 ksi (per NDS-2015 Table 4D, Assume Doug Fir North)

$\nu = F/L$

ν = F/(2)(30 ft)(12 in./ft)

A = 16.88 in.^{2} for a 2 × 12 chord member

G_a = 1.5 k/in. per SDPWS Table 4.2D

δ_{dia} = 5(F kips/720 in)(720 in)^3/[8(1600 ksi)(16.88 in^2)(30 ft)(12in/ft)] + 0.25(F kips/720 in)(720 in.)/(1.5 k/in.)

δ_{dia} = 0.1999F

F = $k\delta$ =>> diaphragm stiffness, k = 5 k/in.

Therefore, in order to investigate the diaphragm stiffness contribution, a spring with a stiffness of 5 k/in is connected to a roof level node of the moment frame models. A similar process was used to determine the spring stiffness for the second floor diaphragm. The second floor diaphragm spring stiffness is 13.3 k/in.; it is higher because the second floor diaphragm is stronger and stiffer.

- Four Scenarios for ASCE/SEI 41-13 demands: ASCE/SEI 41-13 has no drift limit requirements, so the following drift limits examined using ASCE/SEI 41-13 demands are shown below. All of the cases described here include a basic case number 1 to 4 with a suffix -13 or -17 referring to either ASCE/SEI 41-13 or ASCE/SEI 41-17, respectively
    - Case 1-13: No drift limit, design governed by strength
    - Case 2-13: Drift limit = 2.0%
    - Case 3-13: Drift limit = 1.5%
    - Case 4-13: Drift limit = 1.0%
- Two Scenarios for ASCE/SEI 41-17 demands: A drift limit = 1.5% was introduced in ASCE/SEI 41-17 Section 16.2.3.5.6, but it is not explicit as to whether this limit should apply to demands before or after reduction by the *m*-factor. Thus, the two drift limits examined using ASCE/SEI 41-17 demands are as follows.
    - Case 1-17: Drift limit = 1.5% with no *m*-factor.
    - Case 2-17: Drift limit = 1.5% with *m*-factor applied.

Elevations of the steel moment frames designed to comply with each of the four drift limits for ASCE.SEI 41-13 are shown in Figure 1-21 to Figure 1-23. Demands of 19.2 kips and 42.6 kips have been updated from Figure 1-15 to reflect more refined weight determinations.

- Case 1-13 and 2-13: Design governed by strength, ASCE/SEI 41-13 demands, but also met 2% drift demand for Case 2.

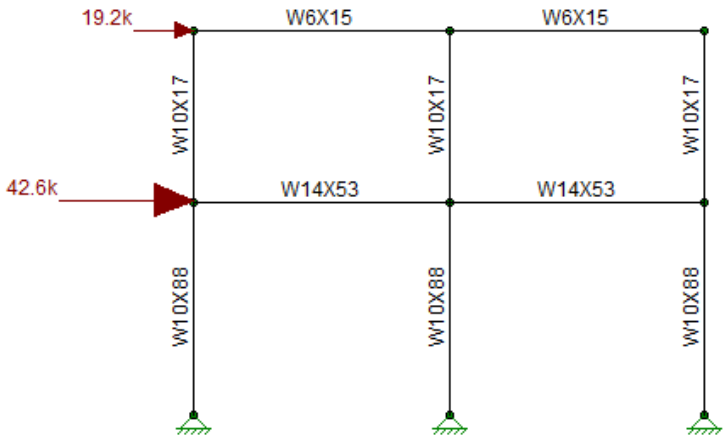

Figure 1-21 Figure showing moment frame design governed by strength and moment frame required to meet 2% drift limit (Case 1-13 and Case 2-13).

Using ASCE/SEI 41-13 demands with no drift limit:

- Story 2 drift = 1.4%
- Story 1 drift = 2.0%

The moment frame attracts 42% of the load at Story 2 and 49% at Story 1 with sections shown in Figure 1-21. Using ASCE/SEI 41-13 demands, the strength governed model also satisfies drift limit = 2.0% for Case 2.

- Case 3-13: For a drift limit = 1.5% using ASCE/SEI 41-13 demands:

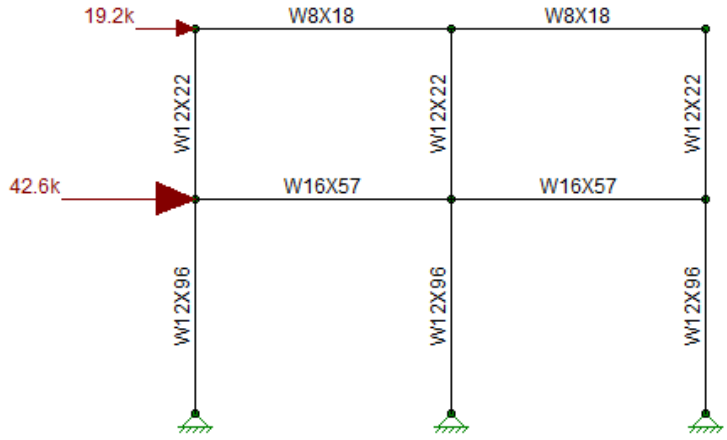

Figure 1-22 Figure showing moment frame required to meet 1.5% drift limit with heavier sections than shown in Figure 1-21 (Case 3-13).

Using ASCE/SEI 41-13 demands and a drift limit = 1.5%:

- Story 2 drift = 0.86%

- Story 1 drift = 1.45%

The moment frame attracts 55% of the load at Story 2 and 60% at Story 1 with sections shown in Figure 1-22.

- Case 4-13: For a drift limit = 1.0% using ASCE/SEI 41-13 demands:

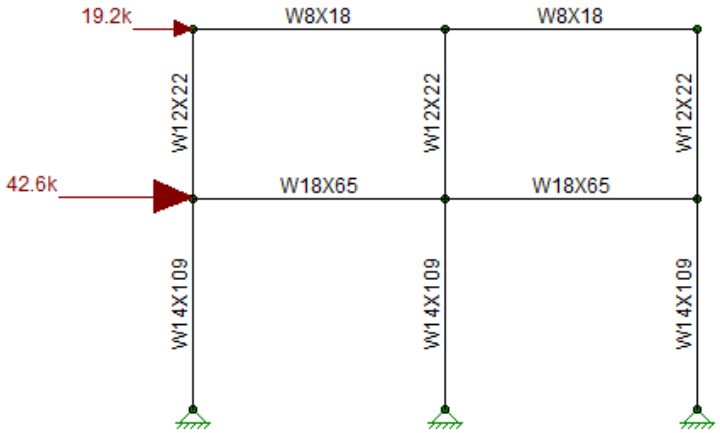

Figure 1-23 Figure showing moment frame required to meet 1% drift limit with heavier sections than either Figure 1-21 or Figure 1-22 (Case 4-13).

Using ASCE/SEI 41-13 demands and a drift limit = 1%:

- Story 2 drift = 0.73%
- Story 1 drift = 1.0%

The moment frame attracts 62% of the load at Story 2 and 67% at Story 1 with sections shown in Figure 1-23.

ASCE/SEI 41-13 Loads Summary: As the drift limits decrease, the moment frame stiffness contribution increases. The following Table 1-2 summarizes the four ASCE/SEI 41-13 cases.

Table 1-2 Retrofit Situation 2b Load Resisted by Moment Frame Based on Drift Limit and Provisions of ASCE/SEI 41-13

Case	Case 1-13	Case 2-13	Case 3-13	Case 4-13
Drift Limit Level 1	No Limit	2%	1.5%	1.0%
Load Resisted by Moment Frame at Level 1	49%	49%	60%	67%

Elevations of the steel moment frames designed to comply with the two drift limits for ASCE/SEI 41-17 are shown in Figure 1-24 and Figure 1-25.

Scenarios for ASCE/SEI 41-17 demands:

- Case 1-17: For a drift limit = 1.5% using ASCE/SEI 41-17 demands with the *m*-factor applied:

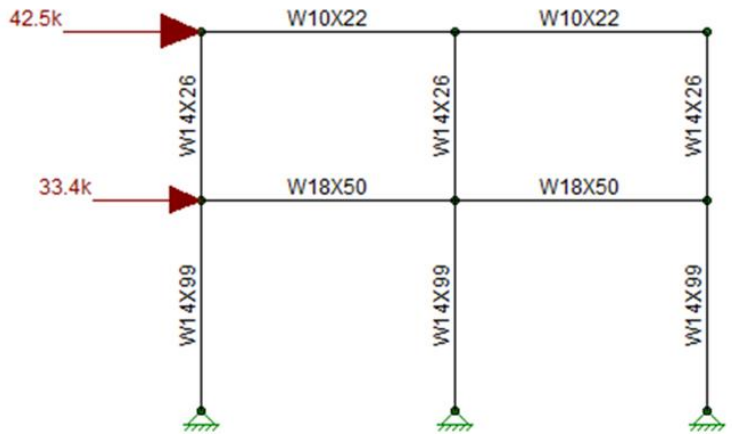

Figure 1-24 Figure showing moment frame required to meet 1.5% drift limit with *m*-factor (Case 1-17).

Using ASCE/SEI 41-17 demands and a drift limit = 1.5% (per ASCE/SEI 41-17 Section 16.2.3.5.6)

- Story 2 drift: 1.0%
- Story 1 drift: 1.5%

The moment frame attracts 73% of the load at Story 2 and 62% at Story 1.

- Case 2-17: For a drift limit = 1.5% using ASCE/SEI 41-17 demands with no *m*-factor applied.

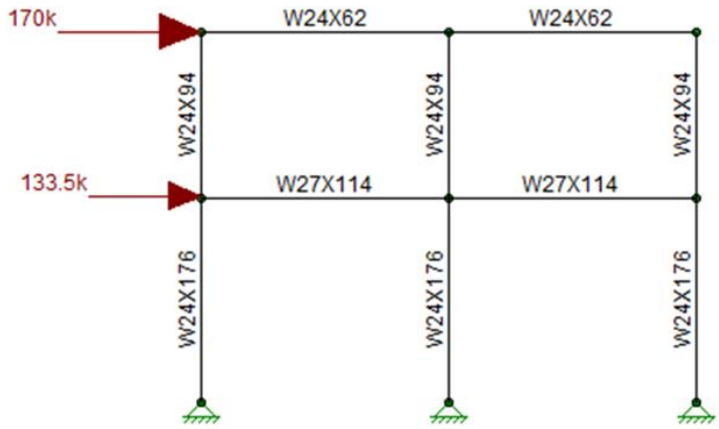

Figure 1-25 Figure showing moment frame required to meet 1.5% drift limit with no *m*-factor (Case 2-17).

Using ASCE/SEI 41-17 demands and a drift limit = 1.5% (per ASCE/SEI 41-17 Section 16.2.3.5.6) with no *m*-factor applied:

- Story 2 Drift: 0.58%
- Story 1 Drift: 1.2% (not optimized)

The moment frame attracts 94% of the load at Story 2 and 89% at Story 1.

In summary, the results for the various conditions initially considered for Retrofit Situation 2b are shown in Table 1-3 and Table 1-4. A summary of the moment frame contribution at Story 1 to resisting load with drift limits ranging from 1.0% to 2.0% and the two codes is given in Table 1-3. A summary of the resulting frame sizes with various drift limits and the two codes in Table 1-4.

Table 1-3 Retrofit Situation 2b Load Resisted by Moment Frame Based on Drift Limit Using Provisions of both ASCE/SEI 41-13 and ASCE/SEI 41-17

Case	ASCE/SEI 41-13				ASCE/SEI 41-17	
	Case 1-13	Case 2-13	Case 3-13	Case 4-13	Case 1-17	Case 2-17
Drift Limit Level 1	No limit	2%	1.5%	1.0%	1.5% w/ *m*-factor	1.5% w/o *m*-factor
Load Resisted by Moment Frame at Level 1	49%	49%	60%	67%	62%	89%

When comparing the two codes for a drift limit of 1.5%, the ASCE/SEI 41-13 values are a bit less conservative than the ASCE/SEI 41-17 values with the *m*-factor applied. However, it is highly dependent on several assumptions regarding which *m*-factors to use and when to apply them.

Summary of member sizes required to meet drift limits: Table 1-4 summarizes the frame sizes for the two-story cases studied. These are the sizes shown Figure 1-21 to Figure 1-25 above.

Table 1-4 Retrofit Situation 2b Moment Frame Beams and Columns Required to Meet Various Drift Limits

Case	Drift Limit	Level 2		Level 1	
		Beam	Column	Beam	Column
Case 1-13: ASCE/SEI 41-13 loads	None	W6×15	W10×17	W14×53	W10×88
Case 2-13: ASCE/SEI 41-13 loads	2.0%	W6×15	W10×17	W14×53	W10×88

Table 1-4 Retrofit Situation 2b Moment Frame Beams and Columns Required to Meet Various Drift Limits (continued)

Case	Drift Limit	Level 2		Level 1	
		Beam	Column	Beam	Column
Case 3-13: ASCE/SEI 41-13 loads	1.5%	W8×18	W12×22	W16×57	W12×96
Case 4-13: ASCE/SEI 41-13 loads	1.0%	W8×18	W12×22	W18×65	W14×109
Case 1-17: ASCE/SEI 41-17 loads and limit, with *m*-factor	1.5%	W10×22	W14×26	W18×50	W14×99
Case 2-17: ASCE/SEI 41-17 loads and limit, no *m*-factor	1.5%	W24×62	W24×94	W27×114	W24×176

When comparing the two codes for a drift limit of 1.5%, the ASCE/SEI 41-13 frame design is more flexible and less conservative than the ASCE/SEI 41-17 frame with the *m*-factor applied. The moment frame design using ASCE/SEI 41-17 without the *m*-factor results in significantly heavier beams and columns. The ASCE/SEI 41-17 approach without the *m*-factor is judged to be too conservative.

1.3.3.3 SUPPLEMENTARY STUDY OF OUT-OF-PLANE WALL STIFFNESS IN 3D ETABS MODELS

A review of the results from the initial Retrofit Situation 2b study shows results that varied depending on modeling assumptions used to characterize the out-of-plane wall stiffness of the longitudinal walls in the two-story building model. Figure 1-26 shows the comparison between two sets of results from 3D ETABS models both with and without the out-of-plane stiffness of the longitudinal masonry walls.

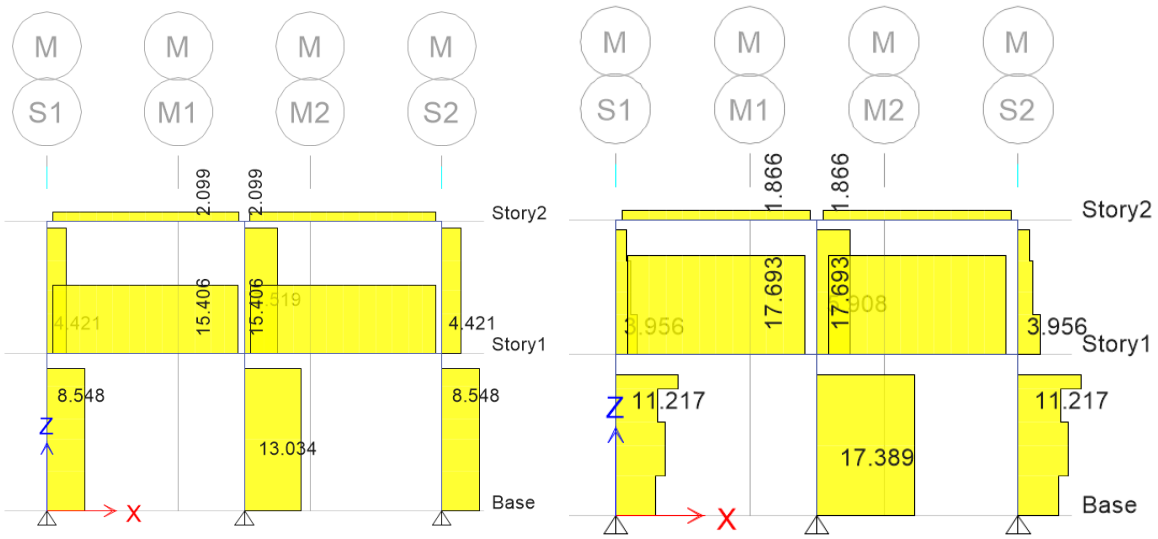

Figure 1-26 ETABS element shears in steel moment frame from 3D models with membrane elements without (left) and thin shell elements with (right) out-of-plane wall stiffness for longitudinal masonry walls in two-story building.

The resulting parametric study considered the following possible variables that could cause the out-of-plane wall reactions shown above:

- Multiple story interaction effects
- Diaphragm stiffness
- Thin shell vs. membrane elements used to model the longitudinal masonry walls
- Out-of-plane spanning capability of thin shell walls

To study these variations, a 3D one-story building was used by eliminating the top floor of the two-story model. The longitudinal walls and diaphragm were modeled with six permutations as shown in Figure 1-27. As the unreinforced masonry walls do not resist out-of-plane loads reliably, the point of the study was to find how to best model these walls to avoid out-of-plane stiffness and not have loads attracted to these walls in a 3D model with transverse loading. The study confirmed that the out-of-plane stiffness characteristics of thin shell elements were inappropriate for modeling the masonry walls that do not resist out-of-plane loads reliably, especially in combination with flexible wood diaphragms. Membrane elements are more appropriate for modeling the in-plane properties of the masonry walls without the out-of-plane properties. The conclusion that the membrane elements provide better results was also confirmed by a comparison of two six-story ETABS models described below.

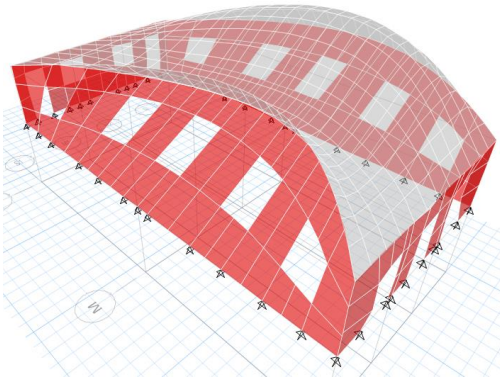

1. **One story, roof (flexible) diaphragm, membrane walls**

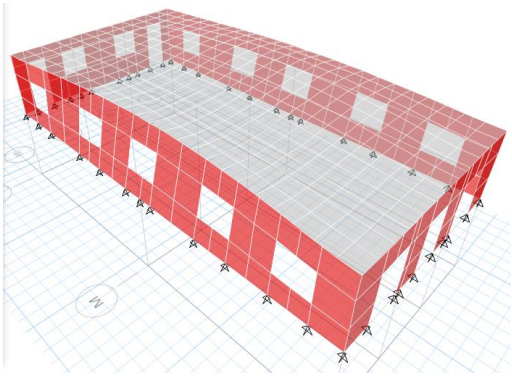

2. **One story, roof (flexible) diaphragm, thin shell walls**

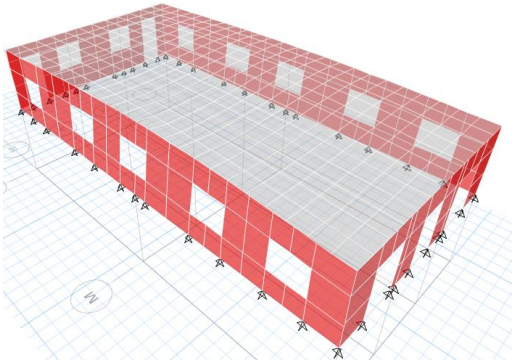

3. **One story, floor (10x stiffer) diaphragm, thin shell walls**

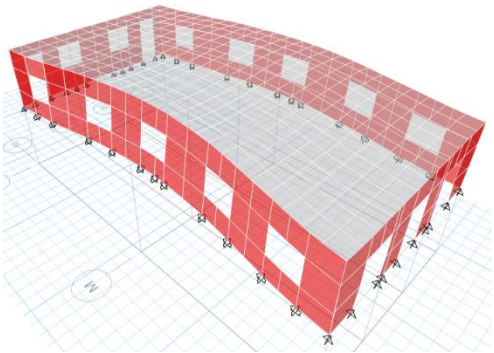

4. **One story, roof (flexible) diaphragm, thin shell walls, side walls on rollers**

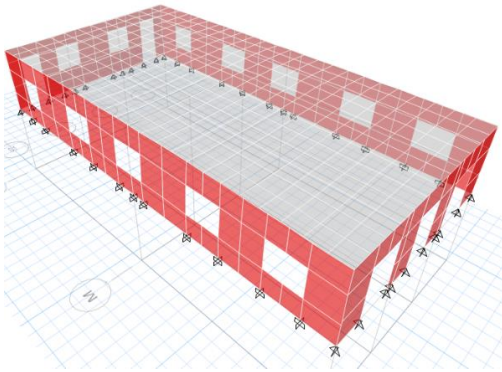

5. **One story, roof (flexible) diaphragm, thin shell walls, side walls fixed at base**

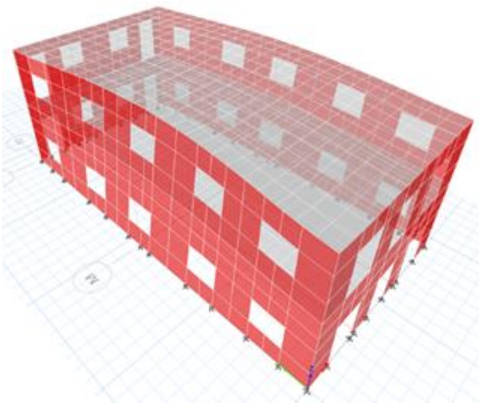

6. **Two-story, thin shell walls (top story)**

Figure 1-27 Six 3D ETABS unretrofitted models used for out-of-plane wall stiffness study.

Table 1-5 Distribution of Loads for Six Unretrofitted Structures from 3D ETABS Models for Loading in Transverse (E-W) Direction

Transverse (E-W) Direction	Rear Wall (k)	Front Wall (k)	Out-of-Plane (k)	Sum (k)	Correlation to Special Procedure
Special Procedure Loads	20	19	-	39	-
1. Flexible diaphragm, membrane wall	20	19	-	39	Good
2. Flexible diaphragm, thin shell wall	22	22	-5	39	Fair
3. Stiff diaphragm, thin shell wall	21	20	-2	39	Good
4. Flexible diaphragm, thin shell wall on rollers	24	24	-9	39	Poor
5. Flexible diaphragm, thin shell walls, fixed side	31	30	-22	39	Poor
6. Two-story, thin shell walls (top story)	31	30	-22	39	Poor

The first and third combination of modeling variables provided results that correlated well with results obtained by using the Special Procedure. The modeling combination of membrane elements for the walls and flexible diaphragms was found to provide better results for the building types in these case studies.

1.3.3.4 SUPPLEMENTARY STUDY OF DIAPHRAGM SPAN LENGTH

The case studies described herein typically involved designs targeting a range of drift limits. These studies were reviewed to determine an appropriate drift limit and to provide and improved definition of the diaphragm span. For retrofit elements placed at midspan $L/2$ that are not sufficiently stiff, the diaphragm may still effectively span the full distance L to the end walls. One of the questions considered in this review was whether the drift limit of 0.75% for moment frames should be revised or extended to cover other or all new vertical elements. The process used for this validation study is shown in Figure 1-28.

- Step 1: Determine loads for a moment frame for Special Procedure demands based on tributary area and diaphragm capacity.

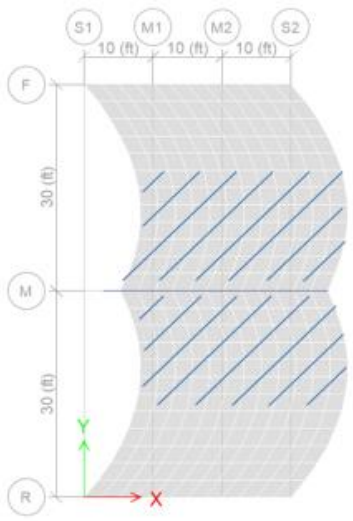

- Step 2: Design the moment frame for Special Procedure demands and a set of specified drift limits. Moment frame design is two-dimensional.

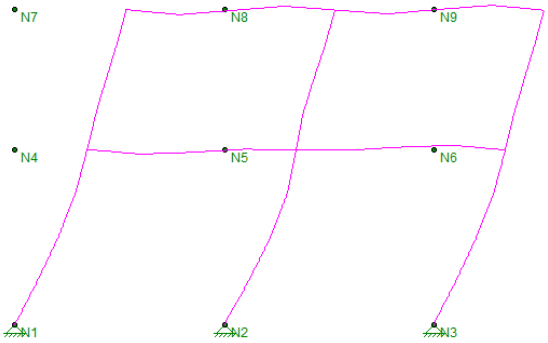

- Step 3: Validation study where each moment frame is added to a 3D model of the building with its masonry walls and wood frames to confirm the adequacy of each design and determine the most appropriate drift limits. The validation study and drift setting are intended to avoid the need for the engineer to do this specifically on their project. They can stay with only having to do Steps 1 and 2, with the knowledge that they will be adequate from the Step 3 validation studies.

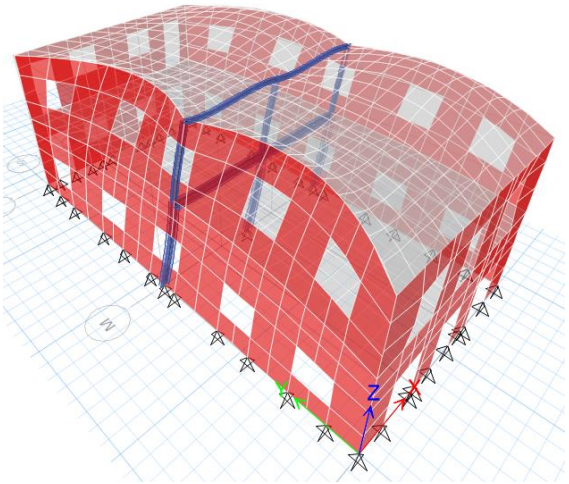

Figure 1-28 Process used to determine appropriate drift limit provision and to define diaphragm span length.

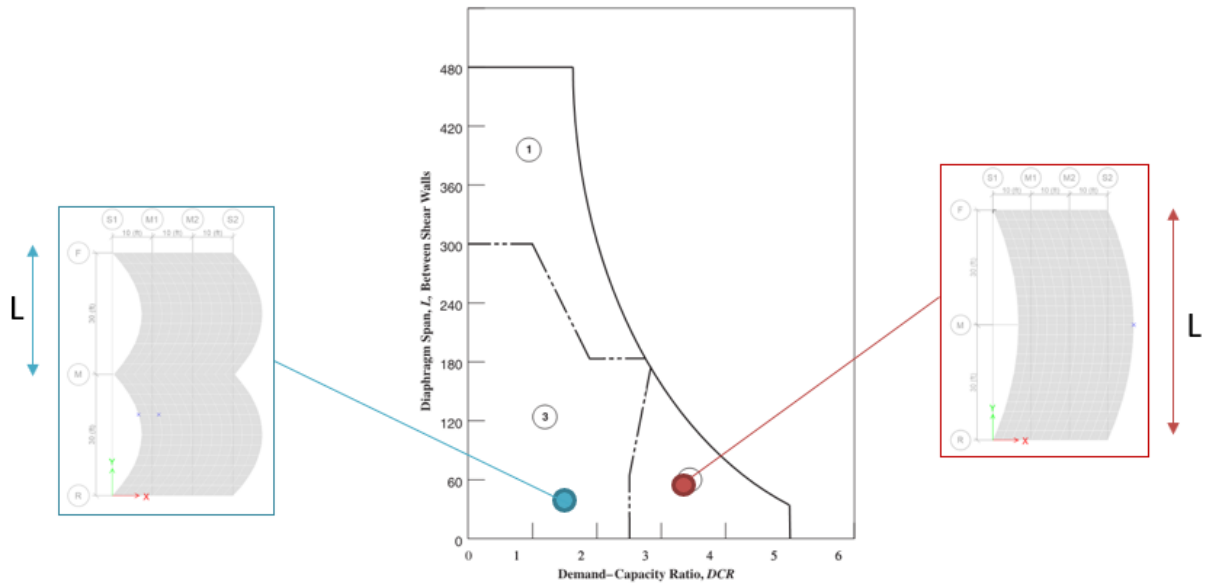

Figure 1-29 Proposed ASCE/SEI 41-23 Figure 16-1. Figure will be modified to clarify the definition of the diaphragm span length as the distance between vertical lateral force-resisting elements that meet the drift limit of 0.75%.

1.3.3.5 SITUATION 2B – STEEL MOMENT FRAME FOR TWO-STORY BUILDING WITH COMPARISON OF RISA-2D VS. ETABS 3D DESIGNS WITH DRIFT LIMIT OF 0.75%

The retrofit design for Situation 2b was repeated using the program RISA-2D for the design of the steel moment frame at the midspan of the 60 ft. long building and using design provisions from the ASCE/SEI 41-13 Special Procedure and combined with the drift limit of 0.75%. This was compared to a similar design using a 3D ETABS model with a stiffer floor diaphragm, more flexible roof diaphragm, and longitudinal walls modeled as membrane elements to eliminate the contribution of the out-of-plane stiffness.

The lateral loading used for the tributary area 2D design and resulting sizes are shown in Figure 1-30. Note that these are heavier and/or deeper member sizes based on a 0.75% drift limit when compared to the previous image in Figure 1-23, which was for Case 4-13 with a drift limit of 1.0%. Both cases use ASCE/SEI 41-13 demands.

The weight of the steel sections shown in Figure 1-30 adds up to 7,188 lb or equivalent to 2.0 psf over the 3,600 sq. ft. building. These additional loads of the retrofit components must be included in the analysis, and that is now noted explicitly in the proposal for ASCE/SEI 41-23 Section 16.2.3.5.4.

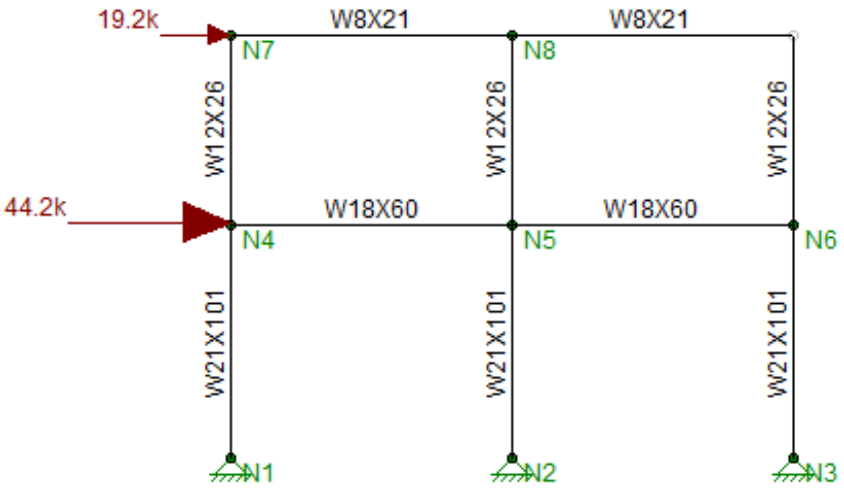

Figure 1-30 Figure showing moment frame required to meet ASCE/SEI 41-13 Special Procedure with 0.75% drift limit with heavier sections than Figure 1-23 above.

The results from the RISA-2D analysis which was controlled by drift were as follows:

- Story 2 drift = 0.64%
- Story 1 drift = 0.72%
- Acceptance Ratio (AR) for worst beam = 0.57 including the AISC 360 ϕ factors or 0.51 with a ϕ = 1.0
- AR for worst column = 0.38 including the AISC 360 ϕ factors or 0.34 with a ϕ = 1.0

The moment frame sizes from the RISA-2D analysis were included in a 3D ETABS model assuming an Ordinary Moment Frame at midspan. An isometric view of both the unretrofitted and retrofitted models along with the 2D view of the moment frame are shown in Figure 1-31.

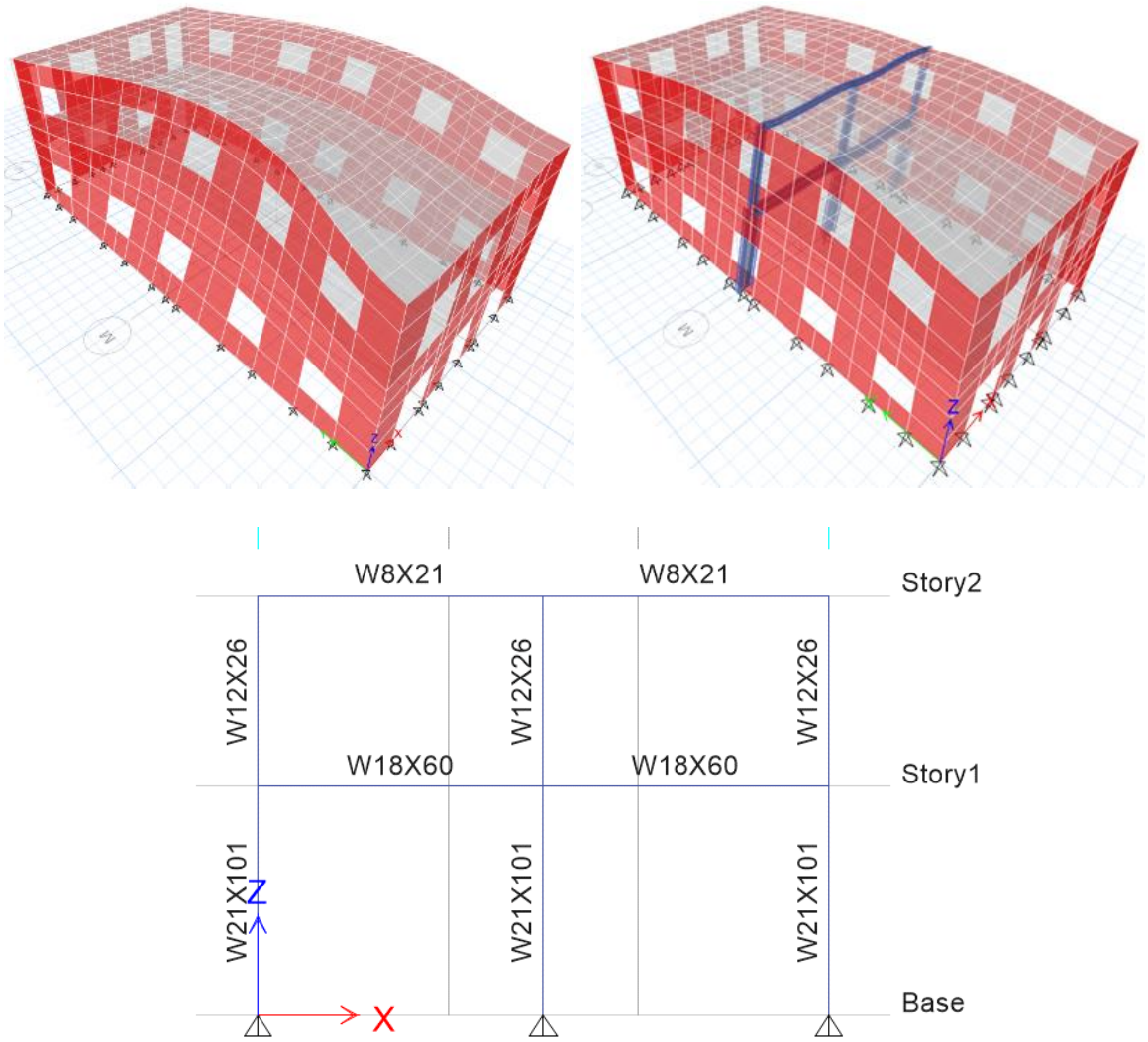

Figure 1-31 Isometric views of unretrofitted (top left) and retrofitted (top right) and 2D view of frame used for 3D ETABS analysis of two-story Retrofit Situation 2b.

Results for the two-story moment frame retrofit using the 3D ETABS models are shown in Table 1-6.

Table 1-6 Midspan Drift Comparison for Two-story Unretrofitted URM Building and MF Retrofit from RISA and ETABS

Level	Unretrofitted URM		Moment Frame Retrofit in URM				
	ETABS Total Displ. X (in.)	ETABS Drift X	Moment Frame Drifts RISA	ETABS Total Displ. X (in.)	ETABS Story Displ. X	ETABS Drift X (in.)	Ratio to Limit
Story 2	1.62	0.60%	0.64%	0.85	0.38	0.32%	0.42
Story 1	0.90	0.63%	0.72%	0.47	0.47	0.33%	0.44

Results in Table 1-6 show that the moment frame retrofit reduces the midspan drift by slightly more than half from 0.63% to 0.33% at Story 1. The "ratio to limit" shown in the far-right column is the comparison of the ETABS midspan drift to the target drift of 0.75% such that 0.32% / 0.75% = 0.42. Importantly, this study shows that a moment frame retrofit designed to meet the 0.75% drift limit with a 2D program, such as RISA-2D, will provide an adequate retrofit design with reduced drifts as seen in the more complex 3D ETABS model. This reduction to the drift limit to 0.75% should alleviate the need for 3D modeling for URM retrofits and will provide retrofits with better behavior. In the rare case where a 3D model of the building is developed perhaps to evaluate project-specific diaphragm strength and stiffness, geometry, and corner wall effects, a 0.75% drift limit in the 3D model would not be sufficiently conservative. For example, in the case summarized in Table 1-6, a 0.75% drift limit is already larger than the 0.60% and 0.63% story drifts in the *unretrofitted* building.

Table 1-7 below shows ratios from the story shears obtained from the ETABS analyses of both the unretrofitted and moment frame retrofit models to the values obtained using the Special Procedure. Values in the table greater than 1 indicate shear forces higher than the result obtained using the Special Procedure and its tributary analysis. Values less than 1 indicate shear forces lower than results obtained using the Special Procedure.

Table 1-7 Story Shears Ratio to Forces from Special Procedure for Two-story Unretrofitted URM Building and Moment Frame Retrofit from ETABS

	Unretrofitted URM		Moment Frame Retrofit in URM		
Level	Rear Wall	Front Wall	Rear Wall	Midspan Moment Frame	Front Wall
Story 2	1.55	1.58	1.50	0.74	1.53
Story 1	0.97	0.99	1.22	0.52	1.20

In summary, the study confirmed that the RISA 2D design using the drift limits of 0.75% provides a moment frame with adequate stiffness that reduces the drift by a factor of approximately two in the 3D ETABS model of the same configuration.

1.3.3.6 SITUATION 2B – STEEL MOMENT FRAME FOR SIX-STORY BUILDING AND COMPARISON OF RISA-2D VS. ETABS 3D DESIGNS WITH DRIFT LIMIT OF 0.75%

The exercise described above for the two-story building was repeated for a six-story ETABS model that was developed by extending the upper story of the two-story model of the masonry portion up four floor levels. The RISA-2D frame used for design is shown in Figure 1-32. The weight of the new moment frame is taken as 3.0 psf and spread over the 10,800 sq. ft. building and included with the analysis. The frame elements were designed using ASCE/SEI 41-13 Special Procedure loads with a 0.75% drift limit as proposed for ASCE/SEI 41-23. The OMF that met those requirements is shown below and was subsequently added to the six-story 3D ETABS model for comparison.

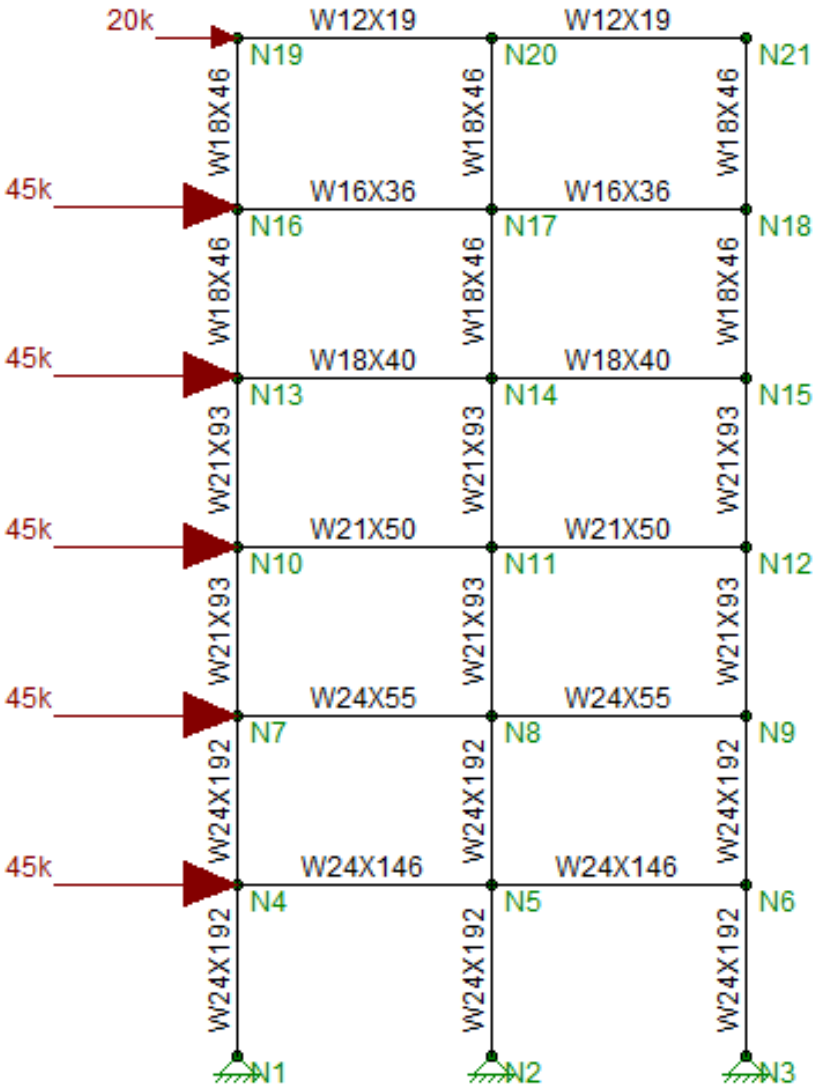

Figure 1-32 **RISA-2D model for six-story moment frame retrofit design using ASCE/SEI 41-13 Special Procedure and a drift limit of 0.75%.**

Table 1-8 **Drift from Six-Story RISA-2D Analysis of Moment Frame Retrofit Situation 2b**

Story	Drift
Story 6	0.51%
Story 5	0.73%
Story 4	0.72%
Story 3	0.73%
Story 2	0.56%
Story 1	0.74%

The results in the frame elements show a maximum AR of 0.91 for the beams and 0.39 for the columns. Drifts from the RISA-2D analysis are shown in Table 1-8 and are all less than the 0.75% target drift.

The moment frame elements were added to the ETABS model for comparison. Note that this retrofit is done with an Ordinary Moment Frame (OMF). Two isometric views and a view of the OMF frame sizes are shown in Figure 1-33. This 3D building has the same stiff floor diaphragms and flexible roof diaphragm as the two-story version.

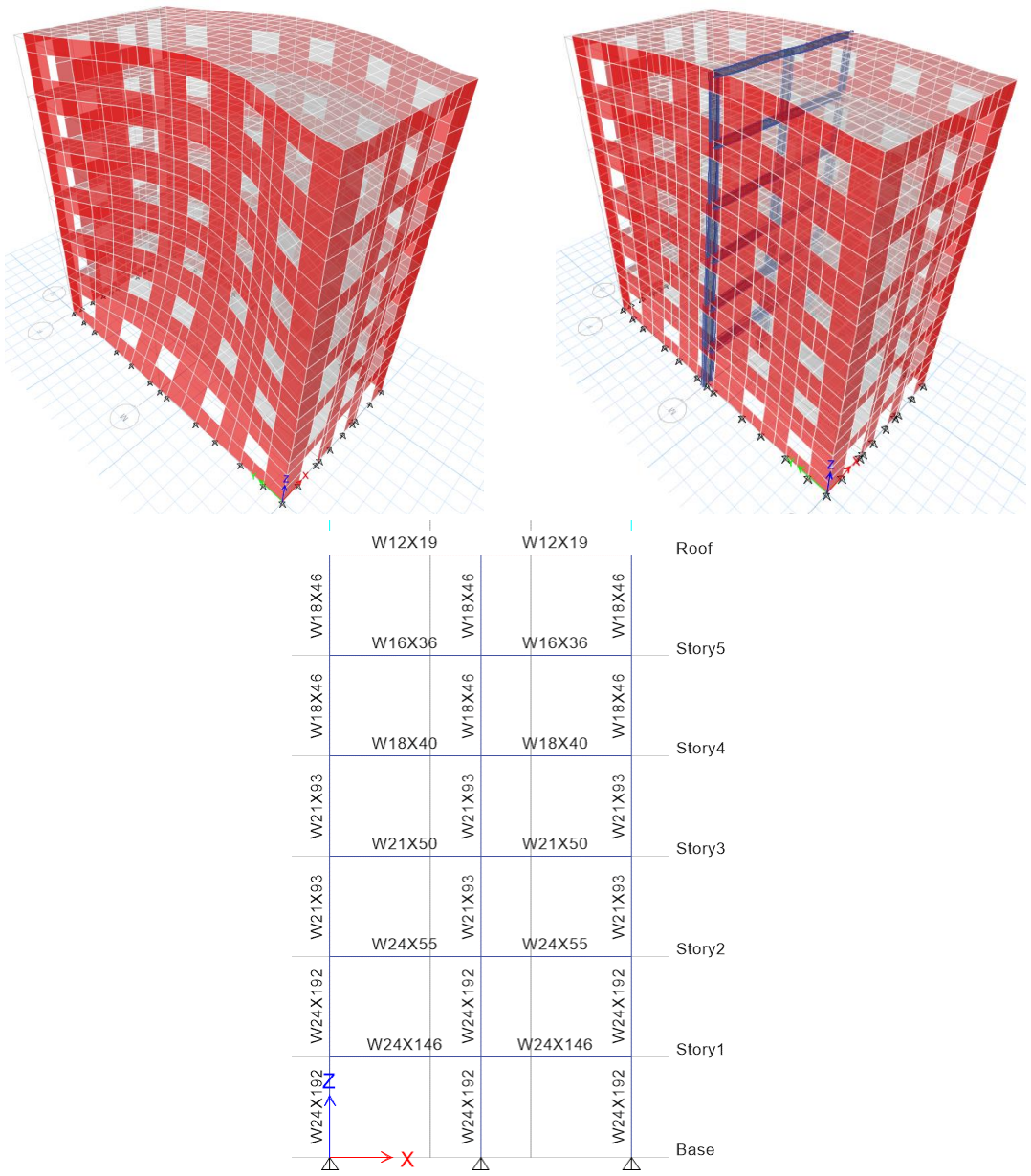

Figure 1-33 Isometric views of unretrofitted (top left) and retrofitted (top right) and 2D view of OMF used for 3D ETABS analysis of six-story Retrofit Situation 2b.

A comparison between the unretrofitted and retrofitted ETABS results in Table 1-9 shows that the OMF retrofit reduces the midspan displacements by approximately half. The comparison of midspan drift varies from floor to floor but the OMF retrofit makes the interstory drifts more uniform up the height of the building and reduces the large interstory at the lower three floors.

Table 1-9 Midspan Displacement and Drift Comparison for Six-story Unretrofitted URM Building and OMF Retrofit from RISA and ETABS

	Unretrofitted URM		OMF Retrofit in URM				
Level	ETABS Total Displ. X (in.)	ETABS Drift X	MF Drifts RISA	ETABS Total Displ. X (in.)	ETABS Story Displ. X (in.)	ETABS Drift X	Ratio to Limit
Story 6	4.23	0.03%	0.51%	2.69	0.32	0.26%	0.35
Story 5	4.19	0.06%	0.73%	2.37	0.41	0.34%	0.46
Story 4	4.13	0.26%	0.72%	1.96	0.46	0.38%	0.51
Story 3	3.81	0.61%	0.73%	1.50	0.50	0.42%	0.56
Story 2	3.07	1.08%	0.56%	1.00	0.43	0.36%	0.48
Story 1	1.78	1.48%	0.74%	0.57	0.57	0.47%	0.63

The OMF retrofit depicted above met the drift criteria imposed in the RISA-2D design and has lower drifts as reflected in the 3D ETABS model. Nevertheless, it is notable from the results in Table 1-10 that while the OMF retrofit building is stiffer and has a 9% increase in base shear, loads to the URM walls are reduced from 48% (285 k / 595 k) to 36% (231 k / 649 k), and the new OMF frame resists 25% (160 k / 649 k) of the retrofit base shear. A tributary area calculation would suggest that the OMF should be designed to resist 50% of the new base shear, but the 3D ETABS analysis confirms that this OMF design provided both adequate strength and adequate stiffness to meet the drift requirements and improve the performance of the URM building.

Table 1-10 ETABS Story Shear Comparison for Six-story Unretrofitted URM Building and OMF Retrofit

	Unretrofitted URM				OMF Retrofit in URM				
Level	Rear Wall (k)	Front Wall (k)	Out-of-plane (k)	Sum (k)	Rear Wall (k)	OMF (k)	Front Wall (k)	Out-of-Plane (k)	Sum (k)
Story 6	37	35	-32	40	38	16	36	-31	59
Story 5	90	88	-28	150	81	29	79	-14	175
Story 4	145	143	-27	261	123	63	125	-16	295

Table 1-10 ETABS Story Shear Comparison for Six-story Unretrofitted URM Building and OMF Retrofit (continued)

Level	Unretrofitted URM				OMF Retrofit in URM				
	Rear Wall (k)	Front Wall (k)	Out-of-plane (k)	Sum (k)	Rear Wall (k)	OMF (k)	Front Wall (k)	Out-of-Plane (k)	Sum (k)
Story 3	200	198	-25	373	163	89	163	-7	408
Story 2	250	252	-15	487	201	144	203	-24	524
Story 1	285	286	24	595	231	160	234	24	649
Story 1 %	48%	48%	4%	100%	36%	25%	36%	3%	100%

Table 1-11 shows these results in a different way by comparing the resulting story shears from the 3D ETABS models with the shears obtained using the Special Procedure. Ratios greater than one indicate 3D ETABS shear forces higher than expected from the Special Procedure. Ratios less than one indicate 3D ETABS shear forces lower than expected using the Special Procedure. Based on the 3D ETABS analysis, the Special Procedure underpredicts shears in the masonry end walls and overpredicts shear forces to the midspan OMF.

Table 1-11 Story Shears Ratio to Forces from Special Procedure for Six-story Unretrofitted URM Building and OMF Retrofit from ETABS

Level	Unretrofitted URM		OMF Retrofit in URM		
	Rear Wall	Front Wall	Rear Wall	Midspan OMF	Front Wall
Story 6	1.85	1.84	1.90	0.84	1.89
Story 5	1.20	1.16	1.47	0.47	1.44
Story 4	1.12	1.08	1.37	0.57	1.34
Story 3	1.08	1.05	1.30	0.57	1.27
Story 2	1.04	1.03	1.26	0.72	1.24
Story 1	0.97	0.95	1.18	0.65	1.16

1.3.4 Case Study: Retrofit Situation 3 with New Vertical Elements at Open Storefront

The case study for Retrofit Situation 3 is based on the same two-story building used previously with the first story front wall replaced by storefront glazing. For this retrofit situation, a new vertical

element is added to the first story at the front of the building. This retrofit is intended to mitigate a soft story deficiency at the first story as shown in Figure 1-34.

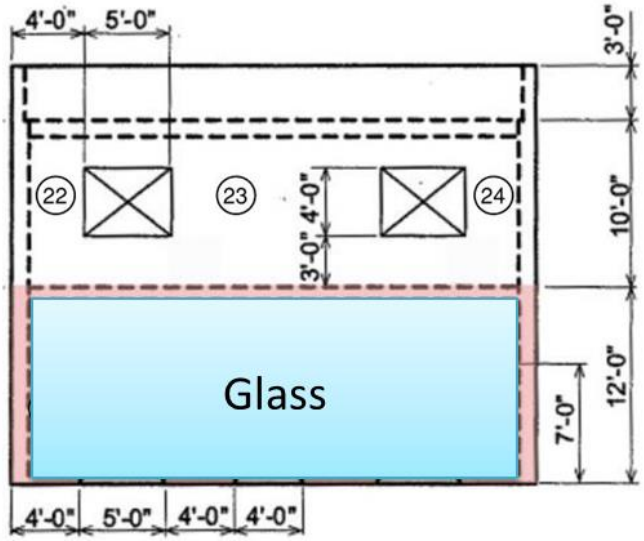

Figure 1-34 Figure showing open front first floor for Retrofit Situation 3.

For this example, a steel braced frame and a steel moment frame will be used at the new vertical elements at the store front.

1.3.4.1 SITUATION 3A – STEEL CHEVRON BRACED FRAME

A steel chevron braced frame is added to the open front at Level 1. Though the braced frame obstructs the opening, and may not be the first choice aesthetically, it is a commonly used retrofit technique, and thus is investigated as a case study.

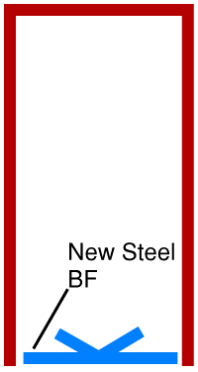

Figure 1-35 Figure showing Retrofit Situation 3a with new steel chevron braced frame.

Per ASCE/SEI 41-17 Table 9-6, the *m*-factor for steel braces varies between 4 and 6. Since the *m*-factor limit for new elements in a URM retrofit is equal to 4 per ASCE/SEI 41-17 Section 16.2.3.5.5, an *m*-factor of 4 is used for all moment frames. See Figure 1-36 for Level 1 seismic demands.

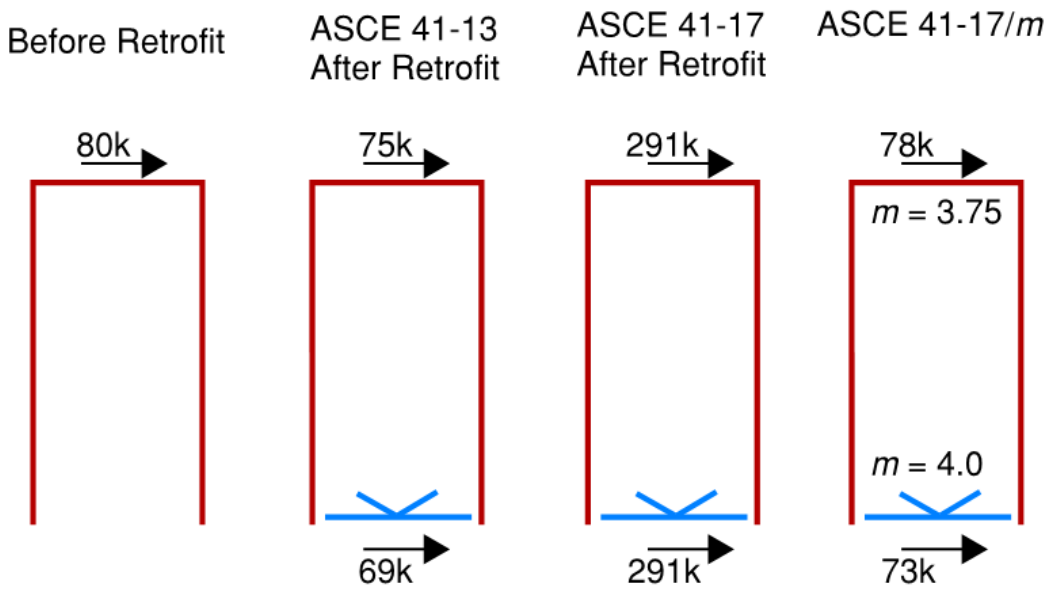

Figure 1-36 Figure showing wall demands per ASCE/SEI 41-13 before the retrofit (same as ASCE/SEI 41-17), per ASCE/SEI 41-13 after the retrofit, per ASCE/SEI 41-17 with no *m*-factor after the retrofit, and per ASCE/SEI 41-17 with *m*-factors after the retrofit (4.0 for the braced frame and 3.75 for the masonry).

Per ASCE/SEI 41-17 Table 9-4 for a brace in compression $m = 4$.

For calculating the base shear using the Linear Static Procedure of Section 7.4.1.3:

$V = C_1C_2C_mS_aW = 582\text{k}$ (ASCE/SEI 41-17 EQ. 7-21)

$F_x = 582\text{k}/2 = 291\text{k}$

$F_x/m = 291\text{k}/4 = 73\text{k}$

After dividing by the *m*-factor, the demands for ASCE/SEI 41-13 (Special Procedure) and for ASCE/SEI 41-17 (Linear Static Procedure) are very similar. However, this is largely dependent on the *m*-factor chosen. Depending on the geometry and failure mode of the URM pier, at the Life Safety Structural Performance Level, the *m*-factor for URM in-plane walls varies from 1.5 to 3.75. Looking at the rear wall, that means the demand could vary from 78k to 194k depending on the *m*-factor.

The variability in demand dependent on *m*-factor is also true for the braced frame. Per ASCE/SEI-41-17 Table 9-6, the *m*-factor for braces varies from 4 to 6. However, the new provision in ASCE/SEI 41-17 Section 16.2.3.5.5 limits the value of *m* to 4.0 so the maximum *m* used must be 4.

Unlike the ASCE/SEI 41-13 method, the ASCE/SEI 41-17 Linear Static Procedure accounts for the ductility of the individual element in the lateral system through the use of these *m*-factors. In the ASCE/SEI 41-13 approach, the values are from capacity-based design, and the demands are limited by what load the system can deliver. It is unclear which approach produces a better, more efficient retrofit.

1.3.4.2 SITUATION 3B – STEEL SPECIAL MOMENT FRAME FOR TWO-STORY BUILDING DESIGNED WITH ASCE/SEI 41-13 AND ASCE/SEI 41-17 WITH VARIOUS DRIFT LIMITS

A steel moment frame is used at the open front at Level 1 for Retrofit Situation 3b. This is a very common choice for soft story retrofits in California. However, adding such a flexible element below the rigid URM system raises concerns with many engineers who, as a result, use stringent drift limits.

Figure 1-37 Figure showing Retrofit Situation 3b with new steel moment frame.

Per ASCE/SEI 41-17 Table 9-6, the *m*-factors for steel moment frame beams and columns vary between 2 and 6. Since the *m*-factor limit for new elements in a URM retrofit is equal to 4 per ASCE/SEI 41-17 Section 16.2.3.5.5 and the average *m*-factor for beams and columns is also equal to 4, an *m*-factor of 4 is used for all moment frames. See Figure 1-38 for Level 1 seismic demands.

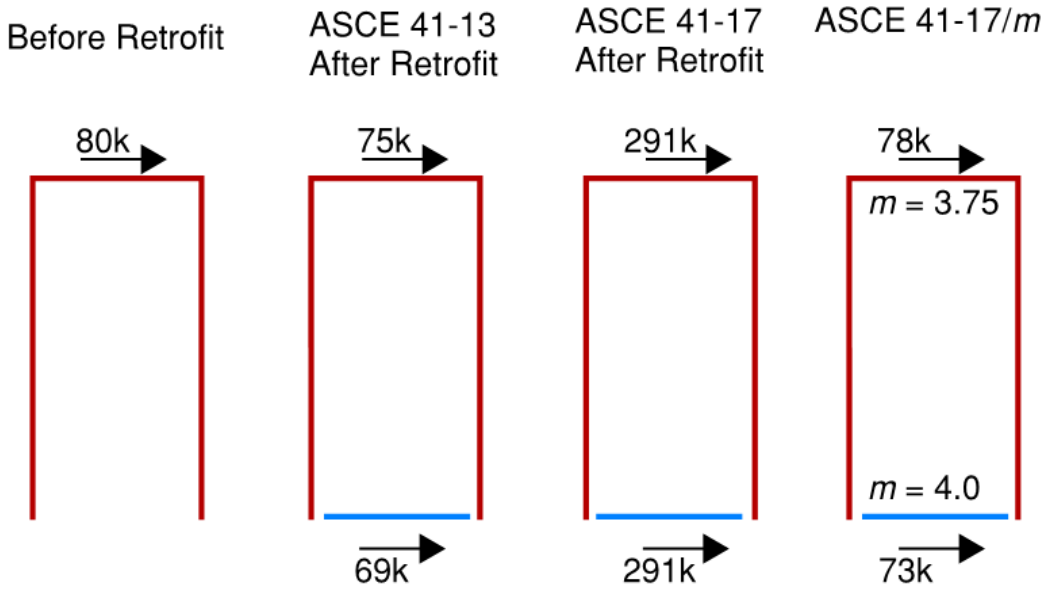

Figure 1-38 Figure showing wall demands per ASCE/SEI 41-13 before the retrofit (same as ASCE/SEI 41-17), per ASCE/SEI 41-13 after the retrofit, per ASCE/SEI 41-17 with no *m*-factor after the retrofit, and per ASCE/SEI 41-17 with *m*-factors after the retrofit (4.0 for the moment frame and 3.75 for the masonry wall).

With the same *m*-factor, the moment frame system has the same demands as the braced frame system.

V = 582k

F_x/m = 73k

Due to the flexibility of the moment frame system, the following examples will be used to evaluate whether the current drift limits in the code are sufficient to ensure the resulting moment frame retrofit actually functions to resist load and limit drift when combined with the existing URM system.

The following drift limits and the moment frames required to resist those limits will be used to illustrate this concept. For context, a design to ASCE/SEI 7-10 is included

- Case 1: No drift limit, strength governed.
- Case 2: Drift limit = 2.5% per ASCE/SEI 7-10 with C_d = 5.5
- Case 3: Drift limit = 1.5% per ASCE/SEI 41-17
- Case 4: Drift limit = 1.5% per ASCE/SEI 41-17 with no *m*-factor applied

Elevations of the steel moment frames designed to comply with Case 1 to Case 4 are shown in Figure 1-39 to Figure 1-42.

- Case 1: No drift limit, strength governed, ASCE/SEI 41-13 demands:

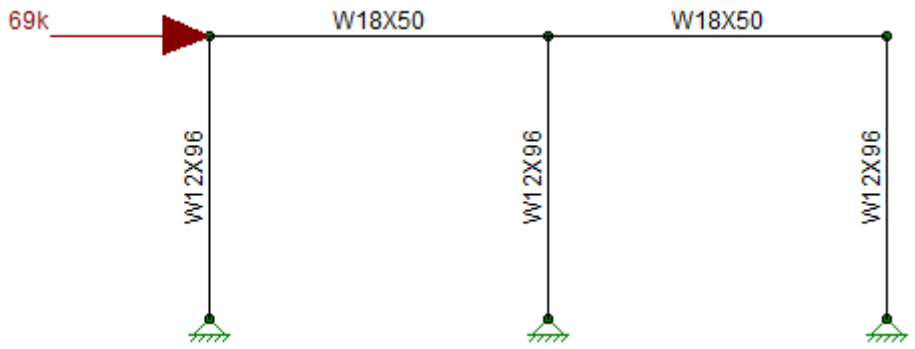

Figure 1-39 Figure showing moment frame governed by strength design.

Drift ratio = (2.168 in)/(150 in) = 1.45%

- Case 2: For a drift limit = 2.5% per ASCE/SEI 7-10 with C_d = 5.5, using ASCE/SEI 41-13 demands:

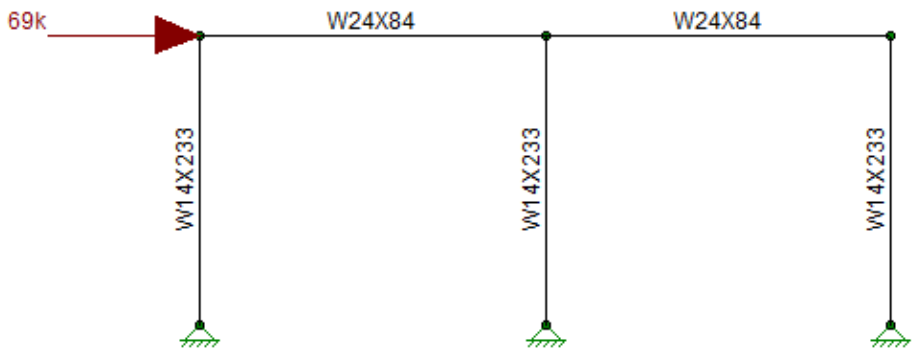

Figure 1-40 Figure showing moment frame required to meet 2.5% drift limit per ASCE/SEI 7-10 with C_d = 5.5.

Drift ratio = (0.664 in) * (5.5in)/(150in) = 2.43%.

- Case 3: For a drift limit = 1.5% per ASCE/SEI 41-17 with *m*-factor = 4:

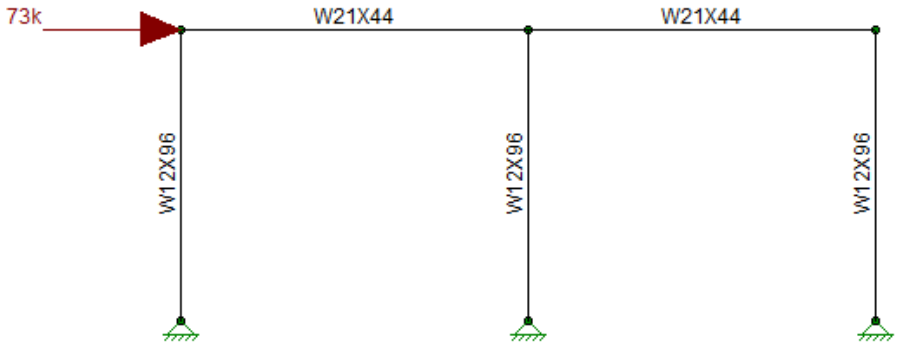

Figure 1-41 Figure showing moment frame required to meet 1.5% drift limit with *m*-factor.

Drift ratio = (2.247 in)/(150 in) = 1.5%.

- Case 4: For a drift limit = 1.5% per ASCE/SEI 41-17 with no *m*-factor applied

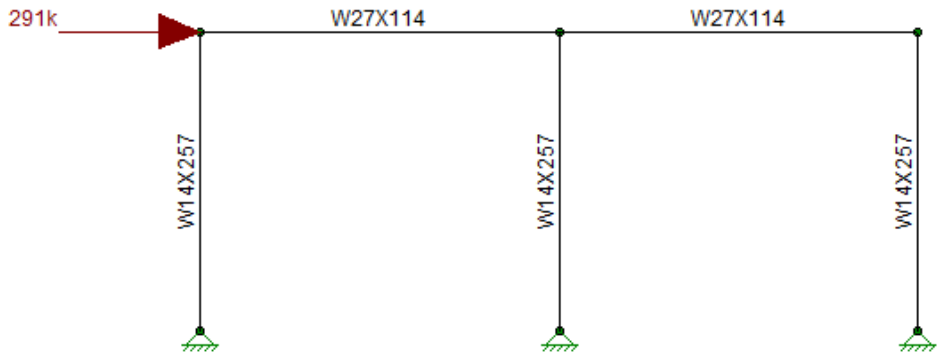

Figure 1-42 Figure showing moment frame required to meet 1.5% drift limit per ASCE/SEI 41-17 with no *m*-factor.

Drift ratio = (2.177in)/(150in) = 1.45%

The beams and columns required to meet these drift limits are summarized in Table 1-12 below.

Table 1-12 Retrofit Situation 3b Moment Frame Beams and Columns Required to Meet Various Drift Limits

Case	Drift Limit	Beam	Column
ASCE/SEI 41-13 loads	none	W18x50	W12x96
ASCE/SEI 41-13 loads, ASCE/SEI 7-10 limit, C_d = 5.5	2.50%	W24x84	W14x233
ASCE/SEI 41-17 loads and limit, with *m*-factor	1.50%	W21x44	W12x96
ASCE/SEI 41-17 loads and limit, no *m*-factor	1.50%	W27x114	W14x257

The ASCE/SEI 7-10 (and 7-16) code drift limit, typically applied to new buildings, is more conservative than the ASCE/SEI 41-17 drift limit of 1.5% with an *m*-factor applied. ASCE/SEI 41-17 is accounting for the ductility, or lack thereof, in a system and assigning an appropriate *m*-factor. The *m*-factor allows engineers to take the existing system into account without redesigning it to meet current code requirements.

The beams and columns are only slightly heavier than the design governed by strength alone with no drift limits. In this example, the limit of 1.5% with the application of the *m*-factor is applicable for an efficient design.

1.3.4.3 SITUATION 3B – STEEL MOMENT FRAME FOR TWO-STORY BUILDING WITH COMPARISON OF RISA-2D VS. ETABS 3D DESIGNS WITH ASCE/SEI 41-13 SPECIAL PROCEDURE AND DRIFT LIMIT OF 0.75%

The design was repeated for Retrofit Situation 3b by doing the initial design using provisions of ASCE/SEI 41-13 Special Procedure with the 0.75% drift limit using RISA-2D. This was compared to the 3D ETABS model with the moment frame at the front wall.

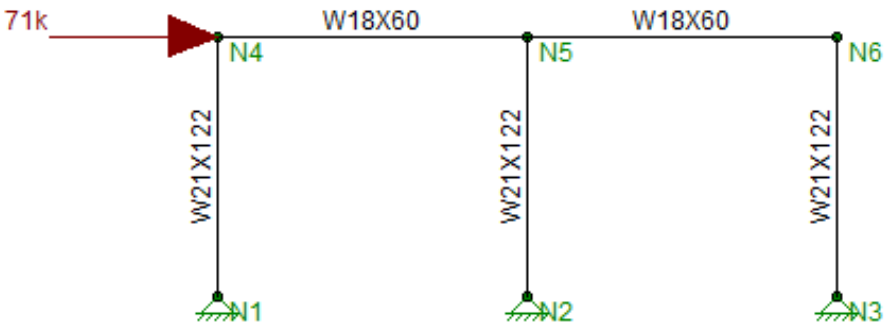

Figure 1-43 Retrofit Situation 3b RISA-2D model for MF at front wall of two-story building.

This design resulted in a story drift of 0.74% at Story 1. The maximum acceptance ratio was 0.60 for the beams and 0.36 for the columns including the phi factors from AISC 360. Note that these resulting sizes differ from the four previous designs shown in Table 1-12. This frame was added to the 3D ETABS model. Two views of the ETABS model are shown in Figure 1-44. Diaphragm displacements at Story 2 and Story 1 are shown in Figure 1-45 and drifts are summarized in Table 1-13. Phi factors were used initially for these studies, but note that the final proposal does not require the use of φ-factors to be consistent with the IEBC. See Section 1.3.5 where the proposed detailing requirements are discussed.

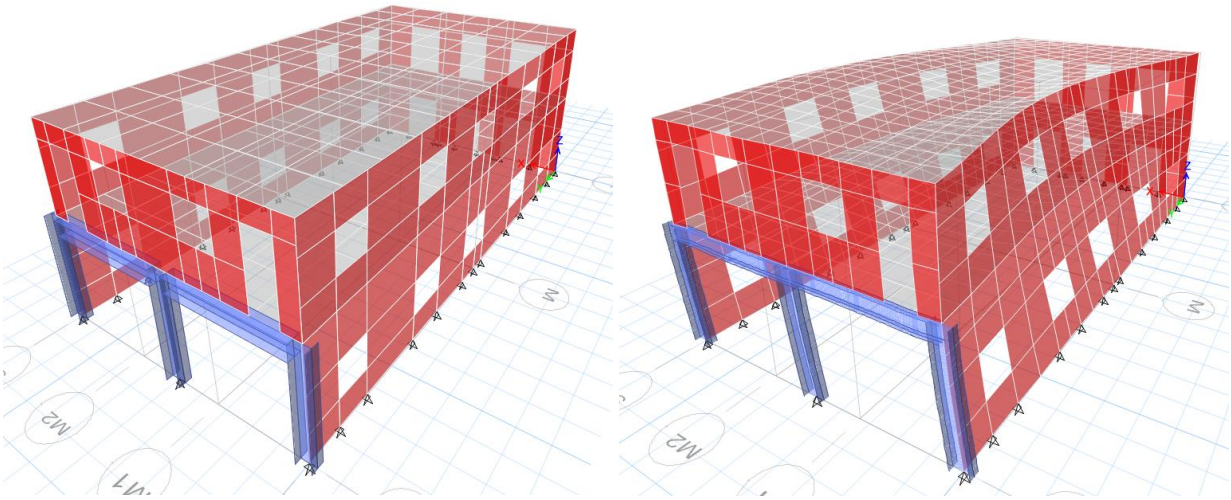

Figure 1-44 Retrofit Situation 3b ETABS model with undeformed shape (left) and deformed shape (right).

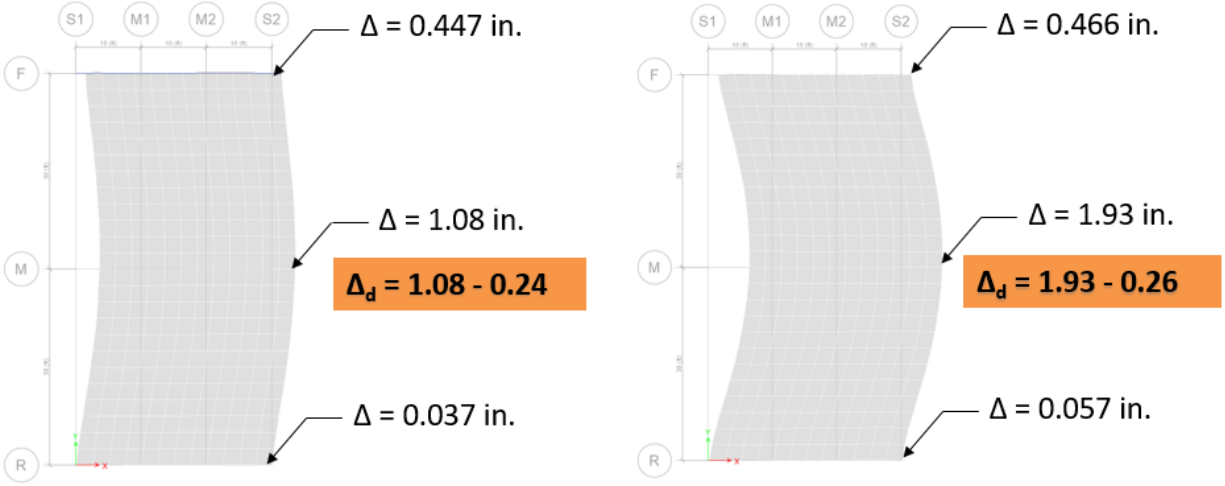

Figure 1-45 Displaced Shape of Story 2 (left) and Story 1 (right) diaphragms from ETABS model with displacements shown in inches. Note that the moment frame is at Line F at the top of the figure.

In Figure 1-45, the diaphragm displacement, Δ_d, is distinguished from the wall displacement. For example, in Story 2, the average of the wall displacements is (0.447 in. + 0.037 in.)/2 = 0.24 in. This is subtracted from the full 1.08-inch midspan displacement to get the displacement due to diaphragm alone.

Table 1-13 Drift and Displacement Comparison for RISA-2D vs. 3D ETABS Models for Stiff MF Designed with Drift Limit 0.75%

Model	Story 2			Story 1		
	Midspan Displ.	Midspan Drift	Rear Wall	Midspan Displ.	Midspan Drift	Rear Wall Drift
RISA 2D MF Stiff	-	-	-	-	-	0.74%
3D ETABS MF Stiff	1.93 in.	0.71%	0.016%	1.08 in.	0.75%	0.31%

The 3D ETABS model for Retrofit Situation 3b was analyzed using both membrane elements and thin shell elements for the longitudinal walls. As concluded earlier with Situation 2b, the membrane walls provided better correlation with the Special Procedure.

Table 1-14 Situation 3b Distribution of Loads for Two 3D ETABS Models for Loading in Transverse (E-W) Direction with Different Out-of-Plane Modeling of Longitudinal Walls

Transverse (E-W) Direction	Rear Wall (k)	Front Wall (k)	Out-of-Plane (k)	Sum (k)	Correlation to Special Procedure
Special Procedure Loads at Story 2	20	19		39	
ETABS stiffer MF, membrane walls	20	19		39	Good
ETABS stiffer MF, thin shell walls	33	42	-36	39	Poor
Special Procedure Loads at Story 1	75	71	-	146	
ETABS stiffer MF, membrane walls	79	67	-	146	Good
ETABS stiffer MF, thin shell walls	78	56	12	146	Fair

In summary, as in the two-story example, the membrane walls used in the 3D ETABS model produced more reliable results and better correlations with results from the Special Procedure. Either the chevron braced frame of Retrofit Situation 3a or the moment frame of Retrofit Situation 3b can be used effectively. The moment frame designed with a drift limit of 0.75% will provide a frame stiff enough to resolve the open front deficiency.

1.3.5 Review of Detailing Requirements

The various case studies prompted additional consideration of provisions present in Chapters 9 to 12 of ASCE/SEI 41 that impose detailing requirements and specify *m*-factors for use in determining acceptance ratios.

- Option 1 – Adopt "Ordinary" Detailing Requirements: New elements and systems shall conform with, at a minimum, the detailing requirements for "ordinary" systems as prescribed in the applicable material standards referenced in Chapters 9 through 12.

- Option 2 - Potential Enhancement: New components in the vertical elements of the seismic force-resisting system shall be designed and detailed such that the corresponding element *m*-factor determined in accordance with Chapters 9 through 12 for a primary element and Collapse Prevention performance is no less than 2.0.

Retrofit Situation 2b provides a useful comparison. The MF designed using the ASCE/SEI 41-13 Special Procedure without a drift limit resulted in a flexible frame. The MF designed using the proposed provisions with the 0.75% drift limit resulted in a significantly stiffer frame. The question is whether special ductility requirements should be imposed on new vertical elements that meet the 0.75% drift limit or whether requirements for "ordinary" systems would be adequate.

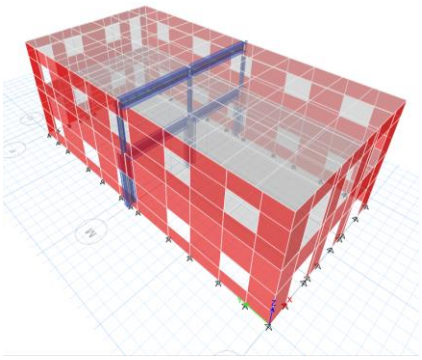

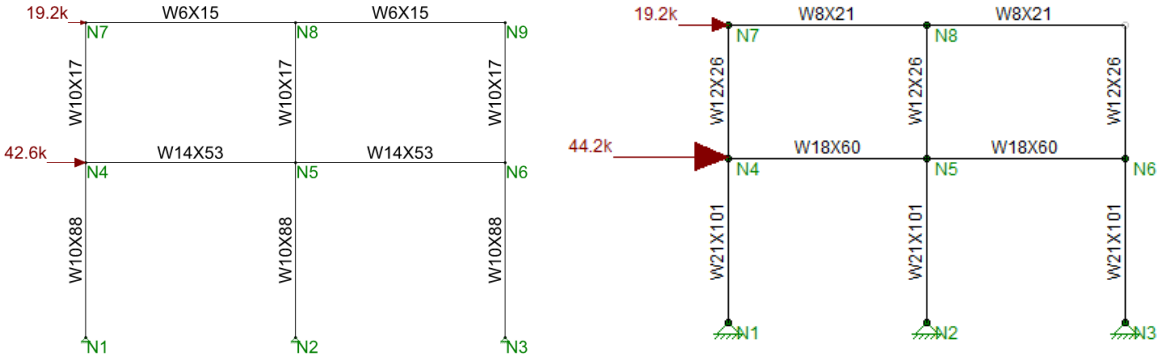

Figure 1-46 Comparison of flexible MF designed with ASCE/SEI 41-13 with no drift limit (Story 1 has 2.1% drift) (image on left) and stiffer MF designed with proposed provisions and 0.75% drift limit (image on right).

Table 1-15 *R*-factors of Common Ordinary vs. Special Systems from ASCE/SEI 7-16

Ordinary System Type	***R***	Ω_0	Ω_0/R	C_d	C_d/R
Concrete Shear Wall (non-bearing)	5	2.5	0.50	4.5	0.90
Concrete OMF	3	3	1.00	2.5	0.83
Steel OMF	3.5	3	0.86	3	0.86
Steel OCBF	3.25	2	0.62	3.25	1.00
Special System Type	***R***	Ω_0	Ω_0/R	C_d	C_d/R
Concrete Shear Wall (non-bearing)	6	2.5	0.42	5	0.83
Concrete Special MF	8	3	0.38	5.5	0.69
Steel Special MF	8	3	0.38	5.5	0.36
Steel Special CBF	6	2	0.33	5	0.83

Table 1-15 shows parameters from ASCE/SEI 7-16 used for new design of several types of Ordinary and Special systems. To highlight the comparison with the two moment frames designed for Situation 2b above, the examples below compare the Steel Special Moment Frame, Steel Ordinary Moment Frame, and stiffer frame above designed with the Special Procedure. Since the stiffer MF from the case studies above was drift controlled, the ductility demands are low.

- ASCE/SEI 7-16 Special Moment Frame (SMF)

  S_{DS}, BSE-1N = 1.401 (Los Angeles site shown above)

  $V/W \leq S_{DS} / (R/I_e) = 1.401 / (8 / 1.0) = 0.175g$

  $V/W \times \Omega_o = 0.175 \times 2.5 = 0.44g$

- ASCE/SEI 7-16 Ordinary Moment Frame (OMF)

  $V/W \leq S_{DS} / (R/I_e) = 1.401 / (3.5 / 1.0) = 0.40g$

  $V/W \times \Omega_o = 0.40 \times 3 = 1.20g$

- ASCE/SEI 41 Special Procedure

  V/W = 61.8 k /173.5 k = 0.36g

  Stiff moment frame (drift governed): Highest D/C = 0.57 (with ϕ = 0.9)

First yield: $(V/W) / \phi = (0.36 / 0.57) / 0.9 = 0.70$

Mechanism would be higher: Say $1.5 \times 0.63 = 1.05$g

Similar to Ordinary Moment Frame overstrength level

A series of proposed detailing requirements were developed for consideration as follows:

- Steel Ordinary Concentric Braced Frame (OCBF) (AISC 341)
  - Braces: moderately ductile, V and inverted V slenderness limits, tension-only permitted
  - Beams and connections: Use omega factor
  - Brace connections: Permits R_yF_y in tension, $1.1F_{cr}A_g$ in compression
- Steel Ordinary Moment Frame (OMF) (AISC 341)
  - No special *b/t* ratios
  - No protected zones
  - Beam-column connections: Demand Critical Welds (DCW) at flange-to-flange connection, design to $1.1R_yM_p$
- Concrete Ordinary Shear Wall (ACI 318-19)
  - Chapter 18: Earthquake Resistant Structures does not apply—no detailing requirements for wall; some detailing and development requirements for foundations.
  - Chapter 11: Walls would apply. It has $\rho_{min} = 0.0025$, bar spacing at maximum of 3h or 18 in., two curtains if over 10 in., not even hooks on horizontal bars at wall ends.
  - Per ASCE/SEI 41-17 Table 10-21 assuming *P* will be low for a URM retrofit, the unconfined "ordinary" wall would have *m*-factors of 2.5 or 4 for the CP condition
  - Per ASCE/SEI 41-17 Table 10-22 assuming *P* will be low for a URM retrofit, the *m*-factor for the CP condition is 3.
- *m*-factor Based Detailing
  - Section 16.2.3.5.5 currently implies detailing and performance for an *m*-factor of 4 but it is proposed that the cross reference to Chapter 7 and the *m*-factor both be dropped.
  - An alternative *m*-factor of 2 was proposed; or an m-factor criteria only applicable for concrete shear walls.

Study participants and reviewers were polled and decided unanimously to opt for Ordinary, not Special, detailing requirements as defined in ASCE/SEI 41-23 Chapters 9 to 12. The reference to an *m*-factor of 4 was dropped. One added requirement was imposed, namely, that OCSW detailing must include 90-degree hooks at wall ends. This could be adapted to 180-degree hooks, such as in single curtain walls.

Adding the bracing requirements at steel beam-column joints required for SMF systems is difficult in URM buildings given the flexibility of the wood diaphragm assemblies. This is not required in an OMF, which simplifies the retrofit and makes it more economical.

1.3.6 Conclusions

Findings for each Retrofit Situation are summarized as follows.

- Retrofit Situation 1: Adding shotcrete overlay to existing masonry
    - Load sharing requirements were not provided in ASCE/SEI 41-13 and have some ambiguity in ASCE/SEI 41-17. This is clarified in the current proposal and would allow design engineers flexibility in allocating the loads to the new elements as long as the existing masonry walls are capable of resisting the loads they attract on the basis of their relative rigidity.
- Retrofit Situation 2: Adding a new vertical element at diaphragm midspan
    - For the introduction of a stiff concrete wall at midspan, as in Retrofit Situation 2a, the ASCE/SEI 41-13 method that is limited by diaphragm capacity appears to be a more rational method where vintage wood diaphragms are involved. For a new shear wall element, the demands with ASCE/SEI 41-17 are significantly higher, resulting in a concrete wall that is twice as long. The ASCE/SEI 41-23 proposed approach will likely result in more cost effective solutions that are still effective in improving performance of URM buildings.
    - For a new moment frame element, as in Retrofit Situation 2b, force demands between ASCE/SEI 41-13 and ASCE/SEI 41-17 are similar, but drift assumptions and detailing requirements can make a substantial difference in final size and stiffness of the moment frames. A moment frame designed with a drift limit of 0.75% was found to produce optimal results by reliably reducing the diaphragm span and limiting the tributary loads sent to the end walls. This approach was studied with both 2D and 3D models with the conclusion that a 2D frame designed with the 0.75% drift limit will be effective in reducing drifts in a similar 3D model configuration by approximately half of the retrofitted drift. For the buildings in these case studies, that represented an effective retrofit strategy without the need for 3D modeling.
- Retrofit Situation 3: Adding a new vertical element at an open front below a masonry wall
    - For a new braced frame, the demands from ASCE/SEI 41-13 are similar to those of ASCE/SEI 41-17. The study confirmed that a chevron brace frame could effectively be designed to

retrofit an open front URM building and also that a moment frame designed using the same 0.75% drift limit would also be an effective retrofit for an open front URM building. These studies similarly showed that a 2D design for the moment frame meeting the 0.75% drift limit compared well to the behavior of a similar 3D model and obviates the need for the more complex 3D analysis model for a URM retrofit. In some cases, the existing masonry elements, such as in heavily punctured shear walls, may have insufficient strength to resist the loads they attract and adding stiff enough new elements is impractical. In these situations, the designer should consider designing the new elements for 100% of the required forces on the wall line and adding truss and beam support per Section 16.2.4.4 and vertical bracing per Section 16.2.4.2.2, even where not required.

The recommended changes described in Section 1.4 address the conclusions summarized above.

1.4 Recommended Changes

Note about Change Proposals

This report documents aspects of change proposals as they were submitted to subcommittees of ASCE's *Seismic Retrofit of Existing Building Standards* Committee. Often, these change proposals were revised, in some cases substantively, by these subcommittees before they were adopted into ASCE/SEI 41-23. Readers should not rely on this report for information about the final version of provisions in ASCE/SEI 41-23.

The strikeout/underline proposed changes to ASCE/SEI 41-23 Sections 16.2.3 and subsections, the new Section 16.2.5, and corresponding sections of the commentary are shown verbatim below. New or modified text is shown in blue.

SCOPE – ASCE 41-17 Section 16.2.3 Analysis and Section 16.2.3.5 New Vertical Elements

16.2.3 Analysis. The URM special procedures for shear wall and diaphragm analysis requirements shall be in accordance with this section. The analysis requirements for other components and systems of URM buildings shall be in accordance with Section 16.2.4.

Material strengths for new elements shall be as prescribed in the applicable material standards referenced in Chapters 9 through 12, unless otherwise required by this section. The strength reduction factor, φ, shall be taken equal to 1.0. Nominal material properties, defined per Section 10.2.2.1.2, as properties specified in construction documents, shall be used in the strength determination, not expected values.

Section 16.2.3.2.3: Acceptability Criteria: The intersection of diaphragm span between ~~walls~~ vertical lateral force-resisting elements that meet the drift requirements of Section 16.2.3.5.6., *L*, and the demand-capacity ratio, DCR, shall be located within Region 1, 2, or 3 on Fig. 16-1.

16.2.3.5 New Vertical Elements

16.2.3.5.1 General. New vertical elements may be added to resist lateral forces.

16.2.3.5.2 Combinations of Vertical Elements

16.2.3.5.2.1 Lateral Force Distribution. Lateral forces shall be distributed among the vertical elements in proportion to the relative rigidities, except that moment-resisting frames shall comply with Section 16.2.3.5.2.2. The existing masonry shall be evaluated and shall be adequate to resist the forces attracted by relative rigidity in accordance with Section 16.2.3.3, regardless of the design force used for new vertical elements.

16.2.3.5.2.2 Moment-Resisting Frames. Moment-resisting frames shall not be used in combination with an unreinforced masonry wall in a single line of resistance unless the wall has piers that have adequate shear capacity to sustain rocking in accordance with Section 16.2.3.3.2. The frames shall be designed to carry 100% of the forces tributary to that line of resistance~~, and the story drift shall be limited to 0.0075.~~.

16.2.3.5.3 *Wood Structural Panels*. Wood structural panels shall not be used to share lateral forces with other materials along the same line of resistance.

16.2.3.5.4 *Forces on New Vertical Elements*. ~~The Linear Static Procedure of Section 7.4.1 shall be used to determine forces on new lateral elements. The building period shall be calculated according to Eq. (7-18) using $C_t = 0.020$ and $\beta = 0.75$. The value of $C_1C_2C_m$ in Eq. (7-21) shall be taken as 1.4.~~ Section 16.2.3.3 shall be used to determine forces on new and existing vertical lateral force-resisting elements. The additional weight of new elements shall be included in the force determination.

16.2.3.5.5 *Acceptance Criteria for New Vertical Elements*. New vertical elements shall satisfy ~~the acceptance criteria provisions of Section 7.5.2.2. The value of m in Eq. (7-36) shall not exceed 4.0.~~ the requirements of Section 16.2.3.

16.2.3.5.6 *Drift Limits*. The story drift ratio for all new vertical elements shall be limited to ~~0.015~~ 0.0075.~~, subject to the limitations of Section 16.2.3.5.2.~~

Section 16.2.5: Detailing for New Elements. New elements and systems shall conform with, at a minimum, the detailing requirements for "ordinary" systems as prescribed in the applicable material standards referenced in Chapters 9 through 12. **EXCEPTION**: For reinforced concrete walls 90-degree hooks shall be provided on horizontal reinforcing at wall ends.

Additionally, seismic force-resisting systems that are not permitted (NP) in Seismic Design Category C of ASCE/SEI 7 are not allowed for new vertical elements in regions of High Seismicity per Section 2.5.

C16.2.3. A general statement regarding material strengths for new elements was missing in the standard. A requirement to use the material standards referenced in Chapter 9 through 12 has been added. A strength reduction factor, φ, equal to 1.0 is included to be consistent with 2018 IEBC Appendix Chapter A1 Section A108.1.2. A clarification was added indicating that specified values are to be used in the strength determination, not expected values, since the concept of lower bound and expected strengths is typically not used in Section 16.2.

C16.2.3.2.3 It is conservative to assume only shear walls are stiff enough to divide the diaphragm span. However, a moment frame designed to meet the 0.0075 drift limit prescribed by this section reduces the diaphragm deflection significantly, effectively dividing the span. Therefore, the provision has been expanded to include other, more flexible systems, provided they meet the 0.0075 drift limit. Diaphragm span lengths, L, are cases with single spans and double spans are illustrated Fig. C16-1.

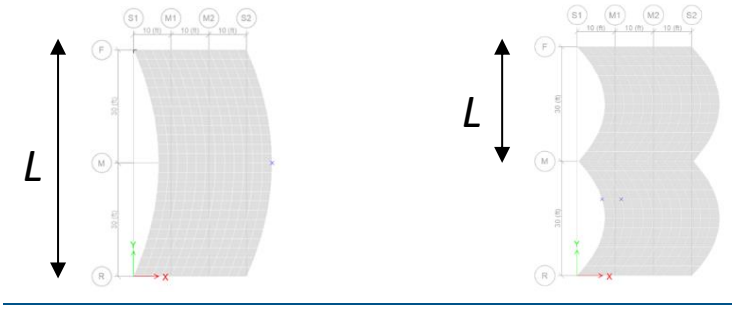

Single Span Double Span

Figure C16-1. Diaphragm Span Length

C16.2.3.5.1 *Forces on New Vertical Elements.* Given the potential differences between the strength and stiffness of new vertical elements and existing masonry wall elements, it is possible that a new wall could be designed to carry 100% of the required forces for the wall line but have insufficient stiffness to attract significant loads away from the masonry elements, leading to substantial damage in the masonry before the new elements provided effective resistance. To address this, the standard requires that loads be shared by relative rigidity between the new and existing elements. An explicit requirement was added to emphasize that, after the loads have been distributed, the masonry must be evaluated using the provisions of Section 16.2.2.3.

In some cases, the existing masonry elements, such as in heavily punctured shear walls, may have insufficient strength to resist the loads they attract and adding stiff enough new elements is impractical. In these situations, the designer should consider designing the new elements for 100% of the required forces on the wall line and adding truss and beam support per Section 16.2.4.4 and vertical bracing per Section 16.2.4.2.2, even where not required.

C16.2.3.5.4 *Forces on New Vertical Elements.* ~~The forces to be used for the design of new elements are intended to be conservative, given the nature of URM buildings, and to keep consistent with the basic assumptions of the modeling of these buildings developed in the original ABK research.~~ The forces to be used for the design of new elements are based on the effective accelerations and diaphragm capacities developed as part of the seismic evaluation using the Special Procedure. This approach is consistent with the traditional standard of practice for retrofitting existing unreinforced masonry wall buildings. It removes the provision that was added in ASCE 41-17 to require new elements to be evaluated per the provisions of Chapter 7 which have a different underlying design basis than was used to develop the Special Procedure demands. ~~The building period calculation is based on a shear wall building, and the modification factors are based on a short period and moderate ductility.~~

C16.2.3.5.5 *Acceptance Criteria for New Vertical Elements.* ~~Consistent with the original assumptions of the ABK research, m-factors for new vertical elements are capped at 4.0. This requirement, along with the associated drift limits, is intended to limit nonlinear behavior in new vertical elements.~~ Capacities of new vertical elements are based on the referenced material standards, except that as indicated in the commentary to Section 16.2.3, a strength reduction factor, φ, of 1.0 is used to be consistent with the 2018 IEBC Appendix Chapter A1 Section A108.1.2.

C16.2.3.5.6 *Drift Limits.* The drift limit of 0.0075, together with the force levels determined in accordance with Section 16.2.3.5.4, was determined as part of three-dimensional two-story and six-story case study analysis models that included in-plane and out-of-plane masonry walls, semi-rigid wood diaphragms, and midspan steel moment frames. Moment frames designed to meet that stiffness were found not to attract the force demands assumed by the tributary area method assumed by the Special Procedure, but they were nonetheless found to be effective in significantly

reducing midspan diaphragm displacements and in attracting substantial force away from parallel in-plane masonry walls. It should be recognized that moment frames, braced frames, or shear walls with lower drifts will further reduce midspan diaphragms and attract more loads. Details on the case studies that were performed are described in FEMA P-2208 (2022).

C16.2.5 *Detailing for New Elements:* Limiting systems to those permitted only in Seismic Design Category C or higher eliminates systems with poor ductility such as plain (unreinforced) concrete and masonry shear wall systems and ordinary concrete moment frames. Other ordinary systems are typically not eliminated by this requirement. However, as described in FEMA P-2208 (2022), case studies have shown that the demands used to design elements in Section 16.2.3 have sufficient strength to place relatively limited ductility demands on new elements. Thus, ordinary detailing requirements are considered sufficient to meet the Limited Performance Objective of Section 16.2.1. The Authority Having Jurisdiction may require detailing that is compliant with current code requirements.

Regarding the exception for reinforced concrete shear walls, for ordinary reinforced concrete shear walls, ACI 318-19 has no special seismic provisions in Chapter 18 Earthquake Resistant Structures. The regular provisions in Chapter 11 Walls in ACI 318-19 require a minimum reinforcing ratio 0.0025, spacing of a maximum of 18" or three times the wall thickness, and two curtains of reinforcing when the wall is over 10", but there are no other detailing requirements, even for hooks at the ends of horizontal bars.

1.5 References

ACI, 2019, *Building Code Requirements for Structural Concrete and Commentary on Building Code Requirements,* ACI 318-19 and ACI 318R-19, American Concrete Institute, Farmington Hills, Michigan.

AISC, 2016*, Seismic Provisions for Structural Steel Buildings,* ANSI/AISC 341-16, American Institute of Steel Construction, Chicago, Illinois.

ASCE, 2010, *Minimum Design Loads for Buildings and Other Structures*, ASCE/SEI 7-10, American Society of Civil Engineers, Reston, Virginia.

ASCE, 2014, *Seismic Rehabilitation of Existing Buildings*, ASCE/SEI 41-13 Report, American Society of Civil Engineers Structural Engineering Institute, Reston, Virginia.

ASCE, 2016, *Minimum Design Loads for Buildings and Other Structures*, ASCE/SEI 7-16, American Society of Civil Engineers, Reston, Virginia.

ASCE, 2017, *Seismic Evaluation and Retrofit of Existing Buildings*, ASCE/SEI 41-17 Report, American Society of Civil Engineers Structural Engineering Institute, Reston, Virginia.

AWC, 2015, Special Design Provisions for Wind and Seismic Standard with Commentary, SDPWS-2015, American Wood Council, Washington, D.C.

CSI, 2016, ETABS Plus, version 17.0.1, Computers and Structures, Inc. Lafayette, California.

RISA, 2020, RISA-2D, version 19.0.0, RISA Tech Inc., Foothill Ranch, California.

FEMA, 2018, *Example Application Guide for ASCE/SEI 41-13 Seismic Evaluation and Retrofit of Existing Buildings with Additional Commentary for ASCE/SEI 41-17*, FEMA P-2006 Report, prepared by the Applied Technology Council for the Federal Emergency Management Agency, Washington, D.C.

FEMA, 2006, *Techniques for the Seismic Rehabilitation of Existing Buildings,* FEMA 547, Federal Emergency Management Agency, Washington, D.C.

ICC, 2018, *International Existing Building Code,* 2018 Edition, International Code Council, Inc. Country Club Hills, Illinois.

SEAOC, 2012, *2009 IEBC SEAOC Structural/Seismic Design Manual,* Structural Engineers Association of California, California.

Chapter 2: Addition of Subdiaphragm Provisions to Chapter 16

2.1 Motivation

ASCE/SEI 41-17 Section 16.2 does not have explicit provisions requiring development of wall anchorage into the diaphragms for URM structures. Separation of diaphragms that were not adequately anchored to URM walls has been a common source of failure in past earthquakes, leading to falling hazards and partial collapse of roof or floor diaphragms. The purpose of the revisions in ASCE/SEI 41-23 Section 16.2.4.3 and Section C16.2.4.3 was to bring the provisions for anchorage of URM walls in Section 16.2 more in line with general wall anchorage provisions in ASCE/SEI 41 Section 7.2.11.1, where anchorage forces are required to be developed in the diaphragm through the use of subdiaphragms, if necessary. A new Section 16.2.4.3.1 has been added to the URM provisions in Chapter 16 that stipulates that the wall anchorage forces must be fully developed into the diaphragm where S_{x1} is greater than 0.2. Development of wall anchorage using subdiaphragms, cross ties, and chords similar to methods in Section 7.2.11.1 is now required for wood floor systems that are not granted explicit exemption to use an alternate prescriptive procedure. The alternate prescriptive anchorage requirements apply to five types of ductile wood floor systems and allow development of wall anchorage over a specified length, but subdiaphragm analysis, cross ties, and chords are not required. The simplified alternate procedure was included for ductile wood diaphragms that have performed well in past earthquakes with the intent to encourage rather than discourage owners from undertaking retrofits for URM buildings. The prescriptive requirements are intended to be compatible with Limited Performance Objectives for URM buildings and purposely do not contain explicit requirements for subdiaphragms, cross ties, and chords currently contained in Section 7.2.11.1.

2.2 Summary of Changes Recommended

The changes occur in ASCE/SEI 41-23 Section 16.2.4.3 and Commentary Section C16.2.4.3 that define requirements for wall anchorage in URM buildings. The new Section 16.4.2.3.1 provides requirements for the transfer of anchorage forces into diaphragms of URM buildings that were not included in previous editions of ASCE/SEI 41. Where S_{x1} is greater than 0.2, the specified anchorage forces must be fully developed. Notably, the new provisions include simplified alternate prescriptive procedures that will apply to five types of wood diaphragms that have demonstrated ductile performance in the past. The new commentary section includes a discussion of out-of-plane failure modes and includes a new figure showing an example of the prescriptive 8’-0” wall anchorage for joists parallel to the URM wall.

2.3 Technical Studies

Parametric studies were undertaken to confirm the specified development length used in the alternate prescriptive method and to bound the applicable limits of the prescriptive method. Variables in the parametric study included diaphragm size and aspect ratio, walls with and without openings, diaphragm capacity either strengthened or unstrengthened, and anchor development lengths.

2.3.1 Case Study

An example building for the purpose of illustrating the proposed problem and calculations was developed and was based on a typical building size in the historic district of Seattle, Washington.

This building is a four-story, unreinforced building with a footprint of 60'-0" by 120'-0". The diaphragm was assumed to consist of wood flooring over straight wood sheathing, which is supported in turn by 3x joists at 16-inches on-center. Heavy timber girders at approximately 20'-0" on-center support the joists and run longitudinally down the building. Heavy timber columns support the girders at approximately 20'-0" on-center. The unreinforced masonry walls are assumed to be 17-inch thick at the first floor and second floor and 13-inch thick at the third floor and fourth floor. A building with this footprint would typically have multiple openings along the transverse walls, while the longitudinal walls would be solid (assuming it is mid-block, with adjacent buildings on each side of the longitudinal walls). The stories are all assumed to be 12'-0" tall, with a 3'-0" tall parapet above the roof. The floor plan is illustrated below in Figure 2-1.

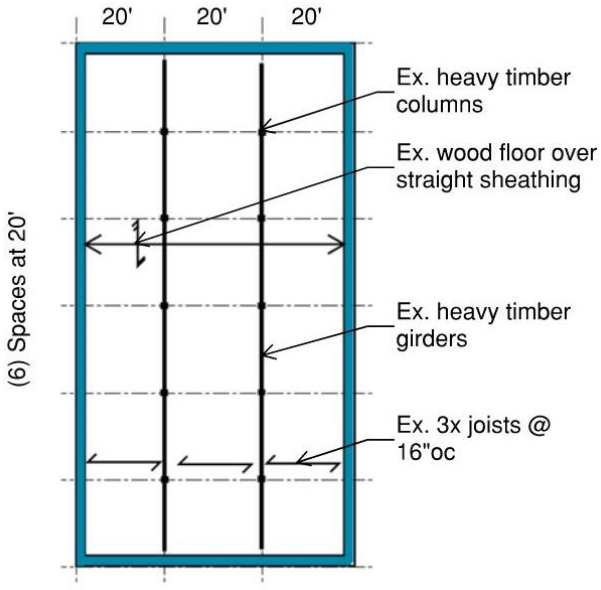

Figure 2-1 Subdiaphragm case study building layout.

For this case study, the building was assumed to be a Risk Category II per the 2018 *International Building Code* (ICC, 2019) and was evaluated using similar seismicity and floor weights to the Unreinforced Masonry Bearing Wall (URM) with Special Procedure example in FEMA P-2006, *Example Application Guide for ASCE/SEI 41-13 Seismic Evaluation and Retrofit of Existing Building* (FEMA, 2018).

Table 2-1 Case Study Weights

Building Component	Weight
Wall Weights	**120 pcf**
13” thick	130 psf
17” thick	170 psf
Floor Weights	
Wood-framed floor	30.5 psf with 10 psf partition load

Based on the Special Procedure method, seismic design parameters are determined per Section 16.2.1 and use the BSE-1E Seismic Hazard Level. The location, latitude, longitude, and site class for the building are as follows:

- Location: Los Angeles, California
- Latitude: 34.0160^{0} North
- Longitude: 118.2682^{0} West
- Site Class D

The following ground motion parameters were obtained for the BSE-1E using ASCE/SEI 41-17 values and the ATC on-line hazard tool:

S_{XS} = 0.861

S_{X1} = 0.489

Unreinforced masonry walls must be adequately connected at each diaphragm to transfer the out-of-plane forces from the wall mass into the diaphragm. ASCE/SEI 41-17 Section 16.2.4.3 provides the required force level for anchors and spacing limitations of anchors and prohibits cross-grain bending in the wood ledgers. The wall anchorage shall have a capacity equal to the larger of $0.9S_{XS}$ or 200 lb/ft. The demand on the anchorage and into the second-floor diaphragm from a solid wall, for example, is calculated as follows.

$F_p = 0.9S_{XS}W$

where:

W = Seismic weight of first floor and second floor wall tributary to the second-floor diaphragm (kips)

= (170 psf)(12 ft)

= 2,040 lb/ft

f_p = 0.9(0.861)(2,040 lb/ft)

= 1,581 lb/ft > 200 lb/ft

Similar calculations can be performed for other levels where the weight may be less due to wall thickness or wall openings, but this worst-case anchorage was used for the initial comparisons.

The next step was to check the subdiaphragm forces. As mentioned earlier, the URM Special Procedure in ASCE/SEI 41-17 Chapter 16 does not include language or requirements for the subdiaphragm checks. However, for a building using the full code approach (and not the Special Procedure), ASCE/SEI 41-17 Section 7.2.11.1 would require development of the anchorage into the diaphragm. If subdiaphragms are used, the shear forces must be evaluated, and there are limitations on length-to-depth ratios. This “full code” approach is one option used in the investigation.

The other option considered is to partially develop the forces into the diaphragm, preventing a failure right at the end of the anchorage point, but relying on the potential overstrength and redundancy of the wood-framed diaphragm to carry higher loads than expected using the published capacities. This “partial code” approach could allow an owner to install anchors and perform the retrofit along the wall, but not extend the work area to the interior of the building. Such an approach could be more economically feasible, thus resulting in more buildings with added wall anchors, and correcting what is a potentially serious hazard.

Figure 2-2 shows the full code and partial code options for the transverse direction of the case study building. The full code option includes wall ties for the out-of-plane force connecting to 20-feet by 20-feet subdiaphragms with cross ties at 18-feet on-center and the existing heavy timber beam acting as the subdiaphragm chord. The partial code option includes wall ties for the out-of-plane forces and, for the initial pass, a minimum 10-foot development into the diaphragm. As the wall ties will be anchored to the joists in this case, and the joists span 20-feet, there will be a 20-foot development into the diaphragm in the transverse direction by default. Deliberate cross ties and subdiaphragm chords are not provided for partial code.

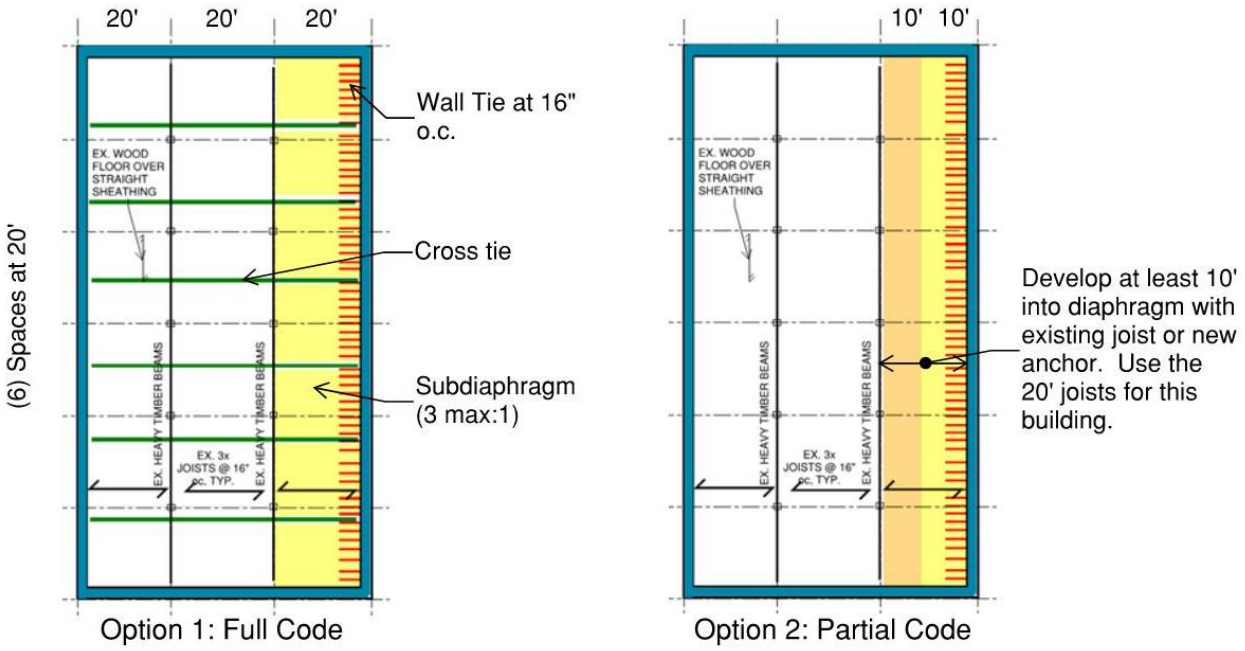

Figure 2-2 Subdiaphragm options in transverse direction.

For the full code option, new tension anchors from the wall to the diaphragm need to meet or exceed the f_p force of 1,581 lb/ft. Tension anchors will be added at 16-inches on-center, resulting in a demand of 2,108 lb per anchor. For ¾-inch adhesive anchors, the allowable tension capacity is 1,200 lb per ICC-AC 60 (ICC, 2015). Using an allowable-to-ultimate conversion factor of 3, as explained in FEMA P-2006 Section 12.16.1, the capacity for strength design is 3,600 lb per anchor, which exceeds the demand.

For the full code option, using a subdiaphragm of 18-feet by 20-feet, the shear stresses in the subdiaphragm are calculated below.

Demand = (1,581 lb/ft)(18 ft)(0.5)/20 ft)

= 711 lb/ft

Capacity = 1,500 lb/ft per ASCE/SEI 41-17 Table 16-3

D/C = Demand/Capacity = 0.47

Chord forces along the existing heavy timber beam line are calculated below. A connection would need to be provided between the timber beams for this load in the full code approach.

Chord axial load = $f_p(L_{sub})^2/(8(b_{sub}))$

where:

f_p = wall tension anchorage demand along wall length

L_{sub} = length of the subdiaphragm = 18 ft

b_{sub} = the width of the subdiaphragm = 20 ft

Chord axial load = (1,581 lb/ft)(18 ft)^2/(8(20 ft))

= 3.20 kips

Cross tie forces between the longitudinal walls are calculated below. A connection would need to be provided between the joists at 18-feet on-center for this load in the full code approach.

Cross tie demand = $f_p(L_{sub})$ = (1,581 ft)(18 ft)

= 28.5 kips

For the partial code option, the new tension anchors must meet the same demands as for the full code option. Thus, the same tension anchors will be added at 16-inches on-center. However, with no cross ties provided, the subdiaphragm is now 20-feet by 120-feet. Performing the calculations similar to the full code method results in a subdiaphragm demand of 4,743 lb/ft and a demand-to-capacity ratio of 3.2. Similarly, the subdiaphragm chord force is 142 kips, if a chord were required. Figure 2-3 illustrates the full code and partial code results.

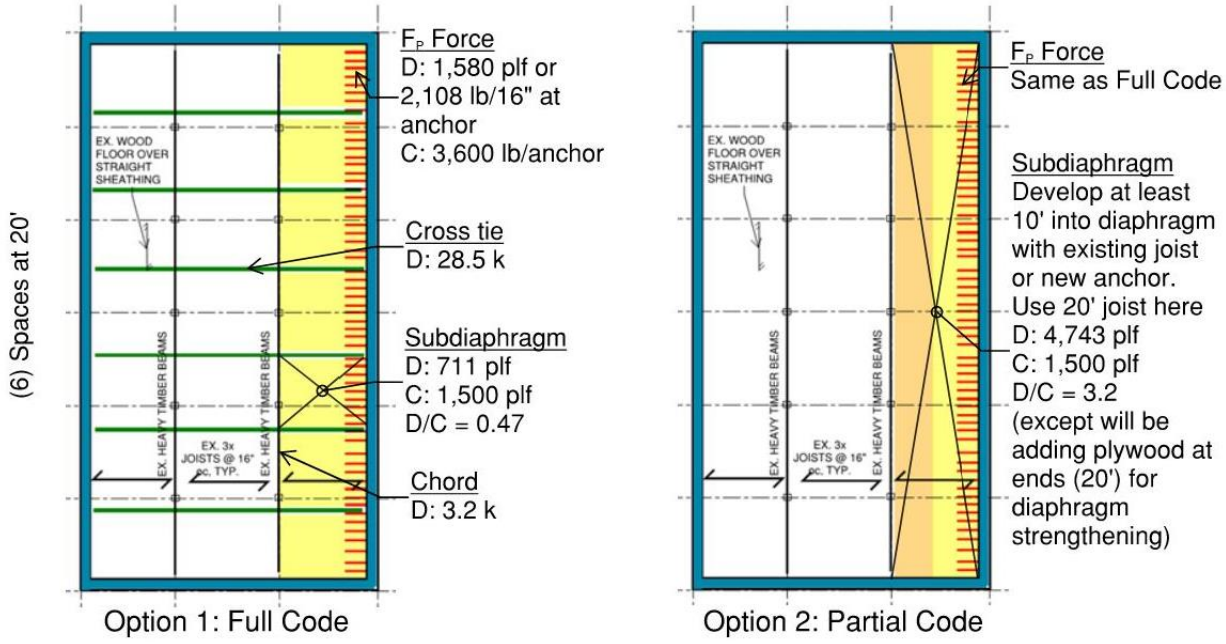

Figure 2-3 Subdiaphragm calculations in transverse direction.

For the longitudinal direction, similar full code and partial code calculations were performed. However, the short walls were assumed to be pierced by two windows per 20-foot bay with 3-foot wide piers and 5-foot tall spandrels. The wall weight and anchorage forces are calculated below.

W = (170 psf)[(5 ft high at spandrel)(7 ft spandrel width)(2 spandrels) + (12 ft story height)(3 ft pier)(2 piers)]/(20 ft)

= 1,207 lb/ft

$f_p = 0.9S_{XS}W = 0.9(0.861)(1{,}207 \text{ lb/ft})$

= 935 lb/ft > 200 lb/ft

Tension anchors will be added at 36-inches on-center, resulting in a demand of 2,805 lb per anchor, which is less than the nominal capacity of 3,600 lb per anchor.

Figure 2-4 shows the full code and partial code options for the longitudinal direction of the case study building. The full code option includes wall ties for the out-of-plane force connecting to 20-feet by 8'-4" subdiaphragms with cross ties at the existing heavy timber girders and joists acting as the subdiaphragm chord. The subdiaphragm aspect ratio is 2.4:1. The partial code option includes wall ties for the out-of-plane forces and, for the initial pass, a minimum 10-foot development into the diaphragm.

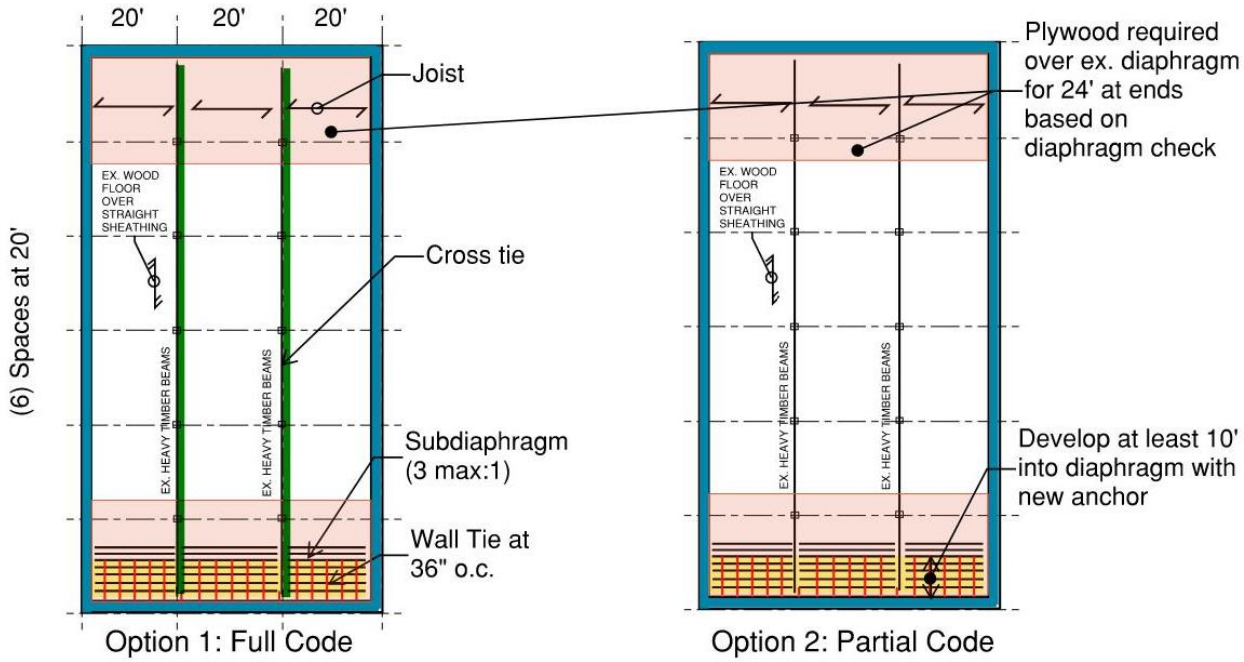

Figure 2-4 Subdiaphragm options in longitudinal direction.

For the full code option, the shear stresses in the subdiaphragm are calculated below.

Demand = (935 lb/ft)(20 ft)(0.5)/(8.33 ft)

= 1,122 lb/ft

The diaphragm capacity is calculated using a rational approach consisting of the existing floor diaphragm value from ASCE/SEI 41-17 Table 16-3 (1,500 lb/ft) plus the expected capacity of the new plywood overlay (as the new overlay will occur at the end subdiaphragms). Per ASCE/SEI 41-17 Section 12.3.2.2, the expected capacity is 1.5 times the Load and Resistance Factor Design (LRFD) procedures from the *ANSI/AWC SDPWS-2015* (AWC 2015) with φ factor equal to 1.0.

Capacity = 1,500 lb/ft + 1.5(600 lb/ft)

= 2,400 lb/ft

D/C = Demand/Capacity = 0.47

Chord forces that must be developed along the joist line at the end of the subdiaphragm are calculated below. Connections would need to be provided between the joists along this line in the full code approach.

Chord axial load = $f_p(L_{sub})^2/(8(b_{sub}))$

= (935 lb/ft)(20 ft)^2/(8(8.33 ft))

= 5.6 kips

Cross tie forces between the transverse walls are calculated below. A connection would need to be provided between the existing heavy timber girders for this load in the full code approach.

Cross tie demand = $f_p(L_{sub})$ = (935 ft)(20 ft)

= 18.7 kips

For the partial code option, the new tension anchors must meet the same demands as for the full code option. Thus, the same tension anchors will be added at 36-inches on-center. However, with no cross ties provided, the subdiaphragm is now 120-feet long and a 10-foot development length was chosen for the initial calculations. Performing the calculations similar to the full code method results in a subdiaphragm demand of 2,805 lb/ft and a demand-to-capacity ratio of 1.2. Similarly, the subdiaphragm chord force is 42.1 kips, if a chord were required. Figure 2-5 illustrates the full code and partial code results.

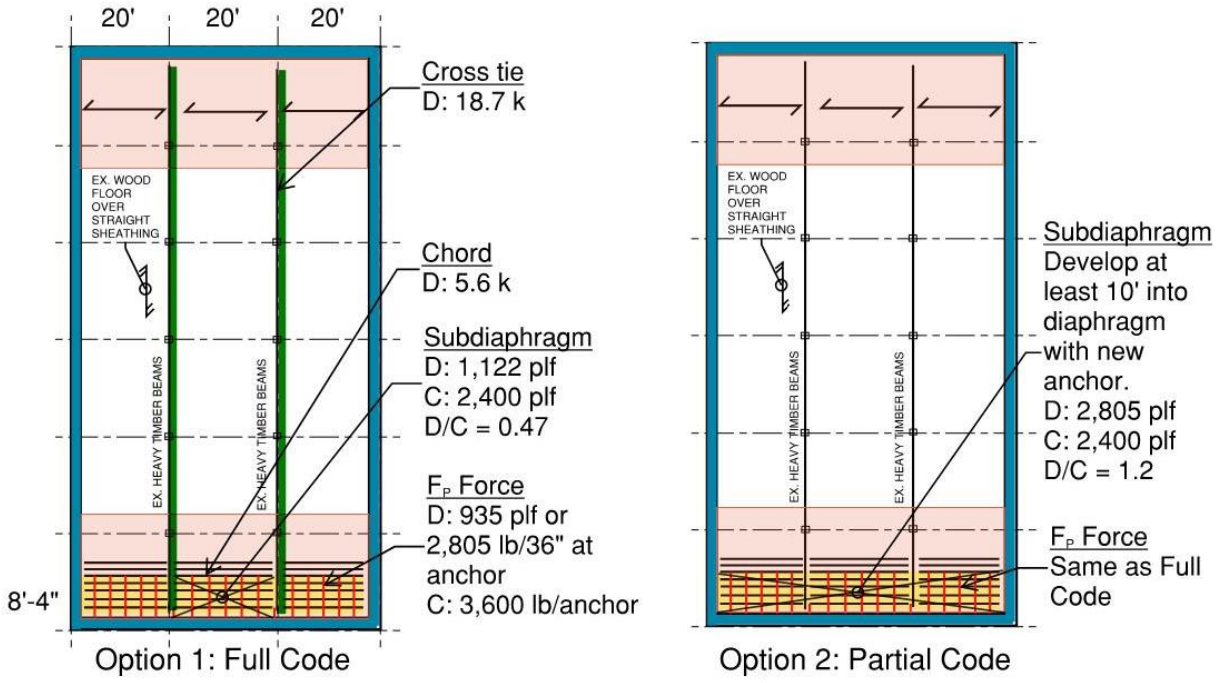

Figure 2-5 Subdiaphragm calculations in longitudinal direction.

While the partial code approach results in a potentially large chord force, if a chord were required, using the traditional subdiaphragm approach, it ignores the redundancy inherent in wood diaphragm connections. Wood diaphragms are connected to each joist and, depending on the number and type of layers, to multiple wood pieces, many of which are continuous across any given joint. Further studies were warranted to look at the actual strength and connectivity of the diaphragm.

2.3.2 Diaphragm Capacity Studies

For the partial code option, subdiaphragm chords and cross ties are not provided. However, the diaphragm is still continuous across the subdiaphragm boundary and could develop the forces beyond the length of the anchorage development. An alternative path for developing the anchorage forces using free-body diagrams of the diaphragm framing was evaluated. The different diaphragm types considered were for wood flooring over straight sheathing, wood flooring over diagonal sheathing, plywood over straight sheathing, straight sheathing, and single diagonal sheathing.

2.3.2.1 WOOD FLOORING OVER STRAIGHT SHEATHING

Wood flooring over straight sheathing consists of straight sheathing laid perpendicular to the joists and a second layer of either straight sheathing or wood flooring laid with joints offset to the first layer. For the purposes of this study, ¾-inch wood flooring laid perpendicular to the bottom layer of sheathing with 8d common nails was assumed. The 8d nails are toe nailed. The bottom layer consists of 1x6 sheathing with 10d common nails to the joists.

In the transverse direction, the wood flooring is continuous across the subdiaphragm boundary. Using this wood flooring to act as cross ties, the worst-case condition would be where a board is spliced at the subdiaphragm boundary. If three 1x4 boards per foot cross the main girder, and each has nails at 6-inches on-center toenailed into the floor sheathing below, there would be six nails per foot. Figure 2-6 shows this approach.

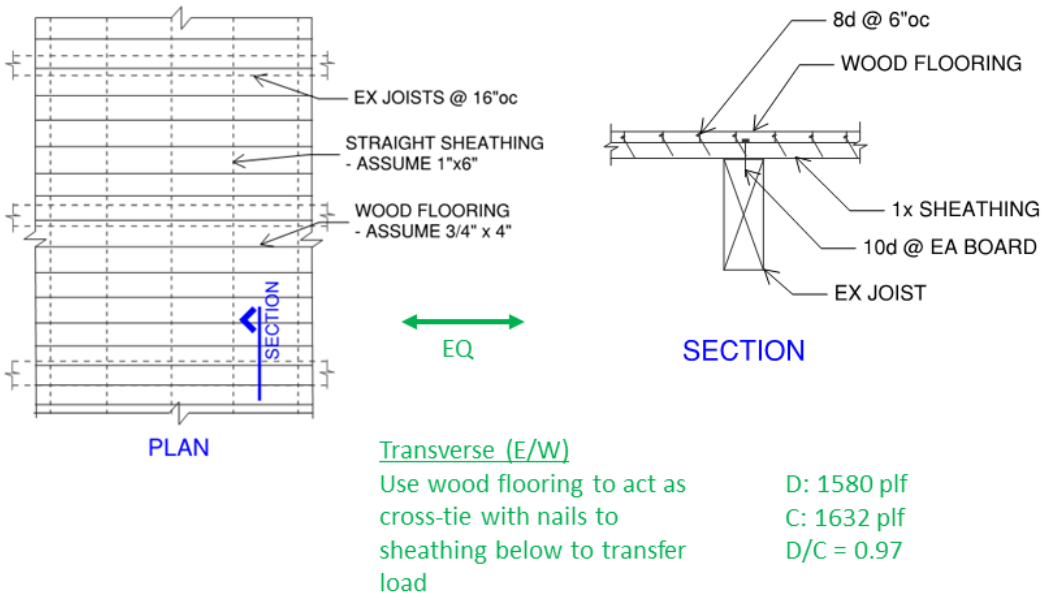

Figure 2-6 Wood flooring over straight sheathing—transverse direction.

The *National Design Specification for Wood Construction with Commentary* (NDS) (American Wood Council, 2018) was used for calculation of the lateral capacity of the nails. Wet service factor, C_M, and temperature factor, C_t, were assumed to be 1.0 as the interior of the building is conditioned and protected from water. The group action factor, C_g, and geometry factors, C_Δ, are also 1.0 as the nails are spaced far enough apart and have a diameter less than ¼-inch. Nails are not installed in the end grain, so the end grain factor, C_{eg}, equals 1.0. The diaphragm factor, C_{di}, of 1.1 is used, as is the toe-nail factor, C_{tn}, of 0.83. Douglas fir wood is assumed. The nominal capacity for one nail is:

$Z' = Z(C_M)C_tC_gC_\Delta C_{eg}C_{di}C_{tn}K_f\phi\lambda$

where:

K_f = Format Conversion Factor = 3.32 per Table 11.3.1 of the NDS

ϕ = Resistance Factor = 1.0 per ASCE/SEI 41-17 Section 12.2.2.5.1

λ = Time Effect Factor = 1.0 for load combinations with earthquake per Section N.3.3 of the NDS

Z' = 90 lb(1.0)(1.0)(1.0)(1.0)(1.0)(1.1)(0.83)(3.32)(1.0)(1.0)

= 272 lb per nail

For the six nails per foot, the total capacity is calculated as follows.

Capacity = 272 lb per nail (6 nails/ft) = 1,632 lb/ft

Demand = 1,581 lb/ft from wall anchorage calculation above

D/C = Demand/Capacity = 0.97

With a demand-to-capacity ratio of less than 1.0, the flooring can act as a continuous cross tie across the building.

In the longitudinal direction, as shown in Figure 2-7, the straight sheathing is continuous across the subdiaphragm boundary. Using this sheathing to act as cross ties, the worst-case condition would be where a board is spliced at the subdiaphragm boundary. A minimum of one nail at the end of a 1x6 board where it is spliced at the joist is assumed (a conservative assumption as two nails is more likely). The capacity of the splice is calculated similar to the nails for the transverse direction, using the NDS with similar factors. In this case, the toenail factor is 1.0, as the nail would have been driven straight down into the joist.

$Z' = Z(C_M)C_tC_gC_\Delta C_{eg}C_{di}C_{tn}K_f\phi\lambda$

where:

K_f = 3.32 per Table 11.3.1 of the NDS

ϕ = 1.0 per ASCE/SEI 41-17 Section 12.2.2.5.1

λ = 1.0 for load combinations with earthquake per Section N.3.3 of the NDS

Z' = 117 lb(1.0)(1.0)(1.0)(1.0)(1.0)(1.1)(1.0)(3.32)(1.0)(1.0)

= 428 lb per nail

Capacity = 428 lb per nail/(0.5 ft.) = 856 lb/ft

Demand = 935 lb/ft from wall anchorage calculation above

D/C = Demand/Capacity = 1.09

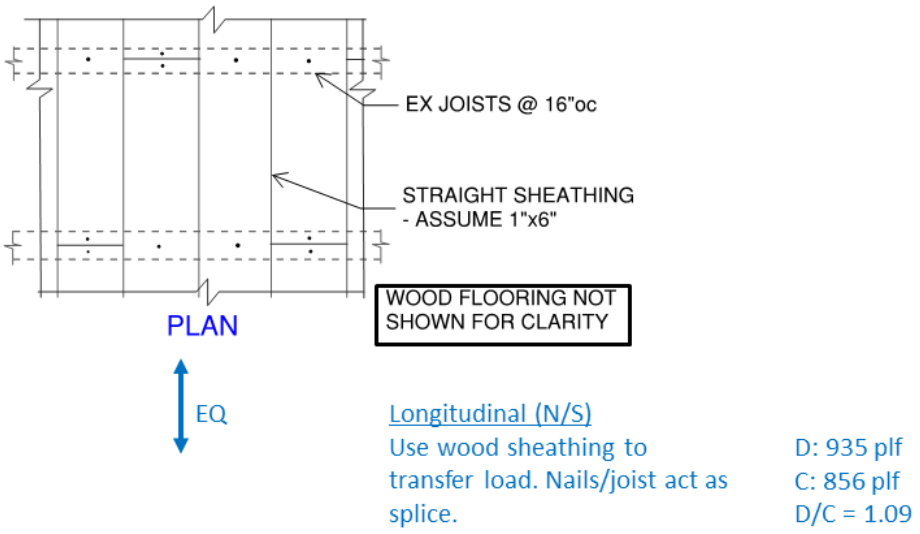

Figure 2-7 Wood flooring over straight sheathing—longitudinal direction.

The demand-to-capacity ratio of 1.09 is close to developing the wall anchorage across the diaphragm and allowing the sheathing to act as a continuous cross tie. In addition, not all the sheathing members will be spliced at the same joist, and the tension capacity of the adjacent sheathing members can compensate for the spliced members.

Using the wood flooring and straight sheathing to act as cross ties for a partial code solution appears feasible for this diaphragm type.

2.3.2.2 WOOD FLOORING OVER DIAGONAL SHEATHING

Wood flooring over diagonal sheathing consists of sheathing laid at approximately forty-five degrees to the joists and a second layer of either straight sheathing or wood flooring laid on top of the first layer. For the purposes of this study, ¾-inch wood flooring laid parallel to the joists with 8d common nails was assumed. The bottom layer consists of 1x6 sheathing at forty-five degrees to the joists with 10d common nails to the joists per Figure 2-8.

In the transverse direction, the wood flooring will behave the same as it did for the wood flooring over straight sheathing case, with the same results.

In the longitudinal direction, as shown in Figure 2-8, the diagonal sheathing is continuous across the subdiaphragm boundary. Using this sheathing to act as cross ties, the worst case condition would be where a board is spliced at the subdiaphragm boundary. A minimum of two nails at the end of a 1x6 board where it is spliced at the joist is assumed (as there is more board over the joists due to the diagonal than for straight sheathing). The capacity of the splice is calculated similar to the straight sheathing case.

$$Z' = Z(C_M)C_tC_gC_\Delta C_{eg}C_{di}C_{tn}K_f\phi\lambda$$

where:

K_f = 3.32 per Table 11.3.1 of the NDS

ϕ = 1.0 per ASCE/SEI 41-17 Section 12.2.2.5.1

λ = 1.0 for load combinations with earthquake per Section N.3.3 of the NDS

Z' = 129 lb(1.0)(1.0)(1.0)(1.0)(1.0)(1.1)(1.0)(3.32)(1.0)(1.0)

= 428 lb per nail

Capacity = (2 nails)(428 lb per nail)/(0.7 ft.) = 1,223 lb/ft

Demand = 935 lb/ft from wall anchorage calculation above

D/C = *Demand*/*Capacity* = 0.76

The demand-to-capacity ratio of 0.76 develops the wall anchorage across the diaphragm and allows the sheathing to act as a continuous cross tie. In addition, not all the sheathing members will be spliced at the same joist, and the tension capacity of the adjacent sheathing members can compensate for the spliced members.

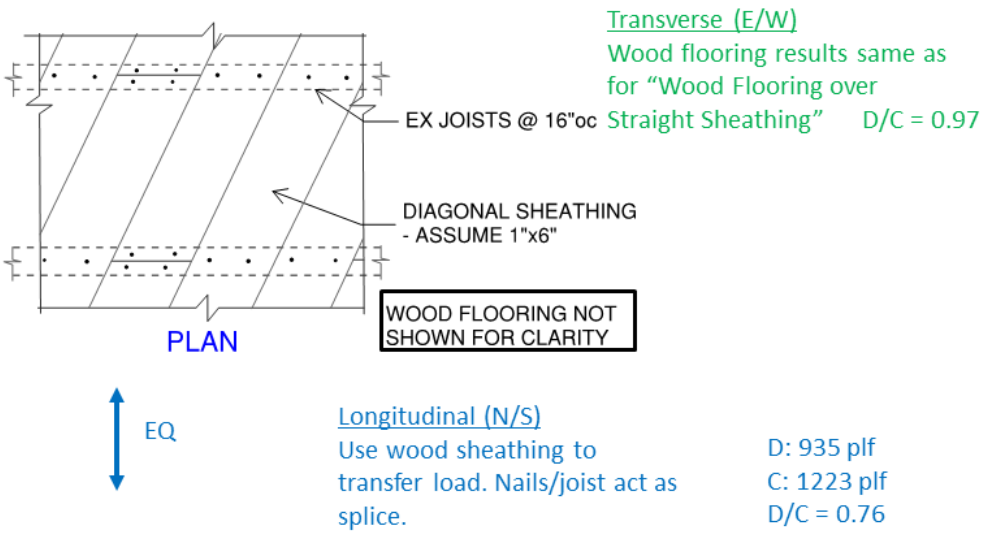

Figure 2-8 Wood flooring over diagonal sheathing.

Using the wood flooring and diagonal sheathing to act as cross ties for a partial code solution appears feasible for this diaphragm type.

2.3.2.3 PLYWOOD OVER STRAIGHT SHEATHING

Plywood over straight sheathing consists of straight sheathing laid perpendicular to the joists and a layer of plywood on top, with edges offset from the straight sheathing. For the purposes of this study, ½-inch plywood with 8d common nails at 6-inches on-center at the edges and at 12-inches on-center to the joists in the field was assumed. The bottom layer consists of 1x6 sheathing with 10d common nails to the joists. See Figure 2-9.

In the transverse direction, as shown in Figure 2-9, the plywood sheathing is continuous across the subdiaphragm boundary. Using this plywood to act as cross ties, the worst case condition would be where a sheet is spliced at the subdiaphragm boundary. The nail capacity is calculated similar to the previous cases, with the nail capacity just accounting for the embed in the main member (not in the straight sheathing).

$Z' = Z(C_M)C_tC_gC_\Delta C_{eg}C_{di}C_{tn}K_f\phi\lambda$

where:

K_f = 3.32 per Table 11.3.1 of the NDS

ϕ = 1.0 per ASCE/SEI 41-17 Section 12.2.2.5.1

λ = 1.0 for load combinations with earthquake per Section N.3.3 of the NDS

Z' = 80 lb(1.0)(1.0)(1.0)(1.0)(1.0)(1.1)(1.0)(3.32)(1.0)(1.0)

= 265 lb per nail

Capacity = 265 lb per nail(2 nails/ft) = 530 lb/ft

Demand = 1,580 lb/ft from wall anchorage calculation above

D/C = Demand/Capacity = 3.0

In the longitudinal direction, the base capacity from the straight sheathing is the same as for the wood flooring over straight sheathing case. However, the plywood capacity can be added to this value. Again, the worst case value at the plywood sheet splice is used.

Capacity = 856 lb/ft + 530 lb/ft = 1,386 lb/ft

Demand = 935 lb/ft from wall anchorage calculation above

D/C = Demand/Capacity = 0.67

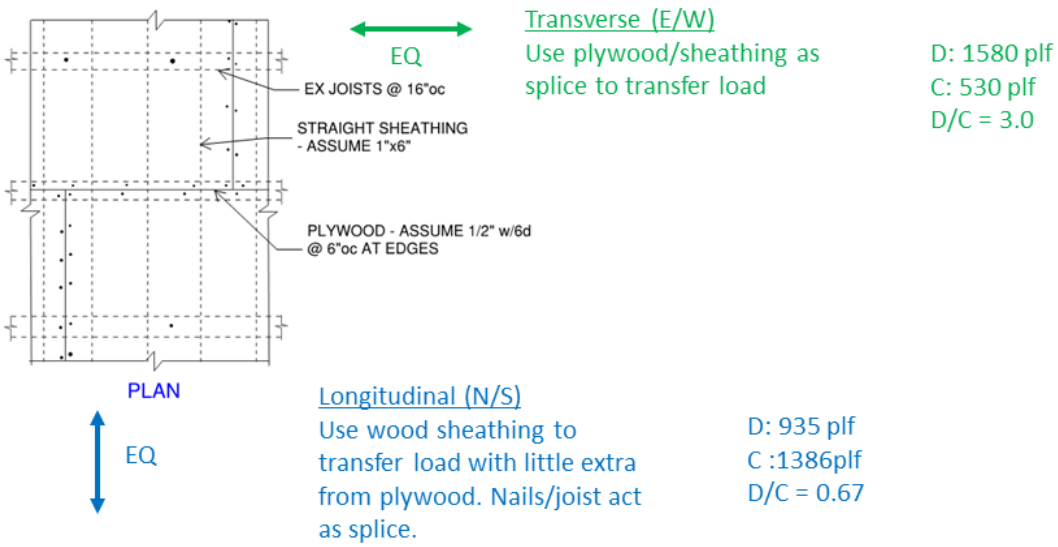

Figure 2-9 Plywood over straight sheathing.

Using the straight sheathing plus plywood to act as cross ties in the longitudinal direction for a partial code solution appears feasible for this diaphragm type. However, the plywood is overstressed in the transverse direction at the splices.

2.3.2.4 STRAIGHT SHEATHING

Straight sheathing consists of straight sheathing laid perpendicular to the joists. For the purposes of this study, 1x6 sheathing with 10d common nails to the joists was assumed.

In the transverse direction, the joists carry the load until the first grid line. However, no alternate load path to transfer the load into the joists in the next bay is obvious. Figure 2-10 shows joists sitting on top of the beam with no positive connection between the joists and no diaphragm members that can act as a splice in this direction. Even if the joists are attached by hangers to the beam, typically the hangers do not provide a consistent out-of-plane strength that could transfer the load. No alternate load path was found for this case.

In the longitudinal direction, the wood flooring will behave the same as it did for the wood flooring over straight sheathing case, with the same results.

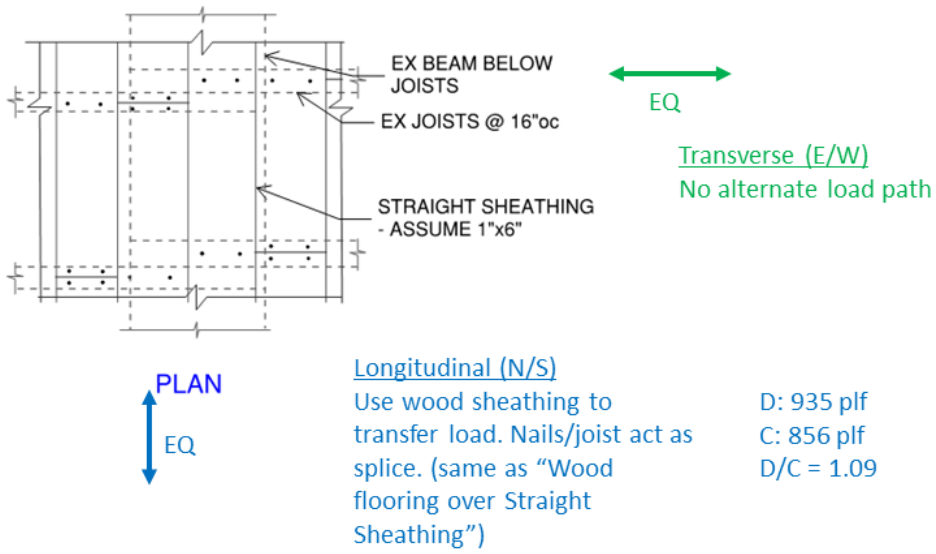

Figure 2-10 Straight sheathing.

Using straight sheathing to act as cross ties is feasible in the longitudinal direction for a partial code solution. However, there is not an alternate load path in the transverse direction for straight sheathing.

2.3.2.5 DIAGONAL SHEATHING

Diagonal sheathing consists of a single layer of sheathing laid at approximately a 45-degree angle to the joists. For the purposes of this study, 1x6 sheathing was assumed with two nails at each joist. See Figure 2-11.

In the transverse direction, a strut-and-tie model was developed and is shown in Figure 2-11 for three out-of-plane anchors. The joists transfer forces to the decking/blocking at the first interior beam line. From there, the forces are then transferred to the joists/blocking at the end walls, and then transferred to the out-of-plane anchor/chord at the walls in the perpendicular direction. This load path tends to agree with the ASCE/SEI 41-17 commentary to diagonal decking (Section C12.5.3.3.2) that indicates chords at the end walls need to be considered.

In the longitudinal direction, the wood flooring will behave the same as it did for the wood flooring over diagonal sheathing case, with the same results.

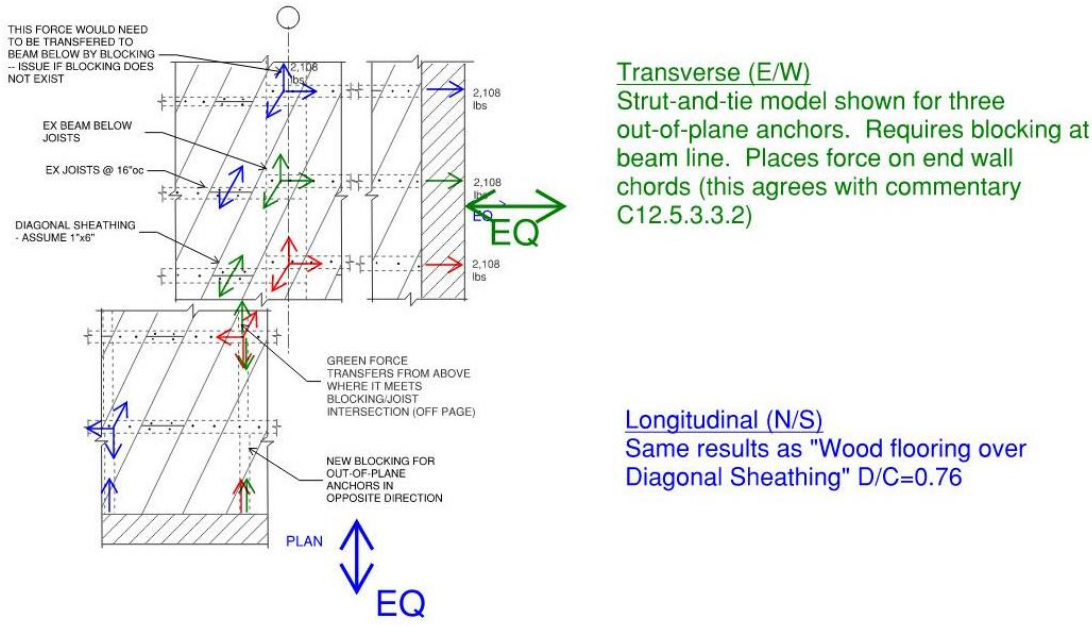

Figure 2-11 Diagonal sheathing.

Using the single diagonal sheathing to act as cross ties for a partial code solution appears feasible for this diaphragm type.

2.3.3 Parametric Study

While the case study building was helpful as a start, information was needed on different building configurations. A parametric study was performed to alter variables on the case study building but perform the same calculations. The following variables were used:

- Building size – The length and width of the building was varied based on the working group's experience. The 150-feet by 100-feet building is unusually large and not common, but has been encountered, so it was included to see the effects.

- Aspect ratios – The aspect ratio is calculated for the longitudinal direction of the building and is found by dividing the building width by the anchor development length. The transverse direction was not included as the joist length, rather than how far back the new connection extended, governed as the joists are typically much longer than the 8- to 10-feet development proposed.

- Solid walls versus walls with openings – Masonry walls may be solid, such as boundary line walls, with no openings and thus have more weight, resulting in larger anchorage forces to be developed into the diaphragm. Solid walls used in the parametric study used an 1,800 lb/ft anchorage force, equivalent to a 17-inch-thick wall with 13'-8" tributary to the diaphragm. The 13'-8" story was used for the larger building as it is more representative of the bigger size, as compared to the 12'-0" story height in the smaller case study. Masonry walls with openings are also encountered, especially along the main street-facing side. Walls with openings were also

considered in the parametric study with an anchorage force of 1,000 lb/ft (rounding up the 935 lb/ft from the case study in the longitudinal direction).

- Diaphragm capacity – Initially two-layers of straight sheathing with offset edges or laid perpendicular was studied (with a capacity of 1,500 lb/ft from Table 16-3 of ASCE/SEI 41-17). Where the diaphragm capacity and span did not meet the requirements of Figure 16-1 of ASCE/SEI 41-17 Chapter 16, the diaphragm was strengthened with a layer of plywood (resulting in a 2,400 lb/ft. capacity). In addition, single diagonal sheathing was studied, with a capacity of 750 lb/ft from Table 16-3 of ASCE/SEI 41-17. Straight sheathing was not studied as no alternate load path was found in the diaphragm studies as discussed above.

- Development length – Initially an anchor development length of 10-feet was considered. After seeing the initial, promising results, a length of 8-feet was also evaluated. The 8-feet length would permit renovations in buildings with smaller, perimeter rooms to keep the work within the room, thus making the provisions more likely to be used.

The above variables were used to calculate the shear demand-to-capacity ratio of the diaphragm, similar to the case study calculations. The chord forces were also calculated similarly. Results are shown in Table 2-2 for the 10-foot anchor development length and in Table 2-3 for the 8-foot anchor development length.

As an example, for the 10-foot anchor development length for the 60-foot by 30-foot building with openings in the wall, the calculations were as follows:

v = subdiaphragm shear = $F(L)/(2w)$

= 1,500 lb/ft

where:

F = anchor force = 1,000 lb/ft

L = subdiaphragm length (in this case, the building width) = 30 ft

w = anchor development length = 10 ft

Capacity = 1,500 lb/ft for the diaphragm, as double-sheathing meets ASCE/SEI 41-17 Figure 16-1 for a building this size and diaphragm strengthening was not required

Shear D/C = Demand/Capacity = v/*Capacity*

= (1,500 lb/ft)(1,500 lb/ft) = 1.0

Chord = $F(L^2)/(8w)$ = (1,000 lb/ft)(30 ft)^2/((8)(10 ft)) = 11. kips

Table 2-2 Partial Code Parametric Study—10-foot Anchor Development

anchor development length, w = 10 ft

Diaphragm capacity

single diagonal sheathing = 750 plf

2-layers straight sheathing w/ offset edges or perpendicular = 1500 plf

2-layers sheathing with plywood = 2400 plf

							unusually large bldg.		single diagonal-sheathed			
Building	60'x30'	60'x30'	60'x60'	60'x60'	120'x60'	120'x60'	150'x100'	150'x100'	60'x30'	60'x30'	60'x60'	60'x60'
Building length (ft)	60	60	60	60	120	120	150	150	60	60	60	60
Building width/subdiaphragm Length, L (ft)	30	30	60	60	60	60	100	100	30	30	60	60
Subdiaphragm Aspect Ratio	3:1	3:1	6:1	6:1	6:1	6:1	10:1	10:1	3:1	3:1	6:1	6:1
Openings in wall or solid?	openings	solid	openings	solid	openings	solid	openings	solid	openings	solid	openings	solid
Diaphragm strengthened? (Y/N)	No	No	No	No	Yes	Yes	Yes	Yes	No	No	No	No
Diaphragm capacity (plf)	1500	1500	1500	1500	2400	2400	2400	2400	750	750	750	750
Anchor force, F (plf)	1000	1800	1000	1800	935	1580	1000	1800	1000	1800	1000	1800
Subdiaphragm shear (plf) v=F*L/(2*w)	1500	2700	3000	5400	2805	4740	5000	9000	1500	2700	3000	5400
shear D/C =v/capacity	**1.00**	**1.80**	**2.00**	**3.60**	**1.17**	**1.98**	**2.08**	**3.75**	**2.00**	**3.60**	**4.00**	**7.20**
Chord (kips) $=F*L^2/(8*w)$	11	20	45	81	42	71	125	225	11	20	45	81

Table 2-3 Partial Code Parametric Study—8-foot Anchor Development

anchor development length, w = 8 ft

Diaphragm capacity

single diagonal sheathing = 750 plf

2-layers straight sheathing w/ offset edges or perpendicular = 1500 plf

2-layers sheathing with plywood = 2400 plf

							unusually large bldg.		single diagonal-sheathed			
Building	60'x30'	60'x30'	60'x60'	60'x60'	120'x60'	120'x60'	150'x100'	150'x100'	60'x30'	60'x30'	60'x60'	60'x60'
Building length (ft)	60	60	60	60	120	120	150	150	60	60	60	60
Building width/subdiaphragm Length, L (ft)	30	30	60	60	60	60	100	100	30	30	60	60
Subdiaphragm Aspect Ratio	3.75:1	3.75:1	7.5:1	7.5:1	7.5:1	7.5:1	12.5:1	12.5:1	3.75:1	3.75:1	7.5:1	7.5:1
Openings in wall or solid?	openings	solid	openings	solid	openings	solid	openings	solid	openings	solid	openings	solid
Diaphragm strengthened? (Y/N)	No	No	No	No	Yes	Yes	Yes	Yes	No	No	No	No
Diaphragm capacity (plf)	1500	1500	1500	1500	2400	2400	2400	2400	750	750	750	750
Anchor force, F (plf)	1000	1800	1000	1800	935	1580	1000	1800	1000	1800	1000	1800
Subdiaphragm shear (plf) v=F*L/(2*w)	1875	3375	3750	6750	3506.25	5925	6250	11250	1875	3375	3750	6750
shear D/C =v/capacity	**1.25**	**2.25**	**2.50**	**4.50**	**1.46**	**2.47**	**2.60**	**4.69**	**2.50**	**4.50**	**5.00**	**9.00**
Chord (kips) $=F*L^2/(8*w)$	14	25	56	101	53	89	156	281	14	25	56	101

A number of observations were made based on these results:

- For typical buildings (120-feet by 60-feet maximum) and not single sheathed, a 10-foot development length resulted in DCRs in the 1 to 2 range. Only a solid 17-inch wall with 60-foot span and no diaphragm strengthening had a DCR above 2.
- Similar results were found for the 8-foot development length, except the DCR range was 1.25 to 2.5.
- Single diagonal sheathing had large DCRs, even for smaller buildings, ranging from 2 to 9.
- For the unusually large building, DCRs are approximately 88% higher than the typical buildings if it has solid walls.

2.3.4 Conclusions

Based on the above studies, the existing wood diaphragms, except for single straight sheathing, meet the anchorage development even at their weakest point (the splices). Combined with the maximum DCRs if the end of the development line did act as a chord, permitting the omission of

specific chords or cross ties at the stronger wood diaphragms appears reasonable. At unusually large buildings, the engineer should consider adding chords and cross ties at solid walls. At single straight sheathed diaphragms, chords and cross ties should still be required, unless plywood sheathing is added to compensate for the lack of connectivity.

2.4 Recommended Changes

Note about Change Proposals

This report documents aspects of change proposals as they were submitted to subcommittees of ASCE's *Seismic Retrofit of Existing Building Standards* Committee. Often, these change proposals were revised, in some cases substantively, by these subcommittees before they were adopted into ASCE/SEI 41-23. Readers should not rely on this report for information about the final version of provisions in ASCE/SEI 41-23.

Based on the above studies, the following strikeout/underline proposed changes to ASCE/SEI 41-23 Sections 16.2.4.3 and C16.4.2.3 shown below were proposed to the ASCE 41 Standards Committee for their consideration. In addition to an expanded commentary, the changes primarily include a new list of building types that are explicitly permitted to use linear procedures and thus exempt from the requirement to determine the application of the limitations described in this section. New or modified text is shown in blue.

The following text is added after the current text in Section 16.2.4.3:

16.2.4.3.1 *Transfer of Anchorage Forces into Diaphragm*

The wall anchorage force in this section shall be fully developed into the diaphragm when S_{X1} exceeds 0.2. If subdiaphragms are used, each subdiaphragm shall be capable of transmitting the shear forces caused by wall anchorage to a continuous diaphragm tie. Subdiaphragms shall have length-to-depth ratios not exceeding 3:1.

Alternatively, wood diaphragms consisting of

- diagonal sheathing overlaid with straight sheathing, finished wood flooring, or wood structural panel sheathing,
- double straight sheathing (with board edges offset or perpendicular),
- straight sheathing overlaid with wood structural panel sheathing (with panel edges offset),
- wood structural panel sheathing, OR
- nail-laminated timber

shall be permitted to develop the wall anchorage as follows, but subdiaphragm analysis, cross ties, and chords are not required:

(1) For joists parallel to the masonry walls, develop the anchorage a minimum of 8-feet into the diaphragm.

(2) For joists perpendicular to the masonry walls, attaching anchors to joists is considered sufficient development. However, if joists are shorter than 8-feet OR if attaching between joists, develop wall anchorage into the diaphragm similar to joists parallel to the masonry walls.

The proposal allows for subdiaphragms, similar to ASCE/SEI 41-17 Chapter 7. In addition, an alternate is permitted for specific diaphragm types that contain redundancy based on the subdiaphragm studies. While a study for nail-laminated timber (NLT) was not shown, given the number and size of the typical spikes connecting the boards, along with the staggered nature of the splices, it is expected to behave in a ductile manner and was thus included. The 8-foot anchor development length from the parametric studies was chosen for the alternate, as the results were similar to 10-feet. Anchoring directly to the joists is encouraged, as it could result in more than 8-feet of development if the joists are longer. However, if the joists are shorter than 8-feet, perhaps due to old, infilled openings or due to a short bay on a diagonal lot edge, the development must still reach at least 8-feet with the alternate.

Currently, ASCE/SEI 41-17 does not contain commentary on wall anchorage. New commentary is proposed to describe the concern, describe the appropriate load path for out-of-plane forces, and explain why the alternate, less-restrictive solution is desired and its basis. Also, commentary recommending cross ties (even if not required) and explaining the basis for the S_{X1} greater than 0.2 limit are added. The following commentary is proposed:

C16.2.4.3 Transfer of Anchorage Forces into Diaphragm

Masonry walls that are not positively anchored to the diaphragms may separate from the structure, leading to a significant falling hazard. If the walls are bearing walls, this separation may also lead to partial collapse of the floors and roof. Adding an anchor from the wall to the diaphragm corrects a portion of the load path, but if the anchor-to-diaphragm connection is not developed far enough into the diaphragm, the diaphragm may fail just beyond the end of the anchor-to-diaphragm connection. Out-of-plane wall failures have occurred where the retrofitted wall anchor and a joist running parallel to the wall pulled away from the diaphragm with the masonry wall because there was insufficient tension capacity in the diaphragm. To show that the out-of-plane force is developed into the diaphragm, the engineer must be able to draw a free-body diagram demonstrating the transfer of anchorage forces from one element to another and demonstrate that each load path element has adequate capacity. One example is transfer from the anchor bolt to a strap, into blocking, and from there into the diaphragm as shown in Figure C16-XXXX. A common assumption is a linear force transfer from the blocking into the diaphragm when checking the blocking length is adequate for the diaphragm capacity.

Section 7.2.11.1 requires the anchorage force to be fully developed into the diaphragm, using subdiaphragms if necessary. As stated in Section C16.2.1, the unreinforced masonry special procedure is intended to reduce risk but at a Limited Performance Objective. Full subdiaphragm analysis with cross ties and chords is not required in the special procedure for the specified wood

diaphragms to increase the likelihood of renovations and because these wood diaphragms are typically stronger. Reasonable development lengths into the diaphragm were developed based on parametric studies [FEMA P-2208]. Single, straight-sheathed diaphragms and single, diagonal-sheathed diaphragms and systems other than those specified were not exempted from the subdiaphragm check because they lack the redundancy and extra strength of the specified wood diaphragms, particularly in the direction perpendicular to the board lay-up. Nail-laminated timber diaphragms consist of dimensional lumber on edge with boards flush next to each other and nails connecting the laminations. Nail-laminated timber diaphragms were historically built in-place, with long, heavy nails passing through multiple boards and typically with sheathing, finish wood floor, or plywood overlay. Nail-laminated timber diaphragms have performed similar to diagonal sheathing with an overlay during seismic events.

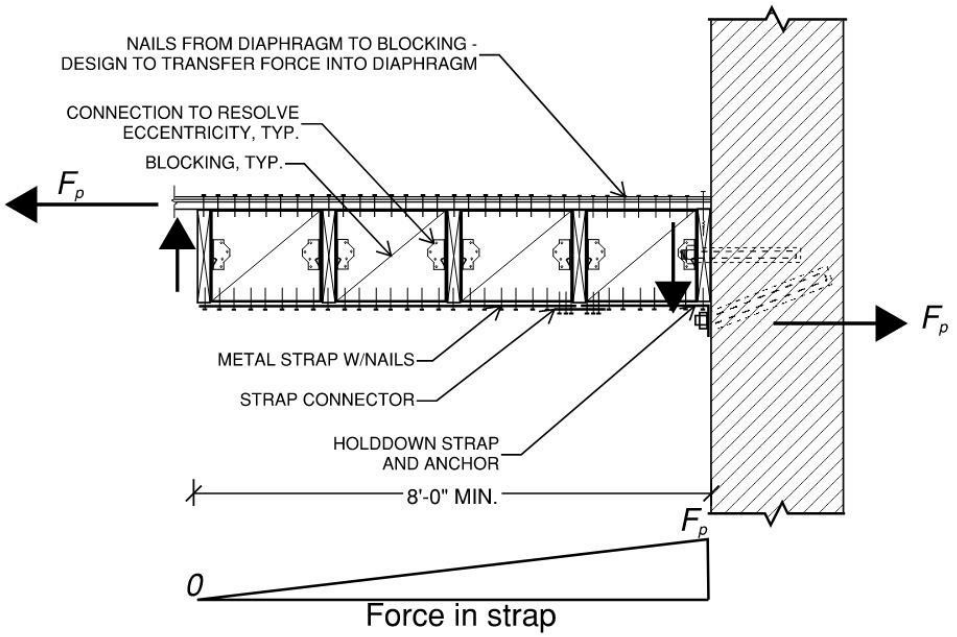

Figure C16-XXXX Out-of Plane Force Transfer from Wall to Diaphragm

While cross ties are not required in the special procedure, adding them will improve the building performance. If adding cross ties is not possible, attaching the walls to longer elements that extend into the diaphragm, such as girders or cross wall top plates that are perpendicular to the walls, will increase the building performance.

Only buildings where S_{x1} is greater than 0.2 are required to develop the anchorage to exempt low-risk locations. The 0.2 limit was chosen to match the diaphragm evaluation limit in Section 16.2.3.2.2.

2.5 References

ASCE, 2017, *Seismic Evaluation and Retrofit of Existing Buildings*, ASCE/SEI 41-17, Structural Engineering Institute of American Society of Civil Engineers, Reston, Virginia.

AWC, 2015, *Special Design Provisions for Wind & Seismic with Commentary, 2015 Edition*, ANSI/AWC SDPWS-2015, American Wood Council, Leeburg, Virginia.

AWC, 2018, *National Design Specification for Wood Construction*, ANSI/AWC NDS-2018, American Wood Council, Leeburg, Virginia.

FEMA, 2018, *Example Application Guide for ASCE/SEI 41-13 Seismic Evaluation and Retrofit of Existing Buildings with Additional Commentary for ASCE/SEI 41-17*, FEMA P-2006 Report, prepared by the Applied Technology Council for the Federal Emergency Management Agency, Washington, D.C.

ICC, 2015, *Acceptance Criteria for Anchors in Unreinforced Masonry Elements*, ICC-Evaluation Service AC 60, International Code Council.

ICC, 2019, *2018 International Building Code*, International Code Council, Country Club Hills, Illinois, Second Printing, January.

Chapter 3: Revisions to Chapter 16 URM Wall Out-of-Plane Provisions

3.1 Motivation

Slender unreinforced masonry bearing walls with large height-to-thickness (*h/t*) ratios have a potential for damage caused by out-of-plane forces that may result in falling hazards and potential localized collapse of the structure. The original table limiting *h/t* ratios was based on research by ABK researchers (ABK et al., 1981a, 1981b) and has been used since the late 1980s to assess the stability of URM walls. More recent research has led to the development of an equation-based check for URM out-of-plane stability, which is the method used in ASCE/SEI 41-17 Chapter 11 for the Life Safety Structural Performance Level and discussed in the ASCE/SEI 41-17 Chapter 11 commentary. This evaluation is based on the procedure proposed by Penner and Elwood (2016b) and includes factors for load on the wall, wall thickness, and diaphragm type as well as *h/t*. Evaluation of the Penner and Elwood (2016a,b) research shows that the *h/t* ratios in ASCE/SEI 41-17 Chapter 16 Table 16-6 are unconservative for S_{D1} values over 0.40g. The goal of the proposal is to incorporate the Penner and Elwood (2016b) findings into an update of ASCE/SEI 41-17 Table 16-6.

3.2 Summary of Changes Recommended

The changes occur in ASCE/SEI 41-23 Section 16.2.4.2 and Commentary Section C16.2.4.2 that define requirements for out-of-plane wall stability in URM buildings. They add two columns to ASCE/SEI 41-17 Table 16-6 for allowable *h/t* ratios for values of S_{D1} over 0.40g: one for $0.50g \leq S_{D1} < 0.60g$ and one for $0.60g \leq S_{D1}$. An option is added such that the procedure in ASCE/SEI 41-17 Section 11.3.3.3.2 can be used for a more accurate, but more involved, determination of allowable *h/t* ratios.

3.3 Technical Studies

The current ASCE/SEI 41-17 Chapter 16 provisions for out-of-plane unreinforced masonry walls require evaluation for values of S_{D1} that exceed 0.133g per ASCE/SEI 41-17 Table 16-6. The evaluation is based on a simple *h/t* ratio, the location of the wall within a building, the seismic acceleration at one second, and, for higher seismicity cases, the diaphragm behavior. Walls located at the top story of a multi-story building have more restrictive ratios as the deformations are amplified at the top of the building plus there is less confining weight, while walls at the ground story have less restrictive ratios due to the rigidity of the base condition plus additional wall weight above providing confinement; walls in between the ground story and top story have in-between *h/t* limits. Walls of one-story buildings have limits similar to the in-between walls, rather than the ground story walls, because there is less weight above providing confinement, though there is the more rigid base condition.

For areas where S_{D1} exceeds 0.4g, the *h/t* ratios are typically more restrictive than lower spectral accelerations. However, these *h/t* ratios may be relaxed if the following conditions are met: the diaphragm is acceptable per ASCE/SEI 41-17 Figure 16-1, the masonry has high shear capacity, there is good mortar coverage of the collar joints, and the building also meets one of the following criteria:

- Has long spans with cross walls in all stories (Region 1 of ASCE/SEI 41-17 Figure 16-1)
- Has short spans and high diaphragm demand-to-capacity ratios (Region 2 of ASCE/SEI 41-17 Figure 16-1)

Values of S_{D1} greater than 0.4g are treated the same. However, as the understanding of seismicity has advanced over the years, large areas along the West Coast, including in major cities, now have S_{D1} values in the 0.50g to 0.70g range for the BSE-1E level.

3.3.1 Penner and Elwood Studies and Method

The ABK method does not account for many other factors, such as wall thickness, increased weight on walls, etc. Also, additional research on walls has been performed since the 1980s study. Penner and Elwood (2016a) performed additional shake table testing, as have others. Penner and Elwood then developed computer modeling calibrated to meet their testing results. With this computer model, a parametric study was performed with over 200,000 parametric runs (Penner and Elwood 2016b). Parameters varied included diaphragm periods, wall thickness, *h/t* ratios, diaphragm damping, diaphragm mass ratios, and axial load. Multiple ground motions per FEMA P695 (FEMA, 2009) were used.

One finding from the study is concerning the use of S_{X1} as the ground motion parameter to use. The distribution of spectral values versus period was evaluated for the reference configuration in Figure 3-1 (Figure 4 of Penner and Elwood, 2016b). The distribution narrows at a period of 1-second. Figure 3-2 (Figure 5 of Penner and Elwood 2016b) shows the coefficient of variation for various periods, *T*. In the 0.75g to 1.25g range, there are sharp minimums and less variance at small intensities. S_{X1} is therefore a logical choice to use, resulting in lower variance and being a number used regularly by design professionals.

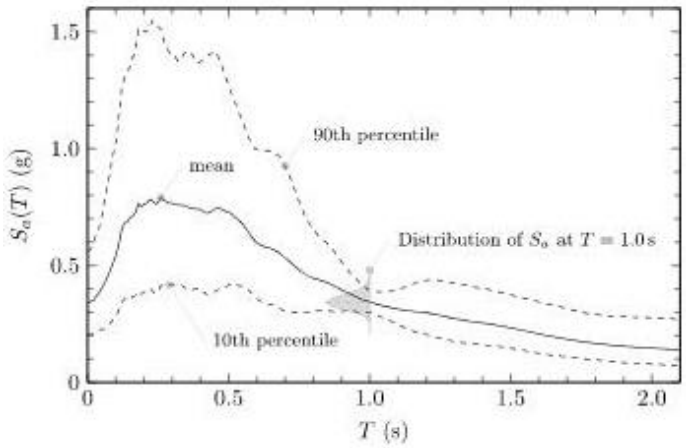

Figure 3-1 S_a at collapse for Penner and Elwood reference configuration (Penner and Elwood, 2016b, Figure 4).

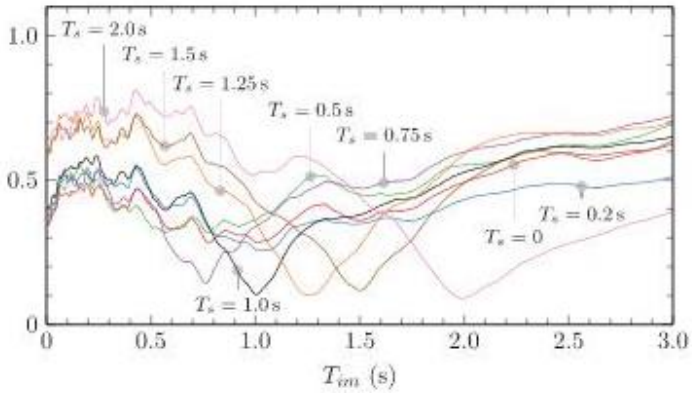

Figure 3-2 Coefficient of variation for varying period, T_{im}, at which the intensity measure, S_a, is evaluated for varying wall-diaphragm system period, T_s (Penner and Elwood, 2016b, Figure 5).

Based on these studies, an equation for checking wall *h/t* ratios was developed. Variables included the following:

- Diaphragm stiffness—either flexible (T_s>0.5-s) or stiff (T_s <0.2-s)
- Height-to-thickness ratio, *h/t*
- Axial load
- An adjustment factor for thin walls that are less than about 13-inches thick
- An adjustment factor for ground story walls as the base connection is more rigid with less movement than a diaphragm

- A correction factor for "exposure level." This factor is based on the probability of collapse calculated from the parametric studies. The recommendations are shown in Table 3-1.

Table 3-1 Exposure Factor, C_e, from Penner and Elwood (2016b)

Exposure	Probability of Collapse	C_e, Stiff Diaphragm	C_e, Flexible Diaphragm
Very high	5%	0.9	0.9
High	10%	1.0	1.0
Low	20%	1.15	1.1
Very low	50%	1.5	1.25

The proposed method results in more stringent requirements for flexible diaphragms than the current ASCE/SEI 41-17 Table 16-6 or Table 11-5 method. For stiff diaphragms, the results are similar to the current tables. The procedure did err on the conservative side, especially for flexible diaphragms.

The method did not include other parameters than can affect the out-of-plane stability of the walls, and the paper recommends further study for the following: diaphragm displacements, response along the diaphragm (more deflection expected at the middle of the diaphragm than at the ends), two-way bending, amplification up the building height, arching action, masonry strength, damping and nonlinearity, in-plane damage, and vertical acceleration.

3.3.2 ASCE/SEI 41-17 Chapter 11 Updates for Life Safety

ASCE/SEI 41-17 Chapter 11 updated the out-of-plane stability for the Life Safety Structural Performance Level based on the Penner and Elwood method, though Collapse Prevention continued to use the table of *h/t* ratio limits developed using the ABK method. The following equation is used for checking the out-of-plane stability for walls with *h/t* ratios greater than 8:

$$S_{X1} \le C_a C_t C_g C_{pl} S_{aDIAPH}(1) \qquad \text{(ASCE/SEI 41-17 11-27a)}$$

where:

$$S_{aDIAPH}(1) = \begin{cases} \dfrac{4}{h/t} & \text{for stiff diaphragms} \\ \dfrac{1.8}{(h/t)^{0.75}} & \text{for flexible diaphragms} \end{cases} \qquad \text{(ASCE/SEI 41-17 11-27b)}$$

C_a = axial load factor

$$= \begin{cases} 1 + C_a'\left(P_D / 685\right)\left(1 - \frac{1}{12}\left(\frac{h}{t} - 8\right)\right) & \text{for } 8 \le h/t \le 20 \\ 1 & \text{for } h/t > 20 \end{cases} \qquad \text{(ASCE/SEI 41-17 11-27c)}$$

C_a' = *0.5 for stiff diaphragms and 0.2 for flexible diaphragms (interpolate as needed)*

P_D = *vertical load on the wall in lb/ft*

C_t = *Modification factor for thin walls = 0.2 + t/15.7 <= 1.0*

t = *wall thickness in inches*

C_g = *Modification factor for ground level walls (1.0 if not at ground level)*

= *1.0 for stiff diaphragms and 1.1 for flexible diaphragms (interpolate as needed)*

C_{pl} = *Modification factor for performance level = 0.9 for Life Safety*

The "exposure factor" from Penner and Elwood (2016b) was renamed to a performance level factor, C_{pl}, and tied to the performance level. For ASCE/SEI 41-17, a Life Safety Structural Performance Level factor of 0.9 was chosen, corresponding to a 5% probability of collapse. Factors for other performance levels are not listed as it is not required for the Collapse Prevention Structural Performance Level (ASCE/SEI 41-17 Table 11-5 is still used) and the Damage Control and Limited Safety Structural Performance Levels were neglected.

One change ASCE/SEI 41-17 made from the Penner and Elwood method is the coefficient for flexible diaphragms was switched from 1.5 to 1.8—an increase of about 20%. Penner and Elwood assumed 5% damping of the diaphragms, but wood diaphragms typically have a higher level of damping, which led to the ASCE/SEI 41-17 increase. Using ASCE/SEI 41-17 Equation 2-3 and assuming 10% damping, β, provides the following results.

$B_{1,10\%}$ = 4/[5.6-ln(100β)]

= 4/[5.6-ln(100(0.10))]

= 1.21

Similarly, B_1 for 5% damping is 1.0. Therefore, slightly less than 10% damping would result in a 20% increase. The study below continues to use the 1.8 factor for increased damping from the wood diaphragm.

3.3.3 Parametric Study

Using ASCE/SEI 41-17 Equation 11-27, a parametric study was conducted to compare various URM wall configurations in out-of-plane behavior to the current Chapter 16 limits. As ASCE/SEI 41-17

Section 16.2 is limited to flexible diaphragms, stiff diaphragms were not considered in the study. The following parameters were varied:

- Wall thickness, *t*: The study used 13-inch and 17-inch walls as these sizes are commonly encountered for multi-story buildings (thinner walls being inadequate). The wall thickness also impacted the axial load and the C_a factor (see below). Using these thicknesses meant C_t=1.0 as this factor is only triggered if wall thickness is less than 13-inches. A 9-inch wall thickness was used for the one-story buildings, where it might potentially be encountered, and those calculations do include the C_t factor per ASCE/SEI 41-17 Equation 11-27d.

- Axial load, C_a, ASCE/SEI 41-17 Equation 11-27c: The axial load is primarily from the masonry wall weight above the floor under consideration. For the "All Other Walls" case, the weight at the 2nd floor wall was used, and the study varied the number of stories above to observe the effects. In other words, a four-story building will have more wall and floor weight above than a three-story building on the 2nd floor or ground floor. The floor weight on a wall is small as the maximum load is one-half of a bay of wood-framed floor, so it was neglected for the "All Other Walls" and the "First Story of a Multi-story Building" cases. For the "Top Story of a Multi-story Building" and "One-story Building" cases, a floor/roof load assuming 30 lb/ft^2 of dead load and the tributary width indicated in the figure legend was added to the wall weight.

- Location of the wall in the building: These match the existing ASCE/SEI 41-17 Table 16-6 cases: top story of a multi-story building, first story of a multi-story building, all other walls in multi-story building, and walls in a one-story building.

The structural performance level chosen is Collapse Prevention, as the intent of the URM Special Procedure is to avoid collapse, and it uses the BSE-1E Seismic Hazard Level at the Collapse Prevention Structural Performance Level. The C_{pl} from ASCE/SEI 41-17 Equation 11-27a was expanded upon, using the Penner and Elwood table shown in Table 3-1. ASCE/SEI 41-17 used the 10% probability of collapse for the Life Safety Structural Performance Level. The 20% probability of collapse was chosen for the Collapse Prevention Structural Performance Level. See Part 6, Chapter 4 for more discussion on C_{pl}.

Table 3-2 Proposed Performance Level Factor, C_{pl}, Adapting Penner and Elwood's C_e Factor

Structural Performance Level	Probability of Collapse	C_{pl}, Stiff Diaphragm	C_{pl}, Flexible Diaphragm
Damage Control		0.8	0.8
Life Safety	5%	0.9	0.9
Limited Safety	10%	1.0	1.0
Collapse Prevention	20%	1.15	1.1
(Not Used)	50%	1.5	1.25

3.3.3.1 ALL OTHER WALLS CONDITION

For the "All Other Walls" condition, three-story, four-story, and five-story buildings were evaluated using ASCE/SEI 41-17 Equation 11-27a. For each building, the *h/t* ratio of the 2nd story was used, as this allowed the effects of the various wall weights above to be considered in the C_a term. The results are shown in Figure 3-3.

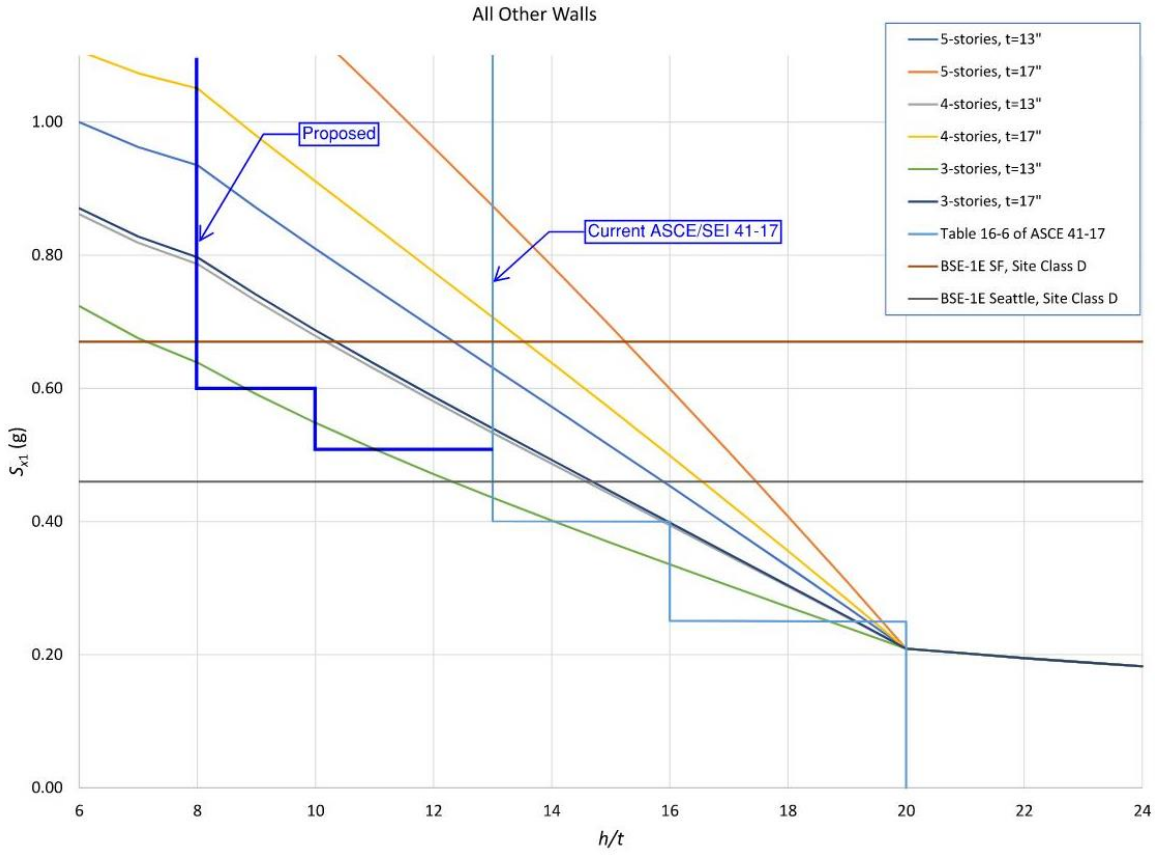

Figure 3-3 Comparison of *h/t* vs S_{X1} for "All Other Walls" category.

The current ASCE/SEI 41-17 Table 16-6 limits are shown on the plot—these stair step due to the nature of the table. In addition, the BSE-1E S_{D1} values for Site Class D are shown for a Seattle site and a San Francisco site for reference. These values are from the updated multi-point spectra developed by the USGS and that are proposed to be adopted into ASCE/SEI 41-23.

As shown in the figure, under ASCE/SEI 41-17 Table 16-6, a building in San Francisco must have an *h/t* ratio of less than 13 for the "All Other Walls" condition to be acceptable. However, using the equations, assuming three stories and a wall thickness of 17-inches, the maximum *h/t* ratio is about 10. If the wall thickness is reduced to 13-inches, the maximum *h/t* ratio is about 8.

Several observations were made regarding the study for the "All Other Walls" condition.

- The existing ASCE/SEI 41-17 Chapter 16 limits follow the more conservative values of the ASCE/SEI 41-17 Chapter 11 equation up to a limit of about S_{X1} of 0.40g.
- Higher values of S_{X1} at around 0.5g start diverging greatly from this conservative value.
- While the equations are shown for *h/t* ratios of less than 8, testing data is not actually available for ratios below this value. In addition, historical data indicates buildings with ratios below 8 have not had significant failures per ASCE 41-17 commentary. Graph values with an *h/t* below 8 should be ignored.
- Buildings with more weight (as in more stories of wall above or thicker walls) behave better under out-of-plane loads than the ASCE/SEI 41-17 Chapter 16 table indicates. The ASCE/SEI 41-17 Chapter 11 equations would allow a user to capture this behavior.

Based on these observations, a recommendation is proposed to refine the *h/t* limits for S_{X1} values between 0.5g and 0.6g and for values greater than 0.6g. The proposed limits would follow the same conservative curve the ASCE/SEI 41-17 Table 16-6 values already follow, up to the *h/t* limit of 8. In addition, use of the ASCE/SEI 41-17 Chapter 11 equations will be allowed for users that would like to refine their calculations.

3.3.3.2 FIRST STORY OF MULTI-STORY BUILDING CONDITION

For the "First Story of Multi-story Building" condition, three-story, four-story, and five-story buildings were evaluated using ASCE/SEI 41-17 Equation 11-27a. For each building, the *h/t* ratio of the first story was used in calculating the C_a term. The results are shown in Figure 3-4.

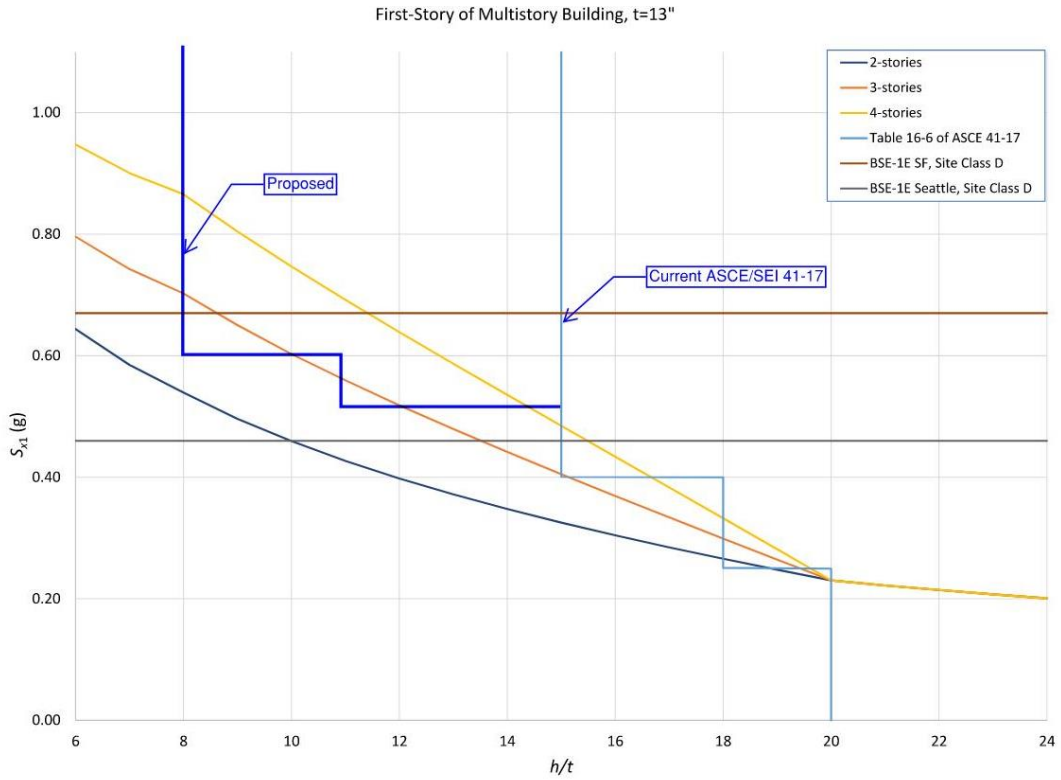

Figure 3-4 Comparison of *h/t* vs S_{X1} for "First Story of Multi-Story Building" category.

Several observations were made regarding the study for the "First Story of Multi-Story" condition.

- The existing ASCE/SEI 41-17 Chapter 16 limits follow the three-story and four-story values of the ASCE/SEI 41-17 Chapter 11 equation up to a limit of about S_{X1} of 0.40g. The most conservative approach of a two-story building is not captured by the table.
- Higher values of S_{X1} at around 0.5g start diverging greatly from the three-story values.
- Buildings with more weight (as in more stories of wall above or thicker walls) could behave better under out-of-plane loads than the ASCE/SEI 41-17 Chapter 16 table indicates. The ASCE/SEI 41-17 Chapter 11 equations would allow a user to capture this behavior.
- Graph values with an *h/t* below 8 should be ignored (see the "All Other Walls" condition).

Based on these observations, a recommendation is proposed to refine the *h/t* limits for S_{X1} values between 0.5g and 0.6g and for values greater than 0.6g. The proposed limits would follow the curve that the ASCE/SEI 41-17 Table 16-6 values already follow, up to the *h/t* limit of 8. In addition, use of the ASCE/SEI 41-17 Chapter 11 equations will be allowed for users that would like to refine their calculations.

3.3.3.3 TOP STORY OF MULTI-STORY BUILDING CONDITION

For the "Top Story of Multi-Story Building" condition, a wall with roof weight tributary and a wall without roof weight tributary were evaluated using ASCE/SEI 41-17 Equation 11-27a. With the added roof weight, the C_a value varied between 1.0 and 1.07, depending on the *h/t* ratio. Walls with the roof joists parallel may experience no added load, except perhaps occasional point loads from girders—these were neglected for the case of no roof weight. Conservatively, no parapet load was assumed, though the weight of a parapet would impact the results beneficially. The results are shown in Figure 3-5.

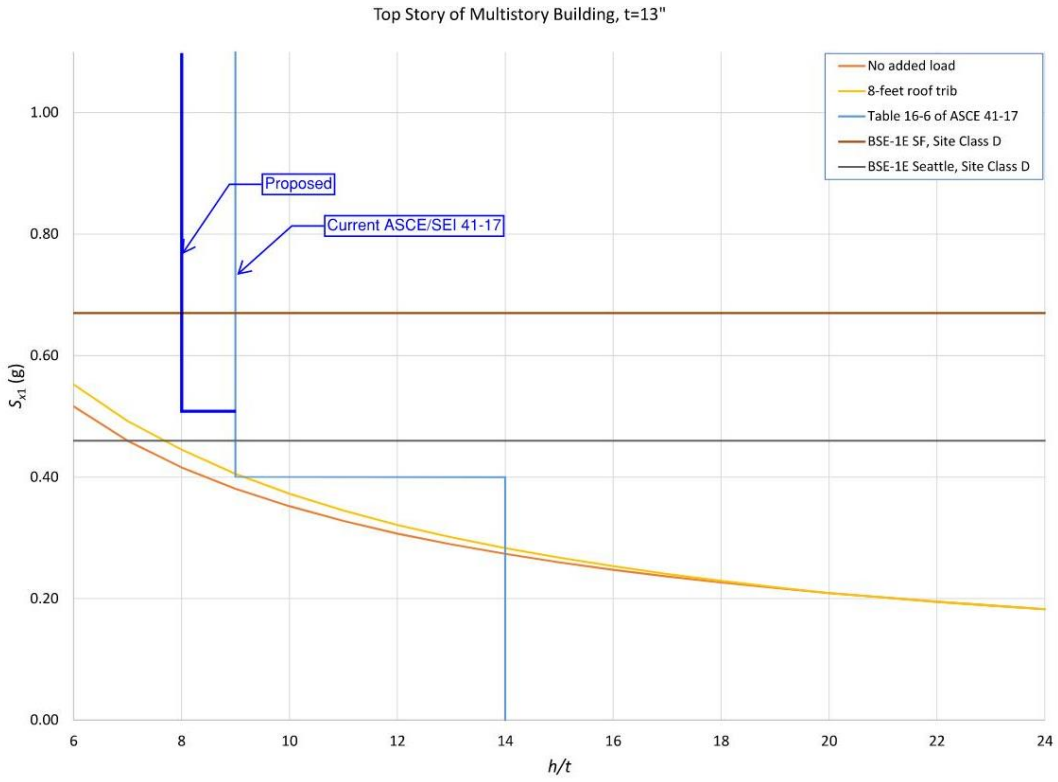

Figure 3-5 Comparison of *h/t* vs S_{X1} for "Top Story of Multi-Story Building" category.

Several observations were made regarding the study for the "Top Story of Multi-Story Building" condition.

- The existing ASCE/SEI 41-17 Chapter 16 limits are conservative for values under 0.35g and match the 0.40g value.
- Higher values of S_{X1} diverge from these conservative values.
- The weight of a roof or floor increases the *h/t* ratio by a very small amount and does not have a large impact.
- Graph values with an *h/t* below 8 should be ignored (see the "All Other Walls" condition).

Based on these observations, a recommendation is proposed to refine the *h/t* limits for S_{X1} values greater than 0.5g. The proposed limits would move to the lower limit of 8. In addition, use of the ASCE/SEI 41-17 Chapter 11 equations will be allowed for users that would like to refine their calculations.

3.3.3.4 ONE-STORY BUILDING CONDITION

For the "One-Story Building" condition, two different wall thicknesses were evaluated using ASCE/SEI 41-17 Equation 11-27a and one included an 8-foot roof tributary weight. The results are shown in Figure 3-6.

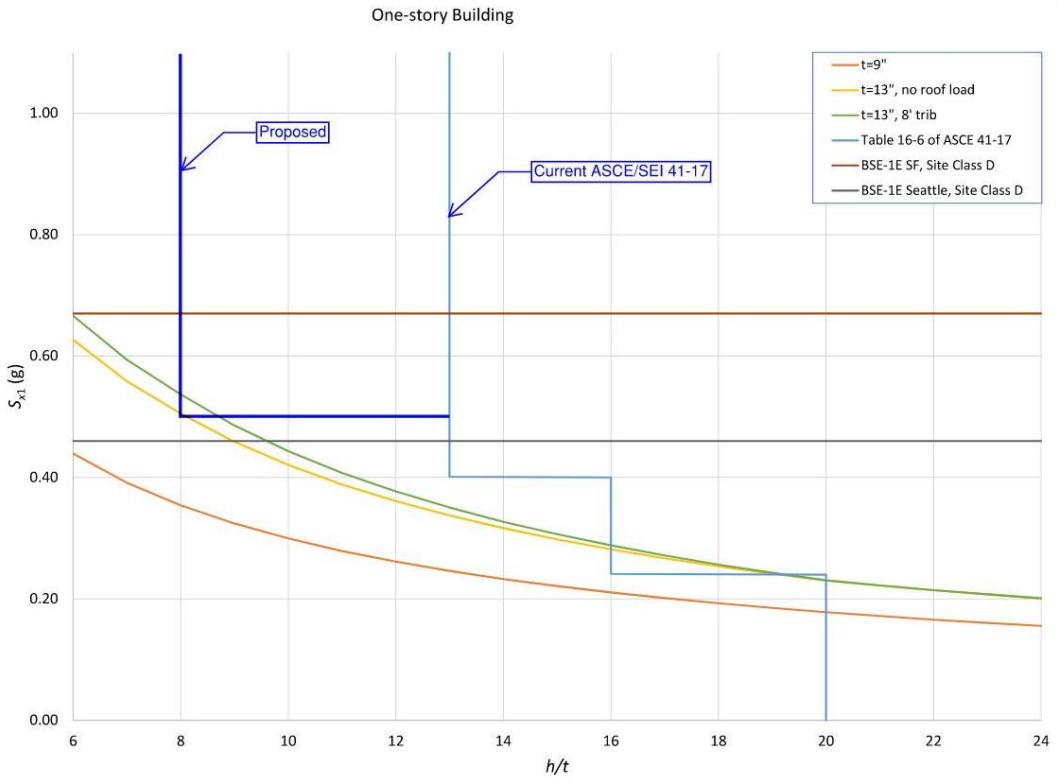

Figure 3-6 Comparison of *h/t* vs S_{X1} for "One-Story Building" category.

Several observations were made regarding the study for the "One-Story Building" condition.

- The existing ASCE/SEI 41-17 Chapter 16 limits are conservative for values under 0.35g and match the 0.40g value.
- Higher values of S_{X1} diverge from these conservative values.
- The weight of a roof or floor increases the *h/t* ratio by a very small amount and does not have a large impact.
- Graph values with an *h/t* below 8 should be ignored (see the "All Other Walls" condition).

Based on these observations, a recommendation is proposed to refine the *h/t* limits for S_{X1} values greater than 0.5g. The proposed limits would move to the lower limit of 8. In addition, use of the ASCE/SEI 41-17 Chapter 11 equations will be allowed for users that would like to refine their calculations.

3.3.4 Diaphragm Spans and Cross Walls

The Penner and Elwood method, and thus the ASCE/SEI 41-17 Chapter 11 equations, were not able to consider all possible variables. One of the items not included was the impact of cross walls on the out-of-plane wall behavior, though it had been included in the original ABK method. Cross walls had been found to decrease diaphragm amplification based on testing (Kariotis, Elwing, and Johnson, 1985). The inelastic behavior of cross wall acts as a damper for flexible, wood floor systems.

In addition, Bruneau (1994) summarizes the masonry testing and analysis that had been performed up to that time and used for the development of the table. It noted that diaphragm amplifications dropped from a range of 3 to 4 down to 1.75 with cross walls. The resulting amplifications correspond to higher damping. With a reduction in amplifications of 3/1.75 = 1.71, the corresponding damping ratio using ASCE/SEI 41-17 Equation 2-3 is about 25%. Engineering judgement was used to extrapolate between the ABK method and the Penner and Elwood equations to determine values for Column A for higher spectral accelerations. This extrapolation allows the special procedure to maintain past methods that are still valid, while updating for newer methods.

3.3.5 Conclusions

Based on the parametric studies using the newer Penner and Elwood method (now incorporated in ASCE/SEI 41 Chapter 11) and the literature review, the allowable *h/t* ratios are to be updated for seismic accelerations greater than 0.50g. In addition, the out-of-plane procedure of Chapter 11 will be explicitly allowed, in case a user would prefer to more accurately calculate the out-of-plane effects.

3.4 Recommended Changes

Note about Change Proposals

This report documents aspects of change proposals as they were submitted to subcommittees of ASCE's *Seismic Retrofit of Existing Building Standards* Committee. Often, these change proposals were revised, in some cases substantively, by these subcommittees before they were adopted into ASCE/SEI 41-23. Readers should not rely on this report for information about the final version of provisions in ASCE/SEI 41-23.

The strikeout/underline proposed changes to ASCE/SEI 41-23 Sections 16.2.4.2 and C16.4.2.2 are shown verbatim below. In addition to new commentary, the changes primarily include the added table columns for S_{X1} between 0.50g and 0.60g and for greater than 0.60g. An additional sentence

is included allowing the user to check the *h/t* ratios using the more accurate ASCE/SEI 41-17 Chapter 11 equations. New or modified text is shown in blue.

16.2.4.2 Out-of-Plane Demands

Where S_{D1} exceeds 0.133, the height-to-thickness ratios of all unreinforced masonry walls shall be less than or equal to the values in Table 16-6. Alternatively, the height-to-thickness ratios shall be permitted to be calculated per Section 11.3.3.3.2 with $C_{pl} = 1.1$. Walls not in compliance shall be strengthened in accordance with Section 16.2.4.2.1.

Table 16-6. Allowable Height-to-Thickness Ratios of Unreinforced Masonry Walls

			~~S_{D1}~~>0.4≤ S_{D1}<0.50		0.50≤S_{D1}<0.6		0.60≤S_{D1}	
Wall Type	0.133≤S_{D1}<0.25	0.25≤S_{D1}<0.4	A	B	A	B	A	B
Walls of one-story building	20	16	16[a,b]	13	13[a,b]	8	8	8
Top story of multi-story building	14	14	14[a,b]	9	9[a,b]	8	8	8
First story of multi-story building	20	18	16	15	15	11	11	8
All other conditions	20	16	16	13	13	10	10	8

[a] Value is permitted to be used when in-plane shear tests in accordance with Section 16.2.2.2.1 have a minimum v_{tL} of 100 lb/in.^{2} or a minimum v_{tL} of 60 lb/in.^{2} and a minimum of 50% mortar coverage of the collar joint.

[b] Values are permitted to be interpolated between columns A and B where in-plane shear tests in accordance with Section 16.2.2.2.1 have a v_{tL} of between 30 and 60 lb/in.^{2} and a minimum of 50% mortar coverage of the collar joint.

Currently, ASCE/SEI 41-17 does not contain commentary on the out-of-plane limits in Chapter 16. New commentary is proposed to describe the concern, explain the original basis of the *h/t* ratio limit table, and explain the updates to the table, including their basis. The following commentary is proposed:

C16.2.4.2 Out-of-Plane Demands.

Slender unreinforced masonry bearing walls with large height-to-thickness (h/t) ratios have a potential for damage caused by out-of-plane forces that may result in falling hazards and potential localized collapse of the structure.

The original table limiting h/t ratios was based on research by the ABK group (ABK, et al., 1981a, 1981b) and has been used since the late 1980s to assess the stability of URM walls. More recent

research has led to the development of an equation-based check for URM out-of-plane stability, which is the method used in Chapter 11 and discussed in the Chapter 11 commentary. This evaluation is based on the procedure proposed by Penner and Elwood (2016) and includes factors for load on the wall, wall thickness, and diaphragm type as well as h/t. For the special procedure, Table 16-6 has been expanded by using this newer procedure as the values in the existing table are unconservative for higher levels of shaking based on the results of recent research. The values in Table 16-6 are typically conservative—using no additional dead load—so the use of Chapter 11 equations is also permitted for those looking to refine their results. C_{pl}=1.1 was chosen as most closely corresponding with the Collapse Prevention level and indicating a Probability of Out-of-Plane Collapse of 20% (see Table C11-1). Due to the limited research, h/t ratios of less than 8 are deemed acceptable regardless of seismicity.

For S_{X1}≥0.4 seconds, the ABK method allowed buildings with cross walls and diaphragms meeting minimum demand/capacity ratios and maximum spans to use higher h/t ratios. These values were based on testing that showed the velocity amplification was reduced due to nonlinear diaphragm behavior under those specific conditions. The paper by Bruneau (Bruneau, 1994) summarizes the masonry testing and analysis that had been performed up to that time and used for the development of the table. When expanding Table 16-6, the Penner and Elwood equations for determining h/t limits did not include variables for cross walls or diaphragm behavior, though these variables do have an influence. Therefore, engineering judgement was used to extrapolate between the ABK method and the Penner and Elwood equations to determine values for Column A at S_{X1}≥0.5 seconds. This extrapolation allows the special procedure to maintain past methods that are still valid, while updating for newer methods.

3.5 References

ABK, 1981a, *Methodology of Mitigation of Seismic Hazards in Existing Unreinforced Masonry Buildings: Diaphragm Testing*, ABK-TR-03, Agbabian Associates, S.B. Barnes & Associates, and Kariotis & Associates, El Segundo, California.

ABK, 1981b, *Methodology of Mitigation of Seismic Hazards in Existing Unreinforced Masonry Buildings: Wall Testing, Out-of-Plane*, ABK-TR-04, Agbabian Associates, S.B. Barnes & Associates, and Kariotis & Associates, El Segundo, California.

ABK, 1984, *Methodology of Mitigation of Seismic Hazards in Existing Unreinforced Masonry Buildings: The Methodology*, ABK-TR-08, Agbabian Associates, S.B. Barnes & Associates, and Kariotis & Associates, El Segundo, California.

Bruneau, M., 1994, "Seismic evaluation of unreinforced masonry buildings—a state-of-the-art report," *Canadian Journal of Civil Engineering*, Volume 21, pp. 512-539.

FEMA, 2009, *Quantification of Building Seismic Performance Factors*, FEMA P695 report, prepared by the Applied Technology Council for the Federal Emergency Management Agency, Washington, D.C.

Kariotis, J.C., Ewing, R.D., and Johnson, A.W., 1985, "Predictions of stability for unreinforced brick masonry walls shaken by earthquakes," *Proceedings of the 7th International Brick Masonry Conference*, Melbourne, Sydney, pp. 1175-1184.

Penner, O. and Elwood, K., 2016a, "Out-of-plane dynamic stability of unreinforced masonry walls in one-way bending: shake table testing," *Earthquake Spectra*, Vol. 32, No. 3, pp. 1675-1697.

Penner, O. and Elwood, K., 2016b, "Out-of-plane dynamic stability of unreinforced masonry walls in one-way bending: parametric study and assessment guidelines," *Earthquake Spectra*, Vol. 32, No. 3, pp. 1699-1723.

Chapter 4: Revisions to Chapter 11 URM Wall Out-of-Plane Provisions

4.1 Motivation

Slender unreinforced masonry (URM) bearing walls with large height-to-thickness (*h/t*) ratios have a potential for damage caused by out-of-plane forces that may result in falling hazards and potential localized collapse of the structure. The ASCE/SEI 41 Chapter 11 out-of-plane wall stability provisions for the Life Safety Structural Performance Level were updated in ASCE/SEI 41-17 using the Penner and Elwood (2016b) methodology, but the Collapse Prevention Structural Performance Level provisions continued to use requirements from previous editions. The Damage Control and Limited Safety Structural Performance Levels were not addressed in the ASCE/SEI 41-17 updates. The proposal for ASCE/SEI 41-23 harmonizes the various structural performance levels using one consistent method, and it revises the height-to-thickness (*h/t*) ratios for high seismic regions which were shown to be unconservative by the Penner and Elwood (2016b) research.

4.2 Summary of Changes Recommended

The changes occur in ASCE/SEI 41-23 Section 11.3.3.3 and Commentary Section C11.3.3.3 provisions that define requirements for out-of-plane wall stability in URM buildings. They remove Table 11-5 which provided *h/t* ratios for the Collapse Prevention Structural Performance Level assessments, and they refine the methodology used for the Life Safety Structural Performance Level for application to the Collapse Prevention, Damage Control, and Limited Safety Structural Performance Levels. A factor to account for the beneficial aspects of cross walls on reducing out-of-plane demands was added to the methodology.

4.3 Technical Studies

For the Collapse Prevention performance level, the current ASCE/SEI 41-17 Chapter 11 provisions for out-of-plane unreinforced masonry walls require evaluation per ASCE/SEI 41-17 Table 11-5. The evaluation is based on a simple *h/t* ratio, the location of the wall within a building, the seismic acceleration at one second, and, for higher seismicity cases, the diaphragm behavior. Walls located at the top story of a multi-story building have more restrictive ratios as the deformations are amplified at the top of the building plus there is less confining weight, while walls at the ground floor have less restrictive ratios due to the rigidity of the base condition plus additional wall weight above providing confinement; walls in between the ground floor and top floor have in-between *h/t* limits. Walls of one-story buildings have limits similar to the in-between walls, rather than the ground floor walls, because there is less weight above providing confinement, though there is the more rigid base condition.

Values of S_{X1} greater than 0.4g are treated the same. However, as the understanding of seismicity has advanced over the years, large areas along the West Coast, including in major cities, now have S_{X1} values in the 0.70g to 1.3g range for the BSE-2E level.

For the Life Safety Structural Performance Level, ASCE/SEI 41-17 included a new method for checking *h/t* ratios based on the Penner and Elwood studies (2016a,b). The Collapse Prevention level was not updated, as mentioned above, and the Damage Control and Limited Safety levels were not addressed.

4.3.1 Penner and Elwood Studies and Method

The ABK method (the basis of Table 11-5) does not account for many other factors, such as wall thickness, increased weight on walls, etc. Also, additional research on walls has been performed since the 1980s study. Penner and Elwood (2016a) performed additional shake table testing, as have others. Penner and Elwood then developed computer modeling calibrated to meet their testing results. With this computer model, a parametric study was performed with over 200,000 parametric runs (Penner and Elwood, 2016b). Parameters varied included diaphragm periods, wall thickness, *h/t* ratios, diaphragm damping, diaphragm mass ratios, and axial load. Multiple ground motions per FEMA P695 (FEMA, 2009) were used.

One finding from the study is concerning the use of S_{X1} as the ground motion parameter to use. Further discussion on this aspect is included in Section 3.3.

Based on these studies, an equation for checking wall *h/t* ratios was developed. Variables included the following:

- Diaphragm stiffness—either flexible (T_s>0.5-s) or stiff (T_s <0.2-s)
- Height-to-thickness ratio, *h/t*
- Axial load
- An adjustment factor for thin walls that are less than about 13-inches thick
- An adjustment factor for ground level walls as the base connection is more rigid with less movement than a diaphragm
- A correction factor for “exposure level”. This factor is based on the probability of collapse calculated from the parametric studies. The recommendations are shown in Table 4-1.

Table 4-1 Exposure Factor, C_e, from Penner and Elwood (2016b)

Exposure	Probability of Collapse	C_e, Stiff Diaphragm	C_e, Flexible Diaphragm
Very high	5%	0.9	0.9
High	10%	1.0	1.0
Low	20%	1.15	1.1
Very low	50%	1.5	1.25

The proposed method results in more stringent requirements for flexible diaphragms than the current ASCE/SEI 41-17 Table 11-5 method. For stiff diaphragms, the results are similar to the current tables. The procedure did err on the conservative side, especially for flexible diaphragms.

The method did not include other parameters than can affect the out-of-plane stability of the walls, and the paper recommends further study for the following: diaphragm displacements, response along the diaphragm (more deflection expected at the middle of the diaphragm than at the ends), two-way bending, amplification up the building height, arching action, masonry strength, damping and nonlinearity, in-plane damage, and vertical acceleration.

4.3.2 ASCE/SEI 41-17 Chapter 11 Updates for Life Safety

ASCE/SEI 41-17 Chapter 11 updated the out-of-plane stability for the Life Safety Structural Performance Level based on the Penner and Elwood method, though the Collapse Prevention Structural Performance Level continued to use the table of *h/t* ratio limits developed using the ABK method. The following equation is used for checking the out-of-plane stability for walls with *h/t* ratios greater than 8:

$$S_{X1} \le C_a C_t C_g C_{pl} S_{aDIAPH}(1) \qquad \text{(ASCE/SEI 41-17 11-27a)}$$

where

$$S_{aDIAPH}(1) = \begin{cases} \dfrac{4}{h/t} & \text{for stiff diaphragms} \\ \dfrac{1.8}{(h/t)^{0.75}} & \text{for flexible diaphragms} \end{cases} \qquad \text{(ASCE/SEI 41-17 11-27b)}$$

C_a = axial load factor

$$= \begin{cases} 1 + C'_a (P_D / 685)\left(1 - \dfrac{1}{12}\left(\dfrac{h}{t} - 8\right)\right) & \text{for } 8 \le h/t \le 20 \\ 1 & \text{for } h/t > 20 \end{cases} \qquad \text{(ASCE/SEI 41-17 11-27c)}$$

C_a' = 0.5 for stiff diaphragms and 0.2 for flexible diaphragms (interpolate as needed)

P_D = vertical load on the wall in lb/ft

C_t = Modification factor for thin walls = 0.2 + t/15.7 <= 1.0

t = wall thickness in inches

C_g = Modification factor for ground level walls (1.0 if not at ground level)

= 1.0 for stiff diaphragms and 1.1 for flexible diaphragms (interpolate as needed)

C_{pl} = Modification factor for performance level = 0.9 for Life Safety

One change ASCE/SEI 41-17 made to the equation from the Penner and Elwood method is the coefficient for flexible diaphragms was switched from 1.5 to 1.8—an increase of about 20%. Penner and Elwood assumed 5% damping of the diaphragms, but wood diaphragms typically have a higher level of damping, which led to the ASCE/SEI 41-17 increase. Using ASCE/SEI 41-17 Equation 2-3 and assuming 10% damping, β, provides the following results.

$B_{1,10\%} = 4/[5.6\text{-}\ln(100\beta)]$

$= 4/[5.6\text{-}\ln(100(0.10))]$

$= 1.21$

Similarly, B_1 for 5% damping is 1.0. Therefore, slightly less than 10% damping would result in a 20% increase. The study below continues to use the 1.8 factor for increased damping from the wood diaphragm.

The primary inputs in the equation are *h/t* ratio, axial load, diaphragm stiffness, wall thickness (for walls less than 13-inches thick), and a factor for the performance level.

Performance Level Correction Factor

The exposure factor from the Penner and Elwood method was renamed to a performance level factor, C_{pl}, and tied to the performance level. For ASCE/SEI 41-17, a Life Safety Structural Performance Level factor of 0.9 was chosen, corresponding to a 5% probability of collapse. Factors for other performance levels are not listed as it is not required for the Collapse Prevention Structural Performance Level (ASCE/SEI 41-17 Table 11-5 is still used) and the Damage Control and Limited Safety Performance Levels were neglected.

If the method is to be expanded to the other performance levels, C_{pl} factors need to be addressed. ASCE/SEI 41 does not have explicit collapse probability values assigned for the various levels. However, the 20% probability of collapse in order to prevent total building collapse appeared reasonable; 50% was briefly discussed, but it was not used as a 50-50 chance of the wall collapsing

did not mesh with the Collapse Prevention Structural Performance Level goal. The Limited Safety Structural Performance Level is defined as using values halfway between the Life Safety and Collapse Prevention Structural Performance Levels in ASCE/SEI Section 2.3.1.4.1, so the 10% probability of collapse values from Penner and Elwood were chosen. Values less than a 5% probability of collapse were not given, so engineering judgement was used to assign a value of 0.8; this also matches the step in C_{pl} between the Life Safety and Limited Safety Structural Performance Levels.

Table 4-2 Proposed Performance Level Factor, C_{pl}, Adapting Penner and Elwood's C_e Factor

Structural Performance Level	Probability of Collapse	C_{pl}, Stiff Diaphragm	C_{pl}, Flexible Diaphragm
Damage Control		0.8	0.8
Life Safety	5%	0.9	0.9
Limited Safety	10%	1.0	1.0
Collapse Prevention	20%	1.15	1.1
(Not Used)	50%	1.5	1.25

These proposed factors were used in the parametric study calculations.

4.3.3 Parametric Study

Using ASCE/SEI 41-17 Equation 11-27, a parametric study was conducted to compare various URM wall configurations in out-of-plane behavior to the current Table 11-5 limits. Only flexible diaphragms were considered at this stage, though stiff diaphragms would result in less-restrictive h/t ratios. The following parameters were varied:

- Wall thickness, t: The study used 13-inch and 17-inch walls as these sizes are commonly encountered for multi-story buildings (thinner walls being inadequate). The wall thickness also impacted the axial load and the C_a factor (see below). Using these thicknesses meant C_t=1.0 as this factor is only triggered if wall thickness is less than 13-inches. A 9-inch wall thickness was used for the one-story buildings, where it might potentially be encountered, and those calculations do include the C_t factor per ASCE/SEI 41-17 Equation 11-27d.

- Axial load, C_a, ASCE/SEI 41-17 Equation 11-27c: The axial load is primarily from the masonry wall weight above the floor under consideration. For the "All Other Walls" case, the weight at the 2nd floor wall was used and the study varied the number of stories above to observe the effects. In other words, a four-story building will have more wall and floor weight above than a three-story building on the 2nd story or ground story. The floor weight on a wall is small as the maximum load is one-half of a bay of wood-framed floor, so it was neglected for the "All Other Walls" and the "First Story of a Multi-story Building" cases. For the "Top Story of a Multi-story Building" and

"One-story Building" cases, a floor/roof load assuming 30 lb/ft^2 of dead load and the tributary width indicated in the figure legend was added to the wall weight.

- Location of the wall in the building: These match the existing ASCE/SEI 41-17 Table 16-6 cases: top story of a multi-story building, first story of a multi-story building, all other walls in multi-story building, and walls in a one-story building.

The structural performance level chosen is Collapse Prevention, as the Life Safety Structural Performance Level had presumably been studied previously. The Limited Safety and Damage Control Structural Performance Levels can be inferred from these results.

Impacts to *h/t* Ratios for the Collapse Prevention Performance Level

The results of the parametric study illustrate the changes to *h/t* ratio limits in switching from the table values to the equations for the Collapse Prevention Structural Performance Level. The current ASCE/SEI 41-17 Table 11-5 limits are shown on the plots—these stair step due to the nature of the table. In addition, the BSE-2E S_{X1} values for Site Class D are shown for a Seattle site and a San Francisco site for reference. These values are from the updated multi-point spectra developed by the USGS and that are proposed to be adopted into ASCE/SEI 41-23.

For the "All Other Walls" condition, three-story, four-story, and five-story buildings were evaluated using ASCE/SEI 41-17 Equation 11-27a. For each building, the *h/t* ratio of the 2nd story was used, as this allowed the effects of the various wall weights above to be considered in the C_a term. The results are shown in Figure 4-1.

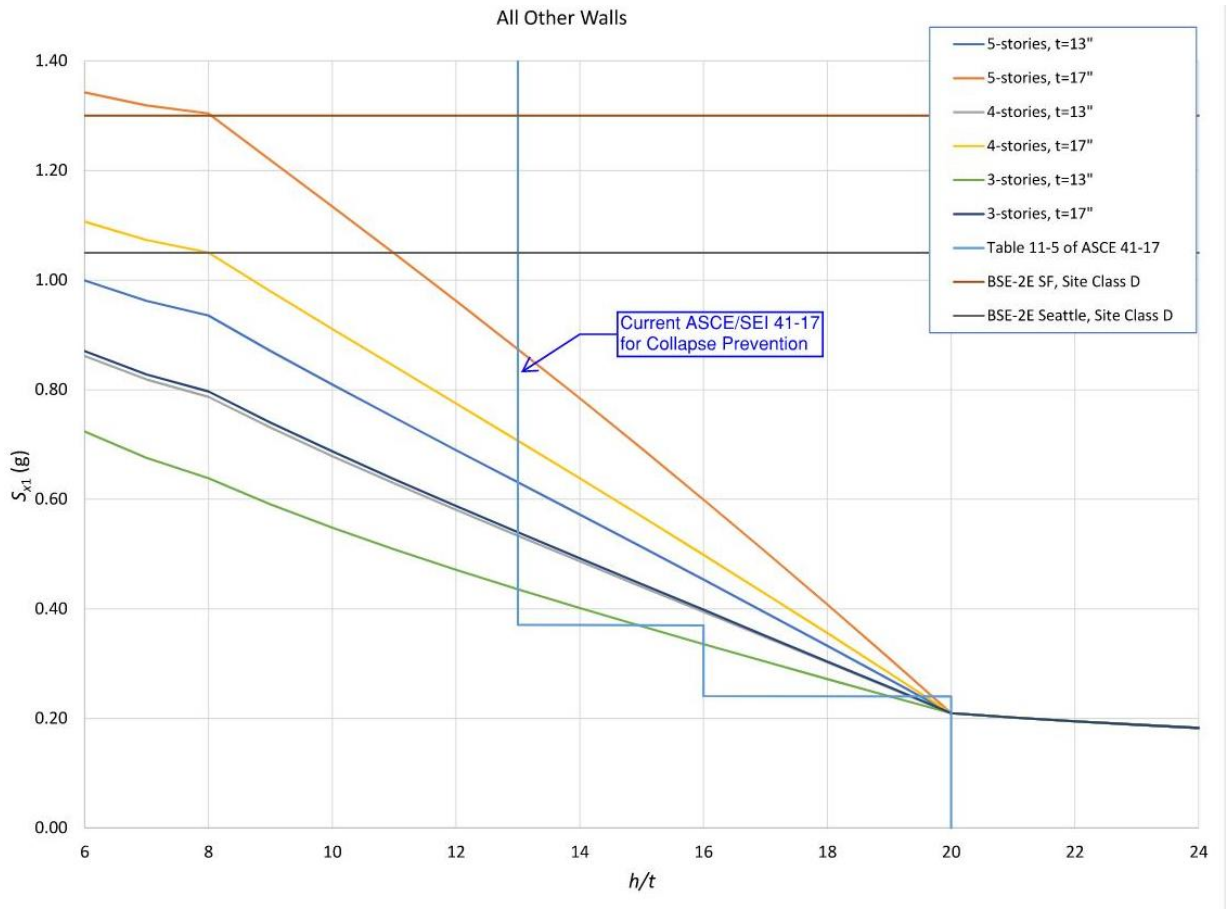

Figure 4-1 Comparison of *h/t* vs S_{X1} for "All Other Walls" category.

As shown in the figure, under ASCE/SEI 41-17 Table 11-5, a building in San Francisco must have an *h/t* ratio of less than 13 for the "All Other Walls" condition to be acceptable. However, using the equations, assuming three-stories and a wall thickness of 17-inches, the maximum *h/t* ratio is about 8.

For the "First Story of Multi-story Building" condition, three-story, four-story, and five-story buildings were evaluated using ASCE/SEI 41-17 Equation 11-27a. For each building, the *h/t* ratio of the first story was used in calculating the C_a term. The results are shown in Figure 4-2.

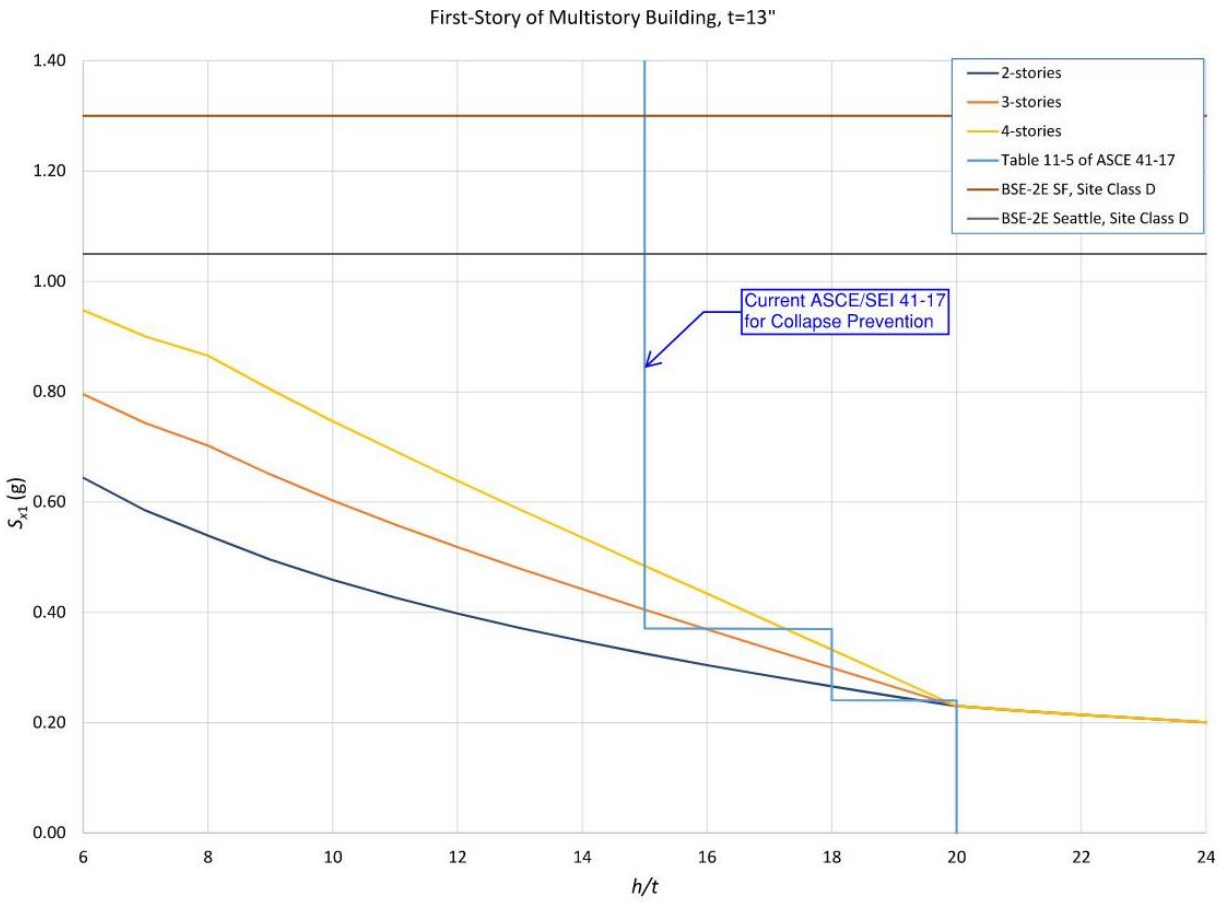

Figure 4-2 Comparison of *h/t* vs S_{X1} for "First Story of Multi-Story Building" category.

For the "Top Story of Multi-Story Building" condition, a wall with roof weight tributary and a wall without roof weight tributary were evaluated using ASCE/SEI 41-17 Equation 11-27a. With the added roof weight, the C_a value varied between 1.0 and 1.07, depending on the *h/t* ratio. Walls with the roof joists parallel may experience no added load, except perhaps occasional point loads from girders—these were neglected for the case of no roof weight. Conservatively, no parapet load was assumed, though the weight of a parapet would impact the results beneficially. The results are shown in Figure 4-3.

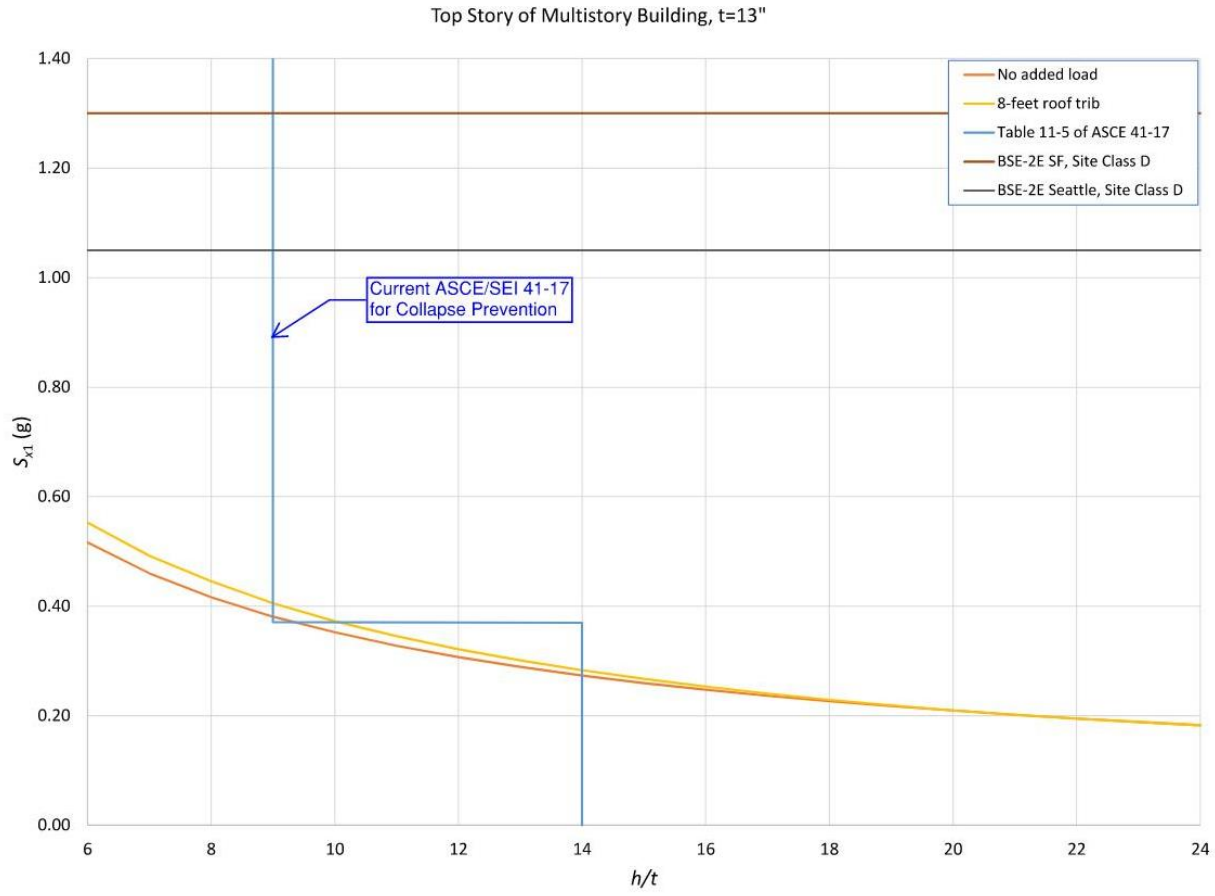

Figure 4-3 Comparison of *h/t* vs S_{X1} for "Top Story of Multi-Story Building" category.

For the "One-Story Building" condition, two different wall thicknesses were evaluated using ASCE/SEI 41-17 Equation 11-27a, and one included an 8-foot roof tributary weight. The results are shown in Figure 4-4.

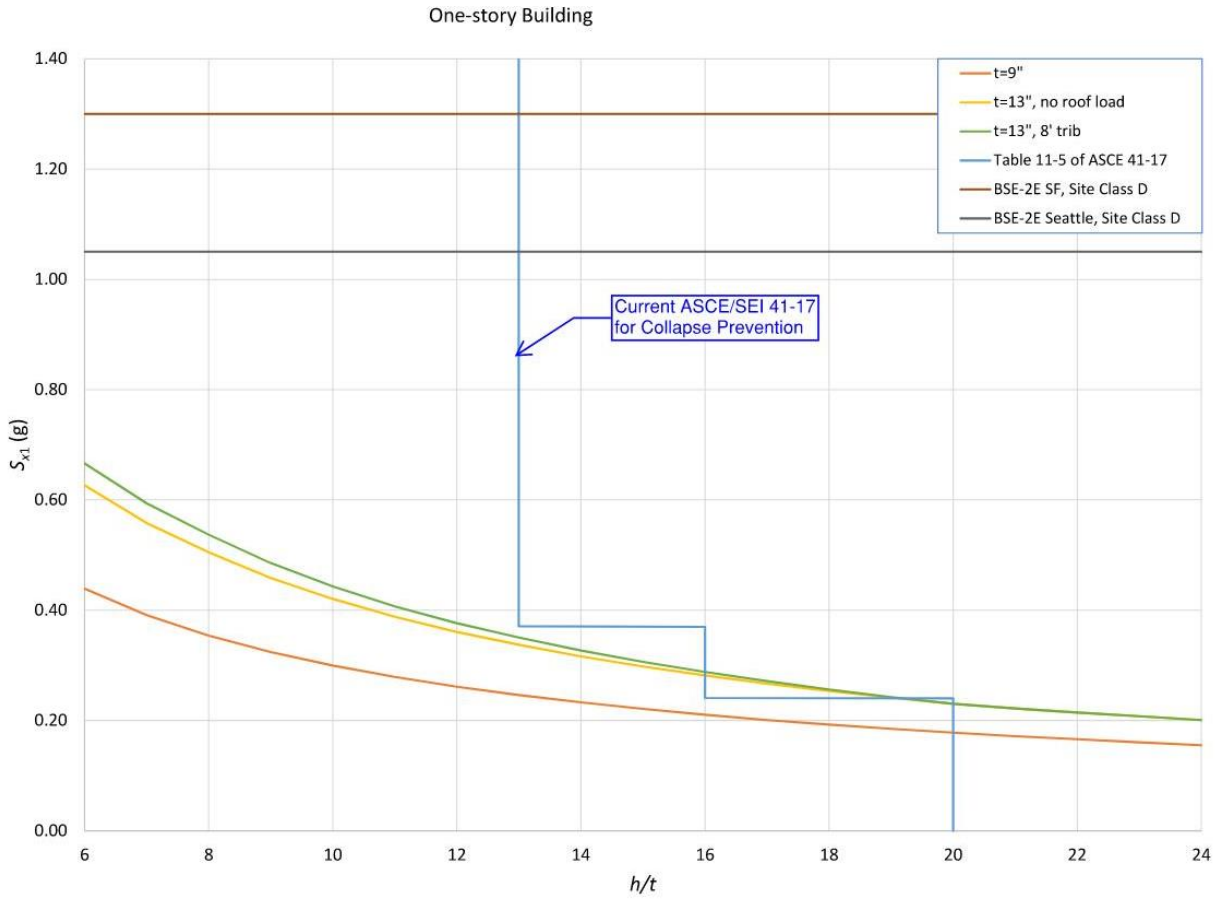

Figure 4-4 Comparison of *h/t* vs S_{X1} for "One-Story Building" category.

Several observations were made regarding the above studies.

- For values of S_{X1} of about 0.40g and below, the existing ASCE/SEI 41-17 Table 11-5 follows the ASCE/SEI 41-17 Equation 11-27 fairly well. For the "All Other Walls" condition, it follows the more conservative line, while in the other categories it tends to follow a moderate line.
- Higher values of S_{X1} at around 0.5g start diverging greatly from the table values.
- Buildings with more weight (as in more stories of wall above or thicker walls) behave better under out-of-plane loads at lower seismicity than the ASCE/SEI 41-17 Table 11-5 table indicates for the "All Other Walls" condition. The ASCE/SEI 41-17 Equation 11-27 results would allow a user to capture this behavior.
- While the equations are shown for *h/t* ratios of less than 8, testing data is not actually available for ratios below this value. In addition, historical data indicates buildings with ratios below 8 have not had significant failures per ASCE 41-17 commentary. Graph values with an *h/t* below 8 should be ignored. ASCE/SEI 41-17 already caps the minimum *h/t* ratio at 8.

- Areas with high seismicity at the Collapse Prevention Structural Performance Level are going to need strongbacking at most URM walls, unless there are multiple stories above providing weight.

4.3.4 Cross Walls

The Penner and Elwood method, and thus the ASCE/SEI 41-17 Chapter 11 equations, were not able to consider all possible variables. One of the items not included was the impact of cross walls on the out-of-plane wall behavior, though it had been included in the original ABK method. Cross walls had been found to decrease diaphragm amplification based on testing (Kariotis, Elwing, and Johnson, 1985).

The inelastic behavior of cross wall acts as a damper for flexible, wood floor systems. Bruneau (1994) summarizes the masonry testing and analysis that had been performed up to that time and used for the development of the table. It noted that diaphragm amplifications dropped from a range of 3 to 4 down to 1.75 with cross walls. With a reduction in amplifications of 3/1.75 = 1.71, the corresponding damping ratio using ASCE/SEI 41-17 Equation 2-3 is about 25%. Using a more conservative damping value of 20% for cross walls, the increase from a building without cross walls to one with cross walls is a change from 10% to 20% damping. Using ASCE/SEI 41-17 Equation 2-3, a damping factor can be calculated of 1.5. Dividing the 1.5 for 20% damping by the 1.2 found for 10% damping (see Section 4.3.2), the increase from 10% to 20% damping is 1.25. Where cross walls meeting limitations similar to the requirements long included in the Special Procedure for Unreinforced Masonry, allowing an increase of 1.25 appears reasonable.

The cross wall requirements in the Special Procedure for Unreinforced Masonry include the following: cross walls shall not be spaced more than 40-feet on-center, they must be perpendicular to the direction under consideration, they must extend the full story height between diaphragms, and meet a minimum aspect ratio. Cross walls are already defined in ASCE/SEI 41-17 Chapter 1 as wood-framed walls with particular sheathing requirements.

Bare steel deck diaphragms, though often meeting the flexible diaphragm parameters, and stiff diaphragms were specifically excluded from the original ABK studies from benefitting from cross walls. Therefore, they are excluded from the increase for cross walls, as are other, flexible, non-wood diaphragms.

4.3.5 Other Considerations

As mentioned above, the method used in ASCE/SEI 41-17 did not include other parameters than can affect the out-of-plane stability of the walls. In addition to cross walls, the following items were considered:

- The Australian masonry code AS 3700:2011 includes a method to potentially account for two-way bending in walls. It uses the virtual work method and idealized crack patterns. However, the method is still computationally intensive and requires checking multiple crack patterns. After review, it was decided the method was too complex to incorporate in the standard.

- The Penner and Elwood method contains provisions for stiff and flexible diaphragms but does not mention rigid diaphragms. The definition of a stiff diaphragm used in this method is that the diaphragm period is less than 0.2 second—different than the definition in Chapter 2 of ASCE/SEI 41-17. For diaphragms that are rigid by the ASCE/SEI 41-17 definition, or that are assumed to meet this definition by inspection (for example, a concrete slab supported by concrete beams), the language has been clarified to state the values for stiff diaphragms shall be used. The language regarding rigid, stiff, and flexible has been reviewed and made consistent throughout the out-of-plane masonry provision.

4.3.6 Conclusions

Table 11-5 with *h/t* ratio limits for the Collapse Prevention Structural Performance Level assessments should be removed and updated using the Penner and Elwood method already adopted for Life Safety. Recommendations for the C_{pl} factor to account for the Collapse Prevention, Damage Control, and Limited Safety Structural Performance Levels are included. In addition, a factor to account for the beneficial aspects of cross walls on reducing out-of-plane demands is recommended to be added to the methodology.

4.4 Recommended Changes

Note about Change Proposals

This report documents aspects of change proposals as they were submitted to subcommittees of ASCE's *Seismic Retrofit of Existing Building Standards* Committee. Often, these change proposals were revised, in some cases substantively, by these subcommittees before they were adopted into ASCE/SEI 41-23. Readers should not rely on this report for information about the final version of provisions in ASCE/SEI 41-23.

The strikeout/underline proposed changes to ASCE/SEI 41-23 Sections 11.3.3.3 and C11.3.3.3 are shown verbatim below. The changes primarily include updating the Damage Control, Limited Safety, and Collapse Prevention Structural Performance Level out-of-plane acceptance criteria to conform to similar standards as the Life Safety Structural Performance Level. A modification factor for buildings containing cross walls is proposed and language regarding rigid and stiff diaphragms is corrected. The change in limit for v_{tl} from less than to greater than 30 lb/in^2 is to correct a known error in the section—the original intent was for walls in good condition with adequate strength to be allowed to crack. New or modified text is shown in blue. Existing text that has been relocated is shown in green.

11.3.3.3 Acceptance Criteria for URM Walls Subject to Out-of-Plane Actions

For the Immediate Occupancy Structural Performance Level, flexural cracking in URM walls caused by out-of-plane inertial loading shall not be permitted. Bed-joint flexural tensile strength is limited by Section 11.3.3.2 or Table 11-2a. If $v_{tL} \leq \geq 30$ lb/in^2 (206.8 kPa), flexural cracking in URM walls caused by out-of-plane inertial loading shall be permitted for the Damage Control, Life Safety, Limited Safety, and Collapse Prevention Structural Performance Levels, provided that cracked wall segments remain stable during dynamic excitation.

~~11.3.3.3.1 Collapse Prevention Acceptance Criteria for URM Walls Subject to Out-of-Plane Actions.~~

~~For the Collapse Prevention Structural Performance Level, walls spanning vertically shall have a height-to-thickness (h/t) ratio less than or equal to that given in Table 11-5.~~

~~Table 11-5. Permissible h/t Ratios for URM Subject to Out-of-Plane Actions for Collapse Prevention Performance~~

~~Wall Types~~	~~$S_{X1} \leq 0.24g$~~	~~$0.24g < S_{X1} \leq 0.37g$~~	~~$S_{X1} > 0.37g$~~
~~Walls of one-story buildings~~	~~20~~	~~16~~	~~13~~
~~First story wall of multistory building~~	~~20~~	~~18~~	~~15~~
~~Walls in top story of multistory building~~	~~14~~	~~14~~	~~9~~
~~All other walls~~	~~20~~	~~16~~	~~13~~

Eqs. (11-27a) through (11-27d) shall be used to assess the ~~Life Safety~~ Structural Performance Levels other than Immediate Occupancy. A wall shall be considered as connected to *stiff diaphragms* if the most flexible diaphragm connected to the wall has a period $T_{DIAPH} \leq 0.2$ s. A wall at a given story shall be considered as connected to *flexible diaphragms* if the most flexible diaphragm connected to the wall has a period $T_{DIAPH} \geq 0.5$ s. Linear interpolation of Sa_{DIAPH} (1), C_a , C_{pl}, and C_g in Eq. (11-27a) based on the diaphragm period shall be permitted for 0.5 s > T_{DIAPH} > 0.2 s. Periods of the diaphragms shall be based on diaphragm stiffnesses and Chapter 7. *Rigid diaphragms* shall use the values and equations for *stiff diaphragms*. Half of the wall height (or any parapet for top-level walls) above and below the diaphragm in question shall be considered in calculation of tributary mass for the diaphragm period.

~~For the Life Safety Structural Performance Level, a~~A cracked wall shall be considered stable during dynamic excitation if h/t ≤ 8 or

$$S_{X1} \leq C_a C_t C_{cw} C_{pl} S_{aDIAPH}(1) \qquad (11\text{-}27a)$$

where

$$S_{aDIAPH}(1) = \begin{cases} \dfrac{4}{h/t} & \text{for stiff diaphragms} \\ \dfrac{1.8}{(h/t)^{0.75}} & \text{for flexible diaphragms} \end{cases} \qquad (11\text{-}27b)$$

and

C_a = Modification factor for axial loads acting on the wall

$$= \begin{cases} 1 + C_a'(P_D / 685) & \text{for } h/t < 8 \\ 1 + C_a'(P_D / 685)\left(1 - \frac{1}{12}\left(\frac{h}{t} - 8\right)\right) & \text{for } 8 \le h/t \le 20 \\ 1 & \text{for } h/t > 20 \end{cases} \quad (11\text{-}27c)$$

where

$$C_a' = \begin{cases} 0.5 \text{ for stiff diaphragms} \\ 0.2 \text{ for flexible diaphragms} \end{cases}$$

P_D = vertical load acting on the wall in lb/ft (not including the self-weight of the wall at the story under consideration);

C_t = Modification factor for thin walls = $0.2 + t/15.7 \le 1.0$ (11-27d)

where t is wall thickness (in.);

C_g = Modification factor for ground-level walls;

$$= \begin{cases} 1.0 & \text{for stiff diaphragms} \\ 1.1 & \text{for flexible diaphragms} \end{cases};$$

C_g = 1.0 for walls not at ground level;

C_{cw} = Modification factor for *cross walls*. *Cross walls* shall not be spaced more than 40 ft (12.2 m) on center, measured perpendicular to the direction under consideration, and shall extend the full story height between diaphragms. *Cross walls* shall have a length-to-height ratio between openings equal to or greater than 1.5;

$$= \begin{cases} 1.0 & \text{for stiff diaphragms and bare steel deck diaphragms} \\ 1.0 & \text{for flexible, wood diaphragms with } \textit{no cross walls} \text{ in direction of evaluating} \\ 1.25 & \text{for flexible, wood diaphragms with } \textit{cross walls} \text{ in direction evaluating} \end{cases}$$

(11-27e)

C_{pl} = Modification factor for Performance Level per Table 11-5;-

~~= 0.9 for Life Safety Performance Level.~~

Table 11-5. C_{pl}, Performance Modification Factor for URM Subject to Out-of-Plane Actions

Performance Levels	Stiff Diaphragms	Flexible Diaphragms
Damage Control	0.8	0.8
Life Safety	0.9	0.9
Limited Safety	1.0	1.0
Collapse Prevention	1.15	1.1

The ASCE/SEI 41-17 commentary is updated to reflect the proposed changes. Commentary shown below in green is not new but has been relocated. The following commentary is proposed:

C11.3.3.3 Acceptance Criteria for URM Walls Subject to Out-of-Plane Actions.

For further information on evaluating the stability of URM walls out-of-plane, refer to *Methodology for Mitigation of Seismic Hazards in Existing Unreinforced Masonry Buildings* (ABK 1984).

The suggested slenderness ratios assume that existing wall-to-diaphragm connections are sufficient to carry inertial forces from the wall into the diaphragm. Timber diaphragms shall be strengthened so that they can carry the forces transferred through connections to out-of-plane loaded walls. Wall-to-diaphragm connections are essential to achieve out-of-plane stability because walls that have inadequate connections to top diaphragms respond in cantilever modes and are much less stable. Research by Lam et al. (1995) and Doherty (2000) has shown that the seismic behavior of freestanding URM walls is analogous to that of a four times more slender simply supported URM wall.

More recent research indicates that h/t ratios in Table 11-5 may be conservative for undamaged URM walls responding to non-near-source ground motions with S_{a1} less than 0.45g (Simsir et al. 2004; Sharif et al. 2007; Dizhur et al. 2010; Derakhshan 2011). However, research on the influence of near-source ground motions with long pulses on out-of-plane actions (Derakhshan 2011) suggests that h/t ratios in high seismic regions can be unconservative. Research has also suggested that the behavior of walls that have the same slenderness ratio but different thickness is different (Sorrentino et al. 2008; Derakhshan 2011). Derakhshan (2011) suggests that of walls having the same slenderness ratio, thicker walls are generally more stable. These findings suggest that future research should be directed to study out-of-plane wall behavior by considering wall thickness.

Sorrentino et al. (2008) and Derakhshan (2011) have suggested that crack height substantially influences wall stability and that analytical models should consider an appropriate crack height. In addition, research to date has not captured all significant variables influencing the performance of out-of-plane URM walls. For example, research is currently under way to address the influence of in-plane demands on out-of-plane actions, overburden eccentricities, and dynamic characteristics of diaphragms (Penner and Elwood 2011).

Research to date has also focused on Collapse Prevention, so the margin between Life Safety and collapse is poorly understood because it has not been explicitly quantified. Localized loss of masonry units may still occur for URM walls that meet these criteria, potentially resulting in falling hazards that can cause serious injury.

Analytical studies that have attempted to capture the response of out-of-plane actions suggest that rigid-body rocking models that account for impact-based collision and restitution can be more reliable than oscillator-based models or displacement-based models (Doherty et al. 2000; Griffith et al. 2003; Lam et al. 2003; Makris and Konstantinidis 2003; Sharif et al. 2007).

~~Table 11-5 is~~ASCE 41 (2017) and earlier editions evaluated out-of-plane actions by h/t ratios based on research by ABK [Agbabian et al. (1981)] ~~and has been used in various forms since the late 1980s to assess the stability of URM walls. For consistency with past Collapse Prevention assessments, these limits are included here only for the Collapse Prevention Performance Level.~~ However, out-of-plane evaluations have been revised in this edition using the assessment procedure from Penner and Elwood (2016), which was added in ASCE 41 (2017) for the Life-Safety case. The procedure has been expanded to include factors for various performance levels.

The limit on S_{X1} in Eq. (11-27a) for the Life Safety Structural Performance Level is based on a proposed assessment procedure by Penner and Elwood (2016). Dynamic wall stability depends on the stiffnesses of the connected diaphragms and is governed by the more flexible of the two connected diaphragms at a given story. The assessment procedure was derived to provide a

consistent probability of collapse based on results from a parametric study of URM wall dynamic stability. The rigid-body rocking model used in the parametric study was calibrated to shake-table collapse tests of six full-scale three-wythe walls in one-way bending. S_{a1} was found to be the best indicator of collapse potential regardless of diaphragm period. Penner and Elwood (2016) assumed 5% damping. Eq. (11-27b) for flexible diaphragms has been adjusted from the Penner and Elwood model to reflect the higher damping levels allowed in ASCE 41 for wood diaphragms (see Section 7.2.3.6). In Eq. (11-27b), the 1.8 value is a 20% increase over Penner and Elwood's (2016) value of 1.5 based on the difference in damping assumptions and the corresponding ratio of response for the suite of ground motions used in that study (Penner 2014). This 20% increase equates to approximately 10% damping using Equation 2-3.

One item not considered by the Penner and Elwood method is the influence of crosswalls. However, the ABK method had included the crosswall effects and they limit amplification of ground motions in higher seismic hazard zones (Kariotis, Elwing, and Johnson, 1985). As noted in the ABK Methodology (ABK 1984), the cross walls act as an inelastic damper for flexible, wood floor systems. As the cross walls increase the damping of the system, an approximate damping of 20% at the level has been assumed, and the damping factor of approximately 1.5 was calculated using Equation 2-3. The 1.5 for 20% damping was divided by the 1.2 increase from the base 10% damping to achieve the cross wall factor of 1.25. This damping increase is only possible for cross walls that occur perpendicular to the masonry walls under consideration and when the diaphragm is constructed of wood. Concrete-framed diaphragms, metal deck diaphragm with structural concrete topping, and bare steel deck diaphragms were specifically excluded from taking advantage of the cross walls in the ABK methodology (ABK 1984).

Probabilities of collapse achieved for different values of C_{pl} and diaphragm stiffnesses are summarized in Table C11-1 based on Penner and Elwood (2016). Values can be interpolated between the table's values for diaphragm stiffness between stiff and flexible.

~~Consideration of possible increases in the probabilities of collapse due to strength and stiffness degradation caused by in-plane actions in URM walls were not included in this research. The provision neglects the expected variations of diaphragm displacements along the spans of the diaphragms, two-way bending action, arching action of walls, interactions with intersecting walls or partitions, all of which are expected to reduce the probabilities of collapse but to an unquantified degree. (Australian Standard for design of unreinforced masonry buildings (AS 3700-2011) provides guidance on consideration of two-way bending, which may be of value to the assessment of walls bounded on three or more sides.) The provision also neglects amplifications of response up the building, but these amplifications are expected to primarily increase short period spectral accelerations, rather than S_{a1}. The effects of varying mortar or masonry unit strengths on collapse probability were beyond the scope of the research. The computer modeling accounted for moderate amounts of spalling at horizontal cracks that form before collapse. The effects of vertical acceleration were not included in this research, but it is expected that its influence on collapse probability is secondary because of the high-frequency, short-period nature of this effect.~~

Table C11-1. Relation between Modification Factor C_{pl} and Probability of Collapse

Probability of Out of Plane Collapse of URM Wall (%)	C_{pl} Factor	
	Stiff Diaphragms	Flexible Diaphragms
5	0.90	0.90
10	1.00	1.00
20	1.15	1.10
50	1.50	1.25

~~While mortar and masonry unit strengths are primary considerations for anchorage performance, other research (Meisl et al. 2007; Lumantarna 2012) suggests that mortar quality and the presence or absence of collar-joint mortar may have little effect on out-of-plane response as long as connection to diaphragms is maintained. However, failures of URM walls in past earthquakes suggest a strong correlation with lack of collar-joint mortar, and low mortar strength, or masonry unit strength, or all three (Deppe 1988; Schmid 1994). Walls with lower strengths may exhibit less integrity and potentially different response characteristics; hence, dynamic stability of cracked walls is not considered reliable for mortar shear strengths less than 30 lb/in.^{2} (206.8 kPa).~~

Penner and Elwood (2016) include no limits on h/t ratios, but some limits may be warranted based on empirical evidence. Empirical data do not exist for h/t values greater than 20. Observations of the acceptable performance of retrofitted URM walls with vertical wall bracing or intermediate wall bracing where h/t ratios are less than 8 in damaging earthquakes with moderate to strong shaking of short durations suggest that 8 is a reasonable lower limit for h/t. Research has not been conducted to determine the effectiveness, required stiffness, and deformation compatibility of wall bracing using vertical bracing members or intermediate wall bracing, but observations from past earthquakes suggest that the latter is less reliable than the former.

Eq. (11-27a) provides an estimate of the ground motion intensity causing collapse of a URM wall adequately attached to the floor diaphragms but without vertical bracing members (strong backs). If the ground motion intensity is exceeded, then vertical bracing members (or similar) should be provided. Spacing of vertical bracing members should be based on ensuring that the vertical bracing can support the inertial forces generated by the out-of-plane URM wall mass. h/t limits based on Eq. (11-27a) should not be used to determine vertical bracing member spacing.

The out-of-plane behavior of URM walls is very complex. A study of past tests, new shake table tests, and over 220,000 parametric runs form the basis of these provisions [Penner, 2014]. These provisions account for diaphragm flexibility, wall overburden pressure, thin walls, cross walls, slenderness ratio, and performance level. However, there are additional variables that can also affect the behavior that have not yet been incorporated. Consideration of possible increases in the probabilities of collapse due to strength and stiffness degradation caused by in-plane actions in URM walls were not included in this research. In addition, the influence of velocity, rather than acceleration, on the wall movement has not been included, though velocity had been the primary parameter in the ABK method. The provision neglects the expected variations of diaphragm displacements and diaphragm response along the spans of the diaphragms, two-way bending action and wall geometry, arching action of walls, and interactions with intersecting walls or partitions, and diaphragms present on both sides of the wall, all of which are expected to reduce the probabilities of collapse but to an unquantified degree. For example, the out-of-plane wall displacements and demands will be less away from the midspan of the diaphragm, thus reducing response of the wall, which would result in less out-of-plane rocking, allowing for potentially higher h/t ratios. (Australian Standard for design of unreinforced masonry buildings (AS 3700-2011) provides guidance on consideration of two-way bending, which may be of value to the assessment of walls bounded on three or more sides.) The provision also neglects amplifications of response up the building, but these amplifications are expected to primarily increase short-period spectral accelerations, rather than S_{a1}. The effects of varying mortar or masonry unit strengths on collapse probability were beyond the scope of the research. The computer modeling accounted for moderate amounts of spalling at horizontal cracks that form before collapse. The effects of vertical acceleration were not included in this research, but it is expected that its influence on collapse probability is secondary because of the high-frequency, short-period nature of this effect.

While mortar and masonry unit strengths are primary considerations for anchorage performance, other research (Meisl et al. 2007; Lumantarna 2012) suggests that mortar quality and the presence or absence of collar-joint mortar may have little effect on out-of-plane response as long as

connection to diaphragms is maintained. However, failures of URM walls in past earthquakes suggest a strong correlation with lack of collar-joint mortar, and low mortar strength, or masonry unit strength, or all three (Deppe 1988; Schmid 1994). Walls with lower strengths may exhibit less integrity and potentially different response characteristics; hence, dynamic stability of cracked walls is not considered reliable for mortar shear strengths less than 30 lb/in.^{2} (206.8 kPa).

4.5 References

ABK, 1981a, *Methodology of Mitigation of Seismic Hazards in Existing Unreinforced Masonry Buildings: Diaphragm Testing*, ABK-TR-03, Agbabian Associates, S.B. Barnes & Associates, and Kariotis & Associates, El Segundo, California.

ABK,1981b, *Methodology of Mitigation of Seismic Hazards in Existing Unreinforced Masonry Buildings: Wall Testing, Out-of-Plane*, ABK-TR-04, Agbabian Associates, S.B. Barnes & Associates, and Kariotis & Associates, El Segundo, California.

ABK, 1984, *Methodology of Mitigation of Seismic Hazards in Existing Unreinforced Masonry Buildings: The Methodology*, ABK-TR-08, Agbabian Associates, S.B. Barnes & Associates, and Kariotis & Associates, El Segundo, California.

Bruneau, M., 1994, "Seismic evaluation of unreinforced masonry buildings—a state-of-the-art report," *Canadian Journal of Civil Engineering*, Volume 21, pp. 512-539.

Deppe, K.,1988, "The Whittier Narrows, California earthquake of October 1, 1987—evaluation of strengthened and unstrengthened unreinforced masonry in Los Angeles City," *Earthquake Spectra*, 4(1), pp. 57–180.

Derakhshan, H., 2011, "Seismic assessment of out-of-plane loaded unreinforced masonry walls," Ph.D. thesis, Faculty of Engineering, Univ. of Auckland, New Zealand.

Dizhur, D., Derakhshan, H., Lumantarna, R., and Ingham, J. M., 2010, "Earthquake-damaged unreinforced masonry building tested in situ," *J. Struct. Eng. Soc.* (SESOC) New Zealand, 23(2), pp. 76–89.

Doherty, K., 2000, *An Investigation of the Weak Links in the Seismic Load Path of Unreinforced Masonry Buildings*, Ph.D. thesis, Dept. of Civil and Environmental Engineering, Faculty of Engineering of the University of Adelaide, Australia.

Doherty, K. T., Rodolico, K. T., Lam, N., Wilson, J., and Griffith, M. C., 2000, "The modeling of earthquake induced collapse of unreinforced masonry walls combining force and displacement principals," *Proceedings of the 12th World Conference on Earthquake Engineering*, Auckland, New Zealand. International Association for Earthquake Engineering, Tokyo.

FEMA, 2009, *Quantification of Building Seismic Performance Factors*, FEMA P695 report, prepared by the Applied Technology Council for the Federal Emergency Management Agency, Washington, D.C.

Griffith, M. C., Magenes, G., Melis, G., and Picchi, L., 2003, "Evaluation of out-of-plane stability of unreinforced masonry walls subjected to seismic excitation," *Journal of Earthquake Engineering,* pp. 141–169.

Kariotis, J.C., Ewing, R.D., and Johnson, A.W., 1985, "Predictions of stability for unreinforced brick masonry walls shaken by earthquakes," *Proceedings of the 7th International Brick Masonry Conference*, Melbourne, Sydney, pp. 1175-1184.

Lam, N., Wilson, J., and Hutchinson, J., 1995, "The seismic resistance of unreinforced masonry cantilever walls in low seismicity areas," *Bulletin of the New Zealand National Society of Earthquake Engineering*, 28(3), pp. 179-195.

Lumantarna, R., 2012, *Material Characterisation of New Zealand Unreinforced Masonry Buildings*, Ph.D. thesis, University of Auckland, New Zealand.

Makris, N., and Konstantinidis, D., 2003, "The rocking spectrum and the limitations of practical design methodologies," *Earthquake Engineering and Structural Dynamics*, 32(2), pp. 265–289.

Meisl, C., Elwood, K., and Ventura, C., 2007, "Shake table tests on the out-of-plane response of unreinforced masonry walls," *Canadian Journal of Civil Engineering*, 34(11), pp. 1381–1392.

Penner, O., 2014, *Out-of-Plane Dynamic Stability of Unreinforced Masonry Walls Connected to Flexible Diaphragms*, Ph.D. thesis, The Faculty of Graduate and Postdoctoral Studies (Civil Engineering), The University of British Columbia.

Penner, O., and Elwood, K. J., 2011, "Effect of diaphragm flexibility on seismic vulnerability of out-of-plane unreinforced masonry walls subjected to ground motions from the 2010 Darfield earthquake." *Proceedings of the 9th Australasian Masonry Conference*, February 15–18, Queenstown, New Zealand.

Penner, O. and Elwood, K., 2016a, "Out-of-Plane Dynamic Stability of Unreinforced Masonry Walls in One-Way Bending: Shake Table Testing," *Earthquake Spectra*, Vol. 32, No. 3, pp. 1675-1697.

Penner, O. and Elwood, K, 2016b, "Out-of-plane dynamic stability of unreinforced masonry walls in one-way bending: parametric study and assessment guidelines," *Earthquake Spectra*, Vol. 32, No. 3, pp. 1699-1723.

Schmid, B., 1994, "URM/UMB and wood buildings, The Northridge earthquake, January 17, 1994." Seminar notes, Structural Engineers Association of California, Sacramento.

Sharif, I., Meisl, C., and Elwood, K. J., 2007, "Assessment of ASCE 41 height to thickness ratio limits for URM walls," *Earthquake Spectra*, 23(4), 893–908.

Simsir, C. C., Ashheim, M. A., and Abrams, D. P., 2004, "Out-of-plane dynamic response of unreinforced masonry bearing walls attached to flexible diaphragms," *Proceedings of the 13th World Conference on Earthquake Engineering*, Vancouver, British Columbia, International Association for Earthquake Engineering, Tokyo.

Sorrentino, L., Kunnath, S., Monti, G., and Scalora, G., 2008, "Seismically induced one-sided rocking response of unreinforced masonry façades," *Eng. Struct.,* 30(8), 2140–2153.

Chapter 5: Addition of Redistribution Provisions for Walls in Section 11.3.2.3.1

5.1 Motivation

Recent earthquakes in New Zealand resulted in extensive damage to URM structures and a renewed interest in evaluation and retrofit of URM buildings. The change proposal is based on assessment guidelines published in New Zealand in 2017 (NZSEE, 2017) and allows redistribution of forces between URM wall piers when they are governed by deformation-controlled actions and analyzed using linear procedures. The New Zealand guidelines permit up to 50% redistribution on wall piers assessed with component ductility capacities analogous to the primary Life Safety acceptance criteria in ASCE/SEI 41-17 Table 11-3. Permitting a similar approach in ASCE/SEI 41-23 for deformation-controlled lines of resistance in the linear procedures of Chapter 11 can allow the user to better utilize the total strength of a line of resistance and is generally consistent with observations of response from nonlinear analyses.

5.2 Summary of Changes Recommended

The changes occur in ASCE/SEI 41-17 Section 11.3.2.3.1 and Commentary Section C11.3.2.3.1 and introduce an application of load sharing or redistribution of forces for deformation-controlled primary wall piers in the same line of resistance when analyzed using linear procedures for in-plane wall actions. The proposal does not delete or modify existing linear analysis provisions; rather, the proposal adds new language to allow up to 20% redistribution of forces for the Collapse Prevention Structural Performance Level under certain circumstances.

5.3 Technical Studies

5.3.1 Mixed Modes of Response

Mixed modes of response, including deformation-controlled and force-controlled actions are commonly encountered in components within the same line of resistance, such as perforated concrete or masonry walls. Deformation-controlled actions can be further classified as flexure, rocking (for unreinforced masonry) or shear-controlled modes of response. For linear procedures, ASCE/SEI 41-17 does not prescribe specific requirements for evaluating mixed modes of response in the same line of resistance and relies upon the component-level evaluation procedures within the material chapters, combined with demands obtained in accordance with the analysis requirements and limitations of Chapter 7. An exception is that ASCE/SEI 41-17 Section 11.3.2.3 requires that rocking wall piers be neglected in lines of resistance that are not classified as all

deformation-controlled. This approach assumes that the performance of lines of resistance with mixed modes of response can be reliably estimated using linear analysis procedures, subject to the prescribed limitations. Linear analysis methods do not explicitly account for changes in stiffness once yielding or force-controlled behaviors initiate and rely upon the acceptance criteria and other provisions to evaluate if the performance is acceptable. This assumption and limitations could be validated for perforated concrete and masonry walls by comparison with nonlinear analysis procedures; however, this was beyond the scope of the study.

This approach differs from that prescribed in the system-specific procedures of ASCE/SEI 41-17 Chapter 16, which utilizes an iterative procedure to classify all wall piers in a line of resistance as rocking, shear-controlled or not contributing (if rocking-controlled in an otherwise shear-controlled line of resistance.) The Chapter 16 procedure can be readily implemented by hand or spreadsheet-based analysis methods. It does not consider force-controlled actions and is limited to use for the Collapse Prevention performance objective at the BSE-1E seismic hazard.

In general, nonlinear analysis of deformation-controlled frames and walls indicates that elastic forces estimated by linear analysis tend to redistribute once yielding in one or more components initiates. The concept of redistribution is permitted by ACI 318-14 by up to 20% for ductile, continuous flexural concrete members and assessment guidelines published in New Zealand for unreinforced masonry buildings in *The Seismic Assessment of Existing Buildings: Technical Guidelines for Engineering Assessments* (NZSEE, 2017). This can result in a more effective utilization of all components in a deformation-controlled line of resistance.

To demonstrate the application of linear analysis procedures to the evaluation of mixed modes of response in the same wall line, an archetypical wall line with four wall piers was studied. The wall piers exhibited mixed modes of response, including rocking (R), bed-joint sliding (BS), toe crushing (TC) and diagonal tension (DT). Additionally, the wall line was used to test the application of the redistribution concept. Refer to Figures 5-1 and 5-2.

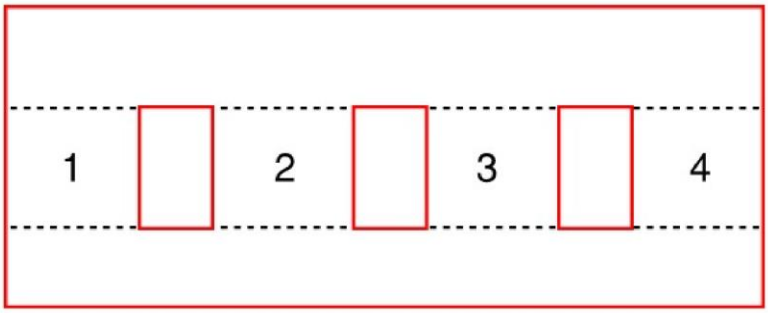

Figure 5-1 Archetypical wall line.

Wall lines with mixed modes of response that are all deformation-controlled (i.e., rocking and bed-joint sliding) are permitted to be evaluated using the corresponding *m*-factors for each action, as illustrated by Figure 5-2. The governing capacity is underlined in red. This specific example was used for validation of the redistribution proposal, as detailed below.

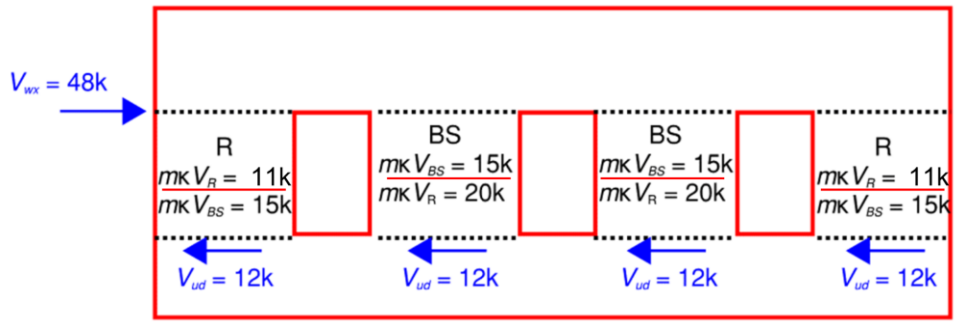

Figure 5-2 Mixed modes: all deformation-controlled.

As illustrated by Figure 5-2, a notional shear force of 48 kips was applied to the line of resistance and distributed equally to the four wall piers due to their equal stiffness (fixed-fixed wall piers.) The end wall piers are classified as rocking-controlled (R), due to the lower relative axial dead load, and the two interior wall piers are classified as bed-joint sliding-controlled (BS). The effective rocking and bed-joint sliding capacities, inclusive of the *m*-factor and κ-factor are listed for each wall pier. The two interior wall piers are acceptable, as the demands are less than the associated capacities. The two exterior wall piers are not acceptable, as the demands on each pier are 1 kip greater than the capacities. The total capacity of the line of resistance is 52 kips (11 kips x 2 exterior piers plus 15 kips x 2 interior piers), which is 4 kips greater than the total applied shear force. If redistribution of forces were permitted between the wall piers, this line of resistance could be found to satisfy the Performance Objective.

Additionally, conditions with mixed modes of response that include a combination of deformation-controlled (e.g., rocking (R) and bed-joint sliding (BS)) and force-controlled (e.g., diagonal tension (DT)) actions were also studied. Refer to Figure 5-3. Due to the brittle (non-ductile) performance of the force-controlled actions, it was determined that the redistribution concept should not be applied to such conditions. This is consistent with the recommendations of the NZSEE (2007) guidelines that only permit redistribution to be applied when all wall piers are deformation-controlled.

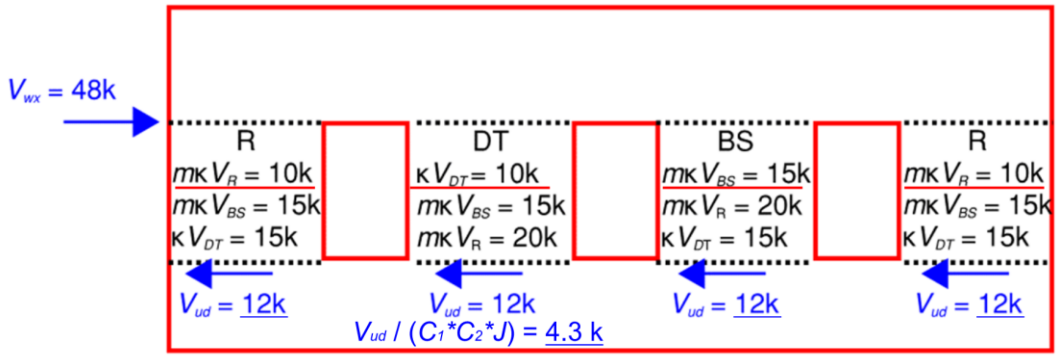

Figure 5-3 Mixed modes: deformation-controlled and force-controlled.

As illustrated by Figure 5-3, the demands on the exterior rocking (R) wall piers are greater than their capacities, while the interior wall piers are governed by Diagonal Tension (DT) and Bed-Joint Sliding (BS), with 5.7 and 3 kips of reserve capacity, respectively. Note that the demand on the DT pier is reduced by C_1C_2J (C_1*C_2 = 1.4, J = 2.0) for a force-controlled action. Thus, the total effective demand on the line of resistance is 40.3 kips (12 + 4.3 + 12 + 12 kips), which is 4.7 kips less than the total capacity of 45 kips (10 + 10 + 15 + 10 kips). However, as the demands on the exterior wall piers exceed their capacities, these piers and the line of resistance do not satisfy the Performance Objective, despite the total demand on the line of resistance being less than the total capacity.

Additionally, ASCE/SEI 41-17 Section 11.3.2.3 requires that the contribution of rocking wall piers be neglected in lines of resistance that are not classified as all deformation-controlled. This increases the demands on the interior wall piers to 24 kips each as illustrated by Figure 5-4.

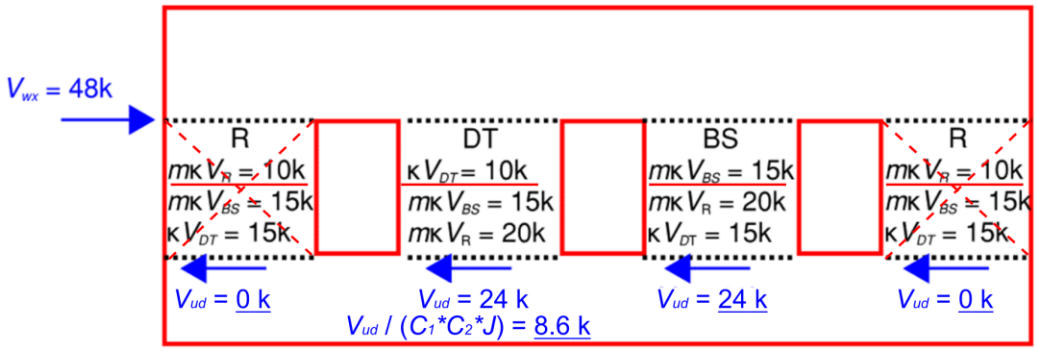

Figure 5-4 Mixed modes: deformation-controlled and force-controlled, considering ASCE/SEI 41-17 Section 11.3.2.3: exclude rocking wall piers.

The total capacity of the two remaining interior wall piers is 25 kips (10 + 15 kips). The effective demand on the DT wall pier is 8.6 kips (accounting for C_1C_2J), which is less than the capacity of 10 kips. The demand on the BS wall pier is 24 kips, which is 60% greater than the capacity of 15 kips. Thus, even if redistribution of load between the DT and BS wall piers were permitted, there is insufficient total capacity to satisfy the Performance Objective.

The requirement of ASCE/SEI 41-17 Section 11.3.2.3 to exclude rocking wall piers from lines of resistance that are not classified as all deformation-controlled is a key limitation of the linear procedures. The commentary to Section 11.3.2.3 does not explain the basis for the limitation; however, it is surmised that this is due to the incompatibility of deformations between rocking and force-controlled actions such as diagonal tension (ie flexible versus relatively stiff) and the potential for the capacity of the force-controlled action being exceeded prior to the rocking capacity being fully developed.

It is unclear if this limitation on mixed-modes of deformation-controlled and force-controlled wall piers on an individual pier leads to overly conservative outcomes for linear procedures (i.e., non-conformance or retrofit.) The interaction of mixed-modes could be investigated with nonlinear analysis, whereby changes in strength, stiffness and load distribution are explicitly accounted for.

This could lead to additional commentary on evaluation of mixed-modes and, possibly, improved linear provisions.

Additionally, the absence of any force-controlled checks in Chapter 16 flowchart procedure may lead to unconservative outcomes and is recommended for further investigation.

5.3.2 Case Study

An additional case study of mixed modes of response was also undertaken on an existing building located in a high-seismic region of Northern California. The study was used to compare the ASCE/SEI 41-17 Chapter 16 (Special Procedure) outcomes with the Chapter 11 provisions. The Chapter 16 provisions evaluate wall lines in aggregate, compared with the component-based approach per Chapter 11.

Demands were obtained based upon the BSE-1E seismic hazard and distributed to the wall piers based upon their relative rigidities, per the requirements of Chapters 11 and 16. The building has flexible diaphragms and two, generally similar, exterior lines of resistance in the longitudinal direction evaluated. The results of this study are summarized in Figures 5-5 and 5-6.

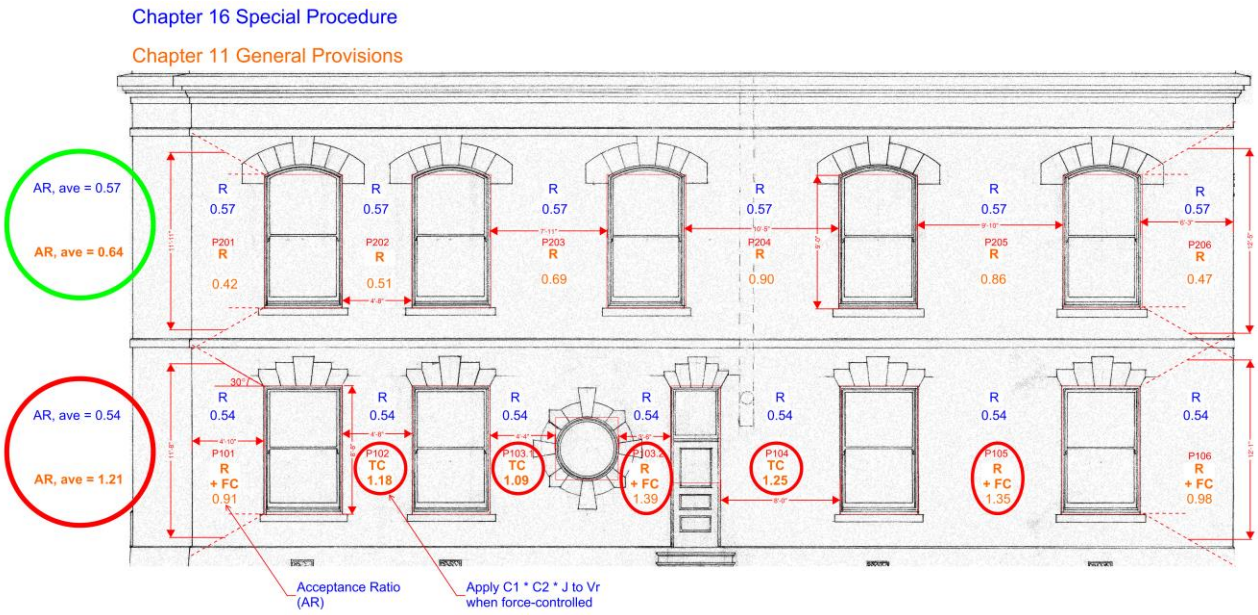

Figure 5-5 Case study: mixed modes: deformation and force-controlled.

As illustrated by Figure 5-5, all second-floor wall piers are rocking-controlled (i.e., deformation-controlled), with similar Acceptance Ratios (AR) on average between the Chapter 11 and 16 procedures. All first-floor wall piers are force-controlled per the Chapter 11 procedures due to relatively high axial load ratios. If the assumed f'_m is set higher than initially assumed (e.g., 900 psi versus 600 psi) then the first-floor wall piers can all be reclassified as deformation-controlled, as illustrated by Figure 5-6.

Per the Chapter 16 procedure, when a line of resistance is classified as rocking-controlled, the AR is determined based on the sum of all contributing wall piers, thus the same AR is reported for all wall piers at each floor. Following the Chapter 16 procedure, all wall piers are rocking-controlled at both the first and second floors, with ARs of 0.54 and 0.57, respectively, as illustrated by Figures 5-5 and 5-6. The ASCE/SEI 41-17 Chapter 16 procedures do not have axial load or f'_m limits for evaluation of existing wall piers; therefore, the Chapter 16 ARs are identical between Figures 5-5 and 5-6. Consideration of axial load limits for the Chapter 16 procedures was beyond the scope of this technical change proposal but may be a topic for future study.

Assuming f'_m equal to 900 psi, the resultant average Acceptance Ratios are comparable between the two procedures and indicate an acceptable outcome (i.e., average and maximum ARs less than 1.0) per Figure 5-6.

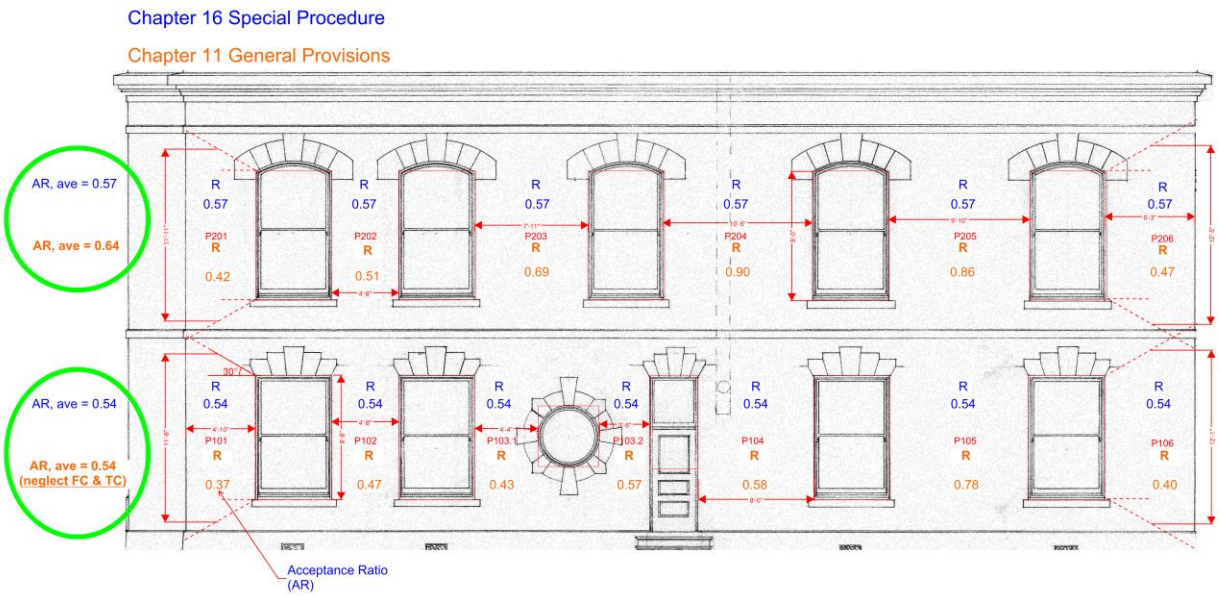

Figure 5-6 All rocking-controlled (deformation-controlled), f'_m = 900 psi.

The case study showed that similar overall evaluation outcomes are achieved using the Chapter 11 and 16 procedures, provided that the more rigorous force-controlled provisions of Chapter 11 do not apply. The aggregate evaluation approach used by Chapter 16 is analogous to the redistribution concept and results in a more effective utilization of all deformation-controlled wall piers in a line of resistance compared with Chapter 11 where each pier is evaluated independently. The latter approach can result in one or two wall piers governing the evaluation on a single line of resistance and the overall building evaluation, even if adjacent wall piers have additional deformation capacity.

5.3.3 Implementation of Redistribution Concept

The change proposal to permit redistribution is based on assessment guidelines published in NZSEE (2017). Similar to the NZSEE (2017) guidelines, the proposal to permit redistribution only applies to lines of resistance where all wall piers are classified as deformation-controlled.

As ASCE/SEI 41-17 Chapter 11 also has provisions for the Collapse Prevention Structural Performance Level and secondary components, the maximum redistribution is capped at 20% (compared with 50% in the New Zealand guidelines) and limited to primary components only. The 20% limit is based on case studies of archetypical wall pier configurations that indicate a reasonable benefit to this level of redistribution, while also noting that ASCE/SEI 41-17 permits the user to consider using secondary acceptance criteria or nonlinear procedures. The New Zealand guidelines do not provide secondary acceptance criteria. Criteria for the Life Safety and Immediate Occupancy Structural Performance Levels are also included.

As an example of permitted redistribution, the wall line from Figure 5-2, with a total shear demand Q_{UD} = 48 kips, is being evaluated for the Collapse Prevention Structural Performance Level, as illustrated by Figure 5-7. Each pier is of equal stiffness, so they each attract 12 kips. The two exterior wall piers are rocking controlled with Q_{CE} = 11 kips, and two interior piers are controlled by bed-joint sliding with Q_{CE} = 15 kips. All wall piers in the line are therefore deformation-controlled. Initially, the wall line would have Acceptance Ratios of 12 kips /11 kips = 1.09 and 12 kips / 15 kips = 0.80, for rocking and bed-joint sliding piers, respectively, and would thus not satisfy the target Performance Objective. Redistribution is permitted up to a 20% increase or decrease in any wall pier, and the total demand on the wall line remains the same. In this wall line, it would be permitted to redistribute 2 kips from the piers governed by rocking to those governed by bed-joint sliding. This would change the demands on the piers governed by rocking to 12 kips – 2 kips = 10 kips and to those governed by bed-joint sliding to 12 kips + 2 kips = 14 kips. Acceptance Ratios would be revised to 10 kips / 11 kips = 0.91 and 14 kips / 15 kips = 0.93, for rocking and bed-joint sliding piers, respectively, thus satisfying the Performance Objective. The change in the rocking piers would be |(10 kips - 12 kips) / 12 kips| = 17%, and the change in the bed-joint sliding piers would be |(14 kips – 12 kips) / 12 kips| = 17%. Both values are below the 20% limit permitted for Collapse Prevention.

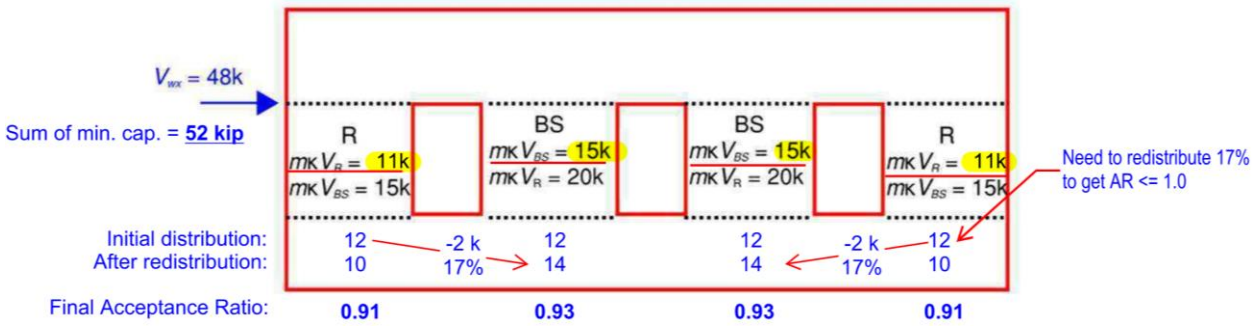

Figure 5-7 Redistribution example.

5.3.4 Conclusions

The proposed approach described above introduces a reasonable application of load sharing or redistribution of forces for deformation-controlled primary wall piers in the same line of resistance when analyzed using linear procedures for in-plane wall actions. An example is provided for wall lines with mixed modes of behavior that include deformation-controlled and force-controlled piers. Future

study is recommended to develop techniques to better address lines with mixed modes of behavior using linear analysis.

5.4 Recommended Changes

Note about Change Proposals

This report documents aspects of change proposals as they were submitted to subcommittees of ASCE's *Seismic Retrofit of Existing Building Standards* Committee. Often, these change proposals were revised, in some cases substantively, by these subcommittees before they were adopted into ASCE/SEI 41-23. Readers should not rely on this report for information about the final version of provisions in ASCE/SEI 41-23.

The strikeout/underline proposed changes to ASCE/SEI 41-17 Sections 11.3.2.3.1 and Commentary Section 11.3.2.3.1 are shown verbatim below. No text has been revised or stricken as part of this proposal; all of the changes involve new text, shown in blue.

SCOPE – ASCE 41-17 Section 11.3.2.3 Acceptance Criteria for URM In-Plane Actions

11.3.2.3 *Acceptance Criteria for URM In-Plane Actions.* In-plane lateral shear of unreinforced masonry walls and wall piers in each line of resistance shall be considered a deformation-controlled action if the expected lateral rocking strength or bed-joint sliding strength of each wall or wall pier in the line of resistance, as specified in Sections 11.3.2.2.1 and 11.3.2.2.2, is less than the lower-bound lateral strength of each wall or wall pier limited by diagonal tension or toe crushing, as specified in Sections 11.3.2.2.3 and 11.3.2.2.4. URM walls that do not meet the criteria for deformation-controlled components shall be considered force-controlled components. Expected rocking strength, V_r, as specified in Section 11.3.2.2.1, shall be neglected in lines of resistance not considered deformation controlled. Axial compression on URM wall components shall be considered a force-controlled action.

11.3.2.3.1 Linear Procedures for In-Plane URM Wall Actions.

For the linear procedures in Sections 7.4.1 and 7.4.2, component actions shall be compared with capacities in accordance with Section 7.5.2.2. When in-plane URM wall response is governed by bed-joint sliding, V_{bjs1} shall be used when assessing component behavior. The m-factors for use with corresponding expected strength shall be obtained from Table 11-3. If v_{tL} is less than 30 lb/in.^{2} (206.8 kPa), the wall or wall pier shall be classified as force controlled or repointed in accordance with Section 11.2.2.5 and retested in accordance with Section 11.2.3.6 to demonstrate that v_{tL} is greater than or equal to 30 lb/in.^{2} (206.8 kPa). Alternatively, m-factors for walls or wall piers with v_{tL} less than 30 lb/in.^{2} (206.8 kPa) shall be based on experimentally obtained response characteristics of representative wall subassemblies in accordance with Section 7.6.

For individual lines of resistance where all wall piers are considered deformation-controlled for in-plane actions and classified as primary, it shall be permitted to redistribute forces between wall piers within the same line of resistance. Redistribution of forces from or to any individual wall pier shall not exceed 20% for Collapse Prevention, 15% for Life Safety, and 0% for Immediate Occupancy, using absolute values. The total demand resisted by the line of resistance shall remain unchanged. Diaphragms and collectors shall be evaluated to transfer the redistributed forces to each wall pier.

C11.3.2.3 *Acceptance Criteria* for URM In-Plane Actions.

The sequence of in-plane actions is difficult to model reliably, particularly when actions have similar strengths or when combinations of actions can occur in one or more piers. Bidirectional effects are also difficult to quantify reliably. The most commonly observed seismic threat posed by URM walls is falling material caused by in-plane shear damage or out-of-plane collapse caused by instability. Stiffness degradation caused by in-plane shear failures adds to the probability of out-of plane instability of the URM walls. Typically, out-of-plane failures initiate earlier than failures caused by in-plane actions.

C11.3.2.3.1 Linear Procedures for In-Plane URM Wall Actions.

m-factors in Table 11-3 are generally based on response characteristics of wall subassemblages with lower-bound bed-joint shear strengths greater than or equal to 30 lb/in.^{2} (206.8 kPa). Walls with lower-strength mortars may exhibit less integrity and potentially different response characteristics and m-factors than are given in Table 11-3.

Rocking. The revisions to Table 11-3 compared with Table 7-3 of ASCE 41-06 are based on test results of individual URM piers that had rocking as primary modes of response and had sufficient information to estimate yield drifts, maximum tested drifts, and axial stress ratios. The maximum m-factors are based on approximately 0.75 times the ratios of maximum tested drift to observed yield drift, and they account for pier aspect ratios. The maximum m-factors are a proxy for limiting allowable drifts of rocking piers. Test results consistently indicate that m-factors are reduced with increased wall and pier axial forces. The m-factors in ASCE 41-06 were generally based on lightly axially loaded piers. The m-factors for primary elements remain the same as those in Table 7-3 of ASCE 41-06, but a new restriction has been added to cap the axial stress ratios in rocking walls and piers because test results indicate that the m-factors generated from test results on piers that have stress ratios beyond this cap are less than the tabulated values. The m-factors for secondary elements have been reduced from the values in Table 7-3 of ASCE 41-06 to correlate with test results and the axial stress ratio limit (Xu and Abrams 1992; Magenes and Calvi 1995; Anthoine et al. 1995; Costley and Abrams 1996; Franklin et al. 2001; Paquette and Bruneau 2003; Yi et al. 2004; Moon et al. 2006).

For guidance on evaluating the adequacy of solid bonded headers in multi-wythe solid brick rocking walls and wall piers, see Section C11.3.2.1.

Sliding. The use of V_{bjs1} provides reasonable estimates of the deformation capacities of walls and wall piers undergoing sliding action when using linear procedures. Strengths eventually reduce to residual bed-joint sliding strengths, V_{bjs2}, after experiencing relatively large deformations, generally well beyond the limits imposed by linear procedures.

Redistribution of forces is an application of Load Sharing, as defined by Chapter 1, and can allow better utilization of the total strength of a line of resistance. This behavior is explicitly captured in nonlinear procedures and is approximated in the linear procedures by allowing limited redistribution of forces between wall piers on deformation-controlled lines of resistance. This approach is similar to that permitted by other guidelines for linear analysis of deformation-controlled lines of resistance with URM wall piers (NZSEE et al, 2017.) Alternatively, the user is permitted to consider whether components can be classified as secondary, in accordance with Chapter 7, and evaluated accordingly. The diaphragm and collector evaluation should be based upon the forces that are required to be transferred to each wall pier, including effects of redistribution. Spandrels are required to be evaluated by Section 11.3.2.2.6, including consideration of any applied axial stresses.

For an individual line of resistance where redistribution is permitted to be applied, the provisions can be expressed algebraically using Eq. (C11-X) and (C11-Y):

For the wall line:

$$\sum_i^n V_{i,initial} = \sum_i^n V_{i,initial} \quad \text{(C11-X)}$$

For any individual wall pier in the wall line, for Collapse Prevention:

$$\left| (V_{i,redistributed} - V_{i,initial}) \right| / V_{i,initial} \le 20\% \quad \text{(C11-Y)}$$

where:

$V_{i,initial}$ = calculated shear force prior to redistribution in wall pier i

$V_{i,redistributed}$ = shear force after redistribution in wall pier i

n = total number of wall piers in the line of resistance

5.5 References

Anthoine, A., Magonette, G, and Magenes, G., 1995, "Shear compression testing and analysis of brick masonry walls," 10th European Conference on Earthquake Engineering, Rotterdam, The Netherlands, 1657-1662.

Costley, A. and Abrams, D., 1996, "Dynamic response of unreinforced masonry buildings with flexible diaphragms," Rep. No NCEER-96-0001, Multidisciplinary Center for Earthquake Engineering Research, State University of New York, Buffalo.

Franklin, S., Lynch, J., and Abrams, D., 2001, *Performance of rehabilitated URM shear walls: Flexural behavior of piers*, Dept. of Civil Engineering, University of Illinois at Urbana-Champaign, Urbana, Illinois.

Magenes, G., and Calvi, G., 1995, "Shaking table tests on brick masonry walls," *Proceedings, 10th European Conference on Earthquake Engineering*, Vol. 3, Vienna, Austria, 2419-2424.

Moon, F., Yi, T., Leon, R., and Kahn, L., 2006, "Recommendations for seismic evaluation and retrofit of low-rise URM structures," *Journal of Structural Engineering*, 132(5), 663-672.

NZSEE, 2017, *The Seismic Assessment of Existing Buildings: Technical Guidelines for Engineering Assessments*, New Zealand Society for Earthquake Engineering (NZSEE), Structural Engineering Society New Zealand, New Zealand Geotechnical Society, New Zealand Ministry of Business, Innovation and Employment, Earthquake Commission [New Zealand], https://www.eq-assess.org.nz/.

Paquette, J., and Bruneau, M., 2003, "Pseudo-dynamic testing of unreinforced masonry building with flexible diaphragm," *Journal of Structural Engineering*, 129(6), 708-716.

Xu, W., and Abrams, D., 1992, “Evaluation of lateral strength and deflection for cracked unreinforced masonry walls,” Report No. 92-26-11, Advanced Construction Technology Center, College of Engineering, University of Illinois, Urbana.

Yi et al., 2004, [Note: This ASCE/SEI 41-17 reference citation does not match the available references in the ASCE/SEI 41-17 reference list. It is possible that the intended citation is Yi, 2004, “Experimental investigation and numerical simulation of an unreinforced masonry structure with flexible diaphragms,” Ph.D. thesis, Georgia Institute of Technology, Atlanta.]

Chapter 6: Revisions to Chapter 11 URM Rocking Axial Stress Provisions

6.1 Motivation

For linear procedures, the *m*-factors for rocking are defined as a function of axial load with a force-controlled limit based on available testing described in ASCE/SEI 41-17 Commentary Section C11.3.2.3.1 and Tremayne et al. (2012). The acceptance criteria for rocking in ASCE/SEI 41-17 Table 11-3 were originally calibrated for a maximum axial load ratio, f_a/f_m', of 4%. Wall piers with axial load ratios greater than 4% are classified as force-controlled.

Anecdotal feedback from users of the provisions were that this limit was occasionally arising as a limitation of the linear procedures for archetypical buildings, due to axial load ratios being slightly greater than 4%. The test data used to generate the *m*-factors in ASCE/SEI 41-13 were reexamined to determine if additional acceptance criteria could be provided for axial load ratios greater than 4%. In general, it was found that the *m*-factor decreases as the axial load ratio increases.

6.2 Summary of Changes Recommended

In summary, the *m*-factors for rocking can be conservatively halved at an axial load ratio of 8%, with a maximum value of 3.0. Interpolation is permitted for axial load ratios between 4% and 8%.

The recommended changes affect the *m*-factors for rocking in ASCE/SEI 41-17 Section 11.3.2.3.1 that appear in Table 11-3. The specific revisions are in Footnote b of ASCE/SEI 41-17 Table 11-3. This is accompanied by a minor addition to ASCE/SEI 41-17 Commentary Section 11.3.2.2.1, *Expected In-Plane Rocking Strength of URM Walls and Wall Piers.*

An editorial correction to the title of Table 11-3 is also proposed, as the acceptance criteria are applicable to any type of linear analysis permitted by Chapter 7 of ASCE/SEI 41-17. This is consistent with the definition of all other linear acceptance criteria in the standard.

6.3 Technical Studies

The current recommended changes are based on a reexamination of the test data used to develop the *m*-factors values that first appeared in ASCE/SEI 41-13 Table 11-3 and work described in a paper by Tremayne et al. (2012).

The acceptance criteria for rocking in Table 11-3 of ASCE/SEI 41-17 were calibrated for a maximum axial load ratio, f_a/f'_m, of 4%. The test data used to generate the *m*-factors that first appeared in

ASCE/SEI 41-13 Table 11-3 and described by Tremayne et al. (2012) were reexamined as presented in Figure 6-1.

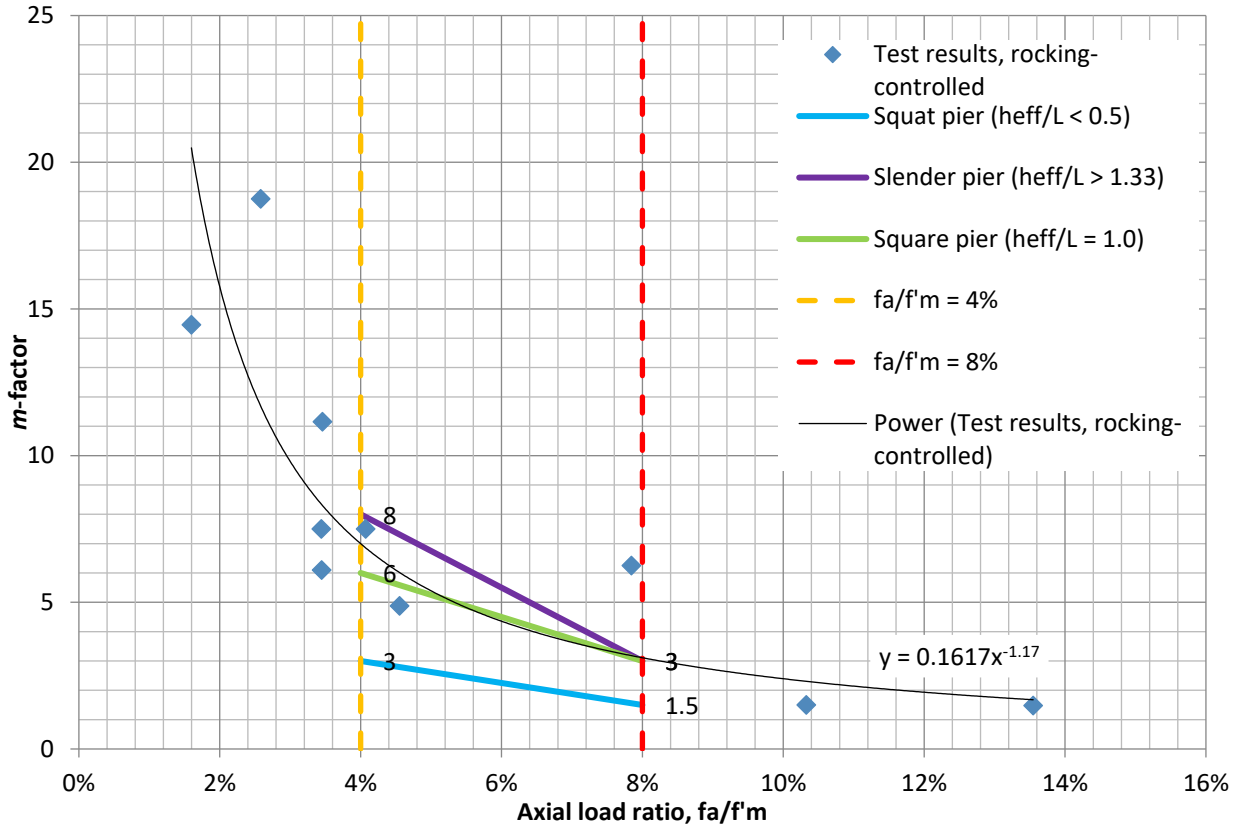

Figure 6-1 *m*-factor versus axial load ratio.

Figure 6-1 illustrates that the *m*-factor decreases as the axial load ratio increases (i.e., ductility capacity is inversely proportional to axial load.) Linear relationships to establish the *m*-factor as a function of wall pier aspect ratio (i.e., consistent with ASCE/SEI 41-17 Table 11-3) are plotted between the 4 and 8% axial load ratios. Note that the *m*-factors are taken as 0.75 times the corresponding nonlinear acceptance criteria, in accordance with ASCE/SEI 41-17 Section 7.6.

Based on the linear relationships illustrated on Figure 6-1, the *m*-factors at 8% axial load ratio are established as follows:

- Square (h_{eff}/L = 1.0) and squat (h_{eff}/L < 0.5) wall piers have an *m*-factor equal to one-half of that at 4% axial stress ratio.
- Slender (h_{eff}/L > 1.33) wall piers have an *m*-factor equal to that of the square pier at 8% axial load ratio. This also aligns with the best-fit curve. This effectively caps the *m*-factor at 3.0.

Extrapolation of the three linear relationships beyond 8% axial load ratio implies *m*-factors of 1.5 or less at 10% axial load ratio. These criteria are likely slightly conservative, as two test results indicate

an *m*-factor of 1.5 at axial load ratios greater than 10%; however, given the limited results (i.e., fewer than three beyond 8%), it was determined that this was insufficient to reliably establish any ductility capacity for axial load ratios greater than 8%.

6.4 Recommended Changes

Note about Change Proposals

This report documents aspects of change proposals as they were submitted to subcommittees of ASCE's *Seismic Retrofit of Existing Building Standards* Committee. Often, these change proposals were revised, in some cases substantively, by these subcommittees before they were adopted into ASCE/SEI 41-23. Readers should not rely on this report for information about the final version of provisions in ASCE/SEI 41-23.

The strikeout/underline proposed changes to ASCE/SEI 41-17 Sections 11.3.2.3.1 and Commentary Section 11.3.2.3.1 are shown verbatim below. New or modified text is shown in blue. Existing text that has been relocated is shown in green.

SCOPE – ASCE 41-17 Section 11.3.2.3 Acceptance Criteria for URM In-Plane Actions

11.3.2.3 *Acceptance Criteria for URM In-Plane Actions.*

In-plane lateral shear of unreinforced masonry walls and wall piers in each line of resistance shall be considered a deformation-controlled action if the expected lateral rocking strength or bed-joint sliding strength of each wall or wall pier in the line of resistance, as specified in Sections 11.3.2.2.1 and 11.3.2.2.2, is less than the lower-bound lateral strength of each wall or wall pier limited by diagonal tension or toe crushing, as specified in Sections 11.3.2.2.3 and 11.3.2.2.4. URM walls that do not meet the criteria for deformation-controlled components shall be considered force-controlled components. Expected rocking strength, Vr, as specified in Section 11.3.2.2.1, shall be neglected in lines of resistance not considered deformation controlled. Axial compression on URM wall components shall be considered a force-controlled action.

11.3.2.3.1 *Linear Procedures for In-Plane URM Wall Actions.*

For the linear procedures in Sections 7.4.1 and 7.4.2, component actions shall be compared with capacities in accordance with Section 7.5.2.2. When in-plane URM wall response is governed by bed-joint sliding, Vbjs1 shall be used when assessing component behavior. The m-factors for use with corresponding expected strength shall be obtained from Table 11-3. If vtL is less than 30 lb/in.2 (206.8 kPa), the wall or wall pier shall be classified as force controlled or repointed in accordance with Section 11.2.2.5 and retested in accordance with Section 11.2.3.6 to demonstrate that vtL is greater than or equal to 30 lb/in.2 (206.8 kPa). Alternatively, m-factors for walls or wall piers with v_{tL} less than 30 lb/in.^{2} (206.8 kPa) shall be based on experimentally obtained response characteristics of representative wall subassemblies in accordance with Section 7.6.

Table 11-3. Linear ~~Static~~ Procedure: m-Factors for URM In-Plane Walls, Wall Piers, and Spandrels

Limiting Behavioral Mode	Performance Level				
	Primary			Secondary	
	IO	LS	CP	LS	CP
Wall and Wall Pier Rocking[a,b]	$1 \le 1.5\ h_{eff}/L \le 1.5$	$1.5 \le 3\ h_{eff}/L^{b} \le 3.75$	$2 \le 4\ h_{eff}/L^{b} \le 5$	$2 \le 4\ h_{eff}/L^{b} \le 5$	$3 \le 6\ h_{eff}/L^{b} \le 8$
Wall and Wall Pier Bed-joint sliding	1	3	4	6	8
Spandrels with Prismatic Lintels	1	1.7	2.2	7.5	10
Spandrels with Shallow Arch Lintels	1	1.7	2.2	4.2	5.6

[a] All rocking-controlled walls and wall piers shall comprise a minimum thickness of 6 in. and, for solid brick masonry, a minimum of two wythes. Multi-wythe solid brick masonry walls and wall piers shall be connected with bonded solid headers.

[b] Tabulated m-factors for rocking apply only for walls and wall piers with f_a/f_m' ratios less than or equal to 4%. For walls and wall piers with f_a/f_m' ratios equal to 8%, the m-factor shall be taken as 50% of the tabulated value but shall not exceed 3.0 and need not be less than 1.0. Linear interpolation shall be used for f_a/f_m' ratios between 4% and 8%. Walls and wall piers with f_a/f_m' ratios greater than 8%~~; otherwise, walls and wall piers~~ shall be considered force controlled, unless it can be demonstrated by analysis using moment curvature or other acceptable means that toe crushing does not occur at the expected pier drift. Alternatively, nonlinear procedures and acceptance criteria should be used, in accordance with Section 11.3.2.3.2.

C11.3.2.2.1 Expected In-Plane Rocking Strength of URM Walls and Wall Piers.

Different methods of modeling the effective height of masonry piers are found in the literature. The rocking equation for expected lateral strength is a revised equation from ASCE 41-06, Eq. (11-8), that explicitly incorporates the weight of the wall or pier and its location. The factor 0.9 is an approximation that accounts for the difference in total pier length compared with the distance between the tension end of the pier and the location of the compression centroid. More accurate estimates of the location of the compression centroid can be used consistent with TMS 402 or can be considered explicitly within a nonlinear analysis building model or component-level moment-curvature analysis.

Assumptions of fixity or cantilever action depend on the stiffness and overall integrity of the spandrels above and below rocking piers. The potential for spandrel uplift along a line of resistance caused by pier rocking and effects of vertical seismic acceleration can also significantly affect pier response (Fig. C11-4). The complete uplift of a spandrel from a pier can result in a loss of stability and shall not be permitted unless an alternate means of maintaining stability is provided.

For URM walls with openings of differing sizes and relatively weaker piers compared with stronger spandrels, Moon (2004) recommends that the effective height of each rocking pier be represented

as the height over which a diagonal compression strut is most likely to develop in the pier at the steepest possible angle that would offer the least lateral resistance. As a result, effective heights for some rocking piers adjacent to unequal size openings vary depending upon the direction of loading. The angles at pier hinges generally depend on bed and head joint dimensions and stair-step cracking along mortar joints (Fig. C11-5a). Using Moon's approach, the locations of the effective heights vary depending on the direction of loading. Dolce (1989) proposed that the effective height be defined by the midpoints of lines representing maximum 30° inclinations of flexural cracks initiating from the corners of openings. This method does not depend on the direction of loading and is a simpler alternative for modeling rocking wall systems for loads in both directions (Fig. C11-5b) compared to Moon's method (Fig. C11-5a). Dolce also proposed further refinements to account for pier–spandrel joint flexibility, but for simplicity the refinements are not included in Fig. C11-5b. The modeling approach based in part on Dolce in Fig. C11-5b will be generally more conservative for perforated wall systems that have rocking piers as the most critical components if the assumed h_{eff} is greater than Moon's modeling approach depicted in Fig. C11-5a. Most walls with rocking piers tend to respond asymmetrically to loads in different directions, so the analysis of rocking actions can benefit from modeling approaches that rely on incremental refinements and reanalysis.

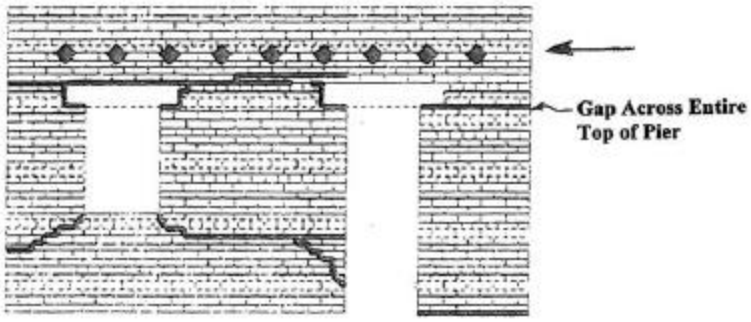

Figure C11-4. Perforated URM Walls with Rocking Piers That Have Dissimilar Aspect Ratios and Relatively Strong Spandrels Can Result in Spandrel Uplift and Gaps Forming across Entire Piers Rendering Relatively Slender Piers Ineffective and Potentially Unstable

Source: Paquette and Bruneau (2003); Copyright ASCE.

Test results of entire wall systems suggest that assumptions of boundary conditions can vary greatly from actual conditions. In addition, where estimated expected strengths for rocking are similar to expected strengths for toe crushing or bed-joint sliding, slight variations in actual conditions may substantially alter the strengths, drifts, and sequences of actions in piers and spandrels. Flanged walls can have considerably higher rocking strengths than those calculated by assuming that no flanges exist, and other actions, particularly force-controlled actions, may control rocking piers with flanges.

For rocking wall piers with relatively high axial loads, toe crushing can often onset as a secondary yield mechanism when the pier is subjected to a sufficiently large drift. For linear procedures, the m-factors for rocking are defined as a function of axial load with a force-controlled limit based on available testing described in C11.3.2.3.1 and Tremayne et al. (2012). For nonlinear procedures the rocking provisions included in this edition of the standard require the yield mechanism hierarchy to be explicitly considered. Given the potential for variation in response, users of this standard are encouraged to consider varying their assumptions about rocking wall and wall pier boundary conditions, effective pier heights, material properties, and yield hierarchy to determine the sensitivity of the expected performance.

6.5 References

Dolce, M., 1989, "Models for in-plane loading of masonry walls," Corso sul consolidamento degli edifice in muratura in zona sismica. Ordine degli Ingegneri (in Italian).

Moon, F., 2004, *Seismic Strengthening of Low-Rise Unreinforced Masonry Structures with Flexible Diaphragms*, Ph.D. thesis, Georgia Institute of Technology, Atlanta.

Paquette, J., and Bruneau, M., 2003, "Pseudo-dynamic testing of unreinforced masonry building with flexible diaphragms," *Journal of Structural Engineering*, 129(6), 708-716.

Tremayne, B., Turner, F., Russel, A., Oliver, S., and Derakhshan, H., 2012, "Proposed update to masonry provisions of ASCE/SEI 41: seismic evaluation and retrofit of existing buildings," *Proceedings of the 15th World Conference on Earthquake Engineering*, Portugal.

Project Participants

Federal Emergency Management Agency

Mike Mahoney (Project Officer, retired)
Federal Emergency Management Agency
400 C Street, SW
Washington, D.C. 20472

Andrew Herseth (Task Monitor)
Federal Emergency Management Agency
400 C Street, SW
Washington, D.C. 20472

Christina Aronson (Task Monitor)
Federal Emergency Management Agency
400 C Street, SW
Washington, D.C. 20472

William T. Holmes (Technical Advisor)
Consulting Structural Engineer
2600 La Cuesta
Oakland, CA 94611

Applied Technology Council

Jon A. Heintz (Project Executive)
Applied Technology Council
201 Redwood Shores Parkway, Suite 240
Redwood City, California 94065

Justin Moresco (Project Manager)
Applied Technology Council
201 Redwood Shores Parkway, Suite 240
Redwood City, California 94065

Project Technical Committee

Terry Lundeen (Project Tech. Director)
Coughlin Porter Lundeen, Inc.
801 Second Ave, Suite 900
Seattle, WA 98104

Russell Berkowitz
Forell/Elsesser Engineers, Inc.
160 Pine Street, 6th Floor
San Francisco, CA 94111

Wassim Ghannoum
The University of Texas at San Antonio
Biotechnology Science and Engineering Building, Room 1.202
One UTSA Circle
San Antonio, TX 78249

Bret Lizundia
Rutherford + Chekene
375 Beale St. Suite 310
San Francisco, California 94105

Roy Lobo
California Department of Health Care Access and Information
2020 West El Camino Avenue
Sacramento, California 95833

Mark Moore
ZFA Structural Engineers
100 Bush Street, Suite 1850
San Francisco, California 94104

James Parker
Simpson Gumpertz & Heger
1055 W. 7th Street, Suite 2500
Los Angeles, California 90017

Bob Pekelnicky
Degenkolb Engineers
375 Beale Street, Suite 500
San Francisco, CA 94105

Peter Somers
Magnusson Klemencic Associates
1301 Fifth Avenue, Suite 3200
Seattle, WA 98101

Bill Tremayne
Holmes Structures
235 Montgomery Street, Suite 1250
San Francisco, CA 94104

Project Review Panel

Michael Cochran (ATC Board Contact)
Thorton Tomasetti
707 Wilshire Blvd, Suite 4450
Los Angeles, CA 90017

Jennifer Goupil
American Society of Civil Engineers/Structural Engineering Institute
1801 Alexander Bell Drive
Reston, VA 20191

Phil Line
American Wood Council
222 Catoctin Circle SE, Suite 201
Leesburg, Virginia 20175

Bonnie Manley
American Iron and Steel Institute
41 Tucker Road
Norfolk, Massachusetts 02081

Khaled Nahlawi
American Concrete Institute
38800 Country Club Drive
Farmington Hills, MI 48331

Jason Thompson
NCMA 13750 Sunrise Valley Drive
Herndon, VA 20171

Working Group 1, Linear Analysis

Bret Lizundia (Team Leader)
Rutherford + Chekene
375 Beale St. Suite 310
San Francisco, California 94105

Russell Berkowitz
Forell/Elsesser Engineers, Inc.
160 Pine Street, 6th Floor
San Francisco, CA 94111

Erick Burgos
Rutherford + Chekene
375 Beale St. Suite 310
San Francisco, California 94105

Garrett Hagen
Degenkolb Engineers
300 South Grand Avenue, Suite 3850
Los Angeles, CA 90071

Stergios Koutrouvelis
Rutherford + Chekene
375 Beale St. Suite 310
San Francisco, California 94105

Terry Lundeen
Coughlin Porter Lundeen, Inc.
801 Second Ave, Suite 900
Seattle, WA 98104

Jie Luo
Rutherford + Chekene
375 Beale St. Suite 310
San Francisco, California 94105

Bob Pekelnicky
Degenkolb Engineers
375 Beale Street, Suite 500
San Francisco, CA 94105

Cynthia Perry
Rutherford + Chekene
375 Beale St. Suite 310
San Francisco, California 94105

Working Group 1, Nonlinear Analysis

Bob Pekelnicky (Team Leader)
Degenkolb Engineers
375 Beale Street, Suite 500
San Francisco, CA 94105

Russell Berkowitz
Forell/Elsesser Engineers, Inc.
160 Pine Street, 6th Floor
San Francisco, CA 94111

Rebecca Collins
Coughlin Porter Lundeen, Inc.
801 Second Ave, Suite 900
Seattle, WA 98104

Greg Deierlein
Stanford University
Dept. of Civil & Environmental Engineering
Blume Earthquake Engineering Center, MC 3037
Stanford, California 94305

Wassim Ghannoum
The University of Texas at San Antonio
Biotechnology Science and Engineering Building,
Room 1.202
One UTSA Circle
San Antonio, TX 78249

Garrett Hagen
Degenkolb Engineers
300 South Grand Avenue, Suite 3850
Los Angeles, CA 90071

Ron Hamburger
Simpson Gumpertz & Heger, Inc.
100 Pine Street, Suite 1600
San Francisco, CA 94111

Bret Lizundia
Rutherford + Chekene
375 Beale St. Suite 310
San Francisco, California 94105

Terry Lundeen
Coughlin Porter Lundeen, Inc.
801 Second Ave, Suite 900
Seattle, WA 98104

Pearl Ranchal
Degenkolb Engineers
375 Beale Street, Suite 500
San Francisco, CA 94105

Charles Roeder
University of Washington
Civil Engineering Department
Seattle, Washington 98195-2700

Nick Skok
Degenkolb Engineers
375 Beale Street, Suite 500
San Francisco, CA 94105

Bill Tremayne
Holmes Structures
235 Montgomery Street, Suite 1250
San Francisco, CA 94104

Working Group 2, Foundations

Roy Lobo (Team Leader)
California Department of Health Care Access and Information
2020 West El Camino Avenue
Sacramento, California 95833

Ryan Bogart
ZFA Structural Engineers
601 Montgomery Street, Suite 1450
San Francisco, CA 94111

John Egan
Senior Principal Geotechnical Engineer
766 Brookside Drive
Danville, California 94526

Bruce Kutter
University of California, Davis
Dept. of Civil and Environmental Engineering
3103 Ghausi Hall
One Shields Avenue
Davis, CA 95616

Bret Lizundia
Rutherford + Chekene
375 Beale St. Suite 310
San Francisco, California 94105

Mark Moore
ZFA Structural Engineers
100 Bush Street, Suite 1850
San Francisco, California 94104

Bob Pekelnicky
Degenkolb Engineers
375 Beale Street, Suite 500
San Francisco, CA 94105

Peter Somers
Magnusson Klemencic Associates
1301 Fifth Avenue, Suite 3200
Seattle, WA 98101

Kate Spiesman
ZFA Structural Engineers
100 Bush Street, Suite 1850
San Francisco, California 94104

Working Group 3, Concrete Structural Walls

Wassim Ghannoum (Team Leader)
The University of Texas at San Antonio
Biotechnology Science and Engineering Building, Room 1.202
One UTSA Circle
San Antonio, TX 78249

Saman Abdullah
University of Sulaimani
Dept. of Civil Engineering
Kirkuk Road, Sulaimani
Kurdistan Region, Iraq

Garrett Hagen
Degenkolb Engineers
300 South Grand Avenue, Suite 3850
Los Angeles, CA 90071

Afshar Jalalian
Rutherford + Chekene
375 Beale St. Suite 310
San Francisco, California 94105

Laura Lowes
University of Washington
Dept. of Civil & Environmental Engineering
201 More Hall, Box 352700
Seattle, Washington 98195

Mohamed Talaat
Simpson Gumpertz & Heger, Inc.
4695 MacArthur Ct, Suite 500
Newport Beach, CA 92660

John Wallace
University of California, Los Angeles
Dept. of Civil and Environmental Engineering
5731C Boelter Hall
Los Angeles, California 90095-1593

Working Group 4, Tier 1 and 2

Peter Somers (Team Leader)
Magnusson Klemencic Associates
1301 Fifth Avenue, Suite 3200
Seattle, WA 98101

Russell Berkowitz
Forell/Elsesser Engineers, Inc.
160 Pine Street, 6th Floor
San Francisco, CA 94111

James Parker
Simpson Gumpertz & Heger
1055 W. 7th Street, Suite 2500
Los Angeles, California 90017

Eugene Trahern
Cascade Crest Consulting Engineers
PO Box 2242
Sisters, OR 97759

Working Group 6, Unreinforced Masonry

Bret Lizundia (Team Leader)
Rutherford + Chekene
375 Beale St. Suite 310
San Francisco, California 94105

Rebecca Collins
Coughlin Porter Lundeen, Inc.
801 Second Ave, Suite 900
Seattle, WA 98104

Terry Lundeen
Coughlin Porter Lundeen, Inc.
801 Second Ave, Suite 900
Seattle, WA 98104

Cynthia Perry
Rutherford + Chekene
375 Beale St. Suite 310
San Francisco, California 94105

Bill Tremayne
Holmes Structures
235 Montgomery Street, Suite 1250
San Francisco, CA 94104

Kylin Vail
Rutherford + Chekene
375 Beale St. Suite 310
San Francisco, California 94105

FEMA

FEMA P-2208